



# Risk and Exposure Assessment for Review of the Secondary National Ambient Air Quality Standards for Oxides of Nitrogen and Oxides of Sulfur

Final

Appendices

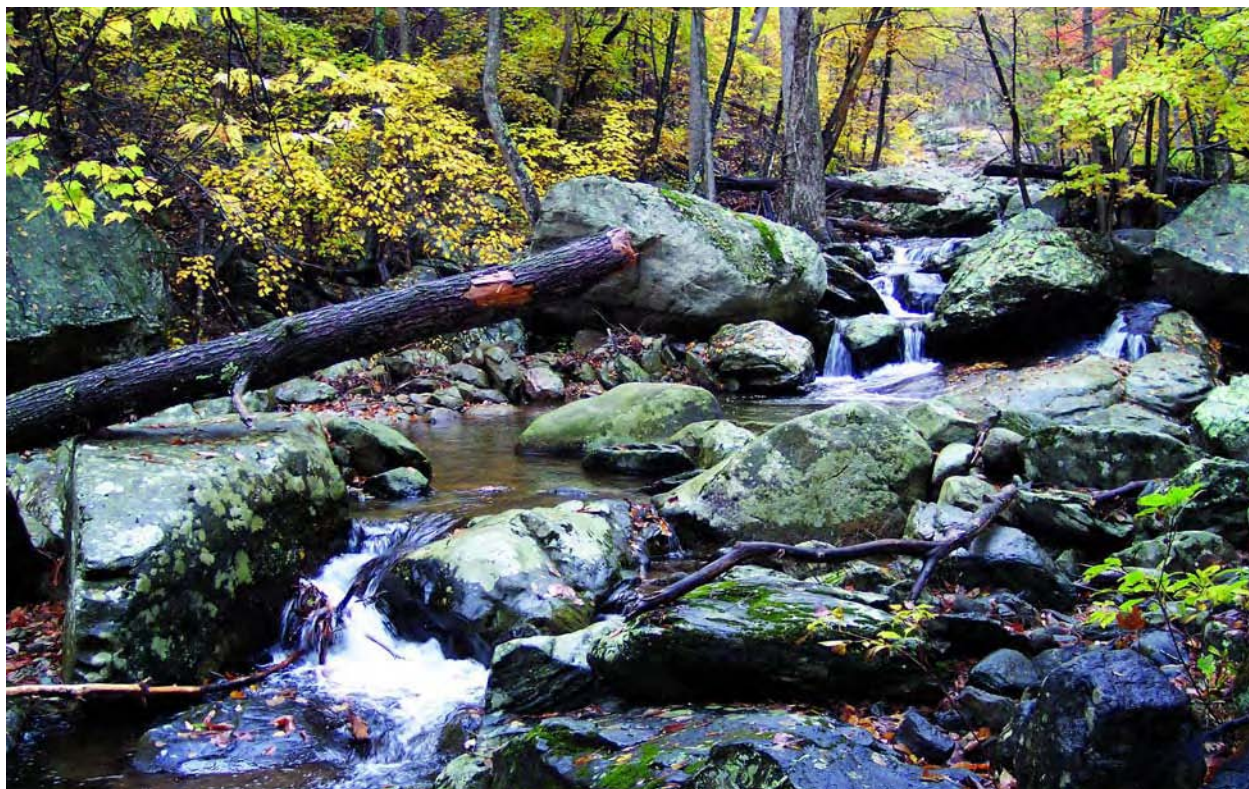


Photo courtesy of the National Park Service



EPA-452/R-09-008b  
September 2009

Risk and Exposure Assessment for Review of the Secondary National Ambient Air Quality  
Standards for Oxides of Nitrogen and Oxides of Sulfur

Final

Appendices

U.S. Environmental Protection Agency  
Office of Air Quality Planning and Standards

Research Triangle Park, NC

## **DISCLAIMER**

This document has been prepared by staff from the Health and Environmental Impacts and Air Quality Analysis Divisions of the Office of Air Quality Planning and Standards, the Clean Air Markets Division, Office of Air Programs, the National Center for Environmental Assessment, Office of Research and Development, and the National Health and Environmental Effects Research Laboratory, Office of Research and Development, U.S. Environmental Protection Agency. Any opinions, findings, conclusions, or recommendations are those of the authors and do not necessarily reflect the views of EPA. This document is being circulated to obtain review and comment from the Clean Air Scientific Advisory Committee (CASAC) and the general public. Comments on this document should be addressed to Dr. Anne Rea, U.S. Environmental Protection Agency, Office of Air Quality Planning and Standards, C539-02, Research Triangle Park, North Carolina 27711 (email: [rea.anne@epa.gov](mailto:rea.anne@epa.gov)).



September 2009

**Appendix 1**  
**Aquatic Nutrient Enrichment Case Study**  
**Community Multiscale Air Quality (CMAQ) Model**

*Final*

**Prepared by**

U.S. Environmental Protection Agency  
Office of Atmospheric Programs  
Washington, DC



## TABLE OF CONTENTS

Acronyms and Abbreviations .....	1-iv
1.0 Introduction.....	1-1
1.1 Overview of CMAQ Model Application.....	1-1
1.2 CMAQ Model Performance Evaluation .....	1-3
1.2.1 CMAQv4.6 2002 Annual Average Predictions versus Observations for the Eastern United States .....	1-5
1.2.2 CMAQv4.6 2002 Annual Average Predictions versus Observations for the Western United States.....	1-9
1.2.3 CMAQv4.7 2002 through 2005 Annual and Monthly Average Predictions versus Observations .....	1-13
1.2.4 Extended Evaluation of CMAQv4.6 2002 Predictions versus Observations .....	1-21
2.0 References.....	1-29

## LIST OF FIGURES

Figure 1.1-1. CMAQ continental United States and eastern and western modeling domains. ....	1-2
Figure 1.2-1. 2002 CMAQv4.6 annual average SO <sub>2</sub> predicted concentrations versus observations at CASTNet sites in the eastern domain. ....	1-6
Figure 1.2-2. 2002 CMAQv4.6 annual average SO <sub>4</sub> <sup>2-</sup> predicted concentrations versus observations at CASTNet sites in the eastern domain. ....	1-6
Figure 1.2-3. 2002 CMAQv4.6 annual average TNO <sub>3</sub> predicted concentrations versus observations at CASTNet sites in the eastern domain. ....	1-7
Figure 1.2-4. 2002 CMAQv4.6 annual average NH <sub>4</sub> <sup>+</sup> predicted concentrations versus observations at CASTNet sites in the eastern domain. ....	1-7
Figure 1.2-5. 2002 CMAQv4.6 annual average SO <sub>4</sub> <sup>2-</sup> predicted wet deposition versus observations at NADP sites in the eastern domain. ....	1-8
Figure 1.2-6. 2002 CMAQv4.6 annual average NO <sub>3</sub> <sup>-</sup> predicted wet deposition versus observations at NADP sites in the eastern domain. ....	1-8
Figure 1.2-7. 2002 CMAQv4.6 annual average NH <sub>4</sub> <sup>+</sup> predicted wet deposition versus observations at NADP sites in the eastern domain. ....	1-9
Figure 1.2-8. 2002 CMAQv4.6 annual average SO <sub>4</sub> <sup>2-</sup> predicted concentrations versus observations at CASTNet sites in the western domain. ....	1-10
Figure 1.2-9. 2002 CMAQv4.6 annual average SO <sub>2</sub> predicted concentrations versus observations at CASTNet sites in the western domain. ....	1-10
Figure 1.2-10. 2002 CMAQv4.6 annual average TNO <sub>3</sub> predicted concentrations versus observations at CASTNet sites in the western domain. ....	1-11

Figure 1.2-11. 2002 CMAQv4.6 annual average $\text{NH}_4^+$ predicted concentrations versus observations at CASTNet sites in the western domain. ....	1-11
Figure 1.2-12. 2002 CMAQv4.6 annual average $\text{SO}_4^{2-}$ predicted wet deposition versus observations at NADP sites in the western domain. ....	1-12
Figure 1.2-13. 2002 CMAQv4.6 annual average $\text{NO}_3^-$ predicted wet deposition versus observations at NADP sites in the western domain. ....	1-12
Figure 1.2-14. 2002 CMAQv4.6 annual average $\text{NH}_4^+$ predicted wet deposition versus observations at NADP sites in the western domain. ....	1-13
Figure 1.2-15. 2002–2005 Domain-wide average $\text{SO}_4^{2-}$ predicted concentrations and observations by month at CASTNet Sites in the eastern domain. ....	1-15
Figure 1.2-16. 2002–2005 Domain-wide monthly aggregate model performance statistics for $\text{SO}_4^{2-}$ concentrations based on CASTNet sites in the eastern domain. ....	1-15
Figure 1.2-17. 2002–2005 Domain-wide average $\text{TNO}_3$ predicted concentrations and observations by month at CASTNet sites in the eastern domain. ....	1-16
Figure 1.2-18. 2002–2005 Domain-wide monthly aggregate model performance statistics for $\text{TNO}_3$ concentrations based on CASTNet Sites in the eastern domain. ....	1-16
Figure 1.2-19. 2002–2005 Domain-wide average $\text{NH}_4^+$ predicted concentrations and observations by month at CASTNet sites in the eastern domain. ....	1-17
Figure 1.2-20. 2002–2005 domain-wide monthly aggregate model performance statistics for $\text{NH}_4^+$ concentrations based on CASTNet sites in the eastern domain. ....	1-17
Figure 1.2-21. 2002–2005 domain-wide average $\text{SO}_4^{2-}$ predicted deposition and observations by month at NADP sites in the eastern domain. ....	1-18
Figure 1.2-22. 2002–2005 domain-wide monthly aggregate model performance statistics for $\text{SO}_4^{2-}$ deposition based on NADP sites in the eastern domain. ....	1-18
Figure 1.2-23. 2002–2005 domain-wide average $\text{NO}_3^-$ predicted deposition and observations by month at NADP sites in the eastern domain. ....	1-19
Figure 1.2-24. 2002–2005 domain-wide monthly aggregate model performance statistics for $\text{NO}_3^-$ deposition based on NADP sites in the eastern domain. ....	1-19
Figure 1.2-25. 2002–2005 domain-wide average $\text{NH}_4^+$ predicted deposition and observations by month at NADP sites in the eastern domain. ....	1-20
Figure 1.2-26. 2002–2005 domain-wide monthly aggregate model performance statistics for $\text{NH}_4^+$ deposition based on NADP sites in the eastern domain. ....	1-20

## LIST OF TABLES

Table 1.1-1. CMAQ Nitrogen and Sulfur Deposition Species .....	1-3
Table 1.1-2. Formulas for Calculating Nitrogen and Sulfur Deposition .....	1-3
Table 1.2-1. Normalized Mean Bias Statistics for Predicted and Observed Pollutant Concentration .....	1-13
Table 1.2-2. Normalized Mean Bias Statistics for Predicted and Observed Pollutant Wet Deposition .....	1-14
Table 1.2-3. CMAQv4.6 Model Performance Statistics for PM <sub>2.5</sub> and Selected Component Species Concentrations .....	1-22
Table 1.2-4. CMAQ v4.6 2002 Model Performance Statistics for Nitric Acid and Sulfur Dioxide.....	1-25
Table 1.2-5. CMAQv4.6 2002 Model Performance Statistics for Annual Sulfate and Nitrate Wet Deposition Model Performance Statistics.....	1-26
Table 1.2-6. CMAQv4.6 Model Performance Statistics for Hourly Ozone Concentrations .....	1-27
Table 1.2-7. CMAQv4.6 Model Performance Statistics for 8-hour Daily Maximum Ozone Concentrations .....	1-28

## ACRONYMS AND ABBREVIATIONS

ANO <sub>3</sub>	particle nitrate
ASO <sub>4</sub>	particle sulfate
CMAQ	Community Multiscale Air Quality
EPA	U.S. Environmental Protection Agency
ha	hectare
HONO	nitrous acid
HNO <sub>3</sub>	nitric acid
kg	kilogram
NADP	National Atmospheric Deposition Program
N <sub>2</sub> O <sub>5</sub>	nitrogen pentoxide
NH <sub>4</sub> <sup>+</sup>	ammonium
NH <sub>x</sub>	total reduced nitrogen
NO	nitric oxide
NO <sub>2</sub>	nitrogen dioxide
NO <sub>3</sub> <sup>-</sup>	nitrate
NO <sub>x</sub>	nitrogen oxides
NO <sub>y</sub>	oxidized nitrogen
NMB	normalized mean bias
NTR	organic nitrate
PAN	peroxyacetyl nitrate
PM	particulate matter
ORD	Office of Research and Development
SO <sub>2</sub>	sulfur dioxide
SO <sub>4</sub> <sup>2-</sup>	sulfate
SO <sub>x</sub>	sulfur oxides

## 1.0 INTRODUCTION

This appendix provides an overview of the Community Multiscale Air Quality (CMAQ) model and the modeling system used for simulating pollutant concentrations and deposition for the years 2002 through 2005. Included in this appendix are the results of a model performance evaluation in which model predictions of sulfur dioxide (SO<sub>2</sub>), nitrogen dioxide (NO<sub>2</sub>), SO<sub>4</sub><sup>2-</sup>, total NO<sub>3</sub><sup>-\*</sup>, and ammonium (NH<sub>4</sub><sup>+</sup>) concentrations and SO<sub>4</sub><sup>2-</sup>, NO<sub>3</sub><sup>-</sup>, and NH<sub>4</sub><sup>+</sup> wet deposition are compared to observations.

### 1.1 OVERVIEW OF CMAQ MODEL APPLICATION

The CMAQ model is a comprehensive, peer-reviewed (Aiyer et al., 2007), three-dimensional grid-based Eulerian air quality model designed to simulate the formation and fate of gaseous and particle (i.e., particulate matter or PM) species, including ozone, oxidant precursors, and primary and secondary PM concentrations and deposition over urban, regional, and larger spatial scales (Dennis et al., 1996; U.S. EPA, 1999; Bryun and Schere, 2006). CMAQ is run for user-defined input sets of meteorological conditions and emissions. For this analysis, we are using predictions from several existing CMAQ runs. These runs include annual simulations for 2002 using CMAQv4.6 and annual simulations for each of the years 2002 through 2005 using CMAQv4.7. CMAQv4.6 was released by the U.S. Environmental Protection Agency's (EPA's) Office of Research and Development (ORD) in October 2007. CMAQv4.7 along with an updated version of CMAQ's meteorological preprocessor (MCIPv3.4)<sup>†</sup> were released in October 2008<sup>‡</sup>. The CMAQ modeling regions (i.e., modeling domains), are shown in **Figure 1.1-1**. The 2002 simulation with CMAQv4.6 was performed for both the Eastern and Western domains. The horizontal spatial resolution of the CMAQ grid cells in these domains is approximately 12 x 12 km. The 2002 through 2005 simulations with CMAQv4.7 were performed for the eastern 12-km domain and for the continental United States domain, which has a grid resolution of 36 x 36 km. The CMAQv4.6 and v4.7 annual simulations feature year-specific meteorology, as well as year-specific emissions inventories for key source sectors, such as utilities, on-road vehicles, nonroad

---

\* Total NO<sub>3</sub><sup>-</sup> includes the mass of nitric acid gas and particulate nitrate.

<sup>†</sup> The scientific updates in CMAQ v4.7 and MCIP v3.4 can be found at the following web links:

[http://www.cmascenter.org/help/model\\_docs/cmaq/4.7/RELEASE\\_NOTES.txt](http://www.cmascenter.org/help/model_docs/cmaq/4.7/RELEASE_NOTES.txt)

[http://www.cmascenter.org/help/model\\_docs/mcip/3.4/ReleaseNotes](http://www.cmascenter.org/help/model_docs/mcip/3.4/ReleaseNotes)

<sup>‡</sup> The differences in nitrogen and sulfur deposition in the case study areas between CMAQ v4.6 and v4.7 for 2002 are small, as described in Chapter 3.



vehicles, wild fires, and natural biogenic sources. Emissions for other sectors of the inventory for each of the years modeled rely on inventories for 2002. Details on the development of emissions, meteorology, and other inputs to the 2002 CMAQv4.6 runs can be found in a separate report (U.S. EPA, 2008). Inputs for the CMAQv4.7 runs for 2002 through 2005 were derived using procedures similar to those for the CMAQv4.6 2002 runs.

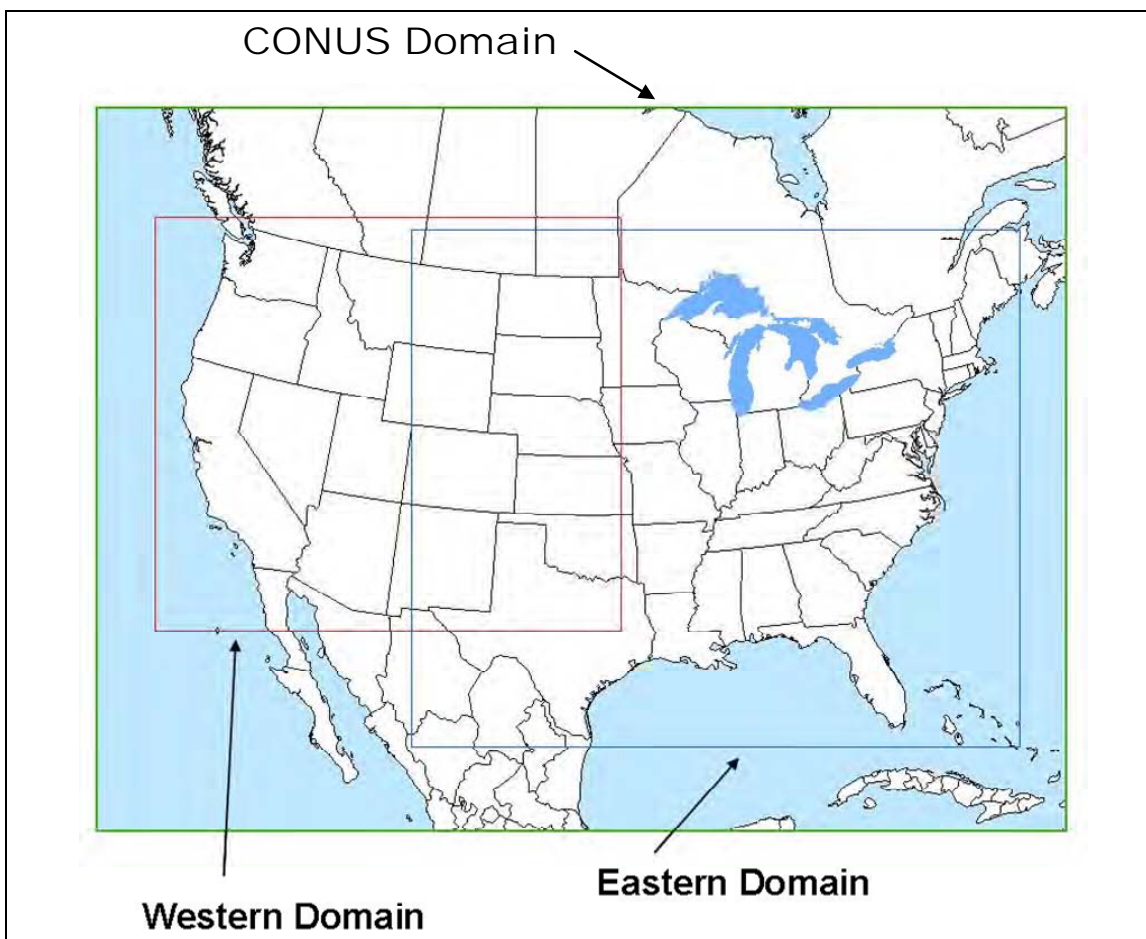


**Figure 1.1-1.** CMAQ continental United States and eastern and western modeling domains.

Each CMAQ model run produces hourly concentrations and wet and dry deposition of individual pollutant species in each grid cell within the domain. Concentration predictions for  $\text{NO}_y^*$  and  $\text{SO}_2$ , both in units of parts per billion (ppb), are produced as part of our standard model output. The CMAQ deposition data for nitrogen and sulfur species are used to calculate oxidized and reduced wet and dry nitrogen deposition, wet and dry sulfur deposition, and total reactive

---

\*  $\text{NO}_y$  is defined as the sum of CMAQ predictions for  $\text{NO}$ ,  $\text{NO}_2$ ,  $\text{HNO}_3$ , and PAN.

nitrogen and total sulfur deposition. These composite deposition variables are derived from the species identified in **Table 1.1-1** as applied in the formulas shown in **Table 1.1-2**. The CMAQ deposition data are in units of kilograms per hectare (kg/ha). We are also including in the analysis gridded precipitation data that were input to the CMAQ runs to help understand the temporal and spatial behavior of wet deposition.

**Table 1.1-1.** CMAQ Nitrogen and Sulfur Deposition Species

CMAQ Species	Chemical Name
ANO <sub>3</sub>	Particle Nitrate
HNO <sub>3</sub>	Nitric Acid
N <sub>2</sub> O <sub>5</sub>	Nitrogen Pentoxide
HONO	Nitrous Acid
NO	Nitric Oxide
NO <sub>2</sub>	Nitrogen Dioxide
PAN	Peroxyacyl Nitrate
NTR	Organic Nitrate
ASO <sub>4</sub>	Particle Sulfate
SO <sub>2</sub>	Sulfur Dioxide

**Table 1.1-2.** Formulas for Calculating Nitrogen and Sulfur Deposition

Deposition Type	Formula
Oxidized Nitrogen	$0.2258 \cdot \text{ANO}_3 + 0.2222 \cdot \text{HNO}_3 + 0.4667 \cdot \text{NO} + 0.3043 \cdot \text{NO}_2 + 0.2592 \cdot \text{N}_2\text{O}_5 + 0.1157 \cdot \text{PAN} + 0.2978 \cdot \text{HONO} + 0.1052 \cdot \text{NTR}$
Reduced Nitrogen	$0.7777 \cdot \text{NH}_4 + 0.8235 \cdot \text{NH}_3$
Sulfur	$0.3333 \cdot \text{ASO}_4 + 0.5000 \cdot \text{SO}_2$

## 1.2 CMAQ MODEL PERFORMANCE EVALUATION

This evaluation of CMAQ focuses on model performance for concentrations and deposition of nitrogen and sulfur species. For the most part, these comparisons are based on predictions and observations using annual average concentrations and deposition, to be consistent with the use of annual predictions in this assessment. A more comprehensive set of

model performance information for the 2002 CMAQ simulation is provided in Section 1-2.5, below.

The purpose of this evaluation is to provide information on how well model predictions of performance for concentrations and deposition of nitrogen and sulfur species match the observed data on a regional basis, and not to evaluate performance for an individual location or area. The CMAQ predictions of  $\text{SO}_2$ ,  $\text{SO}_4^{2-}$ , total  $\text{NO}_3^{-*}$  and  $\text{NH}_4^+$  concentrations, as well as  $\text{SO}_4^{2-}$ ,  $\text{NO}_3^-$ , and  $\text{NH}_4^+$  wet deposition, were compared to the corresponding measured data for the years 2002 through 2005<sup>†</sup>. This analysis compared the annual average predictions of  $\text{SO}_2$ ,  $\text{SO}_4^{2-}$ , total  $\text{NO}_3^-$ , and  $\text{NH}_4^+$  concentrations to measurements from CASTNet sites. It also compared the CMAQ annual total  $\text{SO}_4^{2-}$ ,  $\text{NO}_3^-$ , and  $\text{NH}_4^+$  wet deposition to measurements of these species at National Atmospheric Deposition Program (NADP) sites. In all cases, the model predictions and observations were paired in space and time to align with the corresponding observations.

For the 2002 CMAQv4.6 runs, model performance results are provided for both the eastern and western modeling domains. For the 2002 through 2005 CMAQv4.7, runs have performance results for concentrations and deposition for the eastern modeling domain only.<sup>‡</sup> The CMAQ v4.7 performance results for 2002 through 2005 are courtesy of EPA's ORD. The equations used to calculate model performance statistics for the CMAQv4.6 and v4.7 simulations are described elsewhere (U.S. EPA, 2008).

The "acceptability" of model performance is judged by comparing the CMAQ performance results to the range of performance found in other recent regional photochemical model applications. (U.S. EPA, 2006a; U.S. EPA 2006b; Dentener and Crutzen, 1993) These other modeling studies represent a wide range of modeling analyses, which cover various models, model configurations, domains, years and/or episodes, chemical mechanisms, and aerosol modules. The CMAQv4.6 and v4.7 performance results are within the range found by these other studies. A key limitation of this evaluation, as noted in Section 3.5, is the lack of "true" dry deposition measurements for nitrogen and sulfur that are appropriate for comparison to CMAQ deposition predictions. Thus, this evaluation relies upon the model performance

---

\* Total nitrate includes nitric acid gas and particulate nitrate.

† There are insufficient non-urban measurements of  $\text{NO}_2$  to provide for a meaningful regional evaluation of this pollutant for the purposes of this assessment.

‡ CMAQv4.7 was not run for the Western 12-km domain for 2002 through 2005.

results for various gas and particle species concentrations as well as wet deposition, collectively, to indicate the extent that the modeling system provides a scientifically acceptable approach for use in this assessment.

### **1.2.1 CMAQv4.6 2002 Annual Average Predictions versus Observations for the Eastern United States**

**Figures 1.2-1 through 1.2-7** display the comparison of CMAQv4.6 predictions of annual average concentrations and annual average wet deposition for monitoring CASTNet (concentrations) and NADP (wet deposition) sites the eastern domain. Each data point in the figures represents an annual average paired observation and CMAQ prediction at a particular CASTNet or NADP site. Solid lines indicate the factor of 2 around the 1:1 line shown between them.

Using the normalized mean bias (NMB) statistic, we see the 2002 CMAQ run tends to underpredict concentrations of  $\text{SO}_4^{2-}$  (NMB = -12.0%) and  $\text{NH}_4^+$  (NMB = -3.4%) and overpredict  $\text{SO}_2$  (NMB = 33.8%) and  $\text{TNO}_3$  (NMB = 11.2%) within the eastern domain for 2002. For wet deposition, the 2002 CMAQ run tends to underpredict  $\text{NO}_3^-$  (NMB = -11.4%) and  $\text{NH}_4^+$  (-6.1%) and overpredict  $\text{SO}_4^{2-}$  wet deposition (9.4%).

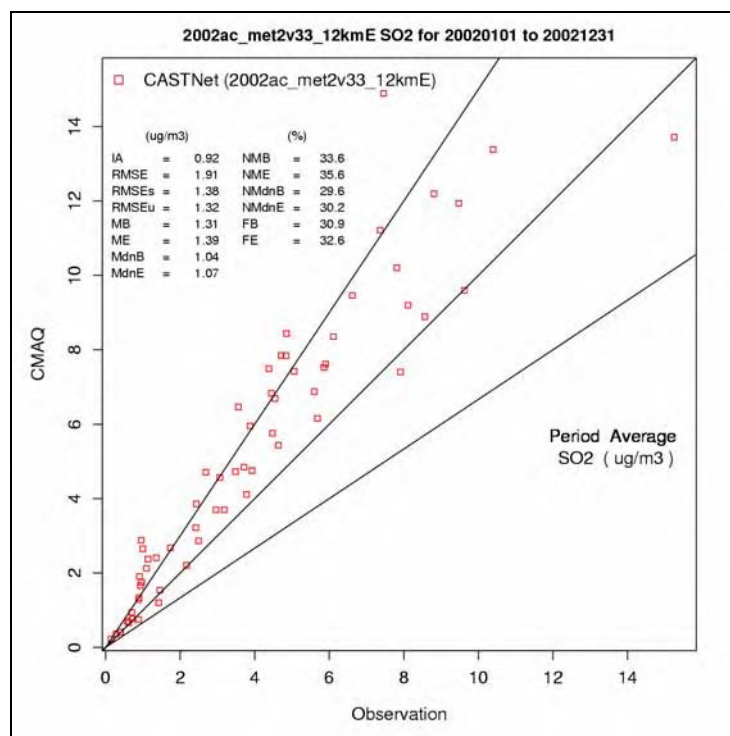


**Figure 1.2-1.** 2002 CMAQv4.6 annual average SO<sub>2</sub> predicted concentrations versus observations at CASTNet sites in the eastern domain.

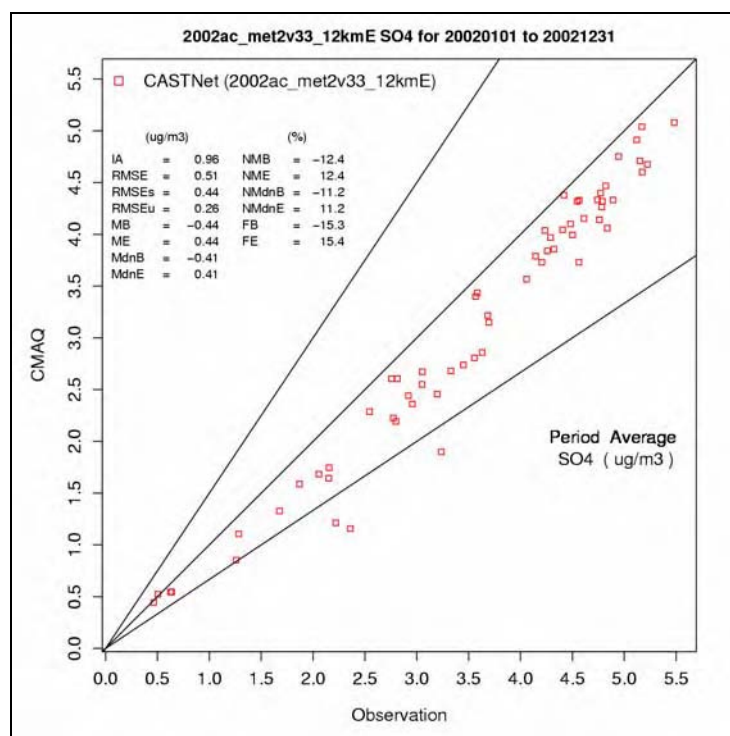


**Figure 1.2-2.** 2002 CMAQv4.6 annual average SO<sub>4</sub><sup>2-</sup> predicted concentrations versus observations at CASTNet sites in the eastern domain.

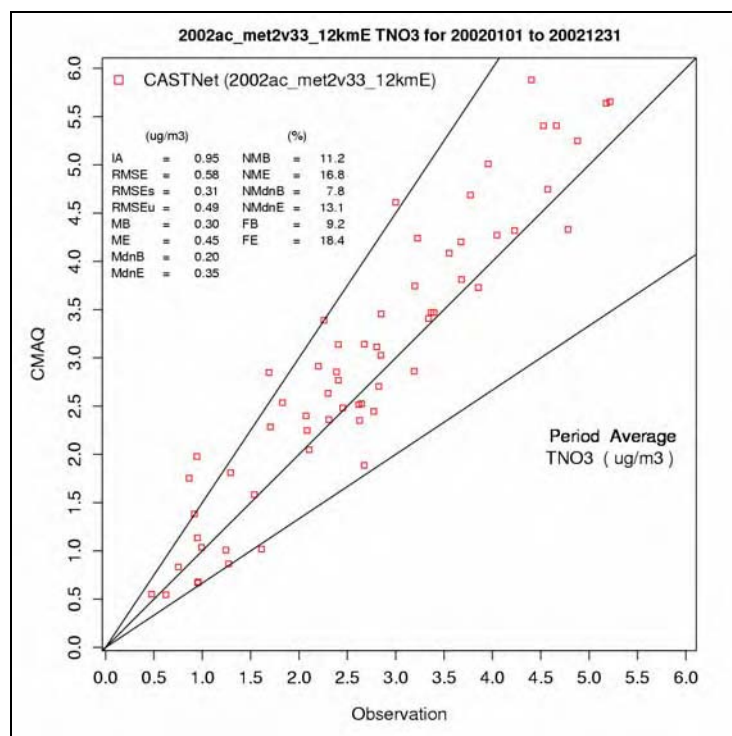


**Figure 1.2-3.** 2002 CMAQv4.6 annual average TNO<sub>3</sub> predicted concentrations versus observations at CASTNet sites in the eastern domain.

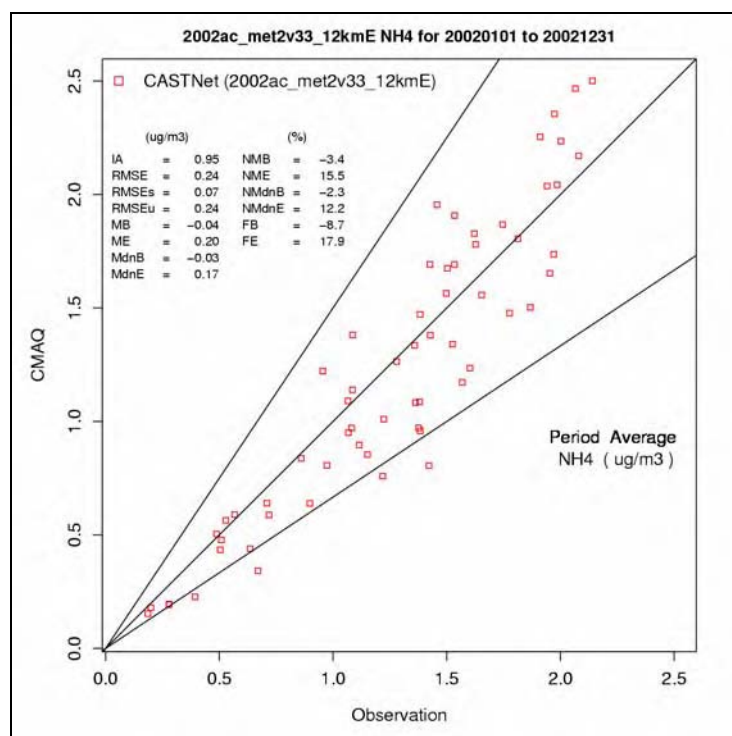


**Figure 1.2-4.** 2002 CMAQv4.6 annual average NH<sub>4</sub><sup>+</sup> predicted concentrations versus observations at CASTNet sites in the eastern domain.

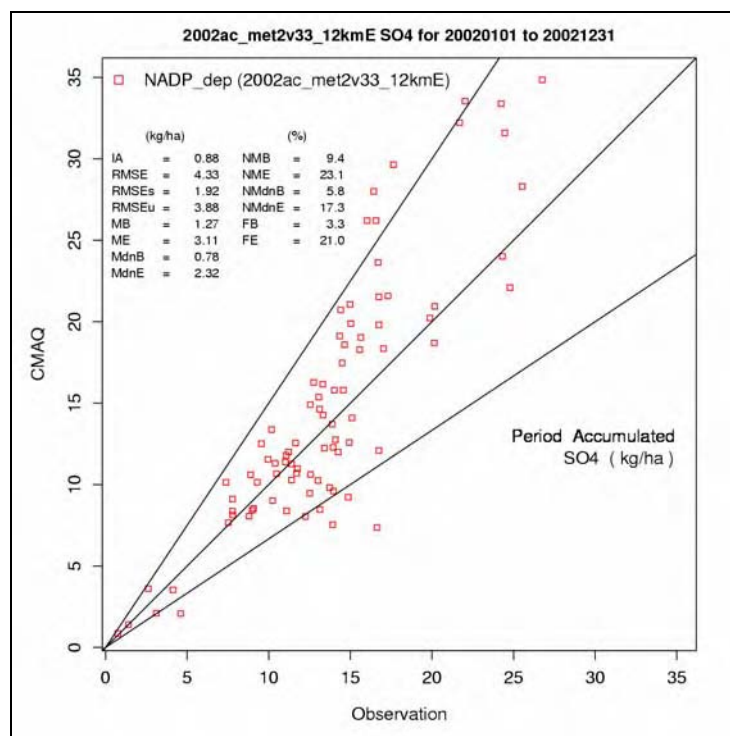


**Figure 1.2-5.** 2002 CMAQv4.6 annual average  $\text{SO}_4^{2-}$  predicted wet deposition versus observations at NADP sites in the eastern domain.

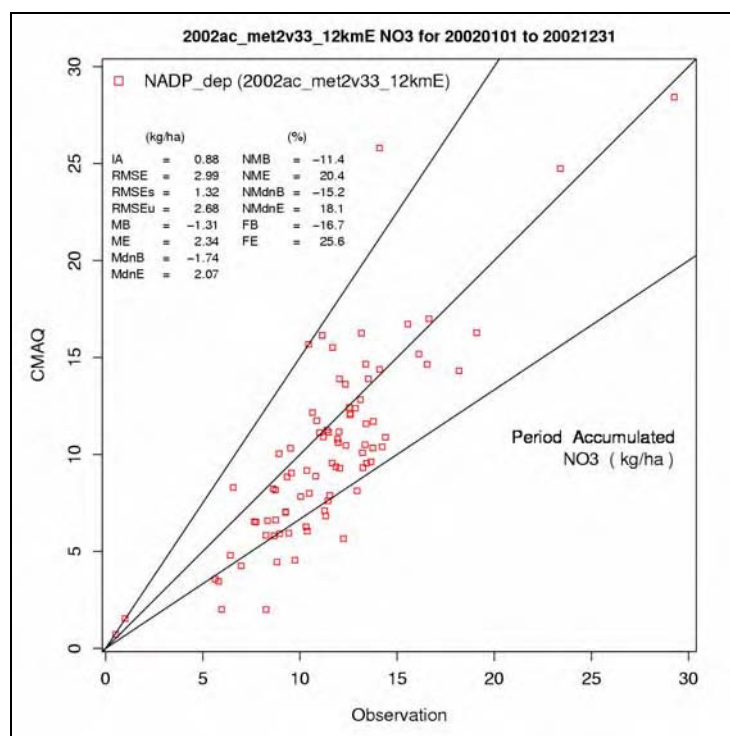


**Figure 1.2-6.** 2002 CMAQv4.6 annual average  $\text{NO}_3^-$  predicted wet deposition versus observations at NADP sites in the eastern domain.



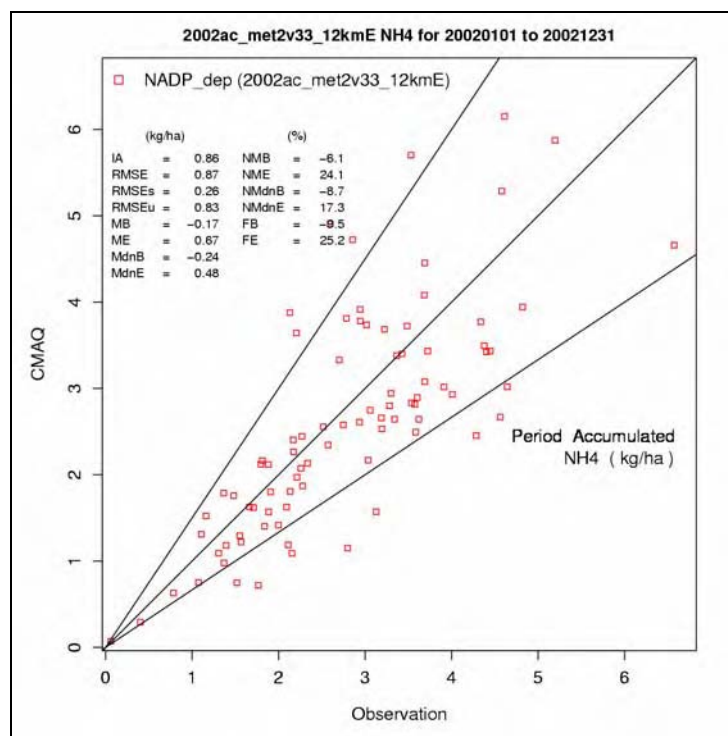


**Figure 1.2-7.** 2002 CMAQv4.6 annual average  $\text{NH}_4^+$  predicted wet deposition versus observations at NADP sites in the eastern domain.

## 1.2.2 CMAQv4.6 2002 Annual Average Predictions versus Observations for the Western United States

Figures 1.2-8 through 1.2-14 display the comparison of CMAQv4.6 predictions of annual average concentrations and annual average wet deposition for monitoring CASTNet (concentrations) and NADP (wet deposition) sites the western domain. Each data point in the figures represents an annual average paired observation and CMAQ prediction at a particular CASTNet or NADP site. Solid lines indicate the factor of 2 around the 1:1 line shown between them.

Using the NMB statistic, the 2002 CMAQ run tends to underpredict concentrations of  $\text{SO}_4^{2-}$  (NMB = -20.8%),  $\text{NH}_4^+$  (NMB = -16.2%), and  $\text{TNO}_3$  (NMB = -19.6%) and to overpredict  $\text{SO}_2$  (NMB = 31.2%) within the western domain for 2002. For wet deposition, the 2002 CMAQ run tends to underpredict  $\text{NO}_3^-$  (NMB = -43.6%),  $\text{NH}_4^+$  (NMB = -43.4%), and  $\text{SO}_4^{2-}$  wet deposition (NMB = -20.5%). In general, model performance for the western domain is degraded somewhat compared to the results found for the eastern domain.

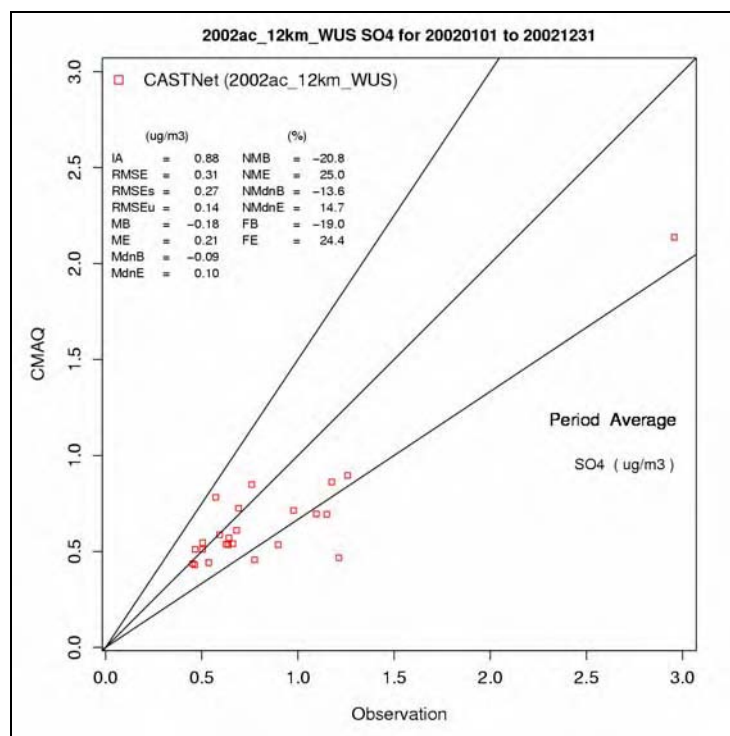


**Figure 1.2-8.** 2002 CMAQv4.6 annual average  $\text{SO}_4^{2-}$  predicted concentrations versus observations at CASTNet sites in the western domain.

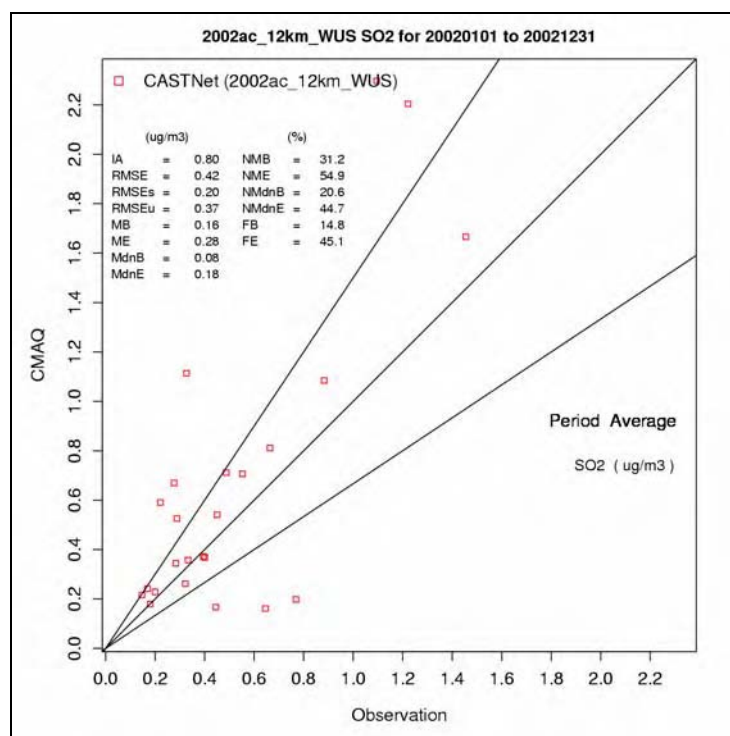


**Figure 1.2-9.** 2002 CMAQv4.6 annual average  $\text{SO}_2$  predicted concentrations versus observations at CASTNet sites in the western domain.

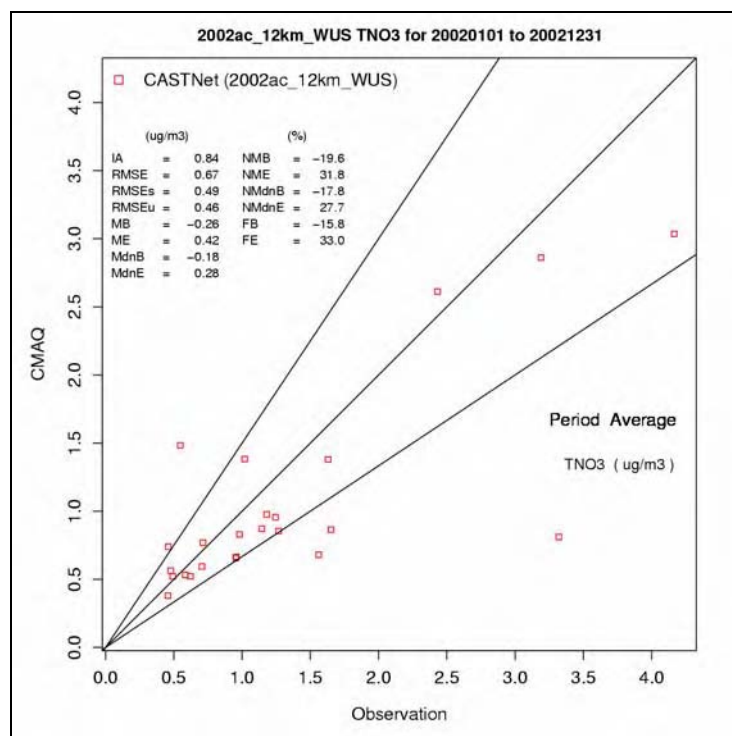


**Figure 1.2-10.** 2002 CMAQv4.6 annual average TNO<sub>3</sub> predicted concentrations versus observations at CASTNet sites in the western domain.

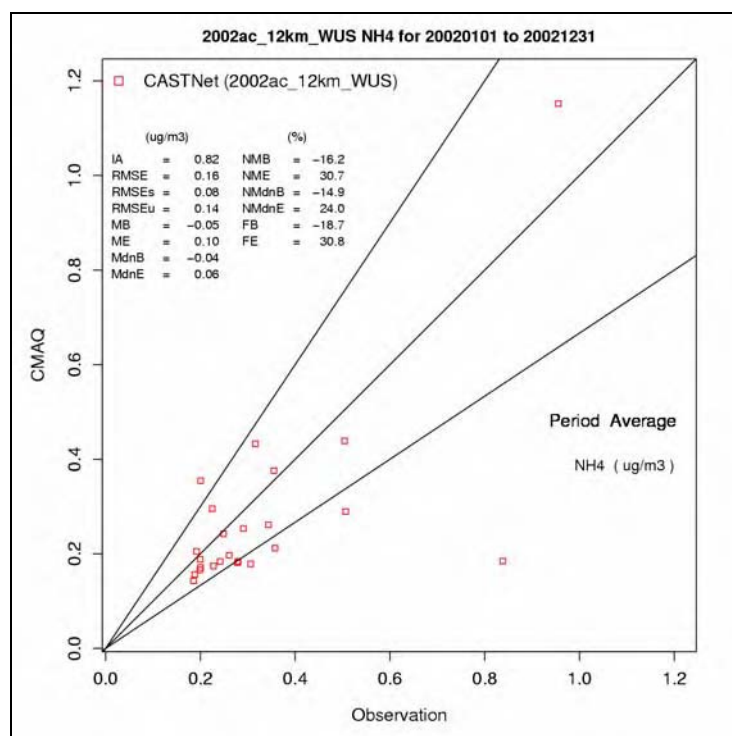


**Figure 1.2-11.** 2002 CMAQv4.6 annual average NH<sub>4</sub><sup>+</sup> predicted concentrations versus observations at CASTNet sites in the western domain.

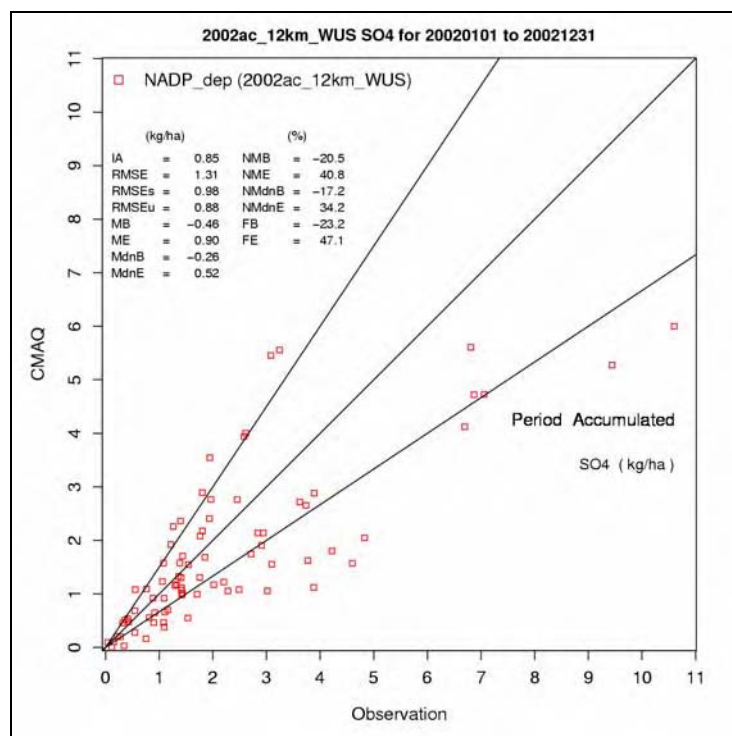


**Figure 1.2-12.** 2002 CMAQv4.6 annual average  $\text{SO}_4^{2-}$  predicted wet deposition versus observations at NADP sites in the western domain.

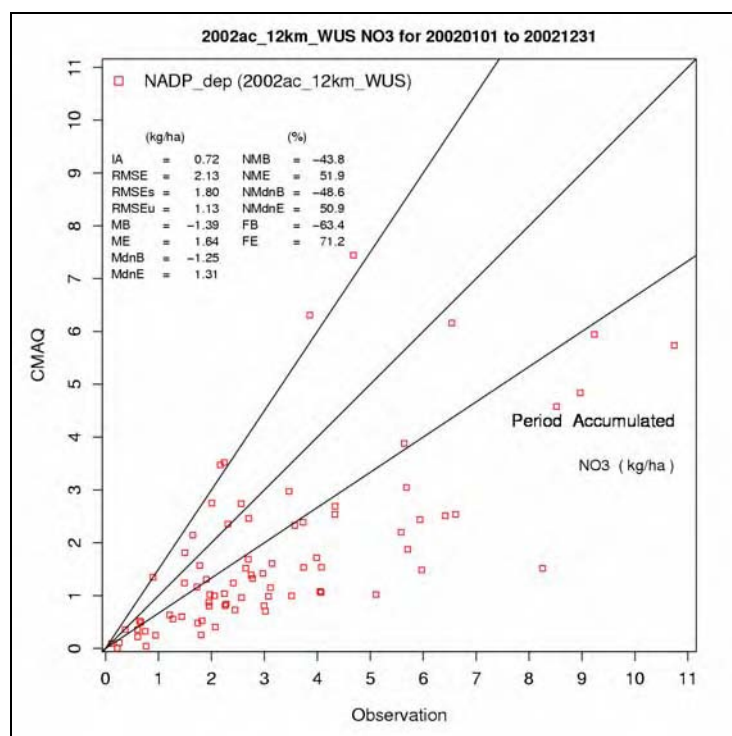


**Figure 1.2-13.** 2002 CMAQv4.6 annual average  $\text{NO}_3^-$  predicted wet deposition versus observations at NADP sites in the western domain.

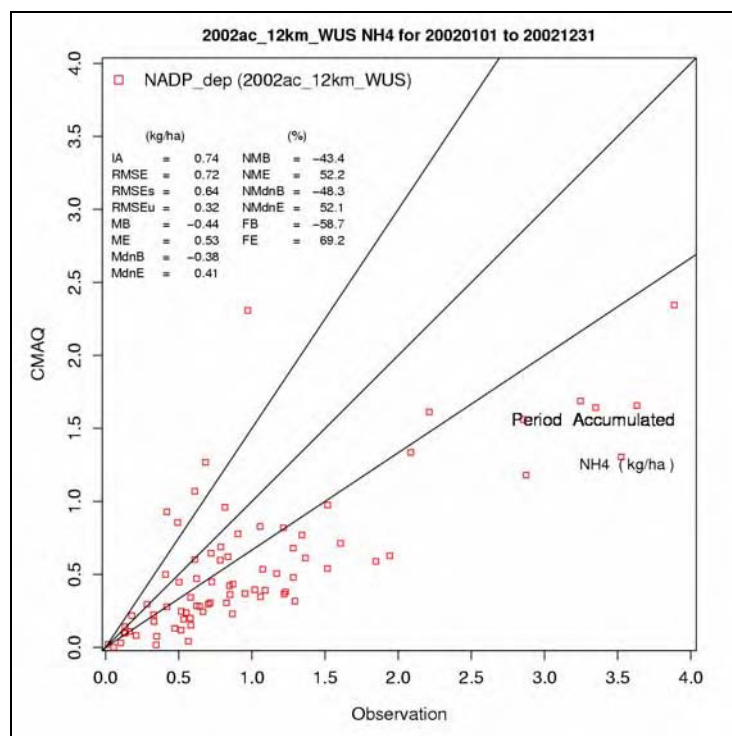


**Figure 1.2-14.** 2002 CMAQv4.6 annual average  $\text{NH}_4^+$  predicted wet deposition versus observations at NADP sites in the western domain.

### 1.2.3 CMAQv4.7 2002 through 2005 Annual and Monthly Average Predictions versus Observations

The annual normalized mean bias statistics for the CMAQv4.7 2002 through 2005 simulations are presented in **Table 1.2-1** and **Table 1.2-2** for annual average concentrations and annual total wet deposition, respectively. In general, model performance for each species is similar in each of the 4 years. The CMAQv4.7 performance for 2002 is similar to that of CMAQv4.6 for most species. Notable differences are seen for concentrations of  $\text{TNO}_3$  and  $\text{NH}_4^+$ . For  $\text{TNO}_3$ , the overprediction in CMAQv4.7 is about twice that of CMAQv4.6. For  $\text{NH}_4^+$ , CMAQv4.7 slightly overpredicts observations (4%), while CMAQv4.6 slightly underpredicts observations (-3%).

**Table 1.2-1.** Normalized Mean Bias Statistics for Predicted and Observed Pollutant Concentration

Pollutant Concentrations	2002	2003	2004	2005
$\text{SO}_2$	45%	39%	47%	41%
$\text{SO}_4^{2-}$	-13%	-9%	-13%	-17%

Pollutant Concentrations	2002	2003	2004	2005
TNO <sub>3</sub>	22%	26%	22%	24%
NH <sub>4</sub> <sup>+</sup>	4%	11%	7%	2%

**Table 1.2-2.** Normalized Mean Bias Statistics for Predicted and Observed Pollutant Wet Deposition

Pollutant Deposition	2002	2003	2004	2005
SO <sub>4</sub> <sup>2-</sup>	11%	6%	11%	6%
NO <sub>3</sub> <sup>-</sup>	-13%	-17%	-14%	-17%
NH <sub>4</sub> <sup>+</sup>	-11%	-16%	-9%	-13%

**Figures 1.2-15 through 1.2-26** provide a comparison of observed and predicted monthly concentrations and monthly total wet deposition for an aggregate of monitoring sites the eastern domain. This time series format is intended to reveal differences and similarities in performance within and across the 4-year period. **Figures 1.2-15 and 1.2-21** indicate that the predictions of SO<sub>4</sub><sup>2-</sup> concentration and SO<sub>4</sub><sup>2-</sup> wet deposition closely track the temporal patterns exhibited by the observations. However, the correlation is higher and the error is lower for SO<sub>4</sub><sup>2-</sup> concentrations than the corresponding statistics for SO<sub>4</sub><sup>2-</sup> wet deposition (see **Figures 1.2-16 and 1.2-22**). Predictions of NO<sub>3</sub><sup>-</sup> concentrations, although highly correlated with the observations in most months, show relatively large error and positive bias in the fall with a peak in October for each year. Model performance for wet deposition of NO<sub>3</sub><sup>-</sup> also has a seasonal pattern, with underprediction of approximately 40% in the late spring and summer and overprediction from October through December. Observed concentrations of NH<sub>4</sub><sup>+</sup> are overpredicted by CMAQ in the spring and fall and underpredicted in the summer. The overprediction in the spring peaks in March/April, while the peak overprediction in the fall occurs in October/November of each year. Model predictions of NH<sub>4</sub><sup>+</sup> wet deposition more closely track the temporal patterns of observations than do the predictions of NH<sub>4</sub><sup>+</sup> concentrations. There does not appear to be strong seasonal differences in performance across the 4 years as seen in NH<sub>4</sub><sup>+</sup> concentrations; however, the greatest underprediction appears to occur in May in each year. The differences and similarities in the seasonal patterns in model performance for various species are being analyzed by EPA to understand and explain these relationships, with the goal of improving model



performance through improvements to emissions and meteorological inputs and scientific formulation.

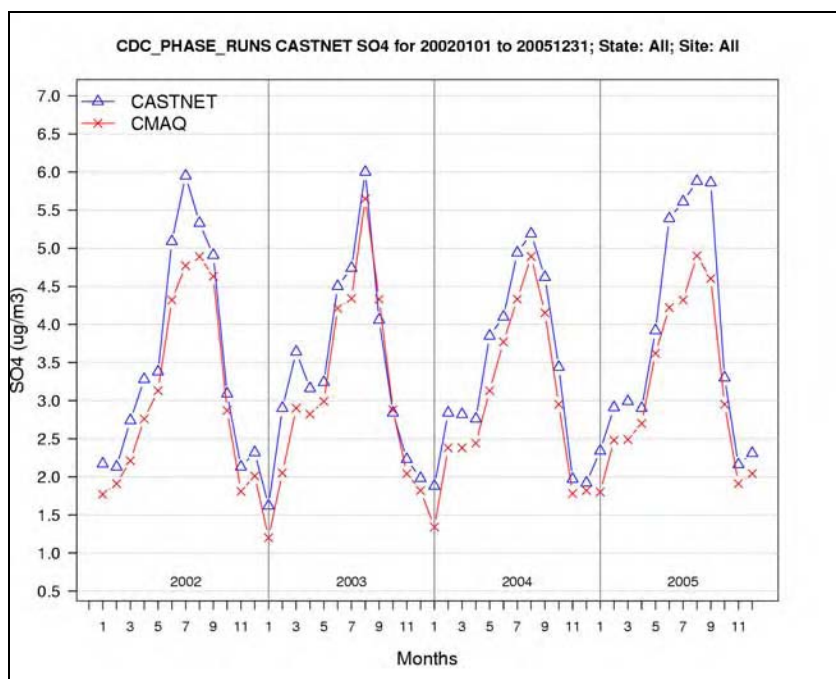


**Figure 1.2-15.** 2002–2005 Domain-wide average  $\text{SO}_4^{2-}$  predicted concentrations and observations by month at CASTNet Sites in the eastern domain.

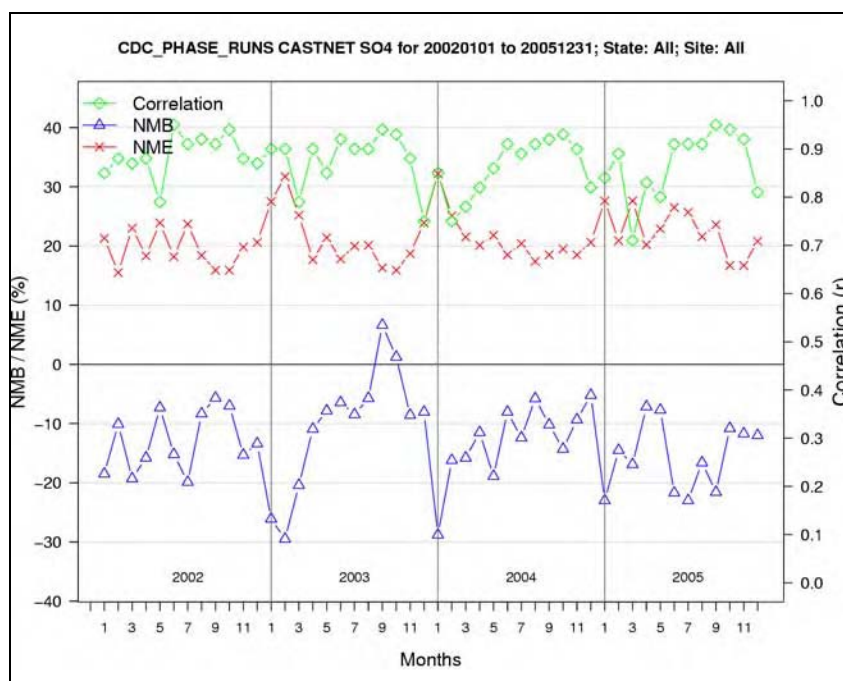


**Figure 1.2-16.** 2002–2005 Domain-wide monthly aggregate model performance statistics for  $\text{SO}_4^{2-}$  concentrations based on CASTNet sites in the eastern domain.



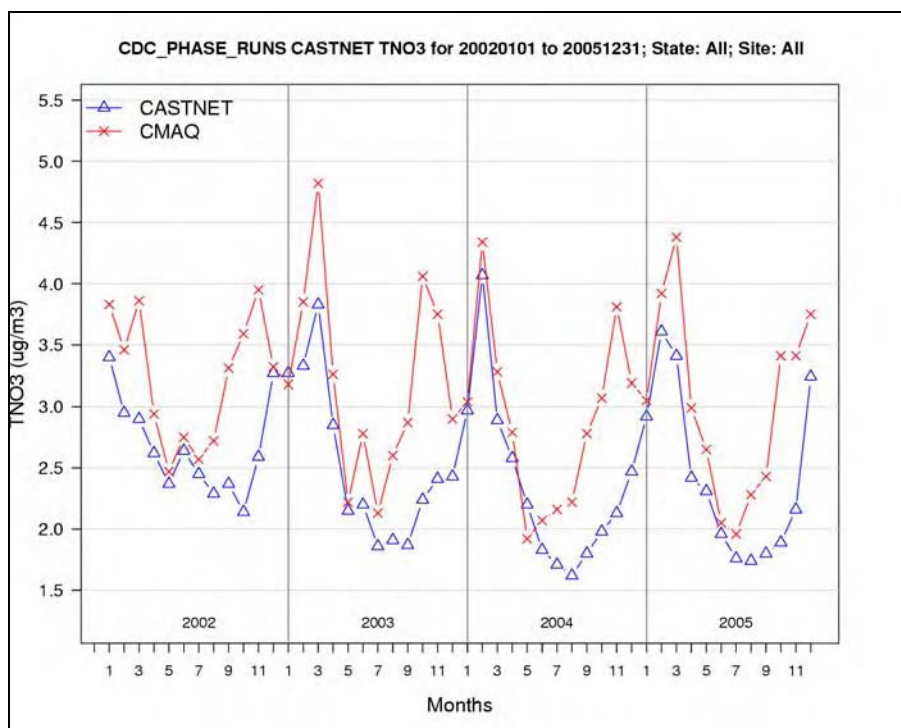


**Figure 1.2-17.** 2002–2005 Domain-wide average TNO<sub>3</sub> predicted concentrations and observations by month at CASTNet sites in the eastern domain.

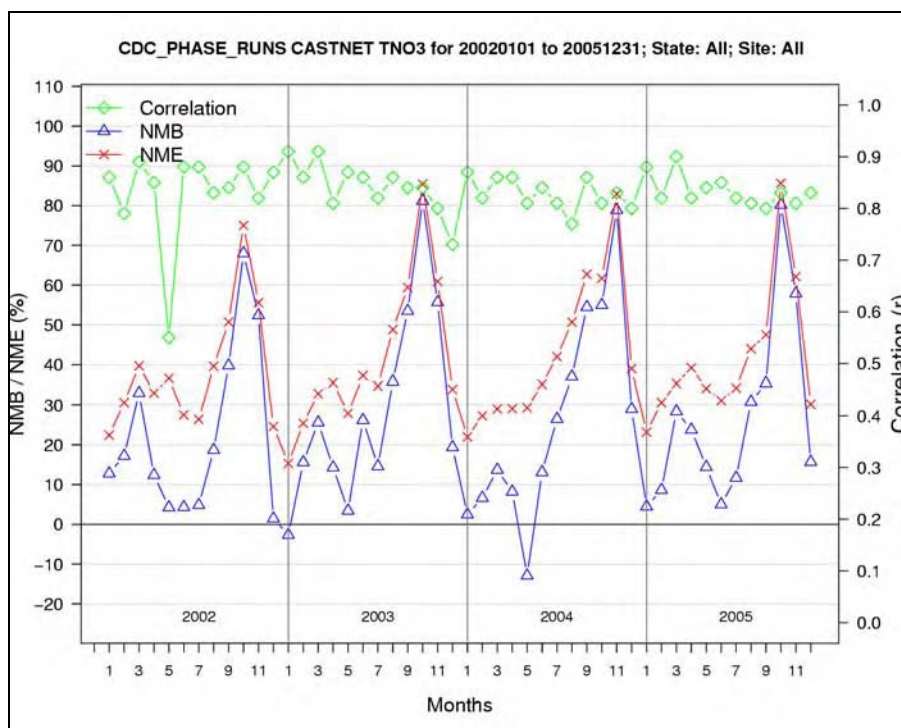


**Figure 1.2-18.** 2002–2005 Domain-wide monthly aggregate model performance statistics for TNO<sub>3</sub> concentrations based on CASTNet Sites in the eastern domain.

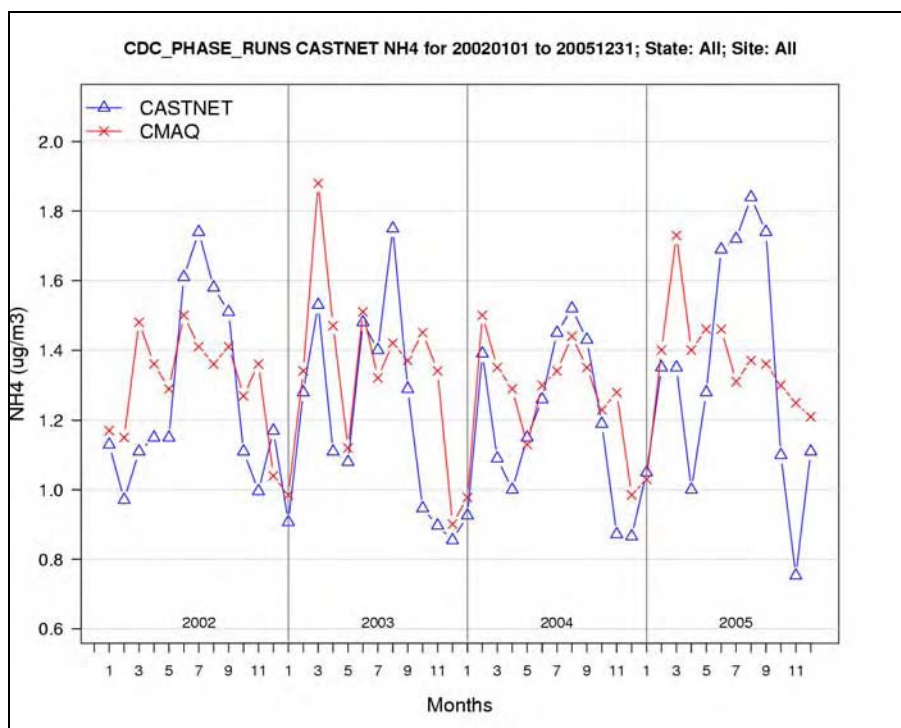


**Figure 1.2-19.** 2002–2005 Domain-wide average  $\text{NH}_4^+$  predicted concentrations and observations by month at CASTNet sites in the eastern domain.

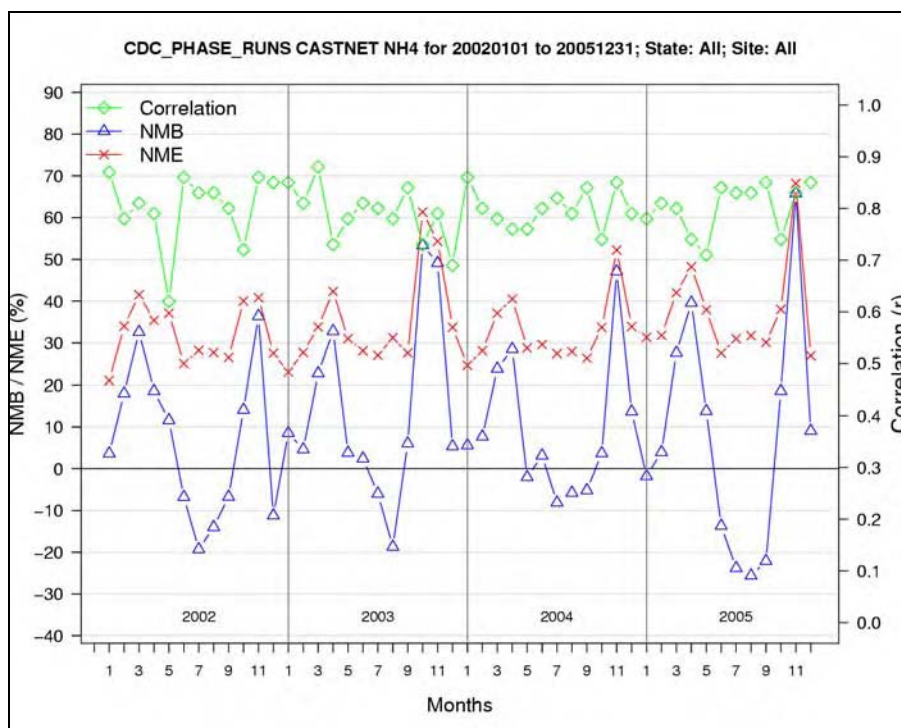


**Figure 1.2-20.** 2002–2005 domain-wide monthly aggregate model performance statistics for  $\text{NH}_4^+$  concentrations based on CASTNet sites in the eastern domain.

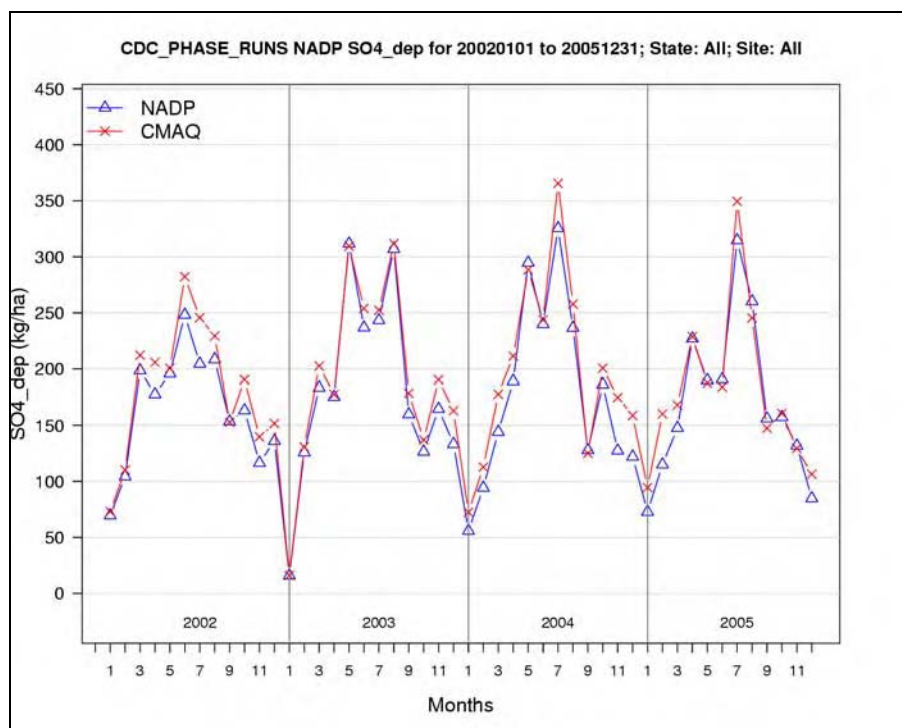


**Figure 1.2-21.** 2002–2005 domain-wide average  $\text{SO}_4^{2-}$  predicted deposition and observations by month at NADP sites in the eastern domain.

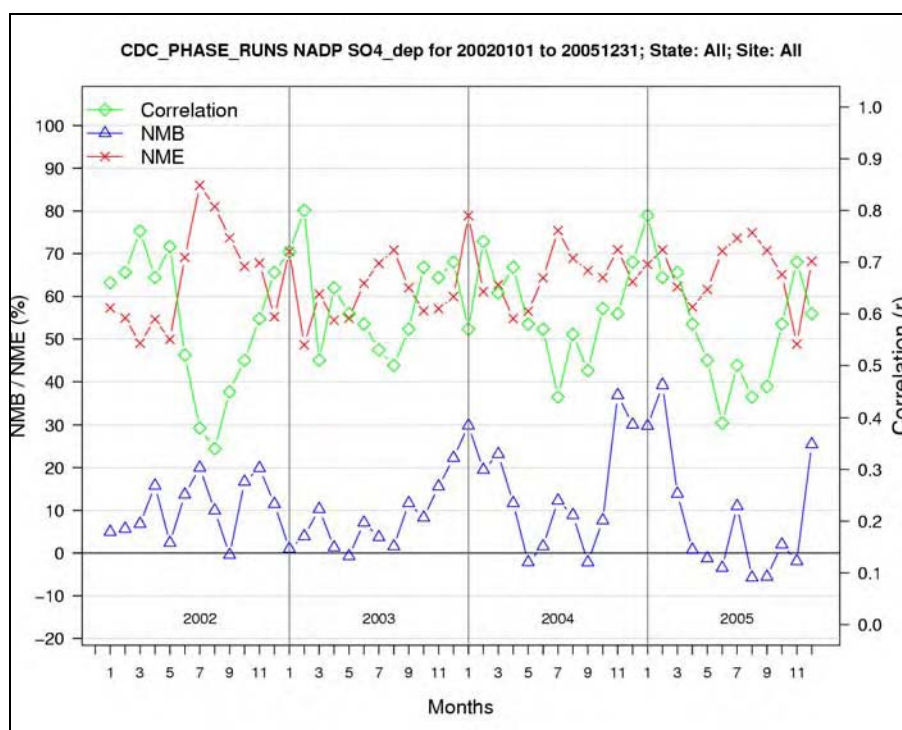


**Figure 1.2-22.** 2002–2005 domain-wide monthly aggregate model performance statistics for  $\text{SO}_4^{2-}$  deposition based on NADP sites in the eastern domain.

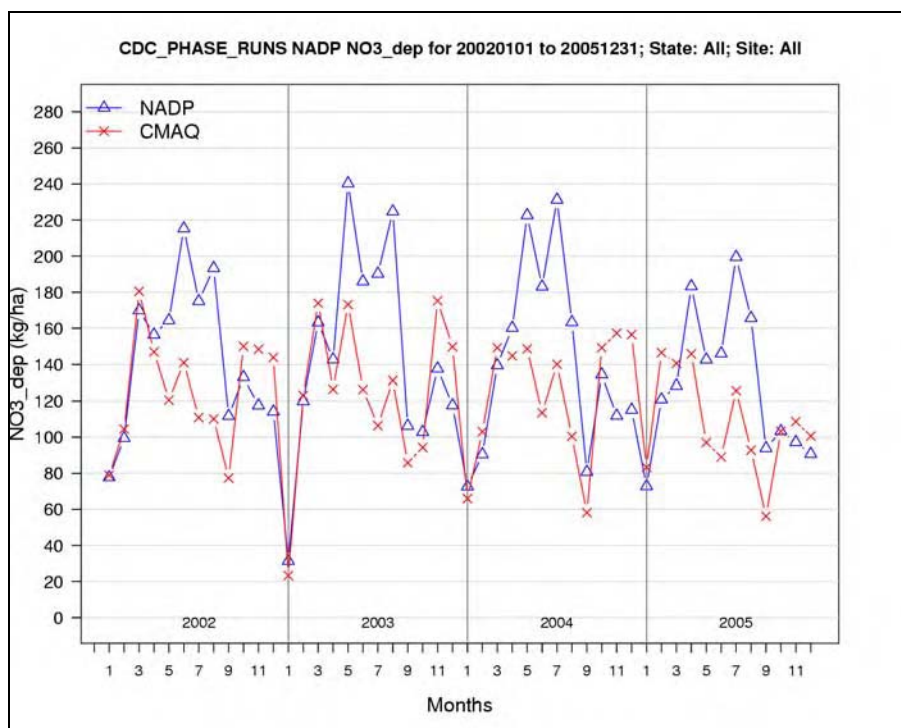


**Figure 1.2-23.** 2002–2005 domain-wide average NO<sub>3</sub><sup>-</sup> predicted deposition and observations by month at NADP sites in the eastern domain.

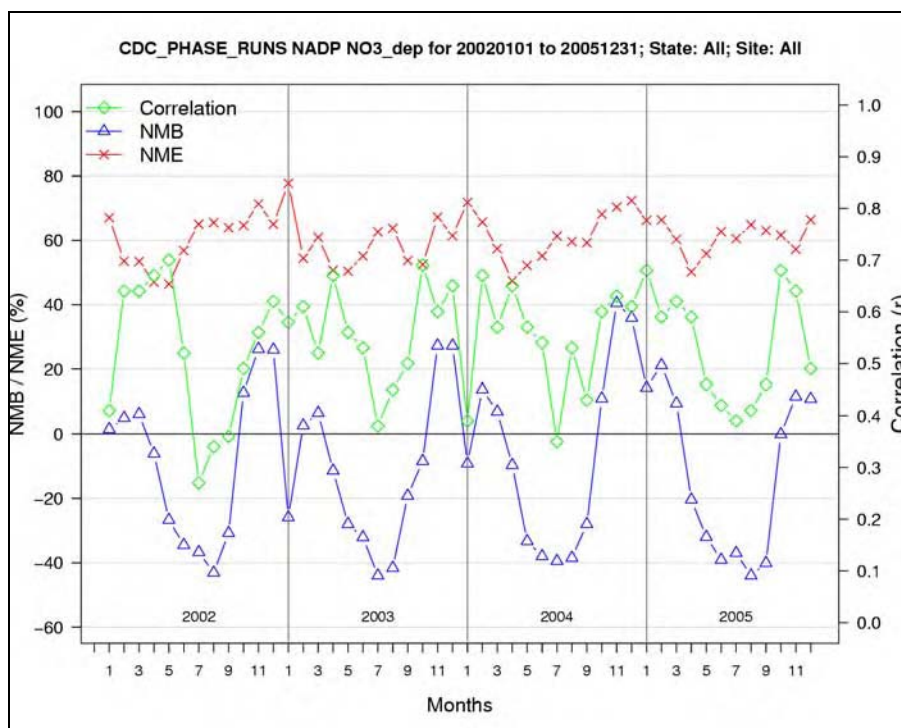


**Figure 1.2-24.** 2002–2005 domain-wide monthly aggregate model performance statistics for NO<sub>3</sub><sup>-</sup> deposition based on NADP sites in the eastern domain.



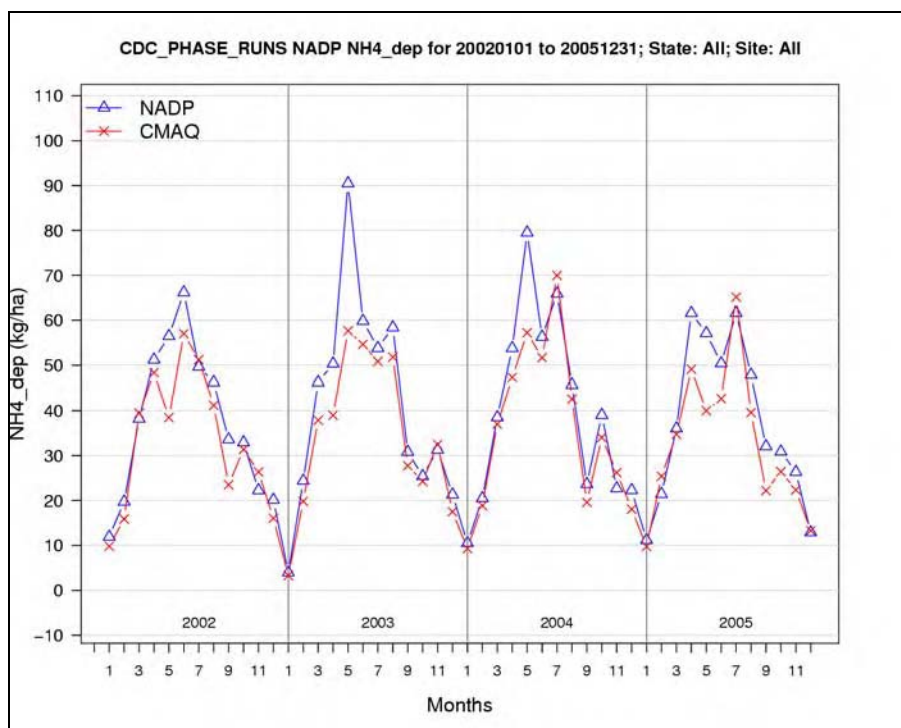


**Figure 1.2-25.** 2002–2005 domain-wide average NH<sub>4</sub><sup>+</sup> predicted deposition and observations by month at NADP sites in the eastern domain.

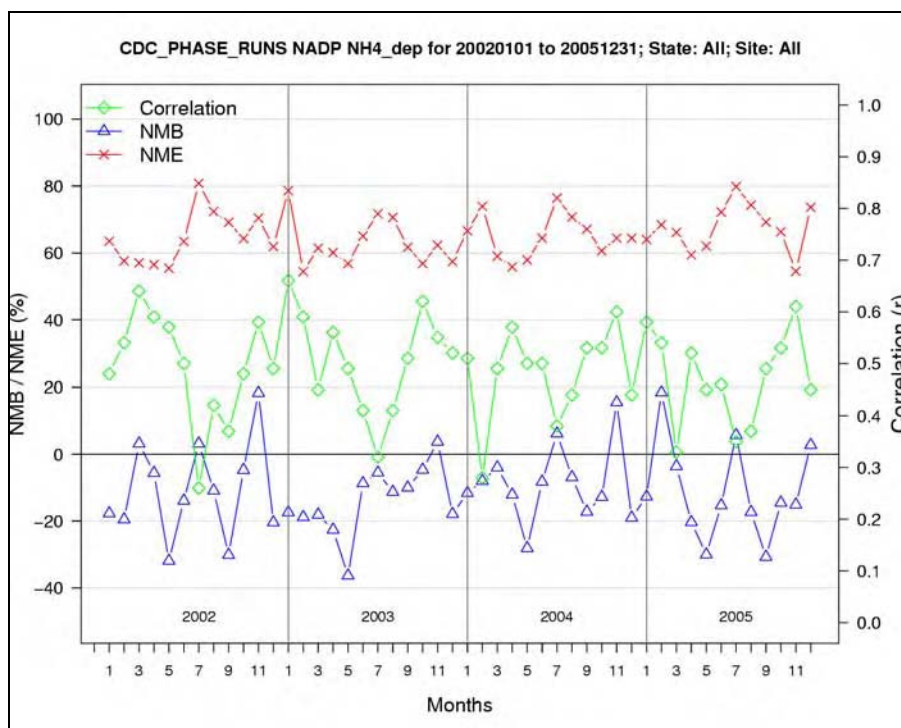


**Figure 1.2-26.** 2002–2005 domain-wide monthly aggregate model performance statistics for NH<sub>4</sub><sup>+</sup> deposition based on NADP sites in the eastern domain.

### 1.2.4 Extended Evaluation of CMAQv4.6 2002 Predictions versus Observations

In addition to the preceding evaluation of annual and monthly average concentrations and deposition for nitrogen and sulfur species, model performance statistics are also calculated and predicted for CMAQv4.6 for a more comprehensive set of species, with comparisons of observations and predictions paired for the native averaging times of the observations (i.e., hourly or weekly)\*. These statistics are presented separately for each of four subregions†: Northeast, Midwest, Southeast, Central, and West for the following species‡: PM<sub>2.5</sub> total mass, selected PM<sub>2.5</sub> component species (i.e., SO<sub>4</sub><sup>2-</sup>, NO<sub>3</sub><sup>-</sup>, NH<sub>4</sub><sup>+</sup>, elemental carbon, and organic carbon), HNO<sub>3</sub>, total nitrate, SO<sub>2</sub>, NO<sub>2</sub><sup>\*</sup>, ozone†, and wet deposition of SO<sub>4</sub><sup>2-</sup>, NO<sub>3</sub><sup>-</sup>, and NH<sub>4</sub><sup>+</sup>. The performance statistics are provided in **Tables 1.2-3 through 1.2-7**. As one way of comparing performance for sulfur and nitrogen containing species across the five subregions, the species/subregion combinations are identified, which had NMB estimates within  $\pm 15\%$ , between  $\pm 15\%$  and  $\pm 30\%$ , and beyond  $\pm 30\%$ . The results of categorizing the statistics in this manner lead to the following findings:

#### 1. Sulfate Concentration

- NMB is within  $\pm 15\%$ , except for the Central subregion and the West subregion, where NMB is between  $-15\%$  and  $-30\%$ .

#### 2. Sulfur Dioxide Concentration

- NMB is between  $+15\%$  and  $+30\%$  in the Northeast and West subregions and greater than  $+30\%$  in the Midwest, Southeast, and Central subregions.

#### 3. Sulfate Wet Deposition

- NMB is within  $+15\%$ , except for the Midwest subregion, where NMD is between  $+15\%$  and  $+30\%$ .

---

\* Measurement sampling periods used in this analysis are as follows: Speciation Trends Network (STN) and IMPROVE - 24-hour average concentrations; CASTNet and NADP - weekly average concentrations and weekly total deposition, respectively; and Air Quality System (AQS) – hourly average concentrations.

† The subregions are defined as groups of states: Midwest includes IL, IN, MI, OH, and WI; Northeast CT, DE, MA, MD, ME, NH, NJ, NY, PA, RI, and VT; Southeast includes AL, FL, GA, KY, MS, NC, SC, TN, VA, and WV; Central includes AR, IA, KS, LA, MN, MO, NE, OK, and TX; and West includes AZ, CA, CO, ID, MT, ND, NM, NV, OR, SD, UT, WY, and WY.

‡ Measurements of NO<sub>2</sub> and NO<sub>y</sub> from sites in the Southeastern Aerosol Research and Characterization (SEARCH) network were not available for use in this assessment.

\* The model performance statistics for NO<sub>2</sub> were not calculated in the West subregion because the results would be disproportionately skewed to California where most of the NO<sub>2</sub> AQS sites in this subregion are located.

† Note that performance statistics for ozone excluded any observed or predicted hourly ozone concentrations less than a threshold of 40ppb.

**4. Nitrate Concentration**

- NMB is within + 15%, except for the Northeast subregion, where NMB exceeds + 30% and the West subregion where NMB is less than - 30%.

**5. Nitric Acid Concentration**

- NMB is within + 15%, except for the Southeast subregion, where NMB is between +15% and + 30%.

**6. Nitrogen Dioxide Concentration**

- NMB is within + 15%, except for the Central subregion, where NMB exceeds + 30%.

**7. Nitrate Wet Deposition**

- NMB is within + 15%, except for the Central subregion, where NMB is between - 15% and - 30%, and the West subregion, where NMB is less than - 30%.

**8. Ammonium Concentration**

- NMB is within + 15%, except for the West subregion, where NMB exceeds + 30%.

**9. Ammonium Wet Deposition**

- NMB is within + 15%, except for the Central subregion, where NMB is between - 15% and - 30%, and the West subregion, where NMB is less than - 30%.

**Table 1.2-3.** CMAQv4.6 Model Performance Statistics for PM<sub>2.5</sub> and Selected Component Species Concentrations

CMAQ 2002			No. of Obs.	NMB (%)	NME (%)	FB (%)	FE (%)
PM <sub>2.5</sub> Total Mass	STN	12-km EUS	10307	2.4	39.5	-3.2	42.1
		12-km WUS	3000	-5.8	46.9	-3.1	45.0
		Northeast	2780	10.7	41.6	7.5	39.3
		Midwest	1516	8.4	32.8	6.2	33.9
		Southeast	2554	-9.4	35.6	-17.2	41.4
		Central	2738	4.4	46.5	-3.4	50.2
		West	2487	-7.4	46.8	-4.5	44.8



CMAQ 2002			No. of Obs.	NMB (%)	NME (%)	FB (%)	FE (%)
PM <sub>2.5</sub> Total Mass (continued)	IMPROVE	12-km EUS	8436	-12.0	44.8	-15.1	50.5
		12-km WUS	10123	-26.4	53.5	-26.3	57.5
		Northeast	2060	4.6	47.2	3.5	45.6
		Midwest	592	-0.8	36.1	-6.0	39.2
		Southeast	1803	-19.7	40.7	-28.8	51.8
		Central	1624	-20.1	48.9	-25.3	58.6
		West	9543	-27.8	53.1	-27.1	57.2
Sulfate	STN	12-km EUS	10157	-5.3	34.1	-11.3	39.3
		12-km WUS	2926	-20.6	41.9	-12.2	43.5
		Northeast	2730	-4.1	29.6	-8.4	33.5
		Midwest	1487	7.1	36.3	0.9	36.9
		Southeast	2541	-9.8	33.7	-18.7	39.8
		Central	2686	-9.2	39.4	-13.0	46.4
		West	2446	-26.1	44.9	-15.8	44.8
	IMPROVE	12-km EUS	8532	-11.7	33.8	-8.8	41.8
		12-km WUS	10232	-7.5	42.4	7.6	45.7
		Northeast	2070	-12.7	30.8	-11.4	37.7
		Midwest	597	-3.1	30.6	-6.9	35.8
		Southeast	1805	-10.8	33.2	-18.8	41.3
		Central	1671	-18.5	37.0	-19.3	44.6
		West	9645	-5.5	43.5	8.6	45.9
Sulfate (continued)	CASTNet	12-km EUS	3173	-12.3	20.3	-17.2	25.7
		12-km WUS	1158	-21.3	34.6	-11.2	35.9
		Northeast	839	-13.3	18.7	-16.9	22.2
		Midwest	663	-8.2	17.9	-14.4	21.6
		Southeast	1085	-12.9	21.4	-19.9	27.4
		Central	229	-22.9	28.6	-29.9	35.8
		West	1118	-20.4	35.3	-10.7	36.1
Nitrate	STN	12-km EUS	8770	0.1	61.1	-39.8	85.8
		12-km WUS	2726	-45.0	63.1	-70.6	95.0
		Northeast	2731	9.8	60.6	-26.2	77.5
		Midwest	1488	2.7	55.9	-14.5	70.4
		Southeast	2540	-5.8	78.2	-70.0	106.9
		Central	1298	-3.8	53.7	-21.5	73.8
		West	2446	-47.5	62.8	-73.8	95.4

CMAQ 2002			No. of Obs.	NMB (%)	NME (%)	FB (%)	FE (%)
Nitrate (continued)	IMPROVE	12-km EUS	8514	13.3	85.1	-66.5	115.4
		12-km WUS	10110	-34.8	80.6	-101.0	130.0
		Northeast	2069	56.3	99.1	-19.6	97.6
		Midwest	597	11.5	72.04	-50.4	101.5
		Southeast	1803	3.8	94.8	-91.4	132.6
		Central	1672	0.8	77.3	-64.7	115.8
		West	9522	-39.6	81.1	-104.0	131.1
Total Nitrate (NO <sub>3</sub> +HNO <sub>3</sub> )	CASTNet	12-km EUS	3171	11.1	30.5	7.2	31.3
		12-km WUS	1157	-19.5	44.2	-12.0	46.0
		Northeast	839	18.1	30.4	15.4	29.7
		Midwest	662	10.2	27.9	7.7	25.6
		Southeast	1085	12.4	33.5	8.3	33.9
		Central	229	-2.9	33.2	-6.5	35.3
		West	1117	-20.4	45.8	-12.1	46.6
Ammonium	STN	12-km EUS	10157	5.0	39.5	7.0	45.7
		12-km WUS	2926	-23.6	55.7	7.2	58.1
		Northeast	2731	5.4	35.3	12.1	40.1
		Midwest	1488	11.8	39.1	17.3	43.4
		Southeast	2540	1.9	38.6	-0.7	43.4
		Central	2685	5.1	46.9	4.7	54.8
		West	2446	-30.6	56.7	2.9	59.7
	CASTNet	12-km EUS	3166	28.2	-3.1	30.8	0.8
		12-km WUS	1156	-16.8	42.5	-13.0	41.1
		Northeast	837	-3.2	27.8	-0.8	28.4
		Midwest	661	7.1	26.5	5.6	26.1
		Southeast	1085	-13.7	29.9	-17.6	35.1
		Central	229	0.5	31.5	-4.2	35.9
		West	1116	-21.1	43.5	-14.4	41.4
Elemental Carbon	STN	12-km EUS	10031	33.0	72.4	12.6	56.1
		12-km WUS	2975	43.1	82.6	18.2	61.3
		Northeast	2744	39.1	68.7	16.1	53.0
		Midwest	1498	25.9	53.1	14.0	47.5
		Southeast	2506	10.1	63.8	-0.1	52.2
		Central	2570	76.4	107.5	31.5	66.1
		West	2475	49.0	86.2	17.1	62.7

CMAQ 2002			No. of Obs.	NMB (%)	NME (%)	FB (%)	FE (%)
Elemental Carbon (continued)	IMPROVE	12-km EUS	8282	48.8	-23.5	-34.1	56.1
		12-km WUS	10069	-14.1	67.2	-29.5	62.1
		Northeast	2056	-4.1	51.8	-15.0	50.6
		Midwest	599	-31.2	39.4	-39.3	51.3
		Southeast	1795	-39.9	47.0	-53.6	62.2
		Central	1532	-31.1	50.4	-38.8	61.2
		West	9493	-15.5	67.8	-31.3	62.7
Organic Carbon	STN	12-km EUS	9726	-45.8	57.5	-50.4	72.8
		12-km WUS	2903	-37.6	60.3	-40.4	69.3
		Northeast	2641	-35.2	58.2	-30.3	66.8
		Midwest	1447	-50.5	60.6	-51.1	75.1
		Southeast	2474	-50.6	56.0	-60.7	73.4
		Central	2504	-49.1	56.2	-61.2	75.6
		West	2408	-36.3	61.4	-37.9	70.2
	IMPROVE	12-km EUS	8287	-41.3	59.0	-49.0	70.6
		12-km WUS	10082	-34.8	60.0	-31.2	63.0
		Northeast	2057	-21.8	58.8	-16.9	57.4
		Midwest	598	-49.6	54.9	-52.5	66.4
		Southeast	1800	-51.9	59.8	-80.9	87.8
		Central	1531	-53.6	63.3	-71.0	85.1
		West	9508	-34.5	59.6	-29.7	61.9

Table 1.2-4. CMAQ v4.6 2002 Model Performance Statistics for Nitric Acid and Sulfur Dioxide

CMAQ 2002			No. of Obs.	NMB (%)	NME (%)	FB (%)	FE (%)
Nitric Acid	CASTNet	12-km EUS	3172	10.0	39.1	9.0	40.3
		12-km WUS	1157	6.1	47.7	17.0	49.0
		Northeast	839	3.8	34.2	4.4	35.4
		Midwest	662	9.2	38.8	3.0	40.4
		Southeast	1086	17.7	44.0	20.5	44.0
		Central	229	2.8	31.3	2.4	31.3
		West	1117	5.5	48.5	17.2	49.5
Sulfur Dioxide	CASTNet	12-km EUS	3174	33.08	46.61	31.6	46.4
		12-km WUS	1157	26.5	71.4	14.9	57.7
		Northeast	839	24.7	39.4	29.7	40.8
		Midwest	663	35.3	47.9	38.7	45.3
		Southeast	1086	39.0	51.6	29.8	51.4
		Central	229	91.6	99.9	48.5	61.0
		West	1117	19.4	68.1	12.9	57.2

CMAQ 2002			No. of Obs.	NMB (%)	NME (%)	FB (%)	FE (%)
Sulfur Dioxide (continued)	SEARCH	12-km EUS	61760	28.1	98.4	24.4	87.1
Nitrogen Dioxide	AQS	12-km EUS	921032	13.6	54.7	4.9	56.5
		Northeast	620014	-2.9	45.2	-13.0	52.5
		Midwest	14913	12.3	44.0	5.8	43.8
		Southeast	342422	7.3	57.2	2.0	60.8
		Central	625924	34.3	70.8	10.9	61.1

**Table 1.2-5.** CMAQv4.6 2002 Model Performance Statistics for Annual Sulfate and Nitrate Wet Deposition Model Performance Statistics.

CMAQ 2002 Annual			No. of Obs.	NMB (%)	NME (%)	FB (%)	FE (%)
Sulfate	NADP	12-km EUS	6896	5.53	63.7	1.0	70.9
		12-km WUS	2354	-18.0	73.5	-23.5	94.7
		Northeast	1405	8.2	57.6	3.0	59.7
		Midwest	1413	17.0	62.9	16.4	64.0
		Southeast	1856	4.8	68.6	1.4	73.2
		Central	1246	-10.2	62.3	-2.5	71.6
		West	2058	-10.5	76.6	-20.5	94.7
Nitrate	NADP	12-km EUS	6896	-16.2	59.2	-22.2	73.3
		12-km WUS	2354	-42.4	72.3	-59.4	99.2
		Northeast	1413	-7.1	56.8	-6.0	66.0
		Midwest	1405	-9.5	52.7	-13.6	60.7
		Southeast	1856	-12.5	64.3	-14.8	74.2
		Central	1246	-25.8	58.9	-24.1	72.8
		West	2058	-45.4	72.0	-59.8	99.3
Ammonium	NADP	12-km EUS	6896	-11.5	65.2	-10.2	76.0
		12-km WUS	2354	-40.4	73.1	-55.5	100.6
		Northeast	1413	-8.0	61.9	0.4	68.5
		Midwest	1405	-2.0	63.1	1.3	67.3
		Southeast	1856	1.1	75.2	-0.2	77.9
		Central	1246	-24.4	60.9	-16.5	75.0
		West	2058	-41.1	74.2	-54.8	100.6

**Table 1.2-6. CMAQv4.6 Model Performance Statistics for Hourly Ozone Concentrations**

<b>CMAQ 2002 Hourly Ozone: Threshold of 40 ppb</b>		<b>No. of Obs.</b>	<b>NMB (%)</b>	<b>NME (%)</b>	<b>FB (%)</b>	<b>FE (%)</b>
<b>May</b>	12-km EUS	241185	-0.7	15.9	-2.0	17.1
	12-km WUS	124931	-3.7	15.9	-5.0	17.3
	Northeast	51055	1.2	17.1	-0.3	18.2
	Midwest	55859	3.3	16.2	2.4	16.9
	Southeast	69073	-2.5	14.1	-3.1	14.8
	Central	41728	-6.4	17.3	-9.2	20.3
	West	111385	-3.9	16.1	-5.2	17.6
<b>June</b>	12-km EUS	256263	-7.5	16.8	-9.0	18.6
	12-km WUS	125662	-8.37	17.7	-9.3	19.1
	Northeast	61354	-8.46	17.3	-9.9	19.1
	Midwest	54515	-7.19	17.9	-8.3	19.6
	Southeast	67867	-7.2	15.3	-7.6	16.3
	Central	46026	-10.0	17.5	-13.5	21.2
	West	109157	-8.8	18.2	-9.9	19.7
<b>July</b>	12-km EUS	257076	-5.3	17.7	-6.6	19.2
	12-km WUS	116785	-12.0	21.5	-14.9	24.3
	Northeast	66774	-3.9	17.0	-4.8	18.0
	Midwest	59360	-10.5	19.4	-12.3	21.7
	Southeast	68619	-3.6	16.5	-3.9	17.2
	Central	36021	-3.6	18.7	-6.3	21.1
	West	104321	-13.6	21.8	-16.8	24.9
<b>August</b>	12-km EUS	235090	-8.7	17.8	-10.2	19.7
	12-km WUS	125575	-7.91	20.1	-10.2	22.1
	Northeast	53837	-6.4	16.7	-7.4	18.0
	Midwest	54179	-10.8	19.1	-12.4	21.4
	Southeast	62506	-9.4	17.3	-9.9	18.5
	Central	41456	-9.3	18.7	-12.8	22.4
	West	110225	-8.5	20.6	-11.1	22.8
<b>September</b>	12-km EUS	179156	-9.9	17.2	-11.8	19.5
	12-km WUS	99710	-10.7	19.0	-12.7	21.1
	Northeast	44678	-8.7	16.3	-10.6	18.4
	Midwest	34285	-11.4	18.5	-12.9	20.4
	Southeast	41627	-8.2	16.5	-9.0	17.8
	Central	41549	-12.8	18.8	-16.6	22.8
	West	83921	-11.7	20.0	-13.8	22.1

<b>CMAQ 2002 Hourly Ozone: Threshold of 40 ppb</b>		<b>No. of Obs.</b>	<b>NMB (%)</b>	<b>NME (%)</b>	<b>FB (%)</b>	<b>FE (%)</b>
<b>Seasonal Aggregate</b>	12-km EUS	1168770	-6.4	17.1	-7.7	18.8
	12-km WUS	592663	-8.4	18.8	-10.3	20.7
	Northeast	277698	-5.4	16.9	-6.5	18.4
	Midwest	258198	-7.3	18.3	-8.4	20.0
	Southeast	309692	-6.0	15.9	-6.4	16.8
	Central	206780	-8.6	18.2	-11.9	21.6
	West	519009	-9.2	19.3	-11.2	21.3

**Table 1.2-7. CMAQv4.6 Model Performance Statistics for 8-hour Daily Maximum Ozone Concentrations**

<b>CMAQ 2002 8-Hour Maximum Ozone: Threshold of 40 ppb</b>		<b>No. of Obs.</b>	<b>NMB (%)</b>	<b>NME (%)</b>	<b>FB (%)</b>	<b>FE (%)</b>
<b>May</b>	12-km EUS	18115	4.0	12.7	4.4	12.7
	12-km WUS	9188	0.1	12.6	0.5	12.8
	Northeast	4123	7.1	13.1	7.4	12.9
	Midwest	5596	13.9	19.7	14.6	19.7
	Southeast	5257	0.5	11.1	0.8	11.2
	Central	2921	0.4	12.3	0.8	12.5
	West	1199	-1.7	11.7	-1.6	11.8
<b>June</b>	12-km EUS	18341	-4.3	12.3	-3.8	12.5
	12-km WUS	8788	-4.9	14.0	-4.3	14.2
	Northeast	4038	-3.0	12.7	-2.0	12.8
	Midwest	5388	-0.8	14.7	2.6	16.4
	Southeast	4901	-5.5	11.9	-5.0	12.1
	Central	3137	-6.1	12.4	-6.2	13.0
	West	7789	-5.4	14.5	-4.8	14.7
<b>July</b>	12-km EUS	19499	-0.9	13.5	-0.5	13.6
	12-km WUS	8809	-7.5	17.0	-8.2	18.0
	Northeast	4300	-5.5	14.0	-4.9	14.2
	Midwest	5612	2.0	13.6	3.1	13.7
	Southeast	5397	-0.6	13.2	-0.1	13.2
	Central	2799	2.1	14.3	1.9	14.6
	West	1242	-14.1	20.3	-16.1	22.2

CMAQ 2002 8-Hour Maximum Ozone: Threshold of 40 ppb		No. of Obs.	NMB (%)	NME (%)	FB (%)	FE (%)
August	12-km EUS	18204	-4.4	13.0	-3.8	13.1
	12-km WUS	9516	-2.9	15.8	-3.2	16.1
	Northeast	3956	-7.3	13.5	-6.7	13.7
	Midwest	5620	2.6	14.3	4.7	14.8
	Southeast	4882	-5.8	13.5	-4.9	13.5
	Central	3104	-3.6	13.0	-3.7	13.6
	West	8283	-3.2	16.1	-3.7	16.4
September	12-km EUS	14921	-5.7	12.6	-5.5	13.0
	12-km WUS	8138	-6.7	15.0	-6.9	15.5
	Northeast	3075	-7.0	13.4	-6.4	13.4
	Midwest	5439	-0.1	14.2	2.6	15.6
	Southeast	3540	-3.7	12.6	-3.1	12.9
	Central	3026	-8.4	13.7	-8.8	14.5
	West	6864	-7.4	15.9	-7.7	16.4
Seasonal Aggregate	12-km EUS	89080	-2.3	12.8	-1.7	13.0
	12-km WUS	44626	-4.3	14.9	-4.3	15.3
	Northeast	19492	-3.3	13.3	-2.3	13.4
	Midwest	27655	3.2	15.1	5.6	16.1
	Southeast	23977	-3.0	12.5	-2.3	12.5
	Central	14987	-3.3	13.2	-3.3	13.6
	West	38823	-5.0	15.3	-5.0	15.7

## 2.0 REFERENCES

- Aiyyer, A, Cohan, D., Russell, A., Stockwell, W., Tanrikulu, S., Vizuete, W., and Wilczak, J. 2007. *Final Report: Third Peer Review of the CMAQ Model*.
- Byun, D.W., and Schere, K.L. 2006. Review of the Governing Equations, Computational Algorithms, and Other Components of the Models-3 Community Multiscale Air Quality (CMAQ) Modeling System. *J. Applied Mechanics Reviews*, 59 (2), 51–77.
- Dennis, R.L., Byun, D.W., Novak, J.H., Galluppi, K.J., Coats, C.J., and Vouk, M.A. 1996. The next generation of integrated air quality modeling: EPA's Models-3. *Atmospheric Environment*, 30, 1925–1938.

- Dentener F. J., and Crutzen P.J. 1993. Reaction of  $\text{N}_2\text{O}_5$  on tropospheric aerosols: impact on the global distributions of  $\text{NO}_x$ ,  $\text{O}_3$ , and OH. *J Geophys Res*, 98, 7149–7163.
- U.S. EPA (Environmental Protection Agency). 1999. *Science Algorithms of EPA Models-3 Community Multiscale Air Quality (CMAQ) Modeling System*. Byun, D.W., and Ching, J.K.S., Eds. EPA/600/R-99/030. Office of Research and Development.
- U.S. EPA (Environmental Protection Agency). 2008. *Technical Support Document for the Final Locomotive/Marine Rule: Air Quality Modeling Analyses*. EPA 454/R-08-002. Office of Air Quality Planning and Standards, Research Triangle Park, NC. January 2008.
- U.S. EPA (Environmental Protection Agency). 2006a. *Technical Support Document for the Final Clean Air Interstate Rule: Air Quality Modeling*. Office of Air Quality Planning and Standards, Research Triangle Park, NC. March 2005 (CAIR Docket OAR-2005-0053-2149).
- U.S. EPA (Environmental Protection Agency). 2006b. *Technical Support Document for the Final PM NAAQS Rule*. Office of Air Quality Planning and Standards, Research Triangle Park, NC.



September 2009

**Appendix 2**  
**Supplemental Deposition Information**  
Wet Deposition Trends in or Near Case Study Areas and  
Supplemental Nationwide Maps Depicting the Ratio of  
Deposition to Concentration and Deposition to Emissions

*Final*

**Prepared by**

U.S. Environmental Protection Agency  
Office of Air Quality Planning and Standards  
Research Triangle Park, NC 27709



## TABLE OF CONTENTS

1.0	Trends in Wet Deposition of Inorganic Nitrogen and Sulfate at National Atmospheric Deposition Program Sites in or Near Case Study Areas .....	1
2.0	Supplemental Nationwide Maps Depicting the Ratio of Deposition to Concentration and Deposition to Emissions .....	17

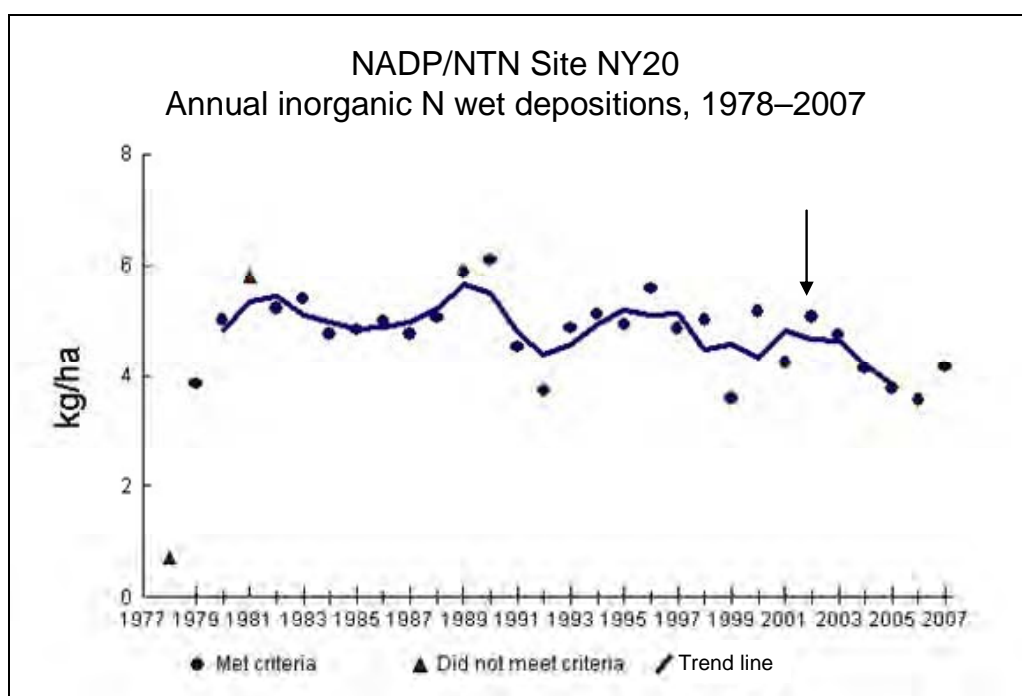
## LIST OF FIGURES

Figure 1-1. Adirondack Case Study Area; Site: Huntington Wildlife Forest, NY NTN = National Trends Network .....	1
Figure 1-2. Adirondack Case Study Area; Site: Whiteface Mountain, NY .....	2
Figure 1-3. Hubbard Brook Experimental Forest Case Study Area; Site: Hubbard Brook, NH.....	2
Figure 1-4. Kane Experimental Forest Case Study Area; Site: Kane Experimental Forest, PA. ....	3
Figure 1-5. Potomac River/Potomac Estuary Case Study Area; Site: Arendtsville, PA .....	3
Figure 1-6. Potomac River/Potomac Estuary Case Study Area; Site: Parsons, WV .....	4
Figure 1-7. Potomac River/Potomac Estuary Case Study Area; Site: Wye, MD .....	4
Figure 1-8. Shenandoah Case Study Area; Site: Shenandoah National Park, VA .....	5
Figure 1-9. Shenandoah Case Study Area; Site: Horton's Station, VA .....	5
Figure 1-10. Neuse River/Neuse River Estuary Case Study Area; Site: Finley Farm, NC .....	6
Figure 1-11. Neuse River/Neuse River Estuary Case Study Area; Site: Beaufort, NC.....	6
Figure 1-12. Rocky Mountain National Park Supplemental Area; Site: Beaver Meadows, CO .....	7
Figure 1-13. Mixed Conifer Forest (Sierra Nevada Range) Case Study Area; Site: Yosemite National Park, CA.....	7
Figure 1-14. Mixed Conifer Forest (Transverse Range) Case Study Area; Site: Joshua Tree National Park, CA.....	8
Figure 1-15. Mixed Conifer Forest (Transverse Range) Case Study Area; Site: Tanbark Flat, CA.....	8
Figure 1-16. Adirondack Case Study Area; Site: Huntington Wildlife Forest, NY .....	9
Figure 1-17. Adirondack Case Study Area; Site: Whiteface Mountain, NY .....	9
Figure 1-18. Hubbard Brook Experimental Forest Case Study Area; Site: Hubbard Brook, NH.....	10
Figure 1-19. Kane Experimental Forest Case Study Area; Site: Kane Experimental Forest, PA. ....	10
Figure 1-20. Potomac River/Potomac Estuary Case Study Area; Site: Arendtsville, PA .....	11
Figure 1-21. Potomac River/Potomac Estuary Case Study Area; Site: Parsons, WV .....	11
Figure 1-22. Potomac River/Potomac Estuary Case Study Area; Site: Wye, MD .....	12
Figure 1-23. Shenandoah Case Study Area; Site: Shenandoah National Park, VA .....	12
Figure 1-24. Shenandoah Case Study Area; Site: Horton's Station, VA .....	13
Figure 1-25. Neuse River/Neuse River Estuary Case Study Area; Site: Finley Farm, NC .....	13
Figure 1-26. Neuse River/Neuse River Estuary Case Study Area; Site: Beaufort, NC.....	14

Figure 1-27. Rocky Mountain National Park (Supplemental Area); Site: Beaver Meadows, CO .....	14
Figure 1-28. Mixed Conifer Forest (Sierra Nevada Range) Case Study Area; Site: Yosemite National Park, CA.....	15
Figure 1-29. Mixed Conifer Forest (Transverse Range) Case Study Area; Site: Joshua Tree National Park, CA.....	15
Figure 1-30. Mixed Conifer Forest (Transverse Range) Case Study Area; Site: Tanbark Flat, CA.....	16
Figure 2-1. Ratio of annual total dry sulfur deposition (kg S/ha/yr) to annual average sulfur dioxide concentrations ( $\mu\text{g}/\text{m}^3$ ). .....	18
Figure 2-2. Ratio of annual total wet sulfur deposition (kg S/ha/yr) to annual average sulfur dioxide concentrations ( $\mu\text{g}/\text{m}^3$ ). .....	19
Figure 2-3. Ratio of annual total wet+dry sulfur deposition (kg S/ha/yr) to annual average sulfur dioxide concentrations ( $\mu\text{g}/\text{m}^3$ ). .....	20
Figure 2-4. Ratio of annual total dry sulfur deposition (kg S/ha/yr) to annual total sulfur dioxide emissions (tons/yr). .....	21
Figure 2-5. Ratio of annual total wet sulfur deposition (kg S/ha/yr) to annual total sulfur dioxide emissions (tons/yr). .....	22
Figure 2-6. Ratio of annual total wet+dry sulfur deposition (kg S/ha/yr) to annual total sulfur dioxide emissions (tons/yr).....	23
Figure 2-7. Ratio of annual total wet oxidized nitrogen deposition (kg $\text{NO}_x$ /ha/yr) to annual average nitrogen dioxide concentrations (ppb). .....	24
Figure 2-8. Ratio of annual total dry oxidized nitrogen deposition (kg $\text{NO}_x$ /ha/yr) to annual average nitrogen dioxide concentrations (ppb). .....	25
Figure 2-9. Ratio of annual total wet+dry oxidized nitrogen deposition (kg $\text{NO}_x$ /ha/yr) to annual average nitrogen dioxide concentrations (ppb). .....	26
Figure 2-10. Ratio of annual total dry oxidized nitrogen deposition (kg $\text{NO}_x$ /ha/yr) to annual total nitrogen dioxide emissions (tons/yr). .....	27
Figure 2-11. Ratio of annual total wet oxidized nitrogen deposition (kg $\text{NO}_x$ /ha/yr) to annual total nitrogen dioxide emissions (tons/yr). .....	28
Figure 2-12. Ratio of annual total wet+dry oxidized nitrogen deposition (kg $\text{NO}_x$ /ha/yr) to annual total nitrogen dioxide emissions (tons/yr). .....	29
Figure 2-13. Ratio of annual total dry nitrogen deposition (kg N/ha/yr) to annual average nitrogen dioxide concentrations (ppb). .....	30
Figure 2-14. Ratio of annual total wet nitrogen deposition (kg N/ha/yr) to annual average nitrogen dioxide concentrations (ppb). .....	31
Figure 2-15. Ratio of annual total wet+dry nitrogen deposition (kg N/ha/yr) to annual average nitrogen dioxide concentrations (ppb). .....	32
Figure 2-16. Ratio of annual total dry nitrogen deposition (kg N/ha/yr) to annual total nitrogen dioxide emissions (tons/yr). .....	33
Figure 2-17. Ratio of annual total wet nitrogen deposition (kg N/ha/yr) to annual total nitrogen dioxide emissions (tons/yr). .....	34
Figure 2-18. Ratio of annual total wet+dry nitrogen deposition (kg N/ha/yr) to annual total nitrogen dioxide emissions (tons/yr). .....	35

## **1.0 TRENDS IN WET DEPOSITION OF INORGANIC NITROGEN AND SULFATE AT NATIONAL ATMOSPHERIC DEPOSITION PROGRAM SITES IN OR NEAR CASE STUDY AREAS**

### **Trends in Wet Deposition of Inorganic Nitrogen (Arrow on plots indicate the year 2002)**



**Figure 1-1.** Adirondack Case Study Area; Site: Huntington Wildlife Forest, NY  
NTN = National Trends Network

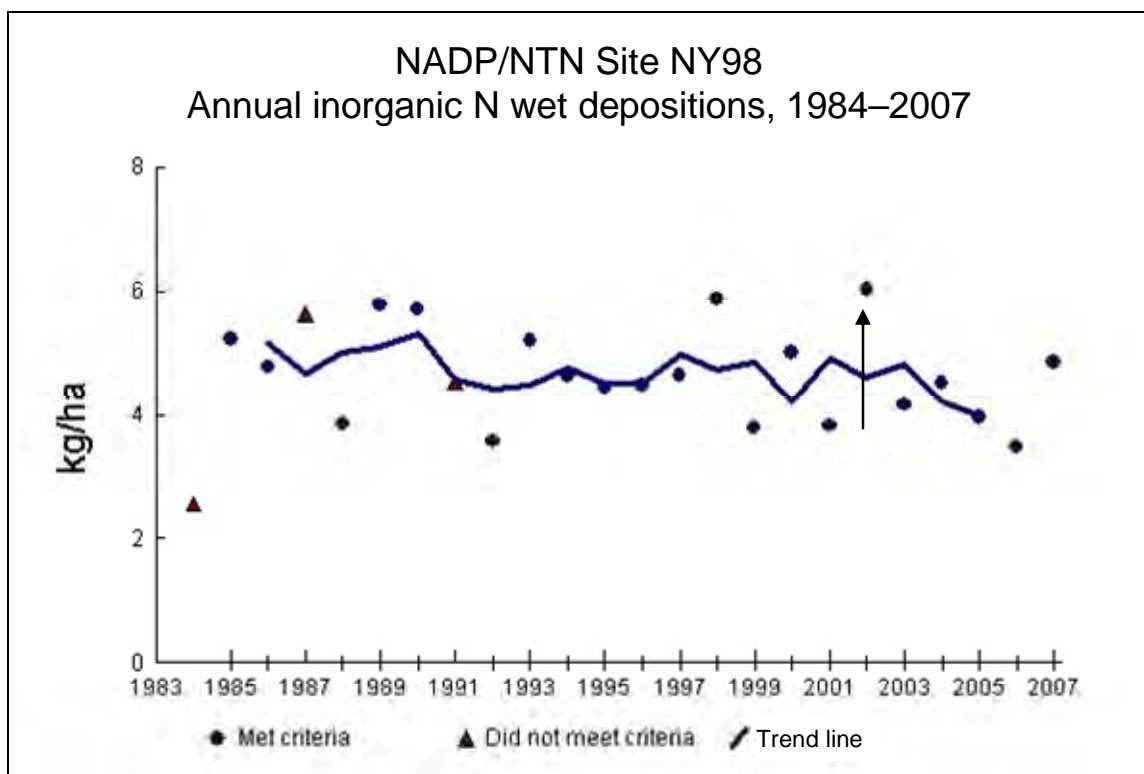


**Figure 1-2.** Adirondack Case Study Area; Site: Whiteface Mountain, NY

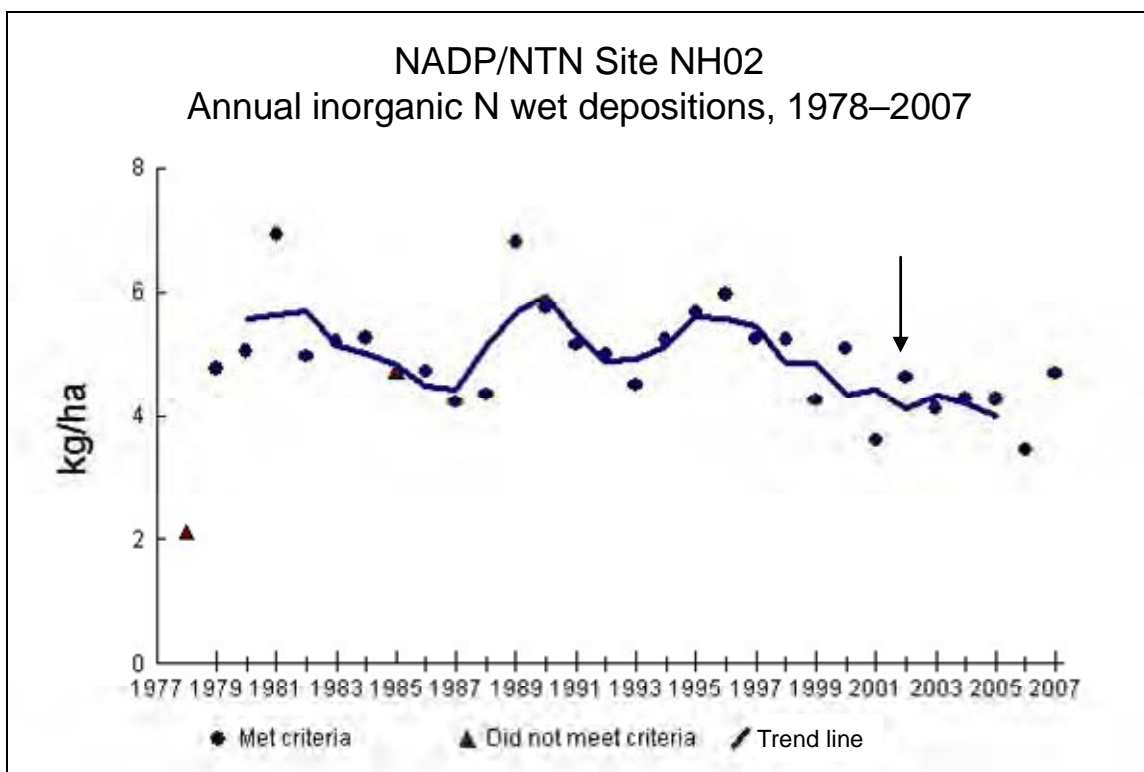


**Figure 1-3.** Hubbard Brook Experimental Forest Case Study Area; Site: Hubbard Brook, NH.

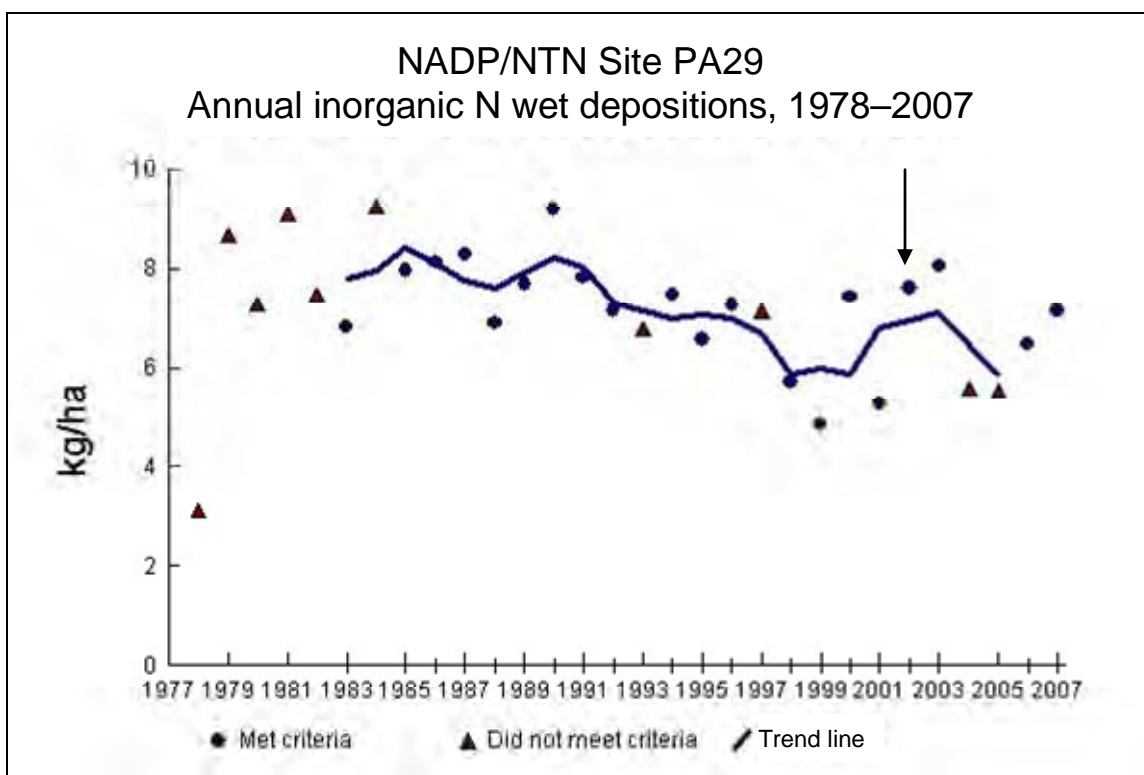


**Figure 1-4.** Kane Experimental Forest Case Study Area; Site: Kane Experimental Forest, PA.

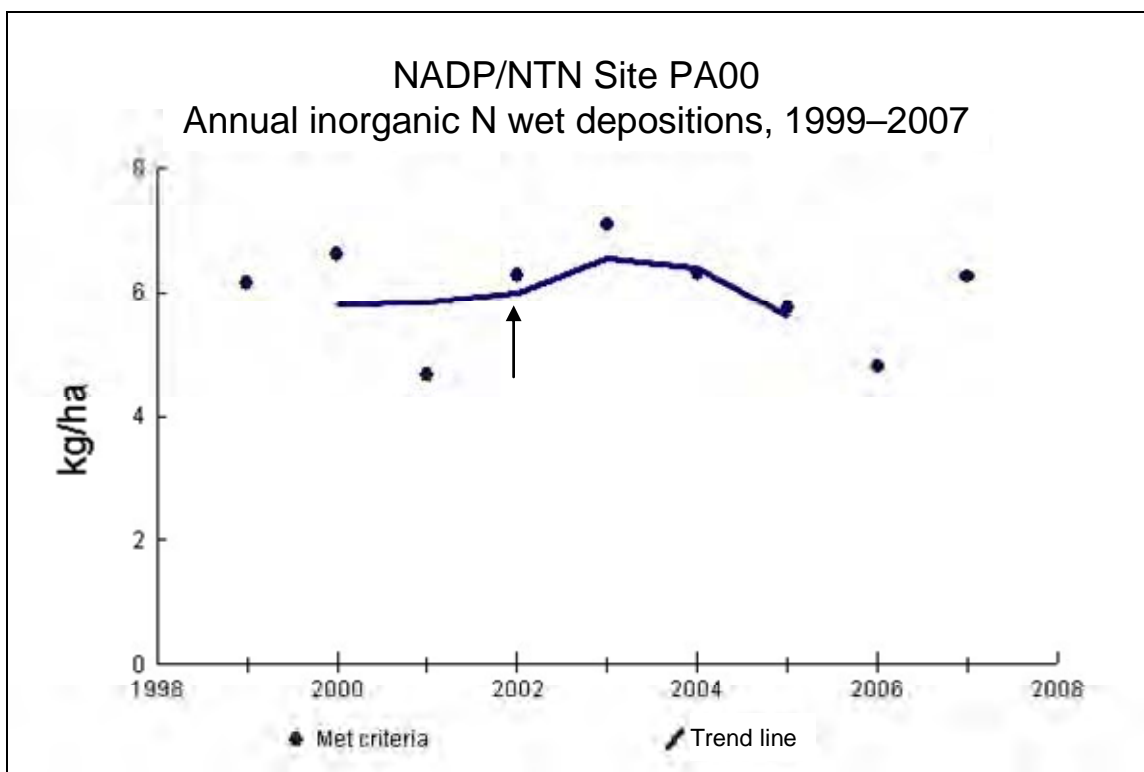


**Figure 1-5.** Potomac River/Potomac Estuary Case Study Area; Site: Arendtsville, PA

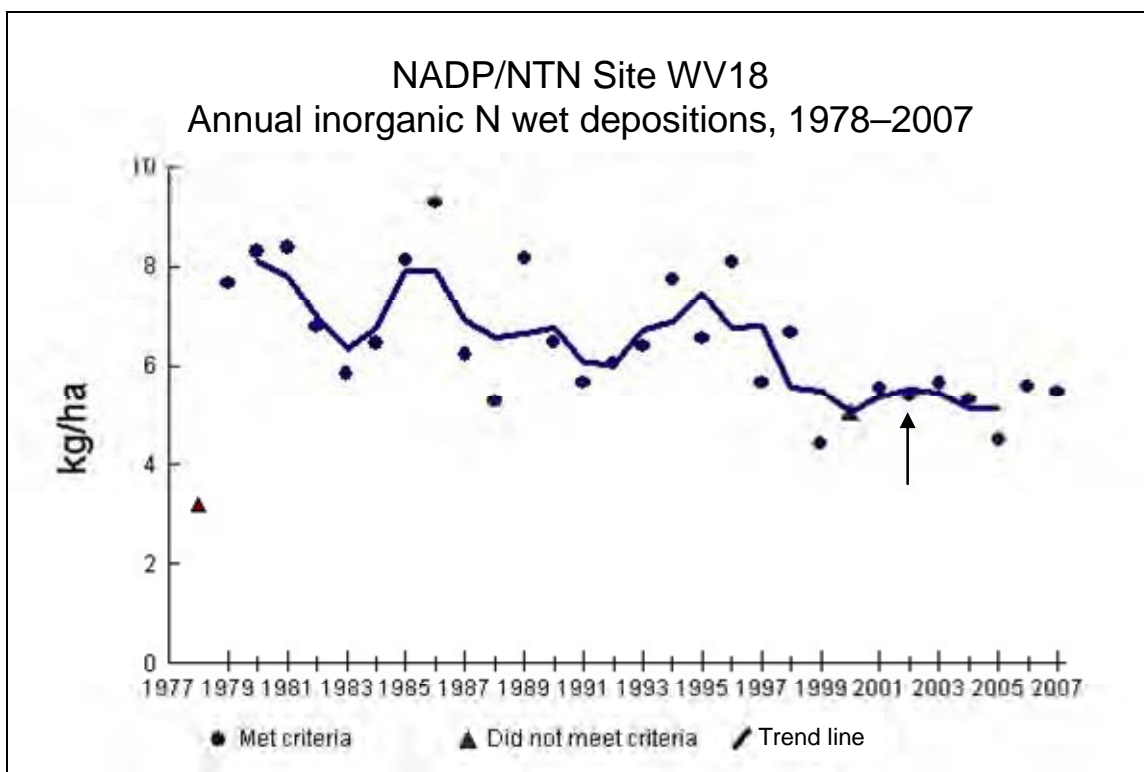


Figure 1-6. Potomac River/Potomac Estuary Case Study Area; Site: Parsons, WV

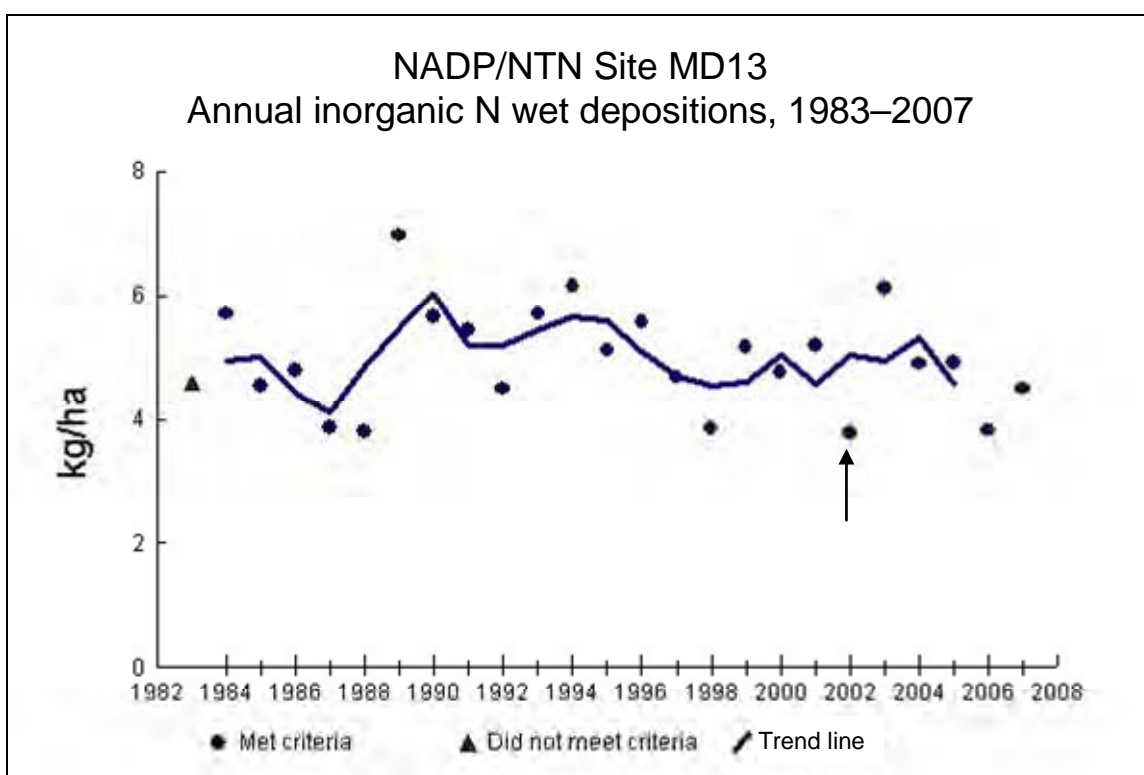


Figure 1-7. Potomac River/Potomac Estuary Case Study Area; Site: Wye, MD



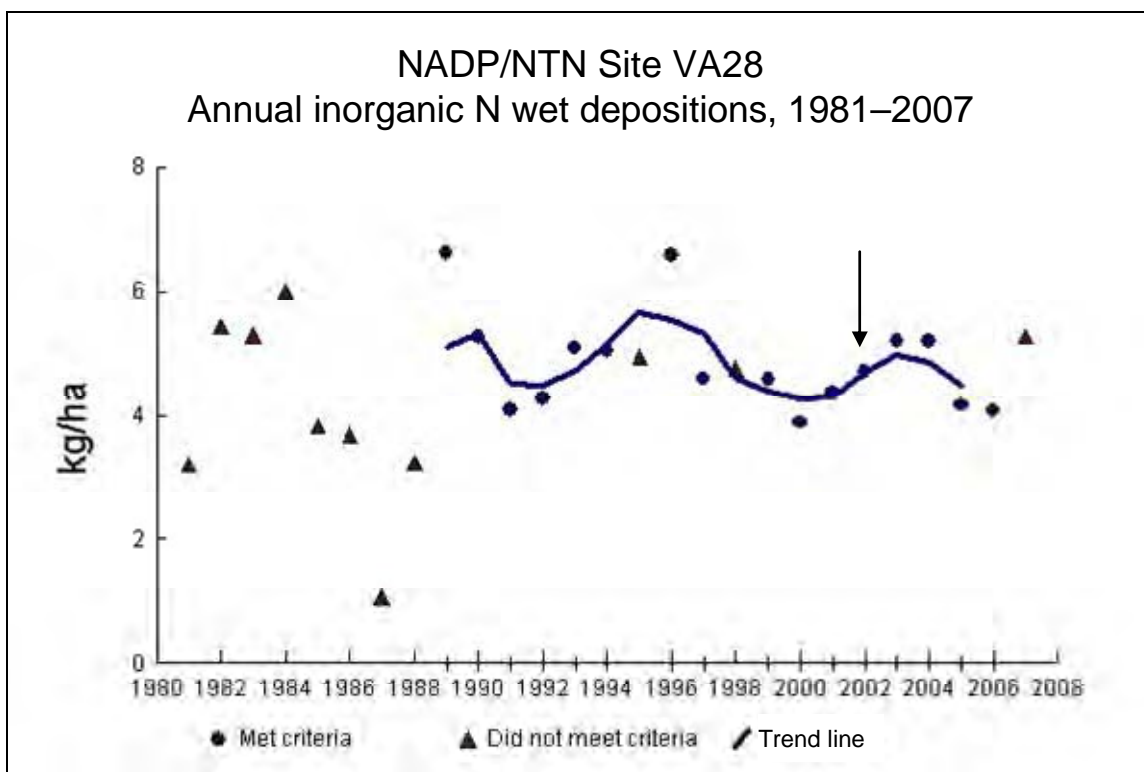


Figure 1-8. Shenandoah Case Study Area; Site: Shenandoah National Park, VA

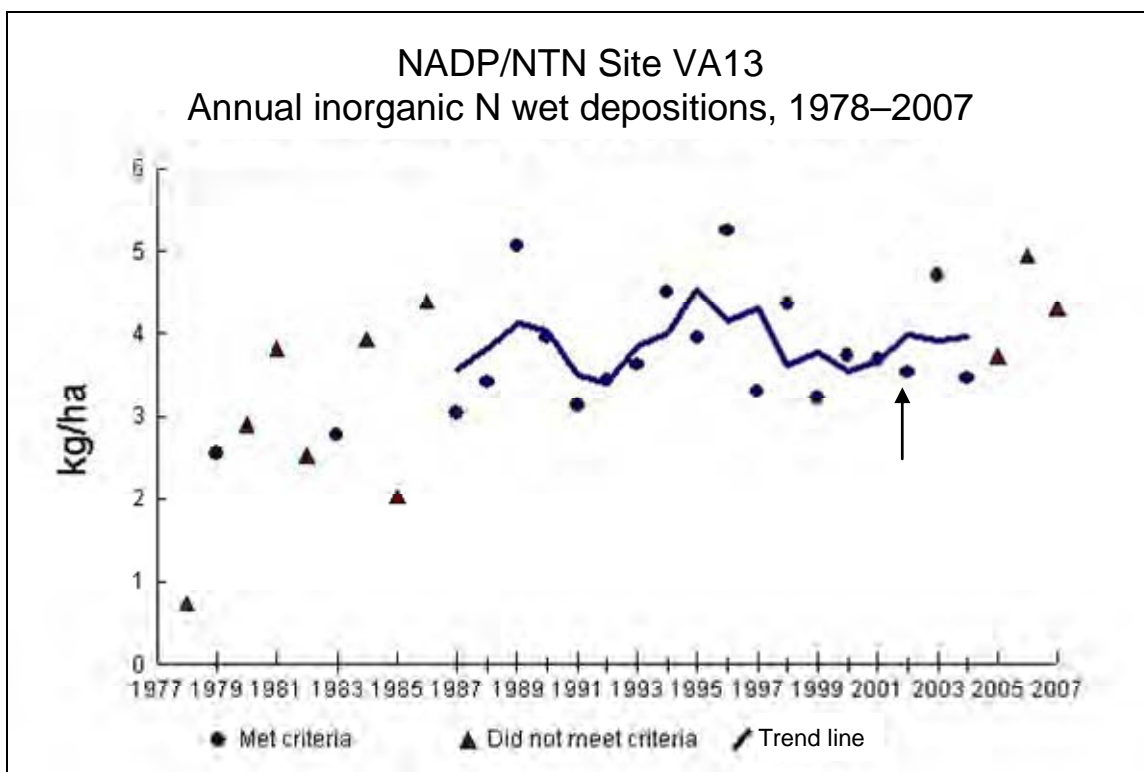
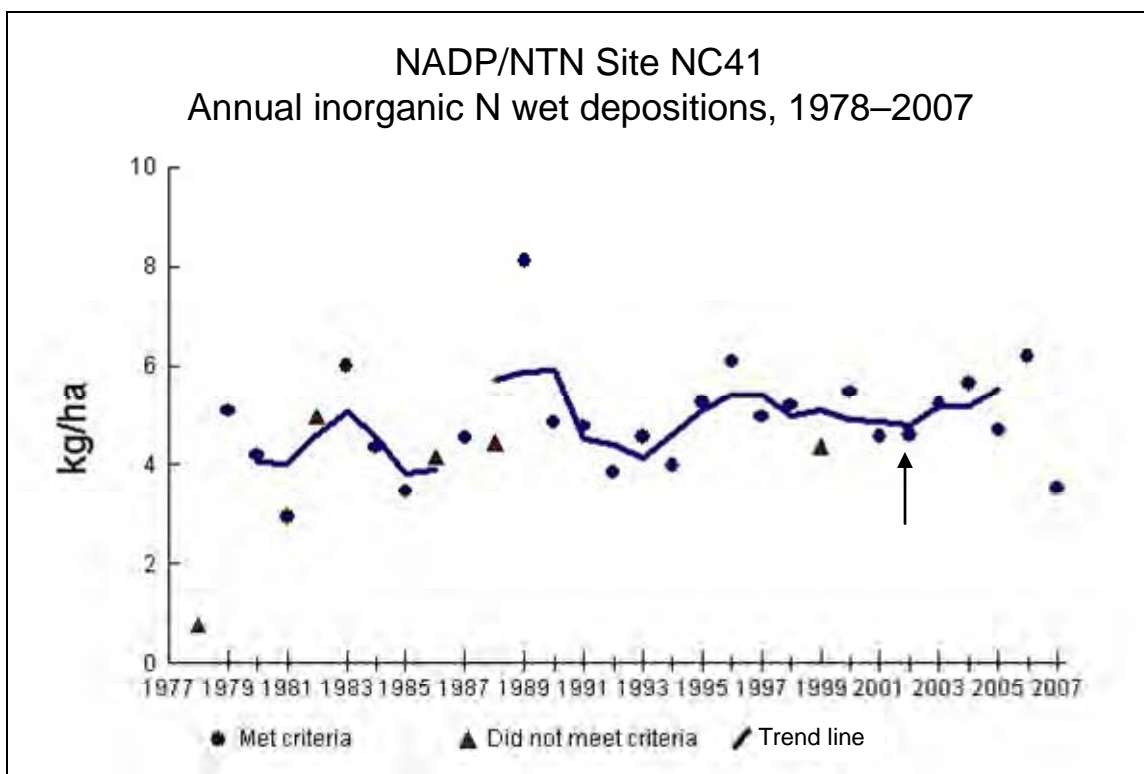
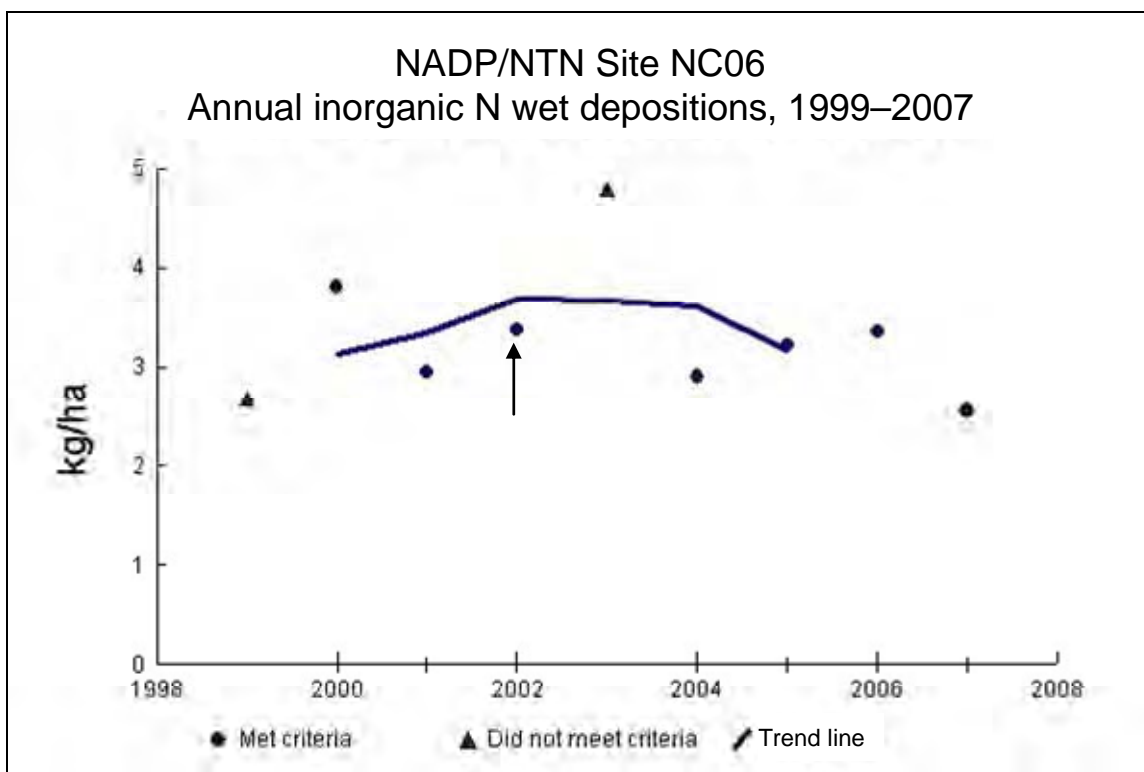


Figure 1-9. Shenandoah Case Study Area; Site: Horton's Station, VA



**Figure 1-10.** Neuse River/Neuse River Estuary Case Study Area; Site: Finley Farm, NC



**Figure 1-11.** Neuse River/Neuse River Estuary Case Study Area; Site: Beaufort, NC

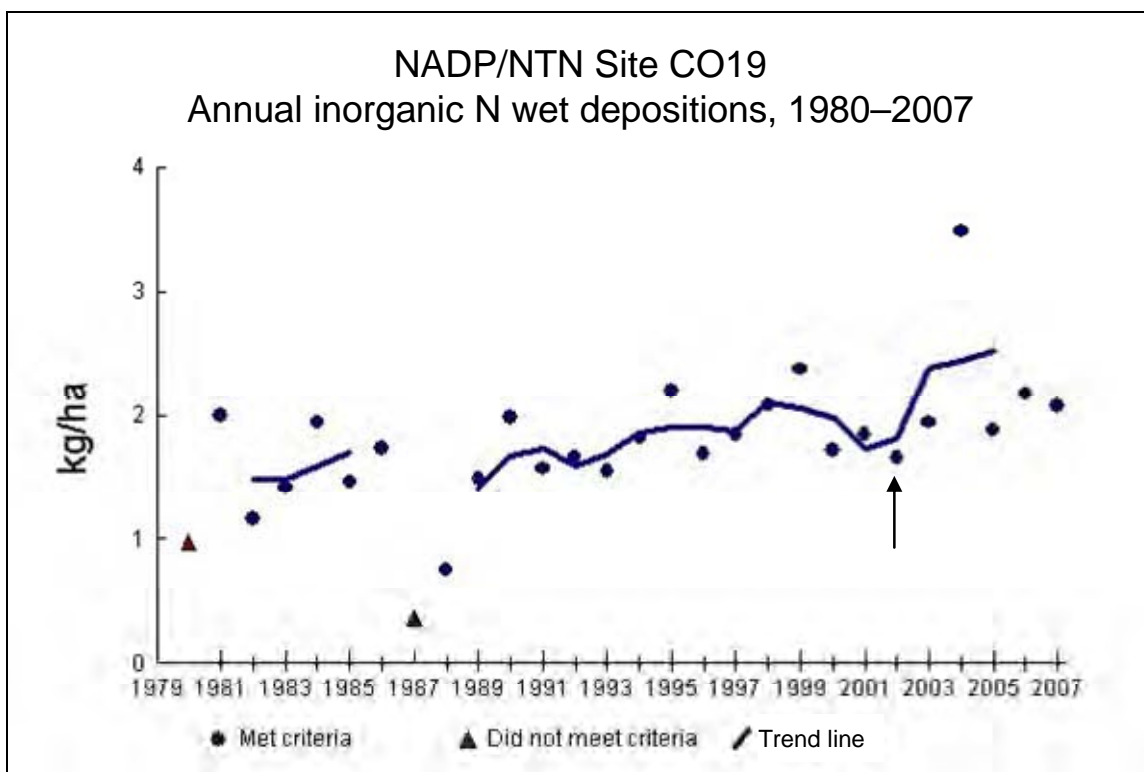


**Figure 1-12.** Rocky Mountain National Park Supplemental Area; Site: Beaver Meadows, CO

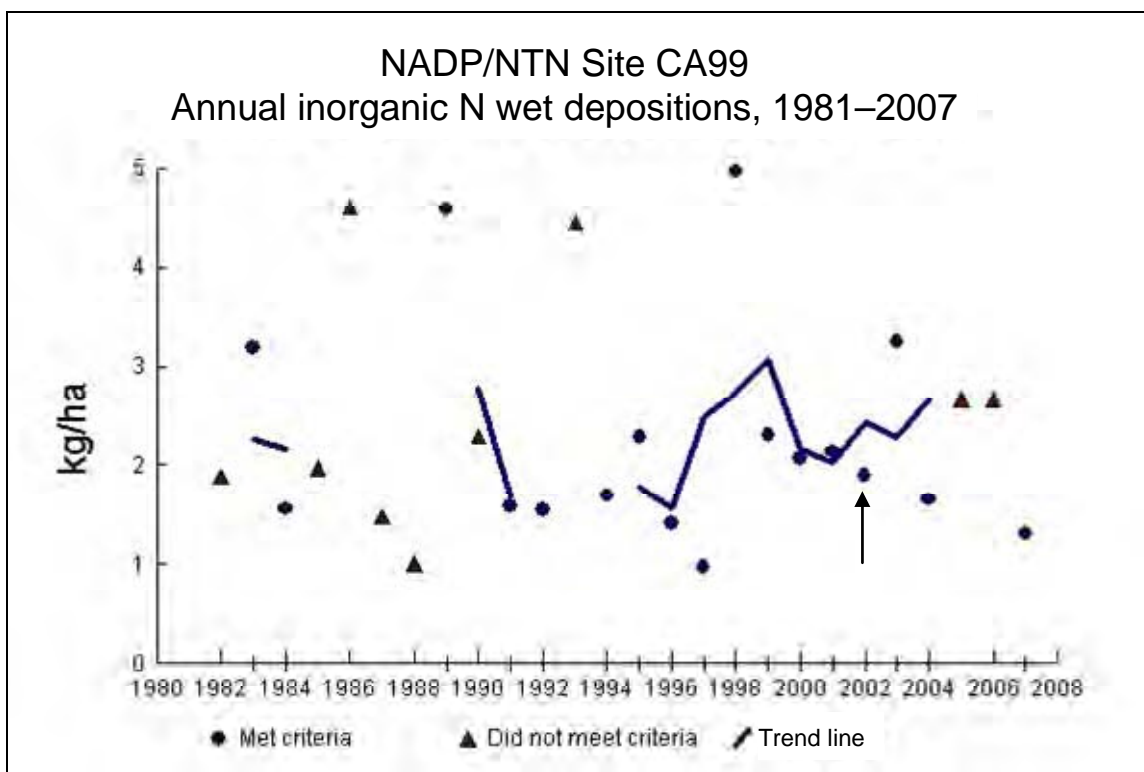


**Figure 1-13.** Mixed Conifer Forest (Sierra Nevada Range) Case Study Area;  
Site: Yosemite National Park, CA

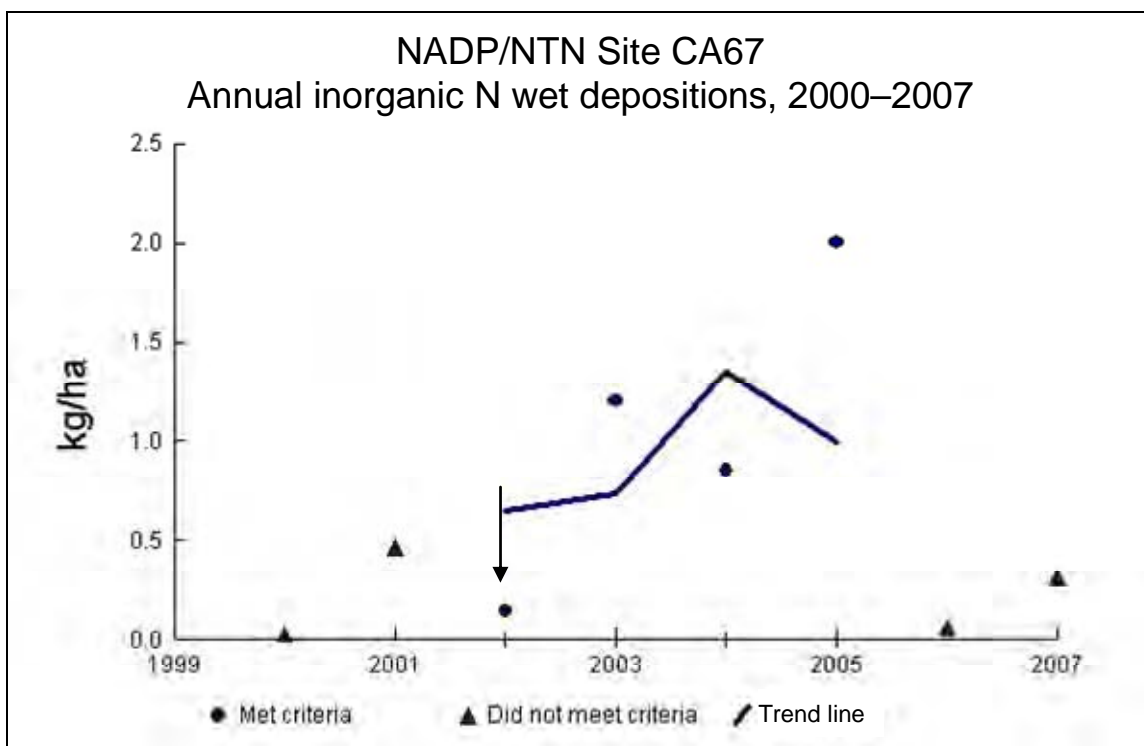


**Figure 1-14.** Mixed Conifer Forest (Transverse Range) Case Study Area;  
Site: Joshua Tree National Park, CA

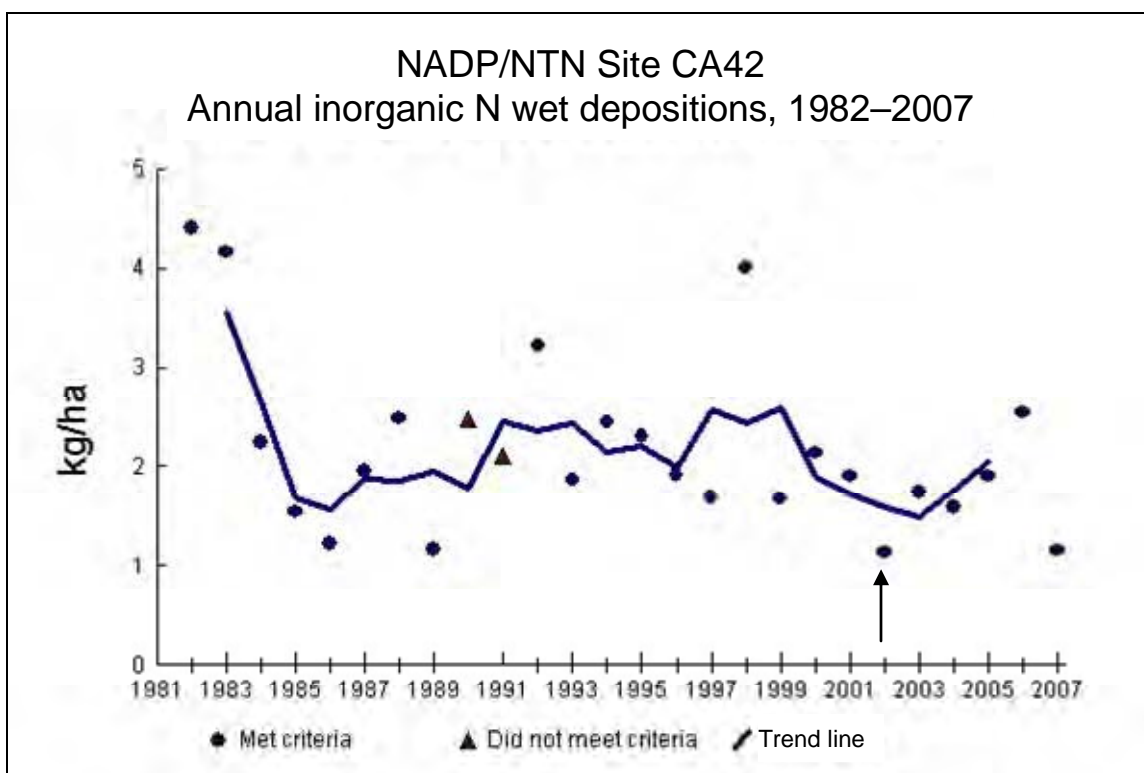


**Figure 1-15.** Mixed Conifer Forest (Transverse Range) Case Study Area;  
Site: Tanbark Flat, CA

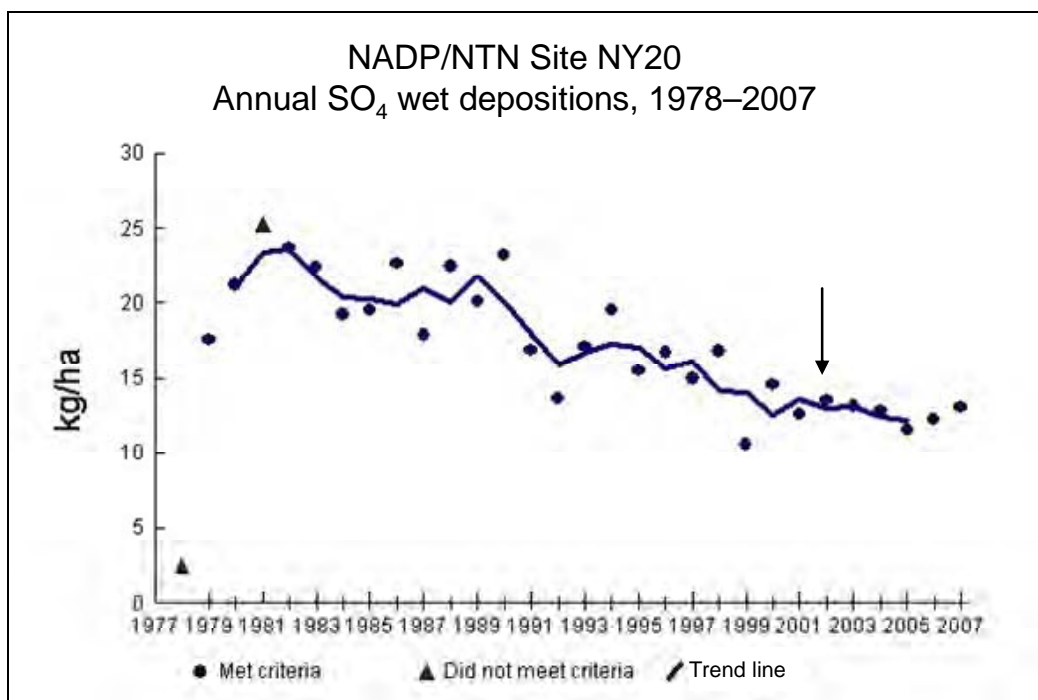


Figure 1-16. Adirondack Case Study Area; Site: Huntington Wildlife Forest, NY

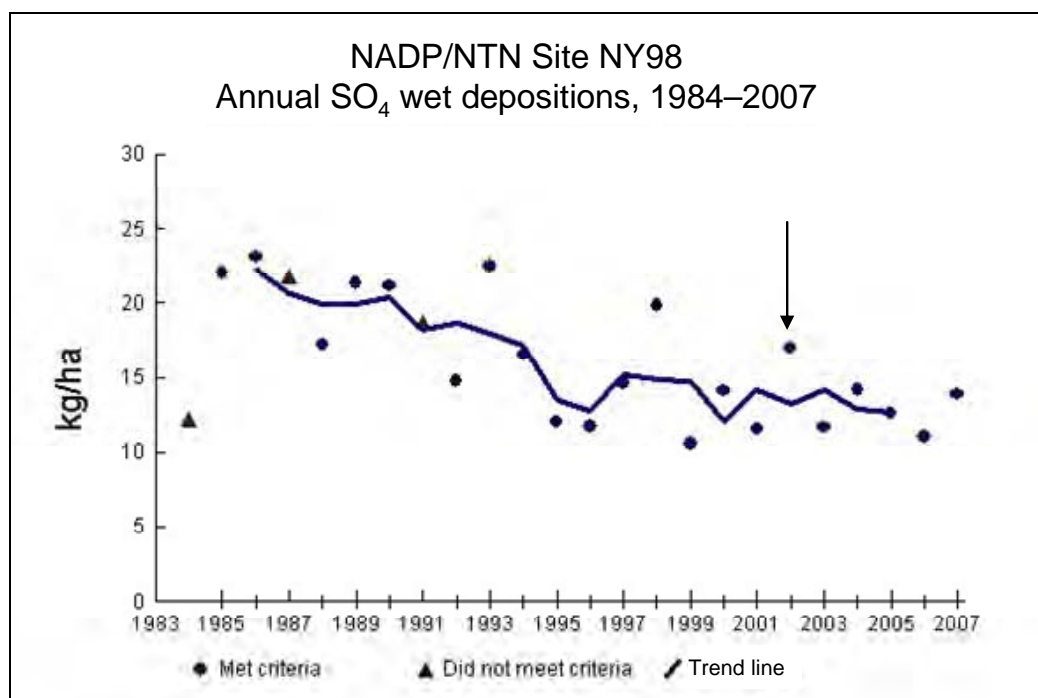
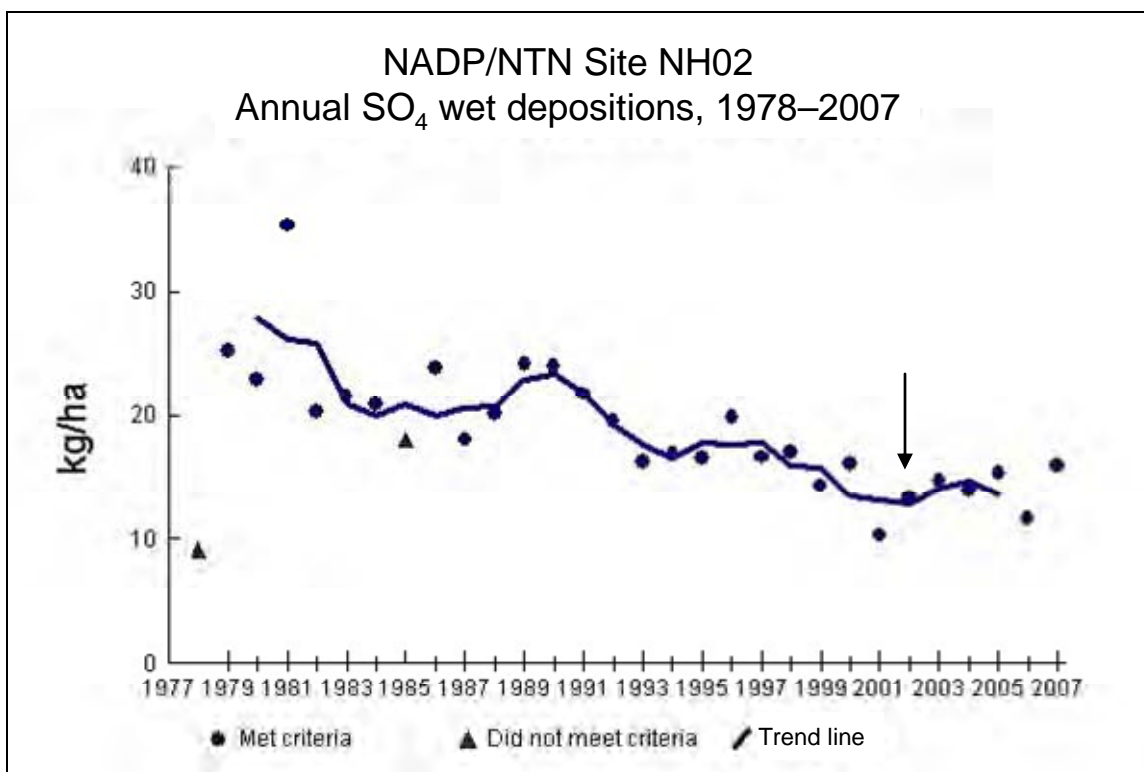
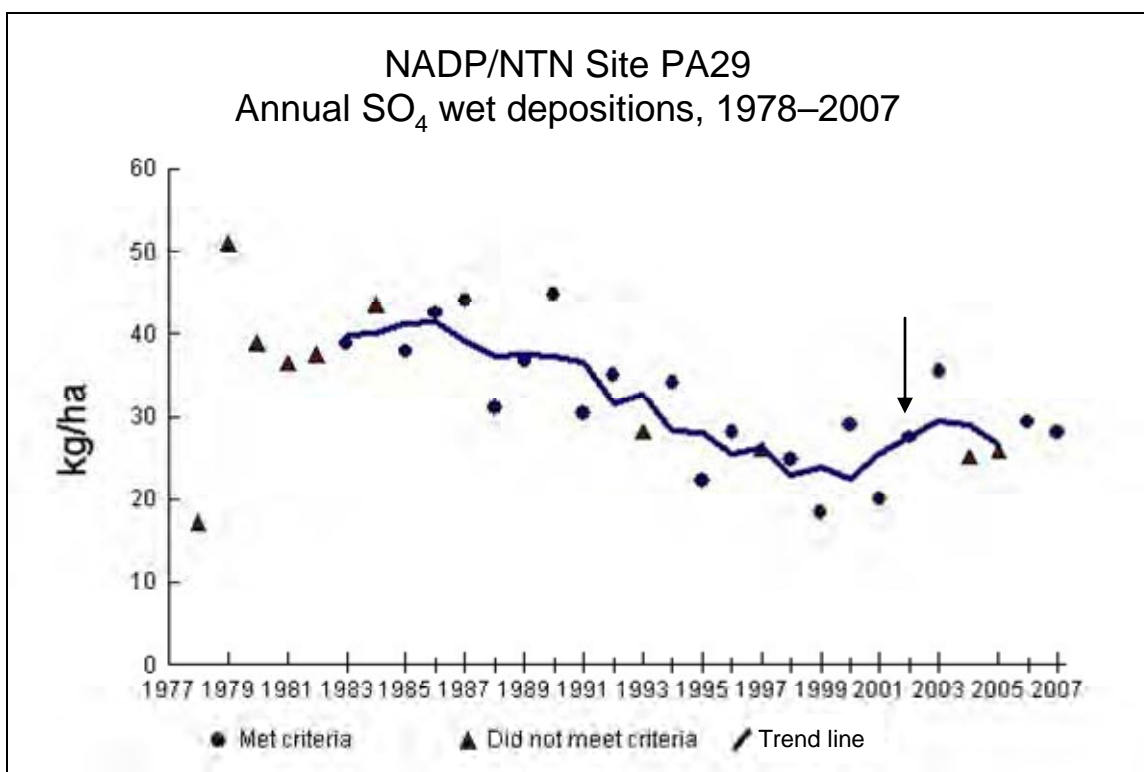


Figure 1-17. Adirondack Case Study Area; Site: Whiteface Mountain, NY



**Figure 1-18.** Hubbard Brook Experimental Forest Case Study Area;  
Site: Hubbard Brook, NH.



**Figure 1-19.** Kane Experimental Forest Case Study Area; Site: Kane Experimental Forest, PA.

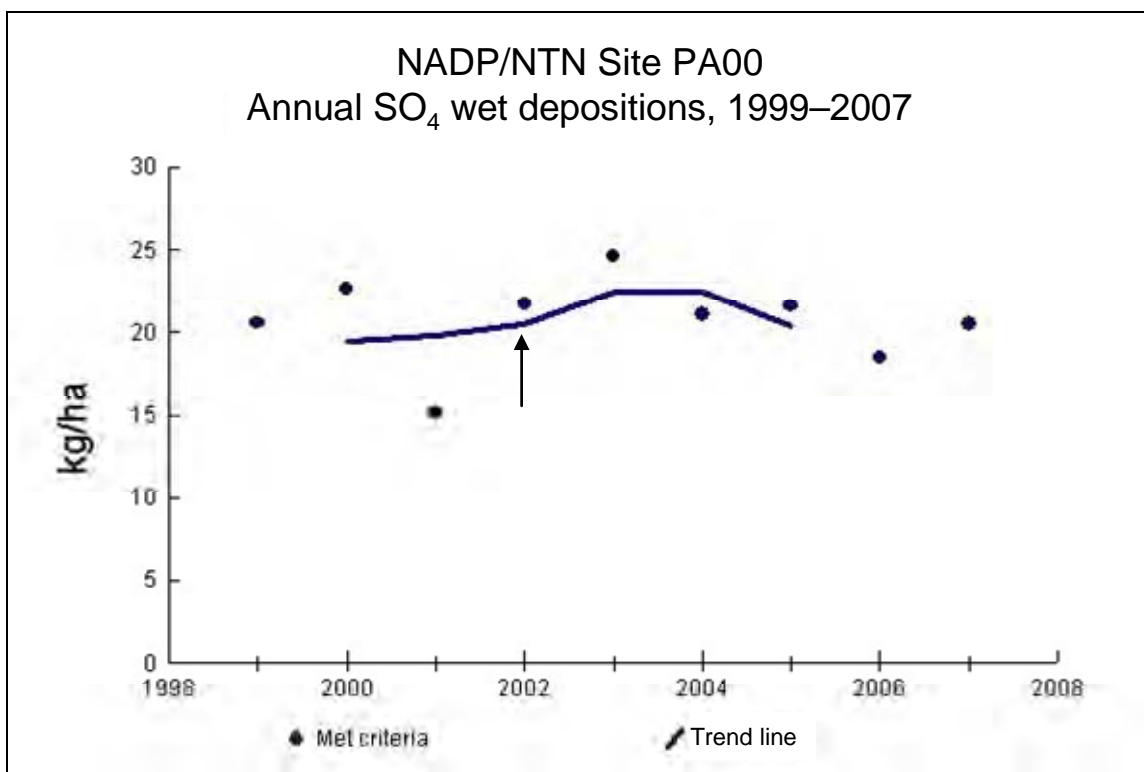


Figure 1-20. Potomac River/Potomac Estuary Case Study Area; Site: Arendtsville, PA

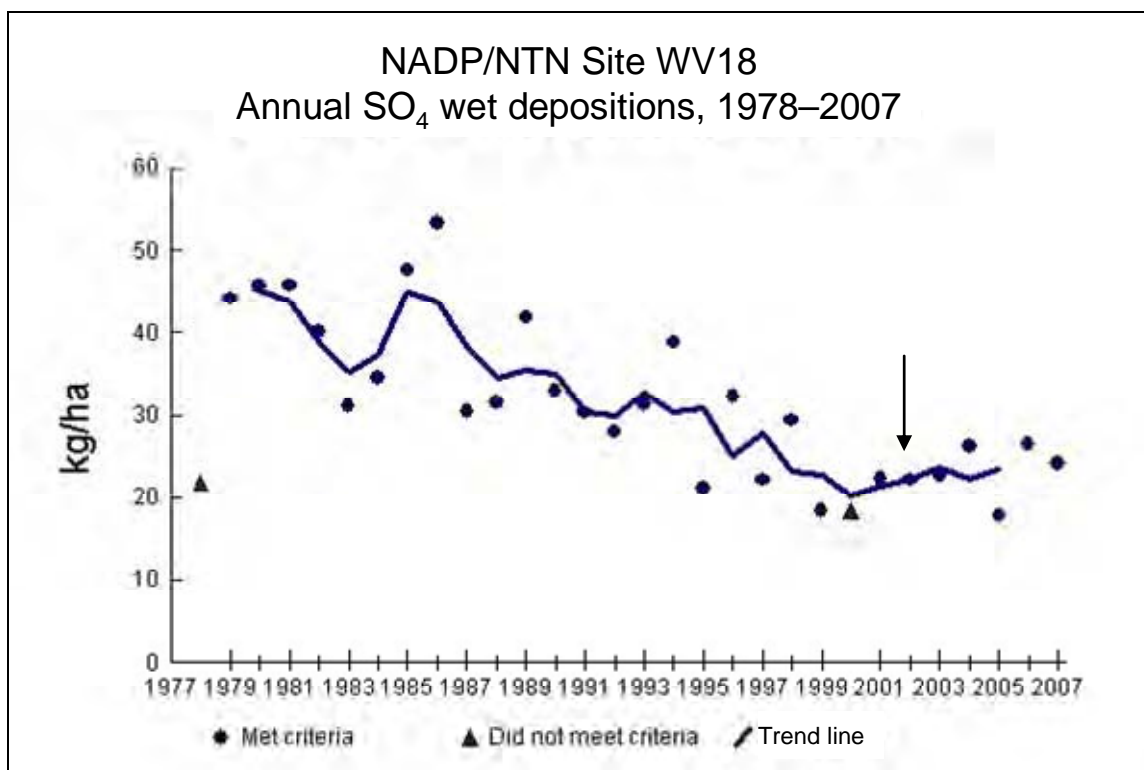


Figure 1-21. Potomac River/Potomac Estuary Case Study Area; Site: Parsons, WV



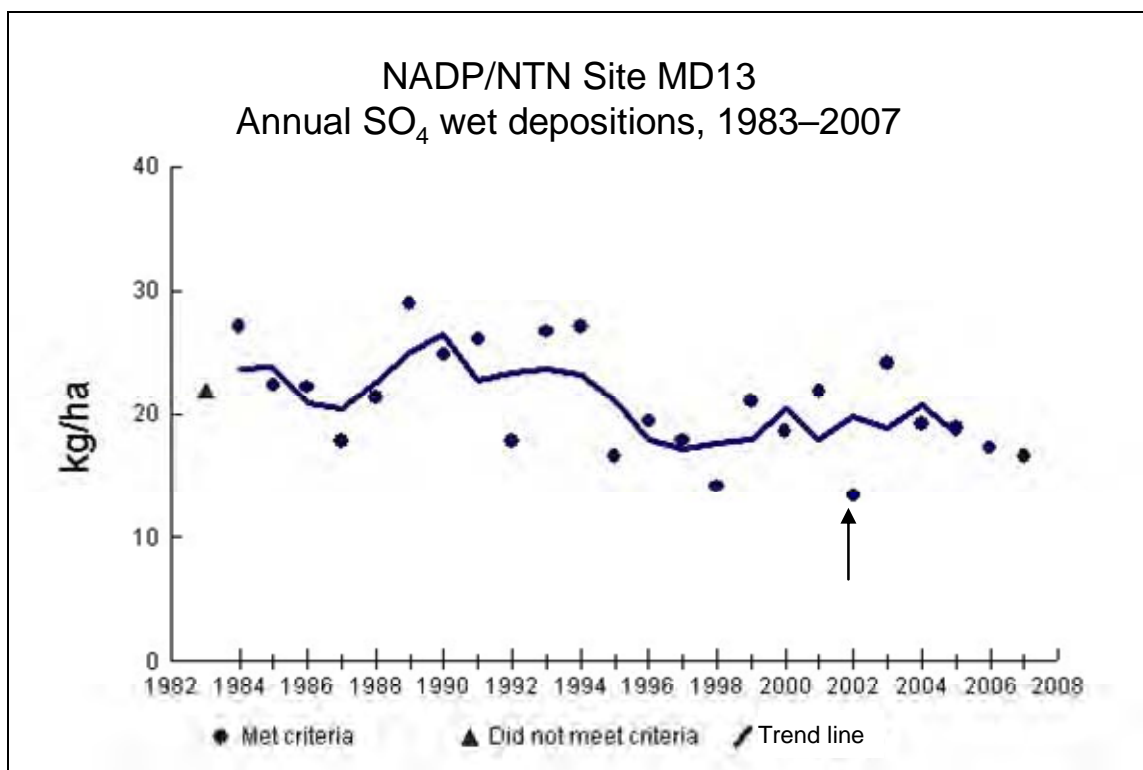


Figure 1-22. Potomac River/Potomac Estuary Case Study Area; Site: Wye, MD

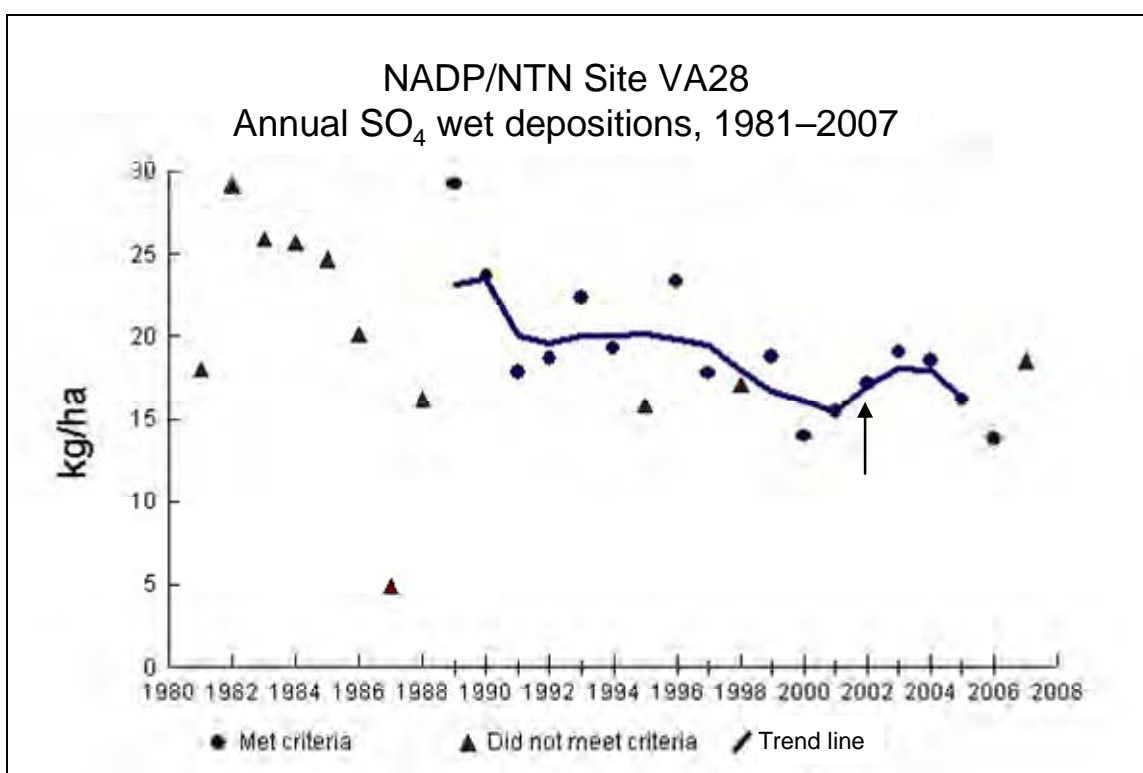


Figure 1-23. Shenandoah Case Study Area; Site: Shenandoah National Park, VA



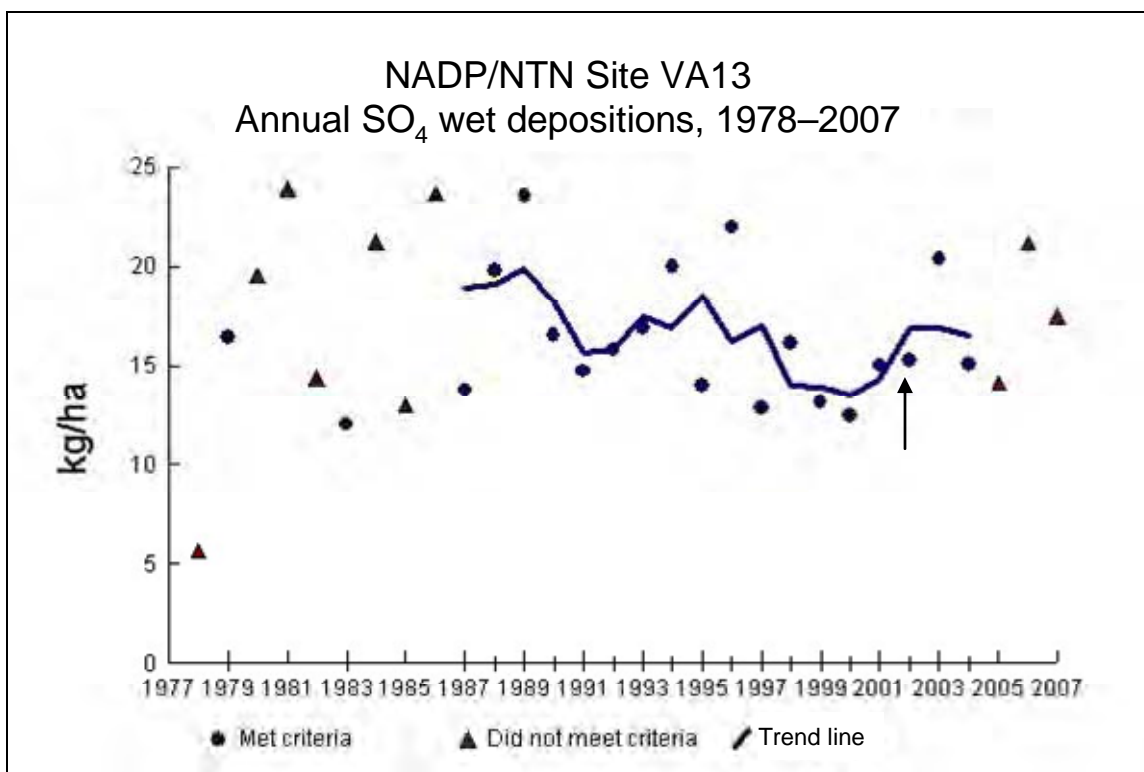


Figure 1-24. Shenandoah Case Study Area; Site: Horton's Station, VA

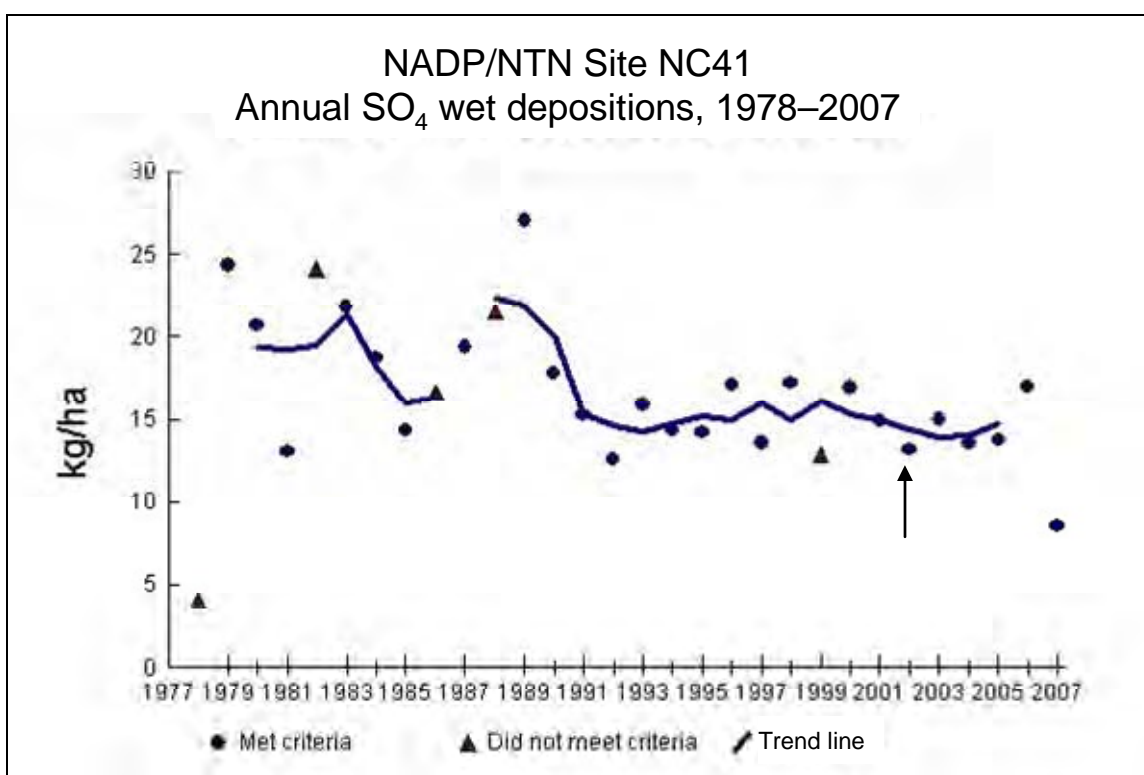


Figure 1-25. Neuse River/Neuse River Estuary Case Study Area; Site: Finley Farm, NC

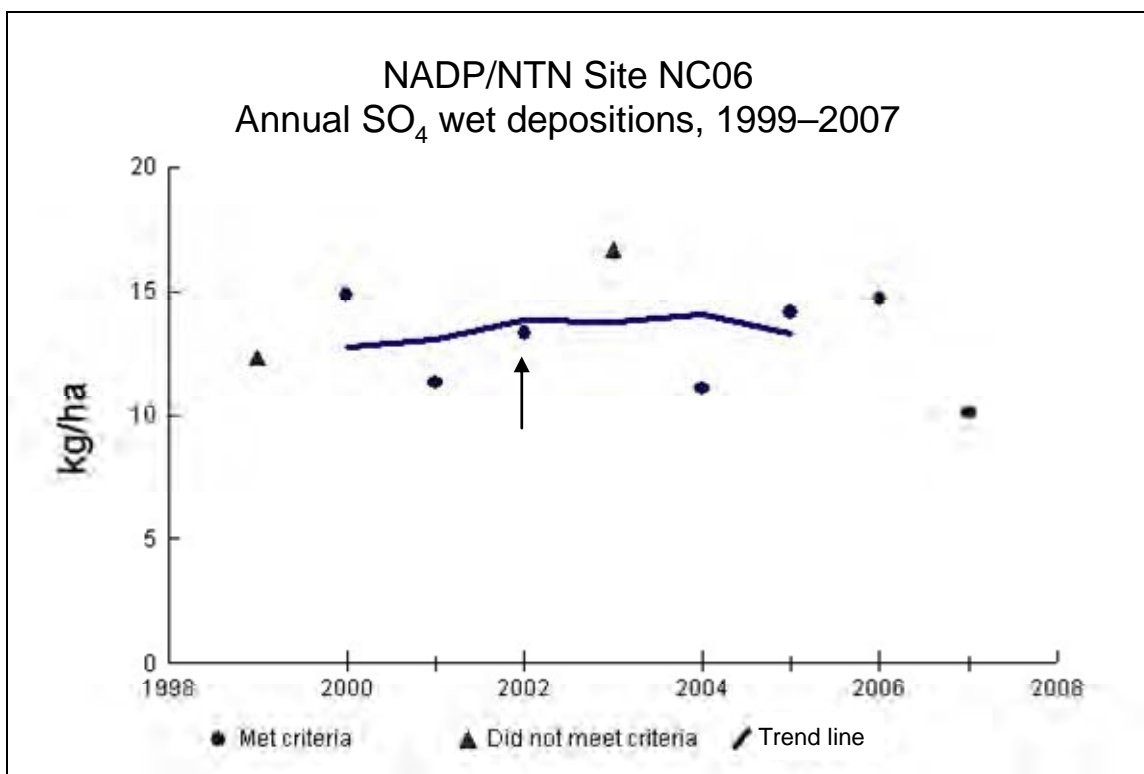


Figure 1-26. Neuse River/Neuse River Estuary Case Study Area; Site: Beaufort, NC

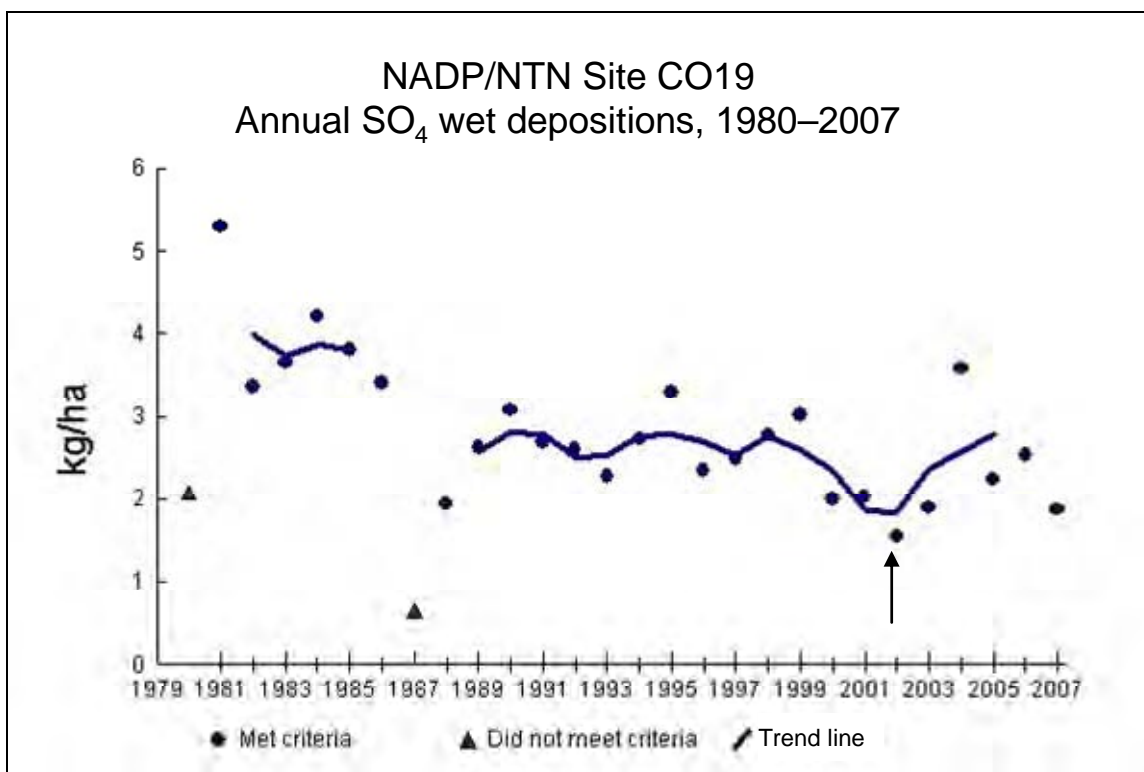
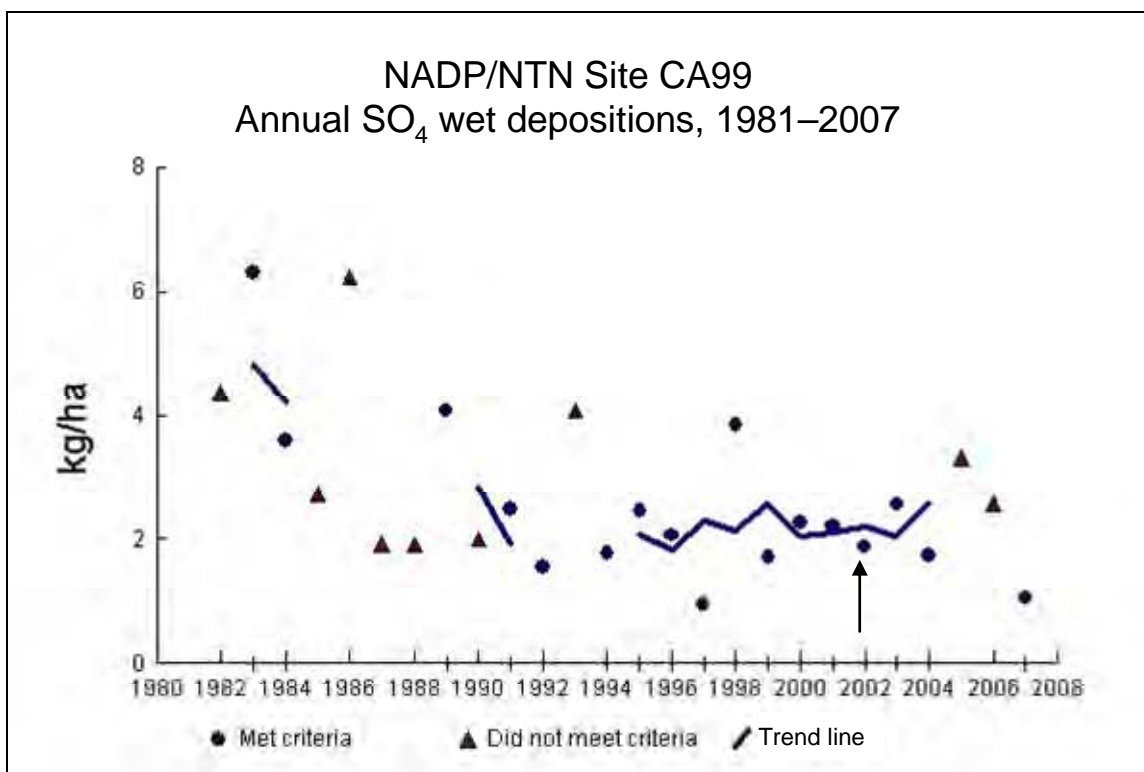
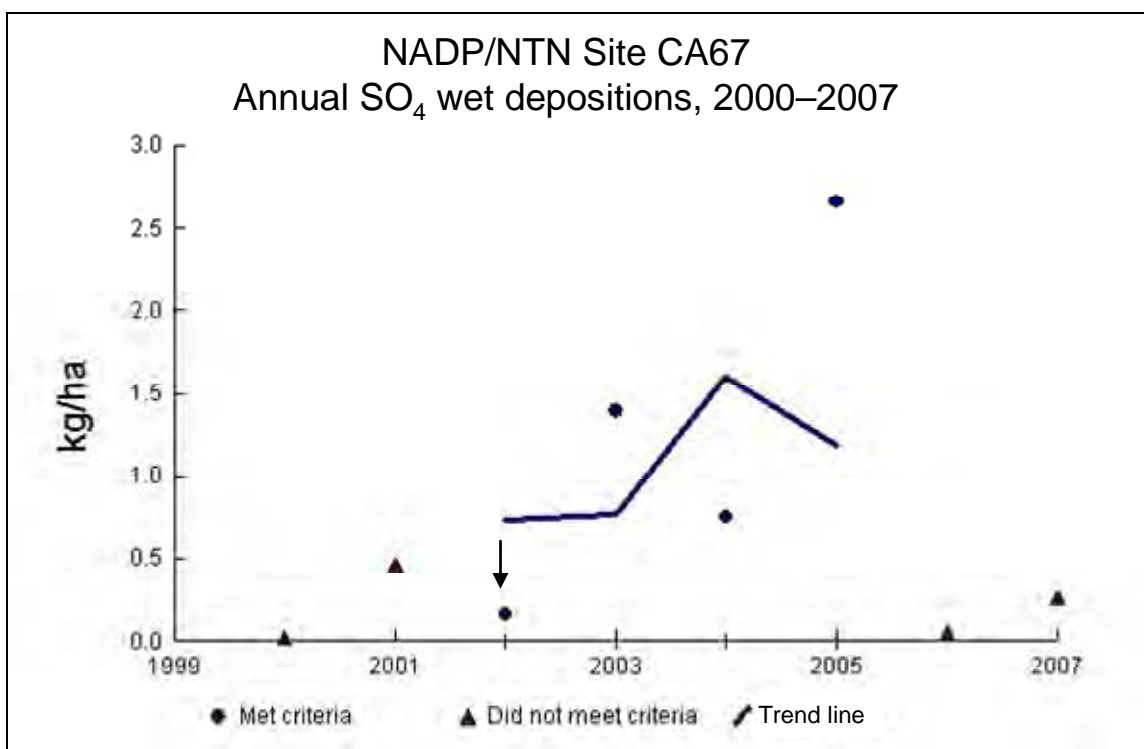


Figure 1-27. Rocky Mountain National Park (Supplemental Area); Site: Beaver Meadows, CO



**Figure 1-28.** Mixed Conifer Forest (Sierra Nevada Range) Case Study Area;  
Site: Yosemite National Park, CA



**Figure 1-29.** Mixed Conifer Forest (Transverse Range) Case Study Area;  
Site: Joshua Tree National Park, CA

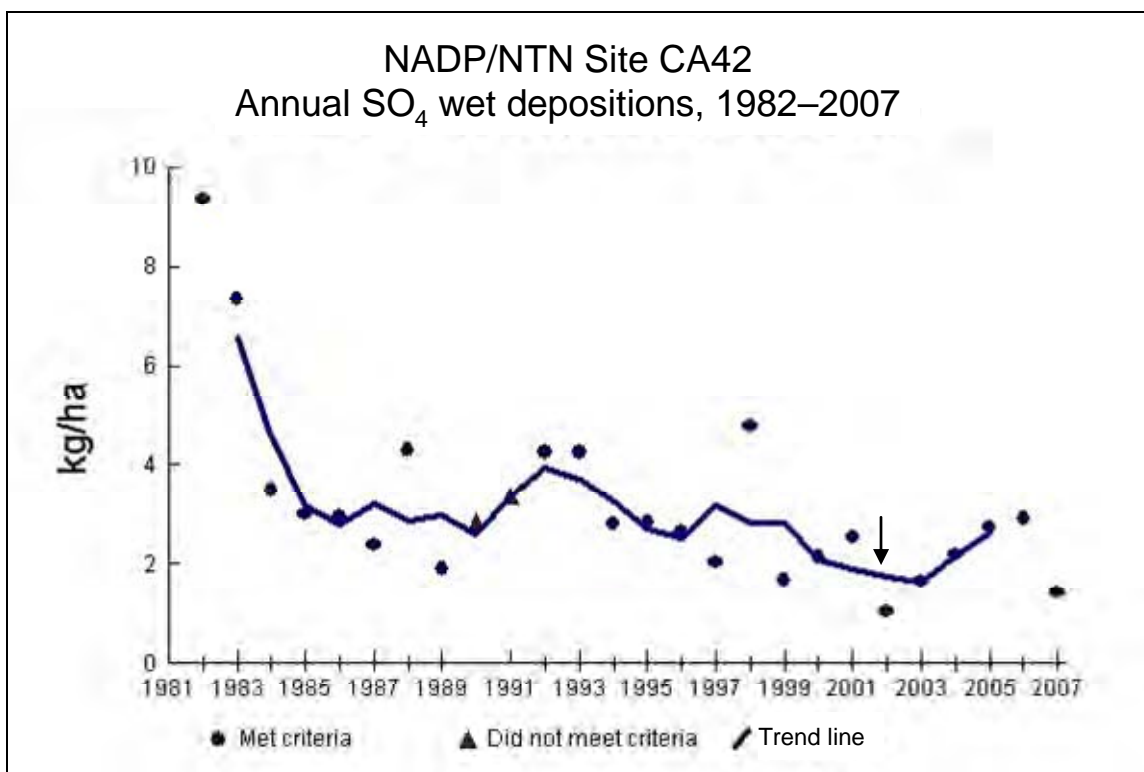


**Figure 1-30.** Mixed Conifer Forest (Transverse Range) Case Study Area;  
Site: Tanbark Flat, CA

## **2.0 SUPPLEMENTAL NATIONWIDE MAPS DEPICTING THE RATIO OF DEPOSITION TO CONCENTRATION AND DEPOSITION TO EMISSIONS**

This section of Appendix 2 contains the following maps (shown by figure number):

- 2-1. Ratio of annual total dry sulfur deposition (kg S/ha/yr) to annual average sulfur dioxide concentrations ( $\mu\text{g}/\text{m}^3$ )
- 2-2. Ratio of annual total wet sulfur deposition (kg S/ha/yr) to annual average sulfur dioxide concentrations ( $\mu\text{g}/\text{m}^3$ )
- 2-3. Ratio of annual total wet+dry sulfur deposition (kg S/ha/yr) to annual average sulfur dioxide concentrations ( $\mu\text{g}/\text{m}^3$ )
- 2-4. Ratio of annual total dry sulfur deposition (kg S/ha/yr) to annual total sulfur dioxide emissions (tons/yr).
- 2-5. Ratio of annual total wet sulfur deposition (kg S/ha/yr) to annual total sulfur dioxide emissions (tons/yr)
- 2-6. Ratio of annual total wet+dry sulfur deposition (kg S/ha/yr) to annual total sulfur dioxide emissions (tons/yr)
- 2-7. Ratio of annual total wet oxidized nitrogen deposition (kg  $\text{NO}_x$ /ha/yr) to annual average nitrogen dioxide concentrations (ppb)
- 2-8. Ratio of annual total dry oxidized nitrogen deposition (kg  $\text{NO}_x$ /ha/yr) to annual average nitrogen dioxide concentrations (ppb)
- 2-9. Ratio of annual total wet+dry oxidized nitrogen deposition (kg  $\text{NO}_x$ /ha/yr) to annual average nitrogen dioxide concentrations (ppb)
- 2-10. Ratio of annual total dry oxidized nitrogen deposition (kg  $\text{NO}_x$ /ha/yr) to annual total nitrogen dioxide emissions (tons/yr)
- 2-11. Ratio of annual total wet oxidized nitrogen deposition (kg  $\text{NO}_x$ /ha/yr) to annual total nitrogen dioxide emissions (tons/yr)
- 2-12. Ratio of annual total wet+dry oxidized nitrogen deposition (kg  $\text{NO}_x$ /ha/yr) to annual total nitrogen dioxide emissions (tons/yr)
- 2-13. Ratio of annual total dry nitrogen deposition (kg N/ha/yr) to annual average nitrogen dioxide concentrations (ppb)
- 2-14. Ratio of annual total wet nitrogen deposition (kg N/ha/yr) to annual average nitrogen dioxide concentrations (ppb)
- 2-15. Ratio of annual total wet+dry nitrogen deposition (kg N/ha/yr) to annual average nitrogen dioxide concentrations (ppb)
- 2-16. Ratio of annual total dry nitrogen deposition (kg N/ha/yr) to annual total nitrogen dioxide emissions (tons/yr)
- 2-17. Ratio of annual total wet nitrogen deposition (kg N/ha/yr) to annual total nitrogen dioxide emissions (tons/yr)
- 2-18. Ratio of annual total wet+dry nitrogen deposition (kg N/ha/yr) to annual total nitrogen dioxide emissions (tons/yr).

These maps were created using CMAQ-predicted 12 x 12 km concentrations and deposition, and CMAQ gridded emissions inputs data.

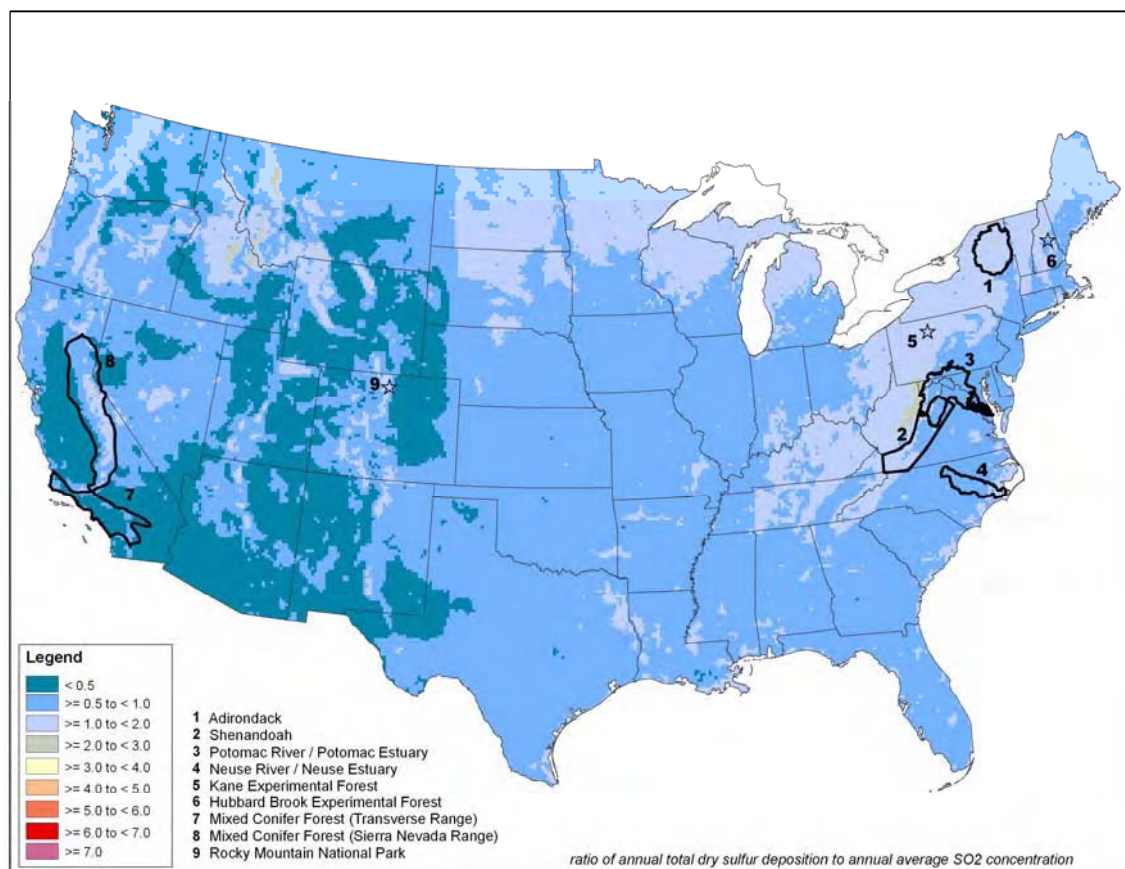


**Figure 2-1.** Ratio of annual total dry sulfur deposition (kg S/ha/yr) to annual average sulfur dioxide concentrations ( $\mu\text{g}/\text{m}^3$ ).



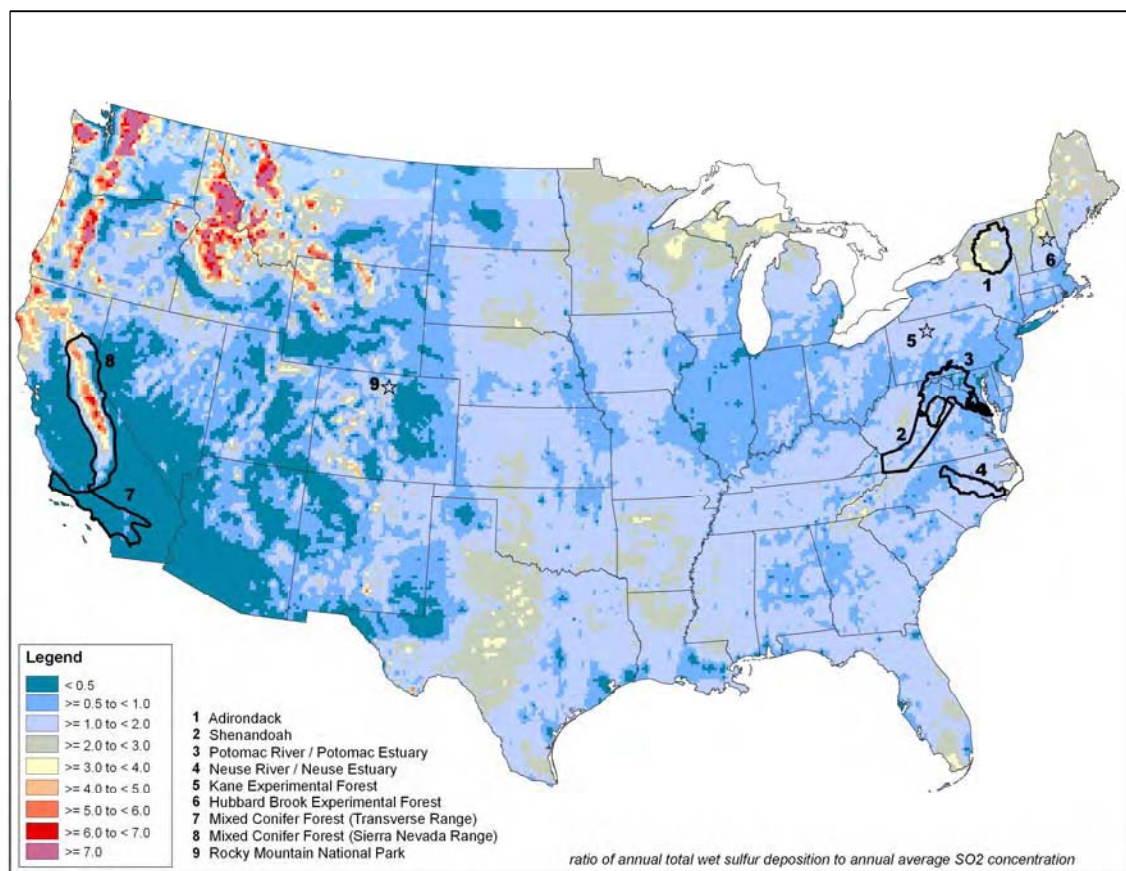


**Figure 2-2.** Ratio of annual total wet sulfur deposition (kg S/ha/yr) to annual average sulfur dioxide concentrations ( $\mu\text{g}/\text{m}^3$ ).

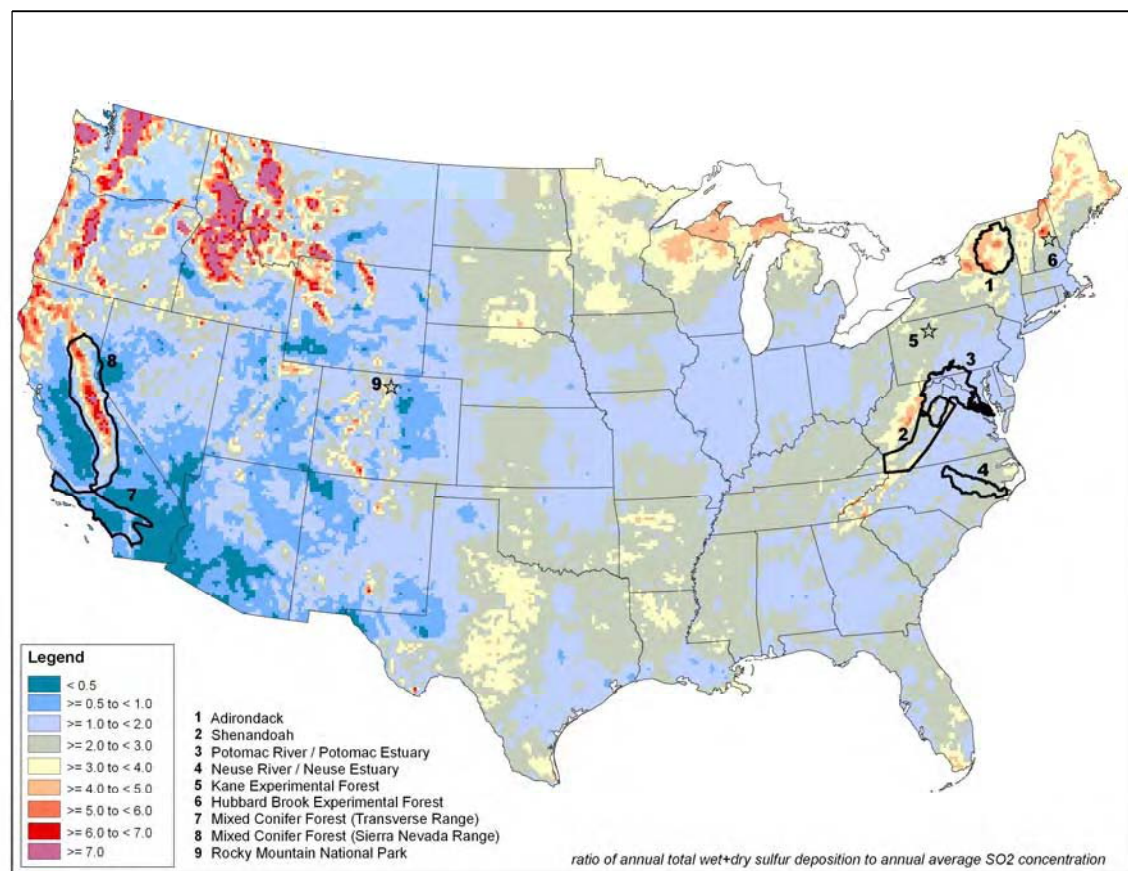


**Figure 2-3.** Ratio of annual total wet+dry sulfur deposition (kg S/ha/yr) to annual average sulfur dioxide concentrations ( $\mu\text{g}/\text{m}^3$ ).



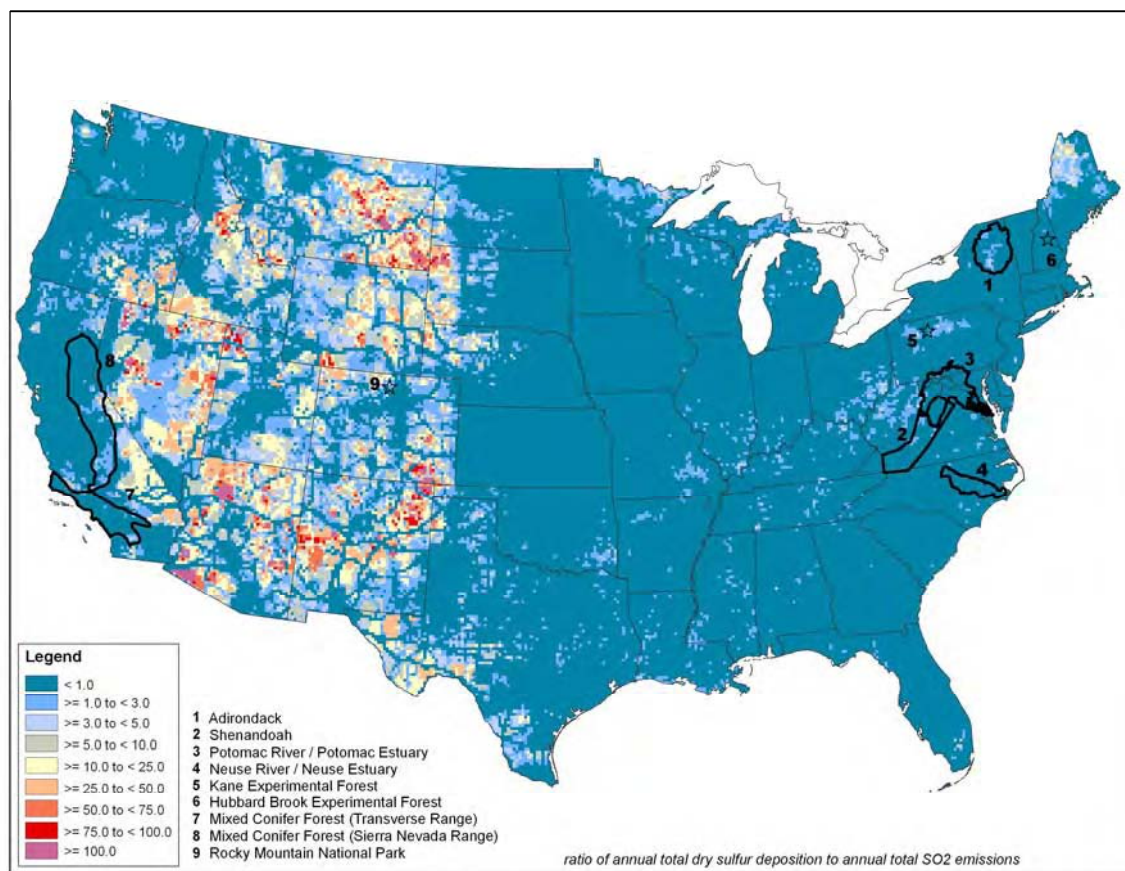


**Figure 2-4.** Ratio of annual total dry sulfur deposition (kg S/ha/yr) to annual total sulfur dioxide emissions (tons/yr).

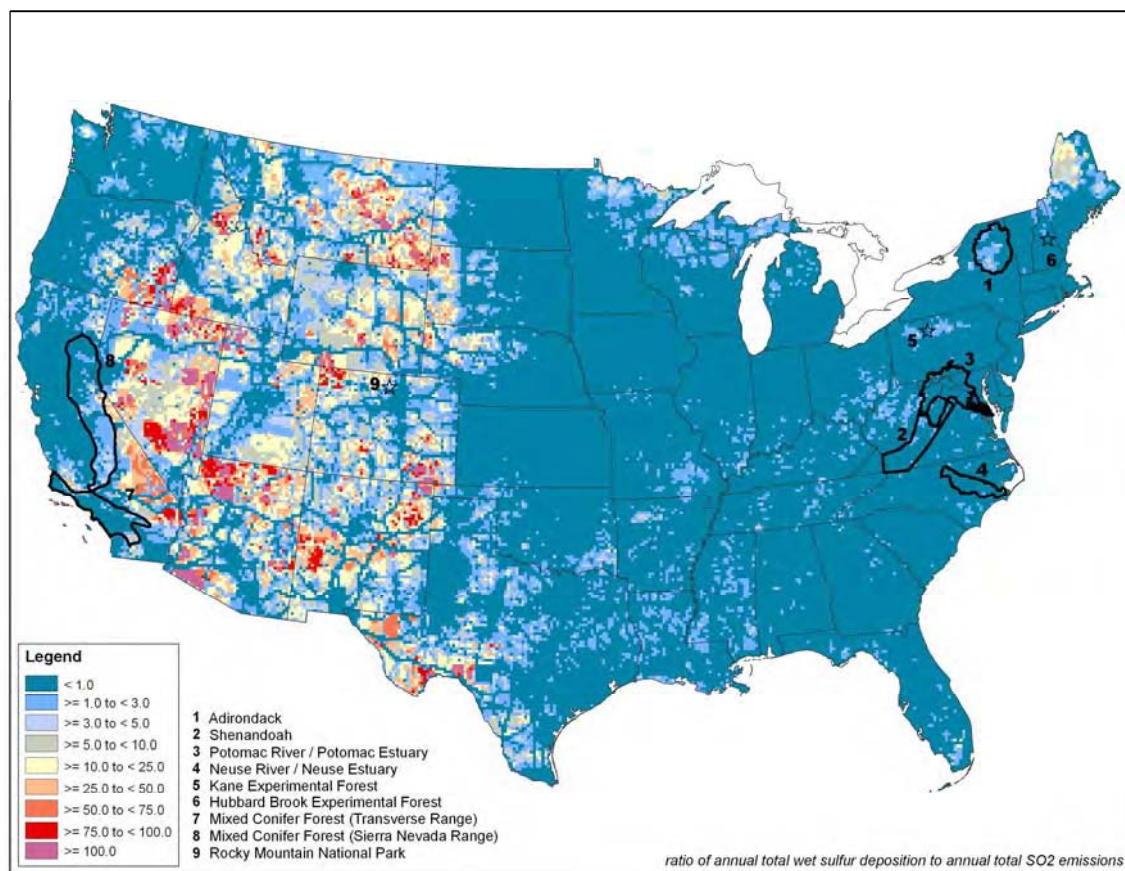


**Figure 2-5.** Ratio of annual total wet sulfur deposition (kg S/ha/yr) to annual total sulfur dioxide emissions (tons/yr).

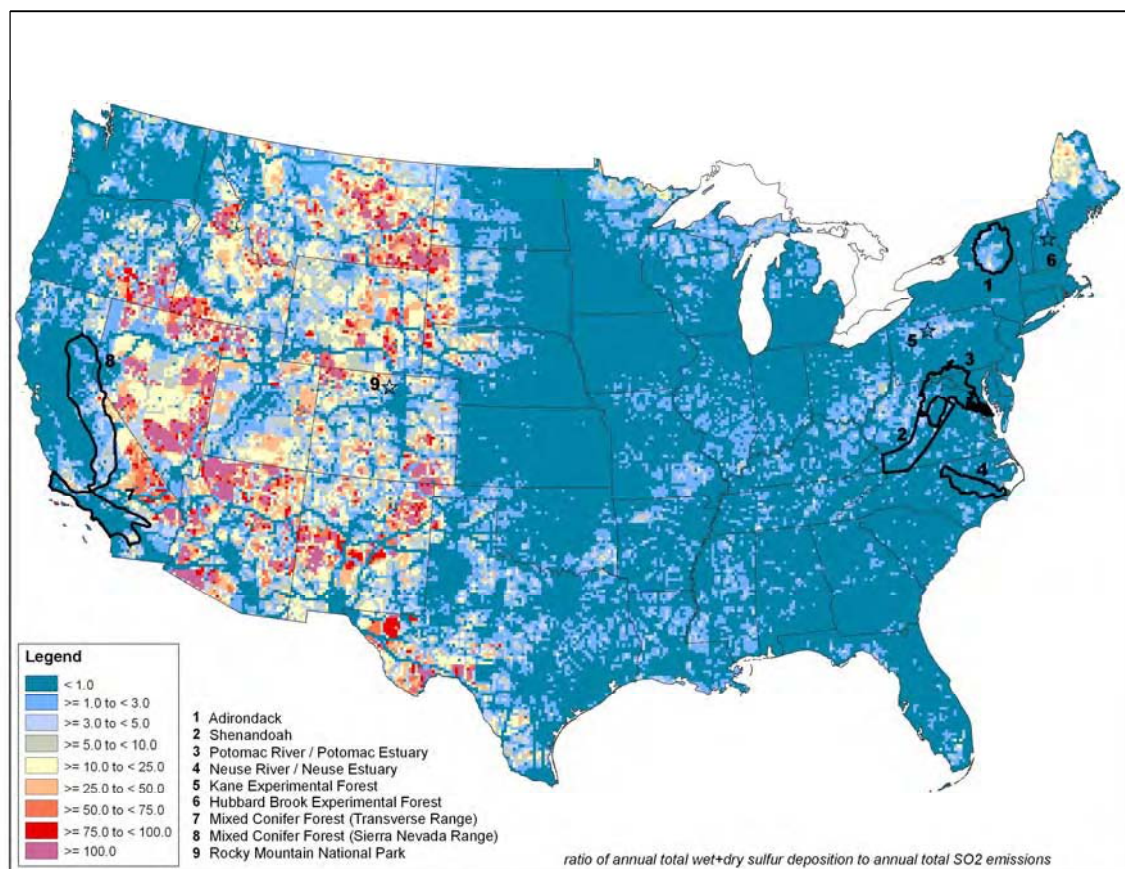


**Figure 2-6.** Ratio of annual total wet+dry sulfur deposition (kg S/ha/yr) to annual total sulfur dioxide emissions (tons/yr).



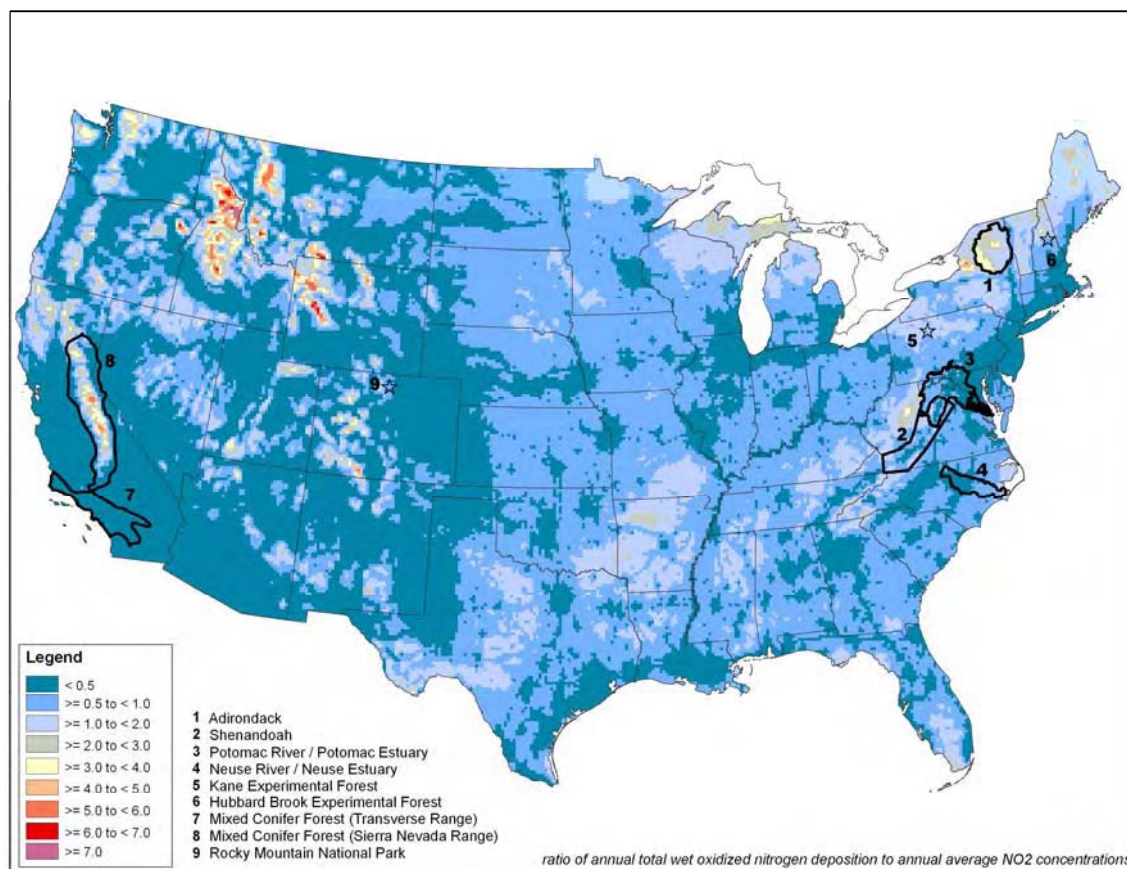


**Figure 2-7.** Ratio of annual total wet oxidized nitrogen deposition (kg NO<sub>x</sub>/ha/yr) to annual average nitrogen dioxide concentrations (ppb).

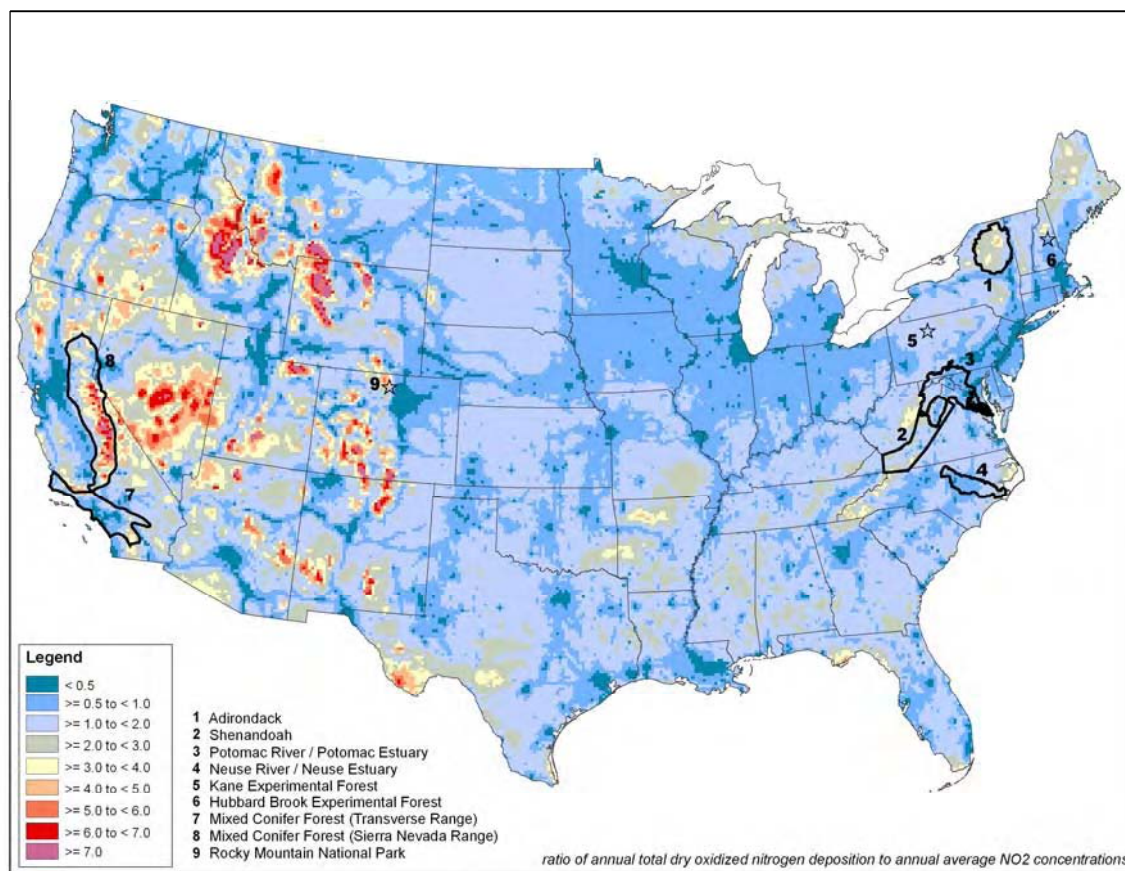


**Figure 2-8.** Ratio of annual total dry oxidized nitrogen deposition (kg NO<sub>x</sub>/ha/yr) to annual average nitrogen dioxide concentrations (ppb).

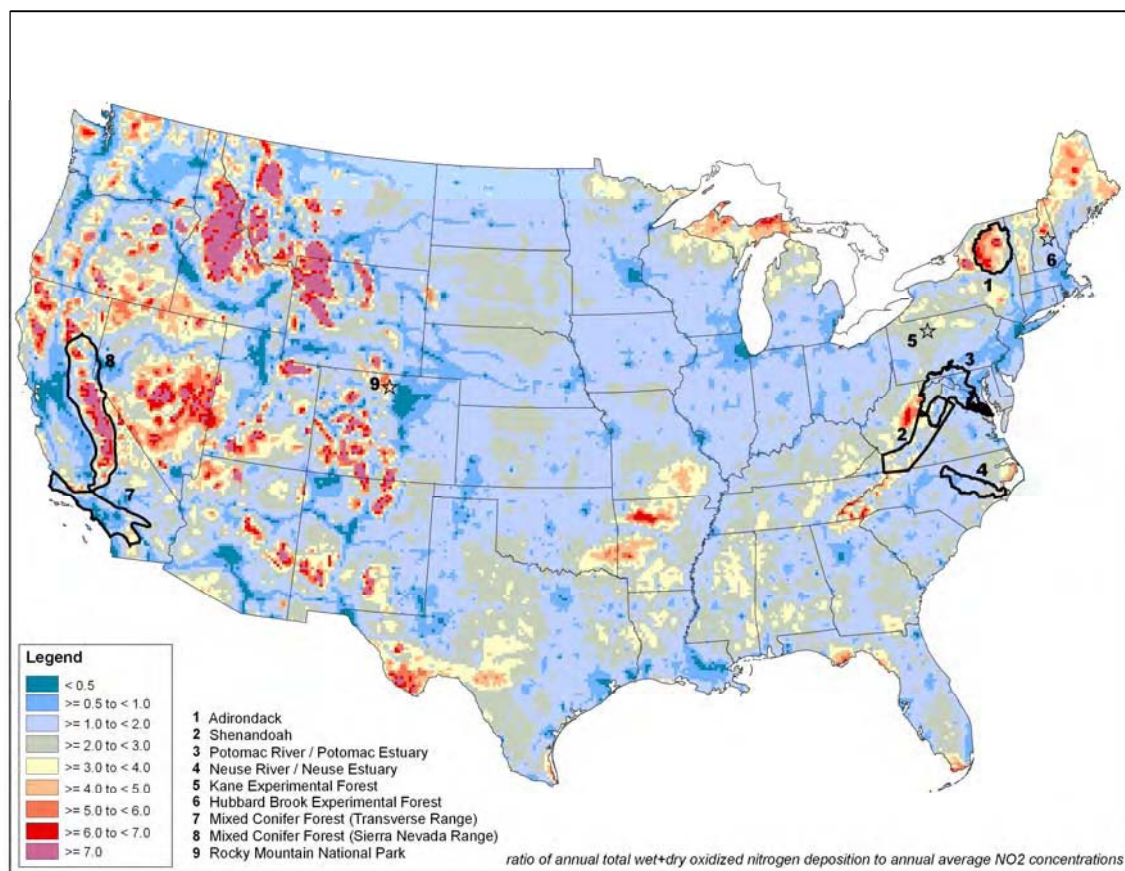


**Figure 2-9.** Ratio of annual total wet+dry oxidized nitrogen deposition (kg NO<sub>x</sub>/ha/yr) to annual average nitrogen dioxide concentrations (ppb).



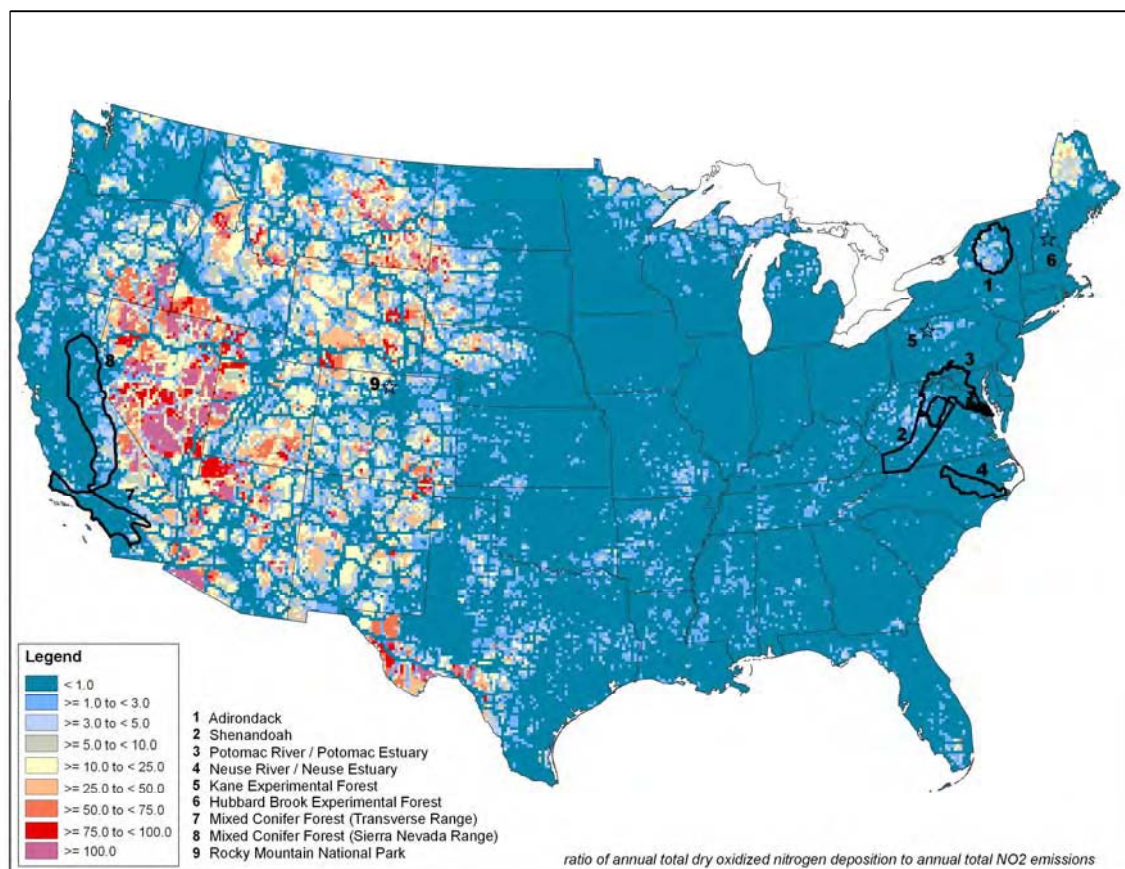


**Figure 2-10.** Ratio of annual total dry oxidized nitrogen deposition (kg NO<sub>x</sub>/ha/yr) to annual total nitrogen dioxide emissions (tons/yr).

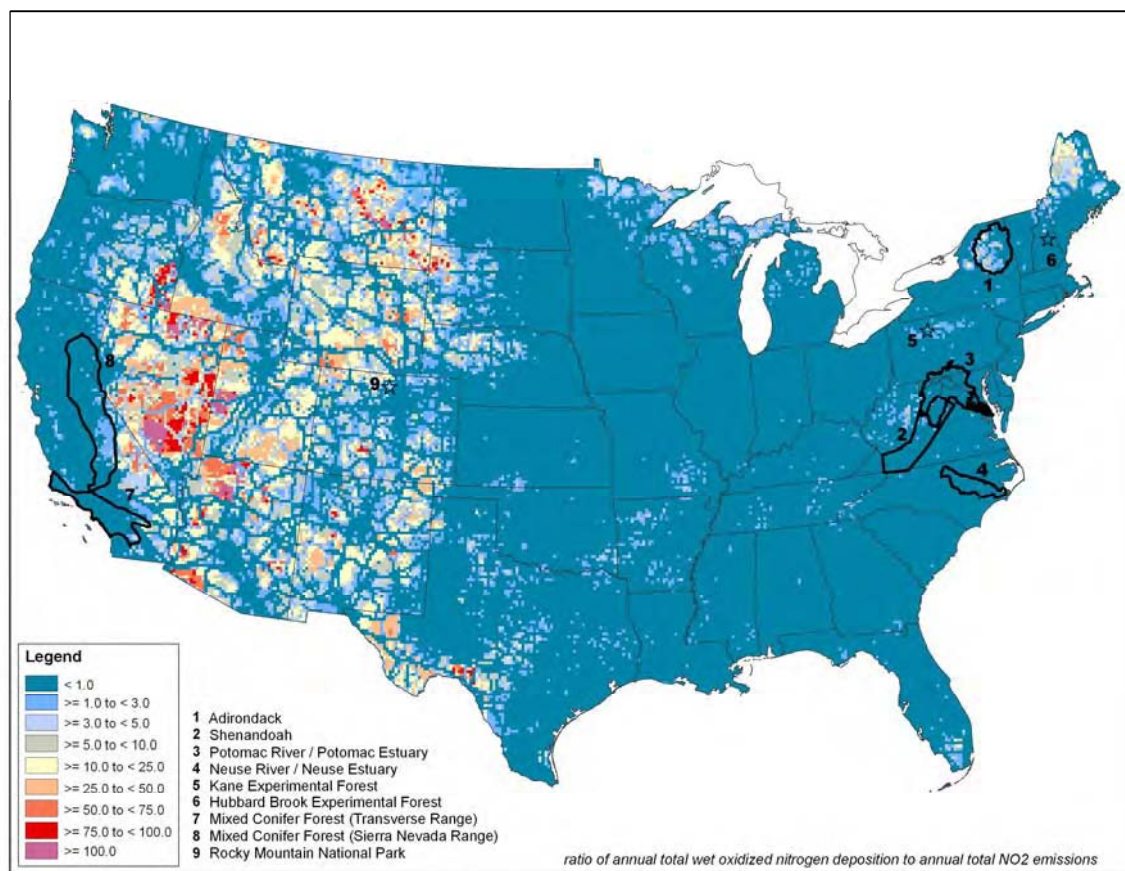


**Figure 2-11.** Ratio of annual total wet oxidized nitrogen deposition (kg NO<sub>x</sub>/ha/yr) to annual total nitrogen dioxide emissions (tons/yr).



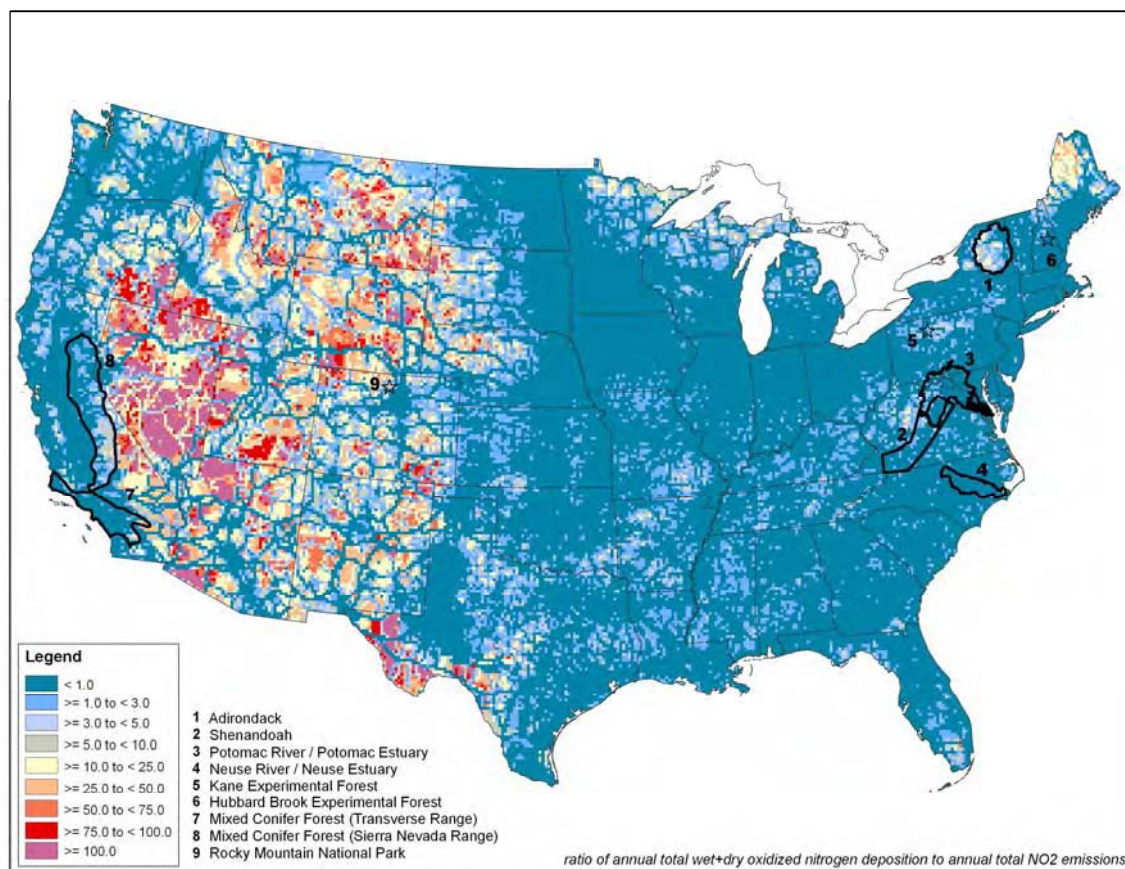


**Figure 2-12.** Ratio of annual total wet+dry oxidized nitrogen deposition (kg NO<sub>x</sub>/ha/yr) to annual total nitrogen dioxide emissions (tons/yr).

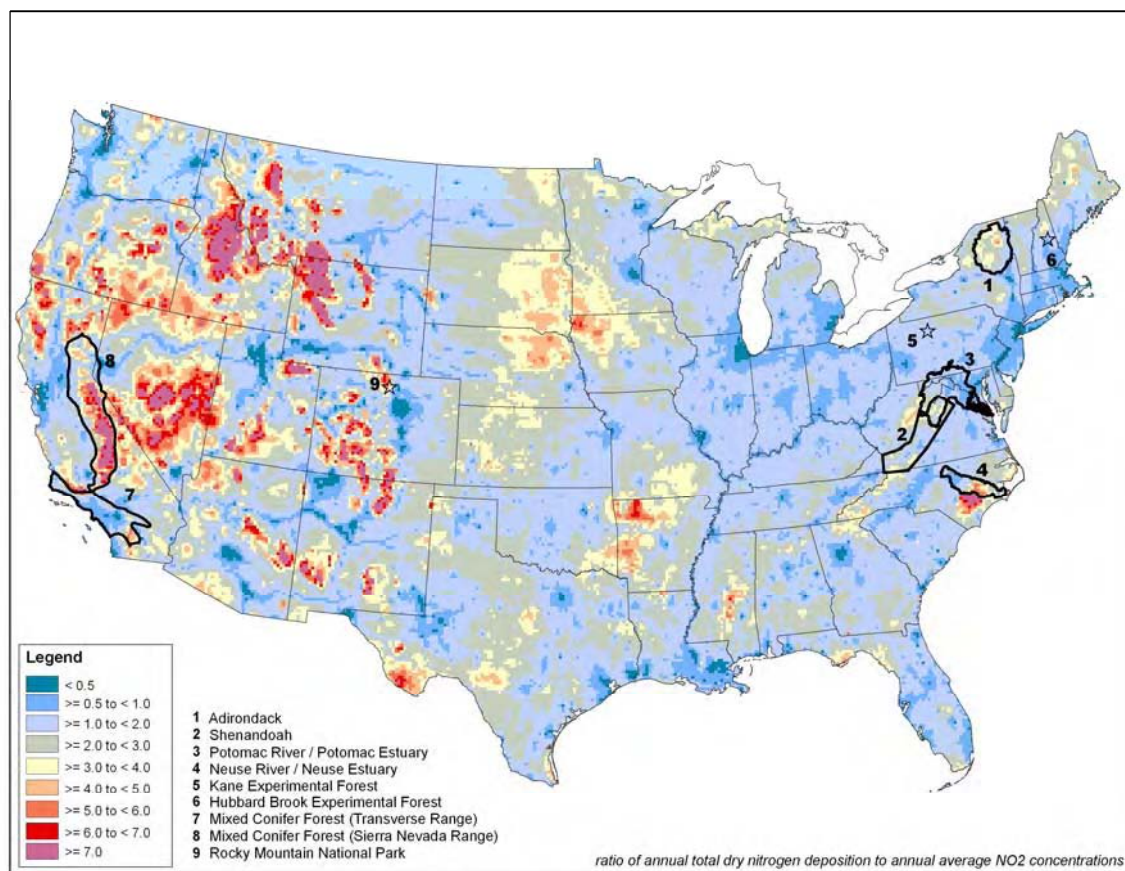


**Figure 2-13.** Ratio of annual total dry nitrogen deposition (kg N/ha/yr) to annual average nitrogen dioxide concentrations (ppb).

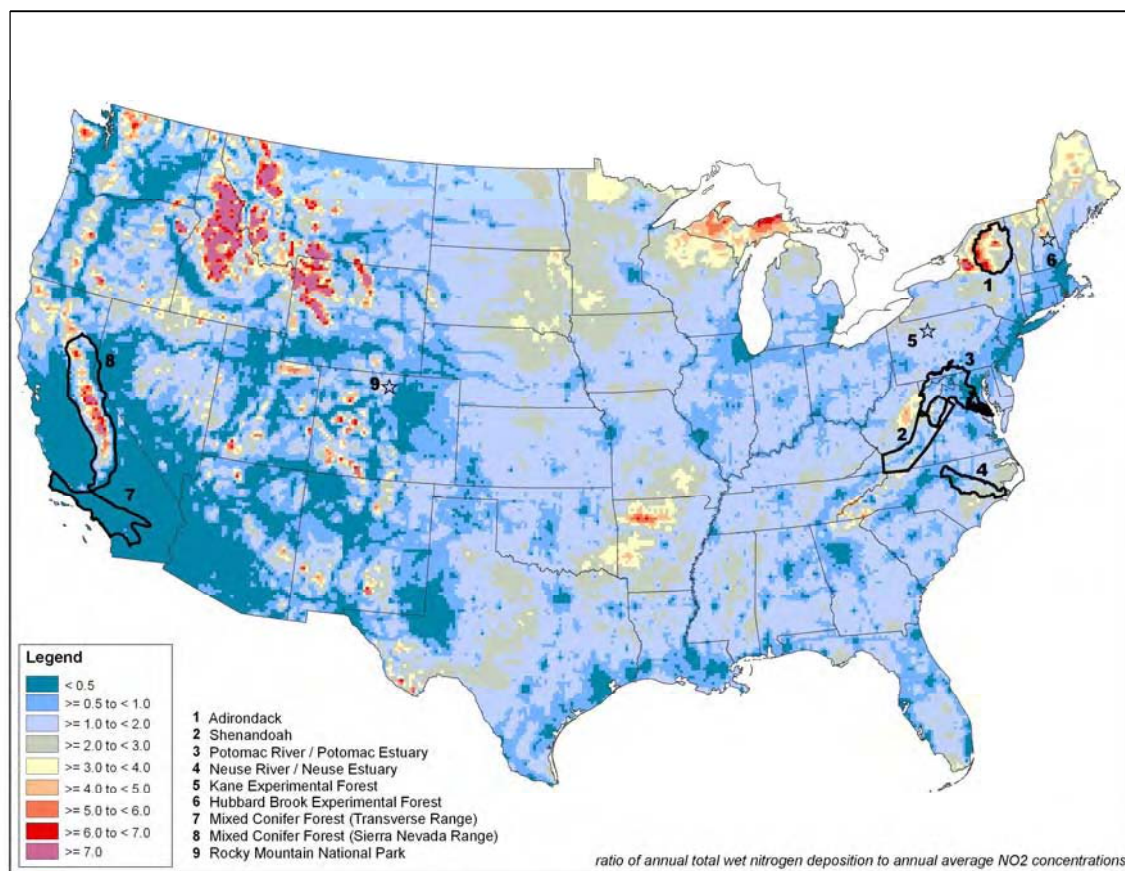


**Figure 2-14.** Ratio of annual total wet nitrogen deposition (kg N/ha/yr) to annual average nitrogen dioxide concentrations (ppb).



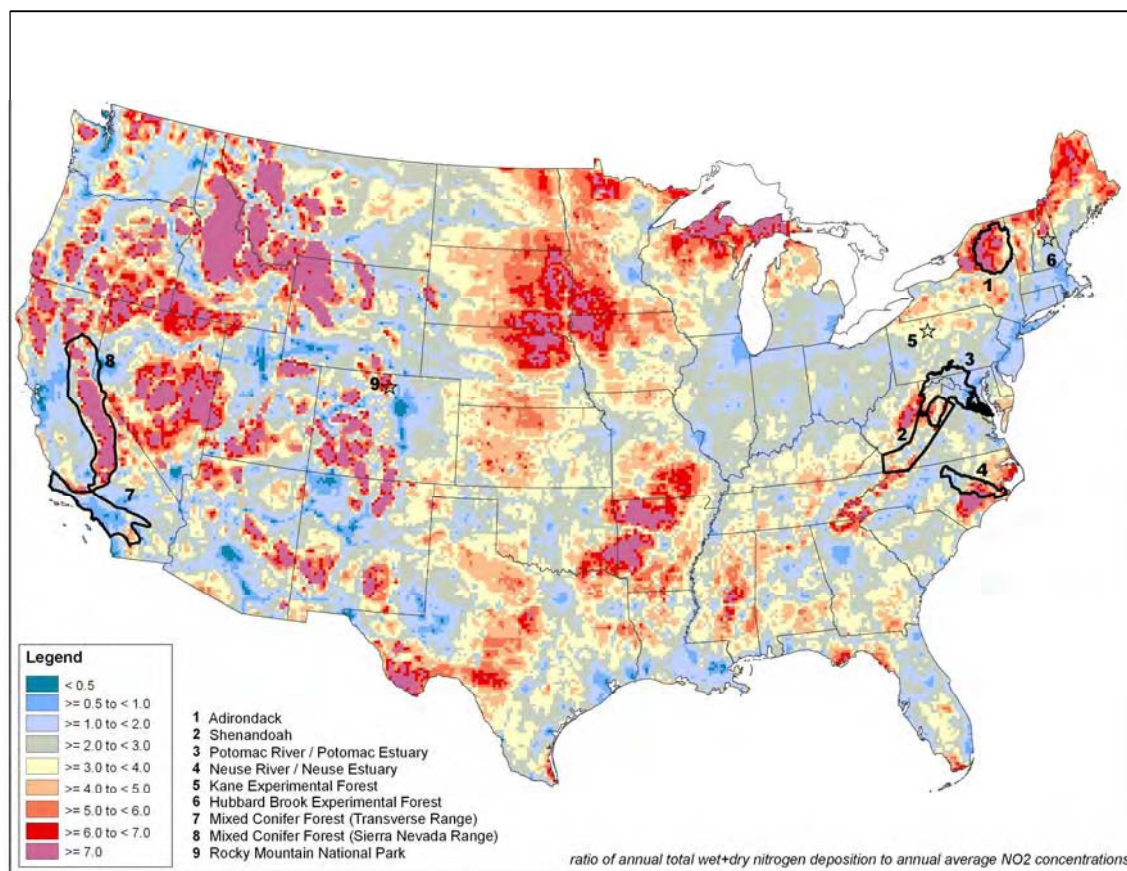


**Figure 2-15.** Ratio of annual total wet+dry nitrogen deposition (kg N/ha/yr) to annual average nitrogen dioxide concentrations (ppb).

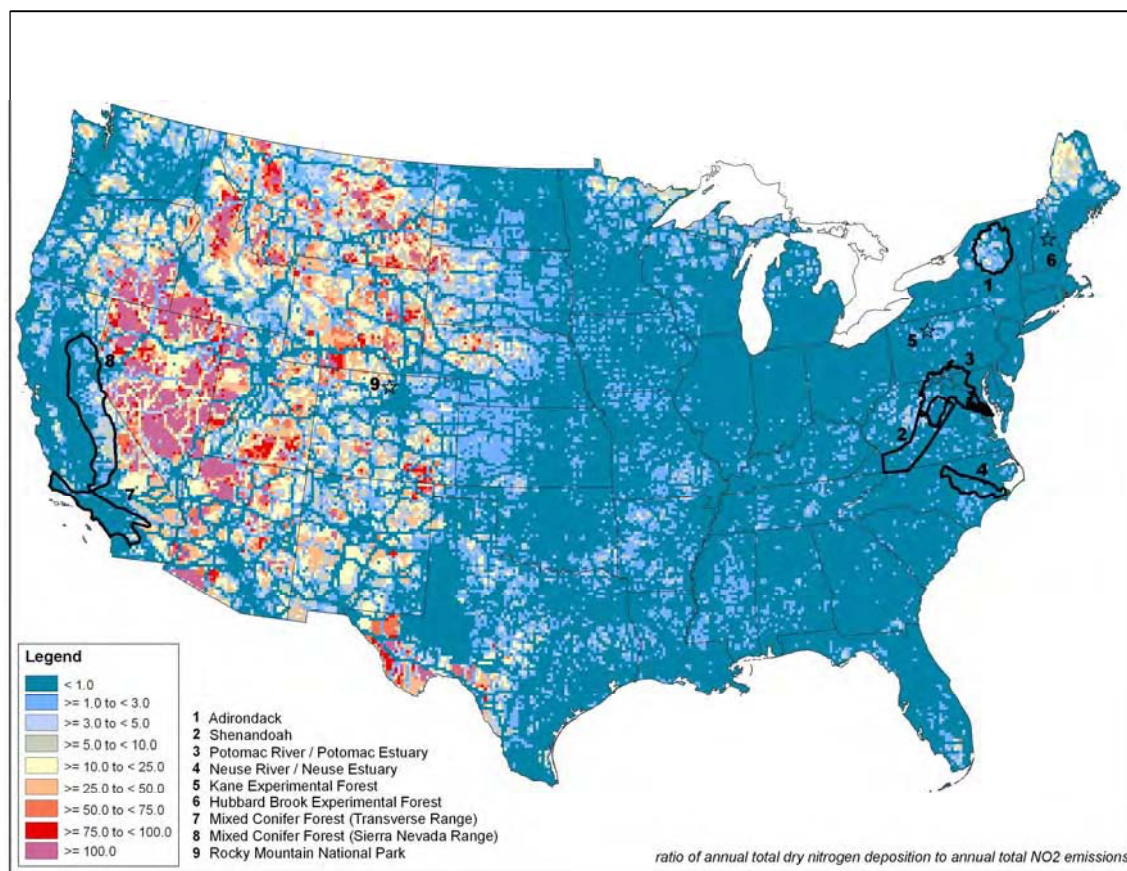


**Figure 2-16.** Ratio of annual total dry nitrogen deposition (kg N/ha/yr) to annual total nitrogen dioxide emissions (tons/yr).

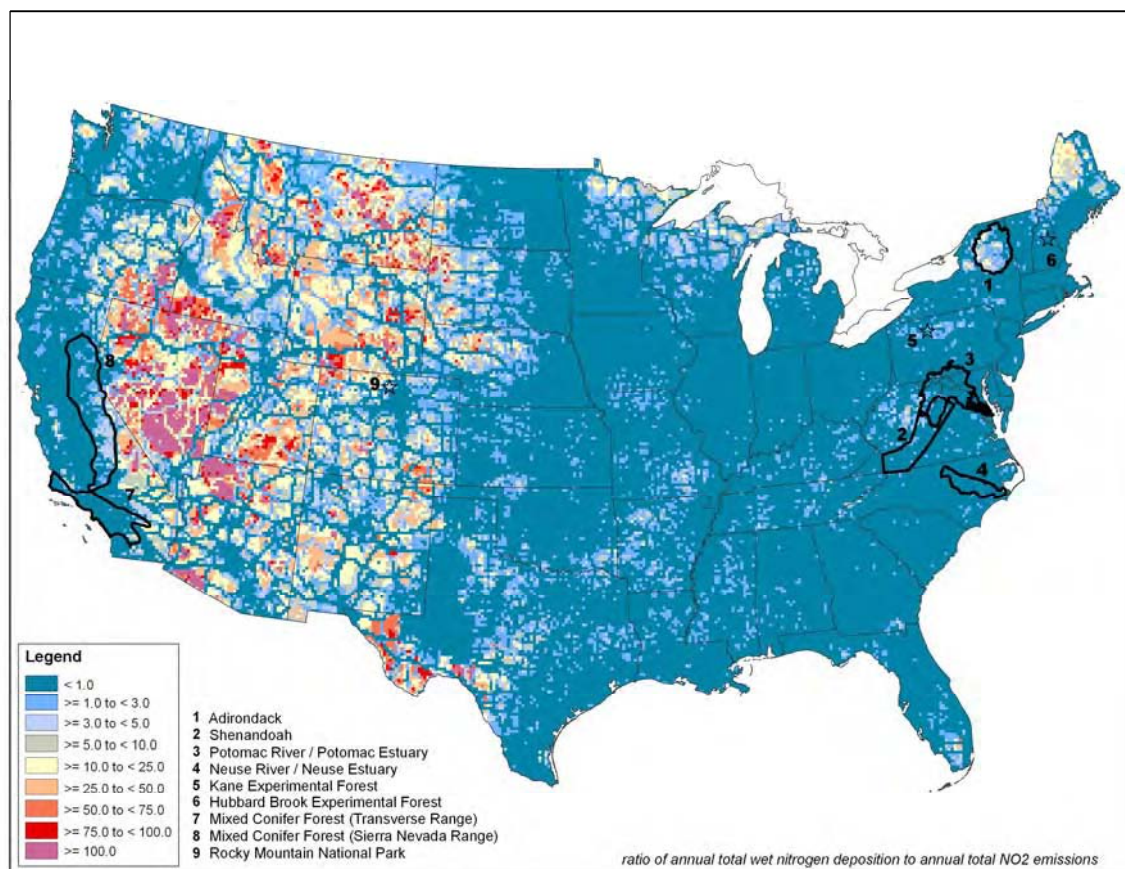


**Figure 2-17.** Ratio of annual total wet nitrogen deposition (kg N/ha/yr) to annual total nitrogen dioxide emissions (tons/yr).



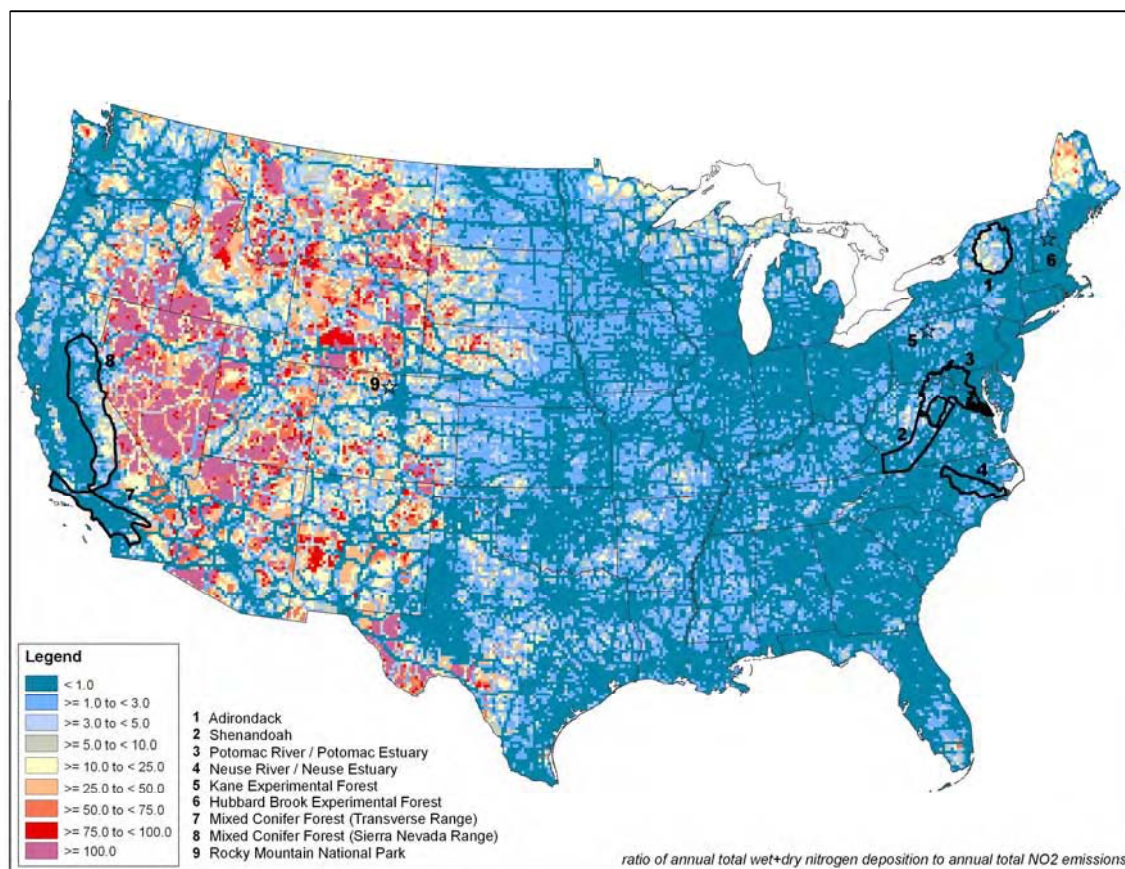


**Figure 2-18.** Ratio of annual total wet+dry nitrogen deposition (kg N/ha/yr) to annual total nitrogen dioxide emissions (tons/yr).





September, 2009

**Appendix 3**  
**Components of Reactive Nitrogen Deposition Based**  
**on Average Deposition Over the Period 2002–2005**  
Dry Deposition from CMAQ/Wet Deposition from NADP

*Final*

**Prepared by**

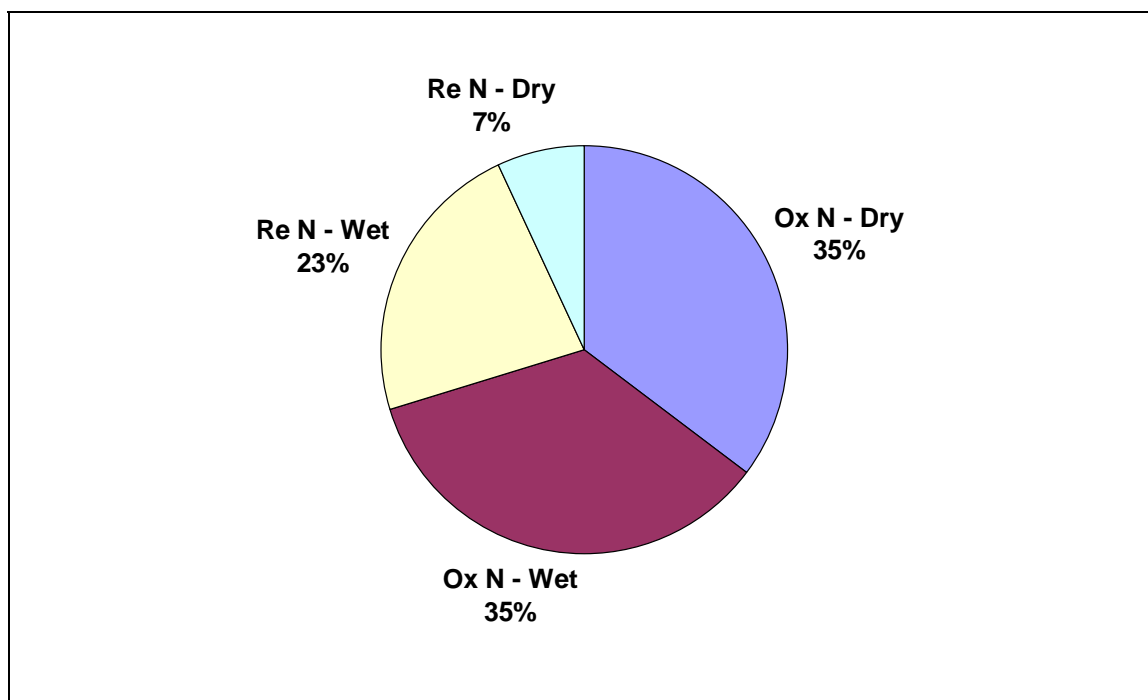
U.S. Environmental Protection Agency  
Office of Air Quality Planning and Standards  
Research Triangle Park, NC 27709



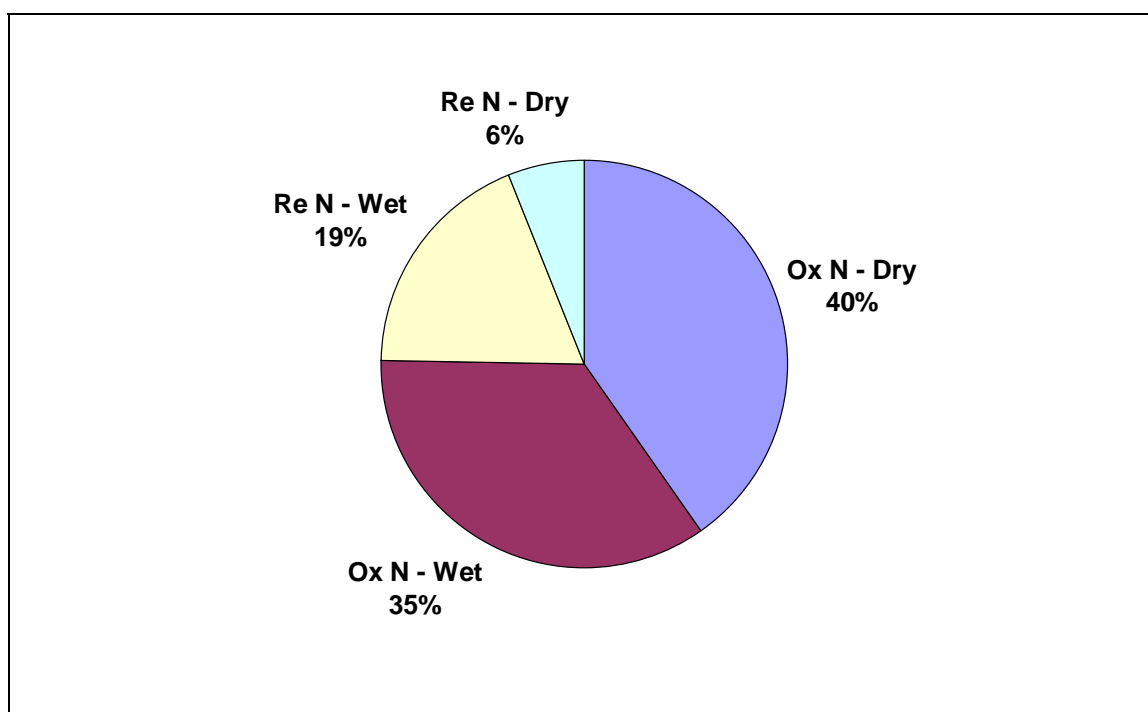
## **LIST OF FIGURES**

Figure 1. Adirondack Case Study Area: 2002–2005.....	1
Figure 2. Hubbard Brook Experimental Forest Case Study Area: 2002–2005. ....	1
Figure 3. Kane Experimental Forest Case Study Area: 2002–2005.....	2
Figure 4. Neuse River/Neuse River Estuary Case Study Area: 2002–2005.....	2
Figure 5. Potomac River/Potomac Estuary Case Study Area: 2002–2005.....	3
Figure 6. Shenandoah Case Study Area: 2002–2005. ....	3
Figure 7. Rocky Mountain National Park (Supplemental Area): 2002–2005. ....	4
Figure 8. Mixed Conifer Forest (Sierra Nevada Range) Case Study Area: 2002–2005.....	4
Figure 9. Mixed Conifer Forest (Transverse Range) Case Study Area: 2002–2005.....	5

*[This page intentionally left blank.]*



**Figure 1.** Adirondack Case Study Area: 2002–2005.



**Figure 2.** Hubbard Brook Experimental Forest Case Study Area: 2002–2005.

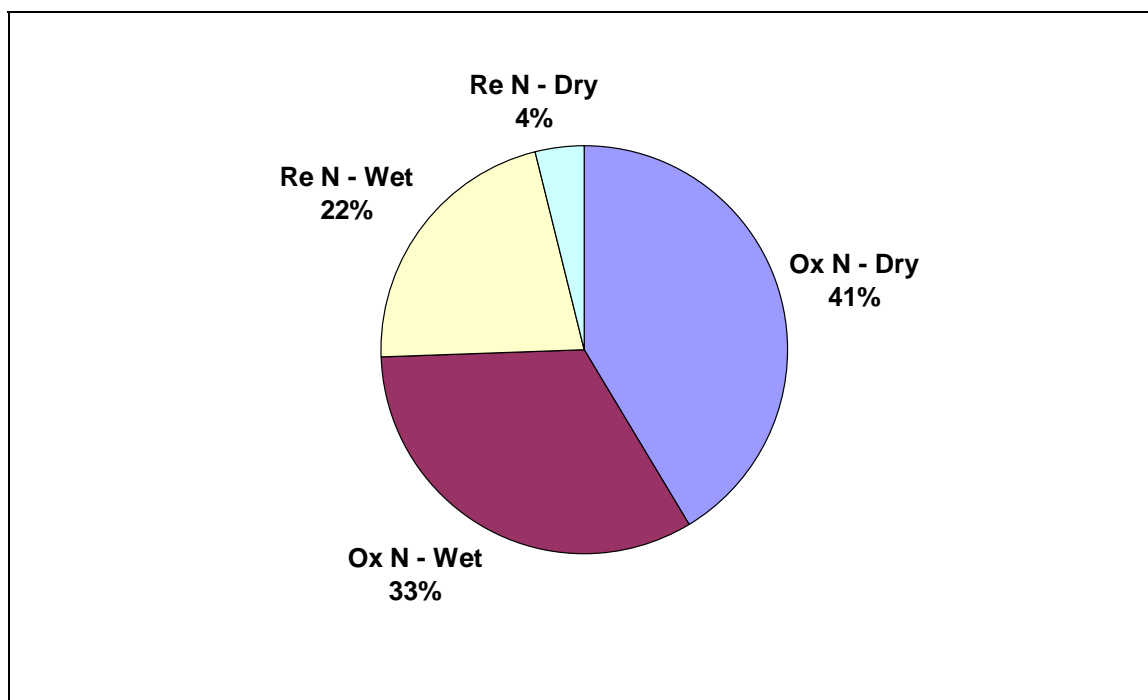


**Figure 3.** Kane Experimental Forest Case Study Area: 2002–2005.

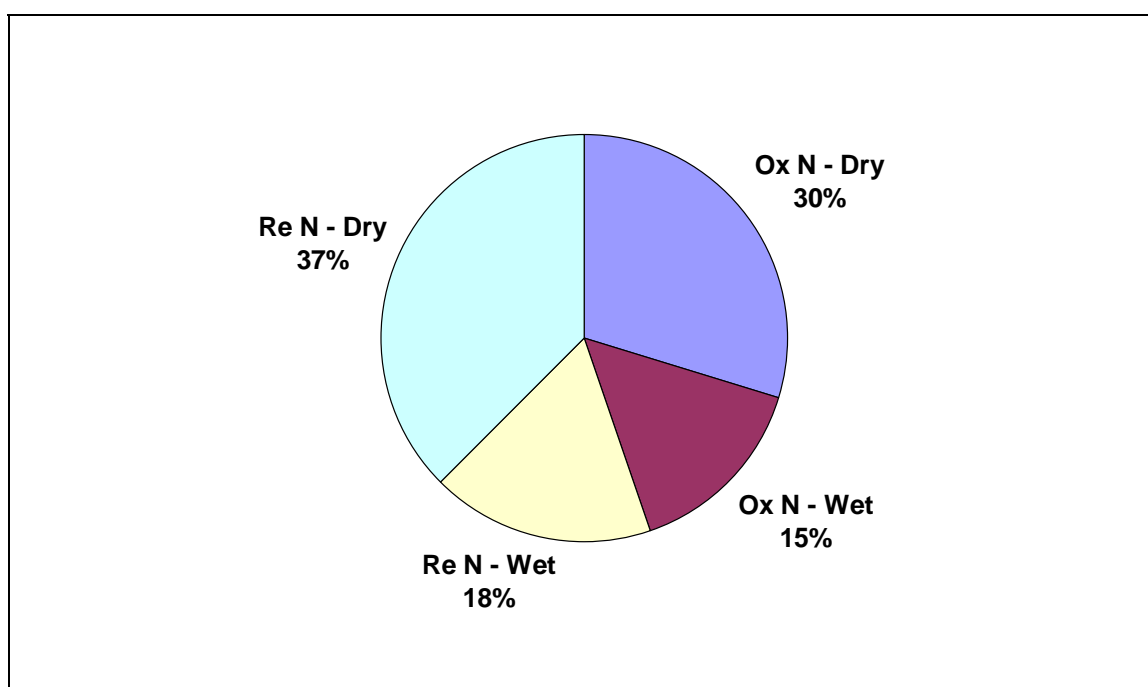


**Figure 4.** Neuse River/Neuse River Estuary Case Study Area: 2002–2005.

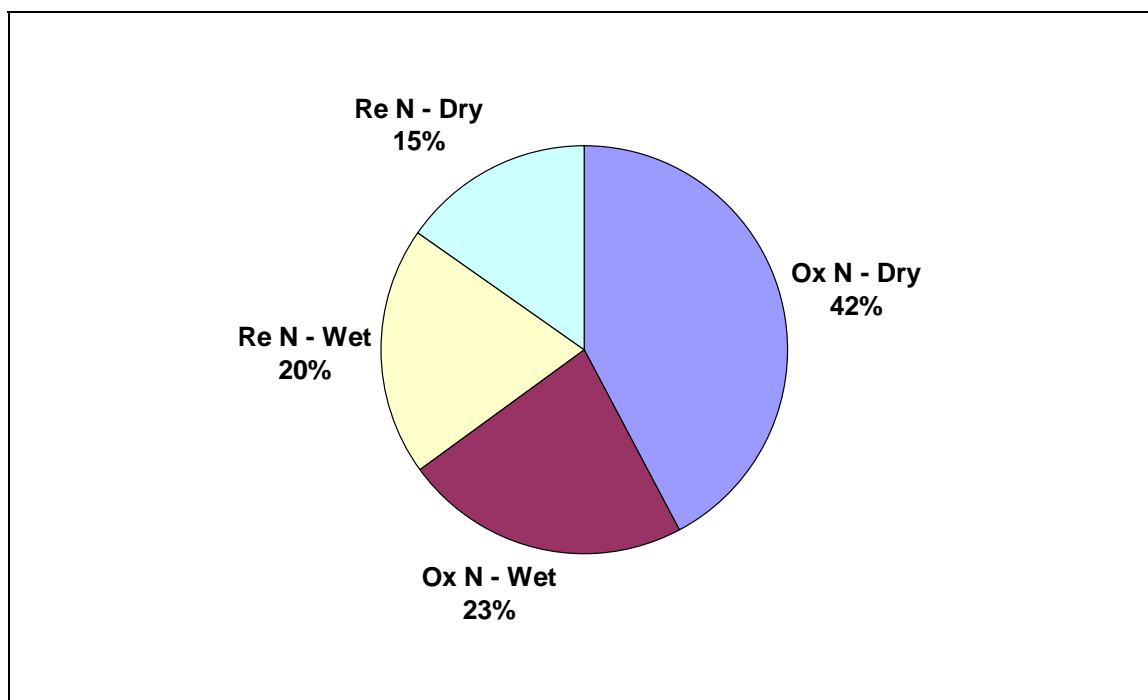


**Figure 5.** Potomac River/Potomac Estuary Case Study Area: 2002–2005.

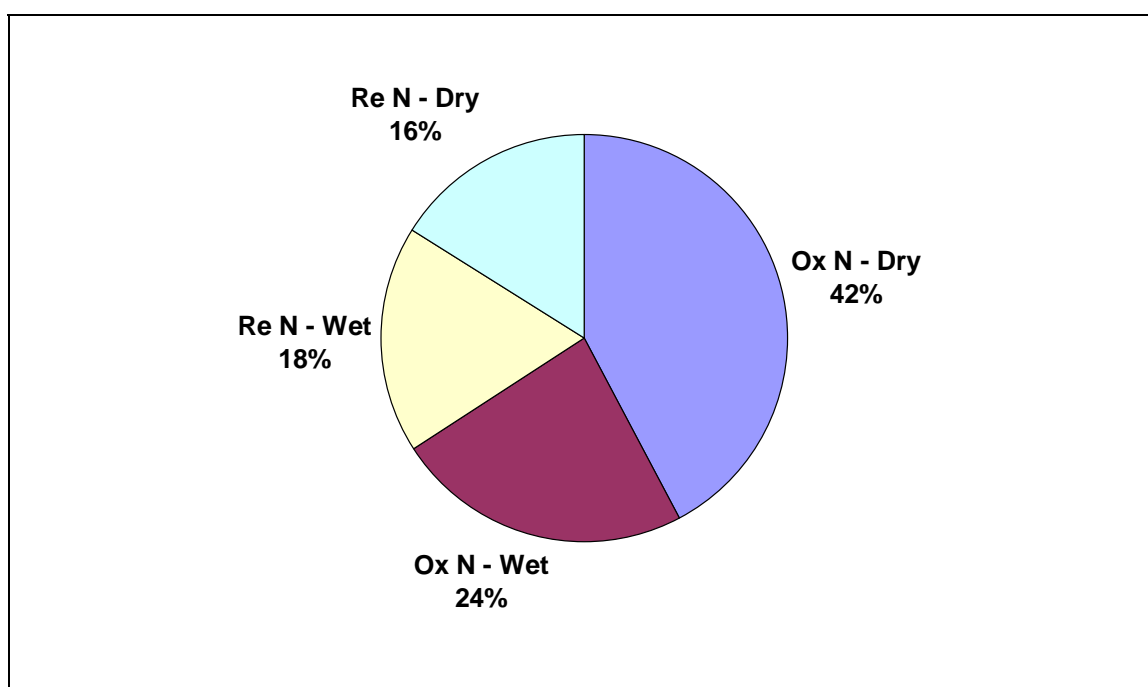


**Figure 6.** Shenandoah Case Study Area: 2002–2005.

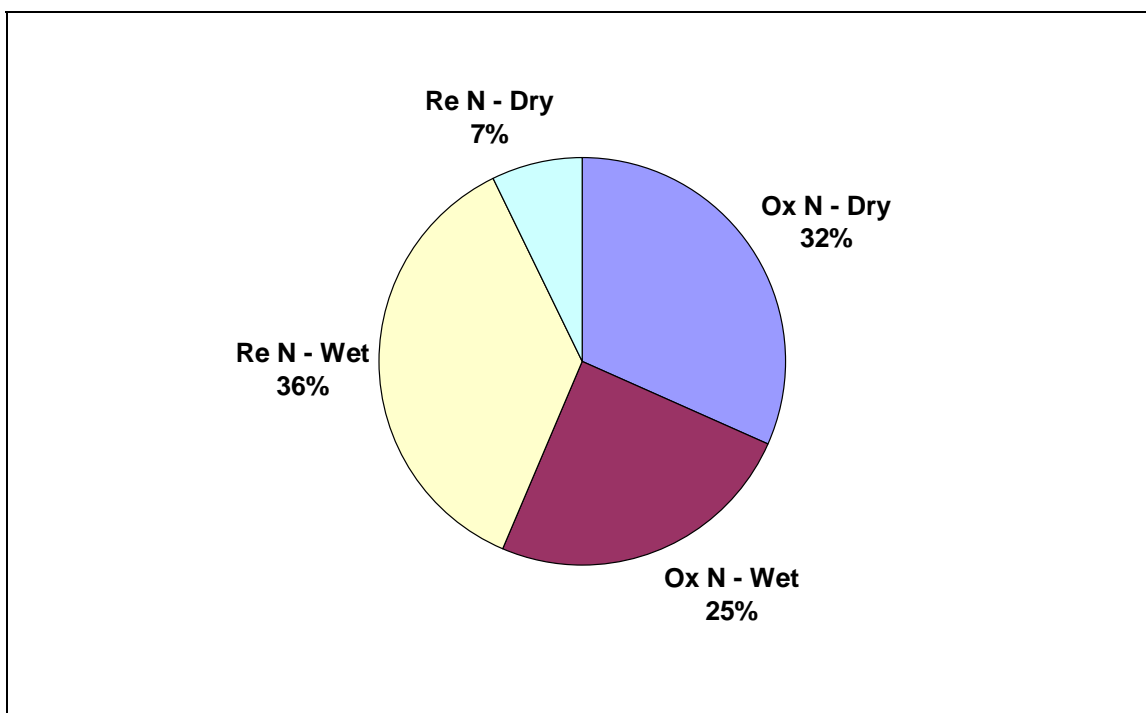


**Figure 7.** Rocky Mountain National Park (Supplemental Area): 2002–2005.

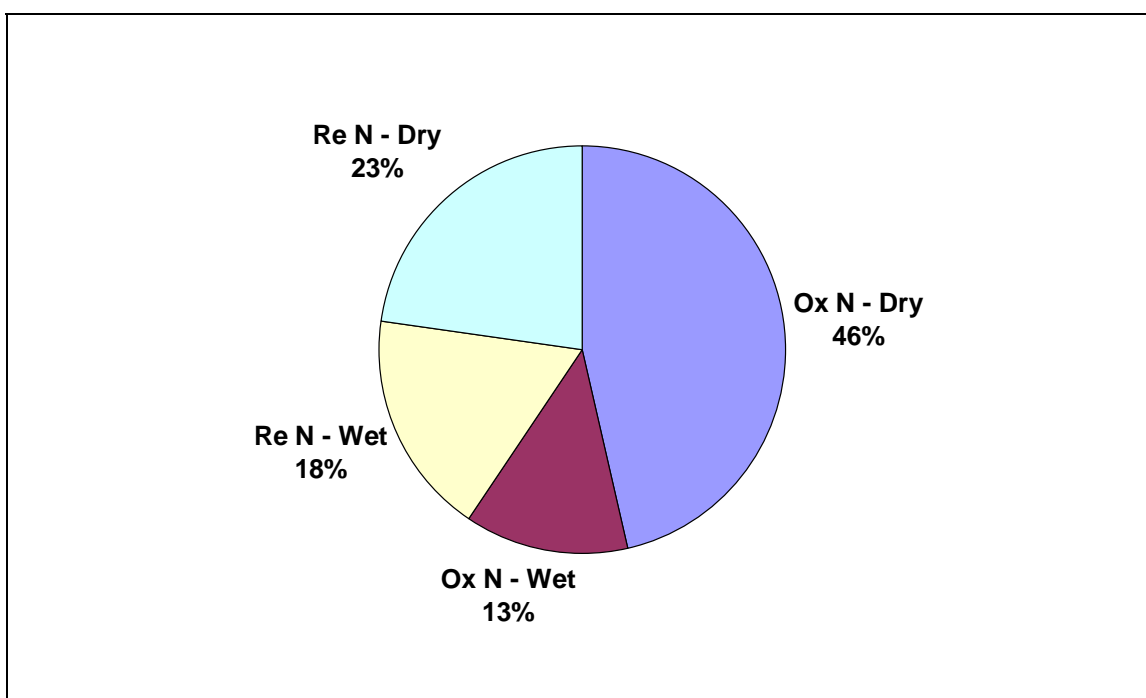


**Figure 8.** Mixed Conifer Forest (Sierra Nevada Range) Case Study Area: 2002–2005.



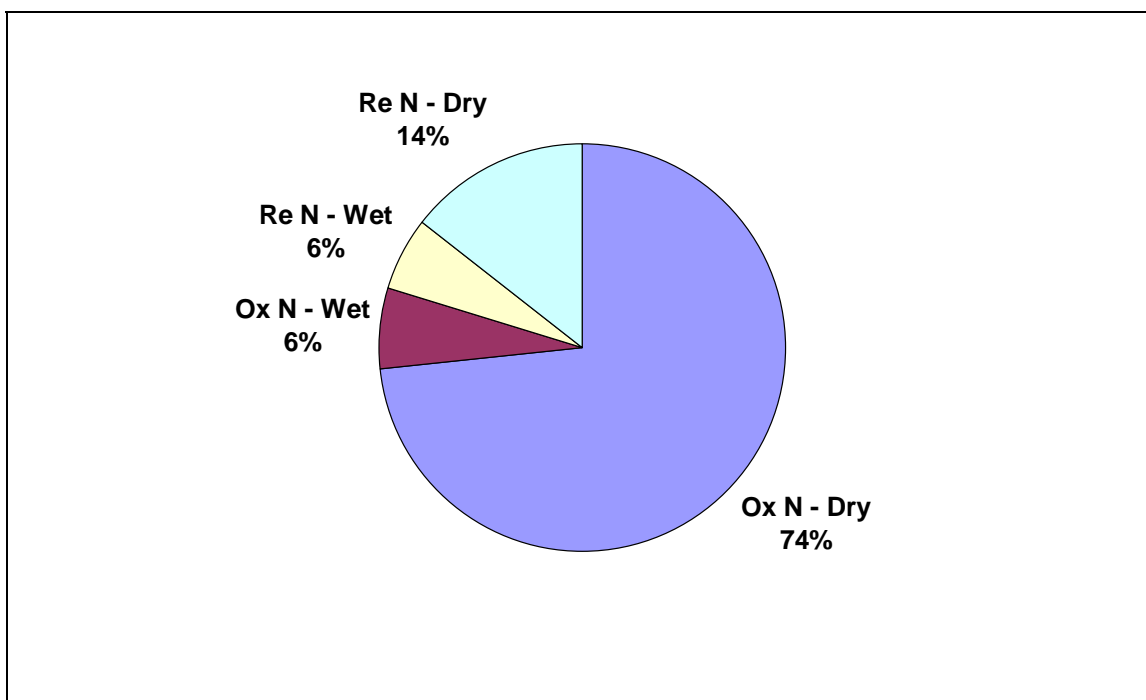


**Figure 9.** Mixed Conifer Forest (Transverse Range) Case Study Area: 2002–2005.



September 2009

# **Appendix 4**

## **Aquatic Acidification Case Study**

*Final*

**Prepared by**

U.S. Environmental Protection Agency  
Office of Atmospheric Programs  
Washington, DC



## TABLE OF CONTENTS

Acronyms and Abbreviations .....	vii
1.0 Purpose.....	1
2.0 Background.....	1
2.1 Acidification .....	1
2.2 Indicators of Acidification .....	2
2.3 Biological Response to Acidification and Acid Neutralizing Capacity.....	4
3.0 Case Studies .....	6
3.1 Surface Waters Acidification in the Eastern United States .....	6
3.2 Objectives .....	8
3.3 Adirondack Case Study Area.....	9
3.3.1 General Description .....	9
3.3.2 Levels of Air Pollution and Acidifying Deposition.....	10
3.3.3 Levels of Sulfate, Nitrate, and ANC Concentrations in Surface Water.....	10
3.4 Shenandoah Case Study Area.....	14
3.4.1 General Description .....	14
3.4.2 Levels of Air Pollution and Acidifying Deposition.....	15
3.4.3 Levels of Sulfate, Nitrate, and ANC Concentrations in Surface Water.....	15
4.0 Methods.....	19
4.1 Biological Response to Acidification .....	19
4.2 Past, Present, and Future Surface Water Chemistry—the MAGIC Modeling Approach.....	23
4.3 Connecting Current Nitrogen and Sulfur Deposition to Acid-Base Conditions of Lakes and Streams: The Critical Load Approach.....	24
4.3.1 Regional Assessment of Adirondack Case Study Area Lakes and Shenandoah Case Study Area Trout Streams .....	27
4.3.1.1 Adirondack Case Study Area.....	27
4.3.1.2 Shenandoah Case Study Area .....	27
5.0 Results.....	29
5.1 Adirondack Case Study Area.....	29
5.1.1 Current and Preacidification Conditions of Surface Waters.....	29
5.1.2 ANC Inferred Condition—Aquatic Status Categories.....	31
5.1.3 The Biological Risk from Current Nitrogen and Sulfur Deposition: Critical Load Assessment .....	33
5.1.4 Representative Sample of Lakes in the Adirondack Case Study Area .....	37
5.1.5 Recovery from Acidification Given Current Emission Reductions .....	38
5.2 Shenandoah Case Study Area.....	39
5.2.1 Current and Preacidification Conditions of Surface Waters.....	39
5.2.2 ANC Inferred Condition—Aquatic Status Categories.....	41
5.2.3 The Biological Risk from Current Nitrogen and Sulfur Deposition: Critical Load Assessment .....	43
5.2.4 Regional Assessment of Trout Streams in the Shenandoah Case Study Area.....	45

5.2.5	Recovery from Acidification Given Current Emission Reductions .....	45
6.	References.....	47
ATTACHMENT A .....		1
1.	Modeling Descriptions.....	1
1.1	MAGIC .....	1
1.1.1	Input Data and Calibration.....	2
1.1.2	Lake, Stream, and Soil Data for Calibration.....	2
1.1.3	Wet Deposition and Meteorology Data for Calibration.....	3
1.1.4	Wet Deposition Data (Reference Year and Calibration Values) .....	5
1.1.5	Dry, Cloud, and Fog Deposition Data and Historical Deposition Sequences .....	6
1.1.6	Protocol for MAGIC Calibration and Simulation at Individual Sites.....	7
1.1.7	Combined Model Calibration and Simulation Uncertainty .....	9
1.1.8	Results of the Uncertainty Analysis.....	10
1.2	Critical Loads: Steady-State Water Chemistry Models .....	15
1.2.1	Preindustrial Base Cation Concentration .....	18
1.2.2	F-factor.....	19
1.2.3	ANC Limits.....	20
1.2.4	Sea Salt Corrections.....	20
1.2.5	Critical load exceedance .....	21
1.2.6	Lake-to-Catchment-Area Ratios .....	23
1.2.7	Denitrification and N Immobilization in Soils.....	23
1.2.8	Uncertainty and Variability.....	23
1.2.8.1	Results of the uncertainty analysis.....	26
ATTACHMENT B .....		1
1.	EMAP/TIME/LTM Programs.....	1
2.	Temporally Integrated Monitoring of Ecosystems and Long-Term Monitoring Programs .....	2
2.1	TIME Program .....	2
2.2	LTM Program .....	3

### LIST OF FIGURES

Figure 2.3-1. (a) Number of fish species per lake or stream versus acidity, expressed as ANC for Adirondack Case Study Area lakes (Sullivan et al., 2006). (b) Number of fish species among 13 streams as a function of ANC in the Shenandoah Case Study Area. Values of ANC are means based on quarterly measurements from 1987 to 1994. The regression analysis shows a highly significant relationship ( $p < .0001$ ) between mean stream ANC and the number of fish species.....	6
Figure 3.1-1. Regions containing ecosystems sensitive to acidifying deposition in the eastern United States (U.S. EPA, based on NAPAP, 2005). .....	7

Figure 3.3-1. Annual average total wet deposition (kg/ha/yr) for the period 1990 to 2006 in $\text{SO}_4^{2-}$ (blue) and $\text{NO}_3^-$ (green) from eight NADP/NTN sites in the Adirondack Case Study Area (shown with linear trend regression lines). .....	10
Figure 3.3-2. Trends over time for annual average $\text{SO}_4^{2-}$ (blue) and $\text{NO}_3^-$ (green) concentrations and ANC (red) in 50 Adirondacks Long-Term Monitoring monitored lakes in the Adirondack Case Study Area (shown with linear trend regression lines). Both $\text{SO}_4^{2-}$ and $\text{NO}_3^-$ concentrations have decreased in surface waters by approximately 26% and 13%, respectively.....	11
Figure 3.3-3. Current yearly average for 2005 to 2006 (a) $\text{SO}_4^{2-}$ concentrations ( $\mu\text{eq/L}$ ), (b) $\text{NO}_3^-$ concentrations ( $\mu\text{eq/L}$ ), and (c) ANC ( $\mu\text{eq/L}$ ) in surface waters from 88 monitored lakes in the Temporally Integrated Monitoring of Ecosystems (38 Lakes) and Adirondacks Long-Term Monitoring (50 Lakes) networks in the Adirondack Case Study Area. ....	13
Figure 3.4-1. Air pollution concentrations and wet deposition for the period 1990 to 2006 using a CastNET (SHN418) and seven NADP/NTN sites in the Shenandoah Case Study Area. (a) Annual average atmospheric concentrations ( $\text{ug/m}^3$ ) of $\text{SO}_2$ (blue), oxidized nitrogen (red), $\text{SO}_4^{2-}$ (green), and reduced nitrogen (black). (b) Annual average total wet deposition (kg/ha/yr) of $\text{SO}_4^{2-}$ (green) and $\text{NO}_3^-$ (blue).....	15
Figure 3.4-2. Trends over time for annual average $\text{SO}_4^{2-}$ (blue) and $\text{NO}_3^-$ (green) concentrations, and ANC (red) in 67 streams in the Surface Water Acidification Study, Virginia Trout Stream Sensitivity Survey, and Long-Term Monitoring programs in the Shenandoah Case Study Area (shown with linear trend regression lines).....	16
Figure 3.4-3. Current yearly average for 2005 to 2006 (a) $\text{SO}_4^{2-}$ concentration, (b) $\text{NO}_3^-$ concentration, and (c) ANC ( $\mu\text{eq/L}$ ) in surface waters from 67 monitored streams in the Surface Water Acidification Study, Virginia Trout Stream Sensitivity, and Long-Term Monitoring network in the Shenandoah Case Study Area. ....	18
Figure 4.1-1. Relationship between summer and spring ANC values at LTM sites in New England, the Adirondack Mountains, and the Northern Appalachian Plateau. Values are mean summer values for each site for the period 1990 to 2000 (horizontal axis) and mean spring minima for each site for the same time period. On average, spring ANC values are at least 30 $\mu\text{eq/L}$ lower than summer values. ....	22
Figure 4.1-2. Number of fish species per lake or stream versus ANC level and aquatic status category (represented by color) for lakes in the Adirondack Case Study Area (Sullivan et al., 2006). The five aquatic status categories are described in Table 4.1-1.....	22
Figure 4.3-1. (a) The location of lakes in the Adirondack Case Study Area used for MAGIC (red circles) and critical load (green circles) modeling. (b) The location of streams in the Shenandoah Case Study Area used for both MAGIC and critical load modeling. ....	25
Figure 5.1-1. Average $\text{NO}_3^-$ concentrations (orange), $\text{SO}_4^{2-}$ concentrations (red), and ANC (blue) for the 44 lakes in the Adirondack Case Study Area modeled using MAGIC for the period 1850 to 2050. ....	29

Figure 5.1-2. (a) NO <sub>3</sub> <sup>-</sup> and (b) SO <sub>4</sub> <sup>2-</sup> concentrations (µeq/L) of preacidification (1860) and current (2006) conditions based on hindcasts of 44 lakes in the Adirondack Case Study Area modeled using MAGIC. ....	31
Figure 5.1-3. Percentage of lakes in the five classes (Acute, Severe, Elevated, Moderate, Low) for years 1860 (preacidification) and 2006 (current) conditions for 44 lakes modeled using MAGIC. Error bars indicate the 95% confidence interval. ....	32
Figure 5.1-4. ANC concentrations of preacidification (1860) and current (2006) conditions based on hindcasts of 44 lakes in the Adirondack Case Study Area modeled using MAGIC. ....	33
Figure 5.1-5. Critical loads of acidifying deposition that each surface water location can receive in the Adirondack Case Study Area while maintaining or exceeding an ANC concentration of 50 µeq/L based on 2002 data. Watersheds with critical load values <100 meq/m <sup>2</sup> /yr (red and orange circles) are most sensitive to surface water acidification, whereas watersheds with values >100 meq/m <sup>2</sup> /yr (yellow and green circles) are the least sensitive sites. ....	34
Figure 5.1-6. Critical load exceedances (red circles) in the Adirondack Case Study Area based on the year 2002 deposition magnitudes for waterbodies where the critical limit ANC concentration is 0, 20, 50, and 100 µeq/L, respectively. Green circles represent lakes where deposition is below the critical load. See Table 5.1-3. ....	36
Figure 5.1-7. Percentage of lakes in each of the five classes of acidification (Acute, Severe, Elevated, Moderate, Low) for the years 2006, 2020, and 2050 for 44 lakes modeled using MAGIC, where current emissions are held constant. Error bars indicate the 95% confidence interval. ....	38
Figure 5.2-1. Average NO <sub>3</sub> <sup>-</sup> concentrations (orange), SO <sub>4</sub> <sup>2-</sup> concentrations (red), and ANC (blue) levels for the 60 streams in the Shenandoah Case Study Area modeled using MAGIC for the period 1850 to 2050. ....	39
Figure 5.2-2. (a) NO <sub>3</sub> <sup>-</sup> and (b) SO <sub>4</sub> <sup>2-</sup> concentrations (µeq/L) of 1860 (preacidification) and 2006 (current) conditions based on hindcasts of 60 streams in the Shenandoah Case Study Area modeled using MAGIC. ....	40
Figure 5.2-3. Percentage of streams in the five classes of acidification (Acute, Severe, Elevated, Moderate, Low) for years 1860 (preacidification) and 2006 (current) conditions for 60 streams modeled using MAGIC. The number of streams in each category is above the bar. Error bars indicate the 95% confidence interval. ....	42
Figure 5.2-4. ANC levels of 1860 (preacidification) and 2006 (current) conditions based on hindcasts of 60 streams in the Shenandoah Case Study Area modeled using MAGIC. ....	42
Figure 5.2-5. Critical loads of surface water acidity for an ANC of 50 µeq/L for Shenandoah Case Study Area streams. Each dot represents an estimated amount of acidifying deposition (i.e., critical load) that each stream's watershed can receive and still maintain a surface water ANC >50 µeq/L. Watersheds with critical load values <100 meq/m <sup>2</sup> /yr (red and orange circles) are most sensitive to surface water acidification, whereas	



watersheds with values $>100 \text{ meq/m}^2/\text{yr}$ (yellow and green circles) are the least sensitive sites. ....	43
Figure 5.2-6. Critical load exceedances for ANC levels of 0, 20, 50, and $100 \text{ } \mu\text{eq/L}$ for Shenandoah Case Study Area streams. Green circles represent streams where current nitrogen and sulfur deposition is below the critical load and that maintain an ANC level of 0, 20, 50, and $100 \text{ } \mu\text{eq/L}$ , respectively. Red circles represent streams where current nitrogen and sulfur deposition exceeds the critical load, indicating they are currently impacted by acidifying deposition. See Table 5.2-3. ....	44
Figure 5.2-7. Percentage of streams in the five categories of acidification (Acute, Severe, Elevated, Moderate, Low) for the years 2006, 2020, and 2050 for 60 streams in the Shenandoah Case Study Area modeled using MAGIC. The number of streams in each category is above the bar. Error bars indicate the 95% confidence interval. ....	46
Figure 1.1-1. Simulated versus observed annual average surface water $\text{SO}_4^{2-}$ , $\text{NO}_3^-$ , ANC, and pH during the model calibration period for each of the 44 lakes in the Adirondacks Case Study Area. The black line is the 1:1 line. ....	12
Figure 1.1-2. Simulated versus observed annual average surface water $\text{SO}_4^{2-}$ , $\text{NO}_3^-$ , ANC, and pH during the model calibration period for each of the 60 streams in the Shenandoah Case Study Area. The black line is the 1:1 line. ....	13
Figure 1.1-3. MAGIC simulated and observed values of ANC for two lakes in the Shenandoah Case Study Area. Red points are observed data and the simulated values are the line. The Root Mean Squared Error (RMSE) for ANC was $11.8 \text{ } \mu\text{eq/L}$ for Helton Creek and $4.0 \text{ } \mu\text{eq/L}$ for Nobusiness Creek. ....	14
Figure 1.1-4. MAGIC simulated and observed values of ANC for two lakes in the Shenandoah Case Study Area. Red points are observed data and the simulated values are the line. The Root Mean Squared Error (RMSE) for ANC was $11.8 \text{ } \mu\text{eq/L}$ for Helton Creek and $4.0 \text{ } \mu\text{eq/L}$ for Nobusiness Creek. ....	15
Figure 1.2-1. The depositional load function defined by the model. ....	22
Figure 1.2-2. The inverse cumulative frequency distribution for Little Hope Pond. The x-axis shows critical load exceedance in $\text{meq/ha/yr}$ and y-axis is the probability. The dashed lines represent zero exceedance. In the case of Little Hope Pond, the dash line divides mostly the probability distribution on the left hand side, indicating Little Hope Pond has a relative low probability of being exceeded (0.3). Critical load and exceedances values were based on a critical level of protection of $\text{ANC} = 50 \text{ } \mu\text{eq/L}$ . ....	25
Figure 1.2-3. Coefficients of variation of surface water critical load for acidity $\text{CL(A)}$ and exceedances ( $\text{EX(A)}$ ). Critical load and exceedances values were based on a critical level of protection of $\text{ANC} = 50 \text{ } \mu\text{eq/L}$ . ....	27
Figure 1.2-4. Probability of exceedance of critical load for acidity for 2002. ....	28

## LIST OF TABLES

Table 4.1-1. Aquatic Status Categories. ....	20
--	----

Table 5.1-1. Estimated Average Concentrations of Surface Water Chemistry for 44 Lakes in the Adirondack Case Study Area Modeled Using MAGIC for Preacidification (1860) and Current (2006) Conditions .....	30
Table 5.1-2. Percentage of Lakes in the Five Aquatic Status Categories Based on Their Surface Water ANC Levels for 44 Lakes Modeled Using MAGIC and 88 Lakes in the TIME/LTM Monitoring Network. Results Are for the Adirondack Case Study Area for the Years 2005 to 2006.....	32
Table 5.1-3. Adirondack Case Study Area Critical Load Exceedances, Where Nitrogen and Sulfur Deposition Is Larger Than the Critical Load for Four Different ANC Critical Limit Thresholds, for 169 Modeled Lakes within the TIME/LTM and EMAP Monitoring and Survey Programs. “No. Exceedances” Indicates the Number of Lakes at or below the Given ANC Critical Limit, and “% Lakes” Indicates the Total Percentage of Lakes at or below the Given ANC Critical Limit. ....	35
Table 5.1-4. Critical Load Exceedances for the Regional Population of 1,842 Lakes in the Adirondack Case Study Area That Are from 0.5 to 2,000 ha in Size and at Least 1 m in Depth for the Four Critical Limit ANC Levels (0, 20, 50, and 100 µeq/L). Estimates Use the Exceedances for the Subset of 169 Lakes Using 2002 Deposition Magnitudes (Table 5.1-3) and Are Extrapolated to the Full Population Based on the EMAP Lake Probability Survey of 1991 to 1994. “No. Exceedances” Indicates the Number of Lakes at or Below the Given ANC Critical Limit; “% Lakes” Indicates the Total Percentage of Lakes at or Below the Given ANC Critical Limit. ....	37
Table 5.2-1. Estimated Average Concentrations of Surface Water Chemistry for 60 Streams in the Shenandoah Case Study Area Modeled Using MAGIC for Preacidification (1860) and Current (2006) Conditions .....	41
Table 5.2-2. Percentage of Streams in the Five Aquatic Status Categories Based on Their Surface Water ANC Concentrations for 60 Streams Modeled Using MAGIC and 67 Streams in the SWAS-VTSSS LTM Network. Results are for the Shenandoah Case Study Area for the Year 2006. ....	41
Table 5.2-3. Critical Load Exceedances (Nitrogen + Sulfur Deposition > Critical Load) for 60 Modeled Streams within the VTSSS LTM Program in the Shenandoah Case Study Area. “No. Exceedances” Indicates the Number of Streams at the Given ANC Limit; “% Streams” Indicates the Total Percentage of Streams at the Given ANC Limit. ....	45
Table 1.2-1. Parameters Used and their Uncertainty Range. The Range of Surface Water Parameters (e.g., CA, MG, CL, NA, NO <sub>3</sub> , SO <sub>4</sub> ) were Determined from Surface Water Chemistry Data for the Period from 1992 to 2006 from the LTM-TIME Monitoring Network. Runoff(Q) and Acidic Deposition were Set at 50% and 25% .....	24
Table 1.2-2. Means and Coefficients of Variation of Critical Loads and Exceedances for Surface Water.....	26

## ACRONYMS AND ABBREVIATIONS

$\text{Al}^{3+}$	aluminum
$\text{Al}(\text{OH})_3$	aluminum hydroxide
ALTM	Adirondack Long-Term Monitoring
ANC	acid neutralizing capacity
ASTRAP	Advanced Statistical Trajectory Regional Air Pollution
$\text{Ca}^{2+}$	calcium
$\text{Cl}^-$	chloride
CL(A)	critical loads of acidity
$\text{CO}_2$	carbon dioxide
DDF	dry and occult deposition factor
EMAP	Environmental Monitoring and Assessment Program
eq/ha/yr	equivalents per hectare per year
$\text{F}^-$	fluoride
FAB	First-Order Acidity Balance
$\text{H}^+$	hydrogen ion
$\text{H}_4\text{SiO}_4$	silicic acid
ha	hectare
ISA	Integrated Science Assessment
$\text{K}^+$	potassium
kg/ha/yr	kilograms/hectare/year
km	kilometer
LTM	Long-Term Monitoring
m	meter
m/yr	meters/year
MAGIC	Model of Acidification of Groundwater in Catchments
MAHA	Mid-Atlantic Highlands Assessment
$\text{meq/m}^2\text{yr}$	milliequivalents per square meter per year
$\text{Mg}^{2+}$	magnesium
$\text{Na}^+$	sodium
NADP	National Atmospheric Deposition Program
$\text{NH}_4^+$	ammonium
$\text{NO}_3^-$	nitrate
$\text{NO}_x$	nitrogen oxides
NSWS	National Lake/Stream Surveys
NTN	National Trends Network
$\text{O}_3$	ozone
PnET-BGC	biogeochemical model
Si	silicon
$\text{SO}_2$	sulfur dioxide
$\text{SO}_4^{2-}$	sulfate
$\text{SO}_x$	sulfur oxides
SWAS	Shenandoah Nation Park Surface Water Acidification Study

SSWC	Steady-State Water Chemistry
TIME	Temporally Integrated Monitoring of Ecosystems
µeq/L	microequivalents per liter
µM	micrometer
VTSSS	Virginia Trout Stream Sensitivity Survey

## **1.0 PURPOSE**

This case study is intended to estimate the ecological exposure and risk to aquatic ecosystems from acidification associated with the deposition of nitrogen and sulfur for two sensitive regions of eastern United States: the Adirondack Mountains in New York (hereafter referred to as the Adirondack Case Study Area) and Shenandoah National Park and the surrounding areas of Virginia (hereafter referred to as the Shenandoah Case Study Area).

## **2.0 BACKGROUND**

### **2.1 ACIDIFICATION**

Sulfur oxides ( $\text{SO}_x$ ) and nitrogen oxides ( $\text{NO}_x$ ) compounds in the atmosphere undergo a complex mix of reactions and thermodynamic processes in gaseous, liquid, and solid phases to form various acidic compounds. These acidic compounds are removed from the atmosphere through deposition: either wet (e.g., rain, snow), fog or cloud, or dry (e.g., gases, particles). Deposition of these acidic compounds leads to ecosystem exposure and effects on ecosystem structure and function. Following deposition, these compounds can, in some instances, leach out of the soils in the form of sulfate ( $\text{SO}_4^{2-}$ ) and nitrate ( $\text{NO}_3^-$ ), leading to the acidification of surface waters. The effects on ecosystems depend on the magnitude of deposition, as well as a host of biogeochemical processes occurring in the soils and waterbodies.

When sulfur or nitrogen leaches from soils to surface waters in the form of  $\text{SO}_4^{2-}$  or  $\text{NO}_3^-$ , an equivalent amount of positive cations, or countercharge, is also transported. This maintains electroneutrality. If the countercharge is provided by base cations, such as calcium ( $\text{Ca}^{2+}$ ), magnesium ( $\text{Mg}^{2+}$ ), sodium ( $\text{Na}^+$ ), or potassium ( $\text{K}^+$ ), rather than hydrogen ( $\text{H}^+$ ) and dissolved inorganic aluminum, the acidity of the soil water is neutralized, but the base saturation of the soil is reduced. Continued  $\text{SO}_4^{2-}$  or  $\text{NO}_3^-$  leaching can deplete the base cation supply of the soil. As the base cations are removed, continued deposition and leaching of  $\text{SO}_4^{2-}$  and/or  $\text{NO}_3^-$  (with  $\text{H}^+$  and  $\text{Al}^{3+}$ ) leads to acidification of soil water, and by connection, surface water. Loss of soil base saturation is a cumulative effect that increases the sensitivity of the watershed to further acidifying deposition. Base cations are replenished through the natural weathering of the rocks and soils, but weathering is a slow process, which results in the depletion of cations in the soil in

the presence of  $\text{SO}_4^{2-}$  and/or  $\text{NO}_3^-$  pollution. A watershed's ability to neutralize acidic deposition is determined by a host of biogeophysical factors, including base cation concentrations, weathering rates, uptake by vegetation, rate of surface water flow, soil depth, and bedrock.

Following deposition,  $\text{SO}_4^{2-}$  can absorb to, or bind with, soil particles, a process that removes it from the aqueous soil solution, and therefore, prevents the leaching of base cations (at least temporarily) and further acidifying of the soil water. This process results in an accumulation of sulfur in the soil. This process is potentially reversible and can contribute to soil acidification if, and when, the  $\text{SO}_4^{2-}$  is desorbed and released back into the soil water solution. The degree to which  $\text{SO}_4^{2-}$  adsorbs on soil is dependent on soil characteristics. The locations of soils in the United States that most effectively adsorb  $\text{SO}_4^{2-}$  are found south of the areas that experienced glaciation during the most recent ice age (Rochelle and Church, 1987; Rochelle et al., 1987).  $\text{SO}_4^{2-}$  adsorption is strongly pH-dependent, and a decrease in soil pH resulting from acidifying deposition can enhance the ability of soil to adsorb  $\text{SO}_4^{2-}$ . Consequently, as deposition increases, the soil potentially stores a disproportionate amount of  $\text{SO}_4^{2-}$ . When deposition decreases, this stored  $\text{SO}_4^{2-}$  is slowly, but continually, released, keeping soil water acidified and/or depleting the base cation supply.

## **2.2 INDICATORS OF ACIDIFICATION**

The chemistry of the surface water is directly related to the biotic integrity of freshwater ecosystems. There are numerous chemical constituents in surface water that can be used to indicate the acidification condition of lakes and streams and to assess the effects of acidifying deposition on ecosystem components. These include surface water pH ( $\log[\text{H}^+]$ ) and concentrations of  $\text{SO}_4^{2-}$ ,  $\text{NO}_3^-$ ,  $\text{Al}^{3+}$ , and  $\text{Ca}^{2+}$ ; the sum of base cations; the recently developed base cation surplus; and the acid neutralizing capacity (ANC). Each of these chemical indicators provides direct links to the health of individual biota and the overall health and integrity of aquatic ecosystems as a result of surface water acidification.

Although ANC does not directly affect the health of biotic communities, it is calculated (or measured) based on the concentrations of chemical constituents that directly contribute to or ameliorate acidity-related stress, in particular, pH,  $\text{Ca}^{2+}$ , and dissolved inorganic aluminum. Furthermore, numerical models of surface water acidification can more accurately estimate ANC than all of the individual constituents that comprise it. Consequently, for the purpose of this case

study, annual average ANC of surface waters was used as the primary metric to quantify the current acidic conditions and biological impacts for a subset of waterbodies in the study areas. The remainder of this section focuses on a description of ANC.

ANC reflects the relative balance between base cations and strong acid anions. It accounts for the cumulative effects of all of the ionic interactions that occur as the acidic compounds are removed from the atmosphere to the catchment and drainage water to emerge in a stream or lake. ANC of surface waters is defined (in this study) as the total amount of strong base ions minus the total amount of strong acid anions:

$$\text{ANC} = (\text{Ca}^{2+} + \text{Mg}^{2+} + \text{K}^+ + \text{Na}^+ + \text{NH}_4^+) - (\text{SO}_4^{2-} + \text{NO}_3^- + \text{Cl}^-) \quad (1)$$

The unit of ANC is microequivalents per liter ( $\mu\text{eq/L}$ ). If the sum of the equivalent concentrations of the base cations exceeds those of the strong acid anions, then the ANC of a waterbody will be positive. To the extent that the base cation sum exceeds the strong acid anion sum, the ANC will be higher. Higher ANC is generally associated with high pH and  $\text{Ca}^{2+}$  concentrations, and lower ANC is generally associated with low pH and high dissolved inorganic aluminum concentrations and a greater likelihood of toxicity to biota.

ANC samples from waterbodies are typically measured using the Gran titration approach. Process-based numerical models, such as Model of Acidification of Groundwater in Catchments (MAGIC) utilize the ANC calculated from the charge balance. For assessment purposes, including resource characterization and Long-Term Monitoring (LTM) programs, it is always best to use both directly measured and numerically estimated ANC values. The difference between the two can be used to quantify uncertainty and reveal the influences of natural organic acidity and/or dissolved inorganic aluminum on the overall acid-base chemistry of the water.

Relative to some individual chemical parameters, such as pH, ANC reflects sensitivity to acidifying deposition input and effects on surface water chemistry in a linear fashion across the full range of ANC values. Consequently, ANC is a preferred indicator variable for surface water acidification. Other parameters, such as surface water pH, can complement the assessment of surface water acidification; however, the response of this parameter to inputs is not necessarily linear throughout its range. For example, at pH values  $>6.0$ , pH is not a good indicator of either sensitivity to acidification or level of biological effect. In addition, pH measurements (especially at these higher values) are sensitive to and can be confounded by the level of dissolved carbon dioxide ( $\text{CO}_2$ ) in the water.

## 2.3 BIOLOGICAL RESPONSE TO ACIDIFICATION AND ACID NEUTRALIZING CAPACITY

Ecological effects occur at four levels of biological organization: (1) the individual; (2) the population, which is composed of a single species of individuals; (3) the biological community, which is composed of many species; and (4) the ecosystem. Low ANC concentrations are linked with negative effects on aquatic systems at all four of these biological levels. For the individual level, impacts are assessed in terms of fitness (i.e., growth, development, and reproduction) or sublethal effects on condition. Surface water with low ANC concentrations can directly influence aquatic organism fitness or mortality by disrupting ion regulation and can mobilize dissolved inorganic aluminum, which is highly toxic to fish under acidic conditions (i.e., pH <6 and ANC <50 µeq/L). For example, research showed that as the pH of surface waters decreased to <6, many aquatic species, including fish, invertebrates, zooplankton, and diatoms, tended to decline sharply causing species richness to decline (Schindler, 1988). Van Sickle et al. (1996) also found that blacknose dace (*Rhinichthy* spp.) were highly sensitive to low pH and could not tolerate inorganic Al concentrations greater than about 3.7 micromolar (µM) for extended periods of time. For example, they found that after 6 days of exposure to high inorganic Al, blacknose dace mortality increased rapidly to nearly 100%.

At the community level, species richness and community structure can be used to evaluate the effects of acidification. Species composition refers to the mix of species that are represented in a particular ecosystem, whereas species richness refers to the total number of species in a stream or lake. Acidification alters species composition and richness in aquatic ecosystems. There are a number of species common to many oligotrophic waterbodies that are sensitive to acidification and cannot survive, compete, or reproduce in acidic waters. In response to small to moderate changes in acidity, acid-sensitive species are often replaced by other more acid-tolerant species, resulting in changes in community composition and richness, but with little or no change in total community biomass. The effects of acidification are continuous, with more species being affected at higher degrees of acidification. At a point, typically a pH <4.5 and an ANC <0 µeq/L, complete to near-complete loss of many classes of organisms occur, including fish and aquatic insect populations, whereas others are reduced to only a few acidophilic forms. These changes in species integrity are because energy cost in maintaining physiological



homeostasis, growth, and reproduction is high at low ANC levels (Schreck, 1981, 1982; Wedemeyer et al., 1990).

Decreases in species richness related to acidification have been observed in the Adirondack Mountains and Catskill Mountains of New York (Baker et al., 1993), the Upper Midwest of the United States (Schindler et al., 1989), New England and Pennsylvania (Haines and Baker, 1986), and Virginia (Bulger et al., 2000). Studies on fish species richness in the Adirondack Case Study Area demonstrated the effect of acidification; of the 53 fish species recorded in Adirondack Case Study Area lakes, only 27 species were found in lakes with a pH <6.0. The 26 species missing from lakes with a pH <6.0 include important recreational species, such as Atlantic salmon, tiger trout (*Salmo trutta* X *Salvelinus fontinalis*), redbreast sunfish (*Lepomis auritus*), bluegill (*Lepomis macrochirus*), tiger musky (*Esox masquinongy* X *lucius*), walleye (*Sander vitreus*), alewife (*Alosa pseudoharengus*), and kokanee (*Oncorhynchus nerka*) (Kretser et al., 1989), as well as ecologically important minnows that are commonly eaten by sport fish. A survey of 1,469 lakes in the late 1980s found 346 lakes to be devoid of fish. Among lakes with fish, there was a relationship between the number of fish species and lake pH, ranging from about one species per lake for lakes having a pH <4.5 to about six species per lake for lakes having a pH >6.5 (Driscoll et al., 2001; Kretser et al., 1989).

These decreases in species richness due to acidifying deposition are positively correlated with ANC concentrations (Kretser et al., 1989; Rago and Wiener, 1986). Most notably, Sullivan et al. (2006) found a logistic relationship between fish species richness and ANC category for Adirondack Case Study Area lakes (**Figure 2.3-1, a**), which indicates the probability of occurrence of an organism for a given value of ANC. In addition, a similar relationship has been found for the Shenandoah Case Study Area, where a statistically robust relationship between ANC and fish species richness was documented (**Figure 2.3-1, b**). In fact, ANC has been found in studies to be the best single indicator of the biological response and health of aquatic communities in acid-sensitive systems (Lien et al., 1992; Sullivan et al., 2006).

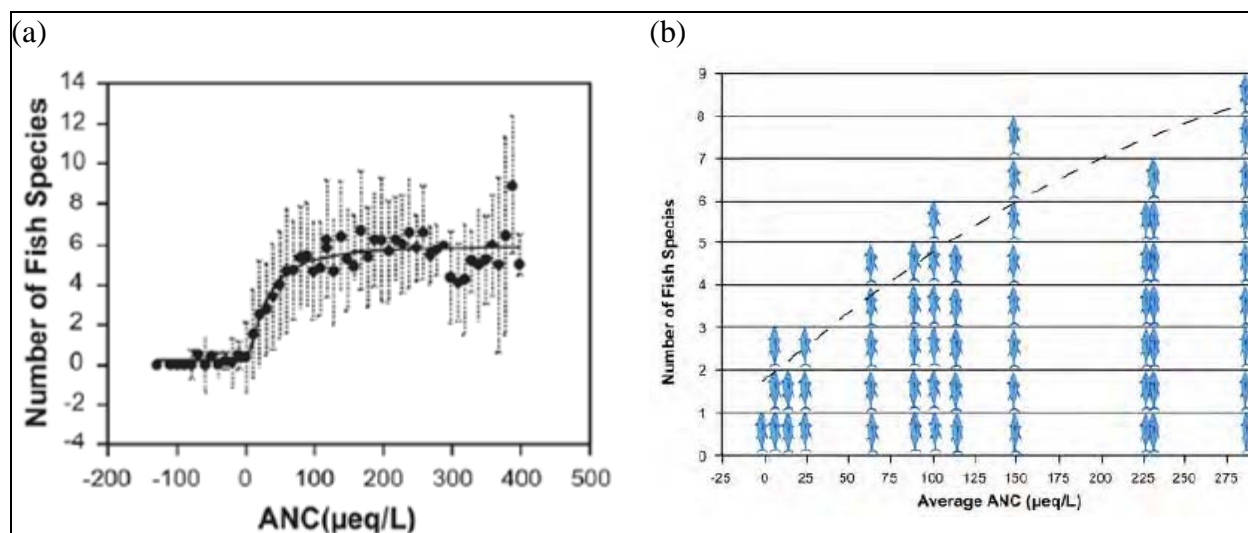


**Figure 2.3-1. (a)** Number of fish species per lake or stream versus acidity, expressed as ANC for Adirondack Case Study Area lakes (Sullivan et al., 2006). **(b)** Number of fish species among 13 streams as a function of ANC in the Shenandoah Case Study Area. Values of ANC are means based on quarterly measurements from 1987 to 1994. The regression analysis shows a highly significant relationship ( $p < .0001$ ) between mean stream ANC and the number of fish species.

### 3.0 CASE STUDIES

#### 3.1 SURFACE WATERS ACIDIFICATION IN THE EASTERN UNITED STATES

The regions of the United States with low average annual surface water ANC values are the locations that are sensitive to acidifying deposition. The majority of lakes and streams in the United States have ANC levels  $>200 \mu\text{eq/L}$  and are not sensitive to the acidifying deposition of  $\text{NO}_x$  and  $\text{SO}_x$  air pollution at their existing ambient concentration levels. **Figure 3.1-1** shows the acid-sensitive regions of the eastern United States with the potential for low surface water ANC, as determined by geology and surface water chemistry.

Freshwater surveys and monitoring in the eastern United States have been conducted by many programs since the mid-1980s, including the National Lake/Stream Surveys (NSWS), EPA's Environmental Monitoring and Assessment Program (EMAP), the Temporally Integrated Monitoring of Ecosystems (TIME) monitoring program (Stoddard, 1990), and LTM project (Ford et al., 1993; Stoddard et al., 1998) (Appendix Attachment B). The purpose of these programs is to determine the current state and document the trends over time in surface water

chemistry for regional populations of lakes or streams impacted by acidifying deposition. Based on extensive surveys and surface water data from these programs, it was determined that the most sensitive lakes and streams (i.e., ANC less than about 50  $\mu\text{eq/L}$ ) in the eastern United States are found in New England, the Adirondack Mountains, the Appalachian Mountains (northern Appalachian Plateau and Ridge/Blue Ridge region), northern Florida, and the Upper Midwest. These areas are estimated to contain 95% of the lakes and 84% of the streams in the United States that have been anthropogenically acidified through deposition (see Annex 4.3.3.2 of the *Integrated Science Assessment (ISA) for Oxides of Nitrogen and Sulfur—Ecological Criteria (Final Report)* (ISA) (U.S. EPA, 2008).

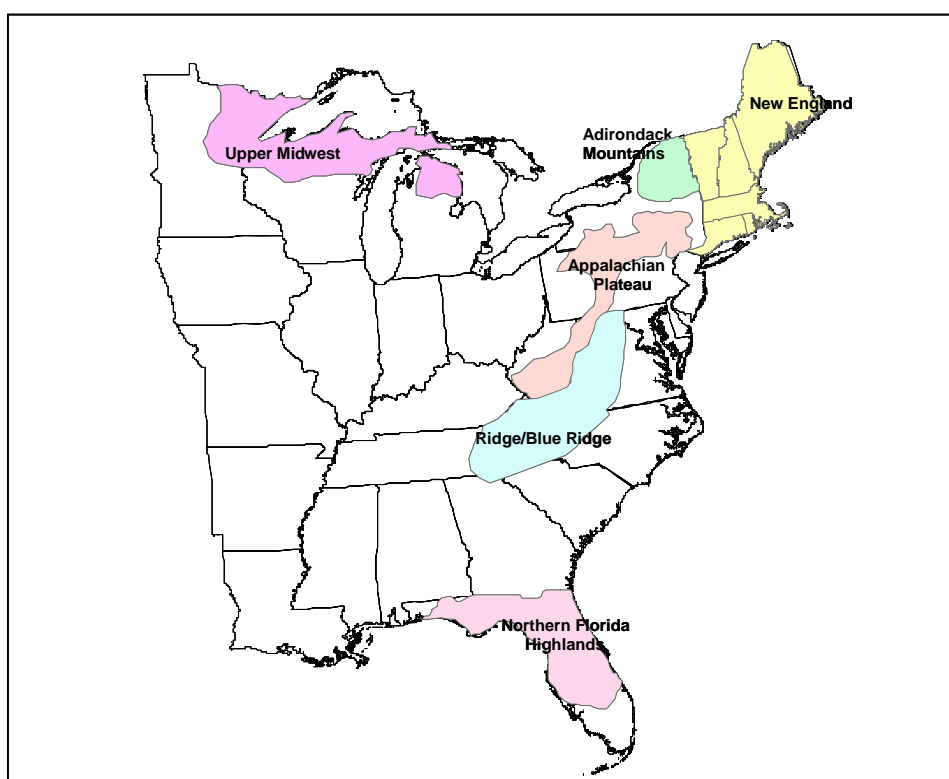


**Figure 3.1-1.** Regions containing ecosystems sensitive to acidifying deposition in the eastern United States (U.S. EPA, based on NAPAP, 2005).

The number and proportion of acidic waterbodies in these regions, defined as having a  $\text{pH} < 5.0$  and  $\text{ANC} < 0 \mu\text{eq/L}$ , are substantial. The Adirondack Case Study Area had a large proportion of acidic surface waters (14%) in the NSWS; from 1984 to 1987, the Adirondack Lakes Survey Corporation sampled 1,469 Adirondack Case Study Area lakes  $> 0.5$  hectares (ha) in size and estimated that many more (26%) were acidic (Driscoll et al., 1991). The proportion of lakes estimated by NSWS to be acidic was smaller in New England and the Upper Midwest (5%

and 3%, respectively), but because of the large number of lakes in these regions, there were several hundred acidic waters in each of these two regions. The Shenandoah Case Study Area had 5.5% and 6% acidic sites, respectively, based on data from the early 1990s. Portions of northern Florida also contain many acidic and low-ANC lakes and streams, although the role of acidifying deposition in these areas is less clear. In 2002, Stoddard et al. (2003) suggested that ~8% of lakes in the Adirondack Mountains and from 6% to 8% of streams in the northern Appalachian Plateau and Ridge/Blue Ridge region were acidic at base-flow conditions.

The Adirondack Case Study Area and the Shenandoah Case Study Area provide ideal areas to assess the risk to aquatic ecosystems from  $\text{NO}_x$  and  $\text{SO}_x$  acidifying deposition. Four main reasons support the selection of these two areas. First, both regions fall within the areas of the United States known to be sensitive to acidifying deposition because of a host of environmental factors that make these regions predisposed to acidification. Second, these areas are representative of other areas sensitive to acidification, which will allow the results of this case study to be generalized. Third, these regions have in the past and continue to experience substantial exposure to  $\text{NO}_x$  and  $\text{SO}_x$  air pollution. Fourth, these areas have been extensively studied (e.g., from atmospheric concentrations, soil characteristics, surface water chemistry, to the changes in biological communities in response to aquatic acidification) over the last 3 decades (see Section 4 of the ISA Report) (U.S. EPA, 2008). For example, extensive water quality data exists from monitoring networks in operation since the 1980s, along with numerous research studies that directly link the biological harm of individuals, populations, communities, and ecosystems to aquatic acidification. The sections below describe each of the case studies areas, in turn, indicating past impacts of acidifying deposition, and identifying research linking biological and acidic conditions for each region.

### **3.2 OBJECTIVES**

For the two case study areas, the Adirondack and the Shenandoah, conditions of the aquatic ecosystems and responses to nitrogen and sulfur deposition were evaluated by using multiple approaches that rely on monitoring data and modeled output. Current conditions were evaluated by a three-step process:

- By evaluating the status and trends of surface water chemistry data to establish linkages between current ambient air pollution levels of nitrogen and sulfur and the total amount of deposition
- By evaluating the biological risk to individuals, populations, and communities from acidification
- By evaluating the response of the aquatic ecosystem to current and future deposition compared with the likelihood for recovery of currently impacted aquatic waterbodies.

In evaluating these conditions, this case study addresses the welfare effects of acidification by building linkages between ambient pollutant levels, deposition, surface water chemistry, and the resulting response in the biological communities.

### **3.3 ADIRONDACK CASE STUDY AREA**

#### **3.3.1 General Description**

The Adirondack Case Study Area is situated in northeastern New York and is characterized by dense forest cover of evergreen and deciduous trees and abundant surface waters, with 46 peaks that extend up to 1,600 meters. The Adirondack Case Study Area has long been a nationally important recreation area for fishing, hiking, boating, and other outdoor activities. The area includes the headlands of five major drainage basins: Lake Champlain and the Hudson, Black, St. Lawrence, and Mohawk rivers, which all draw water from the preserve. There are more than 2,800 lakes and ponds, and more than 1,500 miles of rivers that are fed by an estimated 30,000 miles of brooks and streams. The Adirondack Case Study Area, particularly its southwestern section, is sensitive to acidifying deposition because it receives high precipitation amounts with high concentrations of pollutants, has shallow base-poor soils, and is underlain by igneous bedrock with low weathering rates and buffering ability (Driscoll et al., 1991; Sullivan et al., 2006). This case study area is among the most severely acid-impacted regions in North America (Driscoll et al., 2003; Landers et al., 1988; Stoddard et al., 2003). It has long been used as an indicator of the response of forest and aquatic ecosystems to changes in emissions of sulfur dioxide (SO<sub>2</sub>) and NO<sub>x</sub> resulting, in part, from the Clean Air Act Amendments of 1990 (NAPAP, 1998; U.S. EPA, 1995).

### 3.3.2 Levels of Air Pollution and Acidifying Deposition

Wet deposition in the Adirondack Case Study Area has been monitored by the National Atmospheric Deposition Program/National Trends Network (NADP/NTN) since 1978 at two sites (i.e., Huntington Forest and Whiteface Mountain) and at seven other sites since the 1980s. Since 1990, wet  $\text{SO}_4^{2-}$  and  $\text{NO}_3^-$  deposition at these NADP/NTN sites in the Adirondack Case Study Area has declined by about 45% and 40%, respectively (**Figure 3.3-1**). However, annual total wet deposition is still >15 and 10 kilograms/hectare/year (kg/ha/yr) of  $\text{SO}_4^{2-}$  and  $\text{NO}_3^-$ , respectively.

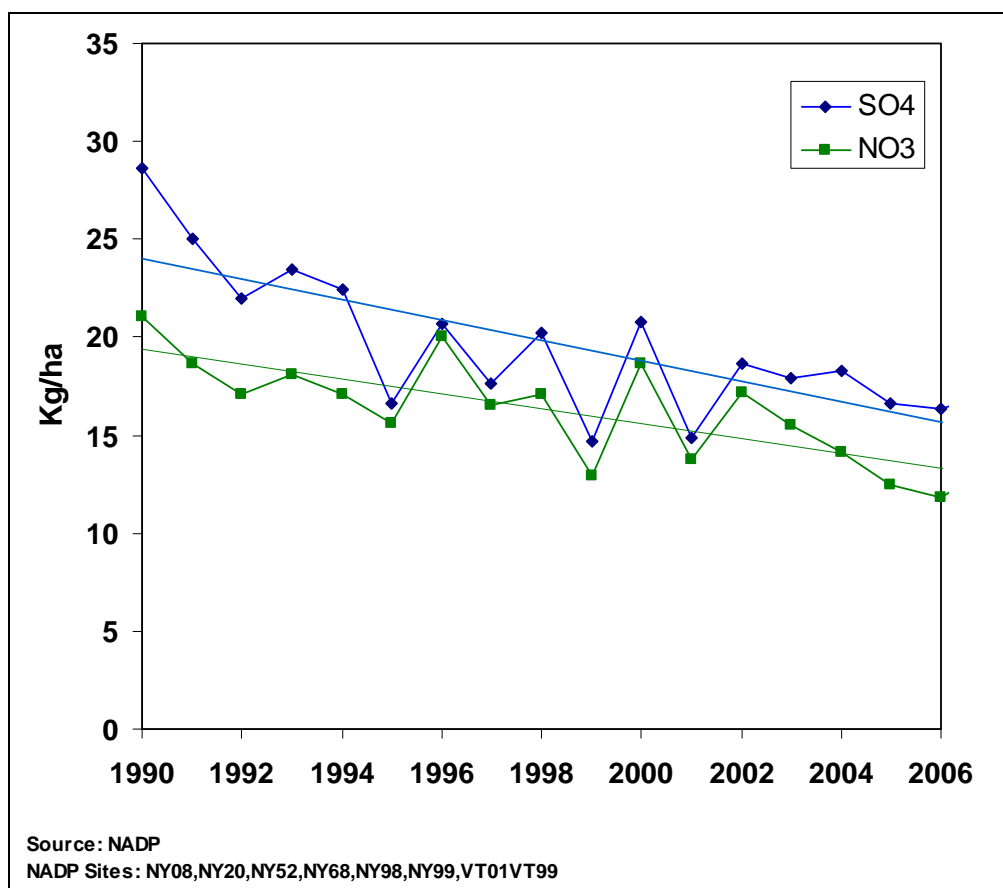


**Figure 3.3-1.** Annual average total wet deposition (kg/ha/yr) for the period 1990 to 2006 in  $\text{SO}_4^{2-}$  (blue) and  $\text{NO}_3^-$  (green) from eight NADP/NTN sites in the Adirondack Case Study Area (shown with linear trend regression lines).

### 3.3.3 Levels of Sulfate, Nitrate, and ANC Concentrations in Surface Water

Environmental monitoring data reported above demonstrate decreasing trends in depositional loading, reflecting decreases in air pollution. **Figure 3.3-2** shows annual average trends since 1990 in  $\text{SO}_4^{2-}$ ,  $\text{NO}_3^-$ , and ANC in surface water from 50 lakes in the Adirondack

Case Study Area monitored through the Adirondack Long-Term Monitoring (ALTM) program. As a result of decreases in air pollution and depositional loading, regional annual average  $\text{SO}_4^{2-}$  concentrations in these lakes has dropped by approximately 26% since the mid-1990s. While inter-annual variability in annual average  $\text{NO}_3^-$  concentrations is evident in the Adirondack Case Study Area monitored lakes, the overall trend is modestly downward (13% over the entire period). An increase in long-term annual average ANC of  $+0.8 \mu\text{eq/L/yr}$  has corresponded to the declines in  $\text{NO}_3^-$  and  $\text{SO}_4^{2-}$ . However, this increase in ANC also correlates with reductions in annual average base cations of calcium ( $\text{Ca}^{2+}$ ) and magnesium ( $\text{Mg}^{2+}$ ) during the same period of time (data not shown). In the Adirondack Case Study Area, toxic levels of dissolved inorganic aluminum also declined slightly (data not shown).

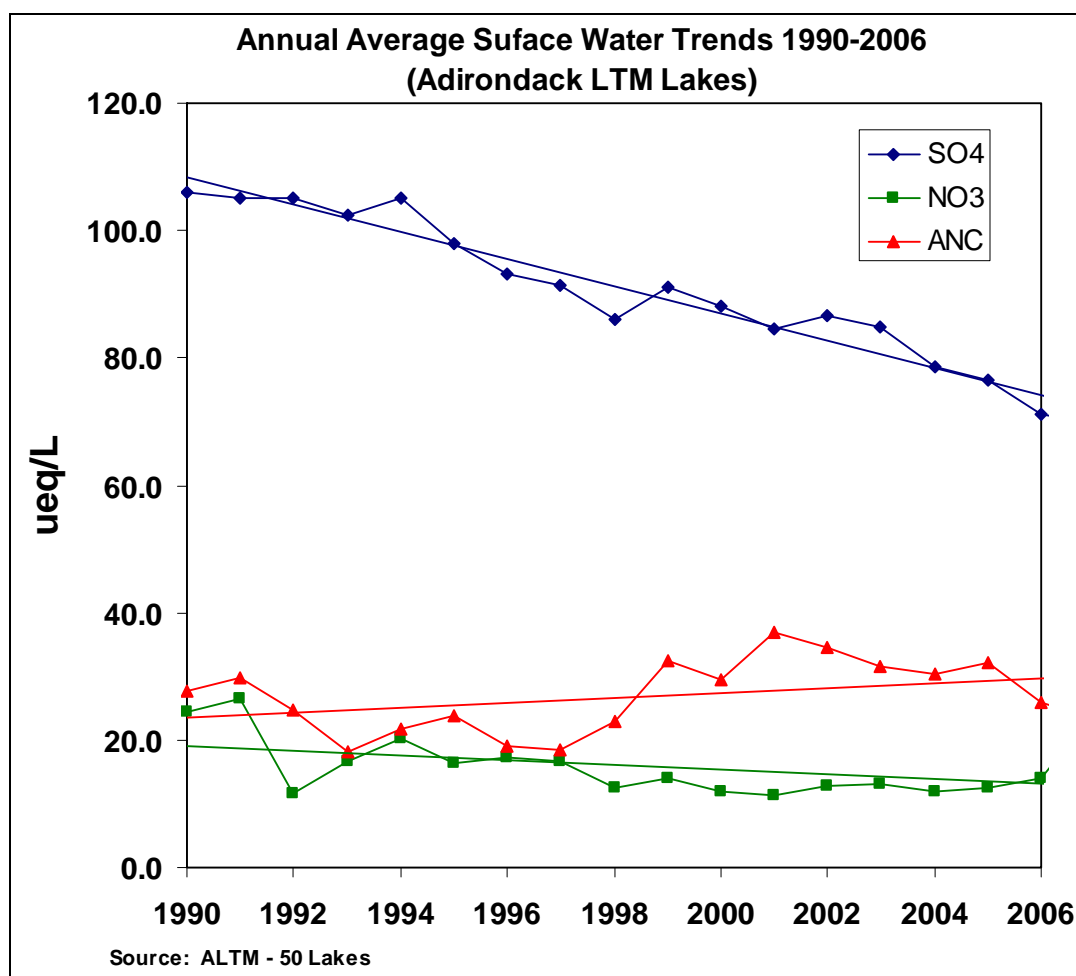


**Figure 3.3-2.** Trends over time for annual average  $\text{SO}_4^{2-}$  (blue) and  $\text{NO}_3^-$  (green) concentrations and ANC (red) in 50 Adirondacks Long-Term Monitoring monitored lakes in the Adirondack Case Study Area (shown with linear trend regression lines). Both  $\text{SO}_4^{2-}$  and  $\text{NO}_3^-$  concentrations have decreased in surface waters by approximately 26% and 13%, respectively.

Despite decreases in deposition and surface water concentrations of  $\text{SO}_4^{2-}$  and  $\text{NO}_3^-$ , levels remain elevated in monitored lakes. **Figure 3.3-3** shows current yearly average (2005 to 2006)  $\text{SO}_4^{2-}$ ,  $\text{NO}_3^-$ , and ANC for 88 Adirondack Case Study Area lakes monitored through the ALTM (50 Lakes) and TIME (38 lakes) programs. The yearly averages for the period from 2005 to 2006 of  $\text{SO}_4^{2-}$ ,  $\text{NO}_3^-$ , and ANC are  $70.88 \pm 19.87$ ,  $9.18 \pm 10.51$ , and  $33.84 \pm 44.40$   $\mu\text{eq/L}$ , respectively.

There is still a substantial number of lakes in the Adirondack Case Study Area that have low ANC values ( $<50$   $\mu\text{eq/L}$ ) based on the observed yearly average of ANC from the years 2005 and 2006 for the waterbodies in the TIME/ALTM monitoring networks. Of the 88 monitored lakes, 24% have ANC values  $>50$   $\mu\text{eq/L}$ , whereas 76% of the monitored lakes have ANC values  $<50$   $\mu\text{eq/L}$ . Of the 73 monitored lakes with  $>50$   $\mu\text{eq/L}$ , 17 are chronically acidic (ANC  $<0$   $\mu\text{eq/L}$ ). Twenty-seven of the lakes have  $<20$   $\mu\text{eq/L}$ , making their biological communities susceptible to episodic acidification.



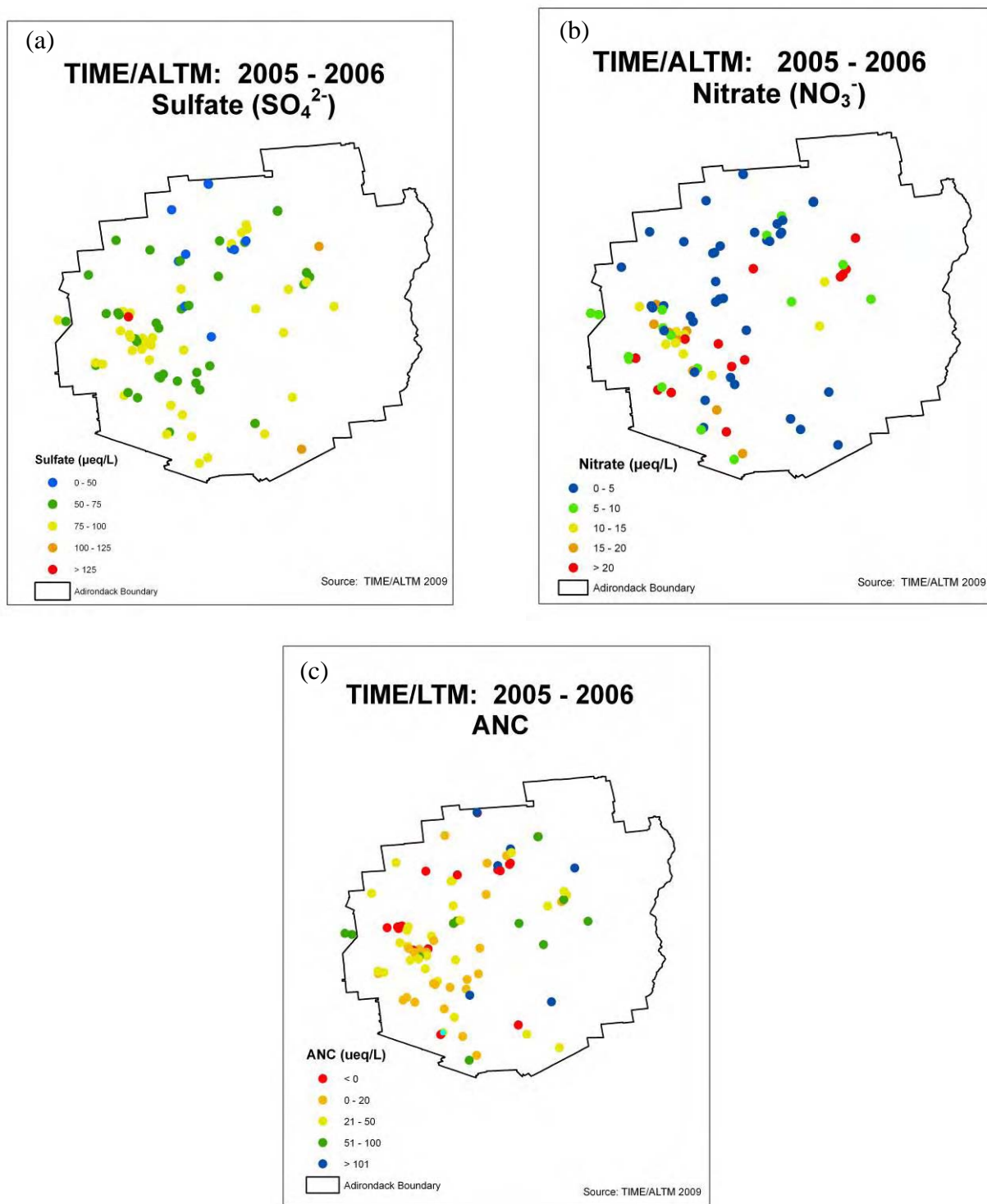


**Figure 3.3-3.** Current yearly average for 2005 to 2006 (a)  $\text{SO}_4^{2-}$  concentrations ( $\mu\text{eq/L}$ ), (b)  $\text{NO}_3^-$  concentrations ( $\mu\text{eq/L}$ ), and (c) ANC ( $\mu\text{eq/L}$ ) in surface waters from 88 monitored lakes in the Temporally Integrated Monitoring of Ecosystems (38 Lakes) and Adirondacks Long-Term Monitoring (50 Lakes) networks in the Adirondack Case Study Area.

### **3.4 SHENANDOAH CASE STUDY AREA**

#### **3.4.1 General Description**

The Shenandoah Case Study Area straddles the crest of the Blue Ridge Mountains in western Virginia, on the eastern edge of the central Appalachian Mountain region. Several areas in Shenandoah National Park have been designated Class 1 Wilderness areas. Shenandoah National Park is known for its scenic beauty, outstanding natural features, and biota. The Skyline Drive, a scenic 165-kilometer (km) parkway, provides the opportunity for views of the Blue Ridge Mountains and surrounding areas. The Appalachian National Scenic Trail is the backbone of the park's trail system. The natural features and biota of the park include the well-exposed rock strata of the Appalachians, which is one of the oldest mountain ranges in the world. The park comprises one of the nation's most diverse botanical reserves and wildlife habitats. A congressionally designated wilderness area within the park is the largest in the mid-Atlantic states and provides a comparatively accessible opportunity for solitude, study, and experience in a natural area.

Air pollution within the Shenandoah Case Study Area, including concentrations of sulfur, nitrogen, and ozone (O<sub>3</sub>), is higher than in most other national parks in the United States. This area is sensitive to acidifying deposition because of the noncarbonate composition and weathering-resistant characteristics of much of the underlying bedrock, which result in base-poor soils with low weathering rates and poor buffering capacity. At base flow conditions, Lynch and Dise (1985) determined that stream water ANC, pH, and base cation concentrations in this region are strongly correlated with bedrock geology. This landscape includes three major bedrock types: siliceous (e.g., quartzite and sandstone), felsic (e.g., granitic), and mafic (e.g., basaltic). Each of these bedrock types influence about one-third of the stream miles in this region. ANC concentrations for streams associated with siliceous bedrock are extremely low. Almost half of the sampled streams had ANC in the chronically acidic range (<0 µeq/L). The balance of the streams associated with siliceous bedrock had ANC in the episodically acidic range (0 to 20 µeq/L). Consequently, this region is among the most severely acid-impacted areas in North America (Stoddard et al., 2003; Webb et al., 2004).

### 3.4.2 Levels of Air Pollution and Acidifying Deposition

Annual average atmospheric concentrations of sulfur dioxide ( $\text{SO}_2$ ),  $\text{NO}_x$ ,  $\text{SO}_4^{2-}$ , and reduced nitrogen at the Big Meadow air monitoring location within the Shenandoah National Park have all decreased since the 1990s, with the exception of reduced nitrogen (**Figure 3.4-1, a**). As a result, wet deposition in the Shenandoah National Park monitored at 7 sites by the NADP/NTN since the 1980s shows wet  $\text{SO}_4^{2-}$  and  $\text{NO}_3^-$  deposition declining by about 28% and 20%, respectively (**Figure 3.4-1, b**). However, annual total deposition is still 15 and 10 kg/ha/yr of  $\text{SO}_4^{2-}$  and  $\text{NO}_3^-$ , respectively.

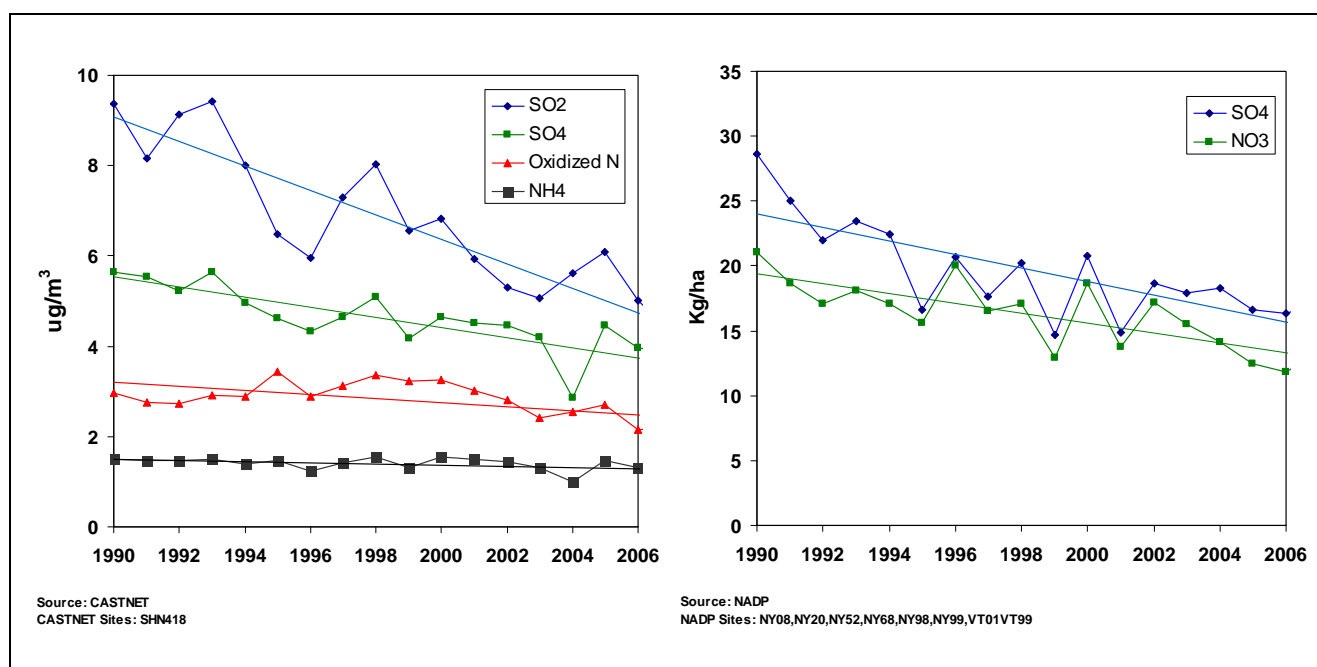


**Figure 3.4-1.** Air pollution concentrations and wet deposition for the period 1990 to 2006 using a CastNET (SHN418) and seven NADP/NTN sites in the Shenandoah Case Study Area. **(a)** Annual average atmospheric concentrations ( $\text{ug}/\text{m}^3$ ) of  $\text{SO}_2$  (blue), oxidized nitrogen (red),  $\text{SO}_4^{2-}$  (green), and reduced nitrogen (black). **(b)** Annual average total wet deposition ( $\text{kg}/\text{ha}/\text{yr}$ ) of  $\text{SO}_4^{2-}$  (green) and  $\text{NO}_3^-$  (blue).

### 3.4.3 Levels of Sulfate, Nitrate, and ANC Concentrations in Surface Water

**Figure 3.4-2** shows trends in annual average surface water concentrations of  $\text{SO}_4^{2-}$  and  $\text{NO}_3^-$  and ANC values for streams in the Shenandoah Case Study Area monitored through the Shenandoah National Park Surface Water Acidification Study (SWAS), Virginia Trout Stream Sensitivity Survey (VTSSS), and LTM programs. The annual average for 67 streams for the period 2005 to 2006 of  $\text{SO}_4^{2-}$ ,  $\text{NO}_3^-$ , and ANC are  $59.29 \pm 28.2$ ,  $3.74 \pm 7.0$ , and  $60.60 \pm 72.7$

$\mu\text{eq/L}$ , respectively (**Figure 3.4-3**). Despite the decreases in pollution and regional acidifying deposition,  $\text{SO}_4^{2-}$  and  $\text{NO}_3^-$  concentrations in these streams have seen slight improvements since the mid-1990s. There is a slight decline in  $\text{SO}_4^{2-}$  concentrations ( $-0.04 \mu\text{eq/L/yr}$ ) in surface waters, whereas  $\text{NO}_3^-$  declined by only  $-0.3 \mu\text{eq/L/yr}$ . On the other hand, average ANC values of the 67 streams increased to  $79 \mu\text{eq/L}$  until the year 2002, from about  $50 \mu\text{eq/L}$  in the early 1990s. However, since 2002, ANC levels have fluctuated by first declining back to early 1990s levels and then increasing to  $67 \mu\text{eq/L}$  in 2006. Despite improvement in deposition, surface water concentrations of  $\text{SO}_4^{2-}$  and  $\text{NO}_3^-$  levels remain elevated in monitored streams in the Shenandoah Case Study Area.

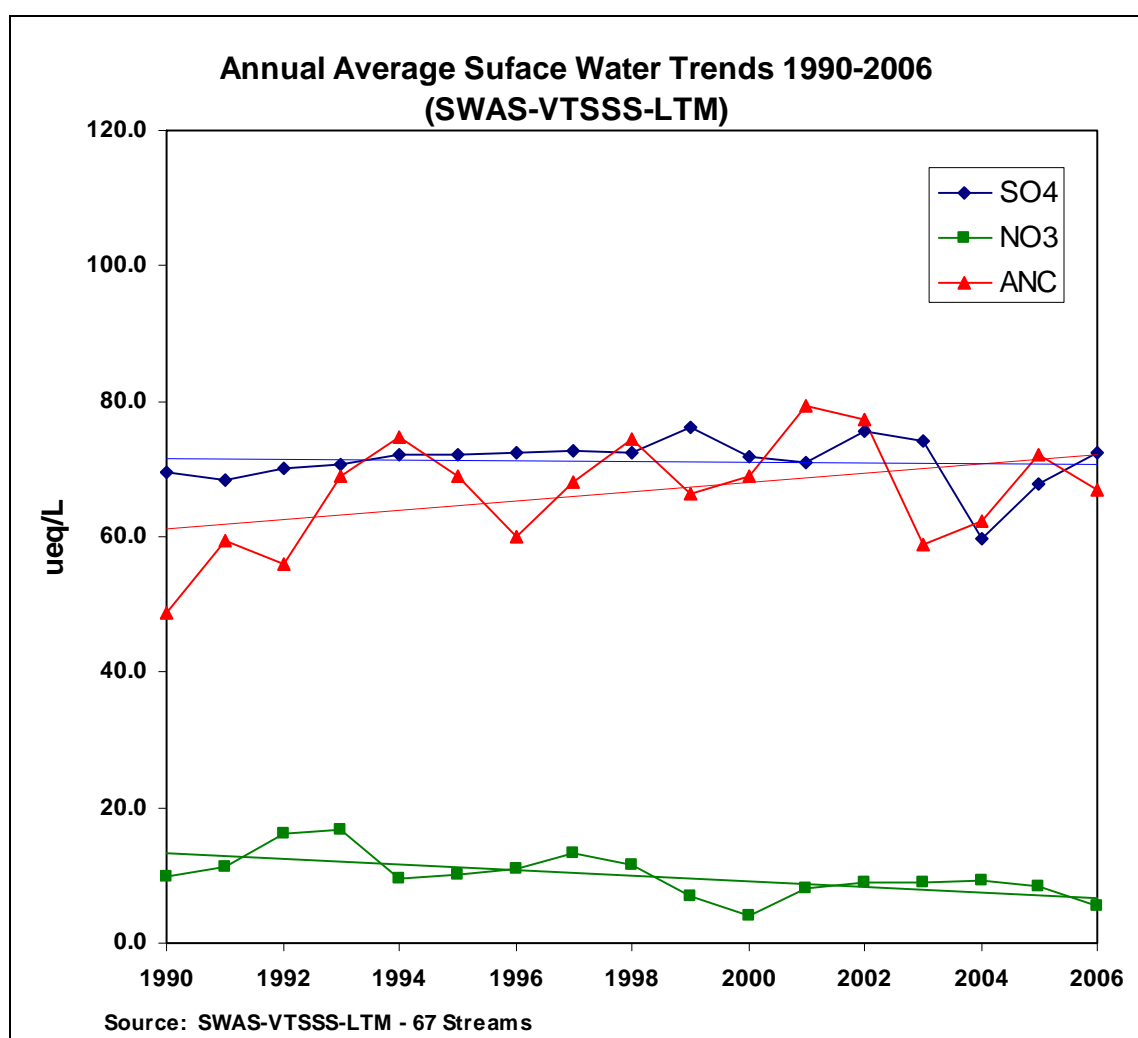


**Figure 3.4-2.** Trends over time for annual average  $\text{SO}_4^{2-}$  (blue) and  $\text{NO}_3^-$  (green) concentrations, and ANC (red) in 67 streams in the Surface Water Acidification Study, Virginia Trout Stream Sensitivity Survey, and Long-Term Monitoring programs in the Shenandoah Case Study Area (shown with linear trend regression lines).

There are a significant number of the 67 streams in SWAS-VTSSS and LTM programs that currently have ANC <50 µeq/L based on the observed annual average ANC concentrations **(Figure 3.4-3)**. Forty-five percent of all monitored streams have ANC values >50 µeq/L, whereas 55% have <50 µeq/L. Of the 55% <50 µeq/L, 18% experience episodic acidification (<20 µeq/L) and 12% are chronically acidic (<0 µeq/L) at the current level of acidifying deposition and ambient concentrations of NO<sub>x</sub> and SO<sub>2</sub>.

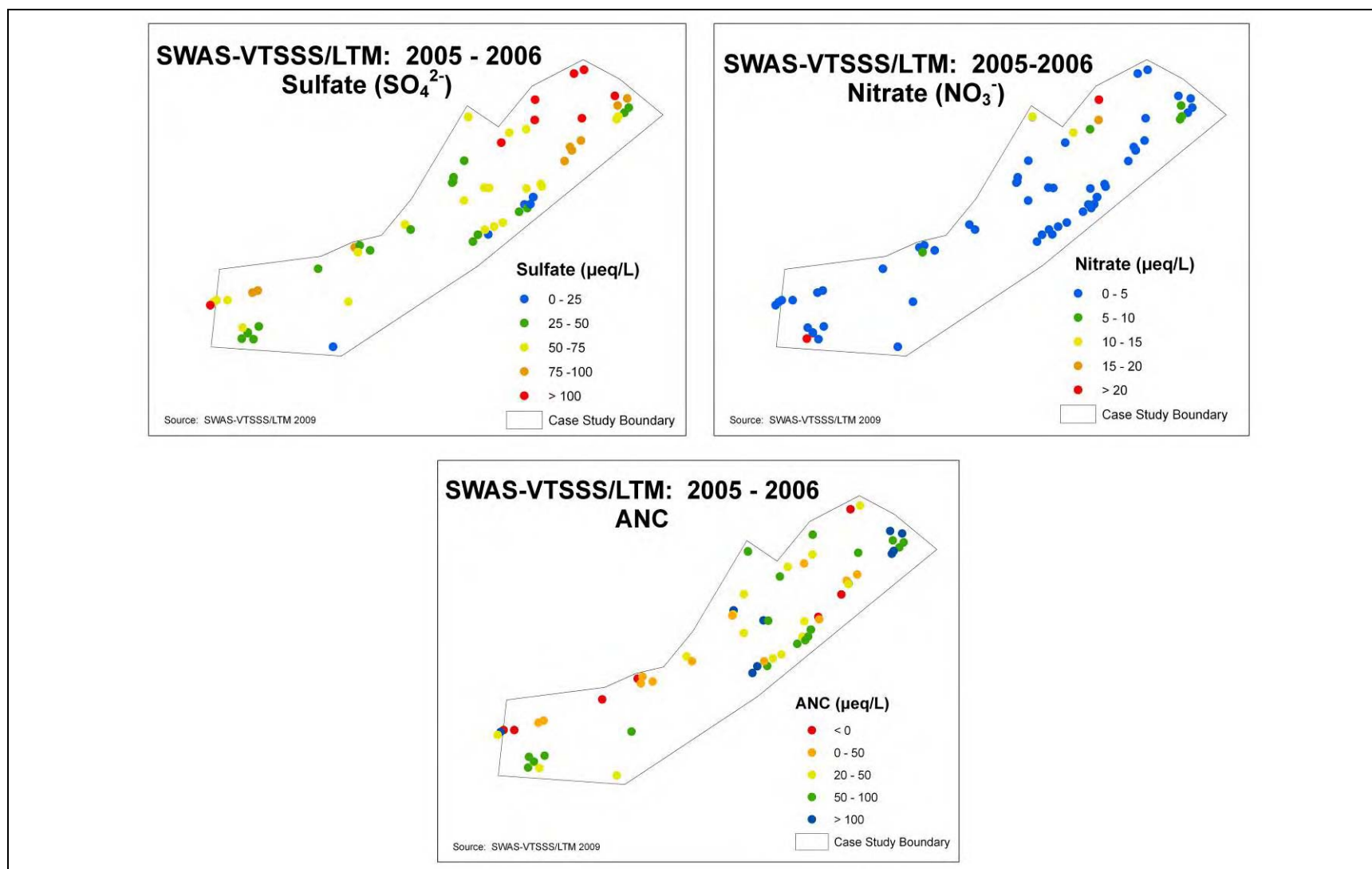


**Figure 3.4-3.** Current yearly average for 2005 to 2006 (a)  $\text{SO}_4^{2-}$  concentration, (b)  $\text{NO}_3^-$  concentration, and (c) ANC ( $\mu\text{eq/L}$ ) in surface waters from 67 monitored streams in the Surface Water Acidification Study, Virginia Trout Stream Sensitivity, and Long-Term Monitoring network in the Shenandoah Case Study Area.

## 4.0 METHODS

### 4.1 BIOLOGICAL RESPONSE TO ACIDIFICATION

Because there is a continuum in the relationship between ANC concentrations and resulting biological effects, a range of ANC values related to specific biological effects is needed for the following reasons:

- (1) ANC values within a waterbody are not constant; there is variation with time and season. For example, during spring, following snowmelt and the resulting influx of acidifying compounds, surface water ANC levels can substantially drop. There is also spatial uncertainty. Consequently, the length of exposure (i.e., chronic vs. episodic) can affect biological responses.
- (2) The biological effects of particular ANC values vary between individual organisms because of differences in developmental stage and size, innate differences between different species of the same general types of organisms, and differences between different kingdoms, phyla, and classes of organisms.

Therefore, five categories of ANC values were used that link specific biological health conditions to the effects of aquatic communities, ranging from no impacts to complete loss of populations. These five classes are based on the relationships among ANC and ecological attributes, including richness, diversity, community structure, and individual fitness of organisms. The following paragraphs describe the biological impacts, given a range of ANC values and the scientific research that supports the grouping. Section AX4 of the Annexes to the ISA (U.S. EPA, 2008) presents a more in-depth description of the biological relationship used in this case study.

For freshwater systems, ANC values are grouped into five major categories: Acute Concern ( $<0$   $\mu\text{eq/L}$ ; acidic), Severe Concern (0 to 20  $\mu\text{eq/L}$ ), Elevated Concern (20 to 50  $\mu\text{eq/L}$ ), Moderate Concern (50 to 100  $\mu\text{eq/L}$ ), and Low Concern ( $>100$   $\mu\text{eq/L}$ ), with each range representing a probability of ecological damage to the community (**Table 4.1-1**).

**Table 4.1-1.** Aquatic Status Categories

Category Label ANC Levels* Expected Ecological Effects		
Acute Concern	<0 µeq/L (Acidic)	Near complete loss of fish populations is expected. Planktonic communities have extremely low diversity and are dominated by acidophilic forms. The number of individuals in plankton species that are present is greatly reduced.
Severe Concern	0–20 µeq/L	Highly sensitive to episodic acidification. During episodes of high acidifying deposition, brook trout populations may experience lethal effects. Diversity and distribution of zooplankton communities decline sharply.
Elevated Concern	20–50 µeq/L	Fish species richness is greatly reduced (i.e., more than half of expected species can be missing). On average, brook trout populations experience sublethal effects, including loss of health, reproduction capacity, and fitness. Diversity and distribution of zooplankton communities decline.
Moderate Concern	50–100 µeq/L	Fish species richness begins to decline (i.e., sensitive species are lost from lakes). Brook trout populations are sensitive and variable, with possible sublethal effects. Diversity and distribution of zooplankton communities also begin to decline as species that are sensitive to acidifying deposition are affected.
Low Concern	>100 µeq/L	Fish species richness may be unaffected. Reproducing brook trout populations are expected where habitat is suitable. Zooplankton communities are unaffected and exhibit expected diversity and distribution.

*Low Concern* – Biota is generally not harmed when ANC values are >100 µeq/L. For example, the number of fish species tend to peak at ANC values >100 µeq/L (Bulger et al., 1999; Driscoll et al., 2001; Kretser et al., 1989; Sullivan et al., 2006). Typically, with ANC concentrations >100 µeq/L, the diversity of the aquatic community is more influenced by other environmental factors, such as habitat availability, than the acid-base balance of the surface water.

*Moderate Concern* – At ANC levels 50 to 100 µeq/L, declines in the fitness and recruitment of species sensitive to acidity (e.g., some fish and invertebrate organisms) have been demonstrated and may result in decreases in community-level diversity as the few highly acid-sensitive species are lost (see **Figure 2.3-1**). However, minimal (no measurable) change in total community abundance or production generally occurs, resulting in good overall health of the community.



*Elevated Concern* – When ANC values drop between 20 and 50  $\mu\text{eq/L}$ , they are generally associated with negative effects on the fitness and recruitment of aquatic biota. Kretser et al. (1989) showed that a 50% reduction in the number of fish species occurred when ANC values dropped to  $<50 \mu\text{eq/L}$  in lakes that were surveyed. Furthermore, Dennis and Bulger (1995) showed that when ANC values drop to between 20 and 50  $\mu\text{eq/L}$ , the overall fitness of most fish species are reduced, such as sensitive species of minnows and daces (e.g., fathead minnow and blacknose dace), and recreation fish species (e.g., lake trout and walleye). In addition to the changes in the fish community, a drop in ANC values can cause some loss of common invertebrate species from zooplankton and benthic communities, which include many species of snails, clams, mayflies, and amphipods. These losses of sensitive species often result in distinct decreases in species richness and changes in species composition of the biota. However, the total community abundance or production remains high, with little if any change.

*Severe Concern* – When ANC levels drop  $<20 \mu\text{eq/L}$ , almost all biota exhibit some level of negative effects. Fish and plankton diversity and the structure of the communities continue to decline sharply to levels where acid-tolerant species begin to outnumber all other species (Driscoll et al., 2001; Matuszek and Beggs, 1988). Loss of several important sport fish species is possible, including lake trout, walleye, and rainbow trout, and losses of additional nongame species, such as creek chub, occur. In addition, several other invertebrate species, including all snails, most slams, and many species of mayflies, stoneflies, and other benthic invertebrates, are lost or greatly reduced in population size, which further depresses species composition and community richness. Also, at  $<20 \mu\text{eq/L}$ , surface waters are susceptible to episodic acidification, and a total loss of biota can occur when ANC concentration goes to  $<0 \mu\text{eq/L}$  for a short period of time. Stoddard et al. (2003) showed that to protect biota from episodic acidification in the spring, base flow (i.e., summer nonstorm event) ANC levels need to have an ANC of at least 30 to 40  $\mu\text{eq/L}$  (**Figure 4.1-1**).

*Acute Concern* – Near complete loss of fish populations and extremely low diversity of planktonic communities occur with ANC levels  $<0 \mu\text{eq/L}$ . Only acidophilic species are present, but their population numbers are sharply reduced. For example, lakes in the Adirondack Case Study Area have been shown to be fishless when the average ANC is  $<0 \mu\text{eq/L}$  (Sullivan et al., 2006). A summary of the five categories of ANC and expected ecological effects can be found in **Figure 4.1-2** and **Table 4.1-1**.

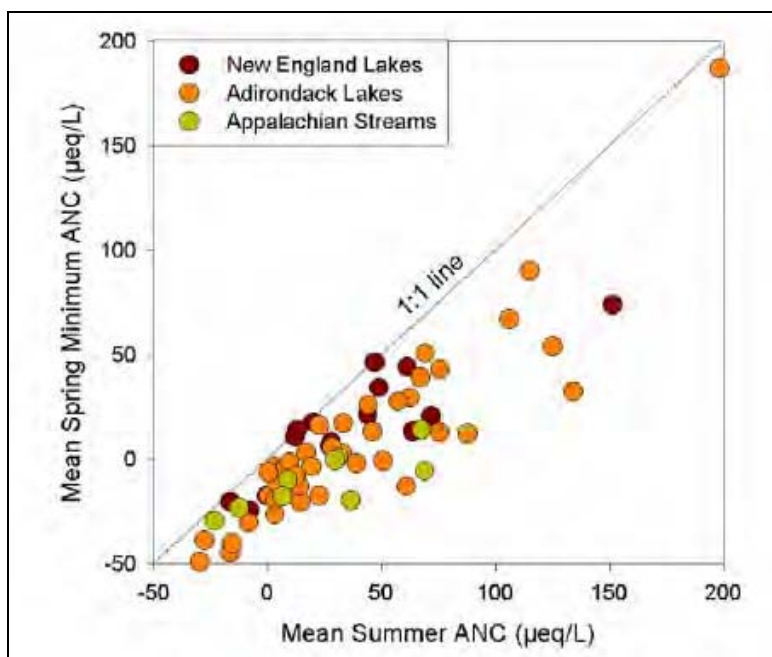


**Figure 4.1-1.** Relationship between summer and spring ANC values at LTM sites in New England, the Adirondack Mountains, and the Northern Appalachian Plateau. Values are mean summer values for each site for the period 1990 to 2000 (horizontal axis) and mean spring minima for each site for the same time period. On average, spring ANC values are at least 30  $\mu\text{eq/L}$  lower than summer values.

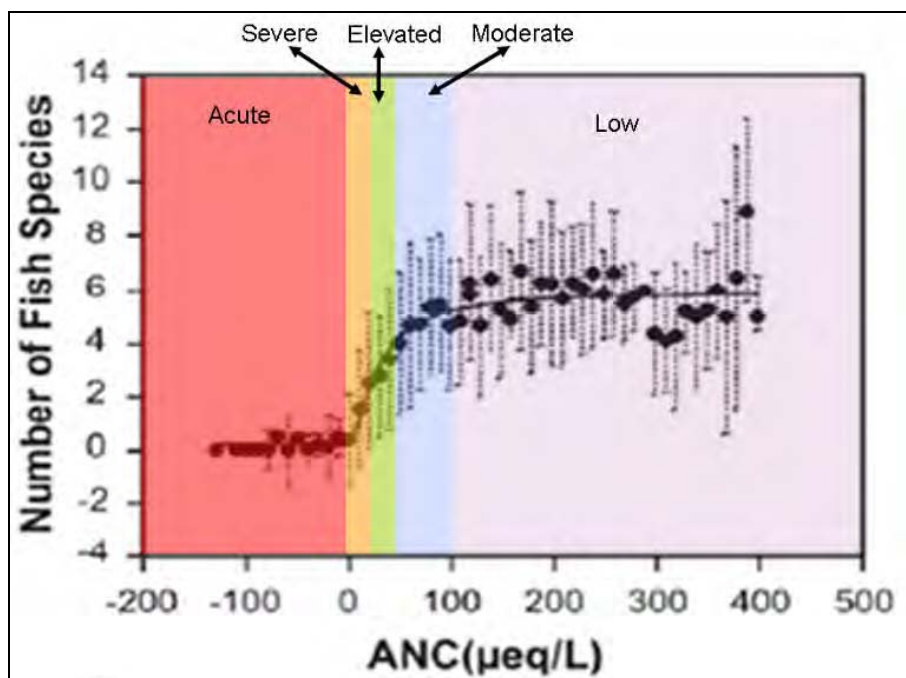


**Figure 4.1-2.** Number of fish species per lake or stream versus ANC level and aquatic status category (represented by color) for lakes in the Adirondack Case Study Area (Sullivan et al., 2006). The five aquatic status categories are described in **Table 4.1-1**.

## **4.2 PAST, PRESENT, AND FUTURE SURFACE WATER CHEMISTRY—THE MAGIC MODELING APPROACH**

The preacidification condition of a waterbody is rarely known because historical measurements are not available. Likewise, it is also difficult to determine if a waterbody has or will recover from acidification as acidifying deposition inputs decline, because recovery may take many years to decades to occur. For these reasons, biogeochemical models, such as MAGIC, enable estimates of past, present, and future water chemistry levels that can be used to evaluate the associated risk and uncertainty of the current levels of acidification compared with estimated preacidification conditions and to evaluate whether a system will recover as a result of reduction in acidifying deposition.

Dynamic hydrological models use surface water measurements of multiple parameters from the long-term record, information about the current exposure (i.e., ambient pollutant concentrations, deposition estimates), and known/measurable biogeochemical factors to characterize a watershed and estimate its preindustrial (i.e., preacidification) state and to estimate its response to changes in deposition in the future.

In both case study areas, MAGIC was used to estimate the past (i.e., preacidification, 1860), present (i.e., the years 2002 and 2006), and future (i.e., the years 2020 and 2050) acidic conditions of 44 lakes in the Adirondack Case Study Area and 60 streams in the Shenandoah Case Study Area (**Figure 4.3-1**). Fewer lakes and streams were modeled with MAGIC because calibration data are not available for all sites in the ALTM and SWAS-VTSSS/LTM monitoring networks. Furthermore, MAGIC was used to quantify the associated uncertainty in these estimates, as well as in input parameters used in MAGIC. The MAGIC model output for each waterbody was summarized into five ANC levels that correspond to the aquatic status categories in **Table 4.1-1**. This grouping permits an assessment of the risk to the biological communities for each of the conditions. The hydrological model, MAGIC, along with all the necessary inputs and calibration procedure, is described in detail in Appendix Attachment A.

### **4.3 CONNECTING CURRENT NITROGEN AND SULFUR DEPOSITION TO ACID-BASE CONDITIONS OF LAKES AND STREAMS: THE CRITICAL LOAD APPROACH**

Critical loads were calculated for lakes and streams in both case study areas. The critical load for a lake or stream provides a means to gauge the extent to which a waterbody has recovered from past acidifying deposition or is potentially at risk because of current deposition levels. The critical load approach provides a quantitative estimate of the level of exposure to one or more pollutants, below which significant harmful effects on specific sensitive elements of the environment do not occur, according to present knowledge.

The critical load approach relates specific amounts of deposition to particular ANC levels for individual waterbodies, using the relationships established between the biogeochemical state of the environment, current pollutant deposition, the surface water chemistry, and the response of the biological communities to deposition. Conversely, it is possible to specify a “critical limit” ANC level and to estimate the “critical load” of deposition required to cause the stream to have that specified ANC level. The past, current, or estimated future levels of deposition can be compared with the critical load estimate. For example, a critical limit ANC value of 50  $\mu\text{eq/L}$  could be specified for a particular stream or lake. The amount of deposition that the stream or lake could take and maintain an ANC of 50  $\mu\text{eq/L}$  would be its critical load. Clearly, if the critical limit ANC value is lower (20  $\mu\text{eq/L}$ ), the critical load would increase—it would take more deposition to lower the stream’s ANC to that new value.

A critical load estimate is analogous to a “susceptibility” estimate, relating the sensitivity of the waterbody to become acidified from the deposition of nitrogen and sulfur to the critical limit ANC concentration. Low critical load values (e.g., less than 50 milliequivalents per square meter per year ( $\text{meq/m}^2/\text{yr}$ )) mean that the watershed has a limited ability to neutralize the addition of acidic anions, and hence, it is at risk or susceptible to acidification and the resulting deleterious effects. The greater the critical load value, the greater the ability of the watershed to neutralize the additional acidic anions and resist acidification, thereby protecting the aquatic ecosystem.

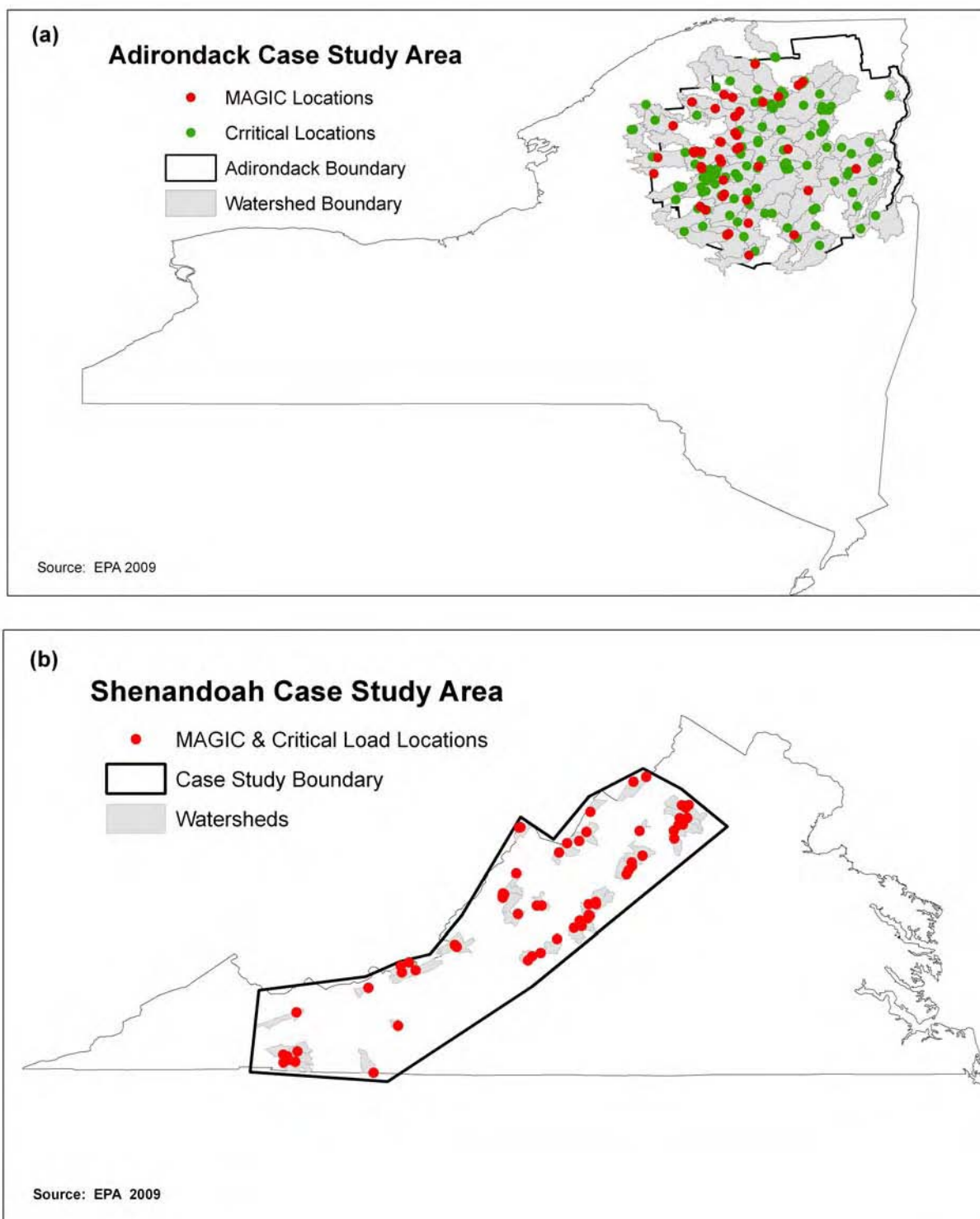


**Figure 4.3-1. (a)** The location of lakes in the Adirondack Case Study Area used for MAGIC (red circles) and critical load (green circles) modeling. **(b)** The location of streams in the Shenandoah Case Study Area used for both MAGIC and critical load modeling.

Applied at locations over a region, the critical load approach provides a method to quantify the number of lakes or streams in a given area that receive harmful levels of deposition. The magnitude of the biological harm is defined by the critical limit ANC level (e.g., ANC of 50  $\mu\text{eq/L}$ ) (see **Table 4.1-1**). Critical load exceedance (i.e., the amount of actual deposition above the critical load, if any) can be calculated for each waterbody in the region. Lakes and streams with positive exceedance values, where actual deposition was above its critical load, are not protected at that critical limit, whereas negative exceedance values, where deposition of nitrogen and sulfur was below its critical load, are protected.

Critical loads and their exceedances were calculated for four critical limit thresholds (i.e., ANC of 0, 20, 50, and 100  $\mu\text{eq/L}$ ), separating the five ANC categories of biological protections (**Table 4.1-1**) for 169 lakes in the Adirondack Case Study Area and 60 streams in the Shenandoah Case Study Area. There are numerous methods and models that can be used to calculate critical loads for acidity. Drawing on the peer-reviewed scientific literature (Dupont et al., 2005), this case study used a steady-state critical load model that uses surface water chemistry as the base for calculating the critical load. A combination of the Steady-State Surface Water Chemistry (SSWC) and First-Order Acidity Balance (FAB) models were used to calculate the critical load. This analysis uses water chemistry data from the TIME and LTM programs that are part of the Environmental Monitoring and Assessment Program (see discussion of surface water trends in Section 5.1.1). This case study focuses on the combined load of sulfur and nitrogen deposition, below which the ANC level would still support healthy aquatic ecosystems. For each waterbody, the actual current total deposition in the year 2002 was compared with the estimated critical loads for the four critical limit thresholds to determine which sites exceed their critical limit of deposition and biological protection level. Estimates of actual current deposition were based on the sum of measured wet deposition values from the year 2002 NADP network and modeled dry deposition values based on the year 2002 emissions and meteorology using the Community Multiscale Air Quality (CMAQ) model, respectively.

The actual deposition was compared with the critical load for each of the waterbodies within the case study areas for each of the critical limit levels, and exceedances were determined. Results for an individual lake were grouped by whether or not the lake exceeded its critical load. For each of two case study areas, the number and percentage of lakes that receive acidifying deposition above their critical load for each of the ANC critical limits of 0, 20, 50, and 100  $\mu\text{eq/L}$

were determined. The critical load models and their inputs are described in detail in Appendix Attachment A.

#### **4.3.1 Regional Assessment of Adirondack Case Study Area Lakes and Shenandoah Case Study Area Trout Streams**

##### ***4.3.1.1 Adirondack Case Study Area***

In the Adirondack Case Study Area, critical load exceedances were extrapolated to lakes defined by the New England EMAP probability survey. The EMAP probability survey was designed to estimate, with known confidence, the status, extent, change, and trends in condition of the nation's ecological resources, such as surface water quality. In probability sampling, the inclusion probability for each sampled lake represents a proportion of the target population. Lakes selected with relatively high probability represent relatively few lakes in the population; therefore, they carry relatively low weight and influence the final inferences less than lakes selected with low probability. These inclusion probabilities (i.e., weighting or expansion factors) are used to infer or estimate population frequency distributions and to evaluate sampling uncertainty.

For the Adirondack Case Study Area, the regional EMAP probability survey of 117 lakes (i.e., weighting factors) were used to infer the number of lakes and percentage of lakes that receive acidifying deposition above their critical load of a target population of 1,842 lakes. The target population of 1,842 lakes represents all lakes from 0.5 to 2,000 ha with a depth of >1 meter (m) and >1,000 m<sup>2</sup> of open water in the Adirondack Case Study Area. ANC limits of 20, 50, and 100 µeq/L were examined.

The 117 lakes in the regional Adirondack probability survey represent a subset of 344 sampled lakes throughout New England (e.g., lakes in Maine, New Hampshire, Vermont, Rhode Island, Massachusetts, Connecticut, New York, New Jersey) from 1991 through 1994. For New England, 11,076 lakes are represented in the target population (Larsen et al., 1994).

##### ***4.3.1.2 Shenandoah Case Study Area***

In the Shenandoah Case Study Area, critical load exceedances were extrapolated using the SWAS-VTSSS LTM quarterly monitored sites to the population of brook trout streams that do not lie on limestone bedrock and/or are not significantly affected by human activity within the

watershed. The total number of brook trout streams represented by the SWAS-VTSSS LTM quarterly monitored sites is approximately 310 streams out of 440 mountain headwater streams known to support reproducing brook trout in the Shenandoah Case Study Area.

The SWAS-VTSSS LTM programs were designed to track the effects of acidifying deposition and other factors that determine water quality and related ecological conditions in the Shenandoah Case Study Area's native trout streams. The SWAS-VTSSS LTM began in spring 1987, when water samples were collected from 440 streams known to have brook trout. Following the 1987 survey, a representative subset of 69 streams was selected for long-term quarterly monitoring of water quality, mostly located on National Forest lands or within the Shenandoah National Park Case Study Area (14 SWAS and 55 VTSSS streams). These streams were selected to achieve geographic distribution and representation of major bedrock types (Webb et al., 1994), allowing the streams to be stratified into bedrock type. This enabled results from the monitored streams ( $n=69$ ) to be extrapolated to the entire regional population of trout streams (440). Webb et al. (1994) identified six bedrock classes that account for much of the spatial variation in ANC among the SWAS-VTSSS LTM quarterly sampled streams. The landscape classes adopted for this study and the number of selected stream sites within each of the classes include Blue Ridge siliciclastic (16 streams), Blue Ridge granitic (18 streams), Blue Ridge basaltic (four streams), and Valley and Ridge siliciclastic (22 streams). Streams in the carbonate classes (13) were not included because they are not considered susceptible to acidification. A weighting scheme based on the number of monitoring streams in each of the bedrock classes was used to extrapolate to the regional population of trout streams. For example, 103 VTSSS streams lie on granitic bedrock, of which 18 were monitored quarterly, resulting in a weighting factor of 5.7 ( $=103/18$ ). The weights for streams in the other bedrock classes are 6.25 ( $= 25/4$ ) for basaltic, 4.3 ( $= 69/16$ ) for Blue Ridge siliciclastic, and 4.86 ( $=107/22$ ) for Valley and Ridge siliciclastic. Thus, the total number of brook trout streams represented in the Shenandoah Case Study Area is approximately 310; these are all brook trout streams that do not lie on limestone (10% of 440 streams) and/or have not been significantly affected by human activity within the watersheds (20% of the streams).



## 5.0 RESULTS

### 5.1 ADIRONDACK CASE STUDY AREA

#### 5.1.1 Current and Preacidification Conditions of Surface Waters

Since the mid-1990s, lakes in the Adirondack Case Study Area have shown signs of improvement in ANC,  $\text{NO}_3^-$ , and  $\text{SO}_4^{2-}$  levels in surface waters, as shown in **Figure 3.3-2**. However, current average surface water concentrations of  $\text{NO}_3^-$  and  $\text{SO}_4^{2-}$  are still well above preacidification conditions based on MAGIC model simulations of 44 lakes (**Figure 5.1-1**), resulting in lower than average ANC surface water chemistry.

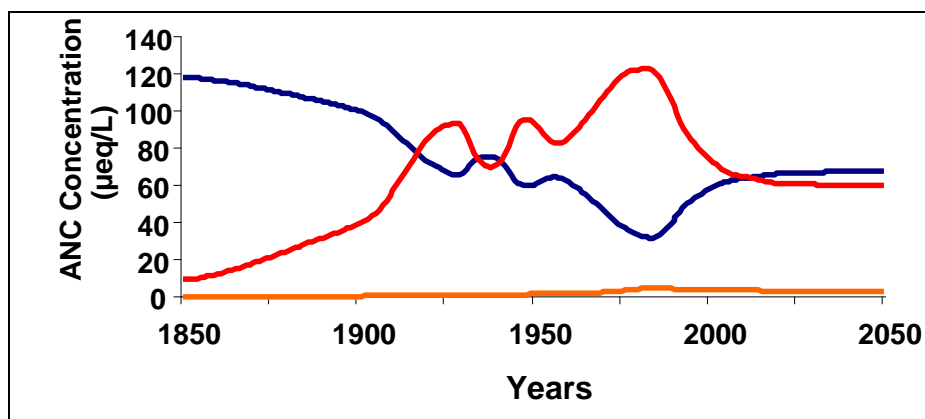


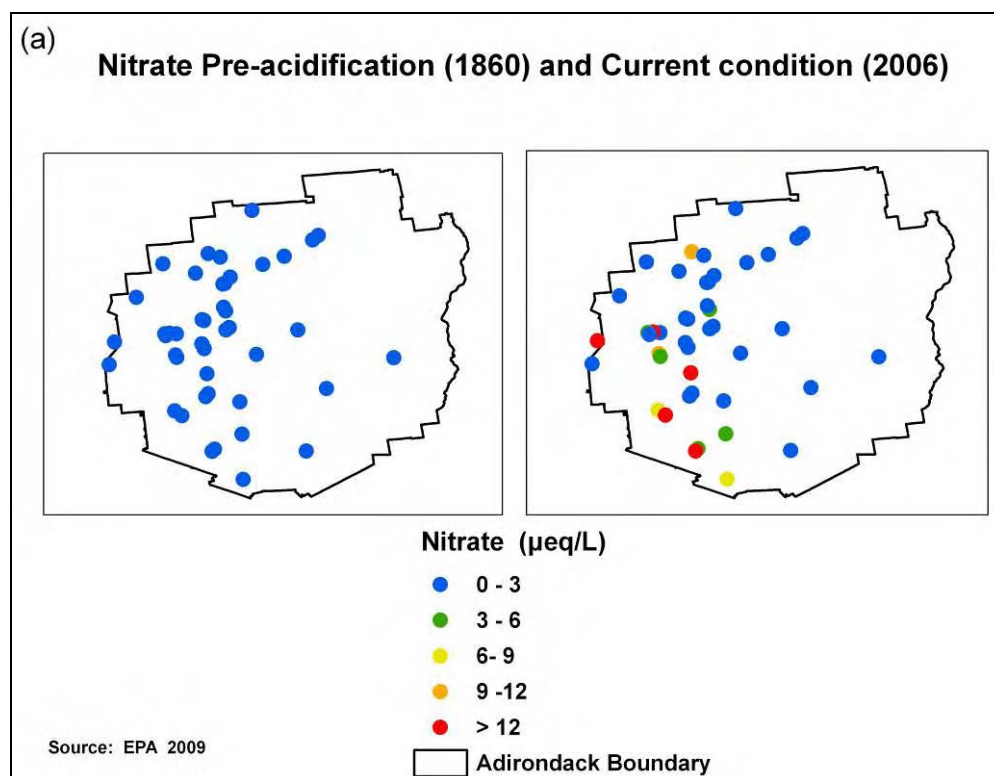
**Figure 5.1-1.** Average  $\text{NO}_3^-$  concentrations (orange),  $\text{SO}_4^{2-}$  concentrations (red), and ANC (blue) for the 44 lakes in the Adirondack Case Study Area modeled using MAGIC for the period 1850 to 2050.

On average, simulated  $\text{SO}_4^{2-}$  and  $\text{NO}_3^-$  surface water concentrations are 5- and 17-fold higher today, respectively, compared with 1860 acidification levels, whereas ANC has dropped by a factor of 2 (**Table 5.1-1**, **Figure 5.1-2**). Although  $\text{NO}_3^-$  deposition can be an important factor in acid precipitation and waterbody acidification, the strong inverse relationship between  $\text{SO}_4^{2-}$  and ANC, in combination with the low levels of  $\text{NO}_3^-$  in surface waters, suggests that acidification in the Adirondack Case Study Area has and continues to be driven by  $\text{SO}_4^{2-}$  deposition.

**Table 5.1-1.** Estimated Average Concentrations of Surface Water Chemistry for 44 Lakes in the Adirondack Case Study Area Modeled Using MAGIC for Preacidification (1860) and Current (2006) Conditions

$\mu\text{eq/L}$	Preacidification		Current	
	Ave.	( $\pm$ )	Ave.	( $\pm$ )
ANC	120.3	13.6	62.1	15.7
$\text{SO}_4^{2-}$	12.4	2.1	66.1	1.24
$\text{NO}_3^-$	0.2	1.7	3.4	14.8
$\text{NH}_4^+$	0.0	0.0	0.1	0.1

An estimate of how much of this current condition is attributed to the effects of industrially generated acidifying deposition can be made by examining the hindcast conditions of the streams. Based on the MAGIC model simulations, the preacidification average ANC concentration of 44 modeled lakes is 120.3  $\mu\text{eq/L}$  (95% CI 106.8 to 134.0) compared with 62.1  $\mu\text{eq/L}$  (95% CI 50.5 to 81.8) for today (**Table 5.1-1**).



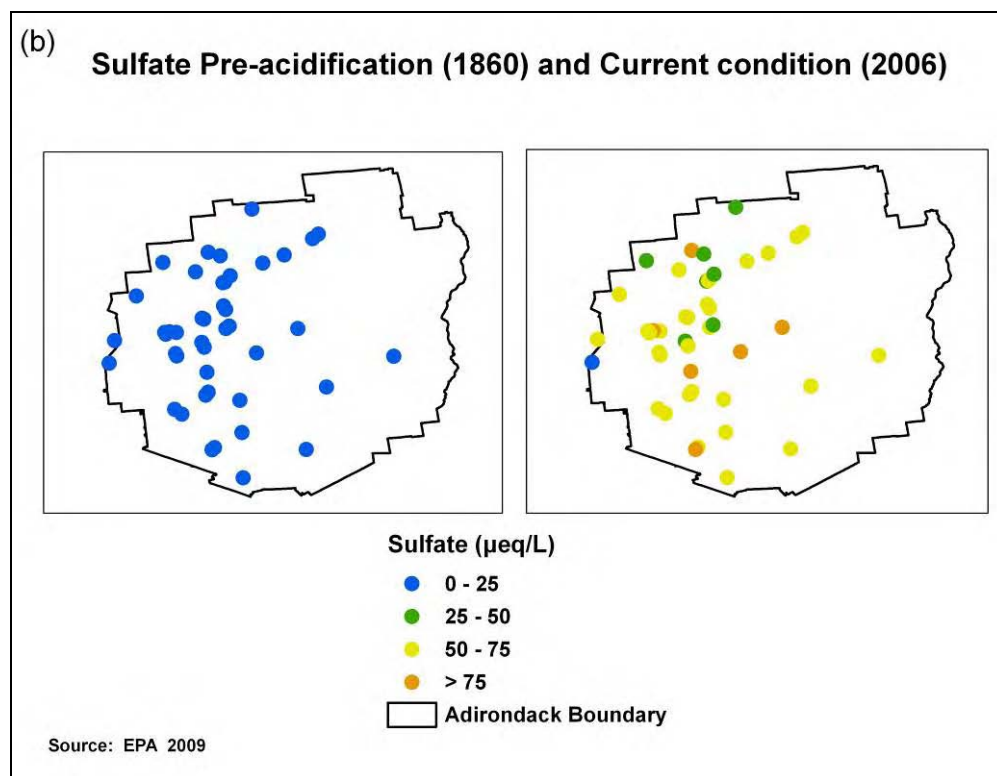


**Figure 5.1-2. (a)  $\text{NO}_3^-$  and (b)  $\text{SO}_4^{2-}$  concentrations ( $\mu\text{eq/L}$ ) of preacidification (1860) and current (2006) conditions based on hindcasts of 44 lakes in the Adirondack Case Study Area modeled using MAGIC.**

### 5.1.2 ANC Inferred Condition—Aquatic Status Categories.

The deposition of sulfur and nitrogen and resulting changes in water quality has effects on ANC values, and by consequence, the biological integrity of the water ecosystem. By comparing their current surface water condition with their preindustrial (i.e., preacidification or 1860) condition through the MAGIC model simulations of 44 lakes, it is possible to estimate how the distribution of affected lakes within the Adirondack Case Study Area has changed over time. Furthermore, grouping each lake into aquatic status categories provides the range of biological condition. The percentage of lakes in each of the five aquatic status categories is shown in **Table 5.1-2**. Eighty-nine percent of the modeled lakes were likely Low Concern or Moderate Concern (i.e., ANC levels  $>50 \mu\text{eq/L}$ ) prior to the onset of acidifying deposition (**Figure 5.1-3**), whereas the remaining 11% of lakes have ANC  $>20 \mu\text{eq/L}$ .

**Table 5.1-2.** Percentage of Lakes in the Five Aquatic Status Categories Based on Their Surface Water ANC Levels for 44 Lakes Modeled Using MAGIC and 88 Lakes in the TIME/LTM Monitoring Network. Results Are for the Adirondack Case Study Area for the Years 2005 to 2006.

Concern	ANC ( $\mu\text{eq/L}$ )	Modeled Pre-Acidification (% of Lakes)	Modeled Current Condition (% of Lakes)	Measured Current Condition (% of Lakes)
Low	>100	50	20	6
Moderate	50–100	39	36	16
Elevated	20–50	11	23	32
Severe	0–20	0	9	29
Acute	<0	0	11	17

In contrast, the current simulated condition of the lakes has shifted toward the chronically acidified categories. Only 20% and 36% of the lakes currently experience the Low Concern or Moderate Concern condition, having ANC concentrations >50  $\mu\text{eq/L}$ , whereas 43% of the lakes are in either the Acute Concern, Severe Concern, or Elevated Concern condition. The result that the hindcast simulations produced no lakes with Acute Concern or Severe Concern preacidification suggests that current and recent historical ambient concentrations of  $\text{NO}_x$  and  $\text{SO}_x$  and their associated levels of  $\text{NO}_3^-$  and  $\text{SO}_4^{2-}$  deposition have substantially contributed to acidification (<50  $\mu\text{eq/L}$ ) to approximately 32% of modeled lakes. **Figure 5.1-4** shows the spatial extent of preacidification and the current annual average ANC levels in the Adirondack Case Study Area.

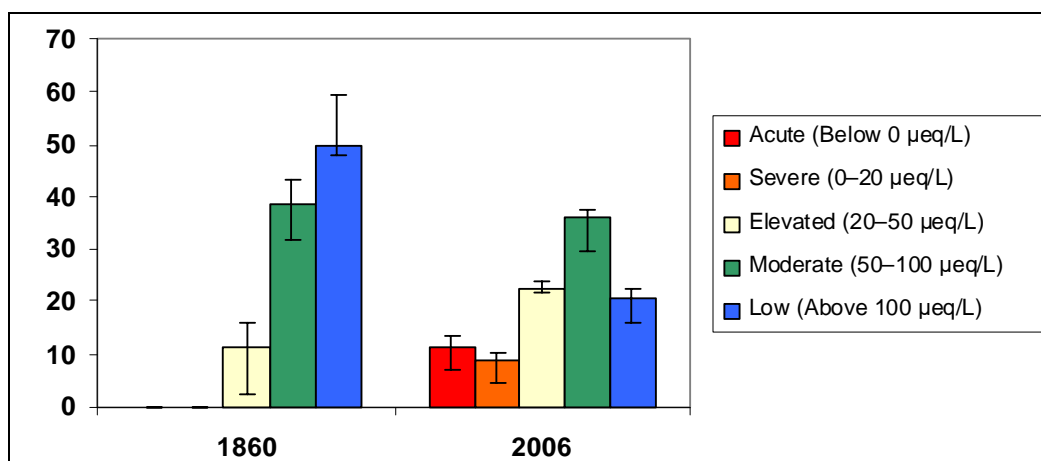


**Figure 5.1-3.** Percentage of lakes in the five classes (Acute, Severe, Elevated, Moderate, Low) for years 1860 (preacidification) and 2006 (current) conditions for 44 lakes modeled using MAGIC. Error bars indicate the 95% confidence interval.

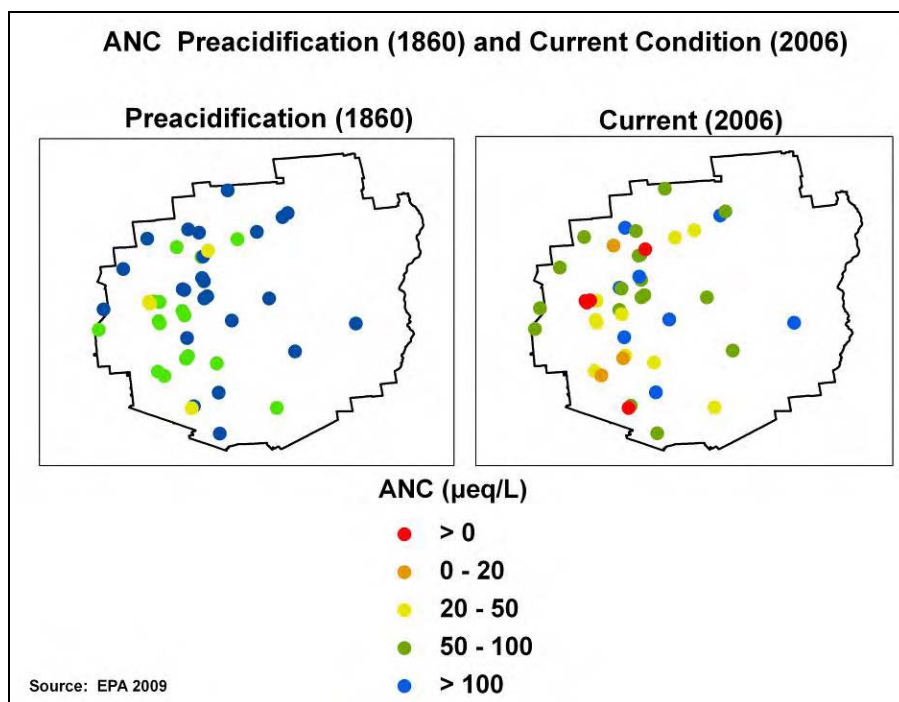


**Figure 5.1-4.** ANC concentrations of preacidification (1860) and current (2006) conditions based on hindcasts of 44 lakes in the Adirondack Case Study Area modeled using MAGIC.

### 5.1.3 The Biological Risk from Current Nitrogen and Sulfur Deposition: Critical Load Assessment

The amount of acidifying deposition of sulfur and nitrogen that a watershed can receive and effectively neutralize varies with location, depending on the biogeochemical properties of the watershed. A critical load of deposition approach, where the amount of deposition that a watershed can receive and maintain an ANC critical limit level, can provide insight into the sensitivity of the waterbody to deposition and can allow an assessment of what the current condition of the lake might be under current deposition loads.

A critical load of deposition analysis for a critical limit ANC threshold level of 50 µeq/L was done for 169 waterbodies in the Adirondack Case Study Area. Sites that are unable to maintain the critical limit ANC level of 50 µeq/L while experiencing 100 meq/m<sup>2</sup>/yr or less of deposition are classified as “highly” or “moderately sensitive,” indicating that they have a limited ANC ability and could shift toward acidic aquatic status levels with modest acidifying deposition inputs. **Figure 5.1-5** shows the locations and relative sensitivity of the 169 waterbodies for the critical load analysis (with the 50 µeq/L ANC critical limit). Sites labeled by red or orange circles have less neutralizing ability than lakes labeled with yellow and green

circles, and therefore, are those lakes most sensitive to acidifying deposition. Approximately 50% of the 169 lakes modeled in the Adirondack Case Study Area are sensitive, or at risk, to acidifying deposition.

In **Figure 5.1-6**, a critical load exceedance “value” indicates combined sulfur and nitrogen deposition for the year 2002 is greater than the amount of deposition the lake could neutralize and still maintain an ANC level at or above the critical limit threshold. For the deposition load for the year 2002, 18%, 28%, 44%, and 58% of the 169 lakes modeled received levels of combined sulfur and nitrogen deposition that exceeded their critical load for the critical limit ANC values of 20, 50, and 100  $\mu\text{eq/L}$ , respectively (**Table 5.1-3**).

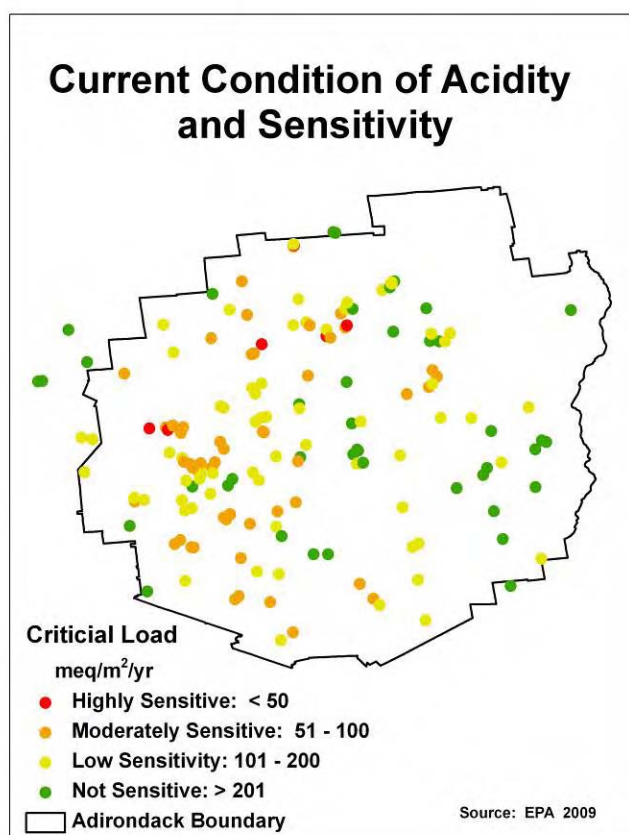


**Figure 5.1-5.** Critical loads of acidifying deposition that each surface water location can receive in the Adirondack Case Study Area while maintaining or exceeding an ANC concentration of 50  $\mu\text{eq/L}$  based on 2002 data. Watersheds with critical load values  $<100 \text{ meq/m}^2/\text{yr}$  (red and orange circles) are most sensitive to surface water acidification, whereas watersheds with values  $>100 \text{ meq/m}^2/\text{yr}$  (yellow and green circles) are the least sensitive sites.

**Table 5.1-3.** Adirondack Case Study Area Critical Load Exceedances, Where Nitrogen and Sulfur Deposition Is Larger Than the Critical Load for Four Different ANC Critical Limit Thresholds, for 169 Modeled Lakes within the TIME/LTM and EMAP Monitoring and Survey Programs. “No. Exceedances” Indicates the Number of Lakes at or below the Given ANC Critical Limit, and “% Lakes” Indicates the Total Percentage of Lakes at or below the Given ANC Critical Limit.

<b>ANC Critical Limit</b>	<b>No. Exceedances (out of 169 Lakes)</b>	<b>% Lakes</b>
100 µeq/L	98	58
50 µeq/L	74	44
20 µeq/L	47	28
0 µeq/L	30	18



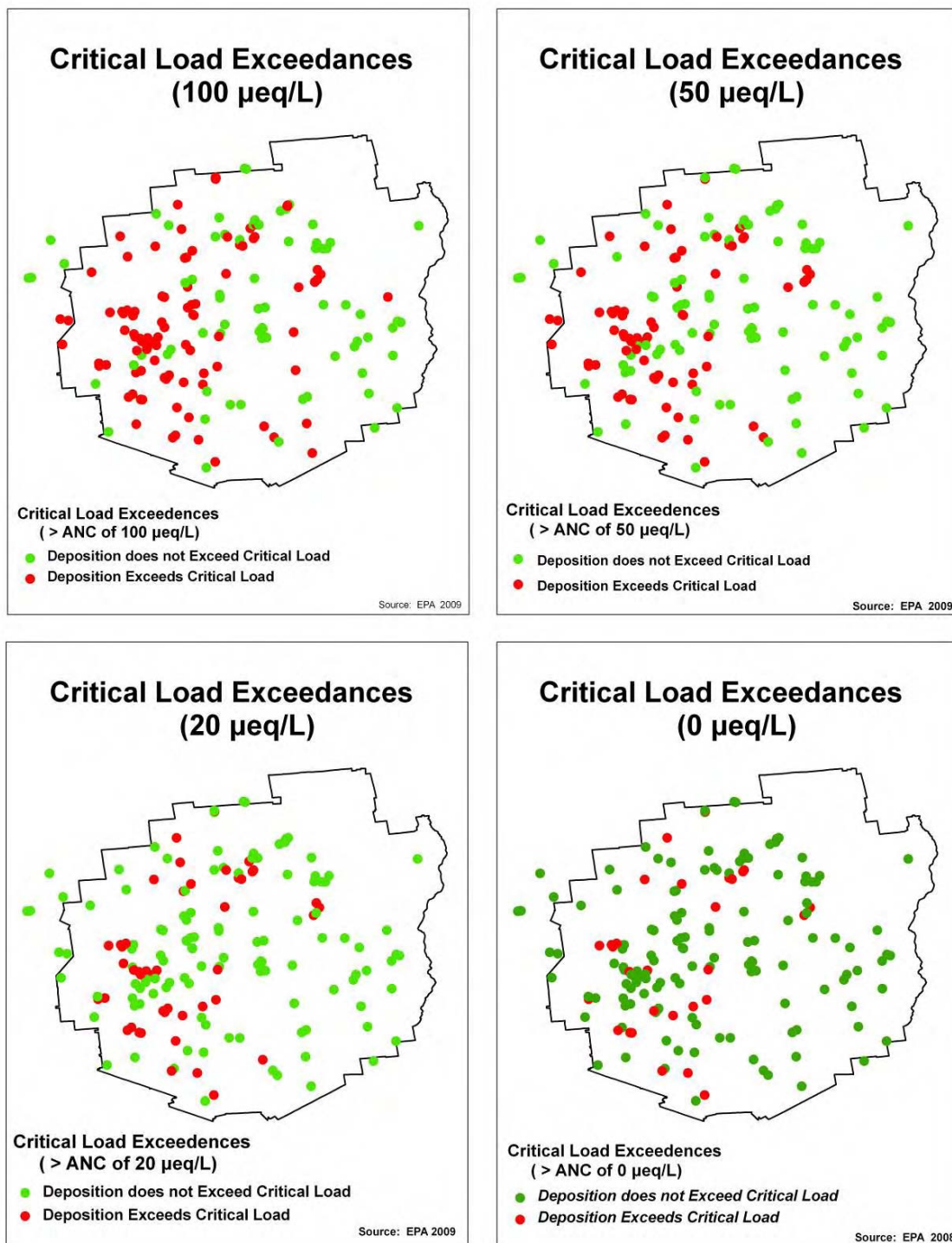


**Figure 5.1-6.** Critical load exceedances (red circles) in the Adirondack Case Study Area based on the year 2002 deposition magnitudes for waterbodies where the critical limit ANC concentration is 0, 20, 50, and 100 µeq/L, respectively. Green circles represent lakes where deposition is below the critical load. See Table 5.1-3.



### 5.1.4 Representative Sample of Lakes in the Adirondack Case Study Area

Estimating the acidification risk to the entire population of lakes in the Adirondack Case Study Area from the current the levels of  $\text{NO}_x$  and  $\text{SO}_x$  ambient concentrations and deposition requires extrapolating from the 169 modeled lakes to the broader population of lakes in the Adirondack Case Study Area. One hundred seventeen lakes of the 169 lakes modeled for critical loads are part of a subset of 1,842 lakes in the Adirondack Case Study Area, which include all lakes from 0.5 to 2000 ha in size and at least 1 m in depth. Using weighting factors for frequency of occurrence derived from the EMAP probability survey and critical load calculations from the 117 lakes, exceedances estimates were derived for the 1,842 lakes in the Adirondack Case Study Area. Based on this approach, 945, 666, 242, and 135 lakes exceed their critical load for the year 2002 deposition with critical limits of 100, 50, 20, and 0  $\mu\text{eq/L}$ , respectively (**Table 5.1-4**). The current effect level for a moderate protective (i.e., ANC limit of 20 and 50  $\mu\text{eq/L}$ ) is 13% of the total population and 36% of the total population, whereas it is 51% of the total population for the most protective level (i.e., ANC limit of 100  $\mu\text{eq/L}$ ).

**Table 5.1-4.** Critical Load Exceedances for the Regional Population of 1,842 Lakes in the Adirondack Case Study Area That Are from 0.5 to 2,000 ha in Size and at Least 1 m in Depth for the Four Critical Limit ANC Levels (0, 20, 50, and 100  $\mu\text{eq/L}$ ). Estimates Use the Exceedances for the Subset of 169 Lakes Using 2002 Deposition Magnitudes (**Table 5.1-3**) and Are Extrapolated to the Full Population Based on the EMAP Lake Probability Survey of 1991 to 1994. “No. Exceedances” Indicates the Number of Lakes at or Below the Given ANC Critical Limit; “% Lakes” Indicates the Total Percentage of Lakes at or Below the Given ANC Critical Limit.

ANC Critical Limit	No. Exceedances (out of 1842)	% Lakes
100 $\mu\text{eq/L}$	945	51
50 $\mu\text{eq/L}$	666	36
20 $\mu\text{eq/L}$	242	13
0 $\mu\text{eq/L}$	13	7

Because some lakes in the Adirondack Case Study Area have natural sources of acidity, they would never have ANC levels >50 or 100  $\mu\text{eq/L}$ , even in the absence of all anthropogenic-derived acidifying deposition. Based on the hindcast simulations of 44 lakes using the MAGIC model, no modeled lakes have ANC levels <20  $\mu\text{eq/L}$ . However, 5 modeled lakes, or 11% of modeled lakes, have ANC concentrations between 22 and 47  $\mu\text{eq/L}$ . This equates to

approximately 300 lakes, or 16%, of the representative population of lakes in the Adirondack Case Study Area that likely had preacidification ANC levels  $<50$   $\mu\text{eq/L}$ . On the other hand, potentially  $>52\%$  of lakes likely had preacidification ANC levels  $<100$   $\mu\text{eq/L}$ . The higher percentage of lakes in the regional population compared with the modeled population is because the lake classes or sizes that are likely to have preacidification ANC levels  $<50$  or  $100$   $\mu\text{eq/L}$  are more abundant in the Adirondack Case Study Area than lakes with preacidification ANC levels  $>50$  or  $100$   $\mu\text{eq/L}$ .

### 5.1.5 Recovery from Acidification Given Current Emission Reductions

The question is whether lakes can recover to healthy systems (i.e., ANC  $>50$ , or  $100$   $\mu\text{eq/L}$ ) given the current surface water and ecosystem conditions of the lakes and current emission and deposition levels in the Adirondack Case Study Area. The forecast model runs of 44 lakes using MAGIC were used to determine if current deposition could lead to recovery of the acidified lakes. Based on a deposition scenario that maintains current emission levels up to years 2020 and 2050, the simulation forecast indicates no improvement in water quality over either of these periods. The percentage of lakes within the Elevated Concern to Acute Concern categories remains the same in the years 2020 and 2050 (**Figure 5.1-7**). Moreover, the percentage of modeled lakes classified as not acidic remains the same, suggesting that current emission levels will not likely improve their recovery from acidification in the Adirondack Case Study Area.

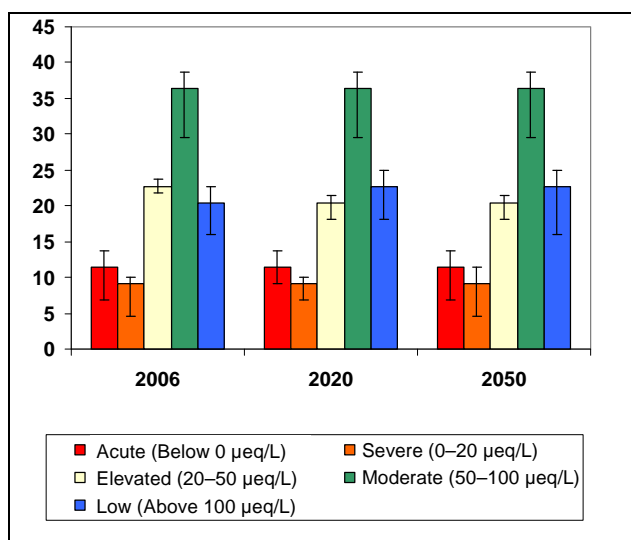


**Figure 5.1-7.** Percentage of lakes in each of the five classes of acidification (Acute, Severe, Elevated, Moderate, Low) for the years 2006, 2020, and 2050 for 44 lakes modeled using MAGIC, where current emissions are held constant. Error bars indicate the 95% confidence interval.

## 5.2 SHENANDOAH CASE STUDY AREA

### 5.2.1 Current and Preacidification Conditions of Surface Waters

Since the mid-1990s, streams in the Shenandoah Case Study Area have shown slight signs of improvement in  $\text{NO}_3^-$  and  $\text{SO}_4^{2-}$  concentrations in surface waters (see **Figure 3.4-2**). However, current concentrations of  $\text{NO}_3^-$  and  $\text{SO}_4^{2-}$  are still well above preacidification conditions based on MAGIC model simulations, resulting in lower ANC levels of surface water (**Figure 5.2-1**).

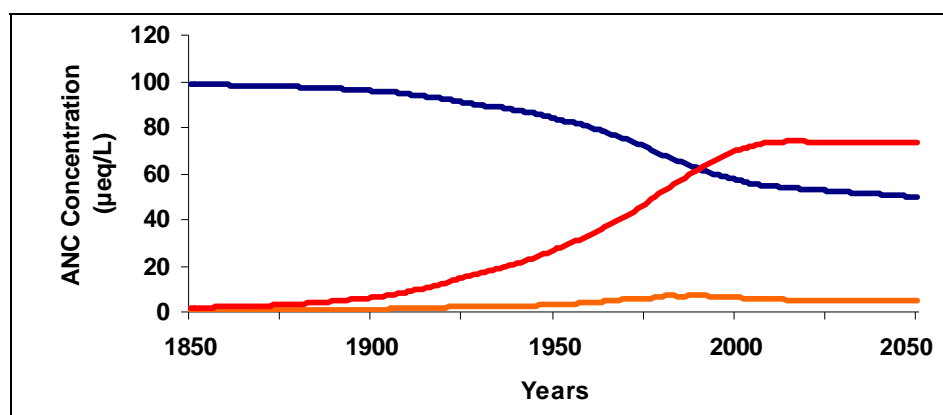


**Figure 5.2-1.** Average  $\text{NO}_3^-$  concentrations (orange),  $\text{SO}_4^{2-}$  concentrations (red), and ANC (blue) levels for the 60 streams in the Shenandoah Case Study Area modeled using MAGIC for the period 1850 to 2050.

**Figure 5.2-2** shows the condition of the streams in the year 1860 (i.e., preacidification) and in the year 2006 (i.e., current) conditions. On average,  $\text{NO}_3^-$  and  $\text{SO}_4^{2-}$  concentrations are 32- and 10-fold higher today (**Table 5.2-1**). These results also demonstrate that acidification in most streams in the Shenandoah Case Study Area are currently being driven by  $\text{SO}_4^{2-}$  deposition because the current average  $\text{SO}_4^{2-}$  concentration is 11-fold greater than  $\text{NO}_3^-$  concentrations in surface waters.

An estimate of how much of this current condition is attributed to the effects of industrially generated acidifying deposition can be made by examining the hindcast conditions of the streams. Based on the MAGIC model simulations, preacidification average ANC level of the 60 modeled streams is 101.4 (95% CI 91.9 to 110.9) µeq/L compared with 57.9 (95% CI 53.4 to 62.4) µeq/L for today (**Table 5.2-1**).

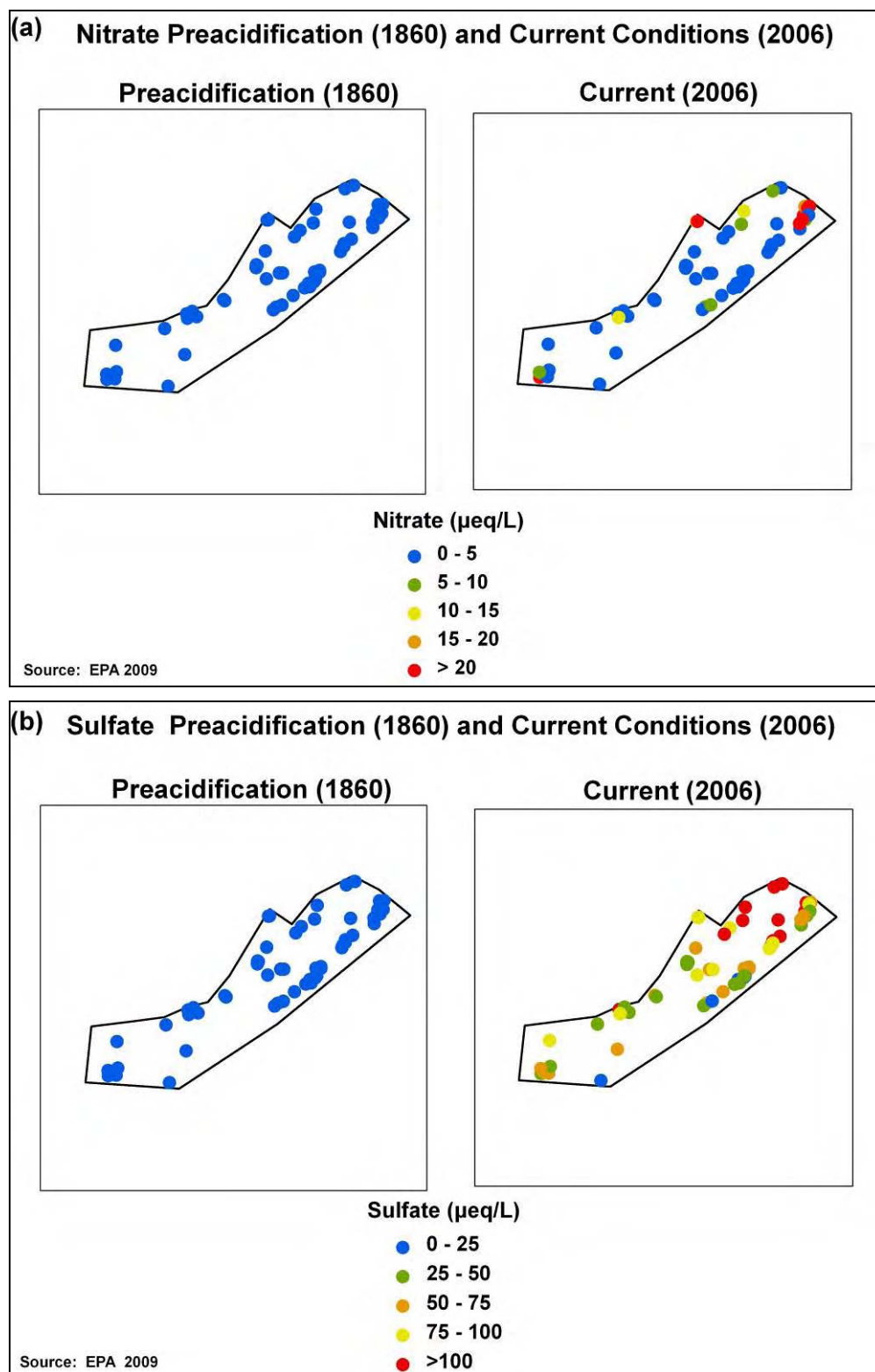


**Figure 5.2-2. (a)  $\text{NO}_3^-$  and (b)  $\text{SO}_4^{2-}$  concentrations (µeq/L) of 1860 (preacidification) and 2006 (current) conditions based on hindcasts of 60 streams in the Shenandoah Case Study Area modeled using MAGIC.**

**Table 5.2-1.** Estimated Average Concentrations of Surface Water Chemistry for 60 Streams in the Shenandoah Case Study Area Modeled Using MAGIC for Preacidification (1860) and Current (2006) Conditions

	Preacidification		Current	
$\mu\text{eq/L}$	Avg.	( $\pm$ )	Avg.	( $\pm$ )
ANC	101.4	9.5	57.9	4.5
$\text{SO}_4^{2-}$	2.1	0.1	68.0	8.4
$\text{NO}_3^-$	0.6	0.01	6.2	0.1
$\text{NH}_4^+$	n/a	n/a	n/a	n/a

### 5.2.2 ANC Inferred Condition—Aquatic Status Categories

The percentage of streams in each of the five aquatic status categories is shown in **Table 5.2-2** and in the graph in **Figure 5.2-3**. Ninety-two percent of the modeled streams likely were at the Low Concern or Moderate Concern conditions prior to the onset of acidifying deposition. The other 8% of streams have ANC of  $>27 \mu\text{eq/L}$ . The hindcast simulations produced no streams with Acute Concern or Severe Concern conditions.

**Table 5.2-2.** Percentage of Streams in the Five Aquatic Status Categories Based on Their Surface Water ANC Concentrations for 60 Streams Modeled Using MAGIC and 67 Streams in the SWAS-VTSSS LTM Network. Results are for the Shenandoah Case Study Area for the Year 2006.

Concern	ANC ( $\mu\text{eq/L}$ )	Modeled Preacidification Condition (% of Streams)	Modeled Current Condition (% of Streams)	Measured Current Condition (% of Streams)
Low	$>100$	42	27	15
Moderate	50–100	50	20	30
Elevated	20–50	8	28	25
Severe	0–20	0	12	18
Acute	$<0$	0	13	12

In contrast, the current simulated condition of the streams has shifted toward the chronically acidified categories. Only 47% of the streams currently experience the Low Concern or Moderate Concern conditions, whereas 53% of the streams experience the Acute Concern, Severe Concern, or Elevated Concern conditions. These results based on model reconstructions suggest that anthropogenic acidifying deposition is responsible for acidifying ( $\text{ANC} < 50 \mu\text{eq/L}$ )

approximately 45% of streams modeled in the Shenandoah Case Study Area. **Figure 5.2-4** shows the spatial extent of preacidification and current annual average ANC levels in the Shenandoah Case Study Area.

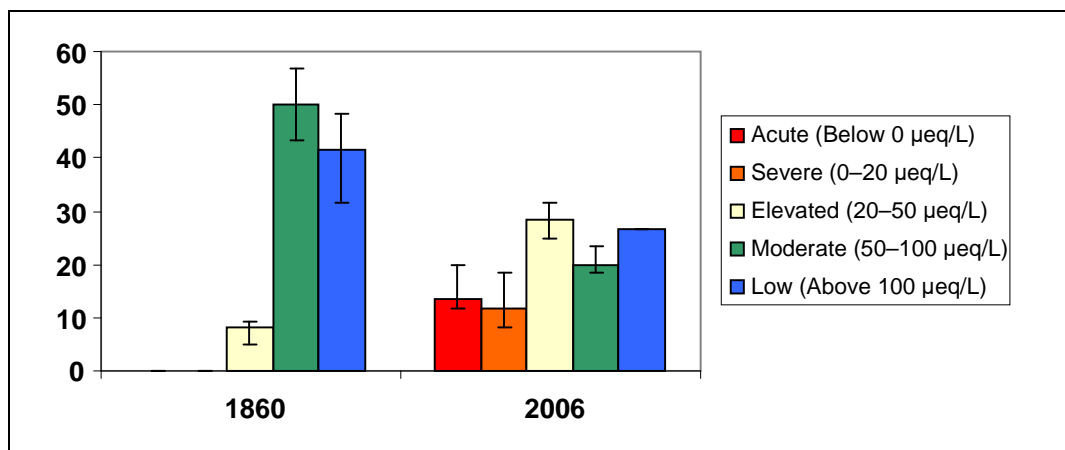


**Figure 5.2-3.** Percentage of streams in the five classes of acidification (Acute, Severe, Elevated, Moderate, Low) for years 1860 (preacidification) and 2006 (current) conditions for 60 streams modeled using MAGIC. The number of streams in each category is above the bar. Error bars indicate the 95% confidence interval.

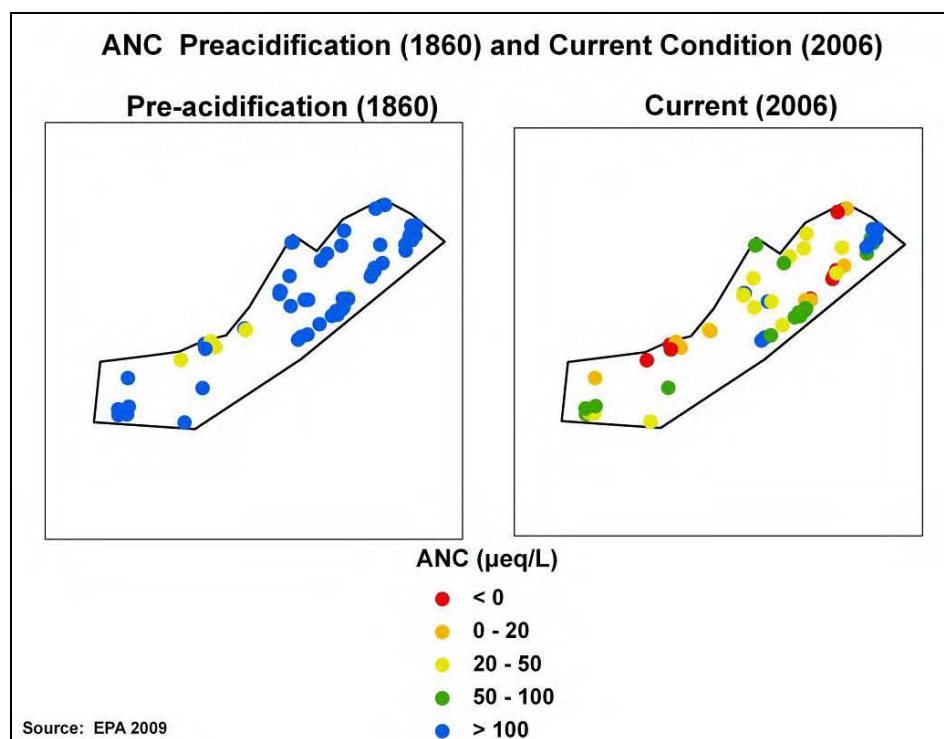


**Figure 5.2-4.** ANC levels of 1860 (preacidification) and 2006 (current) conditions based on hindcasts of 60 streams in the Shenandoah Case Study Area modeled using MAGIC.

### 5.2.3 The Biological Risk from Current Nitrogen and Sulfur Deposition: Critical Load Assessment

In **Figure 5.2-5**, sites labeled by red or orange circles have less ability to neutralize acid inputs than streams labeled with yellow and green circles, and therefore, are streams most sensitive to acidifying deposition. Approximately 75% of the 60 streams modeled in the Shenandoah Case Study Area are sensitive or at risk to acidifying deposition.

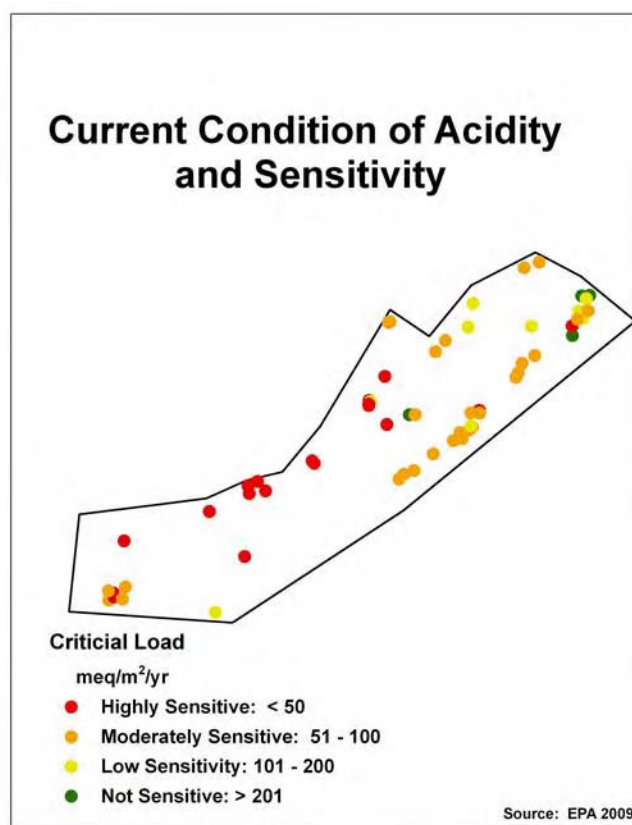


**Figure 5.2-5.** Critical loads of surface water acidity for an ANC of 50  $\mu\text{eq/L}$  for Shenandoah Case Study Area streams. Each dot represents an estimated amount of acidifying deposition (i.e., critical load) that each stream's watershed can receive and still maintain a surface water ANC  $>50 \mu\text{eq/L}$ . Watersheds with critical load values  $<100 \text{ meq/m}^2/\text{yr}$  (red and orange circles) are most sensitive to surface water acidification, whereas watersheds with values  $>100 \text{ meq/m}^2/\text{yr}$  (yellow and green circles) are the least sensitive sites.

In **Figure 5.2-6**, a critical load exceedance “value” indicates combined sulfur and nitrogen deposition in the year 2002 that is greater than the amount of deposition the stream could buffer and still maintain the ANC level of above each of the four different ANC limits of 0, 20, 50, and 100  $\mu\text{eq/L}$ . For the year 2002, 52%, 72%, 85%, and 92% of the 60 streams

modeled receive levels of combined sulfur and nitrogen deposition that exceeded their critical load with critical limits of 0, 20, 50, and 100  $\mu\text{eq/L}$ , respectively (Table 5.2-3).

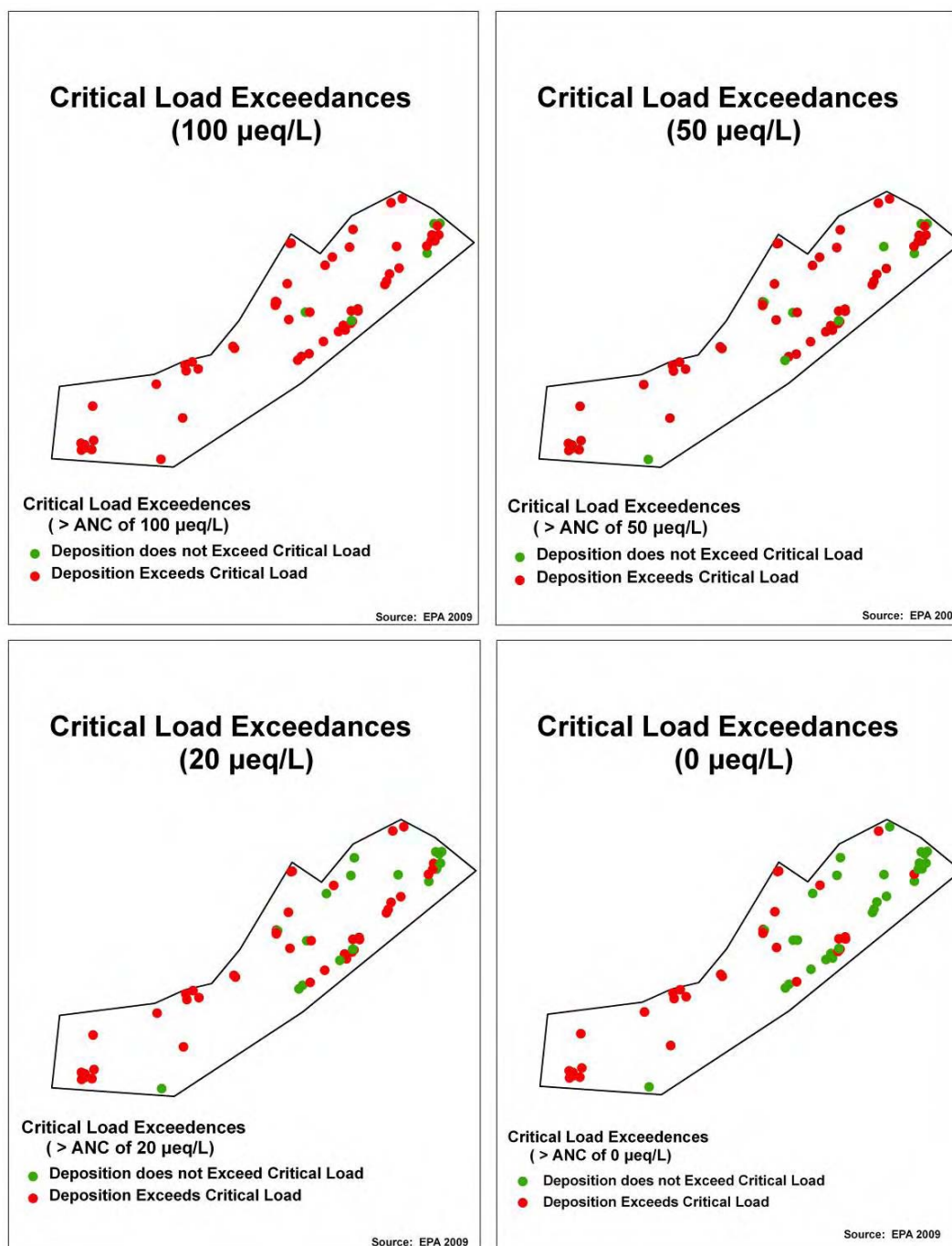


**Figure 5.2-6.** Critical load exceedances for ANC levels of 0, 20, 50, and 100  $\mu\text{eq/L}$  for Shenandoah Case Study Area streams. Green circles represent streams where current nitrogen and sulfur deposition is below the critical load and that maintain an ANC level of 0, 20, 50, and 100  $\mu\text{eq/L}$ , respectively. Red circles represent streams where current nitrogen and sulfur deposition exceeds the critical load, indicating they are currently impacted by acidifying deposition. See Table 5.2-3.



**Table 5.2-3.** Critical Load Exceedances (Nitrogen + Sulfur Deposition > Critical Load) for 60 Modeled Streams within the VTSSS LTM Program in the Shenandoah Case Study Area. “No. Exceedances” Indicates the Number of Streams at the Given ANC Limit; “% Streams” Indicates the Total Percentage of Streams at the Given ANC Limit.

ANC Critical Limit	100 µeq/L	50 µeq/L	20 µeq/L	0 µeq/L
No. Exceedances (out of 60)	55	51	43	31
% Streams	92	85	72	52

#### 5.2.4 Regional Assessment of Trout Streams in the Shenandoah Case Study Area

The 60 trout streams modeled are characteristic of first- and second-order streams on nonlimestone bedrock in the Blue Ridge Mountains of Virginia. Because of the strong relationship between bedrock geology and ANC in this region, it is possible to consider the results in the context of similar trout streams in the Southern Appalachians that have the same bedrock geology and size. In addition, the 60 streams are a subset of 344 streams sampled by the Virginia Trout Stream Sensitivity Study, which can be applied to 304 of the original 344 streams. Using the 304 streams to which the analysis applies directly as the total, 279, 258, 218, and 157 streams exceed their critical load for the year 2002 deposition with critical limits of 100, 50, 20, and 0 µeq/L, respectively. However, it is likely that many more of the ~12,000 trout streams in Virginia would exceed their critical load, given the extent of similar bedrock geology outside of the case study area in the southern Appalachian Mountains.

#### 5.2.5 Recovery from Acidification Given Current Emission Reductions

Based on a deposition scenario that maintains current emission levels to the years 2020 and 2050, there will still be a large number of streams in Virginia that have Elevated Concern to Acute Concern problems with acidity (**Figure 5.2-7**). In the short term (i.e., by the year 2020) and in the long term (i.e., by the year 2050), the response of the 60 modeled streams shows no improvement in the number of streams that have Moderate Concern conditions. In fact, under current emission levels, the modeling suggests that conditions may degrade by the year 2050. In **Figure 5.2-7** the percentage of streams in Acute Concern condition increases by 5%, whereas streams in Moderate Concern condition decreases by 5%.

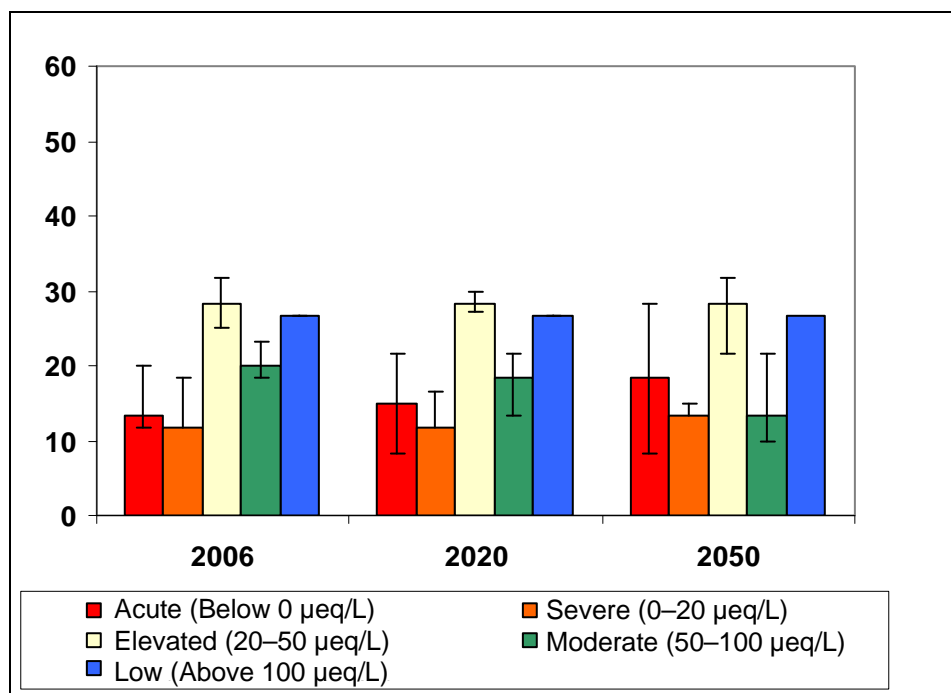


**Figure 5.2-7.** Percentage of streams in the five categories of acidification (Acute, Severe, Elevated, Moderate, Low) for the years 2006, 2020, and 2050 for 60 streams in the Shenandoah Case Study Area modeled using MAGIC. The number of streams in each category is above the bar. Error bars indicate the 95% confidence interval.

## 6. REFERENCES

- Baker, J.P., W.J. Warren-Hicks, J. Gallagher, and S.W. Christensen. 1993. Fish population losses from Adirondack lakes: The role surface water acidity and acidification. *Water Resources Research* 29:861–874.
- Brakke, D.F., A. Henriksen, and S.A. Norton. 1989. Estimated background concentrations of sulfate in dilute lakes. *Water Resources Bulletin* 25(2):247–253.
- Brakke, D.F., A. Henriksen, and S.A. Norton. 1990. A variable F-factor to explain changes in base cation concentrations as a function of strong acid deposition. *International Association of Theoretical and Applied Limnology, Proceedings* 24:146–149.
- Bulger, A.J., B.J. Cosby, C.A. Dolloff, K.N. Eshleman, J.R. Webb, and J.N. Galloway. 1999. *SNP:FISH, Shenandoah National Park: Fish in Sensitive Habitats, Volumes I through IV*. Project final report. Project Completion Report to the National Park Service. Cooperative Agreement CA-4000-2-1007, Supplemental Agreement #2. University of Virginia, Department of Environmental Sciences, Charlottesville, VA.
- Bulger, A.J., B.J. Cosby, and J.R. Webb. 2000. Current, reconstructed past, and projected future status of brook trout (*Salvelinus fontinalis*) streams in Virginia. *Canadian Journal of Fisheries and Aquatic Sciences* 57:1515–1523.
- Cosby, B.J., R.F. Wright, G.M. Hornberger, and J.N. Galloway. 1985a. Modelling the effects of acid deposition: Assessment of a lumped parameter model of soil water and streamwater chemistry. *Water Resources Research* 21:51–63.
- Cosby, B.J., R.F. Wright, G.M. Hornberger, and J.N. Galloway. 1985b. Modelling the effects of acid deposition: Estimation of long-term water quality responses in a small forested catchment. *Water Resources Research* 21:1591–1601.
- Cosby, B.J., G.M. Hornberger, P.F. Ryan, and D.M. Wolock. 1989. *MAGIC/DDRP Final Report*. Project Completion Report. U.S. Environmental Protection Agency, Direct/Delayed Response Project, Corvallis, OR.

- Cosby, B.J., A. Jenkins, R.C. Ferrier, J.D. Miller, and T.A.B. Walker. 1990. Modelling stream acidification in afforested catchments: Long-term reconstructions at two sites in central Scotland. *Journal of Hydrology* 120:143–162.
- Cosby, B.J., S.A. Norton, and J.S. Kahl. 1996. Using a paired-catchment manipulation experiment to evaluate a catchment-scale biogeochemical model. *Science of the Total Environment* 183:49–66.
- Dennis, T.E., and A.J. Bulger. 1995. Condition factor and whole-body sodium concentrations in a freshwater fish: Evidence for acidification stress and possible ionoregulatory overcompensation. *Water, Air, and Soil Pollution* 85:377–382.
- De Vries, W., G. J. Reinds, and M. Posch. 1994. Assessment of critical loads and their exceedance on European forests using a one-layer steady-state model. *Water, Air, and Soil Pollution* 72:357–394.
- DeWalle, D. R. Swistock, B. R. 1994. Causes of episodic acidification in five Pennsylvania streams on the northern Appalachian Plateau. *Water Resources Research* 30: 1955-1963.
- Driscoll C. T. Van Dreason, R. 1993. Seasonal and long-term temporal patterns in the chemistry of Adirondack lakes. *Water Air Soil Pollution* 67: 319-344
- Driscoll, C.T., R.M. Newton, C.P. Gubala, J.P. Baker, and S.W. Christensen. 1991. Adirondack mountains. Pp. 133–202 in *Acidic Deposition and Aquatic Ecosystems: Regional Case Studies*. Edited by D.F. Charles. New York: Springer-Verlag.
- Driscoll, C. T. Postek, K. M., Kretser, E, Raynal, D. J. 1995. Long-term trends in the chemistry of precipitation and lake water in the Adirondack region of New York, USA. *Water Air Soil Pollution* 85: 583-588.
- Driscoll, C.T., G.B. Lawrence, A.J. Bulger, T.J. Butler, C.S. Cronan, C. Eagar, K.F. Lambert, G.E. Likens, J.L. Stoddard, and K.C. Weathers. 2001. Acidic deposition in the northeastern United States: sources and inputs, ecosystem effects, and management strategies. *BioScience* 51:180–198.

- Driscoll, C.T., K.M. Driscoll, K.M. Roy, and M.J. Mitchell. 2003. Chemical response of lakes in the Adirondacks of New York to declines in acidic deposition. *Environmental Science and Technology* 37:2036–2042.
- Dupont, J., T.A. Clair, C. Gagnon, D.S. Jeffries, J.S. Kahl, S.J. Nelson, and J.M. Peckenham. 2005. Estimation of critical loads of acidity for lakes in northeastern United States and eastern Canada. *Environmental Monitoring and Assessment* 109: 275–291
- Ford, J., J.L. Stoddard, and C.F. Powers. 1993. Perspectives in environmental monitoring: an introduction to the U.S. EPA Long-Term Monitoring (LTM) project. *Water, Air, and Soil Pollution* 67:247–255.
- Gran G. Determination of the equivalence point in potentiometric titrations. Part 11. *Analyst* 1952;77:661-671.
- Grimm, J.W., and J.A. Lynch. 2004. Enhanced wet deposition estimates using modeled precipitation inputs. *Environmental Monitoring and Assessment* 90:243–268.
- Haines, T.A., and J.P. Baker. 1986. Evidence of fish population responses to acidification in the Eastern United States. *Water, Air, and Soil Pollution*, 31:605–629
- Henriksen, A. 1984. Changes in base cation concentrations due to freshwater acidification. *International Association of Theoretical and Applied Limnology, Proceedings* 22:692–698.
- Henriksen, A., and M. Posch. 2001. Steady-state models for calculating critical loads of acidity for surface waters. *Water, Air, and Soil Pollution: Focus* 1:375–398.
- Henriksen, A., J. Kämäri, M. Posch, and A. Wilander. 1992. Critical loads of acidity: Nordic surface waters. *Ambio* 21:356–363.
- Herlihy, A.T., Larsen, D.P., Paulsen, S.G., Urquhart, N.S., Rosenbaum, B.J., 2000. Designing a spatially balanced, randomized site selection process for regional stream surveys: the EMAP Mid-Atlantic Pilot Study. *Environmental Monitoring and Assessment* 63: 95–113.

- Hornberger, G.M., B.J. Cosby, and R.F. Wright. 1989. Historical reconstructions and future forecasts of regional surface water acidification in southernmost Norway. *Water Resources Research* 25:2009–2018.
- Jenkins, A., B.J. Cosby, R.C. Ferrier, T.A.B. Walker, and J.D. Miller. 1990a. Modelling stream acidification in afforested catchments: An assessment of the relative effects of acid deposition and afforestation. *Journal of Hydrology* 120:163–181.
- Jenkins, A., P.G. Whitehead, B.J. Cosby, and H.J.B. Birks. 1990b. Modelling long-term acidification: A comparison with diatom reconstructions and the implication for reversibility. *Philosophical Transactions of the Royal Society of London, B* 327:435–440.
- Jenkins, A., P.G. Whitehead, T.J. Musgrove, and B.J. Cosby, 1990c. A regional model of acidification in Wales. *Journal of Hydrology* 116:403–416.
- Kahl, J. S., Norton, S. A., Cornan, C. S. Fernandez, I. J. Bacon, K. C., Haines, T. A. (1991) Maine. In Charles D. F. ed. Acidic deposition and aquatic ecosystems: regional case studies, New York, NY: *Spring-Verlag*: pp. 203-235.
- Kahl, J. S., Haines, T. A., Norton, S. A., Davis R. B. (1993) Recent trends in the acid-base status of surface waters in Maine, USA. *Water Air Soil Pollution* 67: 281-300
- Klemedtsson, L., and B. H. Svensson. 1988. Effects of acidic deposition on denitrification and N<sub>2</sub>O emission from forest soils. Pages 343–362 in J. Nilsson and P. Grennfelt (eds.), Critical loads for sulphur and nitrogen, Nord 1988:97. Nordic Council of Ministers, Copenhagen, Denmark.
- Kretser, W., J. Gallagher, and J. Nicolette. 1989. *Adirondack Lakes Study, 1984–1987: An Evaluation of Fish Communities and Water Chemistry*. Ray Brook, NY: Adirondack Lakes Survey Corporation.
- Landers, D.H., W.S. Overton, R.A. Linthurst, and D.F. Brakke. 1988. Eastern lake survey: Regional estimates of lake chemistry. *Environmental Science and Technology* 22:128–135.

- Larsen B. P., Urquhart, N. S. (1993) A framework for assessing the sensitivity of the EMAP design. In Larsen, D. P., Christie, S. J. eds. EMAP-surface waters 1991 pilot report. Corvallis, OR: U.S. Environmental Protection Agency: pp. 4.1-4.37
- Larsen, D.P., K.W. Thornton, N.S. Urquhart, and S.G. Paulsen. 1994. The role of sample surveys for monitoring the condition of the nation's lakes. *Environmental Monitoring and Assessment* 32:101–134.
- Lepistö, A., P.G. Whitehead, C. Neal, and B.J. Cosby. 1988. Modelling the effects of acid deposition: Estimation of longterm water quality responses in forested catchments in Finland. *Nordic Hydrology* 19:99–120.
- Lien, L., G.G. Raddum, and A. Fjellheim. 1992. *Critical Loads of Acidity to Freshwater: Fish and Invertebrates*. The Environmental Tolerance Levels Programme. Rep. No. 23/1992. Norwegian Ministry of Environment, Oslo, Norway.
- Lynch, D.D. and N.B. Dise. 1985. Sensitivity of stream basins in Shenandoah National Park to acid deposition. Water Resources Investigations Report 85-4115 1985:1]61. U.S. Department of Interior, U.S. Geological Survey, Reston, VA.
- Matuszek, J.E., and G.L. Beggs. 1988. Fish species richness in relation to lake area, pH, and other abiotic factors in Ontario lakes. *Canadian Journal of Fisheries and Aquatic Sciences* 45:1931–1941.
- Murdoch, P. S. Stoddard, J. L. (1993) Chemical characteristics and temporal trends in eight streams of the Catskill Mountains, New York. *Water Air Soil Pollution* 67: 367-395.
- NAPAP (National Acid Precipitation Assessment Program). 2005. *National Acid Precipitation Assessment Program Report to Congress: An Integrated Assessment*. National Acid Precipitation Assessment Program, Washington, DC.
- NAPAP (National Acid Precipitation Assessment Program). 1998. *NAPAP Biennial Report to Congress: An Integrated Assessment*. National Science and Technology Council, Committee on Environment and Natural Resources, Silver Spring, MD.

- Norton, S.A., R.F. Wright, J.S. Kahl, and J.P. Schofield. 1992. The MAGIC simulation of surface water at, and first year results from, the Bear Brook Watershed Manipulation, Maine, USA. *Environmental Pollution* 77:279–286.
- Paulsen, S.G., D.P. Larsen, P.R. Kaufmann, T.R. Whittier, J.R. Baker, D.V. Peck, J. McGue, R.M. Hughes, D. McMullen, D. Stevens, J.L. Stoddard, J. Lazorchak, W. Kinney, A.R. Selle, and R. Hjort. 1991. EMAP-Surface Waters Monitoring and Research Strategy: Fiscal Year 1991. EPA/600/3-91/022, U.S. Environmental Protection Agency, Corvallis, OR: 184 pp.
- Posch, M., J. Kämäri, M. Forsius, A. Henriksen, and A. Wilander. 1997. Exceedance of critical loads for lakes in Finland, Norway and Sweden: Reduction requirements for acidifying nitrogen and sulfur deposition. *Environmental Management* 21: 291–304.
- Rago, P. J., and J.G. Wiener. 1986. Does pH affect fish species richness when lake area is considered? *Transactions of the American Fisheries Society* 115:438–447.
- Reynolds, B., and D.A. Norris. 2001. Freshwater critical loads in Wales. *Water, Air, and Soil Pollution: Focus* 1:495–505.
- Rochelle, B.P., and M.R. Church. 1987. Regional patterns of sulfur retention in watersheds of the eastern U.S. *Water, Air, and Soil Pollution* 36(1–2):61–73.
- Rochelle, B.P., M.R. Church, and M.B. David. 1987. Sulfur retention at intensively studied sites in the U.S. and Canada. *Water, Air, and Soil Pollution* 33:73–83.
- Schindler, D.W. 1988. Effects of acid rain on freshwater ecosystems. *Science* 239:232–239.
- Schindler, D.W., S.E.M. Kaslan, and R.H. Hesslein. 1989. Biological improvement in lakes of the Midwestern and Northeastern United States from acid rain. *Environmental Science and Technology* 23:573–580.
- Schreck, C.B. 1981. Stress and rearing of salmonids. *Aquaculture* 28:241–249.



- Schreck, C.B. 1982. Stress and compensation in teleostean fishes: response to social and physical factors. Pp. 295–321 in *Stress and Fish*. Edited by A.D. Pickering. New York: Academic Press.
- Shannon, J.D. 1998. *Calculation of Trends from 1900 through 1990 for Sulfur and NO<sub>x</sub>-N Deposition Concentrations of Sulfate and Nitrate in Precipitation, and Atmospheric Concentrations of SO<sub>x</sub> and NO<sub>x</sub> Species over the Southern Appalachians*. Report to Southern Appalachian Mountains Initiative, April.
- Stoddard, J.L. 1990. *Plan for Converting the NAPAP Aquatic Effects Long-Term Monitoring (LTM) Project to the Temporally Integrated Monitoring of Ecosystems (TIME) Project*. International report. U.S. Environmental Protection Agency, Corvallis, OR.
- Stoddard, J.L., and J.H. Kellogg. 1993. Trends and patterns in lake acidification in the state of Vermont: evidence from the Long-Term Monitoring project. *Water, Air, and Soil Pollution* 67:301-317.
- Stoddard, J. L., Urquhart, N. S. Newell, A. D. Kugler, D. (1996) The Temporally Integrated Monitoring of Ecosystems (TIME) project design. 2, Detection of regional Acidification trends. *Water Resources* 32: 2529-2538
- Stoddard, J.L., C.T. Driscoll, J.S. Kahl, J.H Kellogg. 1998. A regional analysis of lake acidification trends for the northeastern U.S., 1982–1994. *Environmental Monitoring and Assessment* 51:399–413.
- Stoddard, J., J.S. Kahl, F.A. Deviney, D.R. DeWalle, C.T. Driscoll, A.T. Herlihy, J.H. Kellogg; P.S. Murdoch, J.R. Webb, and K.E. Webster. 2003. *Response of Surface Water Chemistry to the Clean Air Act Amendments of 1990*. EPA 620/R-03.001. U.S. Environmental Protection Agency, Office of Research and Development, National Health and Environmental Effects Research Laboratory, Research Triangle Park, NC.
- Sullivan, T.J., and B.J. Cosby. 1998. Modeling the concentration of aluminum in surface waters. *Water, Air, and Soil Pollution* 105:643–659.

- Sullivan, T.J., and B.J. Cosby. 2004. *Aquatic Critical Load Development for the Monongahela National Forest, West Virginia*. Report Prepared for U.S. Department of Agriculture Forest Service, Monongahela National Forest, Elkins, WV. E&S Environmental Chemistry, Inc., Corvallis, OR.
- Sullivan, T.J., C.T. Driscoll, B.J. Cosby, I.J. Fernandez, A.T. Herlihy, J. Zhai, R. Stemberger, K.U. Snyder, J.W. Sutherland, S.A. Nierzwicki-Bauer, C.W. Boylen, T.C. McDonnell, and N.A. Nowicki. 2006. *Assessment of the Extent to which Intensively-Studied Lakes are Representative of the Adirondack Mountain Region*. Final report. New York State Energy Research and Development Authority (NYSERDA), Albany, NY. Available at <http://nysl.nysed.gov/uhtbin/cgisirsi/Qcwd6NzFby/NYSL/138650099/8/4298474> (accessed November 1, 2007).
- Sverdrup, H., W. de Vries, and A. Henriksen. 1990. *Mapping Critical Loads*. Miljörapport 14. Nordic Council of Ministers, Copenhagen, Denmark.
- Urquhart, N.S., S.G. Paulsen, and D.P. Larsen. 1998. Monitoring for policy-relevant regional trends over time. *Ecological Applications* 8(2):246-257.
- U.S. EPA (Environmental Protection Agency). 1995. *Acid Deposition Standard Feasibility Study*. Report to Congress. EPA 430-R-95-001a. U.S. Environmental Protection Agency, Office of Air and Radiation, Washington, DC.
- U.S. EPA (Environmental Protection Agency). 2008. *Integrated Science Assessment (ISA) for Oxides of Nitrogen and Sulfur—Ecological Criteria (Final Report)*. EPA/600/R-08/082F. U.S. Environmental Protection Agency, National Center for Environmental Assessment—RTP Division, Office of Research and Development, Research Triangle Park, NC. Available at <http://cfpub.epa.gov/ncea/cfm/recordisplay.cfm?deid=201485>.
- Van Sickle, J., J.P. Baker, H.A. Simonin, B.P. Baldigo, W.A. Kretser, and W.E. Sharpe. 1996. Episodic acidification of small streams in the northeastern United States: Fish mortality in field bioassays. *Ecological Applications* 6:408–421.

- Webb J.R., Cosby B.J., Galloway J.N., and Hornberger G.M..1989. Acidification of native brook trout streams in Virginia. *Water Resources Research* 25:1367–1377.
- Webb, J.R., F.A. Deviney, J.N. Galloway, C.A. Rinehart, P.A. Thompson, and S. Wilson. 1994. The acid-base status of native brook trout streams in the mountains of Virginia: a regional assessment based on the Virginia Trout Stream Sensitivity Study. Prepared for the Virginia Department of Game and Inland Fisheries, Richmond, VA.
- Webb, J.R., B.J. Cosby, F.A. Deviney, J.N. Galloway, S.W. Maben, and A.J. Bulger. 2004. Are brook trout streams in western Virginia and Shenandoah National Park recovering from acidification? *Environmental Science and Technology* 38:4091–4096.
- Webster, K. E., Brezonik, P. L., Holdhsen, B. J. 1993. Temporal trends in low alkalinity lakes of the upper Midwest (1983-1989). *Water Air Soil Pollution* 67: 397-414
- Wedemeyer, G.A., B.A. Barton, and D.J. McLeay. 1990. Stress and acclimation. Pp. 178–198 in *Methods for Fish Biology*. Edited by C.B. Schreck and P.B. Moyle. Bethesda, MD: American Fisheries Society.
- Whitehead, P.G., S. Bird, M. Hornung, B.J. Cosby, C. Neal, and P. Paricos. 1988. Stream acidification trends in the Welsh Uplands: A modelling study of the Llyn Brianne catchments. *Journal of Hydrology* 101:191–212.
- Whittier, T.R., S.G. Paulsen, D.P. Larsen, S.A. Peterson, A.T. Herlihy, and P.H. Kaufmann. 2002. Indicators of ecological stress and their extent in the population of northeastern lakes: a regional-scale assessment. *BioScience* 52:235–247.
- Wright, R.F., B.J. Cosby, M.B. Flaten, and J.O. Reuss. 1990. Evaluation of an acidification model with data from manipulated catchments in Norway. *Nature* 343:53–55.
- Wright, R.F., E. Lotse, and E. Semb. 1994. Experimental acidification of alpine catchments at Sogndal, Norway: results after 8 years. *Water, Air, and Soil Pollution* 72:297–315.



## ATTACHMENT A

### 1. MODELING DESCRIPTIONS

#### 1.1 MAGIC

Model of Acidification of Groundwater in Catchments (MAGIC) is a lumped-parameter model of intermediate complexity, developed to predict the long-term effects of acidic deposition on surface water chemistry (Cosby et al., 1985a, b). The model simulates soil solution chemistry and surface water chemistry to predict the monthly and annual average concentrations of the major ions in these waters. MAGIC consists of (1) a 2–10 submodel in which the concentrations of major ions are assumed to be governed by simultaneous reactions involving sulfate ( $\text{SO}_4^{2-}$ ) adsorption, cation exchange, dissolution-precipitation- speciation of aluminum (Al), and dissolution-speciation of inorganic carbon; and (2) a mass balance submodel in which the flux of major ions to and from the soil is assumed to be controlled by atmospheric inputs, chemical weathering, net uptake and loss in biomass, and losses to runoff. At the heart of MAGIC is the size of the pool of exchangeable base cations in the soil. As the fluxes to and from this pool change over time in response to changes in atmospheric deposition, the chemical equilibria between soil and soil solution shift, resulting in changes in surface water chemistry. Thus, the degree and rate of change of surface water acidity depend both on flux factors and the inherent biogeochemical characteristics of the affected soils.

Cation exchange is modeled using equilibrium (Gaines-Thomas) equations with selectivity coefficients for each base cation and Al.  $\text{SO}_4^{2-}$  adsorption is represented by a Langmuir isotherm. Al dissolution and precipitation are assumed to be controlled by equilibrium with a solid phase of aluminum hydroxide ( $\text{Al}(\text{OH})_3$ ). Al speciation is calculated by considering hydrolysis reactions, as well as complexation with  $\text{SO}_4^{2-}$  and fluoride ( $\text{F}^-$ ). The effects of carbon dioxide ( $\text{CO}_2$ ) on pH and on the speciation of inorganic carbon are computed from equilibrium equations. Organic acids are represented in the model as tri-protic analogues. Weathering and the uptake rate of nitrogen are assumed to be constant. A set of mass balance equations for base cations and strong acid anions are included (Cosby et al., 1985).

Given a description of the historical deposition at a site, the model equations are solved numerically to give long-term reconstructions of surface water chemistry (for complete details of

the model, see Cosby et al., 1985 a, b; Cosby et al., 1989). MAGIC was successfully used to reconstruct the history of acidification and to simulate the future trends on a regional basis and in a large number of individual catchments in both North America and Europe (e.g., Cosby et al., 1989, 1990, 1996; Hornberger et al., 1989; Jenkins et al., 1990 a, b, c; Lepisto et al., 1988; Norton et al., 1992; Sullivan and Cosby, 1998; Sullivan and Cosby, 2004; Whitehead et al., 1988; Wright et al., 1990, 1994).

The input data required in this project for aquatic and soils resource modeling with the MAGIC model (i.e., stream water, catchment, soils, deposition data) were assembled and maintained in databases for each site modeled (electronic spreadsheets, text-based MAGIC parameter files). Model outputs for each site were archived as text-based time-series files of simulated variable values. The outputs were also concatenated across all sites and maintained in electronic spreadsheets.

### ***1.1.1 Input Data and Calibration***

The calibration procedure requires that streamwater chemistry, soil chemical and physical characteristics, and atmospheric deposition data be available for each watershed. The surface water chemistry data needed for calibration are the concentrations of the individual base cations (calcium [ $\text{Ca}^{2+}$ ], magnesium [ $\text{Mg}^{2+}$ ], sodium [ $\text{Na}^+$ ], and potassium [ $\text{K}^+$ ]) and acid anions (chlorine [ $\text{Cl}^-$ ],  $\text{SO}_4^{2-}$ , nitrate [ $\text{NO}_3^-$ ]) and the stream pH. The soil data used in the model comprise physical properties, including soil depth and bulk density, and chemical properties, such as soil pH, soil cation-exchange capacity, and exchangeable bases in the soil ( $\text{Ca}^{2+}$ ,  $\text{Mg}^{2+}$ ,  $\text{Na}^+$ , and  $\text{K}^+$ ). The deposition inputs required for calibration include the concentrations and magnitudes of all major ions from wet, dry, and cloud deposition.

The acid-base chemistry modeling for this project was conducted using the year 2002 as the Base Year. The effects models were calibrated to the available atmospheric deposition and water chemistry data and then interpolated or extrapolated to yield Base Year estimates of lake water chemistry in the year 2002, which served as the starting point for modeling of current water chemistry (e.g., the years 2002 to 2100)

### ***1.1.2 Lake, Stream, and Soil Data for Calibration***

Several water chemistry databases were acquired for use in model calibration. Data were derived primarily from the Environmental Monitoring and Assessment Program (EMAP) and

Temporally Integrated Monitoring of Ecosystems (TIME) survey and monitoring efforts. The required lake water and soil composition data for the modeling efforts included the following measurements:

- Stream water composition— pH, acid neutralizing capacity (ANC),  $\text{Ca}^{2+}$ ,  $\text{Mg}^{2+}$ ,  $\text{K}^+$ ,  $\text{Na}^+$ ,  $\text{SO}_4^{2-}$ ,  $\text{NO}_3^-$ , and  $\text{Cl}^-$
- Soil properties— thickness and total cation exchange capacity, exchangeable bases ( $\text{Ca}^{2+}$ ,  $\text{Mg}^{2+}$ ,  $\text{Na}^+$ , and  $\text{K}^+$ ) bulk density, porosity, and pH where available; the stream water chemistry database also included dissolved organic and inorganic carbon, silicic acid ( $\text{H}_4\text{SiO}_4$ ), and inorganic monomeric Al (i.e., Ali).

### ***1.1.3 Wet Deposition and Meteorology Data for Calibration***

MAGIC requires, as atmospheric inputs for each site, estimates of the total annual deposition (eq/ha/yr) of eight ions, and the annual precipitation volume (meters/year [m/yr]). The eight ions are calcium ( $\text{Ca}^{2+}$ ), magnesium ( $\text{Mg}^{2+}$ ),  $\text{Na}^+$ ,  $\text{K}^+$ , ammonium ( $\text{NH}_4^+$ ), wet sulfate ( $\text{SO}_4$ ), chlorine ( $\text{Cl}^-$ ), and nitrate ( $\text{NO}_3$ ). Total deposition of an ion at a particular site for any year can be represented as combined wet, dry, and occult (i.e., cloud and fog) deposition:

$$\text{TotDep} = \text{WetDep} + \text{DryDep} + \text{OccDep}. \quad (1)$$

Inputs to the MAGIC model are specified as wet deposition (the annual flux in  $\text{meq/m}^2/\text{yr}$ ) and a dry, cloud and fog deposition factor (DDF, unitless), which is multiplied by the wet deposition in order to get total deposition:

$$\text{TotDep} = \text{WetDep} \times \text{DDF}, \quad (2)$$

where DDF is the ratio of total deposition to wet deposition. It usually prescribed as equal to a constant fraction of the wet deposition.

Given an annual wet deposition flux (WetDep), the ratio of dry deposition to wet deposition ( $\text{DryDep}/\text{WetDep}$ ), and the ratio of cloud and fog deposition to wet deposition ( $\text{OccDep}/\text{WetDep}$ ) for a given year at a site, the total deposition for that site and year is uniquely determined.

In order to calibrate MAGIC, a time-series of total deposition is needed, beginning with a reference calibration year and including the 140 years preceding the calibration year. The procedure for providing a time-series of total deposition inputs to MAGIC follows.

The absolute values of wet deposition and DDF for each ion are provided for a Reference Year at each site. For all the case study sites, a Reference Year of 2002 was used. Given the Reference Year deposition values, deposition data for the historical and calibration periods, and potentially any future deposition scenarios, can be estimated as a fraction of the Reference Year value. For instance, to calculate the total deposition of a particular ion in some historical or future year, j:

$$\text{TotDep}(j) = [\text{WetDep}(0) \times \text{WetDepScale}(j)] \times [\text{DDF}(0) \times \text{DDFScale}(j)], \quad (3)$$

where:

WetDep(0) = the Reference Year wet deposition (meq/m<sup>2</sup>/yr) of the ion

WetDepScale(j) = the scaled value of wet deposition in year j (expressed as a fraction of the wet deposition in the Reference Year)

DDF(0) = the dry and occult deposition factor for the ion for the Reference Year

DDFScale(j) = the scaled value of the dry and occult deposition factor in year j (expressed as a fraction of the DDF in the Reference Year).

The absolute value of wet deposition used for the Reference Year is time and space specific—varying geographically within the region, varying locally with elevation, and varying from year to year. It is desirable to have the estimates of wet deposition take into account the geographic location and elevation of the site, as well as the year for which calibration data are available. Therefore, estimates of wet deposition used for the Reference Year should be derived from either direct measurements or a procedure (i.e., model) that has a high spatial resolution and considers elevation effects. As described in Section 4.2.1.4, the absolute wet deposition values used for the Reference Year in this project were derived from observed data from NADP hybridized with high-spatially resolved estimates of rainfall.

The value of the DDF used for the Reference Year specifies the ratio between the absolute amounts of wet and total deposition. While the wet deposition component varies spatially and temporally, this ratio is not nearly so responsive. In large part, this is because the varying wet deposition parameter is usually a large component of the total deposition and is included in both the numerator and denominator of the ratio. For example, if in a given year at a particular site, the wet deposition goes up, then the total deposition usually goes up; or, if the elevation or aspect of a given site results in lower wet deposition, the total deposition also will



often be lower. Therefore, estimates of the absolute values of DDF may be derived from a model that has a relatively low spatial resolution and/or temporally smoothes the data. Estimates of the absolute values of the DDF for the Reference Year at each site in this project were derived from the Advanced Statistical Trajectory Regional Air Pollution (ASTRAP) model (Shannon, 1998), as described below.

The long-term scaled sequences used to specify time-series of deposition inputs for MAGIC simulations usually do not require detailed spatial or temporal resolution. Scaled sequences of wet deposition or DDF (normalized to the same reference year) at neighboring sites will be similar, even if the absolute wet deposition or DDF at the sites are different because of factors such as local aspect or elevation. Therefore, if the scaled long-term patterns of any of these do not vary much from place to place, estimates of the scaled sequences (as for estimates of absolute DDF values) may be derived from a model that has a relatively low spatial resolution. As described in the following sections, output from the ASTRAP model was used to construct scaled sequences of both wet deposition and DDF for these case study areas.

#### ***1.1.4 Wet Deposition Data (Reference Year and Calibration Values)***

The absolute values of wet deposition used for defining the Reference Year and for the MAGIC calibrations must be highly site-specific. Estimated wet deposition data was used for each site derived from the spatial interpolation model of Grimm and Lynch (2004), referred to here as the Grimm model. The Grimm model is based on observed wet deposition concentrations at NADP monitoring stations and radar-based precipitation estimates adjusted by elevation effects, and provides a spatially-resolved estimate of wet deposition for each of the eight ions required by MAGIC. The Grimm model makes a correction for changes in precipitation volume (and thus wet deposition) based on the elevation at a given site. This correction arises from a model of orographic effects on precipitation magnitudes derived from regional climatological data.

The latitude, longitude, and elevation of the case study sites were provided as inputs to the Grimm model. Estimates of quarterly and annual wet deposition and precipitation estimates for each modeling site were found for the time period from 1983 through 2002. These annual data were used to define the Reference Year and were used in conjunction with the ASTRAP

historical deposition sequences for MAGIC calibration and simulation. The ASTRAP historical sequences were scaled to match the Grimm estimates at each site.

#### ***1.1.5 Dry, Cloud, and Fog Deposition Data and Historical Deposition Sequences***

Historical sequences of wet deposition and DDF were estimated using the ASTRAP model. The ASTRAP model provided estimates of historical wet, dry, and occult deposition of sulfur and oxidized nitrogen at modeled sites for the two case study areas. The ASTRAP sites included 10 NADP deposition sites. For each of the modeled sites, ASTRAP produced wet, dry, and occult deposition estimates of sulfur and oxidized nitrogen every 10 years, starting in 1900 and ending in 1990. The model outputs are smoothed estimates of deposition roughly equivalent to a 10-year moving average centered on each of the output years. The wet, dry, and occult deposition outputs of ASTRAP were used to estimate the absolute DDF for each site (using the DryDep/WetDep and OccDep/WetDep ratios from the ASTRAP 19 output) and to set up the scaled sequences of historical wet deposition and historical DDF for the calibration of each site modeled in this project. Using the values and rates of change from the year 1900 ASTRAP estimates, values for each time period going back to 1850 were estimated through linear interpolation.

Because the ASTRAP sites are in the same region, but are not in the identical locations as the MAGIC sites, and since deposition magnitudes are spatially- and elevation-sensitive, the historical sequences of deposition at the ASTRAP sites were scaled to align with the deposition estimates from the Grimm model for the MAGIC case study areas. First, the time series of wet deposition estimates for each ASTRAP site were used to construct historical scaled sequences of wet deposition. The absolute wet deposition outputs for the period 1850 to 1990 from each site modeled in ASTRAP were normalized using their year 1990 values, converting them into scaled sequences. It was then necessary to couple these historical scaled wet deposition sequences from the year 1990 to the MAGIC Reference Year 2002. This coupling was accomplished using the observed changes in wet deposition for the period 1983 to 2002 derived from the Grimm model. With these site-specific deposition magnitudes and rates of change, the normalized ASTRAP values were converted back into concentrations, though, now scaled to the deposition at the MAGIC sites.

Because DDF is much less sensitive to location, the actual (nonscaled) estimates from ASTRAP were used at the MAGIC sites. The value of DDF for the year 1990 was used as the value of DDF for the Reference Year (i.e., no change was assumed for DDF for the period 1990 to 2002). The resulting time series of DDF values for the period 1900 to 2002 for each ASTRAP site were normalized to the year 2002 values to provide historical scaled sequences of DDF at each ASTRAP site.

#### ***1.1.6 Protocol for MAGIC Calibration and Simulation at Individual Sites***

The aggregated nature of the MAGIC model requires that it be calibrated with observed data from a system before it can be used to forecast potential system response to changes in deposition. Calibration is achieved by specifying values of certain parameters within the model that can be directly measured or observed in the system of interest (called fixed parameters). The model is then run (using observed and/or assumed atmospheric and hydrologic inputs), and the outputs (streamwater and soil chemical variables called criterion variables) are compared with observed values of these variables. If the observed and simulated values differ, the values of another set of parameters in the model (called optimized parameters) are adjusted to improve the fit. After a number of iterations adjusting the optimized parameters, the simulated-minus-observed values of the criterion variables usually converge to zero (within some specified tolerance, or uncertainty). The model is then considered calibrated.

There are eight observed fixed parameters that are used to drive the estimate (i.e., current soil exchangeable pool size and current output flux of each of the four base cations), and there are eight parameters to be optimized in this procedure (i.e., the weathering and the selectivity coefficient of each of the four base cations). If new assumptions or new values for any of the observed fixed parameters or inputs to the model are adopted, the model must be recalibrated by readjusting the optimized parameters until the simulated-minus-observed values of the criterion variables again fall within the specified tolerance.

Estimates of the fixed parameters, the deposition inputs, and the target variable values to which the model is calibrated all contain uncertainties. A “fuzzy optimization” procedure was used for these case study sites to provide explicit estimates of the effects of these uncertainties. The procedure consists of performing multiple calibrations at each site using random values of the fixed parameters drawn from a *range* of fixed parameter values (representing uncertainty in

knowledge of these parameters) and random values of Reference Year deposition drawn from a *range* of total deposition estimates (representing uncertainty in these inputs). The final convergence (i.e., completion) of the calibration is determined when the simulated values of the criterion variables are within a specified “acceptable window” around the nominal observed value. This acceptable window represents uncertainty in the target variable values being used to calibrate the site.

Each of the multiple calibrations at a site begins with (1) a random selection of values of fixed parameters and deposition, and (2) a random selection of the starting values of the adjustable parameters. The adjustable parameters are then optimized using an algorithm seeking to minimize errors between simulated and observed criterion variables. Calibration success is judged when all criterion values simultaneously are within their specified acceptable windows, (which may occur before the absolute possible minimum error is achieved). This procedure is repeated 10 times for each site.

For this project, the acceptable windows for base cation concentrations in streams were taken as  $\pm 2$  microequivalents per liter ( $\mu\text{eq/L}$ ) around the observed values. Acceptable windows for soil exchangeable base cations were taken as  $\pm 0.2\%$  around the observed values. Fixed parameter uncertainty in soil depth, bulk density, cation exchange capacity, stream discharge, and stream area were assumed to be  $\pm 10\%$  of the estimated values. Uncertainty in total deposition was  $\pm 10\%$  for all ions.

The final calibrated model at the site is represented by the ensemble of parameter values of all of the successful calibrations at the site. When performing a simulation of the site, each of the calibrated parameter sets are run for a given historical or future scenario, generating an ensemble of results. The results include multiple simulated values of each variable for each year, all of which are acceptable in the sense of the calibration constraints applied in the fuzzy optimization procedure. The median of all the simulated values within a year is taken to be “the most likely” response for the site in that year. For this project, whenever single values for a site are presented or used in an analysis, these values are the median of the ensemble values derived from running each of the parameter sets for the site.

An estimate of the uncertainty (or reliability) of a simulated response to a given scenario can also be derived from the multiple simulated values within a year resulting from the ensemble simulations. For any year in a given scenario, the largest and smallest values of a simulated

variable define the upper and lower 95% confidence bounds for that site's response for the scenario under consideration. Thus, for all variables and all years of the scenario, a band of simulated values can be produced from the ensemble simulations at a site that encompasses the likely response (and provides an estimate of the simulation uncertainty) for any point in the scenario. For these case study areas, whenever uncertainty estimates are presented, the estimate is based on the range of values from the ensemble simulations for each of its sites.

In addition, uncertainty estimates for three classes of the major inputs of the model were made through a sensitivity study, examining response of parameters and ability of the model to attain calibration in response to variation in the following inputs:

- Soils data for calibration
- Stream water data calibration
- Deposition data calibration.

#### ***1.1.7 Combined Model Calibration and Simulation Uncertainty***

The sensitivity analyses described above were designed to address specific assumptions or decisions that had to be made to assemble the data for the 44 or 60 modeled sites in a form that could be used for calibration of the model. In all cases, the above analyses address the questions of what the effect would have been if alternate available choices had been taken. These analyses were undertaken for a subset of sites for which the alternate choices were available at the same sites. As such, the analyses above are informative, but they provide no direct information about the uncertainty in calibration or simulation arising from the choices that were incorporated into the final modeling protocol for all sites. That is, having made the choices about soils assignments, high elevation deposition, and stream samples for calibration (and provided an estimate of their inherent uncertainties), the need arises for a procedure for estimating uncertainty at each and all of the individual sites using the final selected calibration and simulation protocol.

These simulation uncertainty estimates were derived from the multiple calibrations at each site provided by the “fuzzy optimization” procedure employed in this project. For each of the modeled sites, 10 distinct calibrations were performed with the target values, parameter values, and deposition inputs for each calibration, reflecting the uncertainty inherent in the observed data for the individual site. The effects of the uncertainty in the assumptions made in

calibrating the model (and the inherent uncertainties in the data available) can be assessed by using all successful calibrations for a site when simulating the response to different scenarios of future deposition. The model then produces an ensemble of simulated values for each site. The median of all simulated values in a year is considered the most likely response of the site. The simulated values in the ensemble can also be used to estimate the magnitude of the uncertainty in the projection. Specifically, the difference in any year between the maximum and minimum simulated values from the ensemble of calibrated parameter sets can be used to define an “uncertainty” (or a “confidence”) width for the simulation at any point in time. All 10 of the successful model calibrations will lie within this range of values. These uncertainty widths can be produced for any variable and any year to monitor model performance.

Direct comparison of simulated versus observed water chemistry values were compared to determine the uncertainty and variability in the MAGIC model output. Average water chemistry ( $\text{SO}_4^{2-}$ ,  $\text{NO}_3^-$ , and ANC) simulated versus observed values during the calibration period (i.e., reference year) were compared for all modeled sites. In addition, simulated versus observed average yearly values for ANC for the period of 1980 to 2007 for 4 sites were completed. The observed water chemistry data were from the, ALTM-LTM, VTSSS-LTM, and TIME water quality measurement programs and represent annual average concentrations. The statistic of Root Mean Squared Error (RMSE) were also calculated for predicted versus observed values for both the calibration period and the period of 1980 to 2007. RMSE is a frequently used measure of the differences between values predicted by a model or an estimator and the values actually observed from the thing being modeled or estimated. The RMSE was based on an annual average ANC over a 5-year period.

#### ***1.1.8 Results of the Uncertainty Analysis***

Based on the MAGIC model simulations, the 95% confidence interval for the pre-acidification and current average ANC concentrations of the 44 modeled lakes was 106.8 to 134.0 and 50.5 to 81.8  $\mu\text{eq/L}$ , respectively, which is on average a 15  $\mu\text{eq/L}$  difference in ANC concentrations, or 10%. The 95% confidence interval for pre-acidification and current average ANC concentrations of the 60 modeled streams was 91.9 to 110.9 and 53.4 to 62.4  $\mu\text{eq/L}$ , respectively, which is on average 8  $\mu\text{eq/L}$  difference in ANC concentration, or 5%.

These direct comparisons show good agreement between simulated and observed water quality values. Results of predicted versus observed average water chemistry during the calibration period (i.e., reference year) are shown in **Figures 1.1-1 and 1.1-2** for MAGIC modeling. The model showed close agreement with measured values at all sites for the 1-year comparison of modeled values. For all sites'  $\text{SO}_4^{2-}$ ,  $\text{NO}_3^-$ , and ANC simulations, the RMSE for predicted versus observed values were 0.1  $\mu\text{eq/L}$ , 0.05  $\mu\text{eq/L}$ , and 3.5  $\mu\text{eq/L}$  for lakes in the Adirondacks Case Study Area and 1.0  $\mu\text{eq/L}$ , 0.06  $\mu\text{eq/L}$ , and 1.0  $\mu\text{eq/L}$  for streams in the Shenandoah Case Study Area. Plots of simulated and observed ANC values for the period of 1980 to 2007 are graphed in **Figures 1.1-3 and 1.1-4** for two lakes in the Adirondacks Case Study Area and for two streams Shenandoah Case Study Area. The RMSE of ANC was 11.8  $\mu\text{eq/L}$  and 4.0  $\mu\text{eq/L}$  for the two lakes in the Adirondacks Case Study Area and was 7.8  $\mu\text{eq/L}$  and 5.1  $\mu\text{eq/L}$  for the two streams in Shenandoah Case Study Area.

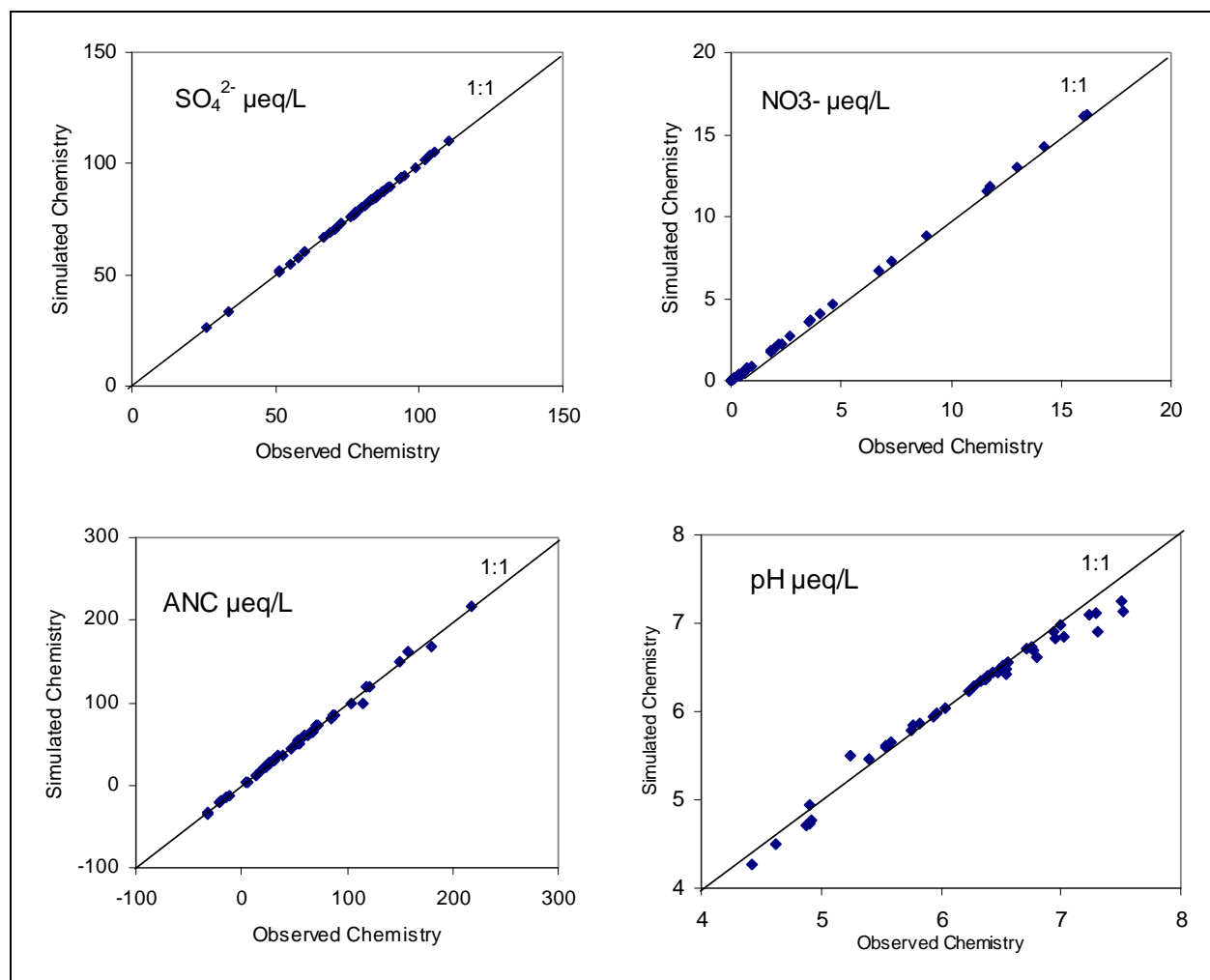


**Figure 1.1-1.** Simulated versus observed annual average surface water SO<sub>4</sub><sup>2-</sup>, NO<sub>3</sub><sup>-</sup>, ANC, and pH during the model calibration period for each of the 44 lakes in the Adirondacks Case Study Area. The black line is the 1:1 line.



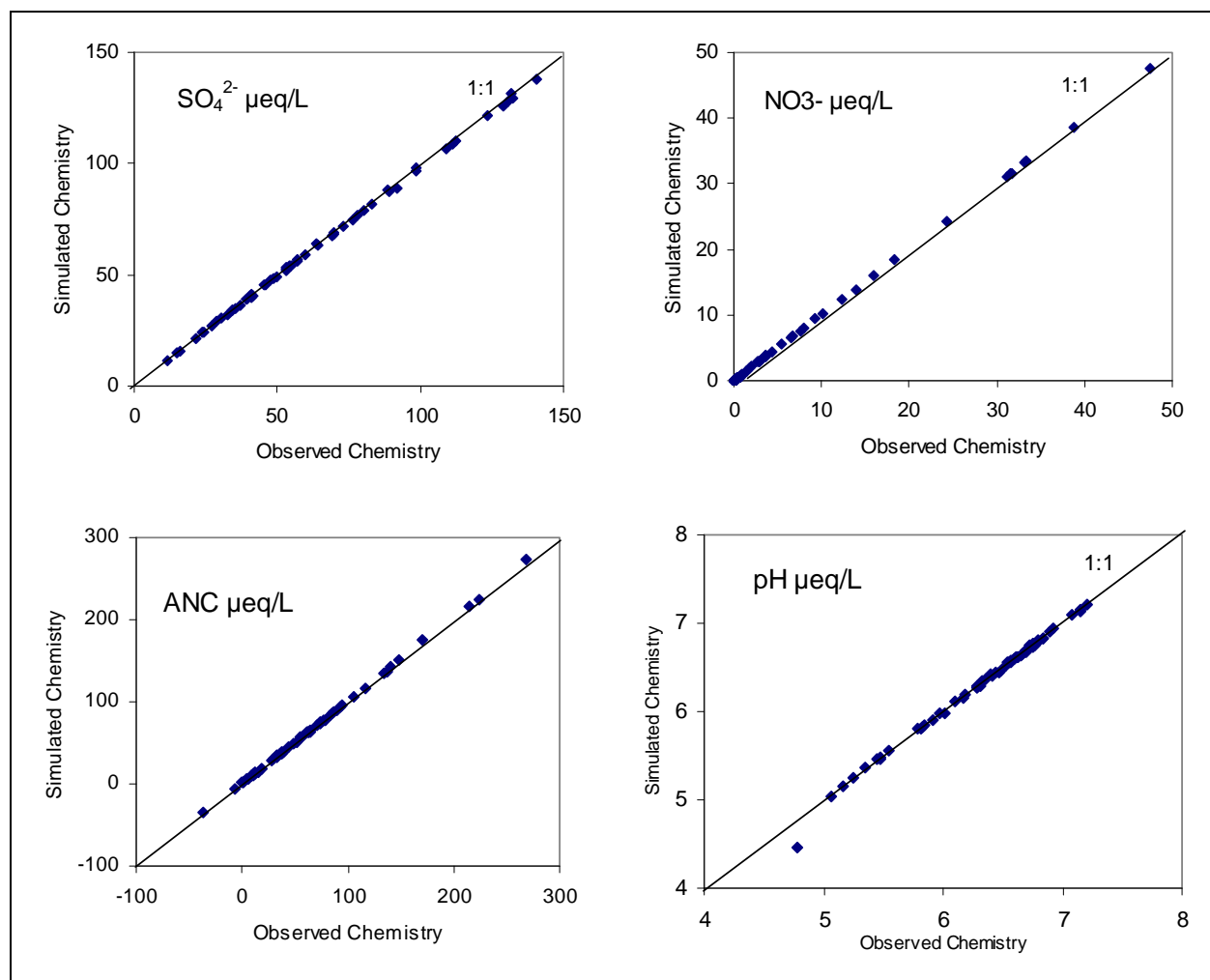


**Figure 1.1-2.** Simulated versus observed annual average surface water SO<sub>4</sub><sup>2-</sup>, NO<sub>3</sub><sup>-</sup>, ANC, and pH during the model calibration period for each of the 60 streams in the Shenandoah Case Study Area. The black line is the 1:1 line.

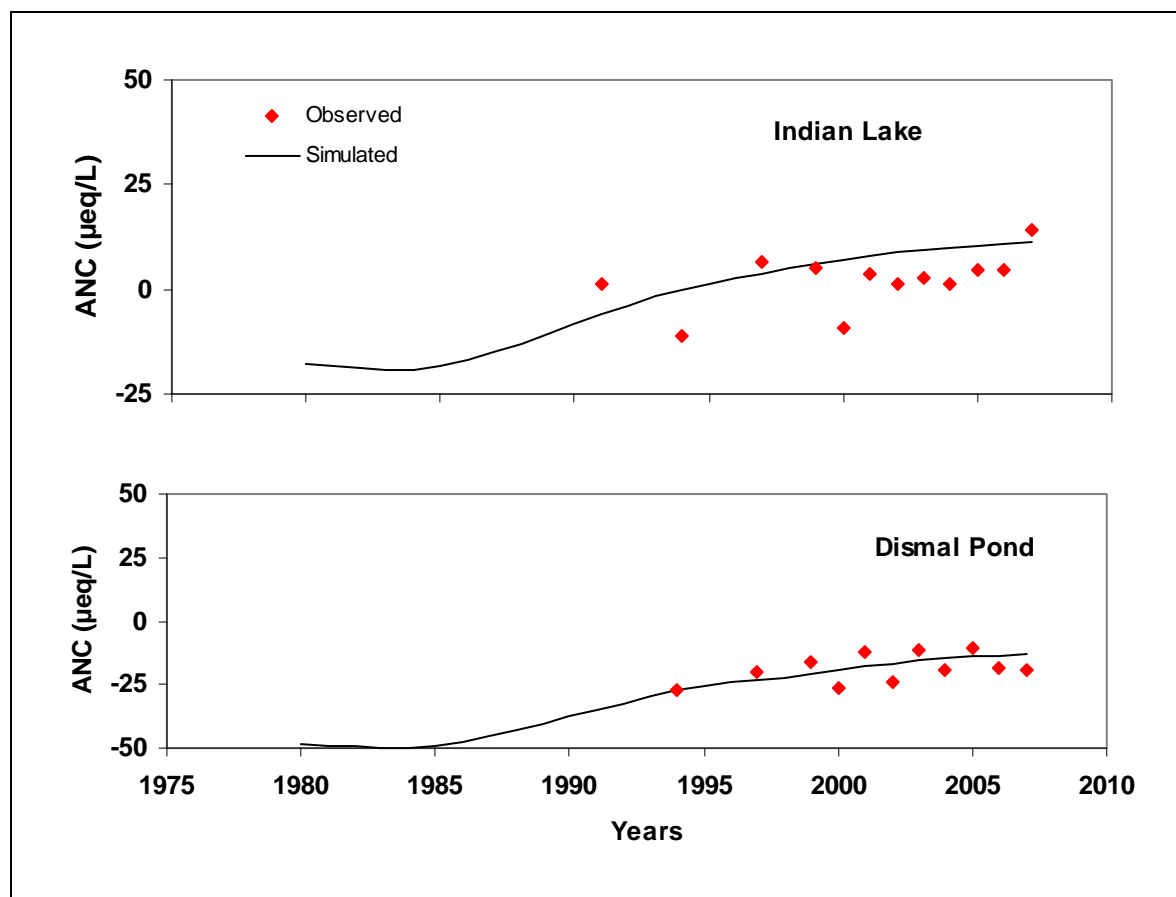


**Figure 1.1-3.** MAGIC simulated and observed values of ANC for two lakes in the Shenandoah Case Study Area. Red points are observed data and the simulated values are the line. The Root Mean Squared Error (RMSE) for ANC was 11.8 µeq/L for Helton Creek and 4.0 µeq/L for Nobusiness Creek.

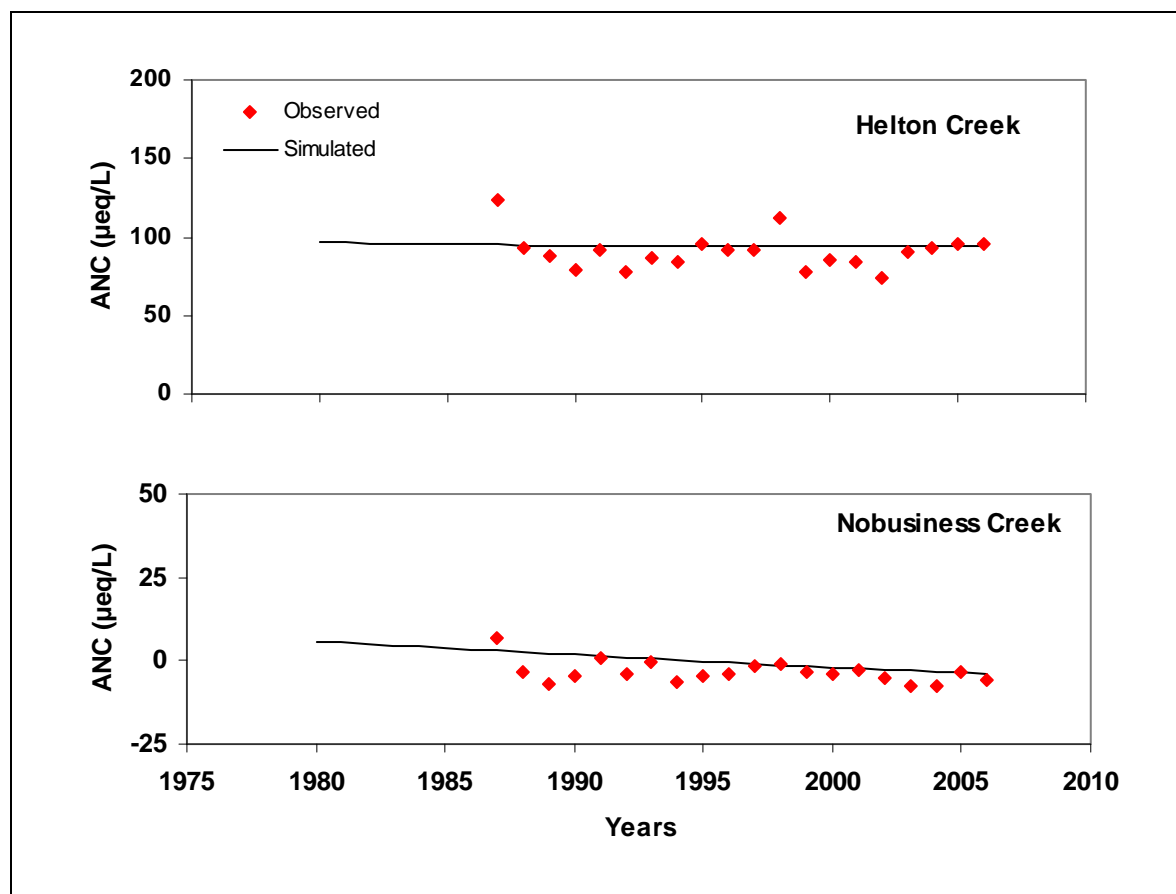


**Figure 1.1-4.** MAGIC simulated and observed values of ANC for two lakes in the Shenandoah Case Study Area. Red points are observed data and the simulated values are the line. The Root Mean Squared Error (RMSE) for ANC was 11.8 µeq/L for Helton Creek and 4.0 µeq/L for Nobusiness Creek.

## 1.2 Critical Loads: Steady-State Water Chemistry Models

The critical load of acidity for lakes or streams was derived from present-day water chemistry using a combination of steady-state models. Both the Steady-State Water Chemistry (SSWC) model and First-order Acidity Balance model (FAB) is based on the principle that excess base-cation production within a catchment area should be equal to or greater than the acid anion input, thereby maintaining the ANC above a preselected level (Reynolds and Norris, 2001; Posch et al. 1997). These models assume steady-state conditions and assume that all  $\text{SO}_4^{2-}$  in runoff originates from sea salt spray and anthropogenic deposition. Given a critical ANC protection level, the critical load of acidity is simply the input flux of acid anions from atmospheric deposition (i.e., natural and anthropogenic) subtracted from the natural (i.e., preindustrial) inputs of base cations in the surface water.

Atmospheric deposition of NO<sub>x</sub> and SO<sub>x</sub> contributes to acidification in aquatic ecosystems through the input of acid anions, such as NO<sub>3</sub><sup>-</sup> and SO<sub>4</sub><sup>2-</sup>. The acid balance of headwater lakes and streams is controlled by the level of this acidifying deposition of NO<sub>3</sub><sup>-</sup> and SO<sub>4</sub><sup>2-</sup> and a series of biogeochemical processes that produce and consume acidity in watersheds. The biotic integrity of freshwater ecosystems is then a function of the acid-base balance, and the resulting acidity-related stress on the biota that occupy the water.

The calculated ANC of the surface waters is a measure of the acid-base balance:

$$\text{ANC} = [\text{BC}]^* - [\text{AN}]^* \quad (1)$$

where [BC]\* and [AN]\* are the sum of base cations and acid anions (NO<sub>3</sub><sup>-</sup> and SO<sub>4</sub><sup>2-</sup>), respectively. Equation (1) forms the basis of the linkage between deposition and surface water acidic condition and the modeling approach used. Given some “target” ANC concentration [ANC<sub>limit</sub>]) that protects biological integrity, the amount of deposition of acid anions (AN) or depositional load of acidity CL(A) is simply the input flux of acid anions from atmospheric deposition that result in a surface water ANC concentration equal to the [ANC<sub>limit</sub>] when balanced by the sustainable flux of base cations input and the sinks of nitrogen and sulfur in the lake and watershed catchment.

Critical loads for nitrogen and sulfur (CL(N) + CL(S) ) or critical load of acidity CL(A) were calculated for each waterbody from the principle that the acid load should not exceed the nonmarine, nonanthropogenic base cation input and sources and sinks in the catchment minus a neutralizing to protect selected biota from being damaged:

$$\text{CL(N)} + \text{CL(S)} \text{ or } \text{CL(A)} = \text{BC}_{\text{dep}}^* + \text{BC}_{\text{w}} - \text{Bc}_{\text{u}} - \text{AN} - \text{ANC}_{\text{limit}} \quad (2)$$

where

BC<sub>dep</sub><sup>\*</sup> = (BC<sup>\*</sup>=Ca<sup>\*</sup>+Mg<sup>\*</sup>+K<sup>\*</sup>+Na<sup>\*</sup>), nonanthropogenic deposition flux of base cations and

BC<sub>w</sub> = the average weathering flux, producing base cations

Bc<sub>u</sub> (Bc=Ca<sup>\*</sup>+Mg<sup>\*</sup>+K<sup>\*</sup>) = the net long-term average uptake flux of base cations in the biomass (i.e., the annual average removal of base cations due to harvesting)

AN = the net long-term average uptake, denitrification, and immobilization of nitrogen anions (e.g. NO<sub>3</sub><sup>-</sup>) and uptake of SO<sub>4</sub><sup>2-</sup>

ANC<sub>limit</sub> = the lowest ANC-flux that protects the biological communities.

Since the average flux of base cations weathered in a catchment and reaching the lake or streams is difficult to measure or compute from available information, the average flux of base cations and the resulting critical load estimation were derived from water quality data (Henriksen and Posch, 2001; Henriksen et al., 1992; Sverdrup et al., 1990). Weighted annual mean water chemistry values were used to estimate average base cation fluxes, which were calculated from water chemistry data collected from the Temporally Integrated Monitoring of Ecosystems (TIME)/Long-Term Monitoring (LTM) monitoring networks, that include Adirondack Long-term Monitoring (ALTM), Virginia Trout Stream Sensitivity Study (VTSSS), and the Shenandoah Watershed Study (SWAS), and Environmental Monitoring and Assessment Program (EMAP) (see Section 4.1.2.1 of Chapter 4).

The preacidification nonmarine flux of base cations for each lake or stream,  $BC^*_0$ , is

$$BC^*_0 = BC^*_{dep} + BC_w - BC_u \quad (3)$$

Thus, critical load for acidity can be rewritten as

$$CL(N) + CL(S) = BC^*_0 - AN - ANC_{limit} = Q([BC^*]_0 - [AN] - [ANC]_{limit}), \quad (4)$$

where the second identity expresses the critical load for acidity in terms of catchment runoff ( $Q$ ) m/yr and concentration ( $[x] = X/Q$ ).

The sink of nitrogen in the watershed is equal to the uptake ( $N_{upt}$ ), immobilization ( $N_{imm}$ ), and denitrification ( $N_{den}$ ) of nitrogen in the catchment. Thus, critical load for acidity can be rewritten as

$$CL(N) + CL(S) = \{fN_{upt} + (1 - r)(N_{imm} + N_{den})\} + ([BC^*]_0 - [ANC]_{limit})Q \quad (5)$$

where  $f$  and  $r$  are dimensionless parameters that define the fraction of forest cover in the catchment and the lake/catchment ratio. The in-lake retention of nitrogen and sulfur was assumed to be negligible.

Equation 5 described the FAB model that was applied when sufficient data was available to estimate the uptake, immobilization, and denitrification of nitrogen and the neutralization of acid anions (e.g.  $NO_3^-$ ) in the catchment. In the case where data was not available, the contribution of nitrogen anions to acidification was assumed to be equal to the nitrogen leaching rate ( $N_{leach}$ ) into the surface water. The flux of acid anions in the surface water is assumed to represent the amount of nitrogen that is not retained by the catchment, which is determined from the sum of

measured concentration of  $\text{NO}_3^-$  and ammonia in the stream chemistry. This case describes the SSWC model and the critical load for acidity is

$$\text{CL(A)} = Q \cdot ([\text{BC}^*]_0 - [\text{ANC}]_{\text{limit}}) \quad (6)$$

where the contribution of acid anions is considered as part of the exceedances calculation (see Section 1.2.5, below).

For the assessment of current condition in both case study areas, the critical load calculation described in Equation 6 was used for most lakes and streams. The lack of sufficient data for quantifying nitrogen denitrification and immobilization prohibited the wide use of the FAB model. In addition, given the uncertainty in quantifying nitrogen denitrification and immobilization, the flux of nitrogen anions in the surface water was assumed to more accurately reflect the contribution of  $\text{NO}_3^-$  to acidification.

Several major assumptions are made: (1) steady-state conditions exist, (2) the effect of nutrient cycling between plants and soil is negligible, (3) there are no significant nitrogen inputs from sources other than atmospheric deposition, (4) ammonium leaching is negligible because any inputs are either taken up by biota or adsorbed onto soils or nitrate compounds, and (5) long-term sinks of sulfate in the catchment soils are negligible.

### ***1.2.1 Preindustrial Base Cation Concentration***

Present-day surface water concentrations of base cations are elevated above their steady-state preindustrial concentrations because of base cation leaching through ion exchange in the soil due to anthropogenic inputs of  $\text{SO}_4^{2-}$  to the watershed. For this reason, present-day surface water base cation concentrations are higher than natural or preindustrial levels, which, if not corrected for, would result in critical load values not in steady-state condition. To estimate the preacidification flux of base cations, the present flux of base cations was estimated,  $\text{BC}_t^*$ , given by

$$\text{BC}_t^* = \text{BC}_{\text{dep}}^* + \text{BC}_w - \text{BC}_u + \text{BC}_{\text{exc}}, \quad (7)$$

where

$\text{BC}_{\text{exc}}$  = the release of base cations due to ion-exchange processes.

Assuming that deposition, weathering rate, and net uptake have not changed over time,  $BC_{exc}$  can be obtained by subtracting Equation 5 from Equation 7:

$$BC_{exc} = BC_t^* - BC_0^* \quad (8)$$

This present-day excess production of base cations in the catchment was related to the long-term changes in inputs of nonmarine acid anions ( $\Delta SO_4^{*2} + \Delta NO_3$ ) by the F-factor (see below):

$$BC_{exc} = F (\Delta SO_4^{*2} + \Delta NO_3) \quad (9)$$

For the preacidification base cation flux, solving Equation 5 for  $BC_0^*$  and then substituting Equation 8 for  $BC_{exc}$  and explicitly describing the long-term changes in nonmarine acid ion inputs:

$$BC_0^* = BC_t^* - F (SO_4^{*4,t} - SO_4^{*4,0} + NO_3^{*3,t} - NO_3^{*3,0}) \quad (10)$$

The preacidification  $NO_3^-$  concentration,  $NO_3^{*3,0}$ , was assumed to be zero.

### 1.2.2 *F-factor*

An F-factor was used to correct the concentrations and estimate preindustrial base concentrations for lakes in the Adirondack Case Study Area. In the case of streams in the Shenandoah Case Study Area, the preindustrial base concentrations were derived from the MAGIC model as the base cation supply in 1860 (hindcast) because the F-factor approach is untested in this region. An F-factor is a ratio of the change in nonmarine base cation concentration due to changes in strong acid anion concentrations (Henriksen, 1984; Brakke et al., 1990):

$$F = ([BC^*]_t - [BC^*]_0) / ([SO_4^{*4}]_t - [SO_4^{*4}]_0 + [NO_3^{*3}]_t - [NO_3^{*3}]_0), \quad (12)$$

where the subscripts t and 0 refer to present and preacidification conditions, respectively. If  $F=1$ , all incoming protons are neutralized in the catchment (only soil acidification); at  $F=0$ , none of the incoming protons are neutralized in the catchment (only water acidification). The F-factor was estimated empirically to be in the range 0.2 to 0.4, based on the analysis of historical data from Norway, Sweden, the United States, and Canada (Henriksen, 1984). Brakke et al. (1990) later suggested that the F-factor should be a function of the base cation concentration:

$$F = \sin (\pi/2 Q[BC^*]_t/[S]) \quad (13)$$

where

$Q$  = the annual runoff (m/yr)

$[S]$  = the base cation concentration at which  $F=1$ ; and for  $[BC^*]_t > [S]$   $F$  is set to 1. For Norway  $[S]$  has been set to 400 milliequivalents per cubic meter ( $\text{meq/m}^3$ ) (circa. 8 mg Ca/L) (Brakke et al., 1990).

The preacidification  $\text{SO}_4^{2-}$  concentration in lakes,  $[\text{SO}_4^*]_0$ , is assumed to consist of a constant atmospheric contribution and a geologic contribution proportional to the concentration of base cations (Brakke et al., 1989). The preacidification  $\text{SO}_4^{2-}$  concentration in lakes,  $[\text{SO}_4^*]_0$  was estimated from the relationship between  $[\text{SO}_4]_0^*$  and  $[\text{BC}]_t^*$  based on work completed by Henriksen et al., 2002 as described by the following equation:

$$[\text{SO}_4]_0^* = 15 + 0.16 * [\text{BC}]_t^* \quad (14)$$

### 1.2.3 ANC Limits

Four classes of ANC limits were estimated: Suitable ANC  $>50 \mu\text{eq/L}$ , Indeterminate ANC 20 to  $50 \mu\text{eq/L}$ , Marginal ANC 0 to  $20 \mu\text{eq/L}$ , and Unsuitable ANC  $<0 \mu\text{eq/L}$ .

### 1.2.4 Sea Salt Corrections

The model applies a sea salt correction to the water chemistry concentrations. The equations below were applied to all lakes and streams, and to all the New England states and eastern Canadian provinces for the New England Governors and Eastern Canadian Premier assessment. The equations correct for sea salt. An asterisk (\*) indicates the value has been corrected for sea salt. Units are in  $\mu\text{eq/L}$ .

$$\text{Ca}^* = (\text{Ca} - (\text{CL} \times 0.0213)) \quad (14)$$

$$\text{Mg}^* = (\text{Mg} - (\text{CL} \times 0.0669)) \quad (15)$$

$$\text{Na}^* = (\text{Na} - (\text{CL} \times 0.557)) \quad (16)$$

$$\text{K}^* = (\text{K} - (\text{CL} \times 0.0206)) \quad (17)$$

$$\text{SO}_4^* = (\text{SO}_4 - (\text{CL} \times 0.14)) \quad (18)$$



### 1.2.5 Critical load exceedance

It is not possible to define a maximal loading for a single total of acidity (i.e., both nitrogen and sulfur deposition) because the acid anions sulfate and nitrate behave differently in the way they are transported with hydrogen ions; one unit of deposition of sulfur will not have the same net effect on surface water ANC as an equivalent unit of nitrogen deposition. However, the individual maximum and minimum critical loads for nitrogen and sulfur are defined when nitrogen or sulfur do not contribute to the acidity in the water. The maximum critical load for sulfur ( $CL_{\max}(S)$ ) is the following:

$$CL_{\max}(S) = [( [BC]_0^* - [ANC_{\text{level}}])Q] \quad (3)$$

when nitrogen deposition does not contribute to the acidity balance. Given the assumption that the long-term sinks of sulfate in the catchment soils are negligible, the amount of sulfur entering the catchment is equal to the amount loaded to the surface water. For this reason, the minimal amount of sulfur is equal to zero:

$$CL_{\min}(S) = 0 \quad (4)$$

In the case of nitrogen,  $CL_{\min}(N)$  is the minimum amount of deposition of total nitrogen ( $NH_x + NO_x$ ) that catchment processes can effectively remove (e.g.,  $N_{\text{upt}} + N_{\text{imm}} + N_{\text{den}} + N_{\text{ret}}$ ) without contributing to the acidic balance:

$$CL_{\min}(N) = fN_{\text{upt}} + (1-r)(N_{\text{imm}} + N_{\text{den}}) \quad (5)$$

The  $CL_{\max}(N)$  is the load for total nitrogen deposition when sulfur deposition is equal to zero:

$$CL_{\max}(N) = fN_{\text{upt}} + (1-r)(N_{\text{imm}} + N_{\text{den}}) + [( [BC]_0^* - [ANC_{\text{level}}])Q]. \quad (6)$$

In reality, neither nitrogen nor sulfur deposition will ever be zero, so the depositional load for the deposition of one is fixed by the deposition of the other, according to the line defining in

**Figure 1.2-1.**

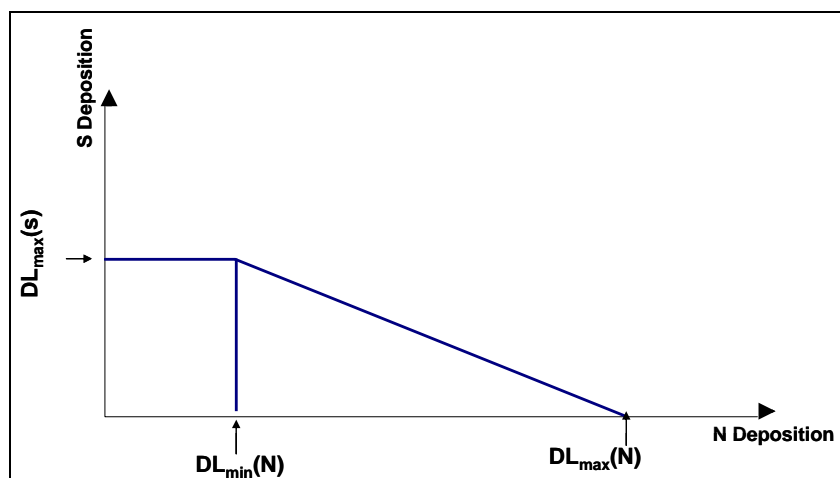


**Figure 1.2-1.** The depositional load function defined by the model.

The thick lines indicate all possible combinations of depositional loads of nitrogen and sulfur acidity that a catchment can receive and still maintain an ANC concentration equal to its  $ANC_{limit}$ . Note that in the above formulation, individual depositional loads of nitrogen and sulfur are not specified; each combinations of depositions ( $S_{dep}$  and  $N_{dep}$ ) fulfilling Equations 2 through 6.

Finally, the calculated exceedances of the critical load of acidity  $Ex(A)$ , when the  $N_{leach}$  is considered the contribution of acid anions acidification is the following:

$$Ex(A) = S_{dep}^* + N_{leach} - CL(A), \quad (11)$$

where  $S_{dep}^*$  is the amount of sulfur deposited in the catchment (assuming that all  $SO_4^{2-}$  deposited leaches into the waterbody) and  $N_{leach}$  is the amount of deposited nitrogen,  $N_{dep}$ , that moves into the water.

While  $SO_4^{2-}$  is assumed to be a mobile anion ( $S_{leach} = S_{dep}^*$ ), nitrogen is to a large extent retained in the catchment by various processes; therefore,  $N_{dep}$  cannot be used directly in the exceedances calculation. Only present-day exceedances can be calculated from the leaching of nitrogen,  $N_{leach}$ , which is determined from the sum of measured concentrations of  $NO_3^-$  and ammonia in the stream chemistry. No nitrogen deposition data are required for exceedance calculations; however,  $Ex(A)$  quantifies only the exceedances at present rates of retention of nitrogen in the catchment.

### **1.2.6 Lake-to-Catchment-Area Ratios**

Lake and catchment areas data are from the Environmental Monitoring and Assessment Program (EMAP) (see Section 4.1.2.1 of Chapter 4).

### **1.2.7 Denitrification and N Immobilization in Soils**

It was assumed that the denitrification fractions are related to the soil types in the catchments. In deeply drained podzolic soils, denitrification values are generally low. However, high values may occur in areas with peatsoils (Klemedtsson and Svensson, 1988; De Vries et al., 1994). Therefore, the average denitrification fraction for each catchment was approximated by the following linear relationship:

$$f_{de} = 0.1 + 0.7f_{peat} \quad (12)$$

where  $f_{peat}$  is the fraction of peatlands in the catchment area.

For the long-term immobilization of nitrogen in forest soils ( $N_{imm}$ ), a constant value of 2 kg N/ha/yr was used. This value represents the lower end of the range suggested for European critical load calculations (Posch et al., 1997).

### **1.2.8 Uncertainty and Variability**

There is uncertainty associated with the parameters in the steady-state critical load model used to estimate aquatic critical loads. The strength of the critical load estimate and the exceedance calculation relies on the ability to estimate the catchment-average base cation supply (i.e., input of base cations from weathering of bedrock and soils and air), runoff, and surface water chemistry. The uncertainty associated with runoff and surface water measurements is fairly well known. However, the ability to accurately estimate the catchment supply of base cations to a waterbody is still poorly known. This is important because the catchment supply of base cations from the weathering of bedrock and soils is the factor that has the most influence on the critical load calculation and also has the largest uncertainty (Li and McNulty, 2007). Although the approach to estimate base cation supply in the case study areas (e.g., F-factor) approach has been widely published and analyzed in Canada and Europe, and has been applied in the United States (e.g., Dupont et al., 2005), the uncertainty in this estimate is unclear and is likely large. For this reason, an uncertainty analysis of the state-steady critical load model was completed to evaluate the uncertainty in the critical load and exceedances estimations.

A probabilistic analysis using a range of parameter uncertainties was used to assess: (1) the degree of confidence in the exceedance values and (2) the coefficient of variation (CV) of the critical load and exceedance values. The probabilistic framework is Monte Carlo, whereby each steady-state input parameter varies according to specified probability distributions and their range of uncertainty (**Table 1.2-1**). The purpose of the Monte Carlo methods was to propagate the uncertainty in the model parameters in the steady-state critical load model.

**Table 1.2-1.** Parameters Used and their Uncertainty Range. The Range of Surface Water Parameters (e.g., CA, MG, CL, NA, NO<sub>3</sub>, SO<sub>4</sub>) were Determined from Surface Water Chemistry Data for the Period from 1992 to 2006 from the LTM-TIME Monitoring Network. Runoff(Q) and Acidic Deposition were Set at 50% and 25%

Parameter	Units	Uncertainty range	Distribution
Q	µeq/L	50%	Normal
CA	µeq/L	65%	Normal
MG	µeq/L	64%	Normal
CL	µeq/L	52%	Normal
NA	µeq/L	58%	Normal
NO <sub>3</sub>	µeq/L	30%	Normal
SO <sub>4</sub>	µeq/L	57%	Normal
Acidic Deposition (NO <sub>x</sub> & SO <sub>4</sub> )	meq/L	25%	Lognormal

Within the Monte Carlo analysis, model calculations were run a sufficient number of times (i.e., 1,000 times) to capture the range of behaviors represented by all variables. The analysis tabulated the number of lakes where the confidence interval is entirely below the critical load, the confidence interval is entirely above the critical load, and the confidence interval straddles zero. Similar results are given for the number of sites with all realizations above the critical load, all realizations below the critical load, and some realizations above and some below the critical load. An inverse cumulative distribution function for exceedances was constructed from the 1000 model runs for each site, which describes the probability of a site to exceed its critical load. For each site, the probability of exceeding its critical load (i.e. probability of exceedance) is determined at the percent of the cumulative frequency distribution that lies above zero. The probability of exceedance, where the percentage of the cumulative frequency

distribution lies above zero, was calculated for all sites and assigned to one of the following five classes:

- 0-5% probability: unlikely to be exceeded;
- 5-25% probability: relatively low risk of exceedance;
- 25-75% probability: potential risk of exceedance;
- 75-95% probability: relatively high risk of exceedance;
- > 95% probability: highly likely to be exceeded.

This gives us a measure of the degree of confidence in whether the site exceeds its critical load. The CDF for Little Hope Pond is shown in **Figure 1.2-2**.

The coefficient of variation (CV) was also calculated on each site for both the critical load and exceedance calculations. The coefficient of variation represents the ratio of the standard deviation to the mean, and it is a useful statistic for comparing the degree of variation in the data. The coefficient of variation allows a determination of how much uncertainty (risk) comparison to its mean.

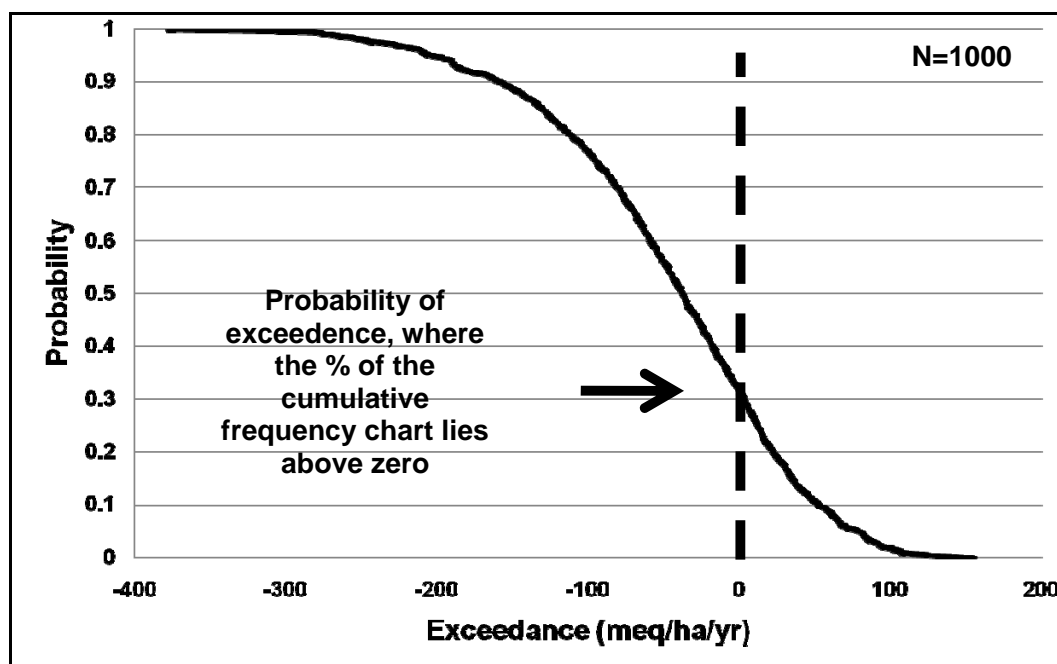


**Figure 1.2-2.** The inverse cumulative frequency distribution for Little Hope Pond. The x-axis shows critical load exceedance in meq/ha/yr and y-axis is the probability. The dashed lines represent zero exceedance. In the case of Little Hope Pond, the dash line divides mostly the probability distribution on the left hand side, indicating Little Hope

Pond has a relative low probability of being exceeded (0.3). Critical load and exceedances values were based on a critical level of protection of ANC = 50  $\mu\text{eq/L}$ .

### 1.2.8.1 Results of the uncertainty analysis

The means and coefficients of variation for critical load (CL(A)) and exceedances (EX(A)) values are shown for all sites in **Table 1.2-2** for four ANC limits (0, 20, 50, 100  $\mu\text{eq/L}$ ). The average coefficients of variation for the various critical load values for all sites are remarkably low except for those calculated using a critical limit of 100  $\mu\text{eq/L}$ . It is noticeable that though all the relevant input parameters have spreads of 25% to 65%, the CVs for CL(A) are only 4%, 5%, 9%, and 100% for critical load limits of 0%, 20%, 50%, and 100%  $\mu\text{eq/L}$ , respectively. In the case of the absolute value of the exceedances (EX(A)), the average CVs for all sites are higher, but still relatively low at 18%, 17%, 25%, and 33%. The individual coefficients of variation for each sites and an ANC limit of 50  $\mu\text{eq/L}$  are shown in **Figure 1.2-3**. Although the average CV is relatively small for the population of sites modeled, individual site CV can varies from 1% to 45% for CL(A) and to 5% to over 100% for EX(A). This difference is due to the high degree of uncertainty in site specific parameters for particular sites and a low degree of confidence in the exceedance value itself for these sites. In addition, when the mean value is near zero, as is the case for exceedance values, the coefficient of variation is sensitive to small changes in the mean, which likely explains why some sites have high CV compare to others.

**Table 1.2-2.** Means and Coefficients of Variation of Critical Loads and Exceedances for Surface Water.

Parameter	Critical load Limit ( $\mu\text{eq/L}$ )	Mean ( $\text{meq/L}$ )	Coefficient of variation (%)
CL(A)	0	247.8	4
	20	227.0	5
	50	196.7	9
	100	140.3	100
EX(A)	0	-178.3	18
	20	-157.6	17
	50	-127.2	25
	100	-75.0	33

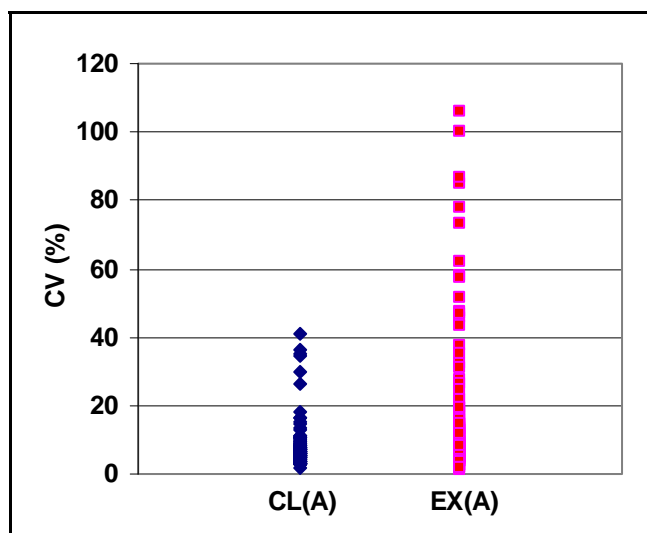


**Figure 1.2-3.** Coefficients of variation of surface water critical load for acidity CL(A) and exceedances (EX(A)). Critical load and exceedances values were based on a critical level of protection of ANC = 50  $\mu\text{eq/L}$ .

The probability of exceedance results, where the percentage of the cumulative frequency distribution lies above zero, are shown in **Figure 1.2-4**. Those areas that have less than 5% probability of exceedance are those with a high degree of confidence that the critical loads are not exceeded; conversely, areas with more than a 95% probability of exceedance are the most certain to be exceeded.

For the sites in the aquatic case study areas, the probability of exceeding the critical load at an ANC limit of 0, 20, 50, and 100  $\mu\text{eq/L}$  were relatively high. The waterbodies that exceeded their critical loads had a greater than 80% probability of doing so. The range of probability of exceedance was from 80% to 98%, indicating a relatively high confidence that these sites exceeded their critical load. The results suggest a relatively robust estimate of critical loads and exceedance rates for the case study areas. It is important to note that this analysis may understate the actual uncertainty because some of the range and distribution types of parameters are not well known for the United States at this time.

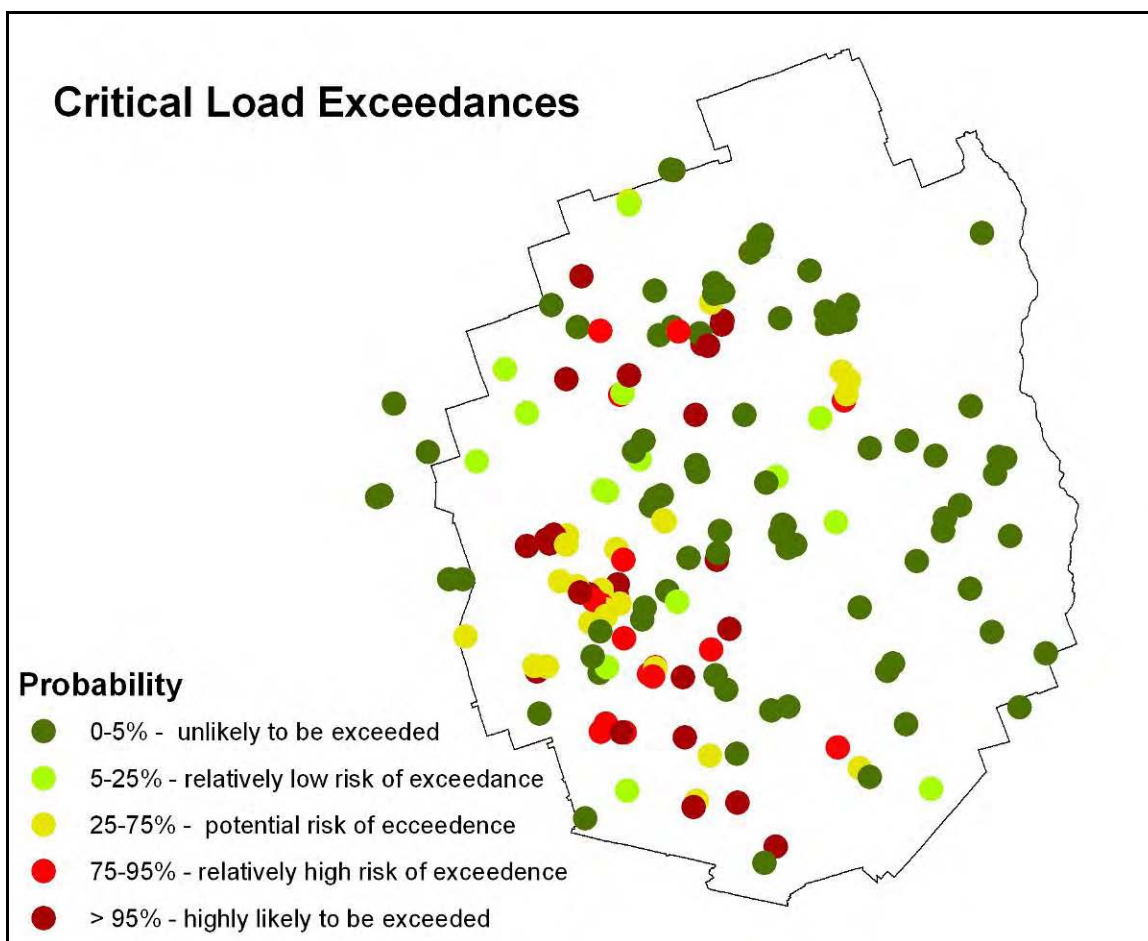


**Figure 1.2-4.** Probability of exceedance of critical load for acidity for 2002.



## **ATTACHMENT B**

### **1. EMAP/TIME/LTM PROGRAMS**

The EPA Environmental Monitoring and Assessment Program (EMAP) began regional surveys of the nation's surface waters in 1991 with a survey of northeastern United States lakes. Since then, EMAP and Regional-EMAP (REMAP) surveys have been conducted on lakes and streams throughout the country. The objective of these EMAP surveys is to characterize ecological condition across populations of surface waters. EMAP surveys are probability surveys where sites are picked using a spatially balanced systematic randomized sample so that the results can be used to make estimates of regional extent of condition (e.g., number of lakes, length of stream). EMAP sampling typically consists of measures of aquatic biota (e.g., fish, macroinvertebrates, zooplankton, periphyton), water chemistry, and physical habitat. Of particular interest with respect to acidifying deposition effects were two EMAP surveys conducted in the 1990s, the Northeastern Lake Survey and the Mid-Atlantic Highlands Assessment of streams (MAHA). The Northeastern Lake Survey was conducted in summer from 1991 to 1994 and consisted of 345 randomly selected lakes in New York, New Jersey, Vermont, New Hampshire, Maine, Rhode Island, Connecticut, and Massachusetts (Whittier et al., 2002). To make more precise estimates of the effects of acidic deposition, the sampling grid was intensified to increase the sample site density in the Adirondack Mountains and New England Uplands areas known to be susceptible to acidic deposition. The MAHA study was conducted on 503 stream sites from 1993 to 1995 in the states of West Virginia, Virginia, Pennsylvania, Maryland, Delaware, and the Catskill Mountain region of New York (Herlihy et al., 2000). Sampling was done during spring baseflow. Sample sites were restricted to first through third order streams as depicted on the USGS 1:100,000 digital maps used in site selection. To make more precise estimates of the effects of acidic deposition, the sampling grid was intensified to increase the sample site density in the Blue Ridge, Appalachian Plateau, and Ridge section of the Valley and Ridge ecoregions. Results from both of these surveys were used to develop and select the sampling sites for the Temporally Integrated Monitoring of Ecosystems (TIME) program, which is described below.

## **2. TEMPORALLY INTEGRATED MONITORING OF ECOSYSTEMS AND LONG-TERM MONITORING PROGRAMS**

There are two surface water chemistry monitoring programs, administered by EPA, that are especially important to inform the assessment of aquatic ecosystem responses to changes in atmospheric deposition. These are the TIME program (Stoddard et al., 2003) and the Long-term Monitoring (LTM) project (Ford et al., 1993; Stoddard et al., 1998). These efforts focus on portions of the United States most affected by the acidifying influence of sulfur and nitrogen deposition, including lakes in the Adirondack Mountains of New York and in New England, and streams in the Northern Appalachian Plateau and Blue Ridge in Virginia and West Virginia. Both projects are operated cooperatively with numerous collaborators in state agencies, academic institutions, and other federal agencies. The TIME program and LTM project have slightly different objectives and structures, which are outlined below. Stoddard et al. (2003) conducted a thorough trends analysis of the TIME and LTM data.

### **2.1 TIME Program**

At the core of the TIME project is the concept of probability sampling, whereby each sampling site is chosen statistically from a predefined target population. Collectively, the monitoring data collected at the sites are representative of the target population of lakes or streams in each study region. The target populations in these regions include lakes and streams likely to be responsive to changes in acidifying deposition, defined in terms of acid neutralizing capacity (ANC), which represents an estimate of the ability of water to buffer acid. Measurement of Gran ANC uses the Gran technique to find the inflection point in an acid-base titration of a water sample (Gran, 1952). In the Northeast, the TIME target population consists of lakes with a Gran ANC <100 microequivalents per liter ( $\mu\text{eq/L}$ ). In the mid-Atlantic, the target population is upland streams with Gran ANC <100  $\mu\text{eq/L}$ . In both regions, the sample sites selected for future monitoring were selected from the EMAP survey sites in the region (Section AX3.2.1.1) that met the TIME target population definition. Each lake or stream is sampled annually (in summer for lakes; in spring for streams), and results are extrapolated with known confidence to the target population(s) as a whole using the EMAP site population expansion factors or weights (Larsen and Urquhart, 1993; Larsen et al., 1994; Stoddard et al., 1996; Urquhart et al., 1998). TIME sites were selected using the methods developed by the EMAP (Herlihy et al., 2000; Paulsen et al.,

1991;). The TIME program began sampling northeastern lakes in 1991. Data from 43 lakes in the Adirondack Mountains can be extrapolated to the target population of low ANC lakes in that region. There are about 1,000 low-ANC Adirondack lakes, out of a total population of 1,842 lakes with surface area greater than 1 hectare (ha). Data from 30 lakes (representing about 1,500 low-ANC lakes, out of a total population of 6,800) form the basis for TIME monitoring in New England. Probability monitoring of mid-Atlantic streams began in 1993. Stoddard et al. (2003) analyzed data from 30 low-ANC streams in the Northern Appalachian Plateau (representing about 24,000 kilometer (km) of low-ANC stream length out of a total stream length of 42,000 km).

The initial 1993 to 1995 EMAP-MAHA sample in the mid-Atlantic was not dense enough to obtain enough sites in the TIME target population in the Blue Ridge and Valley and Ridge ecoregions. In 1998, another denser random sample was conducted in these ecoregions to identify more TIME sites. After pooling TIME target sites taken from both MAHA and the 1998 survey, there are now 21 TIME sites in the Blue Ridge and Ridge and Valley that can be used for trend detection in this aggregate ecoregion in the mid-Atlantic in addition to the northern Appalachian Plateau ecoregion.

## **2.2 LTM Program**

As a complement to the statistical lake and stream sampling in TIME, the LTM Program samples a subset of generally acid-sensitive lakes and streams that have long-term data, many dating back to the early 1980s. These sites are sampled 3 to 15 times per year. This information is used to characterize how some of the most sensitive aquatic systems in each region are responding to changing deposition, as well as giving information on seasonal variation in water chemistry. In most regions, a small number of higher-ANC (e.g., Gran ANC >100 µeq/L) sites are also sampled, and these help to separate temporal changes due to acidifying deposition from those attributable to other disturbances (e.g., climate, land use change). Because of the availability of long-term records (i.e., more than two decades) at many LTM sites, their trends can also be placed in a better historical context than those of the TIME sites, where data are only available starting in the 1990s. Monitored water chemistry variables include pH, ANC, major anions and cations, monomeric aluminum (Al), silicon (Si), specific conductance, dissolved organic carbon, and dissolved inorganic carbon. The field protocols, laboratory methods, and

quality assurance procedures are specific to each team of investigators. This information is contained in the cited publications of each research group. The EMAP and TIME protocols and quality assurance methods are generally consistent with those of the LTM cooperators. Details of LTM data from each region are given below.

**New England lakes:** The LTM project collects quarterly data from lakes in Maine (sampled by the University of Maine) (Kahl et al., 1991; Kahl et al., 1993) and Vermont (data collected by the Vermont Department of Environmental Conservation) (Stoddard and Kellogg, 1993; Stoddard et al., 1998). Data from 24 New England lakes were available for the trend analysis reported by Stoddard et al. (2003) for the period 1990 to 2000. In addition to quarterly samples, a subset of these lakes have outlet samples collected on a weekly basis during the snowmelt season; these data are used to characterize variation in spring chemistry. The majority of New England LTM lakes have mean Gran ANC values ranging from 20 to 100  $\mu\text{eq/L}$ ; two higher ANC lakes (i.e., Gran ANC between 100 and 200  $\mu\text{eq/L}$ ) are also monitored.

**Adirondack lakes:** The trend analysis of Stoddard et al. (2003) included data from 48 Adirondack lakes, sampled monthly by the Adirondack Lake Survey Corporation (Driscoll and Van Dreason, 1993; Driscoll et al., 1995); a subset of these lakes are sampled weekly during spring snowmelt to help characterize spring season variability. Sixteen of the lakes have been monitored since the early 1980s; the others were added to the program in the 1990s. The Adirondack LTM dataset includes both seepage and drainage lakes, most with Gran ANC values in the range -50 to 100  $\mu\text{eq/L}$ ; three lakes with Gran ANC between 100  $\mu\text{eq/L}$  and 200  $\mu\text{eq/L}$  are also monitored.

**Appalachian Plateau streams:** Stream sampling in the Northern Appalachian Plateau is conducted about 15 times per year, with the samples spread evenly between baseflow (e.g., summer and fall) and high flow (e.g., spring) seasons. Data from four streams in the Catskill Mountains (collected by the U.S. Geological Survey) (Murdoch and Stoddard, 1993), and five streams in Pennsylvania (collected by Pennsylvania State University) (DeWalle and Swistock, 1994) were analyzed by Stoddard et al. (2003). All of the northern Appalachian LTM streams have mean Gran ANC values in the range 25 to 50  $\mu\text{eq/L}$ .

**Upper Midwest lakes:** Forty lakes in the Upper Midwest were originally included in the LTM project, but funding in this region was terminated in 1995. The Wisconsin Department of Natural Resources (funded by the Wisconsin Acid Deposition Research Council, the Wisconsin

Utilities Association, the Electric Power Research Institute, and the Wisconsin Department of Natural Resources) has continued limited sampling of a subset of these lakes, as well as carrying out additional sampling of an independent subset of seepage lakes in the state. The data reported by Stoddard et al. (2003) included 16 lakes (both drainage and seepage) sampled quarterly (Webster et al., 1993), and 22 seepage lakes sampled annually in the 1990s. All of the Upper Midwest LTM lakes exhibit mean Gran ANC values from 30 to 80  $\mu\text{eq/L}$ .

Ridge/Blue Ridge streams: Data from the Ridge and Blue Ridge provinces consist of a large number of streams sampled quarterly throughout the 1990s as part of the Virginia Trout Stream Sensitivity Study (Webb et al., 1989), and a small number of streams sampled more intensively (as in the Northern Appalachian Plateau). A total of 69 streams, all located in the Ridge section of the Ridge and Valley province, or within the Blue Ridge province, and all within the state of Virginia, had sufficient data for the trend analyses by Stoddard et al. (2003). The data are collected cooperatively with the University of Virginia and the National Park Service. Mean Gran ANC values for the Ridge and Blue Ridge data range from 15 to 200  $\mu\text{eq/L}$ , with 7 of the 69 sites exhibiting mean Gran ANC  $>100 \mu\text{eq/L}$ .



September 2009

# **Appendix 5**

## **Terrestrial Acidification Case Study**

*Final*

EPA Contract Number EP-D-06-003  
Work Assignment 3-62  
Project Number 0209897.003.062

### **Prepared for**

U.S. Environmental Protection Agency  
Office of Air Quality Planning and Standards  
Research Triangle Park, NC 27709

### **Prepared by**

RTI International  
3040 Cornwallis Road  
Research Triangle Park, NC 27709-2194







## TABLE OF CONTENTS

Acronyms and Abbreviations .....	xi
1.0 Background .....	1
1.1 Indicators, Ecological Endpoints, and Ecosystem Services .....	2
1.1.1 Indicators.....	2
1.1.2 Ecological Endpoints .....	7
1.1.3 Ecosystem Services.....	10
1.2 Case Study Areas.....	11
1.2.1 GIS Analysis of National Sensitivity .....	11
1.2.2 Selection of Case Study Areas .....	12
1.2.3 Sugar Maple .....	17
1.2.3.1 Kane Experimental Forest.....	17
1.2.3.2 Plot Selection for Kane Experimental Forest Case Study Area.....	18
1.2.4 Red Spruce .....	20
1.2.4.1 Hubbard Brook Experimental Forest.....	20
1.2.4.2 Plot Selection for Hubbard Brook Experimental Forest Case Study Area .....	22
2.0 Approach and Methods .....	26
2.1 Chosen Method.....	30
2.1.1 Critical Load Equations and Calculations.....	31
2.1.1.1 Simple Mass Balance Calculations .....	31
2.1.1.2 Deposition Relative to Critical Load Calculations .....	37
2.1.1.3 Critical Load Function .....	38
2.1.2 Critical Load Data Requirements.....	39
2.1.2.1 Data Requirements and Sources .....	39
2.1.2.2 Selection of Indicator Values.....	42
2.1.2.3 Case Study Input Data .....	45
2.2 Critical Load Function Response Curves Associated with the Three Levels of Protection.....	49
3.0 Results.....	50
3.1 Critical Load Estimates .....	50
3.1.1 Sugar Maple .....	50
3.1.2 Red Spruce .....	58
3.2 Recommended Parameter Values and Critical Loads.....	62
3.3 Current Conditions .....	63
4.0 Expansion of Critical Load Assessments for Sugar Maple and Red Spruce .....	75
4.1 Critical Load Assessments.....	75
4.2 Relationship between Atmospheric Nitrogen and Sulfur Deposition and Tree Growth.....	91
5.0 Uncertainty Analysis.....	92
5.1 Kane Experimental Forest and Hubbard Brook Experimental Forest Case Study Areas.....	92
5.2 Expansion of Critical Load Assessments .....	93
6.0 References.....	96

Attachment A: Relationship Between Atmospheric Nitrogen and Sulfur Deposition and Sugar Maple and Red Spruce Tree Growth .....	1
1. Introduction .....	1
2. Source of Data for Analyses .....	2
3. Regression Analyses Methodology and Results .....	7
4. Additional Sources of Variability Influencing the Relationships between Tree Volume Growth and Nitrogen Deposition and Critical Load Exceedance.....	18
4.1 State-Specific Variables.....	18
4.2 Dead Trees .....	19
4.3 Other Factors.....	19
5. Conclusions .....	21

## LIST OF FIGURES

Figure 1.1-1. Conceptual impacts of acidifying deposition on soil $\text{Ca}^{2+}$ depletion, tree physiology, and forest ecosystem health and sustainability (recreated from DeHayes et al., 1999).....	6
Figure 1.1-2. Areal coverages of red spruce and sugar maple tree species within the continental United States (USFS, 2006). .....	10
Figure 1.2-1. Map of areas of potential sensitivity of red spruce and sugar maple to acidification in the United States (see Table 1.2-1 for listing of data sources to produce this map).....	12
Figure 1.2-2. Location of the Kane Experimental Forest (Horsley et al., 2000). .....	17
Figure 1.2-3. The seven plots used to evaluate critical loads of acidity in the Kane Experimental Forest. ....	19
Figure 1.2-4. Location of the Hubbard Brook Experimental Forest.....	21
Figure 1.2-5. Vegetation cover (NLCD, 2001) and location of Watershed 6 of Hubbard Brook Experimental Forest. ....	24
Figure 1.2-6. Grid units within Watershed 6 of Hubbard Brook Experimental Forest. The red outline delineates the spruce-fir forest type. The dotted grid cell areas indicate the grid units with high proportions of red spruce and represents the composite plot area for the Hubbard Brook Experimental Forest Case Study Area. ....	25
Figure 1.2-7. Location of case study plots within Watershed 6 of Hubbard Brook Experimental Forest. ....	26
Figure 2.1-1. The critical load function created from the calculated maximum and minimum levels of total nitrogen and sulfur deposition (eq/ha/yr). The grey areas show deposition levels less than the established critical loads. The red line is the maximum critical level of sulfur deposition (valid only when nitrogen deposition is less than the minimum critical level of nitrogen deposition [blue dotted line]). The flat line portion of the curves	

indicates nitrogen deposition corresponding to the $CL_{min}(N)$ (i.e., nitrogen absorbed by nitrogen sinks within the system). .....	39
Figure 2.1-2. The relationship between the $Bc/Al$ ratio in soil solution and the percentage of tree species (found growing in North America) exhibiting a 20% reduction in growth relative to controls (after Sverdrup and Warfvinge, 1993b). .....	44
Figure 2.1-3. The relationship between soil solution $Bc/Al$ ratio and stem or root growth in sugar maple (from Sverdrup and Warfvinge, 1993b). .....	44
Figure 2.1-4. The relationship between soil solution $Bc/Al$ ratio and biomass or root growth in red spruce (from Sverdrup and Warfvinge, 1993b). .....	45
Figure 2.2-1. An example of the critical load function response curves associated with the three $(Bc/Al)_{crit}$ ratios and the associated levels of protection of tree health. The flat line portion of the curves indicates total nitrogen deposition corresponding to the $CL_{min}$ (nitrogen absorbed by nitrogen sinks within the system). .....	50
Figure 3.1-1. The critical load function response curves detailing the lowest critical load estimates for Plot 1 of the Kane Experimental Forest (refer to Table 3.1-1 for the parameters corresponding to each of the curves). The flat line portion of the curves indicates total nitrogen deposition corresponding to the $CL_{min}(N)$ (nitrogen absorbed by nitrogen sinks within the system). .....	56
Figure 3.1-2. The critical load function response curves detailing the highest critical load estimates for Plot 1 of the Kane Experimental Forest (refer to Table 3.1-1 for the parameters corresponding to each of the curves). The flat line portion of the curves indicates total nitrogen deposition corresponding to the $CL_{min}(N)$ (nitrogen absorbed by nitrogen sinks within the system). .....	57
Figure 3.1-3. The critical load function response curves detailing the lowest critical load estimates for the Hubbard Brook Experimental Forest Case Study Area (refer to Table 3.1-10 for the parameters corresponding to each of the curves). The flat line portion of the curves indicates total nitrogen deposition corresponding to the $CL_{min}(N)$ (nitrogen absorbed by nitrogen sinks within the system). .....	60
Figure 3.1-4. The critical load function response curves detailing the highest critical load estimates for the Hubbard Brook Experimental Forest Case Study Area (refer to Table 3.1-10 for the parameters corresponding to each of the curves). The flat line portion of the curves indicates total nitrogen deposition corresponding to the $CL_{min}(N)$ (nitrogen absorbed by nitrogen sinks within the system). .....	60
Figure 3.3-1. Plot 1 Kane Experimental Forest critical load function response curves, detailing the lowest critical load estimates for Kane Experimental Forest Case Study Area (refer to Table 3.1-1 for the parameters corresponding to each of the curves). The 2002 CMAQ/NADP total nitrogen and sulfur deposition levels $((N+S)_{comb})$ were greater than the critical loads of nitrogen and sulfur at all levels of protection $((Bc/Al)_{crit} = 0.6, 1.2, \text{ and } 2.0)$ . .....	60

- 10.0). The flat line portion of the curves indicates total nitrogen deposition corresponding to the  $CL_{min}(N)$  (nitrogen absorbed by nitrogen sinks within the system). ..... 68
- Figure 3.3-2. Plot 1 critical load function response curves, detailing the highest maximum deposition load estimates for Kane Experimental Forest Case Study Area (refer to Table 3.1-1 for the parameters corresponding to each of the curves). The 2002 CMAQ/NADP total nitrogen and sulfur deposition levels  $((N+S)_{comb})$  were greater than the critical load of total nitrogen and sulfur deposition calculated with the highest level of protection  $(Bc/Al)_{crit} = 10.0)$ . The flat line portion of the curves indicates total nitrogen deposition corresponding to the  $CL_{min}(N)$  (nitrogen absorbed by nitrogen sinks within the system). ..... 69
- Figure 3.3-3. Critical load function response curves, detailing the lowest critical load estimates for the Hubbard Brook Experimental Forest Case Study Area (refer to Table 3.1-10 for the parameters corresponding to each of the curves). The 2002 CMAQ/NADP total nitrogen and sulfur deposition levels  $((N+S)_{comb})$  were greater than the critical load of total nitrogen and sulfur calculated with the highest and the intermediate levels of protection  $((Bc/Al)_{crit} = 1.2 \text{ and } 10.0)$ . The flat line portion of the curves indicates total nitrogen deposition corresponding to the  $CL_{min}(N)$  (nitrogen absorbed by nitrogen sinks within the system). ..... 70
- Figure 3.3-4. Critical load function response curves, detailing the highest critical load estimates for the Hubbard Brook Experimental Forest Case Study Area (refer to Table 3.1-10 for the parameters corresponding to each of the curves). The 2002 CMAQ/NADP total nitrogen and sulfur deposition levels  $((N+S)_{comb})$  were less than the critical loads associated with all three  $(Bc/Al)_{crit}$  ratios. The flat line portion of the curves indicates total nitrogen deposition corresponding to the  $CL_{min}(N)$  (nitrogen absorbed by nitrogen sinks within the system). ..... 71
- Figure 3.3-5. Critical load function response curves for the three selected critical loads conditions (corresponding to the three levels of protection) for the Kane Experimental Forest Case Study Area. The 2002 CMAQ/NADP total nitrogen and sulfur deposition levels  $((N+S)_{comb})$  were greater than the highest and intermediate level of protection critical loads. The flat line portion of the curves indicates total nitrogen deposition corresponding to the  $CL_{min}(N)$  (nitrogen absorbed by nitrogen sinks within the system). ..... 72
- Figure 3.3-6. Critical load function response curves for the three selected critical loads conditions (corresponding to the three levels of protection) for the Hubbard Brook Experimental Forest Case Study Area. The 2002 CMAQ/NADP total nitrogen and sulfur deposition levels  $((N+S)_{comb})$  were greater than the highest level of protection critical loads. The flat line portion of the curves indicates total nitrogen deposition corresponding to the  $CL_{min}(N)$  (nitrogen absorbed by nitrogen sinks within the system). ..... 73

Figure 3.3-7. The influence of the 2002 CMAQ/NADP total nitrogen and sulfur deposition levels ( $\text{NH}_x\text{-N}$ ) on the critical load function response curve, and in turn, the maximum critical loads of sulfur ( $\text{CL}_{\text{max}}(\text{S})$ ) and oxidized nitrogen ( $\text{NO}_x\text{-N}$ ) for the selected highest protection critical load for the Kane Experimental Forest Case Study Area. The critical load of oxidized nitrogen ( $\text{NO}_x\text{-N}$ ) is 661 eq/ha/yr (910 – 249 eq/ha/yr). The $\text{CL}_{\text{min}}(\text{N})$ (nitrogen absorbed by nitrogen sinks within the system) corresponds to the value depicted in Figure 3.3-5. ....	74
Figure 3.3-8. The influence of the 2002 CMAQ/NADP total nitrogen and sulfur deposition levels ( $\text{NH}_x\text{-N}$ ) on the critical load function response curve and, in turn, the maximum critical loads of sulfur ( $\text{CL}_{\text{max}}(\text{S})$ ) and oxidized nitrogen ( $\text{NO}_x\text{-N}$ ) for the selected highest protection critical load for the Hubbard Brook Experimental Forest Case Study Area. The critical load of oxidized nitrogen ( $\text{NO}_x\text{-N}$ ) is 328 eq/ha/yr (487 – 159 eq/ha/yr). The $\text{CL}_{\text{min}}(\text{N})$ (nitrogen absorbed by nitrogen sinks within the system) corresponds to the value depicted in Figure 3.3-6. ....	75
Figure 4.1-1. States where sugar maple is found and where 2002 CMAQ/NADP total nitrogen and sulfur deposition levels exceeded the lowest protection critical load ( $\text{Bc}/\text{Al}_{(\text{crit})} = 0.6$ ) in the following: none of the sugar maple plots, <50% of the sugar maple plots, and >50% of the sugar maple plots. ....	86
Figure 4.1-2. States where sugar maple is found and where 2002 CMAQ/NADP total nitrogen and sulfur deposition levels exceeded the intermediate protection critical load ( $\text{Bc}/\text{Al}(\text{crit}) = 1.2$ ) in the following: none of the sugar maple plots, <50% of the sugar maple plots, and >50% of the sugar maple plots. ....	87
Figure 4.1-3. States where sugar maple is found and where 2002 CMAQ/NADP total nitrogen and sulfur deposition levels exceeded the highest protection critical load ( $\text{Bc}/\text{Al}(\text{crit}) = 10.0$ ) in the following: none of the sugar maple plots, <50% of the sugar maple plots, and >50% of the sugar maple plots. ....	88
Figure 4.1-4. States where red spruce is found and where 2002 CMAQ/NADP total nitrogen and sulfur deposition levels exceeded the lowest protection critical load ( $\text{Bc}/\text{Al}(\text{crit}) = 0.6$ ) in the following: none of the red spruce plots, <50% of the red spruce plots, and >50% of the red spruce plots. ....	89
Figure 4.1-5. States where red spruce is found and where 2002 CMAQ/NADP total nitrogen and sulfur deposition levels exceeded the intermediate protection critical load ( $\text{Bc}/\text{Al}(\text{crit}) = 1.2$ ) in the following: none of the red spruce plots, <50% of the red spruce plots, and >50% of the red spruce plots. ....	90
Figure 4.1-6. States where red spruce is found and where 2002 CMAQ/NADP total nitrogen and sulfur deposition levels exceeded the highest protection critical load ( $\text{Bc}/\text{Al}(\text{crit}) = 10.0$ ) in the following: none of the red spruce plots, <50% of the red spruce plots, and >50% of the red spruce plots. ....	91

## ATTACHMENT FIGURES

Figure 1-1. Hypothesized relationships between tree growth and nitrogen deposition and critical load exceedance. When deposition does not exceed the critical load, growth is stimulated by nitrogen deposition. When deposition exceeds the critical load (deposition is greater than the critical load), growth is reduced. (This figure is a modification of a curve describing forest productivity as a function of long-term chronic nitrogen additions outlined in Aber et al., 1995). .....	A-2
Figure 3-1. Areas of the continental United States that were covered during the last glacial event (~ 20,000 ybp) (Reed and Bush, 2005). .....	A-13

## LIST OF TABLES

Table 1.1-1. Literature Support for Selected Indicators of Acidification .....	2
Table 1.1-2. Key Indicators of Acidification Due to Nitrogen and Sulfur .....	3
Table 1.1-3. Summary of Linkages between Acidifying Deposition, Biogeochemical Processes That Affect $\text{Ca}^{2+}$ , Physiological Processes That Are Influenced by $\text{Ca}^{2+}$ , and Effect on Forest Function .....	8
Table 1.2-1. Summary of Mapping Layers, Selected Indicator, and Selected Ecological Endpoint for the Terrestrial Acidification Case Study .....	12
Table 1.2-2. Compilation of Potential Areas for the Terrestrial Acidification Case Study (i.e., for Studying Red Spruce) as Identified in the Literature.....	14
Table 1.2-3. Major Studies at the Kane Experimental Forest.....	18
Table 1.2-4. Characteristics of the Case Study Plots in the Kane Experimental Forest .....	20
Table 1.2-5. Major Studies at the Hubbard Brook Experimental Forest .....	22
Table 2.1-1. Soil Texture Classes as a Function of Clay and Sand Content.....	34
Table 2.1-2. Parent Material Classes for Common FAO Soil Types.....	34
Table 2.1-3. Weathering Rate Classes as a Function of Texture and Parent Material Classes.....	35
Table 2.1-4. Data Requirements and Sources for Calculating Critical Loads for Total Nitrogen and Sulfur Deposition in Hubbard Brook Experimental Forest and Kane Experimental Forest.....	40
Table 2.1-5. The Three Indicator $(\text{Bc}/\text{Al})_{\text{crit}}$ Soil Solution Ratios Used in This Case Study and the Corresponding Levels of Protection to Tree Health and Critical Loads.....	43
Table 2.1-6. Input Values for the Calculation of Critical Load in Hubbard Brook Experimental Forest and Kane Experimental Forest .....	47

Table 2.1-7. Soil Characteristics in the Seven Plots of the Kane Experimental Forest Case Study Area for the Calculation of the Base Cation Weathering Rate Parameters.....	48
Table 2.1-8. Annual Volume Growth by Tree Species in Each of the Seven Plots of the Kane Experimental Forest Case Study Area for the Calculation of Nutrient Uptake ( $Bc_u$ and $N_u$ ).....	48
Table 2.1-9. Specific Gravity and Nutrient Concentrations by Biomass Component (Bark and Bole Wood) and by Tree Species for the Calculation of Nutrient Uptake ( $Bc_u$ and $N_u$ ) in the Kane Experimental Forest Case Study Area.....	49
Table 3.1-1. Critical Loads Calculated with the Different Base Cation Weathering, Gibbsite Equilibrium Constant ( $K_{gibb}$ ), and Base Cation ( $Bc_u$ ) and Nitrogen ( $N_u$ ) Uptake Parameter Values in Plot 1 of the Kane Experimental Forest Case Study Area.....	51
Table 3.1-2. Critical Loads Calculated with the Different Base Cation Weathering, Gibbsite Equilibrium Constant ( $K_{gibb}$ ), and Base Cation ( $Bc_u$ ) and Nitrogen ( $N_u$ ) Uptake Parameter Values in Plot 2 of the Kane Experimental Forest Case Study Area.....	52
Table 3.1-3. Critical Loads Calculated with the Different Base Cation Weathering, Gibbsite Equilibrium Constant ( $K_{gibb}$ ), and Base Cation ( $Bc_u$ ) and Nitrogen ( $N_u$ ) Uptake Parameter Values in Plot 3 of the Kane Experimental Forest Case Study Area.....	52
Table 3.1-4. Critical Loads Calculated with the Different Base Cation Weathering, Gibbsite Equilibrium Constant ( $K_{gibb}$ ), and Base Cation ( $Bc_u$ ) and Nitrogen ( $N_u$ ) Uptake Parameter Values in Plot 4 of the Kane Experimental Forest Case Study Area.....	53
Table 3.1-5. Critical Loads Calculated with the Different Base Cation Weathering, Gibbsite Equilibrium Constant ( $K_{gibb}$ ) and Base Cation ( $Bc_u$ ) and Nitrogen ( $N_u$ ) Uptake Parameter Values in Plot 5 of the Kane Experimental Forest Case Study Area.....	53
Table 3.1-6. Critical Loads Calculated with the Different Base Cation Weathering, Gibbsite Equilibrium Constant ( $K_{gibb}$ ), and Base Cation ( $Bc_u$ ) and Nitrogen ( $N_u$ ) Uptake Parameter Values in Plot 6 of the Kane Experimental Forest Case Study Area.....	54
Table 3.1-7. Critical Loads Calculated with the Different Base Cation Weathering, Gibbsite Equilibrium Constant ( $K_{gibb}$ ), and Base Cation ( $Bc_u$ ) and Nitrogen ( $N_u$ ) Uptake Parameter Values in Plot 7 of the Kane Experimental Forest Case Study Area.....	54
Table 3.1-8. Ranges of Critical Load Values (eq/ha/yr) (with and without the Influence of Nutrient Uptake and Removal with Tree Harvest) for the Seven Plots of the Kane Experimental Forest Case Study Area (Both $K_{gibb}$ values and methods to estimate $BC_w$ were used in these calculations to present the	

range of critical loads estimated using all combinations of the parameter values.) .....	55
Table 3.1-9. Comparison of the Critical Load Values Determined in This Case Study and the Critical Load Values Determined by McNulty et al. (2007) for the Seven Plots in the Kane Experimental Forest Case Study Area.....	58
Table 3.1-10. Critical Load Calculated with the Different Base Cation Weathering and Gibbsite Equilibrium Constant ( $K_{gibb}$ ) Parameter Values in the Hubbard Brook Experimental Forest Case Study Area .....	59
Table 3.1-11. Summary of the Critical Load Values Determined by Other Studies Conducted in the Hubbard Brook Experimental Forest (negative values are equal to 0 eq/ha/yr) .....	61
Table 3.2-1. Critical Loads Selected to Represent the Three Levels of Protection in the Kane Experimental Forest and Hubbard Brook Experimental Forest Case Study Areas .....	62
Table 3.3-1. Ranges of Differences between the 2002 CMAQ/NADP Total Nitrogen and Sulfur Deposition Levels ( $(N+S)_{comb}$ ) and the Estimated Critical Load Values (with and without the Influence of Nutrient Uptake and Removal [ $N_u$ and $Bc_u$ ]) for the Seven Plots of the Kane Experimental Forest Case Study Area .....	64
Table 3.3-2. Differences between the 2002 CMAQ/NADP Total Nitrogen and Sulfur Deposition Levels ( $(N+S)_{comb}$ ) and the Critical Load Values (with Two Base Cation Weathering Estimation Methods, Two Gibbsite Equilibrium Constants [ $K_{gibb}$ ], and Two Base Cation ( $Bc_u$ ) and Nitrogen ( $N_u$ ) Uptake Parameter Values) in Plot 1 of the Kane Experimental Forest Case Study Area.....	64
Table 3.3-3. Differences between the 2002 CMAQ/NADP Total Nitrogen and Sulfur Deposition Levels ( $(N+S)_{comb}$ ) and the Critical Load Values (with Two Base Cation Weathering Estimation Methods, Two Gibbsite Equilibrium Constants [ $K_{gibb}$ ], and Two Base Cation ( $Bc_u$ ) and Nitrogen ( $N_u$ ) Uptake Parameter Values) in Plot 2 of the Kane Experimental Forest Case Study Area.....	65
Table 3.3-4. Differences between the 2002 CMAQ/NADP Total Nitrogen and Sulfur Deposition Levels ( $(N+S)_{comb}$ ) and the Critical Load Values (with Two Base Cation Weathering Estimation Methods, Two Gibbsite Equilibrium Constants [ $K_{gibb}$ ], and Two Base Cation ( $Bc_u$ ) and Nitrogen ( $N_u$ ) Uptake Parameter Values) in Plot 3 of the Kane Experimental Forest Case Study Area.....	65
Table 3.3-5. Differences between the 2002 CMAQ/NADP Total Nitrogen and Sulfur Deposition Levels ( $(N+S)_{comb}$ ) and the Critical Load Values (with Two Base Cation Weathering Estimation Methods, Two Gibbsite Equilibrium Constants [ $K_{gibb}$ ], and Two Base Cation ( $Bc_u$ ) and Nitrogen ( $N_u$ ) Uptake Parameter Values) in Plot 4 of the Kane Experimental Forest Case Study Area.....	66



Table 3.3-6. Differences between the 2002 CMAQ/NADP Total Nitrogen and Sulfur Deposition Levels ((N+S) <sub>comb</sub> ) and the Critical Load Values (with Two Base Cation Weathering Estimation Methods, Two Gibbsite Equilibrium Constants [ $K_{gibb}$ ], and Two Base Cation (Bc <sub>u</sub> ) and Nitrogen (N <sub>u</sub> ) Uptake Parameter Values) in Plot 5 of the Kane Experimental Forest Case Study Area.....	66
Table 3.3-7. Differences between the 2002 CMAQ/NADP Total Nitrogen and Sulfur Deposition Levels ((N+S) <sub>comb</sub> ) and the Critical Load Values (with Two Base Cation Weathering Estimation Methods, Two Gibbsite Equilibrium Constants [ $K_{gibb}$ ], and Two Base Cation (Bc <sub>u</sub> ) and Nitrogen (N <sub>u</sub> ) Uptake Parameter Values) in Plot 6 of the Kane Experimental Forest Case Study Area.....	67
Table 3.3-8. Differences between the 2002 CMAQ/NADP Total Nitrogen and Sulfur Deposition Levels ((N+S) <sub>comb</sub> ) and the Critical Load Values (with Two Base Cation Weathering Estimation Methods, Two Gibbsite Equilibrium Constants [ $K_{gibb}$ ], and Two Base Cation (Bc <sub>u</sub> ) and Nitrogen (N <sub>u</sub> ) Uptake Parameter Values) in Plot 7 of the Kane Experimental Forest Case Study Area.....	67
Table 3.3-9. Differences between the 2002 CMAQ/NADP Total Nitrogen and Sulfur Deposition Levels ((N+S) <sub>comb</sub> ) and the Critical Load Values (with Two Base Cation Weathering Estimation Methods and Two Gibbsite Equilibrium Constants [ $K_{gibb}$ ]) in the Hubbard Brook Experimental Forest Case Study Area.....	68
Table 4.1-1. Number and Location of USFS FIA Permanent Sampling Plots (each plot is 0.07 ha) Used in the Analysis of Critical Loads For the Full Geographic Ranges of Sugar Maple and Red Spruce.....	76
Table 4.1-2. Gibbsite Equilibrium ( $K_{gibb}$ ) Determined by Percentage of Soil Organic Matter .....	79
Table 4.1-3. Parent Material Acidity Classifications for Base Cation (BC <sub>w</sub> ) Estimations.....	79
Table 4.1-4. Parent Material and Descriptive Modifier Characteristics (within the SSURGO Soils [USDA-NRCS, 2008c] and USGS Geology [USGS, 2009b] Databases) Used to Classify Parent Material Acidity .....	80
Table 4.1-5. Ranges of Critical Load Values by Level of Protection (Bc/Al <sub>(crit)</sub> = 0.6, 1.2, and 10.0) and by State for the Full Distribution Ranges of Sugar Maple and Red Spruce .....	83
Table 4.1-6. Percentages of Plots, by Protection Level (Bc/Al <sub>(crit)</sub> = 0.6, 1.2, and 10.0) and by State, where 2002 CMAQ/NADP Total Nitrogen and Sulfur Deposition Levels Were Greater Than the Critical Loads for Sugar Maple and Red Spruce .....	85
Table 5.2-1. Differences and Percentage Differences in Plot-Level Critical Load Estimates Associated with the Misclassification of Parent Material Acidity for the Full Range Assessment of Sugar Maple.....	94

Table 5.2-2. Differences and Percentage Differences in Plot-Level Critical Load Estimates Associated with the Misclassification of Parent Material Acidity for the Full Range Assessment of Red Spruce.....	95
---	----

## ATTACHMENT TABLES

Table 2-1. Summary of Plot-Level Data Used in the Regression Analyses for Sugar Maple Volume and Growth, Nitrogen Deposition, and Critical Load Exceedances (based on critical loads calculated with $Bc/Al = 10.0$ ) .....	A-4
Table 2-2. Summary of Plot-Level Data Used in the Regression Analyses for Red Spruce Volume and Growth, Nitrogen Deposition, and Critical Load Exceedances (based on critical loads calculated with $Bc/Al = 10.0$ ) .....	A-6
Table 3-1a. Results from the Multivariate Ordinary Least Squares Linear Regression Analyses of Sugar Maple Tree Growth and Nitrogen Deposition (for plots where deposition did not exceed critical loads calculated with $Bc/Al = 10.0$ ) .....	A-8
Table 3-1b. Results from the Multivariate Ordinary Least Squares Linear Regression Analyses of Red Spruce Tree Growth and Nitrogen Deposition (for plots where deposition did not exceed critical loads calculated with $Bc/Al = 10.0$ ) .....	A-9
Table 3-2a. Results from the Multivariate Ordinary Least Squares Linear Regression Analyses of Sugar Maple Tree Growth and Critical Load Exceedance (for plots where nitrogen and sulfur deposition was greater than critical loads calculated with $Bc/Al = 10.0$ ) .....	A-9
Table 3-2b. Results from the Multivariate Ordinary Least Squares Linear Regression Analyses of Red Spruce Tree Growth and Critical Load Exceedance (for plots where nitrogen and sulfur deposition was greater than critical loads calculated with $Bc/Al = 10.0$ ) .....	A-10
Table 3-3. Summary of Plot-Level Data for Sugar Maple Volume and Growth and Critical Load Exceedances North of the Glaciation Line (for plots where nitrogen and sulfur deposition exceeded critical loads calculated with $Bc/Al = 10.0$ ) .....	A-14
Table 3-4. Summary of Plot-Level Data for Red Spruce Volume and Growth and Critical Load Exceedances North of the Glaciation Line (for plots where nitrogen and sulfur deposition exceeded critical loads calculated with $Bc/Al = 10.0$ ) ...	A-16
Table 3-5. Results from the Multivariate Ordinary Least Squares Linear Regression Analyses of Sugar Maple Tree Growth and Critical Load Exceedance North of the Glaciation Line (for plots where deposition exceeded critical loads calculated with $Bc/Al = 10.0$ ).....	A-17
Table 3-6. Results from the Multivariate Ordinary Least Squares Linear Regression Analyses of Red Spruce Tree Growth and Critical Load Exceedance, North of the Glaciation Line (for plots where deposition exceeded critical loads calculated with $Bc/Al = 10.0$ ).....	A-18

## ACRONYMS AND ABBREVIATIONS

Al	aluminum <sup>2+,3+</sup>
Al <sup>3+</sup>	trivalent aluminum
ANC	acid neutralizing capacity
ANC <sub>le,crit</sub>	forest soil acid neutralizing capacity of critical load leaching (calculated value)
Bc	base cation (Ca <sup>2+</sup> + K <sup>+</sup> + Mg <sup>2+</sup> )
(Bc/Al) <sub>crit</sub>	base cation (Ca <sup>2+</sup> + K <sup>+</sup> + Mg <sup>2+</sup> ) to aluminum ratio (selected indicator value)
BC	base cation (Ca <sup>2+</sup> + K <sup>+</sup> + Mg <sup>2+</sup> + Na <sup>+</sup> )
BC <sub>dep</sub>	base cation (Ca <sup>2+</sup> + K <sup>+</sup> + Mg <sup>2+</sup> + Na <sup>+</sup> ) deposition
Bc <sub>u</sub>	uptake of base cations (Ca <sup>2+</sup> + K <sup>+</sup> + Mg <sup>2+</sup> ) by trees
BC <sub>w</sub>	base cation (Ca <sup>2+</sup> + K <sup>+</sup> + Mg <sup>2+</sup> + Na <sup>+</sup> ) weathering
Ca <sup>2+</sup>	calcium
Cl <sup>-</sup>	chloride
Cl <sub>dep</sub>	chloride deposition
CL <sub>max</sub> (N)	maximum critical load of nitrogen
CL <sub>max</sub> (S)	maximum critical load of sulfur
CL <sub>min</sub>	minimum critical load
CL <sub>min</sub> (N)	minimum critical load of nitrogen
CLF	critical load function
CLRTAP	Convention on Long-Range Transboundary Air Pollution
cm	centimeter
CMAQ	Community Multiscale Air Quality
eq/ha/yr	equivalents per hectare per year
FAO	Food and Agriculture Organization
Fe <sup>3+</sup>	trivalent (ferrous) iron
FGROWCFAL	Net annual sound cubic-foot growth of a live tree on forest land
FIA	Forest Inventory and Analysis National Program
ft <sup>3</sup>	cubic feet
GIS	geographic information systems
ha	hectare
HBEF	Hubbard Brook Experimental Forest
HNO <sub>3</sub>	nitric acid
ICP	International Cooperative Programme
ISA	Integrated Science Assessment
K <sup>+</sup>	potassium
K <sub>gibb</sub>	the gibbsite equilibrium constant
KEF	Kane Experimental Forest
kg	kilogram
km	kilometer
m	meter
Mg <sup>2+</sup>	magnesium
mm	millimeter
Mn	manganese <sup>2+,4+</sup>

mol	mole
N	nitrogen
N <sub>de</sub>	denitrification
N <sub>i</sub>	nitrogen immobilization
N <sub>u</sub>	uptake of nitrogen by trees
(N+S) <sub>comb</sub>	combined nitrogen and sulfur deposition
Na <sup>+</sup>	sodium
NADP	National Atmospheric Deposition Program
NEG/ECP	Conference of New England Governors and Eastern Canadian Premiers
NH <sub>4</sub> <sup>+</sup>	ammonium
NH <sub>x</sub>	total reduced nitrogen
NO <sub>3</sub> <sup>-</sup>	nitrate
NO <sub>x</sub>	nitrogen oxides
NO <sub>y</sub>	oxidized nitrogen
NRCS	Natural Resources Conservation Service
OLS	ordinary least squares
S	sulfur
SMB	Simple Mass Balance
SO <sub>2</sub>	sulfur dioxide
SO <sub>4</sub> <sup>2-</sup>	sulfate
SO <sub>x</sub>	sulfur oxides
SSURGO	Soil Survey Geographic Database
STATSGO	State Soil Geographic Database
UNECE	United Nations Economic Commission for Europe
USDA	U.S. Department of Agriculture
USFS	U.S. Forest Service
USGS	U.S. Geological Survey
VOLCFNET	total net volume per tree
ybp	years before present

## **1.0 BACKGROUND**

The selection and performance of case studies represent Steps 3 and 4, respectively, of the 7-step approach to planning and implementing a Risk and Exposure Assessment of total nitrogen, nitrogen oxides ( $\text{NO}_x$ ) (as a component of total nitrogen), and sulfur oxides ( $\text{SO}_x$ ) deposition on ecosystems, as presented in the *April 2008 Scope and Methods Plan for Risk Exposure Assessment* (U.S. EPA, 2008a). Step 4 entails evaluating the current Community Multiscale Air Quality Model (CMAQ) modeling results for 2002 and the 2002 National Atmospheric Deposition Program (NADP) monitoring data for total nitrogen and sulfur deposition loads on, and effects to, a chosen case study assessment area, including ecosystem services. This case study evaluates the current wet and dry atmospheric nitrogen and sulfur deposition load to terrestrial ecosystems and the role atmospheric deposition can play in the acidification of a terrestrial ecosystem.

Deposition of  $\text{NO}_x$  and  $\text{SO}_x$  can result in acidification of certain terrestrial ecosystems. Because ecosystems and species may respond differently, case studies have been used to illustrate potential effects of acidification on sensitive species. This report presents the quantitative approach used to analyze the acidification effects of total nitrogen,  $\text{NO}_x$  (as a component of total nitrogen), and  $\text{SO}_x$  deposition on red spruce and sugar maple.

### **Acidification**

Acidification is the process of increasing the acidity of a system (e.g., lake, stream, forest soil). Within soils, acidification occurs through increases in hydrogen ions or protons. Terrestrial acidification occurs as a result of both natural biogeochemical processes and acidifying deposition where strong acids are deposited into the soil. Acidifying deposition increases concentrations of nitrogen and sulfur in the soil, which accelerates the leaching of sulfate ( $\text{SO}_4^{2-}$ ) and nitrate ( $\text{NO}_3^-$ ) from the soil to drainage water. Under natural conditions (i.e., low atmospheric deposition of nitrogen and sulfur), the limited mobility of anions in the soil controls the rate of base cation leaching. However, acidifying deposition of nitrogen and sulfur species can significantly increase the concentration of anions in the soil, leading to an accelerated rate of base cation leaching, particularly the leaching of calcium ( $\text{Ca}^{2+}$ ) and magnesium ( $\text{Mg}^{2+}$ ) cations. If soil base saturation (i.e., the concentration of exchangeable base cations as a percentage of the total cation exchange capacity. Cation exchange capacity, the sum total of exchangeable cations

that a soil can absorb, is 20% to 25%, or lower, inorganic aluminum<sup>2+,3+</sup> (Al) can become mobilized, leading to the leaching of Al into soil waters and surface waters (Reuss and Johnson, 1985). This is an important effect of acidifying deposition because inorganic Al is toxic to tree roots, fish, algae, and aquatic invertebrates (U.S. EPA, 2008c, Sections 3.2.1.5, 3.2.2.1, and 3.2.3).

## 1.1 INDICATORS, ECOLOGICAL ENDPOINTS, AND ECOSYSTEM SERVICES

### 1.1.1 Indicators

The *Integrated Science Assessment (ISA) for Oxides of Nitrogen and Sulfur–Ecological Criteria (Final Report)* (ISA) (U.S. EPA, 2008c) identified a variety of indicators supported by the literature that can be used to measure the effects of acidification in soils (**Table 1.1-1**). **Table 1.1-2** provides a general summary of these indicators by indicator groups.

**Table 1.1-1.** Literature Support for Selected Indicators of Acidification

Citation	Main Finding
<b>Soil Base Saturation</b>	
Reuss, 1983	When base saturation less than 15% to 20%, then exchange ion chemistry is dominated by inorganic Al.
Cronan and Grigal, 1995	When base saturation below about 15% in the soil, B-horizon could lead to impacts from Al stress.
Lawrence et al., 2005	When base saturation declines from 30% to 20% in the upper soil, B-horizon showed decreases in diameter growth of Norway spruce.
Bailey et al., 2004	Sugar maple mortality found at Ca <sup>2+</sup> saturation less than 2% and Mg <sup>2+</sup> saturation less than 0.5% in the upper soil B-horizon.
Johnson et al., 1991; Joslin and Wolfe, 1992	When base saturation below about 20%, base cation reserves are so low that Al exchange dominates.
<b>Al Concentrations</b>	
Johnson et al., 1991; Joslin and Wolfe, 1992	When base saturation below about 20%, base cation reserves are so low that Al exchange dominates.
Cronan and Grigal, 1995; Eagar et al., 1996	There is a 50% chance of negative effects on tree growth if the molar ratio of Ca <sup>2+</sup> /Al in soil solution is as low as 1.0. There is a 100% chance for negative effects on growth at molar ratio value below 0.2.

Citation	Main Finding
Johnson et al., 1994a, b	Ca <sup>2+</sup> /Al ratios above 1.0 were found in a forestland experiencing high mortality over the course of 4 years.
DeWitt et al., 2001	Ca <sup>2+</sup> /Al ratios of Norway spruce stand below 0.5 showed reduced Mg <sup>2+</sup> concentrations in needles in the third year.
<b>Carbon/Nitrogen Ratio</b>	
Aber et al., 2003; Ross et al., 2004	Increased effects of nitrification occur only in soil with carbon/nitrogen ratio below about 20 to 25.

Source: U.S. EPA 2008c, Section 3.2.2.1.

**Table 1.1-2.** Key Indicators of Acidification Due to Nitrogen and Sulfur

Key Indicator Group	Examples of Indicators	Description
Acid anions	SO <sub>4</sub> <sup>2-</sup> , NO <sub>3</sub> <sup>-</sup>	Trends in these concentrations reflect recent trends in atmospheric deposition (especially SO <sub>4</sub> <sup>2-</sup> ) and in ecosystem responses to long-term deposition (notably NO <sub>3</sub> <sup>-</sup> and desorbed SO <sub>4</sub> <sup>2-</sup> ).
Base cations	Ca <sup>2+</sup> , Mg <sup>2+</sup> , BC (sum of Ca <sup>2+</sup> , Mg <sup>2+</sup> , K <sup>+</sup> and Na <sup>+</sup> ), Bc (sum of Ca <sup>2+</sup> , Mg <sup>2+</sup> , and K <sup>+</sup> )	These cations are mobilized by weathering reactions and cation exchange. They respond indirectly to decreases in SO <sub>4</sub> <sup>2-</sup> and NO <sub>3</sub> <sup>-</sup> because a reduced input of acids will lead to a reduction of neutralizing processes in the soil, thereby reducing the release of base cations to soil water and runoff water. (Base saturation is included within this category.)
Acidity	pH, acid neutralizing capacity	These indicators reflect the outcomes of interactions between the changing concentration of acid anions and base cations.
Carbon	Carbon/nitrogen ratio	The carbon/nitrogen ratio of soil indicates alterations to the nitrogen biogeochemical cycle.
Metals	Al <sup>3+</sup> , Fe <sup>3+</sup>	These metals are mobilized as a response to the deposition of SO <sub>4</sub> <sup>2-</sup> and NO <sub>3</sub> <sup>-</sup> .
Biological	Tree health, community structure, species composition, taxonomic richness, Index of Biotic Integrity	Ecological effects occur at four levels: individual, population, community, and ecosystem. Metrics have been developed for each level to assess the negative effects of acidification.

**Note:** BC = base cation (Ca<sup>2+</sup> + K<sup>+</sup> + Mg<sup>2+</sup> + Na<sup>+</sup>); Bc = base cation (Ca<sup>2+</sup> + K<sup>+</sup> + Mg<sup>2+</sup>); K<sup>+</sup> = potassium; Na<sup>+</sup> = sodium; Al<sup>3+</sup> = trivalent aluminum; Fe<sup>3+</sup> = trivalent (ferrous) iron

Much of the literature discussing terrestrial acidification focuses on Ca<sup>2+</sup> and Al as the primary indicators of detrimental effects for trees and other terrestrial vegetation. As such, this

discussion of indicators of terrestrial acidification focuses on these two parameters and the interaction between them. The use of these indicators—in combination and through the evaluation framework that will be described within this case study—ultimately combines all indicator categories described in **Table 1.1-1** except the carbon category.  $\text{Ca}^{2+}$  and Al are the focus of the analysis because both of these indicators are strongly influenced by soil acidification and both have been shown to have quantitative links to tree health, including aluminum's interference with  $\text{Ca}^{2+}$  uptake and Al toxicity to roots.

A detailed description of the influences of Al on  $\text{Ca}^{2+}$  is provided by Schaberg et al. (2001)<sup>1</sup>:

Decreases in concentrations of exchangeable calcium are generally attributed to displacement by hydrogen ions, which can originate from either acidifying deposition or uptake of cations by roots (Johnson et al., 1994a; Richter et al., 1994). A regional survey of soils in northeastern red spruce forests in 1992-93 (fig. 2)<sup>2</sup> has revealed that decreases in exchangeable calcium concentrations in the Oa horizon (a layer within the forest floor, where uptake of nutrients is greatest) can also result from increased concentrations of exchangeable aluminum, which originated in the underlying mineral soil (Lawrence et al., 1995). By lowering the pH of the aluminum-rich mineral soil, acid deposition can increase aluminum concentrations in soil water through dissolution and ion-exchange processes. Once in solution, the aluminum (although not a nutrient) is taken up by roots and transported through the trees to be eventually deposited on the forest floor in leaves and branches.

A continued buildup of aluminum in the Oa horizon can (1) decrease the availability of calcium for roots (Lawrence et al., 1995), (2) lower the efficiency of calcium uptake because aluminum is more readily taken up than calcium when the ratio of calcium to aluminum in soil water is less than 1 (Cronan and Grigal, 1995), and (3) be toxic to roots at high concentrations (Lawrence et al., 1995).

The relationship between  $\text{Ca}^{2+}$  and Al and tree health is summarized in the ISA (U.S. EPA, 2008c, Section 3.2.2.1), as excerpted below<sup>3</sup>:

Al may be toxic to tree roots. Plants [exposed to] high Al concentration in soil solution often have reduced root growth, which restricts the ability of the plant to take up water and nutrients, especially Ca (Parker et al., 1989) (Figure 3-5 [of U.S. EPA, 2008c]). Ca is well known as an ameliorant for Al toxicity to roots in soil solution, as well as to fish in a stream. However, because inorganic Al tends

---

<sup>1</sup> References contained within this quotation are not included in the References section of this case study report.

<sup>2</sup> Figure 2 is not included in this case study report.

<sup>3</sup> References contained within this quotation are not included in the References section of this case study report.



to be increasingly mobilized as soil Ca is depleted, elevated concentrations of inorganic Al tend to occur with low levels of Ca in surface waters. Mg, and to a lesser extent Na and K, have also been associated with reduced Al toxicity.

Dissolved Al concentrations in soil solution at spruce-fir study sites in the southern Appalachian Mountains frequently exceed 50  $\mu\text{M}$  and sometimes exceed 100  $\mu\text{M}$  (Eagar et al., 1996; Johnson et al., 1991; Joslin and Wolfe, 1992a). All studies reviewed by Eagar [et al.] (1996) showed a strong correlation between Al concentrations and  $\text{NO}_3^-$  concentrations in soil solution. They surmised that the occurrence of periodic large pulses of  $\text{NO}_3^-$  in solution were important in determining Al chemistry in the soils of southern Appalachian Mountain spruce-fir forests.

The negative effect of Al mobilization on Ca uptake by tree roots was proposed by Shortle and Smith (1988). Substantial evidence of this relationship has accumulated over the past two decades through field studies (Kobe et al., 2002; McLaughlin and Tjoelker, 1992; Minocha et al., 1997; Schlegel et al., 1992; Shortle et al., 1997) and laboratory studies (see review by Cronan and Grigal, 1995; Sverdrup and Warfvinge, 1993). Based on these studies, it is clear that high inorganic Al concentration in soil water can be toxic to plant roots. The toxic response is often related to the concentration of inorganic Al relative to the concentration of Ca, expressed as the molar ratio of Ca to inorganic Al in soil solution. As a result, considerable effort has been focused on determining a threshold value for the ratio of Ca to Al that could be used to identify soil conditions that put trees under physiological stress.

Building on the explanation of the relationship between  $\text{Ca}^{2+}$ , Al, and tree health, a figure developed by DeHayes et al. (1999), clearly shows the connections between nitrogen and sulfur acidifying deposition and  $\text{Ca}^{2+}$  within an ecosystem (**Figure 1.1-1**). The authors used solid lines to denote known connections and dotted lines to present potential impacts. While the authors did not specify that increases in Al within the soils would occur with reductions in biologically available  $\text{Ca}^{2+}$  pools, this impact is expected as detailed in the previous paragraphs. The final process represented in **Figure 1.1-1** completes the linkage from the indicator of  $\text{Ca}^{2+}$  (and therefore Al) to the effects on the ecosystem services for the terrestrial area.

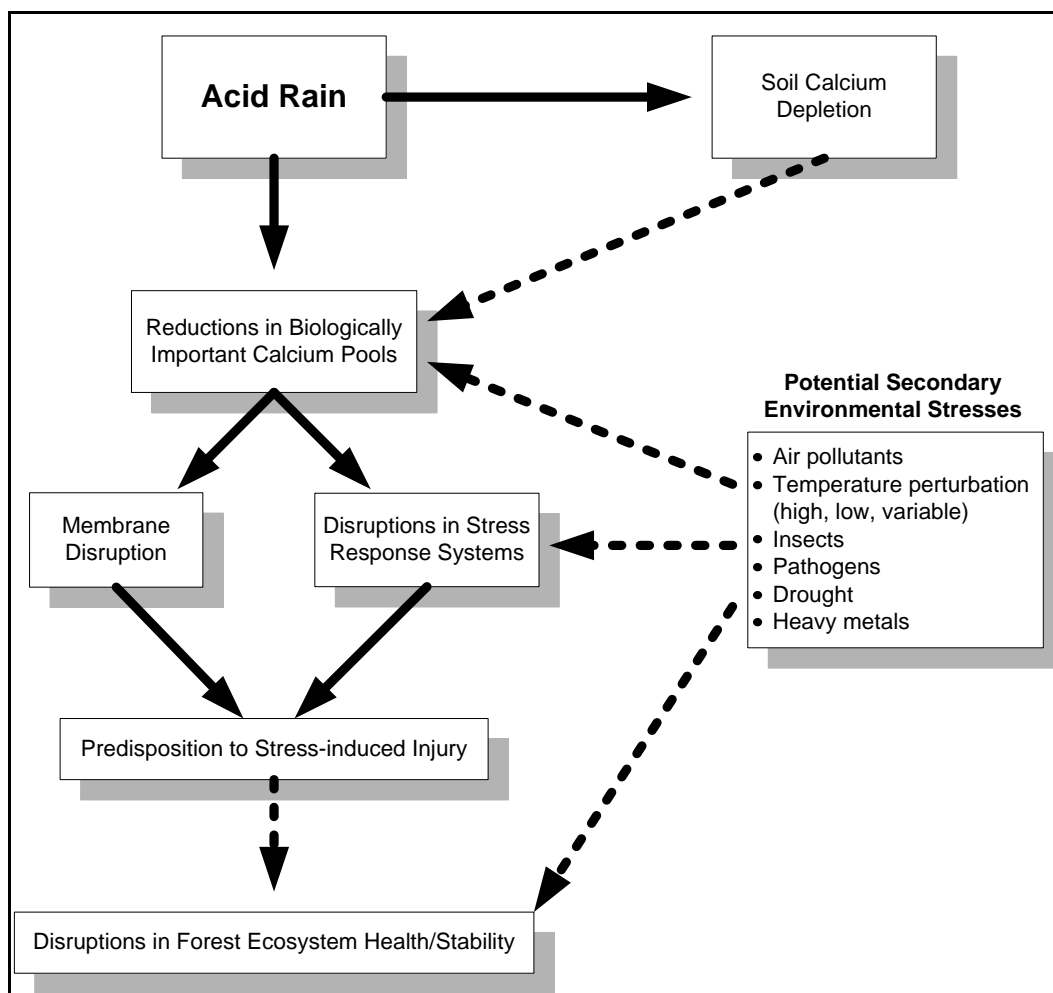


**Figure 1.1-1.** Conceptual impacts of acidifying deposition on soil  $\text{Ca}^{2+}$  depletion, tree physiology, and forest ecosystem health and sustainability (recreated from DeHayes et al., 1999).

In summary, based on the ISA (U.S. EPA, 2008c) and supporting literature, soil  $\text{Ca}^{2+}$  and Al are suitable chemical indicators to represent the impacts of acidification in soils and to provide a linkage between soil acidification and tree health. Therefore, the Ca/Al ratio in soil solution was selected as the basis for the indicator in this case study to evaluate critical loads of acidity in terrestrial systems. Within the calculations of critical loads, the base cation (Bc) to Al ratio (Bc/Al), consisting of molar equivalents of  $\text{Ca}^{2+}$ ,  $\text{Mg}^{2+}$ , and  $\text{K}^{+}$ , was used to represent the Ca/Al indicator. This Bc/Al ratio was selected because it is the most commonly used indicator or critical ratio ( $\text{Bc}/\text{Al}_{\text{crit}}$ ) in the Simple Mass Balance (SMB) model used to estimate critical acid loads in the European Union, Canada, and the United States (McNulty et al., 2007; Ouimet et al., 2006; UNECE, 2004), and the SMB model was applied to this case study (see Section 2.1 for

description of model). In addition, tree species show similar sensitivities to Ca/Al and Bc/Al soil solution ratios. Therefore, the Bc/Al ratio represents a good indicator of the negative impacts of soil acidification on terrestrial vegetation. Sverdrup and Warfvinge (1993b), in a metadata analysis of laboratory and field studies, reported that the critical Bc/Al ratios for a large variety of tree species ranged from 0.2 to 0.8. This range is similar to that described by Cronan and Grigal (1995) for Ca/Al. In their metadata assessment of studies examining sensitivities to the Ca/Al ratio, plant toxicity or nutrient antagonism was reported to occur at Ca/Al ratios ranging from 0.2 to 2.5.

### **1.1.2 Ecological Endpoints**

The tree species most commonly associated with the impacts of acidification due to atmospheric nitrogen and sulfur deposition include red spruce (*Picea rubens*), a coniferous tree species, and sugar maple (*Acer saccharum*), a deciduous tree species. Both species are found in the eastern United States, and soil acidification is widespread throughout this area (Warby et al., 2009).

Red spruce is found scattered throughout high-elevation sites in the Appalachian Mountains, including the southern peaks (**Figure 1.1-2**). Noticeable levels of the canopy red spruce died within the Adirondack, Green, and White mountains in the 1970s and 1980s. Although a variety of conditions, such as changes in climate and exposure to ozone, may impact the growth of red spruce (Fincher et al., 1989; Johnson et al., 1988), acidifying deposition has been implicated as one of the main factors causing this decline. Based on the research conducted to date, acidic deposition can cause a depletion of base cations in upper soil horizons, Al toxicity to tree roots, and accelerated leaching of base cations from foliage (U.S. EPA, 2008c, Section 3.2.2.3). Such nutrient imbalances and deficiencies can reduce the ability of trees to respond to stresses, such as insect defoliation, drought, and cold weather damage (DeHayes et al., 1999; Driscoll et al., 2001), thereby decreasing tree health and increasing mortality. Additional linkages between acidifying deposition and red spruce physiological responses are indicated in **Table 1.1-3**. Within the southeastern United States, periods of red spruce decline slowed after the 1980s, when a corresponding decrease in SO<sub>2</sub> emissions, and therefore acidic deposition, was recorded (Webster et al., 2004).

Sugar maple is found throughout the northeastern United States and the central Appalachian Mountain region (**Figure 1.1-2**). This species has been declining in the eastern United States since the 1950s. Studies on sugar maple have found that one source of this decline in growth is related to both acidifying deposition and base-poor soils on geologies dominated by sandstone or other base-poor substrates (Bailey et al., 2004; Horsley et al., 2000). These site conditions are representative of the conditions expected to be most susceptible to impacts of acidifying deposition because of probable low initial base cation pools and high base cation leaching losses (U.S. EPA, 2008c, Section 3.2.2.3). The probability of a decrease in crown vigor or an increase in tree mortality has been noted to increase at sites with low  $\text{Ca}^{2+}$  and  $\text{Mg}^{2+}$  as a result of leaching caused by acidifying deposition (Drohan and Sharpe, 1997). Low levels of  $\text{Ca}^{2+}$  in leaves and soils were related to lower rates of photosynthesis and higher antioxidant enzyme activity in sugar maple stands in Pennsylvania (St. Clair et al., 2005). Additionally, plots of sugar maples in decline were found to have  $\text{Ca}^{2+}/\text{Al}$  ratios less than 1, as well as lower base cation concentrations and pH values compared to plots of healthy sugar maples (Drohan et al., 2002). Sugar maple regeneration has also been noted to be restricted under conditions of low soil  $\text{Ca}^{2+}$  levels (Juice et al., 2006). These indicators have been shown to be related to the deposition of atmospheric nitrogen and sulfur. Additional linkages between acidifying deposition and sugar maple physiological responses are indicated in **Table 1.1-3**.

**Table 1.1-3.** Summary of Linkages between Acidifying Deposition, Biogeochemical Processes That Affect  $\text{Ca}^{2+}$ , Physiological Processes That Are Influenced by  $\text{Ca}^{2+}$ , and Effect on Forest Function

Biogeochemical Response to Acidifying Deposition	Physiological Response	Effect on Forest Function
Leach $\text{Ca}^{2+}$ from leaf membrane	Decrease the cold tolerance of needles in red spruce	Loss of current-year needles in red spruce
Reduce the ratio of $\text{Ca}^{2+}/\text{Al}$ in soil and soil solutions	Dysfunction in fine roots of red spruce blocks uptake of $\text{Ca}^{2+}$	Decreased growth and increased susceptibility to stress in red spruce
Reduce the ratio of $\text{Ca}^{2+}/\text{Al}$ in soil and soil solutions	More energy is used to acquire $\text{Ca}^{2+}$ in soils with low $\text{Ca}^{2+}/\text{Al}$ ratios	Decreased growth and increased photosynthetic allocation to red spruce roots
Reduce the availability of nutrient cations in marginal soils	Sugar maples on drought-prone or nutrient-poor soils are less able to withstand stresses	Episodic dieback and growth impairment in sugar maple

**Source:** Fenn et al., 2006a.

Although the main focus of the Terrestrial Acidification Case Study is an evaluation of the negative impacts of nitrogen and sulfur deposition on soil acidification and tree health, it should be recognized that, under certain conditions, nitrogen and sulfur deposition can have a positive impact on tree health. Nitrogen limits the growth of many forests (Chapin et al., 1993; Killam, 1994; Miller, 1988); therefore, in such forests, nitrogen deposition may act as a fertilizer and stimulate growth. Forests where critical acid loads are not exceeded by nitrogen and sulfur deposition could potentially be included within this group of forests that respond positively to deposition. These potential positive growth impacts of nitrogen and sulfur deposition are discussed further, and the results of analyses are presented in Attachment A at the end of this Appendix.

In summary, among the potential influencing factors, including elevated ozone levels and changes in climate, the acidification of soils is one of the factors that can negatively impact the health of red spruce and sugar maple. Mortality and susceptibility to disease and injury can be increased and growth decreased with acidifying deposition. Therefore, the health of sugar maple and red spruce was used as the endpoints (ecological responses) to evaluate acidification in terrestrial systems. “Health,” in the context of this case study, is defined as the physiological condition of a tree, which impacts growth and/or mortality.

**End Point:** The health of sugar maple and red spruce was selected as the endpoints to estimate critical deposition loads of acidity in this case study.

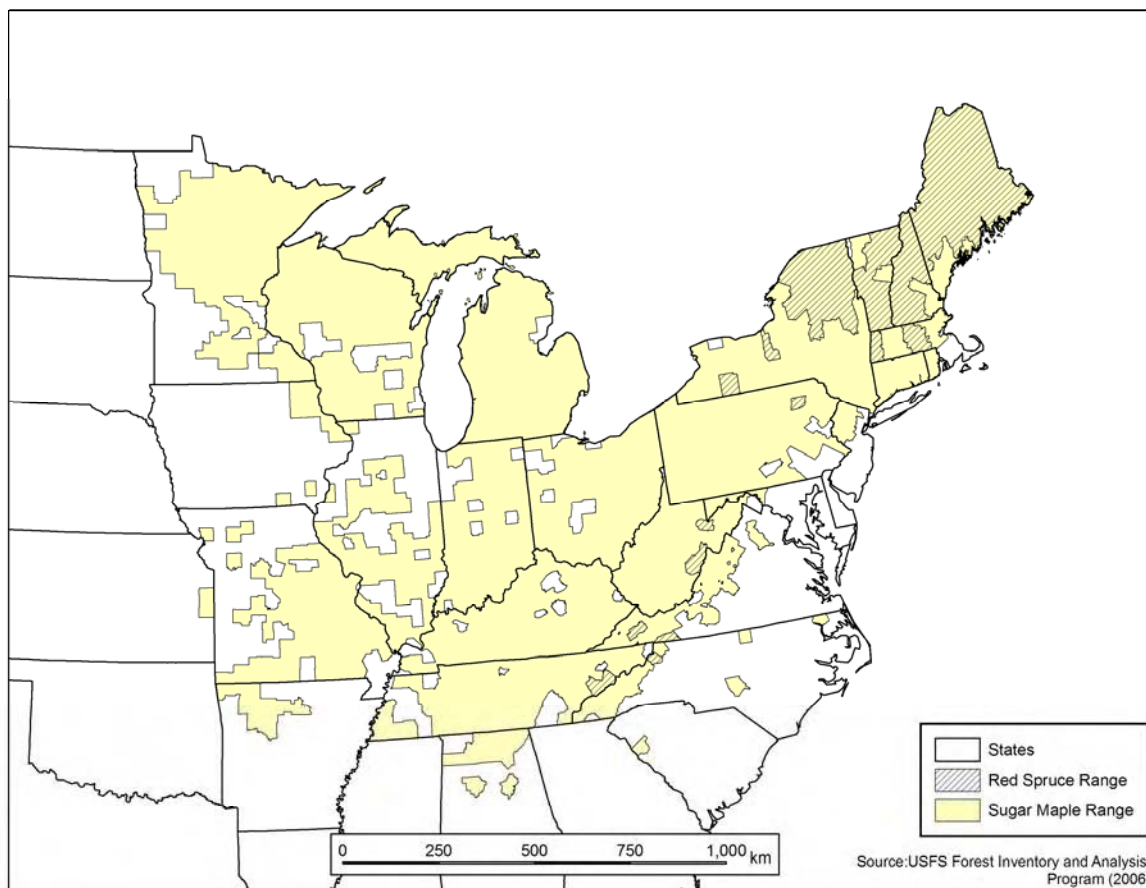


**Figure 1.1-2.** Areal coverages of red spruce and sugar maple tree species within the continental United States (USFS, 2006).

### 1.1.3 Ecosystem Services

Ecosystem services are generally defined as the benefits individuals and organizations obtain from ecosystems. In the Millennium Ecosystem Assessment (MEA, 2005), ecosystem services are classified into four main categories:

- **Provisioning**—includes products obtained from ecosystems
- **Regulating**—includes benefits obtained from the regulation of ecosystem processes
- **Cultural**—includes the nonmaterial benefits people obtain from ecosystems through spiritual enrichment, cognitive development, reflection, recreation, and aesthetic experiences
- **Supporting**—includes those services necessary for the production of all other ecosystem services (MEA, 2005).

A number of impacts on the ecological endpoints of forest health, water quality, and habitat exist, including the following:

- Decline in forest aesthetics—cultural
- Decline in forest productivity—provisioning
- Increases in forest soil erosion and reductions in water retention—cultural and regulating.

Recognizing that many ecosystem services have not been adequately studied, the ecosystem services highlighted in this case study will include economic values associated with red spruce and sugar maple wood volume production.

## **1.2 CASE STUDY AREAS**

The selection of case study areas to evaluate terrestrial acidification was based on geographic information systems (GIS) mapping (locations recommended by the ISA [U.S. EPA, 2008c; Sections 3.2, 4.2, and Annex B]), and the availability of data for the selected indicators and ecological endpoints, as presented in relevant literature and databases.

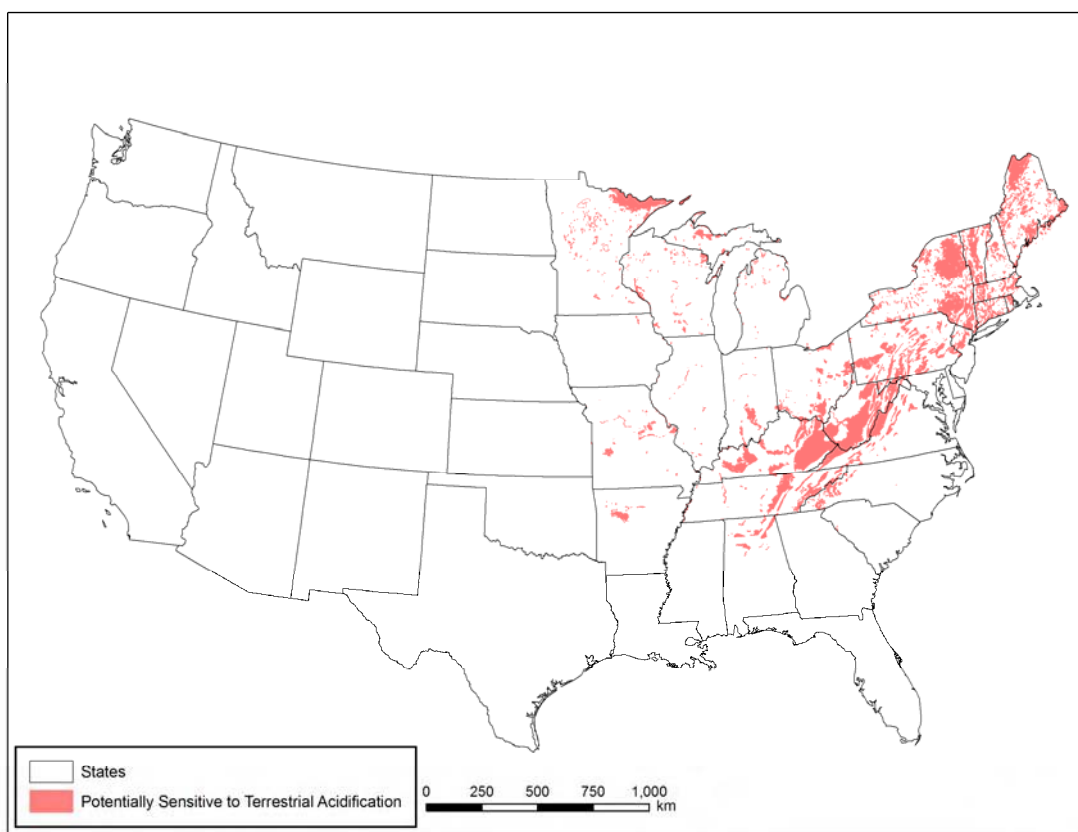
### **1.2.1 GIS Analysis of National Sensitivity**

A GIS analysis was performed on datasets and datalayers of physical, chemical, and biological properties to map areas of potential sensitivity to acidification in the United States (**Table 1.2-1**). Ranges of sugar maple and red spruce were mapped by extracting counties with plots that contained either sugar maple or red spruce from the U.S. Forest Service (USFS) Forest Inventory and Analysis (FIA) database (<http://fia.fs.fed.us/tools-data/>). To characterize soil acidity, soil pH was mapped with State Soil Geographic Database (STATSGO) soils ([http://www.soilinfo.psu.edu/index.cgi?soil\\_data&conus&data\\_cov](http://www.soilinfo.psu.edu/index.cgi?soil_data&conus&data_cov)) and USFS Forest Soils datalayers. Soil thickness was also extracted from the STATSGO soils data. Areas with bedrock with high acid neutralizing capacity (ANC) were determined by using the karst topography dataset from the National Atlas of the United States (Tobin and Weary, 2005). Karst topography is a landscape formed by the dissolution of soluble rock (e.g., limestone, dolomite); caves, springs, and sinkholes are common features of this type of landscape (USGS, 2009a). Locations with sugar maple or red spruce, soil pH  $\leq 5.0$ , soils  $\leq 51$  centimeters (cm) in depth, and low ANC bedrock (not dominated by carbonate rocks) were selected to represent areas with potential sensitivity to acidification (**Figure 1.2-1**).

**Table 1.2-1.** Summary of Mapping Layers, Selected Indicator, and Selected Ecological Endpoint for the Terrestrial Acidification Case Study

Targeted Ecosystem Effect	Selected Indicator	Selected Biological Endpoint	Mapping Layers
Terrestrial acidification due to nitrogen and sulfur	$\text{Ca}^{2+}/\text{Al}$ ratio*	Reduced health of red spruce and sugar maple	Sugar maple and red spruce coverages (USFS, 2006) Soil pH (USDA, 1994; USFS, 2008, Dr. Charles Perry, personal communication) Soil depth (USDA, 1994) Karst topography (Tobin and Weary, 2005)

\*The  $\text{Bc}/\text{Al}$  ( $\text{Bc} = \text{Ca}^{2+}$ ,  $\text{Mg}^{2+}$ , and  $\text{K}^{+}$ ) is used to represent the  $\text{Ca}^{2+}/\text{Al}$  ratio indicator in the acid load calculations (described further at the end of Section 1.1.1).

**Figure 1.2-1.** Map of areas of potential sensitivity of red spruce and sugar maple to acidification in the United States (see **Table 1.2-1** for listing of data sources to produce this map).

### 1.2.2 Selection of Case Study Areas

Following the identification of regions of potential sensitivity to acidification, Risk and Exposure Assessment sites recommended by the Science Advisory Board—Ecological Effects



Subcommittee (U.S. EPA, 2005) and found in the ISA (U.S. EPA, 2008c, Appendix A) and in the body of published and unpublished literature were reviewed to determine the most suitable locations for the Hubbard Brook Experimental Forest (HBEF) and Kane Experimental Forest (KEF) case study areas.

Selection of a location for studying the sugar maple focused on the Allegheny Plateau region in Pennsylvania, where a large proportion of published and unpublished research has been focused. A significant amount of the research work in the Allegheny Plateau region has been sponsored by the USFS and has produced extensive datasets of soil and tree characteristics (Horsley et al., 2000; Bailey et al., 2004; Hallett et al., 2006). The USFS-designated KEF was selected as the area for studying the sugar maple as part of the Terrestrial Acidification Case Study. The KEF has been the focus of several long-term studies since the 1930s.

Selection of a case study area for studying the red spruce involved the review of a variety of regions. Four studies that examined the relationship between the  $\text{Ca}^{2+}/\text{Al}$  soil solution ratio and tree health were identified, and relevant soil and tree information for each of the study regions was compiled (**Table 1.2-2**). A review of this information led to the selection of the HBEF in New Hampshire's White Mountains as the area for the study of red spruce in the Terrestrial Acidification Case Study. The HBEF was also recommended by the ISA (U.S. EPA, 2008c, Appendix A) as a good location for the Risk and Exposure Assessment. This forest has experienced high atmospheric nitrogen and sulfur deposition levels and low  $\text{Ca}^{2+}/\text{Al}$  soil solution ratios. It has been the subject of extensive nutrient investigations and has provided a large dataset from which to work on the case study.

**Table 1.2-2.** Compilation of Potential Areas for the Terrestrial Acidification Case Study (i.e., for Studying Red Spruce) as Identified in the Literature

Site Name	Elevation (m)	Size of Tree Population	Availability of Field Data	Ecological Importance	Reported Impacts	Ca <sup>2+</sup> :Al and Al/Ca <sup>2+</sup> Ratios	Deposition Load (kg/ha/yr)	Source(s)
Balsam High Top, NC	1,641	Spruce-fir forest <sup>e</sup>	University study	Great Smoky Mountains National Park	Nearly 100% chance of negative forest health effects	0.094 <sup>a</sup>	Unknown	Bintz and Butcher, 2007
Clingman's Dome, TN	2,020	Spruce-fir forest <sup>e</sup>	University study	Great Smoky Mountains National Park	Nearly 100% chance of negative forest health effects	0.084 <sup>a</sup>	Unknown	Bintz and Butcher, 2007
Double Spring Gap, TN	1,678	Spruce-fir forest <sup>e</sup>	University study	Great Smoky Mountains National Park	Nearly 100% chance of negative forest health effects	0.053 <sup>a</sup>	Unknown	Bintz and Butcher, 2007
Mount LeConte, TN	2,010	Spruce-fir forest <sup>e</sup>	University study	Great Smoky Mountains National Park	75% chance of a negative forest health effects	0.567 <sup>a</sup>	Unknown	Bintz and Butcher, 2007
Mount Sterling, TN	1,772	Spruce-fir forest <sup>e</sup>	University study	Great Smoky Mountains National Park	Nearly 100% chance of negative forest health effects	0.07 <sup>a</sup>	Unknown	Bintz and Butcher, 2007
Richland Balsam Mountain, NC	1,941	Spruce-fir forest <sup>e</sup>	University study	Blue Ridge Parkway	Nearly 100% chance of negative forest health effects	0.07 <sup>a</sup>	Unknown	Bintz and Butcher, 2007
Spruce Mountain, NC	1,695	Spruce-fir forest <sup>e</sup>	University study	Great Smoky Mountains National Park	Nearly 100% chance of negative forest health effects	0.128 <sup>a</sup>	Unknown	Bintz and Butcher, 2007
Sleepers River, VT	NA	Red spruce dominated with low exchangeable Al/Ca <sup>2+</sup> ratios	Not selected in studies	—	Site did not contain sufficient number of healthy, mature red spruce for study	NA	Unknown	Shortle et al., 1997
Groton, VT	520	Red spruce dominated with a gradient of forest floor exchangeable Al/Ca <sup>2+</sup> ratios	USFS study location	—	No specific references at this time, but disturbances are known to have occurred	0.3 <sup>b</sup>	5.3 <sup>c</sup>	Shortle et al., 1997; Wargo et al., 2003

Site Name	Elevation (m)	Size of Tree Population	Availability of Field Data	Ecological Importance	Reported Impacts	Ca <sup>2+</sup> :Al and Al/Ca <sup>2+</sup> Ratios	Deposition Load (kg/ha/yr)	Source(s)
Howland, ME	60	Red spruce dominated with a gradient of forest floor exchangeable Al/Ca <sup>2+</sup> ratios	USFS study location	—	No specific references at this time, but disturbances are known to have occurred	0.4 <sup>b</sup>	3.1 <sup>c</sup>	Shortle et al., 1997; Wargo et al., 2003
Bartlett, NH	525	Red spruce dominated with a gradient of forest floor exchangeable Al/Ca <sup>2+</sup> ratios	USFS Experimental Forest (1,052 ha); red spruce covers highest slopes	Within the White Mountains	No specific references at this time, but disturbances are known to have occurred	0.8 <sup>b</sup>	4.9 <sup>c</sup>	Shortle et al., 1997; Wargo et al., 2003
Kossuth, ME	100	Red spruce dominated with a gradient of forest floor exchangeable Al/Ca <sup>2+</sup> ratios	USFS study location	—	No specific references at this time, but disturbances are known to have occurred	0.8 <sup>b</sup>	2.8 <sup>c</sup>	Shortle et al., 1997; Wargo et al., 2003
Hubbard Brook, NH	755	Red spruce dominated with a gradient of forest floor exchangeable Al/Ca <sup>2+</sup> ratios	USFS Experimental Forest (3,138 ha); red spruce abundant at higher elevations and on rock outcrops	Within the White Mountains	Acid-extractable Al in the forest floor increased over the past two decades at the HBEF, and ratios of Al to Ca <sup>2+</sup> in mineral soil solutions (but not forest floor solutions) were strongly correlated with exchangeable Al content in the forest floor.	0.8 <sup>b</sup>	6.0 <sup>c</sup>	Shortle et al., 1997; Wargo et al., 2003
Whiteface Mountain, NY	950	Red spruce dominated with a gradient of forest floor exchangeable Al/Ca <sup>2+</sup> ratios	USFS study location	—	Contained neither evidence of unusual mortality or current tree decline; winter injury events reported (Lazarus et al., 2004)	0.8 <sup>b</sup>	7.9 <sup>c</sup>	Shortle et al., 1997; Wargo et al., 2003
Crawford Notch, NH	670	Red spruce dominated with a gradient of forest floor exchangeable Al/Ca <sup>2+</sup> ratios	USFS study location	Within the White Mountains	50% chance of negative forest health effects; mortality of red spruce was significant, but most of the remaining trees were in good to fair health	1.1 <sup>b</sup>	5.5 <sup>c</sup>	Shortle et al., 1997; Wargo et al., 2003

Site Name	Elevation (m)	Size of Tree Population	Availability of Field Data	Ecological Importance	Reported Impacts	Ca <sup>2+</sup> :Al and Al/Ca <sup>2+</sup> Ratios	Deposition Load (kg/ha/yr)	Source(s)
Big Moose Lake, NY	550	Red spruce dominated with a gradient of forest floor exchangeable Al/Ca <sup>2+</sup> ratios	USFS study location	—	50% chance of negative forest health effects	1.2 <sup>b</sup>	6.4 <sup>c</sup>	Shortle et al., 1997; Wargo et al., 2003
Bear Brook, ME	400	Red spruce dominated with a gradient of forest floor exchangeable Al/Ca <sup>2+</sup> ratios	USFS study location	—	75% chance of negative forest health effects	1.9 <sup>b</sup>	3.8 <sup>c</sup>	Shortle et al., 1997; Wargo et al., 2003
Cone Pond, NH	610	Red spruce dominated with a gradient of forest floor exchangeable Al/Ca <sup>2+</sup> ratios	USFS study location	Within the White Mountains	Nearly 100% chance of negative forest health effects	5.2 <sup>b</sup>	5.4 <sup>c</sup>	Shortle et al., 1997; Wargo et al., 2003
Mt. Abraham, VT	NA	Red spruce dominated with a high exchangeable Al/Ca <sup>2+</sup> ratios	Not selected in studies	Within the Green Mountains	Site did not contain sufficient number of healthy, mature red spruce for study; forest floor solution Al/ Ca <sup>2+</sup> ratio above the 50% chance level	7.1 <sup>b</sup>	NA	Shortle et al., 1997
Mt. Ascutney, VT	762	Series of high elevation spruce-fir forest nitrogen addition plots <sup>f</sup>	USFS study location	Nitrogen additions to system	Reduction in live basal area on the high nitrogen addition plots versus control plots	NA	Additions <sup>d</sup>	McNulty et al., 2005

<sup>a</sup> Molar Ca<sup>2+</sup>/Al ratio (Bintz and Butcher, 2007).

<sup>b</sup> Oa horizon Al/Ca<sup>2+</sup> ratios (Wargo et al., 2003).

<sup>c</sup> Estimated wet nitrogen deposition (Lilleskov et al., 2008).

<sup>d</sup> In addition to ambient total nitrogen deposition, paired plots each received 15.7 kilograms (kg) N/ha/yr (low nitrogen addition), 31.4 kg N/ha/yr (high nitrogen addition) or no nitrogen addition (control) from 1988 to 2002.

<sup>e</sup> High elevation sites in the Southern Appalachians—The sites are located in the Great Smoky Mountains National Park and Richland Balsam Mountain on the Blue Ridge Parkway. Sites were selected because of the presence of a spruce-fir forest with a northwest slope aspect within 10 km of a trailhead at elevations between 1,650 and 2,025 meters (m).

<sup>f</sup> Red spruce grew in large patches (>1 ha) at elevations above 725 m. Red spruce comprised > 80% of the total basal area in all plots; the remainder of the other tree species were divided among balsam fir, red maple, mountain maple, and birch.

NA= Not available

### 1.2.3 Sugar Maple

#### 1.2.3.1 Kane Experimental Forest

The KEF (USFS, 1999, 2008b) is located on the eastern edge of the Allegheny National Forest, 5.6 kilometers (km) south of Kane, PA (**Figure 1.2-2**). It is comprised of 703 hectare (ha) of forestland and ranges in elevation from about 550 to 640 meters (m) above sea level, primarily on flat to gently sloping land. The climate of the KEF is humid temperate; the average annual temperature is 6°C. The forest receives approximately 110 cm of precipitation per year, mostly as rain, including 10 cm/month during the growing season.

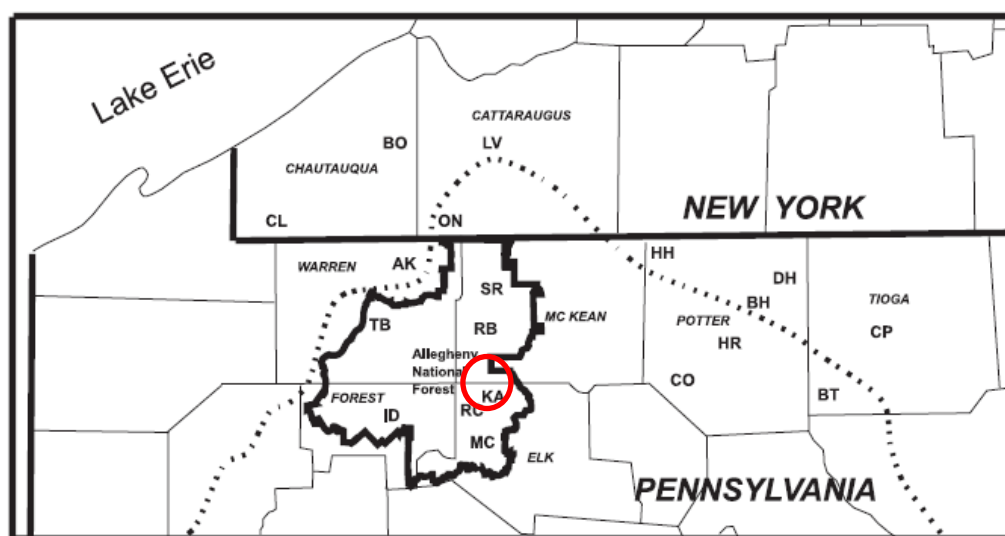


**Figure 1.2-2.** Location of the Kane Experimental Forest (Horsley et al., 2000).

The forest soils on the Allegheny Plateau are derived from shales and sandstones. In general, these soils are very stony and exist as extremely stony loams and sandy loams. They are strongly acidic. The major soil series are the well-drained Hazelton series, the moderately well-drained to somewhat poorly drained Cookport series, and the somewhat poorly drained Cavode series.

The forest stands on the KEF are typical of the Allegheny Plateau. They resulted from a series of cuttings made in the original hemlock-beech-maple stands starting as early as the mid-1880s. Currently, the KEF contains second-growth stands ranging from 60 to about 100 years of age, several third-rotation stands 20 or 40 years old, and one tract with remnant old growth. Most stands are even-aged, with black cherry, maples, and beech being the main overstory species.

The KEF was formally established in 1932, although research there began as early as 1927 or 1928. The forest's primary mission has been forest management research, and the current research focus is centered on three topics: regeneration and forest renewal stand dynamics, silviculture, and sugar maple decline. **Table 1.2-3** summarizes major studies at the KEF related to the sugar maple and chemical criterion that can be used in calculating critical loads of atmospheric nitrogen and sulfur deposition.

**Table 1.2-3.** Major Studies at the Kane Experimental Forest

Authors	Year	Title	Key Finding
Horsley et al.	2000	Factors Associated with the Decline-Disease of Sugar Maple on the Allegheny Plateau	The most important factors determining sugar maple health were foliar levels of $Mg^{2+}$ and Mn and defoliation history. The decline disease of sugar maple appears to be the result of an interaction between $Mg^{2+}$ (and perhaps Mn) nutrition and stress caused by defoliation.
Bailey et al.	2005	Thirty Years of Change in Forest Soils of the Allegheny Plateau, Pennsylvania	Between 1967 and 1997, there were significant decreases in exchangeable $Ca^{2+}$ and $Mg^{2+}$ concentrations and pH at all soil depths. Exchangeable Al concentrations increased at all depths at all sites; however, increases were only significant in upper soil horizons. At most of the sites, losses of $Ca^{2+}$ and $Mg^{2+}$ on a pool basis were much larger than could be accounted for in biomass accumulation, suggesting the leaching of nutrients off site.

**Note:** Mn = manganese.

### ***1.2.3.2 Plot Selection for Kane Experimental Forest Case Study Area***

Plots were selected for the KEF Case Study Area based on the location of permanent sampling plots and the presence of sugar maple trees. Permanent sampling plots are 0.1 acres (0.04 ha) in size and are evenly distributed and spaced (200 m east-west between plots) throughout the forest. Only plots that were not located within an active research study and contained a basal area of at least 20% sugar maple were selected (**Table 1.2-4**). A total of seven plots (0.28 ha total) were identified based on these criteria and were used for the KEF Case Study Area (**Figure 1.2-3**). Site, stand, and soil characteristics of these seven plots are presented in **Table 1.2-4**.

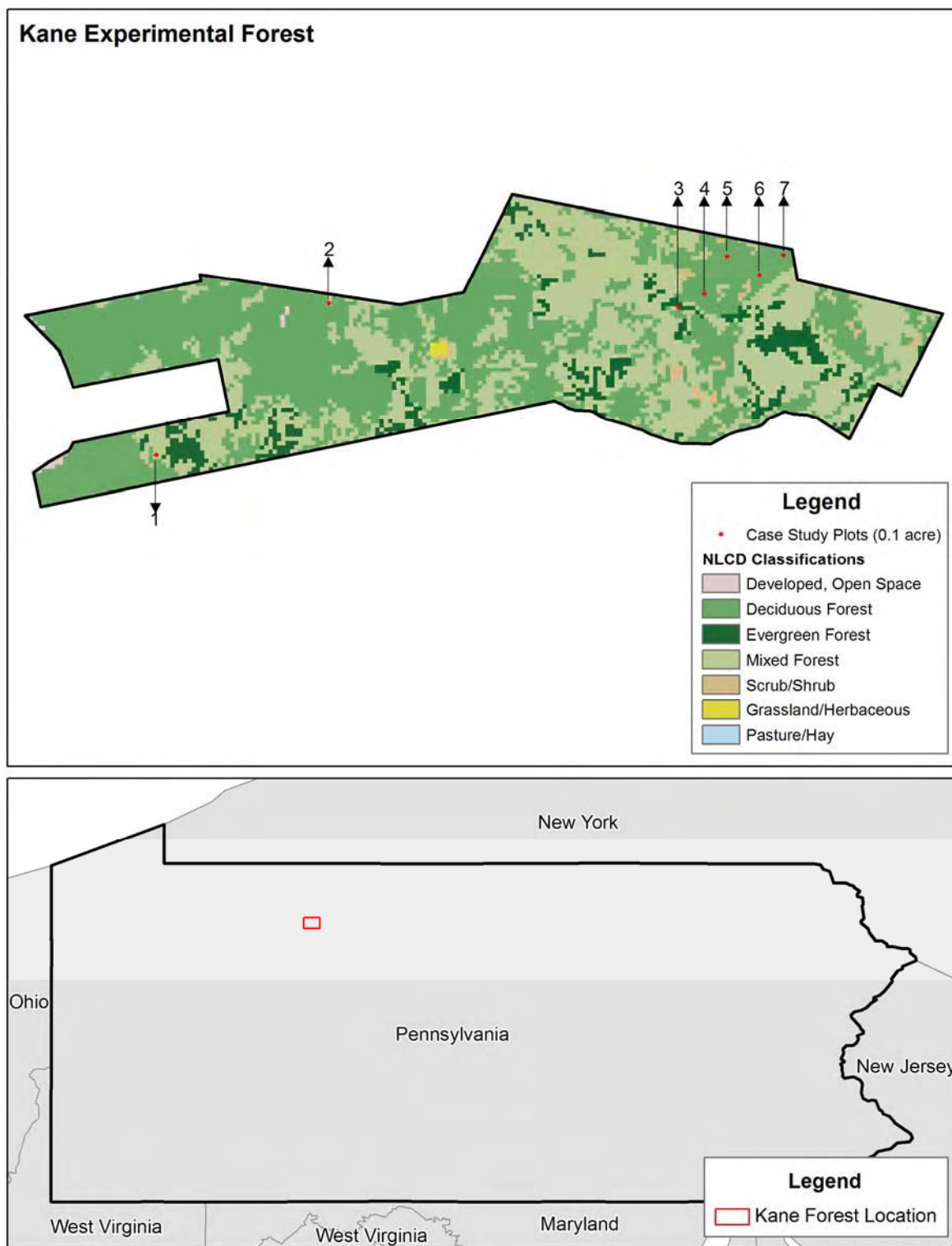


**Figure 1.2-3.** The seven plots used to evaluate critical loads of acidity in the Kane Experimental Forest.

**Table 1.2-4.** Characteristics of the Case Study Plots in the Kane Experimental Forest

Plot Number	KEF Plot ID	Location	Elevation (m)	Stand Basal Area (m <sup>2</sup> /ha)	Representation of Sugar Maple in Stand (% of Basal Area)	Soil Type (Soil Series)
1	2,920	78°47'35"W 41°35'41"N	583.9	62.8	32%	CpB (Cockport)
2	2,150	78°46'33"W 41°36'5"N	616.5	44.8	23%	HaC (Harleton)
3	950	78°44'50"W 41°35'50"N	530.2	28.8	36%	BxD (Buchanan)
4	850	78°44'40"W 41°35'51"N	548.9	22.4	44%	HaF (Harleton)
5	760	78°44'33"W 41°36'01"N	589.0	24.0	28%	CpD (Cockport)
6	650	78°44'24"W 41°35'56"N	530.6	30.7	35%	HaF (Harleton)
7	560	78°44'16"W 41°35'59"N	527.7	23.63	33%	HaF (Harleton)

**Note:** W = west; N = north.

## 1.2.4 Red Spruce

### 1.2.4.1 Hubbard Brook Experimental Forest

The HBEF is located in the southern part of the White Mountain National Forest in Grafton County, central New Hampshire (**Figure 1.2-4**). The experimental forest consists of an oblong basin approximately about 8-km long by 5-km wide, and covers 3,138 ha. Hubbard Brook is the single major stream draining the basin. Elevations within the HBEF range from 222 to 10,015 m. The climate of HBEF is predominantly continental, with a January temperature average of −9°C and an average July temperature of 18°C. Annual precipitation at the HBEF averages about 1,400 millimeters (mm), with one-third to one-quarter as snow.



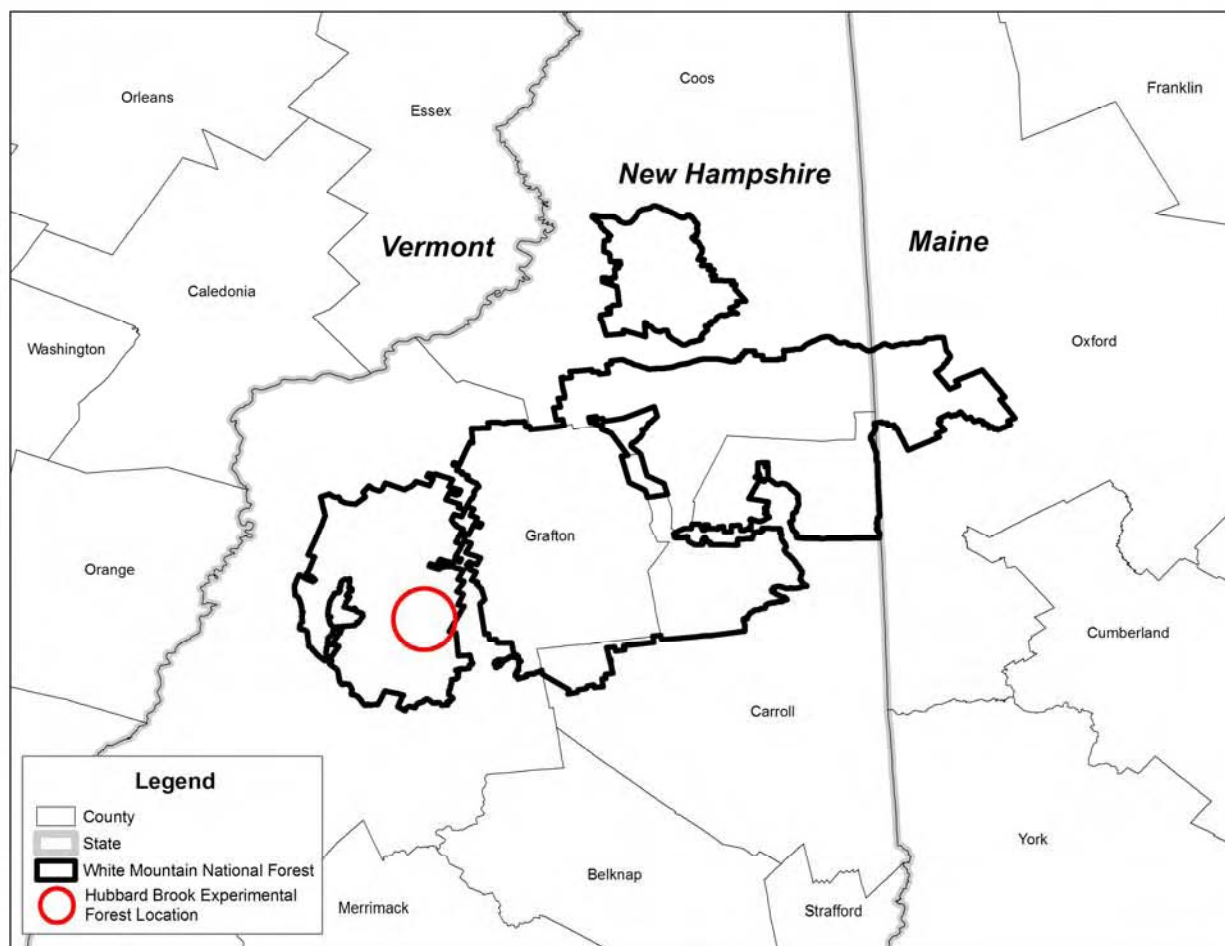


**Figure 1.2-4.** Location of the Hubbard Brook Experimental Forest.

Soils at the HBEF are predominantly well-drained Spodosols (Typic Haplorthods) derived from glacial till, with sandy loam textures. Principal soil series are the sandy loams of the Berkshire series, along with the Skerry, Becket, and Lyman series. These soils are acidic (i.e., pH about 4.5 or less) and relatively infertile (i.e., base saturation of mineral soil ~ 10%). Although highly variable, soil depths, including unweathered till, average about 2.0 m from surface to bedrock.

The HBEF is entirely forested, mainly with deciduous northern hardwoods. Red spruce is abundant at higher elevations and on rock outcrops. Logging in the area began in the late 1880s and ended around 1917. The present second-growth forest is even-aged and composed of about 80% to 90% hardwoods and 10% to 20% conifers.

The HBEF was established in 1955 as a major center for hydrologic research in New England, and in 1963, the Hubbard Brook Ecosystem Study was founded. In 1988, the HBEF

was designated as a Long-Term Ecological Research site. Research at the HBEF has been in progress for more than 50 years and has focused on hydrometeorological monitoring, biogeochemical nutrient cycling, and stand dynamics. **Table 1.2-5** summarizes major studies that were related to red spruce and calculated critical loads of nitrogen and sulfur at the HBEF (HBES, 2008b; Pardo and Driscoll, 1996; USFS, 2008a).

**Table 1.2-5.** Major Studies at the Hubbard Brook Experimental Forest

Authors	Year	Title	Key Finding
Driscoll et al.	1989	Changes in the chemistry of surface waters: 25-year results at the HBEF	A decline in the sum of base cations in surface water paralleled the sulfate decline in atmospheric deposition, preventing any long-term decrease in stream acidity. There have been no significant long-term trends in precipitation inputs or stream outflow of $\text{NO}_3^-$ .
Pardo and Driscoll	1996	Critical loads for nitrogen deposition: case studies at two northern hardwood forests	Critical loads for nitrogen deposition with respect to acidity ranged from 0 to 630 eq/ha/yr; critical loads with respect to effects of elevated nitrogen (eutrophication and nutrient imbalances) ranged from 0 to 1,450 eq/ha/yr.
Palmer et al.	2004	Long-term trends in soil solution and stream water chemistry at the HBEF; relationship with landscape position	Significant declines in strong acid anion concentrations were accompanied by declines in base cation concentrations in soil solutions draining the Oa and Bs soil horizons at all elevations. Persistently low $\text{Ca}^{2+}/\text{Al}_i$ ratios ( $<1$ ) in Bs-horizon soil solutions at these sites may be evidence of continuing Al stress to trees.
Siccama et al.	2007	Population and biomass dynamics of trees in a northern hardwood forest at HBEF	Tree data from 1991 to 2001, including total aboveground biomass, in-growth of $\geq 10$ cm DBH trees, mortality, biomass by type, aboveground net primary productivity, and net ecosystem productivity.

**Note:** eq/ha/yr = equivalents per hectare per year; DBH = diameter at breast height.

#### 1.2.4.2 Plot Selection for Hubbard Brook Experimental Forest Case Study Area

Selection of plots for the HBEF Case Study Area was restricted to Watershed 6 (**Figure 1.2-5**). This watershed is 13.2 ha and is maintained as the biogeochemical control watershed for

research studies. It consists of typical northern hardwood species (e.g., sugar maple, beech, yellow birch) on the lower 90% of its area and by a montane boreal transition forest of red spruce, balsam fir, and white birch (e.g., spruce-fir forest type) on the highest 10% of its area. The watershed is divided into 208 25x25-m<sup>2</sup> grid cells. This grid system and the 2002 Forest Inventory for the watershed were used to identify the nine grid units (units 9, 14, 15, 21 to 24, 32, and 33) within the northeast portion of the watershed that contain large portions of red spruce trees (**Figure 1.2-6**). These nine grid cells were combined into a 0.56-ha plot for the HBEF Case Study Area (**Figure 1.2-7**). This case study plot is located at 43°57'N, 71°44'W and is 762.0 to 769.3 m in elevation. Soils within the plot are from the Tunbridge-Lyman soil association and consist of Tunbridge and Lyman soil series with smaller inclusions of Marlowe and Peru soils. Red spruce accounts for 18.8% of the total basal area (131.3 m<sup>2</sup>/ha) in the plot area.

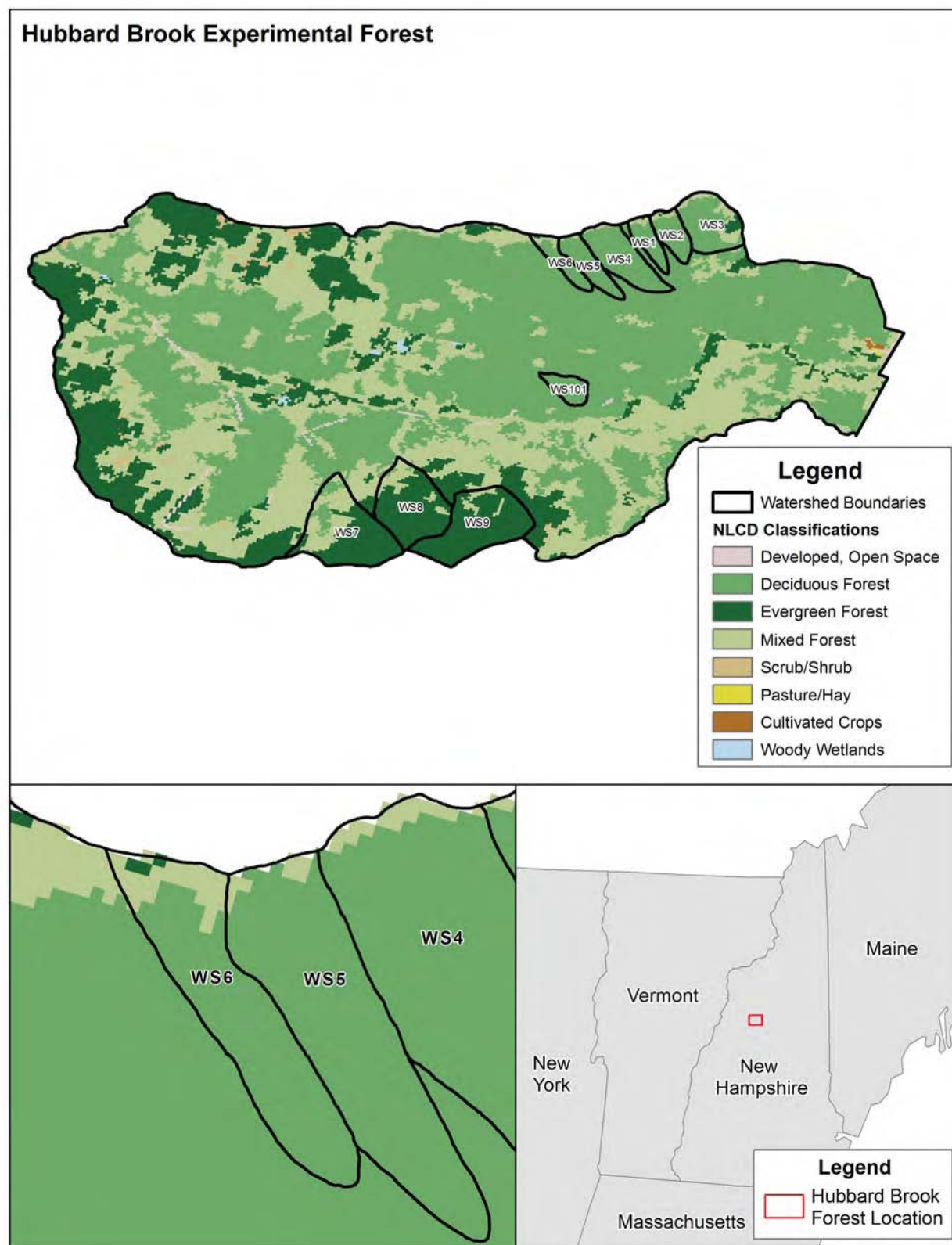


**Figure 1.2-5.** Vegetation cover (NLCD, 2001) and location of Watershed 6 of Hubbard Brook Experimental Forest.

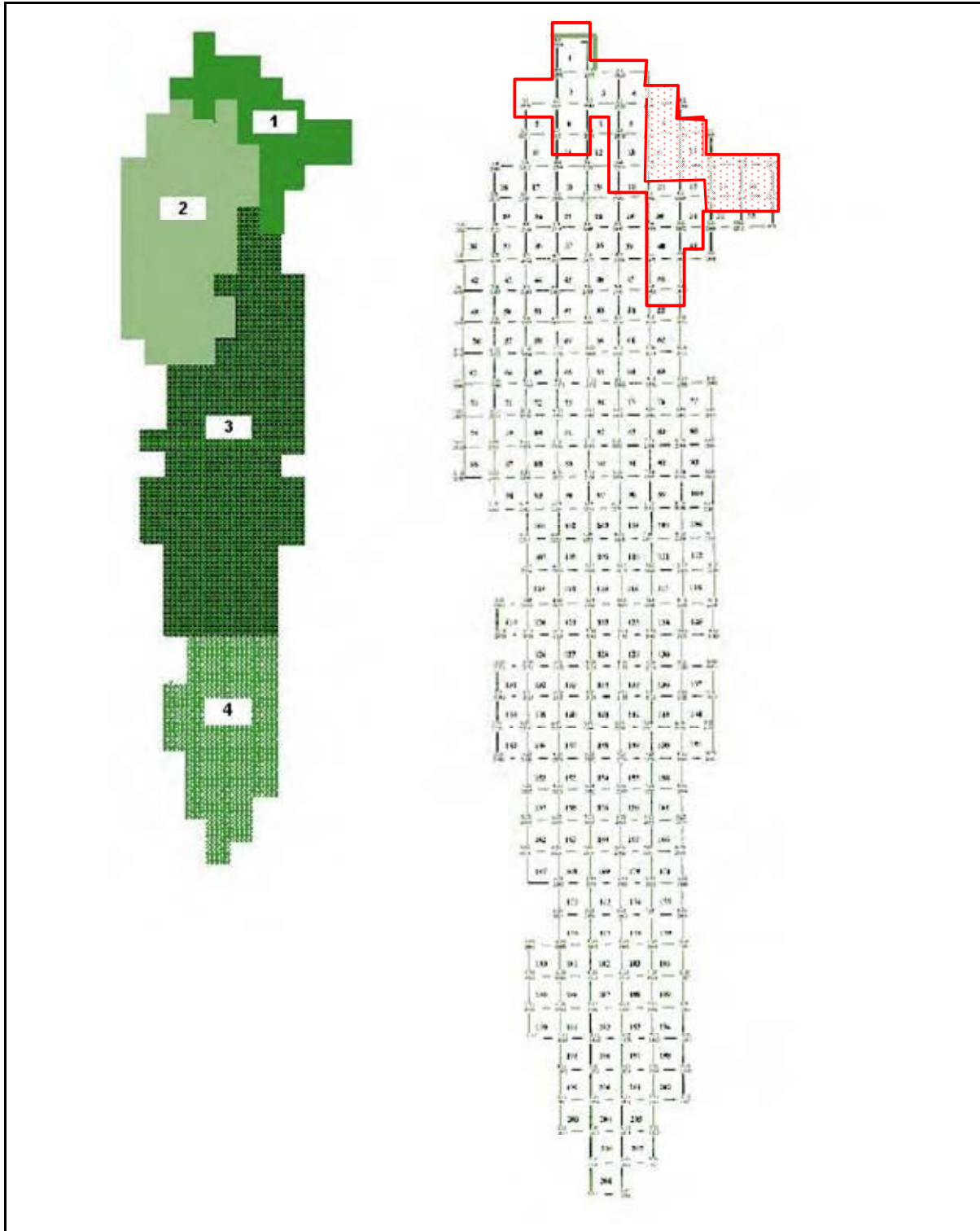


**Figure 1.2-6.** Grid units within Watershed 6 of Hubbard Brook Experimental Forest. The red outline delineates the spruce-fir forest type. The dotted grid cell areas indicate the grid units with high proportions of red spruce and represents the composite plot area for the Hubbard Brook Experimental Forest Case Study Area.

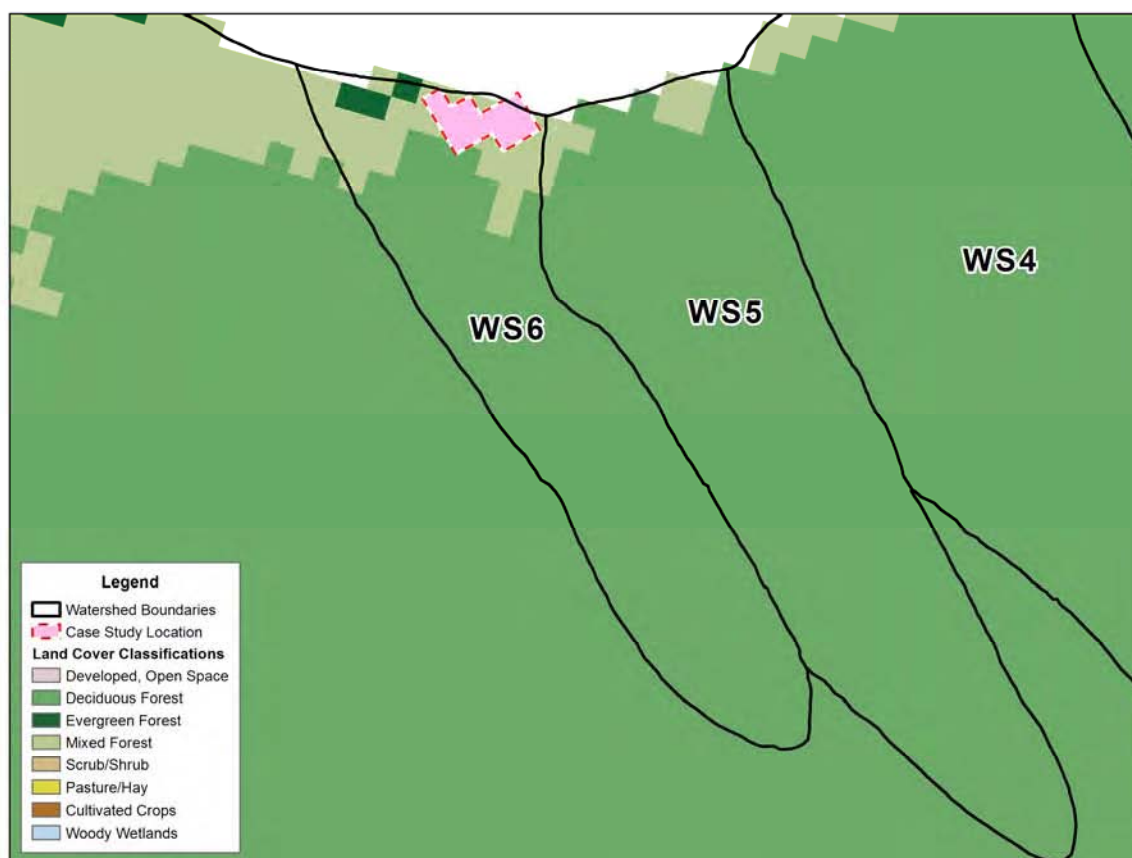


**Figure 1.2-7.** Location of case study plots within Watershed 6 of Hubbard Brook Experimental Forest.

## 2.0 APPROACH AND METHODS

The ISA (U.S. EPA, 2008c, Section 3.1.1) identified critical load assessments as a suitable approach to evaluate the potential impacts of anthropogenic pollution on biological end points and ecosystem impairment. A critical load is “a quantitative estimate of ecosystem exposure to one or more pollutants below which significant harmful effects on specified sensitive elements of the environment do not occur, according to present knowledge” (McNulty et al., 2007). Critical loads of acidity from atmospheric nitrogen and sulfur deposition for an ecosystem have been specifically defined as “the highest deposition of acidifying compounds that will not cause chemical changes leading to long-term harmful effects on ecosystem structure and function” (Nilsson and Grennfelt, 1988). “The basic idea of the critical load concept is to balance the depositions that an ecosystem is exposed to with the capacity of this ecosystem to buffer the

input (e.g., the acidity input buffered by the weathering rate), or to remove it from the system (e.g., nitrogen by harvest) without harmful effects within or outside the system” (UNECE, 2004).

European countries have been using critical load assessments for many years to determine the impacts of atmospheric nitrogen and sulfur deposition in forest ecosystems. These studies have served as the platform for informing policy related to the control and reduction of emissions of acidifying pollutants. The International Cooperative Programme (ICP) on Modelling and Mapping Critical Loads and Levels and Air Pollution Effects, Risks and Trends has published a series of manuals (the most recent in 2004) to provide guidance on calculating and mapping critical loads. These manuals helped parties to the United Nations Economic Commission for Europe (UNECE) Convention on Long-Range Transboundary Air Pollution (CLRTAP) meet their obligations and conduct effects and risk assessments (UNECE, 2004). Canada has also completed critical load evaluations in support of efforts to design emission-reduction programs (Jeffries and Lam, 1993; RMCC, 1990). Critical load modeling was included in the *1997 Canadian Acid Rain Assessment* (Jeffries, 1997) for several regions in eastern Canada.

The establishment and analysis of critical loads within the United States is relatively new. The Conference of New England Governors and Eastern Canadian Premiers (NEG/ECP) funded studies that used critical load-based methods to estimate sustainable acidifying deposition rates and exceedances for upland forests representative of the New England states and the eastern Canadian Provinces in 2000 to 2001 (NEG/ECP Forest Mapping Group, 2001). More recently, McNulty et al. (2007) completed a national critical load assessment for U.S. forest soils at a 1-km<sup>2</sup> scale.

Within the ISA (U.S. EPA, 2008c, Section D.2.2), EPA detailed an 8-step protocol to define the basic critical load question in any analysis. Those steps are repeated here:

1. Identify the *ecosystem disturbance* that is occurring (e.g., acidification, eutrophication).  
Not all disturbances will occur in all regions or at all sites, and the degree of disturbance may vary across landscape areas within a given region or site.
2. Identify the *landscape receptors* that are subjected to the disturbance (e.g., forests, surface waters, crops). Receptor sensitivity may vary locally and/or regionally, and the hierarchy of those receptors that are most sensitive to a particular kind of disturbance may vary as well.



3. Identify the *biological indicators* within each receptor that are affected by atmospheric deposition (i.e., individual organism, species, population, or community characteristics). Indicators will vary geographically and perhaps locally within a given receptor type.
4. Establish the *critical biological responses* that define “significant harm” to the biological indicators (e.g., presence/absence, loss of condition, reduced productivity, species shifts). Significant harm may be defined differently for biological indicators that are already at risk from other stressors or for indicators that are perceived as “more valued.”
5. Identify the *chemical indicators* or variables that produce or are otherwise associated with the harmful responses of the biological indicators (e.g., streamwater pH, lake Al concentration, soil base saturation). In some cases, the use of relatively easily measured chemical indicators (e.g., surface water pH or acid neutralizing capacity [ANC]) may be used as a surrogate for chemical indicators that are more difficult to measure (e.g., Al concentration).
6. Determine the *critical chemical limits* for the chemical indicators at which the harmful responses to the biological indicators occur (e.g., pH < 5, base saturation < 5%, inorganic Al concentration greater than 2  $\mu\text{mol}$ ). Critical limits may be thresholds for indicator responses, such as presence/absence, or may take on a continuous range of values for continuous indicator responses, such as productivity or species richness. Critical limits may vary regionally or locally depending on factors such as temperature, existence of refugia, or compensatory factors (e.g., high  $\text{Ca}^{2+}$  concentration mitigates the toxicity of Al to fish and plant roots).
7. Identify the *atmospheric pollutants* that control (affect) the pertinent chemical indicators (e.g., deposition of  $\text{SO}_4^{2-}$ ,  $\text{NO}_3^-$ , ammonium [ $\text{NH}_4^+$ ], nitric acid [ $\text{HNO}_3$ ]). Multiple pollutants can affect the same chemical variable. The relative importance of each pollutant in producing a given chemical response can vary spatially and temporally.
8. Determine the *critical pollutant loads* (e.g., kg/ha/yr total deposition of sulfur or nitrogen) at which the chemical indicators reach their critical limits. Critical pollutant loads usually include both wet and dry forms of pollutant deposition. The critical pollutant load may vary regionally within a receptor or locally within a site (e.g., as factors such as elevation or soil depth vary) and may vary temporally at the same location (e.g., as accumulated deposition alters chemical responses).



As shown in the eight steps above, a variety of indicators and responses can be incorporated into the estimation of a critical load, the point at which ecological impacts occur. Varying any one of these will result in a different critical load estimate. As a result, there is no single definitive critical load for an ecosystem. In this case study, terrestrial acidification was evaluated using the chemical indicator of the Bc/Al ratio in the soil solution (as a surrogate for  $\text{Ca}^{2+}/\text{Al}$ —discussed earlier at the end of Section 1.1.1) and biological indicators (ecological endpoints) of red spruce and sugar maple tree health and growth. The critical chemical limits discussed above allow for the calculation of multiple critical loads, depending on the level of protection of interest. Three base cation to aluminum ratio – critical load  $(\text{Bc}/\text{Al})_{\text{crit}}$  ratio values were applied in this case study to provide a range of protection (i.e., low, intermediate, high) to tree health and growth, and these values  $(\text{Bc}/\text{Al})_{\text{crit}}$  ratios) are detailed in Section 2.1.2.2.

Several methodological approaches can be taken to estimate critical loads in terrestrial ecosystems. Three of the most commonly used methods are empirically derived estimations, steady-state mass-balance model estimations, and dynamic model estimations (Bull et al., 2001; Bobbink et al., 2003; Jenkins et al., 2003; McNulty et al., 2007; UNECE, 2004).

The UNECE CLRTAP has used the empirically-derived estimation approach within their mapping framework. Empirically derived critical load estimates of atmospheric nitrogen deposition for specific receptor groups within natural and seminatural terrestrial ecosystems and wetland ecosystems were first presented in a background document for the 1992 workshop on critical loads held under the UNECE CLRTAP Convention at Lökeberg (Sweden) (Bobbink et al., 1992). Updates to the empirically derived loads were completed for a 2007 update to the *2004 Manual on Methodologies and Criteria for Modeling and Mapping Critical Loads and Levels and Air Pollution Effects, Risks, and Trends* (henceforth referred to as the ICP Mapping and Modeling Manual) (UNECE, 2004). Empirically derived critical loads can provide good estimates of the impacts of acidifying deposition on terrestrial systems. However, they require data from studies that establish the impacts of varying loads (e.g., amount and duration) on ecosystem processes and attributes and have a limited ability to extrapolate to other systems with different characteristics.

The mass-balance model estimation method to calculate critical loads consists of simple models that relate chemical indicators (e.g., related to or indicative of biological impact of acidifying deposition) to the deposition levels observed in an ecosystem. The chemical indicator

used in the mass balance calculations must have a proven relationship to the biological indicator. With the mass-balance approach, critical loads are calculated by relating the flow of acidifying agents (i.e., base cations and other ions) and nutrients into, out of, and within an ecosystem. These mass-balance models are steady state and offer estimates of critical loads for time frames based on the data used to evaluate the mass balance (UNECE, 2004). To accurately characterize the steady-state ecosystem condition and impacts of acidifying deposition, it is important to use long-term averages of input fluxes in the mass-balance calculations. Benefits of the simple mass-balance approach are its ease of use, moderate data requirements, and applicability over a large area (Pardo and Driscoll, 1996). Disadvantages, however, include an inability to incorporate changes or ecosystem responses into the modeled critical load estimates.

Dynamic-model estimation methods simulate the processes of pollutant fate and transport into, out of, and within a system on a temporally varying basis. They are more data intensive than mass-balance models and require the modeling of temporal rates and processes in addition to the mass balance of acidifying agents, base cations, and nutrients. Some dynamic models involve the integration of hydrologic, geochemical, and biological processes, but such models are still of limited use in determining critical loads (Pardo and Driscoll, 1996). An advantage of dynamic models is that they allow for an estimation or prediction of ecosystem response over time and under different acidifying deposition scenarios (Pardo and Duarte, 2007).

## **2.1 CHOSEN METHOD**

The Simple Mass Balance (SMB) model, outlined in the ICP Mapping and Modeling Manual (UNECE, 2004) to determine terrestrial critical loads, was used to estimate the critical loads of acidifying nitrogen and sulfur deposition in the KEF and HBEF (i.e., for sugar maple and red spruce, respectively) case study areas. This model is currently the most commonly used approach to estimate critical loads and has been widely applied in Europe (Sverdrup and de Vries, 1994), the United States (McNulty et al., 2007; Pardo and Duarte, 2007), and Canada (Watmough et al., 2006; Ouimet et al., 2006). Although a limitation of the SMB model is that it is a steady-state model, as stated by the UNECE (2004), “Since critical loads are steady-state quantities, the use of dynamic models for the sole purpose of deriving critical loads is somewhat inadequate.” In addition, if dynamic models are “used to simulate the transition to a steady state for the comparison with critical loads, care has to be taken that the steady-state version of the

dynamic model is compatible with the critical load model” (UNECE, 2004). Therefore, the selection of the SMB model is the most suitable approach for this case study examining critical loads for sugar maple and red spruce.

The SMB model examines a long-term, steady-state balance of base cation, chloride, and nutrient inputs, “sinks,” and outputs within an ecosystem. With this model, base cation equilibrium is assumed to equal the system’s critical load. It is a single-layer model, where assumptions stipulate that the soil layer is a homogeneous unit at least as deep as the rooting zone, so that the nutrient cycle can be ignored. This allows the model to focus directly on growth and uptake processes. There are several additional assumptions that are included with application of the SMB model (UNECE, 2004):

- All evapotranspiration occurs on the top of the soil profile
- Percolation is constant through the soil profile and occurs only vertically
- Physico-chemical constants are assumed to be uniform throughout the whole soil profile
- Internal fluxes (e.g., weathering rates, nitrogen immobilization) are independent of soil chemical conditions (e.g., pH).

The SMB model relates atmospheric nitrogen and sulfur deposition to a critical load by incorporating mass balances for nitrogen and sulfur within the soils with the charge balance of ions in the soil leaching flux. This model accounts for the processes that add and remove nitrogen and sulfur, as well as base cations and other charged elemental species, from the soil.

Although this model analyzes both total nitrogen and sulfur deposition loads, it does not allow for the analysis of the specific effects of the different total reactive nitrogen species. However, as stated in Chapter 5 of the ICP Mapping and Modeling Manual, “the possible differential effects of the deposited nitrogen species (oxidized nitrogen [ $\text{NO}_y$ ] or reduced nitrogen [ $\text{NH}_x$ ]) are insufficiently known to make a differentiation between these nitrogen species for critical load establishment” (UNECE, 2004). Therefore, attempting an analysis of the impacts of different nitrogen species was not seen as necessary.

## **2.1.1 Critical Load Equations and Calculations**

### ***2.1.1.1 Simple Mass Balance Calculations***

The SMB model used to estimate critical loads of acidity in this case study is presented in Equation 1. The full derivation of this equation is detailed in the ICP Mapping and Modeling

Manual (UNECE, 2004). Unless otherwise stated, all variables are expressed in units of eq/ha/yr. Equivalent, or “eq,” is a unit that removes the influence of molecular weight and is equivalent to “mole.” For example, 1 g of Ca is equal to 0.25 eq (1 g/the molecular weight of Ca = 40.08).

$$CL(S+N) = BC_{dep} - Cl_{dep} + BC_w - Bc_u + N_i + N_u + N_{de} - ANC_{le,crit} \quad (1)$$

where

CL(S+N) = forest soil critical load for combined nitrogen and sulfur acidifying deposition ((N+S)<sub>comb</sub>)

BC<sub>dep</sub> = base cation (Ca<sup>2+</sup> + K<sup>+</sup> + Mg<sup>2+</sup> + Na<sup>+</sup>) deposition<sup>4</sup>

Cl<sub>dep</sub> = chloride deposition

BC<sub>w</sub> = base cation (Ca<sup>2+</sup> + K<sup>+</sup> + Mg<sup>2+</sup> + Na<sup>+</sup>) weathering

Bc<sub>u</sub> = uptake of base cations (Ca<sup>2+</sup> + K<sup>+</sup> + Mg<sup>2+</sup>) by trees

N<sub>i</sub> = nitrogen immobilization

N<sub>u</sub> = uptake of nitrogen by trees

N<sub>de</sub> = denitrification

ANC<sub>le,crit</sub> = forest soil acid neutralizing capacity of critical load leaching

NOTE: There is a distinction between the base cation variables base cation (BC) and Bc. BC includes all four base cations (Ca<sup>2+</sup> + K<sup>+</sup> + Mg<sup>2+</sup> and K<sup>+</sup>), whereas Bc only includes three cations—those that are taken up by vegetation (Ca<sup>2+</sup> + K<sup>+</sup> + Mg<sup>2+</sup>) (UNECE, 2004). Terms in the SMB equations that are directly related to or impact vegetation use the Bc variable.

Some of these parameters had defined or selected input values (BC<sub>dep</sub>, Cl<sub>dep</sub>, N<sub>i</sub>, N<sub>u</sub> and N<sub>de</sub>), while four of these parameters, including BC<sub>w</sub>, Bc<sub>u</sub>, N<sub>u</sub> and ANC<sub>le,crit</sub>, required calculation.

Two methods were used to calculate BC<sub>w</sub> in this case study; the clay-substrate method and the soil type–texture approximation method. The clay-substrate method has been used by many researchers in North America (Ouimet et al., 2006; Watmough et al., 2006; McNulty et al., 2007; Pardo and Duarte 2007), and the soil type–texture approximation is one of the methods outlined in the ICP Mapping and Modeling Manual (UNECE, 2004). Base cation weathering is

<sup>4</sup> The ICP Mapping and Modeling Manual (UNECE, 2004) recommends that wet deposition be corrected for sea salt on sites within 70 km of the coast. Both the HBEF and KEF case study areas are greater than 70 km from the coast, so this correction was not used.

the most influential and most difficult-to-estimate parameter within the SMB model (Whitfield et al., 2006; Li and McNulty, 2007). Therefore, these two methods were chosen to provide a range of  $BC_w$  estimates within which the correct value probably lies (discussed further in Section 5).

Base cation weathering was calculated with the clay-substrate method using equations outlined by McNulty et al. (2007) (Equations 1 to 3). This method relies on a combination of parent material and clay percentage to determine the soil weathering rate. Parent material acidity was determined by silica content (see Table 3 in McNulty et al., 2007).

$$\text{Acid Substrate: } BC_e = (56.7 \times \% \text{ clay}) - (0.32 \times (\% \text{ clay})^2) \quad (2)$$

$$\text{Intermediate Substrate: } BC_e = 500 + (53.6 \times \% \text{ clay}) - (0.18 \times (\% \text{ clay})^2) \quad (3)$$

$$\text{Basic Substrate: } BC_e = 500 + (59.2 \times \% \text{ clay}) \quad (4)$$

where

$BC_e$  = empirical soil base cation ( $Ca^{2+} + K^+ + Mg^{2+} + Na^+$ ) weathering rate (eq/ha/yr)

% clay = the percentage of clay within the soil.

The empirical base cation weathering rate was corrected for soil temperature and depth of the rooting zone soil (Sverdrup and de Vries, 1994; Hodson and Langan, 1999; van der Salm and de Vries, 2001; UNECE, 2004; Watmough et al., 2006; Whitfield et al., 2006; Pardo and Duarte 2007; NEG/ECP Forest Mapping Group, 2001) to determine the final  $BC_w$  as outlined in Equations 5 and 6.

$$BC_c = BC_e \times e^{\left( \left( \frac{A}{2.6+273} \right) - \left( \frac{A}{273+T_m} \right) \right)} \quad (5)$$

$$BC_w = BC_c \times \text{depth} \quad (6)$$

where

$BC_c$  = base cation ( $Ca^{2+} + K^+ + Mg^{2+} + Na^+$ ) weathering rate corrected for temperature (eq/ha/yr/m)

A = Arrhenius constant (3,600 kelvin [K])

$T_m$  = mean annual soil (or air) temperature (°C)

Depth = the depth of rooting zone mineral soil (m).

Base cation weathering was calculated with the soil type–texture approximation method using **Tables 2.1-1, 2.1-2, and 2.1-3** and Equation 7 (UNECE, 2004). Similar to the clay-substrate method, the soil type–texture approximation method also requires a combination of soil texture and parent material acidity to calculate base cation weathering. The soil texture class was determined by percentages of clay and sand (**Table 2.1-1**), and the parent material acidity was classified according to Food and Agriculture Organization (FAO) soil types (**Table 2.1-2**). Soil texture class and parent material acidity was then combined to determine the weathering rate class (**Table 2.1-3**).

**Table 2.1-1.** Soil Texture Classes as a Function of Clay and Sand Content

Texture Class	Name	Definition
1	Coarse	clay <18% and sand $\geq$ 65%
2	Medium	clay <35% and sand >15%, but clay $\geq$ 18% if sand $\geq$ 65%
3	Medium fine	clay <35% and sand <15%
4	Fine	35% $\leq$ clay <60%
5	Very fine	clay $\geq$ 60%

Source: UNECE, 2004.

**Table 2.1-2.** Parent Material Classes for Common FAO Soil Types

Parent Material	FAO Soil Type
Acidic	Ah, Ao, Ap, B, Ba, Bd, Be, Bf, Bh, Bm, Bx, D, Dd, De, Dg, Gx, I, Id, Ie, Jd, P, Pf, Pg, Ph, Pl, Po, Pp, Q, Qa, Qc, Qh, Ql, Rd, Rx, U, Ud, Wd
Intermediate	A, Af, Ag, Bv, C, Cg, Ch, Cl, G, Gd, Ge, Gf, Gh, Gi, Gl, Gm, Gs, Gt, H, Hg, Hh, Hl, J, Je, Jm, Jt, L, La, Ld, Lf, Lg, Lh, Lo, Lp, Mo, R, Re, V, Vg, Vp, W, We
Basic	F, T, Th, Tm, To, Tv
Organic	O, Od, Oe, Ox

Source: UNECE, 2004.

**Table 2.1-3.** Weathering Rate Classes as a Function of Texture and Parent Material Classes

Parent Material	Texture Class				
	1	2	3	4	5
Acidic	1	3	3	6	6
Intermediate	2	4	4	6	6
Basic	2	5	5	6	6
Organic	Class 6 for Oe and class 1 for other organic soils				

Source: UNECE, 2004.

$$BC_w = z \cdot 500 \cdot (WRc - 0.5) \cdot e^{\left(\frac{A}{281} - \frac{A}{273+T}\right)} \quad (7)$$

where

$z$  = rooting zone soil depth (m)

$WRc$  = weathering rate class

$T$  = average annual soil temperature (°C)

$A$  = Arrhenius constant (3,600 K)

Base cation ( $Bc_u$ ) and nitrogen ( $N_u$ ) uptake were calculated for this case study using the equation outlined by McNulty et al. (2007) (Equation 8). These terms represent nutrients that are taken up from the soil and used to support tree growth and maintenance but are eventually returned to the system through litter senescence and decay. In a forest stand that does not experience biomass removal, these nutrients are internally cycled and not lost from the system. Under this scenario, both  $Bc_u$  and  $N_u$  would be given values of 0 equivalents per hectare per year (eq/ha/yr) in the SMB calculations. However, in a managed stand that is harvested, base cations and nitrogen taken up by the trees are removed from the forest system with tree harvesting and are, therefore, considered a loss or output from the system within the SMB calculations.

Watershed 6 in HBEF is a reference watershed and is not harvested. Therefore, for the HBEF Case Study Area, the  $Bc_u$  and  $N_u$  variables were assumed to have a value of 0 eq/ha/yr because biomass and nutrients are not removed from these plots. In contrast, most of the stands in the KEF are harvested, and therefore, as discussed further in Section 3.1.1  $Bc_u$  and  $N_u$  were estimated for the seven plots in the KEF Case Study Area. Equation 8 was modified, as

necessary, to estimate uptake in the bark and bole for nitrogen,  $\text{Ca}^{2+}$ ,  $\text{Mg}^{2+}$ , and  $\text{K}^+$ . These calculations were conducted for each species on each plot.

$$\text{Uptake (eq/ha/yr)} = \text{AVI} \times \text{NC} \times \text{SG} \times \% \text{ bark} \times 0.65 \quad (8)$$

where

AVI = average forest volume increment ( $\text{m}^3/\text{ha/yr}$ )

NC = base cation ( $(\text{Ca}^{2+} + \text{K}^+ + \text{Mg}^{2+})$ ) or nitrogen nutrient concentration in bark and bole (%)

SG = specific gravity of bark and bole wood ( $\text{g}/\text{cm}^3$ )

% bark = percentage of volume growth that is allotted to bark

65% = average aboveground tree volume that is removed from the site (Birdsey, 1992; Hall et al., 1998; Martin et al., 1998).

Acid neutralizing capacity ( $\text{ANC}_{(\text{le}, \text{crit})}$ ) represents the buffering or acid neutralizing capacity of the soil, and the selection of the chemical indicator for the effects on the biological receptor or ecological endpoint occurs within the calculation of  $\text{ANC}_{(\text{le}, \text{crit})}$ . Several formulations for  $\text{ANC}_{(\text{le}, \text{crit})}$  exist, depending on which indicator is being used to examine the critical load for the biological receptor (endpoint), sensitivity to pH conditions, or sensitivity to the toxic effects of Al. A large proportion of the research indicates Al toxicity in relation to  $\text{Ca}^{2+}$  depletion as the main indicator of red spruce and sugar maple mortality and decline. Therefore, for the estimates of critical loads for these two species at HBEF or KEF,  $\text{Ca}^{2+}$  and Al concentrations applied through the base cation to aluminum ( $\text{Bc}/\text{Al}$ )<sub>crit</sub> indicator ratio were used in the  $\text{ANC}_{(\text{le}, \text{crit})}$  calculations according to Equation 9. As outlined in the end of Section 1.1.1, the  $\text{Bc}/\text{Al}$  ratio is a good surrogate for the  $\text{Ca}^{2+}/\text{Al}$  indicator and is the most commonly used indicator ( $\text{Bc}/\text{Al}_{(\text{crit})}$ ) in estimations of acid load (McNulty et al., 2007; Ouimet et al., 2006; UNECE, 2004).

$$\text{ANC}_{(\text{le}, \text{crit})} = -Q^{2/3} \times \left( 1.5 \times \frac{\text{Bc}_{\text{dep}} + \text{Bc}_{\text{w}} - \text{Bc}_{\text{u}}}{K_{\text{gibb}} \times \left( \frac{\text{Bc}}{\text{Al}} \right)_{\text{crit}}} \right)^{1/3} - 1.5 \times \frac{\text{Bc}_{\text{dep}} + \text{Bc}_{\text{w}} - \text{Bc}_{\text{u}}}{\left( \frac{\text{Bc}}{\text{Al}} \right)_{\text{crit}}} \quad (9)$$

where



$Q$	=	annual runoff in m <sup>3</sup> /ha/yr
$Bc_{dep}$	=	base cation (Ca <sup>2+</sup> + K <sup>+</sup> + Mg <sup>2+</sup> ) deposition <sup>5</sup>
$Bc_w$	=	soil base cation (Ca <sup>2+</sup> + K <sup>+</sup> + Mg <sup>2+</sup> ) weathering <sup>6</sup>
$Bc_u$	=	base cation (Ca <sup>2+</sup> + K <sup>+</sup> + Mg <sup>2+</sup> ) uptake by trees
$K_{gibb}$	=	the gibbsite equilibrium constant (a function of forest soil organic matter content that affects Al solubility) (UNECE, 2004)
$(Bc/Al)_{crit}$	=	the base cation to aluminum ratio (indicator)

Base cation weathering ( $Bc_w$ ) in the  $ANC_{(le,crit)}$  parameter was calculated using the two methods described earlier: the clay-substrate and soil type–texture approximation methods. However, sodium (Na<sup>+</sup>) typically accounts for 10% to 30% of base cation weathering ( $BC_w$ ) (Sverdrup and deVries 1994), and therefore, the  $Bc_w$ , which only consists of Ca<sup>2+</sup>, K<sup>+</sup>, and Mg<sup>2+</sup>, was determined by multiplying  $BC_w$  by 0.80, the mid-range of the Na<sup>+</sup> proportional content.

### 2.1.1.2 Deposition Relative to Critical Load Calculations

If total nitrogen and sulfur deposition (combined) ( $(N+S)_{comb}$ ) is greater than the calculated critical load for acidity, the soil is no longer able to neutralize the acidifying deposition, and there is increased likelihood of environmental harm (McNulty et al., 2007). Deposition of  $(N+S)_{comb}$  (expressed as eq/ha/yr) that is greater than the critical load was calculated in this case study by comparing the SMB estimated critical load to the CMAQ/NADP total nitrogen and sulfur deposition levels as outlined in Equation 3.

$$Ex(S + N)_{dep} = S_{dep} + N_{dep} - CL(S + N) \quad (10)$$

where

$Ex$  = exceedance of the forest soil critical nitrogen and sulfur loads

$(S+N)_{dep}$  = the deposition of sulfur and nitrogen.

<sup>5</sup>  $Bc_{dep}$  is **not** the same as  $BC_{dep}$  used in Equation 1.  $BC_{dep}$  includes Ca<sup>2+</sup>, K<sup>+</sup>, Mg<sup>2+</sup>, and Na<sup>+</sup>, whereas  $Bc_{dep}$  includes base cations that are taken up by vegetation (i.e., only includes Ca<sup>2+</sup>, K<sup>+</sup>, and Mg<sup>2+</sup>).

<sup>6</sup>  $Bc_w$  is **not** the same as  $BC_w$  used in Equation 1.  $BC_w$  includes Ca<sup>2+</sup>, K<sup>+</sup>, Mg<sup>2+</sup>, and Na<sup>+</sup>, whereas  $Bc_w$  includes base cations that are taken up by vegetation (i.e., only includes Ca<sup>2+</sup>, K<sup>+</sup>, and Mg<sup>2+</sup>).

### 2.1.1.3 Critical Load Function

The critical load function (CLF) expresses the relationship between all combinations of total nitrogen and sulfur deposition ( $(N+S)_{\text{comb}}$ ) and the critical load of an ecosystem. To define the CLF, minimum and maximum critical load levels for both total nitrogen and sulfur deposition must be determined (UNECE, 2004). These maximum and minimum levels were calculated in this case study using Equations 11 through 13 (UNECE, 2004).

$$CL_{\max}(S) = BC_{\text{dep}} - Cl_{\text{dep}} + BC_w - BC_u - ANC_{\text{le,crit}} \quad (11)$$

$$CL_{\min}(N) = N_i + N_u + N_{\text{de}} \quad (12)$$

$$CL_{\max}(N) = CL_{\min}(N) + \frac{CL_{\max}(S)}{1 - f_{\text{de}}} \quad (13)$$

where

$f_{\text{de}}$  = denitrification fraction ( $0 < f_{\text{de}} < 1$ ); unitless

There is no minimum critical load of sulfur deposition because sulfur cycling processes (e.g., immobilization, uptake, reduction of sulfur) do not significantly contribute to the cycling of nutrients within forests (Johnson, 1984).

The maximum critical load of sulfur ( $CL_{\max}(S)$ ) (Equation 11) occurs when nitrogen deposition does not exceed the nitrogen sinks ( $N_i + N_u + N_{\text{de}}$ ) within the ecosystem. These nitrogen sinks are accounted for by the minimum critical load of nitrogen ( $CL_{\min}(N)$ ) (Equation 12). Above this  $CL_{\min}(N)$  level, nitrogen deposition can no longer be absorbed by the system and acidification effects can occur. The maximum critical load level for nitrogen ( $CL_{\max}(N)$ ) occurs when there is no sulfur deposition and all acidity due to deposition comes from nitrogen. Translated into an equation (Equation 13), this critical load can be calculated as the sum of  $CL_{\min}(N)$  and  $CL_{\max}(S)$  (corrected for denitrification).

An example of a CLF is depicted in **Figure 2.1-1**. All combinations of total nitrogen and sulfur deposition that fall on the black line representing the CLF are at the critical load level. Any deposition combination that falls below the line or within the grey area is below the critical load level. All combinations of total nitrogen and sulfur deposition that are located above the line or within the white area are greater than the critical load.

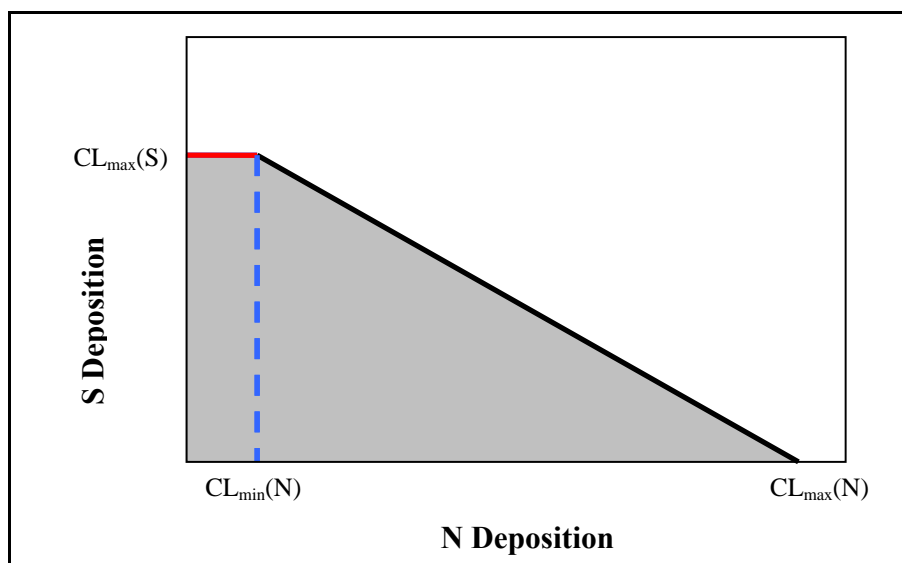


**Figure 2.1-1.** The critical load function created from the calculated maximum and minimum levels of total nitrogen and sulfur deposition (eq/ha/yr). The grey areas show deposition levels less than the established critical loads. The red line is the maximum critical level of sulfur deposition (valid only when nitrogen deposition is less than the minimum critical level of nitrogen deposition [blue dotted line]). The flat line portion of the curves indicates nitrogen deposition corresponding to the  $CL_{min}(N)$  (i.e., nitrogen absorbed by nitrogen sinks within the system).

## 2.1.2 Critical Load Data Requirements

### 2.1.2.1 Data Requirements and Sources

Atmospheric, hydrologic, soil, bedrock geology, and tree measurement data are necessary to evaluate critical loads associated with total nitrogen and sulfur deposition. The specific data requirements to satisfy Equations 1 through 13 and calculate critical loads and CLF for this case study are presented in **Table 2.1-4**. This table also outlines the sources of these data specific to the two case study areas. Cloud deposition of nitrogen was not included in the critical load calculations because of the lack of available data. However, it should be noted that cloud deposition coupled with wet and dry deposition can result in 6 to 20 times greater total nitrogen deposition at high elevation relative to low elevation sites (Baumgardner et al., 2003). Therefore, total nitrogen deposition and the degree to which total nitrogen deposition exceeds the critical load at the HBEF Case Study Area may be underestimated.

**Table 2.1-4.** Data Requirements and Sources for Calculating Critical Loads for Total Nitrogen and Sulfur Deposition in Hubbard Brook Experimental Forest and Kane Experimental Forest

DATA	DATA NAME AND TYPE		DATA SOURCE	
	Name	Type	Hubbard Brook Experimental Forest	Kane Experimental Forest
Total nitrogen and sulfur deposition— wet and dry	CMAQ/ NADP	GIS datalayers	Provided by U.S. Environmental Protection Agency (EPA)/NADP, 2003a, e, h	Provided by EPA/ NADP, 2003a, e, h
Base cation ( $\text{Ca}^{2+}$ , $\text{Mg}^{2+}$ , $\text{Na}^+$ , $\text{K}^+$ ) deposition— wet	NADP	GIS datalayer	NADP, 2003b, d, f, g	NADP, 2003b, d, f, g
Base cation ( $\text{Ca}^{2+}$ , $\text{Mg}^{2+}$ , $\text{Na}^+$ , $\text{K}^+$ ) deposition— dry	CASTNET	GIS datalayer	U.S. EPA, 2008b	U.S. EPA, 2008b
Chlorine ( $\text{Cl}^-$ ) deposition— wet	NADP	GIS datalayer	NADP, 2003c	NADP, 2003c
Chlorine ( $\text{Cl}^-$ ) deposition— dry	CASTNET	GIS datalayer	U.S. EPA, 2008b	U.S. EPA, 2008b
Runoff	Annual run-off (1: 7,500,000 scale)	GIS datalayer	Gebert et al., 1987	Gebert et al., 1987
Mean annual soil temperature	Soil temperature data (HBEF/ KEF)	Database (HBEF)/ Peer-reviewed journal articles (KEF)	HBES, 2008c	Carter and Ciolkosz, 1980
Soil horizon depth	SSURGO	GIS datalayer	USDA-NRCS, 2008b	USDA-NRCS, 2008a
Percentage of clay by soil horizon	SSURGO	GIS datalayer	USDA-NRCS, 2008b	USDA-NRCS, 2008a
Percentage of sand by soil horizon	SSURGO	GIS datalayer	USDA-NRCS, 2008b	USDA-NRCS, 2008a
Percentage of organic matter by soil horizon	SSURGO	GIS datalayer	USDA-NRCS, 2008b	USDA-NRCS, 2008a

DATA	DATA NAME AND TYPE		DATA SOURCE	
	Name	Type	Hubbard Brook Experimental Forest	Kane Experimental Forest
Gibbsite equilibrium constant ( $K_{gibb}$ )	Selected $K_{gibb}$ values	Peer-reviewed journal articles and literature	Ouimet et al., 2006; Watmough et al., 2006; UNECE, 2004	Ouimet et al., 2006; Watmough et al., 2006; UNECE, 2004
Parent material/bedrock	Map of bedrock geology	GIS datalayer	USGS, 2000	PA DCNR, 2001
Food and Agriculture Organization (FAO) soil type	Map of dominant soil types	GIS datalayer	FAO, 2007	FAO, 2007
Nitrogen immobilization ( $N_i$ )	Selected $N_i$ value	Peer-reviewed journal article and literature	McNulty et al., 2007; UNECE, 2004	McNulty et al., 2007; UNECE, 2004
Denitrification ( $N_{de}$ )	Selected $N_{de}$ value	Peer-reviewed journal articles	McNulty et al., 2007; Ouimet et al., 2006; Watmough et al., 2006	McNulty et al., 2007; Ouimet et al., 2006; Watmough et al., 2006
Stand composition	Forest inventory (HBEF)/ SILVAH (KEF)	Database (HBEF)/ mensuration model (KEF)	HBES, 2008a	Thomasma et al., 2008
Annual volume increment (AVI) by species	Forest inventory (HBEF) / SILVAH (KEF)	Database (HBEF)/ mensuration model (KEF)	HBES, 2008a	Thomasma et al., 2008
Percentage allocation of growth to bark by species	Selected % allocation values	Peer-reviewed journal article	McNulty et al., 2007	McNulty et al., 2007
Specific gravity (bark and bole wood) by species	Selected specific gravity values	Peer-reviewed journal article	Jenkins et al., 2001	Jenkins et al., 2001

DATA	DATA NAME AND TYPE		DATA SOURCE	
	Name	Type	Hubbard Brook Experimental Forest	Kane Experimental Forest
Nutrient concentration (bark and bole wood) by species—nitrogen, $\text{Ca}^{2+}$ , $\text{Mg}^{2+}$ , $\text{K}^+$	Nitrogen, $\text{Ca}^{2+}$ , $\text{K}^+$ , $\text{Mg}^{2+}$ concentrations in bark and bole wood by species	Forest Service Report	Pardo et al., 2004	Pardo et al., 2004
Percentage biomass (bark and bole) removal during harvest	Selected value	Peer reviewed journal article	McNulty et al., 2007	McNulty et al., 2007

**Note:** CMAQ = Community Multiscale Air Quality Model; NADP = National Atmospheric Deposition Program; CASTNET = Clean Air Status and Trends Network; GIS = Geographic Information System; SSURGO = Soil Survey Geographic Database; SILVAH = Silviculture of Allegheny Hardwoods

### 2.1.2.2 Selection of Indicator Values

As described at the end of Section 1.1.1, the  $\text{Bc}/\text{Al}$  ratio  $((\text{Bc}/\text{Al})_{\text{crit}})$  in the soil solution was selected as the indicator for the calculation of critical loads in this case study. The  $(\text{Bc}/\text{Al})_{\text{crit}}$  connects the acid-influenced chemical status of the soil with the tree response: as the ratio decreases, tree health and growth can be impaired because of reduced uptake of base cations and increased Al toxicity. Most studies that calculate critical loads of acidity set the  $(\text{Bc}/\text{Al})_{\text{crit}}$  ratio to 1.0 or 10.0 (McNulty et al., 2007; NEG/ECP Forest Mapping Group, 2001; Pardo and Duarte, 2007; UNECE, 2004). The  $(\text{Bc}/\text{Al})_{\text{crit}}$  ratio of 1.0 is a common default value in European forests (UNECE, 2004) and has been applied to coniferous forests in the United States (McNulty et al., 2007). A  $(\text{Bc}/\text{Al})_{\text{crit}}$  ratio of 10.0 is a more conservative ratio and has been applied to hardwood forests in the United States (McNulty et al., 2007), in Canadian forests (Ouimet et al., 2006; Watmough et al., 2006), and in systems where maintained tree health is required (NEG/ECP Forest Mapping Group, 2001). Soil solution  $\text{Bc}/\text{Al}$  ratios of 10.0 are less likely to reduce soil base saturation and are not known to impair tree vigor or growth.

Cronan and Grigal (1995) conducted a meta-analysis of research investigating the relationship between soil solution  $\text{Ca}^{2+}/\text{Al}$  ratio and growth of 18 tree species. They found a 50% chance of negative impacts on tree growth or nutrition when the soil solution  $\text{Ca}^{2+}/\text{Al}$  ratio was

as low as 1.0, a 75% chance when the soil solution ratio was as low as 0.5, and nearly a 100% chance of impaired tree growth or nutrition when the soil solution  $\text{Ca}^{2+}/\text{Al}$  molar ratio was as low as 0.2. In a similar meta-analysis of studies that explored the relationship between  $\text{Bc}/\text{Al}$  and tree growth, Sverdrup and Warfvinge (1993b) reported the  $\text{Bc}/\text{Al}$  ratio at which growth was reduced by 20% relative to control trees. **Figure 2.1-2** presents the findings of Sverdrup and Warfvinge (1993b) based on 46 of the tree species that grow in North America. This summary indicates that there is a 50% chance of negative tree response (i.e., greater than 20% reduced growth) at a soil solution  $\text{Bc}/\text{Al}$  ratio of 1.2. Sverdrup and Warfvinge (1993b) also presented the results of studies conducted on individual tree species. **Figures 2.1-3 and 2.1-4** show growth in sugar maple and red spruce, respectively. According to these figures, sugar maple growth was reduced by 20% and red spruce growth was reduced by 35% (relative to controls) at a  $\text{Bc}/\text{Al}$  ratio of 0.6.

Three  $\text{Bc}/\text{Al}$  ratio ( $(\text{Bc}/\text{Al})_{\text{crit}}$ ) values were used in this case study to evaluate different levels of protection associated with total nitrogen and sulfur deposition: 0.6, 1.2, and 10 (**Table 2.1-5**). The  $(\text{Bc}/\text{Al})_{\text{crit}}$  ratio of 0.6 represents the highest level of impact (lowest level of protection) to tree health and growth; as much as 75% of 46 tree species found in North America experience reduced growth at this ratio (Sverdrup and Warfvinge, 1993b). Both red spruce and sugar maple show at least a 20% reduction in growth at the 0.6  $(\text{Bc}/\text{Al})_{\text{crit}}$  ratio. The  $(\text{Bc}/\text{Al})_{\text{crit}}$  ratio of 1.2 is considered to represent a moderate level of impact; the growth of 50% of tree species (found growing in North America) were negatively impacted at this soil solution ratio (**Figure 2.1-4**). The  $(\text{Bc}/\text{Al})_{\text{crit}}$  ratio of 10.0 was selected to represent the lowest level of impact (greatest level of protection) to tree growth; it is the most conservative value used in studies that have calculated critical loads in the United States and Canada (NEG/ECP Forest Mapping Group, 2001; McNulty et al., 2007; Watmough et al., 2004).

**Table 2.1-5.** The Three Indicator  $(\text{Bc}/\text{Al})_{\text{crit}}$  Soil Solution Ratios Used in This Case Study and the Corresponding Levels of Protection to Tree Health and Critical Loads

Indicator $(\text{Bc}/\text{Al})_{\text{crit}}$ Soil Solution Ratio	Level of Protection to Tree Health	Critical Load
0.6	Low	High
1.2	Intermediate	Intermediate
10.0	High	Low

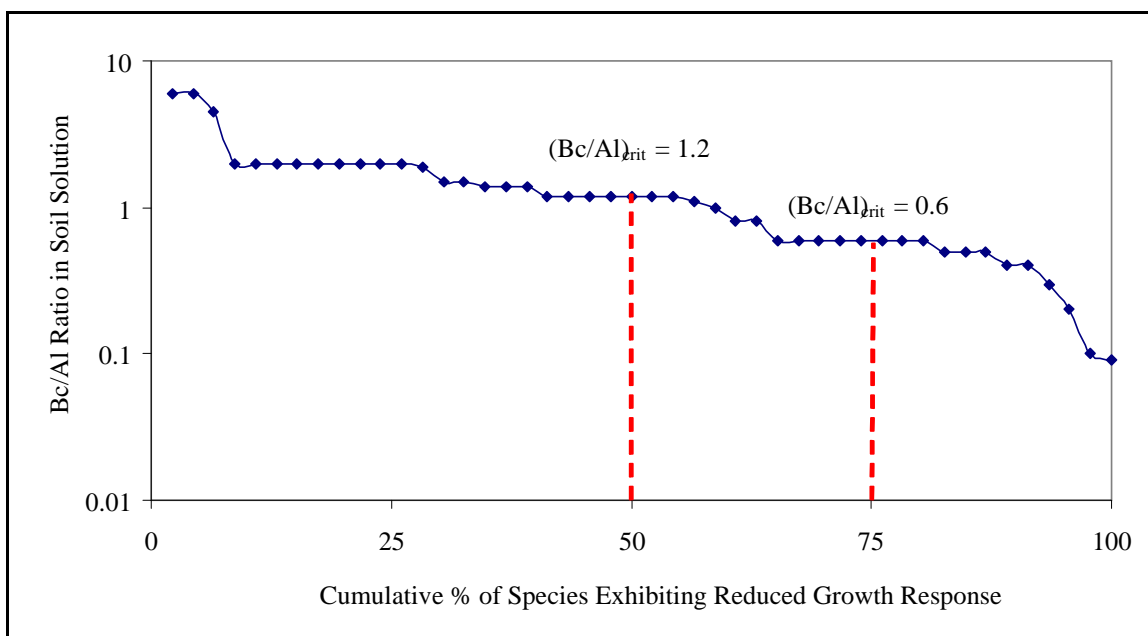


**Figure 2.1-2.** The relationship between the Bc/Al ratio in soil solution and the percentage of tree species (found growing in North America) exhibiting a 20% reduction in growth relative to controls (after Sverdrup and Warfvinge, 1993b).

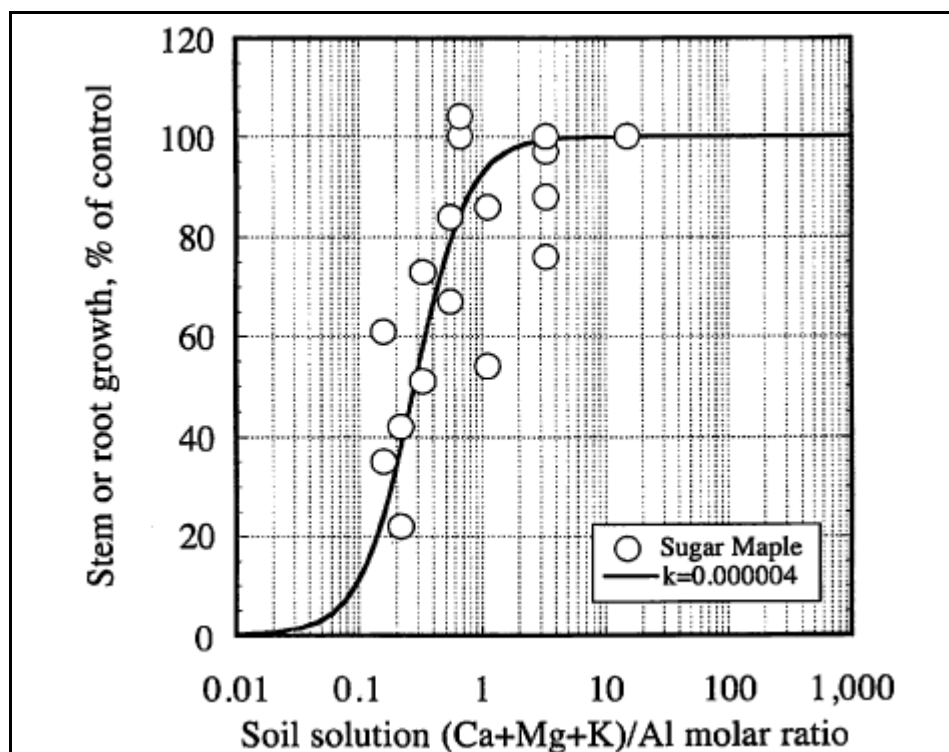


**Figure 2.1-3.** The relationship between soil solution Bc/Al ratio and stem or root growth in sugar maple (from Sverdrup and Warfvinge, 1993b).



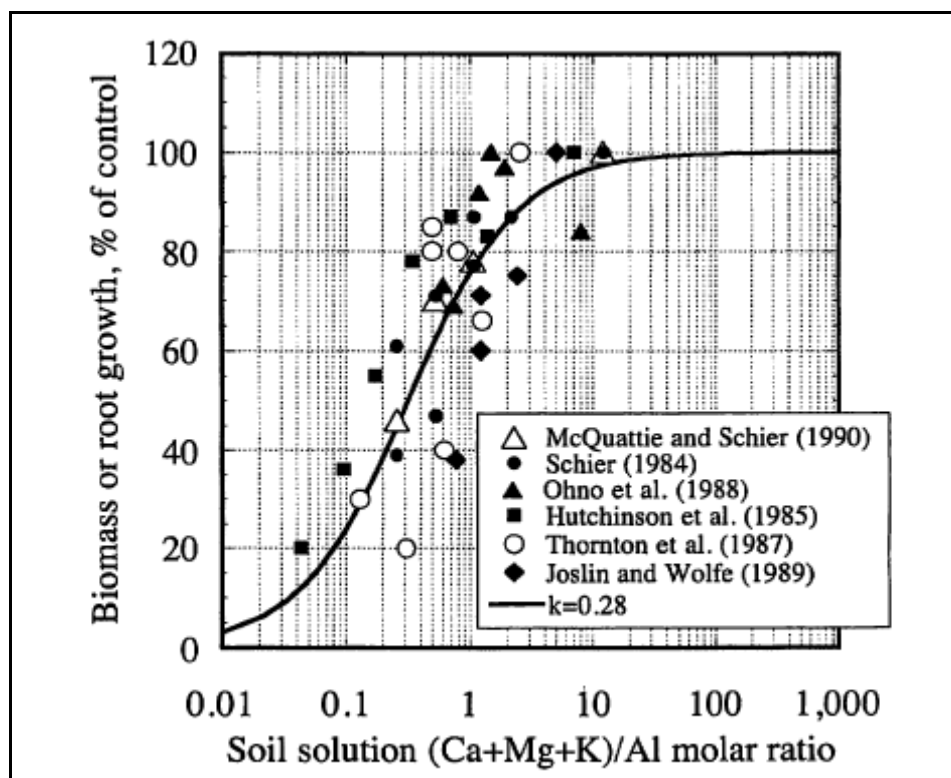


**Figure 2.1-4.** The relationship between soil solution Bc/Al ratio and biomass or root growth in red spruce (from Sverdrup and Warfvinge, 1993b).

### 2.1.2.3 Case Study Input Data

The data used to calculate critical loads for sugar maple and red spruce in the KEF and HBEF of this case study are presented in **Tables 2.1-5, 2.1-6, 2.1-7, and 2.1-8**. The majority of the data was specific to the case study areas and was compiled from published research studies and models, site-specific databases, or spatially-explicit GIS datalayers. However, several of the parameters, including denitrification ( $N_{de}$ ), nitrogen immobilization ( $N_i$ ), the gibbsite equilibrium constant ( $K_{gibb}$ ), and rooting zone soil depth required the use of default values or values used in published critical load assessments. Denitrification loss of nitrogen ( $N_{de}$ ) was assumed to be 0.0 eq/ha/yr because both the KEF and HBEF study plots are upland forests and denitrification is considered negligible in such forests (McNulty et al., 2007; Ouimet et al., 2006; Watmough et al., 2006). The ICP Mapping and Modeling Manual (UNECE, 2004) reported values of  $N_i$  in the soil, ranging from 14.3 to 35.7 eq/ha/yr in colder climates and up to 71.4 eq/ha/yr in warmer climates. Nitrogen immobilization ( $N_i$ ) was set to 42.86 eq/ha/yr (the average of the colder and warmer climate immobilization rates) for both forests in this case study. This approach and value was also used by McNulty et al. (2007) for forests in the United States. Two values of the  $K_{gibb}$ ,

300 and 3,000  $\text{m}^6/\text{eq}^2$ , were used in the calculations of critical loads because the 300  $\text{m}^6/\text{eq}^2$  value is a widely used default value (UNECE, 2004; McNulty et al., 2007), and the 3,000  $\text{m}^6/\text{eq}^2$  value has been used to map critical loads in Canada (Ouimet et al., 2006; Watmough et al., 2006). The 3,000  $\text{m}^6/\text{eq}^2$  constant is also the highest  $K_{\text{gibb}}$  value associated with soils with low organic matter contents (UNECE, 2004). Fifty cm (0.5 m) was selected to represent the depth of the rooting zone layer in this case study. Fine roots, which are responsible for the vast majority of nutrient uptake, are typically concentrated in the upper 10 to 20 cm of soil (van der Salm and de Vries, 2001). These roots are most susceptible to the impacts of acidification. Therefore, a 0.5 m depth has been suggested as a suitable rooting zone depth in the calculation of critical loads for forest soils (Sverdrup and de Vries, 1994; Hodson and Langan, 1999).

As detailed in the preceding section, the three  $(\text{Bc}/\text{Al})_{\text{crit}}$  ratio values, associated with three levels of forest protection, were used in the critical load calculations for this case study. The 0.6, 1.2, and 10.0  $(\text{Bc}/\text{Al})_{\text{crit}}$  ratios were applied to both the KEF and HBEF case study areas.

As outlined earlier, base cation weathering rates were calculated using two methods; the clay-substrate method and the soil type–texture association method. The data presented in **Tables 2.1-6 and 2.1-7** were used for these calculations. Similarly, base cation ( $\text{Bc}_u$ ) and nitrogen ( $\text{N}_u$ ) uptake values were calculated in two different ways for the two case study areas. In HBEF,  $\text{Bc}_u$  and  $\text{N}_u$  were assumed to be 0 eq/ha/yr because Watershed 6 is a reference watershed and does not have a history or future of harvesting. Biomass (and the nutrients contained therein) would, therefore, not have been removed from site. In KEF, two sets of values were used to model two scenarios and estimate  $\text{Bc}_u$  and  $\text{N}_u$  in the SMB model calculations. In the first scenario, it was assumed that the tree biomass was not harvested. Therefore,  $\text{N}_u$  and  $\text{Bc}_w$ , in this scenario, were set to 0 eq/ha/yr. In the second scenario, the case study plots were assumed to be managed and harvested on a regular basis. Values of  $\text{Bc}_u$  and  $\text{N}_u$  for this scenario were therefore calculated using tree data (**Tables 2.1-6, 2.1-8, and 2.1-9**) and Equation 8 in Section 2.1.1.1. The calculation of critical loads with the different  $\text{Bc}_u$  and  $\text{N}_u$  values allowed for a comparison of the influence of forest harvesting on the estimates of critical loads. The removal of nitrogen and base cations with harvesting can significantly reduce the critical load of total nitrogen and sulfur acidifying deposition in an ecosystem; the uptake and removal of base cations reduces the capacity of the system to neutralize acidifying deposition.

**Table 2.1-6.** Input Values for the Calculation of Critical Load in Hubbard Brook Experimental Forest and Kane Experimental Forest

DATA	CASE STUDY AREA	
	Hubbard Brook Experimental Forest	Kane Experimental Forest
2002 CMAQ/NADP total nitrogen and sulfur deposition levels—wet and dry (eq/ha)	Nitrogen = 601.07, Sulfur = 233.0811	Nitrogen = 967.54, Sulfur = 646.37
Average annual (2000 to 2007) base cation ( $\text{Ca}^{2+}$ , $\text{Mg}^{2+}$ , $\text{Na}^+$ , $\text{K}^+$ ) deposition—wet (eq/ha)	$\text{Ca}^{2+} = 15.87$ , $\text{Mg}^{2+} = 5.69$ , $\text{K}^+ = 4.27$ , $\text{Na}^+ = 35.78$	$\text{Ca}^{2+} = 33.03$ , $\text{Mg}^{2+} = 7.96$ , $\text{K}^+ = 6.33$ , $\text{Na}^+ = 18.31$
Average annual (2000 to 2007) base cation ( $\text{Ca}^{2+}$ , $\text{Mg}^{2+}$ , $\text{Na}^+$ , $\text{K}^+$ ) deposition—dry (eq/ha)	$\text{Ca}^{2+} = 0.29$ , $\text{Mg}^{2+} = 0.14$ , $\text{K}^+ = 0.18$ , $\text{Na}^+ = 0.83$	$\text{Ca}^{2+} = 1.08$ , $\text{Mg}^{2+} = 0.38$ , $\text{K}^+ = 0.34$ , $\text{Na}^+ = 0.82$
Average annual (2000 to 2007) chloride ( $\text{Cl}^-$ ) deposition—wet (eq/ha)	45.48	35.36
Average annual chloride ( $\text{Cl}^-$ ) deposition—dry (eq/ha)	(2004 to 2007) 0.37	(2003 to 2007) 0.17
Runoff ( $\text{m}^3/\text{ha}/\text{yr}$ )	7,620	6,350
Average annual soil temperature (to 0.5 m) ( $^{\circ}\text{C}$ )	(1989 to 1998) 7.29	(1976 to 1979) 7.90
Rooting Zone Soil depth (m)	0.5	0.5
Percentage clay (in top 0.5 m of soil) <sup>a</sup>	6.4	See Table 2.1-7
Percentage sand (in top 0.5 m of soil) <sup>a</sup>	57.4	See Table 2.1-7
Percentage organic matter (in top 0.5 m of soil) <sup>a</sup>	3.6	See Table 2.1-7
Gibbsite equilibrium constant ( $K_{\text{gibb}}$ ) ( $\text{m}^6/\text{eq}^2$ )	300 and 3,000	300 and 3,000
Parent material/bedrock <sup>b</sup>	Quartz, mica, schist, and quartzite	Sandstone, conglomerate, and shale
Food and Agriculture Organization (FAO) soil type	Orthic Podzol (Po)	Dystric Cambisol (Bd)
Nitrogen immobilization ( $\text{N}_i$ ) (eq/ha/yr)	42.86	42.86
Denitrification ( $\text{N}_{\text{de}}$ ) (eq/ha/yr)	0	0
Stand composition (in common name alphabetical order)	American Beech ( <i>Fagus grandifolia</i> ), Balsam Fir ( <i>Abies balsamea</i> ), Birch spp. ( <i>Betula</i> spp.), Mountain Ash ( <i>Sorbus americana</i> ), Red Maple ( <i>Acer rubrum</i> ), Red Spruce, Striped Maple ( <i>Acer pensylvanicum</i> ) and Sugar Maple	American Beech ( <i>Fagus grandifolia</i> ), Birch spp. ( <i>Betula</i> spp.), Black cherry ( <i>Prunus serotina</i> ), Cucumber Tree ( <i>Magnolia acuminata</i> ), Eastern Hemlock ( <i>Tsuga canadensis</i> ), Red Maple ( <i>Acer rubrum</i> ), and Sugar Maple

DATA	CASE STUDY AREA	
	Hubbard Brook Experimental Forest	Kane Experimental Forest
Annual volume increment (AVI) by species (m <sup>3</sup> /ha/yr)	—	See Table 2.1-8
Percentage allocation of growth to bark by species	—	11%—coniferous species / 15%—deciduous species
Specific gravity (bark and bole wood) by species (g/cm <sup>3</sup> )	—	See Table 2.1-9
Nutrient concentration (% nitrogen, Ca <sup>2+</sup> , Mg <sup>2+</sup> , K <sup>+</sup> ) (bark and bole wood) by tree species	—	See Table 2.1-9
Percentage biomass (bark and bole) removal during harvest	—	65

<sup>a</sup> Determined by weighted average by horizon depth and soil series coverage

<sup>b</sup> Based on dominant mineralogy

**Table 2.1-7.** Soil Characteristics in the Seven Plots of the Kane Experimental Forest Case Study Area for the Calculation of the Base Cation Weathering Rate Parameters

Soil Attribute (in top 0.5 m of soil)	PLOT						
	1	2	3	4	5	6	7
Percentage Clay	23.3	20.1	21.3	20.1	23.3	20.1	20.1
Percentage Sand	39.9	27.0	26.2	27.0	39.9	27.0	27.0
Percentage Organic Matter	1.4	0.7	1.1	0.7	1.4	0.7	0.7

**Table 2.1-8.** Annual Volume Growth by Tree Species in Each of the Seven Plots of the Kane Experimental Forest Case Study Area for the Calculation of Nutrient Uptake (Bc<sub>u</sub> and N<sub>u</sub>)

PLOT	TREE SPECIES ANNUAL VOLUME GROWTH (m <sup>3</sup> /ha/yr)						
	American Beech	Birch spp.	Black Cherry	Cucumber Tree	Eastern Hemlock	Red Maple	Sugar Maple
1	NA	NA	3.3	NA	NA	0.8	2.8
2	NA	NA	3.0	NA	NA	NA	1.4
3	0.8	0.2	1.3	NA	0.1	0.3	1.3
4	0.9	NA	NA	NA	NA	1.1	0.4
5	0.9	3.0	NA	0	NA	NA	0.6
6	NA	NA	1.8	NA	NA	0.1	1.3
7	0.6	0.1	0.8	NA	0.1	NA	0.7

NA = Not applicable.

**Table 2.1-9.** Specific Gravity and Nutrient Concentrations by Biomass Component (Bark and Bole Wood) and by Tree Species for the Calculation of Nutrient Uptake ( $Bc_u$  and  $N_u$ ) in the Kane Experimental Forest Case Study Area

SPECIES	BARK					BOLE				
	Specific Gravity (g/cm <sup>3</sup> )	% N	% K <sup>+</sup>	% Mg <sup>2+</sup>	% Ca <sup>2+</sup>	Specific Gravity (g/cm <sup>3</sup> )	% N	% K <sup>+</sup>	% Mg <sup>2+</sup>	% Ca <sup>2+</sup>
American Beech	0.50	0.75	0.22	0.05	2.81	0.56	0.11	0.07	0.02	0.07
Birch spp	0.61	0.40	0.12	0.04	0.78	0.61	0.09	0.05	0.02	0.08
Black Cherry	0.50	0.00	0.00	0.00	2.69	0.47	0.00	0.00	0.00	0.08
Cucumber Tree	0.50	0.54	0.21	0.06	2.15	0.52	0.10	0.09	0.02	0.11
Eastern Hemlock	0.34	0.27	0.15	0.03	0.74	0.38	0.08	0.09	0.01	0.07
Red Maple	0.55	0.43	0.20	0.05	1.30	0.49	0.09	0.08	0.02	0.11
Sugar Maple	0.54	0.51	0.31	0.06	2.23	0.56	0.10	0.07	0.02	0.13

**Note:** N = nitrogen.

## 2.2 CRITICAL LOAD FUNCTION RESPONSE CURVES ASSOCIATED WITH THE THREE LEVELS OF PROTECTION

The three  $(Bc/Al)_{crit}$  ratio values (0.6, 1.2, and 10.0) used to evaluate level of protection to tree health and growth correspond to three different critical load values of total nitrogen and sulfur deposition  $((N+S)_{comb})$ . A critical load based on 0.6  $(Bc/Al)_{crit}$  ratio is the least stringent load and offers the least protection to forests of the three critical loads. The 1.2  $(Bc/Al)_{crit}$  ratio results in an intermediate critical load of total nitrogen and sulfur deposition with moderate protection to tree health. A critical load based on a 10.0  $(Bc/Al)_{crit}$  ratio would be the most stringent load and offers the greatest protection to the health of trees.

As outlined in Section 2.1.1.3, critical loads of acidity can be translated into CLF relationships; the CLF defines the combinations of  $(N+S)_{comb}$  that are equal to the calculated combined critical load of an ecosystem. Therefore, to provide an indication of all combinations of total nitrogen and sulfur deposition associated with the three different levels of protection, CLF response curves were produced with the three  $(Bc/Al)_{crit}$  ratios. From the 0.6, 1.2, and 10.0

$(Bc/Al)_{crit}$  ratios, the critical loads of  $(N+S)_{comb}$  and corresponding  $CL_{max}(N)$ ,  $CL_{min}(N)$  and  $CL_{max}(S)$  values were calculated to generate CLF response curves for each case study area.

**Figure 2.2-1** provides an example of the CLF response curves associated with the three levels of protection.

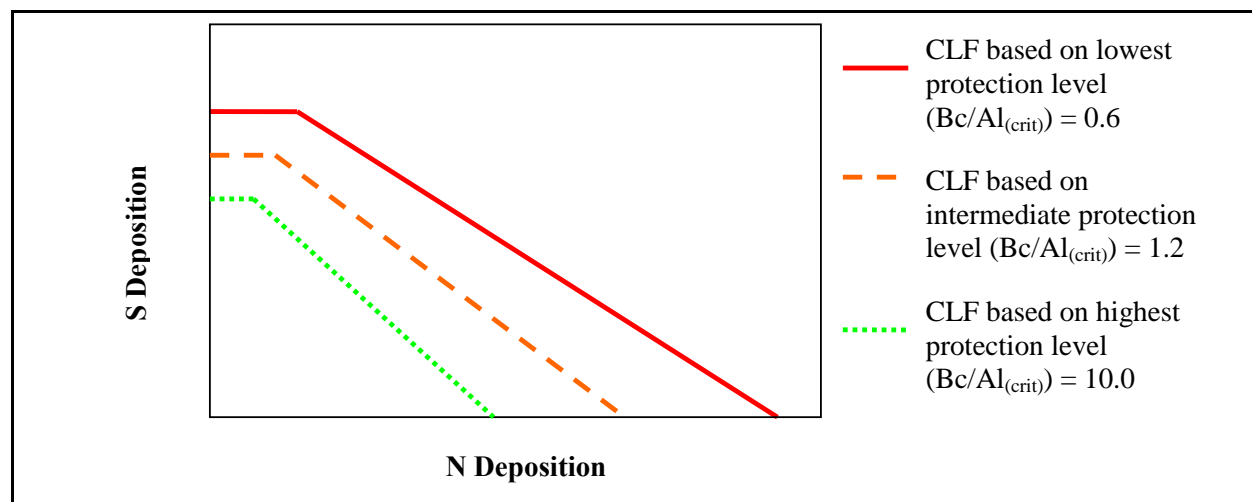


**Figure 2.2-1.** An example of the critical load function response curves associated with the three  $(Bc/Al)_{crit}$  ratios and the associated levels of protection of tree health. The flat line portion of the curves indicates total nitrogen deposition corresponding to the  $CL_{min}$  (nitrogen absorbed by nitrogen sinks within the system).

## 3.0 RESULTS

### 3.1 CRITICAL LOAD ESTIMATES

#### 3.1.1 Sugar Maple

The estimates of critical loads for sugar maple in the seven plots in KEF are presented in **Tables 3.1-1 through 3.1-7**. The critical load estimates for all seven plots are summarized in **Table 3.1-8** and ranged from 728 eq/ha/yr to 2,998 eq/ha/yr of combined total nitrogen and sulfur deposition  $((N+S)_{comb})$ . The ranges of critical loads associated with the three  $(Bc/Al)_{crit}$  ratios differed by level of impact to tree health, but there was some overlap between the ranges of values. The lowest level of protection,  $(Bc/Al)_{crit}$  ratio = 0.6, had the highest critical loads that ranged from 1,132 eq/ha/yr to 2,998 eq/ha/yr of  $(N+S)_{comb}$ . The intermediate level of protection,  $(Bc/Al)_{crit}$  ratio = 1.2, had critical loads ranging from 1,033 eq/ha/yr to 2,079 eq/ha/yr. The  $(Bc/Al)_{crit}$  ratio of 10.0, corresponding to the most protective level for tree health, had critical

load values ranging from 728 eq/ha/yr to 1,139 eq/ha/yr of  $(N+S)_{\text{comb}}$ . Plot location, the two different methods to estimate base cation weathering, the two  $K_{\text{gibb}}$  values, and the inclusion of the influence of nutrient uptake and removal ( $Bc_u$  and  $N_u$  greater than 0 eq/ha/yr) in the critical load calculations all influenced the critical loads for the three  $(Bc/Al)_{\text{crit}}$  ratio values. In general, Plot 1 had both the lowest and highest critical load values. This was largely due to the method used to calculate  $BC_w$  (clay-substrate method) and the relative high percentages of clay and organic matter in the soil, which accounted for the high critical load values. The low critical load values in Plot 1 were caused by the comparatively high amount of base cation and nitrogen uptake by the trees. The  $K_{\text{gibb}}$  constant also influenced the critical load values, with  $300 \text{ m}^6/\text{eq}^2$  causing higher critical loads than  $3000 \text{ m}^6/\text{eq}^2$ . Similarly, the clay-substrate method to estimate  $BC_w$  produced higher critical load values than did the soil type–texture approximation method. The inclusion of the influence of nutrient uptake and removal by trees ( $Bc_u$  and  $N_u$  greater than 0 eq/ha/yr) in the calculations of critical loads resulted in a large decrease in the critical values, especially for the  $(Bc/Al)_{\text{crit}}$  ratio of 0.6, which offers the lowest level of protection to tree health.

**Table 3.1-1.** Critical Loads Calculated with the Different Base Cation Weathering, Gibbsite Equilibrium Constant ( $K_{\text{gibb}}$ ), and Base Cation ( $Bc_u$ ) and Nitrogen ( $N_u$ ) Uptake Parameter Values in Plot 1 of the Kane Experimental Forest Case Study Area

Nutrient Uptake in Critical Load	$(Bc/Al)_{\text{crit}}$ Ratio	Critical Load (eq/ha/yr)			
		Clay-Substrate Method		Soil Type–Texture Approximation Method	
		$K_{\text{gibb}} = 300 \text{ m}^6/\text{eq}^2$	$K_{\text{gibb}} = 3000 \text{ m}^6/\text{eq}^2$	$K_{\text{gibb}} = 300 \text{ m}^6/\text{eq}^2$	$K_{\text{gibb}} = 3000 \text{ m}^6/\text{eq}^2$
$Bc_u$ and $N_u$ NOT Included	0.6	2,998	2,678	2,633	2,328
	1.2	2,079	1,825	1,832	1,591
	10.0	1,139	1,014	1,002	883
$Bc_u$ and $N_u$ Included	0.6	1,940	1,692	1,553	1,332
	1.2	1,473	1,276	1,208	1,033
	10.0	960	862	814	728

**Table 3.1-2.** Critical Loads Calculated with the Different Base Cation Weathering, Gibbsite Equilibrium Constant ( $K_{\text{gibb}}$ ), and Base Cation ( $Bc_u$ ) and Nitrogen ( $N_u$ ) Uptake Parameter Values in Plot 2 of the Kane Experimental Forest Case Study Area

Nutrient Uptake in Critical Load	$(Bc/Al)_{\text{crit}}$ Ratio	Critical Load (eq/ha/yr)			
		Clay-Substrate Method		Soil Type-Texture Approximation Method	
		$K_{\text{gibb}} = 300$ $\text{m}^6/\text{eq}^2$	$K_{\text{gibb}} = 3000$ $\text{m}^6/\text{eq}^2$	$K_{\text{gibb}} = 300$ $\text{m}^6/\text{eq}^2$	$K_{\text{gibb}} = 3000$ $\text{m}^6/\text{eq}^2$
$Bc_u$ and $N_u$ <b>NOT Included</b>	<b>0.6</b>	2,711	2,403	2,633	2,328
	<b>1.2</b>	1,885	1,641	1,832	1,591
	<b>10.0</b>	1,032	911	1,002	883
$Bc_u$ and $N_u$ <b>Included</b>	<b>0.6</b>	2,009	1,749	1,928	1,673
	<b>1.2</b>	1,481	1,275	1,426	1,223
	<b>10.0</b>	910	808	879	779

**Table 3.1-3.** Critical Loads Calculated with the Different Base Cation Weathering, Gibbsite Equilibrium Constant ( $K_{\text{gibb}}$ ), and Base Cation ( $Bc_u$ ) and Nitrogen ( $N_u$ ) Uptake Parameter Values in Plot 3 of the Kane Experimental Forest Case Study Area

Nutrient Uptake in Critical Load	$Bc/Al)_{\text{crit}}$ Ratio	Critical Load (eq/ha/yr)			
		Clay-Substrate Method		Soil Type-Texture Approximation Method	
		$K_{\text{gibb}} = 300$ $\text{m}^6/\text{eq}^2$	$K_{\text{gibb}} = 3,000$ $\text{m}^6/\text{eq}^2$	$K_{\text{gibb}} = 300$ $\text{m}^6/\text{eq}^2$	$K_{\text{gibb}} = 3,000$ $\text{m}^6/\text{eq}^2$
$Bc_u$ and $N_u$ <b>NOT Included</b>	<b>0.6</b>	2,817	2,504	2,633	2,328
	<b>1.2</b>	1,957	1,709	1,832	1,591
	<b>10.0</b>	1,071	949	1,002	883
$Bc_u$ and $N_u$ <b>Included</b>	<b>0.6</b>	2,228	1,954	2,039	1,776
	<b>1.2</b>	1,626	1,408	1,497	1,288
	<b>10.0</b>	983	875	912	809



**Table 3.1-4.** Critical Loads Calculated with the Different Base Cation Weathering, Gibbsite Equilibrium Constant ( $K_{\text{gibb}}$ ), and Base Cation ( $Bc_u$ ) and Nitrogen ( $N_u$ ) Uptake Parameter Values in Plot 4 of the Kane Experimental Forest Case Study Area

Nutrient Uptake in Critical Load	$(Bc/Al)_{\text{crit}}$ Ratio	Critical Load (eq/ha/yr)			
		Clay-Substrate Method		Soil Type–Texture Approximation Method	
		$K_{\text{gibb}} = 300$ $\text{m}^6/\text{eq}^2$	$K_{\text{gibb}} = 3,000$ $\text{m}^6/\text{eq}^2$	$K_{\text{gibb}} = 300$ $\text{m}^6/\text{eq}^2$	$K_{\text{gibb}} = 3,000$ $\text{m}^6/\text{eq}^2$
$Bc_u$ and $N_u$ <b>NOT Included</b>	<b>0.6</b>	2,711	2,403	2,633	2,328
	<b>1.2</b>	1,885	1,641	1,832	1,591
	<b>10.0</b>	1,032	911	1,002	883
$Bc_u$ and $N_u$ <b>Included</b>	<b>0.6</b>	2,388	2,101	2,308	2,025
	<b>1.2</b>	1,707	1,479	1,653	1,429
	<b>10.0</b>	990	878	960	850

**Table 3.1-5.** Critical Loads Calculated with the Different Base Cation Weathering, Gibbsite Equilibrium Constant ( $K_{\text{gibb}}$ ) and Base Cation ( $Bc_u$ ) and Nitrogen ( $N_u$ ) Uptake Parameter Values in Plot 5 of the Kane Experimental Forest Case Study Area

Nutrient Uptake in Critical Load	$(Bc/Al)_{\text{crit}}$ Ratio	Critical Load (eq/ha/yr )			
		Clay-Substrate Method		Soil Type–Texture Approximation Method	
		$K_{\text{gibb}} = 300$ $\text{m}^6/\text{eq}^2$	$K_{\text{gibb}} = 3,000$ $\text{m}^6/\text{eq}^2$	$K_{\text{gibb}} = 300$ $\text{m}^6/\text{eq}^2$	$K_{\text{gibb}} = 3,000$ $\text{m}^6/\text{eq}^2$
$Bc_u$ and $N_u$ <b>NOT Included</b>	<b>0.6</b>	2,998	2,678	2,633	2,328
	<b>1.2</b>	2,079	1,825	1,832	1,591
	<b>10.0</b>	1,139	1,014	1,002	883
$Bc_u$ and $N_u$ <b>Included</b>	<b>0.6</b>	2,545	2,256	2,173	1,903
	<b>1.2</b>	1,849	1,620	1,596	1,382
	<b>10.0</b>	1,118	1,004	978	873

**Table 3.1-6.** Critical Loads Calculated with the Different Base Cation Weathering, Gibbsite Equilibrium Constant ( $K_{gibb}$ ), and Base Cation ( $Bc_u$ ) and Nitrogen ( $N_u$ ) Uptake Parameter Values in Plot 6 of the Kane Experimental Forest Case Study Area

Nutrient Uptake in Critical Load	$(Bc/Al)_{crit}$ Ratio	Critical Load (eq/ha/yr )			
		Clay-Substrate Method		Soil Type–Texture Approximation Method	
		$K_{gibb} = 300$ $m^6/eq^2$	$K_{gibb} = 3,000$ $m^6/eq^2$	$K_{gibb} = 300$ $m^6/eq^2$	$K_{gibb} = 3,000$ $m^6/eq^2$
$Bc_u$ and $N_u$ <b>NOT Included</b>	<b>0.6</b>	2,711	2,403	2,633	2,328
	<b>1.2</b>	1,885	1,641	1,832	1,591
	<b>10.0</b>	1,032	911	1,002	883
$Bc_u$ and $N_u$ <b>Included</b>	<b>0.6</b>	2,212	1,936	2,132	1,861
	<b>1.2</b>	1,599	1,380	1,545	1,329
	<b>10.0</b>	946	838	916	810

**Table 3.1-7.** Critical Loads Calculated with the Different Base Cation Weathering, Gibbsite Equilibrium Constant ( $K_{gibb}$ ), and Base Cation ( $Bc_u$ ) and Nitrogen ( $N_u$ ) Uptake Parameter Values in Plot 7 of the Kane Experimental Forest Case Study Area

Nutrient Uptake in Critical Load	$(Bc/Al)_{crit}$ Ratio	Critical Load (eq/ha/yr )			
		Clay-Substrate Method		Soil Type–Texture Approximation Method	
		$K_{gibb} = 300$ $m^6/eq^2$	$K_{gibb} = 3,000$ $m^6/eq^2$	$K_{gibb} = 300$ $m^6/eq^2$	$K_{gibb} = 3,000$ $m^6/eq^2$
$Bc_u$ and $N_u$ <b>NOT Included</b>	<b>0.6</b>	2,711	2,403	2,633	2,328
	<b>1.2</b>	1,885	1,641	1,832	1,591
	<b>10.0</b>	1,032	911	1,002	883
$Bc_u$ and $N_u$ <b>Included</b>	<b>0.6</b>	2,368	2,082	2,289	2,007
	<b>1.2</b>	1,693	1,466	1,639	1,415
	<b>10.0</b>	981	869	951	840

**Table 3.1-8.** Ranges of Critical Load Values (eq/ha/yr) (with and without the Influence of Nutrient Uptake and Removal with Tree Harvest) for the Seven Plots of the Kane Experimental Forest Case Study Area (Both  $K_{gibb}$  values and methods to estimate  $BC_w$  were used in these calculations to present the range of critical loads estimated using all combinations of the parameter values.)

Nutrient Uptake in Critical Load	$(Bc/Al)_{crit}$ Ratio	Critical Loads (eq/ha/yr )						
		Plot 1	Plot 2	Plot 3	Plot 4	Plot 5	Plot 6	Plot 7
$Bc_u$ and $N_u$ <b>NOT Included</b>	<b>0.6</b>	2,328 to 2,998	2,328 to 2,711	2,328 to 2,817	2,328 to 2,711	2,328 to 2,998	2,328 to 2,711	2,328 to 2,711
	<b>1.2</b>	1,591 to 2,079	1,591 to 1,885	1,591 to 1,957	1,591 to 1,885	1,591 to 2,079	1,591 to 1,885	1,591 to 1,885
	<b>10.0</b>	883 to 1,139	883 to 1,032	883 to 1,071	883 to 1,032	883 to 1,139	883 to 1,032	883 to 1,032
$Bc_u$ and $N_u$ <b>Included</b>	<b>0.6</b>	1,332 to 1,940	1,673 to 2,009	1,776 to 2,228	2,025 to 2,388	1,903 to 2,545	1,861 to 2,212	2,007 to 2,368
	<b>1.2</b>	1,033 to 1,473	1,223 to 1,481	1,288 to 1,626	1,429 to 1,707	1,382 to 1,849	1,329 to 1,599	1,415 to 1,693
	<b>10.0</b>	728 to 960	779 to 910	809 to 983	850 to 990	873 to 1,118	810 to 946	840 to 981

Two series of CLF response curves corresponding to the three  $(Bc/Al)_{crit}$  ratio values (i.e., 0.6, 1.2, and 10.0) for Plot 1 of the KEF Case Study Area are shown in **Figures 3.1-1 and 3.1-2**. Plot 1 had the highest and lowest critical load estimates. Therefore, the extreme values of this plot were graphed to capture the range of critical loads associated with the three levels of protection in the KEF Case Study Area. **Figure 3.1-1** presents the CLF response curves associated with the lowest critical load estimates. This scenario corresponded to the  $BC_w$  calculated using the soil type–texture approximation method, the  $3000 \text{ m}^6/\text{eq}^2$   $K_{gibb}$  constant, and the inclusion of the influence of nutrient uptake and removal ( $Bc_u$  and  $N_u$  greater than 0 eq/ha/yr) in the calculation of critical load. Nitrogen uptake ( $N_u$ ) substantially increased the minimum critical load of nitrogen ( $CL_{min}(N)$ ) in this CLF relationship. **Figure 3.1-2** shows the CLF response curves associated with the highest critical load estimates in Plot 1. These estimates occurred with  $BC_w$  calculated using the clay-substrate method and the  $300 \text{ m}^6/\text{eq}^2$   $K_{gibb}$  constant. Nutrient uptake (i.e.,  $Bc_u$  and  $N_u$ ) was set to 0 eq/ha/yr in this calculation of critical load.

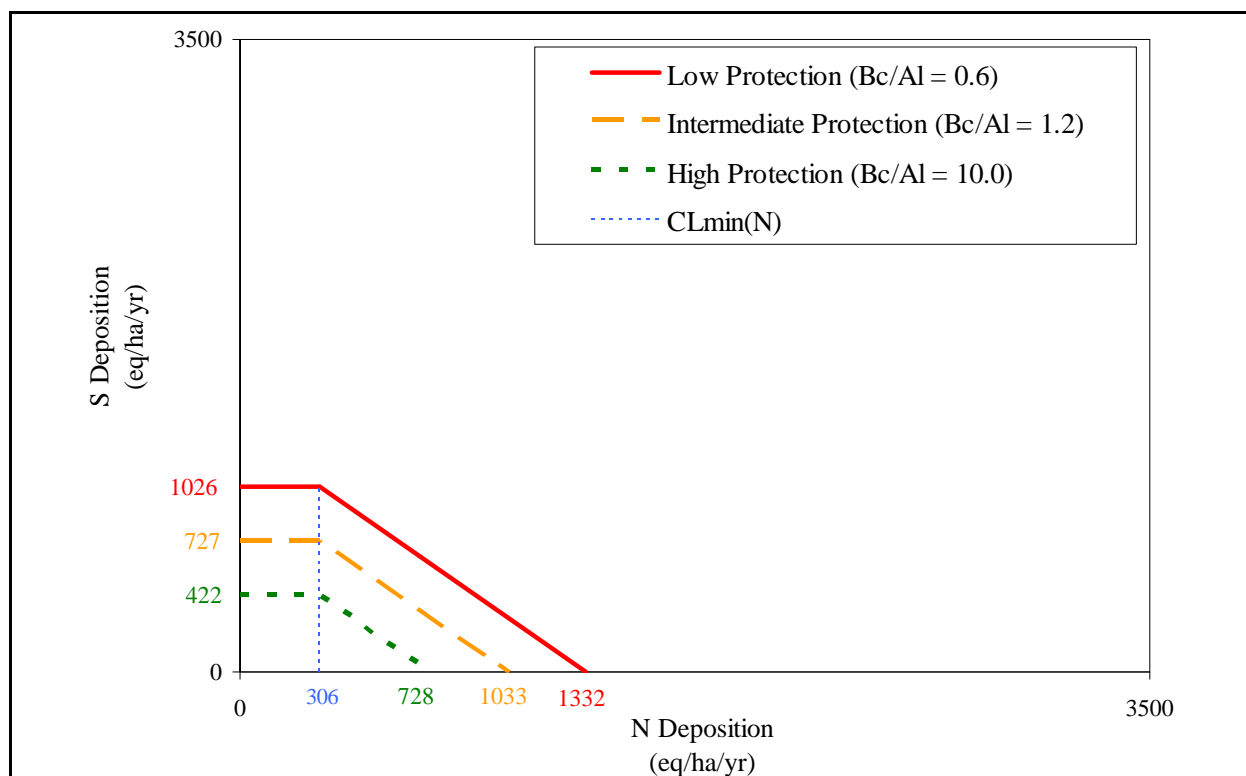


**Figure 3.1-1.** The critical load function response curves detailing the lowest critical load estimates for Plot 1 of the Kane Experimental Forest (refer to **Table 3.1-1** for the parameters corresponding to each of the curves). The flat line portion of the curves indicates total nitrogen deposition corresponding to the  $CL_{min}(N)$  (nitrogen absorbed by nitrogen sinks within the system).

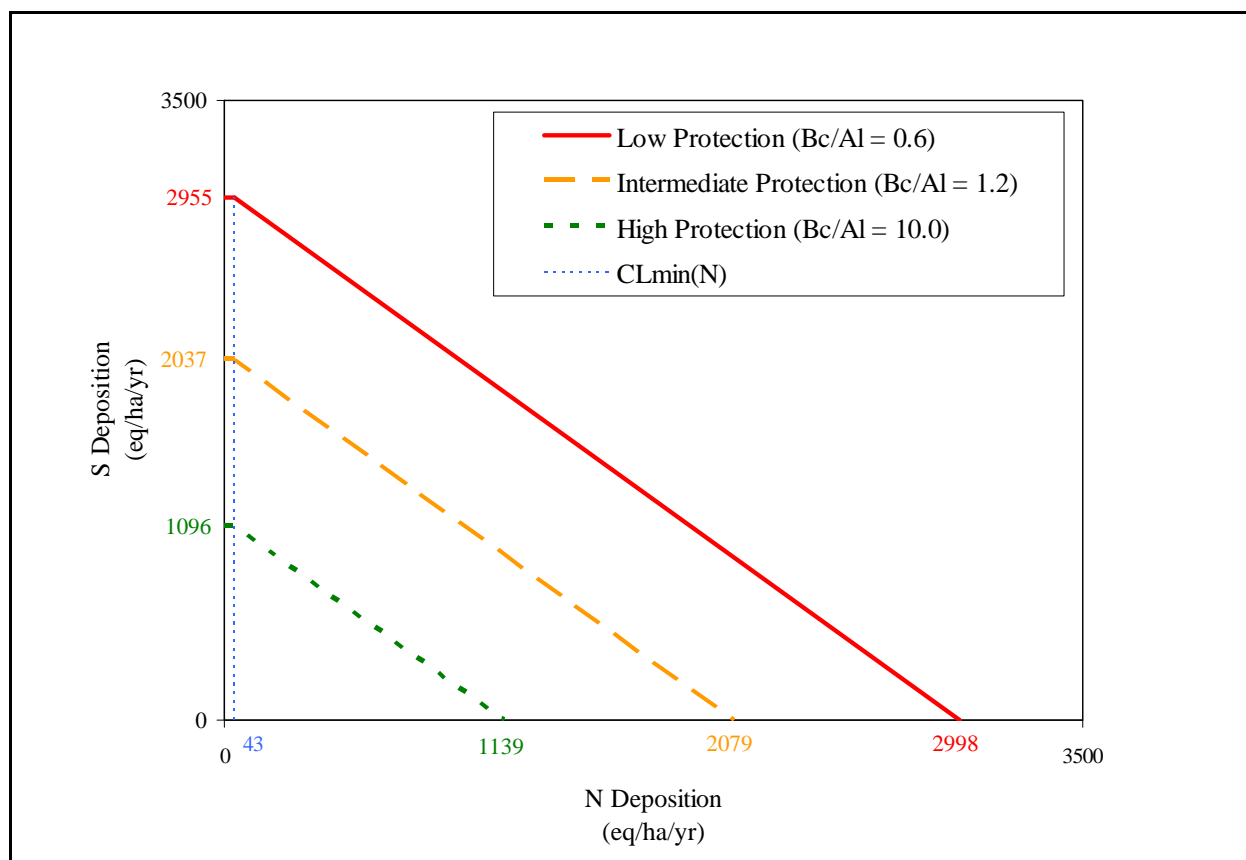


**Figure 3.1-2.** The critical load function response curves detailing the highest critical load estimates for Plot 1 of the Kane Experimental Forest (refer to **Table 3.1-1** for the parameters corresponding to each of the curves). The flat line portion of the curves indicates total nitrogen deposition corresponding to the  $CL_{min}(N)$  (nitrogen absorbed by nitrogen sinks within the system).

The critical loads calculated for the KEF Case Study Area are consistent with critical loads determined by other studies conducted on forests in the Allegheny Plateau. McNulty et al. (2007), in their evaluation of critical loads across the United States, calculated loads of 1,061 to 1,146 eq/ha/yr, corresponding to the location of the seven case study plots in KEF (**Table 3.1-9**). These values are very similar to the ranges (910 to 1,139 eq/ha/yr) determined in this case study, using similar parameter values. McNulty et al. (2007) used the SMB model to calculate critical load, the clay-substrate method to estimate  $BC_w$  and the indicator value of 10.0 for  $(B_c/A_l)_{crit}$  for hardwood tree species. It is not known which  $K_{gibb}$  constant was used or if nutrient uptake and removal ( $B_{c_u}$  and  $N_u$  greater than 0 eq/ha/yr) was included in their calculations.

**Table 3.1-9.** Comparison of the Critical Load Values Determined in This Case Study and the Critical Load Values Determined by McNulty et al. (2007) for the Seven Plots in the Kane Experimental Forest Case Study Area

Case Study Plot	Critical Load (eq/ha/yr)		
	Case Study*		McNulty et al. (2007)
	Nutrient Uptake ( $Bc_u$ and $N_u$ ) NOT Included	Nutrient Uptake ( $Bc_u$ and $N_u$ ) Included	
1	1,139	960	1,146
2	1,032	910	1,144
3	1,071	983	1,061
4	1,032	990	1,061
5	1,139	1,118	1,061
6	1,032	946	1,061
7	1,032	981	1,064

\* The case study values in this table are those calculated with  $K_{gibb} = 300 \text{ m}^6/\text{eq}^2$  and  $(Bc/Al)_{crit} = 10.0$ , and the clay-substrate method to estimate base cation weathering.

### 3.1.2 Red Spruce

The estimates of critical loads of acidity for red spruce in the HBEF Case Study Area are presented in **Table 3.1-10**. The critical load estimates for this case study area were lower than those for KEF, and ranged from 391 eq/ha/yr to 2,568 eq/ha/yr of combined total nitrogen and sulfur deposition ( $(N+S)_{comb}$ ). Similar to the KEF Case Study Area, the ranges of critical loads associated with the three  $(Bc/Al)_{crit}$  ratios differed by level of protection to tree health. The least stringent, least protective level,  $(Bc/Al)_{crit}$  ratio = 0.6, had the highest critical loads that ranged from 991 eq/ha/yr to 2,568 eq/ha/yr of  $(N+S)_{comb}$ . The intermediate level of protection,  $(Bc/Al)_{crit}$  ratio = 1.2, had critical loads ranging from 697 eq/ha/yr to 1,801 eq/ha/yr. The  $(Bc/Al)_{crit}$  ratio of 10.0, corresponding to the most stringent, most protective level for tree protection, had critical load values ranging from 391 eq/ha/yr to 987 eq/ha/yr of  $(N+S)_{comb}$ . The  $K_{gibb}$  and method to calculate  $BC_w$  also influenced the critical load estimates for the HBEF Case Study Area, with the  $K_{gibb}$  value of  $300 \text{ m}^6/\text{eq}^2$  resulting in higher critical load values than  $3000 \text{ m}^6/\text{eq}^2$ . In contrast, the soil type–texture approximation method to estimate  $BC_w$  caused higher critical load values in the HBEF Case Study Area. These trends in the results were largely due to the relatively low clay and organic matter concentrations in the soils in HBEF Case Study Area compared to the

KEF Case Study Area; this lower clay content resulted in much lower  $BC_w$  rates using the clay-substrate compared to soil type–texture method.

**Table 3.1-10.** Critical Load Calculated with the Different Base Cation Weathering and Gibbsite Equilibrium Constant ( $K_{gibb}$ ) Parameter Values in the Hubbard Brook Experimental Forest Case Study Area

$(Bc/Al)_{crit}$ Ratio	Critical Load (eq/ha/yr)			
	Clay-Substrate Method		Soil Type–Texture Approximation Method	
	$K_{gibb} = 300 \text{ m}^6/\text{eq}^2$	$K_{gibb} = 3,000 \text{ m}^6/\text{eq}^2$	$K_{gibb} = 300 \text{ m}^6/\text{eq}^2$	$K_{gibb} = 3,000 \text{ m}^6/\text{eq}^2$
<b>0.6</b>	1,237	991	2,568	2,232
<b>1.2</b>	892	697	1,801	1,534
<b>10.0</b>	487	391	987	856

Two series of CLF response curves that indicate the combined total nitrogen and sulfur deposition ( $(N+S)_{comb}$ ) levels for the three  $(Bc/Al)_{crit}$  ratios (i.e., 0.6, 1.2, and 10.0) for the HBEF Case Study Area are shown in **Figures 3.1-3 and 3.1-4**. These two sets of critical load estimates were selected to provide an indication of the range of critical loads associated with the three levels of protection for red spruce health in the HBEF Case Study Area.

**Figure 3.1-3** shows the CLF response curves corresponding to the lowest critical loads. This scenario occurred with the  $BC_w$  calculated using the clay-substrate method and the  $300 \text{ m}^6/\text{eq}^2$   $K_{gibb}$  constant. **Figure 3.1-4** shows the CLF response curves associated with the highest critical load estimates in the HBEF Case Study Area. These estimates were calculated with  $BC_w$  estimated using the soil type–texture approximation method and the  $3,000 \text{ m}^6/\text{eq}^2$   $K_{gibb}$  constant.

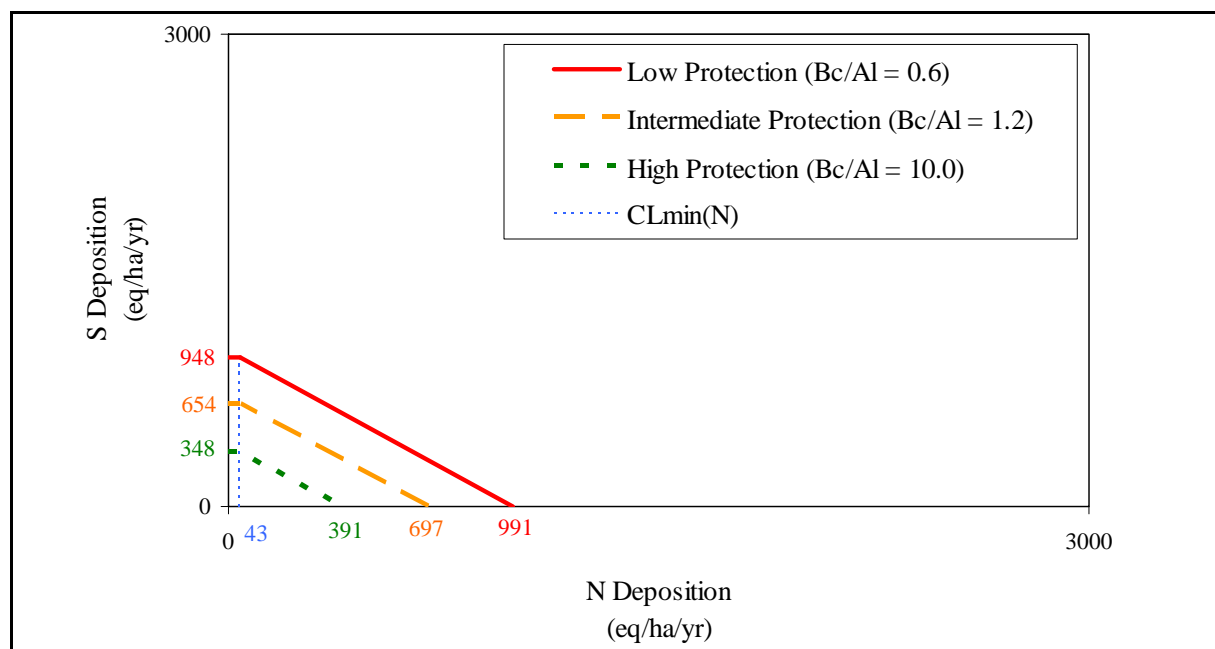


**Figure 3.1-3.** The critical load function response curves detailing the lowest critical load estimates for the Hubbard Brook Experimental Forest Case Study Area (refer to **Table 3.1-10** for the parameters corresponding to each of the curves). The flat line portion of the curves indicates total nitrogen deposition corresponding to the  $CL_{min}(N)$  (nitrogen absorbed by nitrogen sinks within the system).

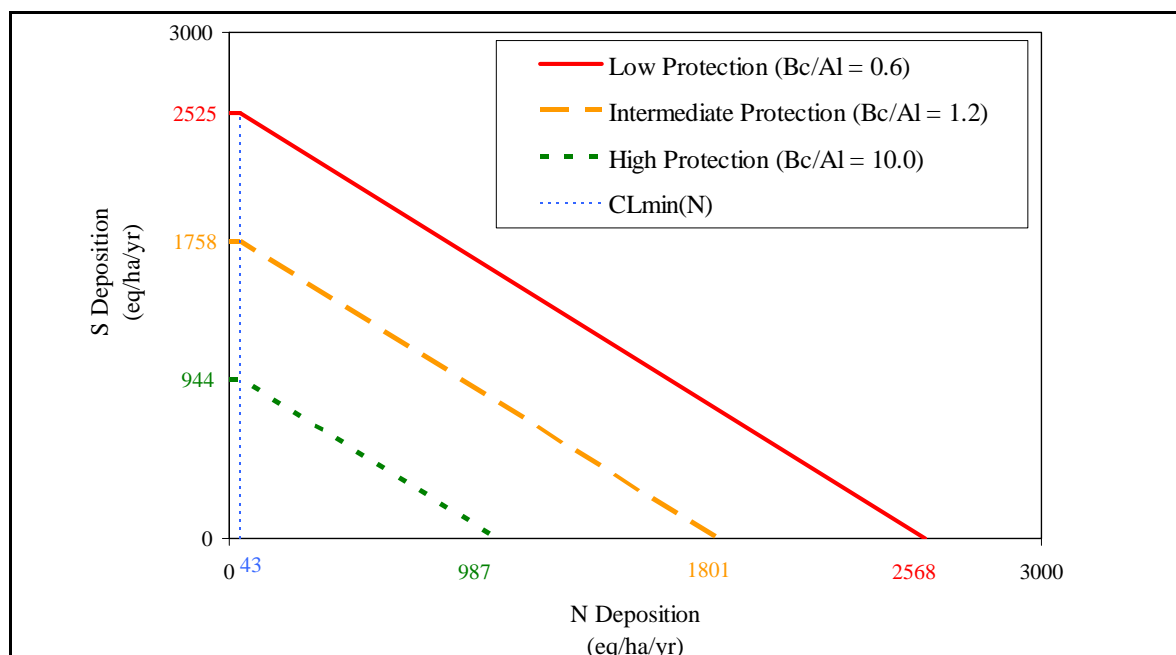


**Figure 3.1-4.** The critical load function response curves detailing the highest critical load estimates for the Hubbard Brook Experimental Forest Case Study Area (refer to **Table 3.1-10** for the parameters corresponding to each of the curves). The flat line portion of the curves indicates total nitrogen deposition corresponding to the  $CL_{min}(N)$  (nitrogen absorbed by nitrogen sinks within the system).



The HBEF Case Study Area has been the site of extensive research, and several studies have estimated critical loads of acidity for the experimental forest (**Table 3.1-11**). Using the SMB model and parameter values similar or equivalent to those used in this case study, McNulty et al. (2007) calculated a critical load of 516 eq/ha/yr for the location of the case study plot. The NEG/ECP Forest Mapping Group (2005) that conducted a detailed assessment of critical loads in several of the northeastern states and the eastern provinces of Canada determined critical load values around 1,500 eq/ha/yr for the area of the case study plot in HBEF (NEG/ECP Forest Mapping Group, 2005). This group used a modified version of the SMB model to estimate critical loads. Pardo and Driscoll (1996) also calculated critical loads for the HBEF. They evaluated four charge- and mass-balance models (steady-state water chemistry, nitrogen mass balance, base cation mass balance, and steady-state mass balance models) over three different time periods (between 1965 and 1988) and found values ranging from -433 to 1,452 eq/ha/yr (negative values are equal to 0 eq/ha/yr). Therefore, the critical load values of 391 to 2,181 eq/ha/yr calculated in this case study are consistent with those from earlier studies that used similar and different methods or models to estimate critical loads. The higher estimates (i.e., 2,568 eq/ha/yr) in this case study can be attributed to the soil type–texture approximation method of calculating  $BC_w$  and the lowest  $(Bc/Al)_{crit}$  (0.6) value.

**Table 3.1-11.** Summary of the Critical Load Values Determined by Other Studies Conducted in the Hubbard Brook Experimental Forest (negative values are equal to 0 eq/ha/yr)

Critical Load Model Used for Estimation	Critical Load Values for Each Study (eq/ha/yr)			
	Pardo and Driscoll (1996)	McNulty et al. (2007)	NEG/ECP Forest Mapping Group (2005)	Case Study
Simple Mass Balance	–	516	~1,500	391 to 2,568
Steady-State Water Chemistry	–4 to 11	–	–	–
Nitrogen Mass Balance	133 to 1,452	–	–	–
Basic Cation Mass Balance	62 to 133	–	–	–
Modified Basic Cation Mass Balance	0 to 1,405	–	–	–
Steady-State Balance	–433 to 630	–	–	–

**Source:** Pardo and Driscoll, 1996.

### 3.2 RECOMMENDED PARAMETER VALUES AND CRITICAL LOADS

Within the ranges of critical loads estimated for the KEF and HBEF case study areas, three critical loads were selected to represent the conditions associated with the three levels of protection ( $Bc/Al_{(crit)} = 0.6, 1.2, \text{ and } 10.0$ ) for sugar maple in KEF and for red spruce in HBEF (**Table 3.2-1**). For the KEF Case Study Area, these critical load values, in order of lowest to highest level of protection were 2,009, 1,481 and 910 eq/ha/yr (for  $Bc/Al_{(crit)} = 0.6, 1.2, \text{ and } 10.0$ , respectively). For the HBEF Case Study Area, these values, in order of lowest to highest level of protection, were 1,237, 892, and 487 eq/ha/yr (for  $Bc/Al_{(crit)} = 0.6, 1.2, \text{ and } 10.0$ , respectively).

These critical load estimates were derived using the clay-substrate method to estimate  $BC_w$  and a  $K_{gibb}$  of  $300 \text{ m}^6/\text{eq}^2$ . For the KEF Case Study Area, nutrient uptake and removal with tree harvest ( $Bc_u$  and  $N_u$ ) was also included in the critical load estimates, and within the constraints of the selected parameters, the plot with the most conservative (i.e., lowest critical load) was selected to represent the full KEF Case Study Area. The parameter values were set to 0 eq/ha/yr in the HBEF Case Study Area because the study plots in this experimental forest are not actively managed or harvested. The selection of these parameters and methods was based on the best available recommendations of scientists and research efforts, to date. When field assessments and measurements are not possible, the clay-substrate method is one of the most commonly used methods to estimate base cation weathering in North America (Ouimet et al., 2006; Watmough et al., 2006; McNulty et al., 2007; Pardo and Duarte 2007), and the  $300 \text{ m}^6/\text{eq}^2$  value of the  $K_{gibb}$  is a recommended default value (UNECE, 2004). For the KEF Case Study Area, the influence of nutrient uptake and removal (i.e.,  $Bc_u$  and  $N_u$  greater than 0 eq/ha/yr) was included because the forest has been and will likely continue to be actively harvested (USFS, 1999).

**Table 3.2-1.** Critical Loads Selected to Represent the Three Levels of Protection in the Kane Experimental Forest and Hubbard Brook Experimental Forest Case Study Areas

Protection Level ( $Bc/Al_{(crit)}$ ratio)	Critical Load Values for Each Case Study Area (eq/ha/yr)	
	KEF	HBEF
Low ( $Bc/Al_{(crit)} = 0.6$ )	2,009	1,237
Medium ( $Bc/Al_{(crit)} = 1.2$ )	1,481	892
High ( $Bc/Al_{(crit)} = 10.0$ )	910	487

### 3.3 CURRENT CONDITIONS

This section discusses the impact of the 2002 CMAQ/NADP total nitrogen and sulfur deposition levels relative to the critical loads estimated for the KEF and HBEF case study areas. The atmospheric deposition of total nitrogen and sulfur ( $(N+S)_{\text{comb}}$ ) in both the HBEF and KEF case study areas was elevated. According to 2002 CMAQ output, the KEF Case Study Area received 13.6 kilograms (kg) N/ha (967.5 eq/ha) and 20.7 kg S/ha (646.4 eq/ha), and the HBEF Case Study Area experienced 8.4 kg N/ha (601.1 eq/ha) and 7.5 kg S/ha (233.1 eq/ha). When these deposition levels were compared to the critical loads calculated using the three  $(Bc/Al)_{\text{crit}}$  ratio values, the CMAQ-modeled  $(N+S)_{\text{comb}}$  deposition loads were found to be both greater than and less than the three critical loads for the two case study areas (**Tables 3.3-1 to 3.3-9, Figures 3.3-1 to 3.3-4**). In all plots of the KEF Case Study Area, the 2002 CMAQ/NADP total nitrogen and sulfur deposition levels ( $(N+S)_{\text{comb}}$ ) were greater than the range of total nitrogen and sulfur allowable for the most stringent critical load (where  $(Bc/Al)_{\text{crit}} = 10.0$ ). Similarly, in the HBEF Case Study Area, the modeled  $(N+S)_{\text{comb}}$  deposition was greater than the critical loads estimated using the  $(Bc/Al)_{\text{crit}} = 10.0$  ratio and the clay-substrate method to estimate  $BC_w$ . However, combined 2002 CMAQ/NADP total nitrogen and sulfur deposition levels were less than the critical loads estimated with  $(Bc/Al)_{\text{crit}} = 10.0$  and  $BC_w$  determined by the soil type–texture approximation. The 2002 CMAQ/NADP total nitrogen and sulfur deposition levels ( $(N+S)_{\text{comb}}$ ) were less than the ranges of total nitrogen and sulfur allowable for the least stringent critical load (where  $(Bc/Al)_{\text{crit}} = 0.6$ ) for both the HBEF Case Study Area and all plots of the KEF Case Study Area. The only exception to this trend was in Plot 1 of the KEF Case Study Area, where the removal of base cations and nitrogen with harvesting ( $Bc_u$  and  $N_u$  greater than 0 eq/ha/yr) were included in the load calculations. The variability in the results comparing 2002 CMAQ/NADP total nitrogen and sulfur deposition levels to calculated acid loads shows the strong influence of the  $Bc/Al_{(\text{crit})}$  indicator ratio (reflecting the level of tree protection) in critical load estimates.

**Table 3.3-1.** Ranges of Differences between the 2002 CMAQ/NADP Total Nitrogen and Sulfur Deposition Levels ((N+S)<sub>comb</sub>) and the Estimated Critical Load Values (with and without the Influence of Nutrient Uptake and Removal [N<sub>u</sub> and Bc<sub>u</sub>]) for the Seven Plots of the Kane Experimental Forest Case Study Area

Nutrient Uptake in Critical Load Estimate	(Bc/Al) <sub>crit</sub> Ratio	Difference between CMAQ/NADP (N+S) <sub>comb</sub> Deposition and Estimated Critical Loads (eq/ha/yr)						
		Plot 1	Plot 2	Plot 3	Plot 4	Plot 5	Plot 6	Plot 7
<i>Bc<sub>u</sub> and N<sub>u</sub> NOT Included</i>	<b>0.6</b>	-1,384 to -714	-1,098 to -714	-1,203 to -714	-1,098 to -714	-1,384 to -714	-1,098 to -714	1,098 to -714
	<b>1.2</b>	-465 to 23*	-271 to 23*	-343 to 23*	-271 to 23*	-465 to 23*	-271 to 23*	-271 to 23*
	<b>10.0</b>	475* to 731*	582* to 731*	543* to 731*	582* to 731*	475* to 731*	582* to 731*	582* to 731*
<i>Bc<sub>u</sub> and N<sub>u</sub> Included</i>	<b>0.6</b>	-327 to 282*	-395 to -59	-614 to -162	-774 to -411	-931 to -289	-598 to -247	-755 to -393
	<b>1.2</b>	141* to 581*	132* to 391*	-12 to 326*	-93 to 185*	-235 to 231*	15* to 285*	-79 to 199*
	<b>10.0</b>	654* to 886*	704* to 835*	631* to 805*	624* to 764*	496* to 741*	668* to 804*	633* to 774*

\* Indicates a positive value or deposition greater than the critical load based on CMAQ-modeled 2002 (N+S)<sub>comb</sub> deposition.

**Table 3.3-2.** Differences between the 2002 CMAQ/NADP Total Nitrogen and Sulfur Deposition Levels ((N+S)<sub>comb</sub>) and the Critical Load Values (with Two Base Cation Weathering Estimation Methods, Two Gibbsite Equilibrium Constants [*K*<sub>gibb</sub>], and Two Base Cation (Bc<sub>u</sub>) and Nitrogen (N<sub>u</sub>) Uptake Parameter Values) in Plot 1 of the Kane Experimental Forest Case Study Area

Nutrient Uptake in Critical Load Estimate	(Bc/Al) <sub>crit</sub> Ratio	Difference between CMAQ/NADP (N+S) <sub>comb</sub> Deposition and Estimated Critical Deposition Loads (eq/ha/yr)			
		Clay-Substrate Method		Soil Type-Texture Approximation Method	
		<i>K</i> <sub>gibb</sub> = 300	<i>K</i> <sub>gibb</sub> = 3,000	<i>K</i> <sub>gibb</sub> = 300	<i>K</i> <sub>gibb</sub> = 3,000
<i>Bc<sub>u</sub> and N<sub>u</sub> NOT Included</i>	<b>0.6</b>	-1,384	-1,064	-1,019	-714
	<b>1.2</b>	-465	-211	-218	23*
	<b>10.0</b>	475*	600*	612*	731*
<i>Bc<sub>u</sub> and N<sub>u</sub> Included</i>	<b>0.6</b>	-327	-78	61*	282*
	<b>1.2</b>	141*	338*	406*	581*
	<b>10.0</b>	654*	751*	800*	886*

\* Indicates a positive value or deposition greater than the critical load based on CMAQ-modeled 2002 (N+S)<sub>comb</sub> deposition.

**Table 3.3-3.** Differences between the 2002 CMAQ/NADP Total Nitrogen and Sulfur Deposition Levels ((N+S)<sub>comb</sub>) and the Critical Load Values (with Two Base Cation Weathering Estimation Methods, Two Gibbsite Equilibrium Constants [ $K_{gibb}$ ], and Two Base Cation ( $Bc_u$ ) and Nitrogen ( $N_u$ ) Uptake Parameter Values) in Plot 2 of the Kane Experimental Forest Case Study Area

Nutrient Uptake in Critical Load Estimate	(Bc/Al) <sub>crit</sub> Ratio	Difference between CMAQ/NADP (N+S) <sub>comb</sub> Deposition and Estimated Critical Loads (eq/ha/yr)			
		Clay-Substrate Method		Soil Type–Texture Approximation Method	
		$K_{gibb} = 300$	$K_{gibb} = 3,000$	$K_{gibb} = 300$	$K_{gibb} = 3,000$
<i>Bc<sub>u</sub> and N<sub>u</sub> NOT Included</i>	0.6	–1,098	–789	–1,019	–714
	1.2	–271	–27	–218	23*
	10.0	582*	703*	612*	731*
<i>Bc<sub>u</sub> and N<sub>u</sub> Included</i>	0.6	–395	–135	–314	–59
	1.2	132*	339*	188*	391*
	10.0	704*	806*	735*	835*

\* Indicates a positive value or deposition greater than the critical load based on CMAQ-modeled 2002 (N+S)<sub>comb</sub> deposition.

**Table 3.3-4.** Differences between the 2002 CMAQ/NADP Total Nitrogen and Sulfur Deposition Levels ((N+S)<sub>comb</sub>) and the Critical Load Values (with Two Base Cation Weathering Estimation Methods, Two Gibbsite Equilibrium Constants [ $K_{gibb}$ ], and Two Base Cation ( $Bc_u$ ) and Nitrogen ( $N_u$ ) Uptake Parameter Values) in Plot 3 of the Kane Experimental Forest Case Study Area

Nutrient Uptake in Critical Load Estimate	(Bc/Al) <sub>crit</sub> Ratio	Difference between CMAQ/NADP (N+S) <sub>comb</sub> Deposition and Estimated Critical Loads (eq/ha/yr)			
		Clay-Substrate Method		Soil Type–Texture Approximation Method	
		$K_{gibb} = 300$ m <sup>6</sup> /eq <sup>2</sup>	$K_{gibb} = 3,000$ m <sup>6</sup> /eq <sup>2</sup>	$K_{gibb} = 300$ m <sup>6</sup> /eq <sup>2</sup>	$K_{gibb} = 3,000$ m <sup>6</sup> /eq <sup>2</sup>
<i>Bc<sub>u</sub> and N<sub>u</sub> NOT Included</i>	0.6	–1,203	–890	–1,019	–714
	1.2	–343	–95	–218	23*
	10.0	543*	665*	612*	731*
<i>Bc<sub>u</sub> and N<sub>u</sub> Included</i>	0.6	–614	–340	–425	–162
	1.2	–12	206*	117*	326*
	10.0	631*	738*	702*	805*

\* Indicates a positive value or deposition greater than the critical load based on CMAQ-modeled 2002 (N+S)<sub>comb</sub> deposition.

**Table 3.3-5.** Differences between the 2002 CMAQ/NADP Total Nitrogen and Sulfur Deposition Levels ((N+S)<sub>comb</sub>) and the Critical Load Values (with Two Base Cation Weathering Estimation Methods, Two Gibbsite Equilibrium Constants [ $K_{gibb}$ ], and Two Base Cation ( $Bc_u$ ) and Nitrogen ( $N_u$ ) Uptake Parameter Values) in Plot 4 of the Kane Experimental Forest Case Study Area

Nutrient Uptake in Critical Load Estimate	(Bc/Al) <sub>crit</sub> Ratio	Difference between CMAQ/NADP (N+S) <sub>comb</sub> Deposition and Estimated Critical Loads (eq/ha/yr)			
		Clay-Substrate Method		Soil Type–Texture Approximation Method	
		$K_{gibb} = 300$ m <sup>6</sup> /eq <sup>2</sup>	$K_{gibb} = 3,000$ m <sup>6</sup> /eq <sup>2</sup>	$K_{gibb} = 300$ m <sup>6</sup> /eq <sup>2</sup>	$K_{gibb} = 3,000$ m <sup>6</sup> /eq <sup>2</sup>
$Bc_u$ and $N_u$ <b>NOT Included</b>	<b>0.6</b>	–1,098	–789	–1,019	–714
	<b>1.2</b>	–271	–27	–218	23*
	<b>10.0</b>	582*	703*	612*	731*
$Bc_u$ and $N_u$ <b>Included</b>	<b>0.6</b>	–774	–487	–694	–411
	<b>1.2</b>	–93	134*	–39	185*
	<b>10.0</b>	624*	736*	654*	764*

\* Indicates a positive value or deposition greater than the critical load based on CMAQ-modeled 2002 (N+S)<sub>comb</sub> deposition.

**Table 3.3-6.** Differences between the 2002 CMAQ/NADP Total Nitrogen and Sulfur Deposition Levels ((N+S)<sub>comb</sub>) and the Critical Load Values (with Two Base Cation Weathering Estimation Methods, Two Gibbsite Equilibrium Constants [ $K_{gibb}$ ], and Two Base Cation ( $Bc_u$ ) and Nitrogen ( $N_u$ ) Uptake Parameter Values) in Plot 5 of the Kane Experimental Forest Case Study Area

Nutrient Uptake in Critical Load Estimate	(Bc/Al) <sub>crit</sub> Ratio	Difference between CMAQ/NADP (N+S) <sub>comb</sub> Deposition and Estimated Critical Loads (eq/ha/yr)			
		Clay-Substrate Method		Soil Type–Texture Approximation Method	
		$K_{gibb} = 300$ m <sup>6</sup> /eq <sup>2</sup>	$K_{gibb} = 3,000$ m <sup>6</sup> /eq <sup>2</sup>	$K_{gibb} = 300$ m <sup>6</sup> /eq <sup>2</sup>	$K_{gibb} = 3,000$ m <sup>6</sup> /eq <sup>2</sup>
$Bc_u$ and $N_u$ <b>NOT Included</b>	<b>0.6</b>	–1,384	–1,064	–1,019	–714
	<b>1.2</b>	–465	–211	–218	23*
	<b>10.0</b>	475*	600*	612*	731*
$Bc_u$ and $N_u$ <b>Included</b>	<b>0.6</b>	–931	–642	–559	–289
	<b>1.2</b>	–235	–6	18*	231*
	<b>10.0</b>	496*	609*	636*	741*

\* Indicates a positive value or deposition greater than the critical load based on CMAQ-modeled 2002 (N+S)<sub>comb</sub> deposition.

**Table 3.3-7.** Differences between the 2002 CMAQ/NADP Total Nitrogen and Sulfur Deposition Levels ((N+S)<sub>comb</sub>) and the Critical Load Values (with Two Base Cation Weathering Estimation Methods, Two Gibbsite Equilibrium Constants [ $K_{gibb}$ ], and Two Base Cation ( $Bc_u$ ) and Nitrogen ( $N_u$ ) Uptake Parameter Values) in Plot 6 of the Kane Experimental Forest Case Study Area

Nutrient Uptake in Critical Load Estimate	(Bc/Al) <sub>crit</sub> Ratio	Difference between CMAQ/NADP (N+S) <sub>comb</sub> Deposition and Estimated Critical Loads (eq/ha/yr)			
		Clay-Substrate Method		Soil Type–Texture Approximation Method	
		$K_{gibb} = 300$ m <sup>6</sup> /eq <sup>2</sup>	$K_{gibb} = 3,000$ m <sup>6</sup> /eq <sup>2</sup>	$K_{gibb} = 300$ m <sup>6</sup> /eq <sup>2</sup>	$K_{gibb} = 3,000$ m <sup>6</sup> /eq <sup>2</sup>
<i>Bc<sub>u</sub> and N<sub>u</sub> NOT Included</i>	0.6	–1,098	–789	–1,019	–714
	1.2	–271	–27	–218	23*
	10.0	582*	703*	612*	731*
<i>Bc<sub>u</sub> and N<sub>u</sub> Included</i>	0.6	–598	–322	–518	–247
	1.2	15*	234*	69*	285*
	10.0	668*	776*	698*	804*

\* Indicates a positive value or deposition greater than the critical load based on CMAQ-modeled 2002 (N+S)<sub>comb</sub> deposition.

**Table 3.3-8.** Differences between the 2002 CMAQ/NADP Total Nitrogen and Sulfur Deposition Levels ((N+S)<sub>comb</sub>) and the Critical Load Values (with Two Base Cation Weathering Estimation Methods, Two Gibbsite Equilibrium Constants [ $K_{gibb}$ ], and Two Base Cation ( $Bc_u$ ) and Nitrogen ( $N_u$ ) Uptake Parameter Values) in Plot 7 of the Kane Experimental Forest Case Study Area

Nutrient Uptake in Critical Load Estimate	(Bc/Al) <sub>crit</sub> Ratio	Difference between CMAQ/NADP (N+S) <sub>comb</sub> Deposition and Estimated Critical Loads (eq/ha/yr)			
		Clay-Substrate Method		Soil Type–Texture Approximation Method	
		$K_{gibb} = 300$ m <sup>6</sup> /eq <sup>2</sup>	$K_{gibb} = 3,000$ m <sup>6</sup> /eq <sup>2</sup>	$K_{gibb} = 300$ m <sup>6</sup> /eq <sup>2</sup>	$K_{gibb} = 3,000$ m <sup>6</sup> /eq <sup>2</sup>
<i>Bc<sub>u</sub> and N<sub>u</sub> NOT Included</i>	0.6	–1,098	–789	–1,019	–714
	1.2	–271	–27	–218	23*
	10.0	582*	703*	612*	731*
<i>Bc<sub>u</sub> and N<sub>u</sub> Included</i>	0.6	–755	–469	–675	–393
	1.2	–79	148*	–25	199*
	10.0	633*	745*	663*	774*

\* Indicates a positive value or deposition greater than the critical load based on CMAQ-modeled 2002 (N+S)<sub>comb</sub> deposition.

**Table 3.3-9.** Differences between the 2002 CMAQ/NADP Total Nitrogen and Sulfur Deposition Levels ( $(N+S)_{\text{comb}}$ ) and the Critical Load Values (with Two Base Cation Weathering Estimation Methods and Two Gibbsite Equilibrium Constants [ $K_{\text{gibb}}$ ]) in the Hubbard Brook Experimental Forest Case Study Area

$(\text{Bc}/\text{Al})_{\text{crit}}$ Ratio	Difference between CMAQ/NADP $(N+S)_{\text{comb}}$ Deposition and Estimated Critical Loads (eq/ha/yr)			
	Clay-Substrate Method		Soil Type–Texture Approximation Method	
	$K_{\text{gibb}} = 300 \text{ m}^6/\text{eq}^2$	$K_{\text{gibb}} = 3,000 \text{ m}^6/\text{eq}^2$	$K_{\text{gibb}} = 300 \text{ m}^6/\text{eq}^2$	$K_{\text{gibb}} = 3,000 \text{ m}^6/\text{eq}^2$
0.6	–403	–157	–1,734	–1,398
1.2	–58	137*	–967	–700
10.0	347*	443*	–153	–21

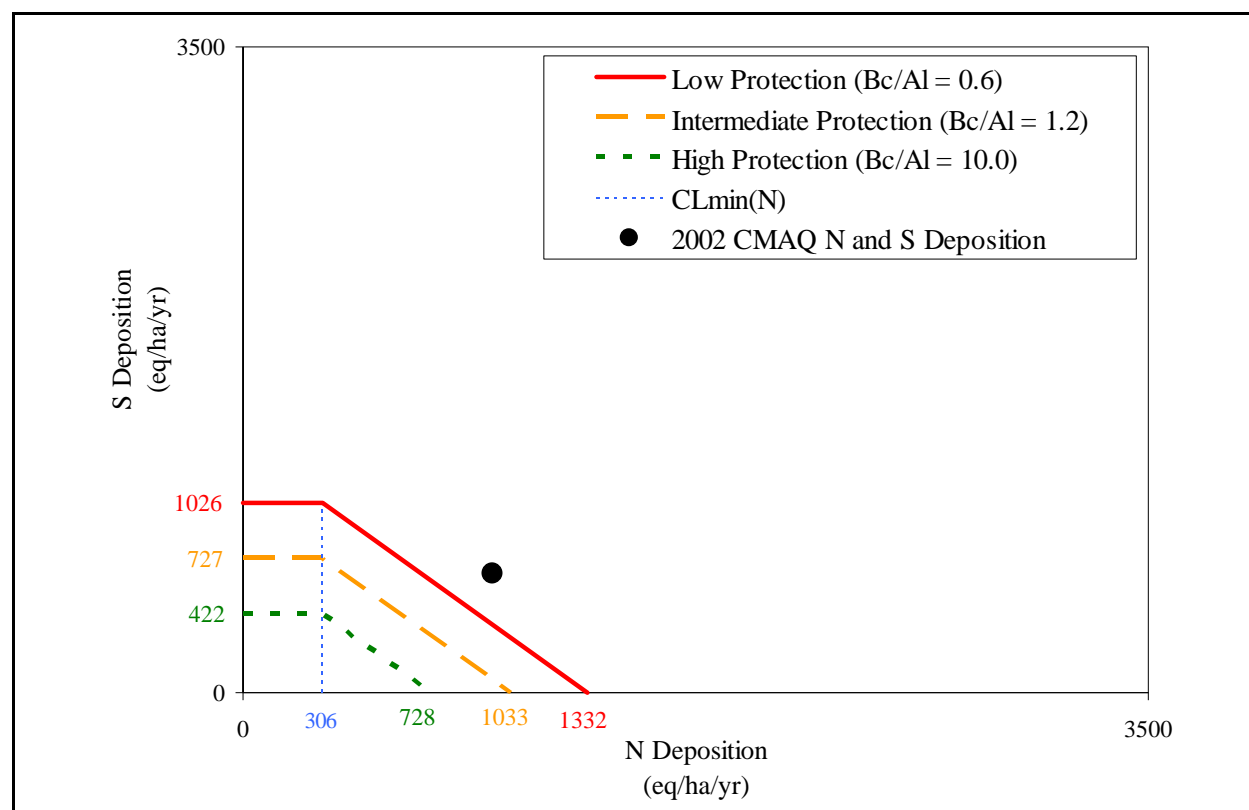


**Figure 3.3-1.** Plot 1 Kane Experimental Forest critical load function response curves, detailing the lowest critical load estimates for Kane Experimental Forest Case Study Area (refer to **Table 3.1-1** for the parameters corresponding to each of the curves). The 2002 CMAQ/NADP total nitrogen and sulfur deposition levels ( $(N+S)_{\text{comb}}$ ) were greater than the critical loads of nitrogen and sulfur at all levels of protection ( $(\text{Bc}/\text{Al})_{\text{crit}} = 0.6, 1.2,$  and  $10.0$ ). The flat line portion of the curves indicates total nitrogen deposition corresponding to the  $\text{CL}_{\text{min}}$  (N) (nitrogen absorbed by nitrogen sinks within the system).



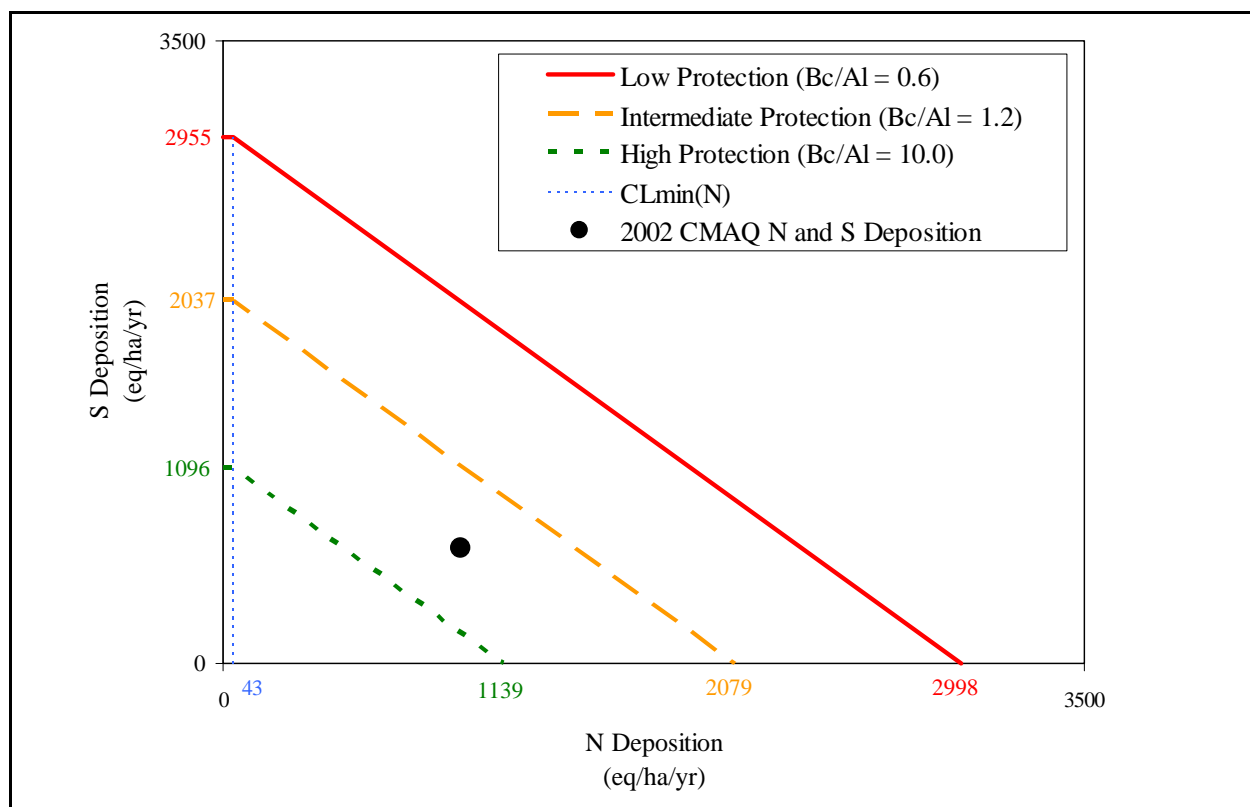


**Figure 3.3-2.** Plot 1 critical load function response curves, detailing the highest maximum deposition load estimates for Kane Experimental Forest Case Study Area (refer to **Table 3.1-1** for the parameters corresponding to each of the curves). The 2002 CMAQ/NADP total nitrogen and sulfur deposition levels  $((N+S)_{\text{comb}})$  were greater than the critical load of total nitrogen and sulfur deposition calculated with the highest level of protection  $(Bc/Al)_{\text{crit}} = 10.0$ . The flat line portion of the curves indicates total nitrogen deposition corresponding to the  $CL_{\text{min}}(N)$  (nitrogen absorbed by nitrogen sinks within the system).

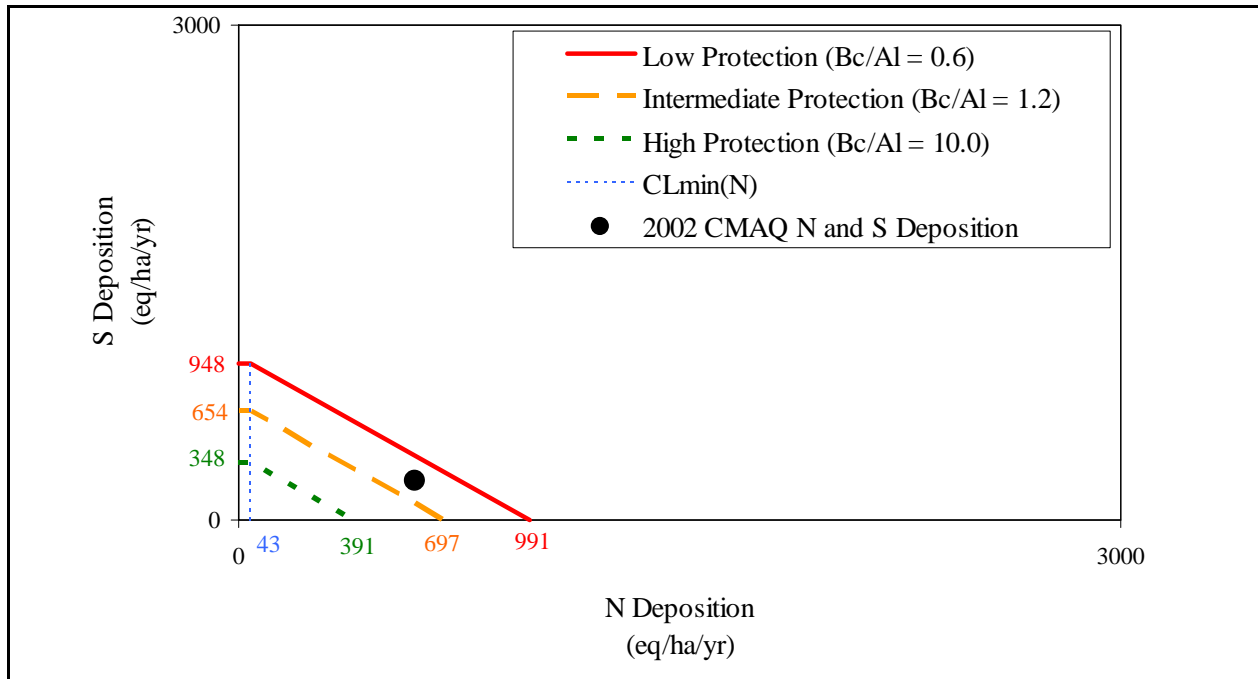


**Figure 3.3-3.** Critical load function response curves, detailing the lowest critical load estimates for the Hubbard Brook Experimental Forest Case Study Area (refer to **Table 3.1-10** for the parameters corresponding to each of the curves). The 2002 CMAQ/NADP total nitrogen and sulfur deposition levels  $((N+S)_{\text{comb}})$  were greater than the critical load of total nitrogen and sulfur calculated with the highest and the intermediate levels of protection  $((Bc/Al)_{\text{crit}} = 1.2 \text{ and } 10.0)$ . The flat line portion of the curves indicates total nitrogen deposition corresponding to the  $CL_{\text{min}}(N)$  (nitrogen absorbed by nitrogen sinks within the system).

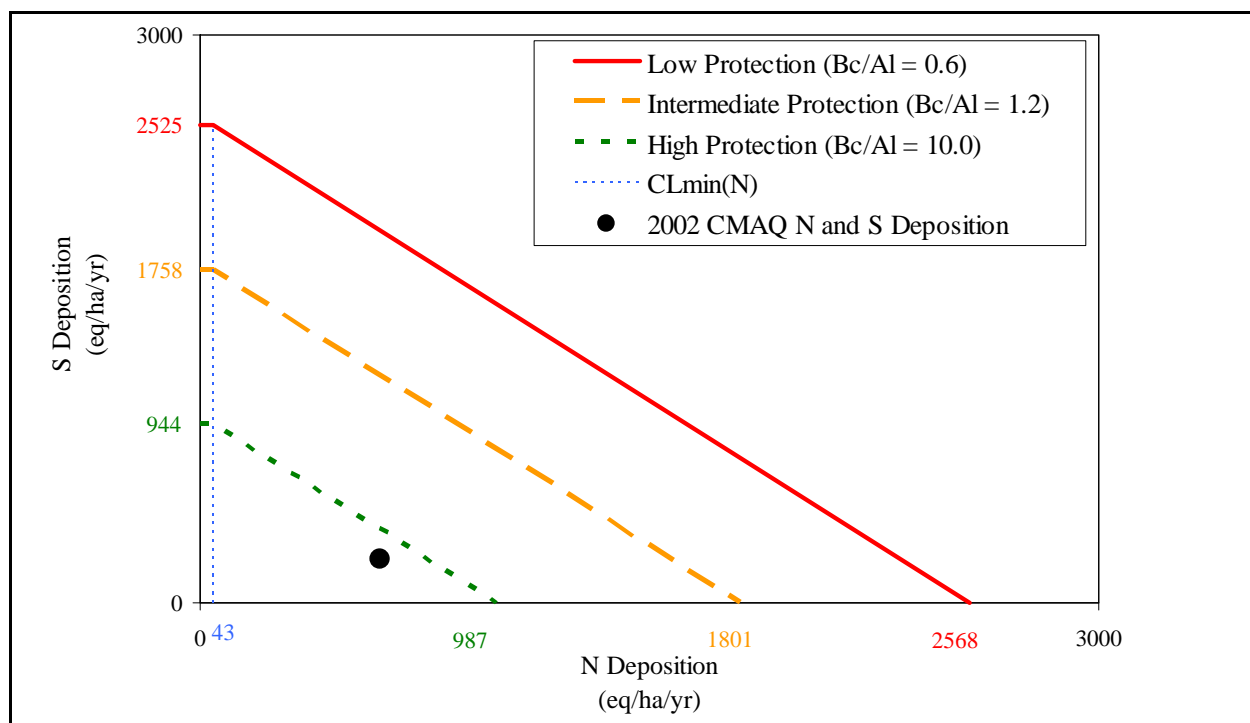


**Figure 3.3-4.** Critical load function response curves, detailing the highest critical load estimates for the Hubbard Brook Experimental Forest Case Study Area (refer to **Table 3.1-10** for the parameters corresponding to each of the curves). The 2002 CMAQ/NADP total nitrogen and sulfur deposition levels ( $(N+S)_{\text{comb}}$ ) were less than the critical loads associated with all three  $(Bc/Al)_{\text{crit}}$  ratios. The flat line portion of the curves indicates total nitrogen deposition corresponding to the  $CL_{\text{min}}(N)$  (nitrogen absorbed by nitrogen sinks within the system).

As outlined in Section 3.2, critical loads of 2,009, 1,481 and 910 eq/ha/yr were selected to represent the three levels of increasing protection for the KEF Case Study Area, and 1,237, 892 and 487 eq/ha/yr were the critical loads selected for the HBEF Case Study Area. These estimates are based on the critical load parameters suggested and most frequently used by scientists and previous research. When compared to the 2002 CMAQ-modeled deposition levels, it was evident that the deposition levels were greater than the most protective critical load ( $Bc/Al_{\text{crit}} = 10.0$ ) for both case study areas and also greater than the intermediate protection critical load ( $Bc/Al_{\text{crit}} = 1.2$ ) for KEF (**Figures 3.3-5 and 3.3-6**). In these comparisons, 2002 CMAQ/NADP total nitrogen and sulfur deposition levels exceeded the KEF Case Study Area critical load by 132 to 704 eq/ha/yr and exceeded the HBEF Case Study Area's critical load by 347 eq/ha/yr. Similar results have been reported in other studies which have assessed the two case study areas. McNulty et al. (2007) and Pardo and Driscoll (1996) found that deposition levels were greater than the estimated critical loads in the HBEF area. McNulty et al. (2007) also

reported that 2002 CMAQ/NADP total nitrogen and sulfur deposition levels in the KEF exceeded the calculated critical loads for the KEF Case Study Area. These results suggest that the health of red spruce at HBEF and sugar maple at KEF may have been compromised by the acidifying nitrogen and sulfur deposition received in 2002.

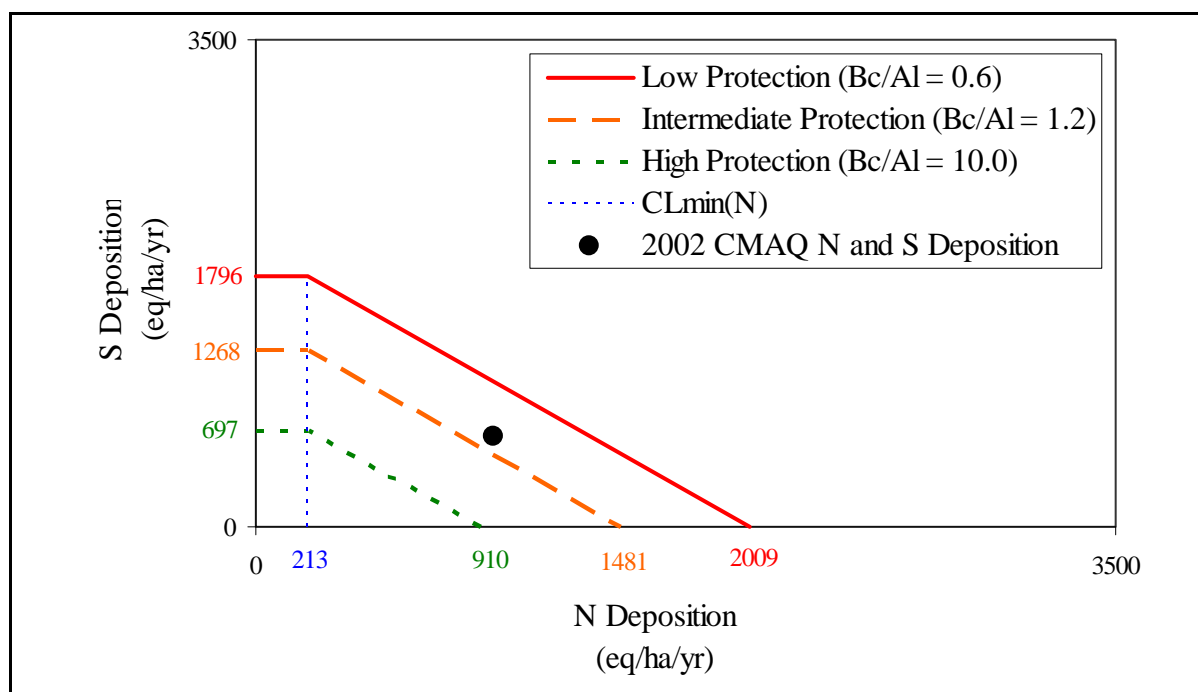


**Figure 3.3-5.** Critical load function response curves for the three selected critical loads conditions (corresponding to the three levels of protection) for the Kane Experimental Forest Case Study Area. The 2002 CMAQ/NADP total nitrogen and sulfur deposition levels  $((N+S)_{comb})$  were greater than the highest and intermediate level of protection critical loads. The flat line portion of the curves indicates total nitrogen deposition corresponding to the  $CL_{min}(N)$  (nitrogen absorbed by nitrogen sinks within the system).

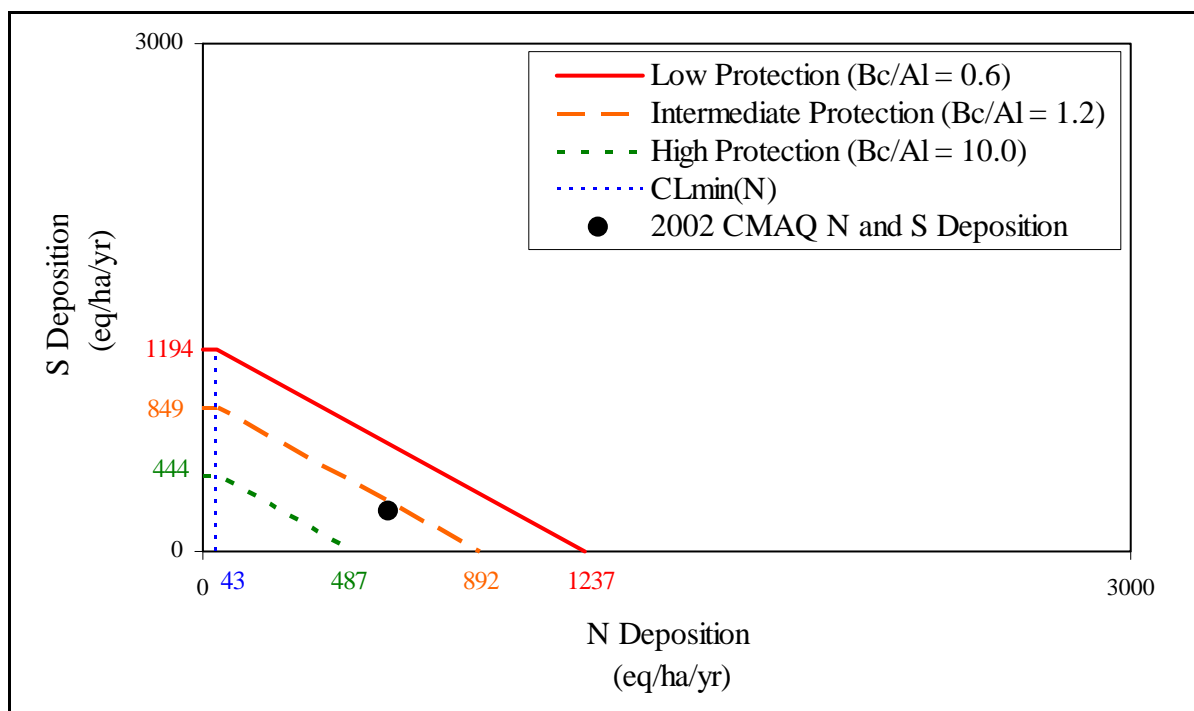


**Figure 3.3-6.** Critical load function response curves for the three selected critical loads conditions (corresponding to the three levels of protection) for the Hubbard Brook Experimental Forest Case Study Area. The 2002 CMAQ/NADP total nitrogen and sulfur deposition levels ((N+S)<sub>comb</sub>) were greater than the highest level of protection critical loads. The flat line portion of the curves indicates total nitrogen deposition corresponding to the CL<sub>min</sub>(N) (nitrogen absorbed by nitrogen sinks within the system).

Acidifying nitrogen deposition consists of both reduced (NH<sub>x</sub>) and oxidized (NO<sub>x</sub>) forms of nitrogen. However, only NO<sub>x</sub> is currently regulated as a criteria pollutant. Therefore, to gain an understanding of the relationship between the two states (i.e., reduced and oxidized) of total nitrogen deposition and the critical loads for the KEF and HBEF case study areas, total nitrogen deposition must be separated into NH<sub>x</sub>-N and NO<sub>x</sub>-N. Examples of the separation of nitrogen species are presented in **Figure 3.3-7** and **Figure 3.3-8** which indicate the CLF response curves for the highest level of protection critical load condition selected for the KEF and HBEF case study areas, respectively. In these relationships, the CLF function has been modified by maintaining NH<sub>x</sub>-N deposition at the 2002 CMAQ-modeled deposition level; only sulfur and NO<sub>x</sub>-N deposition levels vary to indicate the combined critical load. Based on 2002 CMAQ/NADP total nitrogen and sulfur deposition levels, NH<sub>x</sub>-N accounted for 25.7% (249 eq/ha) and 26.4% (159 eq/ha) of total nitrogen deposition in KEF and HBEF case study areas, respectively. These fixed amounts of NH<sub>x</sub>-N influenced the highest protection CLF response

curves for both areas. For both case studies, the maximum sulfur critical load ( $CL_{\max}(S)$ ) and the maximum nitrogen critical load ( $CL_{\max}(N)$ ), as  $NO_x$ , were lowered. In the calculations for the KEF Case Study Area, the  $CL_{\max}(S)$  was reduced by 5% to 661 eq/ha/yr, and in the HBEF Case Study Area calculations, the  $CL_{\max}(S)$  was reduced by 26% to 328 eq/ha/yr. Similarly, the  $CL_{\max}(N)$  (as  $NO_x$ ) for KEF was reduced by 27% to 661 eq/ha/yr, and the  $CL_{\max}(N)$  (as  $NO_x$ ) for HBEF was reduced by 33% to 328 eq/ha/yr.

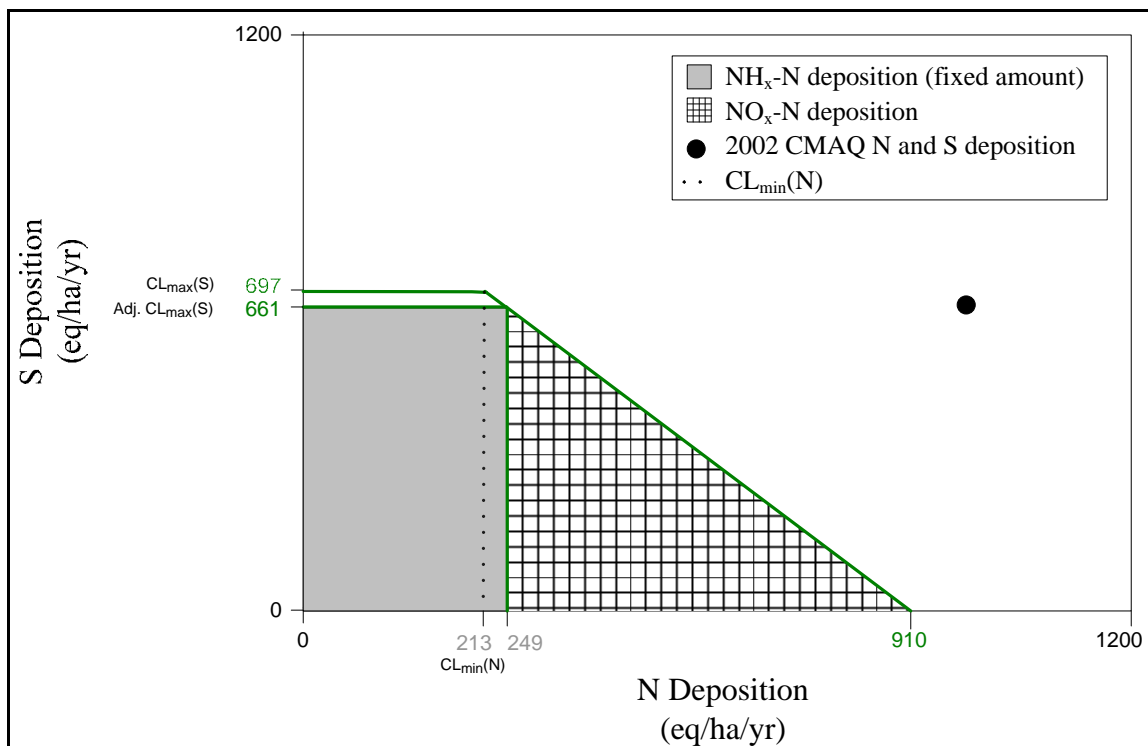


**Figure 3.3-7.** The influence of the 2002 CMAQ/NADP total nitrogen and sulfur deposition levels ( $NH_x-N$ ) on the critical load function response curve, and in turn, the maximum critical loads of sulfur ( $CL_{\max}(S)$ ) and oxidized nitrogen ( $NO_x-N$ ) for the selected highest protection critical load for the Kane Experimental Forest Case Study Area. The critical load of oxidized nitrogen ( $NO_x-N$ ) is 661 eq/ha/yr ( $910 - 249$  eq/ha/yr). The  $CL_{\min}(N)$  (nitrogen absorbed by nitrogen sinks within the system) corresponds to the value depicted in **Figure 3.3-5**.

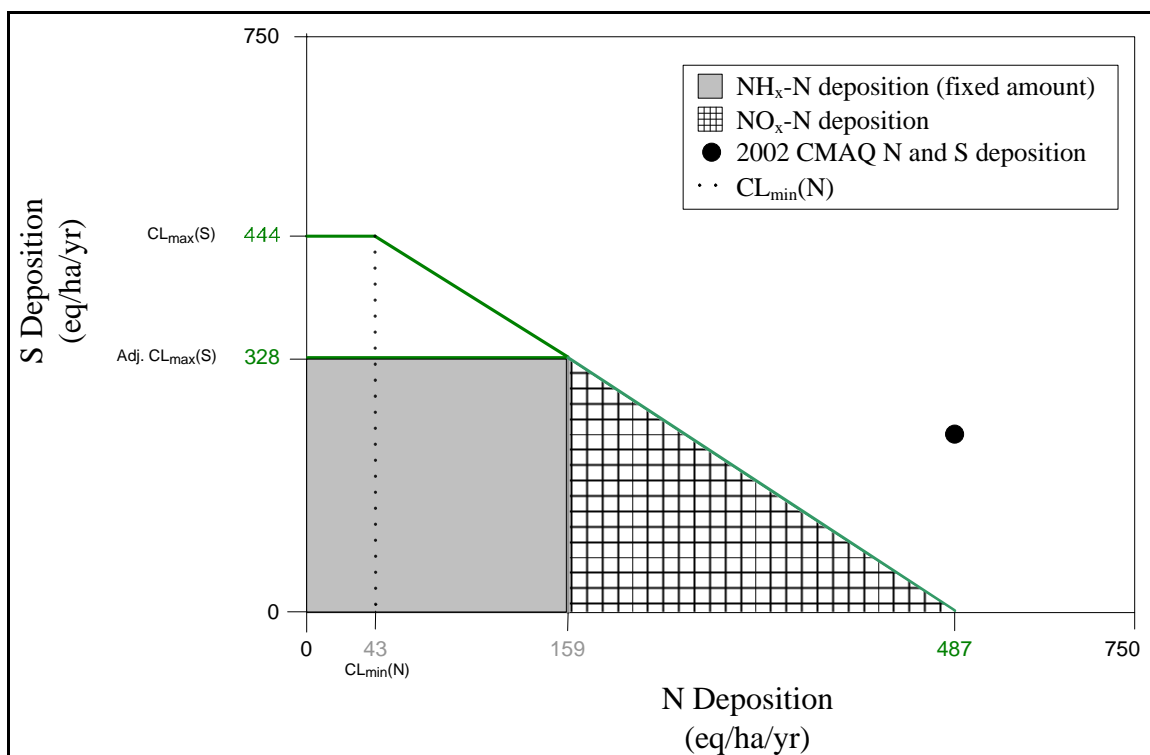


**Figure 3.3-8.** The influence of the 2002 CMAQ/NADP total nitrogen and sulfur deposition levels ( $\text{NH}_x\text{-N}$ ) on the critical load function response curve and, in turn, the maximum critical loads of sulfur ( $\text{CL}_{\text{max}}(\text{S})$ ) and oxidized nitrogen ( $\text{NO}_x\text{-N}$ ) for the selected highest protection critical load for the Hubbard Brook Experimental Forest Case Study Area. The critical load of oxidized nitrogen ( $\text{NO}_x\text{-N}$ ) is 328 eq/ha/yr ( $487 - 159$  eq/ha/yr). The  $\text{CL}_{\text{min}}(\text{N})$  (nitrogen absorbed by nitrogen sinks within the system) corresponds to the value depicted in **Figure 3.3-6**.

## 4.0 EXPANSION OF CRITICAL LOAD ASSESSMENTS FOR SUGAR MAPLE AND RED SPRUCE

### 4.1 CRITICAL LOAD ASSESSMENTS

Although the KEF and HBEF case studies estimated critical loads for red spruce and sugar maple in two locations and established that the 2002 CMAQ/NADP total nitrogen and sulfur deposition levels were greater than the calculated loads, these results cannot be extrapolated directly to represent the critical load condition for the full distribution ranges of the two tree species. Critical loads are largely determined by soil characteristics, and these characteristics vary by location. Therefore, to gain an understanding of the range of critical load

values experienced by sugar maple and red spruce, it is necessary to calculate critical loads in multiple locations throughout the ranges of the two species.

Critical load calculations were applied to multiple locations within 24 states for sugar maple and in 8 states for red spruce. Individual site locations within each State were determined by the USFS FIA database permanent sampling plots' locations on forestland<sup>7</sup> (timberland<sup>8</sup> for New York, Arkansas, Kentucky and North Carolina), each covering 0.07 ha. Only database information for nonunique<sup>9</sup>, permanent sampling plots that supported the growth of sugar maple or red spruce and had the necessary soil, parent material, atmospheric deposition, and runoff data were included in the analyses. With these restrictions, 4,992 of the 14,669 sugar maple plots and 763 of the 2,875 red spruce plots were included in the calculations of the plot-specific critical loads (**Table 4.1-1**). Although only a subset of the total sugar maple and red spruce plots were included in the analyses, the results are thought to capture accurately the range and trends of critical loads of the two species. Due to the randomness of the plot restrictions, it is unlikely that a bias was incorporated into the analyses.

**Table 4.1-1.** Number and Location of USFS FIA Permanent Sampling Plots (each plot is 0.07 ha) Used in the Analysis of Critical Loads For the Full Geographic Ranges of Sugar Maple and Red Spruce

State	Sugar Maple	Red Spruce
Alabama	13	—
Arkansas	10	—
Connecticut	35	—
Illinois	29	—
Indiana	306	—
Iowa	13	—
Kansas	NA	—

<sup>7</sup> Forestland is defined as, “land at least 10 percent stocked by forest trees of any size, or formerly having such tree cover, and not currently developed for non-forest uses, with a minimum area classification of 1 acre.” (USFS, 2002a).

<sup>8</sup> Timberland is defined as, “forest land capable of producing in excess of 20 cubic feet per acre per year and not legally withdrawn from timber production, with a minimum area classification of 1 acre.” (USFS, 2002b).

<sup>9</sup> Nonunique permanent sampling plot locations are those that have critical load attribute values (e.g., soils, runoff, and atmospheric deposition) that are not distinct and are repeated within a 250-acre area of the plot location. This “confidentiality” filter is a requirement of the USFS to prevent the disclosure of data that can be directly linked to a location on private land. To comply with the necessary “confidentiality,” full coverages of the data required for the critical load deposition calculations were given to the USFS, and the USFS matched and provided the data to each nonunique, permanent sampling plot.



State	Sugar Maple	Red Spruce
Kentucky	14	–
Maine	271	560
Maryland	4	–
Massachusetts	33	3
Michigan	633	–
Minnesota	289	–
Missouri	147	–
New Hampshire	82	55
New Jersey	6	–
New York	485	52
North Carolina	17	1
Ohio	374	–
Pennsylvania	285	NA
Rhode Island	NA	–
South Carolina	NA	–
Tennessee	319	1
Vermont	114	11
Virginia	175	NA
West Virginia	378	7
Wisconsin	960	–
TOTAL	4,992	763

**Note:** NA = data not available for State; “–” = tree species not present on forestland in State.

The parameter values selected for the SMB calculations of critical loads for all plots within the ranges of sugar maple and red spruce included wet deposition of base cations ( $\text{Na}^+$ ,  $\text{Ca}^{+2}$ ,  $\text{Mg}^{+2}$ , and  $\text{K}^+$ ) and chlorine, the clay-substrate method to estimate  $\text{BC}_w$ , three levels of protection ( $(\text{Bc}/\text{Al})_{\text{crit}}$  ratio = 0.6, 1.2 and 10.0), a 0.5 m rooting zone soil depth, and the  $\text{N}_i$  (42.86 eq/ha/yr) and  $\text{N}_{\text{de}}$  (0 eq/ha/yr) default values used for the HBEF and KEF case study areas. The  $K_{\text{gibb}}$  constant ranged from 100 to 950  $\text{m}^6/\text{eq}^2$ , and was determined by average organic matter content, as outlined by McNulty et al. (2007) (**Table 4.1-2**). Nutrient ( $\text{N}_u$ ) and base cation ( $\text{BC}_u$ ) uptake were not included in the SMB calculations because it was not possible to determine the harvesting status of the individual sampling plots. Corrections for sea salt influence were not applied to the wet deposition because such corrections were found to over-correct deposition estimates (McNulty et al., 2007).

Similar to the KEF and HBEF case studies, the U.S. Department of Agriculture- Natural Resources Conservation Service (USDA-NRCS) SSURGO soils database (USDA-NRCS, 2008c) was the main source used to estimate  $BC_w$  in the calculations of critical loads for the full distribution ranges of sugar maple and red spruce. The U.S. Geological Survey (USGS) state-level integrated map database for the United States (USGS, 2009b) was used as a secondary source of information, when necessary. Parent material acidity was inferred from the parent material attribute in the SSURGO soils database. The estimated total silica and ferromagnesium content, relative to the mineral assemblage typical of the rock or sediment type, were used to classify parent material as acidic, intermediate, or basic, according to the classification table (**Table 4.1-3**) outlined by McNulty et al. (2007) from Gray and Murphy (1999). When possible, classification of the parent material silica content was determined by the range of rock types provided as examples in **Table 4.1-3**. When rock types were not clearly indicated in the parent material attribute, parent material acidity was classified using a systematic protocol involving the consideration of descriptive modifiers that suggest a probable range of silica or ferromagnesium content (**Table 4.1-4**). In cases where the parent material attribute in the SSURGO soils database was not populated or was too nondescriptive to classify, acidity rating of parent material was inferred from the USGS state-level spatial geology databases. The criteria applied to the soils data were also used in interpretation of these USGS spatial datasets, along with general observation related to spatial patterns of local and regional geologic settings that suggested characteristics of igneous and metamorphic petrogenesis and implied sedimentary depositional mechanisms and environments. If parent material acidity was classified as “organic” or “other” or could not be determined by either the SSURGO or USGS geology databases, the critical load was not estimated for the location. The  $BC_w$  values in the critical load assessments were not corrected for temperature because the soil temperature attribute in the SSURGO soils database was missing data for most of the plot locations. Average air temperature was not used as a substitute because McNulty et al. (2007) determined that corrections for air temperatures were more suitable for northern climates, presumably where the temperature corrections were derived (i.e., Scandinavia).

**Table 4.1-2.** Gibbsite Equilibrium ( $K_{gibb}$ ) Determined by Percentage of Soil Organic Matter

Soil Type Layer	Organic Matter %	$K_{gibb}$ ( $m^6/eq^2$ )
Mineral soils: C layer	<5	950
Soils with low organic matter: B/C layers	5 to 15	300
Soils with some organic material: A/E layers	15 to 70	100
Peaty and organic soils: organic layers	>70	9.5

**Source:** Modification of table from McNulty et al. (2007).

**Table 4.1-3.** Parent Material Acidity Classifications for Base Cation ( $BC_w$ ) Estimations

Parent Material Classification	Parent Material Category	Silica Content	Calcium-Ferromagnesium Content	Examples
Acidic	Extremely siliceous	>90%	Extremely low (generally <3%)	Quartz sands (i.e., beach, alluvial, or Aeolian), chert, quartzite, quartz reefs, and silicified rocks
	Highly siliceous	72% to 90%	Low (generally 3% to 7%)	Granite, rhyolite, adamellite, dellenite, quartz sandstone, and siliceous tuff
Intermediate	Transitional siliceous/Intermediate	62% to 72%	Moderately low (generally 7% to 14%)	Granodiorite, dacite, trachyte, syenite, most greywacke, most lithic sandstone, most argillaceous rocks, and siliceous/intermediate tuff
	Intermediate	52% to 62%	Moderate (generally 14% to 20%)	Monzonite, trachy-andesite, diorite, andesite, intermediate tuff, as well as some greywacke, lithic sandstone, and argillaceous rock
Basic	Mafic	45% to 52%	High (generally 20% to 30%)	Gabbro, dolerite, basalt, and mafic tuff (uncommon)
	Ultramafic	<45%	Very high (generally >30%)	Serpentinite, dunite, peridotite, amphibolite, and tremolite-chlorite-talc schists
	Calcareous	Low*	CaCO <sub>3</sub> dominate other bases variable	Limestone, dolomite, calcareous shale, and calcareous sands

Parent Material Classification	Parent Material Category	Silica Content	Calcium-Ferromagnesium Content	Examples
Organic	Organic	Low*	Organic matter dominates bases variable	Peat, coal, and humified vegetative matter
Other	Alluvial	Variable*	Variable	Variable
	Sesquioxide	Variable*	Variable, dominated by sesquioxides	Laterite, bauxite, ferruginous sandstone, and ironstone
* Category not defined by silica content				

**Source:** Modified from McNulty et al. (2007).

**Table 4.1-4.** Parent Material and Descriptive Modifier Characteristics (within the SSURGO Soils [USDA-NRCS, 2008c] and USGS Geology [USGS, 2009b] Databases) Used to Classify Parent Material Acidity

Parent Material or Modifier Characteristic	Acidity Classification	Rational
Glacial deposits, till, outwash, or drift (without modifiers)	Intermediate	Probable mixture of different mineralogies
Glacial lacustrine (without modifiers)	Intermediate	Probable mixture of different mineralogies
Glaciomarine (without modifiers)	Intermediate	Probable mixture of different mineralogies
Marine deposits (without modifiers)	Intermediate	Probable mixture of different mineralogies
Loess and eolian (without modifiers)	Intermediate	Probable mixture of different mineralogies
Alluvium (without modifiers)	Acidic	Probable composition, predominantly quartz
Residuum (without modifier)	Not able to classify	Mineralogy unknown
Colluvium (without modifiers)	Intermediate	Probable mixture of different mineralogies located close to source area
Deposits, till, or outwash (without modifiers)	Not able to classify	Mineralogy unknown
Saprolite (without modifiers)	Not able to classify	Mineralogy unknown

Parent Material or Modifier Characteristic	Acidity Classification	Rational
Sandy modifier	Acidic	Probable high silica content
Loamy modifier	Intermediate	Equal contributions of chemical properties (intermediate ion exchange capacity) from the three soil textures (i.e., sand, silt, clay)
Skeletal modifier	Classification based on top two layer descriptions	Skeletal layer is very thin and spotty, so top two layers considered main source of parent material
Red, brown, ferric, iron modifier	Basic	Probable high iron content (associated with potentially higher) cation ion-exchange capacity
Opposing mineralogies	Intermediate	Considered average of two mineralogies
Multiple layers described	Classification based on top layer description	Top layer considered main source of soil parent material

The calculated critical loads for the three levels of protection ( $Bc/Al_{crit} = 0.6, 1.2$  and  $10.0$ ) were compared to 2002 CMAQ/NADP total nitrogen and sulfur deposition levels to determine which plots with sugar maple and/or red spruce experienced deposition levels greater than the critical load values.

Based on the SMB calculations for the three levels of protection ( $Bc/Al_{crit} = 0.6, 1.2$  and  $10.0$ ), critical loads of acidifying deposition for sugar maple in the 24 states were found to range from 107 to 6,008 eq/ha/yr (**Table 4.1-5**). Critical loads for red spruce in the 8 states ranged from 180 to 4,278 eq/ha/yr. In a comparison of the 2002 CMAQ/NADP total nitrogen and sulfur deposition levels and calculated critical loads, 3% to 75% of all sugar maple plots and 3% to 36% of all red spruce plots were found to have 2002 CMAQ/NADP total nitrogen and sulfur deposition levels greater than the critical loads; the highest protection critical loads ( $Bc/Al_{crit} = 10.0$ ) had the highest frequency of exceedance (**Table 4.1-6**). Aggregated by State, a large proportion of the sugar maple and red spruce plots showed high levels of critical load exceedance for the highest protection level ( $Bc/Al_{crit} = 10.0$ ) and comparatively lower exceedance frequency at the lowest protection level ( $Bc/Al_{crit} = 0.6$ ) (**Table 4.1-6, Figures 4.1-1 to 4.1-6**). In general, New Hampshire displayed the greatest degree of critical load exceedance at all protection levels for both species.

Collectively, given the limitations and uncertainties associated with the SMB model to estimate critical acid loads (see Section 4.3.9 in Chapter 4 and Section 5 in Appendix 5 for further description), these results suggest that the health of at least a portion of the sugar maple and red spruce growing in the United States may have been compromised with the 2002 CMAQ/NADP total nitrogen and sulfur deposition levels; even with the lowest level of protection, half the states contained sugar maple and red spruce stands that were negatively impacted by acidifying deposition. At the highest level of protection ( $Bc/Al_{crit} = 10.0$ ), the apparent impact of the 2002 CMAQ/NADP total nitrogen and sulfur deposition levels was much greater. A large proportion of sugar maple (>80% of plots in 13 of 24 states) and the majority of red spruce (100% of plots in 5 of 8 states) experienced deposition levels that exceeded the critical loads. If this high protection critical load accurately represents the conditions of the two species, a large proportion of both sugar maple and red spruce, throughout their ranges, were most likely negatively impacted under 2002 CMAQ/NADP total nitrogen and sulfur deposition levels.

**Table 4.1-5.** Ranges of Critical Load Values by Level of Protection ( $Bc/Al_{crit} = 0.6, 1.2, \text{ and } 10.0$ ) and by State for the Full Distribution Ranges of Sugar Maple and Red Spruce

State	Ranges of Critical Load Values (eq/ha/yr)					
	Sugar Maple			Red Spruce		
	$Bc/Al = 0.6$	$Bc/Al = 1.2$	$Bc/Al = 10.0$	$Bc/Al = 0.6$	$Bc/Al = 1.2$	$Bc/Al = 10.0$
Alabama	1,592 to 5,337	1,114 to 3,638	617 to 2,015	–	–	–
Arkansas	2,239 to 4,290	1,536 to 2,913	857 to 1,623	–	–	–
Connecticut	1,519 to 2,468	1,058 to 1,702	581 to 941	–	–	–
Illinois	2,543 to 3,671	1,730 to 2,485	965 to 1,390	–	–	–
Indiana	1,478 to 5,859	1,020 to 3,971	573 to 2,214	–	–	–
Iowa	2,260 to 3,791	1,533 to 2,560	854 to 1,424	–	–	–
Kansas	NA	NA	NA	–	–	–
Kentucky	2,044 to 3,994	1,390 to 2,707	749 to 1,497	–	–	–
Maine	746 to 4,284	535 to 2,983	295 to 1,620	599 to 4,278	439 to 2,979	249 to 1,623
Maryland	2,066 to 3,090	1,417 to 2,122	929 to 1,178	–	–	–
Massachusetts	791 to 2,414	566 to 1,661	319 to 919	1,706 to 1,736	1,191 to 1,213	656 to 669
Michigan	400 to 6,008	294 to 4,070	169 to 2,269	–	–	–
Minnesota	220 to 4,916	166 to 3,318	107 to 1,861	–	–	–
Missouri	978 to 4,891	681 to 3,304	377 to 1,843	–	–	–
New Hampshire	580 to 1,994	419 to 1,439	236 to 780	418 to 1,994	324 to 1,439	180 to 780
New Jersey	1,452 to 2,651	1,029 to 1,824	566 to 1,012	–	–	–
New York	503 to 4,467	370 to 3,039	209 to 1,686	526 to 3,146	386 to 2,156	217 to 1,195
North Carolina	1,415 to 3,444	1,010 to 2,426	558 to 1,319	1256	926	501
Ohio	1,226 to 4,986	855 to 3,366	469 to 1,877	–	–	–
Pennsylvania	1,026 to 4,047	723 to 2,752	402 to 1,530	NA	NA	NA

State	Ranges of Critical Load Values (eq/ha/yr)					
	Sugar Maple			Red Spruce		
	Bc/Al = 0.6	Bc/Al = 1.2	Bc/Al = 10.0	Bc/Al = 0.6	Bc/Al = 1.2	Bc/Al = 10.0
Rhode Island	NA	NA	NA	–	–	–
South Carolina	NA	NA	NA	–	–	–
Tennessee	921 to 5,755	653 to 3,901	351 to 2,175	2,065	1,433	788
Vermont	479 to 5,660	351 to 3,846	201 to 2,142	846 to 2,305	6,016 to 1,648	336 to 888
Virginia	1,036 to 5,852	726 to 3,968	410 to 2,208	NA	NA	NA
West Virginia	369 to 4,134	270 to 2,819	152 to 1,560	2,300 to 3,634	1,610 to 2,533	884 to 1,382
Wisconsin	400 to 5,031	290 to 3,393	166 to 1,898	–	–	–
<b>Combined (all plots)</b>	<b>220 to 6,008</b>	<b>166 to 4,070</b>	<b>107 to 2,269</b>	<b>418 to 4,278</b>	<b>324 to 2,979</b>	<b>180 to 1,623</b>

**Note:** NA = data not available for state; “–” = tree species not present on forestland in state.



**Table 4.1-6.** Percentages of Plots, by Protection Level ( $Bc/AI_{crit} = 0.6, 1.2, \text{ and } 10.0$ ) and by State, where 2002 CMAQ/NADP Total Nitrogen and Sulfur Deposition Levels Were Greater Than the Critical Loads for Sugar Maple and Red Spruce

State	Percentage of Plots Where Critical Load is Exceeded (%)					
	Sugar Maple			Red Spruce		
	$Bc/AI = 0.6$	$Bc/AI = 1.2$	$Bc/AI = 10.0$	$Bc/AI = 0.6$	$Bc/AI = 1.2$	$Bc/AI = 10.0$
Alabama	0	23	31	—	—	—
Arkansas	0	0	10	—	—	—
Connecticut	0	23	100	—	—	—
Illinois	0	0	66	—	—	—
Indiana	0.3	12	87	—	—	—
Iowa	0	0	23	—	—	—
Kansas	NA	NA	NA	—	—	—
Kentucky	0	0	86	—	—	—
Maine	0	0.7	20	0.2	0.5	16
Maryland	0	25	100	—	—	—
Massachusetts	6	33	100	0	100	100
Michigan	6	14	70	—	—	—
Minnesota	2	7	30	—	—	—
Missouri	0.7	2	46	—	—	—
New Hampshire	29	38	84	27	38	78
New Jersey	0	67	100	—	—	—
New York	6	20	95	14	15	79
North Carolina	0	6	71	0	0	100
Ohio	1	16	95	—	—	—
Pennsylvania	7	22	98	NA	NA	NA
Rhode Island	NA	NA	NA	—	—	—
South Carolina	NA	NA	NA	—	—	—
Tennessee	0.3	3	50	0	0	100
Vermont	2	7	99	2	6	100
Virginia	2	9	59	NA	NA	NA
West Virginia	2	8	95	0	0	100
Wisconsin	2	10	82	—	—	—
<b>Combined (all plots)</b>	<b>3</b>	<b>12</b>	<b>75</b>	<b>3</b>	<b>5</b>	<b>36</b>

**Note:** NA = data not available for state; “—” = tree species not present on forestland in state

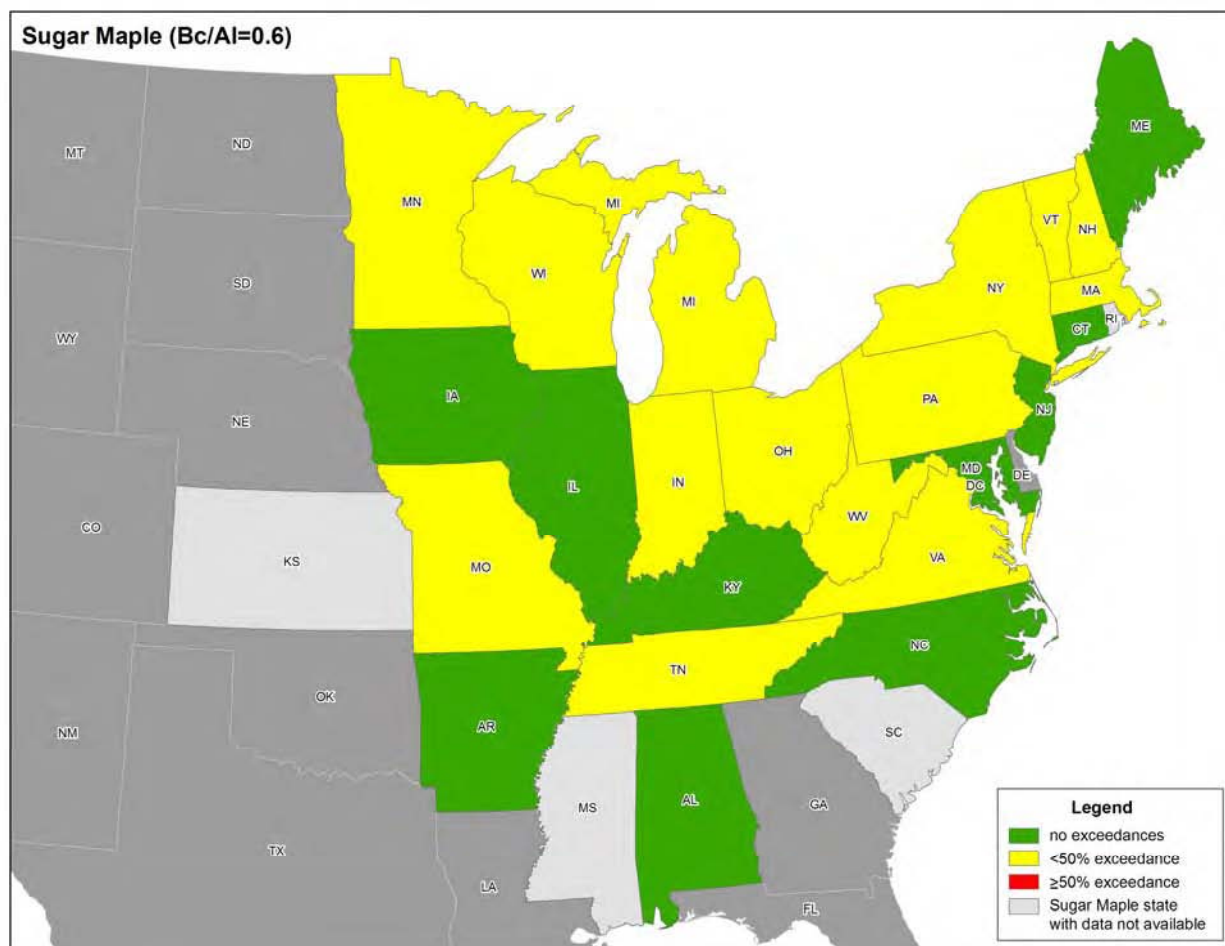


**Figure 4.1-1.** States where sugar maple is found and where 2002 CMAQ/NADP total nitrogen and sulfur deposition levels exceeded the lowest protection critical load ( $Bc/Al_{crit} = 0.6$ ) in the following: none of the sugar maple plots, <50% of the sugar maple plots, and >50% of the sugar maple plots.

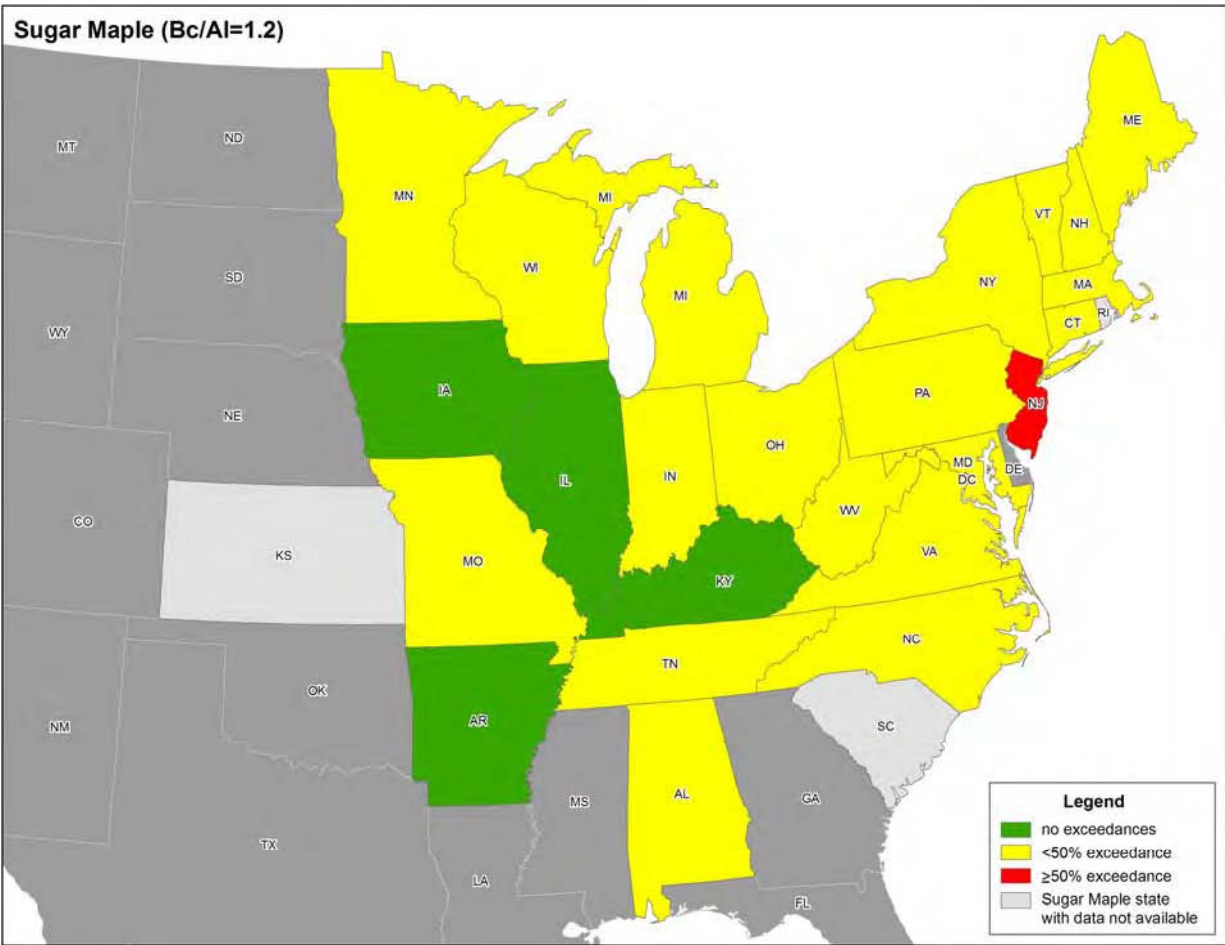


**Figure 4.1-2.** States where sugar maple is found and where 2002 CMAQ/NADP total nitrogen and sulfur deposition levels exceeded the intermediate protection critical load ( $Bc/Al(crit) = 1.2$ ) in the following: none of the sugar maple plots, <50% of the sugar maple plots, and >50% of the sugar maple plots.

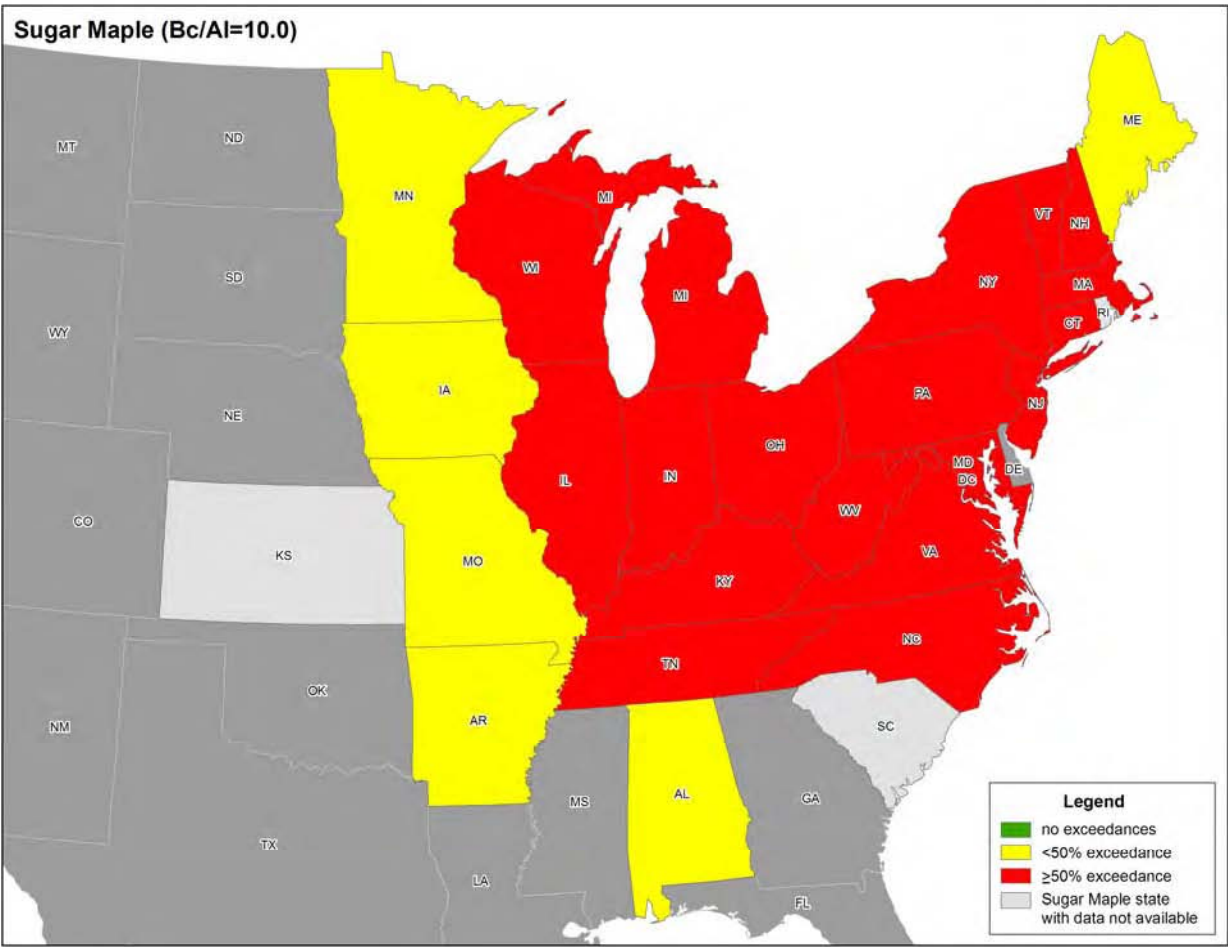


**Figure 4.1-3.** States where sugar maple is found and where 2002 CMAQ/NADP total nitrogen and sulfur deposition levels exceeded the highest protection critical load ( $Bc/Al(crit) = 10.0$ ) in the following: none of the sugar maple plots, <50% of the sugar maple plots, and >50% of the sugar maple plots.

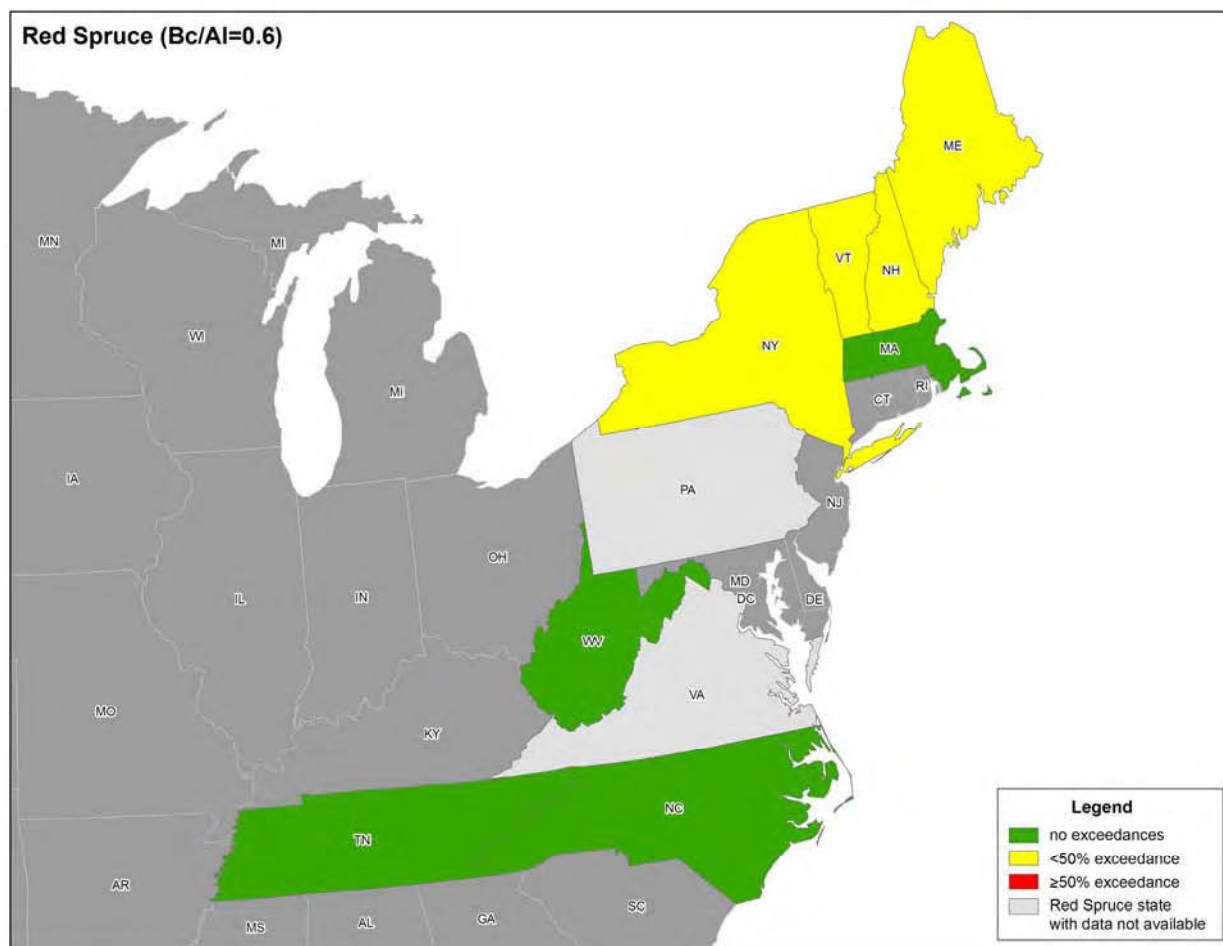


**Figure 4.1-4.** States where red spruce is found and where 2002 CMAQ/NADP total nitrogen and sulfur deposition levels exceeded the lowest protection critical load ( $Bc/Al(crit) = 0.6$ ) in the following: none of the red spruce plots, <50% of the red spruce plots, and >50% of the red spruce plots.

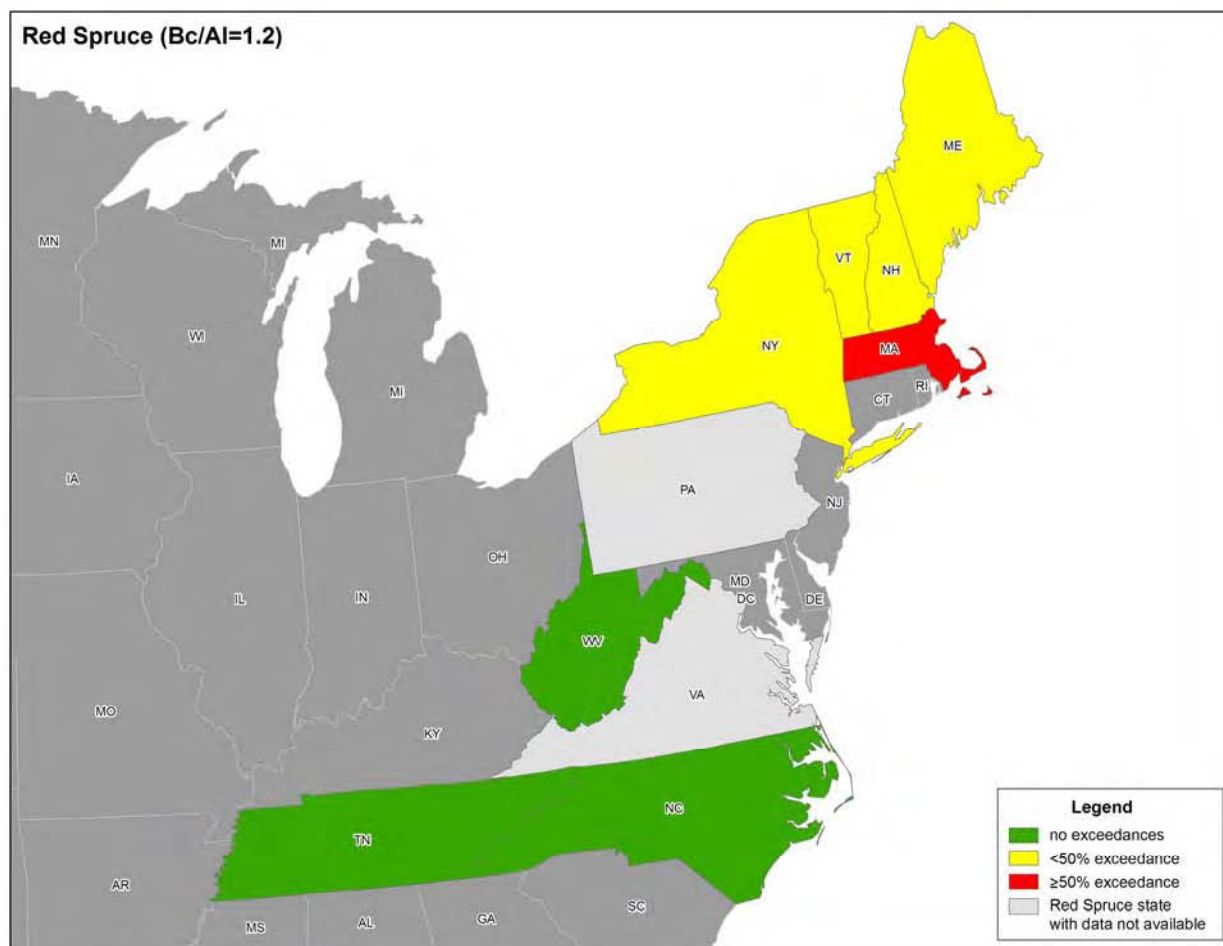


**Figure 4.1-5.** States where red spruce is found and where 2002 CMAQ/NADP total nitrogen and sulfur deposition levels exceeded the intermediate protection critical load ( $Bc/Al(crit) = 1.2$ ) in the following: none of the red spruce plots, <50% of the red spruce plots, and >50% of the red spruce plots.

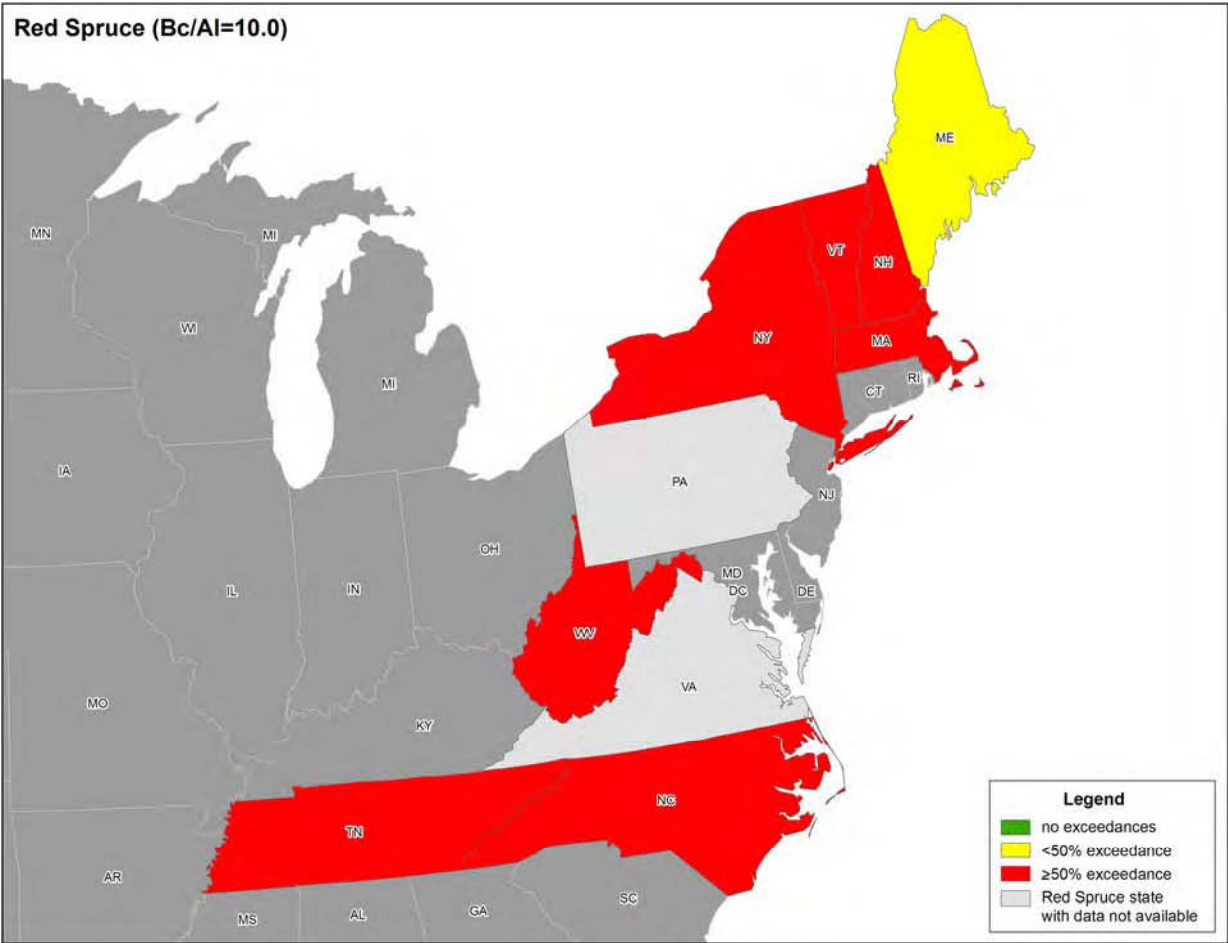


**Figure 4.1-6.** States where red spruce is found and where 2002 CMAQ/NADP total nitrogen and sulfur deposition levels exceeded the highest protection critical load ( $Bc/Al(crit) = 10.0$ ) in the following: none of the red spruce plots, <50% of the red spruce plots, and >50% of the red spruce plots.

## 4.2 RELATIONSHIP BETWEEN ATMOSPHERIC NITROGEN AND SULFUR DEPOSITION AND TREE GROWTH

The impacts of the 2002 CMAQ/NADP total nitrogen and sulfur deposition and critical load exceedances on sugar maple and red spruce growth throughout the full ranges of the two species is presented and discussed in **Attachment A**.

## 5.0 UNCERTAINTY ANALYSIS

### 5.1 KANE EXPERIMENTAL FOREST AND HUBBARD BROOK EXPERIMENTAL FOREST CASE STUDY AREAS

Despite the extensive use of the SMB model to estimate critical loads, there is uncertainty regarding the output from the model and calculations. To a large degree, this uncertainty comes from the dependence of the SMB calculations on assumptions made by the researcher and the use of default values. Parameters including base cation weathering ( $BC_w$  and  $Bc_w$ ),  $ANC_{le,crit}$ ,  $K_{gibb}$ ,  $N_u$ ,  $N_i$ ,  $N_{de}$ , and  $Bc_u$  are rarely measured at each location and must be selected based on the literature or on other calculations and models. In an analysis conducted by Li and McNulty (2007), it was determined that  $BC_w$  and  $ANC_{le,crit}$  were the main sources of uncertainty, with each respectively contributing 49% and 46% to the total variability in critical load estimates. It has, therefore, been suggested that the calculation of critical loads using a relevant range of parameter values can provide the foundation for an uncertainty analysis (Li and McNulty, 2007; Hall et al., 2001; Hodson and Langan 1999); it is likely that the correct critical load of a system will be contained within the range of load estimates from such an approach. If all or a large majority of estimates indicate that the critical load of a system is exceeded with 2002 CMAQ/NADP total nitrogen and sulfur deposition levels, it is likely that deposition is greater than the critical load and that the trees and vegetation in that system are being negatively impacted by acidification. Conversely, if deposition is not greater than the majority of critical load estimates, there can be greater confidence that acidifying deposition is not impacting the system. Under a scenario of a near equal number of estimates indicating exceedance and nonexceedance, it is not possible to determine the actual acidification status of a system with confidence. Nonetheless, such results do suggest that the system is near the critical load level and should be monitored or assessed more thoroughly.

In this case study, multiple values were used for several parameters in the SMB calculations for KEF and HBEF;  $BC_w$  was calculated with two methods, two values of  $K_{gibb}$  constant were used, and three indicator values of  $(Bc/Al)_{crit}$  were evaluated. Therefore, it was possible to use the range of output values from the calculations to assess the certainty of the acidification status of the HBEF and KEF case study areas. For both sugar maple and red spruce, a similar number of estimates indicated deposition levels greater than the critical loads; the



critical loads associated with the most stringent, most protective  $Bc/Al_{crit}$  ratio indicator ( $Bc/Al_{crit} = 10.0$ ) were frequently lower than the 2002 CMAQ/NADP total nitrogen and sulfur deposition levels. Conversely, the critical loads calculated with the  $(Bc/Al)_{crit}$  ratio indicative of a high risk to tree health ( $Bc/Al_{crit} = 0.6$ ) were higher than the 2002 CMAQ/NADP total nitrogen and sulfur deposition levels. The intermediate indicator ratio ( $(Bc/Al)_{crit}$ ) had critical load estimates that were either exceeded or not exceeded by 2002 CMAQ/NADP total nitrogen and sulfur deposition levels. The patterning of the results suggests that the 2002 CMAQ/NADP total nitrogen and sulfur deposition levels were very close to, if not greater than, the critical loads of the two case study areas, and both ecosystems are likely to be sensitive to any future changes in the levels of nitrogen and sulfur acidifying deposition.

A more thorough, quantified uncertainty analysis of the parameters that are selected for the SMB method calculations of critical acid loads is recommended for future analyses.

## **5.2 EXPANSION OF CRITICAL LOAD ASSESSMENTS**

Critical load estimates for individual plots within the distribution ranges of sugar maple and red spruce were calculated using the clay-substrate method to estimate  $BC_w$ . As discussed earlier, the  $BC_w$  term within the SMB model is one of the most influential terms in the calculation of a critical load, and the determination of this  $BC_w$  value is strongly influenced by the classified acidity of the soil parent material. In large-scale analyses, descriptions of the mineralogy of parent material underlying the soil may be missing, nondescriptive, only suggestive of mineralogy, or may only represent the dominant mineralogy in a large area (and therefore not accurately capture the smaller-scale variation in mineralogy). Therefore, it is possible to misclassify the parent material acidity in the  $BC_w$  term.

In the analyses of critical loads for the full distribution ranges of sugar maple and red spruce in this report, two fine-scale databases (i.e., SSURGO soils [USDA-NRCS, 2008c] and USGS state-level geology [USGS, 2009b] databases) were used as the sources for parent material mineralogy to allow for location-specific mineralogy descriptions. In addition, a systematic protocol similar to that used in Europe (UNECE, 2004) and Australia (Gray and Murphy, 1999), and based on known and probable silica and ferromagnesium content, spatial patterns of local and geologic settings, and implied depositional mechanisms and environments was used to determine the parent material acidity classifications. Therefore, steps were taken to

determine accurate, location-specific acidity classifications. Nonetheless, parent material in some of the plots may have been misclassified.

To evaluate the degree to which critical load estimates could change with a misclassification of parent material acidity, a simple analysis of absolute (eq/ha/yr) and percentage change associated with misclassifications of parent materials was conducted, using the critical loads associated with the three levels of protection ( $(\text{Bc}/\text{Al})_{\text{crit}} = 0.6, 1.2 \text{ and } 10.0$ ) for sugar maple and red spruce. The differences between all combinations of critical loads calculated with basic, intermediate, and acidic parent materials were determined, and these difference values were expressed as a percentage of the original critical load estimates (**Tables 5.2-1 and 5.2-2**). For example, the percentage difference associated with the misclassification of an intermediate parent material as acidic would be calculated as the absolute value of  $(\text{CL}_{\text{intermediate}} - \text{CL}_{\text{acid}}) / \text{CL}_{\text{intermediate}}$ .

**Table 5.2-1.** Differences and Percentage Differences in Plot-Level Critical Load Estimates Associated with the Misclassification of Parent Material Acidity for the Full Range Assessment of Sugar Maple

<b>Bc/Al<sub>(crit)</sub> Ratio</b>	<b>Misclassification of Parent Material</b>	<b>Difference between Critical Loads (eq/ha/yr)</b>			<b>% Difference between Critical Loads (%)</b>		
		<b>Range of Values</b>	<b>Average</b>	<b>Median</b>	<b>Range of Values</b>	<b>Average</b>	<b>Median</b>
0.6	<i>Acidic as Intermediate</i>	737 to 1,559	797	784	25 to 492	58	51
	<i>Acidic as Basic</i>	784 to 3,631	1,018	936	42 to 492	70	61
	<i>Intermediate as Basic</i>	0 to 2,072	222	156	0 to 36	8	7
	<i>Intermediate as Acidic</i>	737 to 1,559	797	784	20 to 83	35	34
	<i>Basic as Acidic</i>	784 to 3,631	1,018	936	30 to 83	40	38
	<i>Basic as Intermediate</i>	0 to 2,072	222	156	0 to 26	7	7
1.2	<i>Acidic as Intermediate</i>	493 to 1,045	537	529	24 to 428	56	50
	<i>Acidic as Basic</i>	527 to 2,433	686	634	40 to 428	67	60
	<i>Intermediate as Basic</i>	0 to 1,388	149	105	0 to 36	8	7
	<i>Intermediate as Acidic</i>	493 to 1,045	537	529	19 to 81	34	33
	<i>Basic as Acidic</i>	527 to 2,433	686	634	29 to 81	39	37
	<i>Basic as Intermediate</i>	0 to 1,388	149	105	0 to 26	7	6

<b>Bc/Al<sub>(crit)</sub> Ratio</b>	<b>Bc/Al<sub>(crit)</sub> Ratio</b>	<b>Misclassification of Parent Material</b>			<b>Difference between Critical Loads (eq/ha/yr)</b>		
		<b>Range of Values</b>	<b>Range of Values</b>	<b>Average</b>	<b>Median</b>	<b>Range of Values</b>	<b>Average</b>
10.0	<i>Acidic as Intermediate</i>	275 to 583	298	294	24 to 376	56	50
	<i>Acidic as Basic</i>	293 to 1,357	381	351	41 to 376	67	60
	<i>Intermediate as Basic</i>	0 to 774	83	58	0 to 36	8	7
	<i>Intermediate as Acidic</i>	275 to 583	298	294	20 to 79	34	33
	<i>Basic as Acidic</i>	293 to 1,357	381	351	29 to 79	39	37
	<i>Basic as Intermediate</i>	0 to 774	83	58	0 to 26	7	6

**Table 5.2-2.** Differences and Percentage Differences in Plot-Level Critical Load Estimates Associated with the Misclassification of Parent Material Acidity for the Full Range Assessment of Red Spruce

<b>Bc/Al<sub>(crit)</sub> Ratio</b>	<b>Misclassification of Parent Material</b>	<b>Difference between Critical Loads (eq/ha/yr)</b>			<b>% Difference between Critical Loads (%)</b>		
		<b>Range of Values</b>	<b>Average</b>	<b>Median</b>	<b>Range of Values</b>	<b>Average</b>	<b>Median</b>
0.6	<i>Acidic as Intermediate</i>	772 to 1,340	831	829	27 to 453	69	67
	<i>Acidic as Basic</i>	853 to 1,584	965	932	44 to 453	78	74
	<i>Intermediate as Basic</i>	0 to 655	134	99	0 to 16	6	5
	<i>Intermediate as Acidic</i>	772 to 1,340	831	829	22 to 82	40	40
	<i>Basic as Acidic</i>	853 to 1,584	965	932	31 to 82	43	43
	<i>Basic as Intermediate</i>	0 to 655	134	99	0 to 14	5	5
1.2	<i>Acidic as Intermediate</i>	521 to 969	567	566	27 to 392	66	64
	<i>Acidic as Basic</i>	578 to 1,075	658	637	43 to 392	74	71
	<i>Intermediate as Basic</i>	0 to 444	91	67	0 to 16	5	5
	<i>Intermediate as Acidic</i>	521 to 969	567	566	21 to 80	38	39
	<i>Basic as Acidic</i>	578 to 1,075	658	637	30 to 80	42	42
	<i>Basic as Intermediate</i>	0 to 444	91	67	0 to 14	5	4
10.0	<i>Acidic as Intermediate</i>	289 to 511	312	311	27 to 345	66	65
	<i>Acidic as Basic</i>	320 to 594	362	350	45 to 345	75	73
	<i>Intermediate as Basic</i>	0 to 246	50	37	0 to 16	5	5
	<i>Intermediate as Acidic</i>	289 to 511	312	311	21 to 78	39	39
	<i>Basic as Acidic</i>	320 to 594	362	350	31 to 78	42	42
	<i>Basic as Intermediate</i>	0 to 246	50	37	0 to 14	5	5

The comparisons of critical loads revealed that changes in critical load values could range from 0 to 3,631 eq/ha/yr for sugar maple and 0 to 1,584 eq/ha/yr for red spruce with the misclassification of parent material acidity. These ranges correspond to percentage differences ranging from 0% to 492% and 0% to 453% for sugar maple and red spruce, respectively. The results also indicate that the biggest impacts of a misclassification on critical load estimates would occur with an acidic parent material being misclassified as basic; the average percentage changes in the estimated critical loads, in such a scenario, were 67% to 70% for sugar maple and 74% to 78% for red spruce, and the median percentage changes were 60% to 61% and 71% to 74% for the two species, respectively. In contrast, the smallest impacts on critical load estimates would occur when a basic parent material was incorrectly classified as intermediate and vice versa. In this scenario, the average and median percentage changes in critical load estimates were only 7% to 8% and 6% to 7% for sugar maple and 5% to 6% and 4% to 5% for red spruce. Given the potential significant impacts of a misclassification of parent material acidity on critical load estimates, this potential source of error should be considered in the accuracy and application of the critical load estimates.

## 6.0 REFERENCES

- Aber, J.D., C.L. Goodale, S.V. Ollinger, M.-L. Smith, A.H. Magill, M.E. Martin, R.A. Hall, and J.L. Stoddard. 2003. Is nitrogen deposition altering the nitrogen status of northeastern forests? *Bioscience* 53:375–389.
- Aber, J.D., A. Magill, S.G. McNulty, R.D. Boone, K.J. Nadelhoffer, M. Downs, and R. Hallett. 1995. Forest Biogeochemistry and primary production altered by nitrogen saturation. *Water, Air, and Soil Pollution* 85:1665–1670.
- Allen, H.W. 2001. Silvicultural treatments to enhance productivity. Pp. 129–139 in *The Forests Handbook*. Vol. 2. Edited by J.Evans. Oxford, UK: Blackwell Science Ltd. Available at: [http://books.google.com/books?id=pH47NTIPLVIC&pg=PA129&lpg=PA129&dq=silvicultural+treatments+to+enhance+productivity+the+forests+handbook&source=bl&ots=BeoXcPLqzZ&sig=KPS\\_wT8FX-Y0i9UKhSRop-0K9qs&hl=en#v=onepage&q=&f=false](http://books.google.com/books?id=pH47NTIPLVIC&pg=PA129&lpg=PA129&dq=silvicultural+treatments+to+enhance+productivity+the+forests+handbook&source=bl&ots=BeoXcPLqzZ&sig=KPS_wT8FX-Y0i9UKhSRop-0K9qs&hl=en#v=onepage&q=&f=false) (accessed September 9, 2009).

- Bailey S.W., S.B. Horsley, R.P. Long, and R.A. Hallett. 2004. Influence of edaphic factors on sugar maple nutrition and health on the Allegheny plateau. *Soil Science Society of America Journal* 68:243–252.
- Bailey, S.W., S.B. Horsley, and R.P. Long. 2005. Thirty years of change in forest soils of the Allegheny Plateau, Pennsylvania. *Soil Science Society of America Journal* 69:681–690.
- Baumgardner, R.E., S.S. Isil, T.F. Lavery, C.M. Rogers, and V.A. Mohnen. 2003. Estimates of cloud water deposition at mountain Acid Deposition Program Sites in the Appalachian Mountains. *Journal of Air and Waste Management Association* 53:291–308.
- Bintz, W.W., and D.J. Butcher. 2007. Characterization of the health of southern Appalachian red spruce (*Piceae rubens*) through determination of calcium, magnesium, and aluminum concentrations of foliage and soil. *Microchemical Journal* 87:170–174.
- Birdsey, R.A. 1992. *Carbon Storage and Accumulation in United States Ecosystems*. U.S. Forest Service General Technical Report WO-59. U.S. Department of Agriculture, Forest Service, Northeast Forest Experiment Station, Radnor, PA.
- Bobbink R., D. Boxman, E. Fremstad, G. Heil, A. Houdijk, and J. Roelofs. 1992. Critical loads for nitrogen eutrophication of terrestrial and wetland ecosystems based upon changes in vegetation and fauna. Pp. 111–159 in *Critical Loads for Nitrogen*, Edited by Grennfelt and Thörnelöf. Miljörapport 1992:41. Nordic Council of Ministers, Copenhagen, Denmark.
- Bobbink R., M. Ashmore, S. Braun, W. Flückiger, and I.J.J. Van den Wyngaert. 2003. Empirical nitrogen critical loads for natural and semi-natural ecosystems: 2002 update. Pp. 43–170 in *Empirical Critical Loads for Nitrogen*. Edited by B. Achermann and R. Bobbink. Environmental Documentation 164, Swiss Agency for the Environment, Forests and Landscape (SAEFL), Berne, Switzerland.
- Briggs, R.D., Hornbeck, J.W., Smith, C.T., Lemin, R.C., and McCormack, M.L. 2000. Long-term effects of forest management on nutrient cycling in spruce- fir forests. *Forest Ecology and Management* 138: 285-299.

- Bull, K., B. Achermann, V. Bashkin, R. Chrast, G. Fenech, M. Forsius, H.-D. Gregor, R. Guardans, T. Haussmann, V. Hayes, B. Kvaeven, M. Lorenz, L. Lundin, G. Mills, M. Posch, B.L. Skjelkvale, and M.J. Ulstein. 2001. Coordinated effects monitoring and modeling for developing and supporting international air pollution control agreements. *Water, Air, and Soil Pollution* 130:119–130.
- Carter, B.J., and E.J. Ciolkosz. 1980. Soil temperature regimes of the central Appalachians. *Soil Science Society of America Journal* 44:1052–1058.
- Chapin, F.S., III., L. Moilanen, and K. Kielland. 1993. Preferential use of organic nitrogen for growth by a non-mycorrhizal arctic sedge. *Nature* 361:150–153.
- Cronan, C.S., and D.F. Grigal. 1995. Use of calcium/aluminum ratios as indicators of stress in forest ecosystems. *Journal of Environmental Quality* 24:209–226.
- De Witt, H.A., J. Mulder, P.H. Nygaard, and D. Aamlid. 2001. Testing the aluminum toxicity hypothesis: A field manipulation experiment in mature spruce forest in Norway. *Water, Air, and Soil Pollution* 130:995–1000.
- DeHayes, D.H., P.G. Schaberg, G.J. Hawley, and G.R. Strimbeck. 1999. Acid rain impacts on calcium nutrition and forest health. *Bioscience* 49(10):789–800.
- Driscoll, C.T., G.E. Likens, L.O. Hedin, J.S. Eaton, and F.H. Bormann. 1989. Changes in the chemistry of surface waters: 25-year results at the Hubbard Brook Experimental Forest, NH. *Environmental Science and Technology* 23(2):137–143.
- Driscoll, C.T., G.B. Lawrence, A.J. Bulger, T.J. Butler, C.S. Cronan, C. Eager, K.F. Lambert, G.E. Likens, J.L. Stoddard, and K.C. Weathers. 2001. Acidic deposition in the northeastern United States: Sources and inputs, ecosystem effects, and management strategies. *Bioscience* 51(3):180–198.
- Drohan, J. R., and W.E. Sharpe. 1997. Long-term changes in forest soil acidity in Pennsylvania, U.S.A. *Water, Air, and Soil Pollution* 95:299–311.

- Drohan, P.J., S.L. Stout, and G.W. Petersen. 2002. Sugar maple (*Acer saccharum* Marsh.) decline during 1979-1989 in northern Pennsylvania. *Forest Ecology and Management* 170:1–17.
- Eagar, C., H. Van Miegroet, S.B. McLaughline, and N.S. Nicholas. 1996. *Evaluation of effects of acidic deposition to terrestrial ecosystems in class I areas of the Southern Appalachians*. Technical Report. Southern Appalachian Mountains Initiative, Asheville, NC.
- FAO (Food and Agriculture Organization). 2007. *Digital Soil Map of the World*. GIS datalayer. United Nations, Food and Agriculture Organization, GeoNetwork, Rome, Italy. Available at: <http://www.fao.org/geonetwork/srv/en/main.home> (accessed September 9, 2009).
- Fenn, M.E., V.M. Perea-Estrada, L.I. de Bauer, M. Pérez-Suárez, D.R. Parker, and V.M. Cetina-Alcalá. 2006a. Nutrient status and plant growth effects of forest soils in the Basin of Mexico. *Environmental Pollution* 140(2):187–199.
- Fenn, M.E., Huntington, T.G., McLaughlin, S.B., Eagar, C., Gomez, A., and Cook, R.B. 2006b. Status of soil acidification in North America. *Journal of Forest Science* 52(special issue): 3–13.
- Fincher, J., J.R. Cumming, R. G. Alscher, G. Rubin, and L. Weinstein. 1989. Long-term ozone exposure affects winter hardiness of red spruce (*Picea rubens* Sarg.) seedlings. *New Phytologist* 113:85-96.
- Gebert, W.A., D.J. Graczyk, and W.R. Krug, 1987. *Average Annual Runoff in the United States, 1951-80: U.S. Geological Survey Hydrologic Investigations Atlas HA-710, Scale 1:7,500,000*. GIS datalayer. U.S. Department of Interior, U.S. Geological Survey, Madison, WI. Available at: <http://water.usgs.gov/GIS/dsdl/runoff.e00.gz> (accessed September 9, 2009).
- Gray, J.M., and B.W. Murphy. 1999. *Parent Material and Soils – A Guide to the Influence of Parent Material on Soil Distribution in Eastern Australia*. Technical Report Number 45. NSW Department of Land and Water Conservation, Sydney, Australia. Available at:

- [http://www.dnr.nsw.gov.au/care/soil/soil\\_pubs/parent\\_material.html](http://www.dnr.nsw.gov.au/care/soil/soil_pubs/parent_material.html) (accessed September 9, 2009).
- Hall, J., K. Bull, I. Bradley, C. Curtis, P. Freer-Smith, M. Hornung, D. Howard, S. Langan, P. Loveland, B. Reynolds, J. Ulliyett, and T. Warr. 1998. *Status of UK Critical Loads and Exceedences. Part 1 – Critical Loads and Critical Loads Maps*. Report to the Department of Environment Transport and the Regions. Biological Records Centre, Institute of Terrestrial Ecology, Centre for Ecology and Hydrology, Monks Wood Experimental Station, Abbots Ripton, Huntingdonshire, England.
- Hall, J., B. Reynolds, S. Langan, M. Hornung, F. Kennedy, and J. Aherne. 2001. Investigating the uncertainties in the simple mass balance equation for acidity critical loads for terrestrial ecosystems in the United Kingdom. *Water, Air and Soil Pollution: Focus 1*: 43–56.
- Hallett, R.A., S.W. Bailey, S.B. Horsley, and R.P. Long. 2006. Influence of nutrition and stress on sugar maple at a regional scale. *Canadian Journal of Forest Research* 36:2235–2246.
- HBES (Hubbard Brook Ecosystem Study). 2008a. *Forest Inventory of a Northern Hardwood Forest: Watershed 6 (the biogeochemical reference watershed) 2002*. Online database. Hubbard Brook Ecosystem Study, North Woodstock, NH. Available at: <http://www.hubbardbrook.org/data/dataset.php?id=35> (accessed December 18, 2008).
- HBES (Hubbard Brook Ecosystem Study). 2008b. *Hubbard Brook Ecosystem Study*. Online information. U.S. Department of Agriculture, Forest Service, Water and Ecosystems Project, Northern Research Station, Hubbard Brook Experimental Forest, Durham, NH. Available <http://www.hubbardbrook.org> (accessed June 20, 2008).
- HBES (Hubbard Brook Ecosystem Study). 2008c. *Soil Temperature Data*. Online database. Hubbard Brook Ecosystem Study, North Woodstock, NH. Available at <http://www.hubbardbrook.org/data/dataset.php?id=65> (accessed December 18, 2008).



- Hodson, M.E., and S.J. Langan. 1999. Considerations of uncertainty in setting critical loads of acidity of soils: the role of weathering rate determination. *Environmental Pollution* 106: 73–81.
- Horsley, S.B., R.P. Long, S.W. Bailey, R.A. Hallett, and T.J. Hall. 2000. Factors associated with the decline disease of sugar maple on the Allegheny Plateau. *Canadian Journal of Forest Research* 30:1365–1378.
- Jeffries, D.S. (ed.). 1997. *Canadian Acid Rain Assessment. Volume 3, The Effects of Canada's Lakes, Rivers and Wetlands*. Environment Canada, Gatineau, Quebec.
- Jeffries, D.S., and D.C.L. Lam. 1993. Assessment of the effect of acid deposition on Canadian lakes: determination of critical loads for sulphate deposition. *Water Science Technology* 28:183–187.
- Jenkins, A., B.J. Cosby, R.C. Ferrier, T. Larssen, and M. Posch. 2003. Assessing emission reduction targets with dynamic models: deriving target load functions for use in integrated assessment. *Hydrology and Earth System Services* 7(4):609–617.
- Jenkins, J.C., R.A. Birdsey, and Y. Pan. 2001. Biomass and NPP estimation for the mid-Atlantic region (USA) using plot-level forest inventory data. *Ecological Applications* 11:1174–1193.
- Johnson, A.H., S.B. Andersen, and T.G. Siccama. 1994a. Acid rain and soils of the Adirondacks. I. Changes in pH and available calcium, 1930-1984. *Canadian Journal of Forest Research* 24:39–45.
- Johnson, A.H., A.J. Friedland, E.K. Miller, and T.G. Siccama. 1994b. Acid rain and soils of the Adirondacks. III. Rates of soil acidification in a montane spruce-fir forest at Whiteface Mountain, New York. *Canadian Journal of Forest Research* 24:663–669.
- Johnson, C.E., A.H. Johnson, and T.G. Siccama. 1991. Whole-tree clear-cutting effects on exchangeable cations and soil acidity. *Soil Science Society of America Journal* 55(2):502–508.

- Johnson, A.H., E.R. Cook, and T.G. Siccama. 1988. Climate and red spruce growth and decline in the northern Appalachians. *Proceedings of the National Academy of Sciences* 85: 5369-5373.
- Johnson, D.W. 1984. Sulfur cycling in forests. *Biogeochemistry* 1:29–43.
- Joslin, J.D., and M.H. Wolfe. 1992. Red spruce soil chemistry and root distribution across a cloud water deposition gradient. *Canadian Journal of Forest Research* 22:893–904.
- Juice, S.M., T.J. Fahey, T.G. Siccama, C.T. Driscoll, E.G. Denny, C. Eagar, N.L. Cleavitt, R. Minocha, and A.D. Richardson. 2006. Response of sugar maple to calcium addition to northern hardwood forest. *Ecology* 87:1267-1280.
- Killam, K. 1994. *Soil Ecology*. Cambridge, UK: Cambridge University Press.
- Lawrence, G.B., A.G. Lapenis, D. Berggren, B.F. Aparin, K.T. Smith, W.C. Shortle, S.W. Bailey, D.L. VarlyGuin, and B. Babikov. 2005. Climate dependency of tree growth suppressed by acid deposition effects on soils in northwest Russia. *Environmental Science and Technology* 39:2004–2010.
- Lazarus, B.E., P.G. Schaberg, D.H. DeHayes, and G.J. Hawley. 2004. Severe red spruce winter injury in 2003 creates unusual ecological event in the northeastern United States. *Canadian Journal of Forest Research* 34:1784–1788.
- Li, H., and S.G. McNulty. 2007. Uncertainty analysis on simple mass balance model to calculate critical loads for soil acidity. *Environmental Pollution* 149:315–326.
- Lilleskov, E.A., P.M. Wargo, K.A. Vogt, and D.J. Vogt. 2008. Mycorrhizal fungal community relationship to root nitrogen concentration over a regional atmospheric nitrogen deposition gradient in the northeastern USA. *Canadian Journal of Forest Research* 38: 1260–1266.
- Martin, J.G., B.D. Kloeppel, T.L. Schaefer, D.L. Kimbler, and S.G. McNulty. 1998. Aboveground biomass and nitrogen allocation of ten deciduous southern Appalachian tree species. *Canadian Journal of Forest Research* 28:1648–1659.

- McNulty, S.G., and J. Boggs. In press. A Connectional Framework for Redefining Forest Soil Critical Acid Loads under a Changing Climate. *Environmental Pollution*.
- McNulty, S.G., J. Boggs, J.D. Aber, L. Rustad, and A. Magill. 2005. Red spruce ecosystem level changes following 14 years of chronic nitrogen fertilization. *Forest Ecology and Management* 219:279–291.
- McNulty, S.G., E.C. Cohen, H. Li, and J.A. Moore-Myers. 2007. Estimates of critical acid loads and exceedences for forest soils across the conterminous United States. *Environmental Pollution* 149:281–292.
- MEA (Millennium Ecosystem Assessment Board). 2005. *Ecosystems and Human Well-being: Current State and Trends, Volume 1*. Edited by R. Hassan, R. Scholes, and N. Ash. Washington: Island Press. Available at <http://www.millenniumassessment.org/documents/document.766.aspx.pdf>.
- Miller, H.G. 1988. Long-term effects of application of nitrogen fertilizers on forest sites. Pp. 97–106 in *Forest Site Evaluation and Long-Term Productivity*. Edited by D.W. Cole and S.P. Gessel. Seattle, WA: University of Washington Press.
- NADP (National Atmospheric Deposition Program). 2003a. *Annual Ammonium Wet Deposition, 2002*. GIS datalayer. National Atmospheric Deposition Program, Illinois State Water Survey, Champaign, IL. Available at <http://nadp.sws.uiuc.edu/maps/2002>.
- NADP (National Atmospheric Deposition Program). 2003b. *Annual Calcium Wet Deposition, 2002*. GIS datalayer. National Atmospheric Deposition Program, Illinois State Water Survey, Champaign, IL. Available at <http://nadp.sws.uiuc.edu/maps/2002>.
- NADP (National Atmospheric Deposition Program). 2003c. *Annual Chloride Wet Deposition, 2002*. GIS datalayer. National Atmospheric Deposition Program, Illinois State Water Survey, Champaign, IL. Available at <http://nadp.sws.uiuc.edu/maps/2002>.
- NADP (National Atmospheric Deposition Program). 2003d. *Annual Magnesium Wet Deposition, 2002*. GIS datalayer. National Atmospheric Deposition Program, Illinois State Water Survey, Champaign, IL. Available at <http://nadp.sws.uiuc.edu/maps/2002>.

NADP (National Atmospheric Deposition Program). 2003e. *Annual Nitrate Wet Deposition, 2002*. GIS datalayer. National Atmospheric Deposition Program, Illinois State Water Survey, Champaign, IL. Available at <http://nadp.sws.uiuc.edu/maps/2002>.

NADP (National Atmospheric Deposition Program). 2003f. *Annual Potassium Wet Deposition, 2002*. GIS datalayer. National Atmospheric Deposition Program, Illinois State Water Survey, Champaign, IL. Available at <http://nadp.sws.uiuc.edu/maps/2002>.

NADP (National Atmospheric Deposition Program). 2003g. *Annual Sodium Wet Deposition, 2002*. GIS datalayer. National Atmospheric Deposition Program, Illinois State Water Survey, Champaign, IL. Available at <http://nadp.sws.uiuc.edu/maps/2002>.

NADP (National Atmospheric Deposition Program). 2003h. *Annual Sulfate Wet Deposition, 2002*. GIS datalayer. National Atmospheric Deposition Program, Illinois State Water Survey, Champaign, IL. Available at <http://nadp.sws.uiuc.edu/maps/2002>.

NEG/ECP Forest Mapping Group (Conference of New England Governors and Eastern Canadian Premiers Forest Mapping Group). 2001. *Protocol for Assessment and Mapping of Forest Sensitivity to Atmospheric S and N Deposition: Acid Rain Action Plan – Action Item 4: Forest Mapping Research Project*. Prepared by NEG/ECP Forest Mapping Group. Available at [http://www.nrs.fs.fed.us/clean\\_air\\_water/clean\\_water/critical\\_loads/local-resources/docs/NEGECP\\_Forest\\_Sensitivity\\_Protocol\\_5\\_21\\_04.pdf](http://www.nrs.fs.fed.us/clean_air_water/clean_water/critical_loads/local-resources/docs/NEGECP_Forest_Sensitivity_Protocol_5_21_04.pdf).

NEG/ECP Forest Mapping Group (Conference of New England Governors and Eastern Canadian Premiers Forest Mapping Group). 2005. *Assessment of Forest Sensitivity to Nitrogen and Sulfur Deposition in New Hampshire and Vermont*. Report submitted to the New Hampshire Department of Environmental Services, Concord, NH.

NLCD (National Land Cover Dataset). 2001. *National Land Cover Database 2001*. GIS datalayer. Multi-Resolution Land Characteristics Consortium, U.S. Geological Survey, Sioux Falls, SD. Available at [http://www.mrlc.gov/mrlc2k\\_nlcd.asp](http://www.mrlc.gov/mrlc2k_nlcd.asp).

- Nilsson, J., and P. Grennfelt (eds.). 1988. *Critical Loads for Sulphur and Nitrogen: A Report from a Workshop at Skokloster, Sweden*. Miljørapport 1988:15. Nordic Council of Ministers, Copenhagen, Denmark.
- Ouimet, R., J.-D. Moore, and L. Duchesne. 2008. Effects of experimental acidification and alkalization on soil and growth and health of *Acer saccharum* Marsh. *Journal of Plant Nutrition and Soil Science* 171:868–871.
- Ouimet, R., P.A. Arp, S.A. Watmough, J. Aherne, and I. DeMerchant. 2006. Determination and mapping critical loads of acidity and exceedences for upland forest soils in Eastern Canada. *Water, Air and Soil Pollution* 172:57–66.
- PA DCNR (Pennsylvania Department of Conservation and Natural Resources). 2001. *Digital Bedrock Geology of Pennsylvania*. GIS datalayer. Pennsylvania Bureau of Topographic and Geologic Survey, Department of Conservation and Natural Resources, Harrisburg, PA. Available at <http://www.dcnr.state.pa.us/topogeo/map1/bedmap.aspx>.
- Palmer, S.M., C.T. Driscoll, and C.E. Johnson. 2004. Long-term trends in soil solution and stream water chemistry at the Hubbard Brook Experiment Forest: relationship with landscape position. *Biogeochemistry* 68:51–70.
- Pardo, L.H., and C.T. Driscoll. 1996. Critical loads for nitrogen deposition: case studies at two northern hardwood forests. *Water, Air, and Soil Pollution* 89:105–128.
- Pardo, L.H., and N. Duarte. 2007. *Assessment of Effects of Acidic Deposition on Forested Ecosystems in Great Smoky Mountains National Park using Critical Loads for Sulfur and Nitrogen*. U.S. Department of Agriculture, Forest Service. Prepared for Tennessee Valley Authority, S. Burlington, VT.
- Pardo, L.H., M. Robin-Abbott, N. Duarte, and E.K. Miller. 2004. Tree Chemistry Database (Version 1.0). General Technical Report NE-324. U.S. Department of Agriculture, Forest Service, Northeastern Research Station, Newton Square, PA.

- Reed, J.C. and Bush, C.A. 2005. Generalized Geologic Map of the Conterminous United States Edition 1.2. 1:7,500,000 scale. U.S. Geological Survey. Available at <http://pubs.usgs.gov/atlas/geologic> (accessed on: November 1, 2008).
- Reuss, J.O. 1983. Implications of the calcium-aluminum exchange system for the effect of acid precipitation on soils. *Journal of Environmental Quality* 12:591–595.
- Reuss, J.O., and D.W. Johnson. 1985. Effect of soil processes on the acidification of water by acid deposition. *Journal of Environmental Quality* 14:26–31.
- RMCC (Federal/Provincial Research and Monitoring Coordinating Committee). 1990. *The 1990 Canadian Long-Range Transport of Air Pollutants and Acid Deposition Assessment Report*. Federal/Provincial Research and Monitoring Coordinating Committee, Environment Canada, Ottawa, Canada.
- Ross, D.S., G.B. Lawrence, and G. Fredriksen. 2004. Mineralization and nitrification patterns at eight northeastern USA forested research sites. *Forest Ecology Management* 188:317–335.
- Schaberg, P.G., D.H. DeHayes, and G.J. Hawley. 2001. Anthropogenic calcium depletion: a unique threat to forest ecosystem health? *Ecosystem Health* 7:214–228.
- Shortle, W.C., K.T. Smith, R. Minocha, G.B. Lawrence, and M.B. David. 1997. Acidic deposition, cation mobilization, and biochemical indicators of stress in healthy red spruce. *Journal of Environmental Quality* 26:871–876.
- Siccama, T.G., T.J. Fahey, C.E. Johnson, T.W. Sherry, E.G. Denny, E.B. Girdler, G.E. Likens, and P.A. Schwarz. 2007. Population and biomass dynamics of trees in a northern hardwood forest at Hubbard Brook. *Canadian Journal of Forest Research* 37(4):737–749.
- St. Clair, S.B., J.E. Carlson, and J.P. Lynch. 2005. Evidence for oxidative stress in sugar maple stands growing on acidic, nutrient imbalanced forest soils. *Oecologia* 145:258–369.

- Stone, D.M. 1986. Effect of thinning and nitrogen fertilization on diameter growth of pole-size sugar maple. *Canadian Journal of Forest Research* 16: 1245–1249.
- Sverdrup, H. Personal communication. 2009. Communication between Harald Sverdrup (Lund University, Sweden) and Jennifer Phelan (RTI International, USA) during the Canadian Council of Ministers of the Environment Acid Deposition Critical Loads: Status of Methods and Indicators Workshop, March 18 and 19, 2009. Ottawa, Ontario, Canada.
- Sverdrup, H., and P. Warvfinge. 1993a. Calculating field weathering rates using a mechanistic geochemical model PROFILE. *Applied Geochemistry* 8:273–283.
- Sverdrup, H., and P. Warfvinge. 1993b. *The effect of soil acidification on the growth of trees, grass and herbs as expressed by the (Ca+ Mg+ K)/Al ratio*. Reports in Ecology and Environmental Engineering 2. Lund University, Department of Chemical Engineering, Lund, Sweden.
- Sverdrup, H., and W. de Vries. 1994. Calculating critical loads for acidity with the simple mass balance equation. *Water, Air, and Soil Pollution* 72:143–162.
- Thomasma, S., P. Knopp, and S. Stout. 2008. *SILVAH Version 5.6*. Online computer tool. U.S. Department of Agriculture, Forest Service, North Eastern Forest Experiment Station, Irvine, PA. Available at: <http://www.nrs.fs.fed.us/tools/silvah/> (accessed September 9, 2009).
- Tobin, B.D., and D.J. Weary. 2005. *Engineering Aspects of Karst*. GIS datalayer. National Atlas of the United States, Reston, VA. Available at: <http://www.nationalatlas.gov/mld/karst0m.html> (accessed September 9, 2009).
- UNECE (United Nations Economic Commission for Europe). 2004. *Manual on Methodologies and Criteria for Modeling and Mapping Critical Loads and Levels and Air Pollution Effects, Risks, and Trends*. Convention on Long-Range Transboundary Air Pollution, Geneva Switzerland. Available at <http://www.icpmapping.org> (accessed August 16, 2006).

- U.S. EPA (Environmental Protection Agency). 2005. *Advisory on Plans for Ecological Effects Analysis in the Analytical Plan for EPA's Second Prospective Analysis – Benefits and Costs of the Clean Air Act, 1990-2020*. EPA-COUNCIL-ADV-05-001. U.S. Environmental Protection Agency, Office of the Administrator, Science Advisory Board, Washington, DC. June 23.
- U.S. EPA (Environmental Protection Agency). 2008a. *April 2008 Scope and Methods Plan for Risk Exposure Assessment*. U.S. Environmental Protection Agency, Office of Air Quality Planning and Standards, Research Triangle Park, NC.
- U.S. EPA (Environmental Protection Agency). 2008b. *Clean Air Status and Trends Network (CASTNET)*. GIS datalayer. Clean Air Mapping and Analysis Program, U.S. Environmental Protection Agency, Office of Atmospheric Programs, Clean Air Markets Division, Washington, DC. Available at <http://epamap4.epa.gov/cmap/viewer.htm>.
- U.S. EPA (Environmental Protection Agency). 2008c. *Integrated Science Assessment for Oxides of Nitrogen and Sulfur Environmental Criteria*. Final. EPA/600/R-08/082F. U.S. Environmental Protection Agency, Office of Research and Development, National Center for Environmental Assessment, Research Triangle Park, NC. December.
- USDA (United States Department of Agriculture). 1994. *Soil Information for Environmental Modeling and Ecosystem Management: State Soil Geographic (STATSGO) Database*. Soil datasets. U.S. Department of Agriculture, Natural Resources Conservation Service, National Cartography and Geospatial Center, Washington, DC. Available at [http://www.soilinfo.psu.edu/index.cgi?soil\\_data&conus&data\\_cov](http://www.soilinfo.psu.edu/index.cgi?soil_data&conus&data_cov).
- USDA-NRCS (United States Department of Agriculture-Natural Resources Conservation Service). 2008a. *Soil Survey Geographic (SSURGO) Database for Cameron and Elk Counties, PA*. GIS datalayer. U.S. Department of Agriculture, Natural Resources Conservation Service, Washington, DC. Available at <http://datagateway.nrcs.usda.gov>.
- USDA-NRCS (United States Department of Agriculture-Natural Resources Conservation Service). 2008b. *Soil Survey Geographic (SSURGO) Database for Grafton County Area*,



- New Hampshire*. GIS datalayer. U.S. Department of Agriculture, Natural Resources Conservation Service, Washington, DC. Available at: <http://datagateway.nrcs.usda.gov>.
- USDA-NRCS (United States Department of Agriculture-Natural Resources Conservation Service). 2008c. *Soil Survey Geographic (SSURGO) Database*. U.S. Department of Agriculture, Natural Resources Conservation Service, Fort Worth, TX. Available at: <http://datagateway.nrcs.usda.gov>.
- USFS (U.S. Forest Service). 1999. *Kane Experimental Forest*. Online information. U.S. Department of Agriculture, Forest Service, Kane Experimental Forest, Forestry Sciences Laboratory, Irvine, PA. Available at <http://www.fs.fed.us/ne/warren/kane.html> (accessed June 17, 2008).
- USFS (U.S. Forest Service). 2002a. *Forest Inventory and Analysis National Program: Area of Forest Land, 2002*. U.S. Department of Agriculture, Forest Service, Forest Inventory and Analysis National Program, Arlington, VA. Available at [http://fia.fs.fed.us/tools-data/maps/descr/for\\_land.asp](http://fia.fs.fed.us/tools-data/maps/descr/for_land.asp) (accessed March 3, 2009).
- USFS (U.S. Forest Service). 2002b. *Forest Inventory and Analysis National Program: Area of Timberland, 2002*. U.S. Department of Agriculture, Forest Service, Forest Inventory and Analysis National Program, Arlington, VA. Available at [http://fia.fs.fed.us/tools-data/maps/descr/tim\\_land.asp](http://fia.fs.fed.us/tools-data/maps/descr/tim_land.asp) (accessed March 3, 2009).
- USFS (U.S. Forest Service). 2006. *Forest Inventory Analysis (FIA) Database*. U.S. Department of Agriculture, Forest Service, Forest Inventory and Analysis National Program, Arlington, VA. Available at <http://fia.fs.fed.us/tools-data>.
- USFS (U.S. Forest Service). 2008a. *Hubbard Brook Experimental Forest*. Online information. U.S. Department of Agriculture, Forest Service, Northeastern Research Station, Newtown Square, PA. Available at [http://www.fs.fed.us/ne/newtown\\_square/research/experimental-forest/hubbard-brook.shtml](http://www.fs.fed.us/ne/newtown_square/research/experimental-forest/hubbard-brook.shtml) (accessed June 17, 2008).

- USFS (U.S. Forest Service). 2008b. *Kane Experimental Forest*. Online information. U.S. Department of Agriculture, Forest Service, Northeastern Research Station, Newtown Square, PA. Available at [http://www.fs.fed.us/ne/newtown\\_square/research/experimental-forest/kane.shtml](http://www.fs.fed.us/ne/newtown_square/research/experimental-forest/kane.shtml) (accessed June 17, 2008).
- USFS (U.S. Forest Service) 2008c. The Forest Inventory and Analysis Database: Database Description and Users Manual Version 3.0 for Phase 2. Forest Inventory and Analysis Program, U.S. Department of Agriculture, Forest Service. 243 pp.
- USFS (U.S. Forest Service). 2008. Personal communication from Dr. Charles (Hobie) Perry, USDA Forest Service, Northern Research Station, 1992 Folwell Avenue, St. Paul, MN 55108. August 20.
- USGS (U.S. Geological Survey). 2000. *Bedrock Geologic Map of the Hubbard Brook Experimental Forest, Grafton County, New Hampshire*. GIS datalayer. U.S. Geological Survey, Reston, VA. Available at: <http://pubs.usgs.gov/openfile/of00-045/>.
- USGS (U.S. Geological Survey). 2009a. *Karst*. Online information. U.S. Department of the Interior, U.S. Geological Survey, Office of Ground Water, Reston, VA. Available at <http://water.usgs.gov/ogw/karst/> (accessed February 2009).
- USGS (U.S. Geological Survey). 2009b. *State Geological Map Compilation*. U.S. Department of the Interior, U.S. Geological Survey, Reston, VA. Available at: <http://tin.er.usgs.gov/geology/state> (accessed January 28, 2009).
- Van der Salm, C., and W. de Vries. 2001. A review of the calculation procedure for critical acid loads for terrestrial ecosystems. *The Science of the Total Environment* 271:11–25
- Warby, R.A.F., C.E. Johnson, and C.T. Driscoll. 2009. Continuing acidification of organic soils across the northeastern USA: 1984-2001. *Soil Science Society of America Journal* 73:274–284.
- Wargo, P.M., K. Vogt, D. Vogt, Q. Holifield, J. Tilley, G. Lawrence, and M. David. 2003. Vitality and chemistry of roots of red spruce in forest floors of stands with a gradient of

- soil Al/Ca ratios in the northeastern United States. *Canadian Journal of Forest Research* 33:635–652.
- Watmough, S.A., J. Aherne, and P.J. Dillion. 2004. *Critical Loads Ontario: Relating Exceedance of the Critical Load with Biological Effects at Ontario Forests*. Report 2. Environmental and Resource Studies, Trent University, ON, Canada.
- Watmough, S., J. Aherne, P. Arp, I. DeMerchant, and R. Ouimet. 2006. Canadian experiences in development of critical loads for sulphur and nitrogen. Pp. 33–38 in *Monitoring Science and Technology Symposium: Unifying Knowledge for Sustainability in the Western Hemisphere Proceedings RMRS-P-42CD*. Edited by C. Aguirre-Bravo, P.J. Pellicane, D.P. Burns, and S. Draggan. U.S. Department of Agriculture, Forest Service, Rocky Mountain Research Station, Fort Collins, CO.
- Webster, K.L., I.F. Creed, N.S. Nicholas, and H.V. Miegroet. 2004. Exploring interactions between pollutant emissions and climatic variability in growth of red spruce in the Great Smoky Mountains National Park. *Water, Air, and Soil Pollution* 159:225–248.
- Whitfield, C.J., S.A. Watmough, J. Aherne, and P.J. Dillon. 2006. A comparison of weathering rates for acid-sensitive catchments in Nova Scotia, Canada and their impact on critical load calculations. *Geoderma* 136: 899-911.



# **ATTACHMENT A:**

## **RELATIONSHIP BETWEEN ATMOSPHERIC NITROGEN AND SULFUR DEPOSITION AND SUGAR MAPLE AND RED SPRUCE TREE GROWTH**

### **1. INTRODUCTION**

Nitrogen and sulfur deposition in forest systems can have either positive or negative impacts on tree growth. The growth of many forests in North America is limited by nitrogen availability (Chapin et al., 1993; Killam, 1994; Miller, 1988), and nitrogen fertilization is often a key component of forest management (Allen, 2001). Therefore, in such nitrogen-limited systems, nitrogen deposition may stimulate tree growth. In contrast, nitrogen additions in some systems can sometimes be greater than what trees require and can negatively impact tree health and growth (Aber et al., 1995; McNulty et al., 2005). Forests where atmospheric deposition of nitrogen and sulfur is greater than the critical load may be examples of such a condition. When critical loads are exceeded, tree health and growth may be compromised both directly and indirectly because of soil nutrient deficiencies and imbalances caused by acidic deposition and the leaching of base cations from the soil. Tree growth may be reduced and/or trees may have an increased susceptibility to drought and pest damage, aluminum (Al) toxicity in roots, reduced tolerance to cold, and a greater propensity to frost injury (Driscoll et al., 2001; DeHayes et al., 1999; Fenn et al., 2006b; McNulty et al., 2005; Ouimet et al., 2008). In the context of acidifying deposition of nitrogen and sulfur, the positive versus negative impact of deposition on tree growth may depend largely upon whether the critical load is exceeded by the deposition level and may follow a modified version of the inverted U-shape relationship hypothesized by Aber et al. (1995) for forest systems that receive chronic, long-term nitrogen additions (**Figure 1-1**). If nitrogen and sulfur deposition is less than the critical load, tree growth may be stimulated because of a fertilizer effect of nitrogen deposition. Conversely, when the deposition is greater than the critical load, tree vigor and growth may be reduced because of the negative impacts of soil acidification. The transition point between growth stimulation and impairment would occur when deposition is equal to the critical load.

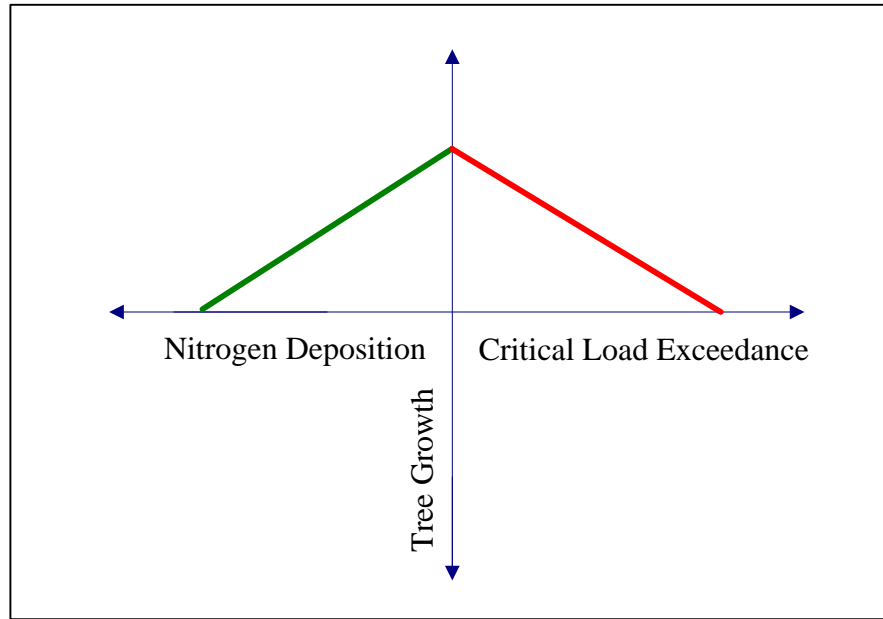


**Figure 1-1.** Hypothesized relationships between tree growth and nitrogen deposition and critical load exceedance. When deposition does not exceed the critical load, growth is stimulated by nitrogen deposition. When deposition exceeds the critical load (deposition is greater than the critical load), growth is reduced. (This figure is a modification of a curve describing forest productivity as a function of long-term chronic nitrogen additions outlined in Aber et al., 1995).

To assess the impacts of nitrogen and sulfur deposition on sugar maple and red spruce in the Terrestrial Acidification Case Study, the relationships between net annual volume growth and (1) nitrogen deposition and (2) critical load exceedance were examined empirically across the geographical ranges of the two species.

## 2. SOURCE OF DATA FOR ANALYSES

Data from plots in the U.S. Forest Service (USFS) Forest Inventory and Analysis (FIA) database used in Section 4 of the Terrestrial Acidification Case Study (Appendix 5) were applied to this assessment. Highest protection level critical loads ( $B_c/AI = 10.0$ ), 2002 CMAQ/NADP nitrogen and sulfur deposition, and USFS FIA database net annual individual tree volume

growth<sup>10</sup> and tree volume<sup>11</sup> for all live sugar maple and red spruce trees in each plot were used in the analyses. Critical load exceedances and nitrogen deposition were determined using the 2002 CMAQ/NADP modeled nitrogen and sulfur deposition estimates. The tree volumes and annual growth values were from the most recent FIA measurement period, and the interval between measurements (to determine growth rates) for the plots ranged from 1 to 11 years. Trees with negative growth values (but that were not dead) were included in the analyses to account for the potential indirect impacts of nitrogen and sulfur deposition. All trees that had “0” volume values were excluded from the analyses. Given these data restrictions, a total of 1,059 sugar maple and 419 red spruce plots were included in the tree volume growth–nitrogen deposition regression analyses, and a total of 2,988 sugar maple and 194 red spruce plots were included in the tree growth–critical load exceedance analyses. Volumes and volume growth for the sugar maple and red spruce trees in each plot were averaged to produce single values of each parameter for each species. **Tables 2-1 and 2-2** summarize the plot-level FIA sugar maple and red spruce data used to model the relationships between tree growth and nitrogen deposition and critical load exceedance.

---

<sup>10</sup> FGROWCFAL or GROWCFAL (i.e., the net annual sound cubic-foot growth of a live tree (of trees  $\geq 12.7$  cm diameter). Growth values may be negative because of loss of volume due to death or damage, rot, broken top, or other natural causes. Source: FIA database (USFS, 2008c).

<sup>11</sup> VOLCFNET (i.e., the net cubic foot volume of wood in the central stem of a tree, beginning at 12.7 cm in diameter or larger up the stem to a minimum 10.16 cm top outer-bark diameter. This measurement does not include rotten, missing, and form cull. Source: FIA database (USFS, 2008c).

**Table 2-1.** Summary of Plot-Level Data Used in the Regression Analyses for Sugar Maple Volume and Growth, Nitrogen Deposition, and Critical Load Exceedances (based on critical loads calculated with Bc/Al = 10.0)

State	Total Number of Plots	NITROGEN DEPOSITION REGRESSION ANALYSIS				CRITICAL LOAD EXCEEDANCE REGRESSION ANALYSIS			
		Number of Plots with N+S Deposition Lower Than CL	Average Nitrogen Deposition (eq/ha/yr)	Average Tree Volume Growth (m <sup>3</sup> /yr)	Average Tree Volume (m <sup>3</sup> )	Number of Plots with N+S Deposition Greater Than CL	Average Critical Load Exceedance (eq/ha/yr)	Average Tree Volume Growth (m <sup>3</sup> /yr)	Average Tree Volume (m <sup>3</sup> )
Alabama	12	9	821.9	0.0111	0.5254	3	434.8	0.0094	0.1171
Arkansas	8	7	676.3	0.0098	0.3469	1	105.7	0.0098	0.3539
Connecticut	33	–	–	–	–	33	487.8	0.0093	0.2787
Illinois	25	8	796.1	0.0093	0.2967	17	145.1	0.0070	0.2009
Indiana	266	31	899.0	0.0177	0.5649	235	439.8	0.0169	0.3856
Iowa	8	6	881.3	0.0114	0.2329	2	48.1	0.0053	0.1234
Kentucky	14	2	815.2	0.0129	0.4126	12	412.3	0.0154	0.3563
Maine	242	191	393.9	0.0079	0.2696	51	130.4	0.0105	0.3229
Maryland	4	–	–	–	–	4	599.9	0.0102	0.3734
Massachusetts	27	–	–	–	–	27	473.3	0.0029	0.3657
Michigan	596	178	563.2	0.0055	0.2995	418	242.2	0.0109	0.3069
Minnesota	257	178	618.8	0.0074	0.2482	79	156.1	0.0101	0.2555
Missouri	122	64	717.9	0.0072	0.2422	58	171.5	0.0051	0.2462
New Hampshire	72	12	457.1	0.0053	0.1963	60	378.4	0.0088	0.3043
New Jersey	6	–	–	–	–	6	601.4	0.0125	0.3569
New York	280	16	677.1	0.0097	0.5243	264	437.9	0.0101	0.3443
North Carolina	13	4	663.7	–0.0038	0.6127	9	299.3	0.0158	0.3777
Ohio	55	1	846.0	0.0033	0.0892	54	554.6	0.0115	0.3854



State	Total Number of Plots	NITROGEN DEPOSITION REGRESSION ANALYSIS				CRITICAL LOAD EXCEEDANCE REGRESSION ANALYSIS			
		Number of Plots with N+S Deposition Lower Than CL	Average Nitrogen Deposition (eq/ha/yr)	Average Tree Volume Growth (m <sup>3</sup> /yr)	Average Tree Volume (m <sup>3</sup> )	Number of Plots with N+S Deposition Greater Than CL	Average Critical Load Exceedance (eq/ha/yr)	Average Tree Volume Growth (m <sup>3</sup> /yr)	Average Tree Volume (m <sup>3</sup> )
Pennsylvania	270	7	707.7	0.0185	0.3778	263	557.9	0.0115	0.3576
Tennessee	264	132	770.4	0.0111	0.3179	132	161.7	0.0128	0.3486
Vermont	162	2	743.4	0.0092	0.2935	160	301.7	0.0077	0.4112
Virginia	104	41	712.2	0.0130	0.2827	63	291.6	0.0126	0.3012
West Virginia	337	19	768.2	0.0148	0.2824	318	352.1	0.0104	0.2825
Wisconsin	870	151	733.0	0.0107	0.3078	719	185.2	0.0087	0.3040
Total Observations (used in calculations)	4,047	1,059	1,059	1,059	1,059	2,988	2,988	2,988	2,988

**Table 2-2.** Summary of Plot-Level Data Used in the Regression Analyses for Red Spruce Volume and Growth, Nitrogen Deposition, and Critical Load Exceedances (based on critical loads calculated with  $Bc/Al = 10.0$ )

State	Total Number of Plots	NITROGEN DEPOSITION REGRESSION ANALYSIS				CRITICAL LOAD EXCEEDANCE REGRESSION ANALYSIS			
		Number of Plots with N+S Deposition Lower Than CL	Average Nitrogen Deposition (eq/ha/yr)	Average Tree Volume Growth (m <sup>3</sup> /yr)	Average Tree Volume (m <sup>3</sup> )	Number of Plots with N+S Deposition Greater Than CL	Average Critical Load Exceedance (eq/ha/yr)	Average Tree Volume Growth (m <sup>3</sup> /yr)	Average Tree Volume (m <sup>3</sup> )
Maine	483	405	390.3	0.0075	0.2487	78	133.1	0.0074	0.2446
Massachusetts	3	–	–	–	–	3	628.5	0.0040	0.2028
New Hampshire	42	10	450.1	0.0060	0.1826	32	369.0	0.0063	0.2451
New York	18	4	615.0	0.0066	0.6146	14	282.5	0.0044	0.2210
Tennessee	1	–	–	–	–	1	420.2	0.0196	0.4634
Vermont	60	–	–	–	–	60	292.4	0.0073	0.3281
West Virginia	6	–	–	–	–	6	257.6	0.0109	0.3289
Total Observations (used in calculations)	613	419	419	419	419	194	194	194	194

### **3. REGRESSION ANALYSES METHODOLOGY AND RESULTS**

The impacts of nitrogen deposition and critical load exceedance on individual tree volume growth of sugar maple and red spruce were examined empirically using multivariate ordinary least squares (OLS) linear regression analyses, testing the positive and negative linear relationships represented in **Figure 1-1**. Plots where 2002 nitrogen and sulfur deposition did not exceed the critical load (based on  $Bc/Al = 10.0$  critical load estimates) were used in the tree volume growth–nitrogen deposition analyses, and plots where deposition exceeded the critical load were used in the regression analyses comparing critical load exceedance and volume growth (**Tables 2-1 and 2-2**). In both sets of analyses for both species, the explanatory variables included the linear term of nitrogen deposition or critical load exceedance (both expressed as equivalents per hectare per year [eq/ha/year]) for each plot, linear and squared terms of average tree volumes in cubic meters ( $m^3$ ), and a categorical (dummy) variable for each State (with Arkansas and Connecticut arbitrarily selected as the reference categories for sugar maple for the nitrogen deposition and critical load exceedance regressions, respectively. For red spruce, New York was selected for the nitrogen deposition regression, and Vermont was selected for the critical load exceedance regression). Tree volume was included as an explanatory variable of tree growth because tree age, the preferred explanatory variable, was not available for this dataset. Tree age and tree volume are highly correlated, and volume growth is influenced by tree size, so tree volume was seen as an appropriate surrogate explanatory variable. The State variables were included in the analyses to control for unobserved sources of variation in tree growth related to a plot's general geographic location. Examples of potential unobserved factors include differences in data collection methods and measurements across reporting State, climatic factors, and geological characteristics.

The results of the linear regression analyses to test the influences of nitrogen deposition and critical load exceedance on sugar maple and red spruce volume growth are presented in **Tables 3-1a–b and 3-2a–b**, respectively.

**Table 3-1a.** Results from the Multivariate Ordinary Least Squares Linear Regression Analyses of Sugar Maple Tree Growth and Nitrogen Deposition (for plots where deposition did not exceed critical loads calculated with Bc/AI = 10.0)

Explanatory Variables	Dependent Variable: Average Tree Growth (m <sup>3</sup> /yr)		
	Coefficient	t-statistic	p-value
Intercept	-0.00278	-0.53	0.5965
Nitrogen Deposition	$1.22 \times 10^{-5}$	3.22	0.0013
Average Tree Volume	0.01296	6.44	<0.0001
Square of Average Tree Volume	$-8.32 \times 10^{-4}$	-1.39	0.1645
Alabama	-0.00242	-0.39	0.6941
Illinois	-0.00131	-0.21	0.8350
Indiana	0.00338	0.65	0.5139
Iowa	$5.19 \times 10^{-4}$	0.08	0.9392
Kentucky	$6.37 \times 10^{-4}$	0.07	0.9479
Maine	0.00249	0.52	0.6034
Michigan	-0.00238	-0.51	0.6134
Minnesota	$-4.20 \times 10^{-4}$	-0.09	0.9286
Missouri	-0.00167	-0.34	0.7302
New Hampshire	$-3.34 \times 10^{-6}$	0.00	0.9995
New York	-0.00190	-0.35	0.7301
North Carolina	-0.01658	-2.17	0.0299
Ohio	-0.00535	-0.41	0.6812
Pennsylvania	0.00790	1.22	0.2241
Tennessee	$5.46 \times 10^{-4}$	0.12	0.9080
Vermont	$-7.88 \times 10^{-4}$	-0.08	0.9356
Virginia	0.00360	0.72	0.4693
West Virginia	0.00468	0.87	0.3847
Wisconsin	$6.76 \times 10^{-4}$	0.14	0.8858
Number of Observations	1,059		
Adjusted R <sup>2</sup>	0.1175		

**Table 3-1b.** Results from the Multivariate Ordinary Least Squares Linear Regression Analyses of Red Spruce Tree Growth and Nitrogen Deposition (for plots where deposition did not exceed critical loads calculated with  $Bc/Al = 10.0$ )

Explanatory Variables	Dependent Variable: Average Tree Growth ( $m^3/yr$ )		
	Coefficient	t-statistic	p-value
Intercept	0.00704	1.57	0.1166
Nitrogen Deposition	$-6.69 \times 10^{-6}$	-1.12	0.2679
Tree Volume	0.00955	3.72	0.0002
Square of Tree Volume	-0.00528	-2.31	0.0215
Maine	0.00121	0.44	0.6626
New Hampshire	$4.5 \times 10^{-4}$	0.15	0.8825
Number of Observations	419		
Adjusted $R^2$	0.0351		

**Table 3-2a.** Results from the Multivariate Ordinary Least Squares Linear Regression Analyses of Sugar Maple Tree Growth and Critical Load Exceedance (for plots where nitrogen and sulfur deposition was greater than critical loads calculated with  $Bc/Al = 10.0$ )

Explanatory Variables	Dependent Variable: Average Tree Growth ( $m^3/yr$ )		
	Coefficient	t-statistic	p-value
Intercept	0.00430	1.35	0.1787
Critical Load Exceedance	$-1.43 \times 10^{-6}$	-0.92	0.3571
Average Tree Volume	0.02001	10.81	<0.0001
Square of Average Tree Volume	$2.58 \times 10^{-4}$	0.34	0.7365
Alabama	0.00341	0.32	0.7523
Illinois	-0.00112	-0.21	0.8347
Indiana	0.00544	1.65	0.0991
Iowa	-0.00142	-0.11	0.9135
Kentucky	0.00449	0.74	0.4564
Maine	$-1.12 \times 10^{-4}$	-0.03	0.9776
Maryland	$-7.89 \times 10^{-4}$	-0.08	0.9337
Massachusetts	-0.00814	-1.76	0.0786
Michigan	$7.77 \times 10^{-4}$	0.24	0.8095
Minnesota	$8.48 \times 10^{-4}$	0.23	0.8194
Missouri	-0.00389	-1.00	0.3192

Explanatory Variables	Dependent Variable: Average Tree Growth (m <sup>3</sup> /yr)		
	Coefficient	t-statistic	p-value
New Hampshire	-0.00120	-0.31	0.7556
New Jersey	0.00190	0.24	0.8108
New York	-5.42 x 10 <sup>-4</sup>	-0.17	0.8685
North Carolina	0.00431	0.64	0.5226
Ohio	1.85 x 10 <sup>-4</sup>	0.05	0.9626
Pennsylvania	8.33 x 10 <sup>-4</sup>	0.25	0.7994
Tennessee	0.00172	0.49	0.6225
Vermont	-0.00448	-1.32	0.1879
Virginia	0.00261	0.68	0.4957
West Virginia	9.14 x 10 <sup>-4</sup>	0.28	0.7783
Wisconsin	-0.00151	-0.48	0.6347
Number of Observations	2,988		
Adjusted R <sup>2</sup>	0.1329		

**Table 3-2b.** Results from the Multivariate Ordinary Least Squares Linear Regression Analyses of Red Spruce Tree Growth and Critical Load Exceedance (for plots where nitrogen and sulfur deposition was greater than critical loads calculated with Bc/Al = 10.0)

Explanatory Variables	Dependent Variable: Average Tree Growth (m <sup>3</sup> /yr)		
	Coefficient	t-statistic	p-value
Intercept	0.00628	5.15	<0.0001
Critical Load Exceedance	-5.62 x 10 <sup>-6</sup>	-2.30	0.0223
Tree Volume	0.00611	1.38	0.1685
Square of Tree Volume	0.00463	1.11	0.2705
Maine	1.26 x 10 <sup>-5</sup>	0.01	0.9890
Massachusetts	-1.73 x 10 <sup>-4</sup>	-0.06	0.9524
New Hampshire	2.68 x 10 <sup>-4</sup>	0.25	0.7993
New York	-0.00200	-1.43	0.1549
West Virginia	0.00331	1.64	0.1020
Number of Observations	194		
Adjusted R <sup>2</sup>	0.2009		

The results of the linear regressions analyzing the relationships between nitrogen deposition and tree volume growth differed by species. For sugar maple, nitrogen deposition had a positive and significant (at the  $p < 0.05$  level,  $p = 0.00013$ ) impact on the aboveground volume growth of individual trees (**Table 3-1a**). These results suggest that the 2002 nitrogen additions, that ranged from 332 to 1,146 eq/ha/yr (4.7 to 16.1 kg N/ha/yr), acted as a fertilizer and stimulated growth on sites where nitrogen and sulfur deposition did not exceed the critical load. On these sites, nitrogen most likely posed a limitation to sugar maple growth. There are few studies that have demonstrated a positive growth response of sugar maple to nitrogen additions. Stone (1986) found that sugar maple diameter growth was not impacted by nitrogen 100 to 300 kg N/ha fertilizers applied three years before or after thinning, and similar results have been determined in other studies (see references in Stone, 1986). In contrast to sugar maple, the red spruce in the tree growth–nitrogen deposition analyses displayed a negative, nonsignificant (at the  $p < 0.05$  level,  $p = 0.2679$ ) relationship between deposition and growth (**Table 3-1b**). These results suggest that red spruce growth may not have been limited by nitrogen on sites where the critical load was not exceeded by nitrogen and sulfur deposition; nitrogen deposition in the range of 255 to 667 eq/ha/yr (3.6 to 9.3 kg N/ha/yr) did not stimulate the growth of red spruce. Briggs et al. (2000) reported that diameter growth of red spruce was unchanged by the application of 200 kg N/ha on pre-commercially thinned spruce-fir stands in Maine. McNulty et al. (2005) found that although ambient nitrogen deposition of 5.4 kg N/ha/yr over the course of 14 years was associated with a 20% increase in basal area of a red spruce–dominated spruce-fir forest, supplemental additions of 15.4 kg N/ha/yr resulted in a 20% decrease in live basal area. Therefore, the documented response of red spruce to nitrogen additions is mixed.

The results of the analyses determining the relationships between critical load exceedance and tree growth showed similar trends for both sugar maple and red spruce; growth declined with increasing levels of critical load exceedance. For red spruce, the relationship was significant at the 5% level ( $p = 0.0223$ ) and negative, indicating that red spruce growth may be negatively impacted by deposition levels that exceed the critical load (**Table 3-2b**). Decreased basal area of red spruce in response to chronic additions of nitrogen have been reported in several other studies (Aber et al., 1995; McNulty et al., 2005), and authors of these studies speculated that these negative growth responses were due to sites reaching a level of nitrogen saturation. Although the tree growth–critical load exceedance relationship was also negative for sugar

maple, it was not statistically significant at the 5% level ( $p=0.3571$ ), suggesting that sugar maple may not be negatively impacted by nitrogen and sulfur deposition levels greater than critical loads (**Table 3-2a**). However, shortcomings of at least one of the variables used within the SMB calculations of critical loads may, in part, have contributed to the lack of a significant relationship between tree growth and critical load exceedance. As discussed in Appendix 5, the base cation weathering ( $BC_w$ ) term that accounts for the contributions of base cations from the weathering of soil minerals and parent material is one of the most influential terms in the SMB model. Li and McNulty (2007) determined that 49% of the variability in critical load estimates was due to this term. Within the United States and Canada,  $BC_w$  for critical load assessments is commonly estimated using the clay-substrate model (Ouimet et al., 2006; Watmough et al., 2006; McNulty et al., 2007; Pardo and Duarte, 2007), and this model was also used in the Terrestrial Acidification Case Study. Critical load experts from both the United States and Canada have commented that the clay-substrate model method performs well in young soils that have formed since the last glaciation (20,000 years before present (ybp)), but may not be suitable for older, more weathered soils south of the most recent glacial advancement. Therefore, to account for the potential influence of a poorer estimation of  $BC_w$  in plots south of the glaciation line (**Figure 3-1**), a second set of multivariate, OLS linear regression analyses were conducted, using the same specifications (i.e., plots where nitrogen and sulfur deposition exceeded the critical load calculated with  $Bc/Al=10.0$ ), as described above. However, these analyses were restricted to data from plots that had been covered by the last glaciation (i.e., north of the glaciation line). Limiting the analysis to plots north of the glaciation line led to analyzing 4% fewer red spruce plots and 26% fewer sugar maple plots (**Tables 3-3 and 3-4**).



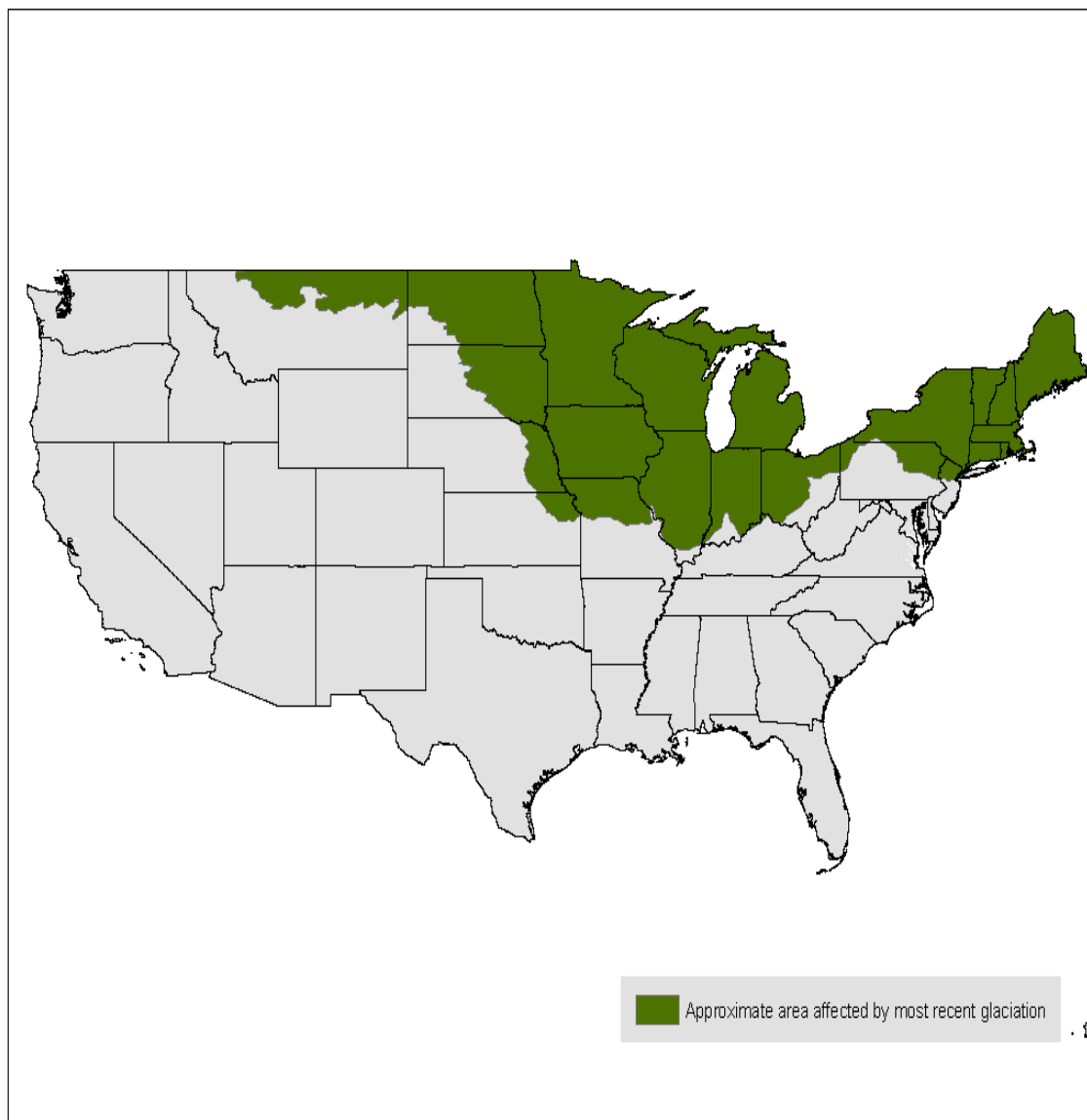


**Figure 3-1.** Areas of the continental United States that were covered during the last glacial event (~ 20,000 ybp) (Reed and Bush, 2005).

**Table 3-3.** Summary of Plot-Level Data for Sugar Maple Volume and Growth and Critical Load Exceedances North of the Glaciation Line (for plots where nitrogen and sulfur deposition exceeded critical loads calculated with Bc/Al = 10.0)

State	Total Number of Plots with N+S Deposition Greater Than CL	Number of Plots North of the Glaciation Line with N+S Deposition Greater Than CL	Average CL Exceedance (eq/ha/yr)	Average Tree Volume Growth (m <sup>3</sup> /yr)	Average Tree Volume (m <sup>3</sup> )
Alabama	3	0	NA	NA	NA
Arkansas	1	0	NA	NA	NA
Connecticut	33	33	487.76	0.009	0.279
Illinois	17	12	117.17	0.007	0.227
Indiana	235	204	390.90	0.018	0.397
Iowa	2	2	48.07	0.005	0.123
Kentucky	12	0	NA	NA	NA
Maine	51	51	130.42	0.011	0.323
Maryland	4	0	NA	NA	NA
Massachusetts	27	27	473.31	0.003	0.366
Michigan	418	418	242.17	0.011	0.307
Minnesota	79	79	156.06	0.010	0.256
Missouri	58	18	84.02	0.012	0.246
New Hampshire	60	60	378.40	0.009	0.304
New Jersey	6	6	601.39	0.013	0.357
New York	264	264	437.94	0.010	0.344
North Carolina	9	0	NA	NA	NA
Ohio	54	26	452.60	0.013	0.545
Pennsylvania	263	126	387.35	0.011	0.366
Tennessee	132	0	NA	NA	NA
Vermont	160	160	301.67	0.008	0.411
Virginia	63	0	NA	NA	NA
West Virginia	318	0	NA	NA	NA
Wisconsin	719	719	185.16	0.009	0.304
Total Observations (used in calculations)	2,988	2,205	2,205	2,205	2,205

NA = not applicable. Average Critical Load Exceedance, Average Tree Volume Growth, and Average Tree Volume values could not be determined because there were no sugar maple plots north of the glaciation line.

State	Total Number of Plots with N+S Deposition Greater than CL	Number of Plots with N+S Deposition Greater than CL North of Glaciation Line	Average CL Exceedance (eq/ha/yr)	Average Tree Volume Growth (m <sup>3</sup> /yr)	Average Tree Volume (m <sup>3</sup> )
Alabama	3	0	NA	NA	NA
Arkansas	1	0	NA	NA	NA
Connecticut	33	33	487.76	0.009	0.279
Illinois	17	12	117.17	0.007	0.227
Indiana	235	204	390.90	0.018	0.397
Iowa	2	2	48.07	0.005	0.123
Kentucky	12	0	NA	NA	NA
Maine	51	51	130.42	0.011	0.323
Maryland	4	0	NA	NA	NA
Massachusetts	27	27	473.31	0.003	0.366
Michigan	418	418	242.17	0.011	0.307
Minnesota	79	79	156.06	0.010	0.256
Missouri	58	18	84.02	0.012	0.246
New Hampshire	60	60	378.40	0.009	0.304
New Jersey	6	6	601.39	0.013	0.357
New York	264	264	437.94	0.010	0.344
North Carolina	9	0	NA	NA	NA
Ohio	54	26	452.60	0.013	0.545
Pennsylvania	263	126	387.35	0.011	0.366
Tennessee	132	0	NA	NA	NA
Vermont	160	160	301.67	0.008	0.411
Virginia	63	0	NA	NA	NA
West Virginia	318	0	NA	NA	NA
Wisconsin	719	719	185.16	0.009	0.304
<b>TOTAL Observations (used in calculations)</b>	<b>2988</b>	<b>2205</b>	<b>2205</b>	<b>2205</b>	<b>2205</b>

**Table 3-4.** Summary of Plot-Level Data for Red Spruce Volume and Growth and Critical Load Exceedances North of the Glaciation Line (for plots where nitrogen and sulfur deposition exceeded critical loads calculated with  $Bc/Al = 10.0$ )

State	Total Number of Plots with N+S Deposition Greater Than CL	Number of Plots with N+S Deposition Greater Than CL North of Glaciation Line	Average CL Exceedance (eq/ha/yr)	Average Tree Volume Growth (m <sup>3</sup> /yr)	Average Tree Volume (m <sup>3</sup> )
Maine	78	78	133.1048	0.007	0.245
Massachusetts	3	3	628.5439	0.004	0.203
New Hampshire	32	32	368.9527	0.006	0.245
New York	14	14	282.5433	0.004	0.221
Tennessee	1	0	NA	NA	NA
Vermont	60	60	292.4329	0.007	0.328
West Virginia	6	0	NA	NA	NA
Total Observations (used in calculations)	194	187	187	187	187

NA = not applicable. Average Critical Load Exceedance, Average Tree Volume Growth, and Average Tree Volume values could not be determined because there were no red spruce plots north of the glaciation line.

The results from the linear regression analyses for sugar maple and red spruce, north of the glaciation line, are presented in **Tables 3-5 and 3-6**, respectively. Similar to the first linear regression analyses that included all critical load exceedance plots, the relationship between tree growth and critical load exceedance was negative for both species and was statistically significant at the 5% level ( $p$ -value of 0.0354) for red spruce. However, in contrast to the first linear regression analyses, the relationship for the sugar maple plots north of the glaciation line was significant at the 10% level ( $p$ -value of 0.1008), and occurred despite the 26% reduction of plots used in the analysis. These results suggest that a larger portion of the variation in sugar maple growth could be accounted for by critical load exceedance when the analysis was restricted to plots north of the glaciation line and lend support to the hypothesis that the clay-substrate model to estimate  $BC_w$  may not be suitable for older soils. Future assessment of critical

loads may, therefore, want to consider exploring other  $BC_w$  models to estimate critical loads of atmospheric nitrogen and sulfur deposition. Models such as PROFILE (Sverdrup and Warfvinge, 1993a), which are based on soil mineralogy, may provide better estimates of the contribution of base cations from soil weathering.

**Table 3-5.** Results from the Multivariate Ordinary Least Squares Linear Regression Analyses of Sugar Maple Tree Growth and Critical Load Exceedance North of the Glaciation Line (for plots where deposition exceeded critical loads calculated with  $Bc/Al = 10.0$ )

Explanatory Variables	Dependent Variable: Average Tree Growth ( $m^3/yr$ )		
	Coefficient	t-statistic	p-value
Intercept	0.004875	1.48	0.1385
Critical Load Exceedance	$-3.344 \times 10^{-6}$	-1.64	0.1008
Average Tree Volume	0.021150	10.12	<.0001
Square of Average Tree Volume	$8.944 \times 10^{-4}$	1.1	0.27
Illinois	-0.001884	-0.31	0.755
Indiana	0.005452	1.63	0.1029
Iowa	-0.002052	-0.16	0.8743
Maine	-0.000895	-0.22	0.8245
Massachusetts	-0.008403	-1.82	0.0685
Michigan	0.000222	0.07	0.9456
Minnesota	0.000210	0.06	0.9553
Missouri	0.001850	0.35	0.7255
New Hampshire	-0.001647	-0.43	0.6696
New Jersey	0.001956	0.25	0.8042
New York	-0.000817	-0.25	0.8035
Ohio	-0.002104	-0.45	0.6522
Pennsylvania	-0.000803	-0.23	0.8177
Vermont	-0.005168	-1.51	0.131
Wisconsin	-0.002195	-0.68	0.4958
Number of Observations	2,205		
Adjusted $R^2$	0.1722		

**Table 3-6.** Results from the Multivariate Ordinary Least Squares Linear Regression Analyses of Red Spruce Tree Growth and Critical Load Exceedance, North of the Glaciation Line (for plots where deposition exceeded critical loads calculated with  $Bc/AI = 10.0$ )

Explanatory Variables	Dependent Variable: Average Tree Growth ( $m^3/yr$ )		
	Coefficient	t-statistic	p-value
Intercept	0.006034	4.96	<.0001
Critical Load Exceedance	$-5.162 \times 10^{-6}$	-2.12	0.0354
Tree Volume	0.005590	1.26	0.2093
Square of Tree Volume	$5.100 \times 10^{-3}$	1.23	0.2218
Maine	0.000285	0.32	0.7489
Massachusetts	-0.000132	-0.05	0.9629
New Hampshire	0.000435	0.42	0.6736
New York	-0.001805	-1.32	0.1897
Number of Observations	187		
Adjusted $R^2$	0.1963		

#### 4. ADDITIONAL SOURCES OF VARIABILITY INFLUENCING THE RELATIONSHIPS BETWEEN TREE VOLUME GROWTH AND NITROGEN DEPOSITION AND CRITICAL LOAD EXCEEDANCE

In addition to potential inaccuracy in the  $BC_w$  variable in the estimation of critical loads, there are additional sources of variation that may have influenced the relationships between critical load exceedance and the growth of red spruce and sugar maple. These sources of variability may have also influenced the relationships between tree growth and nitrogen deposition.

##### 4.1 State-Specific Variables

Although State dummy variables and current tree volume were included as covariates in the regression analyses to account for the influences of location and tree size on tree growth, additional factors could be included in future regression analyses. For example, incorporating latitude/longitude and elevation in analyses could remove the influence of location on tree growth. Similarly, site index could remove the influence of site quality on the growth of red spruce and sugar maple. Total basal area of the stand would remove the influence of stand

density and site occupancy. Measurement year and time between measurements could help remove the influence of year-to-year variation in conditions and measurement methodology on the growth data. Climatic variation (e.g., rainfall, temperature) could be included to account for the influence of drought and frost conditions (McNulty and Boggs, in press) on tree growth. It is recommended that future analyses comparing tree growth and nitrogen deposition or critical load exceedance take additional sources of variability into account. Much of this data is included in the FIA database.

#### **4.2 Dead Trees**

The regression relationship between tree growth and nitrogen deposition or critical load exceedance may also be improved with the inclusion of dead trees in the analyses. In the FIA database, when a tree is recorded as dead for the first time, the total volume of that tree is considered negative volume growth over the most recent measurement period.<sup>12</sup> As described earlier, atmospheric deposition of nitrogen and sulfur can indirectly result in tree mortality. Therefore, it may be appropriate to include tree mortality in an evaluation of the relationship between tree growth and nitrogen deposition or critical load exceedance. However, the validity of including dead tree negative volume growth measurements (as calculated by the FIA database) in the regression analyses was uncertain, and, therefore, the inclusion of dead trees was not pursued in the analyses reported in this Attachment.

#### **4.3 Other Factors**

The FIA sugar maple and red spruce tree data used in the analyses may have also introduced variability and a source of error in the analyses. As discussed in Appendix 5, due to restriction factors, not all sugar maple and red spruce plots were included in the analyses. It is uncertain to what degree, if any, these restrictions may have biased the results. The influence of

---

<sup>12</sup> Dead tree volume growth is calculated as a difference in volumes ( $v_2 - v_1$ ) divided by the time between sequential measurement period ( $t_2 - t_1$ ). When a tree is recorded as dead, it is assigned a  $v_2$  value of "0." Therefore, the associated volume growth is equal to the entire tree volume divided by the difference in the number of years between the current and last measurement cycle.

tree ingress<sup>13</sup> may also not have been completely accounted for in the analyses and may have introduced another source of error. According to USFS FIA database methodology, trees must be at least 12.7 centimeters (cm) in diameter to be included in the VOLCFNET (total net volume per tree) tree volume table. When they reach this size, the full volume of the stem is incorporated into the volume growth measurements, and, in many cases, these measurements would be larger than the actual annual growth rates. Trees with 0 m<sup>3</sup> VOLCFNET volume values were excluded from the analyses to at least partially account for this influence. With the data that were made available for the analyses, it was not possible to determine other possible ingress trees. The use of VOLCFNET tree volume as a covariate of FGROWCFAL (net annual sound cubic-foot growth of a live tree on forest land) tree growth may have also introduced a small source of error. VOLCFNET is based on merchantable volume (e.g., pulp and sawlog), whereas FGROWCFAL is based on growth of sound wood. The difference between the two measurements is cull wood that is sound but not merchantable due to circumstances such as the location on the tree or tree branchiness. The removal of trees with 0 m<sup>3</sup> VOLCFNET volume from the analyses removed at least a portion of the trees that would increase the influence of cull wood on the covariate relationship between the two variables. Measurement error may also have introduced another source of error to the analyses. Tree volumes and volume growth are based on the measurements conducted on the main stem of the tree. Slight differences in measurements conducted by different crews and in different years could have introduced some error to the volume and growth estimates. Based on the FIA data provided by the USFS, it was not possible to determine the degree to which each of these various source of error influenced the data, nor was it possible to determine if reduction or elimination of these sources of error would change and/or improve the regression analyses. Attempts to minimize these potential sources of error are recommended in future analyses of the relationships between tree growth and nitrogen deposition and critical load exceedance.

---

<sup>13</sup> “Ingress” refers to trees that appear that are included in the dataset for the first time. Usually ingress is a result of trees reaching a certain size, but occasionally, ingress can also occur when new trees are included in the measurements. Steps are taken to identify these new trees and estimate previous size and growth, but sometimes they may be missed.



## **5. CONCLUSIONS**

In conclusion, the results from these analyses do suggest that nitrogen and sulfur deposition can result in either a positive or negative impact of tree volume growth. When deposition levels do not exceed the critical load of a site, tree growth may be stimulated by the nitrogen additions, as was seen in the sugar maple analyses. Conversely, when critical loads are exceeded by nitrogen and sulfur deposition, tree growth may be negatively impacted. This negative growth trend was seen in both the red spruce and sugar maple (restricted to plots North of the glaciation line). The trends suggested by these results indicate that large-scale analyses using the USFS FIA database may provide a useful tool with which to examine both the positive and negative impacts of nitrogen and sulfur deposition on tree species in the United States.



September 2009

# **Appendix 6**

## **Aquatic Nutrient Enrichment Case Study**

***Final***

EPA Contract Number EP-D-06-003  
Work Assignment 3-62  
Project Number 0209897.003.062

### **Prepared for**

U.S. Environmental Protection Agency  
Office of Air Quality Planning and Standards  
Research Triangle Park, NC 27709

### **Prepared by**

RTI International  
3040 Cornwallis Road  
Research Triangle Park, NC 27709-2194





## TABLE OF CONTENTS

Acronyms and Abbreviations .....	v
1.0 Background .....	1
1.1 Indicators, Ecological endpoints, and Ecosystem Services .....	4
1.2 Case Studies .....	9
1.2.1 National Overview of Sensitive Areas .....	9
1.2.2 Use of ISA Information and Rationale for Site Selection .....	12
1.2.3 Potomac River and Potomac Estuary .....	17
1.2.4 Neuse River and Neuse River Estuary .....	20
2.0 Approach and Methods .....	26
2.1 Modeling .....	27
2.2 Chosen Method .....	30
2.2.1 SPARROW .....	31
2.2.1.1 Background and Description .....	31
2.2.1.2 Key Definitions for Understanding SPARROW Modeling .....	36
2.2.1.3 Concepts of Importance to Case Study—SPARROW Application .....	38
2.2.2 ASSETS Eutrophication Index .....	39
2.2.2.1 Background and Description .....	39
2.2.2.2 Applications and Updates .....	46
2.2.3 Assessments Using Linked SPARROW and ASSETS EI .....	46
2.2.3.1 Back Calculation Method .....	52
2.2.3.2 Uncertainty Bounds on TN <sub>s</sub> , OEC Min/Max Values .....	53
3.0 Results .....	59
3.1 Current Conditions .....	59
3.1.1 Summary of Results for the Potomac River/Potomac Estuary Case Study Area .....	59
3.1.1.1 SPARROW Assessment .....	60
3.1.1.2 ASSETS EI Assessment .....	66
3.1.2 Summary of Results for the Neuse River/Neuse River Estuary Case Study Area .....	70
3.1.2.1 SPARROW Assessment .....	70
3.1.2.2 ASSETS EI Assessment .....	77
3.2 Alternative Effects Levels .....	80
3.2.1 Potomac River Watershed .....	80
3.2.2 Neuse River Watershed .....	89
4.0 Implications for Other Systems .....	98
5.0 Uncertainty .....	101
6.0 Conclusions .....	105
7.0 References .....	105

## LIST OF FIGURES

Figure 1.1-1. Descriptions of the five eutrophication indicators used in NOAA's NEEA (Bricker et al., 2007a). .....	6
Figure 1.1-2. A simplified schematic of eutrophication effects on an aquatic ecosystem.....	7
Figure 1.1-3. An illustrated representation of eutrophication measures through the use of indicators and influencing factors from NOAA's NEEA (Bricker et al., 2007a). .....	7
Figure 1.2-1. The relationship between mean dissolved inorganic nitrogen concentration and mean wet inorganic nitrogen in unproductive lakes in different regions in North America and Europe (Bergström and Jansson, 2006). .....	11
Figure 1.2-2. Areas potentially sensitive to aquatic nutrient enrichment. ....	12
Figure 1.2-3. The Potomac River Watershed and Potomac Estuary.....	18
Figure 1.2-4. The Neuse River Watershed and Neuse River Estuary.....	23
Figure 2.2-1. Modeling methodology for case study.....	31
Figure 2.2-2. Mass balance description applied to the SPARROW model formulation. ....	32
Figure 2.2-3. Conceptual illustration of a reach network. ....	33
Figure 2.2-4. SPARROW model components (Schwarz et al., 2006).....	35
Figure 2.2-5. Influencing factors/Overall Human Influence index description and decision matrix (Bricker et al., 2007a).....	40
Figure 2.2-6. Overall Eutrophic Condition index description and decision matrix (Bricker et al., 2007a).....	43
Figure 2.2-7. Detailed descriptions of primary and secondary indicators of eutrophication (Bricker et al., 2007a). ....	44
Figure 2.2-8. Determined Future Outlook index description and decision matrix (Bricker et al., 2007a).....	45
Figure 2.2-9. Example response curve of instream total nitrogen concentrations to atmospheric deposition loads.....	48
Figure 2.2-10. Example of response for case study analysis (Bricker et al., 2007b).....	49
Figure 2.2-11. ASSETS EI response curve.....	51
Figure 2.2-12a. Back calculation analysis scenario A: no uncertainty.....	55
Figure 2.2-12b. Back calculation analysis scenario B: uncertainty in ASSETS EI assessment.....	56
Figure 2.2-12c. Back calculation analysis scenario C: uncertainty in both ASSETS EI assessment and nitrogen loading assessment.....	57
Figure 2.2-13. Example of an improvement by one ASSETS EI score category in a back calculation assessment. ....	58
Figure 2.2-14. Example for resulting change in atmospheric nitrogen loads due to improvement in ASSETS EI score in back calculation assessment. ....	59
Figure 3.1-1a. Atmospheric deposition yields of oxidized nitrogen over the Potomac River and Potomac Estuary watershed. ....	62
Figure 3.1-1b. Atmospheric deposition yields of reduced nitrogen over the Potomac River and Potomac Estuary watershed. ....	63
Figure 3.1-1c. Atmospheric deposition yields of total nitrogen over the Potomac River and Potomac Estuary watershed. ....	64

Figure 3.1-2. Total nitrogen yields from all sources as predicted using the Version 3 of the Chesapeake Bay SPARROW application with updated 2002 atmospheric deposition inputs.....	65
Figure 3.1-3. Source contributions to Potomac Estuary nitrogen load. ....	66
Figure 3.1-4. The ASSETS EI scores for the Potomac Estuary (Bricker et al., 2006). ....	68
Figure 3.1-5a. Atmospheric deposition yields of oxidized nitrogen over the Neuse River and Neuse River Estuary watershed. ....	72
Figure 3.1-5b. Atmospheric deposition yields of reduced nitrogen over the Neuse River and Neuse River Estuary watershed. ....	73
Figure 3.1-5c. Atmospheric deposition yields of total nitrogen over the Neuse River and Neuse River Estuary watershed. ....	74
Figure 3.1-6. Total nitrogen yields from all sources in the Neuse River watershed as predicted by a SPARROW modeling application for the Neuse, Tar-Pamlico, and Cape Fear rivers' watersheds with 2002 data inputs.....	76
Figure 3.1-7. Source contributions to Neuse River Estuary total nitrogen load. ....	77
Figure 3.2-1. Response curve relating instream total nitrogen concentration to total nitrogen atmospheric deposition load for the Potomac River watershed. ....	81
Figure 3.2-2. Fitted Overall Eutrophic Condition curve for target ASSETS EI=2, median $TN_{atm\ i}^*$ (i = run 280).....	87
Figure 3.2-3. Response curve relating instream total nitrogen concentration to total nitrogen atmospheric deposition load for the Neuse River/Neuse River Estuary Case Study Area. ....	90
Figure 3.2-4. Fitted Overall Eutrophic Condition curve for target ASSETS EI=2, median $TN_{atm\ i}^*$ (i = run 287).....	95
Figure 3.2-5. Theoretical SPARROW response curves demonstrating relative influence of sources on nitrogen loads to an estuary. ....	97
Figure 4-1. Preliminary classifications of estuary typology across the nation (modified from Bricker et al., 2007a).....	100

## LIST OF TABLES

Table 1.1-1. Key Indicators of Nutrient Enrichment Due to N <sub>r</sub> , Including NO <sub>x</sub> .....	5
Table 1.1-2. Assessment Ecological Endpoints for Nutrient Enrichment Due to Deposition of Total Reactive Nitrogen, Including NO <sub>x</sub> .....	7
Table 1.1-3. Ecosystem Services for Aquatic Systems Affected by Nutrient Enrichment.....	8
Table 1.2-1. Summary of Indicators, Mapping Layers, and Models for Targeted Ecosystems.....	10
Table 1.2-2. Nitrogen Deposition Level vs. EPA Total Nitrogen Criteria for Lakes and Reservoirs .....	11
Table 1.2-3. Science Advisory Board/Ecological Effects Subcommittee Listing of Potential Assessment Areas for Evaluation of Benefits of Decreases in Atmospheric Deposition with Respect to Aquatic Nutrient Enrichment.....	14
Table 1.2-4. Potential Assessment Areas for Aquatic Nutrient Enrichment Identified in the ISA .....	15
Table 1.2-5. Physical Characteristics of the Potomac Estuary .....	18
Table 1.2-6. Hydrological Characteristics of the Potomac Estuary .....	19
Table 1.2-7. Physical Characteristics of the Neuse River Estuary .....	23
Table 1.2-8. Neuse River Watershed Land Use and Population.....	24
Table 1.2-9. Hydrological Characteristics of the Neuse River Estuary .....	25
Table 2.1-1. Examples of SPARROW Applications .....	36
Table 3.1-1. Potomac Estuary Current Condition Overall Human Influence Index Score.....	69
Table 3.1-2. Model Parameters for 2002 Current Condition SPARROW Application for the Neuse River Watershed.....	74
Table 3.1-3. Model Evaluation Statistics for 2002 Current Condition SPARROW Application for the Neuse River Watershed .....	75
Table 3.1-4. Current Condition Overall Eutrophic Condition Index Score for the Neuse River/Neuse River Estuary Case Study Area.....	79
Table 3.2-1. Potomac River Watershed Alternative Effects Levels .....	81
Table 3.2-2. Historical Potomac River Total Nitrogen Loads and Concentrations .....	82
Table 3.2-3. Additional Potomac Estuary Overall Eutrophic Condition Index Scores for Alternative Effects Levels.....	83
Table 3.2-4. Summary Statistics for Target ASSETS EI Scenarios for the Potomac Estuary .....	87
Table 3.2-5. Neuse River/Neuse River Estuary Case Study Area Alternative Effects Levels.....	90
Table 3.2-6. Annual Average Instream Total Nitrogen Concentrations in the Neuse River .....	91
Table 3.2-7. Additional Neuse River Estuary Overall Eutrophic Condition Index Scores for Alternative Effects Levels.....	92
Table 3.2-8. Summary Statistics for Target ASSETS EI Scenarios for the Neuse River/Neuse River Estuary Case Study Area.....	95
Table 4-1. Typology Group Categorizations .....	99



## ACRONYMS AND ABBREVIATIONS

ASSETS EI	Assessment of Estuarine Trophic Status eutrophication index
AQUATOX	a simulation model for aquatic systems
CASTNet	Clean Air Status and Trends Network
CBP	Chesapeake Bay Program
CE-QUAL	a mathematical model of water quality
CMAQ	Community Multiscale Air Quality model.
CO <sub>2</sub>	carbon dioxide
DFO	determined future outlook
DIN	dissolved inorganic nitrogen
EDA	Estuarine Drainage Areas
EES	Ecological Effects Subcommittee
EMAP	Environmental Monitoring and Assessment Program
GIS	geographic information systems
GT/MEL	Georgia Tech Hydrologic Model/Multiple Element Limitation
HAB	harmful algal bloom
HNO <sub>3</sub>	nitric acid
HSPF	Hydrologic Simulation Program-FORTRAN
INCA	Integrated Nitrogen in Catchments
ISA	Integrated Science Assessment
km	kilometer
km <sup>2</sup>	square kilometer
LANDSCAN	a worldwide population database
m	meter
m <sup>2</sup>	square meter
m <sup>3</sup>	cubic meter
MAGIC	Model of Acidification of Groundwater in Catchments
MEA	Millennium Ecosystem Assessment
mg/L	milligrams per liter
mi <sup>2</sup>	square mile
MODMON	Modeling and Monitoring Project
N <sub>2</sub> O	nitrous oxide
NADP	National Atmospheric Deposition Program
NCCR	National Coastal Condition Report
NC DWQ	North Carolina Department of Water Quality
NEEA	National Estuarine Eutrophication Assessment
NH <sub>3</sub>	ammonia gas
NH <sub>4</sub> <sup>+</sup>	ammonium
NOAA	National Oceanic and Atmospheric Administration
NO	nitric oxide
NO <sub>2</sub>	nitrogen dioxide
NO <sub>3</sub> <sup>-</sup>	nitrate
NO <sub>x</sub>	nitrogen oxides
N <sub>r</sub>	reactive nitrogen

OEC	Overall Eutrophic Condition
OHI	Overall Human Influence
psu	practical salinity unit
PnET-BCG	biogeochemical model
QA	quality assurance
QC	quality control
QUAL2K	Enhanced Stream Water Quality Model
RCA/ECOMSED	Row Column AESOP/Estuary and Coastal Ocean Model with Sediment Transport
RF1	Reach File version 1
RHESSys	Regional Hydro-Economic Simulation System
RTI	RTI International
SAGT	Atlantic and the eastern Gulf of Mexico, as well as the Tennessee River basin
SAV	submerged aquatic vegetation
SO <sub>x</sub>	sulfur oxides
SPARROW	Spatially Referenced Regression on Watershed
STORET	STOrage and RETrieval
TN	total nitrogen
TN <sub>atm</sub>	total nitrogen atmospheric deposition load
TN <sub>s</sub>	instream total nitrogen concentration
µg/L	microgram per liter
USGS	U.S. Geological Survey
VIF	Variance Inflation Factor
VIMS	Virginia Institute of Marine Science
WASP	Water Quality Analysis Simulation Program
WATERSN	Watershed Assessment Tool for Evaluating Reduction Strategies for Nitrogen

## 1.0 BACKGROUND

One classification of effects targeted for this Risk and Exposure Assessment is nitrogen and sulfur enrichment of ecosystems in response to deposition of nitrogen oxides ( $\text{NO}_x$ ) and sulfur oxides ( $\text{SO}_x$ ). Nutrient enrichment effects are caused by nitrogen or sulfur deposition, but are dominated by nitrogen deposition, which is the focus of this case study. Nutrient enrichment can result in eutrophication in aquatic systems (see Section 4.3 of the *Integrated Science Assessment (ISA) for Oxides of Nitrogen and Sulfur—Ecological Criteria (Final Report)* (ISA) (U.S. EPA, 2008a).

Because ecosystems may respond differently to nutrient enrichment, it is necessary to first perform Risk and Exposure Assessment case studies unique to the effect and ecosystem type. The feasibility of consolidating the effects and/or ecosystems in the Risk and Exposure Assessment was assessed, and where feasible, a broader characterization was performed. However, some ecosystems and their effects may be too unique to consolidate into a broad characterization.

Upon completion of all risk and exposure assessment case studies, the results of the assessments performed for unique combinations of effects and ecosystem types are presented together to facilitate decision making on the total effects of nitrogen and sulfur deposition. Ecosystem services that relate to the effects are identified and valued, if possible. Ecosystem services provide an additional way to compare effects across various ecosystems.

The selection and performance of case studies represent Steps 3 and 4, respectively, of the seven-step approach to planning and implementing a risk and exposure assessment, as presented in the April 2008 *Draft Scope and Methods Plan for Risk/Exposure Assessment: Secondary NAAQS Review for Oxides of Nitrogen and Oxides of Sulfur* (U.S. EPA, 2008b). Step 4 entails evaluating the current nitrogen and sulfur loads and effects to a chosen case study assessment area, including ecosystems services. This case study evaluates the current nitrogen deposition load to aquatic ecosystems; in particular, estuarine systems and the role atmospheric deposition can play in the eutrophication of an aquatic ecosystem. Note that volatilization of nitrogen from these systems is not considered within the case study because of the lack of quantitative data on denitrification and volatilization rates for estuarine systems across the United States (U.S. EPA, 2008a).

### ***Eutrophication***

Eutrophication is the process whereby a body of water becomes over-enriched in nutrients, resulting in increased productivity. As productivity increases with concomitant increases in organic matter production, dissolved oxygen levels in the waterbody may decrease and result in hypoxia (i.e., low dissolved oxygen levels). Total reactive nitrogen ( $N_r$ ) can promote eutrophication in inland freshwater ecosystems, as well as in estuarine and coastal marine ecosystems, ultimately reducing biodiversity because of the lack of available oxygen needed for the survival of many species of aquatic plants and animals. Total  $N_r$  includes all biologically, chemically, and radiatively active nitrogen compounds in the atmosphere and biosphere, such as ammonia gas ( $NH_3$ ), ammonium ( $NH_4^+$ ), nitric oxide (NO), nitrogen dioxide ( $NO_2$ ), nitric acid ( $HNO_3$ ), nitrous oxide ( $N_2O$ ), nitrate ( $NO_3^-$ ), and organic compounds (e.g., urea, amines, nucleic acids) (U.S. EPA, 2008b).

### ***Freshwater Aquatic Ecosystems***

A freshwater lake or stream must be nitrogen-limited to be sensitive to nitrogen-mediated eutrophication. Although conventional wisdom holds that most lakes and streams in the United States are limited by phosphorus, recent evidence illustrates examples of lakes and streams that are limited by nitrogen and show symptoms of eutrophication in response to nitrogen addition. For example, surveys of lake nitrogen concentrations and trophic status along gradients of nitrogen deposition show increased inorganic nitrogen concentrations and productivity to be correlated with atmospheric nitrogen deposition (Bergström and Jansson, 2006). Additional information supporting the connection between nitrogen loading and eutrophication in freshwater systems is provided in EPA's ISA (U.S. EPA, 2008a, Sections 3.3.2.3 and 3.3.3.2).

### ***Estuarine and Coastal Marine Ecosystems***

Estuarine and coastal marine ecosystems are highly important to human and ecological welfare through the ecosystem services they provide (e.g., fisheries, recreation). "Because the productivity of estuarine and nearshore marine ecosystems is generally limited by the availability of  $N_r$ , an excessive contribution of  $N_r$  from sources of water and air pollution can contribute to eutrophication" (U.S. EPA, 2008a, Section 4.3.4.1). The National Oceanic and Atmospheric Administration's (NOAA's) National Estuarine Eutrophication Assessment (NEEA) examined more than 140 estuaries along the coasts of the conterminous United States. The assessment

examined a range of symptoms of eutrophication, including algal blooms, hypoxia, and vegetation growth. Findings from the study concluded that 65% of the assessed systems had moderate to high overall eutrophic conditions (OECs) (Bricker et al., 2007a). Increasingly, individual estuarine ecosystems have become the center of intensive studies on nutrient enrichment/eutrophication causes and effects. Within the Chesapeake Bay, studies of the frequency of phytoplankton blooms and the extent and severity of hypoxia revealed overall increases in these detrimental effects (Officer et al., 1984). Within the Pamlico Estuary in North Carolina, similar trends have been observed and studied by Paerl et al. (1998). Sources identified within these assessments range from atmospheric deposition to fertilizer applications and other land use-based applications.

Estuarine and coastal marine ecosystems experience a range of ecological problems associated with nutrient enrichment. Because the productivity of estuarine and nearshore marine ecosystems is generally limited by the availability of  $N_r$ , an excessive contribution of  $N_r$  from sources of water and atmospheric pollution can contribute to eutrophication. Some of the most important environmental effects include increased algal blooms, the occurrence of bottom-water hypoxia, and decreases in fishery populations and the abundance of seagrass habitats (Boynton et al., 1995; Valiela and Costa, 1988; Howarth et al., 1996; Paerl, 1995, 1997; Valiela et al., 1990).

There is broad scientific consensus that nitrogen-driven eutrophication in shallow U.S. estuaries has increased over the past several decades and that environmental degradation of coastal ecosystems is now a widespread occurrence (Paerl et al., 2001). For example, the frequency of phytoplankton blooms and the extent and severity of hypoxia have increased in the Chesapeake Bay (Officer et al., 1984), the Pamlico Estuary in North Carolina (Paerl et al., 1998), and along the continental shelf adjacent to the Mississippi and Atchafalaya river discharges to the Gulf of Mexico (Eadie et al., 1994). A recent national assessment of eutrophic conditions in estuaries found that 65% of the assessed systems had moderate to high OECs (Bricker et al., 2007a). Estuaries with high OECs were generally those that received the greatest nitrogen loads from all sources, including atmospheric and land-based sources (Bricker et al., 2007a).

## **1.1 INDICATORS, ECOLOGICAL ENDPOINTS, AND ECOSYSTEM SERVICES**

Major indicators for nutrient enrichment to aquatic systems from atmospheric deposition of total  $N_r$  require measurements based on available monitoring stations for wet deposition (National Atmospheric Deposition Program [NADP]/National Trends Network) and limited networks for dry deposition (Clean Air Status and Trends Network [CASTNet]). Wet deposition monitoring stations can provide more information on an extensive range of nitrogen species than is possible for dry deposition monitoring stations. This creates complications in developing estimates for total nitrogen (TN) deposition levels because dry deposition data sources will likely be underestimated because of the use of fixed deposition velocities that do not reflect local conditions at the time of measurement, under-representation of monitoring sites in certain landscapes, and omission of some  $N_r$  species in the measurements (U.S. EPA, 2008a, Section 2.5).

For aquatic ecosystems, the indicators for “nutrient enrichment” effects reflect a combination of inputs from all media (e.g., air, discharges to water, diffuse runoff, groundwater inputs). Major aquatic system indicators include nutrient loadings (Heinz Center for Science, 2007), excess algal standing crops, or in larger waterbodies, anoxia (i.e., absence of dissolved oxygen) and/or hypoxia in bottom waters (see **Table 1.1-1**). For nitrogen, loadings or concentration values related to total  $N_r$  (a combination of nitrates, nitrites, organic nitrogen, and total ammonia) are encouraged for inclusion in numeric criteria as part of EPA-approved state water quality standards (U.S. EPA, 2000). Given the nature of the major indicators for atmospheric deposition and indicators for aquatic and terrestrial ecological systems, a data-fusion approach that combines monitoring indicators with modeling inputs and outputs is often used (Howarth, 2007).

**Table 1.1-1.** Key Indicators of Nutrient Enrichment Due to N<sub>r</sub>, Including NO<sub>x</sub>






Key Indicator Group	Examples of Indicators	Description
Nitrogen deposition	Nitrate or ammonia	From wet or dry deposition monitoring stations and networks
Nitrogen throughfall deposition	Nitrate, ammonia, organic nitrogen	Special measurements in terrestrial ecosystem with corrections for nitrogen intercepted by plant canopies
Nitrogen loadings and fluxes to receiving waters	Total nitrogen or constituent species combined with flow data from gauged stations	Reflects a combination of inputs from all media (e.g., air, discharges to water, diffuse runoff, and groundwater inputs); relative role of air deposition should ideally be compared with air deposition data and also with available (preferably multimedia) models
Other indicators of aquatic system nutrient enrichment (eutrophication)	Algal standing crop (plankton and periphyton); anoxia/hypoxia for estuaries and large rivers	Reflects a combination of inputs from all media (e.g., air, discharges to water, diffuse runoff, and groundwater inputs); relative role of air deposition should ideally be compared with air deposition data and also with available (preferably multimedia) models

Nitrogen is an essential nutrient for estuarine and marine ecosystem fertility and is often the algal growth-limiting nutrient (U.S. EPA, 2008a; Section 3.3.5.3). Excessive nitrogen contributions can cause habitat degradation, algal blooms, toxicity, hypoxia, anoxia, fish kills, and decreases in biodiversity (Paerl et al., 2002). To evaluate these impacts, five ecological indicators were used in NOAA's recent NEEA of estuary trophic condition: chlorophyll *a*, macroalgae, dissolved oxygen, nuisance/toxic algal blooms, and submerged aquatic vegetation (SAV) (Bricker et al., 2007a).

**Figure 1.1-1**, excerpted from the NOAA's NEEA Update, provides a brief description of each of the indicators. Further interactions between the indicators are described in the following text. For greater detail on each of the indicators, including previous findings and study areas, refer to the ISA (U.S. EPA, 2008a, Sections 3.3.2, 3.3.3, 3.3.5, 3.3.8, 4.3.4, and C.5) and the NEEA Update (Bricker et al., 2007a).

**Figure 1.1-2** provides a simplified progression of the indicators as the estuarine waters become more eutrophic. In the NEEA Update (Bricker et al., 2007a), an illustrated relationship between the OEC, water quality and ecological indicators, and influencing factors (e.g., nitrogen loads) is presented (**Figure 1.1-3**).

Indicators of eutrophication do not provide a direct link to the ecological benefits of the ecosystem. Because of this, the eutrophication-impact ecological endpoints and the ecosystem services affected must be identified and related to the quantifiable indicators. **Table 1.1-2** provides some examples of the ecological endpoints associated with the indicators of eutrophication. As described in the introduction, the ecological endpoints are ecological entities and their impacts. For instance, an indicator may be low dissolved oxygen, but the ecological endpoint or impact of having low dissolved oxygen is a decrease in the populations of fish that are highly sensitive to dissolved oxygen conditions.

Primary symptoms		Description
	<b>Chlorophyll <i>a</i> (Phytoplankton)</b>	A measure used to indicate the amount of microscopic algae (phytoplankton) growing in a water body. High concentrations can lead to low dissolved oxygen levels as a result of decomposition.
	<b>Macroalgal blooms</b>	Large algae commonly referred to as "seaweed." Blooms can cause losses of submerged aquatic vegetation by blocking sunlight. Additionally, blooms may smother immobile shellfish, corals, or other habitat. The unsightly nature of some blooms may impact tourism due to the declining value of swimming, fishing, and boating.
Secondary symptoms		Description
	<b>Dissolved oxygen</b>	Low dissolved oxygen is a eutrophic symptom because it occurs as a result of decomposing organic matter (from dense algal blooms), which sinks to the bottom and uses oxygen during decay. Low dissolved oxygen can cause fish kills, habitat loss, and degraded aesthetic values, resulting in the loss of tourism and recreational water use.
	<b>Submerged aquatic vegetation</b>	Loss of submerged aquatic vegetation (SAV) occurs when dense algal blooms caused by excess nutrient additions (and absence of grazers) decrease water clarity and light penetration. Turbidity caused by other factors (e.g., wave energy, color) similarly affects SAV. The loss of SAV can have negative effects on an estuary's functionality and may impact some fisheries due to loss of a critical nursery habitat.
	<b>Nuisance/toxic blooms</b>	Thought to be caused by a change in the natural mixture of nutrients that occurs when nutrient inputs increase over a long period of time. These blooms may release toxins that kill fish and shellfish. Human health problems may also occur due to the consumption of contaminated shellfish or from inhalation of airborne toxins. Many nuisance/toxic blooms occur naturally, some are advected into estuaries from the ocean; the role of nutrient enrichment is unclear.

**Figure 1.1-1.** Descriptions of the five eutrophication indicators used in NOAA's NEEA (Bricker et al., 2007a).



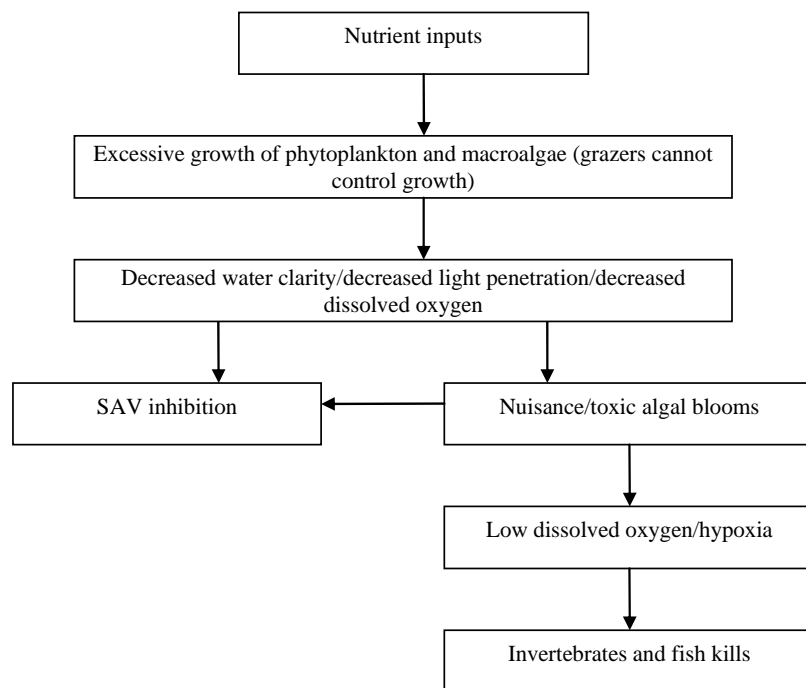


**Figure 1.1-2.** A simplified schematic of eutrophication effects on an aquatic ecosystem.

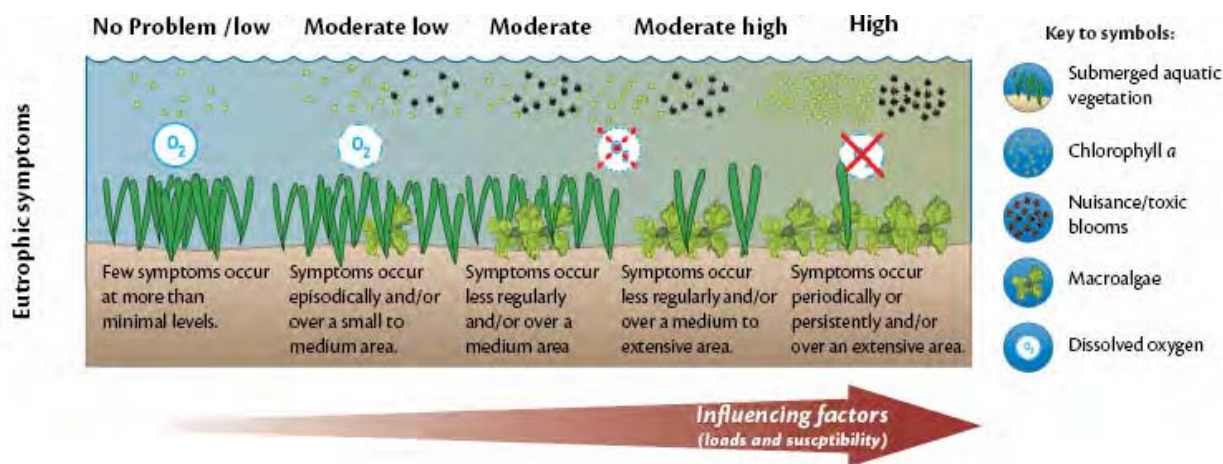


**Figure 1.1-3.** An illustrated representation of eutrophication measures through the use of indicators and influencing factors from NOAA's NEEA (Bricker et al., 2007a).

**Table 1.1-2.** Assessment Ecological Endpoints for Nutrient Enrichment Due to Deposition of Total Reactive Nitrogen, Including NO<sub>x</sub>

Assessment Ecological Endpoint
Fish abundance/population
Water quality, color, clarity
Species richness/community structure

Assessment Ecological Endpoint
Habitat quality, including benthos and shoreline
Surface scum, odors

Continuing to link the indicators and ecological endpoints to the ecological processes of value to society brings us to the ecosystem services related to eutrophication. Examples are provided in **Table 1.1-3**. The example of dissolved oxygen and the resulting decrease in fish population was used to identify the ecosystem services of fish catch rate and fish kills, which support both food and materials and recreational uses of the ecosystem.

**Table 1.1-3. Ecosystem Services for Aquatic Systems Affected by Nutrient Enrichment**

Ecosystem Service
Fisheries <ul style="list-style-type: none"> <li>▪ Fish catch rate</li> <li>▪ Fishable area</li> <li>▪ Size/extent of fish kills</li> </ul>
Recreation <ul style="list-style-type: none"> <li>▪ Boating</li> <li>▪ Swimming</li> <li>▪ Beach conditions</li> </ul>
Tourism <ul style="list-style-type: none"> <li>▪ Aesthetics</li> </ul>
Risk of illness <ul style="list-style-type: none"> <li>▪ Drinking water quality</li> <li>▪ Contaminated fish</li> </ul>

The methods of connecting the ecological endpoints and ecosystem services related to eutrophication are beyond the scope of this case study, but they have been examined in another study (RTI, 2008). Rather, the remaining discussion focuses on determining and detailing the indicator measures as a function of the changing atmospheric deposition inputs of  $N_r$ , including  $NO_x$ .

Ecosystem services are generally defined as the benefits individuals and organizations obtain from ecosystems. In the Millennium Ecosystem Assessment (MEA), ecosystem services are classified into four main categories:

- **Provisioning.** Includes products obtained from ecosystems.
- **Regulating.** Includes benefits obtained from the regulation of ecosystem processes.

- **Cultural.** Includes the nonmaterial benefits people obtain from ecosystems through spiritual enrichment, cognitive development, reflection, recreation, and aesthetic experiences.
- **Supporting.** Includes those services necessary for the production of all other ecosystem services (MEA, 2005).

A number of impacts on the ecological endpoints of fish population, water quality, and habitat quality and the related ecosystem services exist, including the following:

- Fish kills – provisioning and cultural
- Surface scum – cultural
- Fish/water contamination – provisioning and cultural
- Decline in fish population – provisioning and cultural
- Decline in shoreline quality (e.g., erosion) – cultural and regulating
- Poor water clarity and color – cultural
- Unpleasant odors – cultural.

The goal of the Aquatic Nutrient Enrichment Case Study was to focus on fisheries, recreation, and tourism. Attempts have been made to link fisheries (e.g., closings, decreased species richness) quantitatively to eutrophication symptoms through monitoring data, and recreation activities qualitatively through user surveys. The symptoms of eutrophication defined by Bricker et al., (2007a) were pursued as the ecosystem ecological endpoints to link to these ecosystem services.

## **1.2 CASE STUDIES**

### **1.2.1 National Overview of Sensitive Areas**

The selection of case study areas specific to eutrophication began with national geographic information systems (GIS) mapping. Spatial datasets were reviewed that included physical, chemical, and biological properties indicative of eutrophication potential in order to identify sensitive areas of the United States (**Table 1.2-1**). The analysis then led to combining the eutrophic estuaries from NOAA's Coastal Assessment Framework, along with areas that exceed the nutrient criteria for lakes/reservoirs (U.S. EPA, 2002), as compared with wet nitrogen deposition, to define areas of national aquatic nutrient enrichment sensitivity.

**Table 1.2-1.** Summary of Indicators, Mapping Layers, and Models for Targeted Ecosystems

Targeted Ecosystem Effect	Indicator(s)	Mapping Layers	Model(s)
Aquatic nutrient enrichment and eutrophication	<ul style="list-style-type: none"> <li>▪ Nitrate and ammonia, total nitrogen (major reactive nitrogen species)</li> <li>▪ Al toxicity data</li> <li>▪ Chlorophyll <i>a</i> (e.g., algal standing crop)</li> <li>▪ Anoxia/hypoxia (e.g., primarily estuaries and tidal rivers)</li> <li>▪ Nitrogen loadings for sub-watersheds or larger basins and EDAs</li> <li>▪ EPA NCCR Water Quality Index and NOAA Estuarine Coastal Eutrophication Index</li> <li>▪ Diatom data for nitrogen-limited systems</li> </ul>	<ul style="list-style-type: none"> <li>▪ STORET retrievals</li> <li>▪ USGS National Water Quality Assessment Program information</li> <li>▪ USGS SPARROW attributes, information</li> <li>▪ Water quality standards nutrient criteria for rivers and lakes</li> <li>▪ EPA, NCCR, and NOAA estuarine eutrophication indicators</li> <li>▪ NOAA EDAs</li> <li>▪ EPA/NOAA airsheds for major Atlantic and Gulf estuaries CMAQ (e.g., nitrogen) by hydrological unit code</li> </ul>	<ul style="list-style-type: none"> <li>▪ USGS SPARROW</li> <li>▪ PnET-BCG</li> </ul>

**Note:** EDAs = Estuarine Drainage Areas; NCCR = *National Coastal Condition Report*; STORET = STORage and RETrieval; USGS = U.S. Geological Survey; SPARROW = Spatially Referenced Regression on Watershed; CMAQ = Community Multiscale Air Quality; PnET-BCG = a biogeochemical model

Bergström and Jansson (2006) compiled dissolved inorganic nitrogen (DIN) data from 4,296 lakes (i.e., 195 lakes from United States/Canada and 4,101 lakes from Europe). They found that the mean lake DIN concentrations were strongly correlated to the mean wet DIN deposition over large areas of Europe and North America (**Figure 1.2-1**). The equation for this correlation is:

$$\log Y = 1.34 \times \log X - 1.55 \quad (r^2 = 0.70; P < 0.001) \quad (1)$$

where

Y is lake water DIN (microgram per liter [ $\mu\text{g/L}$ ]), and

X is wet deposition (kilograms [ $\text{kg}$ ]  $\text{N/km}^2/\text{yr}$ ).

EPA recommended TN criteria for lakes and reservoirs for 12 aggregated ecoregions in 2002 (U.S. EPA, 2002).

Based on equation (1), nitrogen deposition level (X: kg N/ha/yr) associated with EPA TN criteria (Y: µg/L) for each aggregated ecoregion can be calculated by equation (2), and the results are listed in **Table 1.2-2**.

$$X = 10^{(\log Y + 1.55) / 1.34} / 100 \quad (2)$$

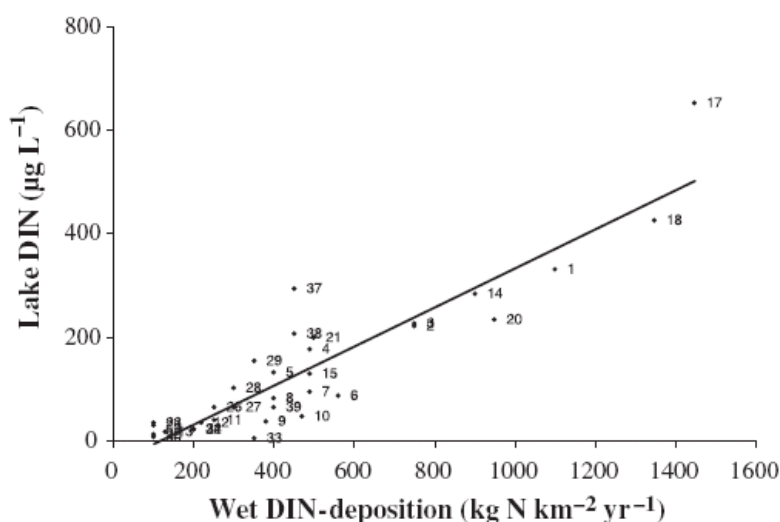


**Figure 1.2-1.** The relationship between mean dissolved inorganic nitrogen concentration and mean wet inorganic nitrogen in unproductive lakes in different regions in North America and Europe (Bergström and Jansson, 2006).

**Table 1.2-2.** Nitrogen Deposition Level vs. EPA Total Nitrogen Criteria for Lakes and Reservoirs

	Agg Ecor II	Agg Ecor III	Agg Ecor IV	Agg Ecor V	Agg Ecor VI	Agg Ecor VII	Agg Ecor VIII	Agg Ecor IX	Agg Ecor XI	Agg Ecor XII	Agg Ecor XIII	Agg Ecor XIV
TN EPA criteria (µg/L)	100	400	440	560	780	660	240	360	460	520	1270	320
N wet dep (kg N/ha/yr)	4.46	12.55	13.47	16.13	20.65	18.23	8.57	11.60	13.93	15.26	29.72	10.62
NADP Mean wet N dep (kg N/ha/yr)	1.19	1.16	2.36	3.02	5.01	6.36	5.21	4.44	4.93	3.28	3.35	4.22

**Source:** Prepared by Lingli Liu, U.S. EPA Office of Research and Development and transmitted in communication from Tara Graever, U.S. EPA Office of Research and Development, May 2008.

(Comparable information was not available for rivers and streams.)

**Note:** kg N/ha/yr = kilograms of nitrogen per hectare per year; µg/L = micrograms per liter.

The resulting map reveals areas of highest potential sensitivity to nitrogen deposition as shown in **Figure 1.2-2**. These areas are identified in blue as nutrient sensitive estuaries contained in NOAA's Coastal Assessment Framework, and in red in areas where deposition exceeds the nutrient criteria. Yellow areas indicate those areas that are below the nutrient criteria, but are within 5 kg/ha/yr of exceeding the criterion. White areas do not have an EPA nutrient criterion for lakes/reservoirs.

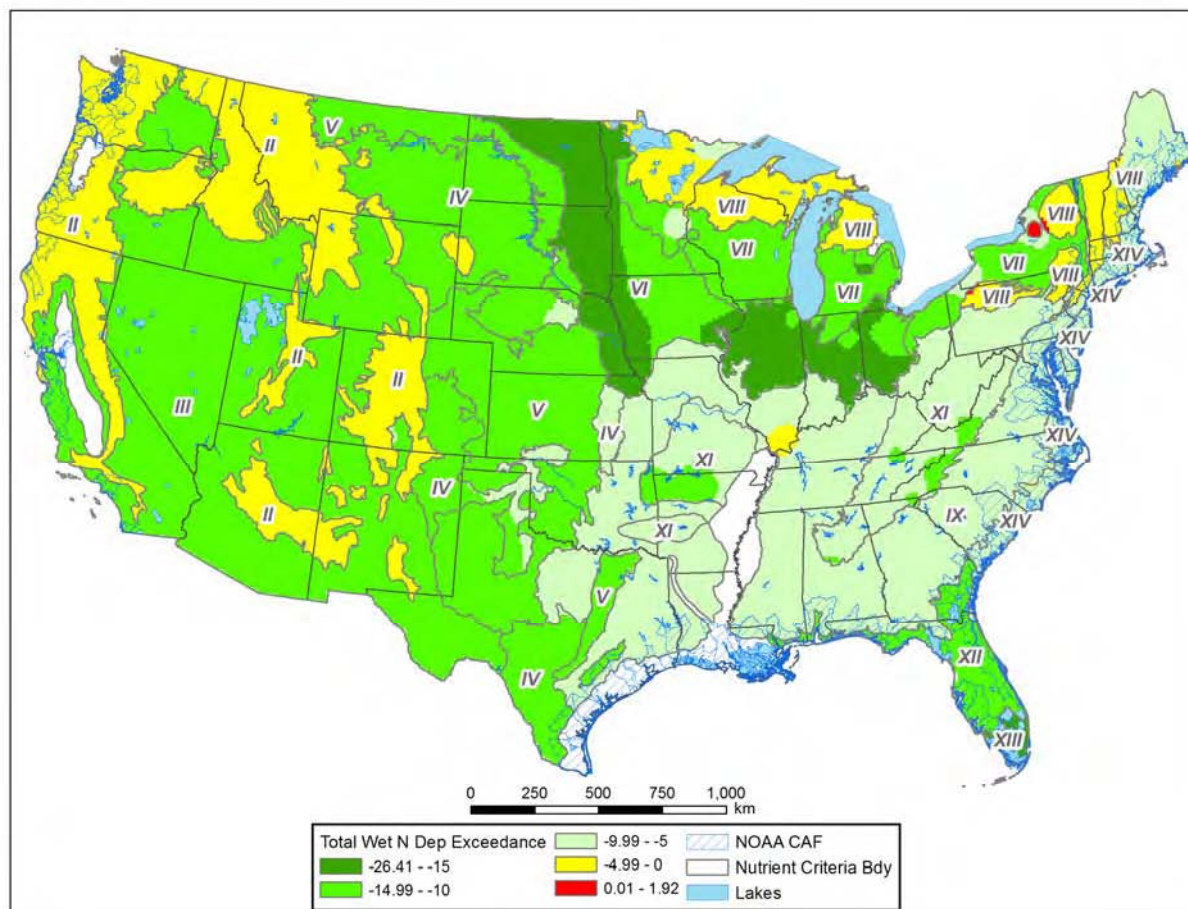


**Figure 1.2-2.** Areas potentially sensitive to aquatic nutrient enrichment.

### 1.2.2 Use of ISA Information and Rationale for Site Selection

The potential case study areas identified by the Ecological Effects Subcommittee (EES) of the Advisory Council on Clean Air Compliance Analysis were considered for examining the ecological benefits of decreasing atmospheric deposition. Nutrient enrichment–relevant case study areas suggested by the EES (U.S. EPA, 2005) are reproduced in **Table 1.2-3**. The ISA (U.S. EPA, 2008b) also recommends case study areas as candidates for risk and exposure

assessments; **Table 1.2-4** contains potential assessment areas for aquatic nutrient enrichment. Additionally, Howarth and Marino (2006) provide a comprehensive summary of the literature and scientific findings on eutrophication over the past 3 decades. This summary has led to the general consensus that freshwater lakes and estuaries differ in terms of nutrient limitation as the cause of eutrophication, and that nitrogen is the limiting element to primary production in coastal marine ecosystems in the temperate zone.

For purposes of the Risk and Exposure Assessment, two regions were selected for case study analysis to which a common methodology could be applied—Chesapeake Bay and the Pamlico Sound. For aquatic nutrient enrichment, special emphasis was given to the Chesapeake Bay region because it has been the focus of many previous studies and modeling efforts, and it is currently one of the few systems within the United States in which economic-related ecosystem services studies have been conducted. The Pamlico Sound, an economically important estuary because of its fisheries, has been studied and modeled greatly by the universities and has also been known to exhibit symptoms of extreme eutrophication. The following factors were considered in choosing these case study areas:

- Availability of atmospheric deposition data
- Availability of existing water quality modeling that accounts for the role of atmospheric deposition
- A large, mainstem river that feeds a system with adequate hydrologic unit code delineation and point- and nonpoint-source input data
- Scientific stature of the case study area
- Scalability and generalization opportunities for risk analysis results from the case studies.

These estuarine ecosystems have been the subjects of extensive research that provides the data needed for a first phase of quantitative analysis of the role of nitrogen deposition in eutrophication. Other candidate estuarine systems could be evaluated for potential future analyses, whereas freshwater ecosystems in the western United States would most likely require a separate analysis.

Because the Chesapeake Bay and Pamlico Sound are fed by multiple river systems, the case study was scaled to one main stem river and associated estuary for each system: the Potomac River and Potomac Estuary for the Chesapeake Bay and the Neuse River and Neuse River Estuary for the Pamlico Sound. Details on each estuarine system are provided below.

**Table 1.2-3.** Science Advisory Board/Ecological Effects Subcommittee Listing of Potential Assessment Areas for Evaluation of Benefits of Decreases in Atmospheric Deposition with Respect to Aquatic Nutrient Enrichment

<b>Ecosystem/ Region</b>	<b>Main CAA Pollutant(s)</b>	<b>Percentage(s) Attributable to Atmospheric Deposition</b>	<b>Quantitative Ecological and Economic Information</b>	<b>EES Comments</b>
<b>Coastal</b>				
Waquoit Bay	Nitrogen	30%	Yes	High priority. Higher loading from nondepositional sources may confound analysis.
Chesapeake Bay	Nitrogen	20% to 30%	Yes	High priority. Loading from diverse sources, particularly agricultural, may confound analysis.
Long Island Sound	Nitrogen; mercury	Nitrogen = 23% to 35%; Mercury = ?	Yes	High priority. High nitrogen loading from wastewater treatment plants may confound analysis.
Barnegat Bay	Nitrogen	50% total; direct deposition 30% to 39%	Yes	High priority. Direct linkage of ecological effects with atmospheric deposition; quantitative economic data exist.
Tampa Bay	Nitrogen; mercury	Nitrogen = 25% to 30%	Yes	Medium priority. Examined in previous EPA efforts. Variability in loading data may confound analysis.
Gulf of Maine	Nitrogen	Low	?	Low priority. Linkage of nitrogen loadings and ecological impacts is not well established. Major source of nitrogen is open-ocean influx.
Casco Bay	Nitrogen; mercury	Nitrogen = 30% to 40% Mercury = 84% to 92%	Yes	Medium priority. Good data on ecological and economic impacts are available.
Rocky Mountains	Nitrogen	Nearly 100%	Yes	Medium priority. Levels of nitrogen loading much lower than for northeastern locations. Economic data may be lacking.



**Table 1.2-4.** Potential Assessment Areas for Aquatic Nutrient Enrichment Identified in the ISA

Area	Indicator	Detailed Indicator	Area Studies	Models	References in U.S. EPA, 2008a	Source
Adirondack Mountains	Aquatic nutrient enrichment; terrestrial nutrient enrichment; mercury methylation	Foliar N concentration; NO <sub>3</sub> <sup>-</sup> leaching; C:N ratio; N mineralization; nitrification; denitrification	PIRLA I and II; Adirondack Lakes Survey; Episodic Response Project; EMAP	MAGIC; PnET-BGC	Baker and Laflen, 1983; Baker et al., 1990b; Baker et al., 1990c; Baker et al., 1996; Benoit et al., 2003; Chen and Driscoll, 2004; Confer et al., 1983; Cumming et al., 1992; Driscoll et al., 1987a; Driscoll et al., 1991; Driscoll et al., 1998; Driscoll et al., 2001a; Driscoll et al., 2001b; Driscoll et al., 2003b; Driscoll et al., 2003c; Driscoll et al., 2007a; Driscoll et al., 2007b; Evers et al., 2007; GAO, 2000; Havens et al., 1993; Ito et al., 2002; Johnson et al., 1994b; Landers et al., 1988; Lawrence et al., 2007; NAPAP, 1998; Siegfried et al., 1989; U.S. EPA, 2003; Sullivan et al., 1990; Sullivan et al., 2006a; Sullivan et al., 2006b; U.S. EPA, 1995b; Van Sickle et al., 1996; Whittier et al., 2002; Wigington et al., 1996; Zhai et al., 2007	ISA, Section 3.2.4, 3.4.1, 4.2.2, Annex B
Chesapeake Bay	Aquatic nutrient enrichment; aquatic nitrogen-limited eutrophication	Watershed N sources; chlorophyll <i>a</i> ; dissolved oxygen; submerged aquatic vegetation	NA	NA	Bricker et al., 1999; Bricker et al., 2007; Boesch et al., 2001; Boyer et al., 2002; Boyer and Howarth, 2002; Cooper and Brush, 1991; Fisher and Oppenheimer, 1991; Harding and Perry, 1997; Howarth, 2007; Kemp et al., 1983; Malone, 1991, 1992; Officer et al., 1984; Orth and Moore, 1984; Twilley et al., 1985	ISA, Section 3.3.2, 3.3.8, 4.3.4, Annex C
Alpine and subalpine communities of the eastern slope of the Rocky Mountains, CO	Aquatic nutrient enrichment; terrestrial nutrient enrichment	Biomass production; NO <sub>3</sub> <sup>-</sup> leaching; species richness	NA	NA	Baron et al., 1994; Baron et al., 2000; Baron, 2006; Bowman, 2000; Bowman and Steltzer, 1998; Bowman et al., 1993; Bowman et al., 1995; Bowman et al., 2006; Burns, 2004; Fenn et al., 2003a; Fisk et al., 1998; Korb and Ranker, 2001; Rueth et al., 2003; Seastedt and Vaccaro, 2001; Sherrod and Seastedt, 2001; Steltzer and Bowman, 1998; Suding et al., 2006; Williams and Tonnessen, 2000; Williams et al., 1996a; Wolfe et al., 2001	ISA, Sections 3.2.1, 3.2.2, 3.3.2, 3.3.3, 3.3.5, 3.3.8, 4.5, Annex C and D

Area	Indicator	Detailed Indicator	Area Studies	Models	References in U.S. EPA, 2008a	Source
Beartooth Mountain, WY	Aquatic nutrient enrichment	Algae composition switch	NA	NA	Saros et al., 2003	ISA, Sections 3.3.5, 4.4.3, 4.5, Annex B and C
Pamlico Estuary, NC	Aquatic nitrogen limited eutrophication	Hypoxia; phytoplankton bloom	NA	NA	Paerl et al., 1998	ISA, Sections 3.3.2, 3.3.3
Rocky Mountain National Park, CO	Aquatic nutrient enrichment	Diatom shifts	NA	NA	Interlandi and Kilham, 1998	ISA, Sections 3.3.3, 3.3.5, 3.3.8, 4.3.3, 4.5, Annex C
Lake Tahoe, CA	Aquatic nutrient enrichment	Primary productivity; chlorophyll <i>a</i>	NA	NA	Goldman, 1988; Jassby et al., 1994	ISA, Sections 3.3.3, 3.3.5, 3.3.8, Annex C

**Source:** U.S. EPA, 2008a

**Note:** CAA = Clean Air Act; PIRLA = paleoecological investigation of recent lake acidification; EMAP = Environmental Monitoring and Assessment Program; MAGIC = Model of Acidification of Groundwater in Catchments; PnET-BGC = a biogeochemical model; NO<sub>3</sub><sup>-</sup> = nitrate; NA = not applicable.

### 1.2.3 Potomac River and Potomac Estuary

The Chesapeake Bay is the largest of 130 estuaries in the United States. This commercial and recreational resource serves more than 15 million people who live in and near its watershed (i.e., drainage basin). The bay produces approximately 500 million pounds of oysters, crabs, and other seafood per year. The richness of its species can be seen in the value of the bay's annual fish harvest, which is estimated at more than \$100 million. The Chesapeake Bay estuary receives approximately 50% of its water from the Atlantic Ocean in the form of saltwater. The other half of the water (i.e., fresh water) drains into the bay from a large 165,800-square-kilometer (km<sup>2</sup>) (64,000-square-mile [mi<sup>2</sup>]) drainage watershed. Among the 150 major rivers and streams in the Chesapeake Bay drainage basin are the James, Potomac, York, Rappahannock, Patuxent, and Susquehanna rivers. The Potomac River watershed comprises about 22% of the land area and 30% of the population of the total Chesapeake Bay watershed. As a result, pollution loads from the Potomac River have a significant impact on the health of the bay. The Chesapeake Bay contains on average more than 68 trillion liters (18 trillion gallons) of water (Atkins and Anderson, 2009).

The Potomac River is approximately 413 miles (665 km) long, with a drainage area of approximately 14,670 mi<sup>2</sup> (38,000 km<sup>2</sup>) and a population of approximately 5,350,000 people. It begins at Fairfax Stone, WV, and runs to Point Lookout, MD. In terms of area, this makes the Potomac River the fourth largest river along the Atlantic Coast of the United States and the twenty-first largest in the United States as a whole (Fact-index.com, 2009). As shown in **Figure 1.2-3**, as well as in **Table 1.2.5** and **Table 1.2-6**, the Potomac River contains diverse watersheds in terms of topography, elevation (e.g., extending into the Shenandoah Mountains), and nutrient point and nonpoint sources (e.g., forestland, farmland, and the Washington, DC, metropolitan area). The Potomac River watershed lies in five geological provinces: the Appalachian Plateau, Ridge and Valley, Blue Ridge, Piedmont Plateau, and Coastal Plain. The watershed is approximately 12% urbanized, 36% agricultural use, and 52% forested. Atmospheric deposition has also been reported to contribute from 5% to 15%–20% of the watershed's TN load (U.S. EPA, 2000; Boyer et al., 2002, respectively).

Atmospheric deposition accounts for between 5% and 15% to 20% of the Potomac River watershed's total nitrogen load according to published research (U.S. EPA, 2000; Boyer et al., 2002, respectively). Additional expert estimates put the contribution by atmospheric deposition at 30% to 40% of the total load.

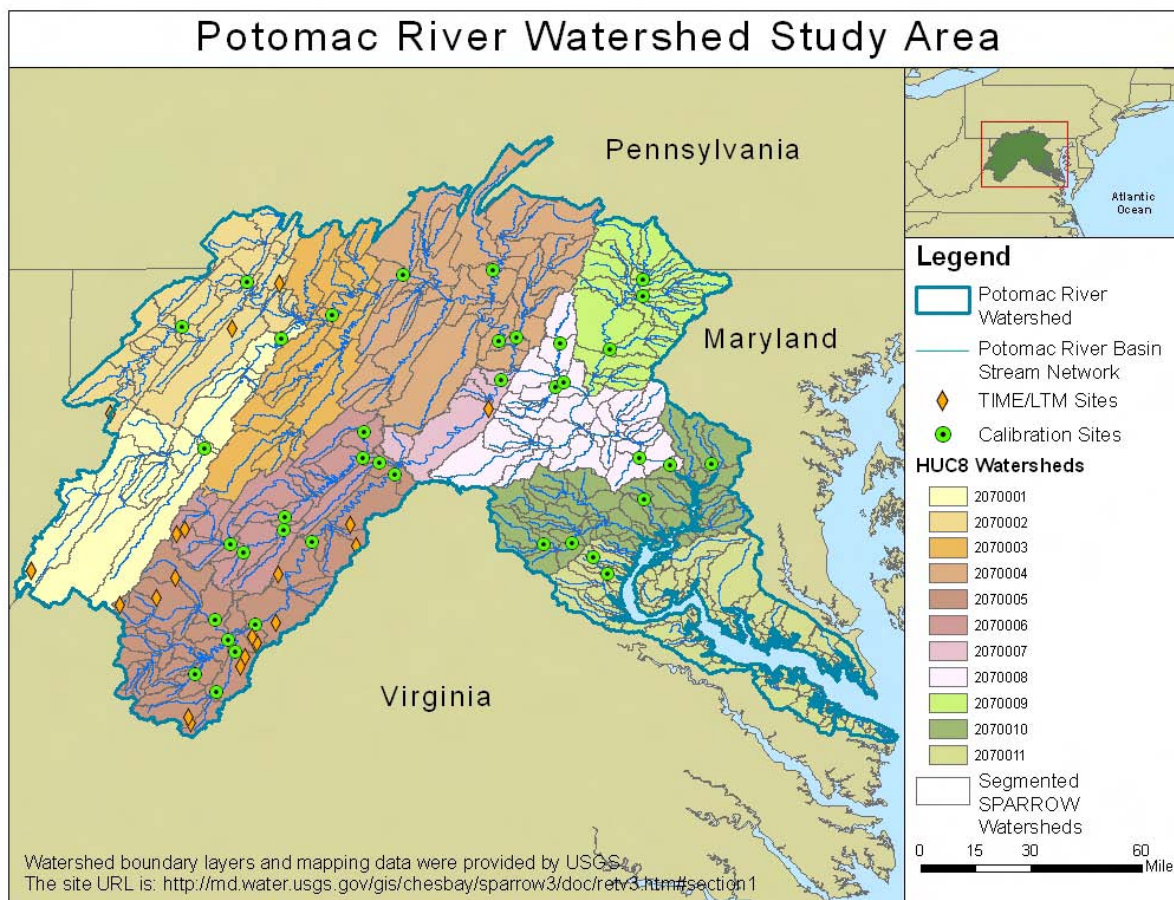


**Figure 1.2-3.** The Potomac River Watershed and Potomac Estuary.

**Table 1.2-5.** Physical Characteristics of the Potomac Estuary

Parameter	Value	Metadata
Estuary area (km <sup>2</sup> )	1,260	Estuary area, calculated from NOAA shapefiles
Tidal fresh zone area (km <sup>2</sup> )	183	Tidal fresh area, calculated from NOAA shapefiles
Mixing zone area (km <sup>2</sup> )	1,077	Mixing zone area, calculated from NOAA shapefiles
Saltwater zone area (km <sup>2</sup> )	0	Saltwater area, calculated from NOAA shapefiles
Estuary volume (m <sup>3</sup> )	$6.46 \times 10^9$	Best estimate of volume from digital bathymetric chart if available; otherwise, NOAA planimetry
Estuary depth (m)	5.13	From digital bathymetric chart if available; otherwise, NOAA planimetry
Estuary perimeter (km)	1,350	Perimeter of estuary, based on shapefile; can be used to calculate various aspect ratios
Percentage of estuary open (%)	1.33	Percentage of the perimeter that is the “open” (or oceanic) boundary; somewhat subjective
Catchment area (km <sup>2</sup> )	36,804	Not available

Parameter	Value	Metadata
Catchment mean elevation (m)	330	Calculated from catchment shapefiles + Hydro1K (a global 1-km grid of elevation)
Catchment maximum elevation (m)	1,433	Calculated from catchment shapefiles + Hydro1K (a global 1-km grid of elevation)
Catchment/estuary area ratio	29.2	Area ratio, based on catchment and area data given above

Source: NEEA Estuaries Database

Note: m = meter

**Table 1.2-6.** Hydrological Characteristics of the Potomac Estuary

Parameter	Value	Metadata
Tide height (m)	0.55	NOAA estimate of tide height, back-calculated from tide volume; in some cases, guessed from nearby systems
Tide volume (m <sup>3</sup> )	$6.93 \times 10^8$	Tide height (m) $\times$ estuary area (km <sup>2</sup> ) $\times 10^6$
Tides/day (#)	2	NOAA designation
Tide volume/day (m <sup>3</sup> .d <sup>-1</sup> )	1,339,130,435	Calculated from tide volume and tides per day
Tide ratio	0.11	Tide height divided by estuary depth; a clean-up of a NOAA variable
Stratification ratio	0.02649	Total freshwater flux per day divided by tide volume per day
Percent freshwater (%)	14.5	Based on NOAA shapefiles of the three zones according to their designation
Percent mixed water (%)	85.5	Based on NOAA shapefiles of the three zones according to their designation
Percent seawater (%)	0	Based on NOAA shapefiles of the three zones according to their designation
Average salinity (psu)	11	Based on NOAA estimate of freshwater volume, but scaled to "local coastal salinity," below
Tidal exchange (days)	121	Exchange time as (Est_V/net fw_V per d) * (coastal_sal - avg_sal)/coastal_sal); a salinity-based estimate of exchange
Tidal freshwater flush (days)	36	NOAA-based calculation, using (daily tide + freshwater volume)/system volume
Daily freshwater/estuary area (m.d <sup>-1</sup> )	27.063	NOAA estimate of daily flow/estuary area
Daily freshwater (m <sup>3</sup> /day) (best)	34,100,000	NOAA estimate above or (if not available) NCPDI estimate
Flow/estuary area (m/day) (best)	27.063	Best estimate/estuary area

Parameter	Value	Metadata
Total freshwater Volume (1/day)	0.00549	Best estimate/estuary volume (= hydraulic exchange rate)
Daily precipitation (m <sup>3</sup> /day)	$3.64 \times 10^6$	Direct precipitation on system, derived from PRISM Shapefile
Daily evaporation (m <sup>3</sup> /day)	$2.26 \times 10^6$	Direct evaporation from system, derived from LOICZ 0.5 degree database, originally from Wilmott
Daily precipitation/estuary area (mm/day)	2.889	Daily precipitation/estuary area
Daily evaporation/estuary area (mm/day)	1.794	Daily evaporation/estuary area
Flow (m <sup>3</sup> /day)	$2.33 \times 10^7$	NCPDI_1982–1991

**Source:** NEEA Estuaries Database

**Note:** m = meter; psu = practical salinity unit; NCPDI = National Coastal Pollution Discharge Inventory; PRISM = Parameter-elevation Regressions on Independent Slopes Model; LOICZ = Land-Ocean Interactions in the Coastal Zone; mm = millimeters.

### 1.2.4 Neuse River and Neuse River Estuary

The Neuse River is the longest river in North Carolina, and the Neuse River watershed is the third largest river watershed in the state (**Figure 1.2-4**). The Neuse River is a mainstem river to the Pamlico Sound—one of the two largest estuaries on the Atlantic Coast. The river originates in north-central North Carolina and flows southeasterly until it reaches tidal waters upstream of New Bern, NC. At New Bern, the river broadens dramatically and changes from a free-flowing river to a sound. While the Neuse River itself is 399 kilometers (km) (248 miles) long, there are 5,628 freshwater stream kilometers (3,497 miles), 6,643 hectares (16,414 acres) of freshwater reservoirs and lakes, 149,724 estuarine hectares (369,977 acres), and 33.8 kilometers (21 miles) of Atlantic coastline within the entire Neuse River watershed. The drainage area for the watershed is approximately 14,210 mi<sup>2</sup> (36,804 km<sup>2</sup>). There are 19 major reservoirs in the Neuse River watershed; most of these are located in the upper portion of the watershed. The watershed starts in the eastern Piedmont physiographic region, with approximately two-thirds of the watershed located in the Coastal Plain (NC DENR, 2002).

The Neuse River watershed encompasses all or portions of 18 counties and 74 municipalities. The watershed has a population of approximately 1,320,379 according to the 2000 census. Fifty-six percent of the land in the watershed is forested, and approximately 23% is in cultivated cropland. Only 8% of the land falls into the urban/built-up category. Despite the

large amount of cultivated cropland and the relatively small amount of urban area, the basin has seen a significant decrease (-72,800 hectares [-180,000 acres]) in cultivated cropland and forest and an increase (+91,900 hectares [+227,000 acres]) in developed areas over the past 15 years (NRCS, 2001). The Neuse River watershed is divided into 14 subbasins (6-digit North Carolina Division of Water Quality [NC DWQ] subbasins) (NC DENR, 2002). **Table 1.2-7** through **Table 1.2-9**, respectively, provide physical, land use and population, and hydrological characteristics of the Neuse River and Neuse River Estuary.

There are 134,540 estuarine hectares (332,457 acres) classified for shellfish harvesting (Class SA [shellfishing]) in the Neuse River Estuary. The Neuse River Estuary is important to the commercial blue crab (*Callinectes sapidus*) fishery in the eastern United States and accounted for approximately one-quarter of the blue crab harvest from 1994 to 2002 (Smith and Crowder, 2005). Eutrophication became a water quality concern in the lower Neuse River and Neuse River Estuary in the late 1970s and early 1980s. Nuisance algal blooms prevalent in the upper estuary prompted investigations by the state. These investigations, as well as other studies, indicated that algal growth was being stimulated by excess nutrients entering the estuarine waters of the system. In 1988, a phosphate detergent ban was put in place, and the lower Neuse River and Neuse River Estuary received the supplemental classification of nutrient-sensitive waters. Phosphorus loading was greatly decreased, and algal blooms in the river and freshwater portions of the system were lowered as a result of this action. However, the 1993 *Neuse River Basin-wide Water Quality Plan* (NC DENR, 1993) recognized that eutrophication continued to be a water quality problem in the estuary below New Bern. Extensive fish kills in 1995 prompted further study of the problem. Low dissolved oxygen levels associated with algal blooms were determined to be a probable cause of many of the fish kills. The algal blooms and correspondingly high levels of chlorophyll *a* prompted the state to place the Neuse River and Neuse River Estuary on the 1994, 1996, 1998, and 2000 303(d) List of Impaired Waters. It was determined that control of nitrogen was needed to decrease the extent and duration of algal blooms.

Atmospheric deposition is believed to play a role in nutrient loading to the Neuse River and Neuse River Estuary. As excerpted from Whitall and Paerl (2001), the following discusses the role of atmospheric deposition to nutrient loading for sensitive waterbodies:

Excessive nitrogen loading to nitrogen-sensitive waters, such as the Neuse River Estuary (North Carolina) has been shown to promote changes in microbial and algal community composition and function (harmful algal blooms), hypoxia and anoxia, and fish kills. Previous studies have estimated that wet atmospheric deposition of nitrogen (WAD-N), as deposition of dissolved inorganic nitrogen (DIN:  $\text{NO}_3^-$ ,  $\text{NH}_3/\text{NH}_4^+$ ) and dissolved organic nitrogen, may contribute at least 15% of the total externally supplied or “new” nitrogen flux to the coastal waters of North Carolina. In a 3-year study from June 1996 to June 1999, Whitall and Paerl calculated the weekly wet deposition of inorganic and organic nitrogen at 11 sites on a northwest–southeast transect in the watershed. The annual mean total (wet DIN + wet organics) WAD-N flux for the Neuse River watershed was calculated to be 956 mg N/m<sup>2</sup>/yr (15,026 Mg N/yr). Seasonally, the spring (March–May) and summer (June–August) months contain the highest total weekly nitrogen deposition; this pattern appears to be driven by nitrogen concentration in precipitation. There is also spatial variability in WAD-N deposition; in general, the upper portion of the watershed receives the lowest annual deposition and the middle portion of the watershed receives the highest deposition. Based on a range of watershed nitrogen retention and in-stream riverine processing values, we estimate that this flux contributes approximately 24% of the total “new” nitrogen flux to the estuary (Whitall and Paerl, 2001).

Of these atmospheric deposition measurements, it is expected that the contributions will be greater from reduced forms of nitrogen than from oxidized forms because of the large amounts of agriculture within the watershed. One of the reasons for selecting this case study area is to evaluate the impact of a  $\text{NO}_x$ -based standard on an area dominated by reduced forms of nitrogen.

According to Whitall and Paerl (2001), atmospheric deposition accounts for approximately 24% of the Neuse River watershed's total nitrogen loading, with reduced forms of nitrogen making up a larger portion of the total than oxidized forms.



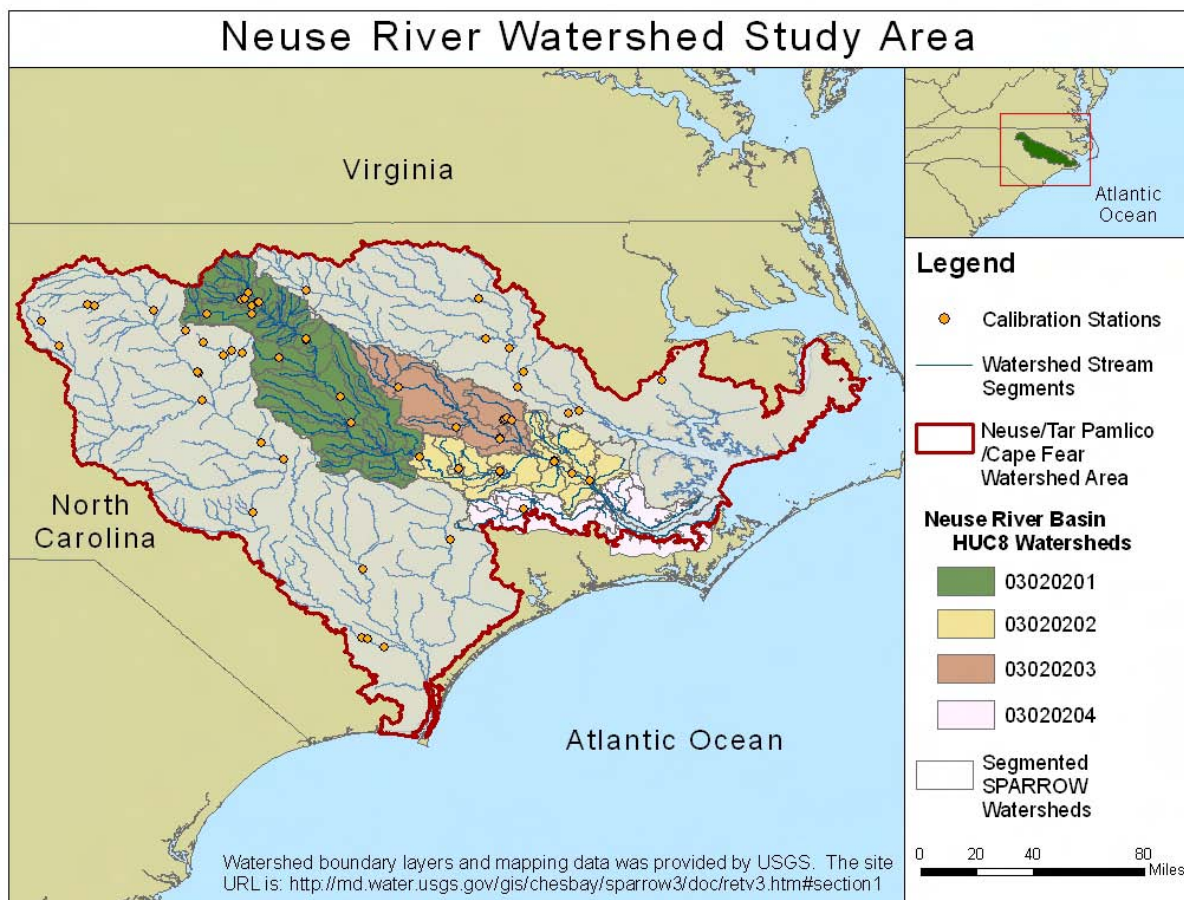


**Figure 1.2-4.** The Neuse River Watershed and Neuse River Estuary.

**Table 1.2-7.** Physical Characteristics of the Neuse River Estuary

Parameter	Value	Metadata
Estuary area (km <sup>2</sup> )	456	Estuary area, calculated from NOAA shapefiles
Tidal fresh zone area (km <sup>2</sup> )	5	Tidal fresh area, calculated from NOAA shapefiles
Mixing zone area (km <sup>2</sup> )	451	Mixing zone area, calculated from NOAA shapefiles
Saltwater zone area (km <sup>2</sup> )	0	Saltwater area, calculated from NOAA shapefiles
Estuary volume (m <sup>3</sup> )	$1.304 \times 10^9$	Best estimate of volume from digital bathymetric chart if available; otherwise, NOAA planimetry
Estuary depth (m)	2.86	From digital bathymetric chart if available; otherwise, NOAA planimetry
Estuary perimeter (km)	523	Perimeter of estuary, based on shapefile; can be used to calculate various aspect ratios
Percentage estuary open (%)	2.1	Percentage of the perimeter that is the “open” (or oceanic) boundary; somewhat subjective

Parameter	Value	Metadata
Catchment area (km <sup>2</sup> )	14,066	Not available
Catchment mean elevation (m)	56	Calculated from catchment shapefiles + Hydro1K (a global 1-km grid of elevation)
Catchment maximum elevation (m)	245	Calculated from catchment shapefiles + Hydro1K (a global 1-km grid of elevation)
Catchment/estuary area ratio	30.8	Area ratio, based on catchment and area data given above

**Source:** NEEA Estuaries Database

**Note:** m = meter

**Table 1.2-8.** Neuse River Watershed Land Use and Population

Parameter	Value	Metadata
Urban (km <sup>2</sup> )	1,328.66 (9.5%)	USGS (LUDA) for entire watershed 1972 with census 1990 information, base year early 1990s
Agriculture (km <sup>2</sup> )	4,983.14 (35.6%)	USGS LUDA for entire watershed 1972 with census 1990 information, base year early 1990s
Forest (km <sup>2</sup> )	6,648.5 (47.5%)	USGS LUDA for entire watershed 1972 with census 1990 information, base year early 1990s
Wetland (km <sup>2</sup> )	1,020.46 (7.3%)	USGS LUDA for entire watershed 1972 with census 1990 information, base year early 1990s
Range (km <sup>2</sup> )	5.17998 (0%)	USGS LUDA for entire watershed 1972 with census 1990 information, base year early 1990s
Total (km <sup>2</sup> )	13,985.93998	USGS LUDA for entire watershed 1972 with census 1990 information, base year early 1990s
Population (#)	1,015,059	Based on gridded (1-km) U.S. 1990 census data, corrected for catchments extending outside the United States (with LANDSCAN)
Population/estuary area (#.km <sup>-2</sup> )	2,226	Population based on gridded (1-km) U.S. 1990 census data, corrected for catchments extending outside the United States (with LANDSCAN). Estuary area, calculated from NOAA shapefiles.

**Source:** NEEA Estuaries Database

**Note:** USGS = U.S. Geological Survey; LUDA = Land Use and Land Cover; LANDSCAN = a global population database

**Table 1.2-9. Hydrological Characteristics of the Neuse River Estuary**

Parameter	Value	Metadata
Tide height (m)	0.15	NOAA estimate of tide height, back-calculated from tide volume; in some cases, guessed from nearby systems
Tide volume (m <sup>3</sup> )	$6.84 \times 10^7$	Tide height (m) $\times$ estuary area (km <sup>2</sup> ) $\times 10^6$
Tides/day (#)	2	NOAA designation
Tide volume/day (m <sup>3</sup> /day)	132,173,913	Calculated from tide volume and tides per day
Tide ratio	0.05	Tide height divided by estuary depth; a clean-up of a NOAA variable
Stratification ratio	0.08318	Total freshwater flux per day divided by tide volume per day
Percent freshwater (%)	1.1	Based on NOAA shape files of the three zones according to their designation
Percent mixed water (%)	98.9	Based on NOAA shape files of the three zones according to their designation
Percent seawater (%)	0	Based on NOAA shape files of the three zones according to their designation
Average salinity (psu)	13	Based on NOAA estimate of freshwater volume, but scaled to “local coastal salinity,” below
Tidal exchange (days)	74	Exchange time as (Est_V/net fw_V per d)*(coastal_sal - avg_sal)/coastal_sal); a salinity-based estimate of exchange
Tidal freshwater flush (days)	73	NOAA-based calculation, using (daily tide + freshwater volume)/system volume
Daily freshwater/estuary area (m/day)	22.368	NOAA estimate of daily flow/estuary area
Daily freshwater (m <sup>3</sup> /day) (best)	10,200,000	NOAA estimate above or (if not available) NCPDI estimate
Flow/estuary area (m/day) (best)	22.368	Best estimate/estuary area
Total freshwater volume (1/day)	0.00843	Best estimate/estuary volume (= hydraulic exchange rate)
Daily precipitation (m <sup>3</sup> /day)	$1.72 \times 10^6$	Direct precipitation on system, derived from PRISM shapefile
Daily evaporation (m <sup>3</sup> /day)	926,000	Direct evaporation from system, derived from LOICZ 0.5 degree database, originally from Wilmott
Daily precipitation/ estuary area (mm/day)	3.772	Daily precipitation/estuary area
Daily evaporation/ estuary area (mm/day)	2.031	Daily evaporation/estuary area

Parameter	Value	Metadata
Flow (m <sup>3</sup> /day)	$7.95 \times 10^6$	NCPDI_1982–1991

**Source:** NEEA Estuaries Database

**Note:** m = meter; psu = practical salinity unit; NCPDI = National Coastal Pollution Discharge Inventory; PRISM = Parameter-elevation Regressions on Independent Slopes Model; LOICZ = Land-Ocean Interactions in the Coastal Zone; mm = millimeters

Ammonia emissions from intensive livestock feeding operations are believed to contribute to nitrogen deposition in eastern North Carolina watersheds. During a 10-year legislative mandated moratorium on new operations, poultry populations increased in two Neuse River watershed counties, according to the U.S. Department of Agriculture's 2002 Ag Census. Statewide, the census reported an increase in poultry farms from 5,094 in 1997 to 6,251 in 2002 statewide (USDA, 2002). (As of this writing, the 2007 Ag Census is not complete.) The continued contribution of poultry operations' growth to nitrogen deposition during the moratoria has not been assessed, particularly in terms of its deposition in the Neuse River watershed.

## 2.0 APPROACH AND METHODS

Since it was necessary for this case study to span both terrestrial and aquatic systems to accommodate indirect (i.e., to the watershed) and direct (i.e., to the water surface) deposition effects, as well as a variety of indicators, a modeling approach was necessary to examine the impacts due to aquatic nutrient enrichment from nitrogen deposition.

There are several complicating factors to carrying out an analysis of eutrophication in waterbodies when one of the requirements is to include modeled output of atmospheric deposition from a high-level, detailed atmospheric model. This analysis is considered a multimedia analysis where the air, land, and water are involved. Typically, models or analysis methods existing in the literature focus on only one of those components. Links between the components with the desired output of eutrophication indicators are rare in the current literature or modeling environments. Additionally, the few instances that are available in the literature tend to focus on specific case study areas or on being highly empirical and difficult to scale or extend to alternate locations. All these facts must be considered when developing a method to examine the effects of N<sub>r</sub>, including NO<sub>x</sub>, deposition on aquatic nutrient enrichment.

## 2.1 MODELING

There are four basic steps necessary to undertake a modeling effort to examine the effects of nitrogen deposition (RTI, 2007):

1. Choose the specific question/problem to address.
2. Choose the best models based on model formulation (e.g., are biological processes considered?), desired output, study area, data availability, and necessary uncertainty/sensitivity analyses for the models.
3. Determine and set up any processes/algorithms necessary to match atmospheric modeling output (assumed to be from Community Multiscale Air Quality [CMAQ]) to the chosen receiving water or terrestrial/watershed model.
4. Obtain the data needed for model parameterization.

The problem to be addressed in this analysis is assessment of the effects of deposition of  $N_r$ , including  $NO_x$ , on aquatic nutrient enrichment. The impacts of both direct (i.e., deposition on the waterbody surface) and indirect (i.e., deposition within the watershed and transport to the waterbody) deposition need to be identified. A method is needed to provide measures of the eutrophication indicators that were previously described in Section 1.1.

A previous RTI International (RTI)<sup>1</sup> report (RTI, 2007) detailed the difficulty, along with the desire, to utilize atmospheric modeling in combination with the receiving-water and terrestrial/watershed models for analyzing the effects of  $N_r$ , including  $NO_x$ , deposition. The multimedia approach to modeling is still in development; therefore, at this time, not many models are set up to immediately accept the output from an atmospheric model such as CMAQ. In the previous model investigation, RTI examined 35 receiving-water and terrestrial/watershed models, which represent a wide diversity of types of ecosystems; history, location, and spatial/temporal scales of application; scientific acceptance levels and organizational and agency support; complexity and requirements; state variables and processes; and management uses.

Several existing models accept atmospheric concentration or flux data, but the time-step, spatial resolution, and exact species required might all differ from the atmospheric model output. The RTI report (2007) provided a list of models that could fulfill the multimedia approach while using CMAQ output as input for the atmospheric component to the model. These models include the Hydrologic Simulation Program-FORTRAN (HSPF), Regional Hydro-Economic Simulation System (RHESys), the Georgia Tech Hydrologic Model/Multiple Element Limitation (GT/MEL), Model of Acidification of Groundwater in Catchments (MAGIC), PnET-BGC,

---

<sup>1</sup> RTI International is a trade name of Research Triangle Institute

Integrated Nitrogen in Catchments (INCA), Spatially Referenced Regression on Watershed (SPARROW) attributes, AQUATOX, Water Quality Analysis Simulation Program (WASP), Enhanced Stream Water Quality Model (QUAL2K), CE-QUAL family of models, and Row Column AESOP/Estuary and Coastal Ocean Model with Sediment Transport (RCA/ECOMSED). These models are very different from one another in terms of the system components included, process representations, data requirements, and output parameters (for comprehensive details for each model, refer to the RTI report [2007]).

After determining which models could utilize CMAQ data, the ecosystem component encompassed by the models was examined. The choice of case study areas that include estuaries dictated that the model chosen must provide nutrient loads to an estuary waterbody and examine the impacts of those loads within the estuary itself. Although AQUATOX and QUAL2K are receiving-water models, they do not function for estuaries, nor do they account for indirect deposition over the contributing watershed. The WASP, CE-QUAL family of models, and RCA/ECOMSED are receiving-water models, which can be parameterized for estuaries, but they do not simulate terrestrial processes. Several of the other models account for indirect deposition and are strictly terrestrial models. These models include Regional Hydro-Economic Simulation System (RHESSys) and GT/MEL. Other models include both the indirect deposition and direct deposition, but only over streams and lakes within the watershed. These models are HSPF, MAGIC, PnET-BGC, INCA, and SPARROW.

From this analysis, it was apparent that a multiple step (i.e., linked processes or calculations) or model (i.e., separate but linked models) analysis would be optimal, including both a step/model to examine the indirect deposition and a step/model to examine the estuarine effects. The challenge was balancing analysis power against data, effort, and scalability requirements. Higher-level modeling approaches could be used to evaluate the eutrophication effects of interest if significant data resources, time, and expertise were available for a specific site. An approach of this kind would not be scalable or applicable to wider regions, but it would provide estimates with less uncertainty for a studied system.

The list of models above was used to identify several models that could be used to produce nutrient loads to the estuary, the obvious critical component of an eutrophication analysis. The best model for determining nitrogen loading to the estuary would track the atmospheric deposition of nitrogen through the watershed and to the estuary. This requirement

eliminated models that did not provide stream networking (i.e., PnET-BGC, MAGIC) or that lumped land-use categories together (i.e., INCA). The remaining models of HSPF and SPARROW are very different. HSPF is a highly parameterized, dynamic model that requires extensive data inputs and calibration. SPARROW is a hybrid statistical and process-based, steady-state model that requires much less data for parameterization, but still includes spatial variation and source investigation. Therefore, the SPARROW model was chosen to estimate nitrogen loadings to the estuaries.

Next, the most applicable method for examining eutrophication effects in an estuary was assessed. The three identified models that could represent estuarine processes (i.e., WASP, CE-QUAL family of models, and RCA/ECOMSED) were systematically ruled out as possibilities. RCA/ECOMSED is a proprietary model with extensive data requirements and requires a high level of expertise. The CE-QUAL family of models has primarily been used by the U.S. Army Corps of Engineers. The various versions of CE-QUAL all have extensive data requirements, and no indications of model integration have been uncovered in the literature. WASP provides the output desired, but requires parameterization for each system of study. Considering that the SPARROW model will provide TN loads to the estuary and the fact that the chosen method needs to be scalable and applicable to a variety of future case study areas, the SPARROW model was selected for this case study.

With the elimination of the three identified dynamic modeling applications, a more descriptive method of evaluation was sought. The method developed by NOAA and used in their NEEA was identified as a likely candidate for eutrophication assessment.

The screening process that led to the decision to use SPARROW and a more descriptive eutrophication evaluation technique considered the level of effort needed for an analysis of this scale in the time available. Additionally, as summarized in recent literature (Howarth and Marino, 2006), the complex processes that cause and express eutrophication within an estuary are not greatly understood and could lead to under- and mis-representation within dynamic models. The loss of a temporally varying analysis with the use of a steady-state or annual average model results in the loss in detailing seasonal changes and some of the intricate processes that may occur on a daily or even monthly time scale rather than over an entire year. This trade-off allows for development toward the ultimate goal of providing a scalable methodology that can be applied to various sites across the nation. With the acknowledged

uncertainties in eutrophication process details across different systems, a more screening-level, scalable approach was deemed appropriate for this initial study to link atmospheric nitrogen deposition to eutrophic conditions.

## **2.2 CHOSEN METHOD**

After examining several estuarine assessment options, the most comprehensive evaluation technique that could be applied on a wide scale was revealed to be an assessment of eutrophication as conducted in NOAA's NEEA. This assessment method is titled Assessment of Estuarine Trophic Status eutrophication index (ASSETS EI) (Bricker et al., 2007a). NOAA's ASSETS EI results in an estimation of the likelihood that the estuary is experiencing eutrophication or will experience eutrophication in the future.

The ASSETS EI incorporates indirect deposition over the watershed through the evaluation of nitrogen loading to the estuary. Thus, a decision was required on how to derive the nitrogen load to the estuary based on the 2002 CMAQ-modeled deposition data. Because the ASSETS EI is more of a screening-level approach to assessing eutrophication, the nitrogen load to the estuary is only required to be an annual estimate of TN loading. For these reasons, The SPARROW model was chosen to provide the estimates of nitrogen loading to the estuary.

The combination of SPARROW modeling and the ASSETS method to developing an EI (**Figure 2.2-1**) provides a sound basis for conducting an eutrophication assessment. Both SPARROW and the ASSETS EI are supported by federal agencies and have been through several improvement iterations. As shown in the following sections, the method provides a screening-level approach that includes an appropriate level of detail for determining the impacts on the degree of eutrophication in an estuary based on changes in atmospheric deposition loadings.



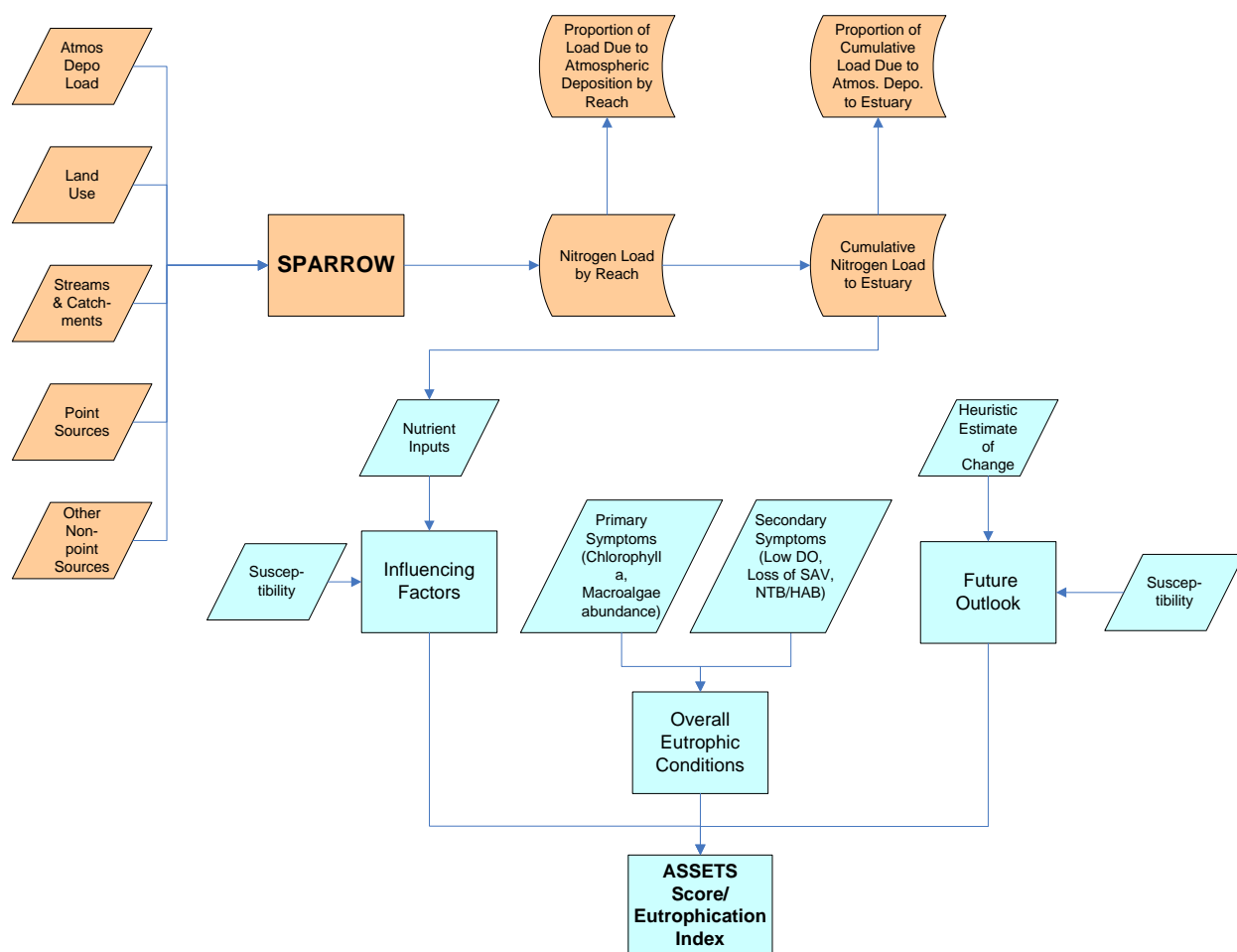


**Figure 2.2-1.** Modeling methodology for case study.

**Note:** DO = dissolved oxygen; HAB = harmful algal bloom.

ASSETS EI scores were available for both the Potomac and Neuse River estuaries, and both estuaries were the subject of past and ongoing SPARROW modeling of point and nonpoint sources, including atmospheric deposition.

## 2.2.1 SPARROW

### 2.2.1.1 Background and Description

SPARROW is a watershed modeling technique designed and supported by the U.S. Geological Survey (USGS). The model relies on a nonlinear regression formulation to relate water quality measurements throughout the watershed of interest to attributes of the watershed. Both point and diffuse sources within the watershed are considered along with nonconservative transport processes (i.e., loss and storage of contaminants within the watershed). SPARROW

follows the rules of mass balance while using a hybrid statistical and process-based approach (**Figure 2.2-2**). “Because the dependent variable in SPARROW models (i.e., the mass of contaminant that passes a specific stream location per unit time) is, in mathematical terms, linearly related to all sources of contaminant mass in the model, all accounting rules relating to the conservation of mass will apply” (Schwarz et al., 2006). Additionally, since SPARROW is a statistical model at its core, it provides measures of uncertainty in model coefficient and water quality predictions. Utilization of the SPARROW model results in estimates of long-term, steady-state water quality in a stream. In most applications, SPARROW estimates represent mean annual stream loadings of a contaminant.

$$\begin{array}{l} \text{Load leaving the} \\ \text{reach} \end{array} = \begin{array}{l} \text{Load generated within} \\ \text{upstream reaches and} \\ \text{transported to the reach via} \\ \text{the stream network} \end{array} + \begin{array}{l} \text{Load originating within the} \\ \text{reach's incremental watershed} \\ \text{and delivered to the reach} \\ \text{segment} \end{array}$$

**Figure 2.2-2.** Mass balance description applied to the SPARROW model formulation.

A key component of SPARROW is its reliance on the spatial distribution of watershed characteristics and sources. The stream reach network is spatially referenced against all monitoring stations, GIS data for watershed properties, and source information. This structure allows for the simulation of fate and transport of contaminants from sources to streams and downstream ecological endpoints. “Spatial referencing and the mechanistic structure in SPARROW have been shown to improve the accuracy and interpretability of model parameters and the predictions of pollutant loadings as compared to those estimated in conventional linear regression approaches” (e.g., Smith et al., 1997; Alexander et al., 2000) (Schwarz et al., 2006). This spatially distributed model structure based on a defined stream network allows separate statistical estimation of land and water parameters that quantify the rates of pollutant delivery from sources to streams and the transport of pollutants to downstream locations within the stream network (i.e., reaches, reservoirs, and estuaries) (Schwarz et al., 2006). **Figure 2.2-3** shows how each watershed and stream reach within the stream network defined for the SPARROW application (represented by different colors in the figure) is processed separately and linked to derive a final loading at a downstream location (the star labeled X). The SPARROW model is calibrated at each monitoring station (represented by stars in **Figure 2.2-3**) by comparing the modeled loads (i.e., a total of loads from each watershed segment and any upstream loads from previous calibrations) against monitored data at the station. In this case, the modeled load at

downstream monitoring station X would include loads from upstream monitoring station Y and the five watershed segments between the two monitoring stations.

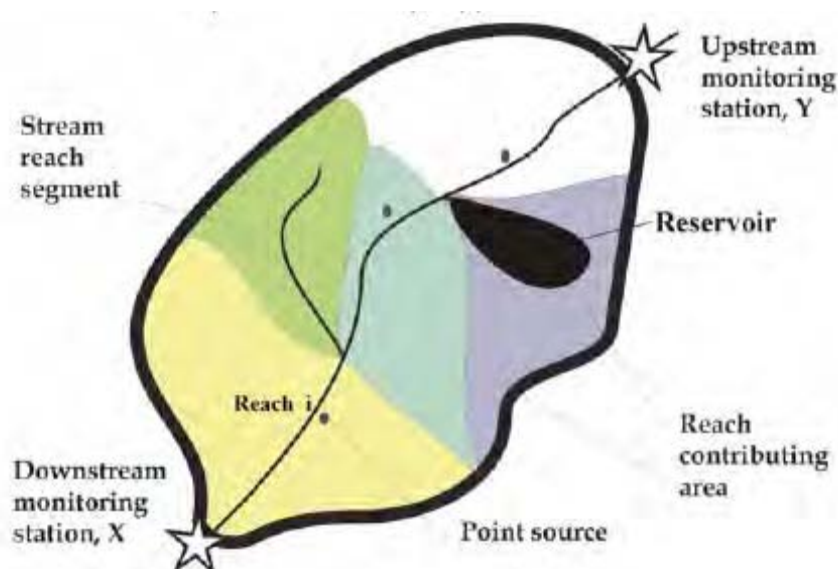


**Figure 2.2-3.** Conceptual illustration of a reach network.

Within this Aquatic Nutrient Enrichment Case Study, the mathematical formulation of the basic version of SPARROW presented by McMahon et al., (2003) is shown for consideration in Equations 3 to 5. “The additive contaminant source components and multiplicative land and water transport terms are conceptually consistent with the physical mechanisms that explain the supply and movement of contaminants in watersheds” (Schwarz et al., 2006). Preservation of mass, accounting for transport and decomposition at individual sources, is accomplished within SPARROW through the spatial referencing of all processes with respect to the stream network and the specific reach in which the process is carried out. Decomposition processes are represented through losses in delivery to the stream and within the stream reach itself (Equation 4) or within a reservoir (Equation 5).

$$Load_i = \sum_{n=1}^N \sum_{j \in J(i)} \beta_n S_{n,j} e^{(-\alpha Z_j)} H_{i,j}^S H_{i,j}^R \varepsilon_i \quad (3)$$

where

- Load = Nitrogen load or flux in reach *i*, measured in metric tons
- n, N* = Source index where *N* is the total number of individual *n* sources
- J(i)* = Set of all reaches upstream, including reach *i*

- $\beta_n$  = Estimated source coefficient for source  $n$   
 $S_{n,j}$  = Nitrogen mass from source  $n$  drainage to reach  $j$   
 $\alpha$  = Estimated vector of land to water delivery coefficients  
 $Z_j$  = Land-surface characteristics associated with drainage to reach  $j$   
 $H_{i,j}^S$  = Fraction of nutrient mass present in water body  $j$  transported to water body  $i$  as a function of first-order loss process associated with stream channels  
 $H_{i,j}^R$  = Fraction of nutrient mass present in water body  $j$  transported to water body  $i$  as a function of first-order loss process associated with lakes and reservoirs  
 $\varepsilon_i$  = Multiplicative error term assumed to be independent and identically distributed across separate subbasins defined by intervening drainage areas between monitoring stations.

$$H_{i,j}^S = \prod_m \exp(-k_m L_{i,j,m}) \quad (4)$$

where

- $k_m$  = First-order loss coefficient ( $\text{km}^{-1}$ ) (A  $k$  value of 0.08, for example, indicates that nitrogen is removed at a rate of approximately 8% per km of channel length.)  
 $m$  = Number of discrete flow classes  
 $L_{i,j,m}$  = Length of the stream channel between water bodies  $j$  and  $i$  in flow class  $m$ .

$$H_{i,j}^R = \prod_l \exp(-k q_l^{-1}) \quad (5)$$

where

- $k$  = Estimated first-order loss rate (or settling velocity; units = m/yr)  
 $q_l^{-1}$  = Reciprocal areal hydraulic load of lake or reservoir (ratio of water-surface area to outflow discharge; units = yr/m) for each of the lakes and reservoirs ( $l$ ) located between water bodies  $j$  and  $i$ .

SPARROW has been designed to identify and quantify pollution sources that contribute to the water quality conditions predicted by the model. Several different types of sources may be examined, and sources may be for an individual stream location or summarized for a grouping of stream locations. Examples of sources modeled within SPARROW include atmospheric deposition, point sources, animal agriculture, or land use–based supply of contamination. “The

ability to develop quantitative information on pollution sources in SPARROW models stems from the ability to trace, for each contaminant category, the predicted in-stream flux through a given stream reach to the individual sources in each of the upstream reach watersheds contributing contamination to that reach” (Schwarz et al., 2006). **Figure 2.2-4** highlights some of these sources in a conceptualization of the SPARROW model process.

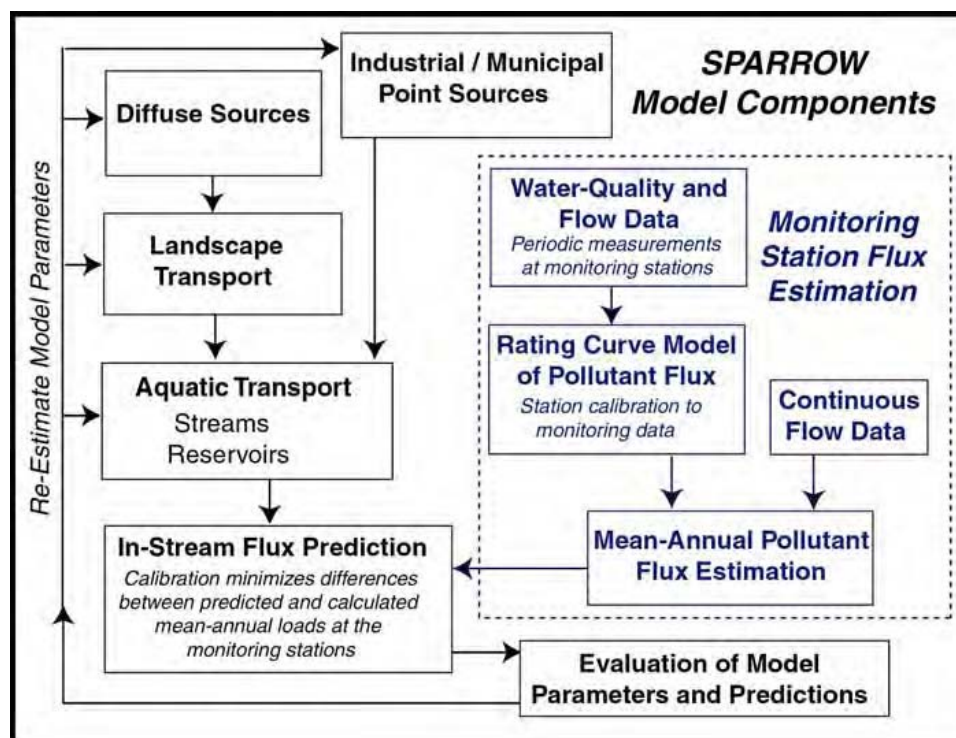


**Figure 2.2-4.** SPARROW model components (Schwarz et al., 2006).

Complete procedures, such as calculation of monitoring station flux estimation (**Figure 2.2-4**) and details on data formatting, will not be discussed here. The reader is pointed to the documentation for the recently released SAS version of the SPARROW model available from the USGS SPARROW Web site (<http://water.usgs.gov/nawqa/sparrow/sparrow-mod.html>) for full details on the model. The reader may also review some of the previous SPARROW applications presented in **Table 2.1-1**. The following sections describing SPARROW provide basic definitions of terms that aid in understanding SPARROW inputs and outputs and discuss some details that pertain to an application focused on atmospheric deposition inputs. Finally, an alternate formulation of SPARROW is described that highlights contributions of ammonia to the total  $N_r$  load for use in the Neuse River watershed.

**Table 2.1-1.** Examples of SPARROW Applications

Location	Citation
National	Smith and Alexander, 2000
Major estuaries of the United States	Alexander et al., 2001
Chesapeake Bay	Preston and Brakebill, 1999; Brakebill and Preston, 2004
State of Kansas waters	Kansas Department of Health and Environment, 2004
Connecticut River Basin	NEIWPCC, 2004
State of New Jersey waters	Smith et al., 1994
New England waters	Moore et al., 2004
New Zealand river basins	Alexander et al., 2002; Elliott et al., 2005
North Carolina coastal watersheds	McMahon et al., 2003
Tennessee and Kentucky watersheds	Hoos, 2005

### ***2.2.1.2 Key Definitions for Understanding SPARROW Modeling***

The following definitions have been summarized from the documentation accompanying the SAS application of the SPARROW model available from the USGS (Schwarz et al., 2006). Additional references are noted when used.

- **Bootstrapping.** This is the practice of estimating the properties associated with the model coefficients by estimating those properties when sampling from a specified distribution using replacement (e.g., the model coefficients are estimated a number of times until the best evaluation properties of the coefficients are found).
- **Delivered Yield (load per area).** This is the amount of nutrients generated locally for each stream reach and weighted by the amount of in-stream loss that would occur with transport from the reach to the receiving water. The cumulative loss of nutrients from generation to delivery to the receiving water is dependent on the travel time and in-stream loss rate of each individual reach (Preston and Brakebill, 1999).
- **Incremental Yield (load per area).** This yield represents the local generation of nutrients. It is the amount of nutrients generated locally (independent of upstream load) and contributed to the downstream end of each stream reach. Each stream reach and associated watershed is treated as an independent unit, quantifying the amount of nutrient generated (Preston and Brakebill, 1999).
- **In-Stream Loss.** This refers to stream attenuation processes that act on contaminant flux as it travels along stream reaches. A first-order decay process implies that the rate of removal of the contaminant from the water column per unit of time is proportional to the concentration or mass

that is present in a given volume of water. According to a first-order decay process, the fraction of contaminant removed over a given stream distance is estimated as an exponential function of a first-order reaction rate coefficient (expressed in reciprocal time units) and the cumulative water time of travel over this distance. Within SPARROW, the in-stream loss rate is assumed to vary as a function of stream channel length and various flow classes.

- **Landscape Variables.** These variables describe properties of the landscape that relate to climatic, or natural- or human-related terrestrial processes affecting contaminant transport. These typically include properties for which there is (1) some conceptual or empirical basis for their importance in controlling the rates of contaminant processing and transport, and (2) broad-scale availability of continuous measurements of the properties for use in model estimation and prediction. Examples include precipitation, evapotranspiration, soil properties like organic content or permeability, topographic index, or slope. Particular types of land-use classes, such as wetlands or impervious cover, may also potentially be used to describe transport properties of the landscape.
- **Land-to-Water Delivery Factor.** This factor describes the influence of landscape characteristics in the delivery of diffuse sources of contamination to the stream. The interaction of particular land-to-water delivery factors with individual sources may also be important to consider in SPARROW models.
- **Monitoring Station Flux Estimation.** This refers to the estimates of long-term flux used as the response variable in the model. Flux estimates at monitoring stations are derived from station-specific models that relate contaminant concentrations from individual water quality samples to continuous records of streamflow and time. These estimates are used to calibrate the model in each application.
- **Non-linear Regression.** The SPARROW model equation is a nonlinear function of its parameters. As such, the model must be estimated using nonlinear techniques. The errors of the model are assumed to be independent across observations and have zero mean; the variance of each observation may be observation-specific. A general method commonly used for these types of problems, one in which it is not necessary to assume the precise distribution of the residuals, is nonlinear weighted least squares. This is the estimation method used by SPARROW.
- **Segmented Watershed Network.** This network relates to the system of joined stream reaches that define the watershed of interest. Previous SPARROW applications have relied on the River Reach File 1 (RF1) hydrography developed by U.S. EPA (1996) and the 1:100,000 scale National Hydrologic Dataset (USGS, 1999). These datasets may be used in their original form or modified as needed depending on application requirements

- **Source.** SPARROW distinguishes between source categories (e.g., point sources, atmospheric sources, and animal agriculture) and individual sources (i.e., the rate of supply of contaminant of a particular category originating in the watershed and draining to a specific stream reach). A variety of sources based on knowledge of the watershed and inferences from literature may be examined with SPARROW.
- **Stream Reach. This is** the most elemental spatial unit of the infrastructure used to estimate and apply the basic SPARROW models. Stream reaches define the stream channel length that extends from one stream tributary junction to another. Each reach has an associated contributing drainage catchment.
- **Total Yield (load per area).** This is the amount of nutrients, including upstream load, contributed to each stream reach. These estimates are calculated by stream reach and account for all potential sources cumulatively and individually (Preston and Brakebill, 1999).

#### ***2.2.1.3 Concepts of Importance to Case Study—SPARROW Application***

Previous SPARROW applications have typically relied on atmospheric deposition measurements from NADP and have used wet  $\text{NO}_3^-$  deposition as a surrogate for nitrogen deposition over the watershed of interest. Within the case studies conducted, CMAQ-modeled and NADP-monitored atmospheric deposition was used. Several differences in the final parameterization of the SPARROW model will most likely result from this variation in input data.

Expected rules of model coefficient estimation based on source type are described below. When using direct measures of contaminant mass as a source estimate, “the source-specific parameter ( $\alpha_n$ ) is expressed as a dimensionless coefficient that, together with standardized expressions of the land-to-water delivery factor, describes the proportion or fraction of the source input that is delivered to streams (note that source and land-to-water delivery coefficients that are standardized in relation to the mean values of the land-to-water delivery variables are necessary to compare and interpret the physical meaning of source coefficients). This fraction would be expected to be  $<1.0$  but  $>0$ , reflecting the removal of contaminants in soils and ground water” (Schwarz et al., 2006).

An example of a source of this type would include atmospheric deposition where the model input would be the mass of nitrogen deposited over the watershed. When using only wet  $\text{NO}_3^-$  deposition as an estimate of nitrogen deposition, the model would be expected to account



for the additional nitrogen species (e.g., organic nitrogen, dry deposition of nitrate) to the extent that they are correlated with the measured inputs of  $\text{NO}_3^-$  (Alexander et al., 2001). This accounting is revealed by estimation within the model application of a land-to-water delivery fraction for wet  $\text{NO}_3^-$  deposition (i.e., product of the deposition coefficient and the exponential land-to-water delivery function) that exceeds 1.0.

Although available estimates for the estuarine watersheds indicate that wet  $\text{NO}_3^-$  deposition is highly correlated with dry  $\text{NO}_3^-$  plus  $\text{NH}_4^+$  and organic wet deposition, and estimates of the ratio of (dry and wet TN) deposition to  $\text{NO}_3^-$  wet deposition for the estuarine watersheds range from 3.2 to 4.0 with an average of 3.6 (Alexander et al., 2001), the use of NADP wet  $\text{NO}_3^-$  measurements requires the assumption that the spatial distribution of the various nitrogen species across a watershed does not vary. With the inclusion of explicit nitrogen species in atmospheric deposition measures, this assumption will not be required, and the land-to-water delivery fraction for the atmospheric deposition source term estimation is expected to be  $<1.0$ . This variation was explored within the case studies as was the general model fit with the improved atmospheric deposition inputs.

## **2.2.2 ASSETS Eutrophication Index**

### **2.2.2.1 Background and Description**

The NEEA Program defined and developed a Pressure-State-Response framework to assess the potential for eutrophication termed the ASSETS EI. It is categorical, where each of three indices results in a score that, when combined, result in a final overall score, also known as the ASSETS EI score or rating, which is representative of the health of the estuary. The indices are as follows:

- **OHI.** Physical, hydrologic, and anthropogenic factors that characterize the susceptibility of the estuary to the influences of nutrient inputs (also quantified as part of the index) and eutrophication.
- **OEI.** An estimate of current eutrophic conditions derived from data for five symptoms linked to eutrophication.
- **DFO.** A qualitative measure of expected changes in the system.

The following excerpt from Whitall et al., (2007) describes the objectives in applying the ASSETS method:

The ASSETS assessment method should be applied on a periodic basis to track trends in nutrient-related water quality over time in order to test management related hypotheses and provide a basis for more successful management. The null hypothesis being tested in this approach is: The change in anthropogenic pressure as a result of management response does not result in a change of state. The hypothesis is tested, e.g., to verify whether decreased pressure improves State, or whether increased pressure deteriorates State. In many cases, a reduction in pressure will result in an improvement of State, but in some cases, such as naturally occurring harmful algal bloom (HAB) advected from offshore, it will not (Whitall et al., 2007).

### ***Influencing Factors/Overall Human Influence***

Influencing factors help to establish a link between a system's natural sensitivity to eutrophication and the nutrient loading and eutrophic symptoms actually observed. This understanding also helps to illustrate the relationship between eutrophic conditions and use impairments (Bricker et al., 2007a). Influencing factors are determined by calculating two factors of susceptibility and nitrogen load, where "susceptibility" provides a measure of a system's nutrient retention based upon flushing and dilution, and "nitrogen loads" are a ratio between the nitrogen input to the system from the oceans versus from the land (Figure 2.2-5).

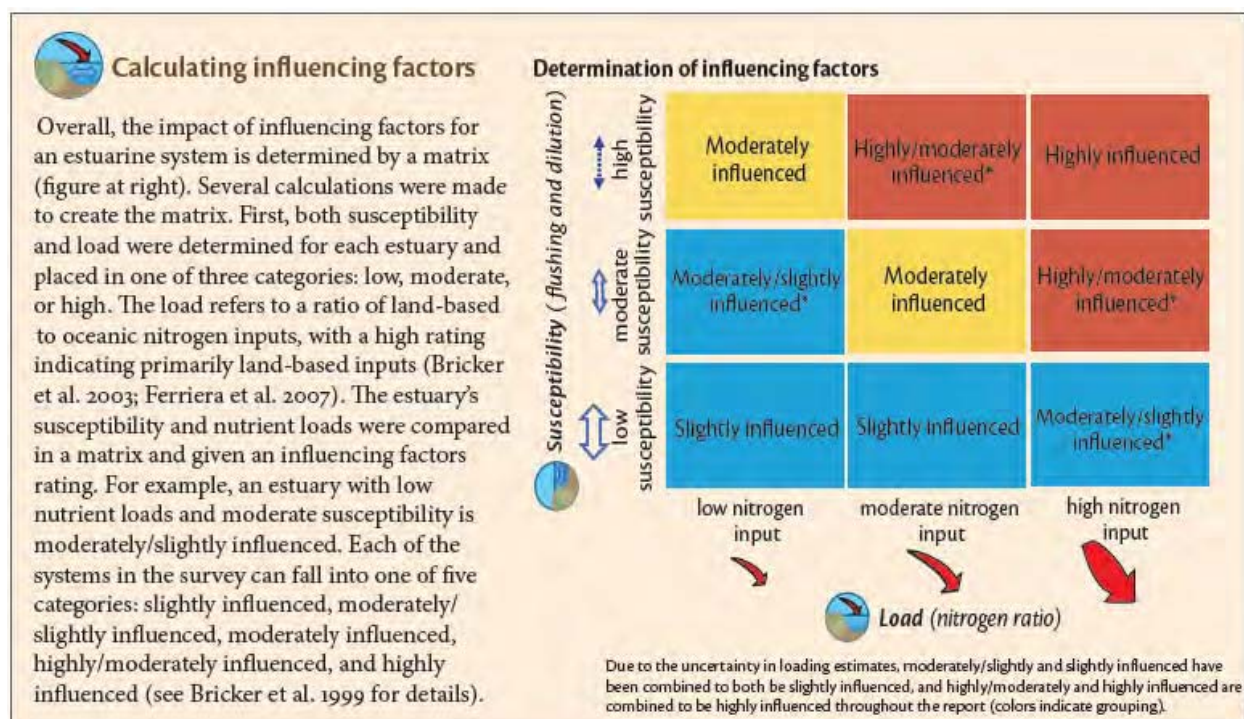


**Figure 2.2-5.** Influencing factors/Overall Human Influence index description and decision matrix (Bricker et al., 2007a).

The following factors take into account both the natural characteristics of and human impacts to systems.

- **Susceptibility.** For a coastal system, susceptibility depends on the flow of water into and out of the system. This flushing capability is determined by the physical properties (e.g., size, mouth) of the system as well as the influence of tidal waters and inflow of freshwater from tributaries. When water flows into and out of the system easily and quickly (i.e., there is a short residence time), nutrients flush out of the system rapidly, and there is not enough time for eutrophic symptoms to develop. Systems with short residence times have low susceptibility. The opposite also holds true. When water, and therefore nutrients, does not flush quickly from the estuary or coastal system, there is time for eutrophication effects to develop.
- **Nitrogen Load.** For this assessment, the loading component is estimated as the ratio of nitrogen coming from the land (i.e., human-related) to that coming from the ocean and is given a rating of low, moderate, or high (Bricker et al., 2003; Ferreira et al., 2007). For example, a high rating means that >80% of the nutrient load comes from land, whereas a low rating signifies a land percentage of <20%. This rating also provides insight into loading management because loads to systems with primarily ocean-derived nitrogen are not easily controlled. Understanding the sizes of current and expected future loads provides further insight into the application and success of management measures.

### ***Overall Eutrophic Condition***

To assess the eutrophic conditions of a system, the NEEA relies on five symptoms. Each of the five symptoms, divided into primary and secondary categories, is assessed based on a combination of the following factors: concentration or occurrence, duration, spatial coverage, frequency of occurrence, and confidence in the data (**Figure 2.2-6**). The two primary symptoms, chlorophyll *a* and macroalgal abundance (**Figure 2.2-7**), were chosen as indicators of the first possible stage in the process of water quality degradation leading to eutrophication. The secondary symptoms, which in most coastal systems will develop from the primary symptoms, include low dissolved oxygen levels, loss of SAV, and occurrences of nuisance/toxic algal blooms (**Figure 2.2-7**). At times, the secondary symptoms may also be present or develop without expression of primary symptoms. Nutrient concentrations are not employed as a symptom indicator because concentrations may vary between low and high values based on a number of factors, such as estuary susceptibility, which invalidates the use of nutrient concentrations alone as an indicator. As stated by Bricker et al., “Through the use of a simple

model, the current framework was established to help understand the sequence, processes, and symptoms associated with nutrient enrichment. Despite its limitations, it represents an attempt to synthesize enormous volumes of data and derive a single value for eutrophication in each estuary, essentially representing a complex process in a simple way” (Bricker et al., 2007a).

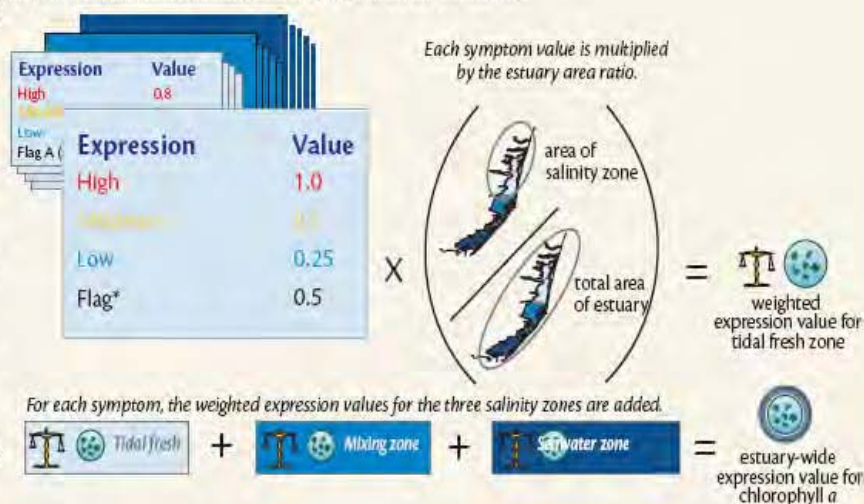


**Step 1: Determine expression value for each eutrophic symptom in each salinity zone.**

Eutrophic symptom expression values are determined for each symptom in each salinity zone (seawater, mixing, and tidal fresh), resulting in a total of 15 calculations. The expression is based on a set of IF, AND, THEN, decision rules that incorporate the symptom level (e.g., concentration), spatial coverage, and frequency.

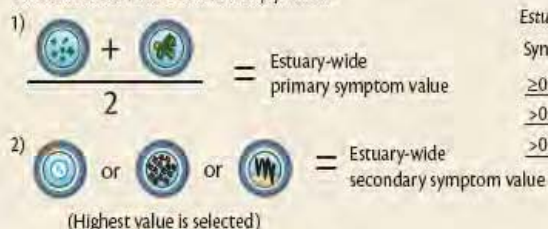

**Step 2: Calculate estuary-wide symptom expressions (using chlorophyll a as an example).**

The expression values are then used to calculate estuary-wide symptom expressions for each symptom. First, each expression value is multiplied by the area of the salinity zone and divided by the entire area of the system to establish the weighted value. Then, the weighted expression values in the tidal fresh, mixing, and seawater zone for each symptom are totaled to calculate the estuary-wide symptom expression value. This process is repeated for all five eutrophic symptoms. Note that "no problem" is the rating assigned if the value is 0, but that "no problem" and low are combined for discussion and tabulation throughout the report.


**Step 3: Assign categories for primary and secondary symptoms.**

The average of the primary symptoms is calculated to represent the estuary-wide primary symptom value. The highest of the secondary symptom values is chosen to represent the estuary-wide secondary symptom expression value and rating. The highest value is chosen because an average might obscure the severity of a symptom if the other two have very low values (a precautionary approach).

Primary and secondary estuary-wide symptom expression values are determined in a two step process:



Estuary-wide symptom rating is determined:

Symptom expression value	Symptom rating
$\geq 0$ to $\leq 0.3$	Low
$> 0.3$ to $\leq 0.6$	Medium
$> 0.6$ to $\leq 1$	High






**Step 4: Determine overall eutrophic condition.**

A matrix is used to combine the estuary-wide primary and secondary symptom values into an overall eutrophic condition rating according to the categories at right. Thresholds between rating categories were agreed on by the scientific advisory committee and participants from the 1999 assessment (Bricker et al. 1999).

1.0 High Primary	Moderate	Moderate high	High
0.6 Moderate Primary	Moderate low	Moderate	High
0.3 Low Primary	Low	Moderate low	Moderate high
	0 Low Secondary	0.3 Moderate Secondary	0.6 High Secondary 1.0

\*Flags are used to identify components for which data were inadequate or unknown. In these cases, assumptions were made based on conservative estimates that unknown spatial coverage is at least 10% of a zone, frequency at least episodic, and duration at least days.

**Figure 2.2-6.** Overall Eutrophic Condition index description and decision matrix (Bricker et al., 2007a).

Symptom	Parameters	Expression									
		Low			Moderate			High			
<div>Chlorophyll <i>a</i> (phytoplankton)</div> <div></div> <div>Typical high concentration (µg L<sup>-1</sup>) in an annual cycle determined as the 90<sup>th</sup> percentile value.</div>	<div>Spatial coverage:</div> <div>High &gt;50%</div> <div>Moderate 25–50%</div> <div>Low 10–25%</div> <div>Very low 0–10%</div> <div>Concentration:</div> <div>High &gt;20 µg L<sup>-1</sup></div> <div>Medium 5–20 µg L<sup>-1</sup></div> <div>Low 0–5 µg L<sup>-1</sup></div>	<div>Frequency:</div> <div>Episodic</div> <div>Periodic</div> <div>Persistent</div>	<div>Low symptom expression:</div> <div>Conc. low</div> <div>Coverage any</div> <div>Frequency any</div> <div>mod. - v. low</div> <div>episodic</div> <div>episodic</div>			<div>Moderate symptom expression:</div> <div>Conc. medium</div> <div>Coverage high</div> <div>Frequency episodic</div> <div>moderate</div> <div>periodic</div> <div>periodic</div> <div>high</div> <div>low - v. low</div> <div>periodic</div> <div>high</div> <div>moderate</div> <div>episodic</div>			<div>High symptom expression:</div> <div>Conc. medium</div> <div>Coverage high</div> <div>Frequency periodic</div> <div>high</div> <div>mod. - high</div> <div>periodic</div> <div>high</div> <div>high</div> <div>episodic</div>		
<div>Macroalgae</div> <div></div> <div>Causes a detrimental impact on any natural resource.</div>	<div>Frequency of problem:</div> <div>Episodic (occasional/random)</div> <div>Periodic (seasonal, annual, predictable)</div> <div>Persistent (always/continuous)</div>		No macroalgal bloom problems have been observed.			Episodic macroalgal bloom problems have been observed.			Periodic or persistent macroalgal bloom problems have been observed.		
<div>Dissolved oxygen</div> <div></div> <div>Typical low concentration (determined as the 10<sup>th</sup> percentile value) in an annual cycle.</div>	<div>Spatial coverage:</div> <div>High &gt;50%</div> <div>Moderate 25–50%</div> <div>Low 10–25%</div> <div>Very low 0–10%</div> <div>State:</div> <div>Anoxia 0 mg L<sup>-1</sup></div> <div>Hypoxia 0–2 mg L<sup>-1</sup></div> <div>Biol. stress 2–5 mg L<sup>-1</sup></div>	<div>Frequency:</div> <div>Episodic</div> <div>Periodic</div> <div>Persistent</div>	<div>Low symptom expression:</div> <div>State anoxia</div> <div>Coverage mod. - low</div> <div>Frequency episodic</div> <div>anoxia</div> <div>very low</div> <div>periodic</div> <div>hypoxia</div> <div>low - v. low</div> <div>periodic</div> <div>hypoxia</div> <div>moderate</div> <div>episodic</div> <div>stress</div> <div>any</div> <div>episodic</div> <div>stress</div> <div>mod. - v. low</div> <div>periodic</div>			<div>Moderate symptom expression:</div> <div>State anoxia</div> <div>Coverage high</div> <div>Frequency episodic</div> <div>anoxia</div> <div>low</div> <div>periodic</div> <div>hypoxia</div> <div>moderate</div> <div>periodic</div> <div>hypoxia</div> <div>high</div> <div>episodic</div> <div>stress</div> <div>high</div> <div>periodic</div>			<div>High symptom expression:</div> <div>State anoxia</div> <div>Coverage moderate - high</div> <div>Frequency periodic</div> <div>anoxia</div> <div>high</div> <div>periodic</div>		
<div>Submerged aquatic vegetation</div> <div></div> <div>A change in SAV spatial area observed since 1990.</div>	<div>Magnitude of change:</div> <div>High &gt;50%</div> <div>Moderate 25–50%</div> <div>Low 10–25%</div> <div>Very low 0–10%</div>		The magnitude of SAV loss is low to very low.			The magnitude of SAV loss is moderate.			The magnitude of SAV loss is high.		
<div>Nuisance/toxic blooms</div> <div></div> <div>Causes detrimental impact on any natural resources.</div>	<div>Duration:</div> <div>Persistent, seasonal, months, variable, weeks, days, weeks to seasonal, weeks to months, or days to weeks</div> <div>Frequency:</div> <div>Episodic, periodic, or persistent</div>		Blooms are either a) short in duration (days) and periodic in frequency; or b) moderate in duration (days to weeks) and episodic in frequency.			Blooms are either a) moderate in duration (days to weeks) and periodic in frequency; or b) long in duration (weeks to months) and episodic in frequency.			Blooms are long in duration (weeks, months, seasonal) and periodic in frequency.		

\*For further technical documentation of the methods, refer to Bricker et al. 1999 and Bricker et al. 2003.

**Figure 2.2-7.** Detailed descriptions of primary and secondary indicators of eutrophication (Bricker et al., 2007a).



### Determined Future Outlook

The future outlook relies on a similar combination of factors as the influencing factors (i.e., a rating of the system susceptibility and nutrient loading in the future). The aim of this index is to estimate future changes in the system through a combination of any physical, hydrologic, or pollutant loadings to the system itself or to its contributing watershed through such actions as watershed management plans, development restrictions, or policy changes resulting in nutrient decreases. The matrix in **Figure 2.2-8** is used to determine the DFO index rating.

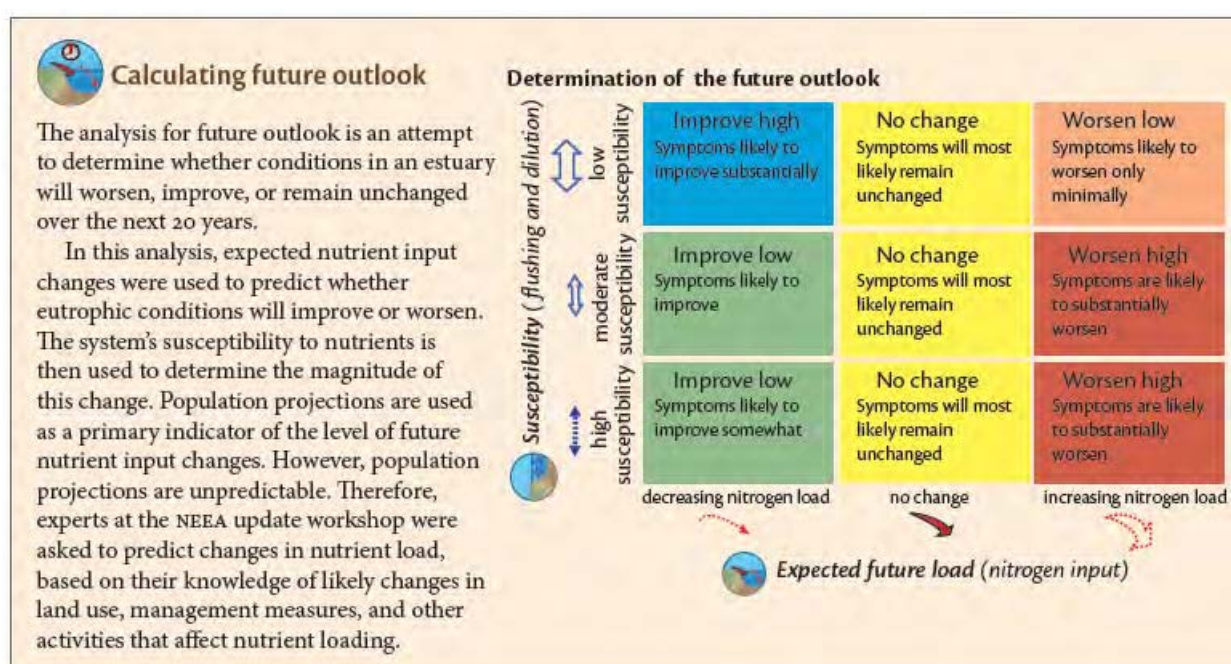


**Figure 2.2-8.** Determined Future Outlook index description and decision matrix (Bricker et al., 2007a).

The last step is to combine the OHI, OEC, and DFO index scores into a single overall ASSETS EI score. The ASSETS EI scores fall into one of six categories: High, Good, Moderate, Poor, Bad, or Unknown. These ratings can be summarized as follows (Bricker et al., 2007a):

- **High:** Low pressure from influencing factors, low OEC, and any expected improvement or no future change in eutrophic condition.
- **Good:** Low to moderate pressure, low to moderate-low eutrophic condition, and any expected future change in condition.

- **Moderate:** Any pressure, moderate-low to moderate-high eutrophic condition, and any expected future change in eutrophic condition.
- **Poor:** Moderate-low to high pressure, moderate to moderate-high eutrophic condition, and any expected future change in condition.
- **Bad:** Moderate to high pressure, moderate-high to high eutrophic condition, and any expected future change in eutrophic condition.
- **Unknown:** Insufficient data for analysis.

### ***2.2.2.2 Applications and Updates***

The ASSETS EI method developed out of the NEEA was first reported in 1999. Since that time, it has been used in several assessments across the country and internationally and has undergone revision and validation (Bricker et al., 1999, 2003, 2007a; Ferreira et al., 2007; Whitall et al., 2007). The original NEEA ASSETS EI assessment relied on questionnaires to experts for each estuary considered (Bricker et al., 1999). Later assessments determined that reliance on monitored data and less on reports from experts provided a more valid assessment tool (Bricker et al., 2006, 2007a). With the NEEA Update in 2007 (Bricker et al., 2007a), an online database was completed in which data users and data holders could access and input data. Additional datasets have also been collected for smaller study areas (Bricker et al., 2006). These data systems provide a wealth of information from which analyses may be conducted.

The original formulation of the ASSETS EI within the NEEA used watershed nutrient model estimates from SPARROW (Bricker et al., 1999). Although the updated ASSETS EI methodology has further apportioned nitrogen sources using the Watershed Assessment Tool for Evaluating Reduction Strategies for Nitrogen (WATERSN) model (Whitall et al., 2007), SPARROW is still appropriate for this study because atmospheric deposition inputs relative to other nitrogen sources can be defined.

### **2.2.3 Assessments Using Linked SPARROW and ASSETS EI**

The link between the SPARROW model and the ASSETS EI occurs when the SPARROW output is used as the nitrogen load in the OHI index calculation of the ASSETS EI score. For the purposes of this study, a complete analysis from atmospheric deposition loading to ecological endpoint of the ASSETS EI score required an assessment of the relative changes in the deposition load, the resulting instream nitrogen load to the estuary, and the change in



ASSETS EI score. An iterative assessment of the various possible ecological endpoints due to changing nitrogen loads has not been previously undertaken. The methods that follow have been designed to allow for set up of a process to link the SPARROW and ASSETS EI assessment, which includes uncertainty analysis. As will be detailed below, at this time the developed process includes an uncertainty analysis for the ASSETS EI assessment, whereas the uncertainty surrounding the corresponding decreased atmospheric deposition loads predicted by SPARROW has not yet been implemented. The process is described beginning with the individual components of each assessment, followed by a description of the iterative processing designed to sample among the assessments, producing a distribution of results.

The first step in setting up the linked analysis was to create a series of response curves. The SPARROW model can be used to assess the different atmospheric deposition loads that will result from changes in the  $\text{NO}_x$  concentrations enforced with any new policy scenarios. Therefore, a change in atmospheric deposition load produces a corresponding change in TN loading at the outlet of the watershed, in this case, to the estuary. Converting the TN load to a concentration value using the flow values employed in the SPARROW modeling allows for the creation of a relationship between decrease in atmospheric deposition load from the current condition scenario and instream total nitrogen concentration ( $\text{TN}_s$ ). A theoretical representation of this relationship in an ideal situation is presented in **Figure 2.2-9** (dotted lines represent uncertainty bounds). The red “x” indicates the nitrogen concentration during the current condition assessment where there is no load decrease in atmospheric deposition. The vertical asymptote of the curve approaches the nitrogen concentration of the river if there were no atmospheric inputs. In theory, the watershed response to changes in any loading would be nonlinear because of various retention and loss processes occurring within the watershed. However, because SPARROW is a statistical model, the empirical representation of these processes does not produce a nonlinear response as shown in **Figure 2.2-9**. As discussed in the results section, the response to changes in atmospheric deposition load is predicted to be linear by SPARROW. This highlights one area of uncertainty due to the steady-state, statistical nature of SPARROW. A benefit of using SPARROW is that the various atmospheric deposition levels can be run through the model in a short amount of time.

A second response curve is set up for the ASSETS EI based on the Influencing Factors/OHI and OEC index scores (Section 2.2.2), which are functions of TN load. The ASSETS EI

assessment is essentially a pressure-state-response scenario (**Figure 2.2-10**) where the pressure is the nitrogen load (represented by  $TN_s$ ) and the state is the current OEC index and ASSETS EI scores for the system. Response would be the change in state of the estuary (represented in the ASSETS EI by the DFO index). Bricker et al. (2007b), noted that the shape of the response curve would vary based on the susceptibility of the system. Therefore, if the susceptibility is known and held constant, a curve can be created.

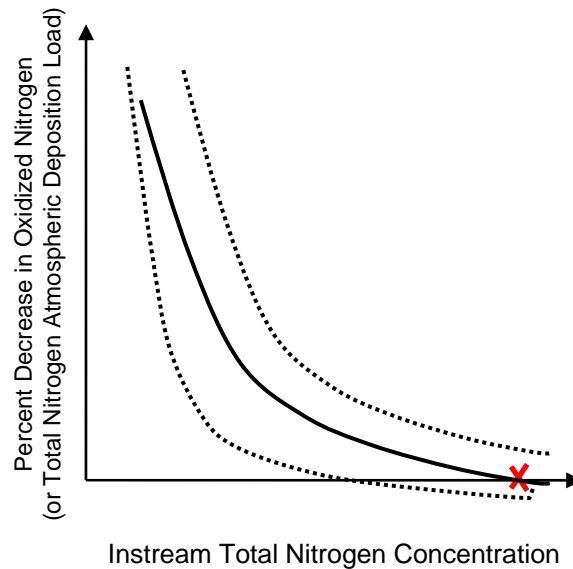


**Figure 2.2-9.** Example response curve of instream total nitrogen concentrations to atmospheric deposition loads.

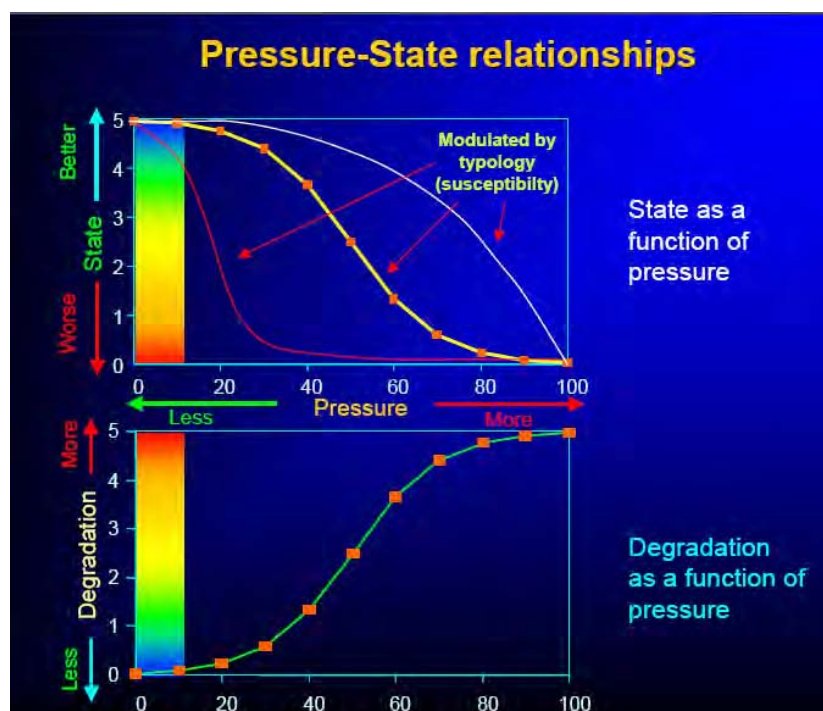


**Figure 2.2-10.** Example of response for case study analysis (Bricker et al., 2007b).

With the case study analysis, response curves were created for two different estuaries where the susceptibility is known. As previously described, the ASSETS EI score is a combination of OEC, OHI, and DFO index scores. It is possible to combine all three of these scores with the ASSETS EI into a single response curve when the susceptibility and DFO are held constant. The DFO may be held constant when alternative effects levels are being evaluated based on a current condition scenario, such as was done in this study. The susceptibility rating is based on physical and hydrological conditions. Physical conditions are unlikely to change. The hydrologic conditions may change because of extreme conditions, such as prolonged drought or hurricane events, but overall the conditions should average to a steady value that can be used in the analysis. **Figure 2.2-11** highlights this combination of scores where the susceptibility is “High” and the DFO is set at “Improve.” Additionally, by holding the susceptibility constant, the OHI index score becomes a function of the  $TN_s$ . This is evident in the double x-axis. The state response is the OEC index score along the y-axis. Underlying these combinations of OHI and OEC index scores is the ASSETS EI score.

The categorical nature of the assessment produces a mix of a continuous curve based on  $TN_s$  and blocks where different ASSETS EI scores are valid. The shape of the curve can be determined by fitting a logistic relationship through a series of points (red “x”s) within the

pressure-state realm based on compilations of historical data. The logistic function is suggested because of the pressure-state-response nature of the system meaning that initial, lower pressures are thought to affect the system slowly, then changes become more rapid up until a point where the pressure is so great that the state changes little because it has almost reached a maximum level. A logistic response to inputs (e.g., nutrients) is a common pattern in biological systems and is well documented. A variety of logistic (or sigmoidal) functions are available. In this case study, the following four-parameter function was used:

$$\text{OEC}(\text{TN}_s) = A + \frac{B}{1 + \exp\left(-\left(\frac{\text{TN}_s - C}{D}\right)\right)} \quad (6)$$

where

$\text{OEC}(\text{TN}_s)$  = OEC index score as a function of  $\text{TN}_s$  (unitless)

$\text{TN}_s$  =  $\text{TN}_s$  (mg N/L)

A, B, C, D = Parameters to be estimated.

Applying this logistic function as in **Figure 2.2-11**, parameter *A* affects the OEC intercept value, **b** in **Figure 2.2-11**; parameters *A* and *B* affect the OEC asymptote value; *C* affects the “S” shape; and *D* shifts the “S” horizontally. The curve is fit through a nonlinear optimization routine using a modified version of Box’s algorithm (Box, 1965). Constraints on the boundary conditions for the function are described below. At this time, 500 iterations of the algorithm were used to define the function. A future assessment must complete a Monte Carlo simulation analysis to determine a justifiable estimate of the number of iterations needed to bring the algorithm to convergence for the problem as thus defined.

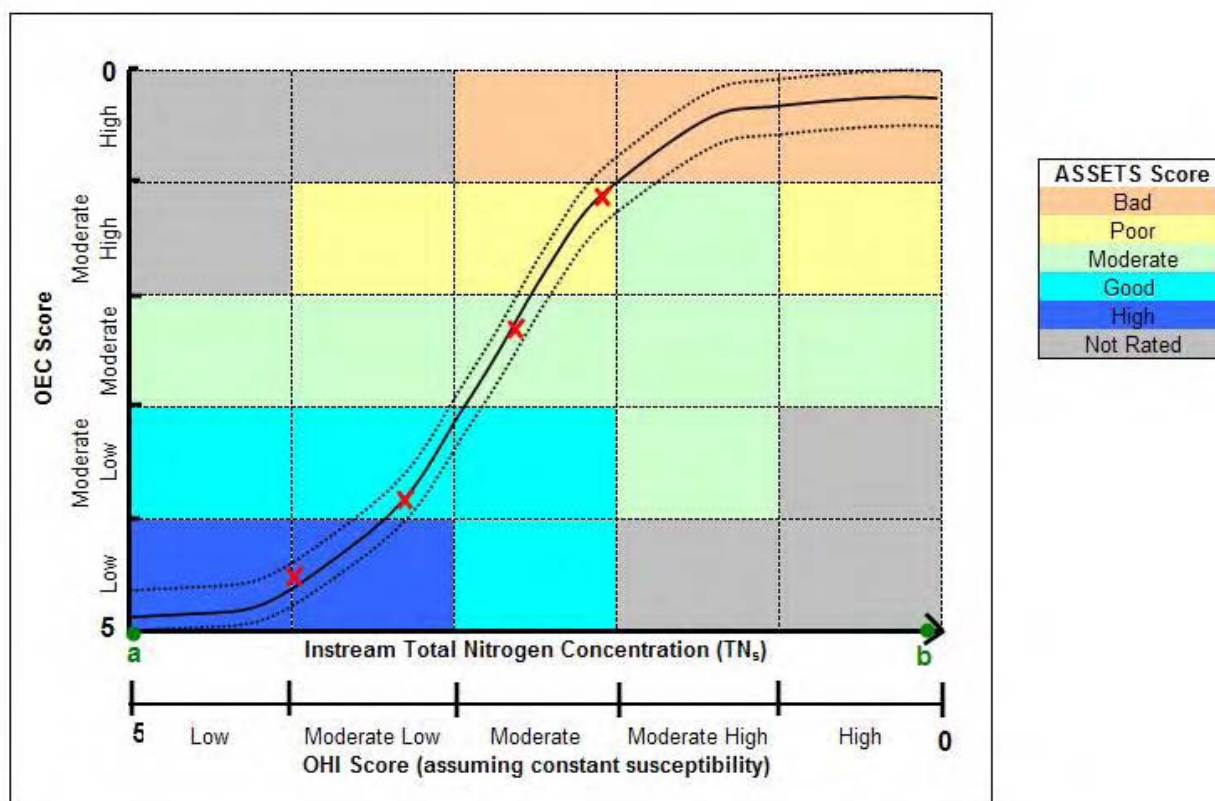


**Figure 2.2-11.** ASSETS EI response curve.

Within the analysis space created by both the OHI and OEC index scores, the axes are limited to the scores of zero (really one) to five, but the corresponding  $TN_s$  must be determined separately. Point “a” represents the background nitrogen concentration that would occur in the system with no anthropogenic inputs (assuming the system is not naturally eutrophic) or the system at a pristine state. In almost all cases, this value will be unknown because of the extent to which anthropogenic inputs have influenced the nation’s ecosystems. A lower bound and upper bound on this value, between which the algorithm randomly selects a different realization for each iteration, were specified. The lower bound was specified as the offshore TN concentration (used in the OHI index score) and the upper bound was specified at 1.0 milligrams per liter (mg/L) for the Potomac River/Potomac Estuary Case Study Area based on best professional judgment and at 0.1 mg/L for the Neuse River/Neuse River Estuary Case Study Area based on a combination of the lowest monitored nitrogen values over a number of years and best professional judgment. The upper bound of the  $TN_s$  is the maximum nitrogen concentration at which the stream is nitrogen-limited; above this point, the nitrogen inputs to the system no longer

affect the eutrophication condition. Several attempts to quantify this limit were made through historical data analysis, examination of nitrogen to phosphorus (N:P) ratios within the estuary, and consideration of the underlying eutrophication processes. For this first assessment, a lower and upper bound on this maximum  $TN_s$  between which the algorithm randomly selects a different realization for each iteration were specified. The lower bound was specified as the maximum observed  $TN_s$ , whereas the upper bound was specified as 50% greater than this value based on best professional judgment.

Further measures of uncertainty could be taken into account using upper and lower bounds on the logistic curve. The horizontal spread at each OEC index score reflects the range of nitrogen concentrations that may relate to that specific OEC index score. The vertical spread relates to the range in OEC index scores that may occur at each nitrogen concentration. As with the  $TN_s$  axis, the lower and upper bounds on both extremes of the OEC scale were specified again. At both ends of the scale (i.e., 0 and 5), the OEC maximum and OEC minimum values could be randomly selected at each iteration within a range of 1 OEC unit or could be set at constant values of 1 and 5. If randomly selected, the actual OEC minimum would be between 0 and 1 at the “0” end of the scale and between 4 and 5 at the “5” end of the scale. This would account for the likelihood that an estuary may not physically be capable of reaching either a “pure, pristine” condition (e.g., OEC = 5) or a “completely hypereutrophic” condition (e.g., OEC = 0). Consideration of this allowance and of holding the scores constant is discussed in the uncertainty section.

### ***2.2.3.1 Back Calculation Method***

The creation of the two response curves allows an analyst to work backward from the ecological endpoint to the source of the impairment; in this case from the ASSETS EI score to the atmospheric deposition loading of oxidized nitrogen. To accomplish this back calculation, a computer program has been generated that processes through a series of user inputs, defined boundary conditions, and set cases for determining the ASSETS EI score to perform the iterative calculations described in setting the logistic curve and determining the  $TN_s$ . Currently, the program is coded in the Visual Basic language and requires an input file defined by the user to contain:

- The desired ASSETS EI ecological endpoint (i.e., score)

- Oceanic nitrogen and salinity values
- Instream salinity values
- The regression equation relating the decrease in atmospheric deposition of nitrogen to  $TN_s$
- The number of realizations on which to iterate the model calculations.

### ***2.2.3.2 Uncertainty Bounds on $TN_s$ , OEC Min/Max Values***

Based on the degree of uncertainty, three different scenarios exist for the analysis (**Figure 2.2-12a** through **Figure 2.2-12c**). There are two relationships, or functions, involving uncertainty in the proposed methodology. The first is the SPARROW-predicted  $TN_s$  at the head of the estuary given a total nitrogen atmospheric deposition load ( $TN_{atm}$ ). (Note that SPARROW model predictions are actually provided in terms of instream TN loads [mass per time]; however, concentrations [mass per volume] can be calculated by dividing the instream TN load by the flow rate.) This functional relationship is denoted as  $TN_s(TN_{atm})$  where the  $TN_s$  is actually evaluated on changes in the loading of oxidized nitrogen, not all nitrogen species, in the TN atmospheric deposition load. This means that decreases are applied to the  $NO_x$  load within the atmospheric load, and a new  $TN_{atm}$  is calculated). (For instance if the  $NO_x$  load contribution is 10 kg N/yr and  $TN_{atm}$  is 20 kg N/yr, then a 40% decrease would result in a  $TN_{atm}$  equal to 16 kg N/yr after decreasing the 10 kg N/yr by 40%.) Because of the SPARROW regression uncertainties, this function is a probability distribution (i.e., given an  $TN_{atm}$ , there are many alternative  $TN_s$  values). This distribution function is denoted as  $TN_s^{pdf}(TN_{atm})$ . Under the standard assumptions of regression modeling, this is a normal distribution with a mean value represented by the SPARROW estimate of TN load. The variability around the mean value represents uncertainty in the SPARROW parameter estimates. However, the SPARROW regression model does not give rise to normally distributed residuals, and some nonparametric methods have been developed by the SPARROW developers to estimate SPARROW's confidence limits on predictions (Schwarz et al., 2006). This measure of uncertainty has not yet been incorporated into this methodology, and that is why the results for the Potomac River/Potomac Estuary Case Study Area and the Neuse River/Neuse River Estuary Case Study Area are based on uncertainty Scenario B (explained below; **Figure 2.2-12b**). Accordingly, the uncertainty presented in those results will be an underestimate of the total uncertainty.

The second uncertain function is the semiquantitative relationship between the ASSETS EI score and the TN<sub>s</sub> load. The ASSETS EI model yields a result based on three index “scores,” the OEC, the OHI, and the DFO index scores as described in Section 2.2.2. The OEC and OHI index scores are functions of TN<sub>s</sub>. Thus, the ASSETS EI model can be written as ASSETS EI = f(OEC(TN<sub>s</sub>), OHI(TN<sub>s</sub>), DFO) where “f” is the functional relationship that is the ASSETS EI methodology. Based on the methodology developed for creation of the response curve, the OEC(TN<sub>s</sub>) function also involves uncertainty, and the OEC index score resulting from any particular TN<sub>s</sub> is also a probability distribution, which can be assumed to be a uniform distribution for this first analysis. Incorporating this uncertainty, the ASSETS EI model can be expressed for this study as ASSETS EI = f(OEC<sup>pdf</sup>(TN<sub>s</sub>), OHI(TN<sub>s</sub>), DFO). **Figure 2.2-12b** and **Figure 2.2-12c** present the iterative steps in which the probability distribution function of OEC results is created in the coded model.

In setting up Scenario B for the evaluation of alternative effects levels, the goal was set to determine the change in oxidized nitrogen load required to improve the ASSETS EI score by one, two, and three categories from its current level set in the 2002 current condition analysis. Improvement in the ASSETS EI score by categorical values means moving along the logistic curve set to data points determined through the gathering of historical monitoring data and reports. **Figure 2.2-13** provides a visualization of what it means graphically to improve by one ASSETS EI score category. In reality, the exact results of improving by one, two, or three categories will vary depending on the estuary and the baseline state of the estuary (i.e., where on the logistic curve the analysis begins). In the example shown in **Figure 2.2-13**, improving the ASSETS EI score by one category also improves the OEC index score by one category but allows for a decrease in the TN<sub>s</sub>, which results in the same OHI index score as the baseline. Also in this example, the baseline for the estuary is an ASSETS EI score of “bad,” thus it is possible to improve by three categories although, in doing so, the OEC and OHI/TN<sub>s</sub> would have to improve to an almost pristine state. If a system begins with an ASSETS EI score of “Moderate” or “Good,” the assessment will only be able to examine an improvement in two or one ASSETS EI score categories, respectively. Also noted in **Figure 2.2-13** is the direction of the category movement. In this example, improvement of the ASSETS EI score along the determined logistic curve is a vertical movement down rather than a horizontal move to the left (not illustrated with this example); therefore, the OHI index score may remain in the same or similar state. If the



movement were to the left, the OHI index score would have to improve, whereas the eutrophic condition of the system (i.e., OEC index score) could remain the same or similar to the baseline conditions.

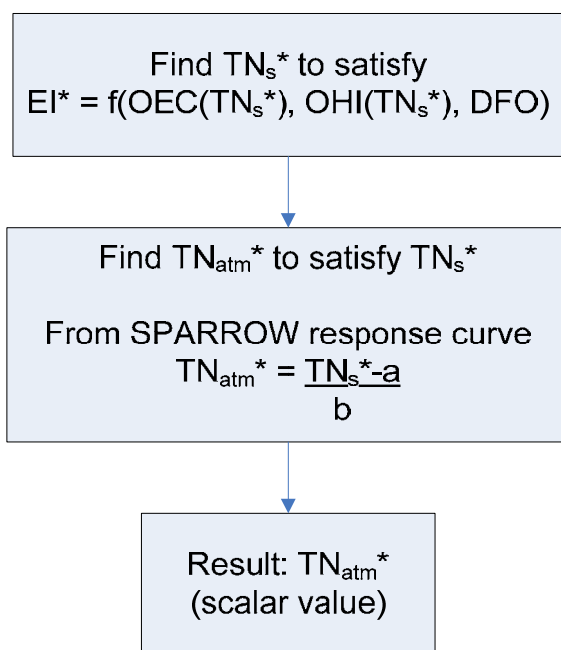
ASSETS model:  $EI = f(OEC(TN_s), OHI(TN_s), DFO)$

SPARROW model response curve:  $TN_s(TN_{atm}) = a + b TN_{atm}$

Terms:

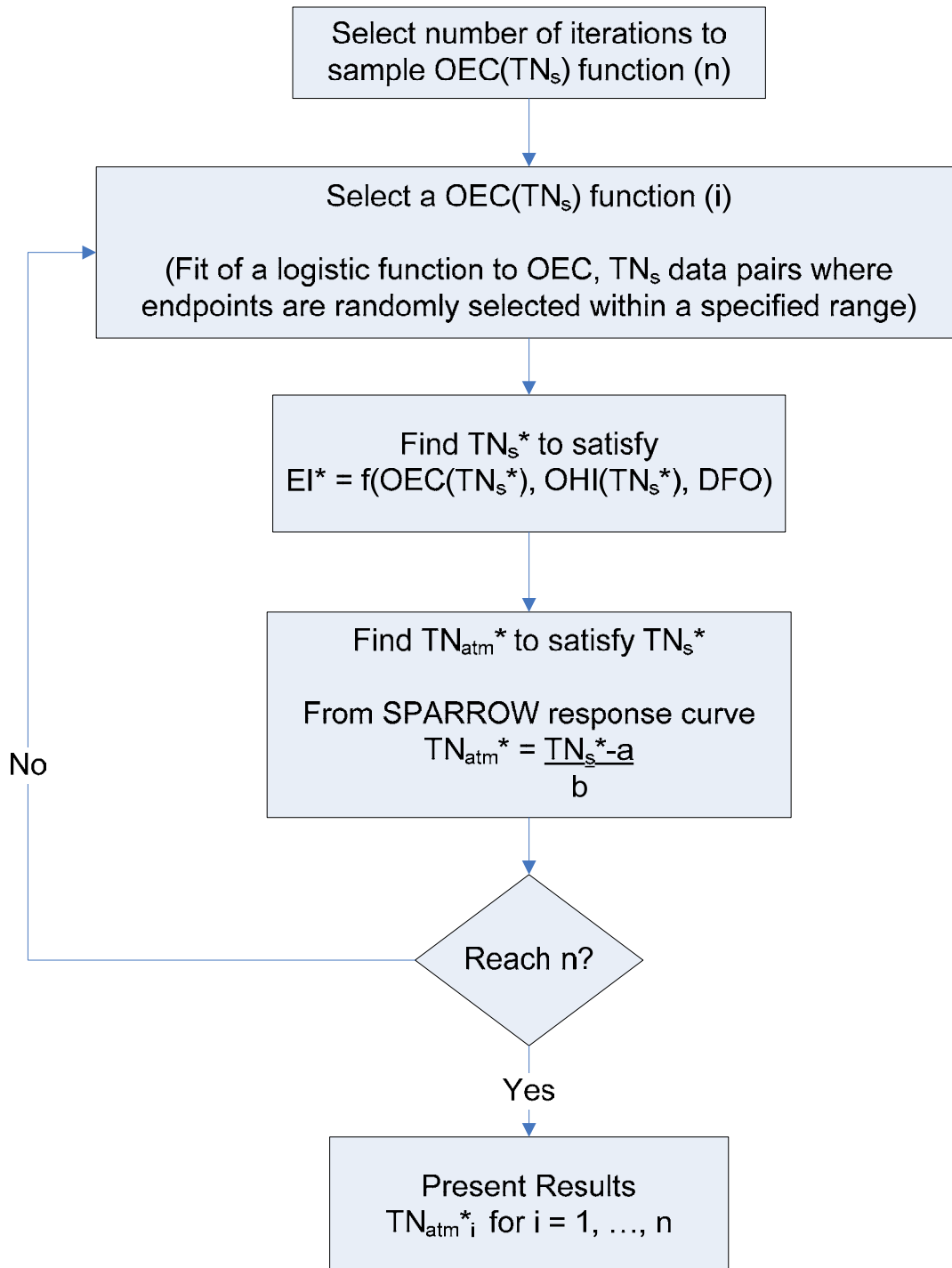
EI	Eutrophication Indicator
f	Denotes functional relationship between parameters (i.e., f is the ASSETS methodology)
OEC	Overall Eutrophic Condition
OHI	Overall Human Influence
DFO	Determined Future Outlook
EI*	Eutrophication Indicator of interest
TN <sub>s</sub> *	Total Nitrogen concentration of interest
TN <sub>atm</sub> *	Total atmospheric nitrogen deposition load <i>evaluated by decreasing the NOx contribution to deposition</i>
a, b	constants
i, j	number of function iterations
CI	Confidence interval

A) No uncertainty in OEC(TN<sub>s</sub>) or in TN<sub>s</sub>(TN<sub>atm</sub>)

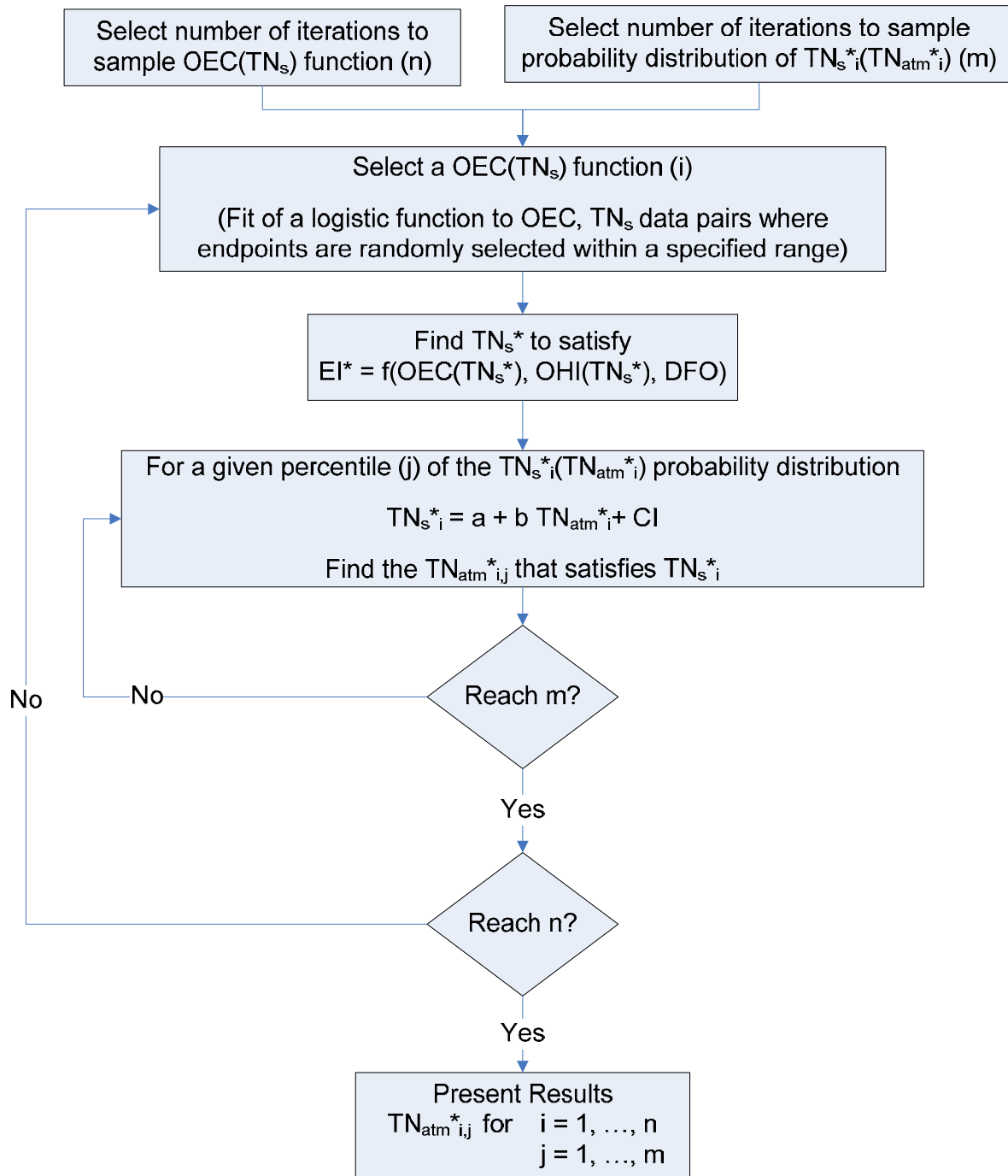


**Figure 2.2-12a.** Back calculation analysis scenario A: no uncertainty.

B) Uncertainty in  $OEC(TN_s)$ ; No uncertainty in  $TN_s(TN_{atm})$



**Figure 2.2-12b.** Back calculation analysis scenario B: uncertainty in ASSETS EI assessment.

C) Uncertainty in OEC(TN<sub>s</sub>) and TN<sub>s</sub>(TN<sub>atm</sub>)


**Figure 2.2-12c.** Back calculation analysis scenario C: uncertainty in both ASSETS EI assessment and nitrogen loading assessment.

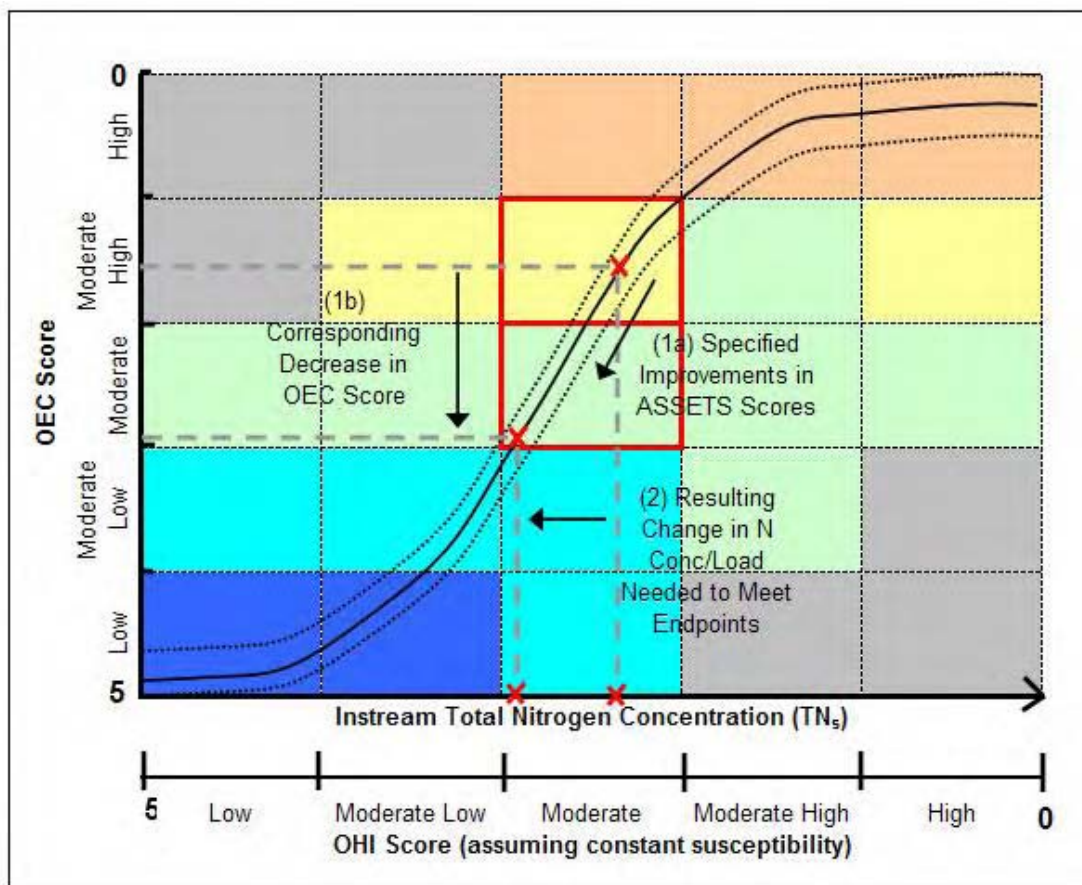


**Figure 2.2-13.** Example of an improvement by one ASSETS EI score category in a back calculation assessment.

In the second piece of the back calculation, the newly determined TN<sub>s</sub> needed to make an improvement in the ASSETS EI score is examined on the response curve of the TN<sub>s</sub> to TN<sub>atm</sub>.

**Figure 2.2-14** presents an example similar to those found in the case studies where the response is linear (note that the axes have been flipped from original representation in **Figure 2.2-9** to reflect how the response curve is handled within the coded program developed for this study). While the linear nature of this curve during this preliminary assessment is a function of the use of SPARROW, a statistical watershed model, valuable information on the required decrease in TN<sub>atm</sub> can still be determined. The scale of the axes of the response curve also provides a great deal of information on the system of interest. For instance, if the TN<sub>s</sub> changes that result from a small change in the TN<sub>atm</sub> are much greater (e.g., 5% change in atmospheric load versus 20% change in instream concentration), then the system is highly influenced by the atmospheric deposition of nitrogen. If the situation is reversed and large changes in TN<sub>atm</sub> result in only small

changes in the  $TN_s$ , then the system is not greatly influenced by the atmospheric deposition of nitrogen.

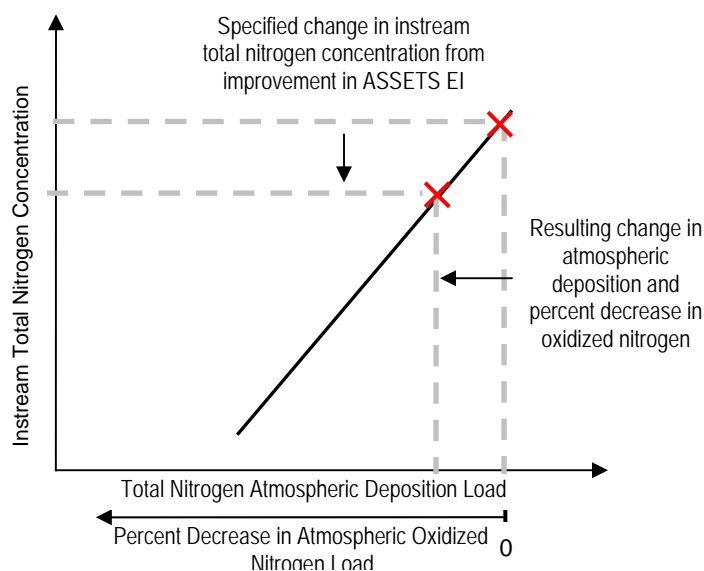


**Figure 2.2-14.** Example for resulting change in atmospheric nitrogen loads due to improvement in ASSETS EI score in back calculation assessment.

## 3.0 RESULTS

### 3.1 CURRENT CONDITIONS

The available air quality data for this review are based on the 2002 CMAQ model year and NADP data; therefore, current conditions for this case study evaluated ecosystem responses for the year 2002. In both case study areas, the best attempts were made to use monitoring and modeling data from that time period. The methods designed for the current condition ecosystem analysis required for this study produce annual averages for 2002.

#### 3.1.1 Summary of Results for the Potomac River/Potomac Estuary Case Study Area

The 2002 current condition analysis of the Potomac River/Potomac Estuary Case Study Area relied on a previous SPARROW application calibrated for the late 1990s in the Chesapeake Bay watershed. The evaluation of the ASSETS EI used raw data compiled from organizations

reporting on various issues in the Chesapeake Bay, including the Chesapeake Bay Program (CBP) and the Virginia Institute of Marine Science (VIMS).

#### **3.1.1.1 SPARROW Assessment**

The Version 3 Chesapeake Bay SPARROW application modeled the watershed for the time period of the late 1990s. Stream nitrogen load estimates from 87 sites were used to calibrate the model. The stream reach network used in this analysis relied on a modified version of the RF1 used in previous Chesapeake Bay SPARROW applications, but included 68 reservoirs that were not previously included. This analysis examined the sources of atmospheric deposition, fertilizer and manure application, point sources, and land use. For details on the compilation of each of these GIS-based datasets, see Brakebill and Preston (2004). Watershed characteristics considered in the model as loss and decay variables include precipitation, temperature, slope, soil permeability, and hydrogeomorphic regions.

The Version 3 calibrated model was selected to create the results for the 2002 current condition analysis because of its temporal proximity to the desired base year. The 5-year difference from 1997 to 2002 was not expected to result in a large change in the model if it were recalibrated to more recent data (S. Preston, personal communication, 2008). Future updates to this study should consider recalibrating the model to 2002 data to ensure that this assumption holds true.

The SPARROW assessment for the 2002 current condition analysis used the same source inputs and watershed characteristics, except in the case of atmospheric deposition. The Version 3 Chesapeake Bay SPARROW application relied on 1997 mean deposition values of wet-deposition atmospheric  $\text{NO}_3^-$  using the 191-point measurements in the NADP program across the country. As described in Section 2.2.1.3, relying on wet  $\text{NO}_3^-$  deposition as a surrogate for TN deposition requires an assumption of spatial homogeneity between the nitrogen species. The 2002 current condition analysis used the CMAQ/NADP data that were prepared for the Risk and Exposure Assessment as atmospheric deposition inputs to the model. Although the Version 3 Chesapeake Bay SPARROW model was calibrated against only wet  $\text{NO}_3^-$  deposition loads, it was decided that the 2002 current condition analysis should incorporate all available forms of nitrogen deposition in order to fully reflect the result of changing oxidized nitrogen loads.

The use of the 2002 atmospheric deposition loads with the 1997 Version 3 of SPARROW introduces a source of uncertainty to the modeled results because the source parameter for atmospheric deposition was calibrated to the spatial variability and magnitude of the original atmospheric source. This degree of uncertainty will be omitted from any future analyses when the time and data exist to recalibrate the SPARROW model to a full set of 2002 current condition data. At this time, the study's goal, which is to reflect on the changes in magnitude of nitrogen loads to the estuary due to changes in the deposition of oxidized nitrogen, can still be assessed and described using this data compilation. The 1997 data used in the original Version 3 Chesapeake Bay SPARROW application shows wet  $\text{NO}_3^-$  yields highest in the western, mountainous region of the Potomac River watershed with lower values around the southern central portion and areas surrounding the Potomac Estuary (Brakebill and Preston, 2004). There is a clear trend of interpolation from the NADP data. In comparison, **Figure 3.1-1a** through **Figure 3.1-1c** reveal highly different spatial patterns in oxidized, reduced, and TN atmospheric deposition yields across the Potomac River and Potomac Estuary watershed. Note that the scales across the three figures use the same increments and colors so that they can be directly compared. For the current condition 2002 analysis of the Potomac River and Potomac Estuary, an estimated 40,770,000 kg of TN was deposited in the 3.2-million hectares (ha) Potomac River watershed, for an average TN deposition of 12.9 kg N/ha/yr.

Application of the SPARROW model provides estimates of the incremental flux derived within each catchment of the Potomac River watershed, as well as estimates of how much of that incremental flux (i.e., delivered flux) ultimately reaches the estuary (**Figure 3.1-2**). By looking at catchment-scale results, the spatial variability among flux/load contributions across the watershed can be shown. Differences between the incremental and delivered yields/loads reflect the instream losses that occur as the load from each catchment travels downstream to the target estuary.

For this first application and analysis of the 2002 current condition case, SPARROW was used to model the loads from the Potomac River and its watershed to the upper portions of the Potomac Estuary. The most downstream modeled catchment in the analysis lies downstream of several major point sources between Washington, DC, and the mixing zone of the estuary. These point sources were major contributors of nutrients to the estuary, and by including them in the analysis a more accurate load from the Potomac River watershed is defined than if the modeling

stopped at the fall line of the river. Direct runoff from catchments surrounding the Potomac Estuary and direct deposition to the estuary were not considered in this preliminary model application. The majority of the nitrogen loading to the estuary was expected to derive within the Potomac River watershed because of its overall larger land area and applications of fertilizer and manure. Additionally, the major point sources to the Potomac Estuary were included in the most downstream watersheds at the mouth of the estuary modeled in this application.

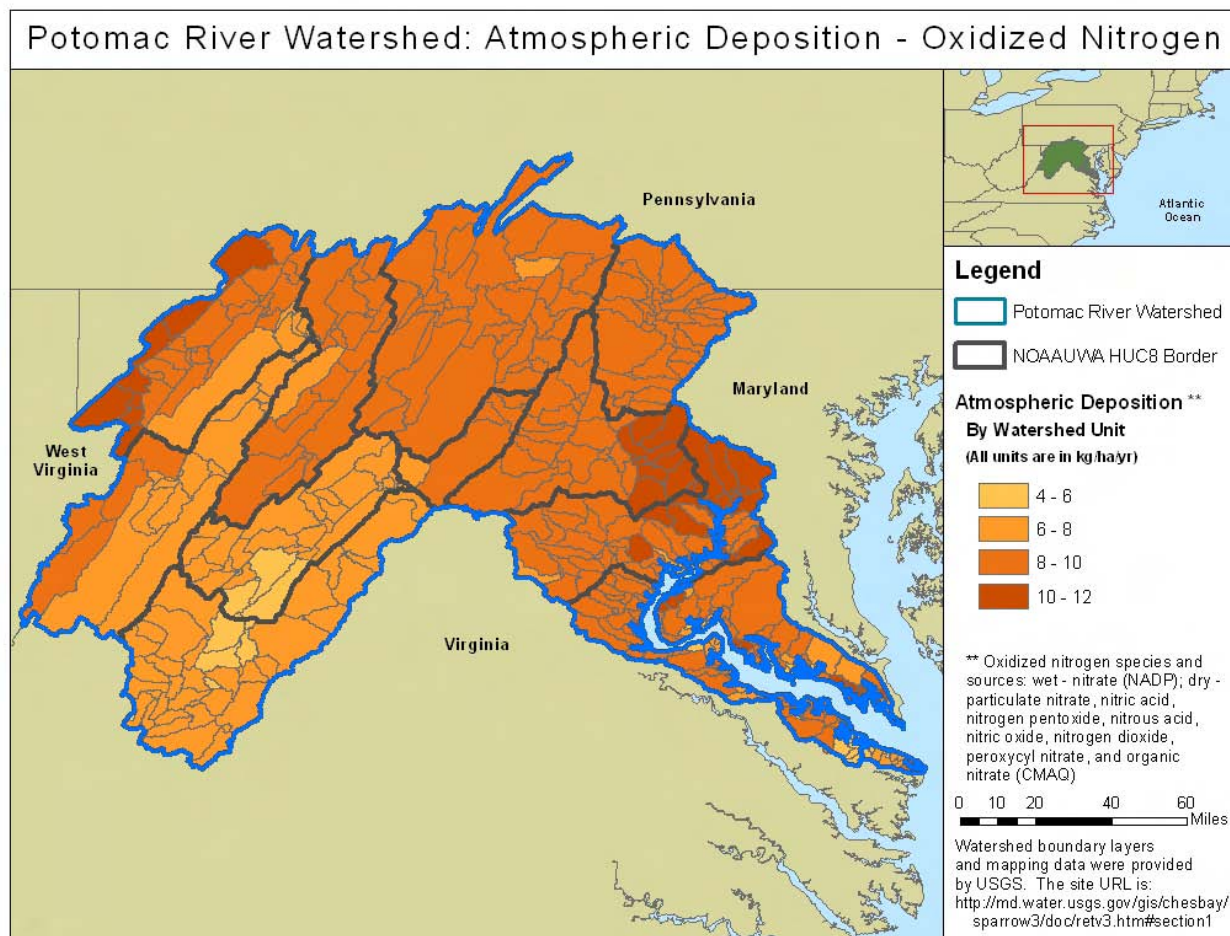


**Figure 3.1-1a.** Atmospheric deposition yields of oxidized nitrogen over the Potomac River and Potomac Estuary watershed.



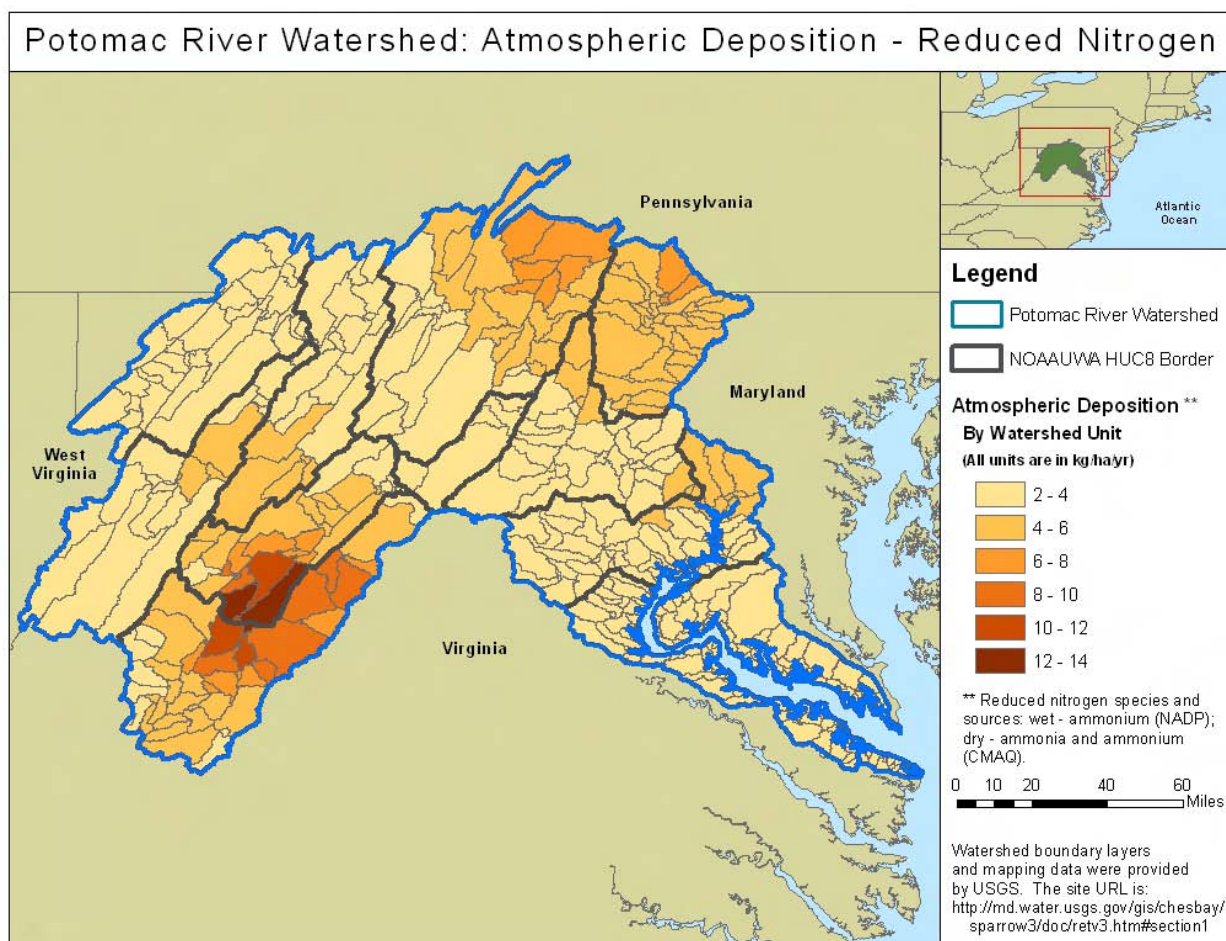


**Figure 3.1-1b.** Atmospheric deposition yields of reduced nitrogen over the Potomac River and Potomac Estuary watershed.

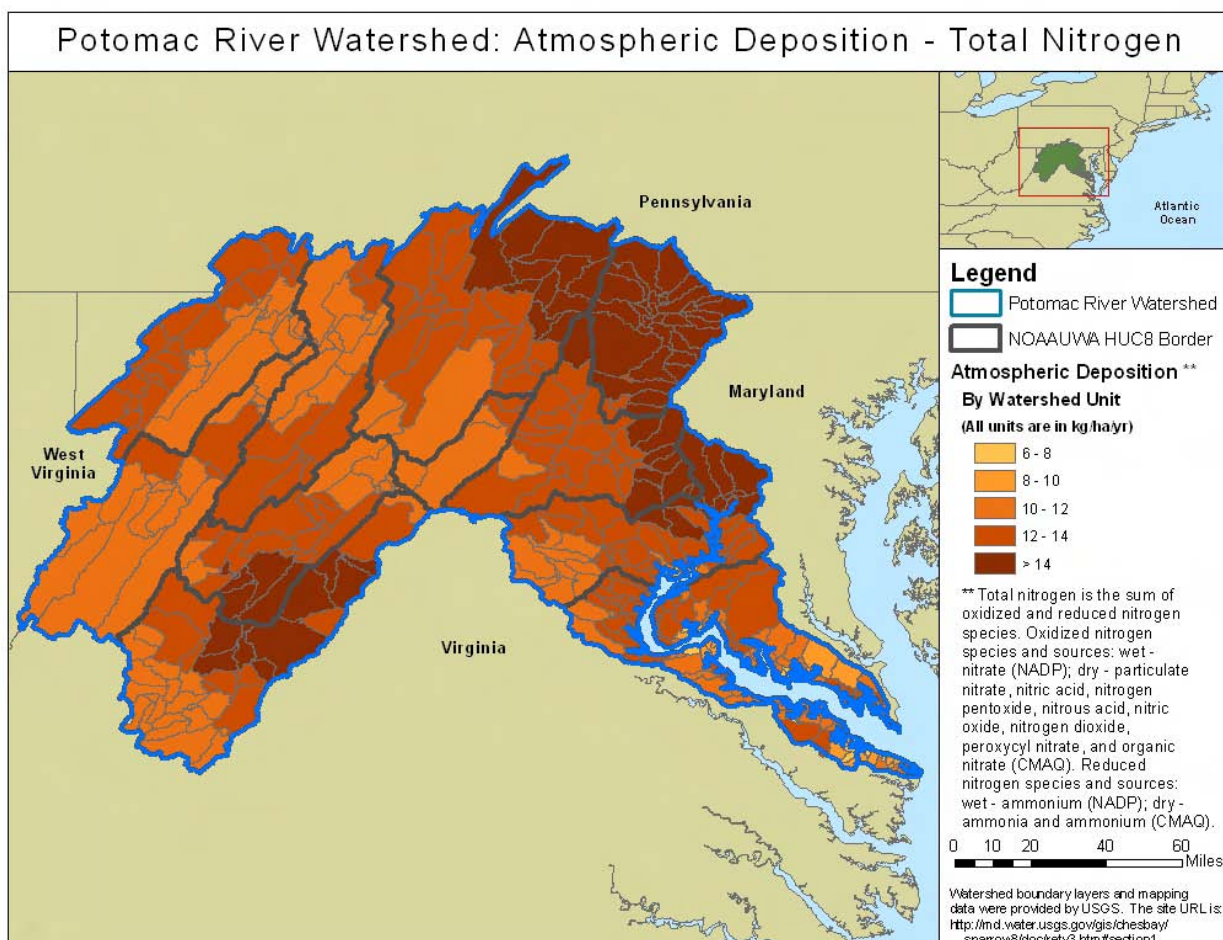


**Figure 3.1-1c.** Atmospheric deposition yields of total nitrogen over the Potomac River and Potomac Estuary watershed.



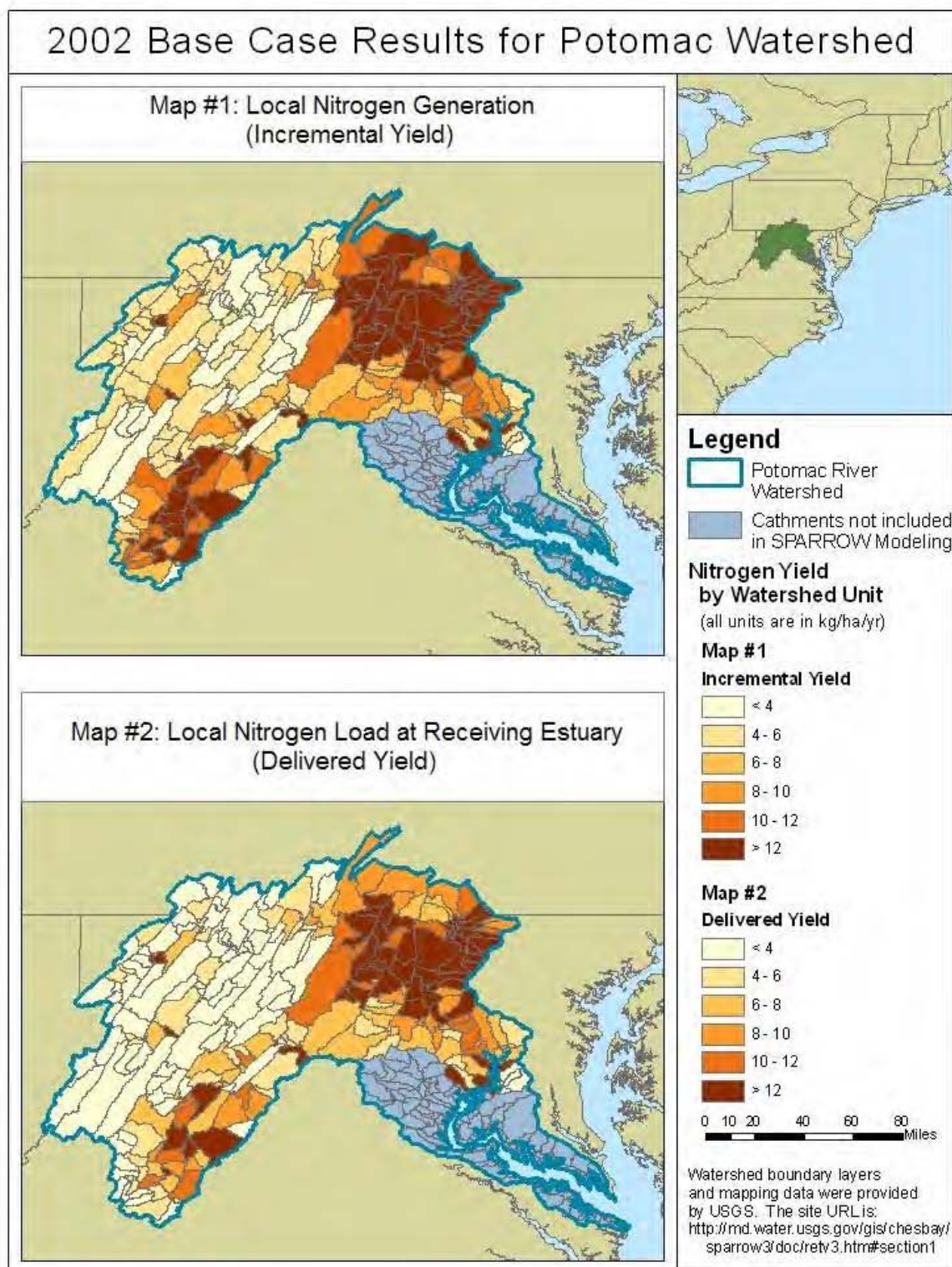


**Figure 3.1-2.** Total nitrogen yields from all sources as predicted using the Version 3 of the Chesapeake Bay SPARROW application with updated 2002 atmospheric deposition inputs.

Overall, the model produced an estimate of TN loading to the Potomac Estuary of 36,660,000 kg N/yr. The atmospheric deposition load was estimated at 7,380,000 kg N/yr or 20% of the total loading (**Figure 3.1-3**). These modeling estimates are consistent with previous modeling estimates for the system (Preston and Brakebill, 1999). The TN<sub>s</sub> resulting from this loading was approximately 3.4 mg/L.

SPARROW modeling for 2002 predicts that atmospheric deposition was 20% of the total nitrogen loading to the Potomac River's estuary, producing an TN<sub>s</sub> of 3.4 mg/L.

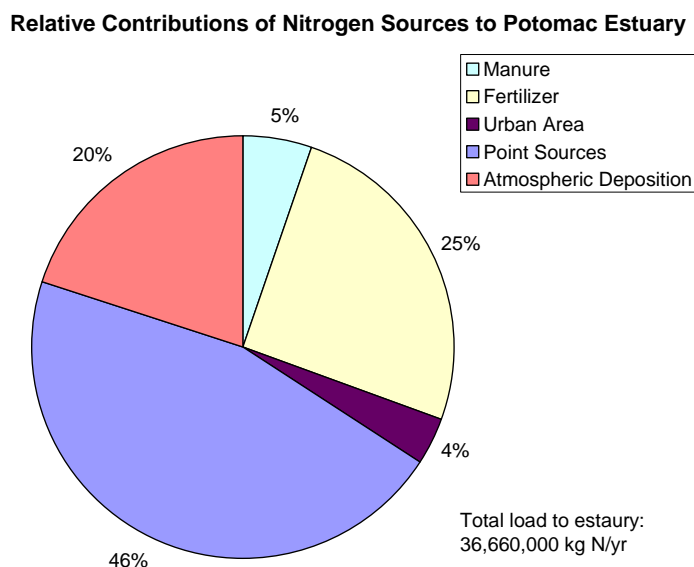


**Figure 3.1-3.** Source contributions to Potomac Estuary nitrogen load.

### 3.1.1.2 ASSETS EI Assessment

An ASSETS EI assessment was completed for the Potomac Estuary (**Figure 3.1-4**) in a 2006 NOAA project on the Gulf of Maine (Bricker et al., 2006). The data used to complete the scoring were from 2002. That assessment showed that the system has a high susceptibility to pressures and a high score for nutrient inputs, resulting in a score of *High* for influencing factors (i.e., OHI index). Individual scores for the primary and secondary indicators varied, but resulted in an overall score of *High* for the OEC (i.e., OEC index). The score of *Improve Low* for the future outlook (i.e., DFO index) is based on the expectations that future nutrient pressures will decrease and there will be significant population and development increases.

The ratings for the nutrient inputs and the OEC index were recreated and verified using methods consistent with the 2007 NEEA Update (**Table 3.1-1**; Bricker et al., 2007a), which included separate areal-weighted consideration of the tidal fresh, mixing, and saltwater zones

within the estuary (Bricker et al., 2007a). (Note that the Potomac Estuary is split approximately between tidal fresh [14.5%] and mixing [85.5%] zones.) Data for dissolved oxygen and chlorophyll *a* were downloaded from the CBP water quality database (CBP, 2008). Harmful algal bloom (HAB) data were taken from data compilations available from VIMS. Conflicting results were found for the SAV coverage where an unreasonably large increase was reported in the original analysis (Bricker et al., 2006). The source of the data for the updated analysis was the VIMS (VIMS, 2008), which was the same source cited for the original analysis. Possible explanations for the discrepancy are different baseline periods for comparisons between the gains and losses in SAV areas. The updated analysis compared only annual changes in areal growth of SAV (in contrast to previous NEEA studies that used a baseline year of comparison [Bricker et al., 1999; Bricker et al., 2007a]). Additionally, the areas of SAV measured for 2001 were listed as partial measures, making the estimates in small gains and losses in the tidal fresh and mixing areas, respectively, of the estuary uncertain. In the 2007 NEEA Update (Bricker et al., 2007a), a value of 0.5 was used for any uncertain index score. A value of 0.5 was, therefore, given to the uncertain loss estimated in the mixing zone of the Potomac Estuary for 2002.

Index scores for the updated analysis were compiled using the scoring methods and matrices as shown in **Figure 2.2-6** and **Figure 2.2-7**. Although there were uncertain/unknown values for macroalgae in the primary symptoms and SAV in the secondary symptoms, the high rankings of chlorophyll *a* within the primary symptoms and HAB in the secondary symptoms overweighed the uncertainty of the other parameters in the final scores. Even if a value of 0.5 (denoting uncertainty) had been used for the macroalgae score, as was done with the mixing zone index for SAV, the overall score for that indicator would have resulted in a primary score greater than 0.6 and a *High* ranking. Combination of the primary and secondary scores (both *High*) provided an overall OEC index score of *High*, which agreed with the original analysis.

The OHI index score (confirmed with the modeled nitrogen load from the 2002 SPARROW application) and the DFO index score remain the same as in the original analysis. Therefore, the ASSETS EI score for the 2002 current condition scenario is *Bad*.

Indices	Methods	Parameters/ Values / EAR			Index category	ASSETS grade
Pressure OHI index	Susceptibility	Dilutionpotential	High	High Susceptibility	High	OHI = 1 OEC = 1 DFO = 4  Bad
		Flushingpotential	Low			
	Nutrient inputs	High				
State OEC index	Primary Symptom Method	Chlorophyll a	High	High	High	
		Macroalgae	No Prob			
	Secondary Symptom Method	Dissolvedoxygen	Low	High		
		Submerged aquaticvegetation	Large Increase			
		Nuisance and Toxic Blooms	Problem (1)			
Response DFO index	Future nutrient pressures	Futurenutrientpressuresdecrease,significantpopulation/ development increases – Improve Low			Improve Low	

**Figure 3.1-4.** The ASSETS EI scores for the Potomac Estuary (Bricker et al., 2006).

**Table 3.1-1.** Potomac Estuary Current Condition Overall Human Influence Index Score

Year	Parameter	Zone	Value	Concentration	Spatial Coverage	Frequency	Expression	Score	Primary/ Secondary Scores	OEC Score
2002	CHLA	MX	13.25	MEDIUM	HIGH	PERSISTENT	HIGH	0.9275	0.9275	HIGH (1)
	CHLA	TF	22.805	HIGH	LOW	PERIODIC	MODERATE			
	Macroalgae	ALL	NA	UNKNOWN	UNKNOWN	UNKNOWN	UNKNOWN			
	DO	MX	3.6	BIO STRESS	HIGH	PERIODIC	MODERATE	0.4275	1	
	DO	TF	5.8	NO PROBLEM	HIGH	PERSISTENT	NO PROBLEM			
	SAV	MX	NA	LOSS (Uncertain)	NA	NA	UNCERTAIN (0.5)			
	SAV	TF	NA	GAIN (Uncertain)	NA	NA	UNCERTAIN (0)	0.43		
	HAB	ALL	NA	NA	NA	NA	HIGH	1		

CHLA: Chlorophyll *a*  
DO: Dissolved Oxygen  
SAV: Submerged Aquatic Vegetation  
HAB: Harmful/Toxic Algal Blooms  
MX: Mixing Zone  
TF: Tidal Fresh Zone  
ALL: All Estuary Zones  
NA: Not Applicable

### **3.1.2 Summary of Results for the Neuse River/Neuse River Estuary Case Study Area**

The 2002 current condition analysis of the Neuse River and Neuse River Estuary used recently released data from the USGS to calibrate a new SPARROW application for 2002 to the Neuse, Tar-Pamlico, and Cape Fear rivers' watersheds. Developing the ASSETS EI score for the Neuse River Estuary proved to be a greater challenge than for the Potomac Estuary because of the availability of data sources that were less consolidated and more varied.

#### **3.1.2.1 SPARROW Assessment**

The release of digital data by the USGS for its Southeast Major River Basin SPARROW Assessment (area includes all of the river basins draining to the south Atlantic and the eastern Gulf of Mexico, as well as the Tennessee River basin [referred to collectively as the SAGT area]) in the summer of 2008 provided the opportunity to calibrate a new SPARROW model for the 2002 current condition analysis (Hoos et al., 2008). The SAGT data were compiled for 2002, providing the necessary data inputs and calibration TN loads for model development. Because of a limited number of calibration points within the Neuse River watershed itself, the SPARROW model was expanded to include the Tar-Pamlico and Cape Fear river watersheds, providing a total of 41 calibration points on which to base the SPARROW model. The river network within these basins was again based on the RF1, with enhancements for calibration points. Source variables investigated in the new model development included atmospheric deposition (modified from the original SAGT dataset to use the CMAQ/NADP data developed for this study), fertilizer application to farmland, manure from livestock production, point sources, and land cover (urban, forest, and nonagriculture categories). Decay and loss terms considered in the model included soil permeability, mean annual temperature, and slope.

**Figure 3.1-5a** through **Figure 3.1-5c** show the atmospheric deposition inputs used within the modeling effort. The model was based on TN loads from deposition, but oxidized and total  $N_r$  yields are also presented to highlight source information within the watershed. The Neuse River watershed is the location of major agricultural operations focusing on swine facilities. These operations are evident in the high levels of reduced nitrogen found within the south-central catchments of the watershed (**Figure 3.1-5b**). For the current condition 2002 analysis of the



Neuse River and Estuary, an estimated 18,340,000 kg of TN was deposited in the 1.3 million-ha Neuse River watershed, for an TN average deposition of 14.0 kg N/ha/yr.

Development of the new SPARROW model used the USGS SAS SPARROW application in predictive mode, with bootstrap analyses completed for additional analysis and exploratory options (Schwarz et al., 2006). The model used two flow classes based on the work by McMahon et al. (2003) and a reservoir decay factor. In model set up, the decay factors were constrained to be nonnegative. **Tables 3.1-2** and **3.1-3** present the calibrated model parameters and model evaluation statistics, respectively. The model used point sources, atmospheric deposition, fertilizer application, manure production, and urban land area. There was some lack of significance in the parameter estimations for manure production and urban land area, but these sources were deemed likely sources based on watershed knowledge and were left in the model. The land-to-water delivery factor used in the model was the soil permeability factor. As expected, the parameter estimate for this factor was less than one. The three decay terms (i.e., two flow classes and reservoir decay) all lacked significance in their parameter estimates but are required for the model as it was configured. Future analyses should consider alternate flow classes to investigate ways to improve statistical significance of these estimates. Overall, the model evaluation criteria reveal a strong significance in the estimated model, with high prediction values (i.e., R-squared values close to 1), little multicollinearity (i.e., Eigen value spread less than 100), and normally distributed weighted model residuals (i.e., probability plot correlation coefficient close to 1).

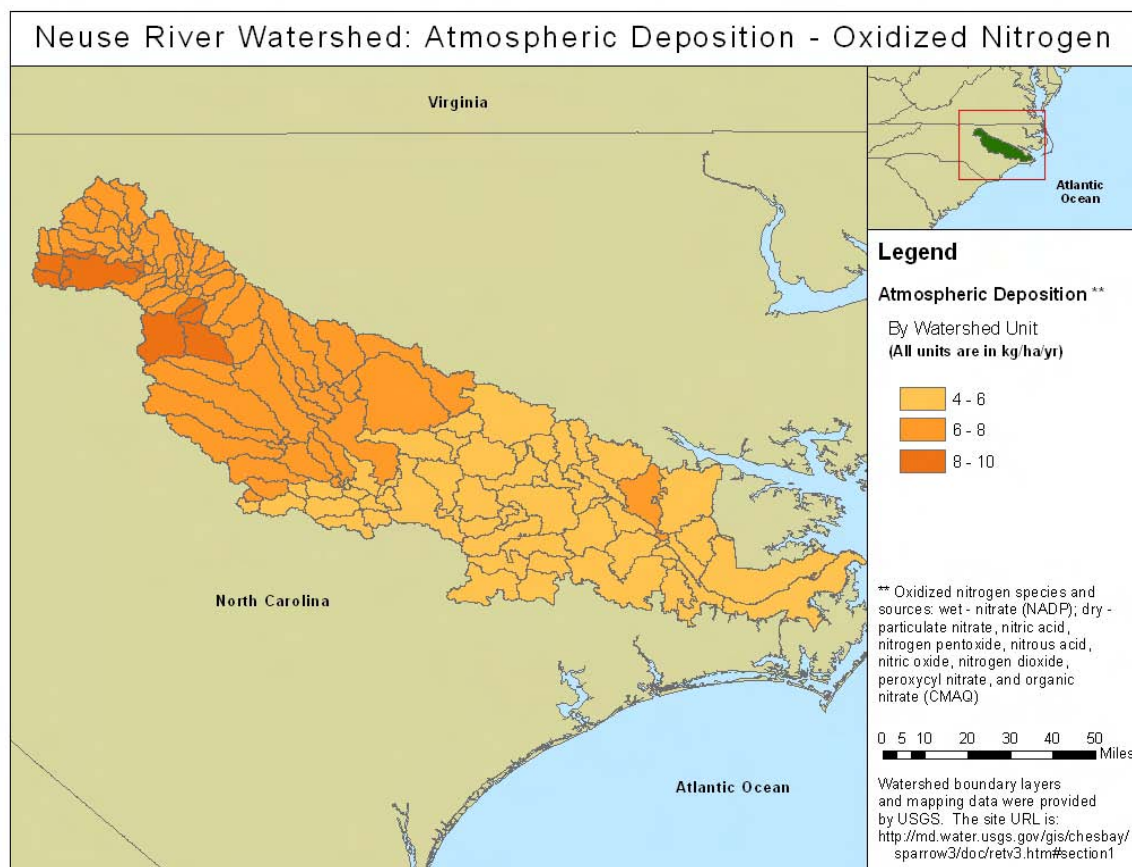


**Figure 3.1-5a.** Atmospheric deposition yields of oxidized nitrogen over the Neuse River and Neuse River Estuary watershed.

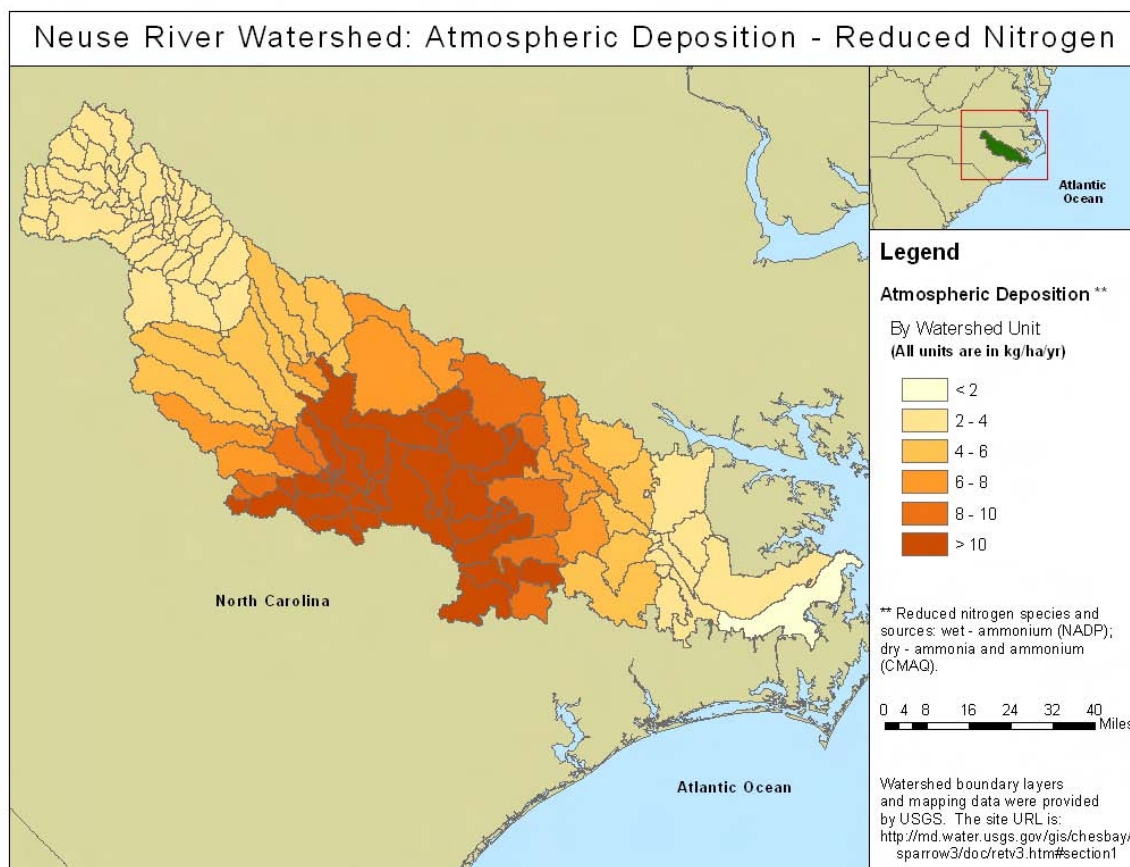


**Figure 3.1-5b.** Atmospheric deposition yields of reduced nitrogen over the Neuse River and Neuse River Estuary watershed.

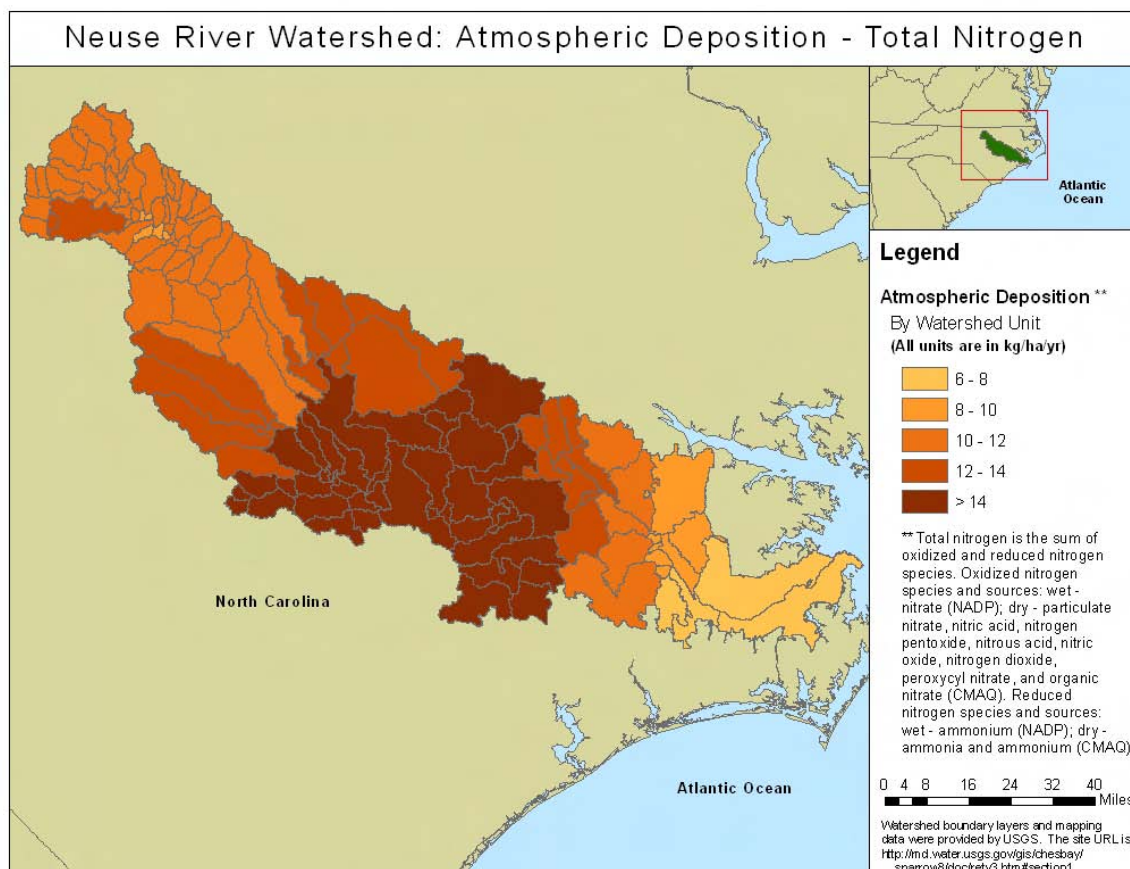


**Figure 3.1-5c.** Atmospheric deposition yields of total nitrogen over the Neuse River and Neuse River Estuary watershed.

**Table 3.1-2.** Model Parameters for 2002 Current Condition SPARROW Application for the Neuse River Watershed

Source Parameters	Parameter Estimate	Standard Error	t-statistic	p-value	VIF
Point Sources	0.84	0.121	6.95	<0.001	1.4
Atmospheric Deposition	0.082	0.045	1.80	0.081	13.3
Fertilizer	0.13	0.038	3.38	0.002	7.1
Manure	0.017	0.019	0.91	0.368	4.6
Urban Area	1.6	1.7	0.96	0.345	2.5
<b>Decay and Loss Parameters</b>					
Soil Permeability	-0.52	0.217	-2.41	0.022	4.8
Reach Decay Group 1	0.17	0.266	0.64	0.528	2.3
Reach Decay Group 2	0.029	0.058	0.49	0.627	2.3
Reservoir Decay	3.4	9.6	0.35	0.728	1.3

**Note:** VIF = Variance Inflation Factor.

**Table 3.1-3.** Model Evaluation Statistics for 2002 Current Condition SPARROW Application for the Neuse River Watershed

Evaluation Criteria	Value
Number of Observations	40
Degrees of Freedom—model error	31
Degrees of Freedom—coefficients	9
Sum of the Squared Errors	1.79
Mean Square Error	0.058
Root Mean Square Error	0.24
R Squared	0.99
Adjusted R Squared	0.98
Eigen Value Spread	84.2
Probability Plot Correlation Coefficient	0.984

As with the Potomac River watershed results, the Neuse SPARROW application modeled watershed loads to the upper edges of the estuary. Both the incremental and delivered yields are presented in **Figure 3.1-6**. The TN load estimated to enter the estuary from the Neuse River is 4,380,000 kg N/yr, equating to a  $TN_s$  of 1.11 mg/L. The load from atmospheric deposition was estimated to be 1,150,000 kg N/yr, or 26% of the total load (**Figure 3.1-7**). These estimates fall in line with instream monitoring data and previous loadings from the Neuse River, estimated at 9.61 million pounds or 4,359,000 kg N/yr (Spruill et al., 2004).

SPARROW modeling for 2002 predicts that atmospheric deposition was 26% of the total nitrogen loading to the Neuse River's estuary, producing a  $TN_s$  of 1.1 mg/L



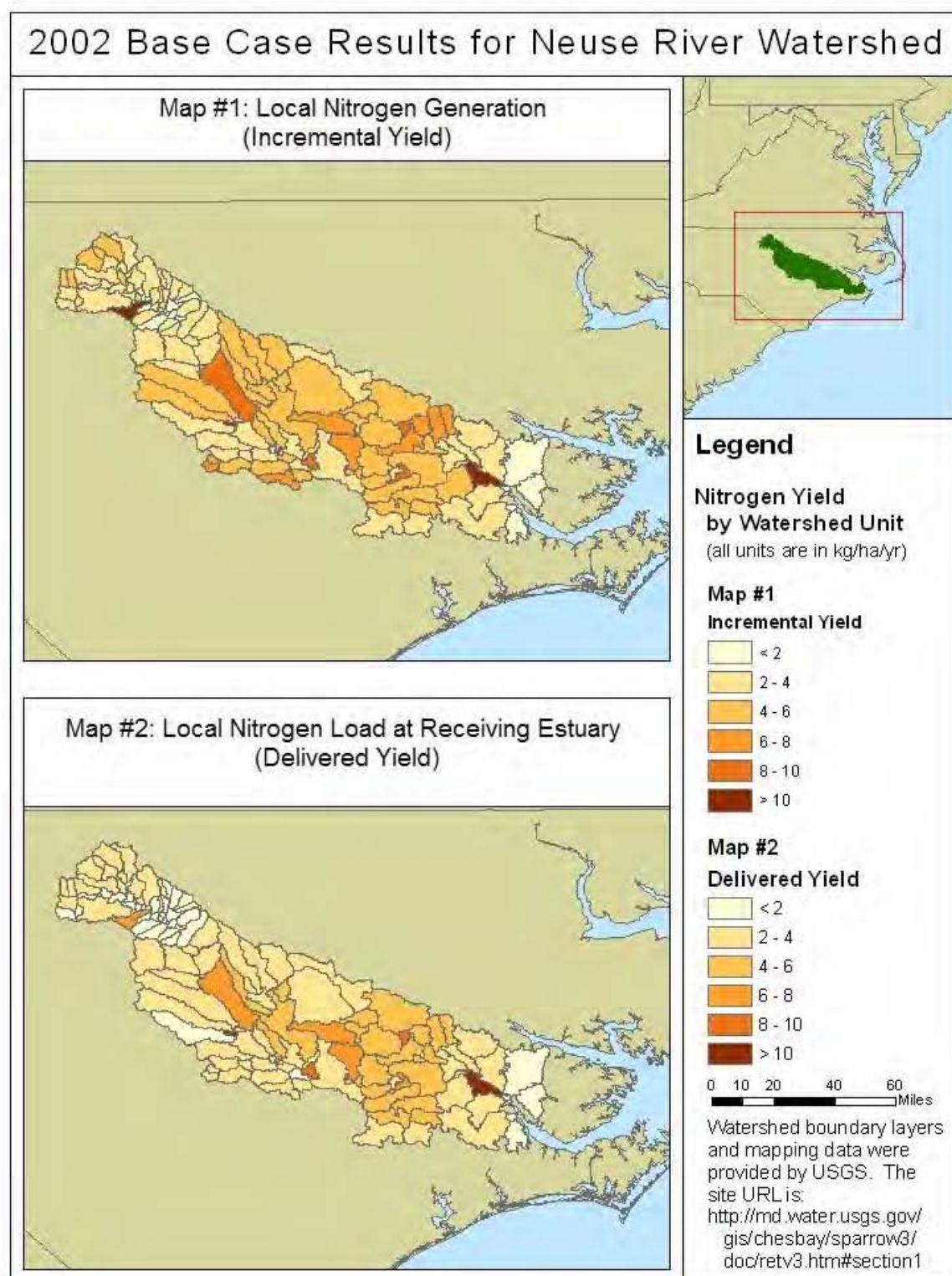


**Figure 3.1-6.** Total nitrogen yields from all sources in the Neuse River watershed as predicted by a SPARROW modeling application for the Neuse, Tar-Pamlico, and Cape Fear rivers' watersheds with 2002 data inputs.

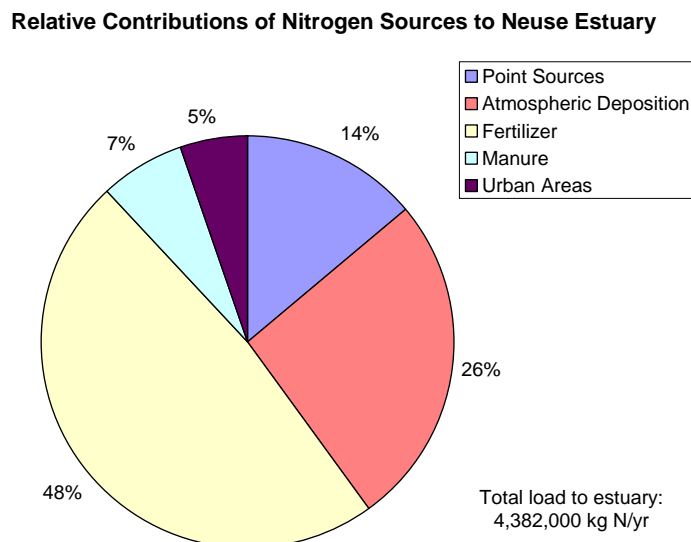


**Figure 3.1-7.** Source contributions to Neuse River Estuary total nitrogen load.

### 3.1.2.2 ASSETS EI Assessment

Previous work was completed using the ASSETS EI assessment on the Neuse River Estuary as part of the NEEA Update (Bricker et al., 2007a). The exact source of this load estimate and the exact timeframe of the data used to calculate the ASSETS EI score are still unknown at this time, although the data should fall within the period of 2000 to 2002 (S. Bricker, personal communication, 2008). That analysis revealed a *Highly/Moderately Influenced* or *High* score for influencing factors (i.e., OHI index) where the nitrogen load was ranked as *Moderate to High* and the ASSETS EI score for the estuary was a *Bad* overall.

To develop an updated ASSETS EI score specific to the 2002 current conditions, raw data were compiled from several sources, including EPA's Storage and Retrieval System (STORET), the Neuse River Estuary Modeling and Monitoring Project (MODMON), NC DWQ, and journal articles. While there were a variety of sources of data, information on macroalgae and SAV for the period of interest could not be obtained. Monitoring data for chlorophyll *a*, dissolved oxygen, and nitrogen were obtained from MODMON records. NC DWQ has only recently begun to measure SAV within defined areas and on defined intervals, so no data were available for the 2002 time period. Monitoring experts within the Neuse River/Neuse River Estuary Case Study Area could not identify any sources of macroalgae data (B. Peierls, personal communication, 2008). HAB data were gleaned from notations in journal papers (Burkholder et al., 2006) and in the reports beginning in 1997 tracked by NC DWQ (NC DWQ, 2008). The

available data were combined to form a 2002 OEC index score (**Table 3.1-4**). Because both the chlorophyll *a* and HAB data were available and overwhelmingly pointed to a system with both *High* primary and secondary scores, a rating of *High* is given to the OEC index with confidence for 2002.

The *High* susceptibility ranking combined with the TN loads estimated by the SPARROW assessment rank the OHI index as *High* as well. The DFO index score set during the 2007 NEEA Update remains unchanged, with a ranking of *Worsen High* due to nutrient decreases from improved management practices in recent years being offset by increases in human populations and factors related to swine production (Burkholder et al., 2006). Combining the three index scores together results in an overall ASSETS EI score of *Bad* for the Neuse River/Neuse River Estuary Case Study Area for 2002.



**Table 3.1-4.** Current Condition Overall Eutrophic Condition Index Score for the Neuse River/Neuse River Estuary Case Study Area

Year	Parameter	Zone	Value	Concentration	Spatial Coverage	Frequency	Expression	Score	Primary/ Secondary Scores	OEC Score	
2002	CHLA	MX	35	HIGH	HIGH	PERSISTENT	HIGH	0.9945	0.9945	HIGH (1)	
2002	CHLA	TF	9.0	MEDIUM	MODERATE	PERIODIC	MODERATE				
2002	Macroalgae	ALL	NA	UNKNOWN	UNKNOWN	UNKNOWN	UNKNOWN				NA
2002	DO	MX	1.6	HYPOXIA	MODERATE	PERIODIC	MODERATE	0.5	1		HIGH (1)
2002	DO	TF	2.7	BIO STRESS	HIGH	PERIODIC	MODERATE				
2002	SAV	ALL	NA	NA	NA	NA	UNKNOWN				
2002	HAB	ALL	NA	NA	NA	NA	HIGH	1			

CHLA: Chlorophyll *a*  
DO: Dissolved Oxygen  
SAV: Submerged Aquatic Vegetation  
HAB: Harmful/Toxic Algal Blooms  
MX: Mixing Zone  
TF: Tidal Fresh Zone  
ALL: All Estuary Zones  
NA: Not Applicable

## 3.2 ALTERNATIVE EFFECTS LEVELS

Alternative effects levels were assessed for both the Potomac River/Potomac Estuary and the Neuse River/Neuse River Estuary case study areas (separately) by applying percentage decreases to the oxidized nitrogen loads in the estimated atmospheric deposition. Model estimates then relied on the SPARROW models used (for the Potomac River/Potomac Estuary Case Study Area) or developed (for the Neuse River/Neuse River Estuary Case Study Area) for the 2002 current condition analysis to determine how the changing atmospheric inputs (i.e., TN load evaluated with changes in oxidized nitrogen deposition,  $TN_{atm}$ ) affect the overall TN load to the estuary of interest. These results were used to create the response curve relating  $TN_s$  to  $TN_{atm}$ , as first described in Section 2.2.3. The second response curve described in Section 2.2.3 was defined for the alternative effects level analysis using historical data compilations of OEC index scores and  $TN_s$ , while holding the susceptibility portion of the OHI index (at its 2002 current condition level—in both cases a ranking of *High*) and the DFO index constant (at a ranking of *No Change* [3]).

Upon creation of the two response curves, the back-calculation–coded program described in Section 2.2.3 (referred to as *BackCalculation* through the remainder of this document) was applied to the curves with the intent of defining the atmospheric loads that are needed to improve the ASSETS EI from a score of *Bad* (1) to *Poor* (2), *Moderate* (3), *Good* (4), or *High* (5). These improvements represent improvements by 1, 2, 3, and 4 categories. The *BackCalculation* program was run under Uncertainty Scenario B (**Figure 2.2-12b**) for both case studies.

The following sections describe the data used to create the two response curves and the application of the *BackCalculation* program for each estuary.

### 3.2.1 Potomac River Watershed

Beginning with the data and model used for the current condition analysis, the atmospheric deposition inputs derived from national coverage of CMAQ and NADP data were altered to create various alternative effects levels by decreasing the oxidized nitrogen loads by rates of 5%, 10%, 20%, 30%, and 40% from their original 2002 levels. A zero percent decrease corresponds to the 2002 current condition analysis (**Table 3.2-1**). The remaining inputs to the SPARROW model remained the same, and the model was rerun for each of these alternative

effects level scenarios. The TN load to the estuary calculated from the model was then converted to  $TN_s$  using the annual average flow of the Potomac River. Plotting these concentrations against the new  $TN_{atm}$  incorporating the oxidized nitrogen decreases leads to the development of the desired response curve and relationship (**Figure 3.2-1**).

**Table 3.2-1.** Potomac River Watershed Alternative Effects Levels

Percent Decrease in Oxidized Nitrogen	Total Nitrogen Atmospheric Deposition Load, $TN_{atm}$ (kg/yr)	Decrease in Oxidized Nitrogen ( $NO_x$ ) Atmospheric Deposition Load (kg/yr)	Instream Total Nitrogen Load (kg/yr)	Instream Total Nitrogen Concentration, $TN_s$ (mg/L)
0	40,770,000	0	36,660,000	3.41
5	39,450,000	1,320,000	36,420,000	3.39
10	38,130,000	2,640,000	36,180,000	3.37
20	35,480,000	5,290,000	35,700,000	3.32
30	32,840,000	7,930,000	35,220,000	3.28
40	30,200,000	10,580,000	34,740,000	3.23

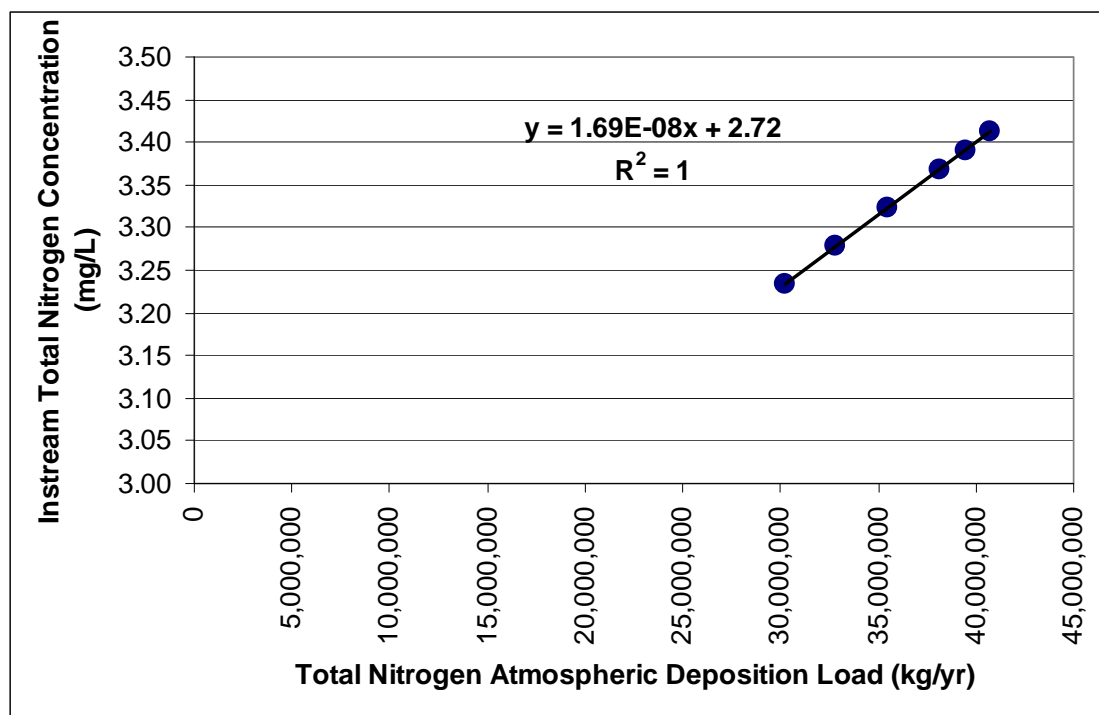


**Figure 3.2-1.** Response curve relating instream total nitrogen concentration to total nitrogen atmospheric deposition load for the Potomac River watershed.

**Table 3.2-2** details the historical modeling data used to determine TN loads to the Potomac Estuary, which are then combined with annual average flow values to calculate a final  $TN_s$ . These instream concentrations were then combined with the OEC index scores, which were also determined from historical data (**Table 3.2-3**), to create the data points needed to create the logistic response curve in the *BackCalculation* program. The years chosen for this analysis relate to those years in which a modeled TN load to the estuary could be estimated. OEC data were then gathered for those years to find the corresponding effects.

**Table 3.2-2.** Historical Potomac River Total Nitrogen Loads and Concentrations

Year	Nitrogen Load to Estuary (kg/yr)	Source	Flow (m <sup>3</sup> /s)	Source	Concentration (mg/L)
1985	32,110,000	CBM Phase 4.3	332	USGS gage records	3.07
1992	49,750,000	CB V2 SPARROW	340	CB V2 SPARROW Input Data	4.63
1997	39,380,000	CB V3 SPARROW	340	CB V3 SPARROW Input Data	3.67
2002	31,160,000	Model Run	196	USGS gage records	5.04
2005	23,790,000	CBM Phase 4.3	307	USGS gage records	2.46

CBM Phase 4.3: Chesapeake Bay Model Phase 4.3 reported results

CB V2 SPARROW: Chesapeake Bay SPARROW Version 2 model results (Brakebill et al., 2001)

CB V3 SPARROW: Chesapeake Bay SPARROW Version 3 model results (Brakebill and Preston, 2004)

Model run: Current condition analysis results as determined using modeling efforts based on CB V3 SPARROW

**Table 3.2-3.** Additional Potomac Estuary Overall Eutrophic Condition Index Scores for Alternative Effects Levels

Year	Parameter	Zone	Value	Concentration	Spatial Coverage	Frequency	Expression	Score	Primary/ Secondary Scores	OEC Score	
1985	CHLA	MX	26	HIGH	MODERATE	PERIODIC	HIGH	1	1	HIGH (1)	
	CHLA	TF	32	HIGH	HIGH	PERIODIC	HIGH				
	Macroalgae	ALL	NA	UNKNOWN	UNKNOWN	UNKNOWN	UNKNOWN	NA	0.86		0.86
	DO	MX	1.6	HYPOXIA	MODERATE	PERIODIC	MODERATE				
	DO	TF	5.6	NO PROBLEM	HIGH	PERSISTENT	NO PROBLEM	0			
	SAV	MX	NA	GAIN	NA	NA	NO PROBLEM				
	SAV	TF	NA	GAIN	NA	NA	NO PROBLEM				
	HAB	ALL	NA	NA	NA	NA	LOW/ UNKNOWN	0.25			
1987	CHLA	MX	26	HIGH	MODERATE/ HIGH	PERIODIC	HIGH	1	1	HIGH (1)	
	CHLA	TF	20	HIGH	MODERATE	PERIODIC	HIGH				
	Macroalgae	ALL	NA	UNKNOWN	UNKNOWN	UNKNOWN	UNKNOWN	NA	0.86		0.86
	DO	MX	2.2	BIO STRESS	HIGH	PERIODIC	MODERATE				
	DO	TF	6.3	NO PROBLEM	HIGH	PERSISTENT	NO PROBLEM	0.04			
	SAV	MX	NA	GAIN	NA	NA	NO PROBLEM				
	SAV	TF	NA	LOSS	NA	NA	VERY LOW				
	HAB	ALL	NA	NA	NA	NA	LOW/ UNKNOWN	0.25			
1992	CHLA	MX	12	MEDIUM	HIGH	PERSISTENT	HIGH	0.93	0.93	MODERATE HIGH (2)	
	CHLA	TF	14	MEDIUM	MODERATE	PERIODIC/ PERSISTENT	MODERATE				
	Macroalgae	ALL	NA	UNKNOWN	UNKNOWN	UNKNOWN	UNKNOWN	NA	0.43		0.43
	DO	MX	2.6	BIO STRESS	HIGH	PERIODIC	MODERATE				
	DO	TF	6.3	NO PROBLEM	HIGH	PERSISTENT	NO PROBLEM	0.07			
	SAV	MX	NA	GAIN	NA	NA	NO PROBLEM				
	SAV	TF	NA	LOSS	NA	NA	MODERATE				

Year	Parameter	Zone	Value	Concentration	Spatial Coverage	Frequency	Expression	Score	Primary/ Secondary Scores	OEC Score
	HAB	ALL	NA	NA	NA	NA	LOW/ UNKNOWN	0.25		
1997	CHLA	MX	28	HIGH	HIGH	PERIODIC/ PERSISTENT	HIGH	1	1	MODERATE HIGH (2)
	CHLA	TF	34	HIGH	HIGH	PERIODIC/ PERSISTENT	HIGH			
	Macroalgae	ALL	NA	UNKNOWN	UNKNOWN	UNKNOWN	UNKNOWN	NA	0.43	
	DO	MX	3.5	BIO STRESS	HIGH	PERIODIC	MODERATE			
	DO	TF	6.6	NO PROBLEM	HIGH	PERSISTENT	NO PROBLEM			
	SAV	MX	NA	GAIN	NA	NA	NO PROBLEM	0.04		
	SAV	TF	NA	LOSS	NA	NA	LOW			
	HAB	ALL	NA	NA	NA	NA	MODERATE/ UNKNOWN	0.5	0.5	
2005	CHLA	MX	21	HIGH	MODERATE	PERIODIC	HIGH	1	1	HIGH (1)
	CHLA	TF	15	MEDIUM	HIGH	PERSISTENT	HIGH			
	Macroalgae	ALL	NA	UNKNOWN	UNKNOWN	UNKNOWN	UNKNOWN	NA	0.43	
	DO	MX	2.2	BIO STRESS	HIGH	PERIODIC	MODERATE			
	DO	TF	5.7	NO PROBLEM	HIGH	PERSISTENT	NO PROBLEM			
	SAV	MX	NA	GAIN	NA	NA	NO PROBLEM	0		
	SAV	TF	NA	GAIN	NA	NA	NO PROBLEM			
	HAB	ALL	NA	NA	NA	NA	HIGH	1	1	

CHLA: Chlorophyll *a*

DO: Dissolved Oxygen

SAV: Submerged Aquatic Vegetation

HAB: Harmful/Toxic Algal Blooms

MX: Mixing Zone

TF: Tidal Fresh Zone

ALL: All Estuary Zones

NA: Not Applicable

The 2002 Potomac Estuary  $TN_{atm}$  (evaluated in terms of decrease in oxidized nitrogen) loading is estimated to be  $4.08 \times 10^7$  kg/yr (**Table 3.2-1**). The response curve relationship between atmospheric deposition and  $TN_s$  ( $TN_s$  [mg/L] =  $2.72 + 1.69 \times 10^{-8} \times TN_{atm}$  [kg/yr]) can be found in **Figure 3.2-1**. Outside data specified for the model include the following:

- Mean salinity in estuary = 11 (relative units)
- Mean salinity offshore = 33 (relative units)
- Mean offshore TN concentration = 0.028 mg/L.

There were five sets of observed OEC and  $TN_s$  data points used to fit the OEC( $TN_s$ ) logistic model (not including ecological endpoints) from the data presented in **Table 3.2-2** and **Table 3.2-3**.

For the purpose of estimating the OEC( $TN_s$ ) function at each iteration, the range on the OEC minimum value was specified as 0 to 0 (i.e., fixed at 0). In addition, the OEC maximum value was fixed at 5. Notwithstanding the capability to vary OEC minimum and OEC maximum from iteration to iteration, the decision was made to not do so. Varying OEC minimum and OEC maximum would ideally be performed to reflect natural limitations on an estuary. For instance, in its most pristine state, it may not fully attain OEC = 5 or, in its most degraded state, it may not fully attain OEC = 1. However, because of the difficulty in knowing these natural limitations, the option to vary these levels was not implemented, but rather left OEC minimum = 0 and OEC maximum = 5. The range on the  $TN_s$  minimum value was specified from 0.028 mg/L (i.e., the offshore value) to 1.0 mg/L (i.e., a value determined by best professional judgment at this time due to lack of supporting data). The  $TN_s$  maximum value range was specified from 4.63 mg/L (maximum observed above) to  $1.5 \times 4.63 = 6.95$  mg/L.

For the purpose of illustrating the overall back calculation uncertainty analysis methodology, each of the four ASSETS EI scores constituting state improvements (i.e., *Poor-2*, *Moderate-3*, *Good-4*, *High-5*) was treated as a “target” ASSETS EI score, and 500<sup>2</sup> iterations were run under each target EI scenario. As previously discussed, at each iteration, the *BackCalculation* program first fits the four-parameter logistic function to the observed data, including the randomly sampled ecological endpoints, using a weighted least squares criterion

<sup>2</sup> A convergence test was performed to see how stable the various quantiles of the resulting  $NO_{x,i}^*$  distribution were to 500 iterations. There was still some variability, suggesting that future analyses should use more than 500 iterations (particularly if SPARROW model uncertainty is included).

(**Figure 3.2-2**). (In this application, only the TN ecological endpoints were varied.) After the nonlinear, least squares optimization is performed (see **Figure 2.2-12b** for an example), the program then iteratively finds that  $TN_s^*$  concentration,  $TN_s^*$ , that satisfies the target ASSETS EI score. Once  $TN_s^*$  is found, the SPARROW response model is then evaluated to find the TN atmospheric deposition load,  $TN_{atm}^*$ , which results in  $TN_s^*$ . That  $TN_{atm}^*$  is saved, and the process is repeated 500 times. The percentage decrease in  $NO_x$  deposition load to reach  $TN_{atm}^*$  is calculated as  $100 \times (TN_{atm} \text{ current load} - TN_{atm}^*) / TN_{atm} \text{ current load}$ , and it is also saved. The result is a distribution of 500  $TN_{atm}^*$  and percentage decrease values, each of which is equally likely to result in the target EI (because the  $OEC(TN_s)$  function is assumed to be uniformly distributed within its uncertain envelope). These 500 values for each result were then rank-ordered (i.e., ascending order) to find statistics of interest (e.g., the mean, median, 5th percentile, and 95th percentile).

It should be carefully noted that the  $TN_{atm}^*$  value is allowed to be determined at each iteration without regard to what the current  $TN_{atm}$  is. Thus, if a  $TN_{atm}^*$  value is greater than the current  $TN_{atm}$  ( $4.08 \times 10^8$  kg/yr), then the implication is that more  $TN_{atm}$  would be required (i.e., added to the system) to attain the target ASSETS EI score. Obviously, in this situation, the estuary is currently at a better/higher ASSETS EI score than the target ASSETS EI score, and the target score represents a more polluted scenario. The  $TN_{atm}^*$  value is not prevented from becoming negative. As can be seen from the general form of the linear, SPARROW response model,  $TN_s = a + b \times TN_{atm}$ , a  $TN_s^*$  value less than parameter “a” would require more than a decrease in  $TN_{atm}$  to zero. It would actually require a “negative”  $TN_{atm}$  load. Clearly, the lower bound on  $TN_{atm}$  load is zero, so the negative  $TN_{atm}^*$  value would represent additional nitrogen (beyond decreasing the  $TN_{atm}$  [i.e., total atmospheric nitrogen] deposition load, including  $NO_x$  to zero) in the system that must be removed to achieve the target ASSETS EI score. (The actual value of the negative load would be valid only if the additional nitrogen removed had the same characteristics [e.g., spatial distribution, speciation, sources/sinks] as the  $TN_{atm}$ . This is unlikely; nonetheless, it is of interest to report the values with this caveat.)



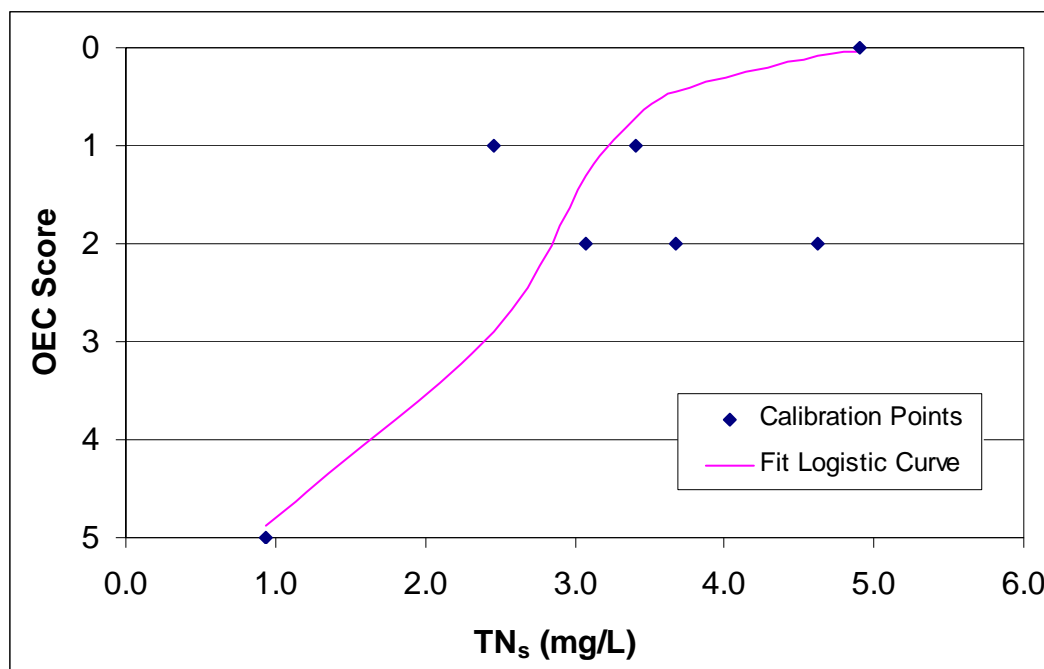


**Figure 3.2-2.** Fitted Overall Eutrophic Condition curve for target ASSETS EI=2, median  $TN_{atm}^* i$  (i = run 280)

The summary statistics of the 500 iterations for each target ASSETS EI scenario for the Potomac Estuary are presented in **Table 3.2-4**.

**Table 3.2-4.** Summary Statistics for Target ASSETS EI Scenarios for the Potomac Estuary

Statistic	$TN_{atm}^* i$ (kg N/yr)	% $TN_{atm}^* i$ Decrease
ASSETS EI = 2 ( <i>Poor</i> )		
Mean	$-1.78 \times 10^6$	104
Median	$-1.46 \times 10^6$	104
5th Percentile	$-3.67 \times 10^6$	109
95th Percentile	$9.02 \times 10^6$	78
ASSETS EI = 3 ( <i>Moderate</i> )		
No feasible solutions found		
ASSETS EI=4 ( <i>Good</i> ) and ASSETS EI = 5 ( <i>High</i> )		
All $TN_{atm}^* i = -1.61 \times 10^8$ , i.e., $TN_s^* i = 0$ mg/L		

Target ASSETS EI = 2 is the most interesting scenario and illustrates the power of the uncertainty analysis. The mean and median  $TN_{atm}^* i$  values are negative, meaning again that not only must all  $TN_{atm}$  (including all  $NO_x$ ) be removed, but additional nitrogen as well. However,

there is a slim chance that ASSETS EI = 2 can be attained only from  $TN_{atm}$  decrease, as indicated by the positive 95th percentile  $TN_{atm}^*$  value of  $9.02 \times 10^6$  kg N/yr (representing a 78% decrease).

Target ASSETS EI = 3 is a unique case because all solutions were infeasible. With a  $TN_s^*$  value of 0 mg/L, the other (i.e., fixed) components of the ASSETS EI scoring methodology (i.e., DFO index and Susceptibility Score) preclude satisfying any of the 95 combinations of DFO, OEC, and OHI indices that comprise the ASSETS EI=3 combinations in the ASSETS EI lookup table. (At  $TN_s^* = 0$ , an ASSETS EI = 4 can be achieved, but not ASSETS EI = 3, according to the 95 score combinations defined by Bricker et al., (2003) for ASSETS EI scores.) Bricker et al. (2003) acknowledge that “not all combinations” were included in the lookup table within their paper, so this scenario falls into that gap. Each of the intermediate scores (i.e., OEC, OHI, and DFO index scores) can take on integer values of 1 to 5. Thus, there are  $5 \times 5 \times 5 = 125$  different possible combinations, yet the lookup tables presented by Bricker et al. (2003) include only 95 combinations, so there are 30 “missing” combinations. (These are evenly distributed among the 5 possible DFO index scores. Each DFO index score has associated with it 19 combinations of OEC and OHI index scores.) It is possible that these combinations were not seen as likely combinations in nature by the experts that defined the scoring matrix (e.g., a  $TN_s^* = 0$  means there is no nitrogen coming in through the surface water and, hence, it is not feasible that a system would score below *Good* in the ASSETS EI score). Future assessments will explore the “missing” combinations further with the ASSETS EI experts.

Target ASSETS EI = 4 and 5 had identical results. All 500 iterations returned a  $TN_s^* = 0$ , and a corresponding  $TN_{atm}^*$  negative load equal to  $TN_{atm}^* = (0 - 2.72)/1.69 \times 10^{-8} = -1.61 \times 10^{-8}$  kg/yr. Clearly, target ASSETS EIs equaling 4 and 5 are very much unattainable when decreasing the  $TN_{atm}$  is the only policy option. To reach the target ASSETS EI, all atmospheric nitrogen (i.e.,  $TN_{atm}$ ) must be removed plus an additional amount (represented by the negative resultant load corresponding to  $TN_s^* = 0$ ) that is approximately equal to one order of magnitude greater than the original atmospheric deposition load. These amounts could be compared to the other nitrogen sources in the watershed (e.g., fertilizer and manure application or point sources) that were used as inputs to the SPARROW model to determine the relative nature of the required removal with other sources in the watershed. However, consideration must be given that this load is a reflection of the characteristics of the source in the SPARROW model (e.g., spatial

distribution, magnitude of loads, sources/sinks), and a decrease required in atmospheric load is not equal to a decrease in another source. Relative proportions can be examined by comparing the source characteristics and model parameters.

The SPARROW response curve can also be used to examine the role of atmospheric nitrogen deposition in achieving specified decreases in TN estuarine load. For example, the SPARROW modeling results predict that the  $41 \times 10^6$  kg N/yr deposited (i.e., atmospheric deposition input) over the Potomac River watershed in 2002 results in a loading of 7,380,000 kg N/yr, or 20% of the annual TN load, to the Potomac Estuary. If a 30% decrease in annual TN load to the estuary (i.e., a decrease of  $11 \times 10^6$  kg N/yr) were desired, a decrease of  $61 \times 10^6$  kg N/yr in nitrogen inputs to the watershed would be required according to the SPARROW response curve based on atmospheric deposition. This represents a 100% decrease in the atmospheric deposition inputs (i.e.,  $41 \times 10^6$  kg N/yr) plus an additional  $20 \times 10^6$  kg N/yr removal of nitrogen from other sources in the Potomac River watershed (i.e., point and nonpoint sources). Note that this value of  $20 \times 10^6$  kg N/yr is an approximate value when applied to the other sources because they differ in characteristics (e.g. spatial distribution and magnitude) from atmospheric deposition which was used to estimate the loading.

### **3.2.2 Neuse River Watershed**

The same methods for creating alternative effects levels were applied to the data from the Neuse River/Neuse River Estuary Case Study Area as to data from the Potomac River/Potomac Estuary Case Study Area. The oxidized nitrogen atmospheric deposition loads were decreased by rates of 5%, 10%, 20%, 30%, and 40% from their original 2002 levels. A zero percent decrease corresponds to the 2002 current condition analysis (**Table 3.2-5**). With the remaining inputs to the SPARROW model kept the same, the SAS-developed model was rerun for each of these alternative effects level scenarios. The TN load to the estuary calculated from the model was then converted to  $TN_s$  using the annual average flow of the Neuse River. Plotting these concentrations against the new  $TN_{atm}$  and incorporating the oxidized nitrogen decreases leads to the development of the desired response curve and relationship (**Figure 3.2-3**). Note that the instream concentration range presented in this figure is discussed at the end of this section.

**Table 3.2-5.** Neuse River/Neuse River Estuary Case Study Area Alternative Effects Levels

Percent Decrease in Oxidized Nitrogen	Total Nitrogen Atmospheric Deposition Load, $TN_{atm}$ (kg/yr)	Decrease in Oxidized Nitrogen Atmospheric Deposition Load (kg/yr)	Instream Total Nitrogen Load (kg/yr)	Instream Total Nitrogen Concentration, $TN_s$ (mg/L)
0	18,340,000	0	4,382,000	1.112
5	17,920,000	410,000	4,378,000	1.111
10	17,510,000	830,000	4,374,000	1.110
20	16,680,000	1,660,000	4,366,000	1.108
30	15,850,000	2,490,000	4,358,000	1.106
40	15,020,000	3,320,000	4,351,000	1.104

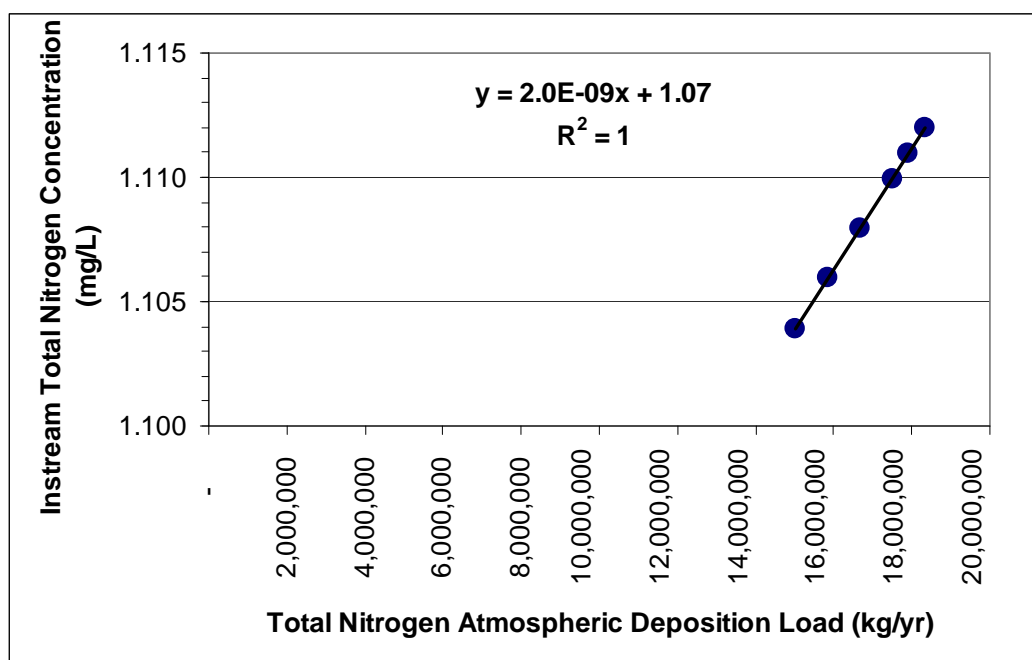


**Figure 3.2-3.** Response curve relating instream total nitrogen concentration to total nitrogen atmospheric deposition load for the Neuse River/Neuse River Estuary Case Study Area.

**Table 3.2-6** details the historical monitoring data used to determine  $TN_s$  at the downstream end of the Neuse River where the SPARROW model was used to determine current condition and alternative effects levels nitrogen loads. The monitoring data were derived from data downloaded from EPA's STORET Web site for monitoring location J8290000 from NC DWQ. These instream concentrations were then combined with the OEC index scores, which

were also determined from historical data (**Table 3.2-7**), to create the data points needed to create the logistic response curve in the *BackCalculation* program. Data from as many years as possible were gathered for both the TN<sub>s</sub> and OEC index scores. However, because of the limited amount of complete data from the various sources identified under the current condition analysis, only three corresponding years of data were found. These years are highlighted in **Table 3.2-6**.

**Table 3.2-6.** Annual Average Instream Total Nitrogen Concentrations in the Neuse River

Year	Annual Average TN <sub>s</sub> (mg/L)
1997	1.08
1998	0.93
1999	0.99
2000	1.10
2001	0.96
2002	0.91
2003	1.02
2004	1.09
2005	1.12
2006	1.07
2007	0.97

NC DWQ Station J8290000; Results from EPA's  
STORET Summation of Total Kjeldahl Nitrogen and  
Nitrate/Nitrite

**Table 3.2-7.** Additional Neuse River Estuary Overall Eutrophic Condition Index Scores for Alternative Effects Levels

Year	Parameter	Zone	Value	Concentration	Spatial Coverage	Frequency	Expression	Score	Primary/ Secondary Scores	OEC Score	
1992	CHLA	MX	28	HIGH	VERY LOW	PERIODIC	MODERATE	0.5	0.5	HIGH(1)	
	Macroalgae	ALL	NA	UNKNOWN	UNKNOWN	UNKNOWN	UNKNOWN	NA			
	DO	MX	6.1	NO PROBLEM	HIGH	PERSISTENT	NO PROBLEM	0.25	1		
	SAV	ALL	NA	NA	NA	NA	UNKNOWN	NA			
	HAB	ALL	NA	NA	NA	NA	HIGH	1			
1993	CHLA	MX	30	HIGH	HIGH	PERIODIC	HIGH	0.99	0.99	HIGH (1)	
	Macroalgae	ALL	NA	UNKNOWN	UNKNOWN	UNKNOWN	UNKNOWN				
	DO	MX	3.4	BIO STRESS	HIGH	PERIODIC	MODERATE	0.5	1		
	SAV	ALL	NA	NA	NA	NA	UNKNOWN	NA			
	HAB	ALL	NA	NA	NA	NA	HIGH	1			
2003	CHLA	MX	46	HIGH	HIGH	PERSISTENT	HIGH	1	1	HIGH (1)	
	CHLA	TF	7.2	MEDIUM	HIGH	PERIODIC	HIGH				
	Macroalgae	ALL	NA	UNKNOWN	UNKNOWN	UNKNOWN	UNKNOWN				NA
	DO	MX	2.0	HYPOXIA	HIGH	PERIODIC	HIGH	0.99	0.99		
	DO	TF	4.5	BIO STRESS	HIGH	PERIODIC	MODERATE				0.99
	SAV	ALL	NA	NA	NA	NA	UNKNOWN				NA
	HAB	ALL	NA	NA	NA	NA	MODERATE				0.5
2007	CHLA	MX	52	HIGH	HIGH	PERSISTENT	HIGH	1	1	MODERATE HIGH (2)	
	CHLA	TF	27	HIGH	MODERATE	PERIODIC	HIGH				
	Macroalgae	ALL	NA	UNKNOWN	UNKNOWN	UNKNOWN	UNKNOWN				NA
	DO	MX	2.6	BIO STRESS	HIGH	PERIODIC	MODERATE	0.5	0.5		
	DO	TF	3.1	BIO STRESS	HIGH	PERIODIC	MODERATE				

Year	Parameter	Zone	Value	Concentration	Spatial Coverage	Frequency	Expression	Score	Primary/ Secondary Scores	OEC Score
	SAV	ALL	NA	NA	NA	NA	UNKNOWN	NA		
	HAB	ALL	NA	NA	NA	NA	<i>LOW/ MODERATE</i>	0.5		

CHLA: Chlorophyll *a*  
 DO: Dissolved Oxygen  
 SAV: Submerged Aquatic Vegetation  
 HAB: Harmful/Toxic Algal Blooms  
 MX: Mixing Zone  
 TF: Tidal Fresh Zone  
 ALL: All Estuary Zones  
 NA: Not Applicable

The current estuary  $TN_{atm}$  (evaluated in terms of decrease in oxidized nitrogen) loading is estimated to be  $1.83 \times 10^7$  kg/yr (**Table 3.2-5**). The response curve relationship between  $TN_{atm}$  and  $TN_s$  ( $TN_s$  [mg/L] =  $1.07 + 2.0 \times 10^{-8} \times TN_{atm}$  [kg/yr]) can be found in **Figure 3.2-3**. Outside data specified for the model include the following:

- Mean salinity in estuary = 13 (relative units)
- Mean salinity offshore = 35 (relative units)
- Mean offshore TN concentration = 0.014 mg/L.

There were three sets of observed OEC and  $TN_s$  data points used to fit the OEC( $TN_s$ ) logistic model (not including ecological endpoints) from the data presented in **Table 3.2-6** and **Table 3.2-7**.

For purposes of estimating the OEC( $TN_s$ ) function at each iteration, the range on the OEC minimum value was specified as 0 to 0 (i.e., fixed at 0). In addition, the OEC maximum value was fixed at 5. Notwithstanding the capability to vary OEC minimum and OEC maximum from iteration to iteration, the decision was made to not do so. The range on the  $TN_s$  minimum value was specified from 0.014 mg/L (i.e., the offshore value) to 0.1 mg/L (i.e., a value determined by best professional judgment at this time due to lack of supporting data). The  $TN_s$  maximum value range was specified from 2.57 mg/L (i.e., maximum observed value from STORET) to  $1.5 \times 2.57 = 3.86$  mg/L.

As for the Potomac River/Potomac Estuary Case Study Area, each of the four ASSETS EI scores representing state improvements (i.e., *Poor-2, Moderate-3, Good-4, High-5*) was treated as a “target” ASSETS EI score, and 500 iterations were run under each target ASSETS EI scenario. **Figure 3.2-4** shows one of the curve fits of the logistic function to the observed OEC and  $TN_s$  data, including the randomly sampled ecological endpoints for  $TN_s$ .

The summary statistics of the 500 iterations for each target ASSETS EI scenario are presented in **Table 3.2-8**.

For target ASSETS EI = 2, all decreases are positive, but exceed 100%, meaning that not only must all  $TN_{atm}$  be removed to meet ASSETS EI = 2, but considerably more nitrogen from other sources must be removed as well. Given these results, the Neuse River Estuary is clearly currently somewhere between these two ASSETS EI scores as was the Potomac Estuary. There is some evidence that it is slightly more eutrophic than the Potomac Estuary because there was at



least a slim chance for the Potomac Estuary (at the 95th percentile) that a decrease in  $TN_{atm}$  (of less than 100%) would achieve ASSETS EI = 2.

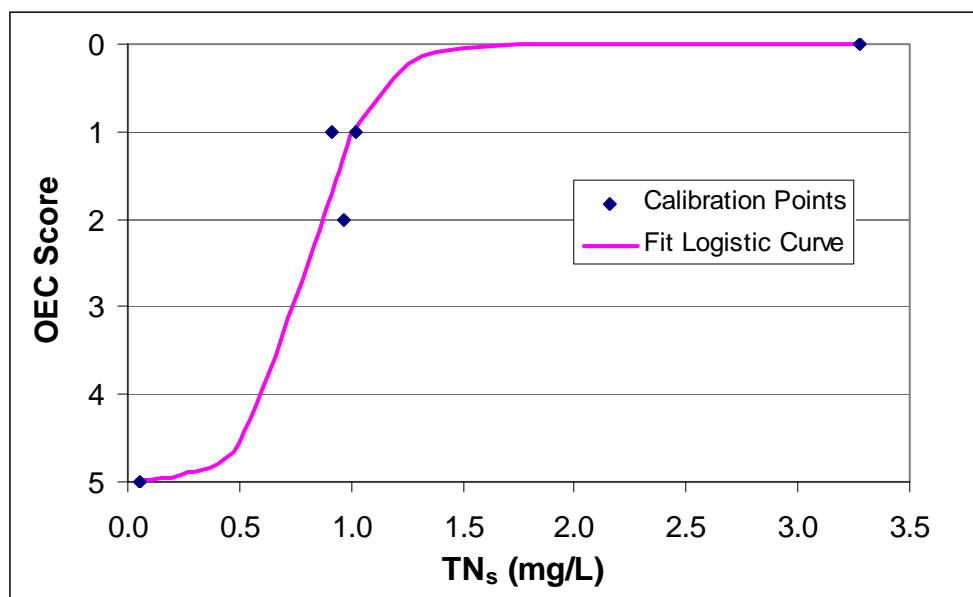


**Figure 3.2-4.** Fitted Overall Eutrophic Condition curve for target ASSETS EI=2, median  $TN_{atm}^*_{i}$  ( $i$  = run 287).

**Table 3.2-8.** Summary Statistics for Target ASSETS EI Scenarios for the Neuse River/Neuse River Estuary Case Study Area

Statistic	$TN_{atm}^*_{i}$ (kg N/yr)	% $TN_{atm}^*_{i}$ Decrease
ASSETS EI = 2 ( <i>Poor</i> )		
Mean	$-1.43 \times 10^8$	880
Median	$-1.43 \times 10^8$	880
5th Percentile	$-1.47 \times 10^8$	901
95th Percentile	$-1.01 \times 10^8$	653
ASSETS EI = 3 ( <i>Moderate</i> )		
No feasible solutions found		
ASSETS EI=4 ( <i>Good</i> ) and ASSETS EI = 5 ( <i>High</i> )		
All $TN_{atm}^*_{i} = -5.35 \times 10^8$ , i.e. $TN_s^*_{i} = 0$ mg/L		

Target ASSETS EI = 3 is again a unique case because all solutions were infeasible. With a  $TN_s^*_{i}$  value of 0 mg/L, the other (i.e., fixed) components of the ASSETS EI scoring methodology (i.e., DFO index and Susceptibility Scores) preclude satisfying any of the 95 combinations of DFO, OEC, and OHI index scores that comprise the ASSETS EI=3

combinations in the ASSETS EI lookup table. This result again depends on the experts who set up the ASSETS EI scoring table, defining only 95 out of 125 possible combinations. The likelihood that any of the 30 “missing” combinations are feasible in nature and could result in reaching Target ASSETS EI = 3 for this scenario will be examined in future analyses.

Target ASSETS EI = 4 and 5 had identical results. All 500 iterations returned a  $TN_{s,i}^* = 0$  mg/L, and a corresponding  $TN_{atm,i}^*$  negative load equal to  $TN_{atm,i}^* = (0 - 1.07)/2.0 \times 10^{-9} = -5.35 \times 10^8$  kg/yr. Clearly, target ASSETS EI equal 4 and 5 are very unattainable when decreasing the  $TN_{atm}$  (including all  $NO_x$ ) is the only policy option. Again, the decrease required includes all of the  $TN_{atm}$  source plus an additional amount that is one order of magnitude greater than the original atmospheric deposition load of  $10^8$  kg/yr). These amounts could be compared to the other nitrogen sources in the watershed that were used as inputs to the SPARROW model, giving consideration to the characteristics of each of these sources.

As with the Potomac River and Potomac Estuary watershed analysis, the SPARROW response curve can be used to examine the role of nitrogen deposition in achieving desired decreases in load to the Neuse River Estuary. In the Neuse River watershed, modeling results indicate that  $7 \times 10^6$  kg N/yr was deposited in 2002. SPARROW modeling predicts that this deposition input results in a loading of  $1.2 \times 10^6$  kg N/yr (i.e., 20% of the annual TN load) to the Neuse River Estuary. Unlike the Potomac River and Potomac Estuary analysis, little change is seen in the TN loading to the Neuse River Estuary with large decreases in the nitrogen deposition. If all atmospheric nitrogen deposition inputs were eliminated (i.e., 100% decrease), the total annual nitrogen load to the Neuse River Estuary would only decrease by 4%. There are two apparent reasons for this lack of change in loadings. The first reason is a characteristic of the Neuse River watershed. The second reason is an inherent characteristic of the SPARROW model formulation.

First, the TN loadings to the Neuse River Estuary are highly dependent on the sources other than atmospheric deposition within the SPARROW model. There are differences in characteristics among the sources within the watershed, where fertilizer, in particular, has a strong signature (i.e., indicating the large influence of agriculture within the watershed). This result demonstrates that the SPARROW response curves of TN load to other sources would be quite different, and the current response curve cannot be used to predict the relative magnitudes of loads needed to produce decreases greater than this 4%. **Figure 3.2-5** illustrates the theoretical

response curves that may result when the SPARROW modeled loads are plotted against the other TN source inputs. The green curve, or least influential source, displays the behavior of the atmospheric deposition for the Neuse River Estuary. The red curve, or highly influential source, likely corresponds to how agricultural sources within the watershed behave. These response curves will depend on the source magnitudes, spatial distributions, and other characteristics.

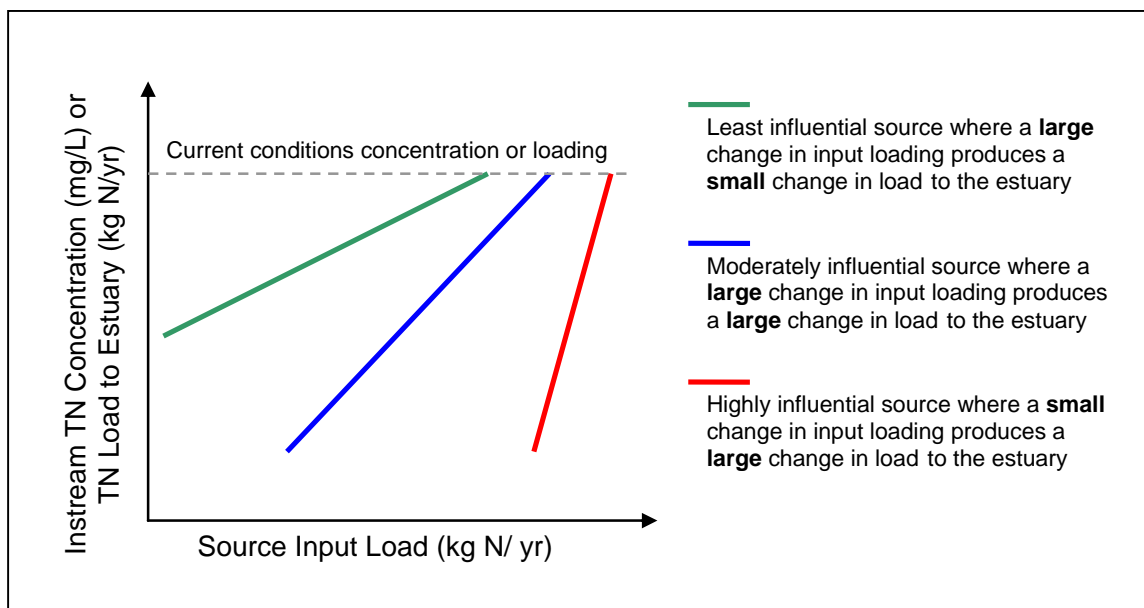


**Figure 3.2-5.** Theoretical SPARROW response curves demonstrating relative influence of sources on nitrogen loads to an estuary.

Second, the decay rates used by SPARROW play a part in the differing percentage decreases seen. The changes in the loadings reaching the estuary in the alternate effects analyses also occur because of the instream and reservoir decay terms. Within SPARROW, the decay term is applied to the total runoff load from each catchment (i.e., the sum of the source loads) in the upstream to downstream cumulative load calculations. When the atmospheric deposition loads are decreased, the TOTAL load from a catchment is decreased, even though the other sources remain constant. The same rate of decay is applied no matter the magnitude of the source loads is because the decay rate is based on stream travel characteristics or reservoir characteristics. So when the total load decreases, the amount of decay decreases, leading to a proportionally higher delivered load. Thus, the same percentage decrease in atmospheric deposition and fertilizer loads would not produce the same decrease in loads to the estuary.

## **4.0 IMPLICATIONS FOR OTHER SYSTEMS**

Selection of the analysis method for aquatic nutrient enrichment considered applications beyond a small number of case studies. The chosen method, consisting of a combination of SPARROW modeling for nitrogen loads and assessment of estuary conditions under the NOAA ASSETS EI, provides a highly scalable and widely applicable analysis method. Both components have been applied on a national scale—the national nutrient assessment using SPARROW (Smith and Alexander, 2000) and the NEEA using the ASSETS EI (Bricker et al., 1999, 2007a). Additionally, both have been used on a smaller scale. These previous analyses supply a large body of work—data, methods, and supporting experts—to draw from when conducting additional analyses or updating past applications.

Requirements for applying this method to other systems include mandatory data inputs, the ability to formulate a SPARROW application on a reliable stream network, and an estuary that is likely to be subject to eutrophication. Data requirements and model formulations have been described and detailed throughout this report.

The method is not currently designed to assess eutrophication impacts on inland waters. SPARROW modeling can still be applied to determine nitrogen loadings to an inland waterway, but the ASSETS EI assessment would not apply, and as such, the indicators and overall likelihood of eutrophication could not be assessed. For these inland waters, an alternate methodology would be necessary to examine the effects of changing nitrogen loads within the waterbody. A variety of methods could possibly be applied, including empirical relationships or dynamic modeling. It is beyond the scope of this case study to further assess these inland waters beyond the sensitive areas analysis in Section 1.2.1. An additional case study in this project examines the effects of aquatic acidification on inland waters using dynamic modeling (See Appendix 4).

The scalability of the methods and approaches taken in these case studies will rely on the ability to group estuaries across the country into patterns of similar behavior either in terms of nitrogen sources or eutrophication effects. In 2003 and 2004, NOAA and the Kansas Geological Survey conducted a series of workshops to develop a type classification system for the 138 estuarine systems assessed in the original NEEA (Bricker et al., 1999). Participants considered 70 classification variables for grouping the estuarine systems. These variables included 51 physical characteristics (e.g., estuary depth and volume, tidal range, salinity, nitrogen and

phosphorus concentrations, estimates of flushing time, evaporation), 10 perturbation characteristics (e.g., population in watershed, estimates of nutrient loading), and nine response characteristics (e.g., SAV loss, presence of nuisance and toxic blooms). Ultimately, the workgroup selected five variables (i.e., depth, openness of estuary mouth, tidal range, mean annual air temperature, and the log of freshwater inflow/estuarine area) deemed to be the most critical physical and hydrological characteristics influencing nutrient processing and the expression of eutrophic symptoms in a waterbody. Based on these five variables, the 138 estuarine systems were classified into 10 groups (**Table 4-1; Figure 4-1**). The two estuary systems included in this case study, the Potomac and Neuse River estuary systems, were in groups one and nine, respectively (Bricker et al., 2007a).

**Table 4-1.** Typology Group Categorizations

Group	Number of Systems	Overriding Characteristics
Group 0	13	Low freshwater inflow:estuarine area ratio; low depth; low estuary mouth openness
Group 1	35	Medium depth, medium openness, high annual air temperature
Group 2	5	High depth, low annual air temperature
Group 3	8	High estuary mouth openness; high depth
Group 4	18	Low estuary mouth openness; high freshwater inflow:estuarine area ratio; low annual air temperature
Group 5	3	High estuary mouth openness; high depth
Group 6	2	High depth; high estuary mouth openness
Group 7	16	High tidal range; medium estuary mouth openness; low annual air temperature
Group 8	17	High freshwater inflow:estuarine area ratio; low depth
Group 9	21	Low depth, medium estuary mouth openness; high annual air temperature

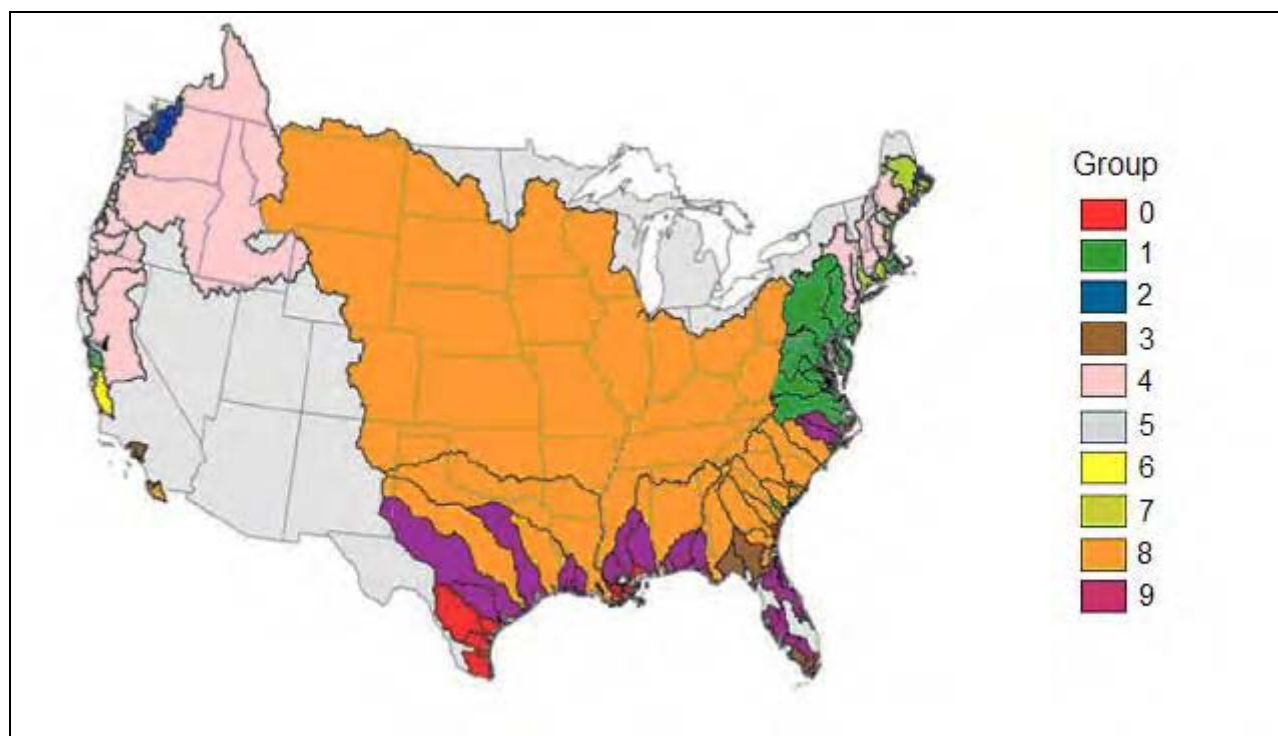


**Figure 4-1.** Preliminary classifications of estuary typology across the nation (modified from Bricker et al., 2007a).

Given that the response curve of the OEC index score to  $TN_s$  is expected to change shapes with different values of susceptibility, the typology classes thus defined in **Table 4-1** provide an opportunity to assess the validity of this expectation. The first step in assessing this statement would be to examine the nutrient loadings in other estuaries that fall within groups 1 or 9, the groups corresponding to the two case study areas. Once the shape and behavior of the response curve for the estuary grouping is confirmed, work can begin to scale the results between estuaries of that group. The ASSETS EI score for an estuary may also be considered within this analysis. For the 48 systems for which an ASSETS EI score was developed in the 2007 NEEA Update, only one system was rated as *High* (i.e., Connecticut River), whereas five were rated as *Good* (i.e., Biscayne Bay, Pensacola Bay, Blue Hill Bay, Sabine Lake, Boston Harbor). Eighteen systems were rated as *Moderate*, and 24 systems were rated as *Poor* or *Bad*. Those estuaries that fall within groups 1 or 9 and are rated as *Poor* or *Bad* would be the most appropriate candidates to start the scaling analysis.

Scaling of results will also need to account for the response of the watershed to atmospheric nitrogen deposition inputs. If SPARROW is used, either through the in-development Web-enabled national SPARROW application or through regional or site-specific applications,

the shape of the response curve will be determined by the model and its parameters. If a different approach is taken to develop TN loadings, then the systems will need to be grouped according to the shape and behavior of the response curve. Additional consideration should be given to the magnitude of the percentage contributions of the atmospheric deposition to the TN load to the watershed and the resulting TN load to the estuary.

## 5.0 UNCERTAINTY

There are several areas of uncertainty with this method of assessment for aquatic nutrient enrichment, which are summarized below.

- **Data inputs to SPARROW.** The compilation of data needed for creation or application of SPARROW relies on geographic and temporal analyses. For this study, the data used were developed under separate studies and published by the USGS. Because the data were independently verified before publication by the USGS, only quality checks were performed on the data rather than full validation exercises. For any future analyses that require new compilations of data, close attention should be paid to the source and geographic and temporal precision and accuracy of the data because SPARROW relies on the distribution of sources across the watershed to create model parameters on the annual average basis.
- **Modeling uncertainty in SPARROW estimates.** With any measured or modeled results, there is a certain amount of uncertainty that should be quantified. Because SPARROW relies on a nonlinear regression basis, a number of parameters can be used to assess the uncertainty within the model and provide confidence intervals around the estimates. The Version 3 Chesapeake Bay SPARROW application met evaluation criteria based on degrees of freedom, model error, and R-squared values. The calibration of the Neuse River watershed SPARROW model using SAS examined the standard deviation, t-statistics, p-values, and VIFs for each estimated parameter. The overall model was evaluated based on minimizing model error, maximizing R-squared values, and ensuring that the Eigen value range was below 100 while the probability plot correlation coefficient was close to one. The model derived for the Neuse River/Neuse River Estuary Case Study Area did produce some model parameters (i.e., manure production, urban area, and decay terms) that did not reach desired statistical significance levels. The estimation of decay term parameters may be rectified by adjusting the flow classes among which the parameters are split. This should be examined in any future analyses. The manure production and urban area source terms should also be examined as to their distribution throughout the watershed and overall contributions to the load.

- **Sensitivity of SPARROW formulation due to atmospheric inputs in the Potomac River/Potomac Estuary Case Study Area.** The parameterization of a SPARROW application for the Potomac River watershed is expected to change when recalibration is completed using the atmospheric deposition of TN based on the combination of CMAQ and NADP data created for this study, rather than the interpolated values of wet deposition of nitrate. As discussed in Section 3.1.1, the spatial gradient as well as the magnitude of the atmospheric deposition of different nitrogen species varies across the watershed. While it is certain that the parameter estimated to apply to the atmospheric deposition source will change, what is uncertain at this point is the extent to which the other model parameters and the overall nitrogen load estimates will be affected by using the CMAQ/NADP estimates in the model calibrated against the wet  $\text{NO}_3^-$  deposition values. Sensitivity of the model parameters and nitrogen load estimate can be evaluated in future studies where SPARROW is recalibrated against the 2002 data.
- **Calibration data for SPARROW estimates.** Monitoring data will be used to calibrate the SPARROW model. By relying on data from federally recognized data systems, the aim is to use data that has undergone quality assurance/quality control (QA/QC) procedures. Additionally, collaboration has been completed with the researchers who have conducted the previous SPARROW applications in each case study area to provide a rigorous check on the data used.
- **Data inputs to the ASSETS EI.** Because of the numerous data requirements and sources required to conduct a full ASSETS EI analysis, there is a large range of uncertainty that can enter into the calculations. For the water quality data evaluation of dissolved oxygen and chlorophyll *a*, the numerical values of the 10th and 90th percentiles used in the evaluation were subjected to QA/QC procedures as processed through regulated databases with checks. The frequency of occurrence of these indicators and HABs events relied more on subjective judgment of temporal variations of concentrations across the year. Best attempts were made to apply standardized evaluation methods in order to minimize any uncertainties due to subjectivity or processing differences.
- **Heuristic estimates of DFO index scores.** The estimation of the DFO index score in the ASSETS EI assessment currently relies on heuristic estimates from systems experts. Future NOAA efforts will seek to provide more scientifically structured estimates for this parameter, but at this time, reliance must be on expert judgment on whether there will be increased or decreased pressures because of nutrient loads, population growth, and land use change.
- **Steady-state estimates/mean annual estimates.** Both SPARROW and the ASSETS EI methods currently provide only longer-term estimates of the system conditions. There is the possibility of conducting the analyses on a seasonal basis, which may be appropriate because the trends in eutrophication indicators are likely to vary seasonally. Producing annual averages actually



introduces some leverage to the uncertainty in the input data as previously discussed. Because the ultimate values used to base the analysis on are averages, there is less reliance on the certainty of individual measures.

- **Use of a screening method.** The methods used in this study are only of the screening level. The screening level was more appropriate for a scalable, widely applicable set of case studies than for a highly detailed modeling effort. Undoubtedly, details, such as the degree to which the soil-groundwater system affects atmospherically deposited nitrogen, will be less quantified than detailed processes using this method. However, for an initial approach to determining the aquatic nutrient enrichment effects on a system, the screening method provides a response curve that can be used in the evaluation of ecosystem services. Additionally, many of the complex concepts linking the indicators of eutrophication to the effects of eutrophication are not highly developed or understood at this time (Howarth and Marino, 2006). While some targeted studies may produce the type of linked results from indicators to ecological endpoints that are the goal of this study, these results cannot be readily expanded to multiple areas in multiple climate zones without great levels of effort. As the base of literature and results expands, the concepts applied in this methodology can be expanded to more deterministic, temporarily varying analyses.
- **Use of a partially empirical framework.** Because SPARROW is, at its core, an empirical relationship, any model obtained using SPARROW is a function of the data used in the calibration. Therefore, the predictions remain valid as long as there is no great change in the conditions (in this case, the nitrogen loadings within each subbasin) underlying the model. This aspect of the model introduces uncertainty into the alternative effects results because they are calculated using a model calibrated under current conditions.

### **Uncertainties in Back Calculation Methods**

- **Missing ASSETS EI scores per combinations of index scores.** The combinations of OHI, OEC, and DFO index scores provided by Bricker et al. (2003) leave out 30 of the possible 125 combinations that represent overall ASSETS EI scores. In both case study analyses, these missing scores have led to a conclusion of infeasible scenarios because an overall ASSETS EI score could not be determined from the resulting instream nitrogen load found during the back calculation method. The methods used to determine the 95 combinations will be investigated, and the missing 30 scores pursued for future case study analyses.
- **Better rationale for TN<sub>s</sub> minimum and maximum uncertainty range.** The uncertainty about how to best quantify the TN<sub>s</sub> ecological endpoint uncertainty is the biggest limitation of the current analyses. This is particularly true for the TN<sub>s</sub> high end (i.e., the maximum TN<sub>s</sub> that would be

expected to result in an OEC index score of 1). The assigned uncertainty ranges were based on best professional judgment, but more research is needed. It is expected for the results of the back calculation methodology to be very sensitive to these ecological endpoint ranges, especially on the maximum  $TN_s$  end. Because of this limitation, the results presented herein for the Potomac and Neuse River estuaries should be interpreted as illustrative of the methodology, not strictly valid.

- **Methodology to incorporate uncertainty in the SPARROW model.** Estimates of  $TN_s$  at the head of the estuary, predicted by SPARROW and driven by the  $TN_{atm}$  (i.e., TN deposition evaluated on decreases in  $NO_x$ ) over the watershed and other nitrogen sources, are uncertain. That uncertainty was not considered in these two case studies; therefore, the probability distributions of  $TN_{atm\ i}^*$  presented are artificially “tight” (i.e., the true distributions would exhibit more variability). There is a need to explore the SPARROW literature more thoroughly to determine how to incorporate the non-parametric confidence limits that have been developed for the SPARROW model. Once such limits are incorporated, it is very unlikely that one would be able to explicitly solve the SPARROW model, including these confidence limit terms explicitly for a  $TN_{atm\ i,j}^*$  as a function of the  $TN_{s\ i}^*$  value and the “jth” probability of confidence limit term. Some sort of implicit, iterative method would be needed. An application of the Newton’s method algorithm has already been developed for these purposes and tested using an artificial confidence limit term. It seems to work remarkably well (i.e., convergence within a few iterations to very tight convergence criteria), and the researchers are optimistic that expanding the overall methodology to include SPARROW uncertainty is very tractable.
- **More convergence testing to determine appropriate numbers of samples.** As briefly mentioned, some modest convergence testing was completed to determine how many samples of the  $OEC(TN_s)$  function need to be used for the statistics of interest for the resulting  $TN_{atm\ i}^*$  distributions to be reasonably stable. The answer is something more than 500, which will undoubtedly increase when SPARROW uncertainty is incorporated. More convergence testing is needed.
- **Crossing of a categorical ranking system with a continuous nitrogen concentration scale.** Several assumptions and considerations had to be made in order to create and evaluate the logistic response curve because the OEC index score is a categorical ranking of 1 through 5, whereas  $TN_s$  is a continuous variable. The functions evaluated in *BackCalculation* treat the OEC index score as a continuous function. Until higher level models are developed to relate the nitrogen concentrations in the system to eutrophication effects, these assumptions are necessary. Future applications with additional data should be used to test and validate these assumptions and results.

## 6.0 CONCLUSIONS

- A screening-level method has been determined to be an appropriate approach to assessing the effects of atmospheric deposition of oxidized nitrogen on eutrophication/nutrient enrichment because there is a lack of a generalized link development between these characteristics in the literature.
- Both the Potomac and Neuse River estuaries have an ASSETS EI score of *Bad* for 2002, meaning that both systems are highly eutrophic and are not expected to improve greatly in the near future. Atmospheric deposition over the watersheds account for approximately 24% and 26% of the instream loads to the Potomac and Neuse River estuaries, respectively.
- The *BackCalculation* program designed and set up for this study succeeded in assessing the links between  $TN_s$  responding to changes in  $TN_{atm}$  and the OEC index and ASSETS EI scores. Results of this assessment for the Potomac Estuary reveal that it is possible to improve the ASSETS EI score by only one category when the only change is in a decrease of the oxidized nitrogen component of the atmospheric deposition (**Table 3.2-4**). This result showed that there was a 5% chance (i.e., 95th Percentile of results) that decreasing the  $TN_{atm}$  by 78% would result in the one category improvement in the ASSETS EI score. Within the Neuse River Estuary, this analysis revealed that it would not be possible to improve the ASSETS EI score by decreasing the oxidized nitrogen in the atmospheric deposition loading to the estuary alone (**Table 3.2-8**; all percentage decreases greater than 100). Additional source decreases would be necessary to produce OHI and OEC index scores good enough to improve the ASSETS EI score.
- Scaling of this methodology was a priority in development. Demonstration of the back calculation methods was the first step to expanding the results to estuaries across the nation. Alternative evaluation methods of eutrophication will be needed to assess nutrient enrichment in inland waters.

## 7.0 REFERENCES

- Alexander, R.B., R.A. Smith, and G.E. Schwarz. 2000. Effect of stream channel size on the delivery of nitrogen to the Gulf of Mexico. *Nature* 403:758–761.
- Alexander, R.B., R.A. Smith, G.E. Schwarz, S.D. Preston, J.W. Brakebill, R. Srinivasan, and P.A. Pacheco. 2001. Atmospheric nitrogen flux from the watersheds of major estuaries of the United States—An application of the SPARROW watershed model. Pp. 119–170 in *Nitrogen Loading in Coastal Water Bodies: An Atmospheric Perspective*. Edited by R.A.

- Valigura, R.B. Alexander, M.S. Castro, T.P. Meyers, H.W. Paerl, P.E. Stacey, and R.E. Turner. American Geophysical Union, Coastal and Estuarine Studies, Washington, DC.
- Alexander R.B., A.H. Elliott, U. Shankar, and G.B. McBride. 2002. Estimating the sources and transport of nutrients in the Waikato River Basin, New Zealand. *Water Resources Research* 38:1268–1290.
- Atkins, W.A., and F. Anderson. 2009. Chesapeake Bay. In *Water Encyclopedia*. Online information. Advameg, Inc., Flossmoor, IL. Available at <http://www.waterencyclopedia.com/Ce-Cr/Chesapeake-Bay.html> (accessed February 2009).
- Bergström, A.K., and M. Jansson. 2006. Atmospheric nitrogen deposition has caused nitrogen enrichment and eutrophication of lakes in the northern hemisphere. *Global Change Biology* 12:635–643.
- Box, M.J. 1965. A new method of constrained optimization and a comparison with other methods. *The Computer Journal* 8:42–52.
- Boyer, E.W., C.L. Goodale, N.A. Jaworski, and R.W. Howarth. 2002. Anthropogenic nitrogen sources and relationships to riverine nitrogen export in the northeastern U.S.A. *Biogeochemistry* 57/58:137–169.
- Boynton, W.R., J.H. Garber, R. Summers, and W.M. Kemp. 1995. Inputs, transformations, and transport of nitrogen and phosphorus in Chesapeake Bay and selected tributaries. *Estuaries* 18:285–314.
- Brakebill, J.W., S.D. Preston, and S.K. Martucci. 2001. *Digital Data Used to Relate Nutrient Inputs to Water Quality in the Chesapeake Bay, Version 2.0*. USGS Open File Report OFR-01-251. U.S. Department of the Interior, U.S. Geological Survey, Baltimore, MD. Available at <http://md.usgs.gov/publications/ofr-01-251/index.htm>.
- Brakebill, J.W., and S.D. Preston. 2004. *Digital Data Used to Relate Nutrient Inputs to Water Quality in the Chesapeake Bay Watershed, Version 3.0*. USGS Open File Report 2004-

1433. U.S. Department of the Interior, U.S. Geological Survey, Baltimore, MD.  
Available at <http://pubs.usgs.gov/of/2004/1433/pdf/sparv3.pdf>.
- Bricker, S.B., C.G. Clement, D.E. Pirhalla, S.P. Orlando, and D.R.G. Farrow. 1999. *National Estuarine Eutrophication Assessment: Effects of Nutrient Enrichment in the Nation's Estuaries*. NOAA—NOS Special Projects Office. U.S. Department of Commerce, National Oceanic and Atmospheric Administration, National Ocean Service, National Centers for Coastal Ocean Science, Center for Coastal Monitoring and Assessment, Silver Spring, MD.
- Bricker, S.B., J.G. Ferreira, and T. Simas. 2003. An integrated methodology for assessment of estuarine trophic status. *Ecological Modelling* 169:39–60.
- Bricker, S., D. Lipton, A. Mason, M. Dionne, D. Keeley, C. Krahforst, J. Latimer, and J. Pennock. 2006. *Improving Methods and Indicators for Evaluating Coastal Water Eutrophication: A Pilot Study in the Gulf of Maine*. NOAA Technical Memorandum NOS NCCOS 20. U.S. Department of Commerce, National Oceanic and Atmospheric Administration, National Ocean Service, National Centers for Coastal Ocean Science, Center for Coastal Monitoring and Assessment, Silver Spring, MD.
- Bricker, S., B. Longstaff, W. Dennison, A. Jones, K. Boicourt, C. Wicks, and J. Woerner. 2007a. *Effects of Nutrient Enrichment in the Nation's Estuaries: A Decade of Change*. NOAA Coastal Ocean Program Decision Analysis Series No. 26. U.S. Department of Commerce, National Oceanic and Atmospheric Administration, National Ocean Service, National Centers for Coastal Ocean Science, Silver Spring, MD.
- Bricker, S., J.G. Ferreira, and R. Pastres. 2007b. *Eutrophication Assessment using ASSETS Approach, Application and Results*. U.S. Department of Commerce, National Oceanic and Atmospheric Administration. Presented at the Venice Water Authority Meeting: Exploring possibilities for collaborative work, December 3. Available at [http://www.eutro.org/presentations/VWA\\_Seminar.pdf](http://www.eutro.org/presentations/VWA_Seminar.pdf).

- Bricker, S. 2008. Personal communication from Suzanne Bricker, National Oceanic and Atmospheric Administration, to Jennifer Schimek, RTI International, Research Triangle Park, NC.
- Bricker, S., B. Buddemeier, S. Smith, B. Maxwell. In prep. *Results of Type Classification Analyses from NOAA Workshop September, 2003 and KGS Work Session January, 2004*. White paper. U.S. Department of Commerce, National Oceanic and Atmospheric Administration, National Ocean Service, Silver Spring, MD.
- Burkholder, J.M., D.A. Dickey, C.A. Kinder, R.E. Reed, M.A. Mallin, M.R. McIver, L.B. Cahoon, G. Melia, C. Brownie, J. Smith, N. Deamer, J. Springer, H.B. Glasgow, and D. Toms. 2006. Comprehensive trend analysis of nutrients and related variables in a large eutrophic estuary: A decadal study of anthropogenic and climatic influences. *Limnology and Oceanography* 51:463–487.
- CBP (Chesapeake Bay Program). 2008. *CBP Water Quality Database (1984-present)*. Online information. Chesapeake Bay Program, Annapolis, MD. Available at [http://www.chesapeakebay.net/data\\_waterquality.aspx](http://www.chesapeakebay.net/data_waterquality.aspx) (accessed December 2008).
- Eadie, B.J., B.A. McKee, M.B. Lansing, J.A. Robbins, S. Metz, and J.H. Trefry. 1994. Records of nutrient-enhanced coastal productivity in sediments from the Louisiana continental shelf. *Estuaries* 17:754–765.
- Elliott, A.H., R.B. Alexander, G.E. Schwarz, U. Shankar, J.P.S. Sukias, and G.B. McBride. 2005. Estimation of nutrient sources and transport for New Zealand using the hybrid physical-statistical model SPARROW. *Journal of Hydrology* 44:1–27.
- Fact-Index.com. 2009. *Potomac River*. Online information. Fact-Index.com. Available at: [http://www.fact-index.com/p/po/potomac\\_river.html](http://www.fact-index.com/p/po/potomac_river.html) (accessed February 2009).
- Ferreira, J.G., S.B. Bricker, and T.S. Castro. 2007. Application and sensitivity testing of a eutrophication assessment method on coastal systems in the United States and European Union. *Journal of Environmental Management* 82:433–445.

- Heinz Center for Science. 2007. *Economics and the Environment: Indicators of Ecological Effects of Air Quality*. Analysis Subcommittee Meeting Summary. Heinz Center for Science, Washington, DC. November.
- Hoos, A.B. 2005. Evaluation of the SPARROW model for estimating transport of nitrogen and phosphorus in streams of the Interior Low Plateau Ecoregion, Tennessee, Kentucky, and Alabama, during 1992-2002. Pp. 2A-47 in *Proceedings of the Fifteenth Tennessee Water Resources Symposium*, Burns, TN, April 13-15. Tennessee Section of the American Water Resources Association.
- Hoos, A.B., S. Terziotti, G. McMahon, K. Savvas, K.G. Tighe, and R. Alkons-Wolinsky. 2008. *Data to Support Statistical Modeling of Instream Nutrient Load Based on Watershed Attributes, Southeastern United States, 2002*. Open File Report 2008-1163. U.S. Department of the Interior, U.S. Geological Survey, Reston, VA.
- Howarth, R.W. 2007. Atmospheric deposition and nitrogen pollution in coastal marine ecosystems. In *Acid in the Environment*. Edited by G.R. Visgilio and D.M. Whitelaw. New York: Springer.
- Howarth, R.W., and R. Marino. 2006. Nitrogen as the limiting nutrient for eutrophication in coastal marine ecosystems: Evolving views over three decades. *Limnology and Oceanography* 51(1 part 2):364-376.
- Howarth, R.W., G. Billen, D. Swaney, A. Townsend, N. Jarworski, K. Lajtha, J.A. Downing, R. Elmgren, N. Caraco, T. Jordan, F. Berendse, J. Freney, V. Kueyarov, P. Murdoch, and Z. Zhao-liang. 1996. Riverine inputs of nitrogen to the North Atlantic Ocean: Fluxes and human influences. *Biogeochemistry* 35:75-139.
- Kansas Department of Health and Environment. 2004. *Surface Water Nutrient Reduction Plan*. Kansas Department of Health and Environment, Bureau of Water, Topeka, KS. Available at [http://www.kdhe.state.ks.us/water/download/ks\\_nutrient\\_reduction\\_plan\\_12\\_29\\_final.pdf](http://www.kdhe.state.ks.us/water/download/ks_nutrient_reduction_plan_12_29_final.pdf) (accessed March 1, 2005).

- McMahon, G., R.B. Alexander, and S. Qian. 2003. Support of total maximum daily load programs using spatially reference regression models. *Journal of Water Resources Planning and Management* 129(4):315–329.
- MEA (Millennium Ecosystem Assessment Board). 2005. *Ecosystems and Human Well-being: Current State and Trends, Volume 1*. Edited by R. Hassan, R. Scholes, and N. Ash. Washington: Island Press. Available at <http://www.millenniumassessment.org/documents/document.766.aspx.pdf>.
- Moore, R.B., C.M. Johnston, K.W. Robinson, and J.R. Deacon. 2004. *Estimation of total nitrogen and phosphorus in New England streams using spatially referenced regression models*. USGS Scientific Investigations Report 2004-5012. U.S. Department of the Interior, U.S. Geological Survey, Pembroke, NH. Available at <http://water.usgs.gov/pubs/sir/2004/5012>.
- NC DENR (North Carolina Department of Environment and Natural Resources). 1993. *Neuse River Basinwide Water Quality Management Plan*. North Carolina Department of Environment and Natural Resources, Division of Environmental Management, Water Quality Section, Raleigh, NC.
- NC DENR (North Carolina Department of Environment and Natural Resources). 2002. *Neuse River Basin-wide Water Quality Plan*. North Carolina Department of Environment and Natural Resources, Division of Water Quality/Planning, Raleigh, NC. Available at <http://h2o.enr.state.nc.us/basinwide/Neuse/2002/Section A Chapter 2.pdf>.
- NC DWQ (Division of Water Quality). 2008. North Carolina Department of Environment and Natural Resources. *Environmental Sciences Section – Fish Kill Event Update*. Online information. North Carolina Department of Environment and Natural Resources, Division of Water Quality, Raleigh, NC. Available at: <http://www.esb.enr.state.nc.us/Fishkill/fishkillmain.htm> (accessed December 2008).
- NEIWPCC (New England Interstate Water Pollution Control Commission). 2004. New England SPARROW water quality model. *Interstate Water Report* 1(3):6–7. Available at [http://www.neiwpcc.org/PDF\\_Docs/iwr\\_s04.pdf](http://www.neiwpcc.org/PDF_Docs/iwr_s04.pdf).



- NRCS (Natural Resources Conservation Service). 2001. *1997 National Resources Inventory, Updated June 2001*. Natural Resources Conservation Service, Washington, DC.
- Officer, C.B., R.B., Biggs, J.L. Taft, L.E. Cronin, M.A. Tyler, and W.R. Boynton. 1984. Chesapeake Bay anoxia: origin, development, and significance. *Science* 223:22–27.
- Paerl, H.W. 1995. Coastal eutrophication in relation to atmospheric nitrogen deposition: current perspectives. *Ophelia* 41:237–259.
- Paerl, H.W. 1997. Coastal eutrophication and harmful algal blooms: Importance of atmospheric deposition and groundwater as “new” nitrogen and other nutrient sources. *Limnology and Oceanography* 42:1154–1165.
- Paerl, H. W. 2002. Connecting atmospheric nitrogen deposition to coastal eutrophication. *Environmental Science and Technology* 36:323A–326A.
- Paerl, H., J. Pinckney, J. Fear, and B. Peierls. 1998. Ecosystem responses to internal and watershed organic matter loading: Consequences for hypoxia in the eutrophying Neuse River Estuary, NC, USA. *Marine Ecology Progress Series* 166:17–25.
- Paerl, H.W., R.S. Fulton, P.H. Moisander, and J. Dyble. 2001. Harmful freshwater algal blooms, with an emphasis on cyanobacteria. *The Scientific World* 1:76–113.
- Paerl, H., J. Dyble, L. Twomey, J. Pinckney, J. Nelson, and L. Kerkhof. 2002. Characterizing man-made and natural modifications of microbial diversity and activity in coastal ecosystems. *Antonie van Leeuwenhoek* 81(1–4):487–507.
- Peierls, B. 2008. Personal communication.
- Preston, S. 2008. Personal communication.
- Preston, S.D., and J.W. Brakebill. 1999. *Applications of Spatially Referenced Regression Modeling for the Evaluation of Total Nitrogen Loading in the Chesapeake Bay Watershed*. USGS Water-Resources Investigations Report 99-4054. U.S. Department of

- the Interior, U.S. Geological Survey, MD-DE-DC Water Science Center, Baltimore, MD. Available at <http://md.usgs.gov/publications/wrir-99-4054>.
- RTI (RTI International). 2007. *Review of Candidate Fate and Transport and Ecological Models*. Report prepared for the U.S. Environmental Protection Agency under Contract No. EP-D-06-003. RTI International, Research Triangle Park, NC.
- RTI (RTI International). 2008. *Methodology Development for Linking Ecosystem Indicators to Ecosystem Services*. Report prepared for the U.S. Environmental Protection Agency, Office of Air Quality Planning and Standards under Contract No. EP-D-06-003. RTI International, Research Triangle Park, NC.
- Schwarz, G.E., A.B. Hoos, R.B. Alexander, and R.A. Smith. 2006. *The SPARROW Surface Water-Quality Model—Theory, Applications and User Documentation*. USGS Techniques and Methods 6-B3, 248 p. and CD –ROM. U.S. Department of the Interior, U.S. Geological Survey, Reston, VA.
- Smith, R.A., and R.B. Alexander. 2000. Sources of nutrients in the nation's watersheds. In *Managing Nutrients and Pathogens from Animal Agriculture*. Proceedings from the Natural Resource, Agriculture, and Engineering Service Conference for Nutrient Management Consultants, Extension Educators, and Producer Advisors, Camp Hill, PA, March 28–30. Natural Resource, Agriculture, and Engineering Service, Cooperative Extension, Ithaca, NY.
- Smith, M.D., and L.B. Crowder. 2005. *Valuing ecosystem services with fishery rents: a lumped parameter approach to hypoxia in the Neuse River Estuary*. Milan, Italy: Fondazione Eni Enrico Mattei (FEEM), NRM Nota di Lavoro (Natural Resources Management Working Papers), 115.05. Available at <http://ssrn.com/abstract=825587> (accessed November 5, 2007).
- Smith, R.A., R.B. Alexander, G.D. Tasker, C.V. Price, K.W. Robinson, and D.A. White. 1994. Statistical modeling of water quality in regional watersheds. Pp. 751–754 in *Proceedings of Watershed '93—A National Conference on Watershed Management*, Alexandria, VA,

- March 21–24, 1993. EPA 840-R-94-002. U.S. Environmental Protection Agency, Washington, DC.
- Smith, R.A., G.E. Schwarz, and R.B. Alexander. 1997. Regional interpretation of water-quality monitoring data. *Water Resources Research* 33(12):2781–2798.
- Spruill, T.B., A.J. Tesoriero, H.E. Mew, Jr., K.M. Farrell, S.L. Harden, A.B. Colosimo, and S.R. Kraemer. 2004. *Geochemistry and Characteristics of Nitrogen Transport at a Confined Animal Feeding Operation in a Coastal Plain Agricultural Watershed, and Implications for Nutrient Loading in the Neuse River Basin, North Carolina, 1999–2002*. Scientific Investigations Report 2004-5283. U.S. Department of the Interior, U.S. Geological Survey, Reston, VA.
- University of North Carolina. 2008. *The Neuse River Estuary Modeling and Monitoring Project (ModMon)*. Online information. University of North Carolina, Institute of Marine Sciences, Morehead City, NC. Available at <http://www.unc.edu/ims/neuse/modmon/index.htm> (accessed December 2008).
- U.S. EPA (Environmental Protection Agency). 1996. *Air quality criteria for ozone and related photochemical oxidants*. EPA/600/AP-93/004aF-cF. 3v. U.S. Environmental Protection Agency, Office of Research and Development, Research Triangle Park, NC. Available at <http://cfpub2.epa.gov/ncea/>.
- U.S. EPA (Environmental Protection Agency). 2000. *Deposition of air pollutants to the great waters. Third report to Congress*. EPA-453/R-00-005. U.S. Environmental Protection Agency, Office of Air Quality Planning and Standards, Research Triangle Park, NC. Available at <http://www.epa.gov/air/oaqps/gr8water/3drpt/> (accessed January 16, 2008).
- U.S. EPA (Environmental Protection Agency). 2002. *Summary Table for Nutrient Criteria Documents*. U.S. Environmental Protection Agency, Office of Water, Washington, DC. Available at: <http://www.epa.gov/waterscience/criteria/nutrient/ecoregions/files/sumtable.pdf>.

- U.S. EPA (Environmental Protection Agency). 2005. *Advisory on Plans for Ecological Effects Analysis in the Analytical Plan for EPA's Second Prospective Analysis—Benefits and Costs of the Clean Air Act, 1990-2020*. U.S. Environmental Protection Agency, Office of the Administrator, Science Advisory Board, Washington, DC. June 23.
- U.S. EPA (Environmental Protection Agency). 2008a. *Integrated Science Assessment for Oxides of Nitrogen and Sulfur—Ecological Criteria*. Final Report. EPA/600/R-08/082F. U.S. Environmental Protection Agency, National Center for Environmental Assessment-RTP Division, Office of Research and Development, Research Triangle Park, NC. Available at <http://cfpub.epa.gov/ncea/cfm/recordisplay.cfm?deid=201485>.
- U.S. EPA (Environmental Protection Agency). 2008b. *Draft Scope and Methods Plan for Risk/Exposure Assessment: Secondary NAAQS Review for Oxides of Nitrogen and Oxides of Sulfur*. U.S. Environmental Protection Agency, Office of Air Quality Planning and Standards, Research Triangle Park, NC Available at [http://www.epa.gov/ttn/naaqs/standards/no2so2sec/cr\\_pd.html](http://www.epa.gov/ttn/naaqs/standards/no2so2sec/cr_pd.html).
- USDA (U.S. Department of Agriculture). 2002. *2002 Census of Agriculture – State Data: Table 13 “Poultry – Inventory and Sales: 2002 and 1997.”* U.S. Department of Agriculture, National Agricultural Statistics Service, Washington, DC. Available at [http://www.nass.usda.gov/census/census02/volume1/us/st99\\_2\\_013\\_013.pdf](http://www.nass.usda.gov/census/census02/volume1/us/st99_2_013_013.pdf).
- USGS (U.S. Geological Survey). 1999. *Digital representation of “Atlas of United States Trees” by Elbert L. Little, Jr.* Digital Version 1.0. U.S. Department of the Interior, U.S. Geological Survey, Denver, CO. Available at <http://esp.cr.usgs.gov/data/atlas/little> (accessed July 25, 2008).
- Valiela, I., and J. Costa. 1988. Eutrophication of Buttermilk Bay, a Cape Cod coastal embayment: Concentrations of nutrients and watershed nutrient budgets. *Environmental Management* 12:539–551.
- Valiela, I., J. Costa, K. Foreman, J.M. Teal, B. Howes, and D. Aubrey. 1990. Transport of groundwater-borne nutrients from watersheds and their effects on coastal waters. *Biogeochemistry* 10:177–197.

- VIMS (Virginia Institute of Marine Science). 2008. *Submerged Aquatic Vegetation (SAV) in Chesapeake Bay and Delmarva Peninsula Coastal Bays*. Online information. Virginia Institute of Marine Science, Gloucester Point, VA. Available at <http://web.vims.edu/bio/sav/?svr=www> (accessed December 2008).
- Whitall, D., and H.W. Paerl. 2001. Spatiotemporal variability of wet atmospheric nitrogen deposition to the Neuse River Estuary, North Carolina. *Journal of Environmental Quality* 30:1508–1515.
- Whitall, D., S. Bricker, J. Ferreira, A.M. Nobre, T. Simas, and M. Silva. 2007. Assessment of eutrophication in estuaries: pressure-state-response and nitrogen source apportionment. *Environmental Management* 40:678–690.



September 2009

# **Appendix 7**

## **Terrestrial Nutrient Enrichment Case Study**

***Final***

EPA Contract Number EP-D-06-003  
Work Assignment 3-62  
Project Number 0209897.003.062

### **Prepared for**

U.S. Environmental Protection Agency  
Office of Air Quality Planning and Standards  
Research Triangle Park, NC 27709

### **Prepared by**

RTI International  
3040 Cornwallis Road  
Research Triangle Park, NC 27709-2194







## TABLE OF CONTENTS

Acronyms and Abbreviations .....	iv
Introduction.....	1
1.0 Background.....	2
1.1 Indicators, Ecological Endpoints, and Ecosystem Services.....	3
1.1.1 What Is Known .....	3
1.1.2 What Is Not Known .....	6
1.1.3 Benchmarks Selected for This Case Study .....	7
1.1.4 Ecosystem Services.....	8
1.2 Case Study Site Selection .....	9
1.2.1 National Overview of Sensitive Areas.....	9
1.2.1.1 Presence of Acidophytic Lichens.....	9
1.2.1.2 Anthropogenic Land Cover.....	9
1.2.1.3 Nitrogen-Sensitive Species Identified in Literature.....	10
1.2.1.4 Excluded Datasets .....	10
1.2.1.5 Overlay Results .....	10
1.2.2 Use of ISA Information and Rationale for Site Selection.....	12
1.3 Ecosystem Overview .....	14
1.3.1 Coastal Sage Scrub .....	14
1.3.2 Mixed Conifer Forest.....	18
1.4 Historical Trends.....	23
1.4.1 Coastal Sage Scrub .....	23
1.4.2 Mixed Conifer Forest.....	24
2.0 Approach and Methodology .....	25
2.1 Published Research .....	26
2.2 GIS Methodology.....	26
2.2.1 Overview.....	26
2.2.2 Available Data Inputs .....	26
2.2.2.1 Nitrogen Deposition.....	26
2.2.2.2 Range of Coastal Sage Scrub.....	27
2.2.2.3 Fire Threat.....	29
2.2.2.4 Changes in Coastal Sage Scrub Communities .....	29
2.2.2.5 Distribution of Invasive Species .....	29
2.2.2.6 Threatened and Endangered Species Habitat.....	29
2.2.2.7 Range of Mixed Conifer Forest .....	30
2.2.2.8 Distribution of Acid-Sensitive Lichens .....	30
3.0 Results.....	30
3.1 Literature Review Findings.....	31
3.1.1 Coastal Sage Scrub .....	31
3.1.1.1 Atmospheric Nitrogen Deposition .....	34
3.1.1.2 Nonnative Grasses .....	36
3.1.1.3 Mycorrhizae .....	36
3.1.1.4 Soil Nitrogen.....	37

3.1.2	Fire .....	38
3.1.3	Coastal Sage Scrub Model .....	39
3.1.4	Mixed Conifer Forest Ecosystems .....	40
3.1.4.1	Nitrogen and Ozone Effects .....	40
3.1.4.2	Nitrogen Effects on Lichens .....	44
3.1.4.3	Nitrogen Saturation .....	46
3.2	Results Summary .....	48
4.0	Implications for Other Systems .....	50
5.0	Uncertainty .....	55
5.1	Coastal Sage Scrub .....	55
5.2	Mixed Conifer Forest .....	56
6.0	Conclusions .....	56
7.0	References .....	57

## LIST OF FIGURES

Figure 1.1-1.	Observed effects from ambient and experimental atmospheric nitrogen deposition loads in relation to 2002 CMAQ/NADP deposition data. Citations for effect results can be found in the ISA, Table 4-4 (U.S. EPA, 2008). .....	5
Figure 1.2-1.	Areas of highest potential nutrient enrichment sensitivity. (Acidophytic lichens, tree species, and the extent of the Mojave Desert are from data obtained from the USFS. The extents of coastal sage scrub and California mixed conifer are from the California Fire and Resource Assessment Program. Grasslands are from the National Land Cover Dataset [USGS]). .....	11
Figure 1.3-1.	Range of coastal sage scrub ecosystems. ....	15
Figure 1.3-2.	Presence of three threatened and endangered species in California's coastal sage scrub ecosystem. ....	16
Figure 1.3-3.	Range of California's mixed conifer forests. ....	19
Figure 1.3-4.	Presence of two threatened and endangered species and mixed conifer forests. ....	19
Figure 1.4-1.	Change in coastal sage scrub extent from 1977 to 2002. ....	24
Figure 3.1-1.	Coastal sage scrub range and total nitrogen deposition using CMAQ 2002 modeling results and NADP monitoring data. ....	35
Figure 3.1-2.	Current fire threats to coastal sage scrub ecosystems. ....	39
Figure 3.1-3.	Model of coastal sage scrub ecosystem in relation to fire and atmospheric nitrogen deposition. ....	40
Figure 3.1-4.	Mixed conifer forest range and total atmospheric nitrogen deposition using CMAQ 2002 modeling results and NADP monitoring data. ....	42
Figure 3.1-5.	Conceptual model for increased susceptibility to wildfire in mixed conifer forests (Grulke et al., 2008). ....	44
Figure 3.1-6.	Importance of lichens as an indicator of ecosystem health (Jovan, 2008). ....	44

Figure 3.1-7. Presence of acidophyte lichens and total nitrogen deposition in the California mountain ranges using CMAQ 2002 modeling results and NADP monitoring data. ....	46
Figure 3.2-1. Illustration of the range of terrestrial ecosystem effects observed relative to atmospheric nitrogen deposition. ....	49
Figure 4.1-1. 2002 CMAQ-modeled and NADP monitoring data for deposition of total nitrogen in the western United States. ....	51
Figure 4.1-2. Benchmarks of atmospheric nitrogen deposition for several ecosystem indicators with the inclusion of the diatom changes in the Rocky Mountain lakes .....	52
Figure 4.1-3. Habitats that may experience ecological benchmarks similar to coastal sage scrub and mixed conifer forest.....	53

## LIST OF TABLES

Table 1.2-1. Potential Assessment Areas for Terrestrial Nutrient Enrichment Identified in the ISA (U.S. EPA, 2008) .....	13
Table 1.3-1. Selected Flora and Fauna Associated with the Coastal Sage Scrub Habitat .....	17
Table 1.3-2. Selected Flora and Fauna Associated with the Mixed Conifer Forest Habitat.....	20
Table 1.3-3. List of Lichen Species Present in the Sierra Nevada Range and San Bernardino Mountains (Jovan, 2008; Sigal and Nash, 1983) .....	22
Table 3.1-1. Summary of Selected Experimental Variables across Multiple Coastal Sage Scrub Study Areas <sup>a</sup> .....	32
Table 3.1-2. Coastal Sage Scrub Ecosystem Area and Nitrogen Deposition .....	36
Table 3.1-3. Research Evidence of Ecosystem Responses to Nitrogen Relevant to Coastal Sage Scrub .....	37
Table 3.1-4. Mixed Conifer Forest Ecosystem Area and Nitrogen Deposition.....	48
Table 4.1-1. Areas of Coastal Sage Scrub and Mixed Conifer Forest That Exceed Benchmark Nitrogen Deposition Levels.....	53

## **ACRONYMS AND ABBREVIATIONS**

AM	arbuscular mycorrhizae
C:N	carbon to nitrogen ratio
cm	centimeter
CMAQ	Community Multiscale Air Quality model
CO <sub>2</sub>	carbon dioxide
CSS	coastal sage scrub
FIA	Forest Inventory and Analysis National Program
FRAP	Fire and Resource Assessment Program
FWS	U.S. Fish and Wildlife Service
GAP	Gap Analysis Project
GIS	geographic information systems
HNO <sub>3</sub>	nitric acid
ISA	Integrated Science Assessment
kg	kilogram
km	kilometer
m	meter
MCF	mixed conifer forest
MEA	Millennium Ecosystem Assessment
mm	millimeter
NADP	National Atmospheric Deposition Program
NH <sub>3</sub>	ammonia gas
NH <sub>4</sub> <sup>+</sup>	ammonium
NH <sub>x</sub>	reduced nitrogen
NO	nitric oxide
NO <sub>3</sub> <sup>-</sup>	nitrate
NO <sub>x</sub>	nitrogen oxides
O <sub>3</sub>	ozone
PNV	Potential Natural Vegetation
SMB	Simple Mass Balance
TM	Thematic Mapper
µg/g	micrograms per gram
USFS	U.S. Forest Service
USGS	U.S. Geological Survey
VTM	Vegetation Type Map

## INTRODUCTION

For the last half century, landscapes in the United States have been exposed to atmospherically deposited nitrogen from anthropogenic activities. Some of the highest deposition has occurred in Southern California, where researchers have documented measurable ecological changes related to atmospheric deposition. This case study investigated the coastal sage scrub (CSS) and the mixed conifer forest (MCF) ecosystems. Research was conducted on these complex ecosystems to understand the relationships among the effects of nitrogen loads, fire frequency and intensity, and invasive plants. The breadth of spatial and temporal data needed for quantitative modeling of ecological response in the CSS and MCF ecosystems is not currently available. However, biologically meaningful ecological endpoints were identified and compared to ecological endpoints identified in the other case studies presented in the *Risk and Exposure Assessment* (Chapters 4 and 5), as well as similar ecological endpoints from ecosystems in different parts of the United States. The results in this case study report are based on geospatial analysis and published empirical research.

Evidence from the two ecosystems discussed in this case study report supports the finding that nitrogen alters the CSS and MCF ecosystems. For this analysis, the loss of the native shrubs in the CSS and the increase in nonnative annual grasses were investigated. In MCF on the slopes of the San Bernardino and Sierra Nevada Range, lichen communities associated with the forest stands and nitrogen saturation were investigated to identify the effects of nitrogen loadings. Changes in nitrogen loading may also affect the ecological services provided by the CSS and MCF ecosystems, including regulation (e.g., water, habitat), cultural and aesthetic value (e.g., recreation, natural landscape, sense of place), and provisioning (e.g., timber) (MEA, 2005). In addition, these locations have the following characteristics that make them good candidates for case studies:

- There is public interest
- Data were available to begin investigation (especially geographic information systems [GIS] datasets)
- Effects observed have implications for other ecosystems and ecosystem services
- Ecological endpoints related to nitrogen deposition can be identified

- Observed effects, such as mycorrhizal responses, increase in nonnative annual grasses, decrease in certain lichen species, and nitrate ( $\text{NO}_3^-$ ) leaching are considered by researchers to be linked to atmospheric nitrogen deposition.

Section 3.3 of the *Integrated Science Assessment (ISA) for Oxides of Nitrogen and Sulfur–Ecological Criteria (Final Report)* (ISA) (U.S. EPA, 2008) describes the ecosystems and species of concern, identifies trends in the ecosystems and the effects of these trends, and discusses research efforts that investigated the variables and driving forces that may affect the communities. The Community Multiscale Air Quality (CMAQ) 2002 modeling results and 2002 National Atmospheric Deposition Program (NADP) data were used to gain an understanding of how atmospheric deposition of nitrogen is spatially distributed. GIS data on the spatial extent of the habitat and changes in that extent, the location of fire threat (an important variable in both CSS and MCF ecosystems), and the location of species of concern were used to compare these patterns to the CMAQ/NADP data. In sum, spatial information and observed, experimental effects were used to help identify the trends in these ecosystems and describe the past and current spatial extent of the ecosystems.

The following ecological endpoints were identified for CSS:

- Loss of CSS native shrubs
- Mycorrhizal (a symbiotic association of fungi and plant roots) responses
- Nonnative annual grass biomass.

The following ecological endpoints were identified for MCF:

- Lichen community species
- $\text{NO}_3^-$  leaching.

## 1.0 BACKGROUND

Current analysis of the effects of terrestrial nutrient enrichment from atmospheric nitrogen deposition in both CSS and MCF seeks to improve scientific understanding of the interactions among nitrogen deposition, fire events, and community dynamics. The available scientific information is sufficient to identify ecological endpoints that are affected by nitrogen deposition. These ecological endpoints can be compared to the ecological endpoints identified

from modeling conducted for other case studies in the *Risk and Exposure Assessment* (Chapters 4 and 5). These ecological endpoints can also be compared to similar ecological endpoints from different ecosystems.

## **1.1 INDICATORS, ECOLOGICAL ENDPOINTS, AND ECOSYSTEM SERVICES**

### **1.1.1 What Is Known**

Determining an acceptable ambient air concentration of nitrogen oxides (NO<sub>x</sub>) for this case study required knowledge of ecosystem sensitivity to subsequent atmospheric deposition. Terrestrial nutrient enrichment research has measured ecosystems' exposure to deposition of various atmospheric nitrogen species, including nitrogen oxides, reduced nitrogen, and total nitrogen. The ISA (U.S. EPA, 2008, Section 3.3) documents current understanding of the effects of nitrogen nutrient enrichment on terrestrial ecosystems. The report concludes that there is sufficient information to suggest a causal relationship between atmospheric nitrogen deposition and biogeochemical cycling and fluxes of nitrogen in terrestrial systems. The ISA further concludes that there is a causal relation between atmospheric nitrogen deposition and changes in species richness, species composition, and biodiversity in terrestrial systems. These conclusions are based on an extensive literature review that is summarized in Table 4-4 of the ISA. The research involves both observational and experimental (e.g., nitrogen addition) projects. Alpine ecosystems, grasslands (e.g., arid and semiarid ecosystems), forests, and deserts were included. This extensive documentation was used to assist in selecting the case study areas to identify and compare ecological endpoints from different habitats.

CSS is subject to several pressures, such as land conversion, grazing, fire, and pollution, all of which have been observed to induce declines in other ecosystems (Allen et al., 1998). Research suggests that both fire and increased nitrogen can enhance the growth of nonnative grasses in established CSS ecosystems. It is hypothesized that many stands are no longer limited by nitrogen and have instead become nitrogen-saturated due to atmospheric nitrogen deposition (Allen et al., 1998; Westman, 1981a). Nitrogen availability may favor the germination and growth of nonnative grasses, which can create a dense network of shallow roots that slow the diffusion of water through soil, decrease the percolation depth of precipitation, and decrease the water storage capability of the soil and underlying bedrock (Wood et al., 2006). Establishment of

CSS species may be decreased because of decreased water and nitrogen availability at depths where more woody CSS tap roots are found (Keeler-Wolf, 1995; Wood et al., 2006).

The ISA (U.S. EPA, 2008, Section 3.3) notes that there are areas of CSS of Southern California where dry nitrogen deposition approaches 30 kilograms (kg) N/ha/yr (Bytnerowicz and Fenn, 1996). Seedlings of native shrubs and nonwoody plants in these areas of high nitrogen deposition are unable to compete with dense stands of exotic grasses, and thus are gradually replaced by grasses, particularly following disturbances, such as fire (Eliason and Allen, 1997; Yoshida and Allen 2001; Cione et al., 2002). CSS has been declining in land area and in shrub density for the past 60 years, and in many places is being replaced by nonnative annual grasses (Allen et al., 1998; Padgett and Allen, 1999). Nitrogen deposition has been suggested as a possible cause or factor in this ecosystem alteration (U.S. EPA, 2008, Section 3.3).

The ISA (U.S. EPA, 2008, Section 3.3) discusses the extensive land areas in the western United States that receive low levels of atmospheric nitrogen deposition and which are interspaced with areas of relatively higher atmospheric deposition downwind of large metropolitan centers and agricultural areas. Fenn et al. (2008) determined empirical critical loads for atmospheric nitrogen deposition in MCF, based on changes in leached  $\text{NO}_3^-$  in receiving waters and decreased fine-root biomass in Ponderosa pine (*Pinus ponderosa*), and based on changes in epiphytic lichen communities. An atmospheric nitrogen deposition of 17 kg N/ha/yr was found to be associated with  $\text{NO}_3^-$  leaching and an approximately 25% reduction in fine root biomass. The study further noted that lichens are good early indicators of atmospheric nitrogen deposition effects on other MCF species because lichens rely entirely on atmospheric nitrogen and cannot regulate uptake. From the lichen data, Fenn et al. (2008) predicted that a critical load of 3.1 kg N/ha/yr would be protective for all components of the forest ecosystem.

**Figure 1.1-1** displays a map of observed effects from ambient and experimental atmospheric nitrogen deposition loads in relation to 2002 CMAQ-modeled deposition results. The map depicts the areas where empirical effects of terrestrial nutrient enrichment have been observed and the area's proximity to elevated levels of nitrogen deposition. The ISA (U.S. EPA, 2008, Section 3.3) also identifies areas of the western United States where atmospheric nitrogen deposition effects have been reported.



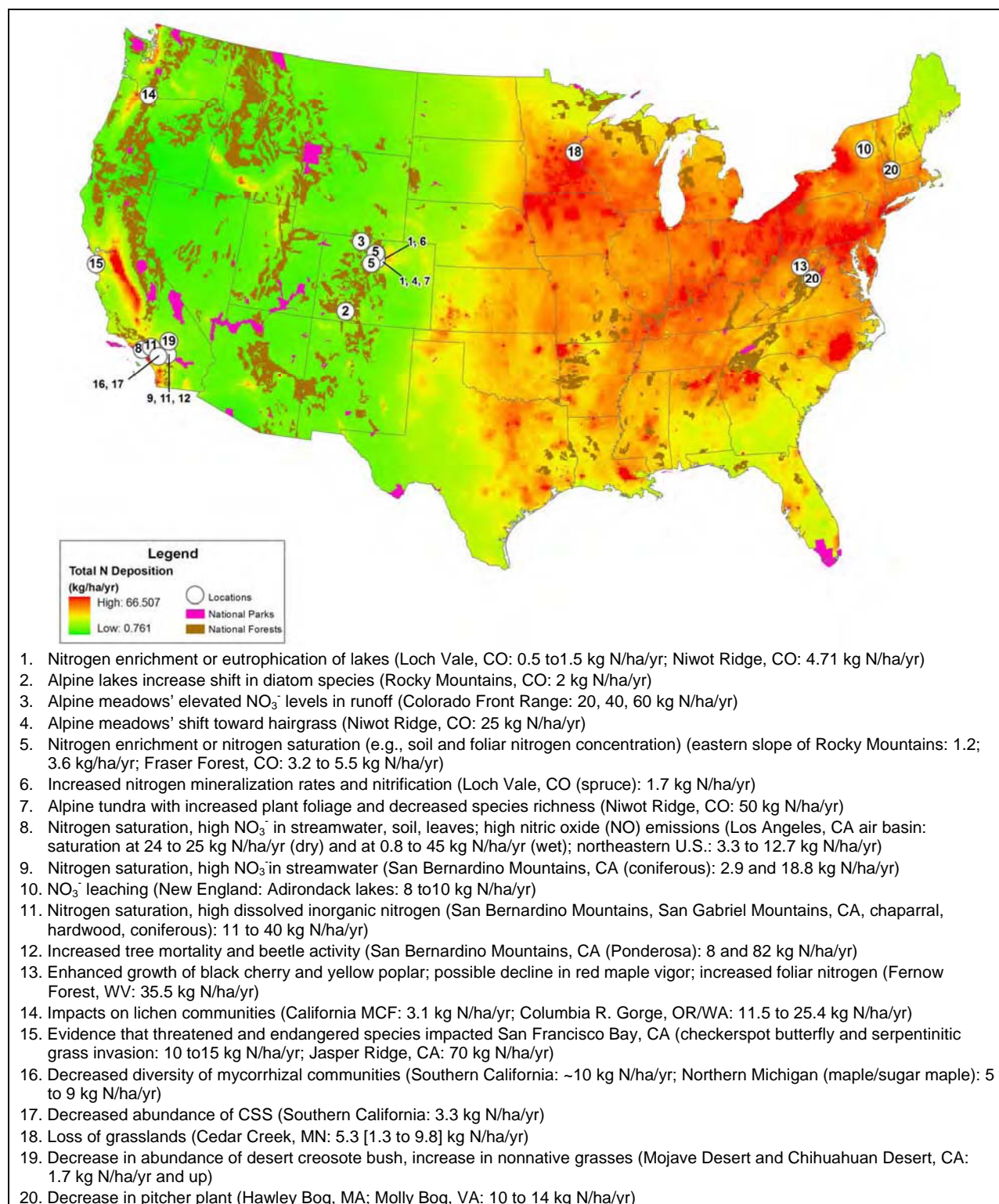


**Figure 1.1-1.** Observed effects from ambient and experimental atmospheric nitrogen deposition loads in relation to 2002 CMAQ/NADP deposition data. Citations for effect results can be found in the ISA, Table 4-4 (U.S. EPA, 2008).

### **1.1.2 What Is Not Known**

The ISA (U.S. EPA, 2008, Section 3.3) indicates that information is limited about the spatial extent and distribution of terrestrial ecosystems most sensitive to nutrient enrichment from atmospheric nitrogen deposition: “Effects are most likely to occur where areas of relatively high atmospheric nitrogen deposition intersect with nitrogen-limited plant communities. The factors that govern the sensitivity of terrestrial ecosystems to nutrient enrichment from atmospheric nitrogen deposition include the degree of nitrogen limitation, rates and form of atmospheric nitrogen deposition, elevation, species composition, length of growing season, and soil nitrogen retention capacity.” Examples of sensitive ecosystems include the following:

- Alpine tundra (low rates of primary production, short growing season, low temperature, wide moisture variation, low nutrient supply).
- Western U.S. ecosystems, such as the alpine ecosystems of the Colorado Front Range, chaparral watersheds of the Sierra Nevada Range, lichen communities in the San Bernardino Mountains and the Pacific Northwest, and CSS communities in Southern California.
- Eastern U.S. ecosystems where sensitivities are typically assessed in terms of the degree of  $\text{NO}_3^-$  leaching from soils into ground and surface waters. These ecosystems are expected to include hardwood forests, semiarid lands, and grassland ecosystems, but effects on individual plant species have not been studied well.

Major indicators for nutrient enrichment to terrestrial systems from atmospheric deposition of total reactive nitrogen, such as those described above, require measurements based on available monitoring stations for wet deposition (NADP/National Trends Network) and limited networks for dry deposition (Clean Air Status and Trends Network [CASTNet]). However, data have been limited, particularly at the spatial scale required for a more accurate analysis. Wet deposition monitoring stations can provide more information on an extensive range of nitrogen species than can dry deposition monitoring stations. In the Mediterranean systems of Southern California where rainfall is concentrated during some months of the year, dry deposition is particularly important. Individual studies measuring atmospheric nitrogen deposition to terrestrial ecosystems that involve throughfall estimates for forested ecosystems

can provide better approximations for total atmospheric nitrogen deposition levels; however, such estimates and related bioassessment data are not available for the entire country.

Finally, in the area of what is still unknown, the exact relationship between atmospheric nitrogen loadings, fire frequency and intensity, and nonnative plants, particularly in the CSS ecosystem, have not been quantified. Various conceptual models linking these factors have been developed, but an understanding of cause and effect, seasonal influences, and benchmarks remains undeveloped. These potential confounders are discussed at greater length in Section 3.

### **1.1.3 Benchmarks Selected for This Case Study**

The data limitations on atmospheric nitrogen deposition (described above), along with current data to describe the full extent and distribution of nitrogen-sensitive U.S. ecosystems, presented a barrier to designing a case study that used quantitative monitoring and modeling tools. Instead, this case study used published research results to identify meaningful ecological endpoints associated with different levels of atmospheric nitrogen deposition.

The ecological endpoints that were identified for the CSS and the MCF are included in the suite of ecological endpoints identified in the ISA (U.S. EPA, 2008, Section 3.3). There are sufficient data to confidently relate the ecological effect to a loading of atmospheric nitrogen.

For the CSS community, the following ecological benchmarks were identified:

- 3.3 kg N/ha/yr—the amount of nitrogen uptake by a vigorous stand of CSS; above this level, nitrogen may no longer be limiting
- 10 kg N/ha/yr—mycorrhizal community changes

For the MCF community, the following ecological benchmarks were identified:

- 3.1 kg N/ha/yr—shift from sensitive to tolerant lichen species
- 5.2 kg N/ha/yr—dominance of the tolerant lichen species
- 10.2 kg N/ha/yr—loss of sensitive lichen species
- 17kg N/ha/yr—leaching of  $\text{NO}_3^-$  into streams.

#### **1.1.4 Ecosystem Services**

Ecosystem services are generally defined as the benefits individuals and organizations obtain from ecosystems. In the 2005 Millennium Ecosystem Assessment (MEA), ecosystem services are classified into four main categories:

- **Provisioning**—includes products obtained from ecosystems
- **Regulating**—includes benefits obtained from the regulation of ecosystem processes
- **Cultural**—includes the nonmaterial benefits people obtain from ecosystems through spiritual enrichment, cognitive development, reflection, recreation, and aesthetic experiences
- **Supporting**—includes those services necessary for the production of all other ecosystem services (MEA, 2005).

Atmospheric nitrogen deposition affects CSS and MCF ecological processes that, in turn, are related to ecosystem services. These processes include the following:

For CSS:

- Decline in CSS habitat, shrub abundance, species of concern—cultural and regulating
- Increased abundance of nonnatives—cultural and regulating
- Increase in wildfires—cultural and regulating.

For MCF:

- Change in habitat suitability and increased tree mortality—cultural and regulating
- Decline in MCF aesthetics—cultural
- Increase in fire intensity, change in forest's nutrient cycling, other nutrients becoming limiting—regulating
- Decline in surface water quality—regulating.

Terrestrial nutrient enrichment for CSS potentially affects ecosystem services, such as biodiversity; threatened and endangered species and rare species (both national and state); landscape view; water quality; and fire hazard mitigation. Linking ecological endpoint to services involves the measurement of changes in biodiversity and abundance and distribution of

threatened and endangered species, comparison of past and present photography, and measurement of the distribution of soil moisture with depth and possible  $\text{NO}_3^-$  leaching. The relationship between fire frequency, CSS ecosystem, and property values will be investigated in the ecosystem services analysis.

The case study approach for MCF focused on ecosystem services, such as visual and recreational aesthetics provided by the CSS community and water quality. Linking ecological endpoints to services includes measurement of the density of stands, shifts in tree dominance, shifts in lichen communities, foliar nitrogen increases, and increased  $\text{NO}_3^-$  concentrations in streams due to leaching.

## **1.2 CASE STUDY SITE SELECTION**

### **1.2.1 National Overview of Sensitive Areas**

The selection of case study areas specific to terrestrial nutrient enrichment began with national GIS mapping. GIS datasets of physical, chemical, and biological properties that were indicative of potential terrestrial nutrient enrichment were considered in order to identify sensitive areas in the United States. The publicly available geospatial datasets outlined in the following paragraphs have been identified as important contributors to terrestrial nutrient enrichment and met the selection criteria.

#### ***1.2.1.1 Presence of Acidophytic Lichens***

Acidophytic lichens are known to be sensitive to increased levels of nitrogen loading. Other species are dependent upon lichens for both food and habitat. For this exercise, the list of acidophytic species from Fenn et al. (2008) was used. Data on these species were available for the years 2001 to 2006. Geospatial data were obtained from the U.S. Forest Service (USFS) Forest Inventory and Analysis National Program (FIA) (USFS, 2008a). Locations where acidophytic lichen were identified were defined as being sensitive.

#### ***1.2.1.2 Anthropogenic Land Cover***

Urban and agricultural land covers were mapped to so that they could be used to exclude areas that are not sensitive to terrestrial nutrient enrichment, such as agricultural areas and urbanized areas. This information was obtained from the U.S. Geological Survey (USGS)

*National Atlas of the United States* (USGS, 2006) and covered the continental United States at a spatial resolution of 1-km grid cells.

#### ***1.2.1.3 Nitrogen-Sensitive Species Identified in Literature***

Although there is no known nationwide species that has shown range loss because of additional nitrogen, it was possible to assemble a “patchwork quilt” of species and forest types from across the United States that are identified as sensitive in the published literature. A range was extracted from national datasets for each species or forest type where the range existed. The cumulative extent of all ranges allowed for the definition of sensitive areas in the United States.

#### ***1.2.1.4 Excluded Datasets***

The publicly available spatial datasets outlined below were considered for inclusion in the national sensitivity assessment, but were not used.

- Soil Nitrogen Content. This pre-1980 dataset was requested but not received at the time of this report’s production. The quality of data is uncertain.
- Presence of Mountains. The physiographic provinces of the United States were considered to provide leeward sides of mountains that tend to receive a greater amount of atmospheric nitrogen deposition. Continental U.S. data identified were from USGS and dated 1946. The spatial resolution was a scale of 1:7,000,000. If used, the benchmark value would have been for mountain ranges only. However, this dataset was not used because terrain is already taken into account by the CMAQ modeling.

#### ***1.2.1.5 Overlay Results***

The extraction of the areas of greatest nutrient enrichment sensitivity was constrained by the relative lack of available national datasets. Therefore, the review involved two steps within the GIS. First, the ranges of sensitive species identified in the literature were combined with a layer of acidophytic lichen distribution. Second, areas of human use (i.e., urban and agricultural land covers) were removed. The resulting map illustrates the area of highest potential sensitivity (see **Figure 1.2-1.**)

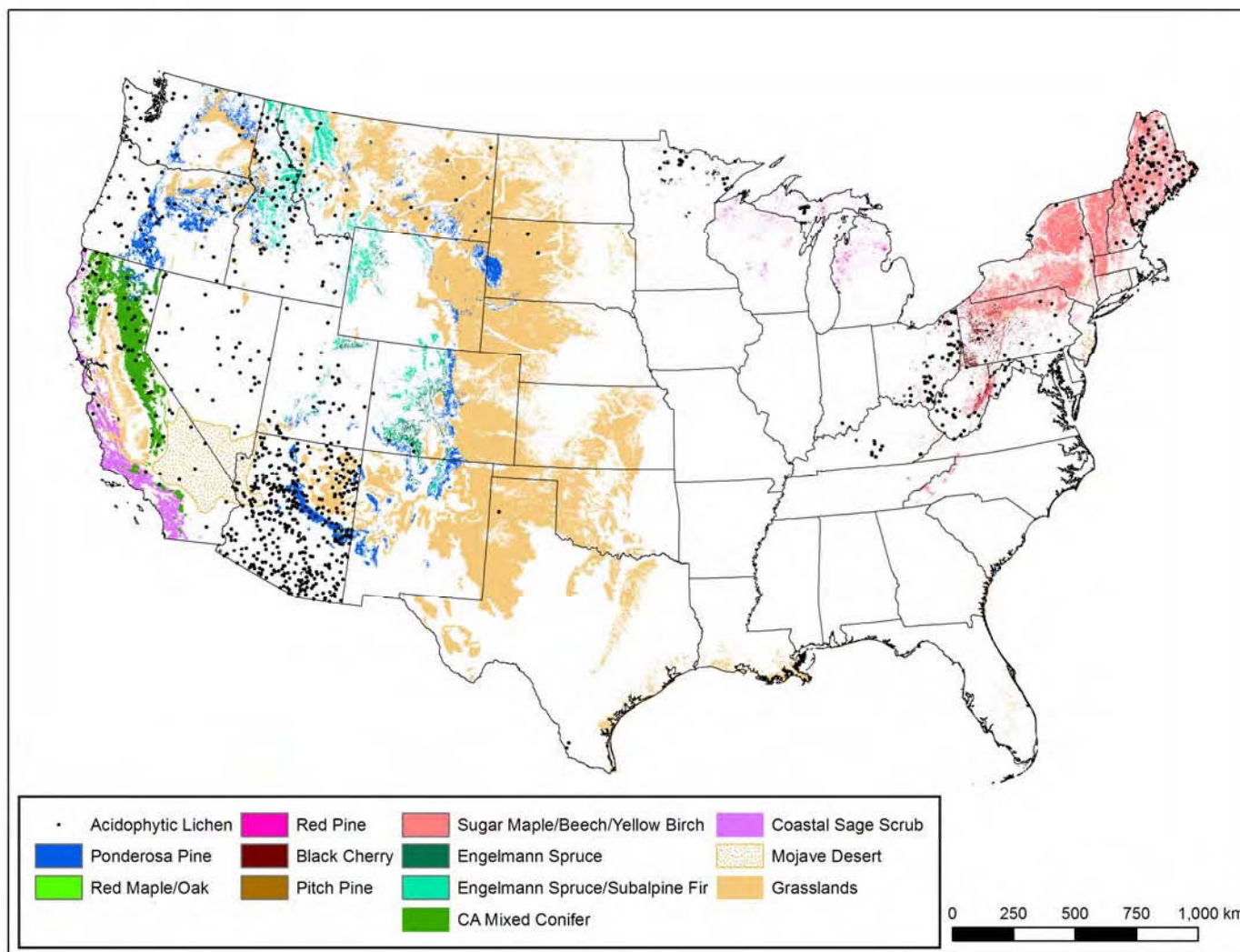


**Figure 1.2-1.** Areas of highest potential nutrient enrichment sensitivity. (Acidophytic lichens, tree species, and the extent of the Mojave Desert are from data obtained from the USFS. The extents of coastal sage scrub and California mixed conifer are from the California Fire and Resource Assessment Program. Grasslands are from the National Land Cover Dataset [USGS]).

### **1.2.2 Use of ISA Information and Rationale for Site Selection**

Potential case study areas identified in the ISA (U.S. EPA, 2008) were considered in site selection along with information gathered in the national GIS analysis. **Table 1.2-1** contains the relevant nutrient enrichment areas identified in the ISA.

After considering this information, California's CSS and MCF ecosystems were selected for this case study analysis. The following selection factors supplement those listed in the Introduction:

- Availability of atmospheric ambient and deposition data (monitored or modeled)
- Availability of digitized datasets of biotic communities; fire-prone areas; and sensitive, rare species
- Scientific results of research on nitrogen effects for the case study area
- Representation of western U.S. ecosystems potentially impacted by atmospheric nitrogen deposition
- Scalability and generalization opportunities for risk analysis results from the case studies.

California's CSS has been the subject of intensive research in the past 10 years, which has provided the data needed for a first phase of GIS analysis of the role of atmospheric nitrogen deposition in terrestrial ecosystems. California's MCF have an even longer record of study that includes investigations into the effects of atmospheric pollution, changes to forest structure, changes to the lichen communities, and measurements of nitrogen saturation. Another ecosystem that was considered but not selected for this case study was the alpine ecosystem in the Rocky Mountains. As noted in the ISA (U.S. EPA, 2008, Section 3.3), results from a number of studies indicate that nitrates may be leaching from alpine catchments, and there appear to be changes in plant communities related to the deposition of atmospheric nitrogen. The amount of data from these alpine ecosystems is more limited than that from the CSS and MCF. However, the ecological benchmarks suggested for alpine ecosystems were comparable to the benchmarks from CSS and MCF ecosystems.

In summary, CSS and MCF were selected as case study areas for the following reasons:

- The two ecosystems have significant geographic coverage and are located where urban areas interface with wilderness areas.



- Both sites are located in areas of sharp atmospheric nitrogen deposition gradients, ranging from low background levels to some of the highest deposition levels recorded in the United States.
- The two ecosystems have been researched for extended periods to understand the interactive effects of deposition, climate change, fire, and other stressors.
- The results of these research investigations for CSS and MCF result are well documented in the peer-reviewed literature.

**Table 1.2-1.** Potential Assessment Areas for Terrestrial Nutrient Enrichment Identified in the ISA (U.S. EPA, 2008)

Area	Indicator	Detailed Indicator	References in U.S. EPA, 2008	Source
Alpine and subalpine communities of the eastern slope of the Rocky Mountains, CO	Terrestrial nutrient enrichment	Biomass production; NO <sub>3</sub> <sup>-</sup> leaching; species richness	Baron et al., 1994; Baron et al., 2000; Baron, 2006; Bowman, 2000; Bowman and Steltzer, 1998; Bowman et al., 1993; Bowman et al., 1995; Bowman et al., 2006; Burns, 2004; Fenn et al., 2003a; Fisk et al., 1998; Korb and Ranker, 2001; Rueth et al., 2003; Seastedt and Vaccaro, 2001; Sherrod and Seastedt, 2001; Steltzer and Bowman, 1998; Suding et al., 2006; Williams and Tonnessen, 2000; Williams et al., 1996a; Wolfe et al., 2001	ISA, Section 3.3, 4.3, Annex A, Annex C, and Annex D
Fernow Experimental Forest near Parsons, WV	Terrestrial nutrient enrichment	Forest growth	Adams et al., 1997, 2000; DeWalle et al., 2006; Edwards and Helvey, 1991; Gilliam et al., 2006; Peterjohn, 1996	ISA, Section 3.3, 4.3, Annex A, Annex B
Bear Brook, ME	Terrestrial acidification	Sugar maple; red spruce	Elvir et al., 2003	ISA, Section 3.3, 4.3, Annex A, Annex B, Annex C
Harvard Forest, MA	Terrestrial nutrient enrichment	Forest growth—species	Magill et al., 2004; Magill, 2004	ISA, Sections 2.8, 2.10, 3.2, 3.3, 4.3, Annex B, Annex C
Southern California	Terrestrial nutrient enrichment	Forest growth—species; coastal sage scrub	Bytnerowicz and Fenn, 1996, 2003a; Takemoto et al., 2001	ISA, Section 3.2, 3.3, 3.4, 4.3, Annex B, Annex C

Area	Indicator	Detailed Indicator	References in U.S. EPA, 2008	Source
Jasper Ridge Biological Preserve, CA	Terrestrial nutrient enrichment	Grasslands	Zavaleta et al., 2003	ISA, Sections 3.3, 4.3
Loch Vale, CO	Terrestrial nutrient enrichment	Old-spruce growth	Rueth et al., 2003	ISA, Section 3.3, 4.3, Annex B
Rocky Mountain National Park, CO	Terrestrial nutrient enrichment	Tundra composition switch	Interlandi and Kilham, 1998	ISA, Section 3.3, 4.3, Annex C

**Source:** U.S. EPA, 2008.

## 1.3 ECOSYSTEM OVERVIEW

### 1.3.1 Coastal Sage Scrub

CSS consists of more than 50 aromatic shrub and subshrub species, which range from approximately 0.5 meters (m) to 2 m in height (Burger et al., 2003; Westman, 1981a). The range of CSS extends from north of San Francisco down to Baja California in the lower elevation coastal range of California (see **Figure 1.3-1**); however, the species composition may vary with location (Westman, 1981b). According to the California Natural Diversity Database, there are 22 floristic alliances of CSS (e.g., Riversidian Sage Scrub, Venturan Sage Scrub, and Diegan Sage Scrub). These alliances consist of similar species that help determine the significance, rarity, and growth patterns of California vegetation types.

CSS grows in a warm Mediterranean climate and is characterized by approximately 300 millimeters (mm) of annual rainfall falling from December through March and little or no rainfall from April through November (Egerton-Warburton and Allen, 2000; Westman, 1981b). Underlying substrate types of CSS vary greatly across the CSS stands, although many CSS floristic alliances are found on unconsolidated sand, sandstone, conglomerate, and shale (Westman, 1981b).

CSS is also known as “soft chaparral” because of its semideciduousness, drought-tolerant nature, and less-rigid leaves, respective to chaparral species (Westman, 1981b). CSS is considered a fire-adapted community; meaning that although vegetation layers may be destroyed in fires, CSS soil seed banks can withstand fire, and in some species, require fire to open the seed cases. However, many CSS species can flourish and propagate in the absence of any fire (Keeler-

Wolf, 1995). CSS has been observed to maintain a permanent cover without fire or other disturbance regimes (e.g., land conversion, grazing) for at least a century (Westman, 1981a).



**Figure 1.3-1.** Range of coastal sage scrub ecosystems.

The resprouting and competition of species post-fire is generally dependent upon fire intensity, fire frequency, and seasonal timing (Keeler-Wolf, 1995). CSS species are generally poor colonizers after a fire (Minnich and Dezzani, 1998). Annual forbs and any grass seedlings present in the post-fire soils are usually dominant in the first few growth cycles. Significant shrub growth is most likely to occur in later cycles, further disturbance notwithstanding (Keeler-Wolf, 1995).

The CSS ecosystem also supports the growth of more than 550 herbaceous annual and perennial species between and beneath the shrub canopy. Of these herbs, nearly half are endangered, sensitive, or of special status (Burger et al., 2003). Additionally, several avian,

arthropod, reptilian, amphibian, and mammalian species depend on CSS habitat for foraging, breeding, and/or residence. These include several threatened and endangered species, such as the coastal California gnatcatcher (*Poliophtila californica californica*), the Stephens' kangaroo rat (*Dipodomys stephensi*), and the Quino checkerspot butterfly (*Euphydryas editha quino*). **Figure 1.3-2** presents the range of these three species. **Table 1.3-1** presents a selected list of flora and fauna species that are associated with CSS habitat.

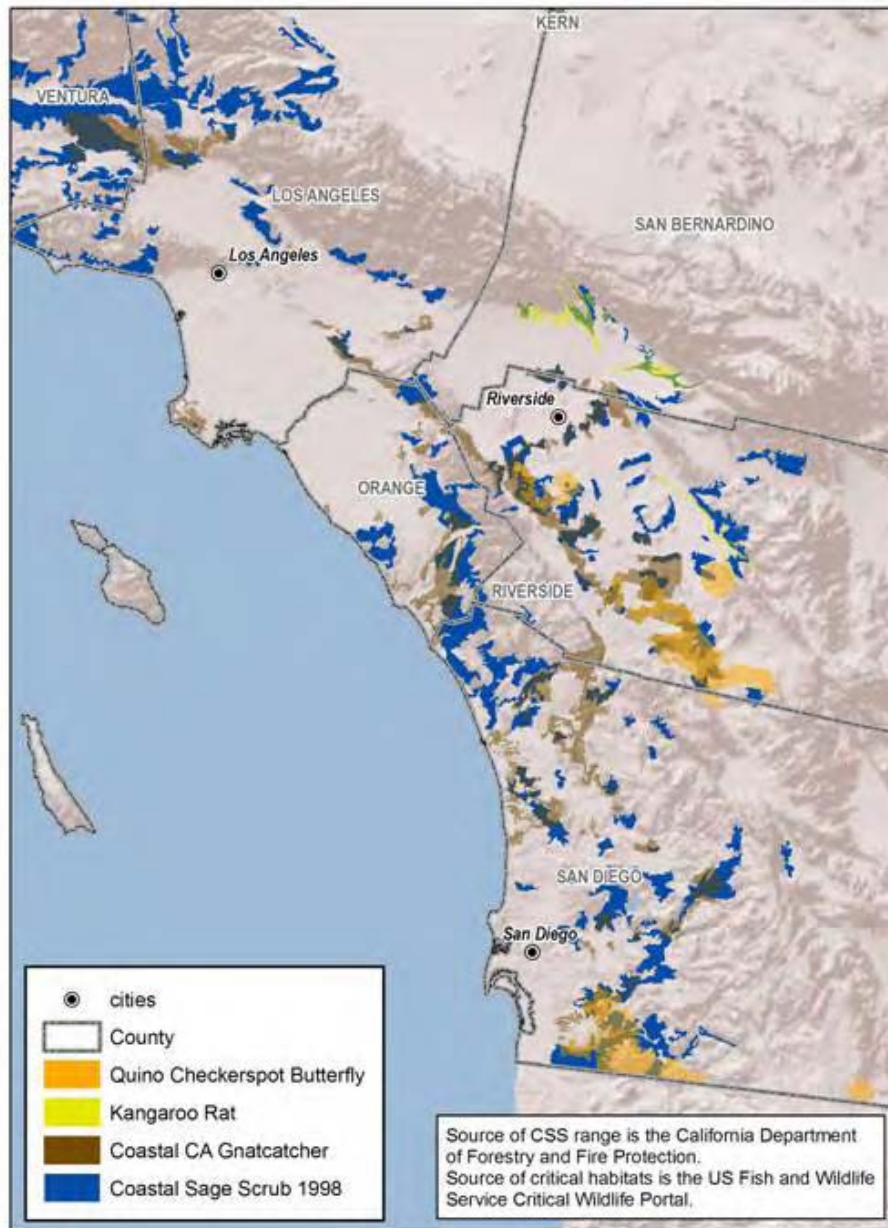


**Figure 1.3-2.** Presence of three threatened and endangered species in California's coastal sage scrub ecosystem.

**Table 1.3-1.** Selected Flora and Fauna Associated with the Coastal Sage Scrub Habitat

Scientific Name	Common Name	Life Form	Federal Listing*	State Listing*
<i>Buteo swainsoni</i>	Swainson's Hawk	Bird	Not listed	Threatened
<i>Poliophtila californica californica</i>	Coastal California Gnatcatcher	Bird	Threatened	Not listed
<i>Dipodomys merriami parvus</i>	San Bernardino Kangaroo Rat	Mammal	Endangered	Not listed
<i>Dipodomys stephensi</i>	Stephens' Kangaroo Rat	Mammal	Endangered	Threatened
<i>Bufo microscaphus californicus</i>	Arroyo Toad	Amphibian	Endangered	Not listed
<i>Euphydryas editha quino</i>	Quino Checkerspot Butterfly	Insect	Endangered	Not listed
<i>Rhaphiomidas terminatus abdominalis</i>	Delhi Sands Flower-Loving Fly	Insect	Endangered	Not listed
<i>Allium munzii</i>	Munz's Onion	Perennial Forb	Endangered	Threatened
<i>Rosa minutifolia</i>	Small-Leaved Rose	Shrub	Not listed	Endangered
<i>Deinandra conjugens</i>	Otay Tarplant	Annual Forb	Threatened	Endangered
<i>Cordylanthus orcuttianus</i>	Orcutt's Bird's Beak	Annual Forb	Not listed	Not listed
<i>Ambrosia pumila</i>	San Diego Ambrosia	Perennial Forb	Proposed Endangered	Not listed
<i>Acanthomintha ilicifolia</i>	San Diego Thorn-Mint	Annual Forb	Threatened	Endangered
<i>Campylorhynchus brunneicapillus couesi</i>	Coastal Cactus Wren	Bird	Not listed	Not listed
<i>Athene cunicularia</i>	Burrowing Owl	Bird	Not listed	Not listed
<i>Cnemidophorus hyperythrus</i>	Orange-Throated Whiptail	Reptile	Not listed	Not listed
<i>Phrynosoma coronatum blainvillei</i>	San Diego Horned Lizard	Reptile	Not listed	Not listed
<i>Masticophis lateralis euryxanthus</i>	Alameda Whipsnake	Reptile	Threatened	Threatened

\* Status listed for threatened and endangered species only. Others may be species of concern, on federal watch lists, or state special status.

The principal source of nitrogen to the CSS ecosystem is atmospheric nitrogen (e.g.,  $\text{NO}_x$ , reduced nitrogen ( $\text{NH}_x$ )). These nitrogen species are transported and deposited onto the historically nitrogen-limited CSS soil in the form of nitrates and nitric acid. In the soil, these nitrogen species are potentially available for plant uptake and nutrient cycles. The effects of increased availability of nitrogen species in the CSS ecosystem were the focus of this case study.

### **1.3.2 Mixed Conifer Forest**

MCF stand approximately 30 to 50 m tall and consist of conifer species that dominate mid-range elevations (1300 to 2800 m) of the California San Bernardino and Sierra Nevada mountain ranges. The San Bernardino Mountains lie east of the Los Angeles air basin, and the Sierra Nevada Range span the majority of the state longitudinally. **Figure 1.3-3** illustrates the range of MCF in California. MCF have historically adapted to withstand fire at low, medium, and even high intensities. As in the range of CSS, the climate is Mediterranean, where 80% of rainfall occurs from October through March (Takemoto et al., 2001).

Dominant tree species shift along a precipitation gradient. Ponderosa pine (*Pinus ponderosa*), white fir (*Abies concolor*), sugar pine (*P. lambertiana*), and incense cedar (*Calocedrus decurrens*) are the predominant species on moist windward slopes, whereas Jeffrey pine (*P. jeffreyi*) and white fir are commonly found on leeward slopes and at higher elevations in the mixed conifer elevation range. Important deciduous components of the MCF are canyon live oak (*Quercus chrysolepis*), black oak (*Quercus kelloggii*), and quaking aspen (*Populus tremuloides*). These stands support a number of shrubs, subshrubs, and annual and perennial forbs, as well as mountain meadows (Minnich, 2007). Federal-listed species, *Rana sierrae* and *Rana muscosa* (both called the mountain yellow-legged frog), and a number of state-listed species, such as the Peninsular bighorn sheep (*Ovis canadensis nelsoni*), utilize MCF habitat. The range of two of these selected species is illustrated in **Figure 1.3-4**. **Table 1.3-2** shows selected flora and fauna associated with MCF habitat.





**Figure 1.3-3.** Range of California's mixed conifer forests.

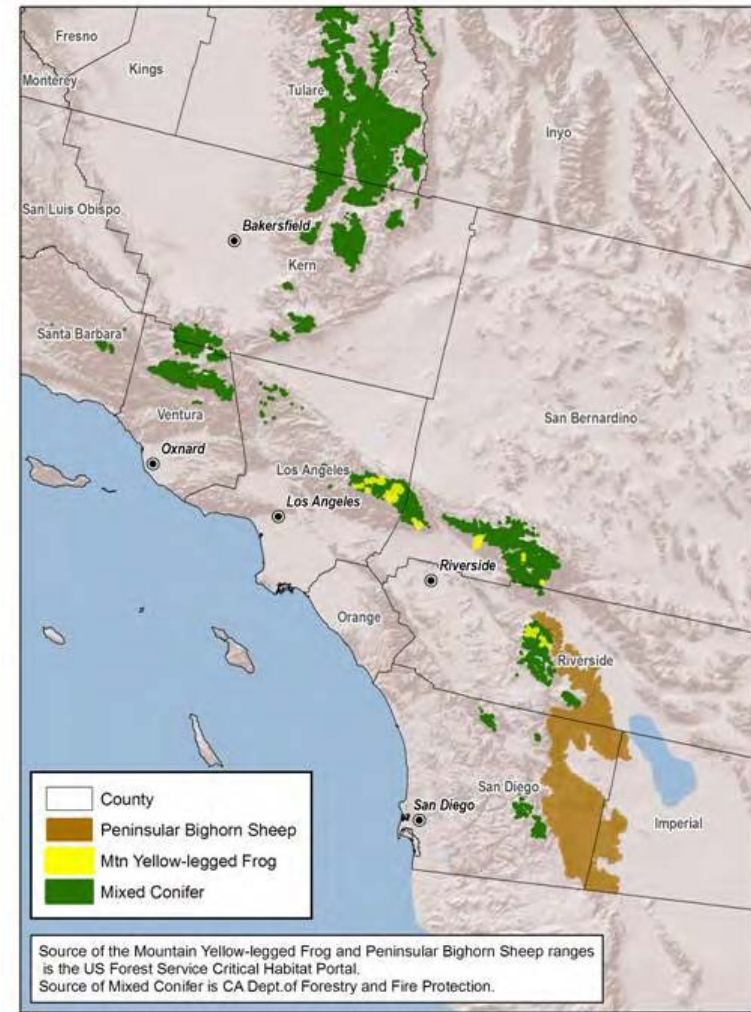


**Figure 1.3-4.** Presence of two threatened and endangered species and mixed conifer forests.

**Table 1.3-2.** Selected Flora and Fauna Associated with the Mixed Conifer Forest Habitat

Scientific Name	Common Name	Life Form	Federal Listing*	State Listing*
<i>Abies concolor</i>	White Fir	Tree	Not listed	Not listed
<i>Pinus ponderosa</i>	Ponderosa Pine	Tree	Not listed	Not listed
<i>Pinus lambertiana</i>	Sugar Pine	Tree	Not listed	Not listed
<i>Calocedrus decurrens</i>	Incense Cedar	Tree	Not listed	Not listed
<i>Rana sierrae</i>	Sierra Madre Yellow-Legged Frog	Amphibian	Endangered	Not listed
<i>Spea hammondi</i>	Western Spadefoot	Amphibian	Not listed	Not listed
<i>Rana muscosa</i>	Sierra Madre Yellow-Legged Frog	Amphibian	Endangered	Not listed
<i>Glaucomys sabrinus</i>	Northern Flying Squirrel	Mammal	Not listed	Not listed
<i>Glaucomys sabrinus californicus</i>	San Bernardino Flying Squirrel	Mammal	Not listed	Not listed
<i>Ovis canadensis nelsoni</i>	Peninsular Bighorn Sheep	Mammal	Endangered	Threatened
<i>Odocoileus hemionus</i>	Black-Tailed Deer	Mammal	Not listed	Not listed
<i>Charina umbratica</i>	Southern Rubber Boa	Reptile	Not listed	Threatened
<i>Packera bernardina</i>	San Bernardino Ragwort	Perennial Forb	Not listed	Not listed
<i>Sidalcea pedata</i>	Bird-Foot Checkerbloom	Perennial Forb	Endangered	Endangered
<i>Perideridia parishii</i> ssp. <i>parishii</i>	Parish's Yampah	Perennial Forb	Not listed	Not listed
<i>Taraxacum californicum</i>	California Dandelion	Perennial Forb	Endangered	Not listed
<i>Gilia leptantha</i> ssp. <i>leptantha</i>	San Bernardino Gilia	Shrub	Not listed	Not listed
<i>Piranga rubra</i>	Summer Tanager	Bird	Not listed	Not listed
<i>Haliaeetus leucocephalus</i>	Bald Eagle	Bird	Delisted	Endangered
<i>Strix occidentalis occidentalis</i>	California Spotted Owl	Bird	Not listed	Not listed
<i>Strix nebulosa</i>	Great Gray Owl	Bird	Not listed	Endangered

\* Status listed for Threatened and Endangered species only. Others may be species of concern, on federal watch lists, or state special status



Additionally, several lichen species are associated with the MCF habitats. Lichens are formed by a symbiotic relationship between fungus and algae or cyanobacterium. In the MCF ecosystem, lichens are generally epiphytic, living on conifers and obtaining nutrients from the atmosphere. Epiphytic lichens serve as food, habitat, and nesting material for various species in the pine stands (Fenn et al., 2008). The presence of individual species is determined by the amount of nitrogen present and the pH of the vegetation on which it grows; however, general categories for lichens have been developed according to species' sensitivity to nitrogen. These categories include nitrophytes, neutrophytes, and acidophytes (Jovan, 2008). Nitrophytes are generally associated with ammonia and high pH environments. Neutrophytes tolerate increased pH and ammonia, but exhibit slower growth patterns than nitrophytes when exposed to these conditions. Acidophytes are sensitive to nitrogen species and deteriorate or die after relatively small increments of exposure to nitrogen species (Fenn et al., 2008). **Table 1.3-3** presents a list of lichen species, classified by nitrogen sensitivity, that have been observed in the San Bernardino Mountains and Sierra Nevada Range.

**Table 1.3-3.** List of Lichen Species Present in the Sierra Nevada Range and San Bernardino Mountains (Jovan, 2008; Sigal and Nash, 1983)

Nitrophytes	Potential Acidophytes	Potential Neutrophytes	Unknown
<i>Candelaria concolor</i>	<i>Bryoria fremontii</i>	<i>Melanelia elegantula</i>	<i>Ahtiana sphaerosporella</i>
<i>Flavopunctelia flaventiorb</i>	<i>Cetraria canadensis</i>	<i>Melanelia exasperatula</i>	<i>Alectoria sarmentosa</i>
<i>Phaeophyscia orbicularis</i>	<i>Cetraria chlorophylla</i>	<i>Melanelia glabra</i>	<i>Collema furfuraceum</i>
<i>Physcia adscendens</i>	<i>Cetraria merrillii</i>	<i>Melanelia subargentifera</i>	<i>Esslingeriana idahoensis</i>
<i>Physcia aipolia</i>	<i>Cetraria orbata</i>	<i>Melanelia subelegantula</i>	<i>Leptogium lichenoides</i>
<i>Physcia dimidiata</i>	<i>Cetraria pallidula</i>	<i>Melanelia subolivacea</i>	<i>Letharia columbiana</i>
<i>Physcia stellaris</i>	<i>Cetraria platyphylla</i>	<i>Parmelia hygrophilab</i>	<i>Letharia vulpina</i>
<i>Physcia tenella</i>	<i>Evernia prunastri</i>	<i>Parmelia sulcata</i>	<i>Nodobryoria abbreviata</i>
<i>Physconia enteroxantha</i>	<i>Hypogymnia enteromorpha</i>	<i>Ramalina subleptocarphab</i>	<i>Nodobryoria oregana</i>
<i>Physconia perisidiosa</i>	<i>Hypogymnia imshaugii</i>	—	<i>Parmelina quercina</i>
<i>Xanthomendoza fallax</i>	<i>Hypogymnia occidentalis</i>	—	<i>Parmelina elegantula</i>
<i>Xanthomendoza fulva</i>	<i>Parmeliopsis ambigua</i>	—	<i>Physcia biziana</i>
<i>Xanthomendoza hasseana</i>	<i>Platismatia glauca</i>	—	<i>Physconia americana</i>
<i>Xanthomendoza oregano</i>	<i>Usnea filipendula</i>	—	<i>Physconia isidiigera</i>
<i>Xanthoria candelaria</i>	—	—	—
<i>Xanthoria polycarpa</i>	—	—	—

## **1.4 HISTORICAL TRENDS**

### **1.4.1 Coastal Sage Scrub**

The CSS ecosystem is a unique system that has experienced a significant decline in coverage since vegetation types in Southern California were inventoried in 1929. Subsequently, this community was designated for special status in California (CA DFG, 1993). This decline is due to urban encroachment and sprawl, increased fire frequencies, and pollution (Minnich and Dezzani, 1998). CSS is decreasing at a higher rate than habitat destruction alone would indicate (Allen et al., 1998; Fenn et al., 2003; Minnich and Dezzani, 1998).

Nonnative grasses were introduced to California by explorer expeditions and Franciscan missionaries arriving in the region prior to documentation of indigenous vegetation. However, accounts of herbaceous vegetation in the coastal range exist from the late 1700s and throughout the 1800s (Minnich and Dezzani, 1998). CSS was first scientifically inventoried during the California Forest and Range Experiment Station Vegetation Type Map (VTM) Survey, beginning in 1929. Recently, 54 of the VTM sites in Southern California that were dominated by CSS cover in the 1930s were resampled (Talluto and Suding, 2008). Since the 1930s, CSS declined 49% and was mainly replaced by nonnative annual grasses (Talluto and Suding, 2008). **Figure 1.4-1** illustrates the decline in CSS from 1977 to 2002.

Based on changes in CSS cover from VTM data since the early 1930s, it is estimated that approximately 18% of the extent of Riverside County CSS had been completely converted to nonnative grasses, and an additional 42% of the cover had nonnative grasses intermixed with CSS. Therefore, only 40% of the original extent of CSS in Riverside County remained intact and contiguous. The 2005 resampling of part of Riverside and Orange counties indicated that 15% of the remaining CSS had not been invaded by annual grasses (Talluto and Suding, 2008). Across the entire CSS range, Westman (1981a) estimated that only 10% to 15% of the historical CSS extent remained in the late 1970s. This estimate is based upon the fraction of potential CSS land cover (in the absence of pressures) in which CSS vegetation was actually observed at the time of the study. The potential CSS land cover estimates may also be supported by the broad range in which specimens of the Quino checkerspot butterfly have historically been observed and collected (Mattoni et al., 1997). Therefore, the remaining extent of CSS is most likely 10% to 82% of the historical CSS coverage, depending on the development pressures and the spread of

nonnative grasses in each stand. Additionally, these nonnative grasses are less diverse and are not likely to support the majority of the sensitive, threatened, and endangered species that currently rely on CSS (Allen et al., 2005).

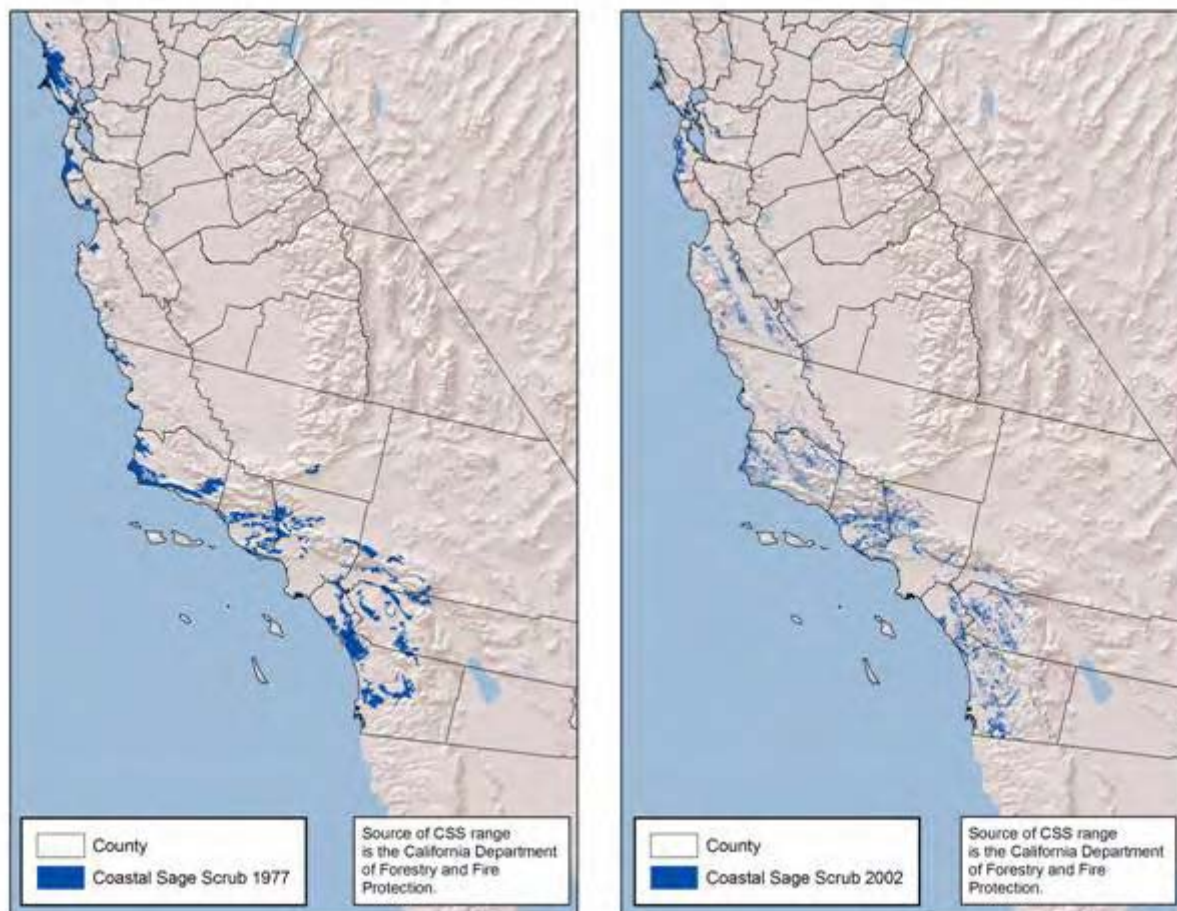


**Figure 1.4-1.** Change in coastal sage scrub extent from 1977 to 2002.

### 1.4.2 Mixed Conifer Forest

The major trends observed in MCF are “densification” and increased litter accumulation. Densification occurs when aboveground biomass is stimulated, resulting in increased numbers of needles, decreased average tree age, decreased overall trunk size, and increased branches (Gulke et al 2008; Minnich et al., 1995; Takemoto et al., 2001). In a retrospective comparison of MCF stands in the San Bernardino Mountains from 1932 to 1992, Minnich et al., (1995) noted significant shifts in age distribution, stand density, and branch density. Tree density increased approximately 77% according to the VTM surveys, and there were 3 to 10 times the number of trees in the younger age brackets when compared to conifer populations 60 years earlier.

Additionally, a 79% increase in the average number of tree branches was reported in the San Bernardino conifer forests. Studies have indicated that increasing stand densities are also occurring within the Sierra Nevada Range (Minnich et al., 1995).

Increased litter on the forest floor has also been observed across the conifer ecosystems, particularly in the MCF stands in the San Bernardino Mountains. These MCF stands have been observed to shed needles approximately six times faster than more remote northern Sierra Nevada Range conifer stands (Takemoto et al., 2001). Additionally, litterfall depths up to 15 centimeters (cm) have been noted in MCF stands near Camp Paivika in the eastern San Bernardino Mountains (Grulke et al., 2008).

Across the San Bernardino Mountains, a tree community composition shift was also noted. In MCF stands where Ponderosa pine has been historically dominant, trees in the youngest age bracket are now predominantly white fir and incense cedar. Additional research is needed to determine if a shift in community composition is also occurring in the Sierra Nevada Range MCF (Minnich et al., 1995). Although research on understory communities revealed no clear trends with atmospheric nitrogen deposition and ozone (O<sub>3</sub>), it was noted that native diversity had declined in those areas receiving the highest loads of atmospheric nitrogen (Allen et al., 2007).

Lichen communities associated with the MCF habitat have also been dramatically altered (Fenn et al., 2003, 2008; Sigal and Nash, 1983). Of the 16 lichen species reported to be associated with the San Bernardino Mountains MCF in the early part of the 20th century, only 8 species were found 60 years later. Additionally, deterioration was observed on some of the lichens, particularly in the areas with the highest levels of air pollution (Sigal and Nash, 1983). Lichens are significant members of the MCF community. They serve as forage for wildlife, and changes in the lichen community are considered by some to be a warning signal for deteriorating conditions in the rest of the forest.

## **2.0 APPROACH AND METHODOLOGY**

Using the approach and methodology described below, a number of significant ecological endpoints have been identified. These results come from empirical results and from spatial databases. Dose/response relationships beyond benchmark values were investigated, but these have not yet been well quantified. Nitrogen deposition data was available at a 12-km resolution,

and many of the ecosystems, especially CSS, are fragmented into smaller areas. The analysis is, therefore, somewhat limited by the discrepancy between resolution of the nitrogen deposition data and the distribution of habitats, as well as by the specific areas where ecological processes were measured. Further, some models have been tested, but with limited results. For example, the steady-state simple mass-balance model (UNECE, 2004) still has many unresolved uncertainties. Uncertainty exists in establishing the linkage between soil and biological impacts and the ability to account for forest management and wildfires (Fenn et al., 2008). The DayCent biogeochemical model is not a watershed-scale model and may not represent  $\text{NO}_3^-$  leaching accurately. Although, application of DayCent yielded results more comparable to empirically based findings than the steady-state model (Fenn et al., 2008).

For the above reasons, empirical data, in tandem with GIS analysis, was deemed more suitable to develop potential correlations between atmospheric nitrogen deposition and ecological endpoints.

## **2.1 PUBLISHED RESEARCH**

The ISA (U.S. EPA 2008, Sections 3.3, 4.3) was used as the basis for identifying the published scientific literature on CSS and MCF ecosystems.

## **2.2 GIS METHODOLOGY**

### **2.2.1 Overview**

For both the CSS and MCF ecosystems, spatially distributed data are available. Some of the variables that are known to influence terrestrial nutrient enrichment and have been cited in the literature are available as either state-level or national-level datasets. It is important that spatial data are temporally and spatially compatible and have well-documented metadata. It is also desirable that they possess the ability to be scaled-up for a national characterization.

### **2.2.2 Available Data Inputs**

#### **2.2.2.1 Nitrogen Deposition**

Wet nitrogen deposition in the forms of  $\text{NO}_3^-$  and ammonium ( $\text{NH}_4^+$ ) are available nationally from the NADP. This national network of 321 sampling stations is the best wet

monitored data available. Scientists at the NADP have created continuous surfaces of deposition values by using interpolation algorithms to estimate values between measurements at known locations. Dry nitrogen deposition can be estimated using the output from the CMAQ 2002 modeling system. This model produced estimates of many nitrogen species aggregated to 12-kilometer (km) squares. Although these data are fairly coarse spatially, they are the best that are currently available.

#### ***2.2.2.2 Range of Coastal Sage Scrub***

Several publicly available spatial vegetation datasets were examined for this analysis. They range in dates from 1945 to 2002 and are compiled from a combination of field data and remotely-sensed imagery.

The Wieslander VTM (USFS, 2008b) collection is a dataset published in 1945 that brought together data recorded on photos, species inventories, plots maps, and vegetation maps. This dataset was obtained from the California Spatial Information Library at the University of California, Davis. It divided the entire state of California into polygons that were attributed with 23 different vegetation types (i.e., communities) such as “coastal sagebrush” or “chaparral.” Individual species were not recorded.

Another vegetation layer named CALVEG (California Vegetation) was created in 1977 from LANDSAT imagery that was used to create 1:1,000,000 scale maps. This dataset is available from the California Department of Forestry and Fire Protection's Fire and Resource Assessment Program (FRAP) Web site (California Department of Forestry and Fire Protection, 2007a). This dataset contains land cover/land use polygons for California digitized from the 1:1,000,000 scale maps. The minimum mapping unit is approximately 400 acres, and the data contains vegetation attributes for series-level species groups only.

A land cover change dataset is also available from the FRAP Web site that uses Thematic Mapper (TM) data from 1993 and 1997 to determine areas of change (California Department of Forestry and Fire Protection, 2007b). This dataset also contains information on the cause of the change. The spatial resolution of this dataset is 30-meter pixels. These data do not contain species-level data; these contain only community-level data.

California Gap Analysis Project (GAP) data is available from the University of California, Santa Barbara Biogeography Lab (Davis et al., 1998). It contains vegetation attributes

for landscape scale map units, including canopy dominant species, canopy density, presence of regional endemic species, and inclusion of wetland habitats. These data were published in 1998 and used a variety of sources including TM data, aerial photography, Wieslander VTM data, and field maps.

The most recent land cover data for the state of California is also available from the FRAP website. It was published in 2002 and was created by compiling the best available land cover data into a single data layer. This agency classified California's vegetation into 59 different categories, including CSS, at a spatial resolution of 100 m. Decision rules were developed that controlled which layers were given priority in areas of overlap. Cross-walks were used to compile the various sources into the common California Wildlife Habitat Relationships system classification. No species specific data are available.

One of the central analytical tasks for this case study was to quantify the amount of CSS and MCF extent loss and to see if loss corresponded spatially to areas of high nitrogen deposition, fire threat, or both. The land cover change layer created by the California Department of Forestry and Fire Protection was used for this case study analysis. While the temporal difference for this layer depicting land cover change was fairly small (i.e., 5 years), the two datasets used to create the change layer were fully compatible, and the results were verified by field confirmation.

The feasibility of using the 1945 VTM, the 1977 CALVEG, the 1998 GAP, and the 2002 FRAP land cover data to determine changes in the extent of CSS and MCF ecosystems was evaluated. In each case, the data sources, spatial resolution, and classification schemes were different enough to prevent any meaningful measurement of change in these communities.

In addition to publicly available datasets, research datasets were obtained and plotted. Field data were obtained directly from Talluto and Suding (2008). While these data provided very detailed measurements of species distribution and percentage ground cover for their study areas, they were not sufficiently spatially dispersed across the CSS range, nor were they compatible with the very spatially coarse (i.e., 12-km grid size) CMAQ-modeled nitrogen deposition data.

Additionally, The Kuchler Potential Natural Vegetation (PNV) Groups (Kuchler, 1988) data layer that was created to show "climax" vegetation was not used because the intent of this case study was to quantify known changes to the extent of CSS. The PNV data illustrates where



the vegetation might potentially be found without disturbance or climate change. PNV is an expression of environmental factors, such as topography, soils, and climate across an area.

#### ***2.2.2.3 Fire Threat***

The California Department of Forestry and Fire Protection's FRAP also compiles data about fire threat. These data consider fire rotation (i.e., how frequently fire occurs) and potential fire behavior, which take into account topography and potential vegetative fuels. Fire threat is classified into four unique categories that range from moderate to extreme.

#### ***2.2.2.4 Changes in Coastal Sage Scrub Communities***

Although spatial datasets mapping CSS communities exist for 1945, 1977, 1998, and 2002, none are compatible enough to calculate meaningful change (e.g., the methods used to ascertain CSS extent and define ecosystems were not consistent across datasets). Therefore, a spatial dataset published by the California Department of Forestry and Fire Protection was chosen. This dataset documented change to CSS and other ecosystems between 1993 and 1997.

#### ***2.2.2.5 Distribution of Invasive Species***

Two data sources for invasive species were found for California. The first is the PLANTS program, which is part of the U.S. Department of Agriculture (USDA) (USDA, 2009; <http://plants.usda.gov/index.html>). This resource posts maps that indicate whether a species is present or not in a given county, but not the distribution of that species within the county. The second is the California Invasive Plant Council (2008), ([http://www.cal-ipc.org/ip/mapping/statewide\\_maps/index.php](http://www.cal-ipc.org/ip/mapping/statewide_maps/index.php)), which lists the relative abundance by county of a select number of species.

#### ***2.2.2.6 Threatened and Endangered Species Habitat***

The U.S. Fish and Wildlife Service (FWS) publishes critical habitat range information for threatened and endangered species by state, county, and species through the Critical Habitat Portal (<http://crithab.fws.gov/>) (U.S. FWS, 2008). For example, the Critical Habitat Portal locates 16 species for Riverside County, 5 of which are associated with CSS habitat.

#### **2.2.2.7 Range of Mixed Conifer Forest**

The most recent (2002) land cover dataset from the California Department of Forestry and Fire Protection's FRAP Web site was used to extract the range of MCF. Research data were also obtained from a series of sample plot locations documented in Fenn et al. (2008). The locations of the field sites were listed as latitude and longitude coordinates, which were converted into a GIS layer with atmospheric nitrogen deposition as an attribute.

#### **2.2.2.8 Distribution of Acid-Sensitive Lichens**

- The USFS FIA datasets were the source of lichen distributions.

### **3.0 RESULTS**

Effects of elevated atmospheric nitrogen deposition on the CSS and MCF ecosystems are the result of increased long-term chronic, rather than short-term pulsed, nitrogen deposition. It is difficult to quantify effects in both ecosystems because of confounding stressors, such as fire and O<sub>3</sub>. The literature available on long-term research and application of robust models on these ecosystems is extremely limited.

The CSS analysis relies upon peer-reviewed literature and spatial analyses to derive major conclusions regarding the effects of nitrogen. Spatial analyses were used to determine the changes in the extent of CSS ecosystems and their associated habitat, as well as to investigate the effects of nitrogen and fire, another driving component in the alteration of the CSS ecosystem. The reviewed literature includes greenhouse experiments, field observations, and field manipulation experiments that document the observed and measured effects of nitrogen.

The MCF analysis also contains a summary of the peer-review literature; however, this case study focused on the empirical loading benchmarks derived from an analysis by Fenn et al. (2008), which employed observational data and the Simple Mass Balance (SMB) model and the DayCent simulation model to estimate critical loads. However, there are identified limitations to both models (e.g., SMB does not account for the effects of prescribed burns or wildfires on nutrient uptake, and DayCent is not a watershed-scale model, and thus, does not accurately represent NO<sub>3</sub><sup>-</sup> concentrations in surface and groundwater). Fenn et al. (2008) conclude that the empirical approach is the most reliable source of information.

### **3.1 LITERATURE REVIEW FINDINGS**

#### **3.1.1 Coastal Sage Scrub**

CSS is subject to several pressures, such as land conversion, grazing, fire, and pollution, all of which have been observed to induce declines in other ecosystems (Allen et al., 1998). At one extreme, development pressure (i.e., the conversion of CSS to residential and commercial land uses) will simply eliminate acres of CSS. Other pressures will come into play in modifying the remaining habitat. Research suggests that both fire and increased atmospheric nitrogen deposition can enhance the growth of nonnative grasses in established CSS ecosystems. Additionally, CSS declines have been observed when fire frequency is held constant and/or nitrogen is held constant, suggesting that both fire and nitrogen play a role in CSS decline when direct destructive factors are not an imminent threat. **Table 3.1-1** contains a summary of selected experimental variables across multiple CSS study areas.

**Table 3.1-1.** Summary of Selected Experimental Variables across Multiple Coastal Sage Scrub Study Areas<sup>a</sup>

Study Locations	Soil Nitrogen	Atmospheric Nitrogen	Vegetation Change	Mycorrhizae Change	Fire Cycle	Author
Riverside-Perris Plain <sup>b</sup>	x	x	x			Allen et al., 1998
Santa Margarita Ecological Reserve			x			Burger et al., 2003
Santa Monica Mountains	x		x			Carrington and Keeley, 1999
Orange County <sup>b</sup>			x			Diffendorfer et al., 2007
Rancho Jamul Ecological Reserve			x			
Voorhis Ecological Reserve			x			Drus, 2004
Riverside-Perris Plain <sup>b</sup>	x			x		Egerton-Warburton and Allen, 2000
Sedgwick Ranch Natural Reserve	x		x			Fierer and Gabet, 2002
Southern California fuel breaks <sup>b</sup>			x		x	Merriam et al., 2006
Critical review <sup>b</sup>			x		x	Keeley, 2001
Southern California burn sites <sup>b</sup>			x		x	Keeley et al., 2005
Riverside-Perris Plain <sup>b</sup>			x		x	Minnich and Dezanni, 1998
Greenhouse experiment	x					Padgett et al., 1999
Riverside-Perris Plain <sup>b</sup>	x	x				Padgett and Allen, 1999
University of California–Riverside Agricultural Research Station			x			Padgett et al., 2000
Riverside-Perris Plain <sup>b</sup>	x			x		Siguenza et al., 2006

Study Locations	Soil Nitrogen	Atmospheric Nitrogen	Vegetation Change	Mycorrhizae Change	Fire Cycle	Author
Riverside-Perris Plain <sup>b</sup>	x			x		Sirulnik et al., 2007a
Lake Skinner	x					Sirulnik et al., 2007b
Riverside-Perris Plain <sup>b</sup>	x					Vourlitis et al., 2007
67 sites across CSS range <sup>b</sup>			x			Westman, 1979, 1981a,b
Riverside-Perris Plain <sup>b</sup>	x					Wood et al., 2006
Lake Skinner Western Riverside County Multi- Species Reserve			x	x		Yoshida and Allen, 2001
Greenhouse experiment			x	x		

<sup>a</sup> Empty cells indicate not studies identified.

<sup>b</sup> Multiple data sites within the study location.

### **3.1.1.1 Atmospheric Nitrogen Deposition**

Increased atmospheric nitrogen deposition has been observed to alter vegetation types when nitrogen is a limiting nutrient to growth. This has been observed in alpine plant communities in the Colorado Front Range, as well as in lichen communities in the western Sierra Nevada region (Fenn et al., 2003, 2008); however, in the case of CSS, it is hypothesized that many stands are no longer limited by nitrogen and have instead become nitrogen-saturated due to atmospheric nitrogen deposition (Allen et al., 1998; Westman, 1981a). This is supported by the positive correlation between atmospheric nitrogen and soil nitrogen, increased long-term mortality of CSS shrubs, and increased nitrogen-cycling rates in soil and litter and soil fertility (Allen et al., 1998; Padgett et al., 1999; Sirulnik et al., 2007a; Vourlitis et al., 2007). **Figure 3.1-1** illustrates the levels of atmospheric nitrogen deposition on CSS ecosystems using 2002 CMAQ/NADP data.

Wood et al. (2006) investigated the amount of nitrogen used by healthy and degraded CSS ecosystems. In healthy stands, the authors estimated that 3.3 kg N/ha/yr was used for CSS plant growth (Wood et al., 2006). It is assumed that 3.3 kg N/ha/yr is near the point where nitrogen is no longer limiting in CSS. Therefore, this amount can be considered an ecological benchmark for CSS. **Figure 3.1-1** displays the spatial extent of CSS where nitrogen deposition is above the ecological benchmark of 3.3 kg N/ha/yr. As shown in **Figure 3.1-1** and **Table 3.1-2**, almost all of CSS receive >3.3 kg N/ha/yr of nitrogen through atmospheric deposition. Note that CSS is observed in areas receiving >3.3 kg N/ha/yr. This distribution may result from time lags (i.e., years may be required for the CSS ecosystem to completely disappear), or it may indicate that 3.3 kg nitrogen, although ecologically meaningful, may not be the benchmark value.

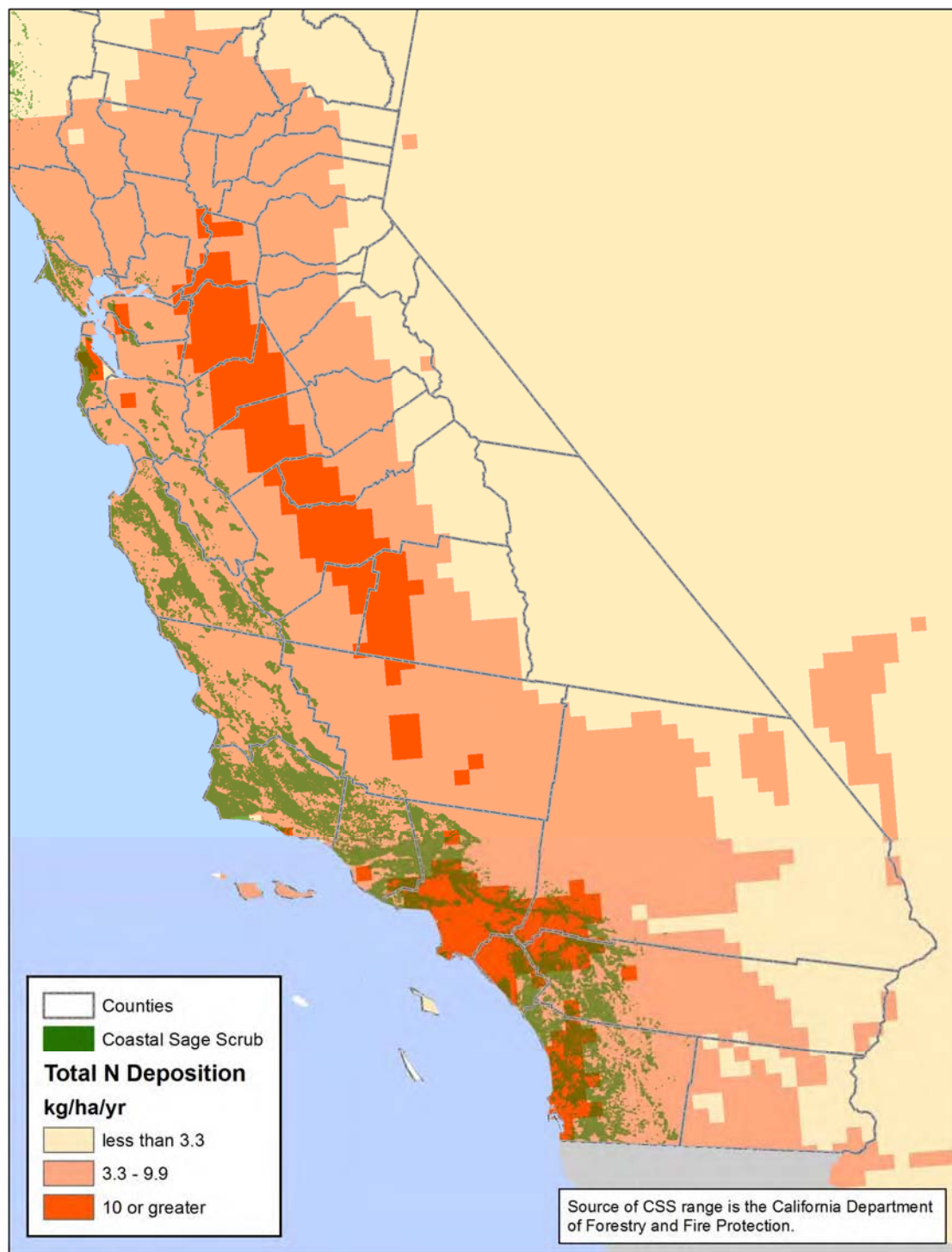


**Figure 3.1-1.** Coastal sage scrub range and total nitrogen deposition using CMAQ 2002 modeling results and NADP monitoring data.

**Table 3.1-2.** Coastal Sage Scrub Ecosystem Area and Nitrogen Deposition

<b>N Deposition (kg/ha/yr)</b>	<b>Area (hectares)</b>	<b>Percent of CSS Area, %</b>
≥3.3	654,048	93.51
≥10	138,019	19.73

### 3.1.1.2 *Nonnative Grasses*

The ecological effects of increased nitrogen are most easily explained by considering the seasonal stages of a semiarid Mediterranean ecosystem. In the rainy, winter season, deposited surface nitrogen is transported deeper into the soil and is rapidly mineralized by microbes, thus making it available for plants. Faster nitrogen availability may favor the germination and growth of nitrophylous colonizers, more specifically nonnative grasses (e.g., *Bromus madritensis*, *Avena fatua*, and *Hirschfeldia incana*). This earlier flourishing of grasses can create a dense network of shallow roots, which slows the diffusion of water through soil, decreases the percolation depth of precipitation, and decreases the amount of water for soil and groundwater recharge (Wood et al., 2006). Growth of CSS species, such as *Artemisia californica*, *Eriogonum fasciculatum*, and *Encelia farinose*, may be decreased because of decreased water and nitrogen availability at the deeper soil layers where more woody CSS tap roots are found (Keeler-Wolf, 1995; Wood et al., 2006). Furthermore, an increased percentage of shrub species is established during wet years, suggesting that percolation of nutrient-carrying water may be limited in years with average or below average precipitation (Keeley et al., 2005).

### 3.1.1.3 *Mycorrhizae*

Elevated nitrogen may also play a role in altering the nutrient uptake of CSS plants by decreasing the species richness and abundance of mutualistic fungal communities, such as arbuscular mycorrhizae (AM) (Egerton-Warburton and Allen, 2000; Siguenza et al., 2006). Although both CSS and nonnative grass species have AM and other mycorrhizal associations, which increase the surface area and capacity for nutrient uptake, CSS is predominantly colonized by a coarse AM species, and nonnative grasses are more likely mutualistic with finer AM species. In the presence of elevated nitrogen, coarse AM colonizations were depressed in number and volume. Egerton-Warburton and Allen (2000) documented shifts in AM species as well as declines in spore abundance and colonization at approximately 10 kg N/ha/yr. In areas with the highest levels of soil nitrogen tested (e.g., 57 micrograms per gram (µg/g) average annual soil



nitrogen present in Jurupa Hills, Riverside County), a shift in the timing of AM growth was also observed. Therefore, it is suggested that these diminished mutualistic associations may contribute to a decline in the overall health of CSS via a loss in nutrient uptake capacity and may represent an ecological endpoint for the CSS ecosystem. **Figure 3.1-1** displays the levels of atmospheric nitrogen deposition on CSS ecosystems above the ecological benchmark of 10 kg N/ha/yr using 2002 CMAQ/NADP data. The 12-km resolution CMAQ/NADP data indicate that CSS within the Los Angeles and San Diego airsheds are likely to experience the noted effects at the 10 kg N/ha/yr ecological benchmark.

#### 3.1.1.4 Soil Nitrogen

In a greenhouse fertilization experiment, soil nitrogen levels of 50 µg/g ammonium NO<sub>3</sub><sup>-</sup> had a 100% mortality rate after 9 months of continuous growth. The plants began to senesce at approximately 6 months, whereas all lower-exposure individuals were still healthy and remained healthy for more than 1 year (Allen et al., 1998). In the field, seasonal changes do not allow for 12 months of uninterrupted growth; therefore, the increased mortality shown in this study may be realized over much longer periods of time *in situ*. Additionally, studies have suggested that soil nitrogen may now be increasing because of soil fertility in conjunction with atmospheric deposition, so that the soil itself becomes an intrinsic source (Padgett et al., 1999). In combination with decreased establishment and the capacity for nutrient uptake, these responses to elevated nitrogen levels may represent a detrimental and long-term pressure on CSS at varying levels of nitrogen additions. **Table 3.1-3** summarizes the various ecosystem responses to nitrogen levels that affect CSS communities.

**Table 3.1-3.** Research Evidence of Ecosystem Responses to Nitrogen Relevant to Coastal Sage Scrub

Environmental Impact	Location	Reference
Enhanced growth of nonnative species	Southern California	Minnich and Dezanni, 1998; Allen et al., 1998; Weiss, 2006; Westman, 1981a,b
Nutrient enrichment of soil and plants	Riverside-Perris Plain, San Diego County	Sirulnik et al., 2007a; Allen et al., 1998; Padgett et al., 1999; Vourlitis et al., 2007
Decreased growth regulation of shrubs	Greenhouse experiment	Padgett and Allen, 1999
Decreased diversity of mycorrhizal communities	Riverside-Perris Plain	Egerton-Warburton and Allen, 2000; Siguenza et al., 2006

Environmental Impact	Location	Reference
Increased runoff and nutrient loss	Santa Barbara	Fierer and Gabet, 2002
Altered fire cycle	Riverside-Perris Plain	Wood et al., 2006
Increased dependent species vulnerability	All CSS; San Diego County	Weiss, 2006; Weaver, 1998
Increased erosion	California shrublands	Keeler-Wolf, 1995

### 3.1.2 Fire

Fire is also an inextricable and significant component in CSS losses. Although CSS species are fire resilient, nonnative grass seeds are quick to establish in burned lands, reducing the water and nutrient amounts available to CSS species for reestablishment (Keeler-Wolf, 1995). Additionally, when nonnative annual grasses have established dominance, these species alter and increase the fire frequency by senescing earlier in the annual season and increasing the dry, ignitable fuel availability (Keeley et al., 2005). With increased fire frequencies and faster nonnative colonizations, CSS seed banks are eventually eradicated from the soil, and the probability of re-establishment decreases significantly (Keeley et al., 2005). **Figure 3.1-2** represents the fire threats to CSS ecosystems.



**Figure 3.1-2.** Current fire threats to coastal sage scrub ecosystems.

### 3.1.3 Coastal Sage Scrub Model

It appears that both atmospheric nitrogen deposition and fire are critical factors involved in the decline of CSS. **Figure 3.1-3** presents a model of CSS ecosystem response to nitrogen and fire. Note that the model indicates that both nitrogen and fire play critical roles, and that there may be positive feedback loops and possible synergies between fire and nitrogen loadings.

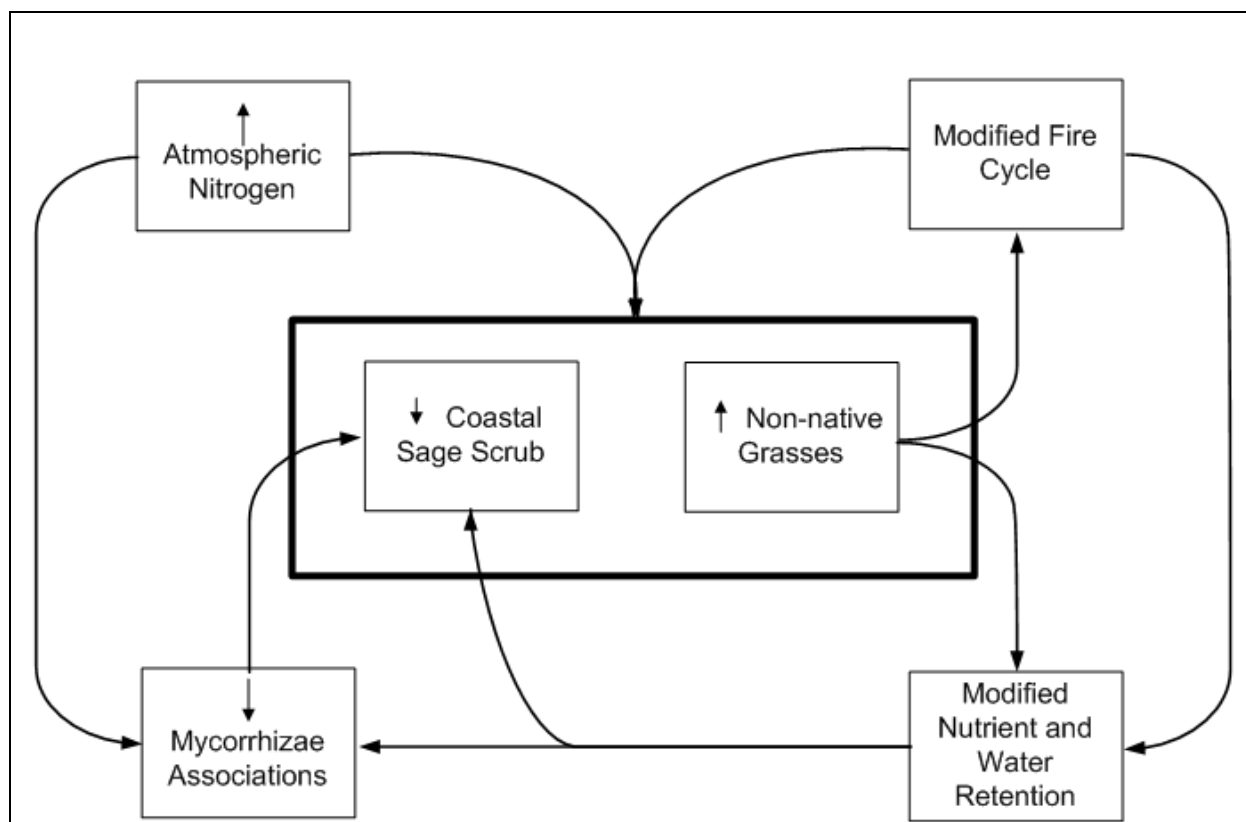


**Figure 3.1-3.** Model of coastal sage scrub ecosystem in relation to fire and atmospheric nitrogen deposition.

### 3.1.4 Mixed Conifer Forest Ecosystems

The MCF ecosystem has been a subject of study for many years. There are a number of important stressors on the community, including atmospheric fire, bark beetles, O<sub>3</sub>, particulates, and nitrogen. Although fire suppression in the 20th century is probably the most significant change that has led to alterations in morphology and perhaps to shifts in forest composition (Minnich et al., 1995), stress from elevated levels of ambient atmospheric nitrogen concentrations is the subject of increasing research.

#### 3.1.4.1 Nitrogen and Ozone Effects

Measurements documenting increases in atmospheric nitrogen deposition have been recorded with some regularity since the 1980s (Bytnerowicz and Fenn, 1996); however, the Los Angeles area has seen elevated ambient atmospheric nitrogen concentrations for the last 50 years (Bytnerowicz and Fenn, 1996). Also, some data have been published for the primary nitrogen species of dry atmospheric nitrogen deposition in the San Bernardino Mountains (i.e., nitric acid

[HNO<sub>3</sub>] and ammonia gas [NH<sub>3</sub>]) from passive samplers (Bytnerowicz et al., 2007). The pressures exerted on MCF ecosystems in California form a gradient across the Sierra Nevada Range and San Bernardino Mountains. Nitrogen throughfall levels in the northern Sierra Nevada Range are as low as 1.4 kg N/ha/yr, whereas forests in the western San Bernardino Mountains experience measured throughfall nitrogen levels up to 33 to 71 kg N/ha/yr. (Note that the high levels of nitrogen seen in some measured throughfall values are not reflected in the CMAQ modeled results. This may be an artifact of using a 12-km grid.) The primary source of nitrogen in the western San Bernardino Mountains stems from fossil fuels combustion, such as vehicle exhaust. Other sources, such as agricultural processes, also play a prominent role in the western portions of the San Bernardino Mountains and Sierra Nevada Range (Grulke et al., 2008).

**Figure 3.1-4** illustrates the current total atmospheric nitrogen deposition on MCF in California.

At the individual tree level, elevated atmospheric nitrogen can shift the ratio of aboveground to belowground biomass. Elevated pollution levels may result in increased uptake of nutrients via the canopy, decreased nitrogen intake requirements on root structures, and increased demand for carbon dioxide (CO<sub>2</sub>) uptake and photosynthetic structures to maintain the carbon balances. Therefore, the increased nutrient availability stimulates aboveground growth and increases foliar production, while reducing the demand for belowground nutrient uptake (Fenn et al., 2000). Carbon allocation gradually shifts from root to shoot, and fine-root biomass is decreased (Fenn and Bytnerowicz, 1997; U.S. EPA, 2008, Section 3.3). Grulke et al. (1998) observed a 6- to 14-fold increase in fine-root mass in areas of low atmospheric nitrogen deposition compared to areas of high deposition. Medium roots also declined at high levels (Fenn et al., 2008).

At the stand level, elevated atmospheric nitrogen has been associated with increased stand density, although other factors, such as fire suppression, also contribute to increased density and can increase mortality rates (U.S. EPA, 2008, Section 3.3). As older trees die, they are replaced with younger, smaller trees. Smaller trees allow more sunlight through the canopy and, combined with an increased availability of nitrogen, may allow for more trees to be established. Increased stand densities with younger-age classes are observed in the San Bernardino Mountains, where air pollution levels are among the highest found in the California MCF ranges studied (Minnich et al., 1995; Fenn et al., 2008). These shifts in stand density and age distribution result in vegetation structure shifts which, in turn, may impact population and

community dynamics of understory plants and animals, including threatened and endangered species.

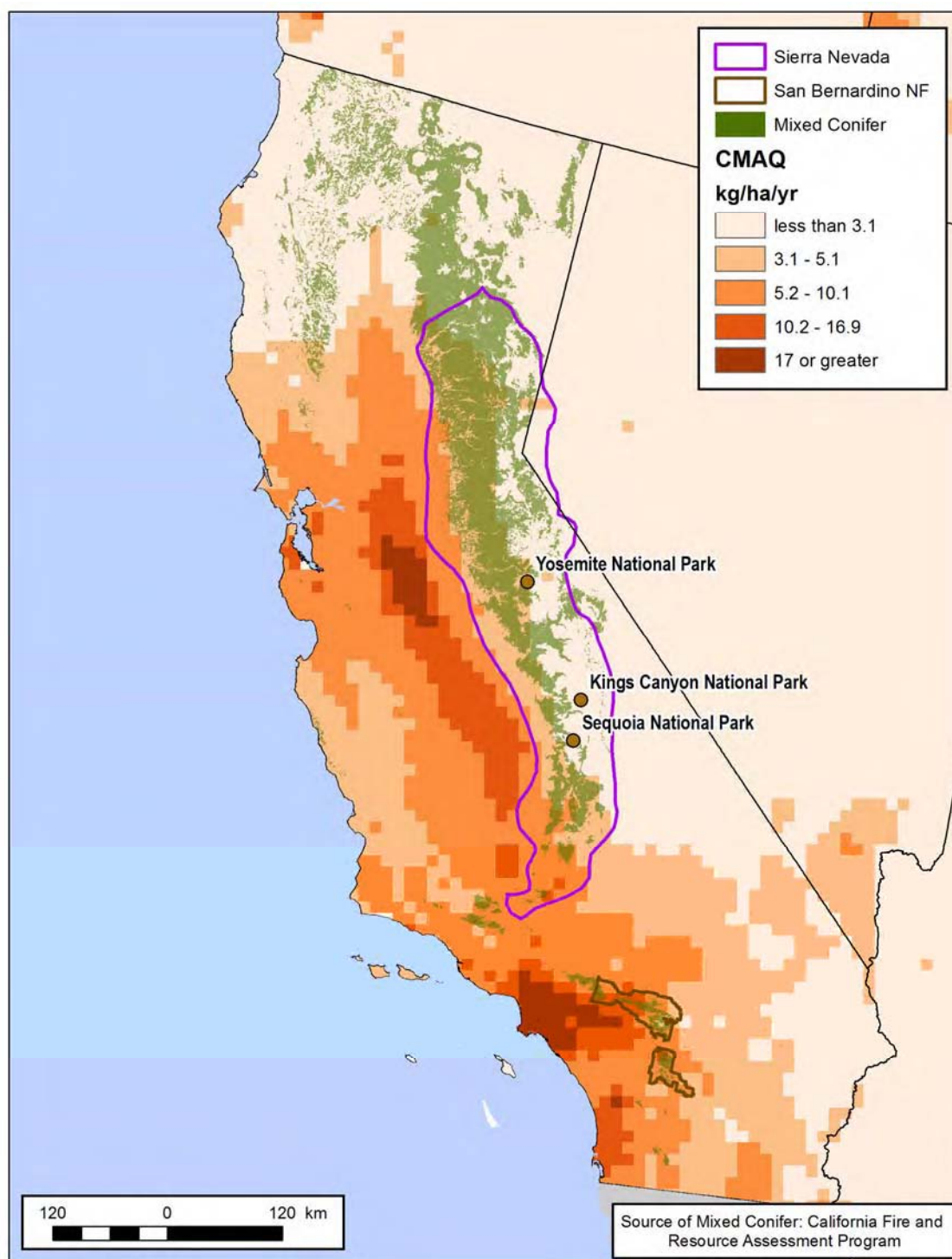


**Figure 3.1-4.** Mixed conifer forest range and total atmospheric nitrogen deposition using CMAQ 2002 modeling results and NADP monitoring data.

It should be noted that the effects of O<sub>3</sub> and atmospheric nitrogen are difficult to separate. The atmospheric transformation of NO<sub>x</sub> can yield moderate concentrations of O<sub>3</sub> as a byproduct (Grulke et al., 2008). Therefore, since elevated nitrogen levels are generally correlated with O<sub>3</sub> concentrations, researchers often report changes in tree growth and vigor as being the result of both (i.e., Grulke and Balduman, 1999).

High concentrations of O<sub>3</sub> and atmospheric nitrogen can generate increased needle and branch turnover. In areas subjected to low pollution, conifers may retain needles across 4 or 5 years; however, in areas of high pollution, such as Camp Paivika in the San Bernardino Mountains, needle retention is generally less than 1 year (Grulke and Balduman, 1999; Grulke et al., 2008). Needle turnover significantly increases litterfall. Litter biomass has been observed to increase in areas with elevated atmospheric nitrogen deposition up to 15 times more than in areas with low deposition, and the litter is seen to have higher concentrations of nitrogen (Fenn et al., 2000; Grulke et al., 2008). Elevated nitrogen levels in litter may facilitate faster rates of microbial decomposition initially, but over the long term, high nitrogen levels slow litter decomposition, and litter accumulates on the forest floor (Grulke et al., 2008; U.S. EPA, 2008). The increased litter depth may then affect subcanopy growth and stand regeneration over long periods of time.

At the highest levels of nitrogen deposition, native understory species were seen to decline (Allen et al., 2007). In addition to this decline in native understory diversity, changes in decreased fine-root mass, increased needle turnover, and the associated chemostructural alterations, MCF that are exposed to elevated pollutant levels have an increasing susceptibility to drought and beetle attack (Grulke et al., 1998, 2001; Takemoto et al., 2001). These stressors often result in the death of trees, producing an increased risk of wildfires. This complex model is displayed in **Figure 3.1-5** as a graphic developed by Grulke et al. (2008).

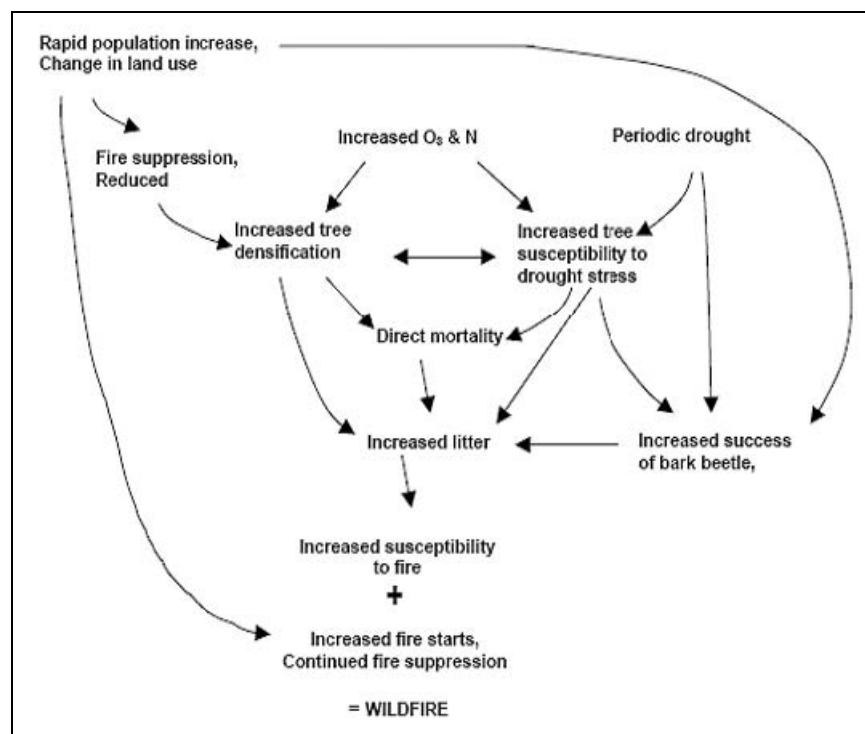


**Figure 3.1-5.** Conceptual model for increased susceptibility to wildfire in mixed conifer forests (Grulke et al., 2008).

#### 3.1.4.2 Nitrogen Effects on Lichens

Lichens emerged as an indicator of nutrient enrichment from the research on the effects of acid rain. Lichen species can be sensitive to air pollution; in particular, atmospheric nitrogen deposition. Since the 1980s, information about lichen communities has been gathered, and lichens have been used as indicators to detect changes in forest communities. Jovan (2008) depicts how lichens might be considered as sentinels in the MCF community (**Figure 3.1-6**).

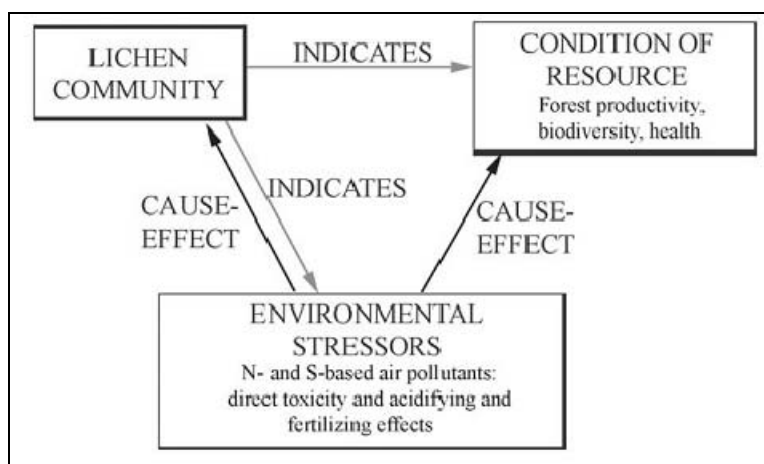


**Figure 3.1-6.** Importance of lichens as an indicator of ecosystem health (Jovan, 2008).



As atmospheric nitrogen deposition increases, the relative abundance of acidophytic lichens decreases, and the concentration of nitrogen in one of those species, *Letharia vulpine*, increases (Fenn et al., 2008). Fenn et al. (2008) were able to quantify the change in the lichen community, noting that for every 1 kg N/ha/yr increase, the abundance of acidophytic lichens declined by 5.6%. **Figure 3.1-7** illustrates the presence of acidophyte lichens and the total atmospheric nitrogen deposition in the California ranges.

In addition to abundance changes, species richness, cover, and health are affected in areas of high O<sub>3</sub> and nitrogen concentrations. Fifty percent fewer lichen species were observed after 60 years of elevated air pollution in San Bernardino Mountains MCF, with the areas of highest pollution levels exhibiting low species richness, decreased abundance and cover, and morphological deterioration of existing lichens (Sigal and Nash, 1983).

Ecological endpoints relating to shifts in the abundance of acidophilic lichens were identified by Fenn et al. (2008). They found that at 3.1 kg N/ha/yr, the community of lichens begins to change from acidophilus to tolerant species; at 5.2 kg N/ha/yr, the typical dominance by acidophilus species no longer occurs; and at 10.2 kg N/ha/yr, acidophilic lichens are totally lost from the community. Additional studies in the Colorado Front Range of the Rocky Mountain National Park support these findings and are summarized in Chapter 5 of the *Risk and Exposure Assessment*. These three values are one set of ecologically meaningful benchmarks for the MCF. As shown in **Figure 3.1-7**, much of the MCF receives nitrogen deposition levels above the 3.1 kg N/ha/yr ecological benchmark according to the 2002 CMAQ/NADP data, with the exception of the easternmost Sierra Nevada Range. MCF in the southern portion of the Sierra Nevada forests and nearly all MCF communities in the San Bernardino forests receive nitrogen deposition levels above the 5.2 kg N/ha/yr ecological benchmark. **Figure 3.1-7** also displays the potential areas where acidophilic lichens are extirpated due to nitrogen deposition levels >10.2 kg N kg/ha/yr.

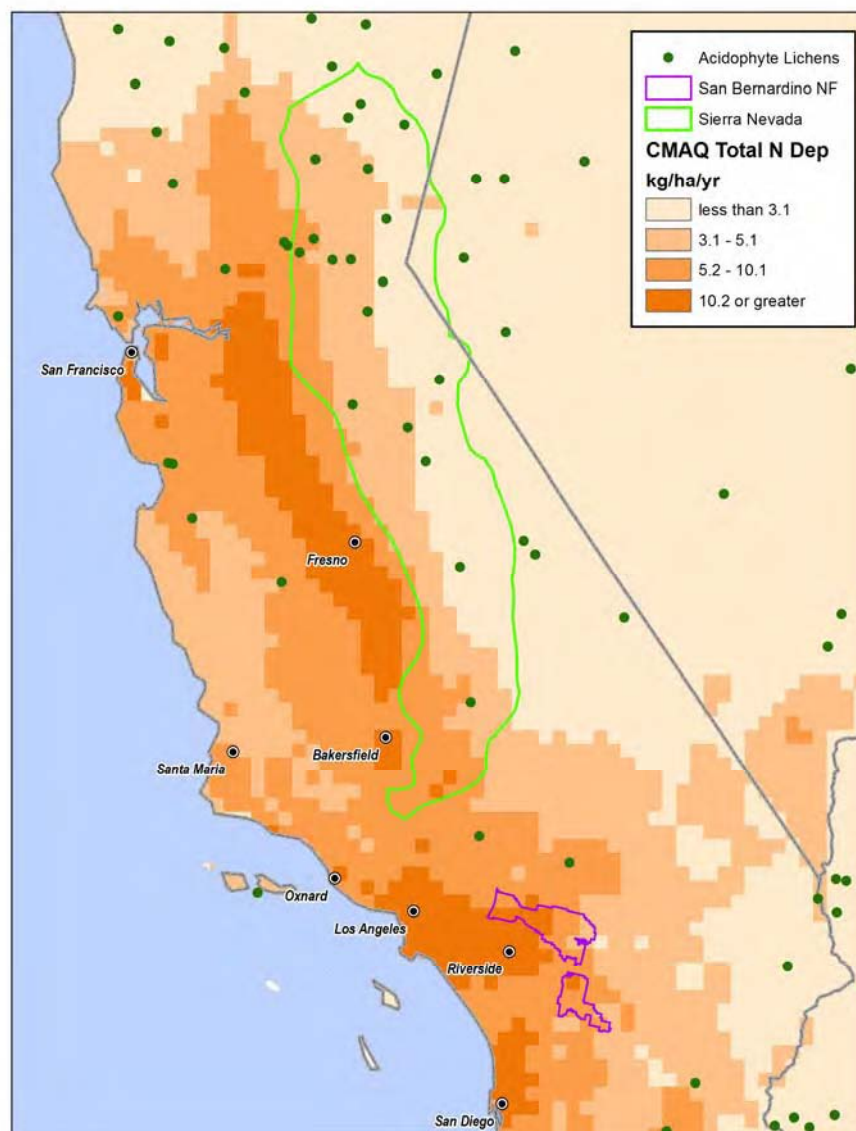


**Figure 3.1-7.** Presence of acidophyte lichens and total nitrogen deposition in the California mountain ranges using CMAQ 2002 modeling results and NADP monitoring data.

#### 3.1.4.3 Nitrogen Saturation

The established signs of nitrogen saturation have been shown within the MCF ecosystem. These symptoms include the following:

- **Increased carbon and nitrogen cycling.** The foliar turnover rates and changes in microbial decomposition both suggest that carbon and nitrogen cycles have been altered as a result of elevated nitrogen. Additionally, nitrogen fluxes in San Bernardino

Mountains soils are elevated when compared to MCF in the northern Sierra Nevada Range (Bytnerowicz and Fenn, 1996).

- **Decreased nitrogen uptake efficiency of plants.** Changes in root:shoot ratio demonstrate structural alterations in response to increasing available nitrogen.
- **Increased loss of forest nitrates to streamwater (i.e.,  $\text{NO}_3^-$  leachate).** Elevated  $\text{NO}_3^-$  leachate levels are estimated to have begun in the late 1950s and have been observed from the western MCF in the San Bernardino Mountains since 1979 (Fenn et al., 2008). These losses are a result of high soil nitrogen driven by the combined litter, needle turnover, and throughfall nitrogen exerted in these areas (Bytnerowicz and Fenn, 1996).

Changes in root biomass and stream leachate, in addition to lichen species compositional shifts, have been used to develop benchmarks for nitrogen benchmarks in the MCF ecosystem. These critical loading benchmarks, or empirical loads, are designed to estimate the levels at which atmospheric nitrogen concentrations and subsequent deposition begin to affect selected components of the ecosystem, such as forest growth, health, and composition. Some benchmarks aim to estimate individual changes to an ecosystem, whereas others assess the levels at which the entire ecosystem will not be altered because of atmospheric nitrogen deposition. The possibility of using the MCF as a model for benchmarking is discussed below.

Fenn et al. (2008) established a critical loading benchmark of 17 kg throughfall N/ha/yr in the San Bernardino Mountains and Sierra Nevada Range MCF ecosystems. This benchmark represents the level of atmospheric nitrogen deposition at which elevated concentrations of streamwater  $\text{NO}_3^-$  leachate or potential nitrogen saturation may occur. At this deposition level, a 26% reduction in fine-root biomass is anticipated (Fenn et al., 2008). Root:shoot ratios are, therefore, altered, and changes in nitrogen uptake efficiencies, litterfall biomass, and microbial decomposition are anticipated to be present at this atmospheric nitrogen deposition level. This benchmark is based on 30 to 60 years of exposure to elevated atmospheric concentrations. At longer exposure levels, the benchmark is lower because of decreased nitrogen efficiencies of the ecosystem. This benchmark is exceeded in areas of the western San Bernardino Mountains, such as Camp Paivika.

$\text{NO}_3^-$  leaching is a symptom that an ecosystem is saturated by nitrogen.  $\text{NO}_3^-$  leaching is also known to cause acidification in adjacent surface waters. The ecological benchmark of 17 kg

N/ha/yr is the last benchmark identified in this study. At this level of atmospheric nitrogen deposition,  $\text{NO}_3^-$  is observed in streams in the MCF (Fenn et al., 2008), denoting a change in ecosystem function.

**Table 3.1-4** displays the area in hectares of MCF experiencing different nitrogen deposition levels.

**Table 3.1-4.** Mixed Conifer Forest Ecosystem Area and Nitrogen Deposition

N Deposition (kg/ha/yr)	Area (hectares)	Percent of MCF Area, %
$\geq 3.1$	1,099,133	38.62
$\geq 5.2$	130,538	4.59
$\geq 10.2$	11,963	0.42
$\geq 17$	0	0.00

## 3.2 RESULTS SUMMARY

A range of ecological benchmarks were developed in the results. All benchmarks are tied to a level of atmospheric nitrogen deposition, but include a number of different ecological processes and ecological endpoints. All of the benchmarks are ecologically significant in that changes are seen that are related to community structure and function. The benchmarks span a range from 3.1 to 17 kg N/ha/yr and include:

- 3.1 kg N/ha/yr—shift in lichen communities are first observed in MCF
- 3.3 kg N/ha/yr—nitrogen no longer limiting in CSS
- 5.2 kg N/ha/yr—dominance of tolerant lichen species in MCF
- 10 kg N/ha/yr—AM community shift in CSS
- 10.2 kg N/ha/yr—loss of acidophilic lichen species from MCF
- 17 kg N/ha/yr— $\text{NO}_3^-$  leaching in MCF.

This range of ecological benchmarks may be used to develop a “green line/red line” schematic, similar to the forest screening model discussed in Lovett and Tear (2007) that illustrates the levels at which ecosystem effects may occur or are known to occur. In **Figure 3.2-1**, the green area/line denotes that point at which there do not appear to be any effects and the red line the point at which known negative effects occur.

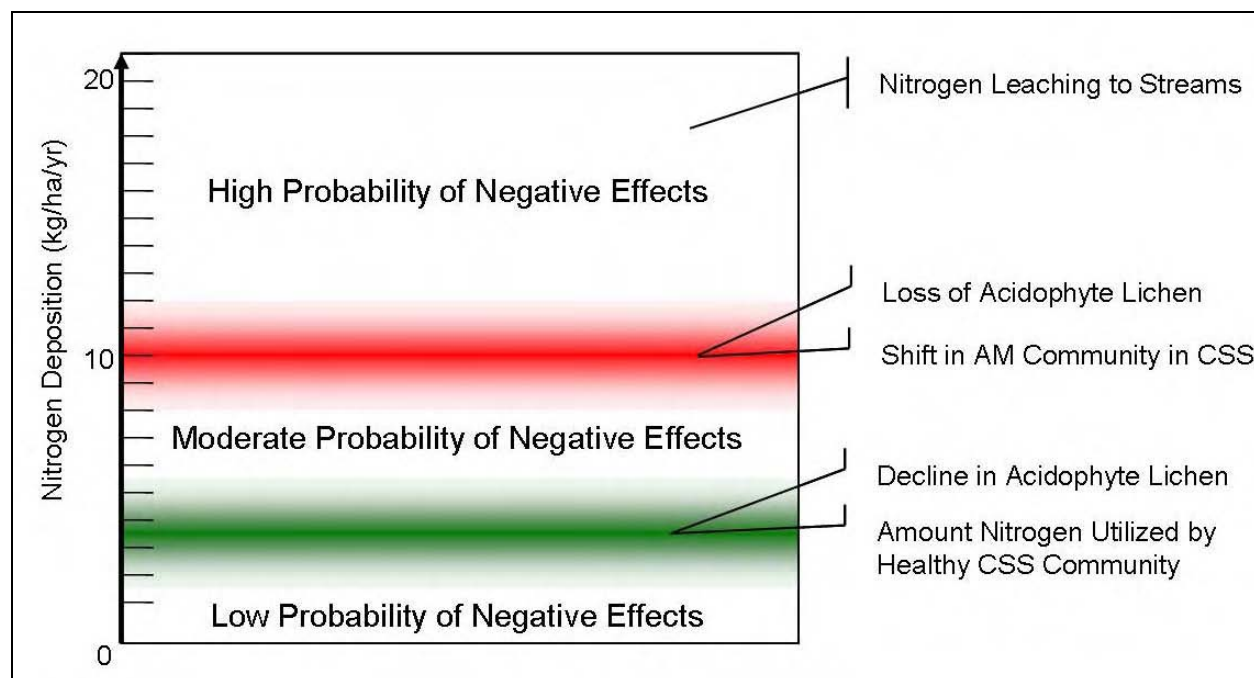


**Figure 3.2-1.** Illustration of the range of terrestrial ecosystem effects observed relative to atmospheric nitrogen deposition.

For the benchmarks identified, effects may occur at the level of atmospheric nitrogen deposition associated with the “green line” illustrated in **Figure 3.2-1**, so the “green line” may be somewhat lower. Whereas, the higher level of atmospheric nitrogen deposition (i.e., both at 10.2 and 17 kg N/ha/yr) better resembles a “red line,” where a known negative effect occurs.

The range of ecological benchmarks in CSS and MCF are not dissimilar from ecological endpoints and benchmarks identified in other ecosystems with related characteristics, such as arid systems, other forested systems, or grasslands. Egerton-Warburton et al. (2001) report that at 10 kg N/ha/yr, nitrogen changes in mycorrhizal communities/grass biomass are observed in chaparral habitats. Nitrates are found to leach into streams from nitrogen-saturated forest soils at deposition levels between 9 and 13 kg N/ha/yr (Aber et al., 2003). Results from several studies suggest ecosystem changes that are related to nitrogen deposition. The capacity of alpine catchments to sequester nitrogen is exceeded at input levels <10 kg N/ha/yr (Baron et al., 1994). Changes in the *Carex* plant community were observed to occur at deposition levels near 10 kg N/ha/yr (Bowman et al., 2006). Clark and Tilman (2008) predict that at 5.3 kg N/ha/yr, there is a loss of species diversity in grasslands. In the Pacific Northwest and in Central California, a number of investigators have observed declines in sensitive lichen species as air pollution

increases (Jovan and McCune, 2005; Geiser and Neitlich, 2007). In Europe, acidophyte decline has been identified in regions with 8 to 10 kg N/ha/yr (Bobbink, 1998; Bobbink et al., 1998).

## **4.0 IMPLICATIONS FOR OTHER SYSTEMS**

This Terrestrial Nutrient Enrichment Case Study examined the effects of atmospheric nitrogen on two ecosystem types in California: CSS and MCF. **Figure 4.1-1** presents the coverage of 2002 CMAQ/NADP data for total nitrogen deposition in the western United States, including California. Ecological effects have been documented across the United States where elevated nitrogen deposition has been observed. Benchmarks documented in the literature for the negative effects on ecosystems are summarized in **Figure 4.1-2** and are discussed in this case study report. Looking across the United States, **Figure 4.1-3** illustrates the occurrence of these ecosystems which are sensitive to nitrogen and/or have similar characteristics to the ecosystems explored in this case study. These ecosystems may also experience levels of atmospheric nitrogen deposition that exceed the benchmark levels identified in **Figure 4.1-2**. **Table 4.1-1** lists the area of CSS and MCF that exceed benchmark nitrogen levels.

In the western United States, other arid and forested ecosystems exposed to deposition at levels discussed in this case study may experience altered effects. As noted in Section 3, research on grasslands and chaparral habitats is underway. These arid systems may respond to benchmarks similar to those observed for CSS, as was shown by Clark and Tilman (2008) for bluestem grasslands in Minnesota.  $\text{NO}_3^-$  leaching in forests with elevated deposition (similar to the range found in this study) may result in nutrient enrichment in streams which can affect aquatic ecosystems (Aber et al., 2003). Research is also being conducted on lichen species in the Pacific Northwest and in Central California that are exposed to elevated levels of atmospheric nitrogen deposition (Jovan, 2008). Extensive research on the eastern Front Range of the Rocky Mountain National Park has been conducted in alpine and subalpine terrestrial and aquatic systems at elevations above 3,300 m, where communities are typically adapted to low nutrient availability but are now being exposed to >10 kg N/ha/yr in some study areas (Baron et al. 2000; Baron, 2006). (Chapters 5 and 6 of the *Risk and Exposure Assessment* also provide discussion on this topic.)

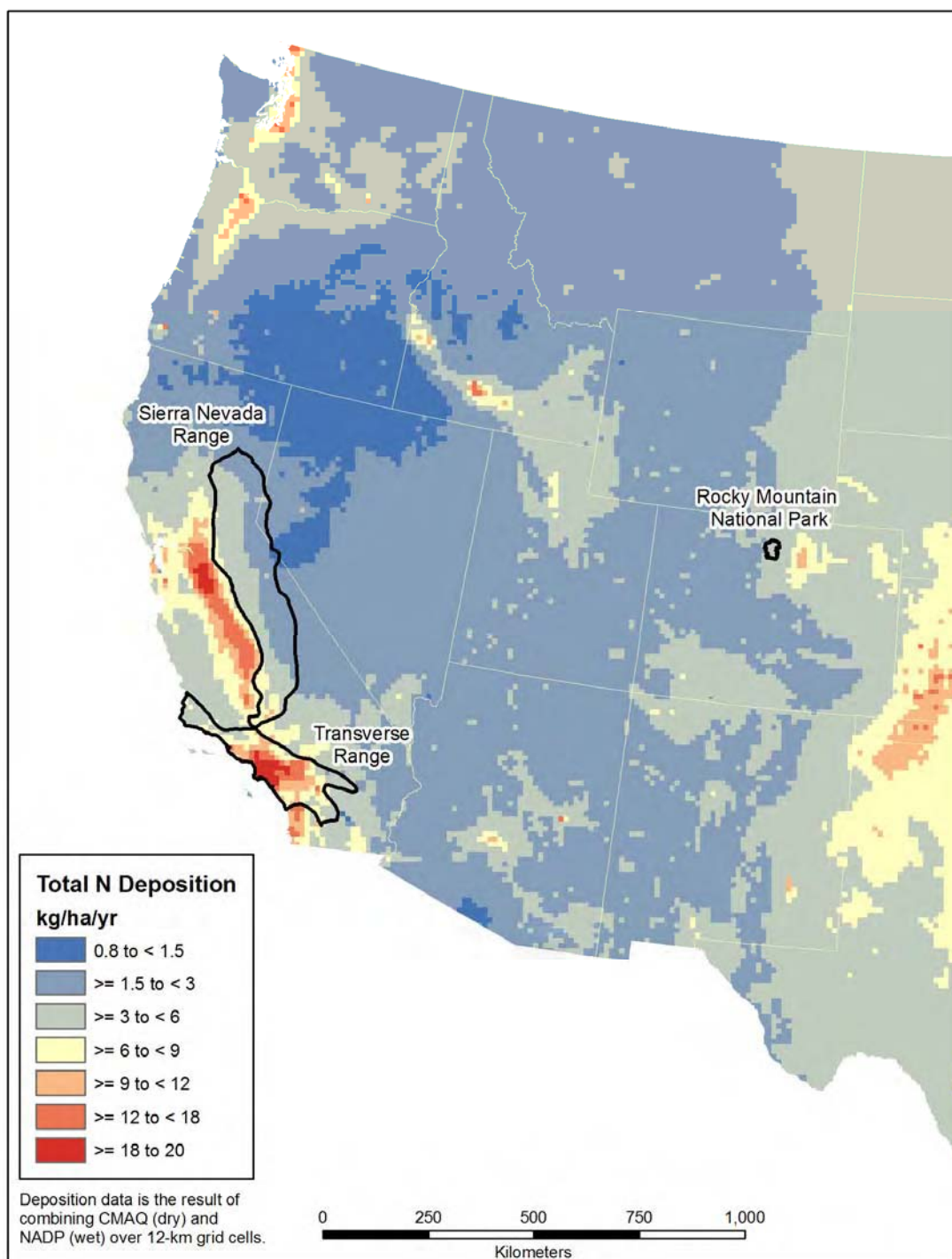


**Figure 4.1-1.** 2002 CMAQ-modeled and NADP monitoring data for deposition of total nitrogen in the western United States.



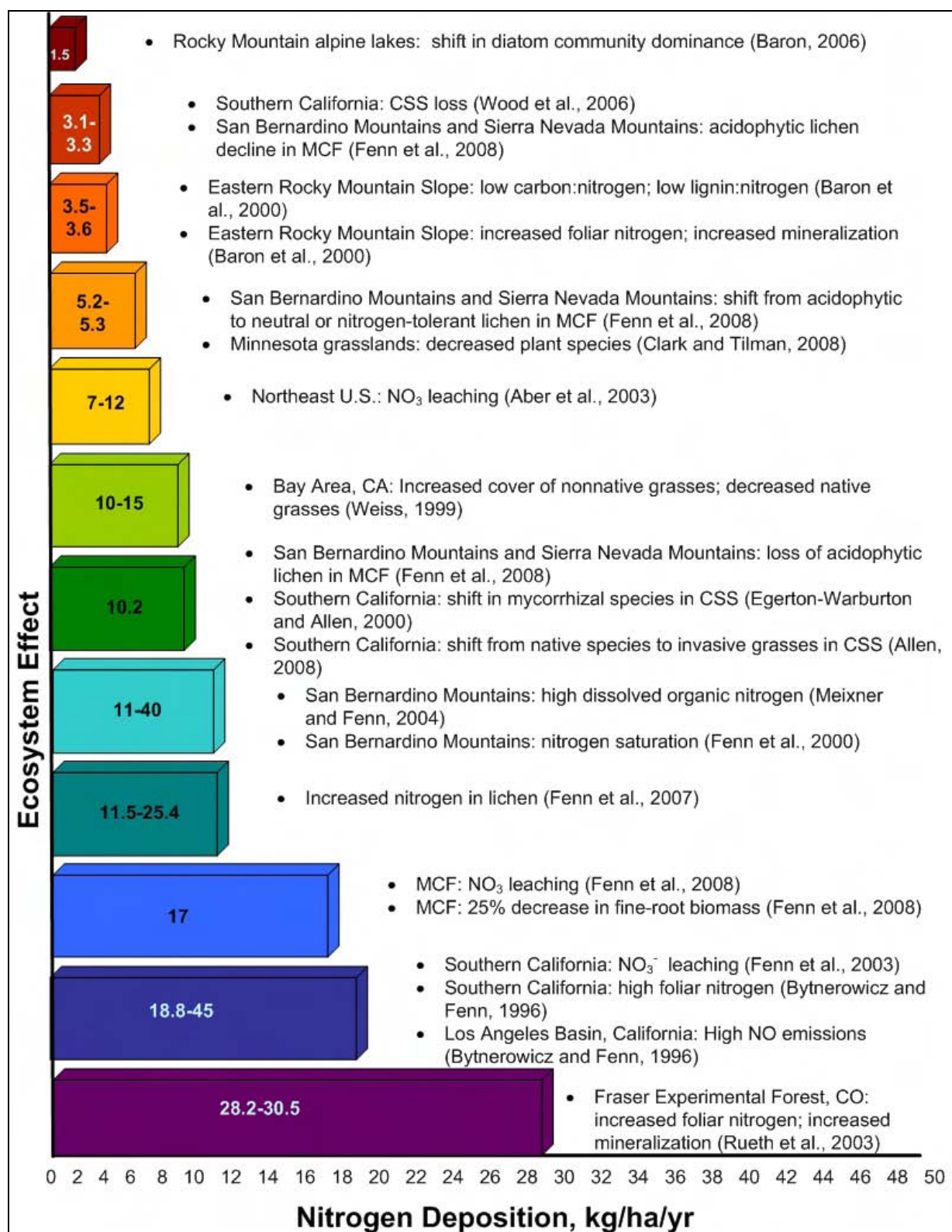
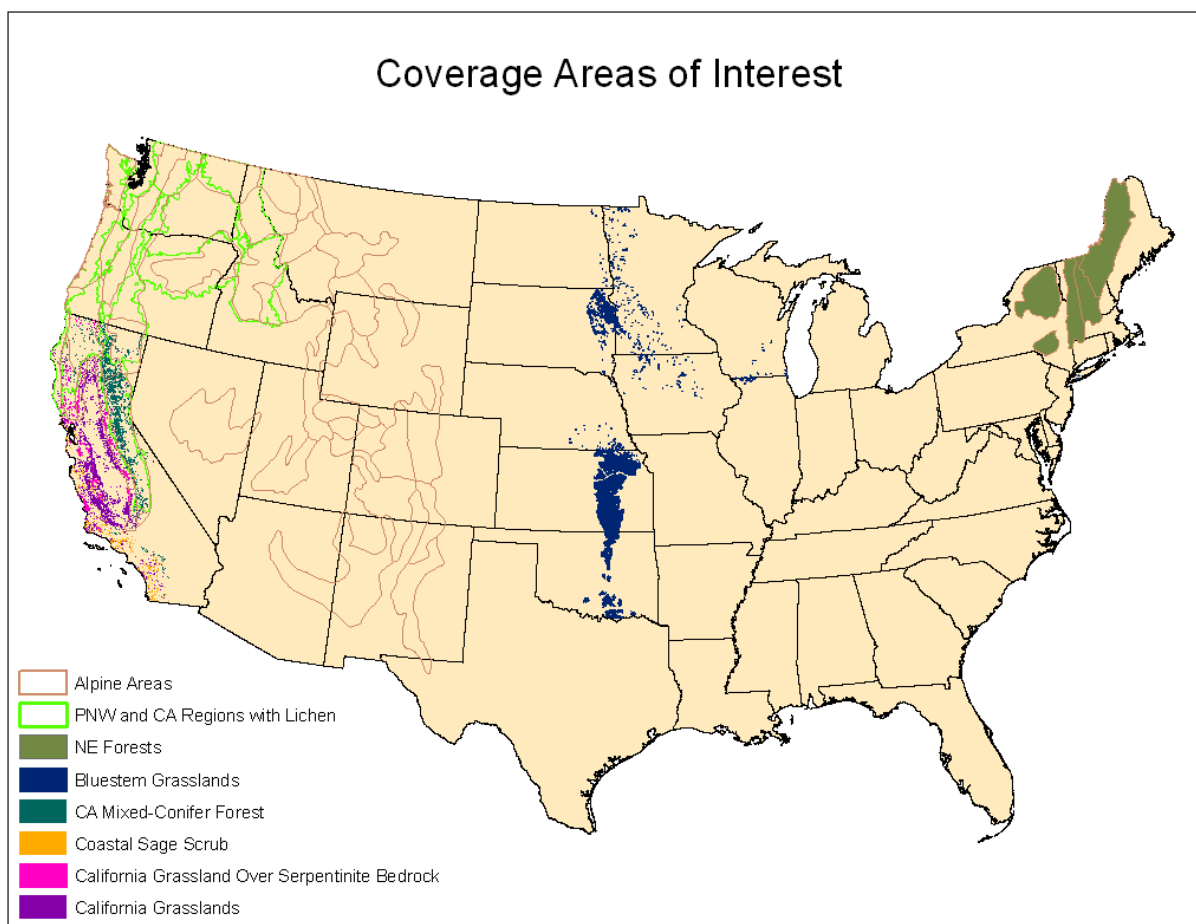


**Figure 4.1-2.** Benchmarks of atmospheric nitrogen deposition for several ecosystem indicators with the inclusion of the diatom changes in the Rocky Mountain lakes.





**Note:** PNW = Pacific Northwest; NE = Northeast.

**Figure 4.1-3.** Habitats that may experience ecological benchmarks similar to coastal sage scrub and mixed conifer forest.

**Table 4.1-1.** Areas of Coastal Sage Scrub and Mixed Conifer Forest That Exceed Benchmark Nitrogen Deposition Levels.

CSS:

N Deposition (kg/ha/yr)	Area (hectares)	Percentage of CSS Area, %
≥3.3	654,048	93.51
≥10	138,019	19.73

MCF

N Deposition (kg/ha/yr)	Area (hectares)	Percentage of MCF Area, %
≥3.1	1,099,133	38.62
≥5.2	130,538	4.59
≥10.2	11,963	0.42
≥17	0	0.00

Other systems with the following characteristics may also be found to be sensitive:

- **Ecosystems with nitrogen-sensitive epiphytes, such as lichens or mycorrhizae.** Such systems may demonstrate shifts in community structure through changes in nutrient availability or modified provisioning services.
- **Ecosystems that may have been exposed to long periods of elevated atmospheric nitrogen deposition.** The established signs of nitrogen saturation are increased leaching of  $\text{NO}_3^-$  into streamwater, decreased nitrogen uptake efficiency of plants, and increased carbon and nitrogen cycling. At prolonged elevated nitrogen levels, ecosystems are generally less likely to use, retain, or recycle nitrogen species efficiently at both the species and community levels.
- **Critical habitats.** Ecosystems that are necessary for endemic species or special ecosystem services should be monitored for possible changes due to nitrogen.
- **Locations where there are seasonal releases of nitrogen.** In both the California CSS and MCF ecosystems discussed in this case study report, a large portion of nitrogen is dry-deposited and remains on the foliage and soil surface until the beginning of the winter rainy season when nitrogen will be flushed into the soil.

Current analysis of the effects of terrestrial nutrient enrichment from atmospheric nitrogen deposition in both CSS and MCF seeks to improve scientific understanding of the interactions among nitrogen deposition, fire events, and community dynamics. The available scientific information is sufficient to identify ecological thresholds that are affected by nitrogen deposition, and ecological thresholds have been identified for CSS and MCF. This case study report has examined the sensitivity and effects of nutrient enrichment on terrestrial ecosystems, and although a diverse array of U.S. ecosystems exist, exposure levels and thresholds for effects appear to be generally comparable to levels identified in other sensitive U.S. ecosystems (e.g., thresholds range from 3.1 to 30.5 kg N/ha/yr), including thresholds identified from modeling conducted for other case studies in the *Risk and Exposure Assessment* (Chapters 4 and 5). Knowledge and understanding of such relevant exposure levels can help inform decision makers.

## **5.0 UNCERTAINTY**

### **5.1 COASTAL SAGE SCRUB**

There are several areas of uncertainty associated with this case study of CSS.

- Although current research indicates that both atmospheric nitrogen deposition and fire have contributed to the decline of CSS, the interaction between the variables and the extent of their contributions requires further research. CSS declines have been observed in the absence of fire when elevated nitrogen levels are present, and declines have also been observed in the absence of elevated nitrogen, but due to fire. Therefore, there is still a need for quantifiable and predictive results to indicate the pressure of each variable, as well as the pressure of the combined variables (if synergism is present). Additional studies are also required to test the proposed nitrogen-fire feedback loop and the associated biogeochemical elements (e.g., changes in water availability and mycorrhizal associations) that contribute to CSS decline.
- Many studies allude to a degradation of CSS by assessing species richness and abundance, but it is not clear that indicators of CSS ecosystem health have been adequately explored. Assessing the health of CSS ecosystems may help to identify a response curve to the factors associated with CSS decline.
- Ongoing experiments are beginning to show changes in CSS in response to elevated nitrogen over relatively long periods of time (Allen, personal communication, 2008). The incremental process may be occurring slower than previous field research experiments have lasted, making the reasons for the decline appear variable or imperceptible over the duration of a typical study.
- At this point, CSS is fragmented into many relatively small parcels. The CMAQ/NADP 2002 data is being modeled at 4-km resolution. The availability of these 4-km resolution data will provide a better sense of the relationship between the current distribution of CSS and atmospheric nitrogen loads and fire threat.
- Very little research exists regarding the effects of O<sub>3</sub> on CSS. Although there is some support that O<sub>3</sub> is negatively correlated with CSS, the role has yet to be quantified or consistently studied (Westman, 1981a).

- The last area of uncertainty is the relationship between current CSS distribution and the changing climate.

## **5.2 MIXED CONIFER FOREST**

The currently known areas of uncertainty for MCF are as follows:

- The long-term consequences of increased nitrogen on conifers are unclear. Although the results indicate an increased susceptibility to wildfire and disease, the long-term health of the stands and risk of cascading effects into the ecosystem require further investigation.
- The effects of O<sub>3</sub> for both MCF and lichens confound the effects of nitrogen.
- The intermingling of fire and nitrogen cycling require additional research.
- Research suggests that critical loading benchmarks can decrease over time if the nitrogen benchmark is exceeded for long periods of time because of decreasing nitrogen efficiencies within nitrogen-saturated ecosystems (Fenn et al., 2008). This may indicate that a sliding-scale approach will be required when evaluating ecosystems of varying nitrogen responses.
- There remains considerable uncertainty in the potential response of soil carbon to increases in total reactive nitrogen additions.

## **6.0 CONCLUSIONS**

Evidence from the two ecosystems discussed in this case study report supports the finding that nitrogen alters CSS and MCF. For this analysis, the loss of the native shrubs in CSS and the increase in nonnative annual grasses were investigated. In MCF on the slopes of the San Bernardino Mountains and Sierra Nevada Range, lichen communities associated with the forest stands and nitrogen saturation were investigated to identify the effects of nitrogen loadings. California's CSS and MCF have important recreational value, protect water resources, and provide habitats for many other species. In the CSS ecosystem, there is compelling evidence that elevated atmospheric nitrogen deposition is a driving force in the degradation of CSS. A CSS model was developed to help identify and parse the pressures and changes occurring within the ecosystem. In the MCF ecosystem, lichen communities and nitrogen saturation can provide a means to monitor and quantify the effects of nitrogen loadings.

Ecological benchmarks for a suite of indicators were identified in both ecosystems:

- 3.1 kg N/ha/yr—shift from sensitive to tolerant lichen species in MCF
- 3.3 kg N/ha/yr—the amount of nitrogen uptake by a vigorous stand of CSS; above this level, nitrogen may no longer be limiting
- 5.2 kg N/ha/yr—dominance of tolerant lichen species in MCF
- 10 kg N/ha/yr—mycorrhizal community changes in CSS
- 10.2 kg N/ha/yr—loss of sensitive lichen species from MCF
- 17 kg N/ha/yr—NO<sub>3</sub><sup>-</sup> leaching in MCF

Because these benchmarks are comparable to levels identified in other sensitive U.S. ecosystems and are also comparable to modeled values found in the other case studies, this set of ecological benchmarks supports the need for continued monitoring, research, and protection of sensitive ecosystems and informs the decision-making process.

## 7.0 REFERENCES

- Aber, J.D., C.L. Goodale, S.V. Ollinger, M.L. Smith, A.H. Magill, M.E. Martin, R.A. Hallett, and J.L. Stoddard. 2003. Is nitrogen deposition altering the nitrogen status of northeastern forests? *Bioscience* 53:375–389.
- Allen, E.B. 2008. Personal communication from E.B. Allen, University of California, Riverside, CA.
- Allen, E.B., P.E. Padgett, A. Bytnerowicz, and R. Minnich. 1998. *Nitrogen Deposition Effects on Coastal Sage Vegetation of Southern California*. General Tech. Rep. PSW-GTR-166. U.S. Department of Agriculture, Forest Service, Albany, CA.
- Allen, E.B., A.G. Sirulnik, L.M. Egerton-Warburton, S.N. Kee, A. Bytnerowicz, P.E. Padgett, P.J. Temple, M.F. Fenn, M.A. Poth, and T. Meixner. 2005. *Air Pollution and Vegetation Change in Southern California Coastal Sage Scrub: A Comparison with Chaparral and Coniferous Forest*. General Tech. Rep. PSW-GTR-1995. U.S. Department of Agriculture, Forest Service, Albany, CA.

- Allen, E.B., P.J. Temple, A. Bytnerowicz, M.J. Arbaugh, A.G. Sirulnik, and L.E. Rao. 2007. Patterns of understory diversity in mixed coniferous forests of Southern California impacted by air pollution. *TheScientificWorldJournal* 7(S1):247-263.
- Baron, J.S. 2006. Hindcasting nitrogen deposition to determine an ecological critical load. *Ecological Applications* 16:433–439.
- Baron, J.S., H.M. Rueth, A.M. Wolfe, K.R. Nydick, E.J. Allstott, J.T. Minear, and B. Moraska. 2000. Ecosystem responses to nitrogen deposition in the Colorado Front Range. *Ecosystems* 3:352–368.
- Baron, J.S., D.S. Ojima, E.A. Holland, and W.J. Parton. 1994. Analysis of nitrogen saturation potential in Rocky Mountain tundra and forest: Implications for aquatic systems. *Biogeochemistry* 27:61–82.
- Bobbink, R. 1998. Impacts of tropospheric ozone and airborne nitrogenous pollutants on natural and semi-natural ecosystems: A commentary. *New Phytologist* 139:161–168.
- Bobbink, R., M. Hornung, and J.G.M. Roelofs. 1998. The effects of air-borne nitrogen pollutants on species diversity in natural and semi-natural European vegetation. *Journal of Ecology* 86:717–738.
- Bobbink, R., M. Ashmore, S. Braun, W. Flückiger, and I.J.J. Van Den Wyngaert. 2003. Empirical nitrogen critical loads for natural and semi-natural ecosystems: 2002 update. Pp. 43–170 in *Empirical Critical Loads for Nitrogen*. Edited by B. Achermann and R. Bobbink. Berne: Swiss Agency for Environment, Forest and Landscape (SAEFL).
- Bowman, W.D., J.R. Gartner, K. Holland, and M. Wiedermann. 2006. Nitrogen critical loads for alpine vegetation and terrestrial ecosystem response: are we there yet? *Ecological Applications* 16:1183–1193.
- Burger, J.C., R.A. Redak, E.B. Allen, J.T. Rotenberry, and M. F. Allen. 2003. Restoring Arthropod Communities in Coastal Sage Scrub. *Conservation Biology* 17(2):460–467.

- Bytnerowicz, A., and M.E. Fenn. 1996. Nitrogen deposition in California forests: a review *Environmental Pollution* 92(2):127–146.
- Bytnerowicz, A., M. Arbaugh, S. Schilling, W. Fraczek, D. Alexander, and P. Dawson. 2007. Air pollution distribution patterns in the San Bernardino Mountains of Southern California: A 40-year perspective. *TheScientificWorldJournal* 7(S1):98–109.
- CA DFG (California Department of Fish & Game). 1993. *Southern California Coastal Sage Scrub NCCP Conservation Guidelines*. California Department of Fish & Game and California Resources Agency, Sacramento, CA. Available at <http://www.dfg.ca.gov/habcon/nccp/cgindex.htm>.
- California Department of Forestry and Fire Protection. 2007a. *Historic 1977 California Vegetation (CALVEG)*. California Department of Forestry and Fire Protection's Fire and Resource Assessment Program, Sacramento, CA. Available at <http://frap.cdf.ca.gov/data/frapgisdata/select.asp>.
- California Department of Forestry and Fire Protection. 2007b. *Thematic Mapper (TM) data from 1993 and 1997*. California Department of Forestry and Fire Protection's Fire and Resource Assessment Program, Sacramento, CA. Available at <http://frap.cdf.ca.gov/data/frapgisdata/select.asp>.
- California Invasive Plant Council. 2008. *Risk Mapping for Early Detection*. California Invasive Plant Council, Berkeley, CA. Available at [http://www.cal-ipc.org/ip/mapping/statewide\\_maps/index.php](http://www.cal-ipc.org/ip/mapping/statewide_maps/index.php).
- Carrington, M.E., and J.E. Keeley. 1999. Comparison of post-fire seedling establishment between scrub communities in Mediterranean and non-Mediterranean climate ecosystems. *Journal of Ecology* 87(6):1025–1036.
- Cione N.K., P.E. Padgett, and E.B. Allen. 2002. Restoration of a native shrubland impacted by exotic grasses, frequent fire and nitrogen deposition in Southern California. *Restoration Ecology* 10:376–384.

- Clark, C.M., and D. Tilman. 2008. Loss of plant species after chronic low-level nitrogen deposition to prairie grasslands. *Nature* 451:712–715.
- Davis, F.W., D.M. Stoms, A.D. Hollander, K.A. Thomas, P.A. Stine, D. Odion, M.I. Borchert, J. H. Thorne, M.V. Gray, R.E. Walker, K. Warner, and J. Graae. 1998. *The California Gap Analysis Project—Final Report*. University of California, Santa Barbara, CA. Available at [http://www.biogeog.ucsb.edu/projects/gap/gap\\_home.html](http://www.biogeog.ucsb.edu/projects/gap/gap_home.html).
- Diffendorfer, J.E., G.M. Fleming, J.M. Duggan, R.E. Chapman, M.E. Rahn, M.J. Mitrovich, and R.N. Fisher. 2007. Developing terrestrial, multi-taxon indices of biological integrity: An example from coastal sage scrub. *Biological Conservation* 140:130–141.
- Drus, G.M. 2004. *Species Richness Patterns in a Coastal Sage Scrub Bird Community*. Master's Thesis. California State Polytechnic University, Pomona, CA. Available at [http://rivrlab.msi.ucsb.edu/drus\\_thesis.pdf](http://rivrlab.msi.ucsb.edu/drus_thesis.pdf).
- Egerton-Warburton, L.M., and E.B. Allen. 2000. Shifts in arbuscular mycorrhizal communities along an anthropogenic nitrogen deposition gradient. *Ecological Applications* 10(2):484–496.
- Egerton-Warburton, L.M., R.G. Graham, E.B. Allen, and M.F. Allen. 2001. Reconstruction of the historical changes in mycorrhizal fungal communities under anthropogenic nitrogen deposition. *Proceedings of the Royal Society of London B* 268:2479–2484.
- Eliason S.A., and E.B. Allen. 1997. Exotic grass competition in suppressing native shrubland re-establishment. *Restoration Ecology* 5:245–255.
- Fenn, M.E., and A. Bytnerowicz. 1997. Summer throughfall and winter deposition in the San Bernardino Mountains in southern California. *Atmospheric Environment* 31(5):673–683.
- Fenn, M.E., M.A. Poth, S.L. Schilling, and D.B. Grainger. 2000. Throughfall and fog deposition of nitrogen and sulfur at an N-limited and N-saturated site in the San Bernardino Mountains, southern California. *Canadian Journal of Forest Research* 30:1476–1488.



- Fenn, M.E., J.W. Baron, E.B. Allen, H.M. Rueth, K.R. Nydick, L. Geiser, W.D. Bowen, J.O. Sickman, T. Meixner, D.W. Johnson, and P. Neitlich. 2003. Ecological effects of nitrogen deposition in the western United States. *Bioscience* 53(4):404–420.
- Fenn, M.E., L. Geiser, R. Bachman, T.J. Blubaugh, and A. Bytnerowicz. 2007. Atmospheric deposition inputs and effects on lichen chemistry and indicator species in the Columbia River Gorge, USA. *Environmental Pollution* 146:77–91.
- Fenn, M.E., S. Jovan, F. Yuan, L. Geiser, T. Meixner, and B.S. Gimeno. 2008. Empirical and simulated critical loads for nitrogen deposition in California mixed conifer forests. *Environmental Pollution* 155(3):492–511.
- Fierer, N.G., and E.J. Gabet. 2002. Carbon and Nitrogen Losses by Surface Runoff following Changes in Vegetation. *Journal of Environmental Quality* 31:1207–1213.
- Geiser, L.H., and P.N. Neitlich. 2007. Air pollution and climate gradients in Western Oregon and Washington indicated by epiphytic macrolichens. *Environmental Pollution* 145:203–218.
- Grulke, N.E., and L. Balduman. 1999. Deciduous conifers: high N deposition and O<sub>3</sub> exposure effects on growth and biomass allocation in ponderosa pine. *Water, Air, and Soil Pollution* 116:235–248.
- Grulke, N.E., C.P. Andersen, M.E. Fenn, and P.R. Miller. 1998. Ozone exposure and nitrogen deposition lowers root biomass of ponderosa pine in the San Bernardino Mountains, California. *Environmental Pollution* 103:63–73.
- Grulke N.E., C. Andersen, W.E. Hogsett. 2001. Seasonal changes in above- and belowground carbohydrate concentrations of ponderosa pine along a pollution gradient. *Tree Physiology* 21:175–184.
- Grulke, N.E., R.A. Minnich, T.D. Paine, S.J. Seybold, D. Chavez, M.E Fenn, P.J. Riggan, and A. Dunn. 2008. Air pollution increases forest susceptibility to wildfires: a case study for the San Bernardino Mountains in southern California. In *Wild Land Fires and Air Pollution*, 8. Edited by A. Bytnerowicz, M. Arbaugh, A. Riebau, C. Andersen. Burlington, MA: Elsevier.

- Jovan, S. 2008. *Lichen bioindication of biodiversity, air quality, and climate: baseline results from monitoring in Washington, Oregon, and California*. General Technical Report. PNW-GTR-737. U.S. Department of Agriculture, Forest Service, Pacific Northwest Research Station, Portland, OR.
- Jovan S., and B. McCune. 2005. Air-quality bioindication in the greater central valley of California, with epiphytic macrolichen communities. *Ecological Applications* 15:1712–1726.
- Keeler-Wolf, T. 1995. Post-fire emergency seeding and conservation in Southern California shrublands. Pp. 127–139 in *Brushfires in California Wildlands: Ecology and Resource Management*. Edited by J.E. Keeley and T. Scott. International Association of Wildland Fire, Fairfield, WA
- Keeley, J.E. 2001. Fire and invasive species in Mediterranean-climate ecosystems of California. Pp. 81–94 in *Proceedings of the Invasive Species Workshop: the Role of Fire in the Control and Spread of Invasive Species*. Edited by K.E.M. Galley and T.P. Wilson. Fire Conference 2000: the First National Congress on Fire Ecology, Prevention, and Management. Miscellaneous Publication No. 11, Tall Timbers Research Station, Tallahassee, FL.
- Keeley, J.E., M.B. Keeley, and C.J. Fotheringham. 2005. Alien plant patterns during postfire succession in Mediterranean-climate California shrublands. *Ecological Applications* 15(6):2109–2125.
- Kuchler, A.W. 1988. Potential natural vegetation of California. Pp. 909–938 and map in *Terrestrial Vegetation of California*. Edited by M.G. Barbour and J. Major. New York: Wiley-Interscience.
- Lovett, G.M., and T.H. Tear. 2007. *Effects of Atmospheric Deposition on Biological Diversity in the Eastern United States*. Workshop Report. Institute of Ecosystem Studies, Millbrook, NY, and The Nature Conservancy, Albany, NY.

- Mattoni, R., G.F. Pratt, T.R. Longcore, J.F. Emmel, and J.N. George. 1997. The endangered quino Checkerspot butterfly, *Euphydryas editha quino*. *Journal of Research on the Lepidoptera* 34:99–118. Available at <http://www.urbanwildlands.org/Resources/Mattonietal1997.pdf>.
- Merriam, K.E., J.E. Keeley, and J.L. Beyers. 2006. Fuel breaks affect nonnative species abundance in Californian plant communities. *Ecological Applications* 16:515–527.
- Meixner, T., and M. Fenn. 2004. Biogeochemical budgets in a Mediterranean catchment with high rates of atmospheric N deposition – Importance of scale and temporal asynchrony. *Biogeochemistry* 70:331–356.
- MEA (Millennium Ecosystem Assessment). 2005. *Ecosystems and human well-being: current state and trends: findings of the Condition and Trends Working Group*. Edited by R. Hassan, R. Scholes, and N. Ash. Washington, DC: Island Press.
- Minnich, R.A. 2007. Southern California coniferous forest. Chapter 18 in *Terrestrial Vegetation of California, 3rd Edition*. Edited M.G. Barbour, T. Keeler-Wolf, and A.S. Schoenherr. University of California Press, Berkeley, CA.
- Minnich, R., and R. Dezzani. 1998. Historical decline of coastal sage scrub in the Riverside-Perris Plain. *Western Birds* 39:366–391.
- Minnich, R.A., M.G. Barbour, J.H. Burk, and R.F. Fernav. 1995. Sixty years of change in conifer forests of the San Bernardino Mountains: Reconstruction of California mixed conifer forests prior to fire suppression. *Conservation Biology* 9:902–914.
- Padgett, P.E., and E.B. Allen. 1999. Differential responses to nitrogen fertilization in native shrubs and exotic annuals common to Mediterranean coastal sage scrub of California. *Plant Ecology* 144:93–101.
- Padgett, P.E., E.B. Allen, A. Bytnerowicz, and R.A. Minnich. 1999. Changes in soil inorganic nitrogen as related to atmospheric nitrogenous pollutants in southern California. *Atmospheric Environment* 33:769–781.

- Padgett, P.E., S.N. Kee, and E.B. Allen. 2000. The effects of irrigation on revegetation of semiarid coastal sage scrub in southern California. *Environmental Management* 26:427–435.
- Rueth, H.M., J.S. Baron, and E.J. Allstott. 2003. Responses of Engelmann spruce forests to nitrogen fertilization in the Colorado Rocky Mountains. *Ecological Applications* 13:664–673.
- Sigal, L.L., and T.H. Nash, III. 1983. Lichen communities on conifers in southern California: an ecological survey relative to oxidant air pollution. *Ecology* 64:1343–1354.
- Siguenza, C., D.E. Crowley, and E.B. Allen. 2006. Soil microorganisms of a native shrub and exotic grasses along a nitrogen deposition gradient in southern California. *Applied Soil Ecology* 32:13–26.
- Sirulnik, A.G., E.B. Allen, T. Meixner, and M.F. Allen. 2007a. Impacts of anthropogenic N additions on nitrogen mineralization from plant litter in exotic annual grasslands. *Soil Biology and Biochemistry* 39:24–32.
- Sirulnik, A.G., E.B. Allen, T. Meixner, M.F. Fenn, and M.F. Allen. 2007b. Changes in N cycling and microbial N with elevated N in exotic annual grasslands of southern California. *Applied Soil Ecology* 36:1–9.
- Takemoto, B.K., A. Bytnerowicz, and M.E. Fenn. 2001. Current and future effects of ozone and atmospheric nitrogen deposition on California's mixed conifer forests. *Forest Ecology and Management* 144:159–173.
- Talluto, M.V., and K.N. Suding. 2008. Historical change in coastal sage scrub in southern California, USA in relation to fire frequency and air pollution. *Landscape Ecology* 23:803–815.
- UNECE (United Nations Economic Commission for Europe). 2004. *Manual on Methodologies and Criteria for Modeling and Mapping Critical Loads and Levels and Air Pollution Effects, Risks, and Trends*. Convention on Long-Range Transboundary Air Pollution,

- Geneva Switzerland. Available at <http://www.icpmapping.org> (accessed August 16, 2006).
- USDA (U.S. Department of Agriculture). 2009. USDA, Natural Resource Conservation Service. 2009. The PLANTS Database (<http://plants.usda.gov>, 22 May 2009). National Plant Data Center, Baton Rouge, LA 70874-4490 USA
- U.S. EPA (Environmental Protection Agency). 2008. *Integrated Science Assessment (ISA) for Oxides of Nitrogen and Sulfur—Ecological Criteria (Final Report)*. EPA/600/R-08/082F. U.S. Environmental Protection Agency, National Center for Environmental Assessment—RTP Division, Office of Research and Development, Research Triangle Park, NC. Available at <http://cfpub.epa.gov/ncea/cfm/recordisplay.cfm?deid=201485>.
- USFS (U.S. Forest Service). 2008a. *Forest Inventory and Analysis National Program*. U.S. Department of Agriculture, Forest Service, Forest Inventory and Analysis National Program, Arlington, VA. Available at <http://fiatools.fs.fed.us/fiadb-downloads/datamart.html>.
- USFS (U.S. Forest Service). 2008b. *Wieslander Vegetation Type Map (VTM)*. U.S. Department of Agriculture, Forest Service, Pacific Northwest Research Station, Forest Inventory and Analysis Program, Portland, OR. Available at <http://vtm.berkeley.edu/data>.
- U.S. FWS (Fish and Wildlife Service). 2008. *FWS Critical Habitat for Threatened and Endangered Species*. U.S. Department of the Interior, U.S. Fish and Wildlife Service, Endangered Species Program, Washington, DC. Available at <http://crithab.fws.gov>.
- USGS (U.S. Geological Survey). 2006. *National Atlas of the United States*. GIS datalayer. U.S. Department of the Interior, U.S. Geological Survey, Reston, VA. Available at <http://nationalatlas.gov>.
- Vourlitis, G.L., G. Zorba, S.C. Pasquini, and R. Mustard. 2007. Carbon and nitrogen storage in soil and litter of southern Californian semi-arid shrublands. *Journal of Arid Environments* 70:164–173.

- Weaver, K.L. 1998. Coastal sage scrub variations in San Diego county and their influence on the distribution of the California gnatcatcher. *Western Birds* 29:392–405.
- Weiss, S.B. 1999. Cars, cows, and checkerspot butterflies: Nitrogen deposition and management of nutrient-poor grasslands for a threatened species. *Conservation Biology* 13:1476–1486.
- Weiss, S.B. 2006. *Impacts of Nitrogen Deposition on California Ecosystems and Biodiversity*. CEC-500-2005-165. California Energy Commission, PIER Energy-Related Environmental Research, Sacramento, CA.
- Westman, W.E. 1981a. Diversity relations and succession in Californian coastal sage scrub. *Ecology* 62:170–184.
- Westman, W.E. 1981b. Factors influencing the distribution of species of Californian coastal sage scrub. *Ecology* 62:439–455.
- Westman, W. 1979. Oxidant effects on California coastal sage scrub. *Science* 205:1001–1003.
- Wood, Y., T. Meixner, P.J. Shouse, and E.B. Allen. 2006. Altered Ecohydrologic response drives native shrub loss under conditions of elevated N-deposition. *Journal of Environmental Quality* 35:76–92.
- Yoshida, L.C., and E.B. Allen. 2001. Response to ammonium and nitrate by a mycorrhizal annual invasive grass and a native shrub in southern California. *American Journal of Botany* 88:1430–1436.

June 5, 2009

# **Appendix 8**

## **Analysis of Ecosystem Services Impacts for the NO<sub>x</sub>/SO<sub>x</sub> Secondary NAAQS Review**

*Final*

### **Prepared for**

U.S. Environmental Protection Agency  
Office of Air Quality Planning and Standards (OAQPS)  
Climate, International and Multi-Media Group (CIMG)  
(MD-C504-04)  
Research Triangle Park, NC 27711

### **Prepared by**

RTI International  
3040 Cornwallis Road  
Research Triangle Park, NC 27709-2194

Maura Flight  
Industrial Economics, Inc.

EPA Contract Number EP-D-06-003

RTI Project Number 0209897.003.066





## TABLE OF CONTENTS

1.0 Introduction.....	5
1.1 Ecosystem Service Categories .....	7
1.1.1 Descriptions and Examples of MEA Ecosystem Services.....	9
1.2 References.....	11
2.0 Aquatic Acidification.....	12
2.1 Overview of Affected Ecosystem Services.....	12
2.1.1 Provisioning Services.....	12
2.1.2 Cultural Services.....	13
2.1.3 Regulating Services .....	13
2.2 Changes in Ecosystem Services Associated with Alternative Levels of Ecological Indicators .....	14
2.2.1 Improvements in Recreational Fishing Services due to Increased Acid Neutralizing Capacity Levels in Adirondack and Other New York Lakes .....	18
2.2.2 Improvements in Total Ecosystem Services due to Increased Acid Neutralizing Capacity Levels in Adirondack Lakes .....	29
2.3 References.....	35
3.0 Terrestrial Acidification.....	37
3.1 Overview of Affected Ecosystem Services.....	37
3.1.1 Provisioning Services.....	37
3.1.2 Cultural Services.....	39
3.1.3 Regulating Services .....	43
3.2 Changes in Ecosystem Services Associated with Alternative Levels of Ecological Indicators .....	44
3.2.1 Increased Provisioning Services from Sugar Maple Timber Harvests due to Elimination of Critical Load Exceedances .....	44
3.3 References.....	57
4.0 Aquatic Enrichment .....	60
4.1 Overview of Affected Ecosystem Services.....	62
4.1.1 Provisioning Services.....	62
4.1.2 Cultural Services.....	66
4.1.3 Regulating Services .....	66
4.2 Changes in Ecosystem Services Associated with Alternative Levels of Ecological Indicators .....	67
4.2.1 The Chesapeake Bay Estuary.....	69
4.2.2 Neuse River Estuary .....	93
4.3 References.....	98
5.0 Terrestrial Enrichment .....	104
5.1 Overview of Affected Ecosystem Services.....	104
5.1.1 Cultural .....	105
5.1.2 Regulating.....	116
5.2 Value of Coastal Sage Scrub and Mixed Conifer Forest Ecosystem Services .....	120

5.3	References.....	121
6.0	Conclusion .....	123
6.1	Benefits from Enhanced Provisioning Services.....	123
6.2	Benefits from Enhanced Cultural Services .....	125
6.3	Benefits from Enhanced Regulating Services.....	126
	Attachment A: Annual Recreational Fishing Benefit Estimates for Reductions in New York Lake Acidification Levels, 2002–2100 .....	A-1

## LIST OF FIGURES

<b>Figure 1.1-1.</b>	Conceptual Framework for Linking Changes in Ambient NO <sub>x</sub> and SO <sub>x</sub> Levels to Changes in Ecosystem Services and Public Welfare .....	6
<b>Figure 1.1-2.</b>	MEA Categorization of Ecosystem Services and their Links to Human Well-Being (Source: MEA, 2005b). .....	9
<b>Figure 2.2-1.</b>	Summary of Acid Neutralizing Capacity Values Relevant for Lake and Fish Health (Source: Industrial Economics, Inc., 2008). .....	17
<b>Figure 3.1-1.</b>	Combined Nitrogen and Sulfur Deposition (from 2002 CMAQ Dry Deposition and NADP Wet Deposition Estimates) and the Range of Sugar Maple in the United States .....	38
<b>Figure 3.1-2.</b>	Combined Nitrogen and Sulfur Deposition (from 2002 CMAQ Dry Deposition and NADP Wet Deposition Estimates) and the Range of Red Spruce in the United States .....	39
<b>Figure 3.1-3.</b>	Annual Value of Sugar Maple and Red Spruce Harvests and Maple Syrup Production, 2006 .....	40
<b>Figure 3.2-1.</b>	Estimated Time Path of Welfare Gains in the Forestry and Agricultural Sector due to Increased Sugar Maple and Red Spruce Growth (2000– 2065) .....	55
<b>Figure 4-1.</b>	Conceptual Model of Eutrophication Impacts in Estuaries (Source: Adapted from Bricker et al. [2007] and Bricker, Ferreira, and Simas [2003]). .....	61
<b>Figure 4.2-1.</b>	Chesapeake Bay Coastal Block Groups .....	86
<b>Figure 5.1-1.</b>	Coastal Sage Scrub Areas and Population .....	106
<b>Figure 5.1-2.</b>	Mixed Conifer Forest Areas and Population.....	107
<b>Figure 5.1-3.</b>	Boundaries of the NCCP Region and Subregions for Coastal Sage Scrub (Source: California Department of Fish and Game, n.d.). .....	108
<b>Figure 5.1-4.</b>	Mixed Conifer Forest Areas and National and State Park Boundaries .....	110
<b>Figure 5.1-5.</b>	Coastal Sage Scrub Areas and Housing Values .....	113
<b>Figure 5.1-6.</b>	Presence of Three Threatened and Endangered Species in California’s Coastal Sage Scrub Ecosystem .....	114
<b>Figure 5.1-7.</b>	Presence of Two Threatened and Endangered Species in California’s Mixed Conifer Forest.....	115
<b>Figure 5.1-8.</b>	Coastal Sage Scrub Areas and Fire Threat.....	118
<b>Figure 5.1-9.</b>	Mixed Conifer Forest Areas and Fire Threat .....	119
<b>Figure 5.1-10.</b>	Mixed Conifer Forest Areas and Major Lakes and Rivers.....	120

## LIST OF TABLES

<b>Table 2.2-1.</b> Participation in Freshwater Recreational Fishing in Northeastern States in 2006.....	14
<b>Table 2.2-2.</b> Acid Neutralizing Capacity Levels (in µeq/L) at 44 MAGIC-Modeled Lakes in the Adirondacks .....	15
<b>Table 2.2-3.</b> Random Effects Model Results .....	20
<b>Table 2.2-4.</b> Count of Impacted Lakes .....	23
<b>Table 2.2-5.</b> Per Capita Willingness to Pay (2007 \$).....	24
<b>Table 2.2-6.</b> Present Value and Annualized Benefits, Adirondack Region .....	26
<b>Table 2.2-7.</b> Present Value and Annualized Benefits, New York State .....	27
<b>Table 2.2-8.</b> Comparison of Resources for the Future Contingent Valuation Scenarios and EPA Zero-Out Scenario .....	30
<b>Table 2.2-9.</b> Aggregate Benefit Estimates for the Zero-Out Scenario .....	33
<b>Table 3.1-1.</b> Participation in Hunting and Wildlife Viewing in Northeastern States in 2006.....	42
<b>Table 3.2-1.</b> Summary of Plot-Level Data on Sugar Maple Growth and Exceedances (for Plots above the Glaciation Line).....	46
<b>Table 3.2-2.</b> Summary of Plot Level Data on Sugar Maple Growth and Exceedances (for Plots above the Glaciation Line).....	47
<b>Table 3.2-3.</b> Linear Exposure–Response Model for Exceedances (above a Critical Load Calculated with Bc/AI = 10) and Sugar Maple Tree Growth: OLS Regression Results (for Plots above the Glaciation Line) .....	48
<b>Table 3.2-4.</b> Linear Exposure–Response Model for Exceedances (above a Critical Load Calculated with Bc/AI = 10) and Red Spruce Tree Growth: OLS Regression Results (for Plots above the Glaciation Line) .....	49
<b>Table 3.2-5.</b> Estimated Increments in Sugar Maple and Red Spruce Timber Volume (Resulting from Elimination of Critical Load Exceedances), by FASOMGHG Region.....	52
<b>Table 3.2-6.</b> Proportions of Hardwood in Sugar Maple Production and Proportions of Softwood in Red Spruce Production, by FASOM Region .....	53
<b>Table 3.2-7.</b> Proportion of Timberland under Private and Public Ownership by FIA Region <sup>a</sup> : 2002.....	54
<b>Table 4.1-1.</b> Annual Values of East Coast Commercial Landings (in millions).....	63
<b>Table 4.1-2.</b> Value of Commercial Landings for Selected Species in 2007 (Chesapeake Bay Region) .....	64
<b>Table 4.2-1.</b> Participation in Selected Marine Recreation Activities in East Coast States in 1999–2000 .....	68
<b>Table 4.2-2.</b> Regression Analysis of the Chesapeake Water Quality Index on Water Quality Parameters.....	71
<b>Table 4.2-3.</b> Average Catch Rate per Fishing Trip in the Chesapeake Bay, by State and Targeted Fish Species .....	73
<b>Table 4.2-4.</b> Aggregate Number of Fishing Trips to the Chesapeake Bay, by State and Targeted Fish Species .....	75
<b>Table 4.2-5.</b> Input Estimates for the Chesapeake Bay Boating Benefit Transfer Model .....	78
<b>Table 4.2-6.</b> Input Estimates for the Chesapeake Bay Beach-Use Benefit Transfer Model .....	82

<b>Table 4.2-7.</b> Summary of Housing Unit Numbers and Average Prices in Chesapeake Coastal Block Groups in 2007 .....	87
<b>Table 5.1-1.</b> Recreational Activities in California in 2006 by Residents and Nonresidents.....	111
<b>Table 6-1.</b> Summary of Aggregate Benefit Estimates for Selected Ecosystem Services and Areas (Zero Out of Nitrogen and Sulfur Deposition) <sup>a</sup> .....	124

## **1.0 INTRODUCTION**

The U.S. Environmental Protection Agency (EPA) is conducting a review of the secondary National Ambient Air Quality Standards (NAAQS) for nitrogen oxides (NO<sub>x</sub>) and sulfur oxides (SO<sub>x</sub>). As part of the review, EPA is interested in linking changes in NO<sub>x</sub> and SO<sub>x</sub> ambient air concentrations to the changes in ecosystem services and ultimately to changes in public welfare. This process of linking changes in ambient NO<sub>x</sub> and SO<sub>x</sub> levels to public welfare through the effects on ecosystem services is illustrated in **Figure 1.1-1**. Reducing NO<sub>x</sub> and SO<sub>x</sub> concentrations will reduce the stresses on aquatic and terrestrial ecosystems by reducing atmospheric deposition of nitrogen and sulfur compounds. As shown in the figure, EPA has identified four main categories of adverse ecosystem effects—aquatic acidification, terrestrial acidification, aquatic nutrient enrichment, and terrestrial nutrient enrichment.<sup>1</sup> For each of these categories, EPA has identified key ecological indicators, which provide quantitative measures of adverse impacts on the affected ecosystems.

The purpose of this report is to identify, characterize, and, to the extent possible, quantify the ecosystem services that are primarily impacted by nitrogen and sulfur deposition (see Section 1.1 for the definition and categorization framework used to define ecosystem services) and the changes in ecosystem services that are expected to result from changes in the ecological indicators. By linking indicators of ecological function to ecosystem service provision through risk and economic assessments, the objective is to inform decisions regarding the adequacy of current NAAQS and the ecosystem protection afforded by potential revisions to the current primary standards for NO<sub>x</sub> and SO<sub>x</sub>.

This report includes four main sections (after this one), each dedicated to one of the main ecosystem effect categories defined above and in Figure 1.1-1. Section 2 focuses on aquatic acidification and provides an overview of the main ecosystem services affected by acidification of freshwater. The section then applies the results of the Aquatic Acidification Case Study of Adirondack lakes to quantify specifically the value of improved recreational fishing and other cultural services caused by reductions in lake acidification in this part of the country.

---

<sup>1</sup> Although other effects exist, the magnitude and/or scientific evidence of these effects is much more limited.

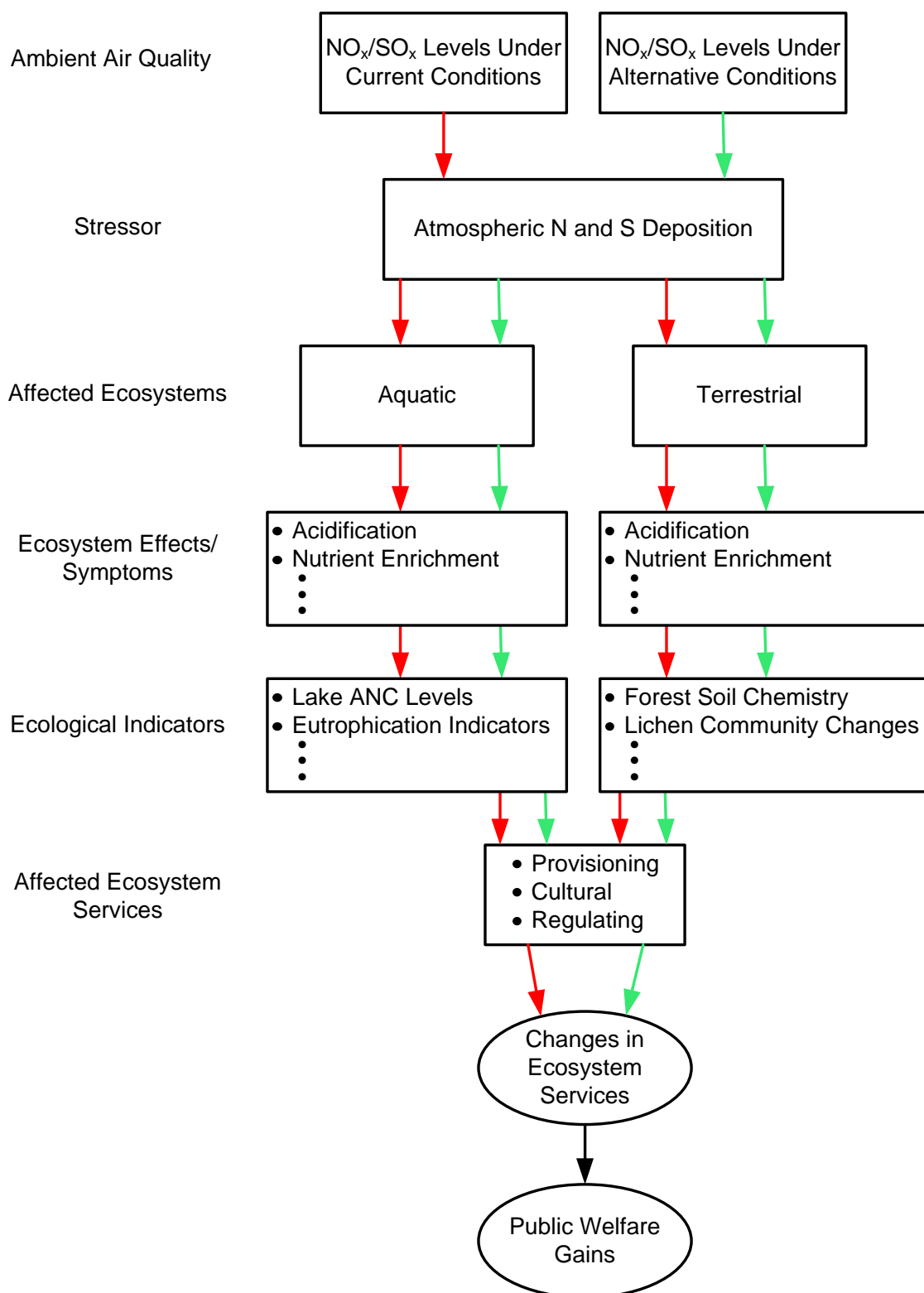


**Figure 1.1-1.** Conceptual Framework for Linking Changes in Ambient NO<sub>x</sub> and SO<sub>x</sub> Levels to Changes in Ecosystem Services and Public Welfare

Section 3 focuses on terrestrial acidification, providing an overview of the main ecosystem services affected by acidification of forest soils. It then applies the results of the Terrestrial Acidification Case Study and additional analyses of impacts on sugar maple trees to quantify the value of improved provisioning services associated with expected enhancements to forest productivity.

Section 4 focuses on aquatic nutrient enrichment. It describes and characterizes the ecosystem services that are primarily affected by the eutrophication processes in estuaries that result from excess nitrogen loadings. It then applies the results of the Aquatic Nutrient Enrichment Case Study of the Potomac River/Potomac Estuary Case Study Area and the Neuse River/Neuse River Estuary Case Study Area to quantify improvements in provisioning and cultural services associated with reduced nitrogen loadings and improvements in eutrophic conditions in the Chesapeake Bay and Neuse estuaries.

Section 5 focuses on terrestrial nutrient enrichment. It provides an overview of the ecosystem services that are primarily affected by excess nitrogen loadings in two main terrestrial ecosystems—California coastal sage scrub (CSS) and mixed conifer forest (MCF) habitats. It also applies the findings from the Terrestrial Nutrient Enrichment Case Study of these affected ecosystems; however, like the case study, because of data limitations and current knowledge gaps, Section 5 does not quantify expected changes due to reductions in nitrogen and sulfur deposition.

## **1.1 ECOSYSTEM SERVICE CATEGORIES**

Ecosystem services are generally defined as the benefits individuals and organizations obtain from ecosystems. This report uses the classification framework for ecosystem services developed by the Millennium Ecosystem Assessment (MEA) (2005a, 2005b). In the MEA, ecosystem services are defined to include both natural and human-modified ecosystems. Services are further defined to encompass both tangible and intangible benefits that individuals and organizations derive from ecosystems. In the MEA, ecosystem services are classified into four main categories:

- **Provisioning:** includes products obtained from ecosystems.

- **Cultural:** includes the nonmaterial benefits people obtain from ecosystems through spiritual enrichment, cognitive development, reflection, recreation, and aesthetic experiences.
- **Regulating:** includes benefits obtained from the regulation of ecosystem processes.
- **Supporting:** includes those services necessary for the production of all other ecosystem services.

**Figure 1.1-2**, taken from the MEA, displays the impact of the ecosystem services on human well-being. The first three categories directly affect human well-being and economic measures of welfare change. Supporting services do not have a direct effect on human well-being but are vital to the functioning of the ecosystem.<sup>2</sup> While other authors have proposed categorizing ecosystem services using different systems, the MEA framework was chosen because it is a well-developed and widely accepted system.<sup>3</sup> The valuation of ecosystem services benefits, however, is based on a careful linking of the MEA framework with neoclassical economics.

---

<sup>2</sup> One of the criticisms of the MEA framework from the perspective of economic analysis is that even some of the regulating services, such as climate regulation, are more like ecosystem functions/processes or “supporting services” that are only indirectly related to welfare (Boyd and Banzhaf [2007], Wallace [2007]).

<sup>3</sup> Alternatives to the MEA ecosystem service classifications include, for example, Daily et al. (1997), National Research Council (2005), and Wallace (2007).



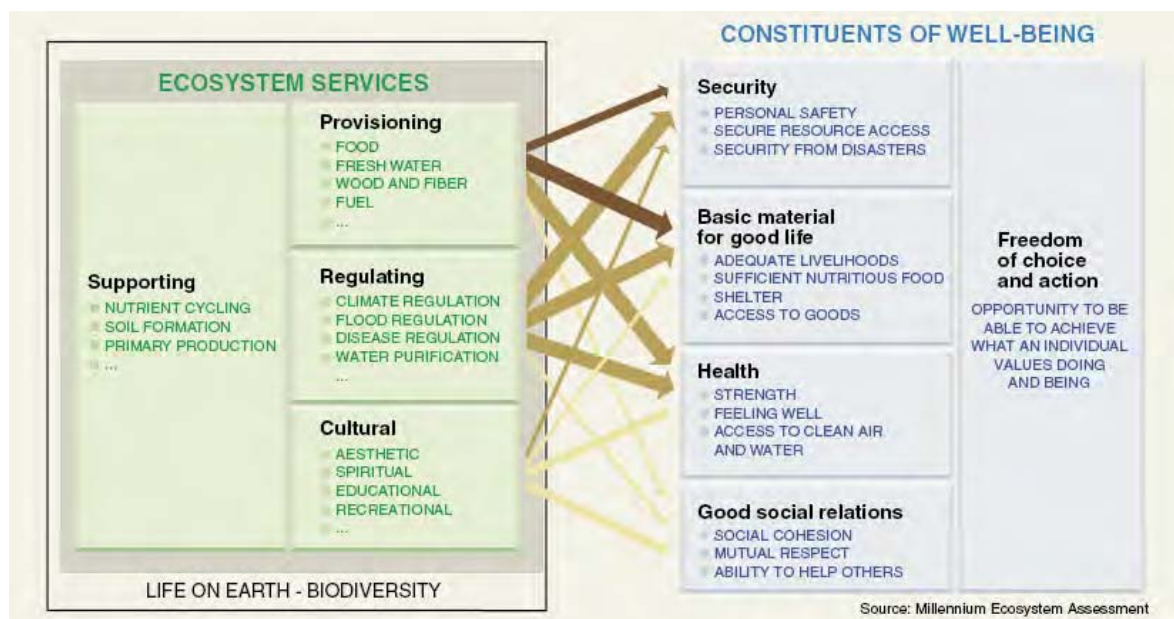


**Figure 1.1-2.** MEA Categorization of Ecosystem Services and their Links to Human Well-Being (Source: MEA, 2005b).

### 1.1.1 Descriptions and Examples of MEA Ecosystem Services

For each service category, the MEA identifies a variety of subcategories. The list below (adapted from MEA [2005b]) highlights the services that are most relevant to this report; however, the MEA framework contains more services than those listed. Note that supporting services, which do not link directly to welfare, are not included, and that there is some overlap between the categories.

#### 1.1.1.1 Provisioning Services

- **Food and fiber:** This includes the vast range of food products derived from plants, animals, and microbes, as well as materials such as wood, jute, hemp, silk, and many other products derived from ecosystems.
- **Fuel:** Wood, manure, and other biological materials serve as sources of energy.
- **Genetic resources:** This includes the genes and genetic information used for animal and plant breeding and biotechnology.
- **Biochemicals, natural medicines, and pharmaceuticals:** Many medicines, biocides, food additives such as alginates, and biological materials are derived from ecosystems.
- **Fresh water:** Fresh water is another example of linkages between categories—in this case, between provisioning and regulating services.

#### ***1.1.1.2 Regulating Services***

- Air quality maintenance: Ecosystems both contribute chemicals to and extract chemicals from the atmosphere, influencing many aspects of air quality.
- Climate regulation: Ecosystems influence climate both locally and globally. For example, on a local scale, changes in land cover can affect both temperature and precipitation. On a global scale, ecosystems play an important role in climate regulation by either sequestering or emitting greenhouse gases.
- Water regulation: The timing and magnitude of runoff, flooding, and aquifer recharge can be strongly influenced by changes in land cover, including, in particular, alterations that change the water storage potential of the system, such as the conversion of wetlands or the replacement of forests with croplands or croplands with urban areas.
- Erosion control: Vegetative cover plays an important role in soil retention and the prevention of landslides.
- Water purification and waste treatment: Ecosystems can be a source of impurities in freshwater but also can help filter out and decompose organic wastes introduced into inland waters and coastal and marine ecosystems.
- Biological control: Ecosystem changes affect the prevalence of crop and livestock pests and diseases.
- Biological control—food chain: Ecosystem changes affect the availability of vegetation and, in turn, animals that comprise and sustain delicate food chains within an ecosystem.
- Storm protection: The presence of coastal ecosystems such as mangroves and coral reefs can dramatically reduce the damage caused by hurricanes or large waves.

#### ***1.1.1.3 Cultural Services***

- Spiritual and religious values: Many religions attach spiritual and religious values to ecosystems or their components.
- Educational values: Ecosystems and their components and processes provide the basis for both formal and informal education in many societies.
- Inspiration: Ecosystems provide a rich source of inspiration for art, folklore, national symbols, architecture, and advertising.

- Aesthetic values: Many people find beauty or aesthetic value in various aspects of ecosystems, as reflected in the support for parks, “scenic drives,” and the selection of housing locations.
- Recreation and ecotourism: People often choose where to spend their leisure time based, in part, on the characteristics of the natural or cultivated landscapes in a particular area.

Environmental economists also have identified a category of services associated with ecological benefits termed “nonuse values” (also referred to as “existence values” or “passive use values”). As the name implies, nonuse values capture those values people have for the environment or natural resources separate from the direct or indirect use value the resources provide. The value some individuals hold for wilderness areas that they will never visit is one type of nonuse value. This report includes nonuse values as a subcategory of cultural services.

## **1.2 REFERENCES**

- Boyd, J., and S. Banzhaf. 2007. “What are Ecosystem Services? The Need for Standardized Environmental Accounting Units.” *Ecological Economics* 63:616-626.
- Daily, G.C., S. Alexander, P.R. Ehrlich, L. Goulder, J. Lubchenco, P.A. Matson, H.A. Mooney, S. Postel, S.H. Schneider, D. Tilman, and G.M. Woodwell. 1997. “Ecosystem Services: Benefits Supplied to Human Societies by Natural Ecosystems.” *Issues in Ecology* 2:1-16.
- Millennium Ecosystem Assessment (MEA). 2005a. *Ecosystems and Human Well-being: Current State and Trends, Volume 1*. R. Hassan, R. Scholes, and N. Ash, eds. Washington, DC: Island Press. Available at <http://www.millenniumassessment.org/documents/document.766.aspx.pdf>.
- Millennium Ecosystem Assessment (MEA). 2005b. *Ecosystems and Human Well-being: Synthesis*. Washington, DC: World Resources Institute.
- National Research Council. 2005. *Valuing Ecosystem Services: Toward Better Environmental Decision-Making*. Washington, DC: National Academies Press.
- Wallace, K.J. 2007. “Classification of Ecosystem Services: Problems and Solutions.” *Ecological Conservation* 139:235-246.

## **2.0 AQUATIC ACIDIFICATION**

High levels of nitrogen and sulfur deposition, particularly in areas with soils containing relatively low levels of alkaline chemical bases such as calcium or magnesium ions, often lead to acidification of surface waters such as lakes and streams. These processes contribute to low pH levels and other chemical changes that can be toxic to fish and other aquatic life. Evidence of both chronic and episodic acidification of surface waters is particularly evident in the Eastern and northeastern United States, where levels of nitrogen and sulfur deposition have also been relatively high in recent decades. These surface waters support a wide variety of ecosystem services, many of which can be affected adversely by acidification.

### **2.1 OVERVIEW OF AFFECTED ECOSYSTEM SERVICES**

Because acidification primarily affects the diversity and abundance of aquatic biota, it also primarily affects the ecosystem services that are derived from the fish and other aquatic life found in these surface waters.

#### **2.1.1 Provisioning Services**

Food and freshwater are generally the most important provisioning services provided by inland surface waters (Millennium Ecosystem Assessment [MEA], 2005). Whereas acidification is unlikely to have serious adverse effects on, for example, water supplies for municipal, industrial, or agricultural uses, it can limit the productivity of surface waters as a source of food (i.e., fish). In the northeastern United States, the surface waters affected by acidification are not a major source of commercially raised or caught fish; however, they are a source of food for some recreational and subsistence fishers and for other consumers. Although data and models are available for examining the effects on recreational fishing (see Section 2.1.2), relatively little data are available for measuring the effects on subsistence and other consumers. For example, although there is evidence that certain population subgroups in the northeastern United States, such as the Hmong and Chippewa ethnic groups, have particularly high rates of self-caught fish consumption (Hutchison and Kraft, 1994; Peterson et al., 1994), it is not known if and how their consumption patterns are affected by the reductions in available fish populations caused by surface water acidification.

### **2.1.2 Cultural Services**

Inland surface waters support several cultural services, such as aesthetic and educational services; however, the type of service that is likely to be most widely and significantly affected by aquatic acidification is recreational fishing, since it depends directly on the health and abundance of aquatic wildlife. Other recreational activities such as hunting and birdwatching are also likely to be affected, to the extent that fish eating birds and other wildlife are harmed by the absence of fish in acidic surface waters.

Recreational fishing in lakes and streams is among the most popular outdoor recreational activities in the northeastern United States. Data from the 2006 National Survey of Fishing, Hunting, and Wildlife Associated Recreation (FHWAR), as summarized in **Table 2.2-1**, indicate that more than 9% of adults in this part of the country participate annually in freshwater (excluding Great Lakes) fishing. The total number of freshwater fishing days occurring in those states (by both residents and nonresidents) in 2006 was 140.8 million days. Roughly two-thirds of these fishing days were at ponds, lakes, or reservoirs in these states, and the remaining one-third were at rivers or streams. Based on studies conducted in the northeastern United States, Kaval and Loomis (2003) estimated an average consumer surplus value per day of \$35.91 for recreational fishing (in 2007 dollars). Therefore, the implied total annual value of freshwater fishing in the northeastern United States was \$5.06 billion in 2006.

### **2.1.3 Regulating Services**

In general, inland surface waters such as lakes, rivers, and streams provide a number of regulating services, such as hydrological regime regulation and climate regulation. There is little evidence that acidification of freshwaters in the northeastern United States has significantly degraded these specific services; however, freshwater ecosystems also provide biological control services by providing environments that sustain delicate aquatic food chains. The toxic effects of acidification on fish and other aquatic life impair these services by disrupting the trophic structure of surface waters (Driscoll et al., 2001). Although it is difficult to quantify these services and how they are affected by acidification, it is worth noting that some of these services may be captured through measures of provisioning and cultural services. For example, these biological control services may serve as “intermediate” inputs that support the production of “final” recreational fishing and other cultural services.

## 2.2 CHANGES IN ECOSYSTEM SERVICES ASSOCIATED WITH ALTERNATIVE LEVELS OF ECOLOGICAL INDICATORS

This section estimates values for changes in ecosystem services associated with reductions in lake acidification in Adirondack State Park and in other lakes in the state of New York. Using the results of the Adirondack Case Study Area of aquatic acidification effects, the value of reducing nitrogen and sulfur deposition in the affected areas to background levels (i.e., a “zeroing out” of anthropogenic sources of nitrogen and sulfur) was estimated. Although this scenario is not realistic from a policy perspective, it allows the examination of the upper bound of ecosystem service gains that would result from reducing the number of acidified (i.e., low acid neutralizing capacity [ANC]) lakes to the lowest possible level.

**Table 2.2-1.** Participation in Freshwater Recreational Fishing in Northeastern States in 2006

State	Participation Rates by State Residents <sup>a</sup>	Activity Days by Residents and Nonresidents (in thousands)		
		Ponds, Lakes, or Reservoirs	Rivers or Streams	Total
Connecticut	7.3%	2,856	2,409	5,265
Delaware	6.4%	764	770	1,534
Illinois	9.5%	10,318	5,088	15,406
Indiana	13.8%	6,843	1,819	8,662
Maine	19.9%	3,734	1,521	5,255
Maryland	6.6%	2,882	2,379	5,261
Massachusetts	6.0%	4,494	978	5,472
Michigan	12.3%	15,175	4,426	19,601
New Hampshire	10.0%	2,144	627	2,771
New Jersey	4.0%	2,377	1,116	3,493
New York	4.6%	8,548	5,086	13,634
Ohio	11.6%	9,781	3,710	13,491
Pennsylvania	8.3%	7,507	6,998	14,505
Rhode Island	5.3%	504	104	608
Vermont	13.2%	1,264	453	1,717
West Virginia	20.9%	3,069	3,617	6,686
Wisconsin	21.4%	13,026	4,439	17,465
Total	9.3%	95,286	45,540	140,826

<sup>a</sup> Ages 16 or older.

Source: U.S. Department of the Interior (DOI), Fish and Wildlife Service, and U.S. Department of Commerce, U.S. Census Bureau, 2007.

The case study analysis focused on 44 lakes in the Adirondacks. It estimated ANC levels at each of these lakes under the alternative scenarios shown in **Table 2.2-2**. Using the MAGIC model, it predicted median ANC levels for the years 2005, 2020, 2050, and 2100 under “business-as-usual” conditions (i.e., accounting for expected emission controls associated with Title IV regulations but no additional measures to reduce nitrogen and sulfur deposition). In contrast, the model run for the year 1860 represents ANC levels for “background” conditions by simulating the effect of zeroing out anthropogenic sources of nitrogen and S.

**Table 2.2-2.** Acid Neutralizing Capacity Levels (in µeq/L) at 44 MAGIC-Modeled Lakes in the Adirondacks

Year:	Observed	MAGIC Model Simulations				
	2002	2005	2020 <sup>a</sup>	2050 <sup>a</sup>	2100 <sup>a</sup>	1860 <sup>b</sup>
Lake Name	(“Background”)					
Clear Pond (61)	218.1	233.0	243.2	246.7	247.6	290.3
Long Pond (65)	66.1	73.5	78.3	80.4	81.2	106.4
Hope Pond	62.6	72.9	78.4	81.1	82.8	126.5
Second Pond	71.3	75.8	77.0	75.3	72.5	121.5
Squaw Lake	19.5	25.6	27.1	24.9	21.3	73.8
Indian Lake	−8.0	1.4	6.2	6.2	5.1	52.2
Big Alderbed	57.4	67.5	72.6	74.5	75.6	124.1
Long Lake	−32.1	−20.8	−15.4	−16.0	−17.6	34.4
Gull Pond	160.9	166.8	170.7	173.0	174.6	208.8
Little Lilly Pond	47.0	54.4	57.9	58.5	58.6	95.5
Upper Sister Lake	31.0	37.4	39.9	39.4	38.0	80.3
Dry Channel Pond	23.8	31.7	34.3	33.2	31.6	78.6
Bennett Lake	33.0	37.5	39.2	37.8	35.0	69.7
Effley Falls Pond	50.8	59.8	64.2	64.2	63.7	132.4
Parmeter Pond	75.6	85.7	91.7	94.3	95.4	134.8
North Lake	−1.6	6.9	10.9	10.0	8.1	66.0
Razorback Pond	33.2	39.6	42.4	40.5	37.4	94.3
Snake Pond	3.6	12.3	15.5	14.5	13.4	78.5
South Lake	−7.7	0.1	3.7	2.3	−0.2	56.6
Boottree Pond	53.2	59.0	63.2	65.3	66.1	84.5
Horseshoe Pond	51.4	63.0	70.0	73.4	74.8	117.6
Rock Pond	86.7	95.1	98.8	99.5	99.5	151.5
Antediluvian Pond	66.2	70.1	72.0	71.4	69.9	95.3
Seven Sisters Pond	−14.1	−9.1	−6.9	−7.2	−8.1	21.9

Year:	Observed	MAGIC Model Simulations				
	2002	2005	2020 <sup>a</sup>	2050 <sup>a</sup>	2100 <sup>a</sup>	1860 <sup>b</sup>
Lake Name	("Background")					
Canada Lake	53.8	69.4	77.6	80.1	81.4	151.2
Bickford Pond	19.9	33.6	41.3	45.2	46.9	101.3
Wolf Pond	-5.7	4.8	9.8	11.2	11.9	58.3
Blue Mountain Lake	118.0	126.7	129.3	127.8	125.2	184.3
Carry Falls Reservoir	121.2	133.2	140.8	144.1	145.8	205.8
Rocky Lake	43.7	58.6	66.3	68.3	68.8	113.7
Bog Pond	88.2	107.0	117.2	120.5	121.6	178.1
Clear Pond (82)	85.9	97.1	104.1	107.4	108.2	145.6
Seventh Lake	198.4	217.3	223.4	227.1	229.1	317.6
Trout Pond	39.9	53.4	61.9	65.7	67.6	127.2
Hitchins Pond	150.2	162.7	170.0	172.6	173.8	214.7
Piseco Lake	98.2	114.7	123.7	127.2	128.6	186.2
Mccuen Pond	37.6	46.0	50.2	51.7	52.4	90.0
Arbutus Pond	88.0	101.6	108.6	111.3	113.1	187.1
Witchhopple Lake	27.2	35.7	39.4	38.9	37.6	91.7
Willys Lake	-48.4	-38.8	-33.5	-33.3	-33.4	47.5
Lower Beech Ridge Pond	-19.6	-10.8	-6.9	-7.4	-8.8	41.5
Dismal Pond	-23.6	-12.0	-7.6	-7.3	-7.6	40.4
Payne Lake	53.5	56.2	58.1	59.0	59.4	75.1
Whitney Lake	22.3	30.7	33.7	32.9	31.5	84.3

<sup>a</sup> Based on predicted future scenarios for nitrogen+sulfur deposition, accounting for Title IV emissions controls.

<sup>b</sup> Represents background levels and levels that would eventually result from a "zero-out" of anthropogenic sources of nitrogen+sulfur deposition.

In the following subsections, ecosystem service gains associated with going from the business-as-usual reference conditions to the zero-out condition are estimated. It was assumed that the zero out of nitrogen and sulfur deposition would occur in 2010 and that it would take 10 years for the full effect of these reductions on lake ANC levels to occur. In other words, by the year 2020, lake ANC levels would increase and fully return to their estimated 1860 background levels, as shown in Table 2.2-2.

In Section 2.2.1, a model that focuses specifically on recreational fishing services is applied, and the value of current and future enhancements to these services from Adirondack and other New York lakes is estimated. In Section 2.2.2, a model that takes a broader perspective on



ecosystem services is applied, and the value of improving all of the ecosystem services that are affected by acidification of Adirondack lakes is estimated.

In both cases, the analysis focuses on ANC and evaluates the sensitivity of different ANC thresholds for aquatic functioning. In general, moderate shifts in ANC levels may result in changes in species composition, where acid-sensitive species are replaced by less sensitive species. At more extreme acidification levels, however, species richness, defined as the total number of species occupying a system, may be affected. Research has shown that the number of fish species present is positively correlated with ANC (Driscoll et al., 2003). In the Adirondacks, recent research indicates that aquatic biota begin to exhibit effects at an ANC of 50 microequivalents per liter ( $\mu\text{eq/L}$ ) (Chen and Driscoll, 2004). Uncertainty exists regarding threshold levels of ANC: the levels at which predictable effects occur. Several ANC thresholds have been observed, however, at which lakes and fish are affected, as summarized in **Figure 2.2-1**. To account for the uncertainty in the threshold level of acidification above which Adirondack lakes may support recreational fishing, this analysis considers three threshold levels: 20  $\mu\text{eq/L}$ , 50  $\mu\text{eq/L}$ , and 100  $\mu\text{eq/L}$ .

ANC THRESHOLD VALUES ( $\mu\text{eq/L}$ )

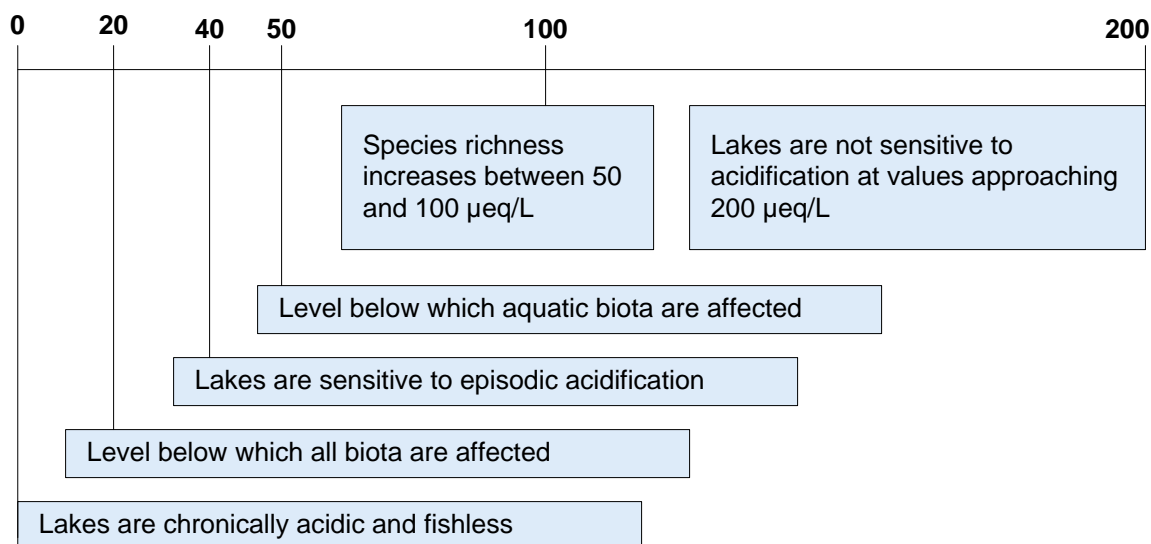


**Figure 2.2-1.** Summary of Acid Neutralizing Capacity Values Relevant for Lake and Fish Health (Source: Industrial Economics, Inc., 2008).

### **2.2.1 Improvements in Recreational Fishing Services due to Increased Acid Neutralizing Capacity Levels in Adirondack and Other New York Lakes**

To estimate the value of improved services, this analysis relied on commonly accepted economic models to relate the predicted changes in lake acidity to a change in recreational fishing behavior throughout the study area. First, a random effects model was used to extrapolate lake ANC levels from the ecological model forecast for a subset of lakes to a broader suite of regional lakes. This random effect model does this by relating acidification levels to lake characteristics and geographic location. That is, the forecast ANC levels of the lakes modeled in MAGIC for each year in the study period are tied to explanatory variables so that the forecast changes in ANC can be extrapolated to other potentially affected lakes in the region. This model was first applied to forecast ANC levels at lakes in the Adirondack region and then repeated to forecast ANC levels for lakes in New York State (with the exception of New York City). The result of this effort is a full time-series dataset of ANC levels for Adirondack and New York State lakes.

The second economic model applied describes changes in behavior of recreational fishers in response to changes in lake acidification levels. This step of the process relies on the assumption that below the specified ANC threshold (of 20 µeq/L, 50 µeq/L, or 100 µeq/L) lakes are no longer fishable. The specific type of model applied here is a “discrete choice model.” Generally, a discrete choice model predicts a binary decision (which may be thought of as “yes” or “no”) regarding whether to fish at a given site made by an individual as a function of a number of independent variables (Greene, 2003). The independent variable is the catch rate at the water body (itself a function of lake acidity). Additional independent variables may include travel time required to reach the site and the concentration of fisherman at the site, among others.

A specific form of discrete choice model called a “random utility model,” or RUM is applied. In the study of economics, utility is defined as a measure of the happiness or satisfaction gained from a good or service. In keeping with the tenets of neoclassical economics, this utility is sought to be maximized subject to a constraint (often represented by income or time). Put more simply, the model assumes that the fisherman will seek the most happiness at the lowest cost. Section 2 describes the application of these models and the results of this analysis.

### **2.2.1.1 Analytic Method**

The following steps were followed to connect the modeled changes in lake ANC levels to the benefits of improved recreational fishing services.

#### **Step 1: Development of the Random Effects Model**

To develop this model, it was first necessary to compare the subset of lakes considered in the ecological model (see Table 2.2-2) with the subset of lakes included in the database of lake characteristics contained within the RUM. Nine of the 44 lakes were not usable for the analysis because they did not appear in the database of lake characteristics within the RUM.<sup>4</sup> As a result, the analysis relied on data for a subset of 35 Adirondack lakes.

Because forecasted ANC levels were provided for the 35 lakes only, the next step of the analysis was extrapolating these forecasts to the broader suite of lakes within the Adirondack region. To this end, a random effects model was developed to determine the statistical relationship between the lakes' ANC levels and their characteristics. Significant uncertainty exists regarding the relationships between lake characteristics and ANC levels. Ecologists at the Environmental Protection Agency (EPA) are researching the characteristics that best explain a lake's sensitivity to acidification.

The random effects model used in this analysis to forecasted lake ANC levels was also limited by the lake characteristic data that are currently available; in this case, elevation, surface area, shoreline, and county location were considered as potential explanatory variables in forecasting ANC levels. The relationship between these characteristics and the forecast ANC levels for the 35 lakes informed the extrapolation of the results from the MAGIC model to the broader population of lakes, first in the Adirondack region and then in New York State. These variables that describe the lake characteristic and geographic location are the explanatory variables in the model. The random effects model helps identify the influences of these explanatory variables, net of other factors that are unknown and cannot be controlled.<sup>5</sup>

---

<sup>4</sup>Those lakes excluded include the following: Bickford Pond, Bog Pond, Hope Pond, Little Lilly Pond, Lower Beech Ridge, Razorback Pond, Seven Sisters Pond, Snake Pond, and Witchhopple Lake.

<sup>5</sup> Several important conditions must be satisfied for the random effects model to be appropriate. In this case, these conditions are met. For both models, the Breusch-Pagan test for random effects rejects the null hypothesis of no random effects in the data. The Hausman specification test (against a fixed effects alternative) rejects the null hypothesis of systematic differences between random and fixed effects models for the Clean Air Interstate Rule (CAIR) and t variables, which indicates that omitted variables are not biasing the coefficients for those variables.

The model cannot perfectly predict ANC levels in lakes; there are not enough available data and there is no existing knowledge about the best determinants of ANC levels. Given that there is some uncertainty and limited information available to explain ANC levels, a method must be used that can remove the net effects of the unknown data and identify the effects of the available information. The random effects model generates estimates of the net effects of the explanatory variables.

Furthermore, random effects models are appropriate for situations where the study sample is a random sample of a larger universe and one wishes to make inferences about the larger universe of data (Kennedy, 2003).<sup>6</sup> In this case, the group of lakes analyzed is sampled from the total number of lakes for which ANC levels are forecast (the lakes to which the ANC levels are forecast is the universe).

The modeled ANC levels for the 35 aforementioned lakes, along with the lake characteristic information, served as inputs for a random effects regression analysis to isolate the impact of each variable on ANC. **Table 2.2-3** details the results of the random effects model.

**Table 2.2-3.** Random Effects Model Results

Variable	Coefficient	Std. Error
constant	-106.171	75.050
elevation	-0.047	0.128
area	0.125	0.074
ln(shoreline)	-36.005	18.802
T	0.108	0.013
Hamilton	9.430	27.760
Essex	55.149	46.894
Fulton	-16.793	80.273
Franklin	49.538	39.176
Herkimer	-38.655	40.142
Lewis	-19.160	45.899
Warren	24.924	66.423

<sup>6</sup> This criterion assumes that there are no omitted variable effects present; the previous footnote explains that there is no evidence of this.

Variables describing elevation, total area, and shoreline length were included to capture physical differences between lakes. While the coefficients are not statistically significant, the variables do lend some explanatory power to the model. The variable identified as “T” is an annual time trend included to capture changes through time manifested in the greater system and not a specific lake. The final seven variables listed in the table are binary variables indicating the counties in which the lakes occur. The omitted variable is for St. Lawrence County. These variables are intended as a proxy for a host of location-specific factors, including subsurface geology and degree of forest cover because data were not available for these variables.

### **Step 2: Extrapolation to All Lakes in Adirondack Region/New York State**

The Montgomery-Needelman RUM includes lake characteristic data for a total of 2,586 lakes in New York State. As described previously, the MAGIC model predicts ANC levels for 35 lakes within the Adirondack region that could be included in the random effects model. These 35 lakes are located in Hamilton, Essex, Fulton, Franklin, Herkimer, Lewis, Warren, and St. Lawrence counties. Their explanatory value for lakes outside of this eight-county region is uncertain. Therefore, this study performed a “tiered” extrapolation, where the random effects model results were first extrapolated only to lakes in the Adirondack region represented by the modeled lakes; this exercise was then repeated for the full suite of New York State lakes.

For the first tier (for the Adirondack region), the analysis was limited by two dimensions: (1) only including lakes within the eight counties containing the 35 modeled lakes and (2) limiting the analysis to lakes within the size range of the modeled lakes. Because none of the 35 modeled lakes occur in Clinton, Saratoga, and Oneida counties (all within the Adirondack region), this analysis did not apply the model to forecast lake acidification in these three counties. This assumption may lead to an understatement of the total benefits associated with decreased lake acidification in the Adirondack region, but it avoids some uncertainty associated with extrapolating ANC outside of the scope of the modeled region.

The second tier of the analysis (for all of New York State except New York City) was also limited to consider only lakes within the size range of the modeled lakes. This portion of the analysis required consideration of lakes outside of the eight-county geographic scope, however. Therefore, an average of the eight-county binary variable coefficients for all lakes outside of the eight counties was used. Further, as with the first tier of the analysis, all lakes with an area

greater than the largest lake in the ecological subset of 35 were “hardwired” to be unimpaired, because changes in their ANC levels are unlikely to be represented by the subset of modeled lakes.<sup>7</sup> A total of 62 lake sites were determined to be too large to be represented by the sample MAGIC data and were, therefore, hardwired.

### **Step 3: Application of ANC Thresholds**

This analysis employs three ANC threshold assumptions—20 µeq/L, 50 µeq/L, and 100 µeq/L—to indicate whether a lake is fishable. A lake was deemed to be affected if it was above the threshold (fishable) in the “zero-out” scenario and below the threshold (impaired) in the baseline scenario. As previously described and shown in Table 2.2-2, zero-out conditions are defined by lake ANC levels in the year 1860 as estimated by MAGIC. MAGIC provided these data for the subset of 35 lakes within the Adirondack region. To determine zero-out conditions for the broader suite of lakes in the Adirondacks and in New York State, a simple ordinary least squares (OLS) regression was run to determine whether lake size is a reasonable indicator of the difference between the observed ANC level in 2002 and the pristine condition in 1860 for the 35 lakes. This analysis determined that no statistically significant relationship existed. Therefore, an average difference in ANC level between the 2002 observed level and the 1860 pristine condition for the 35 lakes was calculated; the average difference is 64.6 µeq/L. This average difference was then added to the 2002 ANC levels for each lake (forecast by extrapolation using the random effects model), and the resulting value was considered to be the “pristine” ANC value in 2020, 2050, and 2100.

**Table 2.2-4** reports the number of “impacted” lakes in each year, where impact means that the lake is predicted to be below the ANC threshold under business-as-usual conditions and above the threshold under zero-out conditions. This definition of impacted lakes is needed because the RUM framework only estimates benefits accruing from lakes that switch from nonfishable to fishable status. The lake counts for 2005 are zero because in this year no change

---

<sup>7</sup> Hardwired lakes (in order of decreasing size) include Lake Ontario, Lake Erie, Great Sacandaga Lake, Oneida Lake, Seneca Lake, Lake Champlain, Cayuga Lake, Lake George, Canandaigua Lake, Ashokan Reservoir, Cranberry Lake, Owasco Lake, Chautauqua Lake, Tupper Lake, Stillwater Reservoir, Keuka Lake, Pepacton Reservoir, Allegheny Reservoir, Raquette Lake, Cannonsville Reservoir, Indian Lake, Skaneateles Lake, Black Lake, Long Lake, Otsego Lake, Saratoga Lake, Mount Morris Reservoir, Salmon River Reservoir, Great Sodus Bay, Conesus Lake, Whitney Point Reservoir, and Onondaga Lake.

occurs in ANC level relative to the baseline (i.e., the reduction in emissions beginning the return to pristine conditions was not assumed to have occurred in those years). The zero-out scenario was assumed to be implemented in 2010, with lakes reaching their pristine conditions by 2020. It should be noted that the nature of this model allows for lakes to switch between impaired and unimpaired between years. As a result, the lake counts reported in Table 2.2-4 are not cumulative counts and, in fact, may reflect different subsets of lakes.

#### **Step 4: Application of the Random Utility Model**

The Montgomery-Needelman model applied in this analysis is a repeated discrete choice RUM that describes lake fishing behavior of New York residents (Montgomery and Needelman, 1997). In particular, the model characterizes decisions regarding (1) the number of lake fishing trips to take each season and (2) the specific lake sites to visit on each fishing trip. The model can be used to develop estimates of economic losses or gains associated with changes in the set of lakes available to anglers.

**Table 2.2-4.** Count of Impacted Lakes

ANC Threshold (in µeq/L)	Year	Lake Count	
		Adirondack Region	New York State
20	2005	0	0
20	2020	107	110
20	2050	95	97
20	2100	74	75
50	2005	0	0
50	2020	244	365
50	2050	222	316
50	2100	200	254
100	2005	0	0
100	2020	430	1,500
100	2050	404	1,399
100	2100	354	1,228

Note: There are 1,076 lakes in the “Adirondack Region” and 2,586 lakes in New York State (less New York City).

The data used to estimate the RUM were obtained from a 1989 repeat-contact telephone survey of New York residents conducted as part of the National Acid Precipitation and

Assessment Program (NAPAP).<sup>8</sup> This survey provided information on the destinations of anglers' fishing trips (day trips only) taken during the 1989 fishing season. The survey data were supplemented with lake characteristics data obtained from New York State Department of Environmental Conservation's (NYSDEC's) *Characteristics of New York State Lakes: Gazetteer of Lakes and Ponds and Reservoirs*, New York State's *Fishing Guide*, and New York's 305(b) report for 1990. Travel distances between anglers' homes and lake fishing sites were calculated using Hyways/Byways. The model and data used in the present analysis are described in greater detail in a 1997 journal article by Montgomery and Needelman.<sup>9</sup>

The list of affected lakes generated in the previous step serves as the primary input to the RUM. The model estimates the economic welfare value of enhancements to recreational fishing services derived from shifting specific lakes from nonfishable to fishable status.<sup>10</sup> The economic benefits estimates represent New York State residents' average willingness to pay (WTP) to improve recreational fishing services by reducing lake acidification levels. **Table 2.2-5** reports the estimated per capita values generated by the RUM. These values have been adjusted from 1989 dollars to 2007 dollars using the Consumer Price Index-All Urban Consumers (CPI-U). Note that the zero-out scenario is assumed to begin at the end of 2010; therefore, the benefits do not begin to accrue until the following year, and they are zero in 2005 and 2010.

**Table 2.2-5.** Per Capita Willingness to Pay (2007 \$)

ANC Threshold (in µeq/L)	Year	Per Capita Benefits of a Return to Pristine Conditions by 2020	
		Adirondack Region	New York State
20	2005	\$0.00	\$0.00
20	2010	\$0.00	\$0.00
20	2020	\$0.41	\$0.47
20	2050	\$0.34	\$0.38
20	2100	\$0.28	\$0.32
50	2005	\$0.00	\$0.00

<sup>8</sup> New York City counties were excluded from the sampling frame.

<sup>9</sup> The published version of the model has had several minor updates, all of which have been discussed with Mark Montgomery.

<sup>10</sup> Since the RUM uses travel distances and travel costs to infer economic values, the benefit estimates are sensitive to the spatial locations and distributions of the impacted lakes (i.e., the benefit estimates do not depend only on the number or percentage of lakes impacted).



ANC Threshold (in µeq/L)	Year	Per Capita Benefits of a Return to Pristine Conditions by 2020	
		Adirondack Region	New York State
50	2010	\$0.00	\$0.00
50	2020	\$0.74	\$2.55
50	2050	\$0.73	\$2.26
50	2100	\$0.70	\$1.47
100	2005	\$0.00	\$0.00
100	2010	\$0.00	\$0.00
100	2020	\$0.79	\$11.05
100	2050	\$0.77	\$10.61
100	2100	\$0.68	\$9.40

### Step 5: Interpolation of RUM Output

The RUM provided per capita loss estimates (reported in 1989 nominal dollars) for 2010, 2020, 2050, and 2100.<sup>11</sup> Rather than running this model separately for each year, estimates for the intervening years (between the four point estimates provided by the RUM) were generated via simple linear interpolations.

### Step 6: Estimation of Aggregate Benefits through Application of Per Capita Results to Affected Population

To estimate aggregate benefits for New York residents, the per capita benefit estimates must be multiplied by the corresponding population of residents. To match the characteristics of the population surveyed in developing the RUM, this analysis required estimating the population of New York State that will be over 18 years old and reside outside of New York City for each year from 2011 through 2100. The U.S. Census Bureau provides estimated population figures for 2002 through 2008 and projected population through 2030 at the state level. Absent projection information, the population was held constant from 2030 through the period of the analysis (through 2100). The ratio of the New York State population residing *outside* New York City (that is, the five counties of Bronx County, Kings County, New York County, Queens County,

<sup>11</sup> As mentioned previously, the CPI-U, provided by the U.S. Bureau of Labor Statistics, was used to inflate these estimates to 2007 dollars.

and Richmond County) was calculated for 2006 and assumed to remain constant throughout the analysis. The U.S. Census also estimates and projects the 18+ population at the state level through 2030. The 18+ population was held constant from 2030 through the end of the analysis in 2100. The ratio of adults (18+) to the entire population was calculated for New York State, and that ratio was applied to the population residing outside New York City.

### **2.2.1.2 Results**

**Table 2.2-6** summarizes the estimated present value and annualized benefits for each acidification threshold assumption applying discount rates of 3% and 7%. The estimated present value of benefits in 2010 range from \$60.1 million to \$298.7 million depending on the threshold and discount rate assumptions applied. In comparison, a previous study of the recreational fishing benefits in the Adirondacks associated with the Clean Air Act Amendments (CAAA) estimated benefits ranging from \$13.7 million to \$100.6 million (EPA, Office of Air and Radiation, 1999).<sup>12</sup> Annualizing these benefits over the period 2010 to 2100 results in annual benefit estimates ranging from \$3.9 million to \$9.3 million per year. Six tables containing detailed results for each scenario (threshold assumption and geographic scope) by year are included in Attachment A.

**Table 2.2-7** describes total present value and annualized benefits associated with reduced lake acidification in all of New York State. Estimated present value benefits in 2010 range from \$68.3 million to \$4.16 billion, depending on the threshold and discount rate assumptions applied. Annualizing these benefits over the period 2010 to 2100 results in annual benefit estimates ranging from \$4.5 million to \$130 million per year.

**Table 2.2-6. Present Value and Annualized Benefits, Adirondack Region**

ANC Threshold (in µeq/L)	Present Value Benefits <sup>a</sup> (in million of 2007 dollars)		Annualized Benefits <sup>b</sup> (in million of 2007 dollars)	
	3% Discount Rate	7% Discount Rate	3% Discount Rate	7% Discount Rate
20	\$142.59	\$60.05	\$4.46	\$3.94
50	\$285.15	\$114.18	\$8.91	\$7.49

<sup>12</sup> For comparison to the results in our analysis, presented in 2007 dollars, the estimated benefits from the Clean Air Act report were inflated from 1999 to 2007 dollars using the GDP deflator (<http://www.bea.gov/bea/dn/nipaweb/SelectTable.asp?Selected=Y>).

ANC Threshold (in µeq/L)	Present Value Benefits <sup>a</sup> (in million of 2007 dollars)		Annualized Benefits <sup>b</sup> (in million of 2007 dollars)	
	3% Discount Rate	7% Discount Rate	3% Discount Rate	7% Discount Rate
100	\$298.67	\$120.61	\$9.33	\$7.91

<sup>a</sup> Annual benefits for 2010 to 2100 discounted to 2010.

<sup>b</sup> Present value benefits annualized over 2009 to 2100.

**Table 2.2-7.** Present Value and Annualized Benefits, New York State

ANC Threshold (in µeq/L)	Present Value Benefits <sup>a</sup> (in million of 2007 dollars)		Annualized Benefits <sup>b</sup> (in million of 2007 dollars)	
	3% Discount Rate	7% Discount Rate	3% Discount Rate	7% Discount Rate
20	\$161.76	\$68.34	\$5.05	\$4.48
50	\$897.20	\$378.00	\$28.04	\$24.78
100	\$4,159.64	\$1,685.80	\$129.98	\$110.52

<sup>a</sup> Annual benefits for 2010 to 2100 discounted to 2010.

<sup>b</sup> Present value benefits annualized over 2010 to 2100.

### 2.2.1.3 Assumptions and Caveats

The following assumptions and caveats are particularly important for interpreting the results and the application of the ecological model for lake acidification:

- This analysis assumed that the level of impairment is binary as applied to a specific lake: that is, the ANC threshold indicates whether a lake is fishable.
- The available literature suggests that ANC levels between 20 and 100 cover the range where ecological effects are realized. Three points within this range (20, 50, and 100) were tested as point estimates at which the fishability of lakes is affected.
- This analysis assumed that the 35 modeled lakes are a representative subset of lakes in the Adirondacks (for the first tier of the analysis) and in New York State (for the second tier of the analysis).
- This analysis used the ANC levels of the 35 modeled lakes in the year 1860 as a proxy for “pristine” acidification levels.
- In the first tier, the analysis is not used to forecast acidification effects in Clinton, Saratoga, and Oneida counties, which are generally considered to be part of the

Adirondack region because they are not represented by the subset of lakes subject to the ecological model. This restriction contributes to an underestimation of total benefits.

- Pristine ANC levels for the full population of New York State lakes are estimated by first finding the average difference between 2002 observed ANC levels and the 1860 ANC values for the 35 lakes modeled by MAGIC and then adding this average difference to the 2002 ANC values for all lakes (as estimated by extrapolating using the random effects model). The ANC levels assumed to represent pristine lake conditions are therefore subject to significant uncertainty.

The following assumptions and caveats are particularly important for interpreting the application of the RUM model for estimating recreational fishing benefits to New York residents:

- The RUM only considers the behavior of New York State residents. It may be reasonable to assume that residents of neighboring jurisdictions (the Canadian provinces of Ontario and Quebec, along with the State of Vermont) may also take day trips to these lakes and respond in a rational manner comparable to New York State residents. This restriction contributes to an underestimation of benefits.
- The output of the RUM is on a per capita basis. The results are presented in terms of impacts to the entire population. This requires an extrapolation of the population through 2100. Absent specific projection information beyond 2030, the population was held constant beyond this year.
- This analysis assumed that the demand for fishing, in other words, an individual's propensity to fish, has remained constant from the time of the survey underlying the RUM to the present. That is, this analysis does not account for any potential change in interest in both recreational fishing and park use since the survey was conducted in 1989. In the case that general demand for recreational fishing has decreased, this analysis may overstate benefits. This restriction contributes to an overestimation of benefits.
- This analysis did not take into account income adjustments through time. The RUM holds income to be constant and a lack of detailed demand elasticity functions precludes the incorporation of an adjustment. Other EPA analyses have shown that increases in real income over time lead to increases in WTP for a wide range of health effects and some

welfare effects, such as recreational visibility. This restriction contributes to an underestimation of benefits.

### **2.2.2 Improvements in Total Ecosystem Services due to Increased Acid Neutralizing Capacity Levels in Adirondack Lakes**

To develop estimates of the overarching ecological benefits associated with reducing lake acidification levels in Adirondacks National Park, researchers at Resources for the Future (RFF) conducted a detailed contingent valuation (CV) survey (Banzhaf et al., 2006). Unlike other valuation studies described in this report, the RFF study did not identify the specific categories of ecosystem services that would be enhanced by improving aquatic conditions. Rather, the survey described and elicited values for specific improvements in acidification-related water quality and ecological conditions in Adirondack lakes. For this reason, and because the survey was administered to a random sample of New York households, in this section the benefit estimates from the RFF study are interpreted as measures that incorporate values for *all* ecosystem services adversely affected by lake acidification.

In this section, the RFF study results were adapted and transferred to estimate the ecological benefits of the zero-out scenario for Adirondack lakes. The fundamental benefit transfer model can be summarized as follows:

$$AggB_{lAdr} = WTP_{Adr} * N_{NY} * \Delta\%IL , \quad (2.1)$$

where

$AggB_{Adr}$  = aggregate annual benefits (in 2007 dollars) to New York households in 2010 due to lake ecosystem improvements resulting from the zero-out scenario,

$WTP_{Adr}$  = average annual household WTP (in 2007 dollars) per unit of long-term change in the percentage of Adirondack lakes impaired by acidification,

$N_{NY}$  = projected total number of households in New York in 2010, and

$\Delta\%IL$  = long-term change in the percentage of Adirondack lakes impaired by acidification as a result of the zero-out scenario.

To develop estimates of  $WTP_{Adr}$ , the estimates from the RFF study were used with results reported in Banzhaf et al. (2006). The CV survey for the study was distributed to a random sample of nearly 6,000 New York residents in 2003 to 2004 through the Internet and mail. As part of the design and development of the survey instrument, experts were interviewed on the

ecological damages, and a summary of the science was used as the foundation for the description of the park's existing condition and the hypothetical changes to be valued. The scientific review indicated that there was significant uncertainty regarding the future status of lakes in the Park in the absence of specific programs to improve lake acidification conditions. To bracket the range of uncertainty in the science as well as to test the sensitivity of respondents' WTP to the scale of ecological improvements, two versions of the survey instrument were developed and randomly administered to separate subsamples.

**Table 2.2-8** summarizes key features of the two survey versions. In both survey versions, respondents were provided with information on the current (circa 2004) condition of the 3,000 lakes in the Park. Both versions describe half (1,500) of them as "lakes of concern" (i.e., unhealthy lakes where "fish and other aquatic life have been reduced or eliminated because of air pollution in the past"), and both versions propose policies that would improve the lakes over a period of 10 years (using lime to neutralize the excess acidity).

**Table 2.2-8.** Comparison of Resources for the Future Contingent Valuation Scenarios and EPA Zero-Out Scenario

Percentage of Adirondack Lakes that Are "Unhealthy"				
	Current (A)	Future		
		No Program <sup>a</sup> (B)	With Program <sup>b</sup> (C)	Reduction (B) – (C)
RFF "Base" Scenario	Year = 2004	Year = 2014		
	50%	50%	30%	20%
RFF "Scope" Scenario	Year = 2004	Year = 2014		
	50%	55%	10%	45%
EPA "Zero-Out" Scenario	ANC Threshold    Year = 2010	Year = 2020		
	20 µeq/L    22%	22%	0%	22%
	50 µeq/L    43%	42%	11%	31%
	100 µeq/L    79%	77%	51%	26%

<sup>a</sup> Business-as-usual conditions.

<sup>b</sup> Lake liming program for the RFF survey scenarios and a zero-out policy for the EPA scenario.

The “base” version of the survey asserts that, in the absence of any direct policy intervention, the condition of the 1,500 unhealthy lakes and 1,500 healthy lakes is expected to remain unchanged over the next 10 years. However, if a liming program is undertaken, it would improve 20% (600) of the lakes in the Park relative to their expected 2014 condition without the program.

In contrast, the “scope” version describes a gradually worsening status quo without the liming program, in which 5% (150) of the healthy lakes are expected to gradually become unhealthy. In other words, without the program, 55% (1,650) of the lakes would be unhealthy in 2014. With the liming program, however, only 10% of the lakes would be unhealthy in 2014, so the program improves 45% (1,350) of the lakes relative to their expected 2014 condition without the program.

Although scientific evidence indicates that a liming policy would not significantly improve the condition of birds and forests, pretesting of the survey indicated that respondents nonetheless tended to assume that these other benefits would occur. Therefore, to make the scenarios more acceptable to respondents, other nonlake effects were added to the two survey versions. In the base case, the red spruce (covering 3% of the forests’ area) and two aquatic bird species (common loon and hooded merganser) are said to be affected. In this version, the health of birds and forests is described as unchanged in the absence of intervention, and minor improvements are said to result from the program. In the scope version, a broader range of damages is associated with acid rain—two additional species of trees (sugar maple and white ash, all together covering 10% of forest area) and two additional birds (wood thrush and tree swallow) are said to be affected. The scope version describes a gradually worsening status quo along with large improvements due to the program.

Each respondent was presented with one of these (base or scope) policy scenarios and then asked how they would vote in a referendum on the program, if it were financed by an increase in state taxes for 10 years. To estimate the distribution of WTP, the annual tax amounts were randomly varied across respondents.

Based on a detailed analysis of the survey data, Banzhaf et al. (2006) defined a range of best WTP estimates, which were converted from 10-year annual payments to permanent annual payments using discount rates of 3% and 5%. For the base version, the best estimates ranged

from \$48 to \$107 per year per household (in 2004 dollars), and for the scope version they ranged from \$54 to \$154.

To specify values for  $WTP_{Adr}$ , these estimates were converted to 2007 dollars using the CPI and each of them was divided by the corresponding change in the percentage of lakes that are unhealthy (20% for the base version and 45% for the scope version). For the base version, the  $WTP_{Adr}$  estimates range from \$2.63 to \$5.87 per percentage decrease in unhealthy lakes, and for the scope version they range from \$1.32 to \$3.76.

To estimate  $N_{NY}$ , the Census population projection for New York for 2010 was used, which is 19.26 million people, and this amount was divided by the ratio of population size to the number of households in New York (2.69) in the year 2000 (assuming that this ratio stays constant from 2000 to 2010).

Finally, to estimate  $\Delta\%IL$  the MAGIC model results reported in Table 2.2-2 were used, and it was assumed that the distribution of ANC levels for these 44 lakes is representative of all 3,000 lakes in the Adirondacks Park. For each of the three ANC thresholds, column (A) of Table 2.2-8 reports the estimated percentage of “unhealthy” (below the ANC threshold) lakes in 2010. In columns (B) and (C), it also reports the percentage of unhealthy lakes in 2020 for the reference and zero-out conditions, respectively. In 2020, the *reduction* in the percentage of lakes that are unhealthy in the zero-out condition compared to the reference condition is 22% for the 20 µeq/L threshold. For the 50 µeq/L, and 100 µeq/L thresholds, it is 31% and 26%, respectively. These 3% reduction values were used as the main estimates of  $\Delta\%IL$ .

To estimate aggregate benefits for the zero-out scenario using the RFF survey results, it is important to use the results from the survey version that most closely match this scenario. Table 2.2-8 provides direct comparisons of the percentage of lakes that are defined as unhealthy under the different conditions and scenarios. Although both RFF survey versions use 2004 as the “current” year instead of 2010, they both use a 10-year horizon, which corresponds to the zero-out scenario. Although no direct matches exist, the closest correspondence is between the zero-out scenario assuming a 50 µeq/L threshold and the RFF scope survey. Under current and future conditions with no additional policy interventions, the RFF scope scenario assumes a small increase in unhealthy lakes from 50% to 55%, whereas the 50 µeq/L threshold is expected to result in a small decrease from 43% to 42%. With the program, the RFF scope survey describes a 45% decrease in unhealthy lakes, whereas the zero-out scenario projects a 31% decrease.



Moreover, although the RFF survey does not specify ANC thresholds, the survey's description of unhealthy lakes is arguably closest to what the science defines for a 50  $\mu\text{eq/L}$  threshold (as summarized in **Figure 2.2-1**).

### 2.2.2.1 Results: Aggregate Benefits from Reduced Acidification in Adirondack Lakes

**Table 2.2-9** reports the aggregate benefit estimates for the zero-out scenario using the 50  $\mu\text{eq/L}$  threshold. As described above, the projected long-term decrease in the percentage of unhealthy lakes ( $\Delta\%IL$ ) for this scenario is 31%. Using the range of  $WTP_{Adr}$  values from the RFF scope survey and the projected number of New York households in 2010 and applying

**Table 2.2-9.** Aggregate Benefit Estimates for the Zero-Out Scenario

ANC Threshold	Reduction in Percentage of Unhealthy Lakes $\Delta\%IL$	Range of Average Household WTP per Percentage Reduction $WTP_{Adr}$		Number of NY Households (in millions) $N_{NY}$	Range of Aggregate Benefits (in millions of 2007 dollars) $AggB_{Adr}$	
20 $\mu\text{eq/L}$	22%	\$2.63	\$5.87	7.162	\$410.6	\$916.4
50 $\mu\text{eq/L}$	31%	\$1.32	\$3.76	7.162	\$291.2	\$829.4
100 $\mu\text{eq/L}$	26%	\$2.63	\$5.87	7.162	\$491.6	\$1,097.2

Equation (2.1), the aggregate annual benefits of the zero-out scenario are estimated to range from \$291 million to \$829 million.

Table 2.2-9 also reports aggregate benefit estimates for the zero-out scenarios using the 20  $\mu\text{eq/L}$  and 100  $\mu\text{eq/L}$  thresholds for ANC. Neither of these scenarios corresponds well with the baseline descriptions of either the base or scope version of the RFF survey. The baseline percentage of unhealthy lakes using the 20  $\mu\text{eq/L}$  threshold (22%) is much lower than in either the survey version. In contrast, the percentage using the 100  $\mu\text{eq/L}$  threshold (77%) is much higher. Nevertheless, the future reductions in the percentage of unhealthy lakes (22% and 26%) are closest to the reductions described in the base version of the RFF survey. Therefore, the aggregate benefits of the zero-out scenario with these thresholds are evaluated using the range of  $WTP_{Adr}$  values from the RFF base survey. With the 20  $\mu\text{eq/L}$  threshold, the aggregate benefits are estimated to range from \$411 million to \$916 million per year. With the 100  $\mu\text{eq/L}$  threshold, the aggregate benefits are estimated to range from \$492 million to \$1.1 billion per year.

### **2.2.2.2 Limitations and Uncertainties**

The benefit transfer model summarized in Equation (2.1) estimates the aggregate benefits to New York households in 2010 due to lake ecosystem improvements resulting from the zero-out scenario. To do this, estimates from two different studies were linked and combined. The measures of improvements in lake ecosystems were obtained from the MAGIC model (as described in Table 2.2-2), and the value estimates were obtained from the RFF survey study. Uncertainties are associated with the estimates drawn from each study, and additional uncertainties arise when these estimates were combined in the analysis. Some of these main uncertainties and limitations are described below.

First, uncertainties are associated with extrapolating results from the 44 MAGIC-modeled lakes to all (roughly 3,000) Adirondack lakes. The 44 modeled lakes are drawn from a larger, randomly drawn sample of lakes; however, the representativeness of these 44 lakes for the Adirondacks as a whole is uncertain.

Second, the time frame required for the zero-out scenario to match 1860 conditions is uncertain. It was assumed that it takes 10 years for lakes to fully adjust to the reductions in nitrogen and sulfur deposition and that conditions equivalent to “background” 1860 conditions are achieved in 2020. The present value and annualized benefits would be lower if a longer time frame were assumed.

Third, there is also some uncertainty related to the exact types of ecosystem services that are included in these RFF study values, particularly regarding provisioning and regulating services, which survey respondents may have been less likely to consider when formulating responses to the CV questions. Importantly though, the values estimated by the RFF study are likely to include (1) recreational fishing services, which means *they cannot be added to the RUM results*, and (2) other cultural services, in particular recreational and nonuse services.

Fourth, the inclusion of other ecosystem changes (trees, birds, etc.) in the RFF CV survey scenarios implies that respondents’ stated values will overstate WTP for just changes in lake acidification. This feature, therefore, contributes to potential overestimation of benefits.

Fifth, the lack of direct correspondence between the RFF CV scenarios and the zero-out scenario requires assumptions for making the benefit transfer. In particular, baseline and future levels (percentage of unhealthy lakes) are very different from those in the RFF survey if one uses a 20 or 100 ANC threshold. Although the percentage changes are reasonably close to the RFF

20% and 45% decline scenarios, they are not exact and may not be applicable when applied to a different baseline (something that was not specifically tested in the CV survey). Rescaling the WTP estimates for different percentage changes in unhealthy lakes also requires the somewhat strong assumption that there is a constant WTP *per percentage* decline in unhealthy lakes.

Finally, the reported results only apply to Adirondack lakes and to New York residents. The Adirondack region is more sensitive to acidity in contrast to many other areas of New York State, which have calcium-rich limestone deposits that neutralize the acid. The bedrock soil and shallow soil deposits have a lower buffering capacity. These geological factors together with high and acidic precipitation levels contribute to the vulnerability of this region to acidification. The uniqueness of the Park makes simple extrapolations of ecological conditions and human values to other lakes very uncertain. Similarly, residents of other states are likely to value improved ecosystem services from Adirondack lakes, but the magnitude of these values is difficult to assess and, therefore, not included in the reported benefit estimates.

## **2.3 REFERENCES**

- Banzhaf, S., D. Burtraw, D. Evans, and A. Krupnick. 2006. "Valuation of Natural Resource Improvements in the Adirondacks." *Land Economics* 82:445-464.
- Chen, L., and C.T. Driscoll. 2004. "Modeling the Response of Soil and Surface Waters in the Adirondack and Catskill Regions of New York to Changes in Atmospheric Deposition and Historical Land Disturbance." *Atmospheric Environment* 38:4099-4109.
- Driscoll, C.T. et al. 2003. "Effects of Acidic Deposition on Forest and Aquatic Ecosystems in New York State." *Environmental Pollution* 123:327-336.
- Driscoll, C.T., G.B. Lawrence, A.J. Bulger, T.J. Butler, C.S. Cronan, C. Eagar, K.F. Lamber, G.E. Likens, J.L. Stoddard, and K.C. Weathers. 2001. Acidic Deposition in the Northeastern United States: Sources and Inputs, Ecosystem Effects and Management Strategies. *BioScience* 51:180-198.
- Greene, W.H. 2003. *Econometric Analysis, 5th Ed.* New Jersey: Prentice Hall.
- Hutchison, R., and C.E. Kraft. 1994. "Hmong Fishing Activity and Fish Consumption." *Journal of Great Lakes Research* 20(2):471-487.

- Industrial Economics, Inc. June 2008. "The Economic Impact of the Clean Air Interstate Rule on Recreational Fishing in the Adirondack Region of New York State." Prepared for the Clean Air Markets Division, Office of Air and Radiation, U.S. EPA.
- Kaval, P., and J. Loomis. 2003. *Updated Outdoor Recreation Use Values With Emphasis On National Park Recreation*. Final Report October 2003, under Cooperative Agreement CA 1200-99-009, Project number IMDE-02-0070.
- Kennedy, P. 2003. *A Guide to Econometrics*, pp. 312-313. Cambridge, MA: MIT Press.
- Millennium Ecosystem Assessment (MEA). 2005. Ecosystems and Human Well-being: Wetlands and Water. Synthesis. A Report of the Millennium Ecosystem Assessment. Washington, DC: World Resources Institute.
- Montgomery, M. and M. Needelman. 1997. "The Welfare Effects of Toxic Contamination in Freshwater Fish." *Land Economics* 73(2):211-223.
- Peterson, D.E., M.S. Kanarek, M.A. Kuykendall, J.M. Diedrich, H.A. Anderson, P.L. Remington, and T.B. Sheffy. 1994. "Fish Consumption Patterns and Blood Mercury Levels in Wisconsin Chippewa Indians." *Archives of Environmental Health* 49(1):53-58.
- U.S. Department of the Interior, Fish and Wildlife Service, and U.S. Department of Commerce, U.S. Census Bureau. 2007. *2006 National Survey of Fishing, Hunting, and Wildlife-Associated Recreation*.
- U.S. Environmental Protection Agency (EPA), Office of Air and Radiation. November 1999. The Benefits and Costs of the Clean Air Act 1990 to 2010: EPA Report to Congress. EPA-410-R-99-001. Washington, DC: U.S. Environmental Protection Agency.

### **3.0 TERRESTRIAL ACIDIFICATION**

Terrestrial acidification is the result of natural processes and anthropogenic sources of acidic deposition. Elevated levels of atmospheric deposition of nitrogen and sulfur can alter the chemical composition of soils by accelerating rates of base cation (e.g., calcium and magnesium) leaching, which depletes available plant nutrients, and by mobilizing and leaching aluminum, which can be toxic to tree roots. Consequently, among the most visible and significant effects of acid deposition are damages to forest health and resulting reductions in tree growth.

Evidence of adverse effects due to terrestrial acidification is particularly strong for two common tree species in the northeastern United States where levels of nitrogen and sulfur deposition have historically been relatively high—sugar maples and red spruce. Therefore, the discussion of ecosystem service effects focuses on these two species; however, more widespread impacts that include other tree species are also possible.

#### **3.1 OVERVIEW OF AFFECTED ECOSYSTEM SERVICES**

The existing ecosystem services that are primarily affected by the terrestrial acidification resulting from nitrogen and sulfur deposition are described and, to the extent possible, quantified using the classification system outlined in Section 1.

##### **3.1.1 Provisioning Services**

Forests in the northeastern United States provide several important and valuable provisioning services, which are reflected in measures of production and sales of tree products.

Sugar maples (also referred to as hard maples) are a particularly important commercial hardwood tree species in the United States. As shown in **Figure 3.1-1**, the main range of the sugar maple covers most of the United States east of the Mississippi River and north of Alabama and Georgia. This range is also the area with the highest levels of nitrogen and sulfur deposition in the country, according to monitored estimates from the National Atmospheric Deposition Network (NADP) and modeled estimates from the Community Multiscale Air Quality (CMAQ) modeling system.

The two main types of products derived from sugar maples are wood products and maple syrup. The wood from sugar maple trees is particularly hard, and its primary uses include

construction, furniture, and flooring (Luzadis and Gossett, 1996). According to data from the U.S. Forest Service's National Forest Inventory and Analysis (FIA) databases (<http://199.128.173.26/fido/mastf/index.html>), in 2006, the total removal of sugar maple saw timber from timberland in the United States was almost 2.12 million cubic meters. Assuming an average price of \$169.5 per cubic meter, the total value of these removals in 2006 was approximately \$358 million.

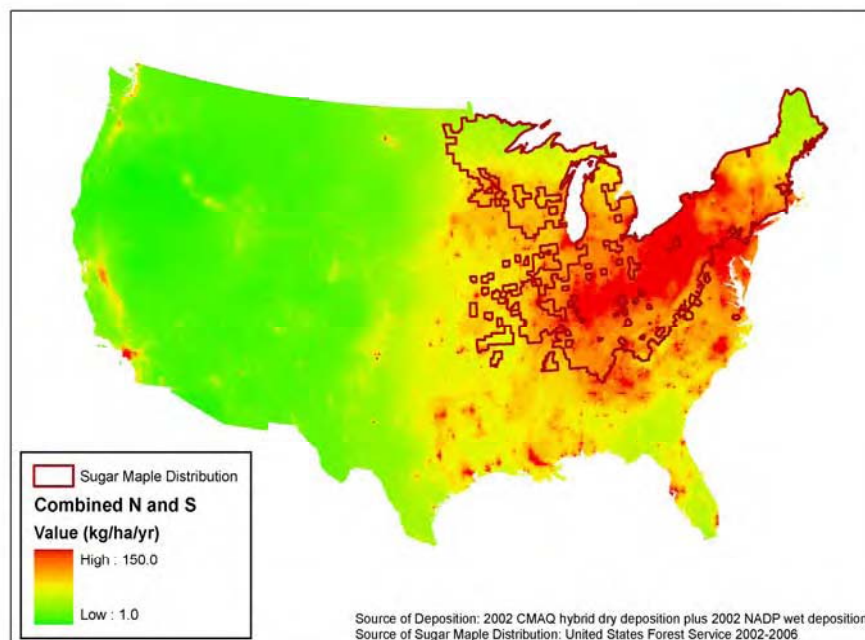


**Figure 3.1-1.** Combined Nitrogen and Sulfur Deposition (from 2002 CMAQ Dry Deposition and NADP Wet Deposition Estimates) and the Range of Sugar Maple in the United States

During winter and early spring (depending, in part, on location and diurnal temperature differences), sugar maple trees also generate sap that is used to produce maple syrup. From 2005 to 2007, annual production of maple syrup in the United States varied between 1.2 million and 5.3 million liters, which accounted for roughly 19% of worldwide production. The total annual value of U.S. production in these years varied between \$157 million and \$168 million (National Agricultural Statistics Service [NASS], 2008).

Red spruce is a common commercial softwood species. As shown in **Figure 3.1-2**, its range in the United States is much more limited than the sugar maple's range, but it also primarily grows in areas with relatively high levels of nitrogen and sulfur deposition. Red spruce

is now mainly found in northern New England, New York, and in a few high-elevation areas of the Appalachian Mountain range. Wood from red spruce is used in a variety of products including lumber, pulpwood, poles, plywood, and musical instruments. According to FIA data, in 2006, the total removal of red spruce saw timber from timberland in the United States was 0.77 million cubic meters. Assuming an average price of \$42.37 per cubic meter, the total value of these removals in 2006 was approximately \$33 million.

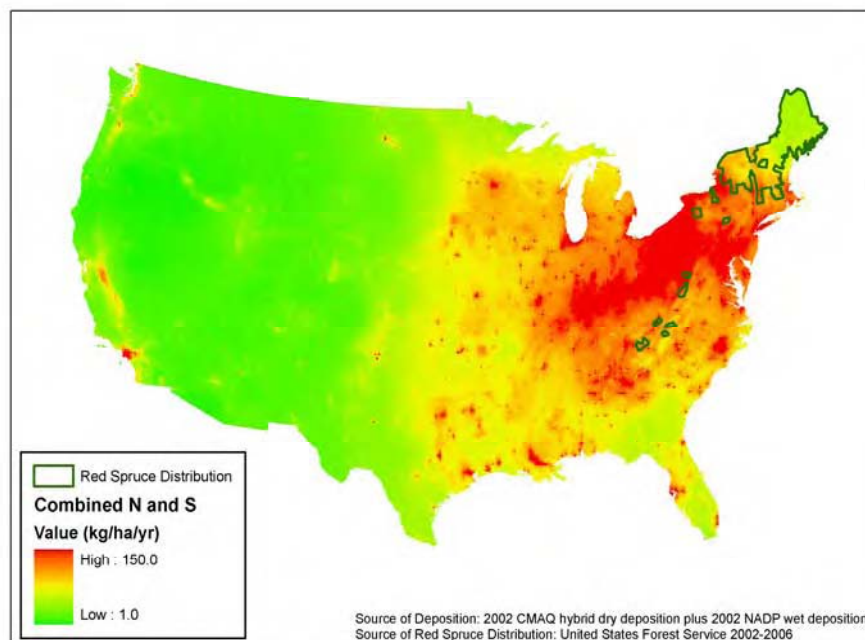


**Figure 3.1-2.** Combined Nitrogen and Sulfur Deposition (from 2002 CMAQ Dry Deposition and NADP Wet Deposition Estimates) and the Range of Red Spruce in the United States

**Figure 3.1-3** shows and compares the value of annual production of sugar maple and red spruce wood products and of maple syrup in 2006. Across states in the northeastern United States, sugar maple timber harvests consistently generated the highest total sales value of the three products. Although total sales of red spruce saw timber and maple syrup were of roughly the same magnitude in the United States as a whole, the red spruce harvest was concentrated in Maine, whereas maple syrup production was largest in Vermont and New York.

### 3.1.2 Cultural Services

Forests in the northeastern United States are also an important source of cultural ecosystem services—in particular recreational and aesthetic services. Forestlands support a wide

variety of outdoor recreational activities, including fishing, hiking, camping, off-road driving, hunting, and wildlife viewing. Regional statistics on recreational activities that are specifically forest based are not available; however, more general data on outdoor recreation provide some insights into the overall level of recreational services provided by forests. For example, most recent data from the National Survey on Recreation and the Environment (NSRE) indicate that, from 2004 to 2007, 31% of the U.S. adult (16 or older) population visited a wilderness or primitive area during the previous year, and 32% engaged in day hiking (Cordell et al., n.d.). From 1999 to 2004, 16% of adults in the northeastern United States<sup>1</sup> participated in off-road vehicle recreation, for an average of 27 days per year (Cordell et al., 2005). Using the meta-analysis results reported by Kaval and Loomis (2003), which found that the average consumer surplus value per day of off-road driving in the United States was \$25.25 (in 2007 dollars), the implied total annual value of off-road driving recreation in the northeastern United States was more than \$9.25 billion.

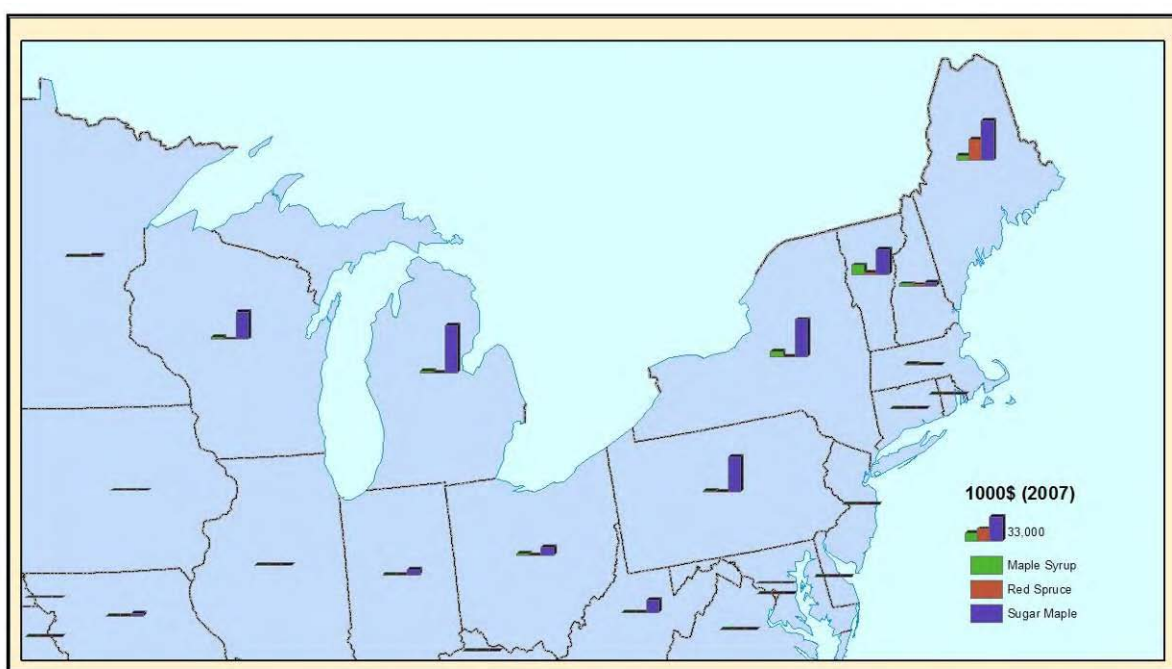


**Figure 3.1-3.** Annual Value of Sugar Maple and Red Spruce Harvests and Maple Syrup Production, 2006

<sup>1</sup> This area includes Connecticut, Delaware, District of Columbia, Illinois, Indiana, Maine, Maryland, Massachusetts, Michigan, New Hampshire, New Jersey, New York, Ohio, Pennsylvania, Rhode Island, Vermont, West Virginia, and Wisconsin.



State-level data on other outdoor recreational activities associated with forests are also available from the 2006 FHWAR (U.S. Department of the Interior [DOI], 2007). As summarized in **Table 3.1-1**, 5.5% of adults in the northeastern United States participated in hunting, and the total number of hunting days occurring in those states was 83.8 million. Data from the survey also indicated that 10% of adults in northeastern states participated in wildlife viewing away from home. The total number of away-from-home wildlife viewing days occurring in those states was 122.2 million in 2006. For these recreational activities in the northeastern United States, Kaval and Loomis (2003) estimated average consumer surplus values per day of \$52.36 for hunting and \$34.46 for wildlife viewing (in 2007 dollars). The implied total annual value of hunting and wildlife viewing in the northeastern United States was, therefore, \$4.38 billion and \$4.21 billion, respectively, in 2006.

As previously mentioned, it is difficult to estimate the portion of these recreational services that are specifically attributable to forests and to the health of specific tree species. However, one recreational activity that is directly dependent on forest conditions is fall color viewing. Sugar maple trees, in particular, are known for their bright colors and are, therefore, an essential aesthetic component of most fall color landscapes. Thus, declines in sugar maple stocks due to terrestrial acidification are expected to have detrimental effects on these landscapes. Statistics on fall color viewing are much less available than for the other recreational and tourism activities; however, a few studies have documented the extent and significance of this activity. For example, based on a 1996 to 1998 telephone survey of residents in the Great Lakes area, Spencer and Holecek (2007) found that roughly 30% of residents reported at least one trip in the previous year involving fall color viewing. In a separate study conducted in Vermont, Brown (2002) reported that more than 22% of households visiting Vermont in 2001 made the trip primarily for the purpose of viewing fall colors. Unfortunately, data on the total number or value of these trips are not available, although the high rates of participation suggest that numbers might be similar to the wildlife viewing estimates reported above.

Although these statistics provide useful indicators of the total recreational and aesthetic services derived from forests in the northeastern United States, they do not provide estimates of how these services are affected by terrestrial and forest acidification. Very few empirical studies have directly addressed this issue; however, two studies have estimated values for protecting high-elevation spruce forests in the Southern Appalachians. Kramer, Holmes, and Haefele (2003)

conducted a CV study estimating households' WTP for programs to protect remaining high-elevation spruce forests from damages associated with air pollution and insect infestation (Haefele, Kramer, and Holmes, 1991; Holmes and Kramer, 1995). The study collected data from 486 households using a mail survey of residents living within 500 miles of Asheville, North Carolina. The survey presented respondents with photographs representing three stages of forest decline and explained that, without forest protection programs high-elevation spruce forests would all decline to worst conditions (with severe tree mortality). The survey then presented two

**Table 3.1-1.** Participation in Hunting and Wildlife Viewing in Northeastern States in 2006

State	Participation Rates by State Residents <sup>a</sup>		Activity Days by Residents and Nonresidents (in thousands)	
	Hunting	Wildlife Viewing <sup>b</sup>	Hunting	Wildlife Viewing <sup>b</sup>
Connecticut	1.2%	11.0%	509	4,184
Delaware	3.1%	7.0%	654	855
Illinois	2.8%	8.0%	4,688	5,686
Indiana	5.3%	13.0%	4,808	24,013
Maine	13.6%	20.0%	2,283	4,778
Maryland	3.5%	7.0%	2,262	4,782
Massachusetts	1.3%	11.0%	1,149	8,461
Michigan	9.2%	11.0%	11,905	10,043
New Hampshire	5.0%	12.0%	1,057	3,165
New Jersey	1.3%	8.0%	1,457	7,965
New York	3.3%	8.0%	10,289	13,521
Ohio	5.4%	13.0%	10,633	7,816
Pennsylvania	9.5%	11.0%	16,863	11,972
Rhode Island	1.2%	11.0%	155	2,948
Vermont	11.3%	16.0%	1,111	2,459
West Virginia	13.6%	9.0%	3,939	4,005
Wisconsin	15.0%	10.0%	10,059	5,547
Total	5.5%	10.0%	83,821	122,200

<sup>a</sup> Ages 16 or older.

<sup>b</sup> Wildlife viewing away from home.

Source: U.S. Department of the Interior (DOI), Fish and Wildlife Service, and U.S. Department of Commerce, U.S. Census Bureau, 2007.

potential forest protection programs—one would prevent further decline in forests along roads and trail corridors (one-third of the at-risk ecosystem) and the other would prevent decline in all at-risk forests. Both programs would be funded by tax payments going to a conservation fund. Median household WTP was estimated to be roughly \$29 (in 2007 dollars) for the first program and \$44 for the more extensive program.

Jenkins, Sullivan, and Amacher (2002) conducted a very similar study in 1995 using a mail survey of households in seven Southern Appalachian states. In this study, respondents were presented with one potential program, which would maintain forest conditions at initial (*status quo*) levels. It was explained that, without the program, forest conditions would decline to worst conditions (with 75% dead trees). In contrast to the previously described study, in this survey the *initial* level of forest condition was varied across respondent. In one version of the survey, the initial condition was described and shown as 5% dead trees, while the other version described and showed 30% dead trees. Household WTP was elicited from 232 respondents using a dichotomous choice and tax payment format. The overall mean annual WTP for the forest protection programs was \$208 (in 2007 dollars), which is considerably larger than the WTP estimates reported by Kramer, Holmes, and Haeefe (2003). One possible reason for this difference is that respondents to the Jenkins, Sullivan, and Amacher (2002) survey, on average, lived much closer to the affected ecosystem. Multiplying the average WTP estimate from this study by the total number of households in the seven-state Appalachian region results in an aggregate annual value of \$3.4 billion for avoiding a significant decline in the health of high-elevation spruce forests in the Southern Appalachian region.

### **3.1.3 Regulating Services**

Forests in the northeastern United States also support and provide a wide variety of valuable regulating services, including soil stabilization and erosion control, water regulation, and climate regulation (Krieger, 2001). As terrestrial acidification contributes to root damages, reduced biomass growth, and tree mortality, all of these services are likely to be affected; however, the magnitude of these impacts is very uncertain. Forest vegetation plays an important role in maintaining soils in order to reduce erosion, runoff, and sedimentation that can adversely impact surface waters. In addition to protecting the *quality* of water in this way, forests also help store and regulate the *quantity* and flows of water in watersheds. Finally, forests help regulate

climate locally by trapping moisture and globally by sequestering carbon. The total value of these ecosystem services is very difficult to quantify in a meaningful way, as is the reduction in the value of these services associated with nitrogen and sulfur deposition.

### **3.2 CHANGES IN ECOSYSTEM SERVICES ASSOCIATED WITH ALTERNATIVE LEVELS OF ECOLOGICAL INDICATORS**

This section estimates values for changes in ecosystem services associated with reductions in damages to commercial forests resulting from terrestrial acidification. With high levels of acidifying nitrogen and sulfur deposition, trees may experience an increased susceptibility to drought and pest damage, aluminum toxicity in roots, a reduced tolerance to cold, and a greater propensity to frost injury (DeHayes et al., 1999; Driscoll et al., 2001; Fenn et al., 2006). As a result, total stand volume and growth may be reduced. The tree growth response and value of reducing nitrogen+sulfur deposition loads across the range of sugar maples and red spruces (as shown in **Figures 3.1-1 and 3.1-2**, respectively) was estimated using a critical load assessment methodology (described in the case study analysis) of terrestrial acidification. More specifically, the beneficial effects of *eliminating* all exceedances of critical load for sugar maples and red spruces in this range were estimated.

#### **3.2.1 Increased Provisioning Services from Sugar Maple Timber Harvests due to Elimination of Critical Load Exceedances**

A three-stage approach was used to estimate the value of increased provisioning services from sugar maple and red spruce timber harvests. In the first stage, exposure–response models<sup>2</sup> for sugar maple and red spruce trees were estimated, which measure the empirical relationship between exceedances of critical loads and growth in volume of live trees. In the second stage, these exposure–response models were applied to estimate the average increase in sugar maple and red spruce growth rates (in three regions) that would result from eliminating critical load exceedances in the range of these tree species. In the third stage, these increased growth rates were incorporated into an existing forest market model for North America and the value (i.e.,

---

<sup>2</sup> See the case study report for alternative models of exposure–response.

increase in consumer and producer surplus) of expected future increases in sugar maple and red spruce timber harvests and sales was estimated. Each of these stages is described below in detail.

### ***3.2.1.1 Stage 1: Estimation of the Exposure–Response Model***

The analysis of the relationship between critical load exceedances and sugar maple and red spruce trees' growth was conducted using data from the USFS FIA database for 16 states in the sugar maple range and 5 states in the red spruce range. Each data point in the analysis corresponds with a permanent sampling plot location on classified forestland (timberland for New York) covering 0.07 ha. Estimation of critical loads for each plot was based on a Simple Mass Balance (SMB) modeling approach (described in the case study). FIA plots were only included in the analysis if they (1) were nonunique<sup>3</sup> permanent sampling plots; (2) provided necessary soil, parent material, atmospheric deposition, and run-off data to apply the SMB model for critical load estimation; (3) were located to the north of the glaciation line (this line represents the southernmost extension of the most recent glacial advancement)<sup>4</sup>; and (4) had positive exceedances in deposition above the most protective critical load (Bc/Al = 10.0).<sup>5</sup> With these restrictions, 2,205 sugar maple plots and 187 red spruce plots were included in the analysis.

**Tables 3.2-1 and 3.2-2** summarize the plot-level FIA sugar maple and red spruce data used to model the exposure–response relationship. For each plot, exceedances of critical loads were calculated by subtracting the results of the SMB analysis (estimated critical loads estimates) from corresponding 2002 CMAQ nitrogen+sulfur deposition estimates. Overall, 74% of sugar maple plots above the glaciation line exceeded the critical loads, ranging from 21% in Maine to over 95% in Connecticut, Massachusetts, New Jersey, New York, Pennsylvania, Ohio, and Vermont. Thirty-one percent of red spruce above the glaciation line exceeded the critical loads, ranging from 16% in Maine to 100% in Massachusetts and Vermont. For sugar maple

---

<sup>3</sup> Nonunique permanent sampling plot locations are those that have maximum critical load attribute values (soils, runoff, and atmospheric deposition) that are not distinct and are repeated within a 250-acre area of the plot location. This “confidentiality” filter is a requirement of the USFS to prevent the disclosure of data that can be directly linked to a location on private land. To comply with the necessary “confidentiality,” full coverages of the data required for the critical load calculations were given to the USFS, and the USFS matched and provided the data for each nonunique permanent sampling plot.

<sup>4</sup> This is because the base cation weathering term, one of the key components of critical load, may not have been accurately estimated for plots from south of the glaciation line (see case study for details) that have older, more weathered soils. Thus, using such plots in the analysis may potentially increase error in the data used.

<sup>5</sup> For analysis using lower levels of protection, see the case study report.

plots with positive exceedances, the average exceedance ranged from less than 100 eq/ha/yr in Missouri and Iowa to over 450 eq/ha/yr in Connecticut, Massachusetts, New Jersey, and Ohio. For red spruce plots with positive exceedances, the average exceedance ranged from less than 150 eq/ha/yr in Maine to over 600 eq/ha/yr in Massachusetts.

Net annual individual tree volume growth and tree volumes for all live sugar maple and red spruce trees<sup>6</sup> (greater than 12.7 cm diameter at 1.3 m) were acquired from the USFS FIA database for each plot. The volume growth calculations were based on the most recent measurement period, and the time interval between measurements for the plots (to determine annual growth rates) ranged from 1 to 11 years. These calculations included the influences of growth and volume reductions or losses due to natural damage (pest, wind, frost) or natural mortality. Average volume growth ranged from 0.1 in Massachusetts to 0.62 in Indiana for sugar maple and from 0.14 in Massachusetts to 0.26 in Maine for red spruce. Volumes and volume growth measures for the sugar maple and red spruce trees in each plot were averaged to produce single values of each measure for each species.

**Table 3.2-1.** Summary of Plot-Level Data on Sugar Maple Growth and Exceedances (for Plots above the Glaciation Line)

State	Total Number of Plots	Number of Plots North of Glaciation Line	Number of Plots with Positive CL Exceedance Values	Number of Plots with Positive CL Exceedance Values North of Glaciation Line	Average CL Exceedance (eq/ha/yr)	Average Tree Volume Growth (m <sup>3</sup> /yr)	Average Tree Volume (m <sup>3</sup> )
Alabama	12	0	3				
Arkansas	8	0	1				
Connecticut	33	33	33	33	487.76	0.009	0.279
Illinois	25	20	17	12	117.17	0.007	0.227
Indiana	266	234	235	204	390.90	0.018	0.397
Iowa	8	8	2	2	48.07	0.005	0.123
Kentucky	14	0	12				
Maine	242	242	51	51	130.42	0.011	0.323
Maryland	4	0	4				
Massachusetts	27	27	27	27	473.31	0.003	0.366

<sup>6</sup> All trees with reported volumes of “0” were excluded from the analyses.

State	Total Number of Plots	Number of Plots North of Glaciation Line	Number of Plots with Positive CL Exceedance Values	Number of Plots with Positive CL Exceedance Values North of Glaciation Line	Average CL Exceedance (eq/ha/yr)	Average Tree Volume Growth (m <sup>3</sup> /yr)	Average Tree Volume (m <sup>3</sup> )
Michigan	596	596	418	418	242.17	0.011	0.307
Minnesota	257	257	79	79	156.06	0.010	0.256
Missouri	122	31	58	18	84.02	0.012	0.246
New Hampshire	72	72	60	60	378.40	0.009	0.304
New Jersey	6	6	6	6	601.39	0.013	0.357
New York	280	280	264	264	437.94	0.010	0.344
North Carolina	13	0	9				
Ohio	55	27	54	26	452.60	0.013	0.545
Pennsylvania	270	133	263	126	387.35	0.011	0.366
Tennessee	264	0	132				
Vermont	162	162	160	160	301.67	0.008	0.411
Virginia	104	0	63				
West Virginia	337	0	318				
Wisconsin	870	870	719	719	185.16	0.009	0.304
<b>TOTAL Observations (used in calculations)</b>	<b>4,047</b>	<b>2,998</b>	<b>2,988</b>	<b>2,205</b>	<b>2,205</b>	<b>2,205</b>	<b>2,205</b>

CL = critical load

**Table 3.2-2.** Summary of Plot Level Data on Sugar Maple Growth and Exceedances (for Plots above the Glaciation Line)

State	Total Number of Plots	Number of Plots North of Glaciation Line	Number of Plots with Positive CL Exceedance Values	Number of Plots with Positive CL Exceedance Values North of Glaciation Line	Average CL Exceedance (eq/ha/yr)	Average Tree Volume Growth (m <sup>3</sup> /yr)	Average Tree Volume (m <sup>3</sup> )
Maine	483	483	78	78	133.1048	0.007	0.245
Massachusetts	3	3	3	3	628.5439	0.004	0.203
New Hampshire	42	42	32	32	368.9527	0.006	0.245
New York	18	18	14	14	282.5433	0.004	0.221
Tennessee	1	0	1	0			
Vermont	60	60	60	60	292.4329	0.007	0.328
West Virginia	6	0	6	0			
<b>TOTAL Observations (used in calculations)</b>	<b>613</b>	<b>606</b>	<b>194</b>	<b>187</b>	<b>187</b>	<b>187</b>	<b>187</b>

The results of a multivariate OLS regression, using average tree growth (measured in cubic meters per year) as the dependent variable, are reported in **Table 3.2-3 and 3.2-4**. The explanatory variables include the critical load exceedance (measured in eq/ha/year) for each plot, linear and squared terms of average tree volumes (measured in cubic meters), and a categorical (dummy) variable for each state (with Connecticut as the reference category for sugar maple and Vermont for red spruce). The purpose of the state variables is to control for other unobserved sources of variation in tree growth, which are related to a plot's general geographic location. Examples of potential unobserved factors include differences in data collection methods and measurements across reporting state, climatic factors, and geological characteristics. An F test applied to the state categorical variables indicated that their coefficients are jointly significant at the 5% level for sugar maple. In general, the growth of a tree rises with age but at a decreasing rate. Because data on the age were unavailable, average tree volume was instead included as a proxy variable in the regression to control for this relationship.

The coefficient of the critical load exceedance was negative for both species and was statistically significant at the 5% level (*p*-value of 0.035) for red spruce and at the 10% (*p*-value of 0.101) for sugar maple, thus supporting the theory that when critical loads are exceeded by atmospheric nitrogen and sulfur deposition, tree health and growth can be impaired.

**Table 3.2-3.** Linear Exposure–Response Model for Exceedances (above a Critical Load Calculated with Bc/Al = 10) and Sugar Maple Tree Growth: OLS Regression Results (for Plots above the Glaciation Line)

Explanatory Variables	Dependent Variable: Average Tree Growth (m <sup>3</sup> /yr)	t-statistic	p-value
	Coefficient		
Intercept	0.004875	1.48	0.1385
Critical load exceedance	-3.344E-06	-1.64	0.1008
Average tree volume	0.021150	10.12	<.0001
Square of average tree volume	8.944E-04	1.1	0.27
Illinois	-0.001884	-0.31	0.755
Indiana	0.005452	1.63	0.1029
Iowa	-0.002052	-0.16	0.8743
Maine	-0.000895	-0.22	0.8245
Massachusetts	-0.008403	-1.82	0.0685
Michigan	0.000222	0.07	0.9456



Explanatory Variables	Dependent Variable: Average Tree Growth (m <sup>3</sup> /yr)	t-statistic	p-value
	Coefficient		
Minnesota	0.000210	0.06	0.9553
Missouri	0.001850	0.35	0.7255
New Hampshire	-0.001647	-0.43	0.6696
New Jersey	0.001956	0.25	0.8042
New York	-0.000817	-0.25	0.8035
Ohio	-0.002104	-0.45	0.6522
Pennsylvania	-0.000803	-0.23	0.8177
Vermont	-0.005168	-1.51	0.131
Wisconsin	-0.002195	-0.68	0.4958
<b>Number of Observations</b>	<b>2,205</b>		
<b>Adjusted R<sup>2</sup></b>	<b>0.1722</b>		

### 3.2.1.2 Stage 2: Estimation of Average Increments in Tree Volume

In this stage of the analysis, the effect of eliminating all critical load exceedances in the range of sugar maples and red spruce was simulated and the resulting average (at a region level) percentage increase in tree volume was estimated.

**Table 3.2-4.** Linear Exposure–Response Model for Exceedances (above a Critical Load Calculated with Bc/AI = 10) and Red Spruce Tree Growth: OLS Regression Results (for Plots above the Glaciation Line)

Explanatory Variables	Dependent Variable: Average Tree Growth (m <sup>3</sup> /yr)	t-statistic	p-value
	Coefficient		
Intercept	0.006034	4.96	<.0001
Critical load exceedance	-5.162E-06	-2.12	0.0354
Tree volume	0.005590	1.26	0.2093
Square of tree volume	5.100E-03	1.23	0.2218
Maine	0.000285	0.32	0.7489
Massachusetts	-0.000132	-0.05	0.9629
New Hampshire	0.000435	0.42	0.6736
New York	-0.001805	-1.32	0.1897
<b>Number of Observations</b>	<b>187</b>		
<b>Adjusted R<sup>2</sup></b>	<b>0.1963</b>		

Based on the results of the regression equation reported in Table 3.2-3 and 3.2-4, for each plot  $i$  with a positive critical loads exceedance, the following equation was first used to estimate what tree volume growth would be under conditions with no critical loads exceedances:

$$g_i^1 = g_i^0 + b * (-CLE_i^0) \quad (3.1)$$

where

$CLE_i^0$  = critical load exceedance at plot  $i$  under observed conditions

$g_i^0$  = annual tree volume growth on plot  $i$  under observed conditions (in m<sup>3</sup>/yr)

$g_i^1$  = annual tree volume growth on plot  $i$  under conditions with no exceedance of critical load ( $CLE_i = 0$ ) (in m<sup>3</sup>/yr)

$B$  = regression coefficient (slope) for critical load exceedance (from Table 3.2-3 and 3.2-4, equals  $-3.344\text{E-}06$  for sugar maple and  $-5.162\text{E-}06$  for red spruce)

Since this study calculated the effects of eliminating positive exceedances with the aim of estimating reductions in *damages* to sugar maple and red spruce forests resulting from terrestrial acidification, it was assumed that there is no change in growth for plots without positive critical load exceedances. In practice, however, some reduced growth may be possible due to lower nitrogen availability in plots that are below the critical load. Thus, the calculations should be interpreted as an upper bound to the value of reducing nitrogen+sulfur deposition loads.

To apply these results in the market model used in the next stage of the analysis, these volume growth estimates were then converted into an average percentage increment in volume. In other words, in each period  $t$ , tree volume on plot  $i$  is expected to be greater (by a factor  $f_i$ ) under conditions with no critical loads exceedance, compared to conditions with currently observed critical loads exceedances. In formal terms:

$$V_{it}^1 = (1 + f_i)V_{it}^0 = (1 + f_i)(1 + (g_i^0 / V_{i,t-1}^0))V_{i,t-1}^0 = (1 + (g_i^1 / V_{i,t-1}^0))V_{i,t-1}^0 \quad (3.2)$$

where

$V_{it}^0$  = average tree volume on plot  $i$  under observed conditions in period  $t$  (in m<sup>3</sup>)

$V_{it}^1$  = average tree volume on plot  $i$  under conditions with no exceedance of critical load in period  $t$  (in m<sup>3</sup>)

Solving Equation (3.2) for  $f_i$  results in

$$f_i = \frac{(1 + (g_i^1 / V_{it-1}^0))}{(1 + (g_i^0 / V_{it-1}^0))} - 1. \quad (3.3)$$

Using the plot-level estimates of  $g^1$ ,  $g^0$ , and  $V^0$ ,  $f_i$  for each plot in the data set was estimated, and these estimates were then averaged across each region.

### ***3.2.1.3 Stage 3: Estimation of Increased Market-Based Benefits from Sugar Maple and Red Spruce Timber Harvests***

The next critical step in establishing the link between changes in nitrogen and sulfur deposition and the changes in forest provisioning services is modeling the effect of the average increase in tree growth (obtained in Stage 2) on public welfare. This section describes the approach to obtaining valuation estimates for this incremental increase in the volume of commercial sugar maple and red spruce stands.<sup>7</sup> To implement this approach, the increase in the percentage volume of timber was applied to all age categories, and FASOMGHG (Forest and Agricultural Sector Optimization Model—Green House Gas version) was used to calculate the resulting market-based welfare effects in the forest and agricultural sectors of the United States. Data obtained from the FIA were used as inputs into FASOMGHG, which enabled the adaptation of the model for this application. The different components of these input data are described below.

FASOMGHG is a price-endogenous, dynamic, nonlinear programming model of the forest and agricultural sectors in the United States (Adams et al., 2005). The model simulates the allocation of land over time to competing activities in these two sectors and the resultant consequences for the commodity markets supplied by these lands. It was developed to evaluate the welfare and market impacts of public policies that cause changes in land use and activities both between and within the two sectors. The results from this model yield a dynamic simulation of prices, production, management, consumption, greenhouse gas (GHG) effects, and other environmental and economic indicators within these two sectors. For this application,

---

<sup>7</sup> Holmes (1992) describes a similar approach to estimate welfare effects for a decline in southern pine forest productivity in the United States.

FASOMGHG's key outputs include economic welfare measures, such as changes in producer and consumer surplus.<sup>8</sup>

The following discussion summarizes the other main features of FASOMGHG and describes how they were used and adapted for this application:

- **Temporal Frame:** The time frame of this model is typically 70 to 100 years, and the model is solved on a 5-year time-step basis. The base year for this model is 2002.
- **Geographical Regions:** FASOMGHG models forest and agricultural activity across the conterminous United States, which is broken into 11 market regions. Forestry production occurs in nine of these regions. The selection of FASOMGHG regions for this model application was determined by comparing maps showing the regions where sugar maples grow with a list of FASOM regions. **Table 3.2-5** lists the states in each of the FASOM regions used in this application. It also shows the average increase in tree growth (obtained from Stage 2) for each of these regions.

**Table 3.2-5.** Estimated Increments in Sugar Maple and Red Spruce Timber Volume (Resulting from Elimination of Critical Load Exceedances), by FASOMGHG Region

Key	Region	States	Average Percentage Increment in Sugar Maple Tree Volume (i.e., average $f_i$ )	Average Percentage Increment in Red Spruce Tree Volume (i.e., average $f_i$ )
NE	Northeast	Connecticut, Delaware, Maine, Maryland, Massachusetts, New Hampshire, New Jersey, New York, Pennsylvania, Rhode Island, Vermont, West Virginia	0.59%	0015%
LS	Lake States	Michigan, Minnesota, Wisconsin	0.28%	
CB	Corn Belt	Illinois, Indiana, Iowa, Missouri, Ohio	0. 57%	

Source: Adams et al., 2005.

- **Types of Forests:** Two types of forests are considered when evaluating policy effects in FASOMGHG—softwood and hardwood. To adapt these categories for the application,

<sup>8</sup> For a detailed documentation of FASOMGHG, please see Adams et al. (2005).

sugar maples and red spruce trees needed to be expressed as a proportion of hardwoods and softwoods, respectively. This was done for each of the regions modeled in this application. These relevant data were obtained from FIA (**Table 3.2-6**) and are a component of the input into FASOMGHG.

**Table 3.2-6.** Proportions of Hardwood in Sugar Maple Production and Proportions of Softwood in Red Spruce Production, by FASOM Region

	FASOM Regions	Proportion of Hardwood/Softwood
Sugar Maple	NE	13%
	LS	11%
	CB	
Red Spruce	NE	14.5% <sup>9</sup>

Source: U.S. Department of Agriculture, Forest Service, 2002.

- **Forestland:** The FASOMGHG model does not track land under forest cover that produces less than 0.57 m<sup>3</sup>/yr (called unproductive forestland) or on timberland that is reserved for other uses, because these are not a part of the U.S. timber base. Endogenous land use modeling is only done for privately held land, not publicly owned or managed timberlands. The model assumes that the amount of public land in forests does not adjust to market conditions but is set by the government. Thus, the average percentage increase in volume is applied to only forests growing on private land. The proportions of the timberland under private and public ownership are shown in **Table 3.2-7** (obtained from FIA data).
- **Welfare Measure:** Mathematically, FASOMGHG solves an objective function to maximize net market surplus. This is represented by the area under the product demand function (an aggregate measure of consumer welfare) less the area under the factor supply curves (an aggregate measure of producer costs). The value of the resultant objective function is consumers' and producers' surplus. The welfare effects of a productivity improvement are obtained from FASOMGHG as the difference in annual net market surplus between a base case (without the policy in place) and a control case (with the policy in place).

<sup>9</sup> The RPA Assessment tables report the proportion of the spruce and balsam fir category as 29%. We assume that half of this is due to red spruce.

To apply FASOMGHG for this analysis, the main input required for the model is the annual percentage increase in *total hardwood* and *total softwood* volume by region. To address this requirement, the estimate of the average percentage increment in *sugar maple tree* volume (average  $f_i$ , shown in Table 3.2-5) was multiplied by the proportion of hardwoods in sugar maple production (shown in Table 3.2-6) for each FASOM region, which ranges from 11% to 13%. Similarly, the estimate of the average percentage increment in *red spruce tree* volume (average  $f_i$ , shown in Table 3.2-5) was multiplied by the proportion of softwoods in red spruce production (shown in Table 3.2-6) for the NE region.

**Table 3.2-7.** Proportion of Timberland under Private and Public Ownership by FIA Region<sup>a</sup>: 2002

FIA Region	Private Timberland	Public Timberland
Northeast	87%	13%
NorthCentral	28%	72%

<sup>a</sup> The states in the Northeast FIA region correspond exactly to states in NE in FASOM.

The states in the NorthCentral FIA region correspond exactly to states in LS and CB in FASOM.

Source: U.S. Department of Agriculture, Forest Service, 2002, Table 10.

#### 3.2.1.4 Results: Aggregate Benefit Estimates

**Figure 3.2-1** summarizes the FASOMGHG model results. These results are reported as the present discounted values of future welfare changes in the forestry sector (in 5-year increments from 2000 to 2065) due to increased tree growth as well as the future welfare changes in the agricultural sector. Summing over this 65-year period, the value of gains to the forestry sector is \$17.1 million (in 2007 dollars, using a 4% discount rate). The agricultural sector has a welfare loss of \$1 million. This loss is possibly due to a shift in land use from agriculture to forestry. The total present value of these welfare changes due to both the sectors is \$16.09 million (in 2007 dollars, using a 4% discount rate). On an annualized basis (at 4%), this is equivalent to \$684,000 per year. **Figure 3.2-1** presents the time path of these welfare estimates for the forestry and agricultural sector as well as the total welfare estimates. The cyclical pattern of the estimates is most likely driven by the fact that if more harvesting is done in any period, this leads to less stock to harvest from in the next period.

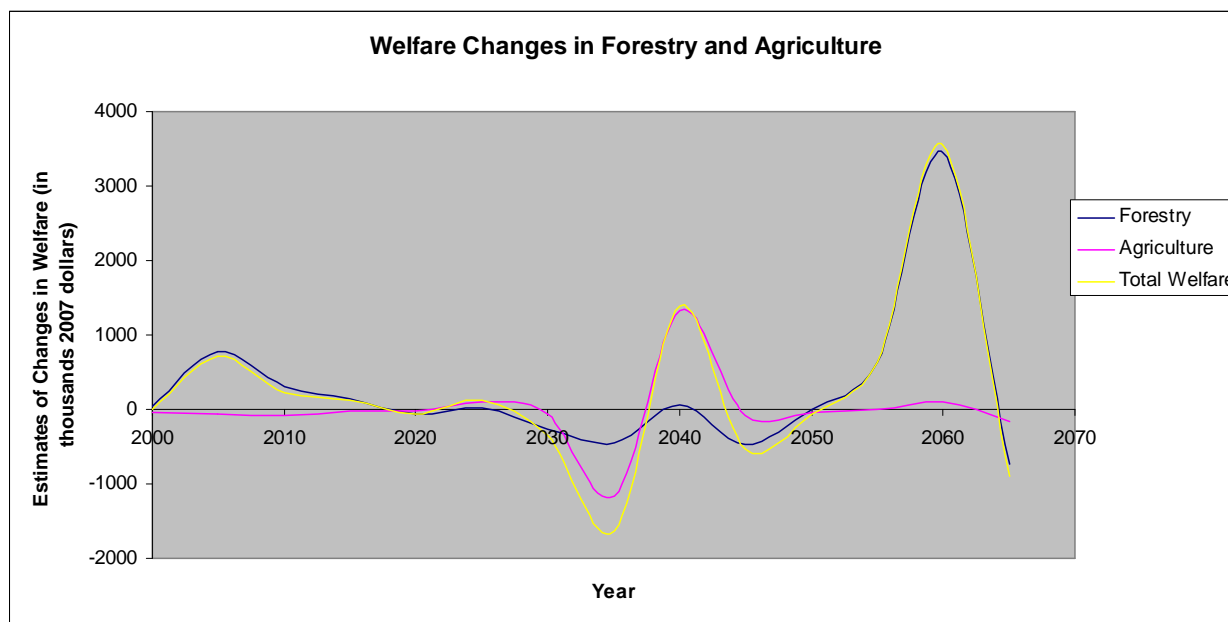


**Figure 3.2-1.** Estimated Time Path of Welfare Gains in the Forestry and Agricultural Sector due to Increased Sugar Maple and Red Spruce Growth (2000–2065)

### Limitations and Uncertainties

This analysis links two separate models to estimate values of reductions in damages to sugar maple forests due to terrestrial acidification. The first is an exposure–response model relating maximum acid deposition load exceedances with tree growth. Simulating the effect of eliminating all exceedances, an average percentage increase in tree volume was obtained. a market model of the forest and agricultural sectors (FASOMGHG) was then used to calculate the welfare effects of this increased volume.

In doing this, certain limitations and uncertainties are associated with each component of the analysis as well as with the linkages between them. These are described below.

Linking changes in deposition levels to changes in tree growth:

- In interpreting the results of this model, readers should keep certain data limitations in mind. First, plot-level data were completely unavailable for some of the states and partially unavailable for others for both the species. Second, only plots that were above the glaciation line were used in this analysis. It is not known whether the plots in other states and also those below the glaciation line that are part of the FASOMGHG regions have characteristics that are correlated with the critical load exceedances, which might lead to biased estimates of the exposure–response relationship.

- The estimated reduction in the forest damages, as explained in Section 3.2.1.2, should be interpreted as an upper bound on the benefits of reducing nitrogen+sulfur deposition, since it only includes the gains from reducing critical load exceedances. Nitrogen deposition below the critical load may actually promote tree growth through fertilization effects; therefore, reducing deposition may have potential counteracting effects on tree growth. The current analysis does not estimate or include these counteracting effects.
- Although this analysis of tree growth response is done for sugar maple and red spruce, gains are also expected for other commercial species. Thus, we are underestimating the total benefits of reducing nitrogen+sulfur deposition.
- Because of data limitations, the exposure–response analysis does not control for other factors that may affect tree growth, such as elevation, slope, density (to account for sunlight and competition among trees for nutrients), age (though tree volume was used as a crude proxy for this variable), different management practices, and climate. Also, differences in measurement and reporting across plots and states may result in discrepancies in the data. Although this study attempted to capture the differences in measurement and in climate by using state dummies, this is not a perfect control, since, for example, there is substantial variation in climate within a state. Inadequate controls for these other factors could potentially lead to omitted variable bias. Other uncertainties and limitations associated with the estimation of the exposure–response relationships are discussed in the case study.

Linking changes in tree growth to economic welfare changes:

- In applying the estimates from the exposure–response model to the FASOM model, it was assumed that the plots used to calculate the percentage increase in tree volume are representative of the FASOMGHG regions. However, because data on all plots in the region are unavailable, there is some uncertainty regarding the representativeness of plots used.
- The tree volume growth estimates used in the exposure–response model were calculated based on live trees on forestland, not timberland, which is what FASOMGHG uses. This may potentially give rise to some uncertainty in applying the results to FASOMGHG because the estimates of the slopes (b) may be different for timberland than for forestland.



- The exposure–response model uses data from both private and public lands, while in FASOMGHG the growth is applied to private lands only. This is an additional source of uncertainty because different management practices could potentially affect the relationship between exposure and growth differently.
- The age structure (and consequently volume of trees) may not be the same. So the stands to which the change in growth rates are applied in FASOMGHG may be different from the ones used in the exposure–response model, and this study may be assuming a change in growth rate that is not realistic for these stands.
- A general limitation when using FASOMGHG is that it is a very aggregated region-level model; thus, effects pertaining to areas particularly vulnerable to acidification cannot be identified. Also, to make future timber market projections, FASOMGHG requires several assumptions regarding future product demands, production capacity, and timber inventory.
- It must also be emphasized that the economic welfare changes reported in this section are only those associated with markets for sugar maple and red spruce timber. They do not include potential gains associated with other provisioning services, such as sugar maple syrup production or production of other hardwood or softwood species affected by terrestrial acidification. They also do not include gains outside the United States (in particular, Canada) or in other sectors of the U.S. economy.

### **3.3 REFERENCES**

- Adams, D., R. Alig, B.A. McCarl, and B.C. Murray. February 2005. FASOMGHG Conceptual Structure, and Specification: Documentation. Available at <http://agecon2.tamu.edu/people/faculty/mccarl-bruce/FASOM.html>. Accessed on October 22, 2008.
- Brown, L.H. 2002. *Profile of the Annual Fall Foliage Tourist in Vermont: Travel Year 2001*. Report prepared for the Vermont Department of Tourism and Marketing. Burlington, VT: Vermont Tourism Data Center, University of Vermont.
- Cordell, H.K., C.J. Betz, G. Green, and M. Owens. 2005. Off-Highway Vehicle Recreation in the United States, Regions and States: A National Report from the National Survey on

- Recreation and the Environment (NSRE). Report prepared for the Forest Service's National OHV Policy & Implementation Teams. USDA Forest Service.
- Cordell, K., B. Leeworthy, G.T. Green, C. Betz, and B. Stephens. n.d. *The National Survey on Recreation & the Environment*. Research Work Unit 4953. Athens, GA: Pioneering Research on Changing Forest Values in the South and Nation USDA Forest Service Southern Research Station. Available at [www.srs.fs.fed.us/trends](http://www.srs.fs.fed.us/trends).
- DeHayes, D.H., P.G. Schaberg, G.J. Hawley, and G.R. Strimbeck, 1999. "Acidic Rain Impacts on Calcium Nutrition and Forest Health." *BioScience* 49:789-800.
- Driscoll, C.T., G.B. Lawrence, A.J. Bulger, T.J. Butler, C.S. Cronan, C. Eagar, K.F. Lamber, G.E. Likens, J.L. Stoddard, and K.C. Weathers. 2001. "Acidic Deposition in the Northeastern United States: Sources and Inputs, Ecosystem Effects and Management Strategies." *BioScience* 51:180-198.
- Fenn, M.E., T.G. Huntington, S.B. McLaughlin, C. Eager, A. Gomez, and R.B. Cook. 2006. "Status of Soil Acidification in North America." *Journal of Forest Science* 52 (special issue):3-13.
- Haefele, M., R.A. Kramer, and T.P. Holmes. 1991. Estimating the Total Value of a Forest Quality in High-Elevation Spruce-Fir Forests. The Economic Value of Wilderness: Proceedings of the Conference. Gen. Tech. Rep. SE-78 (pp. 91-96). Southeastern For. Exper. Station. Asheville, NC: USDA Forest Service.
- Holmes, T.P. 1992. *Economic Welfare Impacts of Air Pollution Damage to Forests in the Southern United States*. Asheville, NC: U.S. Dept. of Agriculture, Forest Service, Southeastern Forest Experiment Station. pp. 19-26.
- Holmes, T., and R. Kramer. 1995. "An Independent Sample Test of Yea-Saying and Starting Point Bias in Dichotomous-Choice Contingent Valuation." *Journal of Environmental Economics and Management* 28:121-132.

- Jenkins, D.H., J. Sullivan, and G.S. Amacher. 2002. "Valuing High Altitude Spruce-Fir Forest Improvements: Importance of Forest Condition and Recreation Activity." *Journal of Forest Economics* 8:77-99.
- Kaval, P., and J. Loomis. 2003. *Updated Outdoor Recreation Use Values With Emphasis On National Park Recreation*. Final Report October 2003, under Cooperative Agreement CA 1200-99-009, Project number IMDE-02-0070.
- Kramer, A., T. Holmes, and M. Haefele. 2003. "Contingent Valuation of Forest Ecosystem Protection." In *Forests in a Market Economy*, E.O. Sills and K.L. Abt, eds., pp. 303-320. Dordrecht, The Netherlands: Kluwer Academic Publishers.
- Krieger, D.J. 2001. *Economic Value of Forest Ecosystem Services: A Review*. Washington, DC: The Wilderness Society.
- Luzadis, V.A. and E.R. Gossett. 1996. "Sugar Maple." In *Forest Trees of the Northeast*, J.P. Lassoie, V.A. Luzadis, and D.W. Grover, eds., pp. 157-166. Cooperative Extension Bulletin 235. Cornell Media Services. Available at <http://maple.dnr.cornell.edu/pubs/trees.htm>.
- National Agricultural Statistics Service (NASS). June 12, 2008. "Maple Syrup Production Up 30 Percent Nationwide." New England Agricultural Statistics, NASS, USDA.
- Spencer, D.M., and D.F. Holecek. 2007. "Basic Characteristics of the Fall Tourism Market." *Tourism Management* 28:491-504.
- U.S. Department of Agriculture, Forest Service. Forest Inventory and Analysis National Program, RPA Assessment Tables. 2002. Available at [http://Ncrs2.Fs.Fed.Us/4801/Fiadb/Rpa\\_Tablet/Draft\\_RPA\\_2002\\_Forest\\_Resource\\_Tables.pdf](http://Ncrs2.Fs.Fed.Us/4801/Fiadb/Rpa_Tablet/Draft_RPA_2002_Forest_Resource_Tables.pdf).
- U.S. Department of the Interior, Fish and Wildlife Service, and U.S. Department of Commerce, U.S. Census Bureau. 2007. *2006 National Survey of Fishing, Hunting, and Wildlife-Associated Recreation*.

## **4.0 AQUATIC ENRICHMENT**

One of the main adverse ecological effects resulting from nitrogen deposition, particularly in the Mid-Atlantic region of the United States, is the effect associated with nutrient enrichment in estuarine waters. A recent assessment of 141 estuaries nationwide by the National Oceanic and Atmospheric Administration (NOAA) concluded that 19 estuaries (13%) suffered from moderately high or high levels of eutrophication due to excessive inputs of both nitrogen and phosphorus, and a majority of these estuaries are located in the coastal area from North Carolina to Massachusetts (NOAA, 2007). By several measures, the aquatic ecosystem of the Chesapeake Bay estuary is particularly suffering from the effects of excessive nitrogen loads, and roughly one-third of these loads are associated with atmospheric deposition of nitrogen in the watershed (Sweeney, 2007).<sup>1</sup> For other estuaries in the Mid-Atlantic region, the contribution of atmospheric distribution to total nitrogen loads is estimated to range between 10% and 58% (Valigura et al., 2001).

Eutrophication in estuaries is associated with a range of adverse ecological effects. Using the conceptual framework developed by NOAA, **Figure 4-1** illustrates the main links between nutrient loadings and ecological symptoms in estuaries. The framework emphasizes four main types of eutrophication effects—low dissolved oxygen (DO), harmful algal blooms (HABs), loss of submerged aquatic vegetation (SAV), and low water clarity.

Low DO (i.e., hypoxia) has become a chronic problem in several estuaries, particularly during summer months. Five of the 22 estuaries evaluated by NOAA in the Mid-Atlantic region suffer from serious DO problems. The mainstem of the Chesapeake Bay has been a particular area of concern. For example, between 2005 and 2007, only about 12% of the Bay met DO standards during the summer months (Chesapeake Bay Program, n.d.). Low DO disrupts aquatic habitats, causing stress to fish and shellfish, which, in the short term, can lead to episodic fish kills and, in the long term, can damage overall growth in fish and shellfish populations. Low DO also degrades the aesthetic qualities of surface water.

---

<sup>1</sup> Phosphorus loads, primarily from agricultural runoff and wastewater dischargers in the Chesapeake Bay watershed, are the other main source of nutrients contributing to eutrophication in the Bay.

HABs were also rated by NOAA as a major problem in five Mid-Atlantic estuaries, including the mainstem of the Chesapeake Bay and the Potomac River estuary. In addition to often being toxic to fish and shellfish and leading to fish kills and aesthetic impairments of estuaries, HABs can, in some instances, also be harmful to human health.

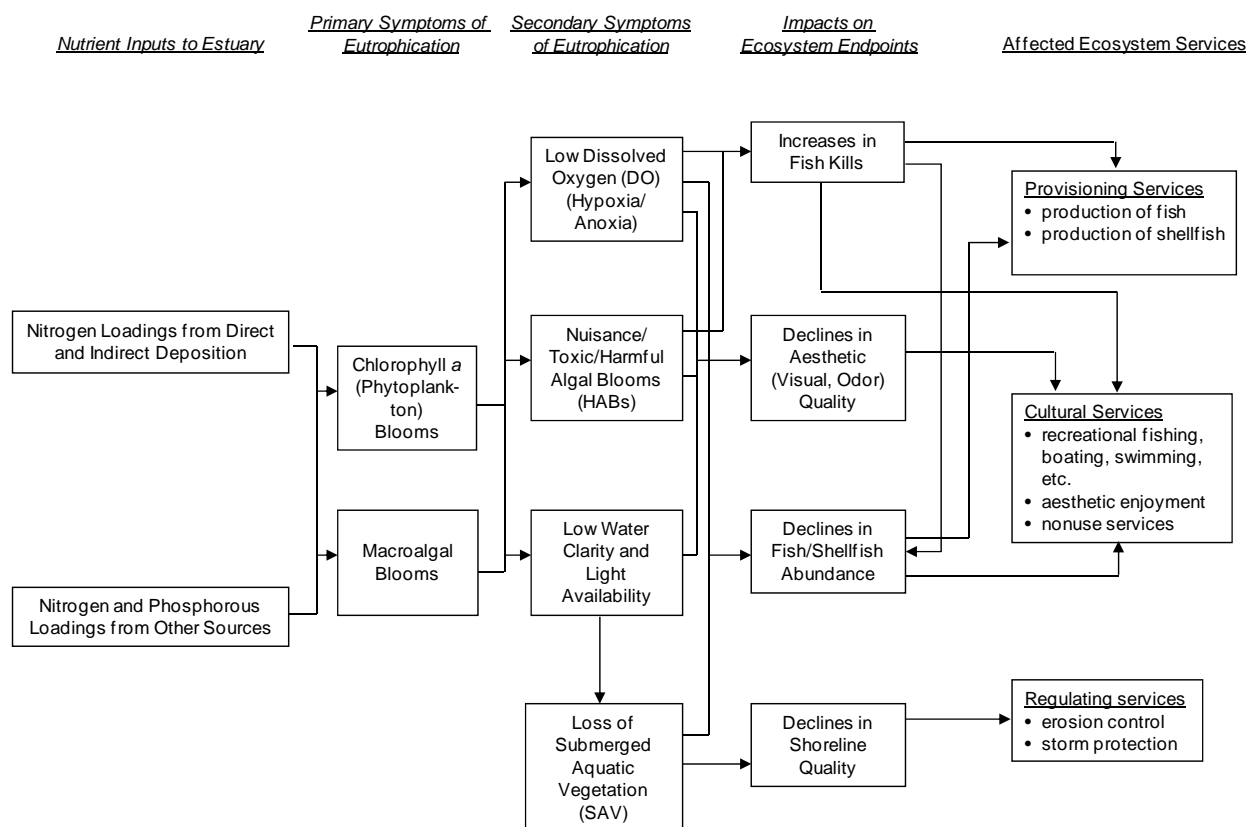


**Figure 4-1.** Conceptual Model of Eutrophication Impacts in Estuaries (Source: Adapted from Bricker et al. [2007] and Bricker, Ferreira, and Simas [2003]).

SAV provides critical habitat for many aquatic species in estuaries and, in some instances, can also protect shorelines by reducing wave strength; therefore, declines in SAV due to nutrient enrichment are an important source of concern. Although less prevalent than low DO and HABs as a problematic symptom of eutrophication, it is nonetheless rated by NOAA as a serious problem in the mainstem of the Chesapeake Bay and the New Jersey Inland Bays.

Low water clarity is the result of accumulations of both algae and sediments in estuarine waters. In addition to contributing to declines in SAV, high levels of turbidity also degrade the aesthetic qualities of the estuarine environment. Although NOAA's assessment of estuaries did not focus on turbidity separately as an indicator of eutrophication, it is nonetheless a common problem in the Mid-Atlantic region.

## **4.1 OVERVIEW OF AFFECTED ECOSYSTEM SERVICES**

**Figure 4-1** also extends the NOAA framework to include links to the main types of ecosystem services that are affected by the primary and secondary symptoms of eutrophication. The following sections provide a discussion and overview of the primarily affected provisioning, cultural, and regulating services.

### **4.1.1 Provisioning Services**

Estuaries in the eastern United States are an important source of food production, in particular fish and shellfish production. The estuaries are capable of supporting large stocks of resident commercial species, and they serve as the breeding grounds and interim habitat for several migratory species.

To provide an indication of the magnitude of provisioning services associated with coastal fisheries, **Table 4.1-1** reports the annual value of commercial landings in recent years for 15 East Coast states. From 2005 to 2007, the average value of total catch was \$1.5 billion per year. It is not known, however, what percentage of this value is directly attributable to or dependent upon the estuaries in these states. **Table 4.1-2** focuses specifically on commercial landings in Maryland and Virginia in 2007, and it reports values for the main commercial species in these states. Although these values also include fish caught outside of the Chesapeake Bay, the values for two key species—blue crab and striped bass—are predominantly from the estuary itself. These data indicate that blue crab landings in 2007 totaled nearly \$44 million in the Bay. The value of striped bass and menhaden totaled about \$9 million and \$25 million, respectively.

To most accurately assess how eutrophication in East Coast estuaries is related to the long-term provisioning services from their fishery resources requires bioeconomic models (i.e., models that combine biological models of fish population dynamics with economic models describing fish harvesting and consumption decisions). In most cases, these models address the dynamic feedback effects between fish stocks and harvesting behavior, and they characterize conditions for a “steady-state” equilibrium, where stocks and harvest levels are stabilized and sustainable over time.

Section 4.2 describes one bioeconomic model linking blue crab harvests to nutrient loads in the Neuse River estuary, and it applies the model to estimate how reductions in nitrogen loads to the estuary would affect the societal value of future blue crab harvests. In practice, however,

very few other studies have developed empirical bioeconomic models to estimate how changes in environmental quality affect fish harvests and the value of these services (Knowler, 2002). One exception is Kahn and Kemp (1985), which estimated a bioeconomic model of commercial and recreational striped bass fishing using annual data from 1965 to 1979, measuring the effects of SAV levels on fish stocks, harvests, and social welfare. They estimated, for example, that a 50% reduction in SAV from levels existing in the late 1970s (similar to current levels [Chesapeake Bay Program, 2008]) would decrease the net social benefits from striped bass by roughly \$16 million (in 2007 dollars).

In a separate analysis, Anderson (1989) developed an empirical dynamic simulation model of the effects of SAV changes on commercial blue crab harvests in the Virginia portion of the Chesapeake Bay. Applying the empirical model results, long-run (15-year) dynamic equilibria were estimated under baseline conditions (assuming SAV area constant at 1987 levels) and under conditions with “full restoration” of SAV (i.e., 284% increase). In equilibrium, the increase in annual producer surplus and consumer surplus with full restoration of SAV was estimated to be \$3.5 million and \$4.4 million (in 2007 dollars), respectively.

**Table 4.1-1.** Annual Values of East Coast Commercial Landings (in millions)

State	2004	2005	2006	2007
Connecticut	\$33.40	\$37.57	\$36.89	\$42.08
Delaware	\$5.42	\$6.11	\$5.69	\$7.58
Florida, East Coast	\$39.98	\$35.49	\$42.00	\$42.74
Georgia	\$14.37	\$13.46	\$11.53	\$10.08
Maine	\$367.09	\$391.90	\$361.85	\$319.52
Maryland	\$49.29	\$63.67	\$53.58	\$52.27
Massachusetts	\$326.00	\$427.07	\$437.05	\$457.18
New Hampshire	\$17.21	\$22.12	\$18.84	\$19.09
New Jersey	\$145.86	\$159.01	\$136.05	\$152.46
New York	\$46.89	\$56.45	\$57.73	\$58.94
North Carolina	\$79.70	\$64.89	\$70.12	\$82.31
Pennsylvania	\$0.07	\$0.04	\$0.10	\$0.13
Rhode Island	\$76.25	\$91.58	\$98.58	\$76.79

State	2004	2005	2006	2007
South Carolina	\$18.54	\$17.57	\$17.03	\$15.57
Virginia	\$160.51	\$155.26	\$109.07	\$130.56
Total	\$1,380.60	\$1,542.20	\$1,456.11	\$1,467.31

Source: National Oceanic and Atmospheric Administration (NOAA), 2007.

**Table 4.1-2.** Value of Commercial Landings for Selected Species in 2007 (Chesapeake Bay Region)

State	Species	Value
Maryland	Blue crab	\$30,433,777
	Striped bass	\$5,306,728
	Clams or bivalves	\$5,007,952
	Sea scallop	\$2,808,984
	Oyster, Eastern	\$2,524,045
	Other	\$6,190,474
	Total	\$52,271,960
Virginia	Sea scallop	\$62,891,848
	Menhaden	\$25,350,740
	Blue crab	\$13,222,135
	Croaker, Atlantic	\$4,615,924
	Striped bass	\$3,834,906
	Clam, Northern Quahog	\$3,691,319
	Summer flounder	\$3,186,229
	Other	\$16,954,893
	Total	\$130,561,765

Source: National Oceanic and Atmospheric Administration (NOAA), 2007.

One study examining the short-term effects of DO levels on crab harvests is Mistiaen, Strand, and Lipton (2003). Focusing on three Chesapeake Bay tributaries—the Patuxent, Chester, and Choptank rivers—they estimated a “stress-availability” model measuring the effects of DO levels on the availability of blue crabs for commercial harvest, given the stock levels and number of fishing vessels. The model results indicated that, below a threshold of 5 mg/L,



reductions in DO cause a statistically significant reduction in commercial harvest and revenues. For the Patuxent River alone, a simulated reduction of DO from 5.6 to 4.0 mg/L was estimated to reduce crab harvests by 49% and reduce total annual earnings in the fishery by \$275,000 (in 2007 dollars). However, this is an upper-bound estimate because it does not account for changes in fishing effort that would likely occur, and if the measured changes are due to migration of crab populations to other areas rather than to crab mortality, then the broader net effects on crab harvests may also be considerably smaller.<sup>2</sup>

In addition to affecting provisioning services through commercial fish harvests, eutrophication in estuaries may also affect these services through its effects on the demand for seafood. For example, a well-publicized toxic pfiesteria bloom in the Maryland Eastern Shore in 1997, which involved thousands of dead and lesioned fish, led to an estimated \$56 million (in 2007 dollars) in lost seafood sales for 360 seafood firms in Maryland in the months following the outbreak (Lipton, 1999). Additional evidence regarding potential losses in provisioning services due to eutrophication-related fish kills is provided by Whitehead, Haab, and Parsons (2003) and Parsons et al. (2006). The survey used in both studies was conducted with more than 5,000 respondents in states bordering the Chesapeake Bay area and in North Carolina. The survey asked respondents to consider how their consumption patterns would change in response to news about a large fish kill caused by a toxic pfiesteria bloom. To address the fact that not all fish kills are the same, the size and type of the described fish kill—either “major,” involving more than 300,000 dead fish and 75% with pfiesteria lesions, or “minor,” involving 10,000 dead fish and 50% with lesions—were randomized across respondents. Based on respondents’ stated behaviors, the studies estimated reductions in consumer surplus per seafood meal ranging from \$2 to \$5.<sup>3</sup> The survey also found that 42% of residents in the four-state area (Maryland, Virginia, Delaware, and North Carolina) were seafood consumers and that the average number of seafood meals per month among these consumers was between four and five. As a result, they estimated

---

<sup>2</sup> The estimated relationship between harvest and DO is discontinuous at 5 mg/L. The size of the measured effect on harvests is relatively small below 5 mg/L and zero above the 5 mg/L threshold; therefore, any sizable benefits would require DO to cross the 5 mg/L threshold. Moreover, the 5 mg/L threshold was an assumption of the model rather than a tested hypothesis, which raises additional questions about the accuracy of benefit estimates for changes across the threshold.

<sup>3</sup> Surprisingly, these estimates were not sensitive to whether the fish kill was described as major or minor or to the different types of information included in the survey.

aggregate consumer surplus losses of \$43 million to \$84 million (in 2007 dollars) in the month after a fish kill.

#### **4.1.2 Cultural Services**

Estuaries in the eastern United States also provide an important and substantial variety of cultural ecosystem services, including water-based recreational and aesthetic services. One of the difficulties with quantifying recreational services from estuaries is that much of the national and regional statistics are jointly collected and reported for estuarine and other coastal areas. Nevertheless, even these combined statistics provide several useful indicators of recreational service flows. For example, data from the FHWAR indicate that, in 2006, 4.8% of the 16 or older population in coastal states from North Carolina to Massachusetts participated in saltwater fishing. The total number of days of saltwater fishing in these states was 26.1 million in 2006. Based on estimates from Kaval and Loomis (2003), the average consumer surplus value for a fishing day was \$35.91 (in 2007 dollars) in the Northeast and \$87.23 in the Southeast. Therefore, the total recreational consumer surplus value from these saltwater fishing days was approximately \$1.28 billion (in 2007 dollars).

Recreational participation estimates for several other coastal recreational activities are also available for 1999 to 2000 from the NSRE. These estimates are summarized in **Table 4.2-1** based on data reported in Leeworthy and Wiley (2001). Almost 6 million individuals aged 16 or older participated in motorboating in coastal states from North Carolina to Massachusetts, for a total of nearly 63 million days annually during 1999–2000. Using a national daily value estimate of \$32.69 (in 2007 dollars) for motorboating from Kaval and Loomis (2003), the aggregate value of these coastal motorboating outings was \$2.08 billion per year. Almost 7 million people participated in birdwatching, for a total of almost 175 million days per year, and more than 3 million participated in visits to nonbeach coastal waterside areas, for a total of more than 35 million days per year. In contrast, fewer than 1 million individuals per year participated in canoeing, kayaking, or waterfowl hunting.

#### **4.1.3 Regulating Services**

Estuaries and marshes have the potential to support a wide range of regulating services, including climate, biological, and water regulation; pollution detoxification; erosion prevention; and protection against natural hazards (Millennium Ecosystem Assessment [MEA], 2005). It is

more difficult, however, to identify the specific regulating services that are significantly impacted by changes in nutrient loadings. One potentially affected service is provided by SAV, which can help reduce wave energy levels and thus protect shorelines against excessive erosion. Declines in SAV may, therefore, also increase the risks of episodic flooding and associated damages to near-shore properties or public infrastructure. In the extreme, these declines may even contribute to shoreline retreat, such that land and structures are lost to the advancing waterline.

## **4.2 CHANGES IN ECOSYSTEM SERVICES ASSOCIATED WITH ALTERNATIVE LEVELS OF ECOLOGICAL INDICATORS**

This section estimates values for changes in several ecosystem services associated with reduced nutrient enrichment effects in the Chesapeake Bay and Neuse River estuaries. Using the results of the Potomac River and Neuse River Case Studies, *the value of removing all atmospheric sources of nitrogen loadings to these estuaries was estimated*. Although such a large change represents an upper bound on possible loading reductions through controls on atmospheric sources, it corresponds with the findings of the case studies, which indicate that reductions of this magnitude are the minimum required to improve the eutrophication index (EI) score (based on NOAA's ASSETS framework) from current "bad" conditions (EI = 1) in these two estuaries to somewhat better "poor" conditions (EI = 2).

**Table 4.2-1.** Participation in Selected Marine Recreation Activities in East Coast States in 1999–2000

State	Visiting Watersides besides Beaches		Motorboating		Canoeing	Kayaking	Bird Watching		Waterfowl Hunting
	N <sup>a</sup>	Days <sup>b</sup>	N <sup>a</sup>	Days <sup>b</sup>	N <sup>a</sup>	N <sup>a</sup>	N <sup>a</sup>	Days <sup>b</sup>	N <sup>a</sup>
Connecticut	0.18	2.41	0.39	6.76	0.05	0.10	0.45	15.19	0.00
Delaware	0.08	— <sup>c</sup>	0.38	4.56	0.04	0.02	0.43	14.03	0.02
Maryland	0.47	5.89	0.97	8.13	0.16	0.03	0.82	19.76	0.03
Massachusetts	0.47	2.93	0.61	6.05	0.07	0.17	1.02	26.10	0.00
New Jersey	0.45	4.58	0.89	12.45	0.07	0.10	0.80	18.80	0.01
New York	0.56	3.74	0.90	9.48	0.07	0.06	0.88	24.55	0.00
North Carolina	0.44	4.16	0.55	7.25	0.04	0.12	1.04	20.52	0.03
Rhode Island	0.27	3.31	0.38	4.37	0.15	0.11	0.56	19.01	0.00
Virginia	0.48	8.27	0.60	4.54	0.15	0.06	0.86	17.00	0.04
Total	3.41	35.29	5.67	63.59	0.79	0.76	6.84	174.96	0.13

<sup>a</sup> Number of resident and nonresident participants annually (in millions).

<sup>b</sup> Number of days by residents and nonresidents annually (in millions).

<sup>c</sup> Insufficient data for estimate.

Source: Leeworthy and Wiley, 2001

#### **4.2.1 The Chesapeake Bay Estuary**

For the Chesapeake Bay analysis, the results of the Potomac River/Potomac Estuary Case Study were applied. Other than the mainstem of the Bay (6,074 km<sup>2</sup>), the Potomac estuary is the largest subestuary within the Chesapeake Bay estuary system (1,260 km<sup>2</sup>), and other than the Susquehanna River, which flows directly into the mainstem, it contributes the largest portion of freshwater (19%) to the Bay. Eutrophic conditions within the Potomac estuary are also reflective of more widespread conditions in the Bay. For example, when assessing estuarine conditions across the country in 2004, NOAA (2007) evaluated nine subestuaries of the Bay, including the mainstem and the Potomac. Five subestuaries in the Bay, including the mainstem and the Potomac, rated “high” with respect to overall eutrophic conditions (the worst level on a 5-point scale from low to high). The remaining four subestuaries were all rated as “moderate high” (the second worst level). Therefore, for this analysis, *it was assumed that the results of the Potomac River estuary case study are representative of the Chesapeake Bay as a whole.*

According to the Aquatic Nutrient Enrichment Case Study, atmospheric deposition is estimated to contribute 24% (7.38 million kg nitrogen/year) of total nitrogen loadings to the Potomac estuary. This percentage falls within the range of the 23% to 33% that has been estimated for the Chesapeake Bay as a whole (Valigura et al., 2001). The case study also estimates that a reduction in nitrogen loadings roughly equivalent to the contribution from atmospheric deposition in the Potomac River watershed would be required to improve the Potomac estuary from “bad” to “poor” on the 5-point ASSETS EI.<sup>4</sup>

For the Chesapeake Bay analysis, the change in selected ecosystem services associated with a 24% reduction in loadings to the Chesapeake Bay as a whole was estimated, and it was assumed that this reduction would also improve the Bay’s overall EI score from “bad” to “poor.” The selection of ecosystem services for this analysis, which includes recreational, aesthetic, and nonuse services (i.e., specific cultural services), was based on availability of existing models, data, and empirical results.

For each of the ecosystem service categories addressed in this section, the geographic extent of aggregate benefits to residents and recreators in Maryland, Virginia, and Washington,

---

<sup>4</sup> The mean and median estimate of required loading reductions is 104% of the annual atmospheric deposition component (almost 25% of all N loadings).

DC (DC) was limited. Because these areas are directly adjacent to the Bay, this approach is expected to include a large majority of the beneficiaries; however, this approach also will unavoidably contribute to some underestimation of aggregate benefits. Other specific limitations and uncertainties in the proposed methods are described in each of the subsections below.

#### **4.2.1.1 Recreational Fishing Services**

This section describes and applies a three-part “benefit transfer” framework for estimating the recreational fishing benefits of improved eutrophic conditions in the Chesapeake Bay. The first component translates changes in the 5-point EI into equivalent changes in average DO levels in the Bay. This step is required to link eutrophic conditions to existing recreational catch rate models.

The second component predicts the effect of changes in average DO levels on recreational fishing catch rates. These catch rates can be interpreted as indicators of the recreational fishing services provided by the Bay. Two catch rate models are described: one based on a study of striped bass fishing in the Bay and the other based on a study of summer flounder fishing in the Maryland coastal bays.

The third component estimates the benefits of catch rate improvements using willingness to pay (WTP) estimates derived from a meta-analysis study by Johnston et al. (2005) and annual fishing trip estimates to the Bay using data from the Marine Recreation Fishing Statistics Survey (MRFSS).

##### **4.2.1.1.1 Converting Changes in EI to Changes in DO**

As described above, low DO is one of several ecosystem symptoms associated with estuarine eutrophication; therefore, DO levels are one of several factors included in the ASSETS framework to derive the composite 5-point EI.

To derive changes in DO that are equivalent to a 1-unit change on the EI, data for a comparable water quality index were used. In collaboration with the University of Maryland’s Center for Environmental Science, NOAA has also developed a 100-point Chesapeake Water Quality Index (CWQI) based on three main eutrophication symptom indicators—chlorophyll *a*, water clarity, and DO (Chesapeake Eco-Check, 2007). Using annual data for the three water quality parameters, a water quality index score was generated for 141 monitoring stations across the Bay in 2007. **Table 4.2-2** reports the results of regressing the CWQI score for each station

against four corresponding water quality measures—(1) average surface DO, (2) average bottom DO, (3) average secchi depth, and (4) average chlorophyll *a*. Both DO measures have positive and statistically significant effects (with a p-value less than 0.05) on the index score, although the estimated effect of bottom DO is somewhat larger. A 1-unit change in both bottom and surface DO is predicted to change the CWQI by a combined effect of 8.3 points. If it was assumed that the 100-point CWQI and the 5-point EI are directly proportional, then a 1-unit change in both bottom and surface DO is predicted to change the EI by 0.415 (= 8.3/20) points. Alternatively, a 1-point increase in the EI (e.g., from “bad” to “good”) would be predicted to result from a 2.41-unit increase in both surface and bottom DO.<sup>5</sup> Therefore, going forward, the effects on recreational fishing resulting from an increase in bottom and surface DO of 2.41 mg/L, which is assumed to be equivalent to a 1-unit increase in the EI, were estimated.

**Table 4.2-2.** Regression Analysis of the Chesapeake Water Quality Index on Water Quality Parameters

Water Quality Parameter	Regression Results		Summary Statistics			
	Coefficient	P-value	Mean	Std. Dev.	Min	Max
CWQI (dependent variable)	—	—	48.85	22.30	9	100
Explanatory variables						
Chlorophyll <i>a</i> (ug/L)	−0.556	0.000	15.99	14.09	2.0	82.0
Secchi depth (m)	0.163	0.443	2.32	7.44	0.1	50.4
Bottom DO (mg/L)	5.069	0.000	5.01	2.00	0.1	9.3
Surface DO (mg/L)	3.235	0.028	6.91	0.97	4.5	9.1
Constant	6.296	0.556	—	—	—	—
Observations	141					
R-squared	0.357					

<sup>5</sup> Based on the results in Table 4.2-2, other combinations of bottom DO and surface DO changes can also produce a 1-point increase in the EI; however, for simplicity, equivalent changes in the two DO measures were considered.

#### 4.2.1.1.2 Estimating Changes in Recreation Services (Catch Rates)

In two related papers, Lipton and Hicks (1999, 2003) reported the results of a travel cost study of recreational striped bass fishing in the Chesapeake Bay. One of the main focuses of the study was measuring the effect of DO levels on striped bass catch rates. The fishing data for this study were drawn from the National Marine Fisheries Service's (NMFS's) 1994 MRFSS, which included 407 intercept sites in the Bay and 1,806 striped bass angler respondents. The DO water quality data were from biweekly summer sampling at 207 locations in the Bay.

The striped bass catch model assumes that the number of fish caught per trip (in logarithmic form) at a site is a linear function of several factors, including the hours spent by the angler at the site on the trip, the angler's experience and skill in saltwater fishing, and water quality conditions at the site. Water quality is characterized in the model by surface temperature ( $ST$ ), bottom temperature ( $BT$ ), surface DO ( $SDO$ ), and bottom DO ( $BDO$ ). According to the functional form of the estimated model, the *change* in the expected striped bass catch rate per trip due to a water quality change can be expressed as

$$\Delta Q = Q_1 - Q_0 = \exp(f_B(\Delta WQ) + \ln Q_0) - Q_0, \quad (4.1)$$

where  $Q_i$  is the expected number of striped bass caught per trip under conditions  $i$ , such that  $i = 0$  represents reference conditions and  $i = 1$  represents conditions after the water quality change. The function  $f_B(\Delta WQ)$  represents the combined effect of changes in temperature and DO on expected catch rates. Using the parameter estimates from the empirical catch rate model, this function for striped bass can be expressed as

$$\begin{aligned} f_B(\Delta WQ) = \ln Q_1 - \ln Q_0 = & -0.2548(ST_1 - ST_0) + 0.3225(BT_1 - BT_0) \\ & + 0.2589(SDO_1 - SDO_0) + 0.2253(BDO_1 - BDO_0) - 0.0167(BDO_1^2 - BDO_0^2) \end{aligned} \quad (4.2)$$

To quantify baseline catch rates ( $Q_0$ ), recent MRFSS data for the Bay, which are summarized in **Table 4.2-3**, were used. The table reports average catch rates for striped bass and other key recreational species for 2001 to 2005. Over the 5-year period, striped bass catch rates averaged 1.65 fish per trip in Maryland and 0.59 fish per trip in Virginia.<sup>6</sup>

---

<sup>6</sup> For comparison, Lipton and Hicks (1999) reported that average catch rates in 1994 were 0.71 in Maryland and 0.66 in Virginia.



With these baseline catch rate estimates, Equations (4.1) and (4.2) can be used to predict the change in average catch rate ( $\Delta Q$ ) associated with specific changes in surface and bottom temperature and DO levels. For example, if average surface and bottom DO levels in the Bay both increase by 2.41 units (with no change in temperature), the striped bass catch rate is predicted to increase by 1.57 in Maryland and by 0.56 in Virginia (a 94.9% increase).

**Table 4.2-3.** Average Catch Rate per Fishing Trip in the Chesapeake Bay, by State and Targeted Fish Species

Fishing Trip	2001	2002	2003	2004	2005	Average 2001–2005
Maryland residents						
Striped bass	1.20	1.58	1.99	1.81	1.70	1.65
Summer flounder	0.09	0.08	0.09	0.34	0.04	0.12
Other species	0.29	0.32	0.32	0.27	0.45	0.33
All species	0.34	0.38	0.40	0.35	0.51	0.39
Virginia residents						
Striped bass	0.42	0.44	0.52	0.82	0.68	0.59
Summer flounder	0.96	0.80	0.91	0.93	0.69	0.86
Other species	0.34	0.40	0.26	0.27	0.34	0.32
All species	0.37	0.42	0.29	0.32	0.36	0.35

Source: National Oceanic and Atmospheric Administration (NOAA), 2009.

It is more difficult to develop catch rate predictions for other recreational species, because of the apparent lack of any other empirical studies that have estimated the relationship between water quality conditions and recreational catch rates in the Bay.<sup>7</sup> One alternative is to assume that the striped bass model described above is applicable to other species; however, the resulting catch rate change estimates would inevitably have higher levels of uncertainty associated with them.

A second approach is to use catch rate models developed in areas outside the Bay; however, only one such study was found.<sup>8</sup> Massey, Newbold, and Gentner (2006) used data from

<sup>7</sup> Bricker et al. (2006) described similar models for the Potomac and Patuxent River estuaries and other East Coast estuaries; however, they did not provide parameter estimates for these models.

<sup>8</sup> Kaoru, Smith, and Liu (1995) also estimated the effects of estuarine water quality on recreational fishing in North Carolina; however, rather than using ambient water quality measures, he used estimates of nutrient and biochemical oxygen demand loadings as proxies for water quality conditions.

the Maryland coastal bays to estimate a catch rate model for recreational summer flounder fishing. They found significant effects from  $DO$ , temperature ( $T$ ), and water clarity (secchi depth [ $SD$ ]) on recreational catch. Using the parameter estimates from this model, the following function summarizes the measured effects of water quality on summer flounder catch rates:

$$f_F(\Delta WQ) = 0.117(DO_1 - DO_0) + 0.126(T_1 - T_0) + 1.392(SD_1 - SD_0). \quad (4.3)$$

Applying this function to Equation (4.1) in place of  $f_B(\Delta WQ)$ , a 2.41-unit increase in  $DO$  (with no change in  $T$  or  $SD$ ) is predicted to increase summer flounder catch by an additional 0.04 fish per trip in Maryland and 0.28 fish per trip in Virginia (a 32.6% increase). Transferring this model from the Maryland coastal bays to the Chesapeake Bay also contributes to the uncertainty in catch rate predictions for summer flounder, although arguably less so than transferring models from other species (i.e., striped bass) within the Bay.

#### 4.2.1.1.3 Valuing Changes in Catch Rates

The second component of the proposed benefit transfer model for recreational fishing can be summarized as follows:

$$AggB_{fish} = \sum_j (WTP_{fish} \times T_j) \times \Delta Q_j, \quad (4.4)$$

where

$AggB_{fish}$  = aggregate annual benefits (in 2007 dollars) to Chesapeake Bay anglers for specified increases in species-specific average catch rates per trip ( $\Delta Q_j$ , where  $j$  is the species indicator),

$\Delta Q_j$  = predicted change in average catch rate per trip for species  $j$  in the Chesapeake Bay (as described in Section 4.2.1.1.2),

$WTP_{fish}$  = average WTP per additional fish caught per trip, and

$T_j$  = total number of annual fishing trips (in 2007) targeting species  $j$  in the Chesapeake Bay.

A large number of revealed- and stated-preference studies have estimated welfare changes associated with changes in recreational fishing catch rates in the United States. Most of these results have been synthesized in a meta-analysis study by Johnston et al. (2006), which estimated meta-regression models controlling for differences across studies in type of water resource, context, angler attributes, and in-study methods. Using these summary models, they

predicted average WTP per fish per trip for different species categories. For both Atlantic small game (including striped bass) and Atlantic flatfish (including summer flounder), they predicted WTP ranging from \$3 to \$11 in 2003 dollars. This meta-analysis study included one WTP estimate from a Chesapeake Bay striped bass study (Bockstael, McConnell, and Strand, 1989), which falls slightly below this range (\$2.23), but it did not include a more recent striped bass estimate from the Lipton and Hicks (1999) study, which falls within the upper end of the range (\$10.91). Johnston et al.'s (2006) study also did not include the estimate for summer flounder in Maryland coastal bays from Massey, Newbold, and Gentner (2006), which falls within the lower end of the range (\$4.22 in 2002 dollars).

Based on these WTP results from the literature, a value range of \$2.50 to \$12.50 for  $WTP_{fish}$ , with a midpoint of \$7.50, was selected.

To quantify annual trips by species ( $T_j$ ), recent MRFSS data for the Bay, which are summarized in **Table 4.2-4**, were again used. The table reports total annual trips for striped bass and other key recreational species from 2001 to 2005. To approximate trips in 2007, the average number of trips from 2001 to 2005 by species were used. The same methodology was used to approximate baseline catch rates for 2007.

**Table 4.2-4.** Aggregate Number of Fishing Trips to the Chesapeake Bay, by State and Targeted Fish Species

Fishing Trip	2001	2002	2003	2004	2005	Average 2001–2005
<b>Maryland residents</b>						
Striped bass	2,594,971	2,014,818	2,579,771	2,176,824	2,351,145	2,343,506
Summer flounder	2,106,810	1,268,048	1,598,484	1,486,154	1,734,101	1,638,719
Other species	33,457,937	31,349,971	48,352,248	39,740,106	34,503,965	37,480,845
All species	38,159,717	34,632,837	52,530,503	43,403,083	38,589,211	41,463,070
<b>Virginia residents</b>						
Striped bass	2,043,025	1,911,180	2,369,576	2,525,057	2,549,248	2,279,617
Summer flounder	2,285,628	1,982,130	2,300,633	2,556,902	2,549,248	2,334,908
Other species	49,915,214	47,535,158	67,839,883	65,345,054	58,036,434	57,734,349
All species	54,243,868	51,428,468	72,510,092	70,427,013	63,134,930	62,348,874

Source: National Oceanic and Atmospheric Administration (NOAA), 2009.

#### **4.2.1.1.4 Results: Aggregate Recreational Fishing Benefits**

Combining the three model components, the aggregate recreational fishing benefits from a 1-point EI increase in Chesapeake Bay from “bad” to “poor” can now be estimated. Assuming that this change is equivalent to a 2.41 mg/L increase in both surface and bottom DO, the result is an annual benefit of \$37.2 million to striped bass anglers in Maryland and Virginia and an annual benefit of \$5.4 million to summer flounder anglers.

Recognizing the uncertainties associated with transferring these models to other species, the same benefit transfer framework can also be applied to other recreational fishing trips. Striped bass and summer flounder fishing only accounted for 7.4% of the total number of trips and 15.5% of the total catch from 2001 to 2005. If the striped bass catch rate model (Equation [4.2]) is applied to all other types of fish species, then a 2.41 mg/L increase in surface and bottom DO would result in an estimated aggregate benefit of \$217 million for recreational anglers targeting these other species in the Bay.

#### **4.2.1.1.5 Limitations and Uncertainties**

Although the objective of the previously described approach is to make the best use of existing research to quantify the relationship between changes in eutrophic conditions and recreational fishing benefits in the Bay, the following limitations and uncertainties must also be noted.

First, the conversion of changes in EI to changes in DO requires several strong assumptions. One key assumption is that the EI and CWQI are directly proportionate to one another. The reasonableness of this assumption rests on the fact that the two indexes use similar symptom indicators (DO, SD, and chlorophyll *a*) and both have been designed and used by NOAA as summary metrics of eutrophic conditions in estuaries. Another key assumption is that the regression model in Table 4.2-2 can be used to generate equivalent changes in DO. Because several water quality parameters besides DO are also measures of eutrophic symptoms, there is no guarantee that a 1-unit change in EI is *uniquely* associated with a 2.41 mg/L change in surface and bottom DO (i.e., that the other factors are held constant).

Second, the catch rate models summarized in Equations (4.2) and (4.3) are most likely to understate the effects of long-term changes (i.e., over several years) in water quality across the

entire Bay. Both models are based on analyses that use spatial and short-term (during a single year's fishing season) temporal variation to measure the relationship between catch rates and water quality conditions. Therefore, these measured relationships cannot be expected to capture the dynamic effects of long-term changes in DO on the overall growth and abundance of the striped bass and summer flounder populations in the Bay.

Third, as previously noted, empirical catch rate models are only available for striped bass and summer flounder, and the model for the latter species is based on data from outside the Bay. Although it is not difficult to apply these models to estimate catch rate changes for other species within the Bay, the resulting estimates are subject to significant uncertainty, because there is little evidence about how well these models transfer to other species.

Fourth, the valuation model summarized in Equation (4.4) uses a number of simplifying assumptions. In particular, the value per fish caught is assumed to be constant, but within a large range—\$2.50 to \$12.50—which can significantly affect the aggregate benefit estimates. In addition, the total number of fishing trips is assumed to be unaffected by changes in catch rates. This restriction is expected to understate the true aggregate benefits of increased catch rates, because higher catch rates would most likely increase the number of fishing trips.

#### **4.2.1.2 Boating**

To estimate benefits to Chesapeake Bay boaters, a benefit transfer approach that uses value estimates developed by Lipton (2004) is described. That study used a CV method and survey data from 755 Maryland boaters in 2000 to estimate the individual and aggregate benefits of a 1-unit improvement in respondents' water quality rating (on a 1 to 5 scale from "poor" to "excellent") for the Bay. The benefit transfer model based on this study can be summarized as follows:

$$AggB_{boat} = \sum_i \sum_j (WTP_{boat,i} \times N_{i,j} \times b_j) \times \Delta WQ_5, \quad (4.5)$$

where

$\Delta WQ_5$  = change in Chesapeake Bay water quality, expressed on a 5-point rating scale (from "poor" to "excellent");

$AggB_{boat}$  = aggregate annual benefits (in 2007 dollars) to Maryland, Virginia, and DC boat owners who use the Chesapeake Bay as their principal boating area for a specified  $\Delta WQ_5$  increase in water quality;

$WTP_{boat,i}$  = average annual WTP (in 2007 dollars) per boater for a 1-unit increase in water quality on the  $WQ_5$  scale ( $i$  = sailboat, trailered powerboat, or in-water powerboat);

$N_{i,j}$  = total number of boats by type  $i$  and location  $j$  ( $j$  = Maryland, Virginia, or DC) of boat ownership in 2007; and

$b_j$  = the ratio of (1) registered boat *owners* whose principal boating area is the Chesapeake Bay to (2) the total number of registered *boats* (by location  $j$ ).

Lipton (2004) reported estimates of average WTP by boat owners in three different categories for a 1-unit increase in water quality ( $\Delta WQ_5 = 1$ ) in the Chesapeake Bay. Sailboat owners had the highest average WTP of \$93.26 (in 2000 dollars). Trailered and in-water powerboat owners had an average WTP of \$30.25 and \$77.98, respectively.

Converting these Lipton (2004) estimates to 2007 dollars with the consumer price index (CPI) results in  $WTP_{boat}$  estimates of \$112.29, \$36.42, and \$93.89 for sailboat, trailered powerboat, and in-water powerboat owners, respectively (**Table 4.2-5**).

**Table 4.2-5.** Input Estimates for the Chesapeake Bay Boating Benefit Transfer Model

Boat Type	Number of Registered Boats			Adjustment Factor			$WTP_{boat}$
	$N_{MD}$	$N_{VA}$	$N_{DC}$	$b_{MD}$	$b_{VA}$	$b_{DC}$	
Sailboat	8,200	9,200	100	60.76%	56.92%	60.76%	\$112.29
Trailered powerboat	93,300	104,600	1,100	60.77%	56.93%	60.77%	\$36.42
In-water powerboat	23,600	26,400	300	60.77%	56.93%	60.77%	\$93.89
Total	125,100	140,300	1,500				

$N_{MD}$  was estimated for the three boater categories using data on Maryland boat ownership from Lipton (2008) and Lipton (2006). The former data source quantifies sailboat and powerboat ownership for 2007, but it does not break out powerboats according to whether they were trailered or in-water boats. To develop separate estimates for these two subcategories, the proportions reported for 2005 (Lipton, 2006), which indicated that 79.8% of powerboats in Maryland were trailered, were applied. To estimate  $N_{VA}$  and  $N_{DC}$ , the total number of registered boats in Virginia and DC in 2006 was obtained from the National Marine Manufacturers Association (2008), and this number was augmented by the observed growth rate in Maryland boat ownership from 2006 to 2007. To separate these total numbers into the three categories of

boat ownership, the same proportions estimated for Maryland registered boats in each category were applied.

The value  $b_{MD}$  represents a two-part adjustment to the total number of registered boats in Maryland, as estimated by Lipton (2004). The first converts the total number of registered boats to the total number of boat owners, because some boat owners own more than one boat. The second adjusts for the fact that, for some Maryland boaters, the Chesapeake Bay is not their principal boating area. Every 100 registered boats correspond to an estimated 60.8 boat owners whose principal boating area is the Chesapeake Bay. The same adjustment factor for registered boaters in DC was applied to estimate  $b_{DC}$ .

To estimate  $b_{VA}$ , the expected 6.3% of registered boats in Virginia Beach (Murray and Lucy, 1981), which is the main Virginia coastal area outside the Bay, was first excluded; then the same adjustment factor developed for Maryland and DC was applied. Thus, in Virginia, for every 100 registered boats, there are 56.9 boat owners whose principal boating area is the Chesapeake Bay.

#### **4.2.1.2.1 Results: Aggregate Recreational Boating Benefits**

To apply the previously described framework, it was first assumed that there is a direct one-to-one correspondence between the 5-point EI and the 5-point subjective  $WQ_5$  index. Based on this assumption, a 1-unit increase in Chesapeake Bay water quality ( $\Delta WQ_5 = 1$  and  $\Delta EI = 1$ ) was estimated to yield an annual aggregate benefit of \$8.2 million for Maryland, Virginia, and DC boat owners whose principal boating area is the Chesapeake Bay.

#### **4.2.1.2.2 Limitations and Uncertainties**

A potential limitation of the proposed benefit transfer model for boating services is the uncertainty associated with directly translating the  $WQ_5$  index into the EI index. Although both metrics are summary 5-point measures of Chesapeake Bay water quality, the first is a subjective index based on boaters' perceptions and experience. These perceptions may be based on observations unrelated to eutrophic conditions (e.g., trash in the water or advisories based on pathogen levels) or boaters may implicitly assign more or less importance to eutrophic conditions than is assigned by the EI.

The other main source of uncertainty is with the number of affected boaters. As in the recreational fishing model, the affected number of recreators is assumed to be unaffected by the

change in water quality. This assumption is likely to lead to an underestimate of the aggregate benefit to boaters of a water quality improvement.

One alternative approach is to use value estimates from Bockstael, McConnell, and Strand (1989), who also estimated changes in consumer surplus for trailered boat owners in Maryland resulting from a 20% decrease in the product of total nitrogen and phosphorus (TNP) levels in the Bay. By rescaling and updating their estimates to 2007 dollars, the implied average WTP per Maryland trailered boat owner per 1% decrease in TNP is \$5.38. Applying this value to the estimated total number of trailered powerboat owners in Maryland, Virginia, and DC (see Table 4.2-1), implies that the aggregate benefits to these boaters per 1% decrease in TNP in the Bay would be \$120,000. Assuming that a 24% decrease in nitrogen loadings would result in a 24% reduction in TNP levels in the Bay, the resulting estimate of annual aggregate benefits is \$2.9 million. The main advantage of this approach compared with the model summarized in Equation (4.5) is that it is based on an objective measure of water quality. The fact that it is based on values estimated through a revealed-preference travel cost model of actual boating behavior, compared with a stated-preference CV approach, may be seen as an advantage. However, this approach also has several drawbacks: (1) it is based on considerably older data (from 1984), (2) it only includes direct estimates for trailered boaters, and (3) it includes a potentially narrower measure of value than the Lipton (2004) study because it uses revealed- rather than stated-preference data. This approach also requires the assumption that decreases in nitrogen loads to the Bay are proportional to decreases in TNP levels in the Bay.

#### **4.2.1.3 Beach Use**

To estimate benefits to Chesapeake Bay beach users, the benefit transfer approaches developed by Morgan and Owens (2001) and Krupnick (1988) were adapted and updated. Both of these studies estimated the aggregate benefits to Maryland, Virginia, and DC households of percentage reductions in levels in the Bay. The fundamental benefit transfer model can be summarized as follows:

$$AggB_{beach} = (WTP_{beach} * (N_1b_1 + N_2b_2) * t_{beach}) * \Delta\%WQ_{TNP}, \quad (4.6)$$

where

$\Delta\%WQ_{TNP}$  = percentage change in Chesapeake Bay water quality, expressed in terms of the average TNP levels, each measured in parts per million (ppm);



$AggB_{beach}$	= aggregate annual benefits (in 2007 dollars) to Maryland, Virginia, and DC households for a specified $\Delta\%WQ_{TNP}$ increase in water quality in the Bay;
$WTP_{beach}$	= average annual household WTP (in 2007 dollars) per trip for a 1% reduction in TNP levels in the Bay;
$N_1$	= total number of households in the 1980 Baltimore and DC standard metropolitan statistical areas (SMSA) in 2007;
$N_2$	= total number of Maryland and Virginia households outside the SMSA in 2007;
$b_1$	= portion of SMSA households with at least one Chesapeake Bay beach trip in the year;
$b_2$	= portion of non-SMSA households in Maryland and Virginia with at least one Chesapeake Bay beach trip in the year; and
$t_{beach}$	= average number of Chesapeake Bay beach trips per year for beach-going Maryland, Virginia, and DC households.

**Table 4.2-6** summarizes value estimates for these model components. Values for  $WTP_{beach}$  were derived using estimates from Bockstael, McConnell, and Strand (1988, 1989). Using data from 408 summer beach users in 1984 at nine Maryland western shore beaches and average county-level summer TNP values, they estimated a varying parameter travel cost model. Based on the model results, they reported *aggregate* annual consumer surplus gains of \$34.66 million (in 1987 dollars) for beachgoers residing in the SMSA associated with a 20% decrease in TNP in the Bay. The study also reported that (1) 401,000 SMSA households per year (in the early 1980s) visited Chesapeake Bay beaches and (2) the average number of trips per year for these beach-going households was 4.35,<sup>9</sup> which implies that there were an estimated 1,745,000 trips to the Bay by SMSA households in 1984. Dividing the aggregate benefit estimate by this number of trips implies an average per-trip benefit of \$19.86 (in 1987 dollars), for a 20% reduction in TNP.

---

<sup>9</sup> This number is actually inferred from a description of values Bockstael, McConnell, and Strand (1989) derived from an alternate model. The value per household user (\$4.70) was divided by the value per trip (\$1.08) to get trips per household (4.35).

**Table 4.2-6.** Input Estimates for the Chesapeake Bay Beach-Use Benefit Transfer Model

Beach Use	Number of Households ( $N$ )	Percentage of Bay Beachgoers ( $b$ )	Average Beach Trips per Year ( $t$ )	$WTP_{beach}$
SMSA	2,744,217	21.00%	4.35	\$1.81
Non-SMSA	2,540,214	3.08%	4.35	\$1.81
Total	5,284,431	12.38%	4.35	\$1.81

To estimate  $WTP_{beach}$ , the \$19.86 estimate was divided by 20 (i.e., it was assumed that each percentage reduction in TNP has the same value), and the estimate was converted to 2007 dollars using the CPI to adjust for inflation. The resulting estimate for  $WTP_{beach}$  is \$1.81.

$N_1$  and  $N_2$  were estimated using the Census estimates of population by county in 2007, multiplied by the ratio of households to population by county in the 2000 U.S. Census. From this calculation, it was estimated that a total of 5.28 million households are in Maryland, Virginia, and DC, and 2.74 million of these are within the SMSA.

For  $b_1$ , the Bockstael, McConnell, and Strand (1989) estimate that 21% of households in the SMSA take at least one beach trip to the Chesapeake Bay a year was applied. To derive  $b_2$ , this estimate was combined with data from the 2006 Virginia Outdoors Survey (Virginia Department of Conservation and Recreation, 2007), which reports that 8% of *all* the households in Virginia take at least one beach trip to the Chesapeake Bay (or other tidal bays) per year. Taken together, these estimates imply that approximately 3% of *non-SMSA* Virginia households take at least one beach trip per year to the Bay. Applying this estimate to Maryland non-SMSA households as well, it was assumed that  $b_2$  equals 3%.

To estimate  $t_{beach}$ , the Bockstael, McConnell, and Strand (1989) estimate of 4.35 trips per year was applied, recognizing that it is most likely an overestimate for non-SMSA beach-going households.

#### 4.2.1.3.1 Results: Aggregate Beach Use Benefits

To apply this benefit estimation framework, it was assumed that changes in nitrogen loads to the Bay are directly proportional to changes in average TNP concentrations in the Bay (i.e., a 24% reduction in loadings results in a 24% decline in TNP). It was estimated that the aggregate annual benefits to Maryland, Virginia, and DC Chesapeake Bay beachgoers

( $AggB_{beach}$ ) per 1% decrease in TNP is \$5.16 million (in 2007 dollars); therefore, the benefit of a 24% decrease is \$124 million.

#### **4.2.1.3.2 Limitations and Uncertainties**

One of the main limitations of the beach-use valuation model described above is that it is based on value estimates that are from 1984 and, therefore, may be outdated. Beach conditions and recreator preferences in the Bay may have changed significantly since then. In addition, several uncertainties are associated with the estimated number of beach trips by Maryland, Virginia, and DC households in 2007. These estimates are based on limited and, in some cases, relatively old data regarding the percentage of households in each state that use the Bay's beaches and the average number of annual beach trips for those who do. A second limitation is that it, again, requires the assumption that decreases in nitrogen loads to the Bay are proportional to decreases in TNP levels in the Bay.

#### **4.2.1.4 Aesthetic Services**

To estimate the benefits of improved aesthetic services due to improvements in Chesapeake Bay water quality, a benefit transfer model that is based on estimates of near-shore residents' values for small water-quality changes was developed and applied. The transfer function has the following form:

$$AggB_{home} = \sum_k MWTP_k \times \Delta DIN_k \times N_k, \quad (4.7)$$

where

$\Delta DIN_k$  = reduction in dissolved inorganic nitrogen (DIN) levels in the portion of the Chesapeake Bay closest to coastal Census block group  $k$ ;

$AggB_{home}$  = aggregate annual benefits (in 2007 dollars) to homeowners in all Chesapeake Bay coastal block groups for specified  $\Delta DIN_k$  changes in water quality;

$N_k$  = estimated number of specified owner-occupied homes in block group  $k$  in 2007; and

$MWTP_k$  = estimated annual marginal WTP (in 2007 dollars) for a 1-unit reduction in water quality,  $\Delta DIN_k = 1$ , in block group  $k$ .

To parameterize this function, results from a hedonic housing price study by Poor, Pessagno, and Paul (2007) were used. Using data on 1,377 residential home sales from 1993 to

2003 in St. Mary's River watershed in Maryland, this study regressed the natural log of real home prices (in 2003 dollars) against structural, neighborhood, and environmental water quality characteristics. It specifically estimated the effect of differences in DIN (mg/L), as measured by the annual average in the year of sale at the closest water monitoring station, on log home prices.<sup>10</sup> The study found a statistically significant effect with a model coefficient estimate of -0.0878.

To convert this semielasticity coefficient, which measures the marginal effect of DIN on the log of home price, to  $MWTP_k$ , which represents the *annualized average dollar* value of a 1-unit reduction in DIN for homes in block group  $k$ , the following conversion equation was used:

$$MWTP_k = 0.0878 * P_k * A(i, T), \quad (4.8)$$

where

$P_k$  = average price of specified owner-occupied homes in block group  $k$  and

$A$  = annualization factor, which is a function of the assumed interest rate ( $r$ ) and average lifetime of homes in years ( $T$ ).<sup>11</sup> For  $r = 0.05$  and  $T = 50$ ,  $A = 0.0522$ .

To implement the model, Chesapeake Bay coastal block groups were defined as those block groups with a Chesapeake Bay coastline, as delineated by the Census block group boundary files (Environmental Systems Research Institute, Inc. [ESRI], 2002), as well as those block groups whose geographic centroids are located within 1 mile of the coast. This second condition was added to ensure that a majority of the included properties are located within roughly 2 miles of the coast. As shown in **Figure 4.2-1**, 1,066 block groups met these criteria.

Within these block groups, the study focused on Census "specified owner-occupied housing units," which include only single-family houses on less than 10 acres without a business or medical office on the property. These properties match best with the types of properties analyzed in the hedonic study described above, and the decennial Census provides both count and property value estimates for these homes. Thirty-six of the identified 1,066 block groups had no specified owner-occupied homes and were excluded from the analysis.

<sup>10</sup> A separate model reported in Poor, Pessagno, and Paul (2007) used total suspended solids (mg/L) instead of DIN as the water quality measure. It was also found to have a statistically significant effect on home prices.

<sup>11</sup>  $A(r, T) = 1 / \left( \sum_{t=1}^T (1+r)^{-(t-1)} \right)$

To estimate  $N_k$ , the number of specified owner-occupied homes in each block group in 2000 was augmented by the growth rate in housing units in the block group's county from 2000 to 2007 (U.S. Census Bureau, 2008b).

To estimate  $P_k$ , the average price of specified owner-occupied homes in 2000 in each block group was adjusted to 2007 using the CPI-Shelter values for Washington-Baltimore, DC-MD-VA-WV.<sup>12</sup> **Table 4.2-7** summarizes the estimated values for  $N_k$  and  $P_k$ .

#### **4.2.1.4.1 Results: Aggregate Aesthetic Benefits to Near-Shore Residents**

To approximate the aggregate annual benefits from a 24% reduction in nitrogen loadings to the Bay, the benefit transfer model summarized in Equations (4.7) and (4.8) was applied, assuming uniform 24% reductions in DIN across all Chesapeake Bay waters. Based on 2005 monitoring data for the Potomac River estuary, the 25<sup>th</sup> and 75<sup>th</sup> percentile values of average DIN levels were 0.46 mg/L and 1.22 mg/L, respectively. Using this range of initial DIN values, a reduction of 24% translates to DIN decreases of between 0.11 mg/L and 0.29 mg/L. It was estimated that these changes would result in aggregate annual benefits of between \$38.7 million and \$102.2 million to residents of specified owner-occupied homes in the Chesapeake coastal block groups.

---

<sup>12</sup> In the decennial Census, values of specified owner-occupied homes were grouped into ranges of values (e.g., from \$250,000 to \$300,000). With the exception of the highest range, which is \$1,000,000 and greater (no upper bound), the midpoint of each range was used to calculate the mean value for each block group. For the highest range, a central value of \$1,250,000 was selected.

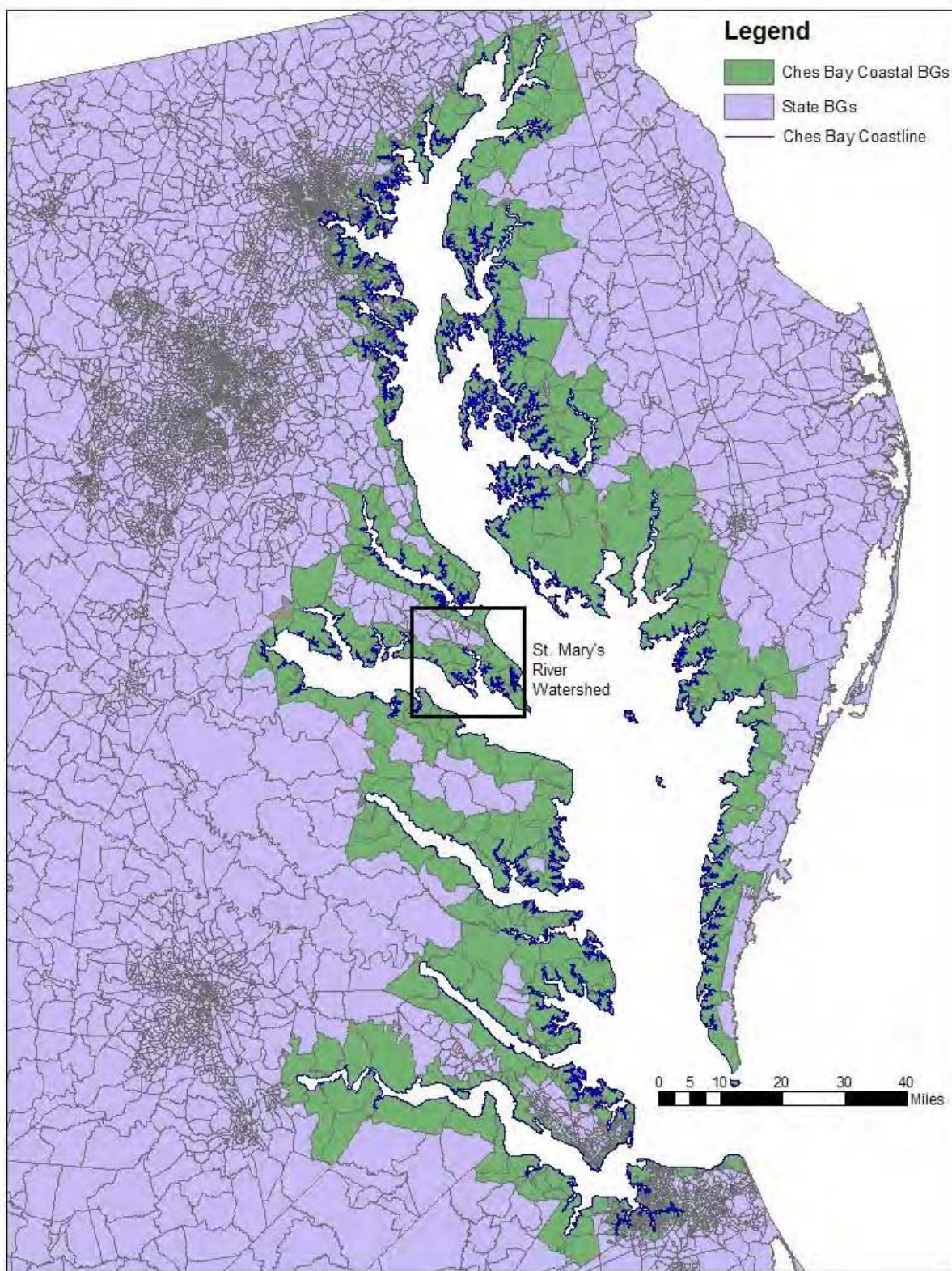


**Figure 4.2-1.** Chesapeake Bay Coastal Block Groups



**Table 4.2-7.** Summary of Housing Unit Numbers and Average Prices in Chesapeake Coastal Block Groups in 2007

State, County	Number of Coastal Block Groups	Number of Specified Single-Unit Dwellings per Block Group ( $N_k$ )				Average Value of Specified Units per Block Group ( $P_k$ )			
		Mean	Std. Dev.	Min	Max	Mean	Std. Dev.	Min	Max
Maryland									
Anne Arundel County	163	470	258	13	1,604	\$298,348	\$128,985	\$81,409	\$686,879
Baltimore County	101	339	160	16	859	\$154,975	\$54,654	\$65,209	\$343,455
Calvert County	25	583	380	190	1,957	\$257,582	\$68,476	\$174,459	\$498,410
Caroline County	2	346	37	310	383	\$145,589	\$3,499	\$142,091	\$149,088
Cecil County	18	408	206	195	1,088	\$206,114	\$41,341	\$138,614	\$270,798
Charles County	6	466	208	302	909	\$263,744	\$46,708	\$196,436	\$319,093
Dorchester County	20	263	125	46	584	\$167,317	\$61,534	\$86,191	\$310,723
Harford County	23	397	296	20	926	\$187,685	\$39,578	\$116,187	\$303,797
Kent County	13	294	105	55	418	\$225,531	\$48,381	\$143,163	\$306,886
Prince George's County	1	175	0	175	175	\$296,739	\$0	\$296,739	\$296,739
Queen Anne's County	18	584	249	158	1,104	\$277,352	\$73,004	\$153,496	\$478,396
St. Mary's County	29	458	195	92	910	\$252,720	\$41,564	\$174,343	\$317,879
Somerset County	14	258	118	81	528	\$130,391	\$30,635	\$77,591	\$181,198
Talbot County	20	431	181	192	943	\$341,180	\$162,586	\$128,864	\$658,874
Wicomico County	7	304	129	163	576	\$145,763	\$29,367	\$110,355	\$186,045
Worcester County	1	148	0	148	148	\$98,596	\$0	\$98,596	\$98,596
Baltimore city	116	168	95	10	436	\$106,483	\$52,800	\$23,628	\$345,380
Virginia									
Accomack County	9	247	93	128	388	\$127,159	\$56,731	\$69,539	\$236,974
Charles City County	4	270	46	219	340	\$163,344	\$43,411	\$104,671	\$227,234
Essex County	5	255	69	135	348	\$175,598	\$52,691	\$132,168	\$278,618
Gloucester County	16	438	248	174	1,063	\$194,628	\$40,091	\$127,058	\$285,437
Isle of Wight County	10	515	204	292	1,076	\$210,389	\$42,265	\$136,806	\$273,345
James City County	7	817	551	85	1,734	\$306,926	\$173,652	\$88,149	\$569,755

State, County	Number of Coastal Block Groups	Number of Specified Single-Unit Dwellings per Block Group ( $N_k$ )				Average Value of Specified Units per Block Group ( $P_k$ )			
		Mean	Std. Dev.	Min	Max	Mean	Std. Dev.	Min	Max
King and Queen County	2	200	7	193	206	\$121,113	\$3,296	\$117,817	\$124,409
King George County	3	227	175	3	431	\$193,030	\$31,483	\$151,588	\$227,847
King William County	1	398	0	398	398	\$128,864	\$0	\$128,864	\$128,864
Lancaster County	11	325	78	145	447	\$255,256	\$51,809	\$157,850	\$339,499
Mathews County	4	700	335	279	1,131	\$203,309	\$28,957	\$153,167	\$220,637
Middlesex County	9	301	88	138	415	\$205,784	\$36,392	\$146,531	\$249,250
New Kent County	1	497	0	497	497	\$188,507	\$0	\$188,507	\$188,507
Northampton County	9	267	48	178	365	\$151,509	\$34,176	\$100,355	\$214,862
Northumberland County	9	363	124	219	670	\$233,922	\$35,330	\$182,242	\$303,884
Prince George County	4	362	220	88	591	\$197,887	\$46,549	\$144,641	\$269,254
Richmond County	3	307	33	276	353	\$172,231	\$19,788	\$157,244	\$200,192
Surry County	2	317	67	250	384	\$172,904	\$12,214	\$160,690	\$185,119
Westmoreland County	13	311	83	181	458	\$161,391	\$32,705	\$98,923	\$228,513
York County	14	549	257	97	1,114	\$239,291	\$54,067	\$123,412	\$333,513
Chesapeake city	29	347	200	38	747	\$140,654	\$51,189	\$61,354	\$261,780
Hampton city	53	301	149	17	810	\$134,117	\$43,962	\$67,363	\$269,833
Newport News city	40	281	287	5	1,374	\$122,332	\$59,341	\$37,130	\$316,437
Norfolk city	109	168	118	7	528	\$168,857	\$98,567	\$51,507	\$590,748
Poquoson city	10	348	150	156	733	\$226,740	\$58,274	\$132,643	\$311,350
Portsmouth city	53	296	242	14	1,031	\$115,948	\$40,479	\$54,008	\$243,782
Suffolk city	5	1,426	644	545	2,198	\$214,610	\$35,399	\$168,310	\$254,324
Virginia Beach city	18	391	210	14	829	\$218,105	\$81,187	\$132,151	\$396,073



#### **4.2.1.4.2 Limitations and Uncertainties**

Many of the limitations and uncertainties surrounding this benefit transfer model are associated with the limitations and uncertainties inherent in the hedonic “implicit price” estimate,  $MWTP_k$ . From a strictly conceptual standpoint, the hedonic implicit price provides a correct measure of the welfare gains to residents of relatively *small* and *localized* improvements in the amenity, in this case changes in DIN water quality. However, caution is required when using this implicit price to estimate the benefits of either a large water-quality change or a change that affects many housing consumers. The accuracy of the benefit transfer model summarized by Equation (4.7) will tend to decline as the value of  $\Delta DIN_k$  increases and as  $N_k$  increases. This is because changes that are larger and that affect more consumers are also more likely to cause shifts in the housing market, resulting in potentially large transaction (e.g., moving) costs and changes in the market price equilibrium. Nevertheless, Bartik (1988) has shown that, under many common conditions, models such as Equation (4.7) can be interpreted as providing an upper-bound estimate of aggregate benefits.

From an empirical standpoint, there are other potential limitations and uncertainties. First, there are potential errors in the hedonic parameter estimate. For example,  $DIN$  may be correlated with other influential housing or neighborhood characteristics that are not included in the hedonic model, in which case the parameter estimate is likely to overstate the implicit price of  $DIN$ . Second, for this benefit transfer model, it was assumed that the Census block groups along the Chesapeake Bay coast represent the areas in which the hedonic estimates can most reasonably be applied; however, this spatial extrapolation has inherent limitations. In particular, the implicit price estimates are expected to be less accurate as a measure of WTP in areas that are farther from the hedonic study area (e.g., St. Mary’s River watershed), particularly areas that are more urban and densely populated. By excluding homes in other noncoastal Census block groups that are also near the Bay, the benefit transfer model is also likely to exclude some beneficiaries of improved aesthetic services and, therefore, underestimate aggregate benefits. Third, the implicit price was measured using data on individual homes and water quality measures within at most a few miles from these homes; however, the model summarized in Equation (4.7) uses properties aggregated at the Census block group level and (most likely) more spatially averaged

water quality. These differences are likely to reduce the accuracy of applying Equation (4.7) to estimate benefits.

It is also important to recognize the expected overlap in ecosystem services captured by the hedonic implicit price estimates and the WTP estimates summarized in Section 4.2. In principle, the hedonic price estimate includes residents' values for *all* of the use-related services they receive that depend on water quality. Therefore, in addition to capturing the aesthetic services received by living near the Bay, the hedonic implicit price should include values for recreational services received by near-shore residents. Unfortunately, the hedonic estimates do not provide separate value estimates for these different use-related services. Decomposing the value estimates into separate use-related categories requires additional assumptions, data, or analysis.

Finally, to specify reductions in DIN levels across the Bay resulting from a 24% reduction in nitrogen loadings, strong assumptions were made that DIN levels decline by the same percentage. In addition, to address variation in initial DIN levels across the Bay, this percentage reduction was applied to the range (25th to 75th percentile) of recently observed values in the Potomac River estuary.

#### **4.2.1.5 Nonuse Services**

Some of the ecosystem services provided by the Chesapeake Bay may be independent of individuals' recreational or other specific uses of the estuary. Measuring values for these nonuse services is more difficult and involves more uncertainty than for recreational and aesthetic services. Nevertheless, several stated-preference studies have estimated water quality values using sample populations that include nonusers. Evidence from these studies indicates that, compared with users of water resources, nonusers have significantly lower but still positive WTP for water quality improvements. Based on this evidence, the following simple benefit transfer equation was specified for estimating nonuse benefits:

$$AggB_{NU} = N_{NU} * WTP_{NU} (\Delta WQ_{10}), \quad (4.9)$$

where

$\Delta WQ_{10}$  = change in Chesapeake Bay water quality, expressed on a 10-point rating scale;

$AggB_{NU}$  = aggregate annual benefits (in 2007 dollars) to nonusers of the Chesapeake Bay in Maryland, Virginia, and DC for a specified  $\Delta WQ_{10}$  increase in water quality;

$WTP_{NU}(\Delta WQ_{10})$  = average annual WTP (in 2007 dollars) per nonuser, as a function of the  $\Delta WQ_{10}$  increase in water quality; and

$N_{NU}$  = total number of nonusers in Maryland, Virginia, and DC in 2007.

To estimate the  $WTP_{NU}$  function, results from two meta-analytic studies summarizing evidence from the water quality valuation literature were used. The first, Johnston et al. (2005), included 81 WTP estimates from 34 stated-preference studies. Although these studies addressed a wide variety of water quality changes, for the meta-analysis, they were all converted to a 10-point index (where 0 and 10 represent the worst and best possible water quality, respectively) based on the “Resources for the Future (RFF) water quality ladder” (Vaughan, 1986). The meta-analysis regressed average WTP estimates on water quality measures (baseline and change), characteristics of the water resource and study population, and several study method descriptors. The resulting WTP function can be simplified and summarized as follows:<sup>13</sup>

$$WTP_{NU} = \exp \left[ \frac{2.45 + (0.6827 * \ln(\Delta WQ_{10})) - (0.129 * WQ_{10base})}{+ (0.005 * INC / CP02)} \right] * CP02, \quad (4.10)$$

where

$WQ_{10base}$  = baseline Chesapeake Bay water quality, expressed on the 10-point rating scale;

$INC$  = average annual household income of Maryland, Virginia, and DC nonusers in 2007; and

$CP02$  = price adjustment factor for 2002 to 2007.

The second study, Van Houtven, Powers, and Pattanayak (2007), conducted a similar meta-analysis using a somewhat different sample of studies (18 studies, including 11 for freshwater resources) and WTP estimates (131). A 10-point index based on the RFF ladder was

---

<sup>13</sup> The function is a simplified version of the translog unweighted parameter estimate model (Model 2) in Johnston et al. (2005). This model includes several explanatory variables and coefficients, which are summarized in the constant term (2.45). To derive this constant, values were assigned to the other explanatory variables as follows: year is 2007 ( $year\_index = 37$ ), study method is a dichotomous choice through a personal interview ( $discrete\_ch = 1$  and  $interview = 1$ ) to a nonuser-only population ( $nonusers = 1$ ) with a high response rate ( $hi\_response = 1$ ), protest and outlier bids are excluded ( $protest\_bids = 1$  and  $outlier\_bids = 1$ ), and the species benefiting from the water quality change are unspecified ( $\ln WQ_{non} = \ln wq\_change$ ).

also used to convert water quality changes to a common scale. The resulting WTP function from this study can also be simplified and summarized as follows:<sup>14</sup>

$$WTP_{NU} = \exp \left[ \begin{array}{l} -1.197 + (0.823 * \ln(\Delta WQ_{10})) + (0.0801 * WQ_{10base}) \\ + (0.8969 * \ln(INC / CP00)) \end{array} \right] * CP00, \quad (4.11)$$

where

$CP00$  = price adjustment factor for 2000 to 2007.

Using these functions,  $WTP_{NU}$  can be estimated for selected values of  $\Delta WQ_{10}$ ,  $WQ_{10base}$ , and  $INC$ . To estimate  $WTP_{NU}$  for a 1-unit change in the 5-point EI scale, it was assumed that the EI scale is directly proportional to the 10-point  $WQ_{10}$  scale. In other words, it was assumed that  $EI = 1$  is equivalent to  $WQ_{10base} = 2$ , and a 1-unit increase in EI is equivalent to  $\Delta WQ_{10} = 2$ . For  $INC$ , U.S. average household income in 2007 of \$67,610 was used (U.S. Census Bureau, 2008a). Based on these inputs,  $WTP_{NU}$  for a 2-unit change in water quality is estimated to be \$16.33 using the Johnston et al. (2005) function and \$27.75 using the Van Houtven, Powers, and Pattanayak (2007) function.

Estimates of the percentage of Maryland, Virginia, and DC residents who are nonusers of the Chesapeake Bay are not readily available; however, they can be roughly approximated from recreational participation statistics for the area. For example, data from the 2006 Virginia Outdoors Survey suggest that (1) 92% of households in Virginia did not take any beach trips to the Chesapeake Bay, (2) 84% did not engage in saltwater fishing, and (3) 92% did not engage in powerboating. Assuming that these proportions represent independent probabilities of nonuse, then the combined probability (proportion) of nonuse for these primary activities is roughly 70%. Applying this percentage to the Maryland, Virginia, and DC population in 2007, which was 13,918,727, suggests that the number of nonusers ( $N_{NU}$ ) is approximately 9,743,109.

---

<sup>14</sup> This function is a simplified version of the parsimonious log-linear model in Table 5 in Van Houtven, Powers, and Pattanayak (2007). This model also includes several explanatory variables and coefficients, which are summarized in the constant term (-1.197). To derive this constant in a way that is consistent with the previous function, values were assigned to the other explanatory variables as follows: year is 2007 ( $studyyr73 = 34$ ), study method is a personal interview ( $inperson = 1$ ) to a nonuser-only population ( $pctuser = 0$ ) with a high response rate ( $responserate = 100$ ), publication outlet is peer reviewed ( $dpubjrlbk = 1$ ), and the water quality change is not expressed in terms of recreational uses ( $lnwq10chru = 0$ ).

#### 4.2.1.5.1 Results: Aggregate Nonuse Benefits

Applying these estimates to the benefit transfer models summarized in Equations (4.9) through (4.11), the aggregate annual nonuse benefits of a 1-unit improvement in the EI scale ( $\Delta WQ_{10} = 2$ ) are estimated to range from \$159.1 million to \$270.4 million.

#### 4.2.1.5.2 Limitations and Uncertainties

As with the recreational boating services model described in Section 4.2.1.2, one of the main practical limitations of applying these meta-analysis models is the water quality index used. Translating changes in the EI scale to the  $WQ_{10}$  metric requires strong assumptions. Another inherent limitation of using the meta-analytic models as benefit transfer functions is their lack of sensitivity to the spatial scale of water quality changes.

In addition to the limitations that primarily contribute uncertainty in the  $WTP_{NU}$  estimates, there is also significant uncertainty associated with the measurement of  $N_{NU}$ . First, defining criteria for distinguishing users and nonusers of the Bay is somewhat inherently subjective. Second, statistics on overall rates of visitation and use of the Bay by Maryland, Virginia, and DC households are not readily available.

A final caveat for this approach to estimating nonuse values for water quality improvements in the Bay is that, by design, it only includes nonuse values for *nonusers*. However, it is not unreasonable to suspect that users also benefit to some extent from nonuse services from the Bay. Whereas these types of nonuse values are likely to be captured in, for example, the Lipton (2004) WTP values for boaters used in Equation (4.5), they are not included in the benefit estimates in Equations (4.4), (4.6), and (4.7) for recreational anglers, beach users, and residents, respectively.

### 4.2.2 Neuse River Estuary

To analyze changes in ecosystem services for the Neuse River, the results of the Neuse River/Neuse Estuary Case Study were applied. This case study concluded that atmospheric deposition contributes 26% (1.15 million kg nitrogen/year) of total nitrogen loadings to the estuary. In contrast to the Potomac River/Potomac Estuary Case Study, it estimates that a much larger reduction in nitrogen loadings than this 26% would be required to improve the Neuse River estuary from “bad” to “poor.” Therefore, for this analysis, the change in selected

ecosystem services associated with a 26% reduction (100% of atmospheric deposition) in nitrogen loadings to the Neuse estuary was estimated.

#### ***4.2.2.1 Provisioning Services from the Blue Crab Fishery***

As discussed in Section 4.1.1, there are few examples of empirical bioeconomic models that link changes in nutrient-related water quality to changes in productivity of commercial fisheries; however, one exception is a study by Smith (2007). This study, which is applied to the Neuse River estuary, estimated the dynamic effects of a 30% reduction in nitrogen loads to the estuary on blue crab stocks, commercial catch levels, and the producer and consumer surplus derived from this fishery.

Smith (2007) applied a two-patch predator-prey model that incorporated both direct and indirect effects of hypoxia (i.e., low DO) on blue crab communities. Direct effects include the movement of blue crab to water habitats with higher DO content. Indirect effects include the dying off of blue crab prey. The model compares producer and consumer surplus changes under the existing open-access institutional structure to a 30% reduction of nitrogen loadings in the same structure. The model was parameterized using results and estimates derived from several other studies. To address uncertainty, the values of three key parameters—economic speed of adjustment under open-access conditions, biological spatial connectivity, and price elasticity of demand—were each allowed to take on three different values. For a 30% reduction in nitrogen loadings to the estuary, the present value (100-year time horizon and 4.5% discount rate) of producer benefits ranged from \$0.7 million to \$5.9 million (in 2002 dollars), and the present value of consumer surplus ranged from \$3.15 million to \$425.20 million. The combined present value of producer and consumer surplus changes was estimated to range from \$3.8 to \$31.0 million.

To estimate the annual aggregate benefits from the blue crab fishery due to a 26% reduction in nitrogen loads, (1) the results reported in Smith (2007) were rescaled by the percentage difference between 30% and 26%, (2) the benefit estimates (using the 100-year horizon and 4.5% discount rate) were annualized, and (3) the estimates were converted to 2007 dollars using the CPI.

#### **4.2.2.1.1 Results: Aggregate Benefits from the Blue Crab Fishery**

Applying this modeling framework, the aggregate annual benefits to Neuse River crab fishers and consumers from a 26% reduction in nitrogen loadings is estimated to range from \$0.12 million to \$1.01 million.

#### **4.2.2.1.2 Limitations and Uncertainties**

The large range of the benefit estimates reported above reflects uncertainty in three key model parameters—economic speed of adjustment under open-access conditions, biological spatial connectivity, and price elasticity of demand. However, the model includes at least 16 other parameters whose values are drawn from other studies; thus, the overall uncertainty in these benefit estimates is most likely understated by this range. In addition, by simply rescaling the results reported in Smith (2007) to address a 26% rather than a 30% reduction in nitrogen loads, it was assumed that benefits are directly proportional to the percentage reduction in nitrogen loads. This assumption adds additional (albeit, most likely small) uncertainty to the reported benefit estimates.

#### **4.2.2.2 Recreational Fishing Services**

To estimate the benefits from improvements in recreational fishing services due to reductions in nitrogen loadings to the Neuse, a benefit transfer model originally developed to assess the nutrient-reduction benefits of EPA's effluent guidelines for Consolidated Animal Feeding Operations (CAFOs) (EPA, 2002) was applied. For that analysis, EPA conducted a case study evaluating the potential economic benefits of a reduction in nutrient loadings via changes in recreational fishing opportunities in North Carolina's Albemarle and Pamlico Sounds (APS) estuary (Van Houtven and Sommer, 2002). The Neuse River estuary is a subestuary within the APS system.

To estimate the value of reductions in nitrogen loads, the APS case study relied on economic value estimates obtained from two related studies—Kaoru (1995) and Kaoru, Smith, and Liu (1995). Both studies used recreational data obtained from a 1981–1982 intercept survey of recreational fishermen conducted at 35 boat ramps or marinas within the APS estuary.

Kaoru (1995) used a three-level nested random utility model (RUM), which broke the recreational fishing decision into three stages: a decision on the duration of the trip (1, 2, 3, or more than 3 days), a decision on which of the five regions to visit, and a decision on which of the

individual sites within the region to visit. The impact of nitrogen (and phosphorus) loadings was specifically investigated in the second stage of the decision process (regional choice). A 25% reduction in nitrogen loadings for the entire APS estuary resulted in a benefit estimate of \$4.70 (in 1982 dollars) per person-trip.

Kaoru, Smith, and Liu (1995) also used a RUM approach to estimate the value of improving water quality. First, a household production function (HPF) was estimated to predict expected catch rates for individuals based on variables such as equipment used; effort exerted; and the physical characteristics of the fishing site, including pollutant loadings. Second, the HPF model was used to predict the impact of a 36% reduction in nitrogen loadings on expected catch rates. The estimated values ranged from \$0.76 to \$6.52 (in 1982 dollars) per person-trip.

Based on a systematic review of the value estimates reported in these studies, the CAFO case study selected three estimates to include in the benefit transfer model—\$4.70 per person-trip, for a 25% reduction in nitrogen loads (Kaoru, 1995) and \$3.95 and \$6.52 per person, for a 36% reduction (Kaoru, Smith, and Liu, 1995).

To apply these estimates, they were converted to comparable units. First, they were converted to 2007 dollars using the CPI. Second, they were rescaled to values per 1% reduction in loadings (i.e., dividing by 25 and 36, respectively). The resulting three unit values are \$0.40, \$0.24, and \$0.39 per person-trip per 1% reduction in nitrogen loads to the APS.

A further adjustment is necessary to convert these values into per-ton units. According to Kaoru (1995), the average nitrogen load to the APS estuary at the time the study was conducted was 1,741 tons per bordering county per year, which translates to a total of 22,633 tons of nitrogen loadings per year because of the 13 counties bordering the APS estuary in North Carolina. The resulting three unit values are \$0.0018, \$0.0010, and \$0.0017 per person-trip per 1-ton reduction in nitrogen loads to the APS.

To estimate the aggregate annual recreational fishing benefits of total reductions in nitrogen loads to the APS estuary, the following benefit transfer equation was specified:

$$AggB_{APSfish} = V \times \Delta L \times T, \quad (4.12)$$

where

$AggB_{APSfish}$  = the aggregate annual recreational fishing benefits from reductions in nitrogen loads to the APS estuary (in 2007 dollars),



- $V$  = the annual per trip value per unit (either in tons per year or percentage) reduction in nitrogen (in 2007 dollars),
- $\Delta L$  = reduction in nitrogen loadings (either in tons per year or percentage) to the APS estuary, and
- $T$  = the total number of annual fishing trips to the APS estuary (person-trips per year).

Although the unit value ( $V$ ) estimates derived from Kaoru (1995) and Kaoru, Smith, and Liu (1995) are based on data only for boating anglers, it was assumed that they apply to *all* recreational fishing trips ( $T$ ) in the APS. Data on visitation rates for recreational anglers in the APS estuary are available from the MRFSS, which contains information on the number, type, and destination of recreational fishers for several coastal regions in the United States. For 2006, the MRFSS data provide an estimate of 753,893 person-trips to the APS for recreational fishing.

#### **4.2.2.2.1 Results: Aggregate Recreational Fishing Benefits**

As noted above, the findings of the Neuse River/Neuse Estuary Case Study indicate that eliminating atmospheric deposition of nitrogen to the Neuse watershed would reduce nitrogen loads to the Neuse estuary (and, thus, the APS estuary as well) by 1.15 million kg per year, which is equivalent to 1,268 tons of nitrogen per year. Assuming that annual recreational fishing levels in the APS remain at 2006 levels and applying Equation (4.12), the resulting aggregate annual benefits ( $AggB_{APSfish}$ ) of such a reduction are estimated to be between \$1.0 million and \$1.7 million.

If the Neuse case study results regarding the portion of nitrogen loadings attributable to atmospheric deposition (26%) are extended to the entire APS system, then this extrapolation implies that eliminating all atmospheric nitrogen loads to the APS watershed would also reduce annual nitrogen loads to the APS estuary by 26%. Applying Equation (4.11) to this scenario suggests that the aggregate recreational fishing benefits of zeroing out nitrogen deposition in the entire APS watershed would be between \$4.6 million and \$7.9 million.

#### **4.2.2.2.2 Limitations and Uncertainties**

The following limitations and uncertainties should be considered when interpreting these recreational fishing benefit estimates. First, the value estimates are based on fishing activity data

that are more than 2 decades old. The analysis assumes that the benefits of water quality changes have remained constant (in real terms) over this period.

Second, the value estimates obtained from the two existing studies were based on percentage reductions in nutrients that were uniform across the APS estuary. By converting these estimates into per-ton terms and applying them only to the Neuse River nitrogen load reductions, the analysis implicitly assumes that average per-trip benefits do not vary with respect to the spatial distribution of the loadings reductions.

Third, the original value estimates are based on data only from boat fishermen; however, the analysis assumes that these values are appropriate for both boat and nonboat fishers.

### **4.3 REFERENCES**

- Anderson, E. 1989. "Economic Benefits of Habitat Restoration: Seagrass and the Virginia Hard-Shell Blue Crab Fishery." *North American Journal of Fisheries Management* 9:140-149.
- Bartik, T.J. 1988. "Measuring the Benefits of Amenity Improvements in Hedonic Price Models." *Land Economics* 64(2):172-183.
- Bockstael, N.E., K.E. McConnell, and I.E. Strand. 1988. "Benefits from Improvements in Chesapeake Bay Water Quality, Volume III." Environmental Protection Agency Cooperative Agreement CR-811043-01-0.
- Bockstael, N.E., K.E. McConnell, and I.E. Strand. 1989. "Measuring the Benefits of Improvements in Water Quality: The Chesapeake Bay." *Marine Resource Economics* 6:1-18.
- Bricker, S., D. Lipton, A. Mason, M. Dionne, D. Keeley, C. Krahforst, J. Latimer, and J. Pennock. 2006. *Improving Methods and Indicators for Evaluating Coastal Water Eutrophication: A Pilot Study in the Gulf of Maine*. NOAA Technical Memorandum NOS NCCOS 20. Silver Spring, MD: National Ocean Service, National Centers for Coastal Ocean Science, Center for Coastal Monitoring and Assessment.
- Bricker, S., Longstaff, B., Dennison, W., Jones, A., Boicourt, K., Wicks, C., and Woerner, J. 2007. *Effects of Nutrient Enrichment in the Nation's Estuaries: A Decade of Change*.

- NOAA Coastal Ocean Program Decision Analysis Series No. 26. National Centers for Coastal Ocean Science, Silver Spring, MD.
- Bricker, S.B., J.G. Ferreira, and T. Simas. 2003. "An Integrated Methodology for Assessment of Estuarine Trophic Status." *Ecological Modelling* 169:39-60.
- Chesapeake Bay Program. n.d. "Chesapeake Bay Program: A Watershed Partnership." Available at <http://www.chesapeakebay.net/>.
- Chesapeake Bay Program. "Bay Grass Abundance (Baywide)." Available at [http://www.chesapeakebay.net/status\\_baygrasses.aspx?menuitem=19652](http://www.chesapeakebay.net/status_baygrasses.aspx?menuitem=19652). Last updated May 21, 2008.
- Chesapeake Eco-Check. 2007. "Indicator Details: 2007. Water Quality Index." Available at [http://www.eco-check.org/reportcard/chesapeake/2007/indicators/water\\_quality\\_index/](http://www.eco-check.org/reportcard/chesapeake/2007/indicators/water_quality_index/).
- Environmental Systems Research Institute, Inc. (ESRI). 2002. "Census Block Groups: DC, DE, MD, and VA." [CD-ROM]. *ESRI Data & Maps 2002*.
- Johnston, R.J., E.Y. Besedin, R. Iovanna, C.J. Miller, R.F. Wardwell, and M.H. Ranson. 2005. "Systematic Variation in Willingness to Pay for Aquatic Resource Improvements and Implications for Benefit Transfer: A Meta-Analysis." *Canadian Journal of Agricultural Economics* 53:221-248.
- Johnston, R.J., M.H. Ranson, E.Y. Besedin, and E.C. Helm. 2006. "What Determines Willingness to Pay per Fish? A Meta-Analysis of Recreational Fishing Values." *Marine Resource Economics* 21:1-32.
- Kahn, J.R., and W.M. Kemp. 1985. "Economic Losses Associated with the Degradation of an Ecosystem: The Case of Submerged Aquatic Vegetation in Chesapeake Bay." *Journal of Environmental Economics and Management* 12:246-263.
- Kaoru, Y. 1995. "Measuring Marine Recreation Benefits of Water Quality Improvements by the Nested Random Utility Model." *Resource and Energy Economics* 17(2):119-136.

- Kaoru, Y., V. Smith, and J.L. Liu. 1995. "Using Random Utility Models to Estimate the Recreational Value of Estuarine Resources." *American Journal of Agricultural Economics* 77:141-151.
- Kaval, P., and J. Loomis. 2003. *Updated Outdoor Recreation Use Values With Emphasis On National Park Recreation*. Final Report October 2003, under Cooperative Agreement CA 1200-99-009, Project number IMDE-02-0070.
- Knowler, D. 2002. "A Review of Selected Bioeconomic Models: With Environmental Influences in Fisheries." *Journal of Bioeconomics* 4:163-181.
- Krupnick, A. 1988. "Reducing Bay Nutrients: An Economic Perspective." *Maryland Law Review* 47(2):453-480.
- Leeworthy, V.R., and P.C. Wiley. 2001. *Current Participation Patterns in Marine Recreation*. Silver Spring, MD: U.S. Department of Commerce, National Oceanic and Atmospheric Administration, National Ocean Service, Special Projects.
- Lipton, D. W. 1999. "Pfiesteria's Economic Impact on Seafood Industry Sales and Recreational Fishing." In *Proceedings of the Conference, Economics of Policy Options for Nutrient Management and Pfiesteria*. B. L. Gardner and L. Koch, eds., pp. 35–38. College Park, MD: Center for Agricultural and Natural Resource Policy, University of Maryland.
- Lipton, D. 2004. "The Value of Improved Water Quality to Chesapeake Bay Boaters." *Marine Resource Economics* 19:265-270.
- Lipton, D. 2006. "Economic Impact of Maryland Boating in 2005." University of Maryland Sea Grant Extension Program. Available at [ftp://ftp.mdsg.umd.edu/Public/MDSG/rec\\_boat05.pdf](ftp://ftp.mdsg.umd.edu/Public/MDSG/rec_boat05.pdf).
- Lipton, D. 2008. "Economic Impact of Maryland Boating in 2007." University of Maryland Sea Grant Extension Program. Available at [ftp://ftp.mdsg.umd.edu/Public/MDSG/rec\\_boat07.pdf](ftp://ftp.mdsg.umd.edu/Public/MDSG/rec_boat07.pdf).

- Lipton, D.W., and R.W. Hicks. 1999. "Linking Water Quality Improvements to Recreational Fishing Values: The Case of Chesapeake Bay Striped Bass." In *Evaluating the Benefits of Recreational Fisheries. Fisheries Centre Research Reports* 7(2), T.J. Pitcher, ed., pp. 105-110. Vancouver: University of British Columbia.
- Lipton, D.W., and R.W. Hicks. 2003. "The Cost of Stress: Low Dissolved Oxygen and the Economic Benefits of Recreational Striped Bass Fishing in the Patuxent River." *Estuaries* 26(2A):310-315.
- Massey, M., S. Newbold, and B. Gentner. 2006. "Valuing Water Quality Changes Using a Bioeconomic Model of a Coastal Recreational Fishery." *Journal of Environmental Economics and Management* 52:482-500.
- Millennium Ecosystem Assessment (MEA). 2005. Ecosystems and Human Well-being: Wetlands and Water. Synthesis. A Report of the Millennium Ecosystem Assessment. Washington, DC: World Resources Institute.
- Mistiaen, J.A., I.E. Strand, and D. Lipton. 2003. "Effects of Environmental Stress on Blue Crab (*Callinectes sapidus*) Harvests in Chesapeake Bay Tributaries." *Estuaries* 26(2a): 316-322.
- Morgan, C., and N. Owens. 2001. "Benefits of Water Quality Policies: The Chesapeake Bay." *Ecological Economics* 39:271-284.
- Murray, T., and J. Lucy. 1981. "Recreational Boating in Virginia: A Preliminary Analysis." Special Report in Applied Marine Science and Ocean Engineering No. 251. Available at <http://www.vims.edu/GreyLit/VIMS/sramsoe251.pdf>.
- National Marine Manufacturers Association (NMMA). 2008. "2007 Recreational Boating Statistical Abstract." Available at <http://www.nmma.org/facts/boatingstats/2007/files/Abstract.pdf>.
- National Oceanic and Atmospheric Administration (NOAA). (2007, August). "Annual Commercial Landing Statistics." Available at [http://www.st.nmfs.noaa.gov/st1/commercial/landings/annual\\_landings.html](http://www.st.nmfs.noaa.gov/st1/commercial/landings/annual_landings.html).

National Oceanic and Atmospheric Administration (NOAA). “Recreational Fisheries.”

Available at [www.st.nmfs.noaa.gov/st1/recreational/overview/overview.html](http://www.st.nmfs.noaa.gov/st1/recreational/overview/overview.html). Last updated February 12, 2009.

Parsons, G., A.O. Morgan, J.C. Whitehead, and T.C. Haab. 2006. “The Welfare Effects of Pfiesteria-Related Fish Kills: A Contingent Behavior Analysis of Seafood Consumers.” *Agricultural and Resource Economics Review* 35(2):1-9.

Poor, P.J., K.L. Pessagno, and R.W. Paul. 2007. “Exploring the Hedonic Value of Ambient Water Quality: A Local Watershed-Based Study.” *Ecological Economics* 60:797-806.

Smith, M.D. 2007. “Generating Value in Habitat-Dependent Fisheries: The Importance of Fishery Management Institutions.” *Land Economics* 83(1):59-73.

Sweeney, J. 2007. “Impacts of CAMD 2020 CAIR on Nitrogen Loads to the Chesapeake Bay.” University of Maryland, Chesapeake Bay Program Office.

U.S. Census Bureau. 2008a. “Annual Social and Economic (ASEC) Supplement.” Available at [http://pubdb3.census.gov/macro/032008/hhinc/new02\\_001.htm](http://pubdb3.census.gov/macro/032008/hhinc/new02_001.htm).

U.S. Census Bureau. 2008b. “Housing Unit Estimates for Counties of MD and VA: April 1/2000 to July 1/2007.” Available at <http://www.census.gov/popest/housing/HU-EST2007-CO.html>.

U.S. Environmental Protection Agency (EPA). 2002. December. Environmental and Economic Benefit Analysis of Final Revisions to the National Pollutant Discharge Elimination System Regulation and the Effluent Guidelines for Concentrated Animal Feeding Operations (EPA-821-R-03-003). Washington, DC: U.S. Environmental Protection Agency, Office of Water, Office of Science and Technology.

Valigura, R.A., R.B. Alexander, M.S. Castro, T.P. Meyers, H.W. Paerl, P.E. Stacy, and R.E. Turner. 2001. *Nitrogen Loading in Coastal Water Bodies: An Atmospheric Perspective*. Washington, DC: American Geophysical Union.

- Van Houtven, G. and A. Sommer. December 2002. Recreational Fishing Benefits: A Case Study of Reductions in Nutrient Loads to the Albemarle-Pamlico Sounds Estuary. Final Report. Prepared for the U.S. Environmental Protection Agency. Research Triangle Park, NC: RTI International.
- Van Houtven, G.L., J. Powers, and S.K. Pattanayak. 2007. "Valuing Water Quality Improvements Using Meta-Analysis: Is the Glass Half-Full or Half-Empty for National Policy Analysis?" *Resource and Energy Economics* 29:206-228.
- Vaughan, W.J. 1986. "The Water Quality Ladder." Included as Appendix B in R.C. Mitchell, and R.T. Carson, eds. *The Use of Contingent Valuation Data for Benefit/Cost Analysis in Water Pollution Control*. CR-810224-02. Prepared for the U.S. Environmental Protection Agency, Office of Policy, Planning, and Evaluation.
- Virginia Department of Conservation and Recreation. 2007. "2006 Virginia Outdoors Survey." Available at [http://www.dcr.virginia.gov/recreational\\_planning/documents/vopsurvey06.pdf](http://www.dcr.virginia.gov/recreational_planning/documents/vopsurvey06.pdf).
- Whitehead, J.C., T.C. Haab, and G.R. Parsons. 2003. "Economic Effects of *Pfiesteria*." *Ocean & Coastal Management* 46(9-10):845-858.

## **5.0 TERRESTRIAL ENRICHMENT**

Terrestrial enrichment occurs when terrestrial ecosystems receive nitrogen loadings in excess of natural background levels, either through atmospheric deposition or direct application. Evidence presented in the Integrated Science Assessment (Environmental Protection agency [EPA], 2008) supports a causal relationship between atmospheric nitrogen deposition and biogeochemical cycling and fluxes of nitrogen and carbon in terrestrial systems. Furthermore, evidence summarized in the report supports a causal link between atmospheric nitrogen deposition and changes in the types and number of species and biodiversity in terrestrial systems.

The Terrestrial Nutrient Enrichment Case Study focuses on the coastal sage scrub (CSS) ecosystem and San Bernardino and Sierra Nevada mixed conifer forests (MCF), both located in California. CSS is a unique and endemic ecosystem that provides habitat to several threatened and endangered species. Additionally, CSS is generally less fire prone than the nitrophyllous species that tend to amass dominance in abundance and richness with increased nutrient enrichment. MCF provide habitat for animals as well as contribute other ecosystem services such as timber, recreation, and water cycling. Nitrogen enrichment occurs over a long time period; as a result, it may take as much as 50 years or more to see changes in ecosystem conditions and indicators. This long time scale also affects the timing of the ecosystem service changes.

The Terrestrial Nutrient Enrichment Case Study differs from the other case studies in that it focuses on geographic information system (GIS) analyses and existing nitrogen loading threshold investigations as the basis for describing endpoints. The CSS investigation analyzed GIS data in conjunction with the results from Community Multiscale Air Quality (CMAQ) 2002 modeling to assess the relationship between atmospheric nitrogen deposition and changes in the CSS ecosystem. In the San Bernardino and Sierra Nevada MCF, nitrogen loading thresholds obtained in situ and through simulation modeling were investigated for potential endpoints and applicability to the San Bernardino and Sierra Nevada MCF system.

### **5.1 OVERVIEW OF AFFECTED ECOSYSTEM SERVICES**

The ecosystem service impacts of terrestrial nutrient enrichment include primarily cultural and regulating services. In CSS, concerns focus on a decline in CSS and an increase in nonnative grasses and other species, impacts on the viability of threatened and endangered species associated with CSS, and an increase in fire frequency. Changes in MCF include changes



in habitat suitability and increased tree mortality, increased fire intensity, and a change in the forest's nutrient cycling that may affect surface water quality through nitrate leaching (EPA, 2008).

Both CSS and MCF are located in areas of California valuable for housing, recreation, and development. CSS runs along the coast through densely populated areas of California (see **Figure 5.1-1**). From **Figure 5.1-2**, MCF covers less densely populated areas that are valuable for recreation. The proximity of CSS and MCF to population centers and recreational areas and the potential value of these landscape types in providing regulating ecosystem services suggest that the value of preserving CSS and MCF to California could be quite high. The value that California residents and the U.S. population as a whole place on CSS and MCF habitats is reflected in the various federal, state, and local government measures that have been put in place to protect these habitats. Threatened and endangered species are protected by the Endangered Species Act. The State of California passed the Natural Communities Conservation Planning Program (NCCP) in 1991, and CSS was the first habitat identified for protection under the program (see [www.dfg.ca.gov/habcon/nccp](http://www.dfg.ca.gov/habcon/nccp)). **Figure 5.1-3** shows the boundaries of the NCCP region and subregions for CSS. Private organizations such as The Nature Conservancy, the Audubon Society, and local land trusts also protect and restore CSS and MCF habitat. According to the 2005 National Land Trust Census Report (Land Trust Alliance, 2006), California has the most land trusts of any state with a total of 1,732,471 acres either owned, under conservation easement, or conserved by other means.

### **5.1.1 Cultural**

The primary cultural ecosystem services associated with CSS and MCF are recreation, aesthetic, and nonuse values. The possible ecosystem service benefits from reducing nitrogen enrichment in CSS and MCF are discussed below, and a general overview of the types and relative magnitude of the benefits is provided.

CSS, once the dominant landscape type in the area, is a unique ecosystem that provides cultural value to California and the nation as a whole. Culturally, the remaining patches of CSS contain a number of threatened and endangered species, and patches of CSS are present in a number of parks and recreation areas. More generally the patches of CSS represent the iconic landscape type of Southern California and serve as a reminder of what the area looked like

predevelopment. Changes that might impact cultural ecosystem services in CSS resulting from nutrient enrichment potentially include

- decline in CSS habitat, shrub abundance, and species of concern;
- increased abundance of nonnative grasses and other species; and
- increase in wildfires.

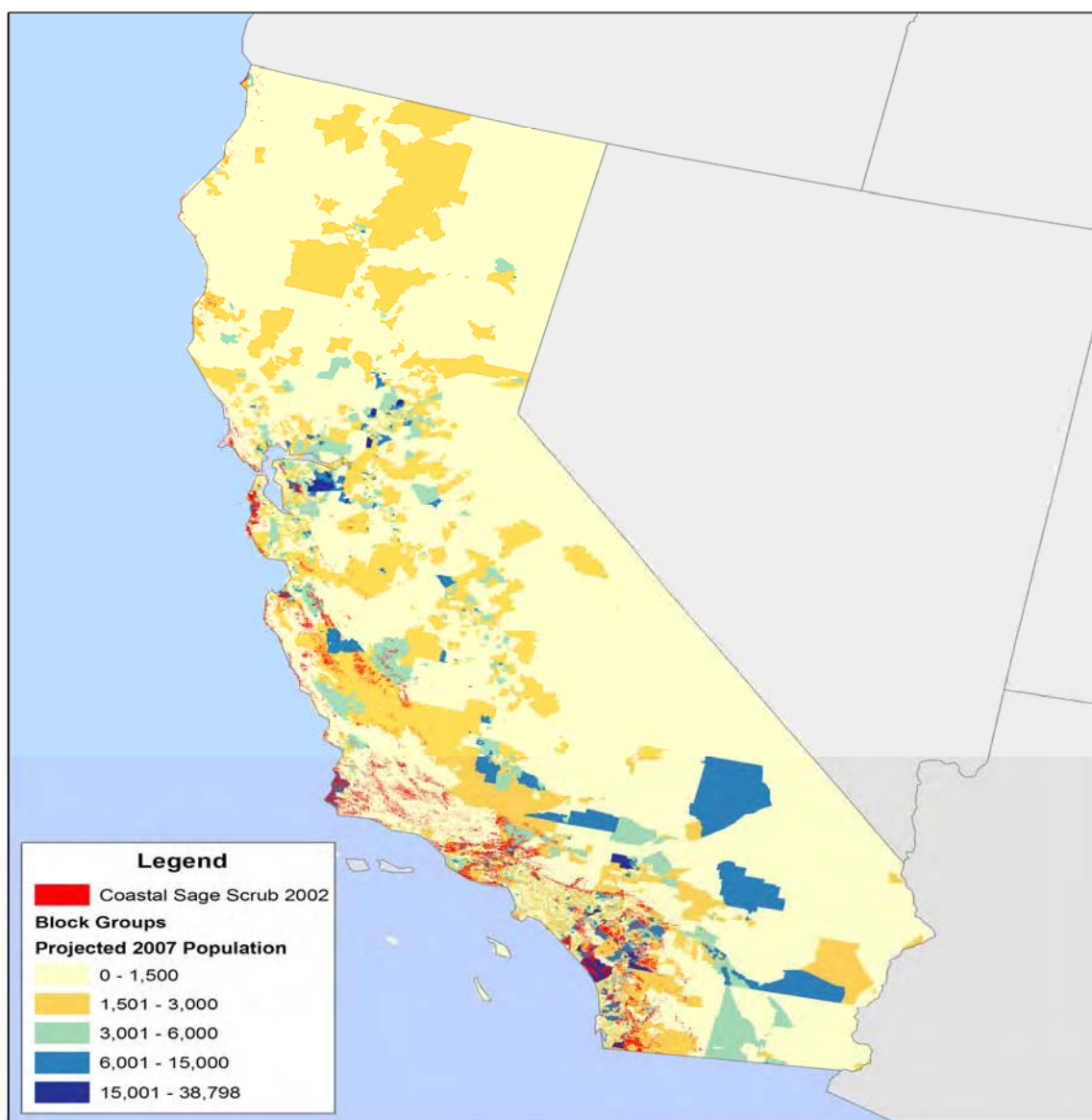


**Figure 5.1-1. Coastal Sage Scrub Areas and Population**

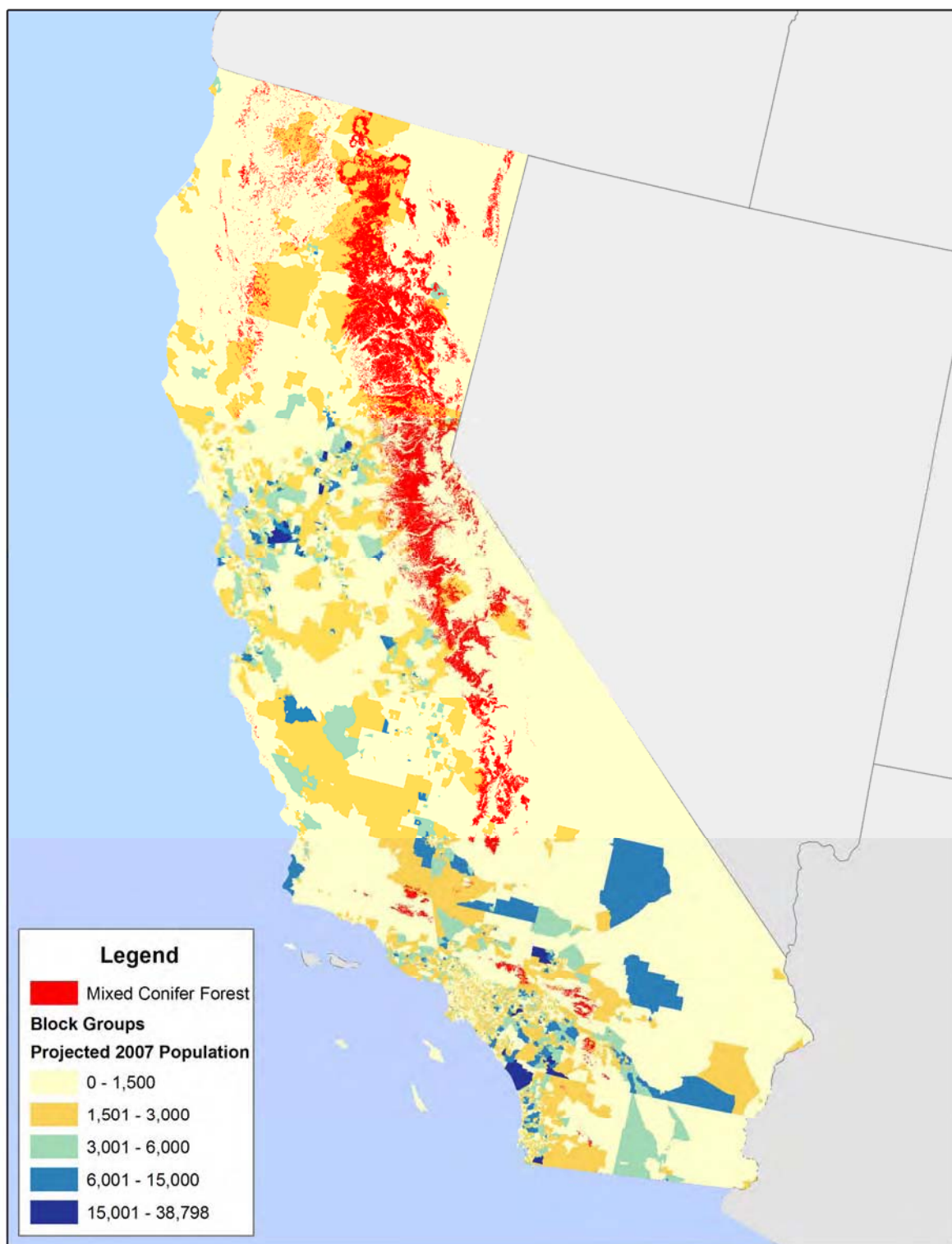


**Figure 5.1-2. Mixed Conifer Forest Areas and Population**



**Figure 5.1-3.** Boundaries of the NCCP Region and Subregions for Coastal Sage Scrub (Source: California Department of Fish and Game, n.d.).

For MCF, the changes from nutrient enrichment that might impact cultural ecosystem services include

- change in habitat suitability and increased tree mortality and
- decline in MCF aesthetics.

#### **5.1.1.1 Recreation**

CSS and MCF are found in numerous recreation areas in California. Three national parks and monuments in California contain CSS, including Cabrillo National Monument, Channel Islands National Park, and Santa Monica National Recreation Area. All three parks showcase CSS habitat with educational programs and information provided to visitors, guided hikes, and research projects focused on understanding and preserving CSS. Together a total of 1,456,879 visitors traveled through these three parks in 2008. MCF is highlighted in Sequoia and Kings Canyon National Park, Yosemite National Park, and Lassen Volcanic National Park, where a total of 5,313,754 people visited in 2008. **Figure 5.1-4** maps national and state parkland against MCF areas.

In addition, numerous state and county parks encompass CSS and MCF habitat. Visitors to these parks engage in activities such as camping, hiking, attending educational programs, horseback riding, wildlife viewing, water-based recreation, and fishing. For example, California's Torrey Pines State Natural Reserve protects CSS habitat (see <http://www.torreypine.org/>).

**Table 5.1-1** reports the results from the 2006 National Survey of Fishing, Hunting, and Wildlife Associated Recreation (FHWAR) for California (DOI, 2007) on the number of individuals involved in fishing, hunting, and wildlife viewing in California. Millions of people are involved in just these three activities each year. The quality of these trips depends in part on the health of the ecosystems and their ability to support the diversity of plants and animals found in important habitats. Based on estimates from Kaval and Loomis (2003), in the Pacific Coast region of the United States, a day of fishing has an *average* value of \$48.86 (in 2007 dollars), based on 15 studies. For hunting and wildlife viewing in this region, average day values were estimated to be \$50.10 and \$79.81 from 18 and 23 studies, respectively. Multiplying these average values by the total participation days reported in Table 5.1-1, the total benefits in 2006 from fishing, hunting, and wildlife viewing away from home in California were approximately \$947 million, \$169 million, and \$3.59 billion, respectively.

In addition, data from California State Parks (2003) indicate that in 2002 68.7% of adult residents participated in trail hiking for an average of 24.1 days per year. Applying these same rates to Census estimates of the California adult population in 2007 suggests that residents in California hiked roughly 453 million days in 2007. According to Kaval and Loomis (2003), the average value of a hiking day in the Pacific Coast region is \$25.59, based on a sample of 49 studies. Multiplying this average-day value by the total participation estimate indicates that the aggregate annual benefit for California residents from trail hiking in 2007 was \$11.59 billion.

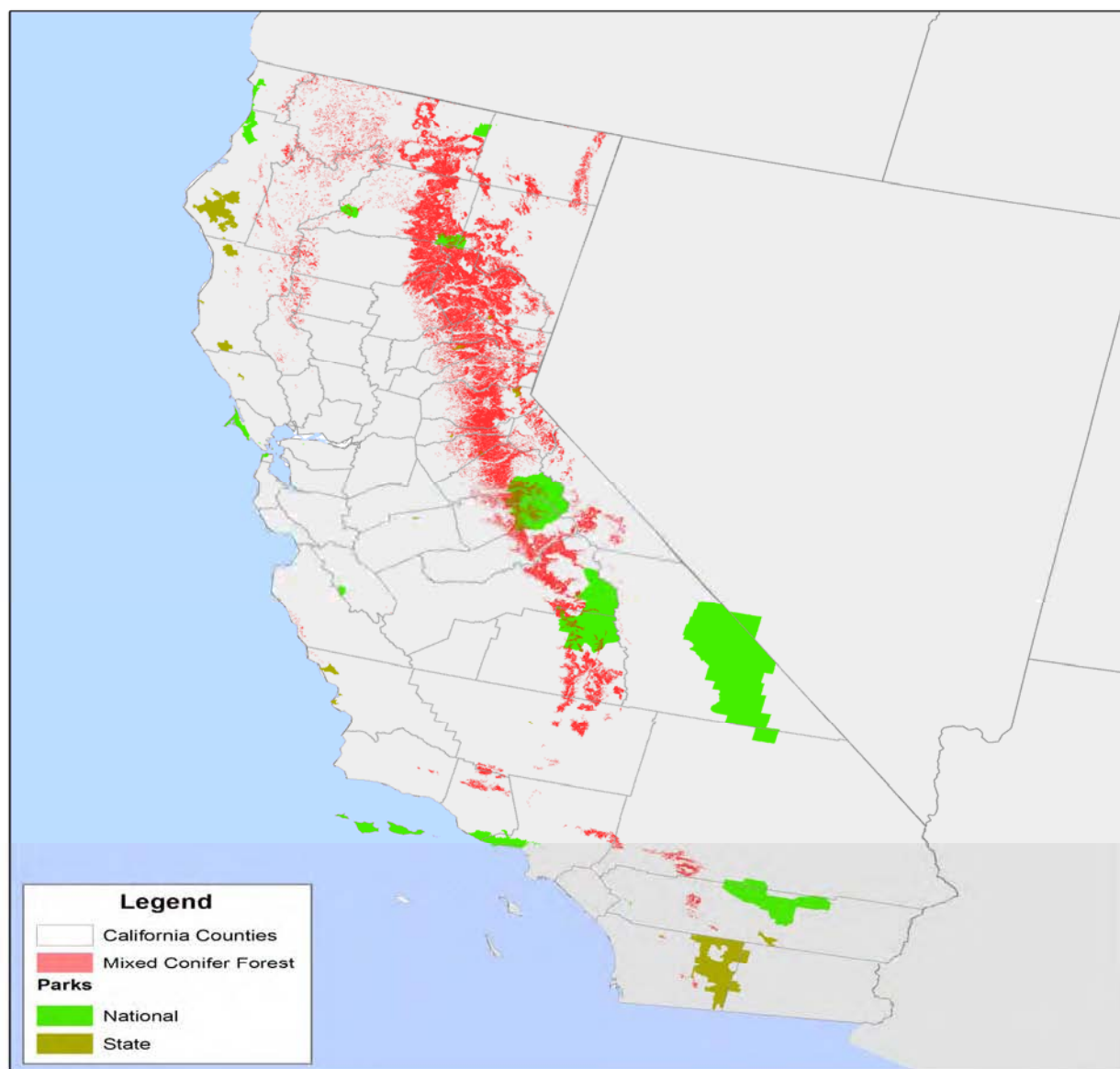


**Figure 5.1-4.** Mixed Conifer Forest Areas and National and State Park Boundaries

**Table 5.1-1. Recreational Activities in California in 2006 by Residents and Nonresidents**

<b>Activities in California by Residents and Nonresidents</b>	
<b>Fishing</b>	
Anglers .....	<b>1,730,000</b>
Days of fishing.....	19,394,000
Average days per angler .....	11
<b>Hunting</b>	
Hunters .....	<b>281,000</b>
Days of hunting .....	3,376,000
Average days per hunter .....	12
<b>Wildlife Watching</b>	
Total wildlife-watching participants .....	<b>6,270,000</b>
Away-from-home participants .....	2,894,000
Around-the-home participants .....	5,259,000
Days of participation away from home.....	45,010,000
Average days of participation away from home .....	16
<b>Activities in California by Residents</b>	
<b>Fishing</b>	
Anglers .....	<b>1,578,000</b>
Days of fishing.....	18,310,000
Average days per angler .....	12
<b>Hunting</b>	
Hunters .....	<b>274,000</b>
Days of hunting .....	3,339,000
Average days per hunter .....	12
<b>Wildlife Watching</b>	
Total wildlife-watching participants .....	<b>5,704,000</b>
Away-from-home participants .....	2,328,000
Around-the-home participants .....	5,259,000
Days of participation away from home.....	41,436,000
Average days of participation away from home .....	18

Source: U.S. Department of the Interior, Fish and Wildlife Service, and U.S. Department of Commerce, U.S. Census Bureau, 2007.

The potential impacts of an increase in wildfires on recreation are discussed in Section 5.1.2, Regulating.

#### **5.1.1.2 Aesthetic**

Beyond the recreational value, the CSS landscape and MCF provide aesthetic services to local residents and homeowners who live near CSS or MCF. Aesthetic services not related to recreation include the view of the landscape from houses, as individuals commute, and as individuals go about their daily routine in a nearby community. Studies find that scenic landscapes are capitalized into the price of housing. Although no studies came to light that look at the value of housing as a function of the view in landscapes that include CSS or MCF, other studies document the existence of housing price premia associated with proximity to forest and open space (Acharya and Bennett, 2001; Geoghegan, Wainger, and Bockstael, 1997; Irwin, 2002; Mansfield, et al., 2005; Smith, Poulos, and Kim, 2002; Tyrvaenen and Miettinen, 2000). The CSS landscape itself is closely associated with Southern California, which should increase the aesthetic value of the landscape in general. **Figure 5.1-5** presents home values in 2000 by Census block and CSS areas. CSS areas border a number of areas along the coast near large cities with very high home values, as well as areas between the cities where home values are lower.

#### **5.1.1.3 Nonuse Value**

Nonuse value, also called existence value or preservation value, encompasses a variety of motivations that lead individuals to place value on environmental goods or services that they do not use. The values individuals place on protecting rare species, rare habitats, or landscape types that they do not see or visit and that do not contribute to the pleasure they get from other activities are examples of nonuse values.

While measuring the public's willingness to pay (WTP) to protect endangered species poses theoretical and technical challenges, it is clear that the public places a value on preserving endangered species and their habitat. Data on charitable donations, survey results, and the time and effort different individuals or organizations devote to protecting species and habitat suggest that endangered species have intrinsic value to people beyond the value derived from using the resource (recreational viewing or aesthetic value). CSS and MCF are home to a number of important and rare species and habitat types. CSS displays richness in biodiversity with more than 550 herbaceous annual and perennial species. Of these herbs, nearly half are endangered,



sensitive, or of special status (Burger et al., 2003). Additionally, avian, arthropod, herpetofauna, and mammalian species live in CSS habitat or use the habitat for breeding or foraging.

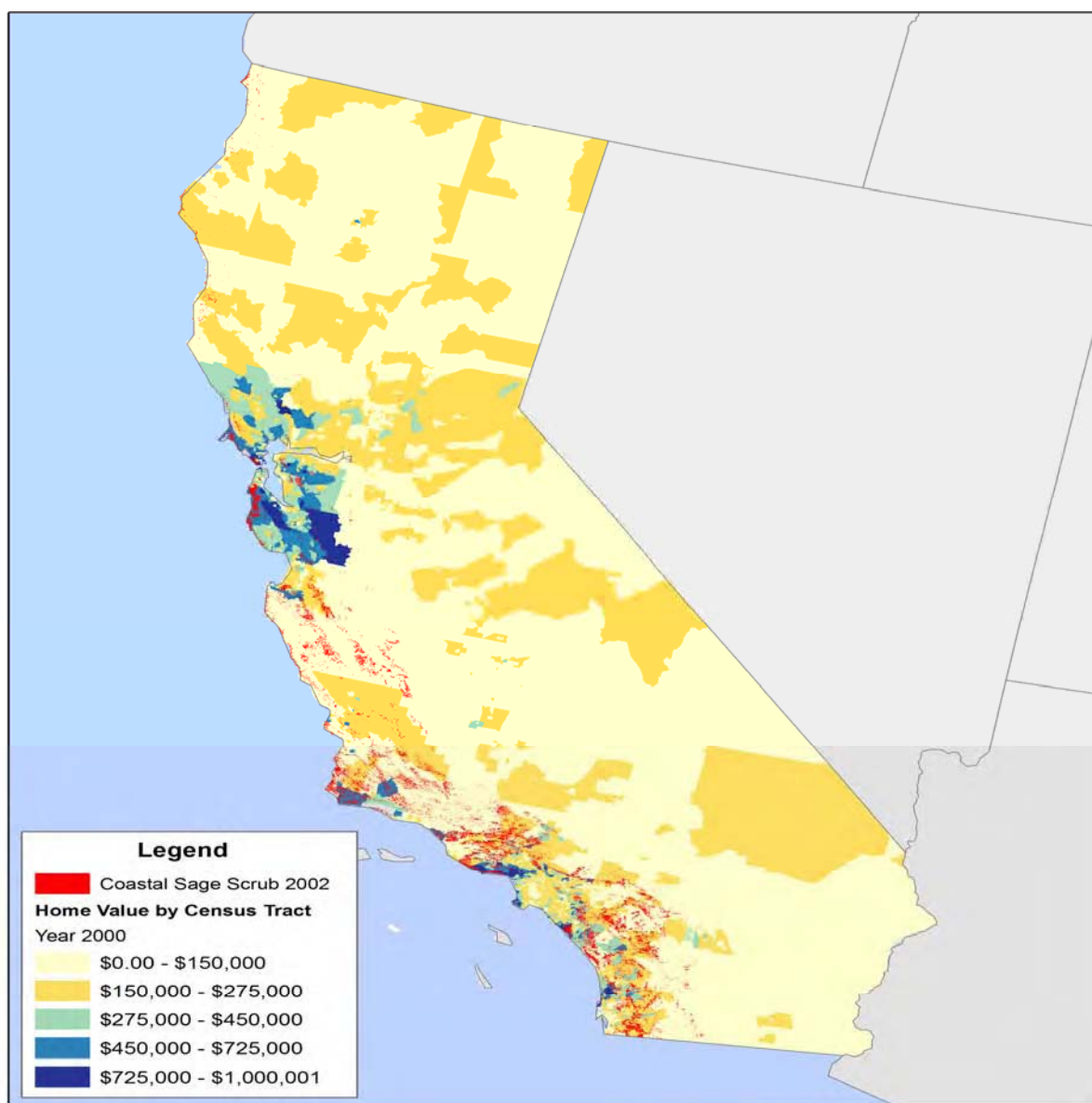


**Figure 5.1-5.** Coastal Sage Scrub Areas and Housing Values

**Figure 5.1-6** shows communities of CSS and three important federally endangered species. MCF is home to one federally endangered species and a number of state-level sensitive species. **Figure 5.1-7** provides a map of MCF habitat and two threatened and endangered species.

species. The Audubon Society lists 28 important bird areas in CSS habitat and at least 5 in MCF in California (<http://ca.audubon.org/iba/index.shtml>).<sup>1</sup>

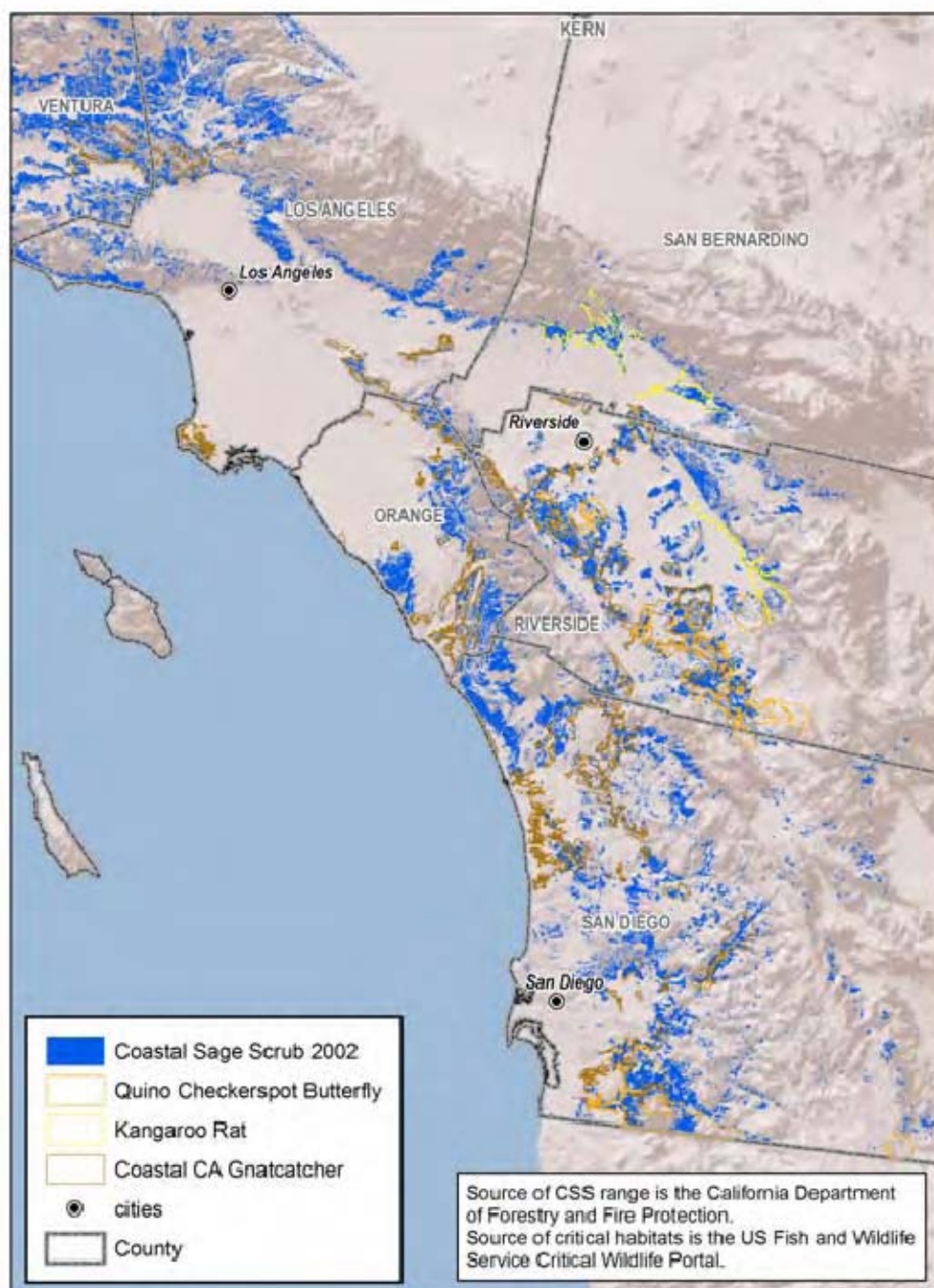


**Figure 5.1-6.** Presence of Three Threatened and Endangered Species in California's Coastal Sage Scrub Ecosystem

<sup>1</sup> Important bird areas are sites that provide essential habitat for one or more species of bird.



**Figure 5.1-7.** Presence of Two Threatened and Endangered Species in California's Mixed Conifer Forest

To the authors' knowledge, only one study has specifically estimated values for protecting CSS habitat in California. Stanley (2005) uses a contingent valuation (CV) survey to measure WTP to support recovery plans for endangered species in Southern California. The survey of Orange County, California, residents asked respondents to value the recovery of a single species (the Riverdale fairy shrimp) and a larger bundle of 32 species found in the county. The acquisition of critical habitat and implementation of the recovery plan were the specific goods being valued in the WTP question and the programs would be financed by an annual tax payment. The average WTP for fairy shrimp recovery was roughly \$29 (in 2007 dollars) and for

all 32 species was \$61 per household, depending on the model used. Aggregating benefits (multiplying average household WTP by the number of households in the county) results in total estimated WTP of over \$27 million annually for protecting fairy shrimp and \$57 million annually for all 32 species.

In a more general study valuing endangered species protection, Loomis and White (1996) synthesize key results from 20 threatened and endangered species valuation studies using meta-analysis methods. They find that annual WTP estimates range from a low of \$11 for the Striped Shiner fish to a high of \$178 for the Northern Spotted Owl (in 2007 dollars). None of the studies summarized by Loomis and White are found in CSS or MCF, but the study provides another indication of the value that the public places on preserving endangered species in general.

### **5.1.2 Regulating**

Excessive nitrogen deposition upsets the balance between CSS and nonnative plants, changing the ability of an area to support the biodiversity found in CSS. The composition of species in CSS changes fire frequency and intensity, as nonnative grasses fuel more frequent and more intense wildfires. More frequent and intense fires also reduce the ability of CSS to regenerate after a fire and increase the proportion of nonnative grasses (EPA, 2008). A healthy MCF ecosystem supports native species, promotes water quality, and helps regulate fire intensity. Excess nitrogen deposition leads to changes in the forest structure, such as increased density and loss of root biomass, which in turn can result in more intense fires and water quality problems related to nitrate leaching (EPA, 2008).

The importance of CSS and MCF as homes for sensitive species and their aesthetic services are discussed in Section 5.1.1. Here the contribution of CSS and MCF to fire regulation and water quality are discussed.

#### **5.1.2.1 Fire Regulation**

The Terrestrial Nutrient Enrichment Case Study identified fire regulation as a service that could be affected by enrichment of the CSS and MCF ecosystems. Wildfires represent a serious threat in California and cause billions of dollars in damage. Over the 5-year period from 2004 to 2008, Southern California experienced, on average, over 4,000 fires a year burning, on average, over 400,000 acres (National Association of State Foresters [NASF], 2009). Improved fire regulation leads to short-term and long-term benefits. The short-term benefits include the value

of avoided residential property damages, avoided damages to timber, rangeland, and wildlife resources; avoided losses from fire-related air quality impairments; avoided deaths and injury due to fire; improved outdoor recreation opportunities; and savings in costs associated with fighting the fires and protecting lives and property. For example, the California Department of Forestry and Fire Protection (CAL FIRE) estimated that average annual losses to homes due to wildfire from 1984 to 1994 were \$163 million per year (CAL FIRE, 1996) and were over \$250 million in 2007 (CAL FIRE, 2008). In fiscal year 2008, CAL FIRE's costs for fire suppression activities were nearly \$300 million (CAL FIRE, 2008). Therefore, even a 1% reduction in these damages and costs would imply benefits of over \$5 million per year.

**Figure 5.1-8** is a map of the overlap between fire threat and CSS habitat. CSS overlaps with areas of very to extremely high fire threat. MCF is found in some areas closer to the coast with extremely high fire threat and in areas up in the mountains also under very high fire threat, as seen in **Figure 5.1-9**.

In the long term, decreased frequency of fires could result in an increase in property values in fire-prone areas. Mueller, Loomis, and González-Cabán (2007) conducted a hedonic pricing study to determine whether increasing numbers of wildfires affect house prices in southern California. They estimated that house prices would decrease 9.71% (\$30,693 in 2007 dollars) after one fire and 22.7% (\$71,722; \$102,417 cumulative) after a second wildfire within 1.75 miles of a house in their study area. After the second fire, the housing prices took between 5 and 7 years to recover. The results come from a sample of 2,520 single-family homes located within 1.75 miles of one of five fires during the 1990s.

Long-term decreases in wildfire risks are also expected to provide outdoor recreation benefits. The empirical literature contains several articles measuring the relationship between wildfires and recreation values; however, very few address fires in California, particularly in CSS areas. One exception is Loomis et al. (2002), which estimates the changes in deer harvest and deer hunting benefits resulting from controlled burns or prescribed fire in the San Bernardino National Forest in Southern California. Using a CV survey of deer hunters in California, they estimated that the net economic value of an additional deer harvested is on average \$122 (in 2007 dollars). Based on predicted changes in deer harvest in response to a prescribed fire, they estimated annual economic benefits for an additional 1,000 acres of prescribed burning ranges from \$3,328 to \$3,893.



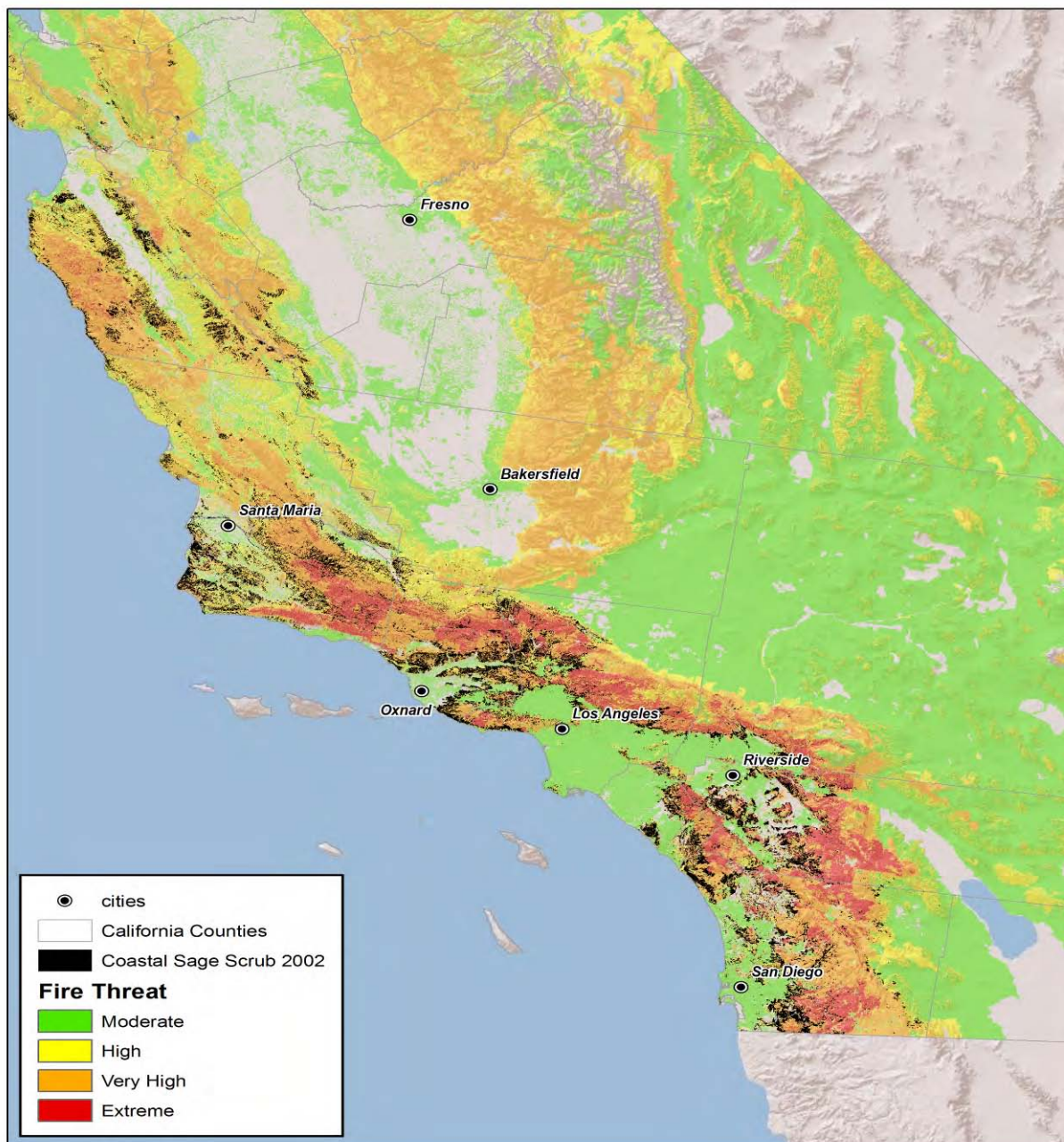


**Figure 5.1-8.** Coastal Sage Scrub Areas and Fire Threat

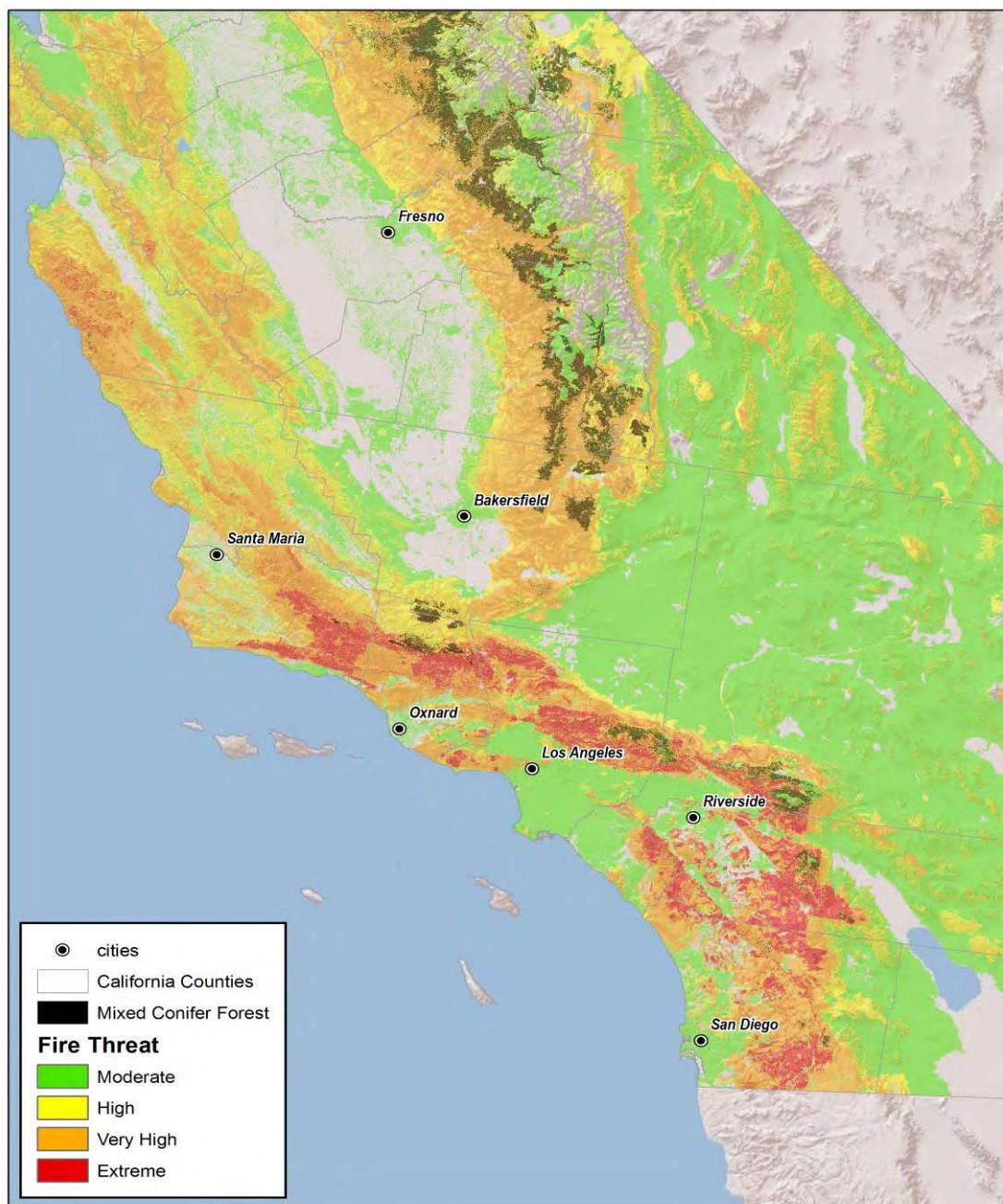


**Figure 5.1-9.** Mixed Conifer Forest Areas and Fire Threat

#### 5.1.2.2 Water Quality

In the MCF case study, maintaining water quality emerged as a regulating service that can be upset by excessive nitrogen. When the soil becomes saturated, nitrates may leach into the surface water and cause acidification. Several large rivers and Lake Tahoe cut through MCF areas, presented in **Figure 5.1-10**. Additional nitrogen from MCF areas could further degrade waters that are already stressed by numerous other sources of nutrients and pollution.



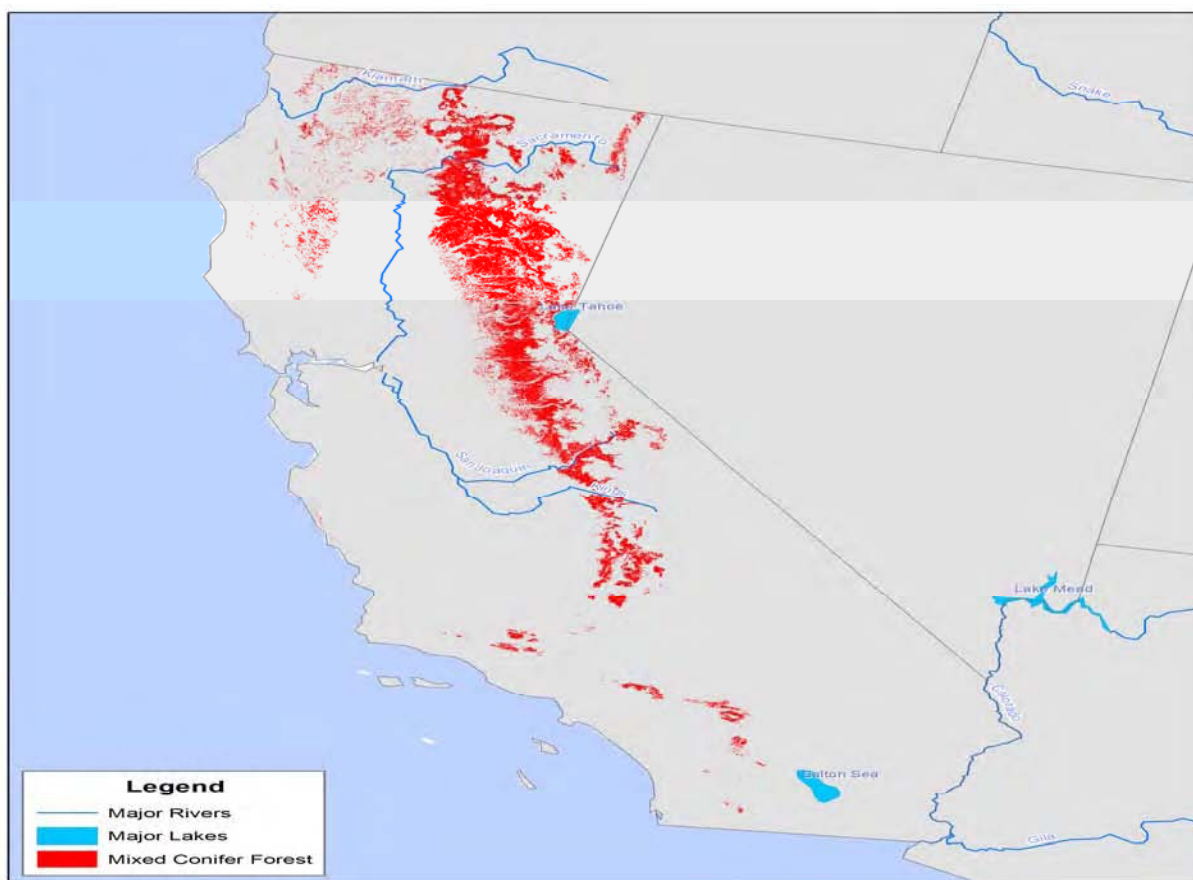


**Figure 5.1-10.** Mixed Conifer Forest Areas and Major Lakes and Rivers

## **5.2 VALUE OF COASTAL SAGE SCRUB AND MIXED CONIFER FOREST ECOSYSTEM SERVICES**

The CSS and MCF were selected as case studies for terrestrial enrichment because of the potential that these areas could be adversely affected by excessive nitrogen deposition. To date, the detailed studies needed to identify the magnitude of the adverse impacts due to nitrogen deposition have not been completed. Based on available data, this report provides a qualitative discussion of the services offered by CSS and MCF and a sense of the scale of benefits associated with these services. California is famous for its recreational opportunities and beautiful landscapes. CSS and MCF are an integral part of the California landscape, and together the ranges of these habitats include the densely populated and valuable coastline and the mountain areas. Through recreation and scenic value, these habitats affect the lives of millions of California residents and tourists. Numerous threatened and endangered species at both the state and federal levels reside in CSS and MCF. Both habitats may play an important role in wildfire



frequency and intensity, an extremely important problem for California. The potentially high value of the ecosystem services provided by CSS and MCF justify careful attention to the long-term viability of these habitats.

### **5.3 REFERENCES**

- Acharya, G., and L.L. Bennett. 2001. "Valuing Open Space and Land-Use Patterns in Urban Watersheds." *Journal of Real Estate Finance and Economics* 22(2/3):221-237.
- Burger, J.C., R.A. Redak, E.B. Allen, J.T. Rotenberry, and M.F. Allen. 2003. "Restoring Arthropod Communities in Coastal Sage Scrub." *Conservation Biology* 17(2):460-467.
- CAL FIRE (California Department of Forestry and Fire Protection). 1996. California Fire Plan. Available at [http://cdfdata.fire.ca.gov/fire\\_er/fpp\\_planning\\_cafireplan](http://cdfdata.fire.ca.gov/fire_er/fpp_planning_cafireplan).
- CAL FIRE (California Department of Forestry and Fire Protection). 2008. CAL FIRE 2007 Wildland Fire Summary.
- California Department of Fish and Game. n.d. <http://www.dfg.ca.gov/habcon/nccp/images/region.gif>.
- Geoghegan, J., L.A. Wainger, and N.E. Bockstael. 1997. "Spatial Landscape Indices in a Hedonic Framework: An Ecological Economics Analysis Using GIS." *Ecological Economics* 23:251-264.
- Irwin, E.G. 2002. "The Effects of Open Space on Residential Property Values." *Land Economics* 78(4):465-480.
- Kaval, P., and J. Loomis. 2003. *Updated Outdoor Recreation Use Values With Emphasis On National Park Recreation*. Final Report October 2003, under Cooperative Agreement CA 1200-99-009, Project number IMDE-02-0070.
- Land Trust Alliance. 2006. *The 2005 National Land Trust Census Report*. Washington, D.C.: Land Trust Alliance, November 30, 2006.

- Loomis, J., D. Griffin, E. Wu, and A. González-Cabán. 2002. “Estimating the Economic Value of Big Game Habitat Production from Prescribed Fire Using a Time Series Approach.” *Journal of Forest Economics* 2:119-29.
- Loomis, J.B., and D.S. White. 1996. “Economic Benefits of Rare and Endangered Species: Summary and Meta-Analysis.” *Ecological Economics* 18(3):197-206.
- Mansfield, C.A., S.K. Pattanayak, W. McDow, R. MacDonald, and P. Halpin. 2005. “Shades of Green: Measuring the Value of Urban Forests in the Housing Market.” *Journal of Forest Economics* 11(3):177-199.
- Mueller, J., J. Loomis, and A. González-Cabán. 2007. “Do Repeated Wildfires Change Homebuyers’ Demand for Homes in High-Risk Areas? A Hedonic Analysis of the Short and Long-Term Effects of Repeated Wildfires on House Prices in Southern California.” *Journal of Real Estate Finance and Economics*, 1-18.
- National Association of State Foresters (NASF). 2009. Quadrennial Fire Review 2009. Washington, DC: NASF. *Quadrennial Fire and Fuel Review Final Report 2009*. National Wildfire Coordinating Group Executive Board January 2009.
- Smith, V.K., C. Poulos, and H. Kim. 2002. “Treating Open Space as an Urban Amenity.” *Resource and Energy Economics* 24:107-129.
- Tyrvaenen, L., and A. Miettinen. 2000. “Property Prices and Urban Forest Amenities.” *Journal of Economics and Environmental Management* 39:205-223.
- U.S. Department of the Interior, Fish and Wildlife Service, and U.S. Department of Commerce, U.S. Census Bureau. 2007. *2006 National Survey of Fishing, Hunting, and Wildlife-Associated Recreation*.
- U.S. Environmental Protection Agency (EPA). 2008. Integrated Science Assessment for Oxides of Nitrogen and Sulfur—Environmental Criteria. EPA/600/R-08/082. U.S. Environmental Protection Agency, Office of Research and Development, National Center for Environmental Assessment – RTP Division, Research Triangle Park, NC.

## **6.0 CONCLUSION**

This report has identified, characterized, and, to the extent possible, quantified the ecosystem services that are primarily affected by changes in nitrogen and sulfur deposition and associated ecological indicators. The discussion has focused on four main categories of ecosystem effects—aquatic and terrestrial acidification and aquatic and terrestrial nutrient enrichment—and on three main categories of ecosystem services—provisioning, cultural, and regulating services.

The report demonstrates that nitrogen and sulfur deposition have wide-ranging detrimental effects on the services provided by ecosystems across the United States; however, there continues to be significant uncertainty regarding the overall magnitude of these effects. To partially address this uncertainty, where data and scientific evidence permit, this study has estimated how reducing nitrogen and sulfur deposition in specific areas would affect the value of selected ecosystem services. These estimates are summarized in **Table 6-1**.

### **6.1 BENEFITS FROM ENHANCED PROVISIONING SERVICES**

Provisioning services are derived from goods and commodities whose production depends directly on inputs from healthy ecosystems. Two main examples of provisioning services that are constrained by nitrogen and sulfur deposition are the production and consumption of forest products and seafood.

Terrestrial acidification has been shown to cause forest damages, and much of the specific evidence has focused on two tree species—sugar maples and red spruce. The value of commercial harvests from these two species in 2006 was roughly \$400 million, but the more relevant question is how much would the value of these services increase with reductions in nitrogen and sulfur deposition? This study estimates that eliminating the growth suppression effects of terrestrial acidification on sugar maples and red spruce would generate market benefits of about \$684,000 per year.

Aquatic enrichment resulting from excess inputs of nitrogen is also known to contribute to eutrophic conditions in surface waters, which limits the growth and abundance of commercial fish species. Evidence regarding the magnitude of these effects is limited, largely due to the complexities involved in modeling the dynamic ecosystem processes and links between fish

stocks and commercial fishing behaviors. One exception is a model of commercial blue crab fishing in the Neuse River estuary (Smith, 2007). Using the results of this study, it is estimated that eliminating the contribution of atmospheric nitrogen deposition to the Neuse would generate market benefits from blue crab fishery ranging between \$0.1 million and \$1 million per year.

**Table 6-1.** Summary of Aggregate Benefit Estimates for Selected Ecosystem Services and Areas (Zero Out of Nitrogen and Sulfur Deposition)<sup>a</sup>

Ecosystem Effect Ecosystem Service Area	Range (in millions of 2007 dollars/year)	
	Low	High
Aquatic Acidification		
Recreational Fishing		
Adirondack Lakes	3.9	9.3
New York Lakes	4.5	130.0
General		
Adirondack Lakes	291.2	1097.2
Terrestrial Acidification		
Commercial Timber (Sugar Maple and Red Spruce)		
Northeastern U.S.	0.684	0.684
Aquatic Enrichment		
Commercial Fishing (Blue Crab)		
Neuse	0.1	1.0
Recreational Fishing		
Chesapeake	42.6	217.0
APS	1.0	7.9
Recreational Boating		
Chesapeake	2.9	8.2
Recreational Beach Use		
Chesapeake	124.0	124.0
Aesthetic (Nearshore Residents)		
Chesapeake	38.7	102.2
Nonuse		
Chesapeake	159.1	270.4

<sup>a</sup> Because of overlaps in the services covered, the value estimates reported in the table should not be added together.

## **6.2 BENEFITS FROM ENHANCED CULTURAL SERVICES**

Cultural services are derived from the nonmaterial benefits that individuals receive from ecosystems, including spiritual enrichment, cognitive development, reflection, recreation, and aesthetic experiences. As this report discusses, acidification and enrichment effects from nitrogen and sulfur deposition have the potential to affect a wide variety of these services; however, most of the available evidence concerns recreation and aesthetic services.

As discussed in Sections 3 and 5, much of the evidence of adverse terrestrial ecosystem impacts from acidification and enrichment centers on forests in the northeastern portion of the United States and coastal sage scrub (CSS) and mixed conifer forest (MCF) ecosystems in the west. These ecosystems support a wide variety of land-based outdoor recreational activities, including hunting, wildlife viewing, and hiking, worth several billions of dollars each year to the general public. Unfortunately, relatively little evidence is available to quantify how the benefits of these recreational services are affected by terrestrial acidification or enrichment due to nitrogen and sulfur deposition.

As discussed in Sections 2 and 4, aquatic ecosystem impacts due to the acidification and nutrient enrichment of surface waters also adversely affect a broad and valuable range of outdoor recreation services. In contrast to terrestrial effects, however, the impacts of these aquatic effects on recreational services are relatively easier to quantify (at least for selected activities and geographic areas). For example, based on the results of an Aquatic Acidification Case Study of the Adirondacks, the benefits to recreational anglers in New York from zeroing out the acidification effects of nitrogen and sulfur deposition on Adirondack lakes are estimated to be roughly equivalent to \$4 million to \$9 million per year. If the zero-out conditions are extended to all New York lakes, the annual benefits could be an order of magnitude higher.

This study also used the results of the aquatic enrichment case studies to estimate the value of enhancements to several recreational activities in the Chesapeake and Albemarle-Pamlico estuaries, as a result of zeroing out nitrogen deposition to their watersheds. In the Chesapeake, the benefits to striped bass and summer flounder anglers were estimated to be roughly \$43 million per year. Extending the estimation methodology to all recreational species implies benefits of nearly \$220 million, but with a much higher degree of uncertainty. For Chesapeake boaters and beach users, the main benefit estimates were \$8 million and \$124 million per year, respectively. In the Albemarle and Pamlico Sounds (APS), the benefits to

recreational anglers were \$1 million if the nitrogen loading reductions only occurred in the Neuse and almost \$8 million if they applied to the entire APS.

In addition to the benefits from enhanced recreational services, this report also examines benefits to other cultural ecosystem services as a result of reduced aquatic acidification and nutrient enrichment effects. Using the results of the Resources for the Future (RFF) contingent valuation (CV) study of New York residents, total annual benefits (assumed to primarily be for improved cultural services, including recreational fishing services) of between \$291 million and \$1.1 billion per year for a zero out of nitrogen and sulfur deposition were estimated. In the Chesapeake Bay, benefits to nearshore residents (assumed to be mainly from improved aesthetic and recreation services) of \$39 million to \$102 million were estimated. Total nonuse benefits of between \$159 million and \$271 million per year were also estimated.

### **6.3 BENEFITS FROM ENHANCED REGULATING SERVICES**

Terrestrial and aquatic ecosystems provide a variety of regulating services, such as fire, flood, and erosion control and hydrological and climate regulation; however, there is relatively little evidence regarding the magnitude of impairments to these services due to the effects of nitrogen and sulfur deposition. Therefore, this report provides more of a qualitative assessment of these services. It describes how aquatic acidification and enrichment can affect biological food chain control services through their effects on the growth and mortality of fish species. It also describes the regulating services provided by forests, including erosion and sedimentation control, water storage, and carbon sequestration, which may be adversely affected by nitrogen and sulfur deposition. Finally, it describes potential changes in wildfire risks and fire regulation services as a result of changes in CSS ecosystems that have been altered through nitrogen enrichment.

**ATTACHMENT A**  
**ANNUAL RECREATIONAL FISHING BENEFIT ESTIMATES**  
**FOR REDUCTIONS IN NEW YORK LAKE ACIDIFICATION**  
**LEVELS, 2002–2100**





**Table A-1.** Adirondack Region—20 µeq/L Threshold

<b>Year</b>	<b>Per Capita Benefit</b>	<b>Population</b>	<b>Undiscounted Benefit</b>
<b>2002</b>	<b>0.0000</b>	<b>8,333,023</b>	<b>\$0</b>
2003	0.0000	8,391,727	\$0
2004	0.0000	8,440,400	\$0
<b>2005</b>	<b>0.0000</b>	<b>8,471,658</b>	<b>\$0</b>
2006	0.0000	8,511,465	\$0
2007	0.0000	8,551,313	\$0
2008	0.0000	8,665,048	\$0
2009	0.0000	8,595,000	\$0
2010	0.0000	8,630,872	\$0
2011	0.0680	8,661,363	\$588,805
2012	0.1360	8,685,935	\$1,180,951
2013	0.2039	8,706,365	\$1,775,593
2014	0.2719	8,721,517	\$2,371,578
2015	0.3399	8,729,057	\$2,967,035
2016	0.4079	8,731,768	\$3,561,548
2017	0.4759	8,731,621	\$4,155,069
2018	0.5438	8,730,281	\$4,747,921
2019	0.6118	8,733,574	\$5,343,426
<b>2020</b>	<b>0.6798</b>	<b>8,733,759</b>	<b>\$5,937,266</b>
2021	0.6760	8,731,785	\$5,903,042
2022	0.6723	8,728,824	\$5,868,169
2023	0.6685	8,725,132	\$5,832,830
2024	0.6647	8,720,953	\$5,797,195
2025	0.6610	8,716,339	\$5,761,304
2026	0.6572	8,712,372	\$5,725,873
2027	0.6534	8,709,340	\$5,691,082
2028	0.6497	8,707,278	\$5,656,945
2029	0.6459	8,705,815	\$5,623,210
2030	0.6421	8,705,075	\$5,589,950
2031	0.6384	8,705,075	\$5,557,169
2032	0.6346	8,705,075	\$5,524,387
2033	0.6309	8,705,075	\$5,491,606
2034	0.6271	8,705,075	\$5,458,824

(continued)

**Table A-1.** Adirondack Region—20 µeq/L Threshold (continued)

<b>Year</b>	<b>Per Capita Benefit</b>	<b>Population</b>	<b>Undiscounted Benefit</b>
2035	0.6233	8,705,075	\$5,426,042
2036	0.6196	8,705,075	\$5,393,261
2037	0.6158	8,705,075	\$5,360,479
2038	0.6120	8,705,075	\$5,327,698
2039	0.6083	8,705,075	\$5,294,916
2040	0.6045	8,705,075	\$5,262,134
2041	0.6007	8,705,075	\$5,229,353
2042	0.5970	8,705,075	\$5,196,571
2043	0.5932	8,705,075	\$5,163,790
2044	0.5894	8,705,075	\$5,131,008
2045	0.5857	8,705,075	\$5,098,226
2046	0.5819	8,705,075	\$5,065,445
2047	0.5781	8,705,075	\$5,032,663
2048	0.5744	8,705,075	\$4,999,882
2049	0.5706	8,705,075	\$4,967,100
<b>2050</b>	<b>0.5668</b>	<b>8,705,075</b>	<b>\$4,934,318</b>
2051	0.5647	8,705,075	\$4,915,346
2052	0.5625	8,705,075	\$4,896,373
2053	0.5603	8,705,075	\$4,877,400
2054	0.5581	8,705,075	\$4,858,428
2055	0.5559	8,705,075	\$4,839,455
2056	0.5538	8,705,075	\$4,820,482
2057	0.5516	8,705,075	\$4,801,510
2058	0.5494	8,705,075	\$4,782,537
2059	0.5472	8,705,075	\$4,763,565
2060	0.5450	8,705,075	\$4,744,592
2061	0.5429	8,705,075	\$4,725,619
2062	0.5407	8,705,075	\$4,706,647
2063	0.5385	8,705,075	\$4,687,674
2064	0.5363	8,705,075	\$4,668,701
2065	0.5341	8,705,075	\$4,649,729
2066	0.5320	8,705,075	\$4,630,756
2067	0.5298	8,705,075	\$4,611,783

(continued)

**Table A-1.** Adirondack Region—20 µeq/L Threshold (continued)

<b>Year</b>	<b>Per Capita Benefit</b>	<b>Population</b>	<b>Undiscounted Benefit</b>
2068	0.5276	8,705,075	\$4,592,811
2069	0.5254	8,705,075	\$4,573,838
2070	0.5232	8,705,075	\$4,554,865
2071	0.5211	8,705,075	\$4,535,893
2072	0.5189	8,705,075	\$4,516,920
2073	0.5167	8,705,075	\$4,497,947
2074	0.5145	8,705,075	\$4,478,975
2075	0.5123	8,705,075	\$4,460,002
2076	0.5102	8,705,075	\$4,441,029
2077	0.5080	8,705,075	\$4,422,057
2078	0.5058	8,705,075	\$4,403,084
2079	0.5036	8,705,075	\$4,384,111
2080	0.5014	8,705,075	\$4,365,139
2081	0.4993	8,705,075	\$4,346,166
2082	0.4971	8,705,075	\$4,327,193
2083	0.4949	8,705,075	\$4,308,221
2084	0.4927	8,705,075	\$4,289,248
2085	0.4906	8,705,075	\$4,270,275
2086	0.4884	8,705,075	\$4,251,303
2087	0.4862	8,705,075	\$4,232,330
2088	0.4840	8,705,075	\$4,213,357
2089	0.4818	8,705,075	\$4,194,385
2090	0.4797	8,705,075	\$4,175,412
2091	0.4775	8,705,075	\$4,156,439
2092	0.4753	8,705,075	\$4,137,467
2093	0.4731	8,705,075	\$4,118,494
2094	0.4709	8,705,075	\$4,099,521
2095	0.4688	8,705,075	\$4,080,549
2096	0.4666	8,705,075	\$4,061,576
2097	0.4644	8,705,075	\$4,042,603
2098	0.4622	8,705,075	\$4,023,631
2099	0.4600	8,705,075	\$4,004,658
<b>2100</b>	<b>0.4579</b>	<b>8,705,075</b>	<b>\$3,985,685</b>

**Table A-2.** Adirondack Region—50 µeq/L Threshold

<b>Year</b>	<b>Per Capita Benefit</b>	<b>Population</b>	<b>Undiscounted Benefit</b>
<b>2002</b>	<b>0.0000</b>	<b>8,333,023</b>	<b>\$0</b>
2003	0.0000	8,391,727	\$0
2004	0.0000	8,440,400	\$0
<b>2005</b>	<b>0.0000</b>	<b>8,471,658</b>	<b>\$0</b>
2006	0.0000	8,511,465	\$0
2007	0.0000	8,551,313	\$0
2008	0.0000	8,665,048	\$0
2009	0.0000	8,595,000	\$0
2010	0.0000	8,630,872	\$0
2011	0.1232	8,661,363	\$1,066,847
2012	0.2463	8,685,935	\$2,139,747
2013	0.3695	8,706,365	\$3,217,170
2014	0.4927	8,721,517	\$4,297,025
2015	0.6159	8,729,057	\$5,375,925
2016	0.7390	8,731,768	\$6,453,113
2017	0.8622	8,731,621	\$7,528,505
2018	0.9854	8,730,281	\$8,602,686
2019	1.1086	8,733,574	\$9,681,672
<b>2020</b>	<b>1.2317</b>	<b>8,733,759</b>	<b>\$10,757,642</b>
2021	1.2310	8,731,785	\$10,748,533
2022	1.2302	8,728,824	\$10,738,213
2023	1.2294	8,725,132	\$10,727,000
2024	1.2287	8,720,953	\$10,715,194
2025	1.2279	8,716,339	\$10,702,859
2026	1.2271	8,712,372	\$10,691,327
2027	1.2264	8,709,340	\$10,680,945
2028	1.2256	8,707,278	\$10,671,759
2029	1.2248	8,705,815	\$10,663,309
2030	1.2241	8,705,075	\$10,655,746
2031	1.2233	8,705,075	\$10,649,090
2032	1.2226	8,705,075	\$10,642,433
2033	1.2218	8,705,075	\$10,635,777
2034	1.2210	8,705,075	\$10,629,121

(continued)

**Table A-2.** Adirondack Region—50 µeq/L Threshold (continued)

Year	Per Capita Benefit	Population	Undiscounted Benefit
2035	1.2203	8,705,075	\$10,622,464
2036	1.2195	8,705,075	\$10,615,808
2037	1.2187	8,705,075	\$10,609,151
2038	1.2180	8,705,075	\$10,602,495
2039	1.2172	8,705,075	\$10,595,839
2040	1.2164	8,705,075	\$10,589,182
2041	1.2157	8,705,075	\$10,582,526
2042	1.2149	8,705,075	\$10,575,869
2043	1.2141	8,705,075	\$10,569,213
2044	1.2134	8,705,075	\$10,562,557
2045	1.2126	8,705,075	\$10,555,900
2046	1.2118	8,705,075	\$10,549,244
2047	1.2111	8,705,075	\$10,542,587
2048	1.2103	8,705,075	\$10,535,931
2049	1.2096	8,705,075	\$10,529,275
<b>2050</b>	<b>1.2088</b>	<b>8,705,075</b>	<b>\$10,522,618</b>
2051	1.2079	8,705,075	\$10,514,670
2052	1.2070	8,705,075	\$10,506,723
2053	1.2061	8,705,075	\$10,498,775
2054	1.2051	8,705,075	\$10,490,827
2055	1.2042	8,705,075	\$10,482,879
2056	1.2033	8,705,075	\$10,474,931
2057	1.2024	8,705,075	\$10,466,983
2058	1.2015	8,705,075	\$10,459,035
2059	1.2006	8,705,075	\$10,451,087
2060	1.1997	8,705,075	\$10,443,139
2061	1.1987	8,705,075	\$10,435,191
2062	1.1978	8,705,075	\$10,427,243
2063	1.1969	8,705,075	\$10,419,296
2064	1.1960	8,705,075	\$10,411,348
2065	1.1951	8,705,075	\$10,403,400
2066	1.1942	8,705,075	\$10,395,452
2067	1.1933	8,705,075	\$10,387,504

(continued)

**Table A-2.** Adirondack Region—50 µeq/L Threshold (continued)

<b>Year</b>	<b>Per Capita Benefit</b>	<b>Population</b>	<b>Undiscounted Benefit</b>
2068	1.1924	8,705,075	\$10,379,556
2069	1.1914	8,705,075	\$10,371,608
2070	1.1905	8,705,075	\$10,363,660
2071	1.1896	8,705,075	\$10,355,712
2072	1.1887	8,705,075	\$10,347,764
2073	1.1878	8,705,075	\$10,339,817
2074	1.1869	8,705,075	\$10,331,869
2075	1.1860	8,705,075	\$10,323,921
2076	1.1851	8,705,075	\$10,315,973
2077	1.1841	8,705,075	\$10,308,025
2078	1.1832	8,705,075	\$10,300,077
2079	1.1823	8,705,075	\$10,292,129
2080	1.1814	8,705,075	\$10,284,181
2081	1.1805	8,705,075	\$10,276,233
2082	1.1796	8,705,075	\$10,268,285
2083	1.1787	8,705,075	\$10,260,338
2084	1.1777	8,705,075	\$10,252,390
2085	1.1768	8,705,075	\$10,244,442
2086	1.1759	8,705,075	\$10,236,494
2087	1.1750	8,705,075	\$10,228,546
2088	1.1741	8,705,075	\$10,220,598
2089	1.1732	8,705,075	\$10,212,650
2090	1.1723	8,705,075	\$10,204,702
2091	1.1714	8,705,075	\$10,196,754
2092	1.1704	8,705,075	\$10,188,806
2093	1.1695	8,705,075	\$10,180,859
2094	1.1686	8,705,075	\$10,172,911
2095	1.1677	8,705,075	\$10,164,963
2096	1.1668	8,705,075	\$10,157,015
2097	1.1659	8,705,075	\$10,149,067
2098	1.1650	8,705,075	\$10,141,119
2099	1.1641	8,705,075	\$10,133,171
<b>2100</b>	<b>1.1631</b>	<b>8,705,075</b>	<b>\$10,125,223</b>

**Table A-3.** Adirondack Region—100 µeq/L Threshold

<b>Year</b>	<b>Per Capita Benefit</b>	<b>Population</b>	<b>Undiscounted Benefit</b>
<b>2002</b>	<b>0.0000</b>	<b>8,333,023</b>	<b>\$0</b>
2003	0.0000	8,391,727	\$0
2004	0.0000	8,440,400	\$0
<b>2005</b>	<b>0.0000</b>	<b>8,471,658</b>	<b>\$0</b>
2006	0.0000	8,511,465	\$0
2007	0.0000	8,551,313	\$0
2008	0.0000	8,665,048	\$0
2009	0.0000	8,595,000	\$0
2010	0.0000	8,630,872	\$0
2011	0.1307	8,661,363	\$1,131,871
2012	0.2614	8,685,935	\$2,270,164
2013	0.3920	8,706,365	\$3,413,256
2014	0.5227	8,721,517	\$4,558,928
2015	0.6534	8,729,057	\$5,703,587
2016	0.7841	8,731,768	\$6,846,430
2017	0.9148	8,731,621	\$7,987,367
2018	1.0454	8,730,281	\$9,127,018
2019	1.1761	8,733,574	\$10,271,769
<b>2020</b>	<b>1.3068</b>	<b>8,733,759</b>	<b>\$11,413,319</b>
2021	1.3056	8,731,785	\$11,400,066
2022	1.3044	8,728,824	\$11,385,532
2023	1.3031	8,725,132	\$11,370,052
2024	1.3019	8,720,953	\$11,353,948
2025	1.3007	8,716,339	\$11,337,287
2026	1.2995	8,712,372	\$11,321,479
2027	1.2982	8,709,340	\$11,306,893
2028	1.2970	8,707,278	\$11,293,575
2029	1.2958	8,705,815	\$11,281,036
2030	1.2946	8,705,075	\$11,269,438
2031	1.2934	8,705,075	\$11,258,798
2032	1.2921	8,705,075	\$11,248,159
2033	1.2909	8,705,075	\$11,237,519
2034	1.2897	8,705,075	\$11,226,879

(continued)

**Table A-3.** Adirondack Region—100 µeq/L Threshold (continued)

<b>Year</b>	<b>Per Capita Benefit</b>	<b>Population</b>	<b>Undiscounted Benefit</b>
2035	1.2885	8,705,075	\$11,216,240
2036	1.2872	8,705,075	\$11,205,600
2037	1.2860	8,705,075	\$11,194,961
2038	1.2848	8,705,075	\$11,184,321
2039	1.2836	8,705,075	\$11,173,681
2040	1.2824	8,705,075	\$11,163,042
2041	1.2811	8,705,075	\$11,152,402
2042	1.2799	8,705,075	\$11,141,763
2043	1.2787	8,705,075	\$11,131,123
2044	1.2775	8,705,075	\$11,120,484
2045	1.2762	8,705,075	\$11,109,844
2046	1.2750	8,705,075	\$11,099,204
2047	1.2738	8,705,075	\$11,088,565
2048	1.2726	8,705,075	\$11,077,925
2049	1.2714	8,705,075	\$11,067,286
<b>2050</b>	<b>1.2701</b>	<b>8,705,075</b>	<b>\$11,056,646</b>
2051	1.2674	8,705,075	\$11,033,188
2052	1.2647	8,705,075	\$11,009,730
2053	1.2621	8,705,075	\$10,986,272
2054	1.2594	8,705,075	\$10,962,814
2055	1.2567	8,705,075	\$10,939,356
2056	1.2540	8,705,075	\$10,915,897
2057	1.2513	8,705,075	\$10,892,439
2058	1.2486	8,705,075	\$10,868,981
2059	1.2459	8,705,075	\$10,845,523
2060	1.2432	8,705,075	\$10,822,065
2061	1.2405	8,705,075	\$10,798,607
2062	1.2378	8,705,075	\$10,775,149
2063	1.2351	8,705,075	\$10,751,691
2064	1.2324	8,705,075	\$10,728,233
2065	1.2297	8,705,075	\$10,704,775
2066	1.2270	8,705,075	\$10,681,317
2067	1.2243	8,705,075	\$10,657,859

(continued)



**Table A-3.** Adirondack Region—100 µeq/L Threshold (continued)

Year	Per Capita Benefit	Population	Undiscounted Benefit
2068	1.2216	8,705,075	\$10,634,400
2069	1.2189	8,705,075	\$10,610,942
2070	1.2162	8,705,075	\$10,587,484
2071	1.2135	8,705,075	\$10,564,026
2072	1.2109	8,705,075	\$10,540,568
2073	1.2082	8,705,075	\$10,517,110
2074	1.2055	8,705,075	\$10,493,652
2075	1.2028	8,705,075	\$10,470,194
2076	1.2001	8,705,075	\$10,446,736
2077	1.1974	8,705,075	\$10,423,278
2078	1.1947	8,705,075	\$10,399,820
2079	1.1920	8,705,075	\$10,376,362
2080	1.1893	8,705,075	\$10,352,903
2081	1.1866	8,705,075	\$10,329,445
2082	1.1839	8,705,075	\$10,305,987
2083	1.1812	8,705,075	\$10,282,529
2084	1.1785	8,705,075	\$10,259,071
2085	1.1758	8,705,075	\$10,235,613
2086	1.1731	8,705,075	\$10,212,155
2087	1.1704	8,705,075	\$10,188,697
2088	1.1677	8,705,075	\$10,165,239
2089	1.1650	8,705,075	\$10,141,781
2090	1.1623	8,705,075	\$10,118,323
2091	1.1597	8,705,075	\$10,094,865
2092	1.1570	8,705,075	\$10,071,406
2093	1.1543	8,705,075	\$10,047,948
2094	1.1516	8,705,075	\$10,024,490
2095	1.1489	8,705,075	\$10,001,032
2096	1.1462	8,705,075	\$9,977,574
2097	1.1435	8,705,075	\$9,954,116
2098	1.1408	8,705,075	\$9,930,658
2099	1.1381	8,705,075	\$9,907,200
<b>2100</b>	<b>1.1354</b>	<b>8,705,075</b>	<b>\$9,883,742</b>

**Table A-4.** New York State—20 µeq/L Threshold

<b>Year</b>	<b>Per Capita Benefit</b>	<b>Population</b>	<b>Undiscounted Benefit</b>
<b>2002</b>	<b>0.0000</b>	<b>8,333,023</b>	<b>\$0</b>
2003	0.0000	8,391,727	\$0
2004	0.0000	8,440,400	\$0
<b>2005</b>	<b>0.0000</b>	<b>8,471,658</b>	<b>\$0</b>
2006	0.0000	8,511,465	\$0
2007	0.0000	8,551,313	\$0
2008	0.0000	8,665,048	\$0
2009	0.0000	8,595,000	\$0
2010	0.0000	8,630,872	\$0
2011	0.0777	8,661,363	\$673,415
2012	0.1555	8,685,935	\$1,350,651
2013	0.2332	8,706,365	\$2,030,742
2014	0.3110	8,721,517	\$2,712,368
2015	0.3887	8,729,057	\$3,393,391
2016	0.4665	8,731,768	\$4,073,334
2017	0.5442	8,731,621	\$4,752,142
2018	0.6220	8,730,281	\$5,430,186
2019	0.6997	8,733,574	\$6,111,264
<b>2020</b>	<b>0.7775</b>	<b>8,733,759</b>	<b>\$6,790,438</b>
2021	0.7727	8,731,785	\$6,747,422
2022	0.7680	8,728,824	\$6,703,667
2023	0.7632	8,725,132	\$6,659,383
2024	0.7585	8,720,953	\$6,614,765
2025	0.7537	8,716,339	\$6,569,857
2026	0.7490	8,712,372	\$6,525,479
2027	0.7442	8,709,340	\$6,481,834
2028	0.7395	8,707,278	\$6,438,935
2029	0.7347	8,705,815	\$6,396,496
2030	0.7300	8,705,075	\$6,354,599
2031	0.7252	8,705,075	\$6,313,245
2032	0.7205	8,705,075	\$6,271,891
2033	0.7157	8,705,075	\$6,230,538
2034	0.7110	8,705,075	\$6,189,184

(continued)

**Table A-4.** New York State—20 µeq/L Threshold (continued)

<b>Year</b>	<b>Per Capita Benefit</b>	<b>Population</b>	<b>Undiscounted Benefit</b>
2035	0.7062	8,705,075	\$6,147,830
2036	0.7015	8,705,075	\$6,106,477
2037	0.6967	8,705,075	\$6,065,123
2038	0.6920	8,705,075	\$6,023,769
2039	0.6872	8,705,075	\$5,982,416
2040	0.6825	8,705,075	\$5,941,062
2041	0.6777	8,705,075	\$5,899,708
2042	0.6730	8,705,075	\$5,858,355
2043	0.6682	8,705,075	\$5,817,001
2044	0.6635	8,705,075	\$5,775,647
2045	0.6587	8,705,075	\$5,734,294
2046	0.6540	8,705,075	\$5,692,940
2047	0.6492	8,705,075	\$5,651,586
2048	0.6445	8,705,075	\$5,610,233
2049	0.6397	8,705,075	\$5,568,879
<b>2050</b>	<b>0.6350</b>	<b>8,705,075</b>	<b>\$5,527,525</b>
2051	0.6327	8,705,075	\$5,508,117
2052	0.6305	8,705,075	\$5,488,710
2053	0.6283	8,705,075	\$5,469,302
2054	0.6261	8,705,075	\$5,449,894
2055	0.6238	8,705,075	\$5,430,487
2056	0.6216	8,705,075	\$5,411,079
2057	0.6194	8,705,075	\$5,391,671
2058	0.6171	8,705,075	\$5,372,264
2059	0.6149	8,705,075	\$5,352,856
2060	0.6127	8,705,075	\$5,333,448
2061	0.6105	8,705,075	\$5,314,041
2062	0.6082	8,705,075	\$5,294,633
2063	0.6060	8,705,075	\$5,275,225
2064	0.6038	8,705,075	\$5,255,818
2065	0.6015	8,705,075	\$5,236,410
2066	0.5993	8,705,075	\$5,217,002
2067	0.5971	8,705,075	\$5,197,595

(continued)

**Table A-4.** New York State—20 µeq/L Threshold (continued)

<b>Year</b>	<b>Per Capita Benefit</b>	<b>Population</b>	<b>Undiscounted Benefit</b>
2068	0.5948	8,705,075	\$5,178,187
2069	0.5926	8,705,075	\$5,158,779
2070	0.5904	8,705,075	\$5,139,372
2071	0.5882	8,705,075	\$5,119,964
2072	0.5859	8,705,075	\$5,100,556
2073	0.5837	8,705,075	\$5,081,149
2074	0.5815	8,705,075	\$5,061,741
2075	0.5792	8,705,075	\$5,042,333
2076	0.5770	8,705,075	\$5,022,926
2077	0.5748	8,705,075	\$5,003,518
2078	0.5726	8,705,075	\$4,984,110
2079	0.5703	8,705,075	\$4,964,703
2080	0.5681	8,705,075	\$4,945,295
2081	0.5659	8,705,075	\$4,925,887
2082	0.5636	8,705,075	\$4,906,480
2083	0.5614	8,705,075	\$4,887,072
2084	0.5592	8,705,075	\$4,867,664
2085	0.5569	8,705,075	\$4,848,257
2086	0.5547	8,705,075	\$4,828,849
2087	0.5525	8,705,075	\$4,809,441
2088	0.5503	8,705,075	\$4,790,034
2089	0.5480	8,705,075	\$4,770,626
2090	0.5458	8,705,075	\$4,751,218
2091	0.5436	8,705,075	\$4,731,811
2092	0.5413	8,705,075	\$4,712,403
2093	0.5391	8,705,075	\$4,692,995
2094	0.5369	8,705,075	\$4,673,588
2095	0.5347	8,705,075	\$4,654,180
2096	0.5324	8,705,075	\$4,634,772
2097	0.5302	8,705,075	\$4,615,365
2098	0.5280	8,705,075	\$4,595,957
2099	0.5257	8,705,075	\$4,576,549
<b>2100</b>	<b>0.5235</b>	<b>8,705,075</b>	<b>\$4,557,142</b>

**Table A-5.** New York State—50 µeq/L Threshold

Year	Per Capita Benefit	Population	Undiscounted Benefit
<b>2002</b>	<b>0.0000</b>	<b>8,333,023</b>	<b>\$0</b>
2003	0.0000	8,391,727	\$0
2004	0.0000	8,440,400	\$0
<b>2005</b>	<b>0.0000</b>	<b>8,471,658</b>	<b>\$0</b>
2006	0.0000	8,511,465	\$0
2007	0.0000	8,551,313	\$0
2008	0.0000	8,665,048	\$0
2009	0.0000	8,595,000	\$0
2010	0.0000	8,630,872	\$0
2011	0.4224	8,661,363	\$3,658,144
2012	0.8447	8,685,935	\$7,337,045
2013	1.2671	8,706,365	\$11,031,452
2014	1.6894	8,721,517	\$14,734,201
2015	2.1118	8,729,057	\$18,433,674
2016	2.5341	8,731,768	\$22,127,279
2017	2.9565	8,731,621	\$25,814,723
2018	3.3788	8,730,281	\$29,498,013
2019	3.8012	8,733,574	\$33,197,783
<b>2020</b>	<b>4.2235</b>	<b>8,733,759</b>	<b>\$36,887,209</b>
2021	4.2077	8,731,785	\$36,740,406
2022	4.1918	8,728,824	\$36,589,530
2023	4.1759	8,725,132	\$36,435,696
2024	4.1601	8,720,953	\$36,279,955
2025	4.1442	8,716,339	\$36,122,540
2026	4.1284	8,712,372	\$35,967,946
2027	4.1125	8,709,340	\$35,817,317
2028	4.0967	8,707,278	\$35,670,765
2029	4.0808	8,705,815	\$35,526,718
2030	4.0649	8,705,075	\$35,385,658
2031	4.0491	8,705,075	\$35,247,618
2032	4.0332	8,705,075	\$35,109,578
2033	4.0174	8,705,075	\$34,971,538
2034	4.0015	8,705,075	\$34,833,498

(continued)

**Table A-5.** New York State—50 µeq/L Threshold (continued)

<b>Year</b>	<b>Per Capita Benefit</b>	<b>Population</b>	<b>Undiscounted Benefit</b>
2035	3.9857	8,705,075	\$34,695,458
2036	3.9698	8,705,075	\$34,557,418
2037	3.9539	8,705,075	\$34,419,378
2038	3.9381	8,705,075	\$34,281,337
2039	3.9222	8,705,075	\$34,143,297
2040	3.9064	8,705,075	\$34,005,257
2041	3.8905	8,705,075	\$33,867,217
2042	3.8747	8,705,075	\$33,729,177
2043	3.8588	8,705,075	\$33,591,137
2044	3.8429	8,705,075	\$33,453,097
2045	3.8271	8,705,075	\$33,315,057
2046	3.8112	8,705,075	\$33,177,016
2047	3.7954	8,705,075	\$33,038,976
2048	3.7795	8,705,075	\$32,900,936
2049	3.7637	8,705,075	\$32,762,896
<b>2050</b>	<b>3.7478</b>	<b>8,705,075</b>	<b>\$32,624,856</b>
2051	3.7216	8,705,075	\$32,397,187
2052	3.6955	8,705,075	\$32,169,517
2053	3.6693	8,705,075	\$31,941,848
2054	3.6432	8,705,075	\$31,714,179
2055	3.6170	8,705,075	\$31,486,509
2056	3.5909	8,705,075	\$31,258,840
2057	3.5647	8,705,075	\$31,031,171
2058	3.5386	8,705,075	\$30,803,502
2059	3.5124	8,705,075	\$30,575,832
2060	3.4863	8,705,075	\$30,348,163
2061	3.4601	8,705,075	\$30,120,494
2062	3.4340	8,705,075	\$29,892,824
2063	3.4078	8,705,075	\$29,665,155
2064	3.3816	8,705,075	\$29,437,486
2065	3.3555	8,705,075	\$29,209,816
2066	3.3293	8,705,075	\$28,982,147
2067	3.3032	8,705,075	\$28,754,478

(continued)

**Table A-5.** New York State—50 µeq/L Threshold (continued)

<b>Year</b>	<b>Per Capita Benefit</b>	<b>Population</b>	<b>Undiscounted Benefit</b>
2068	3.2770	8,705,075	\$28,526,808
2069	3.2509	8,705,075	\$28,299,139
2070	3.2247	8,705,075	\$28,071,470
2071	3.1986	8,705,075	\$27,843,800
2072	3.1724	8,705,075	\$27,616,131
2073	3.1463	8,705,075	\$27,388,462
2074	3.1201	8,705,075	\$27,160,793
2075	3.0940	8,705,075	\$26,933,123
2076	3.0678	8,705,075	\$26,705,454
2077	3.0416	8,705,075	\$26,477,785
2078	3.0155	8,705,075	\$26,250,115
2079	2.9893	8,705,075	\$26,022,446
2080	2.9632	8,705,075	\$25,794,777
2081	2.9370	8,705,075	\$25,567,107
2082	2.9109	8,705,075	\$25,339,438
2083	2.8847	8,705,075	\$25,111,769
2084	2.8586	8,705,075	\$24,884,099
2085	2.8324	8,705,075	\$24,656,430
2086	2.8063	8,705,075	\$24,428,761
2087	2.7801	8,705,075	\$24,201,092
2088	2.7540	8,705,075	\$23,973,422
2089	2.7278	8,705,075	\$23,745,753
2090	2.7017	8,705,075	\$23,518,084
2091	2.6755	8,705,075	\$23,290,414
2092	2.6493	8,705,075	\$23,062,745
2093	2.6232	8,705,075	\$22,835,076
2094	2.5970	8,705,075	\$22,607,406
2095	2.5709	8,705,075	\$22,379,737
2096	2.5447	8,705,075	\$22,152,068
2097	2.5186	8,705,075	\$21,924,398
2098	2.4924	8,705,075	\$21,696,729
2099	2.4663	8,705,075	\$21,469,060
<b>2100</b>	<b>2.4401</b>	<b>8,705,075</b>	<b>\$21,241,390</b>

**Table A-6.** New York State—100 µeq/L Threshold

Year	Per Capita Benefit	Population	Undiscounted Benefit
<b>2002</b>	<b>0.0000</b>	<b>8,333,023</b>	<b>\$0</b>
2003	0.0000	8,391,727	\$0
2004	0.0000	8,440,400	\$0
<b>2005</b>	<b>0.0000</b>	<b>8,471,658</b>	<b>\$0</b>
2006	0.0000	8,511,465	\$0
2007	0.0000	8,551,313	\$0
2008	0.0000	8,665,048	\$0
2009	0.0000	8,595,000	\$0
2010	0.0000	8,630,872	\$0
2011	1.8336	8,661,363	\$15,881,141
2012	3.6671	8,685,935	\$31,852,394
2013	5.5007	8,706,365	\$47,890,966
2014	7.3342	8,721,517	\$63,965,753
2015	9.1678	8,729,057	\$80,026,316
2016	11.0014	8,731,768	\$96,061,405
2017	12.8349	8,731,621	\$112,069,745
2018	14.6685	8,730,281	\$128,060,056
2019	16.5021	8,733,574	\$144,121,906
<b>2020</b>	<b>18.3356</b>	<b>8,733,759</b>	<b>\$160,138,854</b>
2021	18.3111	8,731,785	\$159,888,275
2022	18.2865	8,728,824	\$159,619,755
2023	18.2620	8,725,132	\$159,338,035
2024	18.2374	8,720,953	\$159,047,621
2025	18.2129	8,716,339	\$158,749,471
2026	18.1883	8,712,372	\$158,463,334
2027	18.1638	8,709,340	\$158,194,349
2028	18.1392	8,707,278	\$157,943,136
2029	18.1147	8,705,815	\$157,702,858
2030	18.0901	8,705,075	\$157,475,737
2031	18.0656	8,705,075	\$157,262,020
2032	18.0410	8,705,075	\$157,048,303
2033	18.0165	8,705,075	\$156,834,587
2034	17.9919	8,705,075	\$156,620,870

(continued)



**Table A-6.** New York State—100 µeq/L Threshold (continued)

Year	Per Capita Benefit	Population	Undiscounted Benefit
2035	17.9674	8,705,075	\$156,407,153
2036	17.9428	8,705,075	\$156,193,436
2037	17.9183	8,705,075	\$155,979,720
2038	17.8937	8,705,075	\$155,766,003
2039	17.8691	8,705,075	\$155,552,286
2040	17.8446	8,705,075	\$155,338,569
2041	17.8200	8,705,075	\$155,124,852
2042	17.7955	8,705,075	\$154,911,136
2043	17.7709	8,705,075	\$154,697,419
2044	17.7464	8,705,075	\$154,483,702
2045	17.7218	8,705,075	\$154,269,985
2046	17.6973	8,705,075	\$154,056,269
2047	17.6727	8,705,075	\$153,842,552
2048	17.6482	8,705,075	\$153,628,835
2049	17.6236	8,705,075	\$153,415,118
<b>2050</b>	<b>17.5991</b>	<b>8,705,075</b>	<b>\$153,201,401</b>
2051	17.5589	8,705,075	\$152,851,672
2052	17.5187	8,705,075	\$152,501,943
2053	17.4786	8,705,075	\$152,152,214
2054	17.4384	8,705,075	\$151,802,485
2055	17.3982	8,705,075	\$151,452,756
2056	17.3580	8,705,075	\$151,103,027
2057	17.3179	8,705,075	\$150,753,298
2058	17.2777	8,705,075	\$150,403,569
2059	17.2375	8,705,075	\$150,053,840
2060	17.1973	8,705,075	\$149,704,111
2061	17.1572	8,705,075	\$149,354,382
2062	17.1170	8,705,075	\$149,004,652
2063	17.0768	8,705,075	\$148,654,923
2064	17.0366	8,705,075	\$148,305,194
2065	16.9965	8,705,075	\$147,955,465
2066	16.9563	8,705,075	\$147,605,736
2067	16.9161	8,705,075	\$147,256,007

(continued)

**Table A-6.** New York State—100 µeq/L Threshold (continued)

Year	Per Capita Benefit	Population	Undiscounted Benefit
2068	16.8759	8,705,075	\$146,906,278
2069	16.8358	8,705,075	\$146,556,549
2070	16.7956	8,705,075	\$146,206,820
2071	16.7554	8,705,075	\$145,857,091
2072	16.7152	8,705,075	\$145,507,362
2073	16.6751	8,705,075	\$145,157,633
2074	16.6349	8,705,075	\$144,807,903
2075	16.5947	8,705,075	\$144,458,174
2076	16.5545	8,705,075	\$144,108,445
2077	16.5144	8,705,075	\$143,758,716
2078	16.4742	8,705,075	\$143,408,987
2079	16.4340	8,705,075	\$143,059,258
2080	16.3938	8,705,075	\$142,709,529
2081	16.3537	8,705,075	\$142,359,800
2082	16.3135	8,705,075	\$142,010,071
2083	16.2733	8,705,075	\$141,660,342
2084	16.2331	8,705,075	\$141,310,613
2085	16.1930	8,705,075	\$140,960,883
2086	16.1528	8,705,075	\$140,611,154
2087	16.1126	8,705,075	\$140,261,425
2088	16.0724	8,705,075	\$139,911,696
2089	16.0323	8,705,075	\$139,561,967
2090	15.9921	8,705,075	\$139,212,238
2091	15.9519	8,705,075	\$138,862,509
2092	15.9117	8,705,075	\$138,512,780
2093	15.8716	8,705,075	\$138,163,051
2094	15.8314	8,705,075	\$137,813,322
2095	15.7912	8,705,075	\$137,463,593
2096	15.7510	8,705,075	\$137,113,864
2097	15.7109	8,705,075	\$136,764,134
2098	15.6707	8,705,075	\$136,414,405
2099	15.6305	8,705,075	\$136,064,676
<b>2100</b>	<b>15.5903</b>	<b>8,705,075</b>	<b>\$135,714,947</b>



---

United States  
Environmental Protection  
Agency

Office of Air Quality Planning and Standards  
Health and Environmental Impacts Division  
Research Triangle Park, NC

Publication No. EPA-452/R-09-008b  
September 2009

---